VOLUME 28 / NUMBER 7
APRIL 6, 1990
ACC. NOS. N90-15041 TO N90-15881

STAR

AN ABSTRACT JOURNAL

Scientific and Technical Aerospace Reports

PRODUCED BY THE
SCIENTIFIC AND TECHNICAL
INFORMATION
DIVISION

NASA

NATIONAL AERONAUTICS AND SPACE ADMINISTRATION

WHAT YOU CAN DO FOR *STAR*

All users of this abstract service are urged to forward reports to be considered for announcement in *STAR*. This will aid NASA in its efforts to provide the fullest possible coverage of all scientific and technical publications that might support aeronautics and space research and development. If you have prepared relevant reports (other than those that you will transmit to NASA, DOD, or DOE through the usual contract- or grant-reporting channels), please send them for consideration to the NASA Scientific and Technical Information Facility, P.O. Box 8757, BWI Airport, MD 21240.

Reprints of journal articles, book chapters, and conference papers are also welcome. These will be considered for announcement in *STAR*'s companion journal, *International Aerospace Abstracts*.

You may specify a particular source to be included in a report announcement if you wish; otherwise the report will be placed on public sale at the National Technical Information Service. Copyrighted publications will be announced but not distributed or sold.

PURCHASE OF *STAR*

The semimonthly issues are available to registered users on annual subscription from the NASA Scientific and Technical Information Facility, ATTN: Registration Services, P.O. Box 8757, BWI Airport, MD 21240. *STAR* is publicly available on annual subscription from the Superintendent of Documents, U.S. Government Printing Office, Washington, DC 20402.

PUBLISHED BY:

UNITED STATES GOVERNMENT
NATIONAL AERONAUTICS AND SPACE ADMINISTRATION
SCIENTIFIC AND TECHNICAL INFORMATION DIVISION
Scientific and Technical Aerospace Reports, Volume 28, is prepared by the NASA Scientific and Technical Information Facility operated for the National Aeronautics and Space Administration by RMS Associates.

The Administrator of the National Aeronautics and Space Administration has determined that the publication of this periodical is necessary in the transaction of the public business required by law of this agency. Use of funds for printing this periodical has been approved by the Director of the Office of Management and Budget through March 22, 1991.

US ISSN 0036-8741

Scientific and Technical Aerospace Reports (STAR) is issued twice a month and contains abstracts and indexes of meeting papers, conference proceedings, and unlimited distribution reports that have been added to the NASA Scientific and Technical Information Database during the preceding period. These citations may also be accessed online via NASA/RECON or via AIAA's Aerospace Database (File 108) through Dialog Information Services, Inc.

STAR subject coverage includes all aerospace-related areas that will help NASA achieve its mission. Material is gathered from all over the world and includes significant input from many countries under exchange and access agreements.

Consult the indexes at the back of this volume to help zero in on what you are looking for. These include:

Subject Index
Personal Author Index
Corporate Source Index
Contract Number Index
Report/Accession Number Index

STAR's companion abstract journal *International Aerospace Abstracts* should be used if you are looking for references to periodicals, books, and published meeting papers or conference proceedings.

Questions and comments should be addressed to:

NASA Scientific and Technical Information Facility
User Services
P.O. Box 8757
BWI Airport, MD 21240
301-621-0150

VOLUME 28 NUMBER 7 / APRIL 8, 1990

TABLE OF CONTENTS

AERONAUTICS

Includes aeronautics (general); aerodynamics; air transportation and safety; aircraft communications and navigation; aircraft design, testing and performance; aircraft instrumentation; aircraft propulsion and power; aircraft stability and control; and research and support facilities (air).

For related information see also *Astronautics.*

01 AERONAUTICS (GENERAL) 869

02 AERODYNAMICS 874

Includes aerodynamics of bodies, combinations, wings, rotors, and control surfaces; and internal flow in ducts and turbomachinery.

For related information see also *34 Fluid Mechanics and Heat Transfer.*

03 AIR TRANSPORTATION AND SAFETY 877

Includes passenger and cargo air transport operations; and aircraft accidents.

For related information see also *16 Space Transportation* and *85 Urban Technology and Transportation.*

04 AIRCRAFT COMMUNICATIONS AND NAVIGATION 878

Includes digital and voice communication with aircraft; air navigation systems (satellite and ground based); and air traffic control.

For related information see also *17 Space Communications, Spacecraft Communications, Command and Tracking* and *32 Communications and Radar.*

05 AIRCRAFT DESIGN, TESTING AND PERFORMANCE 879

Includes aircraft simulation technology.

For related information see also *18 Spacecraft Design, Testing and Performance* and *39 Structural Mechanics.* For land transportation vehicles see *85 Urban Technology and Transportation.*

06 AIRCRAFT INSTRUMENTATION 881

Includes cockpit and cabin display devices; and flight instruments.

For related information see also *19 Spacecraft Instrumentation* and *35 Instrumentation and Photography.*

07 AIRCRAFT PROPULSION AND POWER 881

Includes prime propulsion systems and systems components, e.g., gas turbine engines and compressors; and onboard auxiliary power plants for aircraft.

For related information see also *20 Spacecraft Propulsion and Power, 28 Propellants and Fuels,* and *44 Energy Production and Conversion.*

08 AIRCRAFT STABILITY AND CONTROL 882

Includes aircraft handling qualities; piloting; flight controls; and autopilots.

For related information see also *05 Aircraft Design, Testing and Performance.*

09 RESEARCH AND SUPPORT FACILITIES (AIR) 884

Includes airports, hangars and runways; aircraft repair and overhaul facilities; wind tunnels; shock tubes; and aircraft engine test stands.

For related information see also *14 Ground Support Systems and Facilities (Space).*

ASTRONAUTICS

Includes astronautics (general); astrodynamics; ground support systems and facilities (space); launch vehicles and space vehicles; space transportation; space communications, spacecraft communications, command and tracking; spacecraft design, testing and performance; spacecraft instrumentation; and spacecraft propulsion and power.

For related information see also *Aeronautics.*

12 ASTRONAUTICS (GENERAL) N.A.

For extraterrestrial exploration see *91 Lunar and Planetary Exploration.*

13 ASTRODYNAMICS 884

Includes powered and free-flight trajectories; and orbital and launching dynamics.

14 GROUND SUPPORT SYSTEMS AND FACILITIES (SPACE) 885

Includes launch complexes, research and production facilities; ground support equipment, e.g., mobile transporters; and simulators.

For related information see also *09 Research and Support Facilities (Air).*

15 LAUNCH VEHICLES AND SPACE VEHICLES 885

Includes boosters; operating problems of launch/space vehicle systems; and reusable vehicles.

For related information see also *20 Spacecraft Propulsion and Power.*

16 SPACE TRANSPORTATION N.A.

Includes passenger and cargo space transportation, e.g., shuttle operations; and space rescue techniques.

For related information see also *03 Air Transportation and Safety* and *18 Spacecraft Design, Testing and Performance.* For space suits see *54 Man/System Technology and Life Support.*

17 SPACE COMMUNICATIONS, SPACECRAFT COMMUNICATIONS, COMMAND AND TRACKING N.A.

Includes telemetry; space communications networks; astronavigation and guidance; and radio blackout.

For related information see also *04 Aircraft Communications and Navigation* and *32 Communications and Radar.*

18 SPACECRAFT DESIGN, TESTING AND PERFORMANCE 886

Includes satellites; space platforms; space stations; spacecraft systems and components such as thermal and environmental controls; and attitude controls.

For life support systems see *54 Man/System Technology and Life Support.* For related information see also *05 Aircraft Design, Testing and Performance, 39 Structural Mechanics,* and *16 Space Transportation.*

19 SPACECRAFT INSTRUMENTATION N.A.

For related information see also *06 Aircraft Instrumentation* and *35 Instrumentation and Photography.*

20 SPACECRAFT PROPULSION AND POWER 887

Includes main propulsion systems and components, e.g. rocket engines; and spacecraft auxiliary power sources.

For related information see also *07 Aircraft Propulsion and Power, 28 Propellants and Fuels, 44 Energy Production and Conversion,* and *15 Launch Vehicles and Space Vehicles.*

CHEMISTRY AND MATERIALS

Includes chemistry and materials (general); composite materials; inorganic and physical chemistry; metallic materials; nonmetallic materials; propellants and fuels; and materials processing.

23 CHEMISTRY AND MATERIALS (GENERAL) 888

24 COMPOSITE MATERIALS 888

Includes physical, chemical, and mechanical properties of laminates and other composite materials.

For ceramic materials see *27 Nonmetallic Materials.*

25 INORGANIC AND PHYSICAL CHEMISTRY 891

Includes chemical analysis, e.g., chromatography; combustion theory; electrochemistry; and photochemistry.

For related information see also *77 Thermodynamics and Statistical Physics.*

26 METALLIC MATERIALS 897

Includes physical, chemical, and mechanical properties of metals, e.g., corrosion; and metallurgy.

27 NONMETALLIC MATERIALS 908

Includes physical, chemical, and mechanical properties of plastics, elastomers, lubricants, polymers, textiles, adhesives, and ceramic materials.

For composite materials see *24 Composite Materials.*

28 PROPELLANTS AND FUELS 913

Includes rocket propellants, igniters and oxidizers; their storage and handling procedures; and aircraft fuels.

For related information see also *07 Aircraft Propulsion and Power, 20 Spacecraft Propulsion and Power,* and *44 Energy Production and Conversion.*

29 MATERIALS PROCESSING N.A.

Includes space-based development of products and processes for commercial application.

For biological materials see *55 Space Biology.*

ENGINEERING

Includes engineering (general); communications and radar; electronics and electrical engineering; fluid mechanics and heat transfer; instrumentation and photography; lasers and masers; mechanical engineering; quality assurance and reliability; and structural mechanics.

For related information see also *Physics.*

31 ENGINEERING (GENERAL) 916

Includes vacuum technology; control engineering; display engineering; cryogenics; and fire prevention.

32 COMMUNICATIONS AND RADAR 917

Includes radar; land and global communications; communications theory; and optical communications.

For related information see also *04 Aircraft Communications and Navigation* and *17 Space Communications, Spacecraft Communications, Command and Tracking.* For search and rescue see *03 Air Transportation and Safety,* and *16 Space Transportation.*

33 ELECTRONICS AND ELECTRICAL ENGINEERING 920

Includes test equipment and maintainability; components, e.g., tunnel diodes and transistors; microminiaturization; and integrated circuitry.

For related information see also *60 Computer Operations and Hardware* and *76 Solid-State Physics.*

34 FLUID MECHANICS AND HEAT TRANSFER 926

Includes boundary layers; hydrodynamics; fluidics; mass transfer and ablation cooling.

For related information see also *02 Aerodynamics* and *77 Thermodynamics and Statistical Physics.*

35 INSTRUMENTATION AND PHOTOGRAPHY 933

Includes remote sensors; measuring instruments and gauges; detectors; cameras and photographic supplies; and holography.

For aerial photography see *43 Earth Resources and Remote Sensing.* For related information see also *06 Aircraft Instrumentation* and *19 Spacecraft Instrumentation.*

36 LASERS AND MASERS 934

Includes parametric amplifiers.

For related information see also *76 Solid-State Physics.*

37 MECHANICAL ENGINEERING 937

Includes auxiliary systems (nonpower); machine elements and processes; and mechanical equipment.

38 QUALITY ASSURANCE AND RELIABILITY 943

Includes product sampling procedures and techniques; and quality control.

39 STRUCTURAL MECHANICS 944

Includes structural element design and weight analysis; fatigue; and thermal stress.

For applications see *05 Aircraft Design, Testing and Performance* and *18 Spacecraft Design, Testing and Performance.*

GEOSCIENCES

Includes geosciences (general); earth resources and remote sensing; energy production and conversion; environment pollution; geophysics; meteorology and climatology; and oceanography.

For related information see also *Space Sciences.*

42 GEOSCIENCES (GENERAL) N.A.

43 EARTH RESOURCES AND REMOTE SENSING 949

Includes remote sensing of earth resources by aircraft and spacecraft; photogrammetry; and aerial photography.

For instrumentation see *35 Instrumentation and Photography.*

44 ENERGY PRODUCTION AND CONVERSION 950

Includes specific energy conversion systems, e.g., fuel cells; global sources of energy; geophysical conversion; and windpower.

For related information see also *07 Aircraft Propulsion and Power, 20 Spacecraft Propulsion and Power,* and *28 Propellants and Fuels.*

45 ENVIRONMENT POLLUTION 956

Includes atmospheric, noise, thermal, and water pollution.

46 GEOPHYSICS 959

Includes aeronomy; upper and lower atmosphere studies; ionospheric and magnetospheric physics; and geomagnetism.

For space radiation see *93 Space Radiation.*

47 METEOROLOGY AND CLIMATOLOGY 962

Includes weather forecasting and modification.

48 OCEANOGRAPHY 965

Includes biological, dynamic, and physical oceanography; and marine resources.

For related information see also *43 Earth Resources and Remote Sensing.*

LIFE SCIENCES

Includes life sciences (general); aerospace medicine; behavioral sciences; man/system technology and life support; and space biology.

51 LIFE SCIENCES (GENERAL) 965

52 AEROSPACE MEDICINE 966

Includes physiological factors; biological effects of radiation; and effects of weightlessness on man and animals.

53 BEHAVIORAL SCIENCES 967

Includes psychological factors; individual and group behavior; crew training and evaluation; and psychiatric research.

54 MAN/SYSTEM TECHNOLOGY AND LIFE SUPPORT 968

Includes human engineering; biotechnology; and space suits and protective clothing.

For related information see also *16 Space Transportation.*

55 SPACE BIOLOGY N.A.

Includes exobiology; planetary biology; and extraterrestrial life.

MATHEMATICAL AND COMPUTER SCIENCES

Includes mathematical and computer sciences (general); computer operations and hardware; computer programming and software; computer systems; cybernetics; numerical analysis; statistics and probability; systems analysis; and theoretical mathematics.

59 MATHEMATICAL AND COMPUTER SCIENCES (GENERAL) 969

60 COMPUTER OPERATIONS AND HARDWARE 969

Includes hardware for computer graphics, firmware, and data processing.

For components see *33 Electronics and Electrical Engineering.*

61 COMPUTER PROGRAMMING AND SOFTWARE 971

Includes computer programs, routines, algorithms, and specific applications, e.g., CAD/CAM.

62 COMPUTER SYSTEMS 979

Includes computer networks and special application computer systems.

63 CYBERNETICS 981

Includes feedback and control theory, artificial intelligence, robotics and expert systems.

For related information see also *54 Man/System Technology and Life Support.*

64 NUMERICAL ANALYSIS 982

Includes iteration, difference equations, and numerical approximation.

65 STATISTICS AND PROBABILITY 985

Includes data sampling and smoothing; Monte Carlo method; and stochastic processes.

66 SYSTEMS ANALYSIS 986

Includes mathematical modeling; network analysis; and operations research.

67 THEORETICAL MATHEMATICS 987

Includes topology and number theory.

PHYSICS

Includes physics (general); acoustics; atomic and molecular physics; nuclear and high-energy physics; optics; plasma physics; solid-state physics; and thermodynamics and statistical physics.

For related information see also *Engineering.*

70 PHYSICS (GENERAL) 987

For precision time and time interval (PTTI) see *35 Instrumentation and Photography;* for geophysics, astrophysics or solar physics see *46 Geophysics, 90 Astrophysics,* or *92 Solar Physics.*

71 ACOUSTICS 988
Includes sound generation, transmission, and attenuation.
For noise pollution see *45 Environment Pollution.*

72 ATOMIC AND MOLECULAR PHYSICS 989
Includes atomic structure, electron properties, and molecular spectra.

73 NUCLEAR AND HIGH-ENERGY PHYSICS 991
Includes elementary and nuclear particles; and reactor theory.
For space radiation see *93 Space Radiation.*

74 OPTICS 991
Includes light phenomena and optical devices.
For lasers see *36 Lasers and Masers.*

75 PLASMA PHYSICS 993
Includes magnetohydrodynamics and plasma fusion.
For ionospheric plasmas see *46 Geophysics.* For space plasmas see *90 Astrophysics.*

76 SOLID-STATE PHYSICS 997
Includes superconductivity.
For related information see also *33 Electronics and Electrical Engineering* and *36 Lasers and Masers.*

77 THERMODYNAMICS AND STATISTICAL PHYSICS 1006
Includes quantum mechanics; theoretical physics; and Bose and Fermi statistics.
For related information see also *25 Inorganic and Physical Chemistry* and *34 Fluid Mechanics and Heat Transfer.*

SOCIAL SCIENCES

Includes social sciences (general); administration and management; documentation and information science; economics and cost analysis; law, political science, and space policy; and urban technology and transportation.

80 SOCIAL SCIENCES (GENERAL) N.A.
Includes educational matters.

81 ADMINISTRATION AND MANAGEMENT 1007
Includes management planning and research.

82 DOCUMENTATION AND INFORMATION SCIENCE 1009
Includes information management; information storage and retrieval technology; technical writing; graphic arts; and micrography.
For computer documentation see *61 Computer Programming and Software.*

83 ECONOMICS AND COST ANALYSIS N.A.
Includes cost effectiveness studies.

84 LAW, POLITICAL SCIENCE AND SPACE POLICY 1011
Includes NASA appropriation hearings; aviation law; space law and policy; international law; international cooperation; and patent policy.

85 URBAN TECHNOLOGY AND TRANSPORTATION N.A.
Includes applications of space technology to urban problems; technology transfer; technology assessment; and surface and mass transportation.
For related information see *03 Air Transportation and Safety, 16 Space Transportation,* and *44 Energy Production and Conversion.*

SPACE SCIENCES

Includes space sciences (general); astronomy; astrophysics; lunar and planetary exploration; solar physics; and space radiation.
For related information see also *Geosciences.*

88 SPACE SCIENCES (GENERAL) N.A.

89 ASTRONOMY 1011
Includes radio, gamma-ray, and infrared astronomy; and astrometry.

90 ASTROPHYSICS 1012
Includes cosmology; celestial mechanics; space plasmas; and interstellar and interplanetary gases and dust.
For related information see also *75 Plasma Physics.*

91 LUNAR AND PLANETARY EXPLORATION 1014
Includes planetology; and manned and unmanned flights.
For spacecraft design or space stations see *18 Spacecraft Design, Testing and Performance.*

92 SOLAR PHYSICS 1015
Includes solar activity, solar flares, solar radiation and sunspots.
For related information see *93 Space Radiation.*

93 SPACE RADIATION 1015
Includes cosmic radiation; and inner and outer earth's radiation belts.
For biological effects of radiation see *52 Aerospace Medicine.* For theory see *73 Nuclear and High-Energy Physics.*

GENERAL

Includes aeronautical, astronautical, and space science related histories, biographies, and pertinent reports too broad for categorization; histories or broad overviews of NASA programs.

99 GENERAL 1016

Note: N.A. means that no abstracts were assigned to this category for this issue.

SUBJECT INDEX I-1
PERSONAL AUTHOR INDEX I-57
CORPORATE SOURCE INDEX I-65
CONTRACT NUMBER INDEX I-77
REPORT/ACCESSION NUMBER INDEX .. I-81
APPENDIX—ABOUT STAR A-1

TYPICAL CITATION AND ABSTRACT

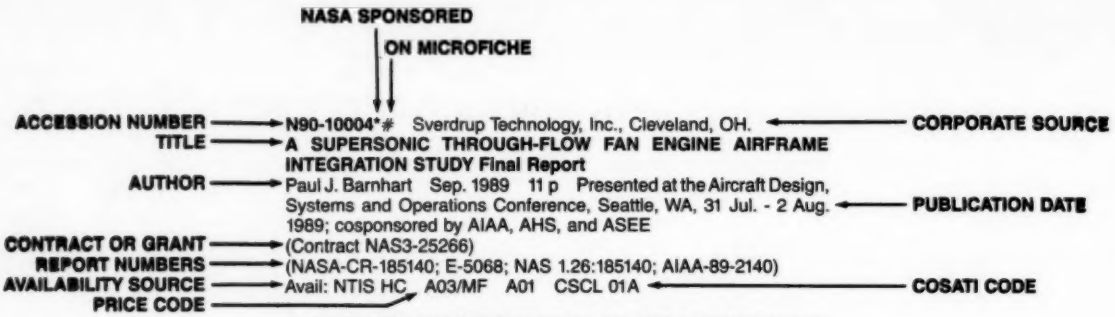
NASA SPONSORED
ON MICROFICHE
ACCESSION NUMBER
N90-10004*# Sverdrup Technology, Inc., Cleveland, OH.
CORPORATE SOURCE
TITLE
A SUPERSONIC THROUGH-FLOW FAN ENGINE AIRFRAME INTEGRATION STUDY Final Report
AUTHOR
Paul J. Barnhart Sep. 1989 11 p Presented at the Aircraft Design, Systems and Operations Conference, Seattle, WA, 31 Jul. - 2 Aug. 1989; cosponsored by AIAA, AHS, and ASEE
PUBLICATION DATE
CONTRACT OR GRANT
(Contract NAS3-25266)
REPORT NUMBERS
(NASA-CR-185140; E-5068; NAS 1.26:185140; AIAA-89-2140)
AVAILABILITY SOURCE
Avail: NTIS HC A03/MF A01 CSCL 01A
COSATI CODE
PRICE CODE

Engine airframe integration effects are investigated for superonsic through-flow fan engines installed on a Mach 3.20 supersonic cruise vehicle. Six different supersonic through-flow fan engine installations covering the effects of engine size, nacelle contour, nacelle placement, and approximate bypass plume effects are presented. The different supersonic through-flow fan installations are compared with a conventional turbine bypass engine configuration on the same basic airframe. The supersonic through-flow fan engine integrations are shown to be comparable to the turbine bypass engine configuration on the basis of installed nacelle wave drag. The supersonic through-flow fan engine airframe integrated vehicles have superior aerodynamic performance on the basis of maximum lift-to-drag ratio than the turbine bypass engine installation over the entire operating Mach number range from 1.10 to 3.20. When approximate bypass plume modeling is included, the supersonic through-flow fan engine configuration shows even larger improvements over the turbine bypass engine configuration. Author

VOLUME 28 NUMBER 7 / APRIL 8, 1990

Scientific and Technical Aerospace Reports

A Semimonthly Publication of the National Aeronautics and Space Administration

01 AERONAUTICS (GENERAL)

N90-15041# Advisory Group for Aerospace Research and Development, Neuilly-Sur-Seine (France). Flight Mechanics Panel.
FLIGHT IN ADVERSE ENVIRONMENTAL CONDITIONS
Sep. 1989 379 p In ENGLISH and FRENCH Symposium held in Gol, Norway, 8-11 May 1989
(AGARD-CP-470; ISBN-92-835-0527-1) Copyright Avail: NTIS HC A17/MF A03; Non-NATO Nationals requests available only from AGARD/Scientific Publications Executive

Four aspects of adverse environmental conditions of interest to the flight mechanics specialist were addressed: atmospheric disturbances, reduced visibility, icing, and electromagnetic disturbances. All four of these can seriously affect flight safety, comfort, and operational capability. The topic was considered to be particularly relevant to the needs of the military community which is putting increased emphasis on the ability of today's and tomorrow's aircraft to fly safely and effectively in the types of adverse conditions. For individual titles, see N90-15042 through N90-15067.

N90-15042# Flight Safety Foundation, Inc., Arlington, VA.
THE HUMAN ELEMENT: THE KEY TO SAFE, CIVIL OPERATIONS IN ADVERSE WEATHER **c05**
John H. Enders *In* AGARD, Flight in Adverse Environmental Conditions Sep. 1989 7 p (For primary document see N90-15041 07-01)
Copyright Avail: NTIS HC A17/MF A03; Non-NATO Nationals requests available only from AGARD/Scientific Publications Executive

The problems of civil flight in adverse weather was discussed in general terms and specific examples were used to illustrate the nature of technical, procedural and human factors, with a view toward the mitigation of serious events. Author

N90-15043# Office National d'Etudes et de Recherches Aerospatiales, Paris (France).
DESCRIPTION OF ATMOSPHERIC TURBULENCE [DESCRIPTION DE LA TURBULENCE ATMOSPHERIQUE] **c46**
Pierre-Marie Hutin *In* AGARD, Flight in Adverse Environmental Conditions Sep. 1989 14 p In FRENCH Previously announced in IAA as A89-48750 (For primary document see N90-15041 07-01)
Copyright Avail: NTIS HC A17/MF A03; Non-NATO Nationals requests available only from AGARD/Scientific Publications Executive

Over one million hours of aircraft flight test data for loading factors in excess of 0.5 g were analyzed using three different methods in order to model coherent atmospheric turbulence. The Houbolt method (using a rigid body with two degrees of freedom for the aircraft flight mechanics) is found to provide a better description of the atmosphere than either the Pratt method (in which turbulence values are obtained from the vertical acceleration of the aircraft) or the Hall method (using only a single degree of freedom for the aircraft motion). The Houbolt method is improved by a calibration using exact calculations for a small number of different aircraft configurations. IAA

N90-15044# Technische Univ., Brunswick (Germany, F.R.). Inst. of Guidance and Control.
WIND SHEAR MODELS FOR AIRCRAFT HAZARD INVESTIGATION **c47**
Manfred Swolinsky *In* AGARD, Flight in Adverse Environmental Conditions Sep. 1989 17 p (For primary document see N90-15041 07-01)
Copyright Avail: NTIS HC A17/MF A03; Non-NATO Nationals requests available only from AGARD/Scientific Publications Executive

Wind shear hazard investigations, flight simulation for pilot training as well as design, development, and testing of flight control systems require suitable wind models. Based on flight test data, airline flight data and meteorological tower measurements, engineering models for dangerous wind shear situations were developed in the frame of different wind shear research projects. Derived from simplified fluid dynamic concepts the engineering models for downburst, frontal wind shear, and low level jet meet the requirements for real-time flight simulation. The comparison of the wind models with measured wind data show good accordance. For the analyses of simulated landing approaches in wind shear conditions a hazard definition is given by means of aircraft energy height deficit, respectively the required energy supply for landing approach on nominal glide slope and constant air speed. Author

N90-15045*# National Aeronautics and Space Administration. Ames Research Center, Moffett Field, CA.
ANALYSIS OF SEVERE ATMOSPHERIC DISTURBANCES FROM AIRLINE FLIGHT RECORDS **c47**
R. C. Wingrove, R. E. Bach, Jr., and T. A. Schultz *In* AGARD, Flight in Adverse Environmental Conditions Sep. 1989 7 p Previously announced as N89-25977 (For primary document see N90-15041 07-01)
Copyright Avail: NTIS HC A17/MF A03; Non-NATO Nationals requests available only from AGARD/Scientific Publications Executive CSCL 04B

Advanced methods were developed to determine time varying winds and turbulence from digital flight data recorders carried aboard modern airliners. Analysis of several cases involving severe clear air turbulence encounters at cruise altitudes has shown that the aircraft encountered vortex arrays generated by destabilized wind shear layers above mountains or thunderstorms. A model was developed to identify the strength, size, and spacing of vortex arrays. This model is used to study the effects of severe wind hazards on operational safety for different types of aircraft. It is demonstrated that small remotely piloted vehicles and executive aircraft exhibit more violent behavior than do large airliners during encounters with high-altitude vortices. Analysis of digital flight data from the accident at Dallas/Ft. Worth in 1985 indicates that the aircraft encountered a microburst with rapidly changing winds embedded in a strong outflow near the ground. A multiple-vortex-ring model was developed to represent the microburst wind pattern. This model can be used in flight simulators to better understand the control problems in severe microburst encounters. Author

N90-15046# Aerodata Flugmesstechnik G.m.b.H., Brunswick (Germany, F.R.).
SYSTEMS FOR AIRBORNE WIND AND TURBULENCE MEASUREMENT **c47**

Peter Voersmann *In* AGARD, Flight in Adverse Environmental Conditions Sep. 1989 12 p (For primary document see N90-15041 07-01)
Copyright Avail: NTIS HC A17/MF A03; Non-NATO Nationals requests available only from AGARD/Scientific Publications Executive

For many years aircraft were equipped for research in wind and turbulence measurements. Very often the system installation consisted of sensors and recording hardware which was spread all over the aircraft. A modern system solution, where all components are integrated in an external pod for aircraft and helicopter applications is described. After a brief description of the principles for airborne wind measurements, advantages and disadvantages for different system solutions will be discussed. The presented pod solution includes a software and hardware concept, which allows to determine all three components of the wind vector in real time on-board the aircraft. Flight test results are presented, which demonstrate the achievable accuracies for the horizontal and especially the vertical wind component. This includes the effects of dynamic aircraft maneuvers. Finally an outlook is given, what kind of precision can be achieved in the future, when satellite navigation systems will be available on a 24 hour basis. Author

N90-15047# Test Group (6520th), Edwards AFB, CA.
THE UNITED STATES AIR FORCE APPROACH TO ALL-WEATHER TESTING **c05**
Clifford D. Tompkins and James A. Ford *In* AGARD, Flight in Adverse Environmental Conditions Sep. 1989 7 p (For primary document see N90-15041 07-01)
Copyright Avail: NTIS HC A17/MF A03; Non-NATO Nationals requests available only from AGARD/Scientific Publications Executive

All-weather test programs historically reveal design deficiencies that impact the operational capabilities of the vehicle involved. Therefore, testing is required to ensure that Air Force weapon systems can be effective under varying or extreme environmental conditions. The major purpose of all-weather testing is to determine to what extent a weapon system, its essential support equipment and crews, can accomplish the design mission in the required climatic conditions. The requirements, purposes, and methods for conducting ground and flight tests under simulated and actual climatic extremes are addressed. The ideal all-weather test program is discussed in sufficient detail for an overall understanding of the major phases. The United States Air Force (USAF) approach to all-weather testing is presented, including regulatory requirements. The current methods of planning, extent of participating test organization involvement, and need for concurrent testing in USAF all-weather test programs of new weapon systems are discussed. Author

N90-15048# Technische Univ., Brunswick (Germany, F.R.). Inst. for Flight Guidance and Control.
INFLUENCE OF WINDSHEAR, DOWNDRAFT AND TURBULENCE ON FLIGHT SAFETY **c03**
Gunther Schaenzer *In* AGARD, Flight in Adverse Environmental Conditions Sep. 1989 19 p (For primary document see N90-15041 07-01)
Copyright Avail: NTIS HC A17/MF A03; Non-NATO Nationals requests available only from AGARD/Scientific Publications Executive

Wind shear, downdraft, and turbulence influences flight safety especially in take-off and landing approach. For a better understanding of the relevant problems, the typical aircraft response in gust and in wind shear will be pointed out and will be compared with real flight situations. In general the airspeed deviation of an aircraft in a wind shear situation is relatively small in contrast to flight path deviations and flight performance is not the limiting factor. Flight simulator studies have shown that it is difficult for the cockpit crew to identify a wind shear situation without any additional display of relevant information in order to control throttle and elevator in a correct manner. A wind shear warning display, based on energy deviation and energy rate can assist the pilot to overcome severe wind shear. Author

N90-15049# Royal Aircraft Establishment, Bedford (England).
CLASSIFICATION OF WINDSHEAR SEVERITY **c47**
A. A. Woodfield *In* AGARD, Flight in Adverse Environmental Conditions Sep. 1989 13 p (For primary document see N90-15041 07-01)
Copyright Avail: NTIS HC A17/MF A03; Non-NATO Nationals requests available only from AGARD/Scientific Publications Executive

A simplified model of aircraft and pilot response to wind shear is used to identify the potential height loss during wind shear encounters. This potential height loss is directly related to the possibility of unscheduled ground contact and is proposed as a primary indicator of wind shear severity. Key factors of wind shear strength and aircraft performance which influence the potential height loss are identified using this simple model. This helps to provide a better understanding of the complex interactions between the pilot/aircraft and the wind shear. Various practical severity factors are examined in relation to both the potential height loss and the probability of encountering various shears. It is shown that severity factors based on pseudo-energy-rate have fundamental problems in resolving the conflict between false alarms and providing timely information to a pilot when used with current sensors on aircraft or sensors that scan and probe (such as Doppler radar or laser). An improved severity factor based on the potential height loss analysis is shown to have a low risk of false or missed alarms, and appropriate threshold values are easily identified for all aircraft types. This improved severity factor requires probe and scan sensors. Author

N90-15050# Aerospatiale, Toulouse (France).
HOW TO FLY WINDSHEAR USING THE FLY-BY-WIRE CONCEPT **c08**
J. L. Bonafe *In* AGARD, Flight in Adverse Environmental Conditions Sep. 1989 16 p (For primary document see N90-15041 07-01)
Copyright Avail: NTIS HC A17/MF A03; Non-NATO Nationals requests available only from AGARD/Scientific Publications Executive

In the past three years, Aerospatiale has developed windshear warning and guidance systems for the A310 and the A300-600; these systems are either newly designed or constructed around the Speed Reference System designed for the A300 and exploited in revenue flight since 1975; they are in accordance with certification rules; and were installed on board the A300-600 since April 1988. Aerospatiale's warning and guidance philosophy regarding the conventional AIRBUS is presented, then the fly-by-wire concept analyzed. The fly-by-wire concept improves the general aircraft situation, and advantage is taken of these new capabilities in the warning and guidance elaboration. Systems will be adapted for the A320 certified and installed onboard in the near future. Author

N90-15051# Instituto Superior Tecnico, Lisbon (Portugal).
A PITCH CONTROL LAW FOR COMPENSATION OF THE PHUGOID MODE INDUCED BY WINDSHEARS **c08**
I. M. B. C. Campos, A. J. N. M. Agular, and J. R. C. Azinheira *In* AGARD, Flight in Adverse Environmental Conditions Sep. 1989 13 p (For primary document see N90-15041 07-01)
Copyright Avail: NTIS HC A17/MF A03; Non-NATO Nationals requests available only from AGARD/Scientific Publications Executive

In a previous paper the development of a flight test facility in Portugal was described. This reference mentioned briefly some of the research projects for which the facility would be initially used, including among other studies in non-linear pitch stability and aircraft response to atmospheric disturbances. The purpose is to discuss in more detail the flight mechanical theory which underlies these research projects: the comparison of theory with flight test data will have to await the availability of the CASA 212 Aviocar aircraft, which is at present already has all sensors installed but is still undergoing final check-out of instrumentation describing pitch stability for flight along a constant glide slope, taking into account the phugoid but neglecting the short period mode. The

model is solved to find pitch control laws for two problems: the non-linear problem of keeping an aircraft on a constant glide slope in still air starting from an arbitrary initial velocity, possibly for removed from the steady flight speeds; and the linearized problem of keeping an aircraft on a constant glide slope in the presence of longitudinal and vertical winds of peak velocity up to 30 percent of the aircraft velocity, which provide a representation of a moderately strong windshear. Author

N90-15052# National Aeronautical Establishment, Ottawa (Ontario). Flight Research Lab.
ADVERSE WEATHER OPERATIONS DURING THE CANADIAN ATLANTIC STORMS PROGRAM c47
J. I. MacPherson and G. A. Isaac (Atmospheric Environment Service, Downsview, Ontario) *In* AGARD, Flight in Adverse Environmental Conditions Sep. 1989 13 p (For primary document see N90-15041 07-01)
Copyright Avail: NTIS HC A17/MF A03; Non-NATO Nationals requests available only from AGARD/Scientific Publications Executive

For cooperative research programs with the Atmospheric Environment Service of Canada, the NRC Twin Otter Atmospheric Research Aircraft was instrumented to measure the motion and thermal structure of the atmosphere and the microphysics of cloud and precipitation. In 1986 the aircraft was flown in the Canadian Atlantic Storms Program to investigate large east-coast storms that typically account for the bulk of the winter-time precipitation in the Maritime provinces, and cause havoc for airborne and surface transportation. A variety of adverse flight conditions were experienced including heavy snow contributing to limited IFR alternates, airframe icing, wind shear and crosswinds on landing. Examples are presented of these incidents analyzed from both a flight research and meteorological perspective using aircraft recorded data. For this project, additional specially-designed deicing boots were installed on the Twin Otter's vertical tail and the wing and landing gear struts. The performance of the enhanced aircraft deicing system will be discussed using data from three deicing encounters. Author

N90-15053# Aeronautica Macchi S.p.A., Varese (Italy). Flight Mechanics and Automatic Control Dept.
CANARD VERSUS AFT-TAIL RIDE QUALITIES PERFORMANCE AND PILOT COMMAND RESPONSE c08
L. V. Cioffi and L. Mangiacasale *In* AGARD, Flight in Adverse Environmental Conditions Sep. 1989 13 p (For primary document see N90-15041 07-01)
Copyright Avail: NTIS HC A17/MF A03; Non-NATO Nationals requests available only from AGARD/Scientific Publications Executive

A comparison between a Close-Coupled configuration and a Close-Coupled Tail configuration was developed in terms of ride qualities and pilot command response in turbulence. Parameters of the study are the mass factor of the airplane, the static stability, and the sign of the trailing-edge flap effectiveness (only for the aft-tail airplane). The known ride quality criteria are used in order to assess the flying qualities of the airplane. Interesting conclusions are derived in terms of configuration sensitivity and attenuation capabilities. Further research is needed in order to add structural flexibility and unsteady aerodynamics to the design model. Pilot command responses are in agreement with the current flying qualities parameters, but a special purpose control law has to be designed for good tracking in presence of discrete gusts. Author

N90-15054# Messerschmitt-Boelkow-Blohm G.m.b.H., Hamburg (Germany, F.R.). Dynamic Dept.
THE INTERFERENCE OF FLIGHTMECHANICAL CONTROL LAWS WITH THOSE OF LOAD ALLEVIATION AND ITS INFLUENCE ON STRUCTURAL DESIGN c08
M. Molzow and R. Moebest *In* AGARD, Flight in Adverse Environmental Conditions Sep. 1989 20 p (For primary document see N90-15041 07-01)
Copyright Avail: NTIS HC A17/MF A03; Non-NATO Nationals requests available only from AGARD/Scientific Publications Executive

Today modern A/C designs use fly-by-wire together with control laws to make the A/C comfortable for handling in service. In addition, this implies an attractive chance for a lot of protections and limitations with the aim to improve handling quality characteristics or to protect the aircraft against overloading. Examples are: overspeed protection; load factor protection; and stall protection. Another chance is the implementation of Load Alleviation Functions (LAF). To optimize the overall A/C design a close cooperation between the different disciplines like: systems, handling quality, aerodynamics, loads, and stressing is needed, not to cancel the benefits in one discipline by handicaps or additional weight in others. The different problems, which have carefully to be watched in relation of interference to each other to reach an overall optimum are described. Author

N90-15055# Oklahoma State Univ., Stillwater. Dept. of Mechanical and Aerospace Engineering.
TURBULENCE EFFECTS OF AIRCRAFT FLIGHT DYNAMICS AND CONTROL c08
Robert L. Swaim *In* AGARD, Flight in Adverse Environmental Conditions Sep. 1989 9 p (For primary document see N90-15041 07-01)
Copyright Avail: NTIS HC A17/MF A03; Non-NATO Nationals requests available only from AGARD/Scientific Publications Executive

Design of aircraft flight control systems requires consideration of many factors including maneuvering, ride and handling qualities, stability augmentation, and control power requirements as well as several others. All the mentioned factors, however, are strongly influenced by the atmospheric turbulence environment through which the aircraft must fly. A unified analytical design method is described which systematically accounts for three-component gust velocity spatial distribution effects, handling qualities in terms of needed closed-loop stability augmentation systems, and the manuevering and stabilization three-axis control power required. These factors are all interrelated. State variable formulations of modern system theory are used for the aircraft and turbulence dynamic models and in stability augmentation system synthesis. Both homogeneous and heterogeneous turbulence are considered. Homogeneous models are described in a statistical sense. Heterogeneous turbulence is discrete due to vortex patterns generated by obstacles such as trees, buildings, or mountains, and is known to result in aircraft upsets and structural failure. Author

N90-15056# Dornier-Werke G.m.b.H., Friedrichshafen (Germany, F.R.).
ACTIVE CONTROL SYSTEM FOR GUST LOAD ALLEVATION AND STRUCTURAL DAMPING c08
Hartmut Boehret and Joachim Winter *In* AGARD, Flight in Adverse Environmental Conditions Sep. 1989 11 p (For primary document see N90-15041 07-01)
Copyright Avail: NTIS HC A17/MF A03; Non-NATO Nationals requests available only from AGARD/Scientific Publications Executive

Based on the Do-228 regional airliner, the improvement in passenger comfort provided by the gust load alleviation system Open Loop Gust Alleviation (OLGA) under adverse weather conditions is shown. The problem of excited structural vibrations is solved with an active structural damper, which eliminates the adverse effect of the gust load alleviation system on structural vibrations and, additionally, diminishes their excitation by maneuvers and gust loads. Author

N90-15057# Deutsche Forschungs- und Versuchsanstalt fuer Luft- und Raumfahrt, Brunswick (Germany, F.R.). Inst. fuer Flugmechanik.
AIRCRAFT RESPONSE AND PILOT BEHAVIOUR DURING A WAKE VORTEX ENCOUNTER PERPENDICULAR TO THE VORTEX AXIS c08
Reinhard Koenig *In* AGARD, Flight in Adverse Environmental

Conditions Sep. 1989 18 p (For primary document see N90-15041 07-01)
Copyright Avail: NTIS HC A17/MF A03; Non-NATO Nationals requests available only from AGARD/Scientific Publications Executive

Vortex systems can be hazardous to trailing aircraft which encounter them in flight. The greatest hazard occurs in areas where aircraft from a wide range of classes operate and where the flight paths are close to the ground. Upwash velocities induced by the wake vortices can be equivalent to the design gust velocities. Furthermore different types of hazardous effects exist when encountering the vortex system, such as imposed rolling and pitching moments, a loss of rate of climb, a loss of altitude and structural loads. Aircraft response and pilot behavior during takeoff are described when a wake vortex is encountered perpendicular to the vortex axis. The aircraft response is calculated by nonlinear digital simulation with a mathematical model of a wake vortex system close to the ground. This real-time vortex model is also used in the Boeing B-737 simulator of Deutsche Lufthansa in order to examine the pilot behavior. Close to the ground, the wake vortex system induces additional horizontal velocities. There exists a critical flight path where very large g-loads are induced by vertical and horizontal vortex velocities and normal vertical acceleration shortly after takeoff. Often the pilot will attempt to counteract these g-loads, but this produces only a small effect.
Author

N90-15058*# Georgia Inst. of Tech., Atlanta. School of Aerospace Engineering.
A STUDY OF THE EFFECTS OF ROTATING FRAME TURBULENCE (RFT) ON HELICOPTER FLIGHT MECHANICS **c05**
D. P. Schrage, J. V. B. Prasad, and G. H. Gaonkar (Florida Atlantic Univ., Boca Raton.) *In* AGARD, Flight in Adverse Environmental Conditions Sep. 1989 13 p (For primary document see N90-15041 07-01)
(Contract NCA2-266)
Copyright Avail: NTIS HC A17/MF A03; Non-NATO Nationals requests available only from AGARD/Scientific Publications Executive CSCL 01C

The turbulence actually experienced by a helicopter blade-element significantly differs from the space-fixed free atmospheric turbulence. The turbulence in the rotor disk requires a rotationally sampled description in a rotating frame of reference. It is referred to as the rotating frame turbulence or RFT which exhibits a striking phenomenon. The RFT spectral density versus frequency shows high peak values at 1P,2P, or 3P, frequencies. The energy increase at these peaks is balanced by an energy decrease primarily at the lower-than-1P frequency range. Particularly for low altitude flight regimes of pure helicopters, such as the nap-of-the-earth maneuvers, the conventional space-fixed description of turbulence is not a good approximation, since the turbulence scale length can have values comparable to the rotor radius. Accordingly the flight mechanics characteristics with RFT description are compared with those based on the conventional space-fixed turbulence description. The results demonstrate that the RFT qualitatively and quantitatively affects the prediction of helicopter flight mechanics characteristics in turbulence. Such comparisons should play an important role in the new development of handling qualities specifications for helicopters.
Author

N90-15059# Technische Univ., Hanover (Germany, F.R.). Inst. fuer Meteorologie und Klimatologie.
MEASUREMENTS OF HORIZONTAL VISIBILITY IN THE LOWEST 300 m OVER NORTHERN GERMANY **c47**
R. Roth and A. R. Siemer *In* AGARD, Flight in Adverse Environmental Conditions Sep. 1989 10 p (For primary document see N90-15041 07-01)
Copyright Avail: NTIS HC A17/MF A03; Non-NATO Nationals requests available only from AGARD/Scientific Publications Executive

In order to establish a climatology of the vertical structure of horizontal visibility in the lowlands of Northern Germany continuous measurements were carried out on radio tower at six different levels up to 300 m above the ground for two and a half year between 1982 and 1985. Ten minute mean values of horizontal visibility, temperature, and dewpoint at each level were recorded automatically as well as the cloud ceiling up to 1500 m above ground. For selected weather situations an additional high resolution vertical sounding system supplied more detailed data on the vertical structure. A statistical analysis of the data was performed showing that there is a relationship between typical patterns of the diurnal variation of the vertical visibility profile and the large scale weather situations in Middle Europe classified according to schemes well established in meteorology. Special cases were examined to study the variation of the vertical visibility profile during fog formation, during the passage of atmospheric fronts and in cases of rapid visibility increases and decreases.
Author

N90-15060# Army Aeromedical Research Lab., Fort Rucker, AL. Aviation Research and Development Activity.
IMAGING PROBABILITIES, GEOMETRY AND ERGONOMICS IN LIMITED VISIBILITY HELICOPTER OPERATIONS **c54**
Robert H. Wright *In* AGARD, Flight in Adverse Environmental Conditions Sep. 1989 11 p (For primary document see N90-15041 07-01)
Copyright Avail: NTIS HC A17/MF A03; Non-NATO Nationals requests available only from AGARD/Scientific Publications Executive

Helicopter pilots using night vision systems have a low probability of seeing the best visual cues that are available for flight control. Even with good visual range, the forward view of current night vision systems looks where visual cues are geometrically insensitive to changes in vehicle states and motions. At terrain flight heights, best visual cues reflecting vehicle states and motions are located directly below the helicopter. As visual range attenuates, the best vision of the terrain retreats toward the same angles below the helicopter where the best flight control cues are found. Image and symbolic cues of night vision systems both preclude effective use of normal spatial-motion visual perception, which quickly processes the entire visual array in parallel with no or very low workload. Downward viewing display concepts should allow normal spatial-motion vision to function effectively, resulting in major reductions in pilot workload and training requirements, and safer flight control with poor visibility. At terrain flight heights most tactical visual cues are visually compressed in elevation angle within just a few degrees at the horizon, but are widely dispersed in azimuth. Terrain obstacles to safe flight are also located within a few degrees of the horizon, but are well defined in azimuth by the velocity vector. It is concluded night vision systems could be improved by designing to better exploit geometric characteristics of visual cues and normal pilot spatial-motion visual processes.
Author

N90-15061# Royal Aircraft Establishment, Bedford (England). Flight Management Dept.
THE ASSESSMENT OF VISIBILITY FROM AUTOMATIC CONTRAST MEASUREMENTS **c04**
A. W. Puffett *In* AGARD, Flight in Adverse Environmental Conditions Sep. 1989 14 p (For primary document see N90-15041 07-01)
Copyright Avail: NTIS HC A17/MF A03; Non-NATO Nationals requests available only from AGARD/Scientific Publications Executive

Visibility and hence runway visual range through the passive and automatic measurement of contrast reduction in a dark target are assessed. Though limited to use from dawn through to dusk the method offers significant advantages over the more usual transmission, or scattering approaches. The advantages arise not only from the measurement process which is intrinsically more robust than that of the transmissometer, but also from the ratiometric manner in which it can be implemented. The result is a self-compensating system which virtually abolishes any requirement for temperature and long term stability in the instrument. Unlike conventional scatter-meters the method may

be used under a wide range of obscuring conditions without doubts in respect of its constancy of sensitivity. Initial comparisons with a human observer have both produced good agreement and confirmed theoretical expectations of behavior. To overcome the night-time deficiency, suggestions are made for ways in which conventional measurements might be integrated into the system. The relaxation in design that would result from night-time only operation show this to be both a practical and economic alternative. Author

N90-15062*# National Aeronautics and Space Administration. Lewis Research Center, Cleveland, OH.

NASA'S PROGRAM ON ICING RESEARCH AND TECHNOLOGY c03

John J. Reinmann, Robert J. Shaw, and Richard J. Ranaudo *In* AGARD, Flight in Adverse Environmental Conditions Sep. 1989 31 p Previously announced as N89-22569 (For primary document see N90-15041 07-01)

Copyright Avail: NTIS HC A17/MF A03; Non-NATO Nationals requests available only from AGARD/Scientific Publications Executive CSCL 01C

NASA's program in aircraft icing research and technology is reviewed. The program relies heavily on computer codes and modern applied physics technology in seeking icing solutions on a finer scale than those offered in earlier programs. Three major goals of this program are to offer new approaches to ice protection, to improve the ability to model the response of an aircraft to an icing encounter, and to provide improved techniques and facilities for ground and flight testing. The following program elements are reviewed: (1) new approaches to ice protection; (2) numerical codes for deicer analysis; (3) measurement and prediction of ice accretion and its effect on aircraft and aircraft components; (4) special wind tunnel test techniques for rotorcraft icing; (5) improvements of icing wind tunnels and research aircraft; (6) ground de-icing fluids used in winter operation; (7) fundamental studies in icing; and (8) droplet sizing instruments for icing clouds. Author

N90-15063# Texas A&M Univ., College Station. Dept. of Aerospace Engineering.

ICE INDUCED AERODYNAMIC PERFORMANCE DEGRADATION OF ROTORCRAFT: AN OVERVIEW c05

K. D. Korkan and R. K. Britton *In* AGARD, Flight in Adverse Environmental Conditions Sep. 1989 34 p (For primary document see N90-15041 07-01)

Copyright Avail: NTIS HC A17/MF A03; Non-NATO Nationals requests available only from AGARD/Scientific Publications Executive

The renewed interest in evaluating the performance degradation of helicopters due to icing has resulted in the development of methodologies to analytically predict the aerodynamic degradation increment. The progress in understanding the basic icing technology is reviewed citing major references. The analytical methodology is then summarized with respect to performance degradation of propellers, helicopter in hover, helicopter in forward flight, and the forerunner of the V-22 Osprey, the XV-15 propulsion mode(s). The experimental studies of the NACA 0012 airfoil with/without generic ice and the model helicopter main rotor experiments with/without generic ice are reviewed. Based upon these results, refinements are suggested to the current methodology with respect to near term/far term. Author

N90-15064# Boeing Commercial Airplane Co., Renton, WA. Configuration and Certification Group.

FLIGHT AND WIND TUNNEL INVESTIGATION OF AERODYNAMIC EFFECTS OF AIRCRAFT GROUND DEICING/ANTIICING FLUIDS c02

L. James Runyan, Thomas A. Zierten, and Eugene G. Hill *In* AGARD, Flight in Adverse Environmental Conditions Sep. 1989 11 p (For primary document see N90-15041 07-01)

Copyright Avail: NTIS HC A17/MF A03; Non-NATO Nationals requests available only from AGARD/Scientific Publications Executive

A flight and wind tunnel investigation of the effects of aircraft ground deicing/anti-icing fluids on the aerodynamic characteristics of a Boeing 737-200ADV airplane was conducted. The flight test was performed in Kuopio, Finland, and the wind tunnel test was carried out in the NASA Lewis Research Center Icing Research Tunnel. Fluids tested in both flight and the wind tunnel include a newtonian deicing fluid and three nonnewtonian anti-icing fluids commercially available during or prior to 1988. Both the flight test results and the wind tunnel results show that fluids remain on the wing after liftoff and cause a measurable lift loss and drag increase. Eight newly developed nonnewtonian fluids, tested only in the wind tunnel, show significantly improved aerodynamic characteristics relative to the existing nonnewtonian fluids that were tested. Wind tunnel results also indicate that the fluid effects are configuration dependent. For a configuration with deflected leading edge high-lift devices, the fluid effect is largest at the maximum lift condition. For a configuration without leading edge high-lift devices, the fluid effect is very small at the maximum lift condition. It was also found that the fluid aerodynamic effects are related to the fluid surface roughness, particularly in the first 30 percent chord. Author

N90-15065*# National Aeronautics and Space Administration. Langley Research Center, Hampton, VA.

EFFECTS OF LIGHTNING ON OPERATIONS OF AEROSPACE VEHICLES c03

Bruce D. Fisher *In* AGARD, Flight in Adverse Environmental Conditions Sep. 1989 14 p (For primary document see N90-15041 07-01)

Copyright Avail: NTIS HC A17/MF A03; Non-NATO Nationals requests available only from AGARD/Scientific Publications Executive CSCL 01C

Traditionally, aircraft lightning strikes were a major aviation safety issue. However, the increasing use of composite materials and the use of digital avionics for flight critical systems will require that more specific lightning protection measures be incorporated in the design of such aircraft in order to maintain the excellent lightning safety record presently enjoyed by transport aircraft. In addition, several recent lightning mishaps, most notably the loss of the Atlas/Centaur-67 vehicle at Cape Canaveral Air Force Station, Florida in March 1987, have shown the susceptibility of aircraft and launch vehicles to the phenomenon of vehicle-triggered lightning. The recent findings of the NASA Storm Hazards Program were reviewed as they pertain to the atmospheric conditions conducive to aircraft lightning strikes. These data are then compared to recent summaries of lightning strikes to operational aircraft fleets. Finally, the new launch commit criteria for triggered lightning being used by NASA and the U.S. Defense Department are summarized. The NASA Research data show that the greatest probability of a direct strike in a thunderstorm occurs at ambient temperatures of about -40 C. Relative precipitation and turbulence levels were characterized as negligible to light for these conditions. However, operational fleet data have shown that most aircraft lightning strikes in routine operations occur at temperatures near the freezing level in non-cumulonimbus clouds. The non-thunderstorm environment was not the subject of dedicated airborne lightning research. Author

N90-15066# Aeroplane and Armament Experimental Establishment, Boscombe Down (England).

AIRCRAFT TESTING IN THE ELECTROMAGNETIC ENVIRONMENT c05

P. M. Newton *In* AGARD, Flight in Adverse Environmental Conditions Sep. 1989 8 p (For primary document see N90-15041 07-01)

Copyright Avail: NTIS HC A17/MF A03; Non-NATO Nationals requests available only from AGARD/Scientific Publications Executive

Testing aircraft flight safety critical systems against the effects of electromagnetic interference (EMI) is normally performed on the ground for reasons of safety, practicality and cost. The threat and the effects of EMI on aircraft systems is discussed. The current ground test methods used at Aeroplane and Armament Experimental Establishment (A and AEE) are reviewed, including

the limitations, uncertainties of measurement and safety margins. A flight test method for assessing the effects on critical systems from both the on-board and external electromagnetic environment is described which should enable the ground test results to be factored thus providing a more precise clearance for service use without compromising safety. Author

N90-15067# Office National d'Etudes et de Recherches Aerospatiales, Paris (France).
PRINCIPAL CHARACTERISTICS OF LIGHTNING ON AIRCRAFT [PRINCIPALES CARACTERISTIQUES DES FOUDROIEMENTS SUR AVIONS] **c03**
J. L. Boulay *In* AGARD, Flight in Adverse Environmental Conditions Sep. 1989 10 p In FRENCH Previously announced in IAA as A89-48744 (For primary document see N90-15041 07-01)
Copyright Avail: NTIS HC A17/MF A03; Non-NATO Nationals requests available only from AGARD/Scientific Publications Executive

The modeling and measurement of lightning on aircraft are considered. Experimental studies were conducted which are based on the launching of small rockets with conducting wires attached to the ground. The study of the lightning-aircraft interaction involves the characterization of the direct effect of lightning on the aircraft, the affect of the electromagnetic field of nearby lightning, the distribution of the electrical and magnetic field components on the aircraft exterior and interior, and the effect of perturbations on on-board equipment. Results are presented for lightning strikes observed on the Transall and CV 580 aircraft. IAA

N90-15068* National Aeronautics and Space Administration, Washington, DC.
AERONAUTICAL ENGINEERING: A CONTINUING BIBLIOGRAPHY WITH INDEXES (SUPPLEMENT 246)
Dec. 1989 182 p
(NASA-SP-7037(246); NAS 1.21:7037(246)) Avail: NTIS HC A08; NTIS standing order as PB89-914100, $10.50 domestic, $21.00 foreign CSCL 01B

This bibliography lists 690 reports, articles, and other documents introduced into the NASA scientific and technical information system in November, 1989. Subject coverage includes: design, construction and testing of aircraft and aircraft engines; aircraft components, equipment and systems; ground support systems; and theoretical and applied aspects of aerodynamics and general fluid dynamics. Author

02 AERODYNAMICS

Includes aerodynamics of bodies, combinations, wings, rotors, and control surfaces; and internal flow in ducts and turbomachinery.

For related information see also *34 Fluid Mechanics and Heat Transfer.*

N90-15069 Mississippi State Univ., State College.
UNSTEADY THREE-DIMENSIONAL THIN-LAYER NAVIER-STOKES SOLUTIONS ON DYNAMIC BLOCKED GRIDS Ph.D. Thesis
Bruce Simpson 1988 164 p
Avail: Univ. Microfilms Order No. DA8909503

An efficient scheme for calculating steady and unsteady solutions on blocked grids for several airfoils and wings is presented. Two algorithms are presented, both of which are based on upwind, finite-volume, flux splitting for the convective terms, and an explicit treatment of the diffusive terms. The first algorithm is based on a flux-vector split (FVS) scheme while the second algorithm is based on a flux-difference split (FDS) scheme. The two algorithms are compared for steady thin-layer Navier-Stokes solutions on a laminar flat plate, RAE 2822 airfoil, and the ONERA M6 wing. The FDS scheme proved to be superior to the FVS in all cases, due to the excessive numerical dissipation in the FVS scheme. A flat plate laminar boundary layer profile is shown with the FDS scheme correctly modeling the boundary layer (compared to a Blasius solution) with only three grid cells internal to the boundary layer. The FVS scheme was not capable of correctly modeling the boundary layer profile. The FDS algorithm was used to evaluate the scheme for unsteady viscous calculations. The diffusive terms are time-lagged in the solution process and therefore are treated as source terms to the convective terms, which behave as a hyperbolic set of equations. The scheme is second order accurate in space and first order accurate in time due to the explicit treatment of the diffusive terms. A Newton subiteration technique was implemented to allow for larger time step sizes and second order temporal accuracy. Dissert. Abstr.

N90-15070 Princeton Univ., NJ.
NONLINEAR PHENOMENA IN COMPUTATIONAL TRANSONIC AEROELASTICITY Ph.D. Thesis
Kenneth Arthur Kousen 1989 154 p
Avail: Univ. Microfilms Order No. DA8908052

An unsteady Euler equation solver was coupled to a typical section airfoil containing pitching and plunging degrees of freedom. A new structural integrator was implemented based on a convolution integral solution of the second order equations of motion for the normal modes of the structure. The aerodynamic model consisted of a finite volume discretization of the unsteady Euler equations, which were integrated with a five-stage Runge-Kutta scheme using artificial dissipation in the first two stages. After coupling the two numerical models together, the combined system was integrated forward in time. Flutter oscillations in the transonic regime fell into a series of limit cycles that generally made up supercritical bifurcations. A weak divergence behavior was also observed, characterized by the slow progression of the system towards finite, nonzero equilibria. For this same system at higher reduced velocities, interactions between the static instability of divergence and the dynamic instability of flutter were demonstrated. A standard two dimensional model for a section of a swept wing was also analyzed. The flutter curve in this case exhibited the transonic dip phenomenon, and the present code verified the existence of multiple flutter points in the transonic range. These multiple points were then seen to be the boundaries of stability regions composed of limit cycle oscillations for the two different flutter modes of the coupled system. Dissert. Abstr.

N90-15071 Illinois Univ., Urbana-Champaign.
A NUMERICAL MODEL FOR THE AXISYMMETRIC EQUILIBRIUM SHAPE OF DROPS IN UNIFORM MOTION: EFFECTS OF EXTERNAL FLOW, ELECTRIC FIELD AND SURFACE CHARGE Ph.D. Thesis
Chien-Hua Catherine Chuang 1989 126 p
Avail: Univ. Microfilms Order No. DA8916231

In the past the best models of raindrop shapes were based on a perturbation form of Laplace's formula valid only for small amplitude distortion from the effect of an aerodynamic pressure around a sphere. In contrast, the current force balance model uses the complete form of differential Laplace's formula and includes adjustments to the aerodynamic pressure distribution for the effects of drop distortion and Reynolds number. The raindrop shapes under the influence of vertical electric fields and drop charges has also been investigated. A finite volume method with numerically generated transformation to a boundary-fitted coordinate system was used to calculate the shape-dependent electric field. Sufficient constraints (viz, drop volume, overall force balance, and shape-dependent surface distributions of aerodynamic and electrostatic stresses) allow the calculation of a unique shape by integration from the upper to lower pole of raindrop using a multiple iteration scheme. Based on the good agreement with wind tunnel observations, it appears that the model axis ratios from aerodynamic distortion provide the best approximation to date for raindrop size up to d = 9 mm. The model shapes closely fit the profiles of rather large raindrops (d = 5 mm). The model has been verified against solutions for a stationary drop in a uniform electric field (Taylor, 1964; Brazier-Smith, 1971; and Zrnic et al., 1984). Numerical shapes of falling drops in electric field show a pronounced extension of the upper pole. The increased fall speed

of electrostatically stretched drops enhances the aerodynamic flattening the base. The resultant triangular drop profiles are similar to wind tunnels observations (Richards and Dawson, 1971; and Rasmussen et al., 1985). Dissert. Abstr.

N90-15072*# Texas A&M Univ., College Station. Dept. of Aerospace Engineering.
A DIRECT-INVERSE METHOD FOR TRANSONIC AND SEPARATED FLOWS ABOUT AIRFOILS Final Report
Leland A. Carlson Washington Jan. 1990 72 p
(Grant NsG-1174)
(NASA-CR-4270; NAS 1.26:4270; TAMRF-3224-85-12) Avail: NTIS HC A04/MF A01 CSCL 01A

A direct-inverse technique and computer program called TAMSEP that can be used for the analysis of the flow about airfoils at subsonic and low transonic freestream velocities is presented. The method is based upon a direct-inverse nonconservative full potential inviscid method, a Thwaites laminar boundary layer technique, and the Barnwell turbulent momentum integral scheme; and it is formulated using Cartesian coordinates. Since the method utilizes inverse boundary conditions in regions of separated flow, it is suitable for predicting the flow field about airfoils having trailing edge separated flow under high lift conditions. Comparisons with experimental data indicate that the method should be a useful tool for applied aerodynamic analyses.
Author

N90-15073 Arizona Univ., Tucson.
NUMERICAL SIMULATION OF THE UNSTEADY TWO-DIMENSIONAL FLOW IN A TIME-DEPENDENT DOUBLY-CONNECTED DOMAIN Ph.D. Thesis
Yen-Ming Chen 1989 291 p
Avail: Univ. Microfilms Order No. DA8919025

Two-dimensional flow in a viscous incompressible fluid, generated by a circular cylinder executing large-amplitude rectilinear oscillations in a plane perpendicular to its axis and parallel to one of the sides of a surrounding rectangular box filled with incompressible fluid is studied numerically. The circular cylinder moves back and forth through its own wake, resulting in an extremely complex flow field. For ease of implementing boundary conditions, a numerically generated body-fitted coordinate system is used. At each time step, the physical domain is doubly-connected, and a cut is introduced in order to map it into a rectangular computational domain. A body-fitted grid is generated by solving a pair of Laplace equations with a simple grid spacing control method which preserves the essential one-to-one property of the mapping. A finite difference/pseudo-spectral technique is used in this work to solve the Navier-Stokes equations in velocity-vorticity formulation. The time integration of the vorticity transport equation is handled by a fully explicit three-level Adams-Bashforth method. The two Poisson equations for the velocity components are 11-banded and block-diagonal in form, and are solved by a preconditioned biconjugate gradient routine. An integral constraint on the vorticity field is used to determine the boundary vorticity that simultaneously satisfies the no-slip and no-penetration conditions. The surface vorticity is uniquely determined by a general solution procedure developed in this study which is valid for flows over multiple solid bodies. With this approach, the physical process of vorticity generation on the solid boundary is properly simulated and the principle of vorticity conservation is satisfied. Results for various tests cases and the complex vortex shedding phenomena generated by an oscillating circular cylinder are presented and discussed. Dissert. Abstr.

N90-15074 Georgia Inst. of Tech., Atlanta.
UNSTEADY AERODYNAMICS OF OSCILLATING AND RAPIDLY PITCHED AIRFOILS Ph.D. Thesis
Ismail Hakki Tuncer 1988 221 p
Avail: Univ. Microfilms Order No. DA8916174

A theoretical method and a computational method are developed and calibrated for the routine and accurate prediction of unsteady aerodynamic forces acting on lifting bodies. These methods are employed to produce improved understanding of the dynamic stall phenomena experienced by large amplitude rapidly pitched or oscillating airfoils. The analysis is based on the unsteady, incompressible, two-dimensional Navier-Stokes equations expressed in terms of velocity and vorticity vectors. The turbulence in high Reynolds number flows is simulated by the Baldwin-Lomax model. The governing differential equations are cast into an integro-differential formulation, which consists of the vorticity transport equation and the integral representation for velocity. This formulation confines the solution domain only to the viscous zone of the flow excluding the potential flow zone and leads to an efficient zonal solution procedure. In the theoretical study, the diffusion of vorticity is neglected. The flow field is represented by a thin surface vortex sheet around the airfoil and concentrated vortex flaments in the wake. Computational demands are greatly reduced by the partial analytic evaluations. In the viscous flow analysis, the vorticity transport equation is discretized on an O-grid around the airfoil. In solving the integral equation for velocity, finite Fourier series are utilized. Unsteady flow fields around rapidly pitched and oscillating airfoils and dynamic stall phenomena are simulated. The predicted flow fields are presented by instantaneous streamlines, vorticity contours and surface pressure distribution curves along the unsteady airfoil motion. The aerodynamic load hysterises are given. The NACA-0012 and SC-1095 airfoils are studied for different reduced pitching rate and reduced frequency motions. The formation and downstream convection of the leading edge vortex and its strong relationship to the dynamic stall phenomenon are assessed. Numerical predictions agree well with experimental data. Dissert. Abstr.

N90-15075 Georgia Inst. of Tech., Atlanta.
FINITE DIFFERENCE TECHNIQUES AND ROTOR BLADE AEROELASTIC PARTIAL DIFFERENTIAL EQUATIONS WITH QUASISTEADY AERODYNAMICS Ph.D. Thesis
Yildirim Kemal Yillikci 1988 181 p
Avail: Univ. Microfilms Order No. DA8916177

A conditionally stable explicit finite difference scheme is used to numerically integrate the nonlinear partial differential equation of motion in space and time to obtain the aeroelastic steady-state and transient responses of a rotor blade. Numerical stability analyses are performed for different blade parameters, flight conditions and spatial discretizations. The effects of different spatial discretizations on blade response and the convergence of the finite difference scheme are also analyzed. Rotor blade responses are calculated for different blade configurations and flight conditions and results are presented and compared with the results of previous analyses. Finally, different aspects of using computational rotor blade aerodynamics in response calculations and one period solution formulation by the use of finite difference equations are discussed without numerical results. Dissert. Abstr.

N90-15076# Sandia National Labs., Albuquerque, NM. Parachute System Div.
AN EXPERIMENTAL INVESTIGATION OF WALL-INTERFERENCE EFFECTS FOR PARACHUTES IN CLOSED WIND TUNNELS
J. Michael Macha and Robert J. Buffington Sep. 1989 25 p
(Contract DE-AC04-76DP-00789)
(DE90-001802; SAND-89-1485) Avail: NTIS HC A03/MF A01

A set of 6-ft-diameter ribbon parachutes (geometric porosities of 7, 15, and 30 percent) was tested in various subsonic wind tunnels covering a range of geometric blockages from 2 to 35 percent. Drag, base pressure, and inflated geometry were measured under full-open, steady-flow conditions. The resulting drag areas and pressure coefficients were correlated with the bluff-body blockage parameter (i.e., drag area divided by tunnel cross-sectional area) according to the blockage theory of Maskell. The data show that the Maskell theory provides a simple, accurate correction for the effective increase in dynamic pressure caused by wall constraint for both single parachutes and clusters. For single parachutes, the empirically derived blockage factor K(sub M) has the value of 1.85, independent of canopy porosity. Derived values of K(sub M) for two- and three-parachute clusters are 1.35 and 1.59, respectively. Based on the photometric data, there was

no deformation of the inflated shape of the single parachutes up to a geometric blockage of 22 percent. In the case of the three-parachute cluster, decreases in both the inflated diameter and the spacing among member parachutes were observed at a geometric blockage of 35 percent. DOE

N90-15077*# North Carolina State Univ., Raleigh.
HYPERSONIC NOZZLE DESIGN Final Report
Wayland C. Griffith Dec. 1989 22 p
(Contract NCC1-109)
(NASA-CR-186261; NAS 1.26:186261) Avail: NTIS HC A03/MF A01 CSCL 01A

Possible experimental facilities appropriate to a university environment that could make meaningful contributions to the solution of problems in hypersonic aerodynamics are investigated. Needs for the National Aerospace Plane and interplanetary flights with atmospheric aerobraking are used to scope the problem. Relevant events of the past two decades in universities and at the national laboratories are examined for their implications regarding both problems and prospects. Most striking is the emergence of computational fluid dynamics, which is viewed here as an equal partner with laboratory experimentation and flight test in relating theory with reality. Also significant are major advances in instrumentation and data processing methods, especially optical techniques. The direction of the study was guided by the concept of a companion program, i.e., the university effort should complement a major area of endeavor at NASA-Langley. Through this, both faculty and student participants gain a natural and effective working relationship. Existing and proposed major hypersonic aerodynamic facilities in industry and at the national laboratories are examined by type; hypersonic wind tunnels, arc-heated tunnels, shock tubes and tunnels, and ballistic ranges. Of these, the free piston tunnel and shock tube/tunnel are most appropriate for a university. Author

N90-15078*# Institute for Computer Applications in Science and Engineering, Hampton, VA.
ON STRONGLY NONLINEAR VORTEX/WAVE INTERACTIONS IN BOUNDARY-LAYER TRANSITION Final Report
Philip Hall and Frank T. Smith (University Coll., London, England) Dec. 1989 37 p Submitted for publication
(Contract NAS1-18605)
(NASA-CR-181963; NAS 1.26:181963; ICASE-89-82) Avail: NTIS HC A03/MF A01 CSCL 01A

The interactions between longitudinal vortices and accompanying waves considered are strongly nonlinear, in the sense that the mean-flow profile throughout the boundary layer is completely altered from its original undisturbed state. Nonlinear interactions between vortex flow and Tollmien-Schlichting waves are addressed first, and some analytical and computational properties are described. These include the possibility in the spatial-development case of a finite-distance break-up, inducing a singularity in the displacement thickness. Second, vortex/Rayleigh wave nonlinear interactions are considered for the compressible boundary-layer, along with certain special cases of interest and some possible solution properties. Both types, vortex/Tollmien-Schlichting and vortex/Rayleigh, are short-scale/long-scale interactions and they have potential applications to many flows at high Reynolds numbers. The strongly nonlinear nature is believed to make them very relevant to fully fledged transition to turbulence. Author

N90-15079# Air Force Wright Research and Development Center, Wright-Patterson AFB, OH.
AN ALTERNATIVE DERIVATION FOR AN INTEGRAL EQUATION FOR LINEARIZED SUBSONIC FLOW OVER A WING Final Report, Feb. 1988 - Jan. 1989
Marc H. Williams, Karl G. Guderley, and Mark R. Lee Aug. 1989 41 p
(AD-A214140; WRDC-TR-89-3097) Avail: NTIS HC A03/MF A01 CSCL 01/1

An integral equation for the time dependent linearized subsonic flow over a wing has been derived in a previous report by K. G. Guderley and Maxwell Blair (AD-A176684). The present alternative derivation due to Marc H. Williams is presented. The difference lies in the sequence of events. The original derivation was carried out in a coordinate system moving with the wing. Williams' derivation makes the crucial step in a coordinate fixed in the undisturbed air and then carries out a transformation to wing coordinates. In addition, this derivation clarifies the relation between the integral equation for steady and unsteady flow, and derives a formulation based on the Lorentz transform. GRA

N90-15080# Naval Postgraduate School, Monterey, CA. Dept. of Aeronautics and Astronautics.
FLOW VISUALIZATION OF THE EFFECT OF PITCH RATE ON THE VORTEX DEVELOPMENT ON THE SCALE MODEL OF A F-18 FIGHTER AIRCRAFT M.S. Thesis
Sung-Nam Park Jun. 1989 145 p Sponsored in part by Naval Air Systems Command
(AD-A214244) Avail: NTIS HC A07/MF A01 CSCL 01/1

Experiments were performed in a water tunnel to visualize the vortex bursting phenomenon on a 1/48th scale model of the F-18 fighter aircraft. Photographs were taken to investigate the effect of pitch rate and yawing on bursting locations of vortices shed from the forebody and the strake during simple pitch up and simple pitch down maneuvers in an angle of attack range up to 50 degrees. It was found that the vortex burst point moves upstream with increasing pitch rate. At the same pitch rate, vortex bursting was usually found to occur earlier for the pitch-down than for the pitch-up maneuver. Aircraft yawing generated significant vortex asymmetries due to earlier vortex bursting on the windward side thus leading to undesirable side forces. GRA

N90-15081 ESDU International Ltd., London (England).
INSTALLED TAILPLANE LIFT-CURVE SLOPE AT SUBSONIC SPEEDS
Oct. 1989 17 p
(ESDU-89029; ISBN-0-85679-701-4; ISSN-0141-397X) Avail: ESDU

ESDU 89029 provides a simple semi-empirical correlation of experimental data from the literature for installed tailplane efficiency for both fin- and body-mounted cases. Efficiency here is installed lift-curve slope normalized by the theoretical free-air value, in this case as predicted by ESDU 70011. The correlation yields two graphs, one for each case, of efficiency against the most appropriate geometric parameter characterizing the airframe interference. Subcritical Mach number effects are accounted for by use of the compressible lift-curve slope from ESDU 70011 but it was found that some improvement in correlation could be achieved by an additional correction factor. The methods apply to cases with or without high-lift devices deployed. Except for fin-mounted tailplanes on close-coupled configurations, the methods will predict lift-curve slope to within 6 percent for any straight-tapered tailplane, as is shown by a sketch of predicted against experimental results for some 70 cases. Two detailed examples illustrate the use of the methods. The techniques used to extract the installed lift-curve slope from the wind-tunnel data are detailed. ESDU

N90-15082 ESDU International Ltd., London (England).
THE MAXIMUM LIFT COEFFICIENT OF PLAIN WINGS AT SUBSONIC SPEEDS
Oct. 1989 24 p
(ESDU-89034; ISBN-0-85679-707-3; ISSN-0141-397X) Avail: ESDU

ESDU 89034 gives an empirical method for estimating the maximum lift of aerodynamically smooth straight-tapered wings with or without camber and/or twist but with high lift devices undeflected. Any shape of section or camber line, both of which may vary spanwise, can be treated. Linear spanwise variation of combined twist (geometric and camber-induced) is assumed, but by means of an equivalent linear twist it can also be applied to wings with non-linear monotonic twist. It can also be applied to wings with cranked or curved edges by use of the equivalent straight-tapered wing concept of ESDU 76003. The method uses the approach of

ESDU 83040 for an unswept, untwisted wing to locate the most highly loaded section. ESDU 84026 is used to find the maximum lift there which is then related to the wing overall lift. Corrections are applied as appropriate for sweep and twist effects and for the influence of Mach and Reynolds numbers. The method has been tested against wing alone wind-tunnel data (including half models) extracted from the literature for a range of wing geometries (aspect ratio 2 to 12, sweeps up to 50 degrees, taper ratios 0.2 to 1.0) for Mach numbers to 0.8, and was found generally to predict the maximum lift coefficient to within 10 percent. ESDU

N90-15064# Boeing Commercial Airplane Co., Renton, WA. Configuration and Certification Group.
FLIGHT AND WIND TUNNEL INVESTIGATION OF AERODYNAMIC EFFECTS OF AIRCRAFT GROUND DEICING/ANTIICING FLUIDS
L. James Runyan, Thomas A. Zierten, and Eugene G. Hill *In* AGARD, Flight in Adverse Environmental Conditions Sep. 1989 11 p (For primary document see N90-15041 07-01)
Copyright Avail: NTIS HC A17/MF A03; Non-NATO Nationals requests available only from AGARD/Scientific Publications Executive

03 AIR TRANSPORTATION AND SAFETY

Includes passenger and cargo air transport operations; and aircraft accidents.

For related information see also *16 Space Transportation* and *85 Urban Technology and Transportation.*

N90-15083# Army Aviation Engineering Flight Activity, Edwards AFB, CA.
EVALUATION OF THE IMPROVED OV-ID ANTI-ICING SYSTEM, PHASE 2 Final Report, 6-23 Mar. 1989
Joseph C. Miess and Gary McVaney Apr. 1989 61 p Sponsored by Army Aviation Systems Command, Saint Louis, MO
(AD-A213928; USAAEFA-87-25-1-Phase-2) Avail: NTIS HC A04/MF A01 CSCL 08/12

The U.S. Army Aviation Engineering Flight Activity re-evaluated the OV-1 modified improved ant-icing system from 6 to 23 March 1989, at Duluth, Minnesota. Six flights (6.4 hours of cloud immersion) in natural icing conditions were conducted. Moderate icing conditions with temperatures less than -12 C were not encountered. One enhancing characteristic, seven deficiencies and five shortcomings were noted. The windshield anti-ice system enhances safe mission accomplishment. The seven deficiencies are as follows: the failure of the pneumatic deicing system to remove wing and empennage leading edge ice accumulations in moderate icing colder than -10 C; the failure of the anti-icing system to keep the engine inlet clear at temperatures colder than -10 C; the ice accretion and shedding characteristics of the propeller spinner afterbody which may result in ice foreign object damage (FOD) to the engine; the numerous converter dropouts during normal operation; the ice accretion characteristics of the pitot tube which result in erroneous airspeed indications; intermittent failure of the ice detector system to activate the anti-icing system; and the actions required to re-establish flight-essential and normal inverter loads following inverter dropout. GRA

N90-15084# Questek, Inc., Centerport, NY.
SEE AND AVOID/COCKPIT VISIBILITY
Walton Graham Oct. 1989 24 p Sponsored by FAA, Atlantic City, NJ
(AD-A214214; DOT/FAA/CT-89/18) Avail: NTIS HC A02/MF A01 CSCL 01/2

This study was conducted in response to the Federal Aviation Administration's (FAA) Office of Aviation Safety and the recommendations of the Interagency Near Midair Collision (NMAC) Working Group, dated July 21, 1986, which suggested a review of see and avoid effectiveness, conspicuity enhancement, and their relationship to cockpit visibility. This report summarizes the salient facts in these areas, based on a review of the literature, and assesses the potential for significant reduction of collision risk. The study was conducted by Walton Graham, Questek, Incorporated, who was previously involved in numerous FAA see and avoid, pilot warning instrument/collision risk studies and analyses of the near midair collision data. GRA

N90-15085# Flight Safety Foundation, Inc., Arlington, VA.
INTERNATIONAL AIRCRAFT OCCUPANT SAFETY CONFERENCE AND WORKSHOP PROCEEDINGS Final Report
Nov. 1988 309 p Conference held in Arlington, VA, 31 Oct. - 3 Nov. 1988
(Contract DTFA01-88-C-0020)
(AD-A214452; DOT/FAA/OV-89/2) Avail: NTIS HC A14/MF A02 CSCL 01/5

These proceedings contain formal conference presentations as well as summaries of informal workshop discussions on how to further improve aircraft cabin occupant safety. Also included are the analysis and future recommendations for occupant safety. Session topics include: Inflight occupant protection; Passenger education; Crashworthiness; and Fire protection. GRA

N90-15048# Technische Univ., Brunswick (Germany, F.R.). Inst. for Flight Guidance and Control.
INFLUENCE OF WINDSHEAR, DOWNDRAFT AND TURBULENCE ON FLIGHT SAFETY
Gunther Schaenzer *In* AGARD, Flight in Adverse Environmental Conditions Sep. 1989 19 p (For primary document see N90-15041 07-01)
Copyright Avail: NTIS HC A17/MF A03; Non-NATO Nationals requests available only from AGARD/Scientific Publications Executive

N90-15062*# National Aeronautics and Space Administration. Lewis Research Center, Cleveland, OH.
NASA'S PROGRAM ON ICING RESEARCH AND TECHNOLOGY
John J. Reinmann, Robert J. Shaw, and Richard J. Ranaudo *In* AGARD, Flight in Adverse Environmental Conditions Sep. 1989 31 p Previously announced as N89-22569 (For primary document see N90-15041 07-01)
Copyright Avail: NTIS HC A17/MF A03; Non-NATO Nationals requests available only from AGARD/Scientific Publications Executive CSCL 01C

N90-15065*# National Aeronautics and Space Administration. Langley Research Center, Hampton, VA.
EFFECTS OF LIGHTNING ON OPERATIONS OF AEROSPACE VEHICLES
Bruce D. Fisher *In* AGARD, Flight in Adverse Environmental Conditions Sep. 1989 14 p (For primary document see N90-15041 07-01)
Copyright Avail: NTIS HC A17/MF A03; Non-NATO Nationals requests available only from AGARD/Scientific Publications Executive CSCL 01C

N90-15067# Office National d'Etudes et de Recherches Aerospatiales, Paris (France).
PRINCIPAL CHARACTERISTICS OF LIGHTNING ON AIRCRAFT [PRINCIPALES CARACTERISTIQUES DES FOUDROIEMENTS SUR AVIONS]
J. L. Boulay *In* AGARD, Flight in Adverse Environmental Conditions Sep. 1989 10 p In FRENCH Previously announced in IAA as A89-48744 (For primary document see N90-15041 07-01)
Copyright Avail: NTIS HC A17/MF A03; Non-NATO Nationals requests available only from AGARD/Scientific Publications Executive

04 AIRCRAFT COMMUNICATIONS AND NAVIGATION

Includes digital and voice communication with aircraft; air navigation systems (satellite and ground based); and air traffic control.

For related information see also *17 Space Communications, Spacecraft Communications, Command and Tracking* and *Communications and Radar.*

N90-15086# Mitre Corp., McLean, VA.
NATIONAL AIRSPACE SYSTEM: AIRPORT MOVEMENT AREA CONTROL OPERATIONAL CONCEPT Final Report
A. Lucille Springen Sep. 1989 37 p
(Contract DTFA01-89-C-00001)
(WP-89W00181; DOT/FAA/DS-89/33; NAS-SR-13211) Avail: NTIS HC A03/MF A01

This concept of operations is one of a set that in total will describe the operation on the National Airspace System (NAS) when the projected upgrades are completed. As described in the National Airspace System System Requirements Specification (NASSRS), Airport Movement Area Control involves the control and separation of aircraft and vehicles on the movement areas of qualifying aerodromes in all weather conditions, and includes the separation of aircraft from obstructions. Described here are specialists' functions necessary for the control of the airport movement area, most importantly, determining the identity and location of vehicles and aircraft on the movement area. This operational concept also describes interactions and information passed between the user, specialists, and NAS subsystems involved with airport movement area control in order to provide a common perspective for those engaged in this control. Author

N90-15087# Sandia National Labs., Albuquerque, NM. Advanced Technology Div.
AUTONOMOUS LAND NAVIGATION IN A STRUCTURED ENVIRONMENT
Paul R. Klarer 1989 7 p Presented at the IEEE International Conference on Systems, Man and Cybernetics, Cambridge, MA, 14-17 Nov. 1989
(Contract DE-AC04-76DP-00789)
(DE90-001625; SAND-89-0319C; CONF-8911102-1) Avail: NTIS HC A02/MF A01

This paper describes a hardware and software system developed to perform autonomous navigation of a land vehicle in a structured environment. The vehicle used for development and testing of the system was the Jeep Cherokee Mobile Robotics Testbed Vehicle. Since obstacle detection and avoidance have not yet been incorporated into the system, a structured environment is postulated that presumes the paths to be traversed are free of obstacles. The system performs path planning and execution based on maps constructed using the vehicle's onboard navigation system and mapmaker. The system software, hardware, and performance data are discussed. DOE

N90-15088# Sandia National Labs., Albuquerque, NM.
GEOMETRIC CONSIDERATIONS FOR A WAYPOINT GUIDANCE METHOD
Farrell J. Perdreauville Sep. 1989 14 p
(Contract DE-AC04-76DP-00789)
(DE90-001803; SAND-89-0623) Avail: NTIS HC A03/MF A01

Waypoint guidance is a technique used to steer an autonomous vehicle along a desired course. Waypoints are designated at intervals along that course. The guidance algorithms issue steering commands that, if followed, result in the vehicle's traveling from waypoint to waypoint. Thus, the vehicle remains on or very close to the desired trajectory. Waypoints can be specified by latitude, longitude, and altitude in geographic coordinates. The vehicle's current location can be described similarly. This is enough information to determine the direction of travel that would take the vehicle to the waypoint. The shortest route from one point on a spherical surface to another on the same surface is a great circle. A great circle lies in a plane that contains the center of the sphere. The plane also is normal to the surface of the sphere along the great circle. The earth actually is distorted slightly from spherical; it is ellipsoidal. An ellipsoidal earth model will be used in this report. Features of the great circle will be applied to effect good approximations of shortest routes to waypoints. Therefore, only the endpoints of long, straight course segments need be specified. DOE

N90-15089# Federal Aviation Administration, Atlantic City, NJ.
IMPROVED LIGHTING OF TAXIWAY/TAXIWAY INTERSECTIONS FOR INSTRUMENT FLIGHT RULES (IFR) OPERATIONS
Eric S. Katz Dec. 1989 13 p
(DOT/FAA/CT-TN89/64) Avail: NTIS HC A03/MF A01

A new visual aid to advise pilots that a taxiway/taxiway intersection is being approached was developed at the Federal Aviation Administration (FAA) Technical Center. Subject pilots were asked to comment on the effectiveness of the new elevated taxiway intersection lights. Results of the evaluation indicate that the lights provide adequate advance warning of the approaching taxiway/taxiway intersection and an indication of where to stop to ensure clearance from aircraft using the intersecting taxiway. Author

N90-15090# Mitre Corp., McLean, VA.
CONTROL OUTSIDE OF INDEPENDENT SURVEILLANCE COVERAGE OPERATIONAL CONCEPT Final Report
Jill B. Randlett Jun. 1989 37 p
(Contract DTFA01-89-C-0001)
(AD-A214163; DOT/FAA/DS-89/26; NAS-SR-1324) Avail: NTIS HC A03/MF A01 CSCL 17/7

This operational concept describes how Air Traffic Control (ATC) will be performed in non-radar (oceanic and mountainous terrain) areas throughout the National Airspace System (NAS). The framework for this document incorporates non-radar ATC requirements from Section 3.2.4 of the NAS System Requirements Specification (NASSRS), the NAS Plan, and the NAS Level 1 Design, as expected to occur during the mid-to-late 1990's. The concept includes the functions provided by the Advanced Automation System (AAS) and Step 1 of the Automatic Dependent Surveillance (ADS) programs. GRA

N90-15091# Rochester Univ., NY. Dept. of Computer Science.
CENTRALIZED AND DECENTRALIZED KALMAN FILTER TECHNIQUES FOR TRACKING, NAVIGATION, AND CONTROL
Christopher M. Brown, Hugh Durrant-Whyte, John Leonard, Bobby Rao, and Barry Steer May 1989 42 p Revised Sponsored in part by RADC, Griffiss AFB, NY
(Contracts DACA76-85-C-0001; F30602-85-C-0008)
(AD-A214245; TR-277-REV) Avail: NTIS HC A03/MF A01 CSCL 17/11

A review of some estimation basics is followed by illustrative applications of Kalman filters for stationary and maneuvering targets. The variable dimension of Kalman filter is used for the maneuvering target. The performance of the nearest neighbor standard filter is compared to that of the probabilistic data association filter for tracking a target in clutter. Multi-target tracking, using sonar sensors to estimate an autonomous robot's distance from walls, is applied to the navigation problem. The Kalman filter equations can be completely decentralized and distributed among the nodes of a multi-sensor system. Each sensing node implements its own local Kalman filter, arrives at a partial decision, and broadcasts it to every other node. Each node then assimilates this received information to arrive at its own local but optimal estimate of the system state. An appendix contains brief implementational notes. GRA

N90-15061# Royal Aircraft Establishment, Bedford (England). Flight Management Dept.
THE ASSESSMENT OF VISIBILITY FROM AUTOMATIC CONTRAST MEASUREMENTS
A. W. Puffett *In* AGARD, Flight in Adverse Environmental Conditions Sep. 1989 14 p (For primary document see

N90-15041 07-01)
Copyright Avail: NTIS HC A17/MF A03; Non-NATO Nationals requests available only from AGARD/Scientific Publications Executive

05 AIRCRAFT DESIGN, TESTING AND PERFORMANCE

Includes aircraft simulation technology.

For related information see also *18 Spacecraft Design, Testing and Performance* and *39 Structural Mechanics*.For land transportation vehicles see *85 Urban Technology and Transportation.*

N90-15092 Texas Univ., Austin.
MODELING AND CONTROL OF THE RAPID DEPLOYMENT OF TOWED AIRBORNE DEVICES Ph.D. Thesis
Don Travis Berry 1989 286 p
Avail: Univ. Microfilms Order No. DA8920662

Recently, the aerospace industry has been interested in the rapid deployment of towed systems. There is a basic physical trade-off between deployment time and the peak loads encountered in the towline during the deployment. Because the aerodynamic forces on the towline are nonlinear functions of the local angle of attack, the equations that describe the system are highly nonlinear, and it is suspected that the change in peak loads with small changes in the deployment control may be rather abrupt. Thus there exists a need for a mathematical model that is specific to the deployment problem, but is quite flexible in its ability to handle different system parameters, flight conditions, and control algorithms. This model is a useful design tool that is developed herein. The partial differential equations that describe the system are developed with an emphasis on physical understanding. Factors suggesting the use of an ordinary differential equation model are mentioned and the ordinary equations are presented with particular attention to the boundary at the towline reel. Studies concerning the size of spatial and temporal steps required are discussed and examples showing how the computer program may be used are presented. Dissert. Abstr.

N90-15093*# ACA Industries, Inc., Rancho Palos Verdes, CA.
APPLICATION OF THE JOINED WING TO TILTROTOR AIRCRAFT
Julian Wolkovitch, Barnaby Wainfan, Yitzhak Ben-Harush, and Wayne Johnson (Johnson Aeronautics, Palo Alto, CA.) Nov. 1989 94 p
(Contract NAS2-12988)
(NASA-CR-177543; NAS 1.26:177543) Avail: NTIS HC A05/MF A01 CSCL 01C

A study was made to determine the potential speed improvements and other benefits resulting from the application of the joined wing concept to tiltrotor aircraft. Using the XV-15 as a baseline, the effect of replacing the cantilever wing by a joined-wing pair was studied. The baseline XV-15 cantilever wing has a thickness/chord ratio of 23 percent. It was found that this wing could be replaced by a joined-wing pair of the same span and total area employing airfoils of 12 percent thickness/chord ratio. The joined wing meets the same static strength requirements as the cantilever wing, but increases the limiting Mach Number of the aircraft from M=0.575 to M=0.75, equivalent to an increase of over 100 knots in maximum speed. The joined wing configuration studied is lighter than the cantilever and has approximately 11 percent less wing drag in cruise. Its flutter speed of 245 knots EAS is not high enough to allow the potential Mach number improvement to be attained at low altitude. The flutter speed can be raised either by employing rotors which can be stopped and folded in flight at speeds below 245 knots EAS, or by modifying the airframe to reduce adverse coupling with the rotor dynamics. Several modifications of wing geometry and nacelle mass distribution were investigated, but none produced a flutter speed above 260 knots EAS. It was concluded that additional research is required to achieve a more complete understanding of the mechanism of rotor/wing coupling. Author

N90-15094*# National Aeronautics and Space Administration. Langley Research Center, Hampton, VA.
SERRATED TRAILING EDGES FOR IMPROVING LIFT AND DRAG CHARACTERISTICS OF LIFTING SURFACES Patent Application
Paul M. H. W. Vijgen, inventor (to NASA) (Kansas Univ., Lawrence.), Floyd G. Howard, inventor (to NASA), Dennis M. Bushnell, inventor (to NASA), and Bruce J. Holmes, inventor (to NASA) 30 Nov. 1989 16 p Sponsored by NASA
(NASA-Case-LAR-13870-1; US-Patent-Appl-SN-429516; NAS 1.71:LAR-13870-1) Avail: NTIS HC A03/MF A01 CSCL 01C

An improvement in the lift and drag characteristics of a lifting surface is achieved by attaching a serrated panel to the trailing edge of the lifting surface. The serrations may have a saw-tooth configuration, with a 60 degree included angle between adjacent serrations. The serrations may vary in shape and size over the span-wise length of the lifting surface, and may be positioned at fixed or adjustable deflections relative to the chord of the lifting surface. NASA

N90-15095# Virginia Univ., Charlottesville. School of Engineering and Applied Science.
EFFECTS OF AEROELASTIC TAILORING ON ANISOTROPIC COMPOSITE MATERIAL BEAM MODELS OF HELICOPTER BLADES M.S. Thesis
Patrick Graham Forrester May 1989 164 p
(AD-A213478) Avail: NTIS HC A08/MF A01 CSCL 01/3

The role of composite materials in modern helicopter blade design has become most important during recent years. By exploiting the directional stiffness properties of these composites, favorable torsion modes or twisting can be achieved. The capability to apply this potential as a design parameter is generally known as aeroelastic tailoring. The bending-torsional coupling of static, hingeless composite rotor blades is investigated using finite element theory. The hingeless blade is treated as a single cell laminated shell beam. Each laminate is composed of different lay-ups of graphite-epoxy composite plies and is categorized as isotropic or anisotropic based upon this lay-up. A systematic study is made to identify the effects of ply orientation and lamina thickness on blade section properties. The results of this study are used to solve the beam equations for composite materials. GRA

N90-15096# Air Force Flight Test Center, Edwards AFB, CA.
SCHLEICHER ASK-21 GLIDER (TG-9) STALL AND SPIN Final Report
Doyle B. Janzen and Charles J. Precourt Jul. 1989 129 p
(AD-A213513; AFFTC-TR-89-27) Avail: NTIS HC A07/MF A01 CSCL 01/1

The results of the Schleicher ASK-21 Glider (TG-9) Stall and Spin Evaluation are documented. Testing included evaluation of the departure and spin susceptibility of the aircraft as a function of weight and cg, definition of spin modes and modes characteristics as well as the control effects on those modes. Stall and spin flight tests of the ASK-21 were conducted between at the Air Force Flight Test Center (AFFTC), Edwards AFB, California. GRA

N90-15097# Air Force Inst. of Tech., Wright-Patterson AFB, OH.
AIRCRAFT PERFORMANCE ENHANCEMENT WITH ACTIVE COMPRESSOR STABILIZATION M.S. Thesis
John G. Seymour 1988 224 p
(AD-A213652; AFIT/CI/CIA-88-228) Avail: NTIS HC A10/MF A02 CSCL 01/1

An engine cycle deck and a mission simulation program were mated to provide the capability to analyze the impact of localized design changes in a systems context. Specifically, the effects of compressor stall alleviation accomplished through the use of active stabilization were analyzed. Since no experimental data exists for compressor performance in the actively stabilized region of

operation, actual compressor performance was bracketed by the examination of two types of compressors; one having steeply sloped speed lines in the actively stabilized region and the other having speed lines with shallow slope. Engines with actively stabilized compressor sections were installed in an advanced tactical fighter and flown through a typical high-low-high attack profile. Mission performance results for the aircraft with controlled compressors were compared to baseline values of mission radius, takeoff gross weight, aircraft operating weight and aircraft total wetted area. Efficiency, engine radius at the fan and bare engine weight were found to be the primary determinants of mission performance. GRA

N90-15098# Army Aviation Research and Development Command, Moffett Field, CA. Aeroflightdynamics Directorate.
AN EXAMINATION OF HELICOPTER ROTOR LOAD CALCULATIONS
Thomas H. Maier 1988 20 p
(AD-A214295) Avail: NTIS HC A03/MF A01 CSCL 20/11

The structural response of three full-scale helicopter rotors has been examined. Airloads predicted by CAMRAD were compared by harmonics with test measurements. Flapwise bending moments were calculated from the CAMRAD airloads using three methods: force integration, curvature, and a finite-difference method. The force-integration and curvature moments were calculated with the CAMRAD program itself; however, the finite-difference method was calculated externally by a forced response program, Blade Response to Aerodynamic Loading (BRAL). The BRAL analysis with measured airloads was shown to agree well with strain-gauge measurements on the CH-34 rotor in a wind tunnel. The CAMRAD/force-integration bending moments were shown to accumulate error as the integration progressed from tip to root. The CAMRAD/curvature moments agreed well with the finite-difference moments over most of the blade; however, at regions of rapidly changing stiffness the agreement was poor. When applied to the BRAL solution, force integration was shown to give excellent results, provided the integration had a small step size. Shear forces calculated by CAMRAD and BRAL showed fair agreement. GRA

N90-15099# Aerolift, Inc., Tillamook, OR.
X.2 LIMITED FLIGHT TEST PLAN
15 Mar. 1989 85 p
(Contract MDA972-88-C-0058)
(AD-A214412) Avail: NTIS HC A05/MF A01 CSCL 01/3

The X.2 Limited Flight Test Plan is for the CycloCrane Program. The principal objectives of the planned tests are to: (1) assess a number of ground handling scenarios for the X.2 system to determine the preferred mix of Ground Support Equipment (GSE) and personnel for efficient and safe field operations, and (2) obtain specific performance data needed to support design development; e.g., hover power of new, four engine configuration. The aerostat has a diameter of 68 feet and is 136 feet long. The fabric is a polyurethane coated dacron. The X.2 CycloCrane is powered by four Hirth F-30 (110 horsepower each) two-stroke engines. The total weight of these four engines with reduction belt drives and exhaust manifolds is 440 pounds. The four propellers are wooden, three-bladed fixed pitch with a diameter of 92 inches. The telemetry subsystem has been upgraded to accommodate the installation of four engines place of the original two. It has a truly remote control operation and is relatively simple but reliable. GRA

N90-15100*# National Aeronautics and Space Administration. Ames Research Center, Moffett Field, CA.
THE EFFECTIVENESS OF VANE-AILERON EXCITATION IN THE EXPERIMENTAL DETERMINATION OF FLUTTER SPEED BY PARAMETER IDENTIFICATION
Eli Nissim (Technion - Israel Inst. of Tech., Haifa.) Jan. 1990 23 p
(NASA-TP-2971; H-1516; NAS 1.60:2971) Avail: NTIS HC A03/MF A01 CSCL 01C

The effectiveness of aerodynamic excitation is evaluated analytically in conjunction with the experimental determination of flutter dynamic pressure by parameter identification. Existing control surfaces were used, with an additional vane located at the wingtip. The equations leading to the identification of the equations of motion were reformulated to accommodate excitation forces of aerodynamic origin. The aerodynamic coefficients of the excitation forces do not need to be known since they are determined by the identification procedure. The 12 degree-of-freedom numerical example treated in this work revealed the best wingtip vane locations, and demonstrated the effectiveness of the aileron-vane excitation system. Results from simulated data gathered at much lower dynamic pressures (approximately half the value of flutter dynamic pressure) predicted flutter dynamic pressures with 2-percent errors. Author

N90-15042# Flight Safety Foundation, Inc., Arlington, VA.
THE HUMAN ELEMENT: THE KEY TO SAFE, CIVIL OPERATIONS IN ADVERSE WEATHER
John H. Enders *In* AGARD, Flight in Adverse Environmental Conditions Sep. 1989 7 p (For primary document see N90-15041 07-01)
Copyright Avail: NTIS HC A17/MF A03; Non-NATO Nationals requests available only from AGARD/Scientific Publications Executive

N90-15047# Test Group (6520th), Edwards AFB, CA.
THE UNITED STATES AIR FORCE APPROACH TO ALL-WEATHER TESTING
Clifford D. Tompkins and James A. Ford *In* AGARD, Flight in Adverse Environmental Conditions Sep. 1989 7 p (For primary document see N90-15041 07-01)
Copyright Avail: NTIS HC A17/MF A03; Non-NATO Nationals requests available only from AGARD/Scientific Publications Executive

N90-15058*# Georgia Inst. of Tech., Atlanta. School of Aerospace Engineering.
A STUDY OF THE EFFECTS OF ROTATING FRAME TURBULENCE (RFT) ON HELICOPTER FLIGHT MECHANICS
D. P. Schrage, J. V. B. Prasad, and G. H. Gaonkar (Florida Atlantic Univ., Boca Raton.) *In* AGARD, Flight in Adverse Environmental Conditions Sep. 1989 13 p (For primary document see N90-15041 07-01)
(Contract NCA2-266)
Copyright Avail: NTIS HC A17/MF A03; Non-NATO Nationals requests available only from AGARD/Scientific Publications Executive CSCL 01C

N90-15063# Texas A&M Univ., College Station. Dept. of Aerospace Engineering.
ICE INDUCED AERODYNAMIC PERFORMANCE DEGRADATION OF ROTORCRAFT: AN OVERVIEW
K. D. Korkan and R. K. Britton *In* AGARD, Flight in Adverse Environmental Conditions Sep. 1989 34 p (For primary document see N90-15041 07-01)
Copyright Avail: NTIS HC A17/MF A03; Non-NATO Nationals requests available only from AGARD/Scientific Publications Executive

N90-15066# Aeroplane and Armament Experimental Establishment, Boscombe Down (England).
AIRCRAFT TESTING IN THE ELECTROMAGNETIC ENVIRONMENT
P. M. Newton *In* AGARD, Flight in Adverse Environmental Conditions Sep. 1989 8 p (For primary document see N90-15041 07-01)
Copyright Avail: NTIS HC A17/MF A03; Non-NATO Nationals requests available only from AGARD/Scientific Publications Executive

06 AIRCRAFT INSTRUMENTATION

Includes cockpit and cabin display devices; and flight instruments.

For related information see also *19 Spacecraft Instrumentation* and *35 Instrumentation and Photography.*

N90-15101*# National Aeronautics and Space Administration. Langley Research Center, Hampton, VA.
TASK-ORIENTED DISPLAY DESIGN: CONCEPT AND EXAMPLE
Terence S. Abbott Dec. 1989 119 p
(NASA-TM-101685; NAS 1.15:101685) Avail: NTIS HC A06/MF A01 CSCL 01D

The general topic was in the area of display design alternatives for improved man-machine performance. The intent was to define and assess a display design concept oriented toward providing this task-oriented information. The major focus of this concept deals with the processing of data into parameters that are more relevant to the task of the human operator. Closely coupled to this concept of relevant information is the form or manner in which this information is actually presented. Conventional forms of presentation are normally a direct representation of the underlying data. By providing information in a form that is more easily assimilated and understood, a reduction in human error and cognitive workload may be obtained. A description of this proposed concept with a design example is provided. The application for the example was an engine display for a generic, twin-engine civil transport aircraft. The product of this concept was evaluated against a functionally similar, traditional display. The results of this evaluation showed that a task-oriented approach to design is a viable concept with regard to reducing user error and cognitive workload. The goal of this design process, providing task-oriented information to the user, both in content and form, appears to be a feasible mechanism for increasing the overall performance of a man-machine system. Author

N90-15102*# National Aeronautics and Space Administration. Langley Research Center, Hampton, VA.
DISPLAY INTERFACE CONCEPTS FOR AUTOMATED FAULT DIAGNOSIS
Michael T. Palmer Dec. 1989 34 p
(NASA-TM-101610; NAS 1.15:101610) Avail: NTIS HC A03/MF A01 CSCL 01D

An effort which investigated concepts for displaying dynamic system status and fault history (propagation) information to the flight crew is described. This investigation was performed by developing several candidate display formats and then conducting comprehension tests to determine those characteristics that made one format preferable to another for presenting this type of information. Twelve subjects participated. Flash tests, or limited time exposure tests, were used to determine the subjects' comprehension of the information presented in the display formats. It was concluded from the results of the comprehension tests that pictographs were more comprehensible than both block diagrams and text for presenting dynamic system status and fault history information, and that pictographs were preferred over both block diagrams and text. It was also concluded that the addition of this type of information in the cockpit would help the crew remain aware of the status of their aircraft. Author

07 AIRCRAFT PROPULSION AND POWER

Includes prime propulsion systems and systems components, e.g., gas turbine engines and compressors; and onboard auxilliary power plants for aircraft.

For related information see also *20 Spacecraft Propulsion and Power, 28 Propellants and Fuels,* and *44 Energy Production and Conversion.*

N90-15103 Virginia Univ., Charlottesville.
SPATIALLY-RESOLVED, NONINTRUSIVE MEASUREMENTS IN A NONREACTING SCRAMJET COMBUSTOR USING LASER-INDUCED IODINE FLUORESCENCE Ph.D. Thesis
Douglas Gerald Fletcher 1989 141 p
Avail: Univ. Microfilms Order No. DA8922432

The theoretical development, calibration, and application of a nonintrusive optical flowfield-diagnostic technique utilizing laser-induced iodine fluorescence (LIIF) is reported. Experimental results from a combination of static cell and gasdynamic studies are used to quantify the thermodynamic scaling of the important collisional phenomena which strongly affect narrow-bandwidth-induced fluorescence of iodine seeded in air. With proper thermodynamic scaling, linecenter fluorescence signal relationships are developed for making measurements of iodine mole fraction, total number density, pressure, and temperature using narrow-bandwidth excitation. Complications in fluorescence signal interpretations arising from high-density broadening of adjacent lines into the linecenter of interest and from departure from the high-density limit are addressed and corrections are developed in order to extend the range of the optical technique. The number density and temperature measurement techniques are combined with velocity measurement into a unified, nonintrusive optical technical for simultaneous measurement of the flow properties in steady, compressible flowfields. A calibration experiment is performed in the known flowfield of an underexpanded jet. Comparison of the measurements with the numerical solution of the flowfield demonstrates the range and accuracy of the optical diagnostic technique. The calibrated technique is then used to characterize the mixing of supersonic streams in a model scramjet combustor. The experimental measurements will be used to quantitatively validate computational fluid dynamic (CFD) codes currently being developed to model the mixing process. Dissert. Abstr.

N90-15104 Council for National Academic Awards (England).
A STUDY OF VARIABLE GEOMETRY IN ADVANCED GAS TURBINES Ph.D. Thesis
J. E. A. Roy-Aikins 1988 226 p
Avail: Univ. Microfilms Order No. BRDX85735

The loss of performance of a gas turbine engine at off-design is primarily due to the rapid drop of the major cycle performance parameters with decrease in power and this may be aggravated by poor component performance. More and more stringent requirements are being put on the performance demanded from gas turbines and if future engines are to exhibit performances superior to those of present day engines, then a means must be found of controlling engine cycle such that the lapse rate of the major cycle parameters with power is reduced. In certain applications, it may be desirable to vary engine cycle with operating conditions in an attempt to re-optimize performance. Variable geometry in key engine components offers the advantage of either improving the internal performance of a component or rematching engine cycle to alter the flow-temperature-pressure relationships. Either method has the potential to improve engine performance. The program was used to study the performance of a number of cycles incorporating variable geometry and it was concluded that variable geometry can significantly improve the off-design performance of gas turbines. Dissert. Abstr.

N90-15105# Florida Univ., Gainesville. Dept. of Environmental Engineering Sciences.
DESIGN AND CALIBRATION OF AN IN-STACK, LOW-PRESSURE IMPACTOR Final Report, Jan. 1985 - Oct. 1987
D. A. Lundgren and R. W. Vanderpool Mar. 1989 131 p
(Contract F08635-83-C-0136)
(AD-A213531; AFESC/ESL-TR-88-31) Avail: NTIS HC A07/MF A01 CSCL 21/5

The purpose was to design, fabricate, calibrate, and field test a low-pressure impactor for sampling and size classifying particulate exhaust from jet engine test cells. All aspects of the effort are covered through an actual field test on a J79 type engine exhaust. A computer code for user prediction of impactor stage outputs is included as well as design drawings for impactor fabrication. GRA

N90-15106# Battelle Columbus Labs., OH.
CHARACTERIZATION OF CHEMICALS ON ENGINE EXHAUST PARTICLES Final Report, Sep. 1986 - Dec. 1987
M. R. Kuhlman and J. C. Chuang Jun. 1989 116 p
(Contract F08635-85-C-0122; AF Proj. 1900)
(AD-A213566; AFESC/ESL-TR-88-50) Avail: NTIS HC A06/MF A01 CSCL 24/1

The objective was to characterize particulate-bound chemicals emitted from military aircraft, both as they are emitted and as the exhaust ages. Three Air Force turbine engines (TF33-P3, TF33-P7, and J79C) were examined, using engine test cells at Tinker AFB, OK. Emissions were collected at power settings of idle, 30 percent, 75 percent, and injected into smog chambers for subsequent aging. Samples were collected from these chambers periodically during the photochemical experiments to permit measurements of the vapor phase and particle associated photochemical experiments to permit measurements of the vapor phase and particle associated polycyclic aromatic hydrocarbon (PAH) and derivatives under experimental conditions. Throughout the course of the experiments, measurements of the concentrations of total hydrocarbons, NO, NOx, and O3 were made. The samples collected on filter and sorbent media were returned to the laboratory for extraction and analysis by gas chromatography/mass spectrometry (GC/MS) to determine masses of specific target compounds collected. The time profiles of these compounds are presented for the various engines, operating powers, sunlight levels, and photochemical reactivities examines. GRA

N90-15107# Pratt and Whitney Aircraft, West Palm Beach, FL. Advanced Engineering Div.
THERMAL MECHANICAL FATIGUE OF COATED BLADE MATERIALS Final Report, 1 Aug. 1984 - 30 Sep. 1988
J. E. Heine, J. R. Warren, and B. A. Cowles 27 Jun. 1989 216 p
(Contract F33615-84-C-5027)
(AD-A214258; PW/FL/FR-20505; WRDC-TR-89-4027) Avail: NTIS HC A10/MF A02 CSCL 21/5

A model capable of predicting thermal mechanical fatigue (TMF) crack initiation and propagation in coated advanced blade materials, with emphasis on crack initiation, was developed and demonstrated. The experimental program included isothermal baseline and TMF tests on one alloy and two coating materials to evaluate the effects of mean stress, frequency, hold periods, and maximum temperature on the TMF life of a coated system. Task 1, Definition of TMF Conditions, was completed using the results of a separately funded program evaluating current and advanced airfoil conditions. Task 2, Alloy/Coating Selection and Isothermal Properties, generated monotonic data for uncoated PWA 1480, freestanding PWA 276 overlay coating, and PWA 275 aluminide coating. GRA

08 AIRCRAFT STABILITY AND CONTROL

Includes aircraft handling qualities; piloting; flight controls; and autopilots.

For related information see also *05 Aircraft Design, Testing and Performance.*

N90-15108*# National Aeronautics and Space Administration. Langley Research Center, Hampton, VA.
RELATIVE MERITS OF REACTIVE AND FORWARD-LOOK DETECTION FOR WIND-SHEAR ENCOUNTERS DURING LANDING APPROACH FOR VARIOUS MICROBURST ESCAPE STRATEGIES
David A. Hinton Washington Feb. 1990 24 p Prepared in cooperation with DOE, Washington, DC
(NASA-TM-4158; L-16622; NAS 1.15:4158; DOT/FAA/DS-89/35)
Avail: NTIS HC A03/MF A01 CSCL 01C

The goal was to quantify the benefits of airborne forward-look windshear detection and to develop and test a candidate set of strategies for recovery from inadvertent microburst encounters during the landing approach, given the utilization of both reactive-only and forward-look windshear detection. Candidate strategies were developed and evaluated using a non-piloted simulation consisting of a simple point-mass performance model of a transport-category airplane flying through an analytical microburst model. The results indicate that the factor which most strongly effects a microburst recovery is the time at which the recovery is initiated. Forward-look alerts given 10 seconds prior to microburst entry permitted recoveries to be made with negligible altitude loss. The results also show that no single microburst scenario can be used to evaluate the relative merits of various recovery strategies. The type of alert used to initiate the recovery (reactive or forward-look) and the altitude of the microburst encounter had an effect on the type of recovery strategy that performed best. These factors may have serious implications for the design and certification of windshear systems. Author

N90-15109 Virginia Polytechnic Inst. and State Univ., Blacksburg.
EFFECT OF MODAL TRUNCATION ON DERIVATIVES OF CLOSED-LOOP DAMPING RATIOS IN STRUCTURAL CONTROL Ph.D. Thesis
Christopher Alan Sandridge 1989 81 p
Avail: Univ. Microfilms Order No. DA8917999

It is well known that Fourier series of discontinuous functions converge slowly and that the derivatives of the series may not converge at all. Since modal expansion of structural response is a generalization of the Fourier series, slow convergence of modal expansion can be expected when the applied loads exhibit discontinuities in time or space. Thus, in a structure controlled by point actuators, slow convergence of derivatives of structural response with respect to system parameters can be expected. To demonstrate this, the sensitivity of the closed-loop response to structural changes is calculated for a multi-span beam with three control systems of increasing complexity that utilize point actuators. Reduced models based on the natural modes of the structure are formed and derivatives of the damping ratios of the closed-loop eigenvalues are calculated. As expected, the convergence of the derivatives of the damping ratios with increasing number of modes is slower than the convergence of the damping ratios themselves. The convergence is improved when distributed actuators replace the point actuators. When the control system is designed based on a reduced model, the damping ratios also converge slowly. In transient response problems, it is known that complementing the vibration modes with a mode representing statis response to the loads can greatly improve convergence. Indeed, for the examples studied, when Rtiz vectors corresponding to statis responses due to unit loads at the actuators are added to the basis vectors, the convergence of the reduced-model derivatives is greatly enhanced. Also, when the control system is designed using a reduced model containing both vibration modes and Ritz vectors, its prediction of the full-model response is greatly improved. Dissert. Abstr.

N90-15110*# National Aeronautics and Space Administration. Langley Research Center, Hampton, VA.
GUIDANCE ANALYSIS OF THE AEROGLIDE PLANE CHANGE MANEUVER AS A TURNING POINT PROBLEM
Christopher Gracey Dec. 1989 29 p
(NASA-TM-101639; NAS 1.15:101639) Avail: NTIS HC A03/MF A01 CSCL 01C

The development of guidance approximations for the atmospheric (aeroglide) portion of the minimum fuel, orbital plane change, trajectory optimization problem is described. Asymptotic methods are used to reduce the two point, boundary value, optimization problem to a turning point problem from the bank angle control. The turning point problem solution, which yields an approximate optimal control policy, is given in terms of parabolic cylinder functions, which are tabulated, and integral expressions, which must be numerically computed. Comparisons of the former, over their region of validity, with optimal control solutions show good qualitative agreement. Additional work and analysis is needed to compute the guidance approximation work. Author

N90-15111*# Boeing Commercial Airplane Co., Seattle, WA.
FLY-BY-LIGHT FLIGHT CONTROL SYSTEM TECHNOLOGY DEVELOPMENT PLAN Final Report
A. Chakravarty, J. W. Berwick, D. M. Griffith, S. E. Marston, and R. L. Norton Jan. 1990 49 p
(Contract NAS1-18027)
(NASA-CR-181953; NAS 1.26:181953) Avail: NTIS HC A03/MF A01 CSCL 01C

The results of a four-month, phased effort to develop a Fly-by-Light Technology Development Plan are documented. The technical shortfalls for each phase were identified and a development plan to bridge the technical gap was developed. The production configuration was defined for a 757-type airplane, but it is suggested that the demonstration flight be conducted on the NASA Transport Systems Research Vehicle. The modifications required and verification and validation issues are delineated in this report. A detailed schedule for the phased introduction of fly-by-light system components has been generated. It is concluded that a fiber-optics program would contribute significantly toward developing the required state of readiness that will make a fly-by-light control system not only cost effective but reliable without mitigating the weight and high-energy radio frequency related benefits. Author

N90-15112*# National Aeronautics and Space Administration. Lewis Research Center, Cleveland, OH.
ADVANCED DETECTION, ISOLATION, AND ACCOMMODATION OF SENSOR FAILURES IN TURBOFAN ENGINES: REAL-TIME MICROCOMPUTER IMPLEMENTATION
John C. DeLaat and Walter C. Merrill Washington Feb. 1990 28 p
(NASA-TP-2925; E-4391; NAS 1.60:2925) Avail: NTIS HC A03/MF A01 CSCL 01C

The objective of the Advanced Detection, Isolation, and Accommodation Program is to improve the overall demonstrated reliability of digital electronic control systems for turbine engines. For this purpose, an algorithm was developed which detects, isolates, and accommodates sensor failures by using analytical redundancy. The performance of this algorithm was evaluated on a real time engine simulation and was demonstrated on a full scale F100 turbofan engine. The real time implementation of the algorithm is described. The implementation used state-of-the-art microprocessor hardware and software, including parallel processing and high order language programming. Author

N90-15113# Virginia Univ., Charlottesville. Dept. of Mechanical and Aerospace Engineering.
ADAPTIVE CONTROL OF HELICOPTER VIBRATIONS VIA THE IMPULSE RESPONSE METHOD Final Report, 1 Jun. 1986 - 31 May 1989
Carl R. Knospe, J. K. Haviland, and W. D. Pilkey Sep. 1989 77 p
(Contract DAAL03-86-G-0043)
(AD-A213728; UVA525167/MAE90/101; ARO-23761.2-EG-F)
Avail: NTIS HC A05/MF A01 CSCL 01/2

An adaptive blade control algorithm for helicopter vibration reduction is developed as an application of an impulse response control method. The method is based on an impulse response formulation which is applicable to any linear system with periodic dynamics. In the investigation of adaptive helicopter vibration control presented, a vertical-axis-only plant is simulated by a model composed of an impulse response matrix and an uncontrolled vibration vector. The adaptive control is implemented by a regulator composed of an estimator and a controller. The model parameters are identified by either Kalman or batch Weighted Least Squares (WLS) filtering in either global or local form. The resulting estimates are used in an optimal control law obtained by the minimization of a constrained, single-step, quadratic performance function. Four control laws are derived: global certainty-equivalent, local certainty equivalent, global cautious, and local cautious. The filters derived are examined in open loop simulations to determine their identification capabilities independent of the control feedback. Two levels of open loop control variation are used to evaluate estimation performance with constant and time-varying plants. The Kalman filters are found to produce lower estimate errors than the WLS filters. GRA

N90-15050# Aerospatiale, Toulouse (France).
HOW TO FLY WINDSHEAR USING THE FLY-BY-WIRE CONCEPT
J. L. Bonafe *In* AGARD, Flight in Adverse Environmental Conditions Sep. 1989 16 p (For primary document see N90-15041 07-01)
Copyright Avail: NTIS HC A17/MF A03; Non-NATO Nationals requests available only from AGARD/Scientific Publications Executive

N90-15051# Instituto Superior Tecnico, Lisbon (Portugal).
A PITCH CONTROL LAW FOR COMPENSATION OF THE PHUGOID MODE INDUCED BY WINDSHEARS
I. M. B. C. Campos, A. J. N. M. Agular, and J. R. C. Azinheira *In* AGARD, Flight in Adverse Environmental Conditions Sep. 1989 13 p (For primary document see N90-15041 07-01)
Copyright Avail: NTIS HC A17/MF A03; Non-NATO Nationals requests available only from AGARD/Scientific Publications Executive

N90-15053# Aeronautica Macchi S.p.A., Varese (Italy). Flight Mechanics and Automatic Control Dept.
CANARD VERSUS AFT-TAIL RIDE QUALITIES PERFORMANCE AND PILOT COMMAND RESPONSE
L. V. Cioffi and L. Mangiacasale *In* AGARD, Flight in Adverse Environmental Conditions Sep. 1989 13 p (For primary document see N90-15041 07-01)
Copyright Avail: NTIS HC A17/MF A03; Non-NATO Nationals requests available only from AGARD/Scientific Publications Executive

N90-15054# Messerschmitt-Boelkow-Blohm G.m.b.H., Hamburg (Germany, F.R.). Dynamic Dept.
THE INTERFERENCE OF FLIGHTMECHANICAL CONTROL LAWS WITH THOSE OF LOAD ALLEVIATION AND ITS INFLUENCE ON STRUCTURAL DESIGN
M. Molzow and R. Moebest *In* AGARD, Flight in Adverse Environmental Conditions Sep. 1989 20 p (For primary document see N90-15041 07-01)
Copyright Avail: NTIS HC A17/MF A03; Non-NATO Nationals requests available only from AGARD/Scientific Publications Executive

N90-15055# Oklahoma State Univ., Stillwater. Dept. of Mechanical and Aerospace Engineering.
TURBULENCE EFFECTS OF AIRCRAFT FLIGHT DYNAMICS AND CONTROL
Robert L. Swaim *In* AGARD, Flight in Adverse Environmental

Conditions Sep. 1989 9 p (For primary document see N90-15041 07-01)
Copyright Avail: NTIS HC A17/MF A03; Non-NATO Nationals requests available only from AGARD/Scientific Publications Executive

N90-15056# Dornier-Werke G.m.b.H., Friedrichshafen (Germany, F.R.).
ACTIVE CONTROL SYSTEM FOR GUST LOAD ALLEVATION AND STRUCTURAL DAMPING
Hartmut Boehret and Joachim Winter *In* AGARD, Flight in Adverse Environmental Conditions Sep. 1989 11 p (For primary document see N90-15041 07-01)
Copyright Avail: NTIS HC A17/MF A03; Non-NATO Nationals requests available only from AGARD/Scientific Publications Executive

N90-15057# Deutsche Forschungs- und Versuchsanstalt fuer Luft- und Raumfahrt, Brunswick (Germany, F.R.). Inst. fuer Flugmechanik.
AIRCRAFT RESPONSE AND PILOT BEHAVIOUR DURING A WAKE VORTEX ENCOUNTER PERPENDICULAR TO THE VORTEX AXIS
Reinhard Koenig *In* AGARD, Flight in Adverse Environmental Conditions Sep. 1989 18 p (For primary document see N90-15041 07-01)
Copyright Avail: NTIS HC A17/MF A03; Non-NATO Nationals requests available only from AGARD/Scientific Publications Executive

09 RESEARCH AND SUPPORT FACILITIES (AIR)

Includes airports, hangars and runways; aircraft repair and overhaul facilities; wind tunnels; shock tubes; and aircraft engine test stands.

For related information see also *14 Ground Support Systems and Facilities (Space).*

N90-15114# Sandia National Labs., Albuquerque, NM.
VIBRAFUGE: COMBINED VIBRATION AND CENTRIFUGE TESTING
J. D. Rogers, F. Cericola, J. W. Doggett, and M. L. Young 1989 11 p Presented at the 60th Shock and Vibration Symposium, Virginia Beach, VA, 14-16 Nov. 1989
(Contract DE-AC04-76DP-00789)
(DE90-001091; SAND-89-1656C; CONF-891152-5) Avail: NTIS HC A03/MF A01

The combined dynamic environments of vibration and linear acceleration are experienced by a large number of devices. Testing such devices has normally been a two step process in which independent vibration and centrifuge tests were performed. Concerns have existed for some time with possible combined effects from these two dynamic environments which could cause failures in the field which were not predicted from either analysis or the independent tests. This paper describes the design and performance of a testing facility which combines vibration and centrifuge testing in an single operation. The test facility is called the VIBRAFUGE and utilizes Sandia's 29 foot underground centrifuge with an attached electrodynamic shaker. DOE

N90-15115# Dundee Univ. (Scotland). Dept. of Civil Engineering.
DESIGN TEMPERATURES FOR FLEXIBLE AIRFIELD PAVEMENT DESIGN Final Report
A. F. Stock Jul. 1989 62 p
(Contract DAJA45-87-M-0484)
(AD-A214141; R/D-5852-EN-01) Avail: NTIS HC A04/MF A01 CSCL 13/3

The mechanistic approach to flexible pavement design recognizes 2 forms of traffic induced structural damage, one being fatigue failure by cracking in the asphalt layer, the other being permanent deformation. The criterion used for ensuring that the pavement does not fail prematurely due to fatigue in the asphalt is based upon tensile strain. It has been shown that the tensile strain due to aircraft loading has a maximum value at the bottom of the asphalt layer, and it is at this depth that the strain is calculated. The position of the maximum strain relative to the aircraft wheels is dependent upon the aircraft gear configuration, the pavement thickness and stiffness, but is readily determined. Extensive laboratory fatigue tests, combined with full scale trials have permitted the development of a fatigue criterion based on a limiting strain value, so that pavements can be designed to give satisfactory performance. GRA

N90-15116# Westinghouse Hanford Co., Richland, WA.
PHYSICAL AND ELECTRICAL STANDARDS LABORATORY GENERAL OPERATING PROCEDURES
J. E. Bongers Mar. 1989 68 p
(Contract DE-AC06-87RL-10930)
(DE90-003515; WHC-SP-0446) Avail: NTIS HC A04/MF A01

Various procedures used in the operation of the Westinghouse Hanford Standards Laboratory are presented. These procedures consist of the following titles: Organization, Operating Directives and Traceability, Preparation and Control of Operating Procedures, Selection and Qualification of Standards Laboratory Personnel, Environmental Guides and Considerations for the Standards Laboratory, Calibration Recall Program, Calibration Reports and Labels, Calibration Stamps, Quality Assurance Records, Nonconforming Equipment in the Standards Laboratory, Receiving/Shipping Instructions, Shipment of Measuring and Test Equipment at Hanford, Offsite Shipment of Standards, and Offsite Shipment of Measuring and Test Equipment. DOE

12 ASTRONAUTICS (GENERAL)

For extraterrestrial exploration see *91 Lunar and Planetary Exploration.*

No abstracts in this category.

13 ASTRODYNAMICS

Includes powered and free-flight trajectories; and orbital and launching dynamics.

N90-15117 Texas Univ., Austin.
ERROR MODELING OF BIAS-TYPE PARAMETERS FOR TOPEX ORBIT DETERMINATION Ph.D. Thesis
C. Rajasenan 1989 241 p
Avail: Univ. Microfilms Order No. DA8920813

The TOPEX mission has a requirement for a radial orbit accuracy of 13 cm over a 10-day period. To achieve this level of accuracy, accurate dynamic and measurement models are required. A large portion of the orbit error is derived from the uncertainty in the apriori values of the constant model parameters, most notably the geopotential coefficients. The major sources of model error affecting the orbit accuracy of TOPEX are identified. This includes the use of the full calibrated covariance matrix of the nominal geopotential model. The results of the parameter identification are used to design an optimal filter for orbit determination. The primary source of orbit error for TOPEX is identified as the geopotential model error followed by error in the solar radiation pressure coefficient. The optical filter that is derived in terms of the accuracy of the filter estimates is one that includes the initial conditions of the orbit, single arc parameters for the coefficient of drag and the reflectivity coefficient of solar radiation pressure and multiple-arc parameters for the density correction model. The accuracy of orbit determination for TOPEX is limited by the geopotential model error which is characterized by the calibrated geopotential covariance matrix. A new method is proposed that would adjust the formal

covariance matrix generated by a gravity model solution for systematic and random errors that affect the orbit accuracy.
Dissert. Abstr.

14 GROUND SUPPORT SYSTEMS AND FACILITIES (SPACE)

Includes launch complexes, research and production facilities; ground support equipment, e.g., mobile transporters; and simulators.

For related information see also *09 Research and Support Facilities (Air).*

N90-15118# Lawrence Livermore National Lab., CA. Shock Physics Program.
DESIGN LIMITATIONS ON ULTRA-HIGH VELOCITY PROJECTILE LAUNCHERS
Lewis A. Glenn 1 Jun. 1989 22 p Presented at the 1989 Hypervelocity Impact Symposium, San Antonio, TX, 12-14 Dec. 1989
(Contract W-7405-eng-48)
(DE89-012933; UCRL-100496; CONF-891214-2) Avail: NTIS HC A03/MF A01

The maximum velocity attainable in a gasdynamic gun is limited by the maximum sound speed in the driver gas. For a conventional 2-stage light gas gun, the limit is approx. 10 km/s. Higher velocities are possible, but probably not without the destruction of the gun barrel. As long as this occurs on a time scale longer than the residence time of the projectile, a useful system may still result. Using a newly developed computer code called IGUN, the performance was evaluated of several multistage designs capable of achieving ultra-high projectile velocities. The main problem is in maintaining the integrity of the projectile. The calculations indicate that 20 km/s should be achievable without fracturing the projectile. If it is only required to retain near original areal density, velocities in excess of 30 km/s appear feasible. DOE

N90-15119# Lawrence Livermore National Lab., CA.
HUGONIOT MEASUREMENTS WITH THE LLNL ELECTRIC GUN FACILITY
G. R. Gathers, H. H. Chau, J. E. Osher, and R. C. Weingart Jul. 1989 4 p Presented at the American Physical Society Topical Conference on Shock Compression of Condensed Matter, Albuquerque, NM, 14-17 Aug. 1989
(Contract W-7405-eng-48)
(DE90-002809; UCRL-100810; CONF-890812-62) Avail: NTIS HC A01/MF A01

A wide class of materials exists with properties that are not consistent enough to justify making very accurate EOS measurements. Some are nonhomogeneous two-phase materials consisting of a matrix and an embedded material. In order to represent these materials in hydrocode simulations, one is usually driven to substituting another material which has (hopefully) similar properties. The Equation of State (EOS) of the material is usually the most important description needed. A technique was developed to make EOS measurements on such materials using the LLNL electric gun facility. DOE

15 LAUNCH VEHICLES AND SPACE VEHICLES

Includes boosters; operating problems of launch/space vehicle systems; and reusable vehicles.

For related information see also *20 Spacecraft Propulsion and Power.*

N90-15120*# National Aeronautics and Space Administration. Langley Research Center, Hampton, VA.
SHUTTLE-C UTILIZATION FOR ASSEMBLY OF THE REPHASED FREEDOM CONFIGURATION
Leonard J. DeRyder, Washito A. Sasamoto, and Patrick A. Troutman Aug. 1989 57 p
(NASA-TM-101658; NAS 1.15:101658) Avail: NTIS HC A04/MF A01 CSCL 22B

The utilization of the Shuttle-C Heavy Lift Launch Vehicle (HLLV) to augment the Shuttle orbiter to deliver to earth orbit elements for assembly of a rephased definition of Space Station Freedom is assessed. A past history of previous HLLV studies performed with respect to Freedom launch and assembly is reviewed and conclusions extrapolated that are appropriate to consider for the new rephased Freedom definition. The rephased Freedom definition is explained, two utilization scenarios are developed and related assessments are provided for Shuttle-C utilization early in the assembly sequence or utilization later in theon-orbit build up phase. Author

N90-15121# Science Applications International Corp., New York, NY.
CURRENT LAUNCH VEHICLE RELIABILITY PRACTICE AND DATA BASE ASSESSMENT. VOLUME 1: EXECUTIVE SUMMARY AND REPORT BODY Final Report, Apr. 1984 - Sep. 1989
Joseph R. Fragola, Lewie Booth, and Yu Shen Jun. 1989 201 p
(Contract F04611-88-C-0014; AF Proj. 3058)
(AD-A213600; AL-TR-89-013-Vol-1) Avail: NTIS HC A10/MF A02 CSCL 19/7

The effort to identify liquid and solid propulsion design parameters, development methodologies, and production/operations techniques related to the improvement of propulsion reliability for future launch vehicles is described. Six key recommendations are made. There is a section on current practice and data base assessment. This is followed by a section on reliability enhancing methods. Finally, there is a section on quantification and prioritization of methodologies. An investigation is included of historical failure correlation factors using the SSME test and flight history as an example, a quick calculation of failure correlation factor versus engine out capability, a reliability analysis of current U.S. launch vehicles, and a history of U.S. launch launch vehicles. GRA

16 SPACE TRANSPORTATION

Includes passenger and cargo space transportation, e.g., shuttle operations; and space rescue techniques.

For related information see also *03 Air Transportation and Safety* and *18 Spacecraft Design, Testing and Performance.* For space suits see *54 Man/System Technology and Life Support.*

No abstracts in this category.

17 SPACE COMM., SPACECRAFT COMM., COMMAND & TRACKING

Includes telemetry; space communications networks; astronavigation and guidance; and radio blackout.

For related information see also *04 Aircraft Communications and Navigation* and *32 Communications and Radar.*

No abstracts in this category.

18 SPACECRAFT DESIGN, TESTING AND PERFORMANCE

Includes satellites; space platforms; space stations; spacecraft systems and components such as thermal and environmental controls; and attitude controls.

For life support systems see *54 Man/System Technology and Life Support.* For related information see also *05 Aircraft Design, Testing and Performance, 39 Structural Mechanics,* and *16 Space Transportation.*

N90-15122# Lawrence Livermore National Lab., CA.
SAFETY EVALUATION REPORT FOR GALILEO: VOLUME 1
John P. Joyce, Leven B. Gray, Darrel A. Huff, Louis J. Ullian, Kenneth L. Kaisler, Frank J. Benz, Robert H. Brown, Dewey B. Channell, Robert F. Fletcher, and John W. Marshall et al Sep. 1989 94 p
(Contract W-7405-eng-48)
(DE90-003086; UCID-21775-Vol-1; INSRP-89-01-Vol-1) Avail: NTIS HC A05/MF A01

Two General Purpose Heat Source Radioisotope Thermoelectric Generators (GPHS RTGs) provide the prime source of electric power for the spacecraft on the Galileo mission. In addition, 120 Light-Weight Radioisotope Heater Units (LWRHUs) provide heat for numerous spacecraft components. The use of radioactive material in RTGs and LWRHUs for the Galileo mission necessitates evaluation of the radiological risks. This Safety Evaluation Report presents the results of the evaluation performed by the Interagency Nuclear Safety Review Panel (INSRP) and its subpanels. Source material consulted for this evaluation included the Galileo Program Office Final Safety Analysis Report, safety test results, and launch vehicle and component historical data. In addition, independent analyses were conducted by INSRP and its subpanels. DOE

N90-15123# Lawrence Livermore National Lab., CA.
SAFETY EVALUATION REPORT FOR GALILEO, VOLUME 2
John P. Joyce, Leven B. Gray, Darrel A. Huff, Louis J. Ullian, Kenneth L. Kaisler, Frank J. Benz, Robert H. Brown, Dewey B. Channell, Robert F. Fletcher, and John W. Marshall et al Sep. 1989 112 p
(Contract W-7405-eng-48)
(DE90-003087; UCID-21775-Vol-2; INSRP-89-01-Vol-2) Avail: NTIS HC A06/MF A01

This report provides a brief overview of the various activities and decisions that were made by the Interagency Nuclear Safety Review Panel (INSRP) coordinators during the development of the Safety Evaluation Report for the Galileo mission. Each of the subpanels has generated a report describing its activities and the results of its portion of the Galileo evaluation. These reports should be reviewed for more indepth understanding of the subpanel activities. To bridge the gap between the subpanel reports and the Safety Evaluation Report, i.e., to assure continuity, this report summarizes the considerations and decisions made by the INSRP Coordinators at various points during the evaluation process. In particular, this report identifies the specific changes made to the Launch Accident Scenario Evaluation Program Version 2 (LASEP2) and EMERGE computer models used by the Department of Energy (DOE) in the development of Volumes 2 and 3 of the Galileo Final Safety Analysis Report and by INSRP in the development of the Safety Evaluation Report. In addition, this report documents decisions made concerning how to best present results obtained from the INSRP evaluation. DOE

N90-15124# Massachusetts Inst. of Tech., Cambridge.
INSTRUMENTATION FOR A FACILITY FOR THE TEST, ANALYSIS AND ACTIVE CONTROL OF SPACECRAFT TRUSS STRUCTURES Final Report, 1 Oct. 1987 - 31 Dec. 1988
Andreas H. VonFlotow 18 Aug. 1989 7 p
(Grant AF-AFOSR-0031-87; AF Proj. 2917)
(AD-A213655; AFOSR-89-1265TR) Avail: NTIS HC A02/MF A01 CSCL 22/2

The report lists in detail the equipment purchased with this instrumentation grant (granted under the DoD-URIP program). Also summarized is the impact this equipment has had upon the work and the reputation of the affected group at MIT. The appendix includes numerous theses and papers which have benefited from the availability of this equipment. GRA

N90-15125# Naval Postgraduate School, Monterey, CA. Dept. of Physics.
STRATEGIC CHARACTERISTICS OF DYNAMICS EXPLORER 1 RETARDING ION MASS SPECTROMETER AND THE CONSEQUENCES FOR CORE PLASMA MEASUREMENTS Technical Report, 1-30 Sep. 1989
R. C. Olsen 14 Sep. 1989 54 p
(AD-A214013; NPS61-89-014) Avail: NTIS HC A04/MF A01 CSCL 21/3

The Retarding Ion Mass Spectrometer (RIMS) on the Dynamics Explorer I (DE I) satellite has provided a new range of data, and challenges for studies of the core plasma of the magnetosphere. Analysis of the RIMS data provides a measure of the satellite potential in the inner magnetosphere. As the satellite leaves the inner plasmasphere, it begins to charge positively, crossing the 0 V mark at about 1000/cc. The potential rises slowly initially, reaching about 1 V near the plasmapause, at the 100/cc point. At lower densities, the potential rises relatively rapidly, reaching +5 V or greater at the 10/cc point. For satellite potentials of +1 to +5 V, portions of the ion distribution function are lost to measurement because the ions are repelled by the satellite. In particular, in a multi-temperature plasma, the cold component is easily lost in this potential (density) regime. It is in this regime where aperture bias techniques were successfully used, particularly in measurements of field aligned ion flows such as the polar wind, which have sufficient kinetic energy to overcome electrostatic barriers in front of the aperture plane. At lower densities (less than 10/cc), the satellite potential can exceed +5 V. At such potentials the core plasma is lost to the RIMS, and even the aperture bias techniques are no lower successful. GRA

N90-15126# Case Western Reserve Univ., Cleveland, OH. Dept. of Systems Engineering.
RELIABILITY ANALYSIS OF THE SPACE STATION FREEDOM ELECTRICAL POWER SYSTEM M.S. Thesis
Michael C. Talbott Aug. 1989 158 p
(AD-A214105) Avail: NTIS HC A08/MF A01 CSCL 10/2

The on-board electrical power system of a space station has to provide the power needed for scientific missions (discretionary loads) and everyday station housekeeping chores (non-discretionary loads). Due to size constraints of the spacecraft, the electrical power system's output, efficiency and reliability will be constrained producing a system that is imperfect. This thesis applies traditional reliability techniques and modified methods to evaluate the reliability of the proposed NASA Space Station electrical power system. The modified methods take into account components and assemblies that have different levels of failure affecting the power output. These components and assemblies with failure levels other than all or nothing power outputs define each power output level between complete failure and expected nominal power. By applying this analysis approach to the proposed space station electrical power system in conjunction with some reasonable assumptions, different levels of the electrical power output are identified along with the exceedance probability that each interval will occur at a specified time. GRA

N90-15127# Air Force Geophysics Lab., Hanscom AFB, MA. Space Physics Div.
SCATHA (SPACECRAFT CHARGING AT HIGH ALTITUDES) ATLAS DATA BASE, VOLUME 1 Environmental Research Papers, 1 Jan. - 30 Jun. 1989
E. G. Mullen, ed. and M. S. Gussenhoven, ed. 1 Sep. 1989 201 p
(AF Proj. 7601)
(AD-A214204; GL-TR-89-0249(1)-Vol-1; GL-ERP-1037-Vol-1)
Avail: NTIS HC A10/MF A02 CSCL 22/5

A study of the plasma environment encountered by the P78-2 Spacecraft Charging At High Altitudes (SCATHA) satellite during

its operation between March 1979 and June 1980 was conducted and reported in the SCATHA Environmental Atlas (AFGL-TR-83-0002). Summary plots of much of the data used in the Atlas are presented in two volumes. The first volume contains magnetic field data and spacecraft frame potential data. The second volume contains low and medium energy range electron and ion data, medium energy range ion composition data and high energy electron data. The data are presented in 24-hour plots. GRA

N90-15128# Air Force Geophysics Lab., Hanscom AFB, MA. Space Physics Div.
SCATHA (SPACECRAFT CHARGING AT HIGH ALTITUDES) ATLAS DATA BASE, VOLUME 2 Environmental Research Papers, 1 Jan. - 30 Jun. 1989
E. G. Mullen, ed. and M. S. Gussenhoven, ed. 1 Sep. 1989 285 p
(AF Proj. 7601)
(AD-A214205; GL-TR-89-0249(2)-Vol-2; GL-ERP-1038-Vol-2)
Avail: NTIS HC A13/MF A02 CSCL 22/5

A study of the plasma environment encountered by the P78-2 Spacecraft Charging At High Altitudes (SCATHA) satellite during its operation between March 1979 and June 1980 was conducted and reported in the SCATHA Environmental Atlas (AFGL-TR-84-0002). Summary plots of much of the data used in the Atlas are presented in two volumes. The first volume contains magnetic field data and spacecraft frame potential data. The second volume contains low and medium energy range electron and ion data, medium energy range ion composition data and high energy electron data. The data are presented in 24-hour plots. GRA

N90-15129# Air Force Systems Command, Wright-Patterson AFB, OH. Foreign Technology Div.
MANNED SPACECRAFT
A. N. Ponomarev 14 Sep. 1989 375 p Transl. into ENGLISH of Pilotiruyemyye Kosmicheskiye Korabli (Moscow, USSR, Voyennoye), 1968 p 1-222
(AD-A214218; FTD-ID(RS)T-0592-89) Avail: NTIS HC A16/MF A02 CSCL 22/5

The book discusses the Soviet spacecraft of the type Vostok, Voskhod, and about American ships Mercury, Gemini, and Apollo, which are intended to be used for the delivery of man to the Moon; about future spacecraft for flight to other planets of solar system; orbital flight vehicles, intended for studying space, engines of space vehicles, are examined. The problems which appear with mastery/adoption of outer space, are briefly illuminated. In description of specific samples and schematics of foreign flight vehicles, their equipment, which relate to the theme in question, there are used data published in the foreign press. The data published in the open Soviet press are used for the examination of Soviet samples of space technology. GRA

N90-15840*# Little (Arthur D.), Inc., Cambridge, MA.
THE SOLAR POWER SATELLITE (SPS): PROGRESS SO FAR
Peter E. Glaser *In* NASA, Langley Research Center, Report of NASA Lunar Energy Enterprise Case Study Task Force Jul. 1989 p 68-83 (For primary document see N90-15836 07-81)
Avail: NTIS HC A09/MF A02 CSCL 22B

19 SPACECRAFT INSTRUMENTATION

For related information see also *06 Aircraft Instrumentation* and *35 Instrumentation and Photography.*

No abstracts in this category.

20 SPACECRAFT PROPULSION AND POWER

Includes main propulsion systems and components, e.g., rocket engines; and spacecraft auxilliary power sources.

For related information see also *07 Aircraft Propulsion and Power, 28 Propellants and Fuels, 44 Energy Production and Conversion,* and *15 Launch Vehicles and Space Vehicles.*

N90-15130*# National Aeronautics and Space Administration. Lewis Research Center, Cleveland, OH.
EXTENDED TEMPERATURE RANGE ROCKET INJECTOR Patent Application
Steven J. Schneider, inventor (to NASA) 30 Nov. 1989 9 p
(NASA-Case-LEW-14846-1; NAS 1.71:LEW-14846-1; US-Patent-Appl-SN-443523) Avail: NTIS HC A02/MF A01 CSCL 21H

A rocket injector is provided with multiple sets of manifolds for supplying propellants to injector elements. Sensors transmit the temperatures of the propellants to a suitable controller which is operably connnected to valves between these manifolds and propellant storage tanks. When cryogenic propellant temperatures are sensed only a portion of the valves are opened to furnish propellants to some of the manifolds. When lower temperatures are sensed additional valves are opened to furnish propellants to more of the manifolds. NASA

N90-15131# Lawrence Livermore National Lab., CA.
A METHODOLOGY FOR EVALUATING HEAVY GAS DISPERSION MODELS Final Report, Nov. 1985 - Feb. 1988
Donald L. Ermak and Michael Merry Jun. 1989 130 p
(Contract W7405-ENG-48; AF Proj. 2103)
(AD-A214009; AFESC/ESL-TR-88-37) Avail: NTIS HC A07/MF A01 CSCL 04/1

The U.S. Air Force uses fuels and other chemicals in their rockets and jet aircraft that are potentially hazardous when emitted to the ambient atmosphere. These chemicals are also stored in tanks and transported within and between USAF installations. Air Force use of dispersion models is primarily concerned with emergency planning for potential accidental releases of toxic and/or combustible gases that could occur during transportation or routine maintenance operations. The development of dependable evaluation techniques and the application of these techniques to verify current Air Force models are essential initial steps in the effort to conduct reliable and meaningful impact studies. A methodology is presented for evaluating the effectiveness of mathematical models in predicting the atmospheric dispersion of heavier-than-air vapor releases. The methodology is based upon ratio comparisons of the model-predicted value to the observed value in field-scale experiments involving continuous releases of denser-than-air gases. Plume characteristics used in the ratio comparisons include maximum concentration, centerline concentration, plume half-width, and plume height, all as a function of downwind distance from the source. Also included in the report is a review of the scientific efforts in the field of atmospheric dispersion model evaluation during the past two decades. GRA

N90-15132# Massachusetts Inst. of Tech., Cambridge. Plasma Fusion Center.
PROPULSION RESEARCH ON THE HYBRID PLUME ROCKET Final Technical Report, 1 Sep. 1988 - 31 Aug. 1989
F. R. Chang-Diaz and T. F. Yang 5 Oct. 1989 61 p
(Grant AF-AFOSR-0190-84; AF Proj. 2308)
(AD-A214420; PFC/RR-89-15; AFOSR-89-1343TR) Avail: NTIS HC A04/MF A01 CSCL 21/2

The construction of a tandem mirror plasma propulsion facility, the numerical modelling of the hybrid plume exhaust, and RF heating of the plasma are discussed. A preliminary experiment of the ICRH (Ion Cyclotron Resonance Heating) heating of plasma ions was performed. For 2.0 KW ECRH (Electron Cyclotron Resonance Heating) power injected into the central cell and 10 KW ICRH power into the end cell, the results obtained from the

probe in the central cell are: n(e) = 2.5 x 10(exp 16)/cu m and T (e) = 80 eV (928,000 K) in the central cell. The estimated values in the end cell are: n(r) = 1.25 x 10(exp 17)/cu m and T(l) = 500 eV (5,797,000 K). The power conversion efficiency was about 80 percent. The results from time dependent 3-D three fluid numerical modeling indicate that a boundary layer can be formed. The formation of this layer is strongly dependent on neutral jet geometry and injection angle. The ICRH heating of plasma was modeled numerically and power absorption efficiency is about 50 percent. Analytical analyses was done on slab geometry. GRA

23 CHEMISTRY AND MATERIALS (GENERAL)

N90-15133# Nevada Univ., Reno.
HIGH TEMPERATURE CHEMISTRY OF AROMATIC HYDROCARBONS Progress Report
L. T. Scott Nov. 1989 2 p
(Contract DE-FG08-88ER-13945)
(DE90-003664; DOE/ER-13945/1) Avail: NTIS HC A02/MF A01

This project focuses on the molecular transformations of aromatic hydrocarbons at high temperatures. Some of the studies make use of readily available compounds; however, others require lengthy organic syntheses. Two studies of each type are summarized herein. DOE

N90-15134# Oklahoma Univ., Norman. Dept. of Botany and Microbiology.
EFFECT OF COMMUNITY STRUCTURE ON THE KINETICS OF ANAEROBIC DEGRADATION OF AROMATIC COMPOUNDS Progress Report, Mar. - Nov. 1989
Michael J. McInerney Nov. 1989 4 p
(Contract DE-FG05-89ER-14003)
(DE90-003666; DOE/ER-14003/1) Avail: NTIS HC A02/MF A01

The kinetics of benzoate degradation by Syntrophus buswellii grown in coculture with Desulfovibrio strain G-11 was determined. At low benzoate concentrations the rate of degradation deviated from that predicted by a first-order decay process and reached a threshold of 2 to 3 microns of benzoate. The S. buswellii was adapted to grow with crotonate and experiments are in progress to isolate this bacterium. An anaerobic bacterium was isolated that catalyzed the cleavage of an aryl ether bond of phenoxyacetate and its chlorinated derivatives forming the respective phenol. The anaerobic fatty acid-degrading bacterium, Syntrophomonas wolfei, catalyzed a rapid formate-bicarbonate exchange reaction and slowly degraded formate. Enzymatic studies showed that the levels of hydrogenase in cell-free extracts of S. wolfei grown in pure culture or in coculture with Methanospirillum hungatei contained very high specific activities of hydrogenase. Formate dehydrogenase activity was present, but the activity was 700 to 900-fold less than hydrogenase activity. The S. wolfei was adapted to grow with mono and di-unsaturated fatty acids 5 to 6 carbons in length. Analysis of the fermentation products showed that part of the substrate was (beta)-oxidized while the remainder was reduced to the corresponding saturated fatty acid. Propionate was produced from a hexadienoate suggesting that another pathway in addition to (beta)-oxidation exists for the degradation of this compound. Labeling studies and analysis of the monomeric composition of poly-beta-hydroxy alkanoate in S. wolfei showed that early in growth PHA was made by the incorporation of an intermediate without cleavage of a C-C bond. Later, PHA was made by a pathway in equilibrium with the acetate pool. DOE

N90-15135# Texas Univ., Austin.
STUDIES OF ORGANO PHOSPHORUS-, NITROGEN-, AND SULFUR-CONTAINING MOLECULES Final Report, 15 Jun. 1986 - 31 Aug. 1989
J. M. White 31 Aug. 1989 5 p
(Contract DAAL03-86-K-0054)
(AD-A213518; ARO-23591.11-CH) Avail: NTIS HC A01/MF A01 CSCL 15/6

This research focused on the surface chemistry of organo phosphorus-, nitrogen-, and sulfur- containing molecules, which have relevance for the Army in the area of hazardous chemical environments. These studies were of a fundamental nature, with efforts to understand the molecular level chemistry occurring on both metal and metal oxide surfaces. In many cases, the surfaces chosen have technical/practical relevance, particularly the metal oxides. Studies were carried out in highly controlled environments where surface composition and structure were controlled and measured. A variety of optical, electron, and mass spectroscopies were employed. GRA

N90-15136# Oak Ridge National Lab., TN. Chemical Technology Div.
DIMENSIONAL ANALYSIS OF CONTINUOUS HIGH-CAPACITY ELECTRODISPERSION OF AQUEOUS BASED LIQUIDS IN AN ORGANIC CONTINUOUS PHASE
Timothy C. Scott 1989 13 p Presented at the 6th Symposium on Separation Science and Technology for Energy Applications, Knoxville, TN, 22-27 Oct. 1989
(Contract DE-AC05-84OR-21400)
(DE90-003714; CONF-891013-9) Avail: NTIS HC A03/MF A01

High-intensity electric fields can be used to disperse aqueous-based solutions in a relatively nonconducting immiscible organic phase. Dimensional analysis of electrical dispersion performance from a single grounded nozzle between two charged electrodes can be characterized in terms of five dimensionless groups: an electrode height; nozzle-electrode distance; a nozzle Reynolds number; an electrical Bond number, which relates electrical to surface forces; and a Taylor number, which relates electrical to viscous forces. Experimental results on the electrodispersion of water in 2-ethyl-1-hexanol indicate that pulsed dc fields can accomplish electrodispersion utilizing a lower rms/voltage than steady dc fields. In addition, the pulsed-field behavior varies with pulse frequency with 200 Hz fields being more effective for higher continuous-phase viscosities while 2000 Hz fields are more effective when the viscosity is lower. A steady dc field displays invariant behavior with changing viscosity. In the case of the 2000 Hz field, the Taylor number remains constant for all cases tested thus indicating that the dispersion behavior is controlled by the dynamic interactions of the forces induced by the transient field with the stability of the liquid stream emanating from the nozzle. DOE

24 COMPOSITE MATERIALS

Includes physical, chemical, and mechanical properties of laminates and other composite materials.

For ceramic materials see *27 Nonmetallic Materials.*

N90-15137 Texas Univ., Austin.
A STUDY OF IMPACT DAMAGE IN COMPOSITE LAMINATES Ph.D. Thesis
Chung-Yue Wang 1989 141 p
Avail: Univ. Microfilms Order No. DA8920862

Damage produced by low velocity impact in a graphite fiber composite plate is analyzed. The distribution of damage produced by impact in each layer of the plate was calculated by employing Di Sciuva's composite laminate theory together with Hashin's failure criterion for fiber reinforced composites. The principle of virtual work was applied in the formulation of the problem. In the analysis the material was regarded as damaged when its designed strength was reduced by the failure of its constituents. The constituent failures consisted of matrix crackings, fiber breakages, and delamination between layers. According to the damage modes, the moduli of materials in the damaged zone were reduced in accordance to the failure criteria. Despite the fact that the stiffness of the entire structure was reduced, the integrity of structure was assumed to be unaffected by the local damage produced by impact.

Only damage produced by low velocity impact was analyzed. The impact velocity was considered to be low when the contact time duration between the impactor and the target plate was long in comparison with the natural period of the target plate so that the effect of wave motions in the plate could be neglected. The dynamic deformation of the target plate was thus represented by the lower vibrational modes of the plate. The deformation of the plate and the corresponding 3-D stress field in all layers of the plate were calculated by employing Di Sciuva's composite laminate plate theory. Dissert. Abstr.

N90-15138 Virginia Univ., Charlottesville.
FATIGUE PROPERTIES OF SiC/Al COMPOSITES Ph.D. Thesis
Jose Pantaleon Gomez, III 1988 152 p
Avail: Univ. Microfilms Order No. DA8913014

Silicon carbide monofilaments, produced by chemical vapor deposition, have several different classifications depending on the surface treatment imparted to the fiber at the final stage of production. The newest of these fibers, designated SCS-8, is produced specifically for aluminum matrix composites in an attempt to improve transverse mechanical properties over the other types. The focus is on the response of SCS-8/6061 Al alloy composites to cyclic loading. Laminates with fibers oriented in the 0, 90, and + or - 45 degree direction were used. Particular emphasis was on elastic modulus changes due to fatigue. Modulus changes could be observed in as few as ten cycles, depending upon stress and laminate orientation. Unnotched specimens were axially loaded in tension-tension (R = 0.1) mode with a sinusoidal waveform at a frequency of 10 Hz. Periodically, cycling was stopped and the specimen elastic modulus determined. Modulus values at N number of cycles, E(sub N), normalized with respect to virgin modulus, E(sub O), were then plotted versus log number of cycles. Conventional fatigue induced fracture behavior was also obtained and reported in the familiar S-N format. Fractographic observation indicates several failure modes: fiber splitting, fiber/matrix debonding, matrix shear failure, interply delaminating, and fiber fracture. Axial tension-tension high cycle fatigue behavior is controlled by the matrix. Low cycle fatigue and static behavior is characterized by progressive failure of the SiC fiber. Modulus change is the result of crack propagation along the fiber-matrix interface. Dissert. Abstr.

N90-15139 California Univ., Berkeley.
THE MECHANICAL BEHAVIOR OF A FIBER-REINFORCED BRITTLE MATRIX COMPOSITE Ph.D. Thesis
Ellice Yeng Luh 1988 119 p
Avail: Univ. Microfilms Order No. DA8916771

The need for materials which can perform in high-temperature, corrosive environments arose with the development of turbine engines. With further progress in the aerospace industry, the available materials were challenged to meet the high demands required for air as well as space vehicles. To meet these demands, many scientists and engineers have turned toward ceramics and ceramic-containing composites in order to fulfill requirements for high strength and toughness at elevated temperatures in corrosive atmospheres. Mechanical properties are examined for a model ceramic-fiber, ceramic-matrix system. An overview of the micromechanics of composite fracture is presented by examining the influence of various parameters on fracture toughness. Included are several approaches to the analysis of fiber bridging as a contribution to composite toughening. Next, an experimental study of fracture trends is conducted by systematically changing interfacial properties by heat treatment. To fully consider toughening contributions made by fiber bridging and pull-out, a statistical analysis of pull-out lengths is incorporated into existing formulations. The effects of heat treatment on interfacial properties are considered photomicrographically to determine physical changes which influence mechanical behavior. The role of subcritical crack growth is examined by cyclic fatigue testing to determine effects in the small crack regime. Finally, conclusions are drawn regarding the role of the fiber-matrix interface in toughness trends and cyclic fatigue behavior. Dissert. Abstr.

N90-15140 California Univ., Berkeley.
CRITICAL AND SUBCRITICAL CRACK-GROWTH BEHAVIOR ALONG TOUGHENED CERAMIC/METAL INFERFACES Ph.D. Thesis
Tae Sung Oh 1988 114 p
Avail: Univ. Microfilms Order No. DA8916822

Toughening of ceramic/metal interfaces through the use of controlled arrays of near-interfacial microcrack-like-voids and interfacial tilts is studied with respect to both critical and subcritical crack growth along glass/copper interfaces. Such near-interfacial microstructures were generated by photolithographic techniques, combined with metal evaporation and diffusion bonding processes, to produce channel- or penny-shaped microcracks, emplaced out-of-plane to the main interfacial crack. Substantial toughening and improved subcritical crack-growth resistance are achieved through the promotion of crack-tip shielding primarily from crack bridging. Plastic void growth within the copper generated bridging ligaments of metal film behind the crack tip; the resulting plastic stretching, and sometimes tearing, of the metal-film ligaments is the dominant toughening mechanism with a small contribution from crack deflection on interfacial tilts. Resistance-curve (R-curve) behavior obtains from the bridging, with interfacial fracture energies rising to an asymptote that varies from 4 to 160 J/m sup 2, compared with inherent fracture energies of approximately 2 J/m sup 2 for plain glass/copper interfaces. Correspondingly, subcritical crack-growth rates with patterned arrays in moist environments are retarded by many orders of magnitude and threshold interfacial fracture energies are enhanced by factor of 6 to 7, compared with those for plain interfaces. Dissert. Abstr.

N90-15141 Stanford Univ., CA.
MECHANICAL BEHAVIOR OF LAMINATED COMPOSITES AT ELEVATED TEMPERATURES Ph.D. Thesis
Sung Kyu Ha 1989 152 p
Avail: Univ. Microfilms Order No. DA8912904

Models are presented for describing the stress-strain relationship of thermoset matrix composites exposed to elevated temperatures. The models describe both elastic and inelastic material behavior. Tests were performed to determine the constants required in the models. The constants for the time independent, nonlinearly elastic stress relationships of Fiberite 976 resin and Fiberite T300/976 graphite epoxy composite were obtained by measuring the tensile, compressive, and shear properties and the Poisson ratios at 75, 250, 300, and 350 F. The constants for the time dependent inelastic stress-strain relationships of fiberite T300/976 composite were determined from data obtained in four point bend tests from 75 to 350 F. Simple expressions are presented for calculating the strengths, initial moduli, and initial Poisson ratios of pure resins and of laminated composites at high temperatures. A procedure is also described which, together with the stress-strain models developed in this study, can be used to calculate the stresses and strains in loaded, high temperature multidirectional laminates. Test data were compared to results calculated by the models, and good agreements were found between the analytical and experimental results. Dissert. Abstr.

N90-15142 California Univ., Berkeley.
AN ANALYSIS OF DRILLING OF COMPOSITE MATERIALS Ph.D. Thesis
Ho-Cheng Hong 1988 148 p
Avail: Univ. Microfilms Order No. DA8916702

Composite materials due to their unique nature, microscopical inhomogeneity, anisotropy, and laminate structure, require a different approach toward machining analysis than that used for metal cutting. In the drilling of composites, interlaminar cracking, or delamination, is the major damage mechanism to be predicted. An analytical model is provided which uses classic plate theory and linear elastic fracture mechanics to predict the critical thrust and cutting force responsible for the onset of the delamination at the exit and entrance respectively. The higher the interlaminar Mode 1 fracture toughness of the modulus of elasticity or the thinner the ply thickness is, the larger the allowable thrust and cutting forces are. A new parameter, k(sub p) the peeling factor,

is defined to show that the model is consistent for different materials (graphite/epoxy and glass/epoxy). Full-scale experiments show satisfactory agreement between the results and the model. Acoustic emission is used to obtain a correlation with delamination energy release rate thereby demonstrating a possible on-line monitoring capability for acoustic emission. A linear relationship between the signal output and the extent of the delamination zone is found from the experiments. Dissert. Abstr.

N90-15143*# National Aeronautics and Space Administration. Lewis Research Center, Cleveland, OH.
EMPIRICAL AND ANALYTICAL DETERMINATION OF THE FRACTURE RESISTANCE OF A TiB2 PARTICLE/SiC MATRIX COMPOSITE
Michael G. Jenkins, Minoru Taya, Albert S. Kobayashi (Washington Univ., Seattle.), and Jonathan A. Salem 1989 7 p Presented at the First International SAMPE Symposium and Exhibition on New Materials and Processes for the Future, Chiba, Japan, 28 Nov. - 1 Dec. 1989
(Contract DE-AC05-84OR-21400)
(NASA-TM-101940; NAS 1.15:101940; DE89-012331; CONF-891116-1) Avail: NTIS HC A02/MF A01 CSCL 11D

The addition of TiB2 particles to an SiC matrix improves machinability and the room temperature fracture resistance of the composite. Empirical tests have revealed, that the fracture resistance of this composite is a function of both loading condition (monotonic or cyclic-type) and temperature (20 to 1400 C) with some dependence on specimen geometry. Both K sub IC and the levels of the flat R-curves decrease with increasing temperature and are dependent on the loading condition. Fractography shows that toughening contributions include particle size effects, micro-cracking at the particle/matrix interface, and crack deflection. Analytical modeling based on the residual stresses within the material due to the thermal mismatch between the particle and matrix materials compares well with the empirical results. DOE

N90-15144# Pacific Northwest Lab., Richland, WA.
EFFECTS OF FILAMENT-MATRIX INTERFACES ON THE MECHANICAL PROPERTIES OF SiC-REINFORCED Si3N4: A REVIEW
C. H. Schilling Sep. 1989 62 p
(Contract DE-AC06-76RL-01830)
(DE90-001863; PNL-7104) Avail: NTIS HC A04/MF A01

The results of a literature review of the effects of filament-matrix interfaces on the mechanical properties of ceramic composites composed of SiC-filament-reinforced Si3N4 are summarized. A general review of the processing and mechanical properties of SiC-filament-reinforced Si3N4 is presented with special emphasis on research pertaining to processing-related effects on filament-matrix interfaces and the resulting effects of these interfaces on fracture behavior. A review of coating techniques for ceramic filaments is also presented, and recommendations are made for future directions in processing SiC-filament-reinforced Si3N4 with mechanical properties that are enhanced by the microstructure of the filament-matrix interface. DOE

N90-15145*# California Univ., Berkeley. Lawrence Berkeley Lab. Materials and Chemical Sciences Div.
ELECTRONIC MATERIALS HIGH-T(SUB c) SUPERCONDUCTIVITY POLYMERS AND COMPOSITES STRUCTURAL MATERIALS SURFACE SCIENCE AND CATALYSTS INDUSTRY PARTICIPATION Annual Report, 1988
1988 190 p Sponsored in part by NASA; Aluminum Co. of America; ARO; Chevron Research Co.; Dow Chemical Co.; Du Pont de Nemours (E. J.) and Co.; EPRI; Ford Motor Co.; Harshaw/Filtrol Partnership; IBM; Lockheed Corp.; LTV Steel; Materials Research Corp.; NADC;
(Contract DE-AC03-76SF-00098)
(NASA-CR-186063; NAS 1.26:186063; DE90-002377; LBL-27657) Avail: NTIS HC A09/MF A02 CSCL 11D

The fifth year of the Center for Advanced Materials was marked primarily by the significant scientific accomplishments of the research programs. The Electronics Materials program continued its work on the growth and characterization of gallium arsenide crystals, and the development of theories to understand the nature and distribution of defects in the crystals. The High Tc Superconductivity Program continued to make significant contributions to the field in theoretical and experimental work on both bulk materials and thin films and devices. The Ceramic Processing group developed a new technique for cladding YBCO superconductors for high current applications in work with the Electric Power Research Institute. The Polymers and Composites program published a number of important studies involving atomistic simulations of polymer surfaces with excellent correlations to experimental results. The new Enzymatic Synthesis of Materials project produced its first fluorinated polymers and successfully began engineering enzymes designed for materials synthesis. The structural Materials Program continued work on novel alloys, development of processing methods for advanced ceramics, and characterization of mechanical properties of these materials, including the newly documented characterization of cyclic fatigue crack propagation behavior in toughened ceramics. Finally, the Surface Science and Catalysis program made significant contributions to the understanding of microporous catalysts and the nature of surface structures and interface compounds. DOE

N90-15146*# Michigan Univ., Ann Arbor. Radiation Lab.
A NEW TECHNIQUE FOR SIMULATING COMPOSITE MATERIAL. TASK 2: ANALYTICAL SOLUTIONS WITH GENERALIZED IMPEDANCE BOUNDARY CONDITIONS (GIBCS) Report, Sep. 1989 - Feb. 1990
M. A. Ricoy and J. L. Volakis Dec. 1989 39 p
(Grant NAG2-541)
(NASA-CR-186249; NAS 1.26:186249; UM-025921-8-T) Avail: NTIS HC A03/MF A01 CSCL 11D

The diffraction problem associated with a multilayer material slab recessed in a perfectly conducting ground plane is formulated and solved via the Generalized Scattering Matrix Formulation (GSMF) in conjunction with the dual integral equation approach. The multilayer slab is replaced by a surface obeying a generalized impedance boundary condition (GIBC) to facilitate the computation of the pertinent Wiener Hopf split functions and their zeros. Both E(sub z) and H(sub z) polarizations are considered and a number of scattering patterns are presented, some of which are compared to exact results available for a homogeneous recessed slab. Author

N90-15147*# National Aeronautics and Space Administration. Lewis Research Center, Cleveland, OH.
IMPROVED PROCESS FOR HIP CANNING OF COMPOSITES Patent Application
John J. Juhas, inventor (to NASA) 9 Nov. 1989 11 p Sponsored by NASA
(NASA-Case-LEW-14990-1-CU; US-Patent-Appl-SN-433863; NAS 1.71:LEW-14990-1-CU) Avail: NTIS HC A03/MF A01 CSCL 11D

A single step is relied on in the canning process for hot isostatic pressing (HIP) metallurgy composites. The composites are made from arc-sprayed and plasma sprayed monotape. The HIP can is of compatible refractory metal and is sealed at high vacuum and temperature. This eliminates outgassing during hot isostatic pressing. NASA

N90-15148*# National Aeronautics and Space Administration. Langley Research Center, Hampton, VA.
NOVEL POLYIMIDE COMPOSITIONS BASED ON 4,4': ISOPHTHALOYLDIPHTHALIC ANAYDRIDE (IDPA) Patent Application
J. Richard Pratt, inventor (to NASA) (PRC Kentron, Inc., Hampton, VA.) and Terry L. SaintClair, inventor (to NASA) 28 Apr. 1989 25 p
(NASA-Case-LAR-14194-1; NAS 1.71:LAR-14194-1; US-Patent-Appl-SN-344877) Avail: NTIS HC A03/MF A01 CSCL 11D

A series of twelve high temperature, high performance polyimide compositions based on 4,4'-isophthaloyl diphthalic anhydride (IDPA)

was prepared and characterized. Tough, film-forming, organic solvent-insoluble polyimides were obtained. Three materials were semicrystalline. Several gave excellent long-term thermooxidative stability by isothermal thermogravimetric analysis (ITGA) at 300 C and 350 C in air when compared to Kapton H film (duPont). One extensively studied material displayed different levels of semicrystallinity over a wide range of final cure time/temperatures. The polyimide from IDPA and 1,3-bis (4-aminophenoxy 4'-benzoyl) benzene exhibited multiple crystallization and melting behavior, implying the existence of two kinetic and two thermodynamic crystallization and melting transitions by differential scanning calorimetry (DSC). NASA

N90-15149# Lawrence Livermore National Lab., CA. Engineering Sciences Div.
COMPOSITE ACTIVITIES AT LAWRENCE LIVERMORE NATIONAL LABORATORY
Scott E. Groves Jul. 1989 7 p Presented at the Joint Operations Weapons Operations Group Conference, Aldermaston, England, 11 Jul. 1989 Submitted for publication
(Contract W-7405-eng-48)
(DE90-002979; UCRL-101381; CONF-8907167-1) Avail: NTIS HC A02/MF A01

At LLNL we have a broad and integrated effort underway to study the behavior of composite materials. We are actively generating material properties for a variety of high performance fibers and resins for use in filament wound structures. We have research programs investigating the three-dimensional failure behavior of these systems, general property evaluations, as well as investigations of the individual behavior of the fibers and resins. We are also investigating the high strain rate properties of some of these materials. We have a complete facility which includes a six-axis filament winding machine, a biaxial test machine for performing tension, torsion, and internal pressurization of composite tubes, 3-D compression fixtures, external ring compression fixtures, rheometer, FTIR, and many other specialized testing fixtures. The focus of this paper will be on the characterization of the three-dimensional failure behavior of the continuous fiber composites utilized at LLNL. DOE

N90-15150# Los Alamos National Lab., NM. Materials Science and Technology Div.
LASER MIXING OF TITANIUM ON SILICON CARBIDE
Thomas R. Jervis, J.-P. Hirvonen, Michael Nastasi, and M. R. Cohen 1989 6 p Presented at the Conference on Beam-Solid Interactions: Physical Phenomena, Boston, MA, 27 Nov. - 2 Dec. 1989 Submitted for publication
(Contracts W-7405-eng-36; DEW-88-24)
(DE90-003216; LA-UR-89-3841; CONF-8911139-1) Avail: NTIS HC A02/MF A01

We have used excimer laser surface processing to melt and mix single Ti layers into the surface of polycrystalline SiC substrates. The mixing of Ti into the surface is very rapid and efficient. Examination of Rutherford backscattering (RBS) data for different mixing conditions shows the formation of a preferred composition at the Ti-substrate interface which propagates from the interface with further mixing. Reconstruction of the RBS spectrum indicates that the composition of the layer is Ti45C37Si18. X ray diffraction demonstrates the formation of Ti silicides and carbides in the surface region. Profiling of C in both mixed and uncoated samples by 5 MeV He+ scattering demonstrates that laser processing of the SiC does not cause major changes in the stoichiometry of the substrate material. DOE

N90-15151# Martin Marietta Space Systems, Inc., Denver, CO.
DAMPING CHARACTERISTICS OF METAL MATRIX COMPOSITES Final Report, 15 Sep. 1985 - 14 May 1989
Suraj P. Rawal, Joseph H. Armstrong, and Mohan S. Misra 25 May 1989 195 p Prepared in cooperation with Texas A and M Univ., College Station and Denver Univ., CO
(Contract N00014-85-C-0857)
(AD-A213712; MCR-89-506) Avail: NTIS HC A09/MF A02 CSCL 11/4

In the present investigation of damping characteristics of metal matrix composites, the objectives were to: (1) Develop an understanding of energy dissipation mechanisms in Gr/Al composites, (2) Characterize fiber/matrix interface structure, (3) Define the role of interfaces in damping, and (4) Identify and evaluate potential high damping metal matrix composite. To accomplish these objectives, initially damping measurement techniques were established to obtain reproducible and reliable test data of Gr/Al composites. These data obtained at different frequency and strain amplitude levels, were analyzed to develop an understanding of damping mechanisms in Gr/Al composites. GRA

N90-15152 ESDU International Ltd., London (England).
TRANSVERSE (THROUGH-THE-THICKNESS) SHEAR STIFFNESSES OF FIBRE REINFORCED COMPOSITE LAMINATED PLATES (COMPUTER PROGRAM)
Dec. 1989 46 p
(ESDU-89013; ISBN-0-85679-684-0; ISSN-0141-4097; ISSN-0958-0360) Avail: ESDU

ESDU 89013 gives a FORTRAN computer program listing to calculate the stiffnesses of laminated plates (or a sandwich panel) from the properties of the layers, with no restriction on the lay-up arrangement. The theory is outlined and assumes that points on a normal to the mid-surface before bending remain in a straight line, although not normal to the mid-surface, after bending. This allows rotation due to shear to be added to rotation due to classical plate bending. Example calculations are included together with graphs showing the effect of lay-up arrangement on the shear stiffnesses. A full description of the input and output of the program is provided, with details of various warning messages that may be generated, and the testing to which the program was subjected is discussed. Values of transverse shear stiffness are important in calculating deflections caused by through-thickness shear stresses, particularly for laminated plates for which the transverse stiffnesses, which depend on the properties of the matrix material bonding the fibers together, are low. The computer program is available on magnetic media as ESDUpac 8913. ESDU

25 INORGANIC AND PHYSICAL CHEMISTRY

Includes chemical analysis, e.g., chromatography; combustion theory; electrochemistry; and photochemistry.

For related information see also *77 Thermodynamics and Statistical Physics.*.

N90-15153*# National Aeronautics and Space Administration. Ames Research Center, Moffett Field, CA.
THE DISSOCIATION ENERGY OF N2
Jan Almloef, Bradley J. DeLeeuw, Peter R. Taylor, Charles W. Bauschlicher, Jr., and Per Siegbahn (Institute for Theoretical Physics, Stockholm, Sweden) 1989 16 p
(Contract NCC2-371; NSF CHE-86-10809)
(NASA-TM-101930; NAS 1.15:101930) Avail: NTIS HC A03/MF A01 CSCL 07D

The requirements for very accurate ab initio quantum chemical prediction of dissociation energies are examined using a detailed investigation of the nitrogen molecule. Although agreement with experiment to within 1 kcal/mol is not achieved even with the most elaborate multireference CI (configuration interaction) wave functions and largest basis sets currently feasible, it is possible to obtain agreement to within about 2 kcal/mol, or 1 percent of the dissociation energy. At this level it is necessary to account for core-valence correlation effects and to include up to h-type functions in the basis. The effect of i-type functions, the use of different reference configuration spaces, and basis set superposition error were also investigated. After discussing these results, the remaining sources of error in our best calculations are examined. Author

N90-15154# Virginia Commonwealth Univ., Richmond.
COMPENSATION FOR PEAK SHIFTS AND VARIABLE BACKGROUND RESPONSES IN FLUORESCENCE SPECTROSCOPY Annual Progress Report No. 2, 1 Oct. 1988 - 1 Oct. 1989
Sarah C. Rutan 1989 4 p
(Contract DE-FG05-88ER-13833)
(DE90-001102; DOE/ER-13833/3) Avail: NTIS HC A01/MF A01

In the past year, we have made significant progress in several areas. Most of our research has focused on improvements in data analysis methodologies for fluorescence spectroscopic detection in thin-layer and high performance liquid chromatographies, although some experiments have extended the applicability of UV-visible detection methods on thin-layer chromatographic plates. One area of research has focused on the development and evaluation of methods for background correction in fluorescence spectroscopy. DOE

N90-15155# Yale Univ., New Haven, CT. Dept. of Mechanical Engineering.
SIMULTANEOUS MULTIPOINT MEASUREMENTS OF DENSITY GRADIENTS AND TEMPERATURE IN A FLAME Final Report, 1 Aug. 1985 - 31 Jul. 1987
Marshall B. Long Sep. 1989 11 p
(Contract DE-FG02-85ER-13427)
(DE90-001719; DOE/ER-13427/2) Avail: NTIS HC A03/MF A01

A summary is given of research directed toward the study of turbulent reacting and nonreacting flows by nonintrusive in situ optical techniques. During the funding period, new diagnostic techniques were developed for the instantaneous mapping of species concentration and temperature in turbulent flames in two and three dimensions. A number of different light scattering mechanisms were utilized including Rayleigh scattering, spontaneous Raman scattering, and fluorescence. Simultaneous measurements of multiple scalars were demonstrated and a method for determining all three components of the scalar gradient was developed. Using advances in high-speed imaging systems, two-dimensional measurements of gas-phase flows were performed at rates high enough to follow their temporal evolution. The data provided by these techniques will be useful for understanding the interaction of turbulence and chemistry in turbulent flames. DOE

N90-15156# California Univ., Berkeley. Lawrence Berkeley Lab. Combustion Group.
A TOMOGRAPHIC STUDY OF PREMIXED TURBULENT STAGNATION POINT FLAMES
I. G. Shepherd, R. K. Cheng, and P. Goix (California Univ., Berkeley.) Oct. 1989 11 p Presented at the Western States Section Meeting of the Combustion Institute, Livermore, CA, 23-24 Oct. 1989
(Contract DE-AC03-76SF-00098)
(DE90-002462; LBL-27904; CONF-8910289-2) Avail: NTIS HC A03/MF A01

The high speed tomographic technique was used to study premixed flame propagation in stagnation flow stabilized flames. Studies are performed on CH4/Air and C2H4/Air flames with equivalence ratios ranging from 0.75 to 1.0. The gas velocity at the nozzle exit is 5 m/s, the turbulence intensity is varied from 5 to 7 percent and the turbulence Reynolds number is 70. The light source is a copper vapor laser which produces 20 ns, 5 mJ pulses at a 4 KHz repetition rate. Cylindrical lenses transform the 38 mm circular laser beam to a sheet 50 mm high and 0.6 mm thick. A high speed Fastax camera is used to record the tomographic images. The films are digitized and the flame front extracted from the images by a thresholding technique. A fractal analysis was performed on the flame boundaries in order to characterize the flame geometry and provide an estimate of the flame surface area. The flame area increase was found to give a reasonable estimate of the burning rate when compared with other methods if the effects of flow tube divergence were considered. Characteristic wrinkle sizes were found to be much larger than the length scales of the turbulence in the reactant stream. DOE

N90-15157# Texas Univ., Austin. Center for Studies in Statistical Mechanics.
THE BEHAVIOR OF MATTER UNDER NONEQUILIBRIUM CONDITIONS: FUNDAMENTAL ASPECTS AND APPLICATIONS Progress Report, 15 Apr. 1989 - 14 Apr. 1990
Ilya Prigogine Oct. 1989 5 p
(Contract DE-FG05-88ER-13897)
(DE90-002522; DOE/ER-13897/10) Avail: NTIS HC A01/MF A01

The properties of nonequilibrium systems and the mechanism of self organization are examined. As is well known, the study of self organization began with the investigation of hydrodynamical or chemical instabilities studied from the point of view of macroscopic physics. The main outcome is that nonequilibrium generates spatial correlations of macroscopic physics. The main outcome is that nonequilibrium generates spatial correlations of macroscopic range whose characteristics length is an intrinsic property and whose amplitude is determined by nonequilibrium constraints. A survey of the macroscopic approach to nonequilibrium states is given in the paper Nonequilibrium States and Long Range Correlations in Chemical Dynamics, by G. Nicolis et al. However, over the last few years important progress has been made in the simulation of nonequilibrium situations using mainly molecular dynamics. It appears now that processes corresponding to self organization as well as the appearance of long range correlations can be obtained in this way starting from a program involving Newtonian dynamics (generally the laws of interaction correspond to hard spheres or hard disks). Examples of such types of studies leading to Benard instabilities, to chemical clocks, or to spatial structure formation are given. As a result, self organization are viewed as a direct expression of an appropriate microscopic dynamics. Tnis is the reason why so much work was devoted to the study of large Poincare systems (LPS) involving continuous sets of resonances. These systems were shown to lead, according to the constraints, either to equilibrium situations or to nonequilibrium states involving long range correlations. LPS are discussed in the frame of classical mechanics. DOE

N90-15158# Pacific Northwest Lab., Richland, WA. Chemical Sciences Dept.
CAPILLARY ELECTROPHORESIS IONIZATION-MASS SPECTROMETRY AND TANDEM MASS SPECTROMETRY
Charles G. Edmonds, Joseph A. Loo, Steven M. Fields, Charles J. Barinaga, Harold R. Udseth, and Richard D. Smith Aug. 1989 24 p Presented at the 2nd International Symposium on Mass Spectrometry in the Health and Life Sciences, San Francisco, CA, 27-31 Aug. 1989
(Contract DE-AC06-76RL-01830)
(DE90-002664; PNL-SA-16838; CONF-8908181-1) Avail: NTIS HC A03/MF A01

The combination of capillary electrophoresis, including capillary zone electrophoresis and capillary isotachophoresis, with electrospray ionization mass spectrometry provides a powerful analytical tool for the analysis of proteins and oligopeptides. The electrospray ionization process provides detection limits in the attomole to femtomole range. The multiple charging phenomena observed in the electrospray ionization mass spectra of large biomolecules also has two important advantageous effects. First, the mass range for analysis with conventional quadrupole mass spectrometers is extended by a factor equal to the extent of charging. This provides mass spectrometric resolution and precision of mass measurement equivalent or superior to mass spectrometric methods dedicated to the measurements at high m/z. Secondly, the efficiency of collisionally induced dissociation (for MS/MS) is markedly enhanced. This provides for an important flexibility and advantage in the qualitative investigation of analytes above the range of mass ordinarily accessible for singly charged analyte parent ions. The experimental results described suggest the possible extension of tandem MS techniques for protein analysis. DOE

N90-15159# Allied-Signal Aerospace Co., Kansas City, MO.
HIGH-TEMPERATURE GEL-PERMEATION CHROMATOGRAPHY OF POLY(4-METHYL-1-PENTENE)
Edward N. Fuller and George Edwards, Jr. 1989 15 p Presented at the Waters '89: International GPC Symposium, Newton, MA, 1-4 Oct. 1989
(Contract DE-AC04-76DP-00613)
(DE90-002967; KCP-613-4127; CONF-8908176-1) Avail: NTIS HC A03/MF A01

A high temperature gel-permeation chromatographic (HTGPC) method was developed for molecular weight (MW) characterization of poly (4-methyl 1-pentene) PMP. Like most high MW polyolefins, PMP is difficult to handle because of solubility problems. Techniques for overcoming the solubility problems are discussed. The effects of sample concentration and of extended analysis temperature exposure on the results obtained by HTGPC were investigated. Thermo-oxidative degradation of the polymer could be readily observed despite the addition of an antioxidant and thermal stabilizer to the carrier solvent. The rate of degradation for PMP appeared to be greater than for polypropylene (PP) or for polyethylene (PE) as was expected based on the branched structure of PMP. Efforts to reduce degradation are described. Results for two commercial grades of PMP, one in pellet form for injection molding and another in bar stock form for machining, are presented. Results from two in-house developmental PMP type resins are compared with those from the pellet type. DOE

N90-15160# California Univ., Berkeley. Lawrence Berkeley Lab. Materials and Chemical Sciences Div.
THEORETICAL METHODS FOR THE STUDY OF CHEMICAL DYNAMICS Ph.D. Thesis
Nancy Makri Apr. 1989 189 p
(Contract DE-AC03-76SF-00098)
(DE90-003122; LBL-27938) Avail: NTIS HC A09/MF A01

Theoretical methods are developed for studying the dynamics of chemical reactions. Many chemical processes can be adequately described as a system of one or two reaction coordinates coupled to a bath of harmonic oscillators. Such a formulation of the problem has obvious advantages as it is often possible to integrate out the harmonic bath, thus reducing the many degree of freedom problem to a one- or two-dimensional calculation. A simple semiclassical model for incorporating tunneling effects in classical trajectory simulations is constructed and shown to give excellent results over a variety of conditions. Feynman path integration provides an exact way of calculating quantum, dynamical properties and is in principle applicable to problems of involving many degrees of freedom. However, the standard Monte Carlo methodology which must be used to evaluate the multidimensional integrals that occur, is not directly applicable to the path integral expression for the real time propagator, because the integrand of the latter is highly, oscillatory. A technique which helps circumvent this problem by sampling about the stationary phase points of the integrand is developed and illustrated with several numerical applications. A new effective real time propagator is also constructed, which is localized and devoid of rapid oscillations. Finally, accurate approximations to the short time propagator are derived, which drastically improve the convergence characteristics of path integrals. These techniques are expected to extend the applicability of path integral calculations to more complex chemical problems. DOE

N90-15161*# National Aeronautics and Space Administration. Langley Research Center, Hampton, VA.
IGNITABILITY TEST METHOD AND APPARATUS Patent Application
Laurence J. Bement, inventor (to NASA), James W. Bailey, inventor (to NASA), and Morry L. Schimmel, inventor (to NASA) (Schimmel Co., Saint Louis, MO.) 25 Oct. 1989 26 p
(NASA-Case-LAR-13996-1-SB; NAS 1.71:LAR-13996-1-SB; US-Patent-Appl-SN-426345) Avail: NTIS HC A03/MF A01 CSCL 21B

An apparatus for testing ignitability of an initiator includes a body with a central cavity, initiator holder for holding the initiator over the central cavity of the body, an ignition material holder disposed in the central cavity of the body and a cavity facing the initiator holder which receives a measured quantity of ignition material to be ignited by the initiator and a chamber in communication with the cavity of the ignition material holder and the central cavity of the body. A measuring system for analyzing pressure characteristics is generated by ignition material by the initiator. The measuring system includes at least one transducer coupled to an oscillograph for recording pressure traces generated by ignition. NASA

N90-15162 ESDU International Ltd., London (England).
SUMMARY PHYSICAL DATA TABLES: ALKANES
Jul. 1989 53 p
(ESDU-PD3; ISBN-0-85679-685-9; ISSN-0141-4070) Avail: ESDU

This data item ESDU PD3, an addition to the Physical Data Subseries, gives equations for the variation with temperature of the vapor pressure and, for the liquid along the saturation line, of specific heat capacity, density, dynamic viscosity and thermal conductivity. The equations apply from the melting point to approximately 0.9 of the critical temperature. The coefficients in the equations for each compound were either derived by fitting them to existing ESDU correlations of measurements in the literature drawn from a wide range of sources, or were already derived as part of existing ESDU correlations. The compounds treated are methane, ethane, propane, n- and iso-butane, n- and iso-pentane, n- and iso-hexane, n- and iso-heptane, octane and nonane. The equations are used to derive tabular presentations of the properties of those alkanes at 10 degree intervals both in Celsius and Kelvin temperatures. The coefficients of the equations are tabulated for each compound together with its critical properties, normal boiling and melting points, molecular weight and acentric factor. ESDU

N90-15163# Ballistic Research Labs., Aberdeen Proving Ground, MD.
STEADY FLOW COMBUSTION MODEL FOR SOLID-FUEL RAMJET PROJECTILES
Michael J. Nusca Apr. 1989 53 p
(DA Proj. 1L1-62618-AH-80)
(BRL-TR-2987) Avail: NTIS HC A04/MF A01

The steady flow Navier-Stokes equations are written in stream function vorticity form and solved using a Gauss-Seidel relaxation scheme. A diffusion flame combustion model is formulated and linked to the Navier-Stokes equations by equations for the conservation of chemical species mass and source terms in the energy equation. Since a steady state solution is produced, solid fuel ignition and depletion events are ignored. Radiation effects due to combustion are also neglected. The diffusion flame combustion model assumes a mass controlled reaction between fuel and oxidizer (air). The reaction occurs in one step and is unidirectional. The reaction is diffusion controlled so that the reaction rate is faster than the diffusion rate. An actual value for the reaction rate is not required since a single equation for the conservation of fuel and oxidizer mass is formulated. The model includes the effects of axial rotation of the combustion chamber. A phenomenological turbulence model is used. Computed solid fuel regression rate and thrust for a solid fuel ramjet projectile agree well with experimental data and in-flight observations. Author

N90-15164# Lawrence Livermore National Lab., CA.
SHOCK TUBE IGNITION OF OCTANES
Alexander Burcat (Technion - Israel Inst. of Tech., Haifa.), William J. Pitz, and Charles K. Westbrook 27 Sep. 1989 60 p Presented at the Western States Section Meeting of the Combustion Inst., Livermore, CA, 23-24 Oct. 1989
(Contract W-7405-eng-48)
(DE90-001167; UCRL-102001; CONF-8910289-3) Avail: NTIS HC A04/MF A01

Ignition delay time measurements were carried out behind reflected shock waves for three isomeric forms of octane, including n-octane, 2,2,4-trimethyl pentane (iso-octane), and 2,3,4-trimethyl

pentane, as well as for 1-octane. The initial concentrations of fuel, oxygen, and argon, and the initial post-shock temperature were varied systematically in order to establish the influences of these parameters on the ignition delay time. A detailed chemical kinetic reaction mechanism was then developed to interpret the experimental results. The overall agreement between experimental and computed results was very good, and the model was then used to explain, in detailed kinetic terms, the elementary reaction paths by which each of these fuels ignite and the kinetic differences between these closely related hydrocarbon fuels. DOE

N90-15165# Sandia National Labs., Albuquerque, NM.
EXCITATION LIFETIMES AND EXCITED-STATE FORCES IN CHEMISORBED MOLECULES
D. R. Jennison, A. R. Burns, and E. B. Stechel 1989 6 p Presented at the 4th International Workshop on Desorption Induced by Electronic Transitions, Gloggnitz, Austria, 2-4 Oct. 1989
(Contract DE-AC04-76DP-00789)
(DE90-002578; SAND-89-1118C; CONF-8910276-2) Avail: NTIS HC A02/MF A01

Quantum state populations and yields for the highest probability (neutral desorbate) channels are now available by laser resonance-ionization spectroscopy (RIS) thus providing an unprecedented opportunity for theoretical progress in electron-stimulated desorption (ESD). In previous work, it was reported that a semi-quantitative explanation of the translational and internal energy distributions of NO (excited state) from Pt(111) based on a detailed microscopic model. More importantly, this work suggested several principles which appear general. After summarizing these, threshold data is presented for the stimulated desorption of NO from (NO+O):Pt(111) and for the stimulated dissociation of NO2:Pt(111), observed by the detection of the NO (excited state) product, NO2(excited state) (a) yields NO(g) + O(a). The assigned excitation is reviewed in the NO:Pt(111) case and argue that coadsorbed oxygen greatly increases the excitation lifetime. For NO2, consideration of the photoelectron spectrum, electronic structure, and excitation lifetimes allows us to assign the two dominant dissociation channels to specific one and two hole excitations. While the holes occupy non-bonding molecular orbitals (MOs), charge transfer screening into a strongly antibonding MO was found. This screening, while far from complete, strongly influences the excitation lifetimes and forces, and affects the two channels differently. DOE

N90-15166# Sandia National Labs., Albuquerque, NM. Dept. of Fluid and Thermal Sciences.
COMMENTS ON ER (ELECTRORHEOLOGICAL) FLUID RHEOLOGY
Andrew M. Kraynik 1989 10 p Presented at the 2nd International Conference on Electrorheological Fluids, Raleigh, NC, 7-9 Aug. 1989
(Contract DE-AC04-76DP-00789)
(DE90-002892; SAND-89-2604C; CONF-8908183-1) Avail: NTIS HC A02/MF A01

The label electrorheological (ER) fluid reflects the salient feature of these materials that continues to attract the attention of scientists and technologists alike. This is the ability to induce significant changes in rheology through an applied electric field. This electrically induced transformation of a fluid-like suspension of nonconducting particles and liquid to a solid-like gel with a yield stress and corresponding high viscosity is as useful as it is striking. The ability to characterize and understand this so-called Winslow effect is fundamental to successful applications. The current interest in ER fluid development provides strong motivation to rheologists. Our purpose here is to discuss briefly some principles of rheology that apply to ER fluids; they range from well-established and familiar to somewhat subtle. We will focus on the measurement of viscosity and yield stress. DOE

N90-15167# Purdue Univ., West Lafayette, IN. School of Chemical Engineering.
GAS-LIQUID-LIQUID EQUILIBRIA IN MIXTURES OF WATER, LIGHT GASES, AND HYDROCARBONS Progress Report, 1 Dec. 1988 - 30 Nov. 1989
K. C. Chao 1989 1 p Revised
(Contract DE-FG02-84ER-13288)
(DE90-003180; DOE/ER-13288/5) Avail: NTIS HC A01/MF A01

A simplified augmented BACK equation of state has been developed for the description of gas-liquid-liquid equilibria in mixtures of water, light, gases, and hydrocarbons. The simplification facilitates application of the equation. In the Augmented BACK equation the polar pressure of water is the difference between two long expressions. One of these is the 26-term BACK equation written for the non-polar core of the water molecule, and the other is the Keeman steam table equation containing 55 equation constants. The complexity is compounded when derivation is made of the equation for fugacity, enthalpy and other thermodynamic quantities, leading to working equations that contain more than one hundred terms. The complexity presents a barrier to useful application. The new simplified equation has been extensively tested. Calculations with the augmented BACK equation (before simplification) are described with example mixtures. Included are mixtures of water + light gases, water + hydrocarbons, and polar substances in general. Phase equilibrium, density, and enthalpy are calculated. DOE

N90-15168# Los Alamos National Lab., NM.
ROBOCAL (ROBOTIC CALORIMETRY): AN AUTOMATED NDA (NONDESTRUCTIVE ASSAY) CALORIMETRY AND GAMMA ISOTOPIC SYSTEM
J. R. Hurd, C. A. Bonner, C. A. Ostenak, P. F. Phelan, W. D. Powell, N. L. Sheer, D. N. Schneider, and H. C. Staley 1989 36 p Presented at the Winter Meeting of the American Nuclear Society, San Francisco, CA, 26-30 Nov. 1989
(Contract W-7405-eng-36)
(DE90-003217; LA-UR-89-3837; CONF-891103-48) Avail: NTIS HC A03/MF A01

ROBOCAL, which is presently being developed and tested at Los Alamos National Laboratory, is a full-scale, prototypical robotic system, for remote calorimetric and gamma-ray analysis of special nuclear materials. It integrates a fully automated, multi-drawer, vertical stacker-retriever system for staging unmeasured nuclear materials, and a fully automated gantry robot for computer-based selection and transfer of nuclear materials to calorimetric and gamma-ray measurement stations. Since ROBOCAL is designed for minimal operator intervention, a completely programmed user interface and data-base system are provided to interact with the automated mechanical and assay systems. The assay system is designed to completely integrate calorimetric and gamma-ray data acquisition and to perform state-of-the-art analyses on both homogeneous and heterogeneous distributions of nuclear materials in a wide variety of matrices. DOE

N90-15169# Oak Ridge Gaseous Diffusion Plant, TN. Enrichment Technical Operations Div.
ISOTOPIC SELECTIVITY OF SURFACE DIFFUSION: AN ACTIVATED DIFFUSION MODEL
L. D. Trowbridge Nov. 1989 43 p
(Contract DE-AC05-84OR-21400)
(DE90-003473; K/ETO-4) Avail: NTIS HC A03/MF A01

Gaseous diffusion systems are designed to separate UF6 isotopes by pumping gas through a microporous membrane. A second mode of transport exists in barrier, namely that of surface diffusion. The primary purpose is to illustrate, with a very simple model, the qualitative behavior of surface diffusion in a way intended to retain the physical insight into how this flow will behave, and to show how it might manifest itself when observed in combination with gas-phase flow. The model developed uses general concepts of activated diffusion and the Langmuir adsorption isotherm to examine surface diffusion from the standpoint of

characteristics important to isotope separation, namely the conductivity and isotopic selectivity of surface flow, as a function of temperature, pressure, and adsorption energy. DOE

N90-15170# Pacific Northwest Lab., Richland, WA.
DEVELOPMENT OF A ROBOTICS SYSTEM FOR AUTOMATED CHEMICAL ANALYSIS OF SEDIMENT, SLUDGES, AND SOILS
B. P. McGrail, M. G. Dodson, J. R. Skorpik, D. M. Strachan, and J. J. Barich (Environmental Protection Agency, Seattle, WA.) Nov. 1989 6 p Presented at the Winter Meeting of the American Nuclear Society, San Francisco, CA, 26-30 Nov. 1989
(Contract DE-AC06-76RL-01830)
(DE90-003637; PNL-SA-16112; CONF-891103-58) Avail: NTIS HC A02/MF A01

The introduction of automation technology into the analytical laboratory holds the promise of higher efficiency, improved productivity, and lower costs. However, the conventional laboratory robot widely used today may not offer the work envelope or reliability required in a high workload laboratory performing quality control or environmental analytical services. To address this need, a demonstration workcell was assembled utilizing an industrial-class robotics system to automate a standard EPA acid digestion protocol. With further development of graphical user interfaces and error recovery software, the technology will significantly enhance the ability of laboratories to meet increasingly complex environmental demands. DOE

N90-15171# Argonne National Lab., IL. Materials Science Div.
PROCESSING AND PROPERTIES OF NANOPHASE OXIDES
J. A. Eastman, Y. X. Liao, A. Narayanasamy, and R. W. Siegel 1989 13 p Presented at the Spring Meeting of the Materials Research Society, Symposium L: Processing Science of Advanced Ceramics, San Diego, CA, 27-28 Apr. 1989 Submitted for publication
(Contract W-31-109-eng-38)
(DE90-003826; CONF-890426-32) Avail: NTIS HC A03/MF A01

Nanophase oxides Al2, O3, MgO, ZnO and TiO2 with typical grain sizes in the range 2 to 20 nm, have been synthesized by the condensation of ultrafine particles in a convective inert gas followed by their collection and in-situ consolidation in vacuum at ambient temperature. These new materials, owing to the reduced scale of their grains along with the enhanced cleanliness of their grain boundaries, are found to have significantly improved properties relative to those of their coarser-grained, conventionally-prepared counterparts. Nanophase rutile TiO2 with an initial mean grain diameter of 12 nm, for example, has been found to sinter at 400 to 600 C, lower temperatures than conventional rutile powders, without the need for compacting or sintering aids, while retaining a small grain size. Additionally, the importance of the extremely clean surfaces obtained with the gas condensation method has been demonstrated by comparing the sintering behavior of powders with and without air exposure prior to consolidation. The research completed on the processing and properties of nanophase ceramics is reviewed, and the potential for engineering advanced ceramics using the nanophase processing method is discussed. DOE

N90-15172# Texas Univ., Austin. Dept. of Chemistry.
ELECTROCHEMISTRY IN NEAR-CRITICAL AND SUPERCRITICAL FLUIDS. 8: METHYL VIOLOGEN, DECAMETHYLFERROCENE, Os(bpy)3(SUP 2+) AND FERROCENE IN ACETONITRILE AND THE EFFECT OF PRESSURE ON DIFFUSION COEFFICIENTS UNDER SUPERCRITICAL CONDITIONS
Carlos R. Cabrera and Allen J. Bard 20 Jul. 1989 25 p Submitted for publication
(Contract N00014-84-K-0428)
(AD-A213407; AD-E501157; TR-15) Avail: NTIS HC A03/MF A01 CSCL 07/4

The cyclic voltammetry (CV) of methyl viologen (MV2+), decamethylferrocence (DMFc), Os(bpy)3(2+) (bpy+2,2'-bipyridine) and ferrocene (Fc) was studied at high temperatures and pressures in a small cell (7.5 ml) where the pressure and temperature could be varied independently. While the CV of MV(2+) and OS(bpy)3(3+) remained well-behaved with reversible of quasi-reversible waves only into the near-critical region (up to ca 230 C), Fc and DMFc showed well-defined behavior under supercritical conditions. The diffusion coefficient of ferrocene was measured at a supercritical temperatures (280 C) as a function of pressure, and the experimental results were correlated to values calculated by the Stokes-Einstein relation. GRA

N90-15173# Northwestern Univ., Evanston, IL. Dept. of Mechanical Engineering.
COMBUSTION CHARACTERISTICS OF SPRAYS Final Report, Dec. 1987 - Jan. 1989
Siavashi H. Sohrab Aug. 1989 124 p
(Contract F04611-87-K-0067)
(AD-A213651; AL-TR-89-015) Avail: NTIS HC A06/MF A01 CSCL 21/8

A general description is provided of the results of research studies aimed at providing a basic understanding of turbulent spray combustion. The environment in a liquid rocket engine can lead to complex flow/flame/droplet interactions which can substantially modify the droplet evaporation and combustion processes which can affect the stability characteristics of the rocket engine. The various studies conducted during this research project were: spray combustion in stagnation point flow, thermo-diffusive flame instabilities, the influence of vorticity on flame stability and/or stabilization, non-planar flame configurations. Areas of future research are presented along with a discussion as to how the results of the investigation can be applied to liquid rocket engine combustion. GRA

N90-15174# National Inst. of Standards and Technology, Gaithersburg, MD. Molecular Spectroscopy Div.
THE PRODUCTION AND SPECTROSCOPY OF MOLECULAR IONS ISOLATED IN SOLID NEON
Marilyn E. Jacox and Warren E. Thompson (National Science Foundation, Washington, DC.) 1989 25 p Submitted for publication
(Contract MIPR-117-89)
(AD-A213723; ARO-25664.5-CH) Avail: NTIS HC A03/MF A01 CSCL 20/5

Although the mass spectrometric detection of molecular ions is common place, relatively little is known about their structures and the properties of their chemical bonds. Studies of the vibrational and electronic spectra of these species are exceptionally well suited to obtaining this information. Such studies would have the bonus of providing a basis for the development of nonintrusive, in situ laser probes for molecular ions in the lower ionosphere and in such important chemical reaction systems as those of chemical vapor deposition and microcircuit etching. Because of their great chemical reactivity, it has been difficult to maintain sufficiently high ion concentrations for molecular spectroscopic study. GRA

N90-15175# Duke Univ., Durham, NC.
CHEMISORPTION UNDER STRESS Final Report, 1 May 1987 - 31 Jul. 1989
Mikael Ciftan 10 Oct. 1989 17 p
(Contract DAAL03-87-C-0009)
(AD-A213785; ARO-21178.15-PH) Avail: NTIS HC A03/MF A01 CSCL 07/4

The ultimate solution of the problem of chemisorption under stress was developed. A first principles theory for the calculation of the energy levels of solids as well as of aggregates of atoms that is analytically exact and computationally efficient, giving the energy levels to unperecedented accuracy with a minimum of computational effort; and a first principles microscopic theory of Quantum Optics that gives the real time dynamical evolution of quantum states of individual atoms and shows how collective states develop are discussed. This theory not only reproduces the well known Quantum Optical phenomena for the first time in such detail and from one single theory, but also predicts new bistable states that promise to be technologically very significant. GRA

N90-15176# Ballistic Research Labs., Aberdeen Proving Ground, MD.
CALCULATION OF EINSTEIN A COEFFICIENTS AND OSCILLATOR STRENGTHS FOR THE A(PERTURBED)(2)A(1)-X(PERTURBED)(2)B(1) TRANSITION OF NH(2) Final Report, Oct. 1988 - Apr. 1989
William R. Anderson Sep. 1989 24 p
(AD-A213837; BRL-TR-3032) Avail: NTIS HC A03/MF A01 CSCL 07/4

The NH2 radical plays an important role in the decomposition chemistry of solid propellants, in particular nitramines. Additives which produce large amounts of NH2 are also known to have burn rate acceleration effects on HMX based propellants, probably due to the reduction of NO by NH2. We believe that these or similar additives may also produce important ignition enhancement effects and are planning studies in this area. In order to spectroscopically probe NH2 in these studies, the strength of individual rovibronic transitions in the molecule's best known electronic transition, A 2A(1) to X 2B(1), must be known. Until recently, however, such information was available for only two lines and these were not precisely known. Recently, a method was presented whereby Einstein coefficients and oscillator strengths may be calculated for the individual lines. The calculation is straightforward, but not readily transparent to the uninitiated. We therefore promised in Reference 3 to make this monograph, which provides example calculations, available. Methods of identifying transitions involving perturbed levels, for which the calculation may not work well, are first discussed. Then an example calculation of a radiative lifetime for a vibrational level in the A state and calculation of the Einstein coefficients and oscillator strengths for two rovibrational lines are given. GRA

N90-15177# George Mason Univ., Fairfax, VA.
ANALYSIS AND EVALUATION OF TECHNICAL DATA ON THE PHOTOCHROMIC AND NON-LINEAR OPTICAL PROPERTIES OF MATERIALS. APPENDIX: EYE/SENSOR PROTECTION BY AN OPTICAL FUSE MIRROR AT A FOCAL PLANE: FEASIBILITY ASSESSMENT
Robert F. Cozzens 7 Aug. 1989 9 p
(Contract DAAB07-89-C-F404)
(AD-A214051) Avail: NTIS HC A02/MF A01 CSCL 09/5

A possible approach to protecting eyes and electrooptical sensors is to use a device having a focal plane with an optical switch or optical fuse at or near the focus. The fuse could be manually reset to a fresh undamaged section following its failure. A variety of optical fuse concepts using a focal plane may be envisioned. One such system employs a thin metal reflector at the focal plane which reflects the image to another optic which reimages the light on the eye. The thin reflector is designed to ablate at a threshold below that which is damaging to the eye, dumping the laser energy behind the destroyed mirror. When the threat has subsided, the optical fuse/mirror may be manually repositioned to a fresh reflective surface. In order for a mirror to serve as a suitable optical fuse for eye protection, it must fail at energy densities lower than the damage threshold of the retina. The system descrioed in this report appears to be borderline feasible for the protection of eyes from pulsed laser radiation if an optical system with a focal plane having a gain of ca. 100,000 or greater were acceptable. The proposed concept using a rapidly decomposing polymer or inorganic crystal coating supporting the reflective mirror layer on a substrate should be investigated further with specific materials and their properties included in the analysis. GRA

N90-15178# George Mason Univ., Fairfax, VA.
ANALYSIS AND EVALUATION OF TECHNICAL DATA ON THE PHOTOCHROMIC AND NON-LINEAR OPTICAL PROPERTIES OF MATERIALS Quarterly Technical Report No. 2
Robert F. Cozzens 1 Jun. 1989 23 p
(Contract DAAB07-89-C-F404; ARPA Order 6631)
(AD-A214212) Avail: NTIS HC A02/MF A01 CSCL 07/4

The overall goal to this effort is to evaluate data on materials, especially polymers, that may be useful in the development of optical limiters for the protection of eyes and electro-optic sensors from exposure to damaging levels of laser radiation. A major task is to assist in the development of a predictive capability in assessing the viability of various protective approaches and to determine the theoretical limitations which may exist in the use of organic materials as optical switches and limiters. GRA

N90-15179# Lehigh Univ., Bethlehem, PA.
EXCIMER EMISSION FROM ALKALI DIATOMIC AND ALKALINE-EARTH-NOBLE-GAS MOLECULES Final Report, 1 Sep. 1986 - 31 Aug. 1989
John P. Huennekens Oct. 1989 102 p
(Contract DAAL03-86-K-0161)
(AD-A214246; ARO-24007.8-PH) Avail: NTIS HC A06/MF A01 CSCL 09/3

Experimental studies involving the interaction of high-power lasers with alkali and alkaline-earth atoms and molecules were performed. The motivation was to evaluate proposed methods for using these systems to create tunable coherent light sources in the near-infrared spectral region. In addition, much fundamental information was obtained about these atomic and molecular systems, and on their interactions with light. The work can be divided into three areas: studies of bound-free triplet emission from alkali molecules, studies of wave mixing processes, and experiments on barium-noble-gas mixtures. In addition, several smaller projects were performed in closely related fields. GRA

N90-15180# Sandia National Labs., Albuquerque, NM.
PREPARATION AND PROPERTIES OF ICOSAHEDRAL BORIDES
T. L. Aselage, D. R. Tallant, J. H. Gieske, S. B. VanDeusen, and R. G. Tissot 1989 15 p Presented at the NATO ARW: The Physics and Chemistry of Carbides, Nitrides, and Borides, Manchester, England, 18-22 Sep. 1989
(Contract DE-AC04-76DP-00789)
(DE90-003574; SAND-89-1791C; CONF-8909274-1) Avail: NTIS HC A03/MF A01

The electronic and thermal transport properties of refractory icosahedral boron-rich solids suggest the utilization of these unique solids as high-temperature semiconductors. Such applications will require high quality, well characterized materials. A variety of techniques were used to prepare powders, ceramics, and single crystals of boron carbides and the icosahedral boron pnictides. X ray diffraction, Raman spectroscopy, and ultrasound measurements were used to probe boron carbide sample quality. Each of these measurements supports the structural model of boron carbides developed from analysis of transport data. Initial electrical conductivity (E(sub a) approx = 0.17 eV) is consistent with a bipolaronic hopping mechanism. DOE

N90-15181# Texas A&M Univ., College Station. Dept. of Chemistry.
CORRELATIONS BETWEEN SURFACE STRUCTURE AND CATALYTIC ACTIVITY/SELECTIVITY Progress Report, 1 Sep. 1988 - 30 Sep. 1989
D. W. Goodman Sep. 1989 27 p
(Contract DE-FG05-88ER-13954)
(DE90-003755; DOE/ER-13954/1) Avail: NTIS HC A03/MF A01

The work now underway is directed toward the study of structural effects on catalytic activity and selectivity. For example, one of the projects addresses the effects of the presence of coordinatively unsaturated metal sites present at the reconstructed surface of platinum on the selectivity for ethane in the hydrogenolysis of butane. This work is proceeding toward the goal of generating these special sites using structural promoters on surfaces such as rhodium. Several projects are underway which are examining the novel structure and chemistry of monolayer metal films, particularly regarding their use in delineating structural effects in catalysis. One project is examining the structure and chemisorptive properties of binary overlayers of Cu and Ni on a Mo substrate. DOE

N90-15182# Oak Ridge National Lab., TN. Solid State Div.
ON THE CHOICE OF TRIAL FUNCTION IN THEORETICAL CALCULATIONS OF THE THERMAL CONDUCTIVITY
S. Pettersson Oct. 1989 18 p Presented at the 21st International Thermal Conductivity Conference, Lexington, KY, 15-18 Oct. 1989 Prepared in cooperation with Tennessee Univ., Knoxville, TN
(Contract DE-AC05-84OR-21400)
(DE90-001733; CONF-8910319-1) Avail: NTIS HC A03/MF A01

The dispersion relations for 17 alkali halides are calculated throughout the entire Brillouin zone with a deformation dipole model. The linearized Boltzmann equation, including only three-phonon scattering processes, is solved by a variational method. Several trial functions and linear combinations are tested. Separate trial functions are assumed for the acoustic and optic branches, respectively, which gives an improved estimate of the importance of optic phonons as heat carriers. The amount of heat carried by optic phonons differs greatly among the investigated crystals, from 2 percent up to 34 percent. The introduction of linear combination of trial functions increases the thermal conductivity values by 10 to 300 percent. DOE

N90-15183 ESDU International Ltd., London (England).
THERMAL CONDUCTIVITY OF GASEOUS ALIPHATIC HYDROCARBONS. PART 1: ALKANES
Oct. 1989 58 p
(ESDU-89035-Pt-1; ISBN-0-85679-708-1; ISSN-0141-4062) Avail: ESDU

ESDU 89035 presents the results of correlating experimental data extracted from the literature using a procedure that makes use of the critical temperature and pressure (taken from ESDU 87028) and the specific heat capacity at constant pressure of the ideal gas (taken from values published by Texas A and M University). Close agreement of the data over a wide range of sources and experimental methods was found and allowed results to be extended to cover a temperature range from 0.4 to 1.5 of critical at atmospheric pressures. The correlated data were fitted by a third order polynomial in temperature, the coefficients for which are tabulated for all 23 alkanes treated. The equations are used to compute two tables of thermal conductivity in SI units for each alkane at intervals of either 20 K or 20 C. The sources of the data for each compound are listed. The effect of pressure is discussed in general terms and a source for high pressure data is recommended. ESDU

N90-15184 ESDU International Ltd., London (England).
ORTHOBARIC DENSITIES AND MOLAR VOLUMES OF LIQUIDS: ALCOHOLS
Nov. 1989 70 p
(ESDU-89037; ISBN-0-85679-710-3; ISSN-0141-4062) Avail: ESDU

This data item tabulates density and molar volumes for 31 alcohols (the normal straight-chain, C1 to C6 alcohols and their isomers). The tables are in units of kg/cu m and cu cm/mol respectively at 10 K intervals from near the normal melting point to within a few degrees of the critical point. The data were obtained by fitting an equation to the experimental data for density for each compound taken from a wide range of sources in the literature; values established for the coefficients in the equation for each compound are also tabulated. Estimates of the accuracy of the predictions are included, as is the list of the sources of data actually used for each compound. ESDU

26 METALLIC MATERIALS

Includes physical, chemical, and mechanical properties of metals, e.g., corrosion; and metallurgy.

N90-15185# Advisory Group for Aerospace Research and Development, Neuilly-Sur-Seine (France). Structures and Materials Panel.
NEW LIGHT ALLOYS
Aug. 1989 364 p In ENGLISH and FRENCH Meeting held in Mierlo, Netherlands, 3-5 Oct. 1988
(AGARD-CP-444; ISBN-92-835-0519-0) Copyright Avail: NTIS HC A16/MF A02; Non-NATO Nationals requests available only from AGARD/Scientific Publications Executive

The status of current developments in aluminum-lithium alloys, the characterization of commercially available products, and their likely applications in aircraft structures were reviewed. Also considered were developments in other lightweight metallic materials such as magnesium alloys, aluminum powder metallurgy alloys and aluminum metal matrix composites. For individual titles, see N90-15186 through N90-15209.

N90-15186# Cegedur Pechiney Centre de Recherche et Developpement, Voreppe (France).
Al-Li ALLOY DEVELOPED BY PECHINEY
M. Doudeau, P. Meyer, and D. Constant *In* AGARD, New Light Alloys Aug. 1989 17 p (For primary document see N90-15185 07-26)
Copyright Avail: NTIS HC A16/MF A02; Non-NATO Nationals requests available only from AGARD/Scientific Publications Executive

An up-to-date view of Al-Li development is presented in terms of both properties and production readiness. Successes achieved to date, mostly where damage tolerance and medium strength targets are concerned, will be outlined. Design allowables, properties, and product size capabilities will be presented for some alloy/product form combinations which are close to commercialization. As certification has started on some product forms, the introduction of Al-Li alloys on the aerospace market is under way. Author

N90-15187# Virginia Univ., Charlottesville. School of Engineering and Applied Science.
THE MICROSTRUCTURE AND PROPERTIES OF ALUMINUM-LITHIUM ALLOYS
Edgar A. Starke, Jr. and William E. Quist (Boeing Commercial Airplane Co., Seattle, WA.) *In* AGARD, New Light Alloys Aug. 1989 23 p (For primary document see N90-15185 07-26)
Copyright Avail: NTIS HC A16/MF A02; Non-NATO Nationals requests available only from AGARD/Scientific Publications Executive

The advantage to be gained by weight reduction of aerospace structures have encouraged the aluminum industry to develop a family of aluminum alloys which contain lithium as one of the alloying elements. When alloyed with aluminum, lithium can reduce the density by approximately three percent and increase the elastic modulus by six percent for every weight percent added. A new series of aluminum alloys, typified by 2090, 2091, 8090, and 8091, were developed and are currently being produced in commercial quantities. These alloys have densities between 7 and 10 percent lower than the conventional alloy 7075 with correspondingly higher stiffness. Although a combined set of specific properties of the Al-Li-X alloys often exceeds those of the conventional aluminum materials used in aerospace, these properties seem to be much more sensitive to processing parameters. The strong processing-property relationship is associated with sharp crystallographic textures that are developed during primary processing and very complex precipitate microstructures whose distributions are sensitive to quench rates and degree of deformation prior to aging. The processing-microstructure property relationships of the new Al-Li-X alloys are described and the focus is on strength, ductility, fracture toughness, fatigue and stress corrosion properties. Author

N90-15188# National Aerospace Lab., Emmeloord (Netherlands). Structures and Materials Div.
MECHANICAL PROPERTIES AND FRACTURE TOUGHNESS OF 8090-T651 PLATE AND 2091 AND 8090 SHEET
W. G. J. tHart, L. Schra, D. S. McDarmaid, and M. Peters (Deutsche Forschungs- und Versuchsanstalt fuer Luft- und Raumfahrt, Cologne, Germany, F.R.) *In* AGARD, New Light Alloys Aug. 1989 17 p (For primary document see N90-15185 07-26)

Copyright Avail: NTIS HC A16/MF A02; Non-NATO Nationals requests available only from AGARD/Scientific Publications Executive

The strength and toughness properties of the medium strength Al-Li plate alloy 8090-T651 were determined and compared to those of damage tolerant 2000 series plate alloys. For the LT and TL orientations similar K(sub Ic) values were obtained but 8090-T651 was inferior in terms of short transverse fracture toughness. Tensile tests through-the-thickness and with respect to rolling direction indicated considerable anisotropy. Residual strength tests were performed on center cracked sheet panels of the Al-Li alloys 2091 and 8090 in different tempers and 2024-T3 reference material. Fracture modes and characteristics were analyzed using fractography and resulted in a better understanding of the fracture behavior of the Al-Li alloys. Recrystallized Al-Li sheet in specific tempers achieved plane stress fracture toughness values similar to those of 2024-T3, but at somewhat lower yield strengths. Author

N90-15189# Deutsche Forschungs- und Versuchsanstalt fuer Luft- und Raumfahrt, Cologne (Germany, F.R.). Inst. fuer Werkstoff-Forschung.

FATIGUE PROPERTIES OF Al-Li ALLOYS

M. Peters, K. Welpmann, D. S. McDarmaid, and W. G. J. tHart (National Aerospace Lab., Emmeloord, Netherlands) *In* AGARD, New Light Alloys Aug. 1989 18 p (For primary document see N90-15185 07-26)

Copyright Avail; NTIS HC A16/MF A02; Non-NATO Nationals requests available only from AGARD/Scientific Publications Executive

Results are presented on fatigue properties of Al-Li 8090 plate material generated at DFVLR, NLR and RAE in the frame of a GARTEUR activity on Al-Li alloys. High cycle fatigue results are discussed as well as fatigue crack growth properties. Comparison is made to conventional high strength Al alloys. In most cases the Al-Li alloy showed at least equivalent high cycle fatigue properties and improved resistance to fatigue crack growth, primarily due to crack closure effects. Author

N90-15190# Royal Aerospace Establishment, Farnborough (England). Materials and Structures Dept.

CORROSION AND STRESS CORROSION OF ALUMINIUM-LITHIUM ALLOYS

C. J. E. Smith, J. A. Gray, L. Schra, J. A. M. Boogers, R. Braun, H. Buhl, and G. J. H. Vaessen (Fokker B.V., Schipol-Oost, Netherlands) *In* AGARD, New Light Alloys Aug. 1989 20 p (For primary document see N90-15185 07-26)

Copyright Avail: NTIS HC A16/MF A02; Non-NATO Nationals requests available only from AGARD/Scientific Publications Executive

A program of research to evaluate the corrosion and stress corrosion resistance of experimental, pre-production and production quality aluminum-lithium sheet and plate alloys is described. Accelerated laboratory tests and outdoor trials were used to compare the corrosion behavior of aluminum-lithium alloys with conventional aerospace alloys. Author

N90-15191# Laboratoire Central Aerospatiale, Suresnes Cedex (France). Section Metallurgie.

PROPERTIES OF Al-Li ALLOYS [PROPRIETES DES ALLIAGES AL-LI]

Y. Barbaux *In* AGARD, New Light Alloys Aug. 1989 18 p In FRENCH Sponsored by Service Technique des Programmes Aeronautiques, France (For primary document see N90-15185 07-26)

Copyright Avail: NTIS HC A16/MF A02; Non-NATO Nationals requests available only from AGARD/Scientific Publications Executive

Investigations of commercial aluminum lithium alloys conducted by Aerospatiale in the last five years are summarized. The characterization and application of thin metal sheets of 2091 CPH T8X and 8090C T81, medium-thickness sheets of 2091 T8x51, and structural sections of 8090 and 2091 T8511 are discussed. The eventual application of some of these materials in the A-340 Airbus is also discussed. Transl. by M.G.

N90-15192# Messerschmitt-Boelkow-Blohm G.m.b.H., Bremen (Germany, F.R.). Transport Aircraft Group.

INVESTIGATION ON SHEET MATERIAL OF 8090 AND 2091 ALUMINIUM-LITHIUM ALLOY

W. Zink, J. Weilke, L. Schwarmann, and K. H. Rendigs *In* AGARD, New Light Alloys Aug. 1989 15 p (For primary document see N90-15185 07-26)

Copyright Avail: NTIS HC A16/MF A02; Non-NATO Nationals requests available only from AGARD/Scientific Publications Executive

The new aluminum-lithium alloys offer an attractive alternative of reducing structural weight for civil aircraft components. For fuselage application the damage tolerant version of aluminum-lithium as substitution of 2024 T3 material is of greatest interest. Due to the responsibility of MBB/UT for fuselage structures within the Airbus production sharing investigations on damage tolerant 8090 and 2091 sheet material was carried out a few years ago. The Al-Li alloys 2091 and 8090, developed by Pechiney, Alcoa, and Alcan for 2024 T3 substitution will be presented in view of mechanical properties and damage tolerant behavior with special emphasis placed on the comparison with conventional alloys. Fracture toughness data from R-Curves performed on CCT-specimens as well as crack propagation behavior and fatigue results will be discussed. Finally, a summary will be given on the different corrosion behaviors. Author

N90-15193# Naval Air Development Center, Warminster, PA.

ALUMINUM LITHIUM ALLOYS FOR NAVY AIRCRAFT

E. W. Lee and J. Waldman *In* AGARD, New Light Alloys Aug. 1989 10 p (For primary document see N90-15185 07-26)

Copyright Avail: NTIS HC A16/MF A02; Non-NATO Nationals requests available only from AGARD/Scientific Publications Executive

Ingot metallurgy alloys of aluminum with lithium additions offer large gains in structural efficiency due to reduced density together with increased strength and elastic modulus. Several alloys are now commercially available. The Navy was sponsoring research and development activities in these alloys since the mid-seventies. Current efforts include ongoing multi-laboratory evaluations of aluminum alloys to replace 7075-T6 and 7075-T73. The Navy is also conducting research and development on thermal mechanical processing and superplastic forming on these alloys. Additional testing is being conducted to determine their corrosion resistance in an aircraft carrier environment. Author

N90-15194# Pisa Univ. (Italy). Dept. of Aerospace Engineering.

FATIGUE, FRACTURE MECHANICS AND CORROSION PROPERTIES OF SOME ALUMINIUM-LITHIUM ALLOYS

G. Cavallini, L. Lazzeri, M. Scolaris, F. Boschetti, A. Solina, M. DeSanctis, and G. Zennaro (Divisione Aerea Studi Ricerche e Sperimentazioni, Pratica di Mare, Italy) *In* AGARD, New Light Alloys Aug. 1989 18 p Sponsored in part by Italian National Research Council, Rome (For primary document see N90-15185 07-26)

Copyright Avail: NTIS HC A16/MF A02; Non-NATO Nationals requests available only from AGARD/Scientific Publications Executive

A research program for the evaluation of the main characteristics of the newly developed Al-Li alloys was undertaken under the sponsorship of the Italian National Research Council (CNR). Many Italian aeronautical industries and research institutes take part in this program which comprises a large variety of experimental activities: static tests, fatigue tests, crack propagation tests, fracture toughness, corrosion susceptibility, formability, workability, and other tests. Different producers provided the alloys tested in this program; 2091, 8090 and 2090 alloys were the objects of investigation. Some of the results obtained so far in the CNR program and some results obtained by Aeritalia in its own programs are described. The results are relevant to fatigue

tests carried out both on notched and unnotched specimens, under constant amplitude loading (R=0.1). Fatigue tests, together with structural (TEM) and fractographic (SEM) studies, were performed also for assessing the influence of different ageing on both mechanical properties and failure modes of materials. Crack propagation tests were carried out under both C.A. loading and FALSTAFF sequence and are here presented, together with results from fracture toughness tests. Corrosion properties were assessed by measuring the free corrosion potential according to ASTM G 69 standard method and also in neutral salt solution of Na2SO4 (0.1M). Preliminary results obtained show that Li-containing materials exhibit an intermediate behavior between traditional 2024 and 7075 alloys and that the presence of Li does not influence appreciably the corrosion mechanism. Author

N90-15195# Industrieanlagen-Betriebsgesellschaft m.b.H., Ottobrunn (Germany, F.R.).
FATIGUE AND FRACTURE BEHAVIOUR OF A PM Al-Li ALLOY
Rainer Schaefer and Brigitte Weiss (Wien Univ., Austria) *In* AGARD, New Light Alloys Aug. 1989 13 p Sponsored by BMFT, Fed. Republic of Germany and BMWF, Austria (For primary document see N90-15185 07-26)
Copyright Avail: NTIS HC A16/MF A02; Non-NATO Nationals requests available only from AGARD/Scientific Publications Executive

The fatigue life, fatigue crack growth behavior, and fracture toughness properties of the experimental mechanically alloyed Al-Mg-Li alloy Al 905 XL were investigated. This material was developed, above all, for being fabricated into structural components by forging. HCF as well as LCF data were determined at room temperature and elevated temperature (180 C). Crack growth rates were measured including near threshold behavior. The mean values of fatigue life at room temperature were found to be slightly better than the values of conventional high strength aluminum alloys. Internal defects, however, like inclusions or pores, may reduce fatigue life considerably. At 180 C fatigue strength decreased to approximately 60 percent of room temperature values. Crack propagation was noticeably faster in Al 905 XL than in conventional ingot alloy 7075, for example. Fracture toughness tests finally resulted in rather low K(sub Ic) values compared to conventional Al alloys. Author

N90-15196# Fokker B.V., Schipol-Oost (Netherlands). Material and Fabrication Technology.
FABRICATION OF TEST-ARTICLES FROM Al-Li 2091 FOR FOKKER 100
G. J. H. Vaessen, C. vanTilborgh, and H. W. vanRooijen *In* AGARD, New Light Alloys Aug. 1989 12 p (For primary document see N90-15185 07-26)
Copyright Avail: NTIS HC A16/MF A02; Non-NATO Nationals requests available only from AGARD/Scientific Publications Executive

The technical requirements for introduction of aluminum-lithium alloys in secondary structures of aircraft are formulated. The general corrosion behavior, stress-corrosion properties, and mechanical properties of the alloy 2091-T3 from Cegedur-Pechiney meet these requirements. The successful fabrication of access doors in the underwing fairing of the Fokker 100 is described. The same manufacturing techniques as for 2024 can be used for 2091, i.e., machining, blanking, bending, chemical milling, surface pretreatments, adhesive bonding, solution heat treatment and drop-hammer forming, stretch forming, painting and riveting. Operational in-service trial on Fokker 100 and F28 operated by major airlines as Swissair and Garuda has started. An estimate of the cost-effectiveness of the access doors out of 2091 is given. Author

N90-15197# Avions Marcel Dassault-Breguet Aviation, Saint-Cloud (France).
PUTTING ALLOY 2091 TO WORK [MISE EN OEUVRE DE L'ALLIAGE 2091]
J. Bevalot *In* AGARD, New Light Alloys Aug. 1989 7 p In FRENCH (For primary document see N90-15185 07-26)
Copyright Avail: NTIS HC A16/MF A02; Non-NATO Nationals requests available only from AGARD/Scientific Publications Executive

Assessments leading to the replacement of alloy 2024 T3 with the aluminum-lithium alloy 2091 in aircraft applications are discussed. Formability, metallurgical characteristics, and fatigue properties of alloy 2091 are discussed and compared with those of alloy 2024. Alloy 2091 has very good deformation characteristics allowing the formation of panels in one pass with cold tempering instead of two passes for alloy 2024. The working time with cold tempering is very long with the 2091 alloy -- on the order of three days. In addition, alloy 2091 was found to have very good spot weld properties, good chemical machinability, and the same protection ranges as alloy 2024. Transl. by M.G.

N90-15198# British Aerospace Public Ltd. Co., Bristol (England). Production Development and Methods.
FABRICATION CHARACTERISTICS OF 8090 ALLOY
V. H. Mould *In* AGARD, New Light Alloys Aug. 1989 10 p (For primary document see N90-15185 07-26)
Copyright Avail: NTIS HC A16/MF A02; Non-NATO Nationals requests available only from AGARD/Scientific Publications Executive

Some of the experience gained so far, by a user, during a production process evaluation of 8090 medium strength Al-Li alloy is collated. The four primary production processes, machining, forming, joining, and construction, in this sense finishing, treatments, painting, plating classed as secondary processes are examined. Sufficient work was completed to give confidence in the ability of this material to respond to these four basic processes, and produce a quality article. No fundamental changes will be required of machine tools, cutting tools, plant, or equipment. Some techniques will change from conventional alloy requirements, particularly with forming, where further work is required, as 8090 does not form well in the cold condition. It is concluded that 8090 medium strength Al-Li alloy is becoming available in sufficient quantity and quality to enable design engineers to specify the material for applications that can exploit the proven weight and strength advantages. The final responsibility resting with the manufacturing engineers is to ensure that Al-Li can be utilized as an economic proposition. Author

N90-15199# Superform Metals Ltd., Worcester (England).
SUPERPLASTIC PERFORMANCE AND PROPERTIES OF THE LITAL ALLOYS
R. G. Butler and B. J. Dunwoody *In* AGARD, New Light Alloys Aug. 1989 7 p (For primary document see N90-15185 07-26)
Copyright Avail: NTIS HC A16/MF A02; Non-NATO Nationals requests available only from AGARD/Scientific Publications Executive

The requirements in a superplastic sheet material are either to possess a fine uniform grain size or to be capable of developing such a grain structure during the course of superplastic deformation. The lital alloys processed by the optimum route to produce superplastic grade sheet fall into the latter category. The evolution, superplastic performance, and properties of 8090 SPF produced by a commercial production route are described. The sheet produced by this processing route has good isotropic superplastic properties, the ability to be formed at the solution heat treatment temperature, and low quench sensitivity. Properties determined on components formed with hydrostatic confining pressure are presented. The low flow stress of the material enables cavitation to be controlled during forming by this process. Author

N90-15200# Airbus Industrie, Blagnac (France). Advanced Structures and Materials.
POINT OF VIEW OF A CIVIL AIRCRAFT MANUFACTURER ON Al-Li ALLOY
Johannes Koshorst *In* AGARD, New Light Alloys Aug. 1989 5 p (For primary document see N90-15185 07-26)
Copyright Avail: NTIS HC A16/MF A02; Non-NATO Nationals requests available only from AGARD/Scientific Publications Executive

The process of evaluating a new material for use in a civil transport aircraft is rather complex and long. The introduction of Al-Li appears as being a particular difficult item. Initially developed for application in combat aircraft aiming for high strength properties, a civil transport airplane however requires Al-Li in a damage tolerant version. Equivalence to existing alloys is requested (equal or better) but Al-Li demands a compromise between major properties as strength, damage tolerance and corrosion resistance. Progress in achieving acceptable and harmonized material quality is very slow and time constraints have prevented introduction in a planned way in a number of programs. The question is raised whether a cost effective use of Al-Li can be envisaged over the next years.
Author

N90-15201# Westland Helicopters Ltd., Yeovil (England).
USES AND PROPERTIES OF AI-LI ON THE NEW EH101 HELICOPTER
A. F. Smith *In* AGARD, New Light Alloys Aug. 1989 19 p (For primary document see N90-15185 07-26)
Copyright Avail: NTIS HC A16/MF A02; Non-NATO Nationals requests available only from AGARD/Scientific Publications Executive

The EH101 is a long range, large capacity helicopter developed and built to meet the needs of civil, naval, and utility operations and in which many new aerodynamic, electronic and structural design concepts are successfully combined. In order to effect significant structural weight reductions, extensive use will be made of aluminum-lithium based alloys which are now becoming commercially available. The results of a weight-saving cost analysis favor the use of aluminum-lithium sheet, extruded profiles and forgings on the EH101, while corresponding plate and extruded bar will not be used due to the combined effects of low utilization rate and the inherently higher material cost of aluminum-lithium. Accordingly, greater emphasis is being placed upon the use of die forgings, particularly for the manufacture of components hitherto machined from non-lithium containing aluminum plate. Extensive evaluation programs are currently in progress covering AA 8090 and AA 2091 sheet, together with specific EH101 extruded profiles and forgings also in AA 8090 but with additional studies in alloy AA 8091; comparisons will be made with alloys AA 2014, 2024, 7075 and 7010 where appropriate. Notwithstanding the lower ductilities and anisotropic effects characteristic of aluminum-lithium, the results to date show that direct substitution of current aluminum alloys may be realistically pursued, particularly as superior fatigue properties are indicated in the new materials. The use of aluminum-lithium based alloys on the EH101 are reviewed and the findings of the current studies reported. Author

N90-15202# McDonnell Aircraft Co., Saint Louis, MO. Materials and Process Development Branch.
ALUMINUM-LITHIUM: APPLICATION OF PLATE AND SHEET TO FIGHTER AIRCRAFT
Byron A. Davis *In* AGARD, New Light Alloys Aug. 1989 11 p (For primary document see N90-15185 07-26)
(MCAIR Proj. 7-220)
Copyright Avail: NTIS HC A16/MF A02; Non-NATO Nationals requests available only from AGARD/Scientific Publications Executive

The potential for weight savings resulting from the low density and high stiffness of aluminum-lithium (Al-Li) alloys led to the consideration of Al-Li alloys for use on both new and existing aircraft. The successful fabrication, and flight testing of several demonstration parts on both the F-15 and F/A-18 increased interest in these alloys. In support of these and other applications of Al-Li plate and sheet, the mechanical properties, conventional formability, and superplastic formability of 2090 and 8090 were evaluated. With a few notable exceptions, such as the anisotropy in sheet, these Al-Li alloys were comparable to conventional aluminum alloys. Chemical processing and corrosion resistance of 2090 and 8090 were also investigated and again were found comparable to conventional aluminum. Author

N90-15203# Royal Aerospace Establishment, Farnborough (England). Materials and Structures Dept.
CURRENT STATUS OF THE APPLICATION OF CONVENTIONAL ALUMINIUM-LITHIUM ALLOYS AND THE POTENTIAL FOR FUTURE DEVELOPMENTS
C. J. Peel *In* AGARD, New Light Alloys Aug. 1989 9 p (For primary document see N90-15185 07-26)
Copyright Avail: NTIS HC A16/MF A02; Non-NATO Nationals requests available only from AGARD/Scientific Publications Executive

Commercial aluminum-lithium alloys are now entering service use and, while it cannot be claimed that they are yet fully achieving their maximum potential, it is now appropriate to consider the limitations to their further development and the possibilities for the development of other systems and composites based on light alloys, especially suited for aerospace structures. All the commercial aluminum-lithium alloys presently offered were designed to present a reduction in density and an increase in elastic modulus as their main benefits to the designers contemplating their application. The other important metallurgical properties of the alloys, such as strength and fracture toughness were matched to the performance of existing 2000 and 7000 series alloys. The possibilities for further density reductions and increases in mechanical properties, comparing the potential improvements with those offered by non-metallic composites are considered. Three types of structure are considered generically namely damage tolerant structure, typified by a pressurized fuselage skin, structure limited by inadequate material stiffness in either the case of aeroelastic performance or resistance to buckling and structure limited by currently obtainable strength levels at both ambient and elevated temperatures. It transpires from the following brief analysis that future developments may well have to be optimized against the special requirements of the three simple categories outlined and that the simple principle underlying the development of the conventional aluminum-lithium alloys cannot be extended greatly.
Author

N90-15204# Drexel Univ., Philadelphia, PA. Dept. of Materials Engineering.
HIGH PERFORMANCE POWDER METALLURGY ALUMINUM ALLOYS: AN OVERVIEW
M. J. Koczak and M. K. Premkumar *In* AGARD, New Light Alloys Aug. 1989 18 p Sponsored by Naval Air Development Center, Warminster, PA and AFOSR, Washington, DC (For primary document see N90-15185 07-26)
Copyright Avail: NTIS HC A16/MF A02; Non-NATO Nationals requests available only from AGARD/Scientific Publications Executive

The historic development of aluminum powder metallurgy dates back to the early 1900s with initial flake powder production and has matured to the present day production of viable aerospace alloys. Primary powder production and processing techniques, such as atomization and mechanical alloying are reviewed. Processing-microstructure property relationships in four classes of high performance powder metallurgy (P/M) aluminum alloys are considered. These are high strength alloys (AlZnMgCuCo); high specific modulus alloys (AlLiCu); high temperature alloys (ALFeCo, AlFeNi); mechanically alloyed material (AlMg), and composite alloys. Direct property comparisons with counterpart ingot metallurgy alloys are presented where ever appropriate. Aluminum powder metallurgy alloy development is now at a mature stage of growth where commercial and aerospace application are being sought and developed in competition with traditional aluminum ingot metallurgy, titanium and composite structures. The future growth and development of these alloy systems is vested in reliable economic processing. Author

N90-15205# Calgary Univ. (Alberta). Dept. of Mechanical Engineering.
MICROSTRUCTURE/MECHANICAL PROPERTY RELATIONS IN A MECHANICALLY ALLOYED ALUMINUM
W. J. D. Shaw *In* AGARD, New Light Alloys Aug. 1989 12 p (For primary document see N90-15185 07-26)

Copyright Avail: NTIS HC A16/MF A02; Non-NATO Nationals requests available only from AGARD/Scientific Publications Executive

Mechanically alloyed aluminum has not lived up to its initial expectations and very little progress was made in understanding, controlling, and improving this material over the last decade. The complexities of the reactions that occur in this material are presented in terms of the present state of knowledge. This current understanding is linked to the mechanical properties of the material. It is necessary that an understanding of the mechanisms regarding the role of oxygen and carbon or hydrocarbon in the material be obtained before further development is undertaken. Once an understanding of the inherent reactions taking place in these materials is determined, then major advances in research and development will occur resulting in an unlimited potential of engineered materials. Author

N90-15206# Institut National des Sciences Appliquees de Lyon, Villeurbanne (France).

METAL MATRIX COMPOSITES WITH LONG INORGANIC FIBERS [COMPOSITES A MATRICE METALLIQUE ET A FIBRES LONGUES INORGANIQUES]

P. F. Gobin *In* AGARD, New Light Alloys Aug. 1989 17 p In FRENCH (For primary document see N90-15185 07-26)

Copyright Avail: NTIS HC A16/MF A02; Non-NATO Nationals requests available only from AGARD/Scientific Publications Executive

The general characteristics and problems associated with inorganic-fiber metal-matrix composites are reviewed and recent French investigations related to these materials are summarized. The nature and properties of both metal matrices and reinforcing fibers are discussed along with compatibility factors and fiber-matrix interaction in general. Finally, production methods for this class of composite materials are addressed. Transl. by M.G.

N90-15207# Nottingham Univ. (England). Dept. of Metallurgy and Materials Science.

SHORT FIBRE AND PARTICULATE REINFORCED METAL MATRIX COMPOSITES

S. J. Harris *In* AGARD, New Light Alloys Aug. 1989 13 p (For primary document see N90-15185 07-26)

Copyright Avail: NTIS HC A16/MF A02; Non-NATO Nationals requests available only from AGARD/Scientific Publications Executive

Short fibers, whiskers, or particles of ceramic materials, e.g., silicon carbide and alumina, when dispersed in a more or less random manner in a metallic matrix can promote increases in stiffness and strength at ambient and elevated temperatures without imposing a weight penalty. The available routes for the fabrication of such composites, e.g., by squeeze casting, spray forming, powder technologies and hot working are considered. Influences of type and amount of reinforcement, matrix alloy selection, and processing route on strength, creep, and fatigue resistance are discussed. Comparisons are made with conventional metals and alloys, and polymers and metals reinforced with continuous fibers. Attention is drawn to the behavior of these materials under compressive loading as well as to their expansion and conductivity. The majority of the matrices considered are aluminum-based. Author

N90-15208# Deutsche Forschungs- und Versuchsanstalt fuer Luft- und Raumfahrt, Cologne (Germany, F.R.). Inst. of Material Science.

METAL MATRIX COMPOSITES: A PROMISING ALTERNATIVE TO CONVENTIONAL ALLOYS

K. Schulte and W. Bunk *In* AGARD, New Light Alloys Aug. 1989 16 p (For primary document see N90-15185 07-26)

Copyright Avail: NTIS HC A16/MF A02; Non-NATO Nationals requests available only from AGARD/Scientific Publications Executive

Conventional metallic materials were tailored in the past close to their ultimate properties. New technological requirements ask for further improved materials. Metal-matrix composites (MMC) promise to reach this goal. MMC can be described as materials whose microstructure comprise a continuous metallic phase (the matrix) into which a second phase is artificially introduced during processing, as reinforcement. Presently the interest in MMC is primarily focused on light alloys reinforced with fibrous or particulate phases to achieve major jumps in selected mechanical properties or thermal stability. This new interest is mainly related to the fact that ceramic based reinforcement constituents became recently available, which are comparatively inexpensive. Al2O3- or SiC-based fibers, whiskers, and particles, but also carbon fibers are used to reinforce aluminum, magnesium, or titanium matrix alloys. Author

N90-15209# Royal Aerospace Establishment, Farnborough (England). Materials and Structures Dept.

MAGNESIUM ALLOY TECHNOLOGY FOR AEROSPACE APPLICATIONS

D. J. Bray *In* AGARD, New Light Alloys Aug. 1989 9 p (For primary document see N90-15185 07-26)

Copyright Avail: NTIS HC A16/MF A02; Non-NATO Nationals requests available only from AGARD/Scientific Publications Executive

Recent developments in magnesium alloy technology for aerospace applications are reviewed. Most of the current requirements are met by cast alloys and two new alloys were introduced; WE54 for high temperature applications up to 300 C, and high purity AZ91 with improved corrosion resistance. Improvements in casting technology permit the manufacture of more complex castings with wall thicknesses as low as 3.5 mm. A new polyimide coating was developed for gearbox casings which resists attack by lubricating oils at temperatures over 200 C. Rapidly solidified magnesium alloys are at an early stage of development, but their potential is illustrated by the improvements in mechanical properties and corrosion resistance which were obtained. The new rapidly solidified alloy EA55RS is reported to have a 0.2 percent proof stress of 435 MPa, a UTS of 472 MPa, 13 percent elongation, and a corrosion rate in salt spray of 8 mils/year. Author

N90-15210 Virginia Univ., Charlottesville.

THE EFFECTS OF Mo2C MORPHOLOGY AND STRAIN DISTRIBUTION ON THE FATIGUE PROPERTIES OF Fe-C-Mo DUAL-PHASE STEELS Ph.D. Thesis

John Henry Beatty 1988 189 p

Avail: Univ. Microfilms Order No. DA8913016

The effects of Mo2C morphology and distribution on the low cycle fatigue and fatigue crack growth behavior of Fe-C-Mo dual-phase steels were studied in two alloys, Fe(0.2)C4Mo and Fe(0.2)C2Mo. The interactions between the carbides and other microstructural components that occur during fatigue were examined. Isothermal transformations produced both a fibrous carbide structure and an interphase needle carbide structure in the 4Mo alloy. Similar heat treatments produced needle interphase carbides in the 2Mo alloy with different carbide sheet spacings. Transmission electron microscopy revealed that the fibrous morphology increased the homogeneity of cyclic deformation in the ferrite. Increased slip localization was seen as the spacings of the needle carbide sheets were increased. Scanning electron microscopy determined that crack initiation occurred at prior austenite grain boundaries in the fibrous microstructure and along intrusions/extrusions in microstructures with interphase needle carbides. Carbide interactions with the stress and strain distribution in the ferrite-martensite dual-phase structure was examined with finite element methods (FEM). Both LCF and FCG loading conditions were considered. The concentration of strain in critical regions of the microstructures, as predicted by the LCF FEM model, agreed well with reductions in LCF life with increasing martensite volume fraction. The observed cyclic hardening/softening behavior can also be explained by the FEB strain distributions, which show that martensite softening can accompany ferrite hardening depending on their relative strengths. The FCG FEM model examined R ratio effects in dual-phase microstructures near threshold growth rates, and gave additional support for an intrinsic R effect in dual-phase materials. Dissert. Abstr.

N90-15211*# National Aeronautics and Space Administration. Lewis Research Center, Cleveland, OH.
SECONDARY ELECTRON EMISSION CHARACTERISTICS OF MOLYBDENUM-MASKED, ION-TEXTURED OFHC COPPER
Arthur N. Curren, Kenneth A. Jensen, and Robert F. Roman Jan. 1990 15 p
(NASA-TP-2967; E-5009; NAS 1.60:2967) Avail: NTIS HC A03/MF A01 CSCL 11F

A method for producing a uniform, highly textured surface on oxygen-free, high conductivity (OFHC) copper by ion bombardment using sputtered molybdenum as a texture-inducing masking film was developed and used to provide samples for study. The purpose was to develop a basically OFHC copper surface having very low secondary electron emission characteristics. Surfaces having low secondary electron emission are a requirement for the electrodes of very high efficiency multistage depressed collectors (MDC's). Such MDC's are used in microwave amplifier traveling wave tubes for space communications and other applications. OFHC copper is the material most commonly used for MDC electrodes because it has high thermal conductivity, it is easy to machine, and its fabrication and brazing procedures are well established. However, its untreated surface displays relatively very high levels of secondary electron emissions. Textured OFHC copper samples were tested for true secondary electron emission and relative reflected primary electron yield at primary electron beam energy levels from 200 to 2000 eV and at direct (0 deg) to oblique (60 deg) beam impingement angles. The test results for three of the samples, each of which was processed in a slightly different way, are compared with each other and with test results for a machined OFHC copper sample. Although the textured samples are not represented here as having been processed optimally, their measured secondary electron emission characteristics are significantly lower than those of the untreated OFHC copper sample over the range of conditions studied. Importantly, the relative reflected primary electron yield of one of the textured samples is conspicuously lower than that of the others. Clearly, with further development, the molybdenum-masked ion-textured OFHC copper surface will be a promising material for high-efficiency MDC electrodes. Author

N90-15212# Oak Ridge National Lab., TN.
MICROSTRUCTURAL EVOLUTION OF MARTENSITIC STEELS DURING FAST NEUTRON IRRADIATION
P. J. Maziasz 1989 6 p Presented at the Winter Meeting of the American Nuclear Society, San Francisco, CA, 26-30 Nov. 1989
(Contract DE-AC05-84OR-21400)
(DE89-016231; CONF-891103-24) Avail: NTIS HC A02/MF A01

Irradiation of martensitic/ferritic steels with fast neutrons (E greater than 0.1 MeV) to displacement damage levels of 30 to 50 dpa at temperatures of 300 to 500 C produces significant changes in the as-tempered microstructure. Dislocation loops and networks can be produced, irradiation-induced precipitates can form, the lath/subgrain boundary structure and the thermal precipitates produced during tempering can become unstable, and if helium is present, bubbles and voids can form. These microstructural changes caused by irradiation can have important effects on the properties of this class of steels for both fast breeder reactor (FBR) and magnetic fusion reactor (MFR) applications. The purpose of this paper is to compare reactor-irradiated and long-term thermally aged 9Cr--1MoVNb specimens, in order to distinguish effects due to displacement damage from those caused by elevated-temperature exposure alone. DOE

N90-15213# Tennessee Univ., Knoxville. Dept. of Physics.
MAGNETIC BEHAVIOR OF CURIUM AND AMERICIUM-CURIUM ALLOYS
S. E. Nave, R. G. Haire, and J. R. Moore (Oak Ridge National Lab., TN.) Sep. 1989 3 p Presented at Actinides '89, Tashkent, USSR, 24-29 Sep. 1989
(Contract DE-FG05-88ER-13834)
(DE89-017808; DOE/ER-13834/8; CONF-8909225-1) Avail: NTIS HC A01/MF A01

The magnetic interactions, electronic properties and structures of the transplutonium metals, curium and americium are briefly described. DOE

N90-15214# Brookhaven National Lab., Upton, NY. Dept. of Physics.
EXCHANGE COUPLING IN METALS AS UNDERSTOOD THEN AND NOW
R. E. Watson 1989 18 p Presented at the 34th Conference on Magnetism and Magnetic Materials, Boston, MA, 28 Nov. - 1 Dec. 1989
(Contract DE-AC02-76CH-00016)
(DE90-001271; BNL-43296; CONF-891117-3) Avail: NTIS HC A03/MF A01

The first U.S. magnetism conference occurred in 1952 and featured an invited session on exchange coupling in metals with Zener, Slater, Wohlfarth and Van Vleck speaking. All were concerned with intra- and interatomic exchange with Zener discussing coupling via conduction electron polarization while Wohlfarth and Slater were preoccupied with itinerant ferromagnetism. Van Vleck verbalized the Hubbard Hamiltonian (prior to its derivation). That meeting may be viewed as the ultimate discussion of magnetism prior to modern day computation and many of the ideas expressed there underlie our computational activities today. Solutions of the Hubbard Hamiltonian and electronic structure calculations, as applied to magnetism, come to mind. We will concentrate on the latter here, since solving the Hubbard Hamiltonian will be of great concern elsewhere in this meeting, and we will attempt to juxtapose current findings with some of the thoughts of that pioneering meeting. DOE

N90-15215# Oak Ridge National Lab., TN.
DEFORMATION AND FRACTURE OF LOW ALLOY STEELS AT HIGH TEMPERATURE Final Report, 1 May 1982 - 30 Apr. 1985
Douglas L. Marriott, James F. Stubbins, Frederick A. Leckie, and Barrie Muddle Dec. 1988 118 p
(Contract DE-AC05-84OR-21400)
(DE90-001274; ORNL/Sub-82-22239/01; UILU-ENG-88-4019)
Avail: NTIS HC A09/MF A01

This project formed part of the initiative in the Advanced Research and Technology Development (AR and TD) program to characterize high temperature, time-dependent damage processes in low alloy steels, for use in the construction of a coal-gasification plant. This project was broadly aimed at adding to the knowledge base for this bainitic form of 2.25Cr 1Mo steel, as it related to time-dependent performance at elevated temperature. Its original intention was to obtain information in specific grades of 2.25Cr 1Mo steel, in particular those containing reduced residual elements and microalloyed modifications, which were being considered as candidate materials at the time. This objective was subsequently modified to a more generic study of bainitic steel, using the 2.25Cr 1Mo material as a representative of the class. The main thrust of the project was directed initially at the detrimental effect of cyclic loading on creep resistance and manifesting itself in an apparently severe creep-fatigue interaction. Three subtasks were eventually identified. These are: a study of the evolution of microstructural changes in bainitic materials during steady load creep and under constant amplitude cyclic deformation, investigation of the effect of cyclic softening on the fatigue and creep strength of complex geometries, focusing on circumferentially notched bars, and investigation of the influence of environment as a possible cause of observed fatigue/elevated temperature interaction through its effects on crack initiation and propagation, using EDM notched specimens tested in air and vacuum. Results are discussed. DOE

N90-15216# Oak Ridge National Lab., TN.
A REVIEW OF THE EFFECTS OF MICROALLOYING CONSTITUENTS ON THE FORMATION AND BREAKDOWN OF PROTECTIVE OXIDE SCALES ON HIGH-TEMPERATURE ALLOYS AT TEMPERATURES BELOW 700 C

I. G. Wright and J. A. Colwell (Battelle Columbus Labs., OH.) 15 Sep. 1989 92 p
(Contract DE-AC05-84OR-21400)
(DE90-001277; ORNL/Sub-86-57444/01) Avail: NTIS HC A05/MF A01

In this literature review, the state of understanding the effects of microalloying additions on the behavior of protective oxide scales is examined. Particular emphasis is placed on scale formation and degradation at temperatures in the range 500 to 700 C, and in environments ranging from simple oxidation to those involving complex gas mixtures and mechanical components. DOE

N90-15217# Oak Ridge National Lab., TN.
REPORT OF THE ADVANCED NEUTRON SOURCE (ANS) ALUMINUM CLADDING CORROSION WORKSHOP
G. H. Hanson, G. W. Gibson, J. C. Griess, R. E. Pawel, N. E. Pace, and J. M. Ryskamp (Idaho National Engineering Lab., Idaho Falls.) Feb. 1989 44 p Workshop held in Idaho Falls, ID, 16-17 Nov. 1988
(Contract DE-AC05-84OR-21400)
(DE90-001281; CONF-8811203) Avail: NTIS HC A03/MF A01

The Advanced Neutron Source (ANS) Corrosion Workshop on aluminum cladding corrosion in reactor environments is summarized. The workshop was held to examine the aluminum cladding oxidation studies being conducted in support of the ANS design. This report was written principally to provide a record of the ideas and judgments expressed by the workshop attendees. The ANS operating heat flux is significantly higher than that in existing reactors, and early experiments indicate that there may be an aluminum cladding oxidation problem unique to higher heat fluxes or associated cladding temperatures that, if not solved, may limit the operation of the ANS to unacceptably low power levels. The information presented by each speaker is described along with a compilation of the most significant ideas and recommended research areas. The appendices contain a copy of the workshop agenda and a list of attendees. DOE

N90-15218# Oak Ridge National Lab., TN.
SURFACE MODIFICATION OF METALS BY ION BEAMS
Foreign Trip Report, 24 Aug. - 11 Oct. 1988
C. J. McHargue 20 Oct. 1988 9 p
(Contract DE-AC05-84OR-21400)
(DE90-001285; ORNL/FTR-3096) Avail: NTIS HC A02/MF A01

Structure-Property Relationships in Surface Modified Ceramics were studied. The effects of ion beam treatments in ceramics that arise from the structure and bonding in this class of materials that are different from those in metals and semiconductors were examined. An up-to-date assessment of the status of this research was made, and needs and opportunities for further research were identified. An invited paper, Ion Implanted Ceramics, was presented at the international meeting on Surface Modification of Metals by Ion Beams. Much of the emphasis of this meeting has shifted to ion beam assisted deposition. The visits to the three universities was for the purpose of analyzing data obtained in collaborative research. DOE

N90-15219# Westinghouse Savannah River Co., Aiken, SC.
HELIUM-INDUCED WELD CRACKING IN IRRADIATED 304 STAINLESS STEEL
A. K. Birchenall 1989 27 p Presented at the Metallurgical Society Fall Meeting: Materials Week, Indianapolis, IN, 1-5 Oct. 1989
(Contract DE-AC09-89SR-18035)
(DE90-001312; DP-MS-89-41; CONF-891024-3) Avail: NTIS HC A03/MF A01

Slide notes are presented which were used for presentation to The Metallurgical Society of the American Institute of Mining, Metallurgical and Petroleum Engineers (AIME). This presentation was the second of three consecutive talks contributed by SRL personnel dealing with helium-induced weld cracking. DOE

N90-15220# Lockheed Missiles and Space Co., Palo Alto, CA. Research and Development Div.
NICKEL BERYLLIDES AND THEIR PROPERTIES
T. G. Nieh, J. Wadsworth, and C. T. Liu (Oak Ridge National Lab., TN.) 1989 10 p Presented at the Metallurgical Society Fall Meeting: Materials Week, Indianapolis, IN, 1-5 Oct. 1989
(Contract DE-AC05-84OR-21400)
(DE90-001736; CONF-891024-2) Avail: NTIS HC A02/MF A01

The elastic properties of nickel beryllide were evaluated from room temperature to 1000 C. The room temperature modulus is measured to be 186 GPa which is relatively low by comparison with other B2 aluminides such as NiAl and CoAl. Hardness measurements were carried out on specimens that had compositions over the range from 49 to 54 at. percent Be, using both a Vickers microhardness tester and a nanoindentor. It was found that the hardness of NiBe exhibits a minimum at the equiatomic composition. This behavior is similar to that of aluminides of the same crystal structure, e.g., NiAl and CoAl. The effect of interstitial oxygen on the hardness of NiBe was also studied and the results show that the presence of oxygen in NiBe can cause a significant increase in hardness. It is demonstrated that the hardness increase for the off-stoichiometric compositions is primarily caused by interstitial oxygen and can only be attributed partially to anti-site defects generated in off-stoichiometric compositions. Oxidation properties of both equiatomic NiBe and pure Be were characterized at temperatures ranging from 800 to 1200 C. At temperatures below 1100 C, nickel beryllide formed a thin, protective BeO scale and exhibited excellent oxidation resistance. The good oxidation resistance is believed to be a result of the small lattice mismatch between BeO and NiBe. The effect of oxygen partial pressure on the oxidation of NiBe was also evaluated. DOE

N90-15221# Argonne National Lab., IL. Materials and Components Technology Div.
ACCELERATED AGING EMBRITTLEMENT OF CAST DUPLEX STAINLESS STEEL: ACTIVATION ENERGY FOR EXTRAPOLATION
H. M. Chung and O. K. Chopra May 1989 35 p Presented at the 4th International Symposium on Environmental Degradation of Materials in Nuclear Power Systems: Water Reactors, Jekyll Island, GA, 6-10 Aug. 1989 Sponsored in part by Nuclear Regulatory Commission
(Contract W-31-109-eng-38)
(DE90-001773; CONF-890820-5) Avail: NTIS HC A03/MF A01

Cast duplex stainless steels, used extensively in Light Water Reactor systems for primary pressure boundary components such as primary coolant pipes, valves, and pumps, are susceptible to thermal aging embrittlement at reactor operating or higher temperatures. Since a realistic aging embrittlement for end-of-life or life-extension conditions (i.e., 32 to 50 yr of aging at 280 to 320 C) cannot be produced, it is customary to simulate the metallurgical structure by accelerated aging at approx. 400 C. Over the past several years, extensive data on accelerated aging have been reported from a number of laboratories. The most important information from these studies is the activation energy, namely, the temperature dependence of the aging kinetics between 280 and 400 C, which is used to extrapolate the aging characteristics to reactor operating conditions. The activation energies (in the range of 18 to 50 kcal/mole) are, in general, sensitive to material grade, chemical composition, and fabrication process, and a few empirical correlations, obtained as a function of bulk chemical composition, have been reported. Herein, a mechanistic understanding of the activation energy is described on the basis of the results of microstructural characterization of various heats of CF-3, -8, and -8M grades that were used in aging studies at different laboratories. The primary mechanism of aging embrittlement at temperatures between 280 and 400 C is the spinodal decomposition of the ferrite phase, and M23C6 carbide precipitation on the ferrite/austenite boundaries is the secondary mechanism for high carbon CF-8 grade. DOE

N90-15222# California Univ., Berkeley. Lawrence Berkeley Lab. Center for Advanced Materials.
CRYOGENIC MECHANICAL PROPERTIES OF LOW DENSITY SUPERPLASTIC Al-Mg-Sc ALLOYS
S. L. Verzasconi (Aluminum Co. of America, Alcoa Center, PA.) and J. W. Morris, Jr. Jun. 1989 12 p Presented at the International Cryogenic Materials Conference, Los Angeles, CA, 24-28 Jul. 1989
(Contract DE-AC03-76SF-00098)
(DE90-002120; LBL-27381; CONF-890701-13) Avail: NTIS HC A03/MF A01

Spacecraft cryogenic fuel tankage made from superplastic materials is a possible new application for low density aluminum alloys such as Al-Mg-Sc. Examples from this alloy system were examined for cryogenic strength and toughness. Alloys studied were received in the superplastically formable condition, in sheet form. Alloy 2219-T87 sheet was also tested for comparison, since 2219-T8X is currently used in cryogenic tankage. Five compositions of Al-Mg-Sc alloys were tested at 77 and 4 K. Alloys showed the expected increase in strength with decreasing temperature, accompanied by a general slight decrease in elongation and the Kahn tear-yield ratio toughness indicator; however, the strength-tear toughness relationship of this alloy class was as good as or better than that of 2219-T87. Correlations found between the properties, microstructure, and fracture surfaces are discussed. DOE

N90-15223# National Inst. of Standards and Technology, Gaithersburg, MD.
MAGNETIC VISCOSITY IN Ni/Cu COMPOSITIONALLY-MODULATED ALLOYS
L. H. Bennett, L. J. Swartzendruber, H. Ettedgui, U. Atzmony, D. S. Lashmore, and R. E. Watson (Brookhaven National Lab., Upton, NY.) 1989 8 p Presented at the 34th Conference on Magnetism and Magnetic Materials, Boston, MA, 28 Nov. - 1 Dec. 1989
(Contract DE-AC02-76CH-00016)
(DE90-002303; BNL-43108; CONF-891117-6) Avail: NTIS HC A02/MF A01

The existence of a magnetic aftereffect (magnetic viscosity) in Ni/Cu multilayered alloys was established using a vibrating sample magnetometer at room temperature and at 86 K. It was shown that the effect is strongly dependent on the step field, H2 (i.e., the value the field is reduced to after the magnetic moment has been aligned in high field) and exhibits a maximum relaxation rate for values of H2 around the reverse coercive field, -H(sub c). Aftereffect behavior of this type has been observed in other materials, though most often for systems composed of superparamagnetic particles, where the relaxation freezes out at low temperatures. In contrast, the relaxation in the CMA was shown to be enhanced at 86 K over its value at room temperature. New measurements over a wider temperature range show that the enhancement in this sample reaches a maximum near 120 K, but below that temperature the relaxation does freeze out. The temperature of maximum enhancement varies from sample to sample. DOE

N90-15224# Oak Ridge Gaseous Diffusion Plant, TN. Computing and Telecommunication Div.
CALCULATION OF SURFACE HEAT TRANSFER PARAMETERS DURING QUENCHING FROM SURFACE THERMOCOUPLE SIGNALS
J. E. Park and G. M. Ludtka 1989 11 p Presented at the ASME Winter Annual Meeting, San Francisco, CA, 10-15 Dec. 1989
(Contract DE-AC05-84OR-21400)
(DE89-011620; K/CSD/INF-89/5; CONF-891208-3) Avail: NTIS HC A03/MF A01

High peak heat flux values (8 to 9 W/sq mm) of short duration were measured during cold water quenching of a 152.4-mm (6-in.)-dia nickel tube from an initial temperature of 810 C. Temperatures were measured using thermocouples installed on and beneath the outer surface of the cylinder. The transient boiling surface heat flux was calculated from these data using an initial least squares smoothing of the data and an inverse heat transfer technique. The experimental apparatus and technique and the data reduction technique are described. The data are presented, discussed, and compared with previous results from other investigators. The peak heat flux values occurred at a driving temperature difference of about 40 to 90 C. The peak heat flux moves up the cylinder as the cylinder cools. Cooling is controlled by convection currents generated in the quench bath by the buoyant steam and hot water. DOE

N90-15225# International Centre for Theoretical Physics, Trieste (Italy).
ELECTRON THEORY OF LONG WAVELENGTH CONCENTRATION FLUCTUATIONS IN LIQUID METAL ALLOYS
Wang Li and M. P. Tosi (Trieste Univ., Italy) May 1989 8 p Submitted for publication Sponsored in part by Ministero della Pubblica Istruzione and Consiglio Nazionale delle Richerche, Italy
(DE89-636213; IC-89/77) Avail: NTIS (US Sales Only) HC A02/MF A01

Long-wavelength concentration fluctuations in a binary liquid metal alloy are determined by a pair interchange free energy w, which is exactly given by the sum of an elastic strain term and of the concentration-concentration direct correlation function. The latter is evaluated in an alloy of homovalent components by electron screening theory in the pseudopotential approach of Shaw and Harrison and shown to be entirely determined by non-local terms reflecting charge transfer to the more electronegative alloy component. Numerical calculations for the liquid Na-K alloy show strong cancellation between the two contributions to w at all concentrations, in qualitative agreement with experiment. DOE

N90-15226# Oak Ridge National Lab., TN.
AN INVESTIGATION OF THE SENSITIZATION BEHAVIOR OF Fe-Mn-Cr AUSTENITIC STEELS
G. E. C. Bell, P. F. Tortorelli, and E. A. Kenik 1989 11 p Presented at the 4th International Conference on Fusion Reactor Materials, Kyoto, Japan, 4-8 Dec. 1989
(Contract DE-AC05-84OR-21400)
(DE90-002719; CONF-891204-3) Avail: NTIS HC A03/MF A01

Standard chemical immersion (modified Strauss) tests and analytical electron microscopy (AEM) showed that reduced activation austenitic steels based on Fe-20Mn-12Cr-0.25C (wt percent) are extremely prone to thermal sensitization and intergranular corrosion because of their high carbon contents and low chromium concentrations. This susceptibility to sensitization after thermal aging, fabrication, or irradiation makes their use in aqueous and other certain environments problematical. Excellent correlation between intergranular corrosion induced by immersion in the acidified CuSO sub 4 solution and the presence of narrow chromium-depleted zones around grain boundaries, as determined by AEM, was found. Due to the need to meet reduced activation requirements, the opportunities to increase the sensitization of fully austenitic Fe-Mn-Cr steels by alloy design are limited. DOE

N90-15227*# National Aeronautics and Space Administration. Marshall Space Flight Center, Huntsville, AL.
DIRECTIONAL SOLIDIFICATION OF SUPERALLOYS Patent Application
Deborah Diane Schmidt, inventor (to NASA), Wendy Sue Alter, inventor (to NASA), and William David Hamilton, inventor (to NASA) 7 Sep. 1989 13 p
(NASA-Case-MFS-28314-1; NAS 1.71:MFS-28314-1; US-Patent-Appl-SN-404289) Avail: NTIS HC A03/MF A01 CSCL 11F

This invention relates to the directional solidification of superalloys, in particular nickel-based superalloys, by imposition of a predetermined temperature profile in the solidification front and, depending on the desired results, a predetermined rate of advance of said solidification front, whereas castings of markedly superior fatigue resistance are produced. NASA

N90-15228# Sandia National Labs., Albuquerque, NM.
HEAT TREATMENT OF PULSED Nd: YAG LASER WELDS IN A Ti-14.8 WT PCT Al-21.3 WT PCT Nb TITANIUM ALUMINIDE
W. A. Baeslack, III (Ohio State Univ., Columbus.), M. J. Cieslak, and T. J. Headley 1989 6 p Presented at the 2nd International Conference on Trends in Welding Research, Gatlinburg, TN, 14-18 May 1989
(Contract DE-AC04-76DP-00789)
(DE90-003484; SAND-89-1764C; CONF-8905118-13) Avail: NTIS HC A02/MF A01

The influence of postweld heat treatment (PWHT) on the structure, mechanical properties and fracture characteristics of pulsed, Nd: YAG laser welds in a Ti-14.8 wt percent Al-21.3 wt percent Nb titanium aluminide was investigated. Significant microstructure variations within the fusion zone (FZ) of all heat-treated welds were attributed primarily to the influence of local compositional fluctuations on decomposition of the metastable-(beta) microstructure present in the as-welded FZ. An increase in PWHT temperature promoted a decrease in the maximum FZ hardness and an increase in the longitudinal-weld bend ductility. Correspondingly, the proportion of ductile tearing to cleavage fracture within the FZ increased with an increase in PWHT temperature. DOE

N90-15229# Argonne National Lab., IL. Materials Science Div.
DYNAMICAL STRUCTURE OF LIQUID AND AMORPHOUS METALS
David L. Price Aug. 1989 11 p Presented at the 7th International Conference on Liquid and Amorphous Metals, Kyoto, Japan, 4-8 Sep. 1989
(Contract W-31-109-eng-38)
(DE90-003805; CONF-8909267-2) Avail: NTIS HC A03/MF A01

Our current understanding of the dynamics of disordered metals is reviewed, including collective excitations, single-particle motions and diffusive modes. Examples are given for liquid metals, metallic glasses and quasicrystals. DOE

N90-15230# Massachusetts Inst. of Tech., Cambridge. Dept. of Materials Science and Engineering.
THE EFFECT OF NITROGEN AND TITANIUM ON THE TOUGHNESS OF HIGH STRENGTH SAW WELD DEPOSITS M.S. Thesis
Stephen W. Stanko 12 May 1989 158 p Sponsored by ONR, Washington, DC
(AD-A213400; AD-E501157) Avail: NTIS HC A08/MF A01 CSCL 11/6

Nitrogen titanium additions were stiudied during submerged arc welding of HY-100 steel alloy. By comparing the properties of butt-welded HY-100 plate under various levels of nitrogen and titanium contamination, quantitative conclusions about the effects of these elements were achieved. The ultimate goal of this work was to further the development of consumables and procedures for joining high strength steels. In this endeavor, ten butt-welded HY-100 sample plates were produced using the submerged arc welding process. With the exception of incremental increases in the nitrogen and titanium concentrations, the welding parameters were held constant for all the test welds. Evaluating and quantifying these compositional variations required comprehensive metallographic examinations, chemical analyses and mechanical testing. GRA

N90-15231# Massachusetts Inst. of Tech., Cambridge. Dept. of Ocean Engineering.
REDUCTION OF RESIDUAL STRESS AND DISTORTION IN HY100 AND HY130 HIGH STRENGTH STEELS DURING WELDING M.S. Thesis
Richard A. Bass Jun. 1989 250 p
(Contract N00228-89-G-0580)
(AD-A213532) Avail: NTIS HC A11/MF A01 CSCL 11/6

An experimental study was carried out with the specific intention of reducing the undesirable effects of both high residual stresses and distortion in HY100 and HY130 high strength steels during welding. Tests were also conducted on Mild Steel for comparison. The goal of these tests was to first ascertain the distortion and residual stresses during and after welding of test pieces of the three different steels. Test specimens were: 5.5' wide by 18' long and 0.5' thick. A nominal 20 KJ/inch heat input was used in all experiments. Bead on edge was utilized as representative of a butt weld. An automated GMA process was utilized for welding with 98 percent argon and 2 percent oxygen as shielding gas. GRA

N90-15232# Ohio State Univ., Columbus. Dept. of Welding Engineering.
ULTRASONIC EVALUATION OF POROSITY IN ALUMINUM CAST MATERIALS Final Report, Oct. 1985 - Dec. 1987
L. Adler, P. B. Nagy, D. V. Rypien, and J. H. Rose May 1989 84 p
(Contract MIPR-FY1457-89-N-5014; AF Proj. 2418)
(AD-A213548; WRDC-TR-89-4023) Avail: NTIS HC A05/MF A01 CSCL 11/6

A new quantitative ultrasonic method was developed for gas porosity evaluation. The method, which is based on ultrasonic attenuation measurements and spectroscopic analysis of the ultrasonic reflected pulse, is capable of determining gas porosity in the range from 0.1 to 6 percent volume fraction and for pore sizes from 50 to 55 microns. The range is actually defined by the applied ultrasonic frequency which was from 1 to 20 MHz in this work, which can be extended (i.e., for smaller pores) by using high frequencies. This is the range encompassing all premium aluminum casting used in aerospace applications. This method can be used in plate-like geometries with thicknesses up to 3 to 4 inches. The technique can also be automated and controlled by a computer. GRA

N90-15233# Army Lab. Command, Watertown, MA. Material Technology Lab.
ENERGETICS OF BCC-FCC LATTICE DEFORMATION IN IRON Final Report
Genrich L. Krasko and Gregory B. Olson Sep. 1989 15 p
(AD-A213801; MTL-TR-89-86) Avail: NTIS HC A03/MF A01 CSCL 20/5

The BCC-FCC phase transformation in iron lies at the core of the unique properties of iron-based materials. This transformation, being a typical representative of the family of Martensitic Transformations (MT), has been studied for decades. Unlike most of the polymorphic transformations in solids, the MT is a diffusionless process involving a correlated motion of many atoms. One important aspect of such motion is the energetics of large-strain homogeneous lattice deformation. This contributes a local energy density of importance to interfacial energy and mobility, as well as the energetics of potential nonclassical nucleation mechanisms. The homogeneous deformation mechanism allows continuous crystallographic transition from initial to final phase. In the case of the BCC-FCC MT, a few homogeneous strain paths have been suggested. The simplest one, known as the Bain deformation, consists of a continuous expansion of the BCC lattice along one of the cubic axes with a contraction along the two others. Due to its simplicity, the mechanism is a very convenient tool of investigating the energetics of the transformation. GRA

N90-15234# Rensselaer Polytechnic Inst., Troy, NY. Dept. of Materials Engineering.
THE EFFECT OF DISSOLVED CHLORINE ON THE PITTING BEHAVIOR OF 304L STAINLESS STEEL IN A 0.5 N NaCl SOLUTION Technical Report, No. 1, Oct. 1986 - Oct. 1989
H. H. Lu and D. J. Duquette Oct. 1989 40 p
(Contract N00014-89-J-1125)
(AD-A213803) Avail: NTIS HC A03/MF A01 CSCL 11/6

Electrochemical experiments were performed on a 304L stainless steel alloy in a 0.5 N Sodium Chloride solution as a function of chlorine content (0-180 mg/1). Experiments performed included a measurement of the corrosion potential as a function of time, the determination of the breakdown potential, and of the repassivation potential, utilizing cyclic polarization curves; and the

use of a scratching electrode technique to measure the kinetic aspects of the breakdown of passivity. The addition of chlorine to a solution of pH5 in the concentration range of 20 to 60 ppm chlorine resulted in a significant shift in the corrosion potential in the noble direction. At higher concentrations of chlorine the corrosion potential shifts back toward that observed without chlorine additions. Chlorine also results in a monotonic shift in the breakdown potential, suggesting that the passive film is rendered more stable against the initiation of localized corrosion. However, the repassivation potential exhibits a minimum in the chlorine concentration range where the corrosion potential exhibits a maximum. The data suggest that the rate of propagation of localized corrosion should be maximized in this chlorine regime (20 to 60 mg.1). When scratching electrode experiments are performed, the number of pits is minimized but the size of the pits is maximized. GRA

N90-15235# Rensselaer Polytechnic Inst., Troy, NY. Dept. of Materials Engineering.
THE EFFECT OF DISSOLVED OZONE ON THE CORROSION BEHAVIOR OF Cu-30 Ni AND 304L STAINLESS STEEL IN 0.5 N NaCl SOLUTIONS Technical Report, No. 2, Oct. 1986 - Oct. 1989
H. H. Lu and D. J. Duquette Oct. 1989 37 p
(Contract N00014-89-J-1125)
(AD-A213804) Avail: NTIS HC A03/MF A01 CSCL 11/6

Electrochemical experiments on the effect of dissolved ozone on the corrosion behavior of Copper-30 Nickel and 304 L stainless steel have been performed in 0.5 N Sodium chloride solutions at room temperature. The experiments performed included measurements of corrosion potential as a function of time and ozone concentrations, cyclic polarization experiments, iso-potential measurements of current densities and Auger electron spectroscopy studies of the chemical composition of the corrosion product films. The results of these experiments have shown that for both Cu-based alloy and the stainless steel, the corrosion potential exhibits a marked shift to more noble values (approx. 300 mv) for ozone concentrations less the 0.2 - 0.3 mg/l. At higher ozone concentrations the corrosion potential is virtually independent of the level of ozone dissolved in the solution. The presence of dissolved ozone resulted in a reduction in the corrosion rate for the Cu-30 Ni alloy, as measured by a significant decrease in the current density at a constant applied potential. This improvement in the corrosion resistance appears to be related to a reduction in the corrosion product film thickness and a higher fraction of oxygen to chloride in the corrosion product film. For the stainless steel, Auger electron spectroscopy indicated no appreciable differences between the passive film produced in ozonated solutions versus those in unozonated solutions. GRA

N90-15236# United Technologies Research Center, East Hartford, CT.
DISPERSION STRENGTHENING OF HIGH TEMPERATURE NIOBIUM ALLOYS Final Report, May 1986 - Apr. 1989
31 Jul. 1989 89 p
(Contract F49620-86-C-0053)
(AD-A213829; UTRC-R89-917437-3; AFOSR-89-1267TR) Avail: NTIS HC A05/MF A01 CSCL 11/6

Niobium base alloys are very attractive as high temperature materials for advanced gas turbine applications. After many conventional metallurgical approaches, a high temperature creep resistant alloy has yet to be identified which will replace nickel base superalloys. The best chance for obtaining high temperature creep resistance in these alloys is through dispersion strengthening with a stable precipitate that is introduced through rapid solidification. This would result in a very fine dispersion of nonshearable precipitates that would not coarsen upon long term exposure at temperatures in excess of 1200 C. A study was conducted here to identify such a stable dispersion, fabricate alloys through solidification approach and characterize the coarsening of the resulting precipitates. A thermodynamic argument is presented to select candidate dispersions for evaluation. Arc melted and splat quenched alloys were fabricated and evaluated through micro-hardness measurements. An indirect assessment of particle stability is introduced which resulted in a coarsening parameter determined for each candidate precipitate at 1400 C. Microscopic examination of the more stable alloys were made via optical and thin foil TEM analyses. Tensile and strain-rate sensitivity tests were run on these alloys at 1400 C. GRA

N90-15237# Rensselaer Polytechnic Inst., Troy, NY. Dept. of Electrical, Computer, and Systems Engineering.
RESEARCH ON MERCURY CADMIUM TELLURIDE Annual Report, 14 Feb. 1988 - 14 Feb. 1989
Sorab K. Ghandhi 5 Sep. 1989 66 p
(Contract N00014-85-K-0151)
(AD-A213924) Avail: NTIS HC A04/MF A01 CSCL 11/6

Work done during the fourth year is summarized. Conventional growth of this material was achieved with plus or minus 0.001 composition control over a 1 dia., using a rotating susceptor. A computer program was written to evaluate anomalous Hall data. Techniques were developed to achieve full annealing of these layers. Use of a new Te-alkyl has allowed growth of HgCdTe in the 250 to 320 C range. Extrinsic p-doping of HgCdTe was achieved, for the first time, in layers grown by OMVPE. Arsenic was used as the acceptor, and its presence confirmed by SIMS data and by its stability with heat treatment (15 hours at 205 C). GRA

N90-15238# California Univ., Los Angeles. Dept. of Materials Science and Engineering.
SOLID-STATE PHASE EQUILIBRIA IN THE ZnS-Ga2S3 SYSTEM
Jimin M. Zhang, William W. Chen, Alan J. Ardell, and Bruce Dunn
1 Oct. 1989 19 p Submitted for publication
(Contract N00014-87-K-0531)
(AD-A213944; TR-4) Avail: NTIS HC A02/MF A01 CSCL 20/6

ZnS is commercially used as an infrared transmitting material because of its good optical transmission up to 12 microns and adequate mechanical strength. However, ceramics with improved fracture toughness, thermal-shock resistance and erosion resistance are absolutely essential for certain IR-window applications. There are several possible approaches to the engineering of ceramics with this combination of improved mechanical properties while retaining infrared transmittance comparable to that of ZnS. Our approach is to explore the possibilities of strengthening and toughening ZnS by the addition of dispersions of particles of a second-phase, with the dispersoids introduced into the microstructure by the appropriate heat-treatment of densified samples. GRA

N90-15239# Army Lab. Command, Watertown, MA. Material Technology Lab.
HEAT TREATMENT INVESTIGATION OF 4330 VANADIUM-MODIFIED STEEL Final Report
Charles F. Hickey, Jr., David W. Dix, and Mary E. ODonovan
Aug. 1989 17 p
(AD-A214290; MTL-TR-89-84) Avail: NTIS HC A03/MF A01 CSCL 11/6

The shear pin material for the T5106 155-mm torsional impact round was originally specified to have been 4340 steel. It was determined by the authors that the required properties of an ultimate shear strength of 150 ksi and Charpy impact value of 20 ft-lb at 40 F were not obtainable in 4340. The decision to employ 4330 vanadium-modified steel as a substitute shear pin material initiated this heat treatment and mechanical property investigation. The 4340 steel is a low alloy, martensitic, ultrahigh strength steel developed from the modification in composition of 4340 steel. The reduction of the carbon level in this alloy increases its performance, relative to its predecessor in the areas of fracture toughness, weldability, and general fabrication. Mechanical properties were determined from 1/2-in and 5/8-inch-diameter bar stock for austenitizing temperatures of 1500 and 1600 F and tempering temperatures ranging from 375 and 675 F. The material

was evaluated for the specification requirements mentioned above in addition to being tested for hardness, fracture toughness, and tensile properties. GRA

N90-15240# Department of the Navy, Washington, DC.
METAL FILM COATINGS ON AMORPHOUS METALLIC ALLOYS Patent Application
Lawrence T. Kabacoff, inventor (to Navy) 11 Jul. 1989 15 p
(AD-D014308; US-Patent-Appl-SN-377997) Avail: NTIS HC A03/MF A01 CSCL 11/3

Fe-metalloid amorphous metallic alloy ribbons, when properly annealed in a transverse magnetic field, exhibit extremely high magnetomechanical coupling. Other amorphous metallic alloys (or glassy metals) have desirable properties such as high strength, corrosion resistance, high magnetic permeabilities, etc. Coating of crystalline metals (Silver, Gold, Copper, Aluminum) are formed on amorphous metallic alloys (glassy metals) by cathode magnetron sputtering. The process can be used to produce new products such as copper coated amorphous metallic alloy wires for torpedo controls, shielding materials for electromagnetic waves, and anticorrosion coatings for Fe-metalloid magnetostrictive elements. GRA

N90-15241# Argonne National Lab., IL. Materials and Components Technology Div.
CAST STAINLESS STEEL AGING: MECHANISMS AND PREDICTIONS
O. K. Chopra and H. M. Chung Oct. 1989 30 p Presented at the 17th Water Reactor Safety Information Meeting, Rockville, MD, 23-25 Oct. 1989
(Contract W-31-109-eng-38)
(DE90-003772; CONF-8910222-9) Avail: NTIS HC A03/MF A01

Charpy impact and J-R curve data are presented for several experimental and commercial heats, as well as for reactor-aged material of CF-3, CF-8, and CF-8M grades of cast stainless steel. The effects of material variables on the embrittlement of cast stainless steels are evaluated. In general, the low carbon CF-3 grades of cast stainless steels are the most resistance and molybdenum-containing high carbon CF-8M grades are the most susceptible to low temperature embrittlement. The ferrite morphology has a strong effect on the extent or degree of embrittlement, while material composition influences the kinetics of embrittlement. The kinetics of embrittlement can vary significantly with small changes in the constituent elements of the cast material. The mechanisms of embrittlement were also established. Mechanical property data were analyzed to develop the procedure and correlations for predicting the kinetics and extent of embrittlement of reactor components from known material parameters. The method and examples of estimating the impact strength and fracture toughness of cast components during reactor service are described. The lower-bound values of impact strength and fracture toughness for cast stainless steels at LWR operating temperatures are defined. DOE

N90-15242# Argonne National Lab., IL. Chemistry and Materials Science Div.
NEW ORGANIC SYNTHETIC METALS DERIVED FROM BEDT-TTF, Ni(dsit)2 AND BEDO-TTF
Mark A. Beno, Aravinda M. Kini, Urs Geiser, Hau H. Wang, K. Douglas Carlson, and Jack M. Williams 1989 4 p Presented at the 1st ISSP International Symposium on the Physics and Chemistry of Organic Superconductors, Tokyo, Japan, 27-30 Aug. 1989
(Contract W-31-109-eng-38)
(DE90-003793; CONF-8908191-1) Avail: NTIS HC A01/MF A01

Three strategies have been employed by us to synthesize new organic synthetic metals and superconductors. On the basis of structure-property correlations derived for the beta-(BEDT-TTF)2X salts, new charge transfer salts of BEDT-TTF with large, polarizable anions have been synthesized. The occurrence of molecular dimers has been engineered into salts of the new organic acceptor molecule, Ni(dsit)2(bis(4,5 dislenolate-1,3 dithiole-2-thione) nickelate), to synthesize salts with acceptor packing similar to the donor packing in kappa-(BEDT-TTF)2Cu(SCN)2. Finally, two charge transfer salts of bis(ethylenedioxy)tetrathiafulvalene, BEDO-TTF, namely (BEDO-TTF)2AuBr2 and (BEDO-TTF)2AuI2 have been synthesized. The AuBr2- salt, the first BEDO-TTF salt to be structurally characterized, is semiconducting below 263 K, while the AuI2- salt shows metallic conductivity to low temperatures. DOE

N90-15243# Westinghouse Savannah River Co., Aiken, SC. Materials Technology Section.
PROPERTIES OF ALUMINUM-URANIUM ALLOYS
H. B. Peacock and R. L. Frontroth Aug. 1989 71 p
(Contract DE-AC09-89SR-18035)
(DE90-003889; WSRC-RP-89-489) Avail: NTIS HC A04/MF A01

Enriched aluminum-uranium alloys were used for nuclear reactor fuel elements at the Savannah River Site (SRS) for over 30 years. The alloy also was used for fuel in research and test reactors in the international community. Over 200,000 elements were successfully irradiated at SRS without incident. No known accidents related to the fuel have occurred during irradiation with the exception of a few cladding penetrations due to localized corrosion. Aluminum-uranium fuel elements are proposed for the New Production Reactor (NPR). To carry out design and study irradiation behavior, physical, mechanical and chemical properties were obtained from the literature and assembled into a manual so a consistent set of data are available. DOE

N90-15244# Westinghouse Savannah River Co., Aiken, SC. Scientific Computations Section.
INTERACTION OF HYDROGEN IN PALLADIUM AS PRESCRIBED BY THE EMBEDDED ATOM METHOD
Ralph J. Wolf 1989 14 p Presented at the Annual Westinghouse Computer Symposium, Pittsburgh, PA, 6-7 Nov. 1989 Submitted for publication
(Contracts DE-AC09-89SR-18035; DE-AC09-76SR-00001)
(DE90-003893; WSRC-RP-89-476; CONF-891192-24) Avail: NTIS HC A03/MF A01

The embedded atom method (EAM) is a technique developed at Sandia National Laboratories for the construction of many-body potential models for metals. This description provides a computationally efficient method for the calculation of physical properties of materials. Structural properties for the hydrogen/palladium system were studied as a function of H:Pd stoichiometry and compared to first principle electronic structure calculations. The qualitative behavior is visualized using 3D graphics. DOE

N90-15245 ESDU International Ltd., London (England).
GUIDE TO THE SELECTION OF SURFACE TREATMENTS FOR THE IMPROVEMENT OF FATIGUE STRENGTH OF STEELS
Sep. 1989 38 p
(ESDU-89031; ISBN-0-85679-703-0; ISSN-0141-4089) Avail: ESDU

This Data Item ESDU 89031, an addition to the Stress and Strength Subseries, provides comprehensive guidance for the selection of surface treatments that improve the fatigue strength of steels primarily by inducing surface compressive stresses that inhibit the initiation and growth of cracks. Three main groups of treatments are covered, each itself further subdivided. They are mechanical methods of cold working (shot peening, thread and fillet rolling, and pressing for holes), thermal treatments (induction, flame, laser or electron beam hardening) that induce the stresses by surface contraction during transition on quenching from the austenitic to the matensitic state, and thermochemical treatments (carburizing, carbonitriding, nitriding and ferritic nitrocarburizing) that enhance the surface properties and also induce the compressive stresses through the expansion due to chemical change at the surface. Tables summarize the major advantages and limitations of each of the methods, and indicate the potential fatigue strength improvement to be expected. A separate table shows, according

to component, the current treatments usually applied to a wide range of commonly-met parts, such as pistons, shafts, springs, and so on. A systematic procedure for selecting a treatment appropriate to the component is illustrated by a flowchart, although it is recognized that the final decision will be influenced by cost, convenience and availability, as well as the technical issues.
ESDU

27 NONMETALLIC MATERIALS

Includes physical, chemical, and mechanical properties of plastics, elastomers, lubricants, polymers, textiles, adhesives, and ceramic materials.

For composite materials see *24 Composite Materials.*

N90-15246# National Inst. of Standards and Technology, Gaithersburg, MD. Polymers Div.
STUDIES ON SOME FAILURE MODES IN LATEX BARRIER FILMS Final Report, 1 Oct. 1987 - 30 Sep. 1988
Charles M. Guttman, Gregory B. McKenna, Kathleen M. Flynn, and Todd K. Trout Oct. 1988 50 p
(Contract FDA-224-79-5023)
(PB89-209308; NISTIR-89/4084) Avail: NTIS HC A03/MF A01 CSCL 11C

The report covers work on a 1988 contract with the FDA to study failure modes of latex barrier films in their use as condoms or medical gloves. Two areas are reported on: the change in the failure of latex barrier films as a result of swelling in bodily fluid simulants and the cross-link density variation in condoms on the 0.1 mm scale.
Author

N90-15247# Lawrence Livermore National Lab., CA. Chemistry and Materials Science Dept.
MECHANISTIC MODELING OF EPOXY RESINS
Leroy Chiao 16 Jun. 1989 40 p Presented at the 2nd Topical Conference on Emerging Technologies in Materials, San Francisco, CA, 6-9 Nov. 1989
(Contract W-7405-eng-48)
(DE89-015119; UCRL-101108; CONF-891153-1) Avail: NTIS HC A03/MF A01

Epoxy resins are an important class of materials, particularly when used as the matrix for advanced fiber composites. Because material performance is directly related to processing, it is useful to study the cure kinetics of these resins for use in process modeling, design and control. Mechanistic modeling of the cure reactions are shown to offer more flexibility than the empirical rate laws currently used, without being cumbersome or impractical. In this work, amine catalyzed epoxy reactions are studied. A kinetic model is developed, based on an accepted reaction mechanism, and applied to experimental data from the literature. This model is shown to be able to describe the cure of real-world systems, and unlike the empirical rate laws, can account for variations in the resin formulations. Moreover, the mechanistic model, unlike the empirical ones, is capable of estimating the concentrations of linkages formed during the cure reactions. These data offer insight into the cured resin morphology, which determines the chemical and physical properties of the material. A composite cure model is developed using the mechanistic kinetics. Results from the model are compared to experimental data from the literature, and the effects of resin formulation and cure cycle changes are investigated.
DOE

N90-15248# Oak Ridge National Lab., TN.
POTENTIAL APPLICATIONS OF STRUCTURAL CERAMIC COMPOSITES IN GAS TURBINES Final Report
W. P. Parks, Jr., R. R. Ramey, D. C. Rawlins, J. R. Price, and M. vanRoode (Solar Turbines, Inc. San Diego, CA.) Sep. 1989 205 p
(Contract DE-AC05-84OR-21400)
(DE90-001273; ORNL/Sub-88-SA798/01) Avail: NTIS (US Sales Only) HC A10/MF A02

A Babcock and Wilcox-Solar Turbines Team has completed a program assessing the potential for structural ceramic composites in turbines for direct coal-fired or coal gasification environments. A review is made of the existing processes in direct coal firing, pressurized fluid bed combustors, and coal gasification combined cycles. Materials requirements in these areas are also assessed. The program examines the state-of-the-art in ceramic composites materials and the most promising materials for use in coal-fired turbines are identified. These materials are based upon Al2, O3, ZrO2, Si3 N4, SiC, or glass ceramics. Use of ceramic composites could produce performance and efficiency gains within the turbine. Utilization of ceramic composites in the rotor blades and nozzles vanes would provide the most benefit to the turbines. A research program designed to introduce ceramic composite components to these turbines was recommended.
DOE

N90-15249# Oak Ridge National Lab., TN.
CERAMIC POWDER CHARACTERIZATION Foreign Trip Report, 7-14 Oct. 1988
V. J. Tennery 20 Oct. 1988 15 p
(Contract DE-AC05-84OR-21400)
(DE90-001282; ORNL/FTR-3097) Avail: NTIS HC A03/MF A01

The author attended the conference, 2nd International Conference on Ceramic Powder Processing Science, and participated in the Subtask 2 working group meeting on ceramic powder characterization being conducted by the United States, the Federal Republic of Germany (FRG), and Sweden under terms of the Annex 2 agreement. In addition, the author participated in an unscheduled meeting with Dr. R. Neumann, KFA, Juelich, FRG, and Dr. A. Bruechner-Foit, KFK, University of Karlsruhe, FRG, to review major problems encountered in receiving mechanical property data from the FRG under Subtask 4 of the Annex.
DOE

N90-15250# Oak Ridge National Lab., TN.
SURFACE ENGINEERING BY HIGH ENERGY BEAMS Foreign Trip Report, 23 Sep. - 6 Oct. 1989
C. J. McHargue 23 Oct. 1989 11 p
(Contract DE-AC05-84OR-21400)
(DE90-001296; ORNL/FTR-3422) Avail: NTIS HC A03/MF A01

A paper entitled Structure-Mechanical Property relationships in Ion Implanted Ceramics was presented at the 2nd International Seminar on Surface Engineering by High Energy Beams in Lisbon, Portugal. This seminar was sponsored by the International Federation of Heat Treatment and Surface Engineering and included discussions on surface modifications using laser, electron, and ion beams. The visit to the University of Lisbon and LNETI-Sacavem included discussions regarding collaborative research in which Professor J.C. Soares and Dr. M.F. da Silva would conduct perturbed angular correlation studies on ion implanted samples supplied by the traveler. The collaboration between researchers at ORNL and the University Claude Bernard-Lyon 1 (France) continues. Data were analyzed during this visit, plans for further experiments were developed, and a paper was drafted for publication.
DOE

N90-15251# Oak Ridge National Lab., TN. Metals and Ceramics Div.
CERAMIC TECHNOLOGY FOR ADVANCED HEAT ENGINES PROJECT Semiannual Progress Report, Oct. 1988 - Mar. 1989
Aug. 1989 558 p
(Contract DE-AC05-84OR-21400)
(DE90-001852; ORNL/TM-11239) Avail: NTIS HC A23/MF A01

The Ceramic Technology for Advanced Heat Engines Project was developed by the Department of Energy's Office of Transportation Systems (OTS) in Conservation and Renewable Energy. This project, part of the OTS's Advanced Materials Development Program, was developed to meet the ceramic technology requirements of the OTS's automotive technology programs. Significant accomplishments in fabricating ceramic components for the Department of Energy (DOE), National

Aeronautics and Space Administration (NASA), and Department of Defense (DoD) advanced heat engine programs have provided evidence that the operation of ceramic parts in high temperature engine environments is feasible. However, these programs have also demonstrated that additional research is needed in materials and processing development, design methodology, and data base and life prediction before industry will have a sufficient technology base from which to produce reliable cost effective ceramic engine components commercially. DOE

N90-15252# Idaho National Engineering Lab., Idaho Falls.
SUPERCONDUCTING FILM FABRICATION BY THE SOL-GEL PROCESS Final Report, 1 Oct. 1987 - 30 Sep. 1989
J. C. Debsikdar, E. G. Samsel, C. H. Sellers, K. L. Telschow, and D. V. Miley Sep. 1989 42 p
(Contract DE-AC07-76ID-01570)
(DE90-002069; EGG-MS-8696) Avail: NTIS HC A03/MF A01

A sol-gel approach based on polymerization chemistries of alkoxide precursors was used to produce yttrium barium cuprate YBa2Cu3O(7-x) superconducting films. The alkoxide precursors were also synthesized either because they were not commercially available or because the available alkoxides were not suitable for sol-gel synthesis. It was demonstrated that the chemical homogeneity of sol-gel derived YBa2Cu3O(7-x) is superior to that produced by the conventional solid state chemistry approach, even though both powders appeared to be single phase YBa2Cu3O(7-x) by x ray diffraction analysis. Superconducting thin films were fabricated from partially polymerized alkoxide solution on polycrystalline and single crystal substrates. The characteristics of these films were reported. The precursor solution used for thin film fabrication produced a paste-like viscous, stable fluid which could be used as a potential material for fabricating superconducting fiber and/or wire. DOE

N90-15253# Argonne National Lab., IL. Tribology Section.
SOLID LUBRICATION OF CERAMIC SURFACES BY IAD (ION-ASSISTED DEPOSITION)-SILVER COATINGS FOR HEAT ENGINE APPLICATIONS
A. Erdemir, G. R. Fenske, F. A. Nichols, and R. A. Erck 1989 31 p Presented at the Joint American Society of Mechanical Engineers/Society of Tribologists and Lubrication Engineers Tribology Conference, Ft. Lauderdale, FL, 16-19 Oct. 1989
(Contract W-31-109-eng-38)
(DE90-002860; CONF-891036-2) Avail: NTIS HC A03/MF A01

An investigation was made of the tribological characteristics of alumina ceramics coated with silver by means of ion assisted deposition (IAD). Tests were performed at temperatures up to 400 C on an oscillating-slider wear test machine capable of simulating the reciprocating motion of a ring/cylinder system. The results showed that higher test temperatures caused greater wear damage and increased friction for uncoated alumina. At 400 C, the wear rates of the alumina-alumina test pairs were 8 to 10 times higher than those tested at room temperature. The steady state friction coefficients were also fairly high, typically ranging from 0.8 to 1.1. In contrast, the wear rate of IAD silver coated flats was virtually zero and the wear rates of the counterface pins were reduced by a factor of 72. Friction was also reduced to about half to one third of those for the uncoated pairs. Surface and structure analytical investigations together with the hot-hardness testing of substrate alumina at temperatures up to 600 C were performed to ascertain the mechanisms responsible for the friction and wear behavior of both alumina-alumina and alumina-IAD-silver coated alumina pairs. DOE

N90-15254# Oak Ridge National Lab., TN. Engineering Technology Div.
CRACK TIP TOUGHENING BY INCLUSIONS WITH PAIRS OF SHEAR TRANSFORMATIONS
S.-J. Chang and P. F. Becher 1989 35 p Presented at the Winter Annual Meeting of the American Society of Mechanical Engineers, San Francisco, CA, 10-15 Dec. 1989
(Contract DE-AC05-84OR-21400)
(DE89-007845; CONF-891208-1) Avail: NTIS HC A03/MF A01

The deviatoric transformation strain of an inclusion is modeled by applying an equivalent distribution of dislocations along a surface which exhibits a discontinuous change in the transformation strains. This method is applied to qualitatively model the twin structures generated in transformation toughened ceramics. For this case, the transformation shear strain of the inclusion is assumed to consist of a number of symmetrical pairs of (twinning) shears in a rectangular grain. The elastic energy is derived and expressed in terms of elementary functions. With one pair of shears, the inclusion induced toughening effect in the presence of a crack is calculated by applying a recent solution of the crack-dislocation interaction problem. Numerical results show that the toughening due to the inclusion (as compared to that due to dilatation) is not negligible if the inclusion is located within a distance equal to several grain sizes from the crack tip. Moreover, the toughening depends strongly on the orientation of the inclusion relative to the crack. DOE

N90-15255# Sandia National Labs., Albuquerque, NM.
THE ELASTIC PROPERTIES OF WOVEN POLYMERIC FABRIC
William E. Warren 1989 20 p Presented at the Symposium on Mechanics of Plastics and Plastic Composites, San Francisco, CA, 10-15 Dec. 1989
(Contract DE-AC04-76DP-00789)
(DE89-015391; SAND-89-1820C; CONF-891230-1) Avail: NTIS HC A03/MF A01

The in-plane linear elastic constants of woven fabric are determined in terms of the specific fabric microstructure. The fabric is assumed to be a spatially periodic interlaced network of orthogonal yarns and the individual yarns are modeled as extensible elastica. These results indicate that a significant coupling of bending and stretching effects occurs during deformation. Results of this theoretical analysis compare favorably with measured in-plane elastic constants for Vincel yarn fabrics. DOE

N90-15256# Westinghouse Savannah River Co., Aiken, SC.
PREDICTING THE PERFORMANCE OF CERAMIC FILTERS BY THE USE OF SILT DENSITY INDEX
Steven M. Cain 1989 16 p Prepared for presentation at the South Carolina Junior Academy of Sciences and the CSRA Science Fair, Apr. 1990
(Contract DE-AC09-89SR-18035)
(DE90-001316; WSRC-RP-89-792) Avail: NTIS HC A03/MF A01

A series of experiments were conducted to study the rate of filter fouling of several simulants. These solutions contained hydroxides of iron, aluminum, silica, and zinc, using a range of concentration of each under various conditions. Total Solids (TS), Total Suspended Solids (TSS), Total Dissolved Solids (TDS), Silt Density Index (SDI), and conductivity were measured in the studies. The purpose of these experiments was to find out whether or not SDI could be used to accurately predict the performance of ceramic filters. The preliminary results show that SDI alone cannot be used, but can be used in conjunction with the total filtration time. The procedure is limited and can only be used for preliminary screening. DOE

N90-15257# Lawrence Livermore National Lab., CA.
LASER GLASS (1989)
Marvin J. Weber Oct. 1989 10 p Presented at the 2nd International Symposium on New Glass, Tokyo, Japan, 29-30 Nov. 1989
(Contract W-7405-eng-48)
(DE90-002754; UCRL-102044; CONF-8911121-1) Avail: NTIS HC A02/MF A01

Glasses play many and varied roles in laser systems, both passive and active. Properties of special interest include the transparency for transmitting optical components, absorption and emission spectra and excited state lifetimes of paramagnetic ions for amplifying media, magnetooptic properties for optical isolators, acoustooptic properties for optical modulators, and nonlinear optical properties for controlling beam propagation and for photonic switching. The role and extent to which glasses have been used for lasing are briefly reviewed. Although the exploitation of glass

for lasers is a mature activity, it is not exhausted. The number of glass lasers actually demonstrated is much smaller, and the number of commercial laser glasses is smaller still. DOE

N90-15258# Lawrence Livermore National Lab., CA. Polymers Section.
BONDING AEROGELS WITH POLYURETHANES
Florida Matthews and D. Mark Hoffman 1 Nov. 1989 11 p Presented at the Society of Plastics Engineers Annual Technical Conference, Dallas, TX, 7-11 May 1989
(Contract W-7405-eng-48)
(DE90-003050; UCRL-101602; CONF-8905241-1) Avail: NTIS HC A03/MF A01

Aerogels, porous silica glasses with ultra-fine cell size (30 nm), are made by a solution gelation (sol-gel) process. The resulting gel is critical point dried to densities from 0.15 to 0.60 g/cc. This material is machinable, homogeneous, transparent, coatable and bondable. To bond aerogel an adhesive should have long cure time, no attack on the aerogel structure, and high strength. Several epoxies and urethanes were examined to determine if they satisfied these conditions. Bond strengths above 13 psi were found with double bubble and DP-110 epoxies and XI-208/ODA-1000 and Castall U-2630 urethanes. Hardman Kalex Tough Stuff A-85 hardness urethane gave 18 psi bond strength. Hardman A-85, Tuff-Stuff was selected for further evaluation because it produced bond strengths comparable to the adherend cohesive strength. DOE

N90-15259*# National Aeronautics and Space Administration. Langley Research Center, Hampton, VA.
WET SPINNING OF SOLID POLYAMIC ACID FIBERS Patent Application
William E. Dorogy, Jr., inventor (to NASA) (PRC Kentron, Inc., Hampton, VA.) and Anne K. SaintClair, inventor (to NASA) 21 Sep. 1989 21 p
(NASA-Case-LAR-14162-1; NAS 1.71:LAR-14162-1; US-Patent-Appl-SN-410572) Avail: NTIS HC A03/MF A01 CSCL 11C

The invention is a process for the production of solid aromatic polyamic acid and polyimide fibers from a wet gel or coagulation bath wet gel using N,N-dimethylacetamide (DMAc) solution of the polyamic acid derived from aromatic dianhydrides such as 3,3',4,4'-benzo phenone tetracarboxylic dianhydride (BTDA) and aromatic diamines such as 4,4'oxydianiline (4,4'-ODA). By utilizing the interrelationship between coagulation medium and concentration, resin inherent viscosity, resin percent solids, filament diameter, and fiber void content, it is possible to make improved polyamic acid fibers. Solid polyimide fibers, obtained by the thermal cyclization of the polyamic acid precursor, have increased tensile properties compared to fibers containing macropores from the same resin system. NASA

N90-15260*# National Aeronautics and Space Administration. Langley Research Center, Hampton, VA.
POLYIMIDES WITH CARBONYL AND ETHER CONNECTING GROUPS BETWEEN THE AROMATIC RINGS Patent Application
Paul M. Hergenrother, inventor (to NASA) and Stephen J. Havens, inventor (to NASA) (PRC Kentron, Inc., Hampton, VA.) 9 Nov. 1989 24 p
(NASA-Case-LAR-14001-1; NAS 1.71:LAR-14001-1; US-Patent-Appl-SN-433812) Avail: NTIS HC A03/MF A01 CSCL 11C

New polyimides have been prepared from the reaction of aromatic dianhydrides with novel aromatic diamines containing carbonyl and ether connecting groups between the aromatic rings. Several of these polyimides are shown to be semi-crystalline as evidenced by wide angle x ray diffraction and differential scanning calorimetry. Most of the polyimides form tough solvent resistant films with high tensile properties. Several of these materials can be thermally processed to form solvent and base resistant moldings. NASA

N90-15261*# National Aeronautics and Space Administration. Goddard Space Flight Center, Greenbelt, MD.
CERAMIC HEAT PIPE WICK Patent Application
Benjamin Seidenberg, inventor (to NASA) and Theodore Swanson, inventor (to NASA) 31 Jan. 1989 18 p
(NASA-Case-GSC-13199-1; US-Patent-Appl-SN-304147; NAS 1.71:GSC-13199-1) Avail: NTIS HC A03/MF A01 CSCL 11C

A wick for use in a capillary loop pump heat pipe is disclosed. The wick material is an essentially uniformly porous, permeable, open-cell, silicon dioxide/aluminum oxide inorganic ceramic foam having a silica fiber ratio, by weight, of about 78 to 22, respectively, a density of 6 lbs/cu ft, and an average pore size of less than 5 microns. A representative material having these characteristics is Lockheed Missile and Space Company, Inc.'s HTP 6-22. This material is fully compatible with the freons and anhydrous ammonia and allows for the use of these very efficient working fluids, and others, in capillary loops. NASA

N90-15262*# National Aeronautics and Space Administration. Lewis Research Center, Cleveland, OH.
BROMINATED GRAPHITIZED CARBON FIBERS Patent Application
Ching-Chen Hung, inventor (to NASA) 30 Nov. 1989 13 p
(NASA-Case-LEW-14698-2; NAS 1.71:LEW-14698-2; US-Patent-Appl-SN-443289) Avail: NTIS HC A03/MF A01 CSCL 11C

Low cost, high break elongation graphitized carbon fibers having low degree of graphitization are inert to bromine at room or higher temperatures, but are brominated at -7 to 20 C, and then debrominated at ambient. Repetition of this bromination-debromination process can bring the bromine content to 18 percent. Electrical conductivity of the brominated fibers is three times of the before-bromination value. NASA

N90-15263*# National Aeronautics and Space Administration. Pasadena Office, CA.
MOLECULES WITH ENHANCED ELECTRONIC POLARIZABILITIES BASED ON DEFECT-LIKE STATES IN CONJUGATED POLYMERS Patent Application
David N. Beratan, inventor (to NASA) (Jet Propulsion Lab., California Inst. of Tech., Pasadena.) 10 Oct. 1989 22 p
(Contract NAS7-918)
(NASA-Case-NPO-17633-1-CU; NAS 1.71:NPO-17633-1-CU; US-Patent-Appl-SN-418611) Avail: NTIS HC A03/MF A01 CSCL 11C

Highly conjugated organic polymers typically have large non-resonant electronic susceptibilities, which give the molecules unusual optical properties. To enhance these properties, defects are introduced into the polymer chain. Examples include light doping of the conjugated polymer and synthesis, conjugated polymers which incorporate either electron donating or accepting groups, and conjugated polymers which contains a photoexcitable species capable of reversibly transferring its electron to an acceptor. Such defects in the chain permit enhancement of the second hyperpolarizability by at least an order of magnitude. NASA

N90-15264# Los Alamos National Lab., NM.
SESAME EQUATION OF STATE FOR A POLYMER COMPOSITE: PHENOLIC REFRASIL
J. C. Boettger Mar. 1989 14 p
(Contract W-7405-eng-36)
(LA-11512-MS) Avail: NTIS HC A03/MF A01

An equation of state (EOS) for phenolic refrasil was constructed for the SESAME library as material number 7580. It is shown that the principal Hugoniot for this polymer composite cannot be described by simply mixing separate EOS for the two constituents (phenolic and fiber glass). This result has serious implications for future work on composites and for the range of applicability of EOS number 7580. An EOS for phenolic was also constructed as material number 7570. Author

N90-15265# Sandia National Labs., Albuquerque, NM.
CHARACTERIZATION AND IN SITU TESTING OF DIAMOND FILMS
D. E. Peebles and Larry E. Pope 1989 19 p Presented at the Air Force Tribology Technical Review, Fairborn, OH, 27-30 Nov. 1989
(Contracts DE-AC04-76DP-00789; FY1457-89-O-5004)
(DE90-003155; SAND-89-2767C; CONF-8911129-2) Avail: NTIS HC A03/MF A01

Diamond films deposited on silicon wafers have been evaluated by a variety of analytical and mechanical procedures in preparation for tribological studies of these films. For in situ wear studies of diamond films, analysis techniques must be developed that do not damage the films. An ion sputter-cleaning procedure has been found (200 eV acceleration energy) which allows reduction of surface contaminants and a cleaning up of the sp(sup 3) bonding. Preliminary tribological pin-on-plate studies have been completed for a hardened 440 C stainless steel pin sliding on the diamond films in laboratory air. DOE

N90-15266# State Univ. of New York, Stony Brook. Dept. of Chemistry.
PHASE TRANSITION IN POLYMER BLENDS AND STRUCTURE OF IONOMERS Performance Report, 1 Apr. - 25 Oct. 1989
Benjamin Chu 1989 24 p
(Contract DE-FG02-86ER-45237)
(DE90-003525; DOE/ER-45237/T1) Avail: NTIS HC A03/MF A01

Progress is briefly reported on small angle x ray scattering measurements (SAXS) of the following: solutions of polystyrene-polyisoprene AB block copolymer in aniline; gelatin; sulfonated polystyrene ionomers; and lead sulfides. DOE

N90-15267# Pacific Northwest Lab., Richland, WA.
OPTICAL PROPERTIES AND LASER DAMAGE MEASUREMENTS OF INORGANIC POLYMER FILMS
Gregory J. Exarhos and Kevin M. Crosby (Beloit Coll., WI.) Nov. 1989 9 p Presented at the 21st Annual Symposium on Optical Materials for High Power Lasers, Boulder, CO, 1-3 Nov. 1989
(Contract DE-AC06-76RL-01830)
(DE90-003633; PNL-SA-17327; CONF-891163-1) Avail: NTIS HC A02/MF A01

Linear phosphorus-nitrogen bases polymers were synthesized and deposited as thin films from solution on silica or silicon substrates using dip-coating or spin-casting methods. Most materials transmit well into the ultraviolet region of the spectrum and have refractive indices (1.5 to 1.7 at 500 nm) which are controlled by the functionality of chemical substituents introduced at the phosphorus atom. Films exposed to pulsed laser irradiation (1064 nm, 8ns pulsewidth) exhibit damage morphologies ranging from severe cratering to delamination. The chloro-substituted polymer shows a spheroidal surface morphology after exposure to a 25 J/sq cm pulse suggesting melting or condensation of ablated material. The relative stability of these materials to laser irradiation is discussed in terms of chemical bond ionicity which is influenced by atom electronegativity and the nature of substituent groups. Preliminary measurements of the non-linear optical response observed in several of these materials (SHG) is also discussed. DOE

N90-15268# Pacific Northwest Lab., Richland, WA.
CERAMIC PROCESSING USING INORGANIC POLYMERS
J. J. Lannutti, I. A. Aksay (Washington Univ., Seattle.), and C. H. Schilling Oct. 1989 8 p Presented at the Spring Meeting of the Materials Research Society, San Diego, CA, 24-28 Apr. 1989
(Contract DE-AC06-76RL-01830)
(DE90-003638; PNL-SA-17607; CONF-890426-31) Avail: NTIS HC A02/MF A01

Inorganic polymers are used in the formation of green compacts via sedimentation of colloidal alumina suspended in chloroform. Polymers containing highly polar components tend to produce constant density profiles of greater than 55 percent density, while those containing nonpolar, reactive components produce profiles with a large gradient in packing density. Density profiles describing the sedimentation behavior versus time and the final dried density of the compacts are generated via the use of gamma ray densitometry. These polymers have the potential not only to increase green compact density but also to reduce burnout and subsequent sintering requirements by pyrolyzing to useful ceramic. DOE

N90-15269# Argonne National Lab., IL. Materials and Components Technology Div.
DEVELOPMENT OF NMR (NUCLEAR MAGNETIC RESONANCE) IMAGING PROBES FOR ADVANCED CERAMICS
N. Gopalsami, G. A. Forster, S. L. Dieckman, W. A. Ellingson, and R. E. Botto Sep. 1989 18 p Presented at the Conference on Review of Progress in Quantitative NDE, Brunswick, ME, 23-28 Jul. 1989
(Contract W-31-109-eng-38)
(DE90-003812; CONF-890770-7) Avail: NTIS HC A03/MF A01

The purpose of this paper is to present the design and test results of a special imaging probe built at Argonne for ceramics characterization. The imaging probe is designed to be used in an 89-mm vertical-bore, 2.35-T superconducting magnet in conjunction with a Bruker CXP-100 spectrometer. The probe must accommodate samples up to 28 mm in diameter, in accordance with our present requirements. The probe includes an RF coil for excitation and detection of the nuclear signals, and a set of gradient coils to create gradient fields with respect to the x, y, and z spatial coordinates. At high field strengths, the gradient coils will generate considerable heat owing to resistive losses; hence, a provision for cooling the probe is included. DOE

N90-15270# Texas Univ., Arlington. Dept. of Chemistry.
ELECTRONIC AND IONIC TRANSPORT IN POLYMERS Quarterly Report, 1 Jul. - 30 Sep. 1989
Martin Pomerantz, John R. Reynolds, Krishnan Rajeshwar, and Dennis S. Marynick 3 Oct. 1989 7 p
(Contract N00014-86-K-0769)
(AD-A213410; AD-E501157; TR-17) Avail: NTIS HC A02/MF A01 CSCL 07/4

By employing Sodium Hydroxide dedoping, high/low conductivity interfaces have been prepared. Optoelectrochemical properties of several thiophene-phenylene-thiophene polymers have been studied. Blends of poly(3-decylthiophene) with polyethylene or poly(ethylene terephthalate) have been prepared. The ion binding properties of copolymers of pyrrole and 3-(1-pyrrolyl)propane-sulfonate have been studied for the first time using Ru(NH3)6(3+) and Ru(bpy)3(2+)(bpy=2,2'-bipyridyl) as the ion probes. Molecular orbital calculations have been used to estimate the equilibrium ground state geometries of alternating copolymers of substituted phenylenes and bithiophenes. Calculated spin populations suggest possible Alpha-Beta and/or Beta-Beta linkages in addition to Alpha-Alpha linkages. Calculated band gaps are between those of poly(p-phenylene) and polythiophene. GRA

N90-15271# Army Materials Technology Lab., Watertown, MA.
IEA/ANNEX 2 POWDER CHARACTERIZATION COOPERATIVE PROGRAM Final Report
Theresa M. Resetar, James W. McCauley, Glenn E. Schafer, Alan L. Dragoo, Steven M. Hsu, D. Ray Johnson, Hans Hausner, and Robert Pompe (Swedish Inst. for Silicate Research, Gotheborg.) Jun. 1989 17 p
(Contract DE-AI05-84OR-21411)
(AD-A213540; MTL-TR-89-53) Avail: NTIS HC A02/MF A01 CSCL 11/2

Materials characterization will play a key role in such critical issues as quality, reliability, and manufacturing cost reduction of emerging high performance ceramic materials. The identification of better analytical standards and standard procedures for obtaining the true values of powder characteristics is an important component of this overall thrust. The U.S. Department of Energy, with the Oak Ridge National Laboratory has initiated an international program to comprehensively characterize Silicon Nitride, Silicon,

Silicon Carbide, and Zirconium Oxide powders in laboratories in the United States, the Federal Republic of Germany, and Sweden to expedite the accomplishment of these objectives. GRA

N90-15272# Massachusetts Inst. of Tech., Cambridge. Dept. of Chemistry.
NEW POLYMERS MADE WITH WELL-CHARACTERIZED ORGANOMETALLIC CATALYSTS Final Report
Richard R. Schrock 16 Oct. 1989 4 p
(Contract N00014-87-K-0099; NSF DMR-84-18718)
(AD-A213592) Avail: NTIS HC A02/MF A01 CSCL 07/6

In the first publication we reported that Mo(CH-t-Bu)(NAr)(O-t-Bu)2 was a good catalyst for the ring opening metathesis polymerization of endo,endo-5,6-dicarbo methoxynorbornene to give homopolymers with polydispersities in the range 1.11 to 1.22, as well as block copolymers containing endo,endo-5,6-dicarbo methoxynorbornene and norbornene with similar low polydispersities. In the second publication we reported additional details of the metathesis of functionalized monomers by molybdenum, and also that 7.8-bis (trifluoromethyl) tricyclo(4.2.2.0)deca 3,7,9-triene could be ring opened and the polymer cleaved with pivaldehyde to give (after pyrolysis) soluble polyenes, (t-Bu)(CH=CH)2x+1(t-Bu). Triblocks containing a 40-ene (average) central chain, capped by two polynorbornene chains also were prepared. GRA

N90-15273# Rensselaer Polytechnic Inst., Troy, NY. Dept. of Chemical Engineering.
A NOVEL HEAT RESISTANT BLEND PRODUCED BY COMPOSITIONAL QUENCHING: A THERMOPLASTIC POLYIMIDE IMPACT MODIFIED WITH A FLUOROELASTOMER Final Report, 1 Jun. 1986 - 31 May 1989
John S. Furno and E. Bruce Nauman 15 Aug. 1989 28 p
(Contract DAAL03-86-G-0055)
(AD-A213724; ARO-23797.2-MS-F) Avail: NTIS HC A03/MF A01 CSCL 07/6

The polymers used in this work are Ultem, a thermoplastic polyimide produced by General Electric, and Viton A, a fluoroelastomer made by Dupont. Both the polymer and rubber were chosen for this study because of their excellent thermal stability. Ultem is a heat and chemical resistant polymer that suffers from poor impact strength. The addition of a dispersed rubber phase to Ultem significantly reduces this problem. Compositional quenching is a process in which a single-phase solution consisting of two (or more) polymers dissolved in a common solvent is heated and then flashed in a vacuum chamber. Rapid devolatilization of the solvent results, leaving behind a two-phase polymer blend in which the minor component is microdispersed within the major component through the action of spinodal decomposition. Through the process of compositional quenching, Ultem-Viton blends were produced that contained relatively uniform-sized, spherical Viton particles approximately one-half micron in diameter. GRA

N90-15274# Ceramic Process Systems Corp., Milford, MA.
COMPOSITE CERAMIC SUPERCONDUCTING WIRES FOR ELECTRIC MOTOR APPLICATIONS Quarterly Report No. 5, 1 Jul. - 30 Sep. 1989
John W. Halloran 10 Oct. 1989 51 p
(Contract N00014-88-C-0512; DARPA Order 9525)
(AD-A213742; CPS-89-013) Avail: NTIS HC A04/MF A01 CSCL 20/12

This is a progress report on developing Y-123 wire for an HTSC motor. Y-123 powder lot size was increased to 10 kilograms. Spools of 125-micron diameter green fiber (50 to 60 vol percent Y-123) are routinely produced. Wire development is focused on co-fired silver coated monofilaments. The silver coating has improved thickness and uniformity. Continuous coated green fiber was made at lengths up to 150 feet. The major emphasis was on continuous co-firing of wire in a reel-to-reel operation. The length of the heated zones in the furnace limits wire length, furnace modifications are being designed. Continuously sintered Ag-clad wire was produced. The longest length without a break was 19 feet. Design was completed for a drum dc homopolar with an iron magnetic current. Parts and equipment were ordered or are being machined. The motor will be assembled and tested with copper coils in the following quarters. GRA

N90-15275# Army Construction Engineering Research Lab., Champaign, IL.
ARC-SPRAYED COATINGS FOR ELECTROMAGNETIC PULSE PROTECTION: ASSESSMENT OF PHYSICAL AND ELECTRICAL PROPERTIES Final Report
Howard S. Savage and Ray G. McCormack Sep. 1989 78 p
(AD-A213825; CERL-TR-M-89/15) Avail: NTIS HC A05/MF A01 CSCL 09/7

The Army is studying methods of protecting sensitive electronic equipment against electromagnetic pulse (EMP) and radiofrequency interference (RFI) events. Part of this work focuses on metal arc-spray techniques as a potentially low-cost alternative to traditional EMP/RFI protection. Arc-sprayed metal coatings were used for several years in different applications; however, little is known about the physical and electrical properties of these coatings. A better understanding of these properties would allow spraying parameters to be optimized, ensuring the most effective coatings at the lowest cost. Aluminum, aluminum bronze, copper, low-carbon steel, 13 percent chrome steel, nickel, nickel chrome, tin, and zinc were sprayed onto paper and aluminum foil substrates using the two-wire arc-spray process to determine the physical and electrical characteristics of these materials when sprayed on ordinary rooms composed of common construction materials. GRA

N90-15276# California Univ., Los Angeles. Dept. of Materials Science and Engineering.
HARDENING AND TOUGHENING OF ZnS-Ga2S3 CERAMICS BY SOLID-STATE REACTIONS Technical Report No. 3, Sep. 1988 - Sep. 1989
Alan J. Ardell, Bruce Dunn, William W. Chen, and J. Zhang 1 Oct. 1989 10 p Presented at the 5th European Electromagnetic Windows Conference, Toulon, France, Sep. 1989 Submitted for publication
(Contract N00014-87-K-0531)
(AD-A213875; TR-3) Avail: NTIS HC A02/MF A01 CSCL 11/2

The first results of research on the hardness and toughness of ZnS containing 16 mol percent Ga2S3, which is the eutectoid composition, are reported. Hot-pressed material of 97 to 99 percent of theoretical was heat-treated for various times in the temperature range 700 to 790 C to stimulate eutectoid decomposition below th eutectoid temperature (818 C). Hardness and toughness were evaluated by the indentation method. The heat-treated material is significantly harder than pure ZnS, but the fracture toughness is about the same, although there is some evidence that toughness increases at longer reaction times. GRA

N90-15277# Texas A&M Univ., College Station. Dept. of Chemistry.
ELECTROCHEMICAL INVESTIGATION OF ELECTRONICALLY CONDUCTIVE POLYMERS
Charles R. Martin, Reginald M. Penner, and Leon S. VanDyke 11 Oct. 1989 23 p
(Contract N00014-82-K-0612)
(AD-A214019; TR-41) Avail: NTIS HC A03/MF A01 CSCL 07/6

A small amplitude current-pulse method which is uniquely suited for solving the myriad problems associated with electrochemical analyses of electronically conductive polymers has been developed. This method was used to obtain Dapp values for the electronically conductive polymer, polypyrrole. The results of these experiments are described here. In addition, a procedure for controlling the morphologies of electronically conductive polymers has been developed. This procedure involves the electrochemical growth of the conductive polymer at an electrode surface which has been masked with a microporous polymer membrane. The pores in this membrane act as templates for the nascent electronically conductive polymer. Because the template membrane contains

linear cylindrical pores, cylindrical conductive polymer fibrils are obtained. We will show in this manuscript that microfibrillar polypyroole films prepared via this approach can support higher rates of charge-transport than conventional polypyrrole. GRA

N90-15278# Department of the Navy, Washington, DC.
SILVER COATED SUPERCONDUCTING CERAMIC POWDER Patent Application
William Ferrando, inventor (to Navy) 2 Aug. 1989 16 p
(AD-D014300; US-Patent-Appl-SN-389220) Avail: NTIS HC A03/MF A01 CSCL 20/3

A process for silver coating superconducting ceramic powder by: (1) coating the superconducting ceramic powder particles with silver nitrate; (2) melting the AgNO3 so that it wets and forms a uniform coating over the surfaces of the particles; and (3) decomposing the AgNO3 to form a thin, uniform coating of silver metal on the surfaces of the particles. The product is a loose powder of superconducting ceramic particles which are uniformly coated with silver metal. The powder can be cold worked (e.g., swaged, forged, etc.) to form superconducting structures such as rods or wires. GRA

N90-15279# Oak Ridge National Lab., TN. Metals and Ceramics Div.
TOUGHENING BEHAVIOR AND INTERFACIAL PROPERTIES OF FIBER-REINFORCED CERAMIC COMPOSITES
Chun-Hway Hsueh 1989 31 p Presented at the 13th Energy-Sources Technology Conference and Exhibition, New Orleans, LA, 14-18 Jan. 1990
(Contract DE-AC05-84OR-21400)
(DE89-015351; CONF-900102-2) Avail: NTIS HC A03/MF A01

Toughening of ceramics by incorporating strong fibers has become an established technology, resulting in the creation of a new generation of tough ceramic composites. This toughening effect is primarily due to bridging of the crack surfaces by intact fibers when the composite is subjected to tension. The fiber bridging mechanisms, which are contingent upon the stress transfer phenomena between the fiber and the matrix, are reviewed. The critical role of the properties at the fiber/matrix interface in controlling the stress transfer phenomena is examined. Finally, evaluations of the interfacial properties of the composite by the indentation technique and the corresponding analysis are presented. DOE

N90-15280# IIT Research Inst., Bartlesville, OK. National Inst. for Petroleum and Energy Research.
CROSSLINKED, FLEXIBLE, LOW-MOLECULAR-WEIGHT POLYACRYLAMIDE GELS FOR MOBILITY CONTROL
H. W. Gao Dec. 1989 15 p
(Contract DE-FC22-83FE-60149)
(DE90-000202; NIPER-432) Avail: NTIS HC A03/MF A01

This project is a continuation of a research program initiated in FY88 to develop shear-resistant flexible gels based on crosslinking a low-molecular-weight polyacrylamide for mobility control. Polyacrylamide was crosslinked with aluminum citrate and chromium citrate. This report is divided into three parts: (1) gelation tests; (2) shear degradation and rehealability tests; and (3) porous media studies. Gelation tests showed that crosslinked low-molecular-weight polyacrylamide gels for mobility control can be formulated at pH = 7.0 using a low-molecular-weight polyacrylamide polymer, HPAM1 (molecular weight = 400,000 daltons) at concentrations from 10,000 to 20,000 ppm and a crosslinker, aluminum citrate, at aluminum concentrations from 150 to 2,400 ppm. Porous media studies showed that weak gels were injectable through porous media. Shear degradation tests for a weak gel in a porous medium (permeability = 197 darcies) consisting of a pack of five 100-mesh stainless steel screens showed that crosslinked bonds were broken under a high shear condition and rehealed under a low shear condition. DOE

28 PROPELLANTS AND FUELS

Includes rocket propellants, igniters, and oxidizers; their storage and handling procedures; and aircraft fuels.

For related information see also *07 Aircraft Propulsion and Power, 20 Spacecraft Propulsion and Power,* and *44 Energy Production and Conversion.*

N90-15281# Lawrence Livermore National Lab., CA.
USING SMALL SCALE TESTS TO ESTIMATE THE FAILURE DIAMETER OF A PROPELLANT
Craig M. Tarver and Leroy G. Green 18 Aug. 1989 9 p Presented at the 9th International Symposium on Detonation, Portland, OR, 28 Aug. - 1 Sep. 1989
(Contract W-7405-eng-48)
(DE90-001166; UCRL-101953; CONF-890811-39) Avail: NTIS HC A02/MF A01

Electric gun and gas gun shock initiation experiments using embedded manganin pressure gauges were employed to determine high pressure reaction rates of propellants. This reaction rate data was used to develop ignition and growth reactive flow computer models, which then predict the unconfined failure diameter of these propellants. Two ammonium perchlorate/binder/aluminum propellants were studied: one containing no HMX and one containing 12 percent HMX. The propellant containing no HMX exhibited no reaction in any of the experiments. In the short pulse duration electric gun and the lower pressure gas gun experiments, the HMX-containing propellant exhibited partial reactions indicating that only the 12 percent HMX reacted. At 20 GPa input pressures the rest of the propellant mixture reacted and the reaction rates were quantitatively measured and calculated. Using these reaction rates, the unconfined failure diameter of the 12 percent HMX propellant was calculated to be between 2.5 and 3 inches. DOE

N90-15282# Mound Lab., Miamisburg, OH.
CRITICAL TEMPERATURE ANALYSIS FOR A HEMISPHERICAL CHARGE OF A BINARY EXPLOSIVE
James M. Pickard 1989 7 p Presented at the 18th North American Thermal Analysis Society Conference, San Diego, CA, 24-27 Sep. 1989
(Contract DE-AC04-88DP-43495)
(DE90-001447; MLM-3608(OP); CONF-8909169-3) Avail: NTIS HC A02/MF A01

The adiabatic induction period for a hemispherical charge of a binary explosive (13.9 wt percent pentaerythritol tetranitrate (PETN) and 86.1 wt percent plastic bonded explosive (PBX9407)) enclosed in an aluminum/ceramic housing was measured by conventional cook-off tests over the temperature range of 150 to 250 C. Simulated adiabatic induction time curves for an intimate mixture of PETN and PBX9407 were recorded with accelerating rate calorimetry (ARC). Apparent heat-transfer coefficients approximating conductive and convective modes of heat-transfer were calculated from cooling curves recorded for the charge housing loaded with mock explosive powder (diphenyl silane diol) and water, respectively. Predicted critical temperatures based on models utilizing Semenov and Frank-Kamenetskii boundary constraints were in good agreement with experimental results determined from the cook-off test. DOE

N90-15283# Sandia National Labs., Albuquerque, NM. Systems Engineering Div.
STUDIES OF THE ADSORPTION/DESORPTION BEHAVIOR OF EXPLOSIVE-LIKE MOLECULES
Bernard T. Kenna and Frank J. Conrad Oct. 1989 36 p
(Contract DE-AC04-76DP-00789)
(DE90-001867; SAND-86-0141) Avail: NTIS HC A03/MF A01

The adsorption/desorption behavior of explosive-like molecules are described as a function of temperature. Capillary column gas chromatography was used in conjunction with bare fused silica and borosilicate glass columns. Adsorption rate constants and energies of adsorption/desorption are estimated. A possible adsorption mechanism is addressed which involves a Lewis acid-base type of interaction between the molecules and substrate coupled with island formation by the adsorbed molecules. DOE

N90-15284# Central Research Inst. of Electric Power Industry, Tokyo (Japan). Energy and Environment Lab.
SURVEY ON SYNTHESIS TECHNOLOGIES OF METHANOL AS AN ALTERNATIVE FUEL
Seiichi Oyama, Yasushi Ozawa, and Hisashi Fukuzawa Oct. 1988 44 p In JAPANESE; ENGLISH summary
(DE89-901303; CRIE-T-87110) Avail: NTIS (US Sales Only) HC A03/MF A01

To provide for future utilization of methanol in the electric power industry, the present circumstances on synthesis technologies of methanol were surveyed. Gas phase methanol synthesis process (the conventional process) uses natural gas or petroleum as the feed, and the reaction conditions are as follows; reaction temperature of 230 to 400 C, reaction pressure of 50 to 400 atmospheres, and Cu or Zn system catalyst is used. However the process has low points such as; low yield of the product (10 to 15 percent), necessity of recirculation of the unreacted gases, complicated process, poor control of the reaction temperature, and no effective catalyst for the low temperature and low pressure reaction. Recently, liquid phase synthesis process was proposed. The process is said to show high yield of 90 percent under the reaction conditions of 100 C, 10 atmospheres with inactive solvent such as tetrahydrofuran. Furthermore, the feed stocks with wide range of CO/H2 ratio can be used with effective reaction temperature and the low manufacturing costs are expected. However, the process is still under development and the subjects to be solved are as follows: catalyst activity at low temperature, high selectivity, long life catalyst, effects of impurities on the catalyst and its measures. DOE

N90-15285# Sandia National Labs., Albuquerque, NM. Explosive Projects and Diagnostics Div.
SHOCK-WAVE CHARACTERIZATION OF ENERGETIC BOOSTER-ROCKET PROPELLANT WAK-2 AND ITS SIMULANT UGS
L. J. Weirick Oct. 1989 34 p
(Contract DE-AC04-76DP-00789)
(DE90-002633; SAND-89-0917) Avail: NTIS HC A03/MF A01

A series of shock loading experiments on an energetic propellant and its simulant was conducted on a light gas gun. The shock sensitivity of WAK-2, which is a composite modified, double based, booster rocket propellant was characterized along with its simulant UGS. The initial objectives were to obtain Hugoniot data, to investigate the pressure threshold at which a reaction occurs, and to measure spall threshold at various impact velocities. The Hugoniot data obtained for the propellant fits the Hugoniot curve provided by the manufacturer of the propellant. A Hugoniot curve developed for the simulant was found to match that of the propellant. The initial density, rho (sub 0), initial bulk sound velocity, C(0), and constant S values for the energetic propellant WAK-2 and its simulant UGS were 1.85 g/cu cm, 2.2 mm/microns and 2.66, respectively. The ignition threshold pressure of the WAK-2 was found to be in the range of 3 kbar. A violent reaction was observed for a sample impacted at a pressure of 22 kbar. In spall tests, impact pressures in the range of 1.1 to 3.1 kbar were applied to the propellant/simulant. The propellant exhibited spall strengths approx. 0.33 kbar, with its simulant being somewhat weaker, approx. 0.22 kbar. Scanning electron microscopy and electron microprobe analysis were used to characterize the microstructures of the materials and to determine the details of the spall events. DOE

N90-15286# Lawrence Livermore National Lab., CA.
BURNING RATES OF TWO CAST NITRAMINE EXPLOSIVES USING A HYBRID CLOSED BOMB-STRAND BURNER
William C. Tao, Marc S. Costantino, and Donald L. Ornellas Aug. 1989 12 p Presented at the 9th International Symposium on Detonation, Portland, OR, Sep. 1989
(Contract W-7405-eng-48)
(DE90-002785; UCRL-101879; CONF-890926-3) Avail: NTIS HC A03/MF A01

The burn rate of two HMX-based cast explosives, RX-08-EL and RX-40-AP, is measured to pressures above 650 MPa using a hybrid closed bomb-strand burner. The hybrid design allows the simultaneous measurement of pressure and regression rate, in each experiment, over a large range of pressures. RX-08-EL is a high performance extrusion cast explosive with low sensitivity, and RX-40-AP is a cast-cured explosive with a mono-modal HMX particle size distribution. Up to 650 MPa, both explosives exhibit a planar burning mechanism with the regression rate obeying the classical aP(sup n) formalism. Upon cycling to 400 MPa, unloading, and re-pressurizing, the RX-08-EL explosive exhibited a significant increase (an order of magnitude) in its burn rate. DOE

N90-15287# Oak Ridge National Lab., TN. Chemical Technology Div.
PROPERTIES AND THERMAL DECOMPOSITION OF THE DOUBLE SALTS OF URANYL NITRATE-AMMONIUM NITRATE
Karl J. Notz and Paul A. Haas 1989 17 p Presented at the International Chemical Congress of Pacific Basin Society Symposium on Polymer Rheology and Processing (PACIFICHEM '89), Honolulu, HI, 17-22 Dec. 1989
(Contract DE-AC05-84OR-21400)
(DE89-004909; CONF-891206-1) Avail: NTIS HC A03/MF A01

The formation of ammonium nitrate-uranyl nitrate double salts has important effects on the thermal denitration process for the preparation of UO(sub 3) and on the physical properties of the resulting product. Analyses were performed, and properties and decomposition behavior were determined for three double salts: NH4UO2(NO3)3, (NH4)2UO2(NO(3)4, and (NH4)2UO2(NO3)-4-2H2O. The trinitrate salt decomposes without melting at 270 to 300 C to give a gamma UO3 powder of approx. 3 micron average size, with good ceramic properties for fabrication into UO2 nuclear fuel pellets. The tetranitrate dihydrate melts at 48 C; it also dehydrates to the anhydrous salt. The anhydrous tetranitrate decomposes exothermically, without melting, at 170 to 270 C by losing one mole of ammonium nitrate to form the trinitrate salt. DOE

N90-15288# Pennsylvania State Univ., University Park. Coll. of Earth and Mineral Sciences.
THERMAL STABILITY OF JET FUEL Quarterly Report No. 4, Jul. - Sep. 1989
Semin Eser, Janice Perison, Ronald M. Copenhaver, and Harold H. Schobert 1989 54 p
(Contract DE-AC22-88PC-88827)
(DE90-002760; DOE/PC-88827/T4) Avail: NTIS HC A04/MF A01

The overall objective of this program is to investigate the effect of chemical components on the thermal stability of jet fuel. Six model compounds were heat treated in microautoclave reactors lined with pyrex tubes to investigate the effect of the reactor surface on thermal degradation reactions. These experiments were carried out at 350 to 450 C for 1 to 2 hours in 100 psig cold nitrogen pressure. Reactions products were analyzed by H-1 and C-13 NMR spectroscopy to compare their chemical constitution with those obtained under the same conditions without the glass liners in the reactors. The thermal treatments in air were extended to cover a wider temperature and time range than those indicated in the second quarterly report. The treatment temperature varied between 150 and 450 C for reaction times ranging from 93 hours to 1 hour, respectively. This set of reactions were performed under 100 psig cold air pressure. Reaction products were characterized by H-1 and C-13 NMR spectroscopy and GC-MS analysis. The degradation of 2,6-dimethylphenol is discussed. DOE

N90-15289# Mound Lab., Miamisburg, OH.
SIMULTANEOUS THERMAL ANALYSIS TECHNIQUES FOR CHARACTERIZATION OF ENERGETIC MATERIALS
Ruth B. Whitaker, Charles R. Brown, Cherng Chang, John A. McDaniel, and Juanita R. Tackett 1989 8 p Presented at the American Defense Preparedness Association's (ADPA) International Joint Symposium on Compatibility of Plastics and Other Materials With Explosives, Propellants and Pyrotechnics, and Processing Propellants, Explosives, and Ingredients
(Contract DE-AC04-88DP-43495)

(DE90-003028; MLM-3612(OP); CONF-8910157-3) Avail: NTIS HC A02/MF A01

Simultaneous thermal analysis techniques for characterization of materials has become widespread, with increased availability of instrumentation for such analyses. EG and G Mound has the capability to do simultaneous thermogravimetry-differential/scanning calorimetry (TG/DSC) to 825 C, simultaneous thermogravimetry/mass spectrometry (TG/MS) to 1000 C, and temperature thermogravimetry/differential thermal analysis (TG/DTA) to 2400 C. Advantages of these simultaneous techniques include the exact correlation of TG weight loss data with observed enthalpic transitions and with evolved gas analysis. These thermal analysis techniques have proven to be very useful in the characterization and study of reactions of energetic materials. In this study, several secondary explosives have been examined by TG/DSC to determine weight losses during melting and decomposition, and by TG/MS to identify the decomposition products. Reactions of two pyrotechnic blends were studied by TG/DTA under varying analysis conditions. DOE

N90-15290# Lawrence Livermore National Lab., CA.
A FUTURE FOR LLNL (LAWRENCE LIVERMORE NATIONAL LABORATORY) RESEARCH IN COMPOSITE HIGH EXPLOSIVES
Robert G. Hickman Oct. 1989 43 p
(Contract W-7405-eng-48)
(DE90-004442; UCID-21763) Avail: NTIS HC A03/MF A01

The purpose was to provide direction for research in composite high explosives at LLNL. This category of explosives was known for hundreds of years and it potentially can provide performance higher than HMX and still be insensitive. The reasons to seek such a material are set forth in the context of programmatic benefit. Explosive performance is reviewed along with some fundamental limits and possibilities for the future. It is concluded that the research should continue for the purpose of enhanced safety and that a reasonable goal is to produce an explosive with 20 percent greater performance than TATB. DOE

N90-15291# Argonne National Lab., IL. Energy and Environmental Systems Div.
PRODUCTS OF THE HYPOCHLORITE OXIDATION OF HYDRAZINE FUELS Final Report, Oct. 1984 - Sep. 1986
Kenneth L. Brubaker, Jose V. Bonilla, and Amrit S. Boparai Jun. 1989 39 p
(AF Proj. 1900)
(AD-A213557; AFESC/ESL-TR-87-51) Avail: NTIS HC A03/MF A01 CSCL 07/4

Neutralization of hydrazine fuels with hypochlorite is a recommended procedure for the treatment of fuel spills prior to disposal. Previous research has shown that incomplete reaction of hypochlorite with the methylated hydrazine fuels monomethylhydrazine (MMH) and unsymmetrical dimethylhydrazine (UDMH) leads to a wide variety of byproducts, including N-nitrosoamines, which are believed to be highly carcinogenic. The results presented were obtained as part of a program to assess the environmental implications of using the hypochlorite method for the treatment and disposal of hydrazine fuel spills. The fuels examined were hydrazine, MMH, UDMH, and Aerozine-50. The neutralization products were determined under experimental conditions comparable to those expected for actual spills. The effects of varying the temperature and the pH as well as of aging the final reaction mixture were determined. Quantitative measurements of the nitrosoamines produced are presented. Major and environmentally significant minor products were identified using gas chromatography/mass spectroscopy. GRA

N90-15292# Ballistic Research Labs., Aberdeen Proving Ground, MD.
SPECTRAL STUDIES OF SOLID PROPELLANT COMBUSTION. 2: EMISSION AND ABSORPTION RESULTS FOR M-30 AND HMX1 PROPELLANTS Final Report, Jun. 1988 - Jun. 1989
John A. Vanderhoff 1989 58 p
(AD-A213857; BRL-TR-3055) Avail: NTIS HC A04/MF A01 CSCL 19/1

A windowed strand burner with a propellant feed mechanism has been used to characterize the steady-state burning of two composite propellants, M-30 and HMXI, at moderate pressure. Both emission and absorption spectroscopy have yielded profile data on three important combustion species: OH, NH, and CN. Relative appearance of these three species are inferred from emission intensity profiles, and absolute concentration profiles are calculated from the absorption data. This is the first absolute determination of these combustion intermediates in a propellant flame. These concentration measurements for OH indicate that the propellant flame temperatures are about 200 K below adiabatic. A maximum value of 40 ppm NH is found for the M-30 propellant flame. Fluctuations in the flame front of HMXI compromised the determination of maximum concentrations for NH and CN. GRA

N90-15293# Clarkson Univ., Potsdam, NY.
FUNDAMENTAL MECHANISM OF ATOMIZATION Final Report, 15 May 1986 - 30 Jul. 1989
S. P. Lin 31 Jul. 1989 99 p
(Contract DAAL03-86-K-0072; NSF MSM-88-17372)
(AD-A213859; ARO-23297.10-EG) Avail: NTIS HC A05/MF A01 CSCL 21/4

The physical mechanism of atomization is investigated. A problem statement is given in Section 1. The research has resulted in 6 papers. They are given in the Appendices. The results of the research are summarized in Section 2. The list of publications and the personnel involved in the research are given respectively in Section 3 and 4. The relevant bibliographies on the subject are listed in the references section of each journal article. GRA

N90-15294# Rockwell International Corp., Canoga Park, CA. Rocketdyne Div.
INORGANIC HALOGEN OXIDIZERS Final Report, 19 Sep. 1983 - 30 Sep. 1989
K. O. Christe 4 Oct. 1989 13 p
(Contract N00014-83-C-0531)
(AD-A213990; RI/RD89-241) Avail: NTIS HC A03/MF A01 CSCL 07/4

The purpose of this program was to explore the synthesis and properties of energetic inorganic halogen oxidizers. Although the program was directed toward basic research, applications of the results generated major technological breakthroughs. Thus, the first chemical synthesis of elemental fluorine was achieved, pure fluorine solid-propellant gas generators were developed, and a continuous ion exchange process for the production of advanced NF_4^+ salts was worked out. GRA

N90-15295# Chemical Research and Development Center, Aberdeen Proving Ground, MD.
MUTAGENIC RESPONSES OF SOME PETROLEUM-BASE OBSCURANTS IN THE AMES TEST Technical Report, Oct. 1986 - Dec. 1987
Fred K. Lee, Jr., William T. Muse, Jr., and Bernard J. Brown Sep. 1989 21 p
(DA Proj. 1C1-62622-A-552)
(AD-A214201; CRDEC-TR-071) Avail: NTIS HC A02/MF A01 CSCL 06/11

In the Ames test, five petroleum fractions diesel fuel (DF) 25 percent distilled, DF with approximately 6 percent tetraethoxysilane, Jet-A, 75 percent bottoms product and Fog Oil, and methylene chloride extractions of combusted DF were evaluated for their mutagenic potential. The five fractions were dissolved in ethanol containing 1 percent Tween 80. One hundred milligrams of the residue from combusted DF was extracted with 25 mL of methylene chloride for 24 hr. After that time, the methylene chloride was replaced with acetone by evaporation. Each of five materials was tested in the four standard tester strains; TA97, TA98, TA100, and TA102, metabolically activated (aroclor 1254 induced rat liver S9) and nonactivated. Five concentrations, ranging upwards to the approximate level of cytotoxicity, of each material were tested,

and the results in each case were confirmed with a similar nonconcurrent test. Positive results were not demonstrated in any of the materials tested. GRA

N90-15296# Delaware Univ., Newark. Dept. of Chemistry.
CHARACTERIZATION OF THE THERMAL DEGRADATION OF SELECTED ENERGETIC MATERIALS AND MIXTURES BY RAPID-SCAN FOURIER TRANSFORM INFRARED (RSFTIR) SPECTROSCOPY Final Report, Jun. 1988 - Jun. 1989
Thomas B. Brill and Thomas P. Russell Sep. 1989 23 p
(Contract F08635-87-C-0130; AF Proj. 2303)
(AD-A214411; AFATL-TR-89-55) Avail: NTIS HC A02/MF A01 CSCL 07/4

There is considerable interest in ethylene diammonium dinitrate (EDD) as a component of mixtures with other nitrate salts and various organic molecules for use in melt castable explosives. Most of this work is described in the international patent literature. EDD mixtures with ammonium nitrate (AN) are more thermally stable than EDD alone, and have better performance than AN alone. The eutectic mixture has a lower melting point than either component making it suitable for melt casting. However, EDD/AN mixtures suffer from volume changes with temperature because of the phase transitions of AN. The addition of potassium nitrate (KN) stabilizes the AN and counters the expansion of AN at 32 C caused by one of the solid-solid phase transitions. The fast thermal decomposition processes are described for AN, EDD and two heterogeneous mixtures: EDD/AN (50/50) and EDD/AN/KN (46/46/8), called EAK. The techniques employed are rapid scan Fourier Transform Infrared (FTIR) Spectroscopy/Temperature Profiling as the main technique and differential scanning calorimetry (DSC) to support the temperature profiling data obtained at the high heating rates. GRA

N90-15297# Systems Research Labs., Inc., Dayton, OH. Research Applications Div.
SURFACE THERMOMETRY OF ENERGETIC MATERIALS BY LASER-INDUCED FLUORESCENCE Final Technical Report, Feb. 1987 - Aug. 1989
Michael E. Post and Larry P. Goss Sep. 1989 69 p
(Contract F49620-87-C-0040; AF Proj. 2308)
(AD-A214423; SRL-5510-F; AFOSR-89-1351TR) Avail: NTIS HC A04/MF A01 CSCL 09/3

The laser-induced fluorescence from Dy: YAG was employed for the measurement of temperature on reacting and nonreacting surfaces. Point, line, and two-dimensional mapping of the surface temperature was demonstrated utilizing the tripled output (355 nm) of a Nd:YAG laser. The temporal and spatial distribution of the temperature was recorded with a two-dimensional intensified imaging system. The technique was also utilized for the measurement of the thermal depth profile of a plastic material undergoing rapid heating by a CO2 laser. A fiber-optic temperature probe was developed. Fluorescent crystals bonded to the fiber-optic tip with a ceramic adhesive provide a 300 to 1100 K temperature range for the probe. GRA

N90-15298# EG and G Mound Applied Technologies, Miamisburg, OH.
MORE EFFICIENT SENSITIVITY TESTING
Barry T. Neyer 20 Oct. 1989 31 p
(Contract DE-AC04-88DP-43495)
(DE90-002639; MLM-3609) Avail: NTIS HC A03/MF A01

A new sensitivity test which has many advantages over the previously defined tests was developed. Computer simulation demonstrated that this new test provides better estimates (less bias and smaller variance) of both the mean, (mu), and the standard deviation, (sigma), than the other known tests. Theoretical analysis and simulation suggest that this test will generally be the most efficient sensitivity test possible. Thus, use of this test should result in savings of both time and components without loss of precision. DOE

29 MATERIALS PROCESSING

Includes space-based development of products and processes for commercial applications.
For biological materials see *55 Space Biology*.

No abstracts in this category.

31 ENGINEERING (GENERAL)

Includes vacuum technology; control engineering; display engineering; cryogenics; and fire prevention.

N90-15299# Allied-Signal Aerospace Co., Kansas City, MO.
A STRATEGY FOR CONCURRENT PRODUCT AND PROCESS DESIGN OF AEROSPACE COMPONENTS
David H. Brewer, A. SherifEl-Gizawy, and Jeng-Yih Hwang (Missouri Univ., Columbia.) Jul. 1989 22 p Presented at the Winter Annual Meeting of the American Society of Mechanical Engineers, San Francisco, CA, 10-15 Dec. 1989
(Contract DE-AC04-76DP-00613)
(DE90-002926; KCP-613-4145; CONF-891208-24) Avail: NTIS HC A03/MF A01

A strategy is presented for concurrent product and process design of aerospace components that require high strength and light weight. A modular modeling technique that combines physical and computer models was developed to implement the concurrent product and process design approach. The strategy provides for timely evaluation of the product and process design changes on manufacturing performance as measured by cost effectiveness and productivity indices. Implementation of the strategy is illustrated by a case study from the aerospace industry. Three different product designs for manufacture were tested with eight different processing conditions. The selected processes included conventional hot forging coupled with heavy machining, net-shape forming, and near-net-shape forming plus finish machining. The results indicated that the product and preform geometries, interface friction condition, and speed of deformation used design parameters that could be optimized to reduce costs and improve productivity. The study illustrates clearly the advantage of the strategy realized through reduction of lead time and development costs for product, process, and tooling. DOE

N90-15300# Allied-Signal Aerospace Co., Kansas City, MO. Technical Communications.
AUTOMATED CONVECTION SOLDERING
C. G. Harte Jan. 1989 104 p
(Contract DE-AC04-76DP-00613)
(KCP-613-4005) Avail: NTIS HC A06/MF A01

The critical process parameters are defined which are involved in soldering multiwire/flat flex cables and the feasibility of process control through automated convection soldering is examined. Evolution of the automated process including determination of critical parameters relate to setup, calibration, and operation is addressed. Tests conducted revealed no detrimental effects to the connector insulation from heating connector pins using either a production soldering iron or a focused, heated stream of nitrogen gas. The results also showed that automated convection soldering can be used to improve the quality of solder joints by controlling critical soldering process variables. Full automation of the soldering process using programmable x-y-z tables and a solder paste dispensing system was achieved for flat flex cables. There were a number of advantages gained by using an automated soldering process. The soldering used for reflowing a joint was eliminated, eliminating possible cold solder joint formation. The size of the flux inclusions in the bottom of the solder cup caused by a temperature gradient on the cup when heat was applied was reduced. There was better control of the soldering time and temperature and the quantity of flux and solder added to each

joint. The study became a starting point for the incorporation of new technologies and processes. Author

N90-15301# Lawrence Livermore National Lab., CA.
BENEFITS FROM COMBINING ELECTROPLATING AND PHYSICAL VAPOR DEPOSITION TECHNOLOGIES
J. W. Dini 19 Apr. 1989 12 p Presented at the 3rd International Conference on Surface Modification Technologies, Neuchatel, Switzerland, 28 Aug. - 1 Sep. 1989 Submitted for publication
(Contract W-7405-eng-48)
(DE90-002700; UCRL-100649; CONF-8904292-1) Avail: NTIS HC A03/MF A01

Synergism can be obtained by combining the coating technologies of electroplating and physical vapor deposition. In a number of cases, better coatings and improved adhesion have been obtained with the two processes combined than by using either one by itself. For some applications, parts that could not be fabricated by either process could be produced by combining the two coating methodologies. Quantitative adhesion tests revealed that PVD followed by electroplating produced adherent deposits on Ti, Mo and W. With this combined coating scheme, overall finishing steps are simplified because etching and heating operations are eliminated from the process cycle. Another recent benefit from combining the coating technologies is the demonstrated ability to coat glass with thick copper (1.0 mm) which can be precision machined to an optic surface. These and other examples of combining electroplating and PVD will be discussed in this paper. DOE

32 COMMUNICATIONS AND RADAR

Includes radar; land and global communications; communications theory; and optical communications.

For related information see also *04 Aircraft Communications and Navigation* and *17 Space Communications, Spacecraft Communications, Command and Tracking.* For search and rescue see *03 Air Transportation and Safety,* and *16 Space Transportation.*

N90-15302# National Inst. of Standards and Technology, Boulder, CO. Electromagnetic Fields Div.
ALTERNATIVE TECHNIQUES FOR SOME TYPICAL MIL-STD-461/462 TYPES OF MEASUREMENTS
J. E. Cruz and E. B. Larsen Mar. 1989 43 p Sponsored by Army Aviation Systems Command, Saint Louis, MO
(PB89-235139; NIST/TN-1320) Avail: NTIS HC A03/MF A01; SOD HC $2.50 as 003-003-02946-7 CSCL 20N

Antenna factors determined in a screenroom which was partially loaded with radio frequency (RF) absorbing material, using the two antenna insertion loss technique, are presented. These antenna factors are compared with the antenna factors obtained in an unloaded screenroom, a fully loaded screenroom (anechoic chamber), and at an open field site. In addition, measurements at the 8 corners of a cube were made in partially loaded and fully loaded screenroom to determine the field deviation at the 8 corners of the cube with respect to its center. Also, measurement improvements are quantified for the electric field strength beneath a single wire transmission line, in a partially loaded screenroom. Finally, electric field measurements were made on top of the grounded table in a partially loaded screenroom to determine the field strength variation above the table. Author

N90-15303# Royal Signals and Radar Establishment, Malvern (England).
ON THE PRIVACY PROBLEMS INVOLVED IN ALLOWING ACCESS TO COMPUTERS VIA THE PUBLIC TELEPHONE SYSTEM
S. C. Giess Apr. 1988 15 p
(RSRE-88006; BR106837) Copyright Avail: NTIS HC A03/MF A01

Privacy problems involved in allowing access to computers over the Public Switched Telephone Network (PSTN) are discussed. The relevant aspects of current land-line PSTN and cellular radio operations are described and the weaknesses of the access controls of current computer systems are discussed. Possible solutions that would allow access under a limited set of conditions are described. Author

N90-15304# Massachusetts Inst. of Tech., Lexington. Lincoln Lab.
SLCSAT (SUBMARINE LASER COMMUNICATION SATELLITE) COMMUNICATION SYSTEM DESIGN STUDY
S. L. Bernstein, R. S. Bondurant, E. A. Bucher, V. W. Chan, and F. G. Walther 23 Aug. 1989 103 p
(Contract F19628-85-C-0002)
(AD-A213403; AD-E501157; TR-872) Avail: NTIS HC A06/MF A01 CSCL 25/5

This report summarizes the results of a Lincoln Laboratory study of issues affecting Submarine Laser Communication Satellite (SLCSAT) implementation. The study compares alternative SLCSAT downlink implementations using semiconductor and solid-state lasers in terms of the satellite transmitter power required to provide a given level of communication service. Signal coding is applied to increase transmitter design flexibility by accommodating a wider range of peak-to-average power trade-offs. Adaptive signaling structures which allow more efficient use of transmitter optical power in the face of channel variations are illustrated. Receiver atomic resonance filter alternatives compatible with operation in solar Fraunhofer lines are discussed. Power efficient tunable transmitter technologies, particularly frequency doubled AlGaAs diode lasers, are found to be very attractive. SLCSAT system size estimates are presented for the various technologies presented. High leverage SLCSAT technology development areas are identified. GRA

N90-15305# Massachusetts Inst. of Tech., Lexington. Lincoln Lab.
N-PORT THEORY APPLIED TO BACKSCATTER POLARIMETRY AND DEPOLARIZATION IN FOLIAGE PENETRATION
Richard M. Barnes 1 Aug. 1989 38 p
(Contract F19628-85-C-0002)
(AD-A213437; TT-75; ESD-TR-89-173) Avail: NTIS HC A03/MF A01 CSCL 17/9

The N-port network theory is used to prove results that are frequently stated without proof in the literature, including the symmetry of the polarization scattering matrix in backscattering, the equation for received voltage, and the equations defining Stokes vectors and backscatter Mueller matrices. Appropriate N-port networks are defined for a single-polarized antenna, a dual-polarized antenna, and a backscattering target. An important result is demonstrated: reciprocity (symmetry of the polarization scattering matrix) is meaningful only in the context of the monostatic convention, for which the coordinate system is the same for both transmit and receive. This, in turn, implies a change in the handedness of the coordinate system, so that scattered fields and Stokes vectors are expressed in opposite handedness from incident fields and Stokes vectors. These results are used as tools in the derivation of a new technique for measuring depolarization in foliage penetration (FOPEN). Four polarimetric active radar calibrators (PARCs) are used with an algorithm to completely measure the Mueller matrices describing downward-going and upward-going foliage penetration. GRA

N90-15306# Massachusetts Inst. of Tech., Lexington. Lincoln Lab.
POLARIMETRIC SAR ANTENNA CHARACTERIZATION
Richard M. Barnes and Dennis J. Blejer 28 Jul. 1989 31 p
(Contract F19628-85-C-0002)
(AD-A213438; STD-15; ESD-TR-89-166) Avail: NTIS HC A03/MF A01 CSCL 17/9

A procedure is described for obtaining the two-way polarimetric properties of a Synthetic Aperture Radar (SAR) antenna from one-way measurements in a compact antenna test range. The two-way properties are determined by involving reciprocity and

computing a polarization distortion matrix (PDM). Next, one-way antenna-only measurements are combined with boresight measurements of the complete system to find an overall PDM. Polarimetric distortions caused by the antenna can be compensated using the inverse of the PDM; however, the Advanced Detection Technology Sensor antenna was found to have adequately low crosspolarization without the need for crosspolarization compensation. GRA

N90-15307# Massachusetts Inst. of Tech., Lexington. Lincoln Lab.
FLASHLIGHT RADAR: A THREE-DIMENSIONAL IMAGING RADAR
Dennis J. Blejer, Richard L. Ferranti, Richard M. Barnes, William W. Irving, and Shawn M. Verbout 10 Aug. 1989 46 p
(Contract F19628-85-C-0002)
(AD-A213439; TT-74; ESD-TR-89-167) Avail: NTIS HC A03/MF A01 CSCL 17/9

In support of several programs at Lincoln Laboratory, a small focused-beam polarimetric, millimeter-wave radar scatterometer (an instrument for measuring radar cross section) has been developed. An overview of the design of this Flashlight Radar is presented. Theoretical and empirical studies of antenna performance are discussed. The backscatter theory relating to the characteristics of the Flashlight Radar as a scatterometer is presented, and experimental RCS measurements are compared with theoretical predictions. The data processing steps (polarimetric calibration and compensation, signal processing, and image formation) are described. We show the results of two representative experiments using the Flashlight Radar. The first is a measurement of dihedral and trihedral reflectors with and without radar camouflage. The second is a faster scan of a truck tire, highlighting the radar's fine resolution and its ability to collect three-dimensional data. GRA

N90-15308# Syracuse Univ., NY.
NETWORK SIMULATOR DEFINITION Final Technical Report, Oct. 1986 - Sep. 1987
Pramod K. Varshney Oct. 1989 32 p
(Contract F30602-81-C-0169)
(AD-A213463; RADC-TR-89-167) Avail: NTIS HC A03/MF A01 CSCL 25/5

A white paper was delivered to RADC which provided a detailed analysis of a technique utilizing state transition probability matrices that provided a realistic model of a digital communications channel. As such, the technique offers a computationally viable method for implementing a large number of realistic channel models. This work will feed or transition to efforts eventually implementing this technique to perform network survivability analyses. The results will be incorporated in more comprehensive reports resulting from this work and in the actual implementation of these techniques in RADC's Network Design Laboratory. GRA

N90-15309# Syracuse Univ., NY.
BASEBAND DEVELOPMENT SYSTEM IMPLEMENTATION Final Technical Report, Oct. 1986 - Sep. 1987
Kamal Jabbour Oct. 1989 25 p
(Contract F30602-81-C-0169)
(AD-A213464; RADC-TR-89-168) Avail: NTIS HC A03/MF A01 CSCL 25/5

The real-time implementation of a voiceband communication channel simulator on the TMS32020 digital signal processor is presented. Several channel characteristics are simulated including attenuation distortion, group delay distortion, harmonic distortion, listener echoes, frequency offset, gaussian noise, and impulsive noise. One of the problems encountered in evaluating the performance of various communications equipment such as group delay meters, channel equalizers, and voiceband modems is the need to test them under realistic operating conditions, similar to those encountered during their actual use. These tests could be carried out on actual channels, but the cost and the need to access both ports of a channel make it prohibitive and impractical for all but a few equipment designers. Even then, using real lines gives the designer a limited choice of channel responses. Channel simulation then becomes not only a viable alternative, but a desirable one as well. GRA

N90-15310# Defence and Civil Inst. of Environmental Medicine, Downsview (Ontario).
THE APPLICATION OF QUEUING THEORY TO THE MODELLING OF CP-140 AIRCRAFT COMMUNICATIONS
E. L. Campbell Jun. 1989 39 p
(AD-A213479; DCIEM-89-TR-23) Avail: NTIS HC A03/MF A01 CSCL 12/4

Several authors have argued that queueing models can be used to predict workload and performance of operators under the single channel hypothesis of man's information processing capability. A simple exponential, single server queueing model is used to investigate the application of queueing theory to communication and navigation tasks performed aboard the CP-140 Aurora aircraft. It was anticipated that the model would provide insight into how individual tasks with low workloads combine to create high workload situations. The results, however, indicated problems originating from the data and the model. A new model was recommended as well as an appropriate data collection technique for the application of queueing theory to multi-task situations. GRA

N90-15311# Southern Methodist Univ., Dallas, TX. Dept. of Electrical Engineering.
SPREAD SPECTRUM MOBILE RADIO COMMUNICATIONS Final Report, 1 Sep. 1982 - 31 Aug. 1989
S. C. Gupta, C. Sandeep, and W. Refai 20 Sep. 1989 70 p
(Grant AF-AFOSR-0309-82; AF Proj. 2305)
(AD-A213726; AFOSR-89-1286TR) Avail: NTIS HC A04/MF A01 CSCL 25/2

Two problems are studied. The first is concerned with evaluating the performance of a class of bandwidth efficient modulation schemes in a frequency reuse mobile radio channel. The second problem is concerned with formulating and evaluating the performance of a class of known delay multipath diversity receivers for indoor wireless communication. Several partial response (PRCPM) schemes such as TFM, GMSK and 3RC are compared with regard to their performance in the presence of Adjacent Channel Interference (ACI) and CoChannel Interference (CCI). The performance criteria chosen were average probability of bit error and mean-square cross talk ratio. A comparison of three receiver filters with regard to their ability to reject ACI is also provided. Results indicate that receiver filter length is very important parameter for good performance. The performance of PRCPM schemes is analyzed by considering the combined effects of ACI, CCI and Rayleigh fading. The analysis is extended to the case when space diversity is employed. Results indicate that by using space diversity and maximal Ration Combining significant performance gains can be achieved. GRA

N90-15312# California Univ., Davis. Dept. of Civil Engineering.
THE RADAR-BASED SHORT TERM PREDICTION OF THE TIME-SPACE EVOLUTION OF RAIN FIELDS Final Report, Jan. 1988 - Dec. 1988
M. L. Kavvas and Z. Chen Mar. 1989 24 p
(Contract MIPR-FY7121-88-03752; AF Proj. ILIR)
(AD-A213802; GL-TR-89-0103) Avail: NTIS HC A03/MF A01 CSCL 17/9

A new method is developed in order to track and predict in short term (15 min to hr lead times) the spatial configurations, the velocity vectors and the rain intensity textures of the potentially flood producing rain fields that are detected on a radar scope. First, the rain field is decomposed into simple, tractable elements. Then a statistical adaptive forecasting scheme is developed in order to predict the evolution of each of these elements in time and space. The composition of these elements forms the complete rain field with respect to its spatial configuration, location and rain intensity texture at each prediction lead time. The method is currently being applied to the radar data of rain fields. Some application results are given. GRA

N90-15313# Rome Air Development Center, Griffiss AFB, NY.
PROCEEDINGS OF THE ANTENNA APPLICATIONS SYMPOSIUM, VOLUME 2 Final Report
Paul Mayes Jun. 1989 596 p Symposium held at Illinois Univ., IL, 21-23 Sep. 1988; sponsored in part by RADC and Illinois Univ.
(AD-A213815; RADC-TR-89-121-Vol-2) Avail: NTIS HC A25/MF A04 CSCL 09/1

The Proceedings of the 1988 Antenna Applications symposium is a collection of state-of-the-art papers relating to phased array antennas, multibeam antennas, satellite antennas, microstrip antennas, reflector antennas, HF, VHF, UHF and various other antennas. GRA

N90-15314# Vista Research Corp., Mountain View, CA.
MF/HF MULTISTATIC MID-OCEAN RADAR EXPERIMENTS IN SUPPORT OF SWOTHR (SURFACE-WAVE OVER-THE-HORIZON RADAR) Final Technical Report, Nov. 1987 - Nov. 1988
Alan A. Burns and Daniel S. Naar 15 Sep. 1989 133 p
(Contract DASG60-88-C-0014)
(AD-A213830) Avail: NTIS HC A07/MF A01 CSCL 17/9

A shoreline based multistatic MF/HF radar experiment was fielded in a mid-ocean environment with the objectives of evaluating and demonstrating several aspects of the surface-wave over-the-horizon radar (SWOTHR) concept. Data were collected at 2.8 and 7.8 MHz. A-4 aircraft were used on cooperative targets, whose calculated radar cross reactions were -15 dBsm at 2.8 MHz. An A-4 flying at 300 ft altitude. GRA

N90-15315# Naval Ocean Systems Center, San Diego, CA.
VOICE MULTIPLEX SYSTEM (VMS)
R. J. Kochanski Sep. 1989 3 p Presented at the DOD Fiber Optics Conference, Mar. 1988 Submitted for publication
Sponsored by Naval Sea Systems Command, Washington, DC
(AD-A213902) Avail: NTIS HC A01/MF A01 CSCL 25/5

A three node aircraft status fiber optic Local Area Network (LAN) aboard the USS Constellation will provide interior voice communication and data display information. Point to Point voice communications and aircraft status (normally done on translucent boards and grease pencils) will be supplied to various areas of the ship. System users fall into three categories. Two users, AIR OPS and STRIKE OPS, will construct, modify and broadcast flight schedules; two users, CIC TAO and FDC, will be able to update selected display field e.g. launch time; the remaining users will be constrained to viewing a variety of display files. Each user can scroll through one of ten display files he wishes to view. GRA

N90-15316# Defence Research Establishment, Ottawa (Ontario). Nuclear Effects Section.
DESIGN OF A BOUNDED WAVE EMP (ELECTROMAGNETIC PULSE) SIMULATOR
P. A. A. Sevat Jun. 1989 106 p
(AD-A214137; DREO-1006) Avail: NTIS HC A06/MF A01 CSCL 20/15

Electromagnetic Pulse (EMP) simulators are used to simulate the EMP generated by a nuclear weapon and to harden equipment against the effects of EMP. At present, DREO has a 1 m EMP simulator for testing computer terminal size equipment. To develop the R and D capability for testing larger objects, such as a helicopter, a much bigger threat level facility is required. This report concerns the design of a bounded wave EMP simulator suitable for testing large size equipment. Different types of simulators are described and their pros and cons are discussed. A bounded wave parallel plate type simulator is chosen for it's efficiency and the least environmental impact. Detailed designs are given for 6 m and 10 m parallel plate type wire grid simulators. Electromagnetic fields inside and outside the simulators are computed. Preliminary specifications for a pulse generator required for the simulator are also given. Finally, the electromagnetic fields radiated from the simulator are computed and discussed. GRA

N90-15317# Environmental Research Inst. of Michigan, Ann Arbor. Advanced Concepts Div.
HIGH RESOLUTION IMAGING BY PHASE RETRIEVAL AND DISCRIMINATION USING SPECKLE, VOLUME 1 Final Report, Aug. 1987 - Jan. 1989
J. N. Cederquist, J. R. Fienup, and J. C. Marron Mar. 1989 132 p
(Contract N00014-86-C-0587)
(AD-A214243; ERIM-201600-11-F-Vol-1) Avail: NTIS HC A07/MF A01 CSCL 09/3

Concepts for unconventional sensors capable of high-resolution imaging and parameter estimation for the SDI midcourse discrimination application were developed. The basic sensor consists of a large filled array of small-aperture receivers that measure a laser-illuminated object's Fourier intensity in the aperture of the receiver. Reconstruction of a high-resolution image using a phase retrieval algorithm was investigated via theoretical analysis, computer simulations, and laboratory experiments. In particular, modification of the basic sensor to include a small-aperture, diffraction-limited imager within the array was studied. A method was developed to use the additional low resolution image data in the process of reconstructing a high resolution image. This method first retrieves the Fourier phase over the small aperture of the low resolution imager using the Gerchberg-Saxton algorithm and then proceeds with phase retrieval over the entire array aperture using the iterative Fourier transform algorithm. This method was successfully demonstrated via computer simulations. Reconstruction of the image of a simple two-part object from Fourier intensity data gathered in a laboratory experiment was also achieved. Non-imaging, speckle correlation methods were developed which use the data provided by the large array of receivers to measure rotation rates and separation rates for multiple objects. GRA

N90-15318# Naval Research Lab., Washington, DC. Target Characteristics Branch.
ADAPTIVE CANCELLER LIMITATIONS CAUSED BY I,Q MISMATCH ERRORS Interim Report
Karl Gerlach 5 Sep. 1989 43 p
(AD-A214287; NRL-9115) Avail: NTIS HC A03/MF A01 CSCL 17/9

The effects of I and Q phase, amplitude, and low pass filter (LPF) errors on adaptive cancellers are investigated. The I,Q errors occur because of errors in the synthesis process of the mixers and LPFs designed to be identical for each input channel. These I,Q errors among the channels result in cancellation degradation. Tapped delay line transversal filters have been proposed as a way to compensate for these errors and thus improve cancellation performance. However, it is shown that if there is any LPF mismatch, then transversal filter has a small effect on improving canceller performance. The method of individual I,Q adaptive transversal filter weighting is suggested as a means of eliminating the phase and amplitude errors and making the canceller performance responsive to transversal filter compensation. In addition, the cancellation performance of cascaded mismatched IF and I,Q filters is briefly considered. GRA

N90-15319# Naval Research Lab., Washington, DC.
VOICE/DATA INTEGRATION IN MOBILE RADIO NETWORKS: OVERVIEW AND FUTURE RESEARCH DIRECTIONS
Jeffrey E. Wieselthier and Anthony Ephremides 30 Sep. 1989 83 p
(AD-A214289; NRL-9189) Avail: NTIS HC A05/MF A01 CSCL 25/4

This report gives the results of preliminary background investigations into the problem of voice/data integration in mobile radio networks. The nature of these networks creates a totally new environment, in which the problems of voice/data integration have scarcely been addressed. We review the basics of the voice/data integration problem, and we discuss some of the approaches that have been developed in recent years. Few accurate models are available for optimization and control, and these have generally been limited to operation at a single network

node. The problem of overall network operation and control is extremely complicated, even when issues related to mobile radio network operation are not addressed. We outline our future research plans for this basic research task, which will stress the development of accurate analytical models for performance evaluation and control. Optimization models will be developed by using techniques such as Markovian decision process models. An important goal of this study is the development of a framework for overall network modeling. Toward this goal we plan to develop new network models based on the use of discrete event dynamic systems techniques. GRA

N90-15320# Naval Research Lab., Washington, DC. Human Computer Interaction Lab.
DUAL TASK PERFORMANCE WITH LPC (LINEAR PREDICTIVE CODING) DEGRADED SPEECH IN A SENTENCE VERIFICATION TASK
Astrid Schmidt-Nielsen, Howard J. Kallman, and Corinne Meijer (Maryland Univ., College Park.) 20 Oct. 1989 11 p
(AD-A214298; NRL-MR-6557) Avail: NTIS HC A03/MF A01 CSCL 25/4

The results of a preliminary study on the effects of reduced speech intelligibility on dual task performance are reported. The speech task was a sentence verification task, and the speech degradation was accomplished using a narrowband digital voice transmission system operating with and without random bit errors. The second task was a visual picture sorting task. There was a dual task decrement on the sorting task, and in addition, there was a further decrease in sorts per minute as the speech was increasingly degraded. Reaction time for the speech task increased with the concurrent sorting task, but the dual task condition did not affect speech task error rates. GRA

N90-15321# Air Force Weapons Lab., Kirtland AFB, NM. Aircraft and Missile Div.
PROPOSED ACTIVITIES TO PREPARE FOR TESTING ADVANCED/STEALTH WEAPONS SYSTEMS Technical Publication, Aug. - Sep. 1989
Harold T. Bishop Aug. 1989 21 p
(AF Proj. 3763)
(AD-A214453; WL/NTA-TP-89-001) Avail: NTIS HC A02/MF A01 CSCL 20/15

The B-2 brings new challenges for Electromagnetic Pulse (EMP) Testing. This paper discusses the unique characteristics of the B-2 and develops a time line of activities that need to be completed by the AF Weapons Laboratory before EMP testing of the B-2 begins. GRA

N90-15322# Department of the Navy, Washington, DC.
FOCAL PLANE ANTENNA ARRAY FOR MILLIMETER WAVES Patent Application
William M. Waters, inventor (to Navy) 29 Jun. 1989 26 p
(AD-D014306; US-Patent-Appl-SN-372963) Avail: NTIS HC A03/MF A01 CSCL 09/1

A millimeter wave imaging system receives millimeter wave radiation and provides video imaging signals based thereon. The system comprises an imaging lens for receiving incoming radiation; a focal plane antenna array disposed at the focal plane of the lens on which radiation received by the lens is focussed; and signal processing and display circuitry for processing the output of the antenna array and for producing and displaying corresponding video imaging signals. The focal plane antenna array comprises a planar array of a plurality of conical horns and circular waveguides which, in use, are disposed at the focal plane of the lens; and a stripline detector assembly coupled to the waveguides for detecting the radiation received thereby. The stripline detector assembly comprises a dielectric substrate having a plurality of microstrip conductors embedded therein, each microstrip conductor being coupled to a respective one of the waveguides, and a diode detector being connected to each microstrip conductor. A solid state commutator samples the output of the detectors and provides a resultant video imaging control signal. GRA

33 ELECTRONICS AND ELECTRICAL ENGINEERING

Includes test equipment and maintainability; components, e.g., tunnel diodes and transistors; microminiaturization; and integrated circuitry.

For related information see also *60 Computer Operations and Hardware* and *76 Solid-State Physics*.

N90-15323# Helsinki Univ. of Technology, Espoo (Finland). Radio Lab.
THE 22 GHz RADIOASTRON RECEIVER: DEVELOPMENT OF PROTOTYPE COMPONENTS DURING THE YEAR 1988 Progress Report
Antti Raeisaenen, Juhani Peltonen, Ari Lahtinen, Anne-Tuulia Leino, Petri Piironen, Juhana Ylinen, Petri Jukkala, Seppo Kangasmaa, Ossi Poellaenen, and Hans Somerma Mar. 1989 37 p Prepared in cooperation with Ylinen Electronics Co., Espoo, Netherlands
(PB89-212583; S-177; ISBN-951-754-825-7; ISSN-0355-5712)
Avail: NTIS HC A03/MF A01 CSCL 09C

The progress made in the 22 GHz low noise Radioastron receiver project during the year 1988 is described. A receiver for satellite very long base interferometry radio astronomy is being designed and constructed. The LNA utilizing high electron mobility transistors will be cooled to 80 K, the other parts of the receiver including a phase locked LO at 21.72 GHz, down-conversion to 512 MHz IF, total power detector and noise injection calibration system stay at 300 K physical temperature. Author

N90-15324# Sandia National Labs., Albuquerque, NM.
MEMBRANE AND DURABILITY STUDIES FOR THE ZINC/BROMINE BATTERY
C. Arnold, Jr., R. A. Assink, and P. C. Butler 1989 7 p Presented at the 9th Battery and Electrochemical Contractors' Conference, Alexandria, VA, 13-17 Nov. 1989
(Contract DE-AC04-76DP-00789)
(DE89-016181; SAND-89-1914C; CONF-891132-4) Avail: NTIS HC A02/MF A01

Zinc/bromine flow batteries are being developed for vehicular and utility load leveling applications by Johnson Controls Co. and Energy Research Corp. Problems that were encountered with the zinc/bromine efficiency brought about by permeation of bromine through the separator and limited life caused by attack of the bromine-containing electrolyte on plastic parts, particularly the flow frame. It is shown that large decreases in the bromine transport rates through microporous separators can be achieved with only a minimal loss of conductivity and identify a chemically stable replacement for PVC, a flowframe material. DOE

N90-15325# California Univ., Berkeley. Lawrence Berkeley Lab.
NOVEL HIGH-RATE, ALL SOLID-STATE, SODIUM AND LITHIUM/ORGANOSULFUR BATTERIES
Steven J. Visco, Meilin Liu, Michel B. Armand, and Lutgard C. DeJonghe Aug. 1989 4 p Presented at the 9th Battery and Electrochemical Contractors' Conference, Alexandria, VA, 13-17 Nov. 1989
(Contract DE-AC03-76SF-00098)
(DE90-001014; LBL-27593; CONF-891132-6) Avail: NTIS HC A02/MF A01

This paper is an abstract for a talk to be given at the Battery and Electrochemical Contractor's Conference. The paper gives a brief description of sodium and lithium/organosulfur batteries. DOE

N90-15326# Los Alamos National Lab., NM.
RF TRANSISTOR THERMAL/ELECTRICAL CHARACTERIZATION
Gloria A. Bennett, M. Clark Thompson, Timothy H. Larkin, and James C. Hedstrom Sep. 1989 53 p
(Contract W-7405-eng-36)
(DE90-001427; LA-11633-MS) Avail: NTIS HC A04/MF A01

In recent years there has been a dramatic increase in

semiconductor device power density and dissipated power. The typical result has been to push high-power RF transistors beyond their thermal limit because thermal time constants are much longer than the electrical ability to deposit heat. Dissipated heat removal is complicated by the desire to keep junction temperatures at a low level to maintain a predefined reliability. The purpose of our work was to improve the thermal performance of high-power RF semiconductor devices and their cooling systems. This required developing a series of numerical models to predict device thermal performance. Input for the thermal models was provided by a series of very careful electrical and thermal measurements made on several single transistors mounted in a single-stage amplifier test bed and on a large multistage amplifier. The models were validated using electrical and thermal experimental data taken during the testing. With an accurate quantity for dissipated power and an accurate surface temperature measurement in the radar and transient modes, appropriate thermal resistances were determined. We have determined that transient, or pulse sampling, is a more accurate electrical performance measurement technique than the conventional bench test methods. DOE

N90-15327# Brookhaven National Lab., Upton, NY.
A VERSATILE STEPPING MOTOR CONTROLLER FOR SYSTEMS WITH MANY MOTORS
Shuchen K. Feng and D. Peter Siddons 1989 6 p Presented at the 7th Synchrotron Radiation Instrumentation National Conference, Berkeley, CA, 6-10 Aug. 1989
(Contract DE-AC02-76CH-00016)
(DE90-001556; BNL-43328; CONF-890802-8) Avail: NTIS HC A03/MF A01

A versatile system for controlling beamlines or complex experimental setups is described. The system as currently configured can control up to 32 motors, with all motors capable of full speed operation concurrently. There are 2 limit switch inputs for each motor, and a further input to accept a reference position marker. The motors can be controlled via a front panel keyboard with display, or by a host computer over an IEEE-488 interface. Both methods can be used together if required. There is an emergency stop key on the front panel keyboard to stop the motion of all motors without losing track of the motors' position. DOE

N90-15328# Sandia National Labs., Albuquerque, NM.
NEW DEVICES USING FERROELECTRIC THIN FILMS
C. E. Land, M. A. Butler, and S. J. Martin 1989 4 p Presented at the IEEE International Electron Devices Meeting, Washington, DC, 3-6 Dec. 1989
(Contract DE-AC04-76DP-00789)
(DE90-000789; SAND-89-1607C; CONF-891205-1) Avail: NTIS HC A02/MF A01

Recent developments in the fabrication technologies of ferroelectric thin films in general and of PZT (lead zirconate titanate) and PLZT (lead lanthanum zirconate titanate) thin films in particular have suggested the feasibility of several new devices. Integrated optical devices for information processing and high-speed switching, high-density optical information processing and storage devices and spatial light modulators are some of the applications currently being investigated for these films. Ongoing studies of the longitudinal electrooptic effects and the photosensitivities of PZT and PLZT thin films have established the feasibility of erasable/rewritable optical memories with fast switching and potentially long lifetimes compared to current magneto-optic thin film devices. Some properties of PZT thin films and of new devices based on those properties are described in this paper. DOE

N90-15329# Argonne National Lab., IL. Chemical Technology Div.
STATUS AND RESULTS OF ANL LIFE EVALUATION OF VALVE-REGULATED LEAD-ACID LOAD-LEVELING BATTERIES
W. H. DeLuca, J. F. Miller, C. E. Webster, and R. L. Hogrefe 1989 6 p Presented at the 9th Battery and Electrochemical Contractors' Conference, Alexandria, VA, 13-17 Nov. 1989
(Contract W-31-109-eng-38)
(DE90-001918; CONF-891132-8) Avail: NTIS HC A02/MF A01

Argonne National Laboratory has developed and initiated a three-year life evaluation of both gelled-electrolyte and absorbed-electrolyte valve-regulated lead-acid (VRLA) battery technologies for deep-discharge applications. The objectives are: (1) to use accelerated testing techniques to obtain data within 6 months on VRLA battery life expectancy; and (2) to determine VRLA battery life within a 2 to 3 year time period under temperature and depth-of-discharge (DOD) conditions that simulate those encountered in a utility load-leveling environment. The accelerated life test uses a matrix of operating conditions designed to increase the stress of known failure modes, thereby accelerating the mechanisms that cause battery end-of-life. The primary failure mode is expected to be active material changes caused by charge-discharge cycling (i.e., microstructural and morphological changes, sulfation, mass isolation, loss of surface area, loss of porosity, etc). The test matrix consists of four sets of operating conditions (80 and 100 percent DOD and 30 C and 50 C temperature, which include the stress factors to accelerate failure. DOE

N90-15330# Sandia National Labs., Albuquerque, NM.
SINGLE FLUID SIMULATIONS OF PLASMA OPENINGS SWITCH BEHAVIOR
Michael H. Frese, Steven S. Payne, and Robert E. Peterkin, Jr. (Mission Research Corp., Albuquerque, NM.) Sep. 1989 119 p
(Contract DE-AC04-76DP-00789)
(DE90-002643; SAND-89-7106) Avail: NTIS HC A06/MF A01

The bulk of this report summarizes a study of plasma opening switch (POS) behavior using a two-dimensional single fluid code known as MACH2. This effort developed a model for the plasma motion during injection and the resultant mass distribution at the time of accelerator during that was consistent with the plasma diagnostic information obtained from experiments performed on the PBFA II accelerator at Sandia National Laboratories. The emphasis in this follow-on effort has been on developing a single fluid model of the switching process itself. The ability to model a POS in a reasonable manner with a single fluid code was first demonstrated with the two-dimensional HAM code. Subsequent studies of the operation of a POS that employ HAM and were performed during the last quarter of this research effort are also discussed in this report. Most of the MACH2 simulations discussed in this report were performed on Cray supercomputers at Los Alamos National Laboratory. During the course of this research effort, MACH2 was installed on the Sandia Cray computer. The HAM code already existed on the Sandia Cray and all HAM simulations took place on that computer. The model described here produced current histories qualitatively like those of the PBFA II experiments. DOE

N90-15331# California Univ., Berkeley. Lawrence Berkeley Lab. Engineering Div.
RETRACTABLE GAS COOLED LEADS FOR ASTROMAG
W. L. Pope and M. A. Green Jul. 1989 8 p Presented at the International Cryogenic Materials Conference, Los Angeles, CA, 24-28 Jul. 1989
(Contract DE-AC03-76SF-00098)
(DE90-002679; LBL-27746; CONF-890701-19) Avail: NTIS HC A02/MF A01

This paper discusses retractable gas cooled leads for the ASTROMAG experiment superconducting solenoid which will operate on the space station. The ASTROMAG magnet will be cooled by superfluid helium pumped from a storage tank by a fountain effect pump. Since it is desirable to keep the helium consumption low, retractable gas cooled leads are proposed for the ASTROMAG magnet. These leads, which will be in the cryostat vacuum space, will connect directly with the helium flow circuitry which cools the magnet. The leads will operate in a flow circuit separated from the shields. DOE

N90-15332# Oregon State Univ., Corvallis. Dept. of Electrical and Computer Engineering.
ADJUSTABLE SPEED DRIVE STUDY, JUNE 1985 TO SEPTEMBER 1988. PART 2: APPENDICES
Alan Wallace Aug. 1989 230 p Prepared for Bonneville Power Administration, Portland, OR
(Contract DE-AI79-85BP-23169)
(DE90-002771; DOE/BP-23169/2) Avail: NTIS HC A11/MF A02

Advances in speed control for motors in recent years, notably those in power electronics, have widened the range of application for several adjustable speed drive (ASD) types to include the smaller horsepower sizes. The dc motor drive, formerly in almost universal use for speed control, is being challenged by the high efficiency induction motor/pulse width modulation (PWM) drive; and for special small horsepower size applications, by the permanent magnet motor/PWM inverter drive or by the switched reluctance motor drive. The main characteristics of the several ASD types suitable for small horsepower size applications are discussed, as well as their unwanted side effects: poor power factor, harmonic distortion of the supply, acoustic noise, and electromagnetic interference. A procedure is recommended for determining which, if any, ASD to use. DOE

N90-15333# Lawrence Livermore National Lab., CA.
DESIGN OF A HIGH-GAIN FLUX-COMPRESSION GENERATOR
P. A. Pincosy, D. K. Abe, and J. B. Chase 1 Sep. 1989 10 p Presented at the 5th International Conference on Megagauss Magnetic Field Generation and Related Topics, Novosibirsk, USSR, 3-7 Jul. 1989
(Contract W-7405-eng-48)
(DE90-002795; UCRL-100432; CONF-890710-22) Avail: NTIS HC A02/MF A01

The current gain of a high gain, high explosive helical magnetic-flux-compression generator (HEG) is limited both by nonuniformities in stator expansion and by armature-stator misalignment. Three goals were explored: (1) an output current of at least 2 MA with a current gain greater than 1000 to drive a 150- to 300-nH load; (2) a generator with an acceptably small volume and length; and (3) generator output of a reliable magnitude. DOE

N90-15334# Lawrence Livermore National Lab., CA.
ENHANCEMENT OF MICROCHANNEL PLATE GAIN BY DEPOSITION OF CsI ON THE CHANNEL WALLS
G. D. Power and R. Bonner 1989 12 p Presented at the International Conference on Optical and Opto-electronics and Applied Science, San Diego, CA, 14-18 Aug. 1989
(Contract W-7405-eng-48)
(DE90-003051; UCRL-101663; CONF-8908185-1) Avail: NTIS HC A03/MF A01

Microchannel plate (MCP) detectors of x rays have been in use for several years. The voltage is applied by a coating on the MCP which needs to be thick enough that the propagation losses are small. To enhance the gain loss of a thick Au coating CsI is used to enhance the gain and quantum efficiency of the MCP. It was recently discovered that thick coatings of CsI (2 (mu)m) in both the front and back side of the MCP (normal to bias angle) greatly increases the gain. DOE

N90-15335# Allied-Signal Aerospace Co., Kansas City, MO. Technical Communications.
COMPONENT PRESENCE-ABSENCE DETECTION FOR AUTOMATED VISUAL INSPECTION OF HYBRID MICROCIRCUITS Final Report
D. L. Cheray Feb. 1989 90 p
(Contract DE-AC04-76DP-00613)
(KCP-613-4050) Avail: NTIS HC A05/MF A01

An image-processing algorithm was developed to effectively detect component presence or absence on thin-film hybrid microcircuits by using an IBM-PC-XT-based vision system consisting of a microscope, computer controlled X-Y stage, digital camera, and a commercial image processing board. The algorithm acquires pixel cross section data from each component and determines how well the acquired data correlate with data from an ideal signal. The accuracy of the algorithm relies on classical hypothesis/significance testing concepts used to establish pixel gray level acceptance values for specific types of components, such as chip capacitors, beam lead devices, and gold ribbons. These values define the threshold of visual acceptance. Devices falling below the established threshold level are rejected. Author

N90-15336# Argonne National Lab., IL. Chemical Technology Div.
LIFE EVALUATION OF VALVE-REGULATED LEAD-ACID BATTERIES FOR LOAD-LEVELING APPLICATIONS
W. H. DeLuca, J. F. Miller, C. E. Webster, and R. L. Hogrefe 1989 17 p Presented at the 2nd International Conference on Batteries for Utility Energy Storage, Newport Beach, CA, 24-28 Jul. 1989
(Contract W-31-109-eng-38)
(DE90-002188; CONF-8907170-1) Avail: NTIS HC A03/MF A01

Argonne National Laboratory (ANL) has initiated a test program to evaluate the suitability of valve-regulated lead-acid (VRLA) batteries for use in deep-discharge cycling applications. The program includes the examination of VRLA batteries of the gelled-electrolyte design and the absorbed-electrolyte type. This work is sponsored by the Electric Power Research Institute (EPRI) and the International Lead Zinc Research Organization (ILZRO). While VRLA batteries have found use in standby and uninterruptable power source applications, insufficient data are available to determine their performance and life in repetitive cycling applications. The objectives of the ANL test plan are: (1) to use accelerated testing techniques to obtain evidence within a 6 month test period that indicate an expected life in a utility operating environment; (2) to determine VRLA battery life within a 2 to 3 year time period under conditions (temperature and depth-of-discharge) that closely simulate those encountered in load-leveling operations; and (3) to assess the applicability and usefulness of accelerated testing procedures for deep-discharge cycling applications. DOE

N90-15337# Lawrence Livermore National Lab., CA.
AVALANCHE PHOTOCONDUCTIVE SWITCHING
M. D. Pocha, R. L. Druce, M. J. Wilson, and W. W. Hofer 1989 5 p Presented at the 7th IEEE Pulsed Power Conference, Monterey, CA, 11-14 Jul. 1989 Submitted for publication
(Contract W-7405-eng-48)
(DE90-002980; UCRL-100354; CONF-8907168-1) Avail: NTIS HC A02/MF A01

This paper describes work being done at Lawrence Livermore National Laboratory on the avalanche mode of operation of laser triggered photoconductive switches. We have been able to generate pulses with amplitudes of 2 kV to 35 kV and rise times of 300 to 500 ps, and with a switching gain (energy of output electrical pulse vs energy of trigger optical pulse) of 10(exp 3) to over 10(exp 5). Switches with two very different physical configurations and with two different illumination wavelengths (1.06 micrometer, 890 nm) exhibit very similar behavior. The avalanche switching behavior, therefore, appears to be related to the material parameters rather than the optical wavelength or switch geometry. Considerable further work needs to be done to fully characterize and understand this mode of operation. DOE

N90-15338# Argonne National Lab., IL. Materials and Component Technology Div.
FABRICATION OF SUPERCONDUCTOR COILS
S. E. Dorris, J. T. Dusek, J. J. Picciolo, H. J. Leu, J. P. Singh, A. Cazzato, and R. B. Poeppel Oct. 1989 11 p Presented at the 1st International Ceramic Science and Technology Congress, Anaheim, CA, 31 Oct. - 3 Nov. 1989
(Contract W-31-109-eng-38)
(DE90-003571; CONF-8910120-4) Avail: NTIS HC A03/MF A01

Small coils of superconducting YBa2Cu3O(7-x)(123) can be

formed in the green state using a layered superconductor/insulator tape. In this approach, the insulator prevents contact between the turns of the coil during firing. The insulator must be chemically compatible with 123 during firing, and ideally should match 123 with respect to firing shrinkage and thermal expansion. Fabrication of small coils from the layered superconductor/insulator composites 123/Y2BaCuO5 and 123/BaCuO2 will be discussed. The issue of chemical compatibility will be addressed, and measurements of the firing shrinkage and thermal expansion will be presented for 123 and the two insulators Y2BaO5 and BaCuO2. In addition, the superconducting properties of 123 in the composites will be presented. DOE

N90-15339# Argonne National Lab., IL. Electrochemical Technology Program.
RECHARGABLE MOLTEN-ELECTROLYTE LITHIUM BATTERIES Status Report
T. D. Kaun 1989 15 p Presented at the Electrochemical Society Fall Meeting, Hollywood, FL, 15-20 Oct. 1989
(Contract W-31-109-eng-38)
(DE90-003774; CONF-8910107-4) Avail: NTIS HC A03/MF A01

Lithium-alloy/metal sulfide cells with on molten-halide electrolytes, which are operated in a temperature range of 375 to 474 C, have undergone many improvements in recent years. Cycle life now exceeds 1000 cycles. The Li-alloy/LiCl-LiBr-KBr eutectic (25:37:38 mol percent)/upper-plateau (U.P.) FeS2 cell operated at 400 C has shown excellence performance prospects: 200 Wh/kg specific energy and 200-W/kg specific power. Electrolyte composition has played a dominant role in attaining long-term stable electrochemical performance. A modified LiCl-LiBr-KBr composition (34:32.5:33.5 mol percent) was found to exhibit 25 percent increased ionic conductivity over that of the eutectic. This higher-conductivity electrolyte approximately compensates for the reduced electrolyte content of the electrolyte-starved FeS2 cell. Such a cell has attained of 95 percent utilization of U.P. FeS2 electrode capacity at a comparable cell impedance (0.8 to 1.0 ohm sq cm) to that of an electrolyte-flooded cell. Advancements in cell design and materials application have reduced materials costs and increased battery durability. Both FeS and FeS2 cell tests have demonstrated overcharge tolerance (3 to 5 mA/sq cm) for electrolyte-starved operation with MgO powder separators. DOE

N90-15340# Lawrence Livermore National Lab., CA.
DESIGN OF A CUSTOM LOAD CELL FOR A PRECISION ASSEMBLY APPLICATION
John J. Scott 25 Oct. 1989 26 p
(Contract W-7405-eng-48)
(DE90-004439; UCID-21619) Avail: NTIS HC A03/MF A01

A custom load cell was designed for a precision assembly application where high sensitivity and minimum deflections were required in two orthogonal directions. The application required that the load cell be integrated into existing micropositioning equipment. The aluminum alloy 2024-T81 was used as the spring material to maximize both strain output and gage heat dissipation. Large area, high resistance gages were selected to minimize heat generation and maximize dissipation. Dual Wheatstone bridge circuits were used to resolve the two orthogonal directions. The spring element was designed for optimal mechanical sensitivity, heat dissipation, and ease of fabrication. The described hardware was fabricated and successfully used to support a major LLNL research program. This paper was written as a case study to benefit future designers of such hardware. DOE

N90-15341# Giner, Inc., Waltham, MA.
ADVANCED DOUBLE LAYER CAPACITOR Quarterly Interim Technical Report No. 5, 1 May - 31 Jul. 1989
Anthony B. LaConti, Philip Lessner, and S. Sarangapani Oct. 1989 20 p
(Contract N00014-88-C-0391)
(AD-A213406; AD-E501157; C87A-25) Avail: NTIS HC A03/MF A01 CSCL 09/1

The overall goal of this project is to develop electrochemical capacitors with no liquid electrolyte present. The liquid electrolyte is replaced by a solid ionomer electrolyte. An advantage of these devices over conventional electrochemical capacitors containing free acid would be greater safety and reliability. In the fifth quarter, efforts were concentrated in five areas: preparation and characterization of electrode materials, fabrication of membrane and electrode (M and E) assemblies, development of sealed-cell hardware, capacitance determination by constant load discharge, and determination of cell internal resistance. GRA

N90-15342# Emory Univ., Atlanta, GA.
TRANSPORT PROCESSES THROUGH MONOMOLECULAR FILMS Final Report, 1 Jun. 1986 - 31 May 1989
Frederic M. Menger 5 Sep. 1989 5 p
(Contract DAAL03-86-G-0037)
(AD-A213609; ARO-23780.1-CH-F) Avail: NTIS HC A02/MF A01 CSCL 09/1

Conductance at the water/air interface is unaffected by lipid monolayers at low film pressures and impeded by the monolayers at high film pressures. The conductance data are in conflict with previously published results and, more importantly, they imply that surfaces of biological membranes, in the absence of carriers, serve as poor conduits for ion movement. The results bear on modern theories of energy transduction. GRA

N90-15343# California Univ., San Diego. Dept. of Electrical and Computer Engineering.
COMPUTER AIDED DESIGN OF MONOLITHIC MICROWAVE AND MILLIMETER WAVE INTEGRATED CIRCUITS AND SUBSYSTEMS Final Report, 1 Sep. 1986 - 30 Nov. 1988
Walter H. Ku May 1989 110 p
(Grant AF-AFOSR-0339-86; AF Proj. 2305)
(AD-A213656; AFOSR-89-1266TR) Avail: NTIS HC A06/MF A01 CSCL 09/1

The objectives of this research are to develop analytical and computer aided design techniques for monolithic microwave and millimeter wave integrated circuits (MMIC and MIMIC) and subsystems and to design and fabricate those ICs. Emphasis was placed on heterojunction-based devices, especially the High Electron Mobility Transition (HEMT), for both low noise and medium power microwave and millimeter wave applications. Circuits to be considered include monolithic low noise amplifiers, power amplifiers, and distributed and feedback amplifiers. Interactive computer aided design programs were developed, which include large signal models of InP MISFETs and InGaAs HEMTs. Further, a new unconstrained optimization algorithm POSM was developed and implemented in the general Analysis and Design program for Integrated Circuit (ADIC) for assistance in the design of largesignal nonlinear circuits. GRA

N90-15344# Colorado Univ., Boulder. Dept. of Electrical and Computer Engineering.
INVESTIGATION OF BROADBAND MICROSTRIP ANTENNA STRUCTURES FOR APPLICATION IN MONOLITHIC MILLIMETER WAVE ARRAYS Final Report, 16 May 1986 - 15 Mar. 1989
David C. Chang and E. F. Kuester 15 Oct. 1989 20 p
(Contract N00014-86-K-0417)
(AD-A213856) Avail: NTIS HC A03/MF A01 CSCL 09/1

The development of several ways of accurately yet efficiently modeled behavior of closely spaced microstrip antenna elements is shown. The accuracy was verified by comparison with brute force numerical procedures, and thus suggests that wideband microstrip antennas should be designable with much less difficulty than previously believed. Further, both experimental and numerical evidence was obtained for the proposition that wider bandwidth, and even lower frequency operation of a microstrip patch antenna element can be achieved by arranging many closely coupled narrow strip dipoles together in an appropriate way. An understanding of these effects is not completed; especially since there was no study of the frequency dependence of the radiation properties of these new elements. Design and optimization is also in a very

primitive stage, as accurate modeling of their properties requires numerically intensive methods at this time. Questions of this nature deserve more investigation. GRA

N90-15345# Polytechnic Univ., Brooklyn, NY. Dept. of Electrical Engineering and Computer Science.
ARRAY SIGNAL PROCESSING: NEW TECHNIQUES FOR DIRECTION FINDING AND SPECTRUM ESTIMATION Annual Report, Jan. - Oct. 1989
S. Unnikrishna Pillai Oct. 1989 88 p
(Contract N00014-89-J-1512)
(AD-A213883) Avail: NTIS HC A05/MF A01 CSCL 09/1

New algorithms for estimating signals from sensor output measurements are studied. A complete performance analysis of the proposed algorithms is developed in Appendix A together with new results for resolving two and three uncorrelated/coherent signals. Appendix B concerns with the problem of extending a given set of n autocorrelations so that the power spectral density associated with one-step predictors, the natural extension of maximizing the MMSE for r-step predictors compatible with the given correlations is studied. It is shown here for the first time that the resulting spectrum corresponds to that of a stable ARMA (n, r - 1) process. GRA

N90-15346# Diamond Materials, Inc., State College, PA.
DEVELOPMENT OF HIGH PERFORMANCE BETA-SiC FIELD-EFFECT TRANSISTORS Quarterly Report No. 1, 20 Jul. - 20 Oct. 1989
Richard Koba 26 Oct. 1989 7 p
(Contract N00014-89-C-0207)
(AD-A213885; DMI-TR-89014) Avail: NTIS HC A02/MF A01 CSCL 09/1

On July 20, 1989, Diamond Materials, Inc. (DMI), began work on its SBIR Phase 2 program entitled Development of High-Performance Beta-SiC Field-Effect Transistors. This program is funded by SDIO/IST and is monitored by the Office of Naval Research. During the first quarter of this program, work has concentrated on designing and installing engineering upgrades to DMI's Beta-SiC reactor. These upgrades include an inverted rotating platen and expansion of the gas control system to handle three different dopant source gases. Additionally, the gas plumbing system has been rebuilt to permit instant turn-on and turn-off of dopant gases in order to make p-n junction and doped/undoped junctions during in situ growth. It is anticipated that growth experiments into the formation of undoped Beta-SiC will begin early in the next quarter. GRA

N90-15347# Polytechnic Univ., Farmingdale, NY.
SCANNABLE MILLIMETER WAVE ARRAYS, VOLUME 1 Final Technical Report, Apr. 1984 - Jan. 1987
Arthur A. Oliner Apr. 1989 283 p
(Contract F19628-84-K-0025; AF Proj. 2305)
(AD-A213895; POLY-WRI-1543-88-Vol-1; RADC-TR-89-8-Vol-1)
Avail: NTIS HC A13/MF A02 CSCL 09/1

The complexity usually associated with scanning arrays at millimeter wavelengths produces fabrication difficulties, so that alternative methods are needed that employ simpler structures. Such an alternative scanning approach is described, and a group of new and simpler radiating structures suitable for millimeter-wave applications is presented. The new class of scanning arrays described here achieves scanning in 2-D by creating a 1-D array of leaky wave line source antennas. The individual line sources are fed from one end and are scanned in elevation by electronic means or by varying the frequency. Scanning in the cross plane, and therefore in azimuth, is produced by phase shifters arranged in the feed structure of the 1-D array of line sources. Within the sector of space over which the arrays can be scanned, the radiation has negligible cross polarization, no blind spots and no grating lobes. These are significant and also unusual advantages. The novel features herein relate mainly to the new structures employed for the individual leaky wave line sources and their combination into arrays, but also to analysis of the interactive effects produced when scanning occurs in both planes simultaneously. GRA

N90-15348# Polytechnic Univ., Farmingdale, NY.
SCANNABLE MILLIMETER WAVE ARRAYS, VOLUME 2 Final Technical Report, Apr. 1984 - Jan. 1987
Arthur A. Oliner Apr. 1989 240 p
(Contract F19628-84-K-0025; AF Proj. 2305)
(AD-A213896; POLY-WRI-1543-88-Vol-2; RADC-TR-89-8-Vol-2)
Avail: NTIS HC A11/MF A02 CSCL 09/1

The complexity usually associated with scanning arrays at millimeter wavelengths produces fabrication difficulties, so that alternative methods are needed that employ simpler structures. An alternative scanning approach is described and a group of new and simpler radiating structures suitable for millimeter wave applications is presented. The new class of scanning arrays described here achieves scanning in 2-D by creating a 1-D array of leaky wave line source antennas. The individual line sources are fed from one end and are scanned in elevation by electronic means or by varying the frequency. Scanning in the cross plane, and therefore in azimuth, is produced by phase shifters arranged in the feed structure of the 1-D array of line sources. Within the sector of space over which the arrays can be scanned, the radiation has negligible cross polarization, no blind spots and no grating lobes. GRA

N90-15349# Johns Hopkins Univ., Laurel, MD. Applied Physics Lab.
RECTANGULAR-TO-CIRCULAR WAVEGUIDE TRANSITIONS FOR HIGH-POWER CIRCULAR OVERMODED WAVEGUIDES
William A. Huting Sep. 1989 30 p
(Contract N00039-89-C-5301)
(AD-A213925; JHU/APL-TG-1375) Avail: NTIS HC A03/MF A01 CSCL 09/1

Circular overmoded waveguide is being investigated at The Johns Hopkins University Applied Physics Laboratory (JHU/APL) for low loss, high power microwave transmission near 3.0 GHz. Unfortunately, most microwave power sources and receivers are compatible with single-mode rectangular waveguide rather than overmoded circular waveguide. This problem is usually solved by using metallic waveguide transitions. Design objectives for such transitions include high power carrying capability, low mode conversion, low reflectivity, and low transmission loss. An overview of the theory of waveguide transition operation is presented. It is concluded that a prerequisite for a comprehensive waveguide transition analysis is to solve the uniform waveguide problem for the various cross sections of the transition. A review is included that describes some of the difficulties encountered in developing a computer program package that analyzes uniform waveguides with arbitrary cross sections. A overview is included of important waveguide design issues, several proposed designs, and several different tasks and problem areas one might encounter in a long-term study. GRA

N90-15350# Texas Instruments, Inc., Dallas.
RESEARCH ON GaAs QUANTUM-COUPLED STRUCTURES THAT CAN BE USED AS ELECTRON DEVICES Final Technical Report, 16 Jun. 1987 - 31 Dec. 1988
R. T. Bate, W. R. Frensley, and M. A. Reed 26 Jan. 1989 153 p
(Contract N00014-87-C-0700)
(AD-A214015; TI-08-89-54) Avail: NTIS HC A08/MF A01 CSCL 20/12

The objective of this program was to conduct a theoretical and experimental investigation of the physics of quantum coupled semiconductor structures, with the ultimate goal of developing an integrated circuit technology based on quantum coupled devices. The prototype structure on which both the theoretical and experimental efforts were based was the quantum well resonant tunneling diode. The theoretical work answered questions concerning the dc and small signal ac behavior of this device and some very fundamental questions concerning the theory of open quantum system. The theory of open system is a necessary part of the development of quantum device technology because all electron devices are open systems. The experimental part of the program focused on two areas. The first on the behavior of quantum

dot structures, which are resonant-tunneling diodes whose lateral dimensions (perpendicular to the direction of current flow) have been reduced to quantum scales by microlithography and etching. The spectroscopy of these structures is explained as revealed in their I-V characteristics. The second area of investigation compared the I-V curves of structurally well-characterized resonant-tunneling diodes to theoretical models. The resonant peak voltage sensitively depended on the precise details of the epitaxial structure. The fitting of the theoretical model to the experimental I-V curve appears to be a more precise way to determine these details than any existing direct technique. GRA

N90-15351# Massachusetts Inst. of Tech., Cambridge. Lab. for Computer Science.
VLSI THEORY AND PARALLEL SUPERCOMPUTING
Charles E. Leiserson May 1989 18 p
(Contract N00014-87-K-0825)
(AD-A214035; MIT/LCS/TM-402) Avail: NTIS HC A03/MF A01 CSCL 09/1

Since its inception, VLSI theory has expanded in many fruitful and interesting directions. One major branch is layout theory which studies the efficiency with which graphs can be embedded in the plane according to VLSI design rules. In this survey paper, I review some of the major accomplishments of VLSI layout theory and discuss how layout theory engendered the notion of area and volume-universal networks, such as fat-trees. These scalable networks offer a flexible alternative to the more common hypercube-based networks for inter-connecting the processors of large parallel supercomputers. GRA

N90-15352# Massachusetts Univ., Amherst. Dept. of Electrical and Computer Engineering.
A STUDY OF INTER-INJECTION-LOCKED PHASED ARRAYS Final Report, 1 Aug. 1986 - 31 Jul. 1989
Karl D. Stephan 10 Oct. 1989 27 p
(Contract DAAL03-86-K-0087)
(AD-A214097; ARO-23397.14-EL) Avail: NTIS HC A03/MF A01 CSCL 09/1

Progress in monolithic fabrication of microwave integrated circuits has led to reduced size and weight as well as improved performance of many microwave systems. At the shorter microwave and millimeter wavelengths, however, currently available solid-state devices often fail to deliver the required amount of power, so innovative power-combining schemes are still needed. A study of phased arrays driven by individual active solid-state devices has led to a number discoveries. It was found that the phases of a number of oscillators, if coupled together properly, can be controlled by means of only one master source and phase shifter. In addition to this experimental demonstration, power combing of planar oscillators in a quasioptical cavity was demonstrated and several effects of coupled oscillators were explored. Finally, the potential of resonant-tunnelling-diode oscillators as self-oscillating mixers was investigated. GRA

N90-15353# Pennsylvania State Univ., University Park. Dept. of Electrical Engineering.
TECHNOLOGY OF FAST SPARK GAPS Final Report, Oct. 1987 - Jul. 1988
Ronald B. Standler Sep. 1989 45 p
(Contract DAAL03-87-K-0078)
(AD-A214199; HDL-CR-89-078-1) Avail: NTIS HC A03/MF A01 CSCL 09/1

To protect electronic systems from the effects of electromagnetic pulse (EMP) form nuclear weapons and high-power microwave (HPM) weapons, it is desirable to have fast responding protection components. The gas-filled spark gap appears to be an attractive protection component, except that it can be slow to conduct under certain conditions. This report reviews the literature and presents ideas for construction of a spark gap that will conduct in less than one nanosecond. The key concept to making a fast-responding spark gap is to produce a large number of free electrons quickly. Seven different mechanisms for production of free electrons are reviewed, and several that are relevant to miniature spark gaps for protective applications are discussed in detail. These mechanisms include: inclusion of radioactive materials, photoelectric effect, secondary electrode emission from the anode, and field emission from the cathode. GRA

N90-15354# Paris Univ. (France).
FIRST INTERNATIONAL SYMPOSIUM ON ELECTROCHEMICAL IMPEDANCE SPECTROSCOPY. EXTENDED ABSTRACTS
26 May 1989 202 p Symposium held in Paris, France, 22-26 May 1989
(Contract DAJA45-89-M-0187)
(AD-A214406; R/D-6204-CH-02) Avail: NTIS HC A10/MF A02 CSCL 09/1

First, a brief discussion of Impedance Spectroscopic, its definitions, history, and limits, is presented, integrated with similar material on its subfield, Electrochemical Impedance Spectroscopy. The distinction between unsupported and supported electrolyte conditions is particularly emphasized and theoretical models for unsupported situations, appropriate for most solid electrolytes, is discussed and their implications illustrated. GRA

N90-15355# Department of the Navy, Washington, DC.
LARGE-APERTURE SPARSE ARRAY DETECTOR SYSTEM FOR MULTIPLE EMITTER LOCATION Patent Application
W. F. Gabriel, inventor (to Navy) 25 Nov. 1989 13 p
(AD-D014303; US-Patent-Appl-SN-275873) Avail: NTIS HC A03/MF A01 CSCL 17/11

A detector beamformer array system having a sparse array and a reference array is discussed. The reference array is adapted, according to known principles, to have an output response with one main lobe significantly larger than all other side lobes, and with a substantially flat response. Signals received by both arrays are cross-correlated with one another, and only signals sufficiently correlated are annunciated. The resulting adaptive array system has a resolution even better than that of the sparse array's aperture, and with directional sector selectivity corresponding to the angular width of the reference array's mainlobe, providing a system having high resolution and directional selectivity, but with far fewer sensors than with filled arrays used for this purpose. GRA

N90-15356# Oak Ridge National Lab., TN.
TUNED-CIRCUIT JOHNSON NOISE THERMOMETRY
M. J. Roberts, T. V. Blalock (Tennessee Univ., Knoxville.), and R. L. Shepard 1989 6 p Presented at the 7th Symposium on Space Nuclear Power Systems, Albuquerque, NM, 7-11 Jan. 1990
(Contract DE-AC05-84OR-21400)
(DE89-016221; CONF-900109-5) Avail: NTIS HC A02/MF A01

Three tuned circuits that can be used in Johnson noise thermometry have been analyzed; series resistance-inductance-capacitance (RLC), parallel RLC, and transformer coupled. Tuned circuits allow the temperature of the sensor to be determined by a single noise voltage, which is ideally independent of the resistance of the sensor, thereby reducing the complexity of temperature-measuring systems for space applications. Direct-coupled and transformer-coupled tuned circuits may offer advantage to the SP-100 system designer interfacing with data systems. A study was performed to establish whether the advantages of the ideal tuned circuits would be obtained with real, lossy inductive components and would provide a measurement system independent of aging and temperature effects on sensor resistance. Theoretical mean-squared output voltage dependence on sensor temperature and resistance, output capacitor value, and inductor temperature and resistance are derived for the series and parallel RLC cases. It is shown for tuned circuits using lossless inductors that the mean squared voltage is kT sub R/C, where T sub R is the sensor temperature and C is the capacitance of the capacitor. For lossy inductors and transformers, the mean-squared capacitor voltage is a function of sensor resistance, which may change in an unknown manner during an extended mission. DOE

N90-15357# Sandia National Labs., Albuquerque, NM.
OVERVIEW ON RADIATION EFFECTS IN ELECTRONICS
William R. Dawes, Jr. 1989 7 p Presented at the 7th Symposium on Space Nuclear Power Systems, Albuquerque, NM, 7-11 Jan. 1990
(Contract DE-AC04-76DP-00789)
(DE90-000841; SAND-89-2277C; CONF-900109-6) Avail: NTIS HC A02/MF A01

The radiation spectrum constituents of interest to microelectronics are prompt gamma or x ray, total dose, neutrons (or protons), and cosmic radiation. Each of these constituents has a unique effect upon microelectronic components and requires unique techniques to improve the microelectronic radiation tolerance to such an exposure. The radiation effects are reviewed which are associated with the natural space and nuclear reactor radiation environment, that is to say, total dose, neutrons, and cosmic rays. DOE

N90-15358# Sandia National Labs., Albuquerque, NM.
A NICKEL/HYDROGEN BATTERY FOR PV SYSTEMS
Donald M. Bush 1990 11 p Presented at the 5th Annual Battery Conference on Applications and Advances, Long Beach, CA, 16-18 Jan. 1990
(Contract DE-AC04-76DP-00789)
(DE90-001537; SAND-89-2214C; CONF-900138-1) Avail: NTIS HC A03/MF A01

The nickel/hydrogen battery was developed in the early 1970's as an energy storage subsystem for commercial communication satellites. The advantages offered by nickel/hydrogen batteries, including long life, low maintenance and high reliability, make it very attractive for terrestrial applications such as stand-alone photovoltaic systems. The major drawback to the wider use of the nickel/hydrogen battery is its high initial cost. Sandia National Laboratories has placed cost-shared contracts with Comsat Laboratories and Johnson Controls, Inc., to reduce the cost, and a battery consisting of prismatic cells in a common pressure vessel has evolved. A 7-kWh battery has been on test at Sandia since January 1988 using a flat-plate photovoltaic array for charging. DOE

N90-15359# Sandia National Labs., Albuquerque, NM.
SINTERING STUDIES ON HIGH FIELD VARISTORS
T. J. Garino, B. A. Tuttle, M. S. Harrington, and J. L. Yio Oct. 1989 31 p
(Contract DE-AC04-76DP-00789)
(DE90-002626; SAND-89-0782) Avail: NTIS HC A03/MF A01

We studied the sintering behavior of high field chem-prep ZnO varistors using dilatometry and determined how sintering conditions influence the varistor's electrical properties. The dilatometric results indicated that 95 percent theoretical densities could be obtained with a soak time of only 0.5 hour above 752 C, using a 3 C/min ramp rate; greater shrinkage did not occur for soak temperatures above 752 C. A variety of soak times and temperatures was found to be capable of producing varistors with acceptable electrical properties. The variation in the switching field, E sub s at a current density of 10 A/cm (2), with soak temperature was found to be significantly less for short soak times than for the standard 16 hour soak time. Annealing sintered pellets at 700 C for 4 hours raised the nonlinearity coefficients by approximately 25 percent and decreased E sub s by approximately 10 percent. This uniform decrease in E sub s led to a further reduction in the slope of E sub s vs soak temperature for values of E sub s in the specified range of interest. Further testing of more samples, of samples from different powder batches, and of samples annealed at various temperatures needs to be performed to verify these results. DOE

34 FLUID MECHANICS AND HEAT TRANSFER

Includes boundary layers; hydrodynamics; fluidics; mass transfer; and ablation cooling.

For related information see also *02 Aerodynamics* and *77 Thermodynamics and Statistical Physics.*

N90-15360 Pennsylvania State Univ., University Park.
AN EXPERIMENTAL, ANALYTICAL, AND COMPUTATIONAL INVESTIGATION OF TURBOMACHINERY ROTOR FLOW FIELDS Ph.D. Thesis
Jianjun Zhang 1988 225 p
Avail: Univ. Microfilms Order No. DA8910090

Turbomachinery rotor flow is one of the most complex flow fields. The flow has distinct characteristics in different regions of the flow field. This thesis deals with rotor tip clearance flow, rotor wakes, and a computational study of rotor blade boundary layers. In the experimental investigation, the detailed measurement of a compressor rotor tip clearance region is carried out at two different tip clearance heights. For both clearance heights, the relative stagnation pressure and the axial and tangential velocity components of relative velocities are measured upstream, inside the passage and downstream the rotor, up to about 20 percent of the blade span from the annulus wall. It is found that there are substantial differences in the flow field as the clearance is varied. The losses increase within the passage and their values increase in proportion to tip clearance height. In the analytical study, a momentum integral technique is developed for prediction of two and three dimensional turbulent wakes. The analysis is valid for both near and far wakes. The only assumption involved in the analysis is the existence of similarity in the velocity profiles. This analysis is used to predict the decay characteristics of the wake velocity defect and the variation of wake width. Dissert. Abstr.

N90-15361 Arizona Univ., Tucson.
NUMERICAL INVESTIGATION OF TRANSITION CONTROL OF A FLAT PLATE BOUNDARY LAYER Ph.D. Thesis
Linda Dee Kral 1988 408 p
Avail: Univ. Microfilms Order No. DA8907965

A numerical model has been developed for investigating boundary layer transition control for a three-dimensional flat plate boundary layer. Control of a periodically forced boundary layer in an incompressible fluid is studied using surface heating techniques. The spatially evolving boundary layer is simulated. The Navier-Stokes and energy equations are integrated using a fully implicit finite difference/spectral method. The Navier-Stokes equations are in vorticity-velocity form and are coupled with the energy equation through the viscosity dependence on temperature. Both passive and active methods of control by surface heating are investigated. In passive methods of control, wall heating is employed to alter the stability characteristics of the mean flow. Both uniform and nonuniform surface temperature distributions are studied. In the active control investigations, temperature perturbations are introduced locally along finite heater strips to directly attenuate the instability waves in the flow. A feedback control loop is employed in which a downstream sensor is used to monitor wall shear stress fluctuations. A receptivity study is performed to study how localized temperature perturbations are generated into Tollmien-Schlichting waves. It is shown that narrow heater strips are more receptive in that they maximize the amplitude level of the disturbances in the flow. It is also found that the local temperature fluctuations cause mainly a strong normal gradient in spanwise vorticity. Dissert. Abstr.

N90-15362 Stanford Univ., CA.
DYNAMICS OF A CLASS OF VORTEX RINGS Ph.D. Thesis
Karim R. Shariff 1989 296 p
Avail: Univ. Microfilms Order No. DA8919472

The contour dynamics method is extended to axisymmetric regions containing vorticity varying linearly from the symmetry axis. The method tracks boundaries of vorticity regions, reducing the

dimensionality of the problem by one. A model that retains only the elliptic mode in the core shapes is developed to explain features observed with contour dynamics. Passage and collision interactions of two identical rings are studied, focusing on core deformation, sound generation and stirring of fluid elements. With respect to core deformation, it is found that not only the strain rate but how rapidly it varies is important and accounts for greater susceptibility to vortex tearing than in two-dimensions. For slowly varying strain, core deformations are elastic in the sense that cores remain in equilibrium. With respect to sound generation, good agreement with measurements for colliding rings is obtained and a feature thought to be due to viscosity is shown to be an effect of inviscid core deformation. For passages, core pulsations lead to a component of high frequency and amplitude. Evidence for the presence and importance of this noise source in measured jet noise spectra is provided. Finally, transport of fluid elements in time periodic flows is studied using techniques from non-linear dynamics. The processes of fluid engulfment and rejection for an unsteady vortex ring are studied using the invariant manifolds.
Dissert. Abstr.

N90-15363*# Georgia Inst. of Tech., Atlanta. School of Mechanical Engineering.
FEASIBILITY ANALYSIS OF RECIPROCATING MAGNETIC HEAT PUMPS Final Report
A. V. Larson, J. G. Hartley, Sam V. Shelton, and M. M. Smith Dec. 1989 59 p
(Grant NAG3-600)
(NASA-CR-186205; NAS 1.26:186205) Avail: NTIS HC A04/MF A01 CSCL 20D

A reciprocating gadolinium core in a regeneration fluid column in the warm bore of a superconducting solenoidal magnet is considered for magnetic refrigeration in 3.517 MW (1000 ton) applications. A procedure is presented to minimize the amount of superconducting cable needed in the magnet design. Estimated system capital costs for an ideal magnetic refrigerator of this type become comparable to conventional chillers as the frequency of reciprocation approaches 10 Hertz. A 1-D finite difference analysis of a regenerator cycling at 0.027 Hertz is presented which exhibits some of the features seen in the experiments of G. V. Brown.
Author

N90-15364*# Calspan-Buffalo Univ. Research Center, NY.
DEVELOPMENT OF AN INTEGRATED BEM APPROACH FOR HOT FLUID STRUCTURE INTERACTION Annual Report, Nov. 1988 - Nov. 1989
G. F. Dargush and P. K. Banerjee (State Univ. of New York, Buffalo.) 1989 119 p
(Grant NAG3-712)
(NASA-CR-186214; NAS 1.26:186214) Avail: NTIS HC A06/MF A01 CSCL 20D

The progress made toward the development of a boundary element formulation for the study of hot fluid-structure interaction in Earth-to-Orbit engine hot section components is reported. The convective viscous integral formulation was derived and implemented in the general purpose computer program GP-BEST. The new convective kernel functions, in turn, necessitated the development of refined integration techniques. As a result, however, since the physics of the problem is embedded in these kernels, boundary element solutions can now be obtained at very high Reynolds number. Flow around obstacles can be solved approximately with an efficient linearized boundary-only analysis or, more exactly, by including all of the nonlinearities present in the neighborhood of the obstacle. The other major accomplishment was the development of a comprehensive fluid-structure interaction capability within GP-BEST. This new facility is implemented in a completely general manner, so that quite arbitrary geometry, material properties and boundary conditions may be specified. Thus, a single analysis code (GP-BEST) can be used to run structures-only problems, fluids-only problems, or the combined fluid-structure problem. In all three cases, steady or transient conditions can be selected, with or without thermal effects. Nonlinear analyses can be solved via direct iteration or by employing a modified Newton-Raphson approach.
M.G.

N90-15365# Sandia National Labs., Albuquerque, NM. Fluid and Thermal Sciences Dept.
GELLED PROPELLANT FLOW: BOUNDARY LAYER THEORY FOR POWER-LAW FLUIDS IN A CONVERGING PLANAR CHANNEL
Andrew M. Kraynik, A. S. Geller, and J. H. Glick Oct. 1989 19 p
(Contract DE-AC04-76DP-00789)
(DE90-000923; SAND-89-1720) Avail: NTIS HC A03/MF A01

A boundary layer theory for the flow of power-law fluids in a converging planar channel has been developed. This theory suggests a Reynolds number for such flows, and following numerical integration, a boundary layer thickness. This boundary layer thickness has been used in the generation of a finite element mesh for the finite element code FIDAP. FIDAP was then used to simulate the flow of power-law fluids through a converging channel. Comparison of the analytic and finite element results shows the two to be in very good agreement in regions where entrance and exit effects (not considered in the boundary layer theory) can be neglected.
DOE

N90-15366# Lawrence Livermore National Lab., CA.
TIME-DEPENDENT FREE CONVECTION IN LIQUID METALS
Matthew A. McClelland and Pamela J. Meyer Sep. 1989 5 p
(Contract W-7405-eng-48)
(DE90-000957; UCID-21800) Avail: NTIS HC A01/MF A01

A numerical analysis is given for the time dependent free convection of highly conductive liquids in a rectangular cavity. The results are relevant to the electron beam vaporization of metals. The spatial problem is solved with the Galerkin finite element method, and the time integration is performed with a backward Euler method incorporating step-size control. Streamwise dispersion is introduced for cases involving large convection and numerical instabilities. Results are given for flows in the transition region between laminar and turbulent flow.
DOE

N90-15367# Oak Ridge National Lab., TN. Energy Div.
LABORATORY STUDY OF THE DYNAMIC LOSSES OF A SINGLE SPEED, SPLIT SYSTEM AIR-TO-AIR HEAT PUMP HAVING TUBE AND PLATE FIN HEAT EXCHANGERS, 1985 TO 1986
W. A. Miller Aug. 1989 121 p
(Contract DE-AC05-84OR-21400)
(DE90-000970; ORNL/CON-253) Avail: NTIS HC A07/MF A01

An air-to-air split-system residential heat pump of nominal 9.7-kW (2 3/4-ton) capacity was instrumented and tested in the laboratory. The coefficient of performance capacity, and component efficiencies were measured during cooling and heating mode steady state and cycling conditions and under frosting and defrosting conditions. Improvement in cycling COP and capacity was observed by controlling off-cycle refrigerant migration. Best cycling COP and capacity performance occurred for cycling tests conducted with refrigerant isolated in the indoor heat exchanger during the off cycle, coupled with 2 min of extended indoor blower operation during the off-cycle. The frosting-defrosting experiments were conducted at outdoor ambient temperatures of 4.4, 1.7, and minus 3.8 C (40, 35, and 25 F) and for discrete humidity levels ranging from 60 through 80 percent. Frosting and defrosting algorithms were developed from the data for use in seasonal analysis simulations. Seasonal analysis calculations revealed that the reduction of frosting, defrosting, and cycling losses would result in a 3-year payback of roughly $150 to $300 to the consumer for most climatic regions in the United States.
DOE

N90-15368# Lawrence Livermore National Lab., CA.
IRREVERSIBLE PROCESSES FROM REVERSIBLE MECHANICS
William G. Hoover, Carol G. Hoover, Will J. Evans, Bill Moran, Joanne A. Levatin, and Errol A. Craig Aug. 1989 76 p Presented

at the Conference on Microscopic Simulation of Complex Flows, Brussels, Belgium, 21-25 Aug. 1989
(Contract W-7405-eng-48)
(DE90-001057; UCRL-101907; CONF-8908158-1) Avail: NTIS HC A05/MF A01

We describe and illustrate methods for treating many-body irreversible processes using time-reversible deterministic Nose-Hoover thermostats. In phase space, Lyapunov-unstable multifractal strange attractors are the common feature representing any of these nonequilibrium flows, be they steady, periodic, or transient. This generic behavior is illustrated here for three prototypical one-body problems: steady field-driven diffusive flow in a Galton Board, time-periodic boundary-driven viscous flow of a Lorentz gas, and transient, but time-periodic, compressible flow characterizing a one-dimensional free expansion followed by compression and thermalization. DOE

N90-15369# Institute of Gas Technology, Chicago, IL.
DETERMINATION OF FLOW-REGIME BOUNDARIES FOR COHESIVE PARTICLES Quarterly Report, 20 Dec. 1988 - 19 Mar. 1989
T. M. Knowlton Oct. 1989 40 p
(Contract DE-AC22-88PC-88951)
(DE90-001405; DOE/PC-88951/2) Avail: NTIS HC A03/MF A01

The purpose of this work is to develop a hydrodynamic model capable of predicting the choking/non-choking flow regime boundary for cohesive solids. There are six tasks: (1) preparation of a project work plan, (2) hydrodynamic model development, (3) determination of solid rheological properties for incorporation into the hydrodynamic model, (4) small scale flow tests, (5) large scale flow tests, and (6) comparison of model with data and preparation final report. This quarter the hydrodynamic model was tested (Task 2) against the literature results of Bader, Findlay, and Knowlton (1988). In Task 3, the commercial Hosokawa cohetester was received. Initial testing was conducted to determine the interparticle forces (cohesive forces) of oil shale with an average particle size of 5 microns. DOE

N90-15370# Argonne National Lab., IL. Materials and Components Technology Div.
RECENT ADVANCES IN MAGNETIC HEAT PUMP TECHNOLOGY
Kenneth L. Uherka, John R. Hull, and Paul E. Scheihing (Department of Energy, Washington, DC.) 1989 20 p Presented at the 1989 ASME Winter Annual Meeting, San Francisco, CA, 10-15 Dec. 1989
(Contract W-31-109-eng-38)
(DE89-013289; CONF-891208-7) Avail: NTIS HC A03/MF A01

Magnetic heat pump (MHP)/refrigeration systems, incorporating state-of-the-art superconducting magnet technology, were assessed for industrial applications ranging from the liquefaction of gases (20 K to 100 K range) to cold storage refrigeration for food preservation (250 K to 320 K range). Initial market penetration of MHP technology is anticipated to occur in the gas liquefaction sector, since the performance advantages of magnetic refrigeration cycles relative to gas compression cycles and other conventional systems are more pronounced in the lower temperature ranges. Design options for rotary MHP devices include alternative regeneration schemes to obtain the temperature spans necessary for industrial applications. The results of preliminary design assessment studies indicate that active magnetic regenerator concepts, in which the magnetic working material also serves as the regenerative medium, offer advantages over alternative MHP designs for industrial applications. DOE

N90-15371# Oak Ridge Gaseous Diffusion Plant, TN. Dept. of Systems and Equipment Technology.
COMMENTS ON COMPRESSIBLE FLOW THROUGH BUTTERFLY VALVES
John G. Blakenship 1989 5 p Presented at the ASME Winter Annual Meeting, San Francisco, CA, 10-15 Dec. 1989
(Contract DE-AC05-84OR-21400)
(DE89-015730; K/QT-279; CONF-891208-10) Avail: NTIS HC A01/MF A01

In the flow analysis of process piping systems, it is desirable to treat control valves in the same way as elbow, reducers, expansions, and other pressure loss elements. In a recently reported research program, the compressible flow characteristics of butterfly valves were investigated. Fisher Controls International, Inc., manufacturer of a wide range of control valves, publishes coefficients that can be used to calculate flow characteristics for the full range of valve movement. The use is described of the manufacturer's data to calculate flow parameters as reported by the researchers who investigated compressible flow through butterfly valves. The manufacturer's data produced consistent results and can be used to predict choked flow and the pressure loss for unchoked flow. DOE

N90-15372# Associacao Brasileira de Ciencias Mecanicas, Rio de Janeiro. Dept. Tecnologia de Reatores.
EXPERIMENTAL DETERMINATION OF THE FLUID VELOCITY BY SPECTRAL ANALYSIS OF TEMPERATURE FLUCTUATIONS
Michel Jean Foucrier and Artur J. G. Faya Dec. 1988 4 p In PORTUGESE Presented at the 2nd National Meeting of Thermal Science, Aguas de Lindoia, Brazil, 6-8 Dec. 1988 Submitted for publication
(DE89-636430; INIS-BR-1578; CONF-8812106) Avail: NTIS (US Sales Only) HC A01/MF A01

Local velocities of turbulent closed channel flow were measured applying the noise analysis technique to signals coming from two sensors separated by a known distance. Good agreement was found when comparing experimental data to more accurate measurements. Ranges of Reynolds number and thermocouple spacial separation are recommended. DOE

N90-15373# Associacao Brasileira de Ciencias Mecanicas, Rio de Janeiro.
LAMINAR FORCED CONVECTION INSIDE EXTERNALLY FINNED TUBES
C. A. C. Santos, R. M. Cotta, and M. N. Ozisik (North Carolina State Univ., Raleigh.) Dec. 1988 4 p Presented at the 2nd National Meeting of Thermal Science, Aguas de Lindoia, Brazil, 6-8 Dec. 1988
(DE89-636431; INIS-BR-1579; CONF-8812106) Avail: NTIS (US Sales Only) HC A02/MF A01

Analytical solutions are obtained for thermal entry region problems inside ducts with axially varying heat transfer coefficient, by making use of the ideas in the recently advanced generalized integral transform technique. The analysis is applied to stepwise variations of Biot number that simulate intermitent rows of external fins. Numerical results are obtained for different fin arrangements, in a systematic manner, so as to critically examine the relative merits of wider and/or more numerous fin rows. DOE

N90-15374# Associacao Brasileira de Ciencias Mecanicas, Rio de Janeiro.
STATIC PRESSURE DISTRIBUTION IN AN ANGULAR CHANNEL WITH HELICOIDAL WIRE
Marcelo J. S. deLemos (Instituto Tecnologico de Aeronautica, Sao Paulo, Brazil) Dec. 1988 4 p Presented at the 2nd National Meeting of Thermal Science, Aguas de Lindoia, Brazil, 6-8 Dec. 1988
(DE89-636474; !NIS-BR-1577; CONF-8812106) Avail: NTIS (US Sales Only) HC A02/MF A01

This work reports data on pressure drop distribution along a channel formed by a wire-wrapped rod placed inside a circular tube. This geometry simulates the flow field in the vicinity of a tropical fuel rod of a LMFBR (Liquid-Metal Fast Breeder Reactor) fuel assembly. The working fluid was air and the range for the Reynolds number extended from 2.26 x 10(4) to 4.52 x 10(4). The aspect ratio, P/D and the lead-to-diameter ratio, 1/D, were 1.2 and 15, respectively. DOE

N90-15375# Idaho National Engineering Lab., Idaho Falls.
HEAT TRANSFER IN CONDENSATION OF LITHIUM VAPORS
C. H. Oh and R. P. Wadkins 1988 5 p Presented at the 26th AIAA Aerospace Conference, Reno, NV, 10-14 Jan. 1988 Previously announced in IAA as A88-22257
(Contract DE-AC07-76ID-01570)
(DE90-002081; EGG-M-36587; CONF-880139-5) Avail: NTIS HC A01/MF A01

The results of an experimental investigation into lithium condensation are presented. The objective of the investigation is to find the condensing side heat transfer coefficients of lithium on the vertical flow configuration and to explain the discrepancy between the Nusselt's theory and experimental results. The heat fluxed in these experiments varied from about 13,000 W/sq m at 833 K to 1130,000 W/sq m at 898 K, giving heat transfer coefficients of 4078 W/sq m K to 37805 W/sq m K. These values appear 0.3 to 3 percent of those predicted by the Nusselt theory. Condensate film thickness was calculated by the Nusselt theory. Boiling and condensing of lithium at low, less than atmospheric pressure, appears to be an efficient energy transport mechanism that may find use in space applications or cooling of the first wall in fusion reactors. DOE

N90-15376# California Inst. of Tech., Pasadena.
RAYLEIGH-TAYLOR INSTABILITY IN COMPRESSIBLE FLUIDS Final Report, 1 Oct. 1988 - 30 Sep. 1989
B. Sturtevant 15 Jun. 1989 180 p Prepared for LLNL, CA
(Contract W-7405-eng-48)
(DE90-003027; UCRL-21230) Avail: NTIS HC A09/MF A02

The interaction of shock waves with a contact surface between gases of different densities has been studied experimentally and theoretically. The basic mechanism for the instability of perturbations at the interface is baroclinic vorticity generation resulting from the misalignment of the pressure gradient of the shock and the density gradient of the interface. In the present study, the effects of interface density contrast and initial thickness, and incident wave strength on the development of the instability at the interface are investigated. The experiments were performed in a new vertical shock tube facility where the interaction of a shock wave with either a discontinuous interface, formed by a thin (0.5 (mu)m) plastic membrane, or a continuous interface, created by retracting a metal plate initially separating the two gases, was studied. Air was used on one side of the interface and either helium, carbon dioxide, refrigerant-22 or sulphur hexafluoride was used on the other side as the test gas. Experiments to study the time evolution of quasi-sinusoidal perturbations on a continuous interface have shown that the growth rates are reduced as the interface thickness is increased. Experiments were also performed to observe the schlieren visual thickness of plane discontinuous or continuous interfaces with random small-scale perturbations after interaction with the incident shock wave and its reverberations. DOE

N90-15377# Lawrence Livermore National Lab., CA.
TIME-DEPENDENT FREE CONVECTION IN LOW PRANDTL NUMBER FLUIDS
Matthew A. McClelland 25 Oct. 1989 41 p Presented at the American Institute of Chemical Engineers Annual Meeting, San Francisco, CA, 5-10 Nov. 1989
(Contract W-7405-eng-48)
(DE90-003053; UCRL-100847; CONF-891113-7) Avail: NTIS HC A03/MF A01

A numerical analysis is given for time-dependent free convection in a fluid with small Prandtl number. Consideration is given to a long two-dimensional cavity with vertical walls maintained at different temperatures. The results are relevant to the electron beam vaporization of liquid metals. The spatial problem is solved with the Galerkin finite element method. A backward Euler method with step-size control is used to perform the time integration. For cases involving large convection and numerical instabilities, streamwise diffusion is introduced with an approach sharing some features in common with the Taylor-Galerkin and Petrov-Galerkin methods. Solutions are given for a Prandtl number of 0.015 and Grashof numbers between 10(exp 4) and 10(exp 7), corresponding to the transition region between steady-state laminar and turbulent flow. The results reveal the effects of added streamwise diffusion along with mesh and time-step refinement. DOE

N90-15378# International Centre for Theoretical Physics, Trieste (Italy).
STRUCTURE PROPERTIES OF CONFINED SYSTEMS. HARD SPHERES BETWEEN IDEAL WALLS
M.-E. Boudh-hir May 1989 17 p Submitted for publication
(DE90-600818; IC-89/69) Avail: NTIS (US Sales Only) HC A03/MF A01

An iterative development of the one-particle distribution function, for hard sphere fluids confined between two parallel ideal walls, is proposed. This development allows us to study the confinement effect. It is shown that the confinement has two components. The first, which remains even when the superposition approximation is used, is called compatibility term. The second, due to the fact that the particles may be correlated to the two walls simultaneously, is referred to as coupling term. The latter disappears when the superposition approximation is introduced. These two terms have different magnitudes and ranges. They are governed by the parameters, L, the distance between the walls along which the particles are free to move, (sigma), the hard sphere diameter; and, eta, the packing fraction of the fluid. DOE

N90-15379# Japan Atomic Energy Research Inst., Tokyo. Dept. of Reactor Safety Research.
STABILITY OF NUMERICAL SOLUTIONS FOR STRATIFIED TWO-PHASE FLOW
Tadashi Watanabe and Masashi Hirano Mar. 1989 19 p
(DE90-701646; JAERI-M-89-029) Avail: NTIS (US Sales Only) HC A03/MF A01

The stability of numerical solutions for stratified two-phase flow is studied. The one-dimensional two-fluid model equations with two phasic pressures are solved by using the MINCS code. The stability analysis based on Neumann's method is carried out for the implicit upwind scheme. The stability criterion is shown in terms of the eigenvalue of amplification matrix for the discretized equation system. Through numerical examples, not only the short-wavelength instability but also the long-wavelength wave growth are shown to be well described by the stability limit determined by the eigenvalue. DOE

N90-15380*# Notre Dame Univ., IN. Aerodynamics Lab.
EXPERIMENTAL MEASUREMENTS OF THE LAMINAR SEPARATION BUBBLE ON AN EPPLER 387 AIRFOIL AT LOW REYNOLDS NUMBERS Final Report, 1 Sep. 1988 - 31 Dec. 1989
Gregory M. Cole and Thomas J. Mueller Jan. 1990 149 p
(Grant NsG-1419)
(NASA-CR-186263; NAS 1.26:186263; UNDAS-1419-FR) Avail: NTIS HC A07/MF A01 CSCL 20D

An experimental investigation was conducted to measure the flow velocity in the boundary layer of an Eppler 387 airfoil. In particular, the laminar separation bubble that this airfoil exhibits at low Reynolds numbers was the focus. Single component laser Doppler velocimetry data were obtained at a Reynolds number of 100,000 at an angle of attack of 2.0 degree. Static Pressure and flow visualization data for the Eppler 387 airfoil were also obtained. The difficulty in obtaining accurate experimental measurements at low Reynolds numbers is addressed. Laser Doppler velocimetry boundary layer data for the NACA 663-018 airfoil at a Reynolds number of 160,000 and angle of attack of 12 degree is also presented. Author

N90-15381*# Old Dominion Univ., Norfolk, VA.
EXPLICIT AND IMPLICIT CALCULATIONS OF TURBULENT CAVITY FLOWS WITH AND WITHOUT YAW ANGLE M.S. Thesis
Guan-Wei Yen Aug. 1989 123 p Prepared in cooperation with National Cheng-Kung Univ., Tainan (Taiwan)

(Grant NAG1-664)
(NASA-CR-186293; NAS 1.26:186293) Avail: NTIS HC A06/MF A01 CSCL 20D

Computations were performed to simulate turbulent supersonic flows past three-dimensional deep cavities with and without yaw. Simulation of these self-sustained oscillatory flows were generated through time accurate solutions of the Reynolds averaged complete Navier-Stokes equations using two different schemes: (1) MacCormack, finite-difference; and (2) implicit, upwind, finite-volume schemes. The second scheme, which is approximately 30 percent faster, is found to produce better time accurate results. The Reynolds stresses were modeled, using the Baldwin-Lomax algebraic turbulence model with certain modifications. The computational results include instantaneous and time averaged flow properties everywhere in the computational domain. Time series analyses were performed for the instantaneous pressure values on the cavity floor. The time averaged computational results show good agreement with the experimental data along the cavity floor and walls. When the yaw angle is nonzero, there is no longer a single length scale (length-to-depth ratio) for the flow, as is the case for zero yaw angle flow. The dominant directions and inclinations of the vortices are dramatically different for this nonsymmetric flow. The vortex shedding from the cavity into the mainstream flow is captured computationally. This phenomenon, which is due to the oscillation of the shear layer, is confirmed by the solutions of both schemes. Author

N90-15382# Massachusetts Inst. of Tech., Cambridge. Dept. of Ocean Engineering.

GAS TURBINE REGENERATORS: A METHOD FOR SELECTING THE OPTIMUM PLATE-FINNED SURFACE PAIR FOR MINIMUM CORE VOLUME M.S. Thesis

Joseph F. Campbell, Jr. Jun. 1989 91 p
(Contract N00228-89-G-0580)
(AD-A213430) Avail: NTIS HC A05/MF A01 CSCL 21/5

Based on a power law curve fit for the Soland et al. 2 modification of the Kays-London 1 way of presenting heat exchanger performance, a closed-form for sizing counterflow regenerators is derived. After applying this method to many Kays-London plate-finned surfaces, the optimum surface pair for minimum heat exchanger core volume is found to be 1/9 to 24.12 and 1/10 to 19.35. In general, the minimum core volume will be obtained by following a three step process: select a surface for the high pressure side having the minimum plate spacing commensurate with cleaning constraints; list all other available surfaces with plate spacings nearly equal to the selected high pressure side plate spacing; and select from this list the surface with the minimum hydraulic diameter for use on the low pressure side. GRA

N90-15383# Massachusetts Inst. of Tech., Cambridge. Dept. of Ocean Engineering.

A CONING MOTION APPARATUS FOR HYDRODYNAMIC MODEL TESTING IN A NON-PLANAR CROSS-FLOW M.S. Thesis

David C. Johnson Jun. 1989 140 p
(Contract N00228-89-G-0580)
(AD-A213431) Avail: NTIS HC A07/MF A01 CSCL 20/4

As part of continuing research into the flow about slender bodies of revolution, a coning motion apparatus for hydrodynamic model testing was built and demonstrated. This is the first known use of a rotary balance apparatus for external flow hydrodynamic applications. The vorticity shed by the hull and appendages creates a wake field that interacts with the velocity distribution over the vehicle's surface. This in turn effects the surface pressure distribution and thus, when integrated over the body's surface, the total force on the hull/appendage combination. It is this interaction that prevents a closed-form analytic solution to the problem. GRA

N90-15384# Massachusetts Inst. of Tech., Cambridge. Dept. of Ocean Engineering.

AN EXPERIMENTAL STUDY OF THE TIME-DEPENDENT BEHAVIOR OF THE APPENDAGE-BODY JUNCTION VORTEX M.S. Thesis

Joseph F. Fallone Jun. 1989 97 p
(Contracts N00014-86-J-1218; N00014-87-K-0422)
(AD-A213465) Avail: NTIS HC A05/MF A01 CSCL 20/4

The 3-D flow in the region where a turbulent boundary layer encounters an appendage is characterized by the formation of a junction root vortex. The formation of this vortex can be attributed to the adverse pressure gradient upstream of the appendage. One major area of concern is the temporal behavior of the vortex. Fluctuations in the size and/or location of the vortex can cause degradation of downstream components or excitation of local structures. Recent studies in wind tunnels have identified a bi-modal characteristic in the structure of the vortex. An experimental investigation of the time dependent behavior of the junction root vortex was conducted using MIT's variable pressure water tunnel and laser doppler anemometry system. Data was collected at various points forward of a modified NACA 0020 section appendage mounted on a splitter plate and analyzed using off-line Discrete Fourier Transform (DFT) analysis. The data was gathered at tunnel speeds of 10 and 20 ft/sec using an analog-to-digital acquisition system. Velocity probability distributions using a fully digital acquisition system were also plotted to identify the bi-modal structure. The spectra generated from the DFT analysis were inconclusive. No distinct frequencies or pattern of frequencies attributable to the flow could be identified. Fluctuations within the spectra made their accuracy questionable. The existence of the bi-modal structure was confirmed by the velocity probability distributions. GRA

N90-15385# Wisconsin Univ., Madison. Center for Mathematical Sciences.

NEW TRANSIENT ALGORITHMS FOR NON-NEWTONIAN FLOWS Technical Summary Report

David S. Malkus, Yi-Cheng Tsai, and Robert W. Kolkka (Michigan Technological Univ., Houghton.) 11 Oct. 1989 31 p
(Contract DAAL03-87-K-0036; AF-AFOSR-0141-85; AF-AFOSR-0191-87; AF-AFOSR-0220-89; NSF DMS-86-20303; NSF DMS-89-07264; NSF DMS-87-12058; NSF CTS-89-10518)
(AD-A213494; CMS-TSR-90-14) Avail: NTIS HC A03/MF A01 CSCL 20/4

A fully dynamic method for shear flows is presented that treats the short time scales associated with Newtonian viscosity (or short relaxation processes) and shear wave propagation implicitly, while treating the long relaxation processes explicitly. The method is generalized to flows with non-constant strain rate histories in the context of the well known fiber drawing problem. The linearized stability of the methods is analyzed, and extension of these methods to planar flows is given. The approach taken in the case of non-trivial deformation histories is that of an Oldroyd Difference Quotient (ODQ) that approximates the convected derivatives of the differential constitutive equation in Lagrangian fashion along the portion of the streamline upstream of the stress evaluation point. Techniques based on earlier ideas of drift function tracking are used to develop a weighting scheme for the ODQ that permits the use of low order, C sub 0 stress elements. The numerical methods are discussed and analyzed in the context of a Johnson-Segalman fluid model with added Newtonian viscosity. The resulting initial boundary value problem is globally well posed and possesses the key feature: the steady shear stress is a non-monotone function of the strain rate. Such models will be seen to display the spurt phenomenon in plane Poiseuille flow and apparently related phenomena in step strain experiments. GRA

N90-15386# Kentucky Univ., Lexington. Dept. of Mechanical Engineering.

HIGH POWER DENSITY SPRAY COOLING Interim Report, Jul. 1987 - Aug. 1988

Donald E. Tilton, Martin R. Pais, and Louis C. Chow Jul. 1989

69 p
(Contract F33615-87-C-2777)
(AD-A213575; UK-ME-88-07; WRDC-TR-89-2082) Avail: NTIS HC A04/MF A01 CSCL 13/9

The research reported describes experimental and theoretical investigations of high power density evaporative spray cooling. Preliminary experiments demonstrating heat fluxes greater than 1,000 W/sq cm were conducted. Extensive laser phase Doppler measurements of spray characteristics were also taken. These measurements provided valuable insight into the heat transfer process. An in-depth analysis was conducted to determine the mechanisms responsible for critical heat flux. Theoretical modeling was also conducted to determine the most desirable heat transfer conditions. After analysis of these results, an improved experimental apparatus was designed and fabricated. The new apparatus provided greater experimental control and improve accuracy. New tests were conducted in which the critical heat flux was increased, and the heat transfer efficiency was greatly improved. These results are compared to those of previous researchers, and indicated substantial improvement. GRA

N90-15387# Michigan Univ., Ann Arbor. Gas Dynamics Labs.
DENSE-SPRAY PROPERTIES: STRUCTURE AND TURBULENCE MODULATION Final Report, 15 Jul. 1985 - 14 Jul. 1989
G. A. Ruff, R. N. Parthasarathy, and G. M. Faeth Aug. 1989 119 p
(Grant AF-AFOSR-0244-85; AF Proj. 2308)
(AD-A213671; AFOSR-89-1284TR) Avail: NTIS HC A06/MF A01 CSCL 20/4

A theoretical and experimental study of aspects of dense sprays is described, considering: the structure and mixing properties of the near injector, dense spray region of pressure atomized sprays; and the direct effect of particle (drop) motion on the turbulence properties of multiphase flows (which is often called turbulence modulation). The structure of dense sprays was studied using large scale (9.5 and 19.1 mm jet exit diameters) water sprays in still air. Measurements included: flow visualization using flash photography; liquid volume fractions using gamma ray absorption; streamwise mean and fluctuating velocities at the injector exit, and entrainment velocities, using laser velocimetry; and dispersed phase properties using single- and double-flash holography. Predictions based on the locally homogeneous flow (LHF) approximation of multiphase flow theory were evaluated using the measurements. Measurements showed that mixing was strongly influenced by the degree of flow development at the injector exit and the breakup regime: fully developed flow and atomization breakup yielded the fastest mixing rates. Turbulence modulation was studied by considering nearly monodisperse spherical glass particles falling in a stagnant water bath, where effects of turbulence modulation were responsible for the entire turbulence field. Measurements included phase velocities, as well as the temporal and spatial correlations of continuous phase velocities, using a two-point phase discriminating laser velocimeters, and calibration of particle motion properties using motion picture shadowgraphs. GRA

N90-15388# Ergenics, Inc., Wyckoff, NJ.
DESIGN AND FABRICATE A METALLIC HYDRIDE HEAT PUMP WITH A COOLING CAPACITY OF 9000 BTU/H Final Report
P. M. Golben and E. L. Huston 7 Feb. 1989 236 p
(Contract DAAK70-86-C-0123)
(AD-A213756) Avail: NTIS HC A11/MF A01 CSCL 13/1

Existing Environmental Control Equipment (ECE) for truck mounted electronic communication shelters are powered by Army generator sets. Fully 50 percent of the generated power is consumed by the ECE. Innovative ECE technology was sought to reduce this electrical load. The heat content of the diesel generator exhaust gas was viewed as a potential waste heat source for thermally driven ECE systems. Metal hydride heat pumps were proposed as for this application. The purpose of this contract was to produce a prototype metal hydride air conditioner of 9000 BTU/H capacity and compare system size, weight, electric power requirements and performance with a standard Army air conditioner of the same capacity. GRA

N90-15389# Ballistic Research Labs., Aberdeen Proving Ground, MD.
AN ALGEBRAIC TURBULENCE MODEL FOR FLOW SEPARATION CAUSED BY FORWARD AND BACKWARD FACING STEPS
James E. Danberg and Nisheeth R. Patel Dec. 1989 34 p
(AD-A213800; BRL-MR-3791) Avail: NTIS HC A03/MF A01 CSCL 20/4

The Baldwin-Lomax algebraic turbulence model is currently widely used in numerical Navier-Stokes codes primarily because it avoids the problems of calculating a boundary layer thickness. However, two of its disadvantages are: (1) it requires the evaluation of a maximum in the moment of vorticity with respect to the surface which is ambiguous under certain conditions and, (2) its applicability to some separated flows is unclear. The basis for the Baldwin-Lomax method is reviewed in detail particularly as it applies to locally separated flows. This leads to a reformulation of the Baldwin-Lomax method. The modification uses a velocity scale, at each separated flow station, which is the difference between the maximum velocity and the minimum velocity (considered negative in separated flows with recirculation regions). The length scale is defined in terms of the ratio of this velocity scale to the maximum vorticity. Other modifications are included which adapt the model to forward and rearward facing step applications. GRA

N90-15390# Air Force Inst. of Tech., Wright-Patterson AFB, OH. School of Engineering.
SOLUTION OF POTENTIAL FLOW PAST AN ELASTIC BODY USING THE BOUNDARY ELEMENT TECHNIQUE M.S. Thesis
Norma F. Taylor Dec. 1988 128 p
(AD-A213843; AFIT/GAE/AA/88D-37) Avail: NTIS HC A07/MF A01 CSCL 20/4

This thesis describes the development of a Fortran computer code which models the interaction between an incompressible, potential flow and a homogeneous, elastic structure. The boundary element technique was chosen because of its ability to numerically approximate both the fluid and structural behavior with a common definition of the fluid/structure boundary. The ability to accurately model solid and fluid boundaries can be quite important in the fields of aeroelasticity and structural analysis. The nature of these boundaries is what determines the final solution to a problem of fluid flow past an elastic body. Often the complexity of defining and tracking the boundary and its associated boundary conditions has led the user to assumptions of rigid bodies, and therefore rigid boundaries. Certainly the tasks of defining the domain grids for finite difference and finite element techniques have not simplified this process. In the computer code developed for this thesis the fluid and structural governing equations are simultaneously solved to determine the pressure about the structure and the corresponding elastic deformations. The deformations are applied to the original boundary, resulting in a new geometry. This new geometry is used to recalculate the pressure field about the structure, and the process is iterated until a final steady-state solution is obtained. GRA

N90-15391# Pennsylvania State Univ., University Park. Applied Research Lab.
MODIFICATIONS OF THE PENN STATE BOUNDARY LAYER RESEARCH FACILITY FOR BOUNDARY LAYER/STRUCTURE INTERACTION EXPERIMENTAL RESEARCH
C. B. Burroughs 23 Aug. 1989 71 p
(Contract N00039-88-C-0051)
(AD-A213874; TM-89-38) Avail: NTIS HC A04/MF A01 CSCL 20/4

Modifications to the Penn State Boundary Layer Research Facility (BLRF) were made so that low wavenumber Turbulent Boundary Layer (TBL) wall pressure fluctuation spectra can be measured. In addition, fundamental experimental research on boundary layer/structure interaction can be conducted.

Modifications include the design and fabrication of a new test section to accommodate a long flat elastic test plate in contact with the boundary layer and extensive treatments to reduce background vibration levels in the test plate. The design, fabrication and installation of these modifications are described. GRA

N90-15392# Iowa Univ., Iowa City. Inst. of Hydraulic Research.
NONLINEAR VISCOUS WAVES PRODUCED BY AN IMPULSIVELY MOVING PLATE Technical Report, 1 Feb. - 30 Sep. 1989
S. A. Yang and Allen T. Chwang Sep. 1989 86 p
(Contract N00014-89-J-1581)
(AD-A214014; IIHR-332) Avail: NTIS HC A05/MF A01 CSCL 20/4

The free surface flow generated by an impulsively accelerating, surface piercing, vertical plate are studied numerically as well as experimentally. The 2-D, unsteady Navier-Stokes equations are discretized using the finite analytic scheme which incorporates the analytic solution into the locally linearized differential equations. The continuity equation and the dynamic boundary conditions on normal and tangential stresses at the free surface are applied to determine the pressure and two velocity components at the free surface. The kinematic boundary condition on the free surface provides the movement of the free surface. A series of experiments is carried out. The flat vertical plate is fixed on a towing carriage which is set off by suddenly dropping a weight bucket through a connecting steel cable in a pulley system. A data acquisition system is used for controlling the sampling process and for recording the signal output. The agreement of the free surface profile and the pressure distribution between the numerical results and the experimental measurements is fairly good. The mathematical singularity, which is predicted by the potential flow theory, at the contact line between the plate and the free surface is not observed in the physical experiments. The water surface in front of the vertical plate simply rises up during the initial stage of the acceleration of the plate. GRA

N90-15393# New York Univ., New York. Inst. of Mathematical Sciences.
ENHANCED RESOLUTION CONCEPTS IN LARGE SCALE SCIENTIFIC COMPUTING Final Report, 1 Sep. 1986 - 31 Aug. 1989
James Glimm 31 Oct. 1989 9 p
(Contract DAAL03-86-G-0026)
(AD-A214095; ARO-23770.1-MAF) Avail: NTIS HC A02/MF A01 CSCL 20/4

Efficient numerical procedures were found for the solution of shock wave interactions in gas dynamics. The wave interactions were idealized as point interactions and were thus equivalent to the solution of Riemann problems. The equation of state was taken in a very general form, as tabular data. The essential problem solved was the use of tabular equation of state data for description real materials and the efficient solution of Riemann problems in this context. GRA

N90-15394# West Virginia Univ., Morgantown. Dept. of Mechanical and Aerospace Engineering.
REDUCTION OF EROSION IN ELBOWS DUE TO FLOW MODIFICATIONS, PHASE 2 Final Report
E. K. Johnson and K. H. Means Jun. 1989 57 p
(Contract DE-AC21-84MC-21349)
(DE89-011702; DOE/MC-21349/2738) Avail: NTIS HC A03/MF A01

The objective of this project was the reduction of erosion in elbows (bends), in pneumatic transport systems, due to flow field modification. Air was to be injected into a bend, thus modifying the flow so that the eroding particles are kept from the surfaces. The goal was to achieve erosion rates less than those of blind tees. A fluidized blind tee and two different air injection bends were selected for detailed investigation. The detailed investigation demonstrated that the air injection bends significantly reduced erosion rates, but never developed an erosion rate less than that for a blind tee. Although the air injection bends' erosion rates approached those for a blind tee; technically the blind tee represents a simpler system and consequently will probably remain the choice of engineers concerned with erosion of bends. DOE

N90-15395# Associacao Brasileira de Ciencias Mecanicas, Rio de Janeiro. Dept. de Engenharia Mecanica.
INVESTIGATION OF LOADS GENERATED BY TEMPERATURE TRANSIENTS IN PIPES
C. E. Maneschy Dec. 1988 4 p Presented at the 2nd National Meeting of Thermal Science, Aguas de Lindoia, Brazil, 6-8 Dec. 1988
(DE89-636433; INIS-BR-1581; CONF-8812106) Avail: NTIS (US Sales Only) HC A02/MF A01

The effect of a transient temperature on the stress distribution due to a fluid flowing through a pipe is analytically determined using the definition of a variable called in this paper shifted time. This variable, which is related to the axial coordinate, the average fluid velocity and the real time, is defined to make the transient thermal problem one-dimensional. The stresses are then calculated from the temperature solution using the linear theory of viscoelasticity. DOE

N90-15396# Los Alamos National Lab., NM. Advanced Engineering Technology Dept.
RADIAL HEAT FLUX LIMITS IN POTASSIUM HEAT PIPES: AN EXPERIMENTAL AND ANALYTICAL INVESTIGATION
K. A. Woloshun, J. Tom Sena, E. S. Keddy, and Michael A. Merrigan 1989 6 p Presented at the 7th Symposium on Space Nuclear Power Systems, Albuquerque, NM, 7-11 Jan. 1990
(Contract W-7405-eng-36)
(DE90-002655; LA-UR-89-3365; CONF-900109-14) Avail: NTIS HC A02/MF A01

A radial flux limit of 147 W/sq cm at the wetted inner tube wall has been demonstrated with a Nb-1 percent Zr/K heat pipe, a flux 5 times greater than the previously accepted safe design level of 25 to 30 W/sq cm. The wick structure was an annular gap type fabricated from 100 times 100 mesh Nb-1 percent Zr screen. Rigorous fabrication and cleaning procedures are believed to be critical to good wetting, resulting in significantly reduced active nucleation site size and a higher boiling limit. The procedure used to clean this heat pipe included acid wash, Freon-TF degrease, ethanol wash, high-vacuum firing, and operation as a lithium heat pipe. A heat pipe boiling limit model, based on the active nucleation site radius, is described. An active nucleation site radius of 6 times 10(exp -6) m 2.4 times 10(exp -4) in. correlates the radial flux boiling limit measured in these tests. DOE

N90-15397 ESDU International Ltd., London (England).
REFLUX CONDENSATION IN VERTICAL TUBES
Nov. 1989 41 p
(ESDU-89038; ISBN-0-85679-711-1; ISSN-0141-402X) Avail: ESDU

ESDU 89038 summarizes the advantages and disadvantages of reflux condensation in vertical tubes, in which the vapor enters the heat exchanger tube bundle at the bottom and the condensate flows down under gravity. The mechanism of flooding, when the condensate is carried upwards rather than draining to the bottom is discussed and available flooding data are compared with two successful correlations to establish their accuracy. Limitations of the recommended correlation are stressed and methods of improving the flooding performance are suggested. Data for condensate film heat transfer are also compared with an existing correlation for co-current flow of vapor and condensate and suggest that the correlation can be used in the reflux situation. Pressure drop is discussed, and it is concluded that under most operating conditions it will be low and often negligible. A step-by-step calculation procedure for the design of a reflux condenser, or for performance rating an existing condenser, is given for either a single- or a multicomponent vapor, and is illustrated with an example. ESDU

35 INSTRUMENTATION AND PHOTOGRAPHY

Includes remote sensors; measuring instruments and gages; detectors; cameras and photographic supplies; and holography.

For aerial photography see *43 Earth Resources and Remote Sensing.* For related information see also *06 Aircraft Instrumentation,* and *19 Spacecraft Instrumentation.*

N90-15398# Transportation Research Board, Washington, DC.
GEOTECHNICAL INSTRUMENTATION
G. E. Green, P. E. Mikkelsen, P. W. Mayne, D. D. Frost, and C. H. Dowding 1988 97 p
(PB89-198675; TRB/TRR-1169; ISBN-0-309-04705-6; LC-88-34472) Avail: NTIS HC A05/MF A01 CSCL 14B

The 11 papers in the report deal with the following areas: deformation measurements with inclinometers; dilatometer experience in Washington, D.C., and vicinity; ground vibration monitoring instrumentation and computerized surveillance; instrumentation for tests of piles subjected to axial loading; use of the wave equation by the North Carolina Department of Transportation; NYSDOT's construction control of pile foundations with dynamic pile testing; discussion of procedures for the determination of pile capacity; modern specification of driven pile work; analysis of laterally loaded piles with nonlinear bending behavior; unified design of piles and pile groups, and LTBASE, a computer program for the analysis of laterally loaded piers including base and slope effects. Author

N90-15399*# National Aeronautics and Space Administration. Ames Research Center, Moffett Field, CA.
CALIBRATION OF SEVEN-HOLE PRESSURE PROBES FOR USE IN FLUID FLOWS WITH LARGE ANGULARITY
Gregory G. Zilliac Dec. 1989 46 p
(NASA-TM-102200; A-89163; NAS 1.15:102200) Avail: NTIS HC A03/MF A01 CSCL 14B

Described here is the calibration of a non-nulling, conical, seven-hole pressure probe over a large range of flow onset angles. The calibration procedure is based on the use of differential pressures to determine the three components of velocity. The method allows determination of the flow angle to within 0.5 deg and velocity magnitude to approximately 1.0 percent. Also included is an examination of the factors which limit the use of the probe, a description of the measurement chain, an error analysis, and a typical experimental result. In addition, a new general analytical model of pressure probe behavior is described and the validity of the model is demonstrated by comparing it with experimentally measured calibration data for a three-hole yaw meter and a seven-hole probe. Author

N90-15400*# Cornell Univ., Ithaca, NY. Dept. of Computer Science.
IMPLEMENTING FAULT-TOLERANT SENSORS
Keith Marzullo May 1989 23 p
(Contract NAG2-593; N00140-87-C-8904; ARPA Order 6037)
(NASA-CR-186251; NAS 1.26:186251; TR-89-997) Avail: NTIS HC A03/MF A01 CSCL 14B

One aspect of fault tolerance in process control programs is the ability to tolerate sensor failure. A methodology is presented for transforming a process control program that cannot tolerate sensor failures to one that can. Additionally, a hierarchy of failure models is identified. Author

N90-15401*# National Aeronautics and Space Administration. Langley Research Center, Hampton, VA.
PORTABLE DIGITAL PRESSURE INDICATOR FOR CALIBRATING MAGNETIC TAPE RECORDERS
Royce F. McCormick and Bradley D. Leighty Nov. 1989 10 p
(NASA-TM-101650; NAS 1.15:101650) Avail: NTIS HC A02/MF A01 CSCL 14B

The design of a portable Digital Pressure Indicator (DPI) to be used for calibrating the pressure systems on Langley's magnetic tape recorders is described. High-speed magnetic tape recorders require pressure (0 to 20 psig) for providing an air cushion across the tape guides and a slight vacuum (30 inch H2O) for maintaining the proper number of tape loops in the advance and feed chamber. The DPI is a hand-held device that can be quickly coupled to a magnetic tape recorder and includes a two-position switch for selecting either measured pressure or vacuum, to be displayed digitally in engineering units (psig or inches H2O). The DPI is currently in use in Langley's Analysis and Computation Division. Author

N90-15402# Naval Research Lab., Washington, DC. Beam Physics Branch.
REVIEW OF QUASI-OPTICAL GYROTRON DEVELOPMENT
A. W. Fliflet, T. A. Hargreaves (Mission Research Corp., Newington, VA.), R. P. Fischer, W. M. Manheimer, and P. Sprangle 18 Oct. 1989 94 p
(AD-A213491; NRL-MR-6538) Avail: NTIS HC A05/MF A01 CSCL 09/1

There is currently a need for megawatt average power sources of 100 to 600 GHz radiation for electron cyclotron heating of fusion plasmas. One of the leading candidates for such a source, the conventional waveguide cavity gyrotron, has produced impressive output powers and efficiencies at frequencies up to about 300 GHz. However, this gyrotron configuration is limited at high frequencies by high ohmic heating and problems with transverse mode competition due to the highly overmoded configuration, and with beam collection, since the beam must be collected along a section of the output waveguide. The quasi-optical gyrotron (QOG) features an open resonator formed by a pair of spherical mirrors instead of a waveguide resonator and has the potential for overcoming each of these limitations. The resonator mirrors can be well removed from the beam-wave interaction region, allowing a large volume for the interaction and low ohmic heating densities at the mirrors. The beam direction is transverse to the resonator so that beam collection is separate from the output waveguide. GRA

N90-15403# Washington Univ., Seattle. Applied Physics Lab.
A COMPACT ACOUSTIC RECORDER
Ronald Stein 21 Sep. 1989 5 p Submitted for publication
Sponsored by Office of Navy Technology
(AD-A213581; NORDA-CONTRIB-PR-89; Rept-047; Rept-242)
Avail: NTIS HC A02/MF A01 CSCL 14/3

The design and operation of a portable compact acoustic recorder is discussed. Designed to be used in arctic conditions for applications that require portable equipment, the device is configured to fit into a lightweight briefcase. It will operate for eight hours at -40 F with heat provided by a hot water bottle. It has proven to be an effective scientific tool in the measurement of underwater acoustic signals in arctic experiments. It has also been used successfully in warmer climates, e.g., in recording acoustic signals from small boats with no ac power. The acoustic recorder's cost is moderate since it is based on a Sony Walkman Professional (WM-D6C) tape recorder playback unit. A speaker and battery assembly and a hydrophone interface electronic assembly complete the system electronics. The interface assembly supplies a number of functions, including a calibration tone generator, an audio amplifier, and a hydrophone interface. Calibrated acoustic recordings can be made by comparing the calibration tone amplitude with the acoustic signal amplitude. The distortion of the recording is minimized by using a high quality, consumer tape recorder. GRA

N90-15404# Air Force Systems Command, Wright-Patterson AFB, OH. Foreign Technology Div.
A NEW KIND OF HETERODYNE FIBER-OPTIC GYROSCOPE
Gangding Peng, Shangyuan Huang, and Zhongqi Lin 23 Aug. 1989 12 p Transl. into ENGLISH from Guangxue Xuebao (China), v. 7, no. 7, Jul. 1987 p 662-666
(AD-A213953; FTD-ID(RS)T-0574-89) Avail: NTIS HC A02/MF A01 CSCL 09/5

In this paper a novel fiber optic heterodyne detection technique

of rotation rate is described. Using electro-optic frequency and highly birefringent single mode fiber, the heterodyne fiber optic gyroscope system no more needs the use of acousto-optic devices and is free from the direct current drift in the electronics. In addition, the reciprocity of the optical path in the system is improved. Preliminary experiments have shown a good linearity of the scale factor. GRA

N90-15405# Department of the Navy, Washington, DC.
A SCHEINER-PRINCIPLE VERNIER OPTOMETER Patent Application
William B. Cushman, inventor (to Navy) 23 Jun. 1989 20 p (AD-D014304; US-Patent-Appl-SN-370521) Avail: NTIS HC A03/MF A01 CSCL 06/12

A method and optometer apparatus is disclosed for measuring the dark focus of accommodation. In a preferred embodiment, the optometer apparatus includes: a pinhole aperture plate having first and second horizontally positioned apertures disposed on opposite sides of a first optical axis; first and second orthogonally-oriented polarizing filters respectively covering the first and second horizontally positioned apertures; a positive lens having an optical axis on the first optical axis and being positioned at a distance of approximately one focal length from the pinhole aperture plate; a lens system having an optical axis on the first optical axis; a slit aperture plate having a vertical slit and being disposed on the first optical axis and between the positive lens and the lens system; third and fourth vertically positioned polarizing filters selectively disposed adjacent to the slit aperture plate to divide the slit vertically, a monochromatic light source for propagating light along the first optical axis through the lens system; and movable means attached to the slit aperture plate, the lens system and the monochromatic light source for moving the slit aperture plate. GRA

36 LASERS AND MASERS

Includes parametric amplifiers.
For related information see also *76 Solid-State Physics*.

N90-15406# Lawrence Livermore National Lab., CA.
THE 17.1-GHz FREE-ELECTRON LASER AS A MICROWAVE SOURCE FOR TeV COLLIDERS
R. A. Jong, R. D. Ryne, G. A. Westenskow, S. S. Yu, D. B. Hopkins, and A. M. Sessler (California Univ., Berkeley. Lawrence Berkeley Lab.) 11 Sep. 1989 26 p Presented at the 11th International Free Electron Laser Conference, Naples, FL, 28 Aug. - 1 Sep. 1989
(Contracts W-7405-eng-48; DE-AC03-76SF-00098)
(DE90-001506; UCRL-101193; CONF-8908134-7) Avail: NTIS HC A03/MF A01

The proposed development of a 17.1-GHz microwave source based on an induction-linac driven free electron laser that is expected to produce peak power levels at the several gigawatt level is described. This system is being designed to serve as the power source for a tera-electron-volt (TeV) linear collider or for other high gradient accelerators. The power source requirements for TeV colliders are discussed and the initial design of an FEL that will produce the desired power are presented. In addition, efficiency enhancement schemes are discussed such as a relativistic klystron afterburner, the requirements for beam reacceleration, and concepts for extraction of the microwave power while preserving key properties of the beam such as emittance and phase. DOE

N90-15407# Lawrence Livermore National Lab., CA.
ANHARMONIC BETATRON MOTION IN FREE ELECTRON LASERS
John J. Barnard 25 Sep. 1989 19 p Presented at the 11th International Free Electron Laser Conference, Naples, FL, 28 Aug. - 1 Sep. 1989 Submitted for publication
(Contracts W-7405-eng-48; W31RPD-9-D5007)
(DE90-001515; UCRL-101066; CONF-8908134-6) Avail: NTIS HC A03/MF A01

We calculate the trajectory of an electron in a free electron laser (FEL), including non-linear, off-axis focusing terms in the transverse equations of motion. We estimate the emittance growth due to the non-linear terms. DOE

N90-15408# Los Alamos National Lab., NM. Theoretical Div.
HAMILTONIAN CHAOS IN A NONLINEAR POLARIZED OPTICAL BEAM
D. David, D. D. Holm, and M. V. Tratnik 1989 21 p Presented at the Santa Fe Institute Summer School on Complex Systems, Santa Fe, NM, 5-30 Jun. 1989
(Contract W-7405-eng-36)
(DE90-002437; LA-UR-89-3337; CONF-8906239-1) Avail: NTIS HC A03/MF A01

This lecture concerns the applications of ideas about temporal complexity in Hamiltonian systems to the dynamics of an optical laser beam with arbitrary polarization propagating as a traveling wave in a medium with cubically nonlinear polarizability. We use methods from the theory of Hamiltonian systems with symmetry to study the geometry of phase space for this optical problem, transforming from C squared to S cubed x S(sup 1), first, and then to S squared x (J, theta), where (J, theta) is a symplectic action-angle pair. The bifurcations of the phase portraits of the Hamiltonian motion on S squared are classified and displayed graphically. These bifurcations take place when either J (the beam intensity), or the optical parameters of the medium are varied. After this bifurcation analysis has shown the existence of various saddle connections on S squared, the Melnikov method is used to demonstrate analytically that the traveling-wave dynamics of a polarized optical laser pulse develops chaotic behavior in the form of Smale horseshoes when propagating through spatially periodic perturbations in the optical parameters of the medium. DOE

N90-15409# Berkeley Research Association, CA.
THEORY FOR HIGH GAIN, HIGH POWER FREE ELECTRON LASERS Final Report
William B. Colson 1989 31 p Prepared in cooperation with Lawrence Livermore Lab., CA
(Contract W-7405-eng-48)
(DE90-003024; UCRL-21254; BRA-89-342R) Avail: NTIS HC A03/MF A01

The research on high gain, high power free electron lasers (FELs) was fruitful. The findings have resulted in publications, presentations, and some important new research topics in progress. The new research proposed is also coordinated closely with specific LLNL FEL project physicists, and the upcoming high gain, high power amplifier experiments during the next year on the Paladin FEL. The research includes analysis of the initial ELF experiments, identification of new FEL physics in Paladin at 5m length, electron beam distributions from future induction linacs, electron beam distributions in weak optical fields, a major FEL review paper, a simple understanding of FEL optical guiding, multimode analysis applied to single pass FEL amplifiers, a LLNL review talk on FEL sidebands and electron distribution functions. DOE

N90-15410# Lawrence Livermore National Lab., CA.
THE SEARCH FOR SOLID STATE FUSION LASERS
Marvin J. Weber Apr. 1989 11 p Presented at the French-Israeli Workshop on Solid State Lasers, Jerusalem, Israel, 12-14 Dec. 1989 Submitted for publication
(Contract W-7405-eng-48)
(DE89-012301; UCRL-98989; CONF-891220-1) Avail: NTIS HC A03/MF A01

Inertial confinement fusion (ICF) research puts severe demands on the laser driver. In recent years large, multibeam Nd:glass lasers have provided a flexible experimental tool for exploring fusion target physics because of their high powers, variable pulse length and shape, wavelength flexibility using harmonic generation, and adjustable focus. Advances in solid state lasers technology indicates that Nd:glass lasers can be scaled up to provide a single-phase, multi-megajoule, high gain laboratory microfusion

facility, and gas cooled slab amplifiers with laser diode pump sources are viable candidates for an efficient, high repetition rate, megawatt driver for an ICF reactor. In both applications requirements for energy storage and energy extraction drastically limit the choice of lasing media. Nonlinear optical effects and optical damage are additional design constraints. New laser architectures applicable to ICF drivers and possible laser materials, both crystals and glasses, are surveyed. DOE

N90-15411# Lawrence Livermore National Lab., CA.
NTES (NUCLEAR TEST AND EXPERIMENTAL SCIENCES) PROGRAM LASER FACILITY FOR PHYSICS EXPERIMENTS BUILDING 391 HIGH BAY OPTION
D. J. Christie, R. J. Foley, D. N. Frank, M. A. Henesian, G. L. Hermes, J. T. Hunt, W. G. Labiak, D. W. Larson, J. K. Lawson, and S. E. Mayo et al 31 Aug. 1989 47 p
(Contract W-7405-eng-48)
(DE90-001795; UCID-21810) Avail: NTIS HC A04/MF A01

This report discusses the following topics: a high energy laser driver; the NTES laser and experiment facilities; systems control and data acquisition; and auxiliary lasers. DOE

N90-15412# Lawrence Livermore National Lab., CA.
LASER-SUPPORTED DETONATION WAVES AND PULSED LASER PROPULSION
Jordin T. Kare 1989 8 p Presented at the 17th International Symposium on Shock Waves and Shock Tubes, Bethlehem, PA, 17-21 Jul. 1989
(Contract W-7405-eng-48)
(DE90-002753; UCRL-101677; CONF-890756-4) Avail: NTIS HC A02/MF A01

A laser thermal rocket uses the energy of a large remote laser, possibly ground-based, to heat an inert propellant and generate thrust. Use of a pulsed laser allows the design of extremely simple thrusters with very high performance compared to chemical rockets. The temperatures, pressures, and fluxes involved in such thrusters (10 exp 4 K, 10 exp 2 atmospheres, 10 exp 7 w/sq cm) typically result in the creation of laser supported detonation (LSD) waves. The thrust cycle thus involves a complex set of transient shock phenomena, including laser-surface interactions in the ignition if the LSD wave, laser plasma interactions in the LSD wave itself, and high temperature nonequilibrium chemistry behind the LSD wave. The SDIO Laser Propulsion Program is investigating these phenomena as part of an overall effort to develop the technology for a low cost earth-to-orbit laser launch system. The program's approach to developing a high performance thruster, the double pulse planar thruster is summarized, and an overview is presented of some results obtained to date, along with a discussion of the many research questions still outstanding in this area. DOE

N90-15413# Lawrence Livermore National Lab., CA.
INTEGRATION OF A GATED MICROCHANNEL PLATE DETECTOR INTO THE NOVA LASER SYSTEM
J. D. Wiedwald, R. L. Hanks, G. L. Tietbohl, D. O. Bishop, G. D. Power, F. R. Kelly, and P. M. Bell 11 Aug. 1989 10 p Presented at the 33rd SPIE Annual International Technical Symposium on Optical and Optoelectronic Applied Science and Engineering, San Diego, CA, 6-11 Aug. 1989
(Contract W-7405-eng-48)
(DE90-002981; UCRL-101630; CONF-890836-19) Avail: NTIS HC A02/MF A01

In recent years the measurements of Inertial Confinement Fusion (ICF) target dynamics using x ray imaging have grown in both quality and quantity. One instrument being used increasingly at the Lawrence Livermore National Laboratory's Nova facility is the Gated X Ray Imager. This imager uses a microchannel plate as detector, amplifier, and gating element to allow x ray photographs with aperture times under 100 ps. In anticipation of as many as 16 imagers installed on Nova within the next year, an electronic control system has been developed. This system simplifies operator interface when in a stand-alone mode while synchronizing with the Nova sequence clock when in the shot mode. The system is also expected to be fully integrated into the Nova computer system within the next year. This will allow remote parameter input and the monitoring and archiving of system status. DOE

N90-15414# Los Alamos National Lab., NM. Physics Div.
COMPREHENSIVE, NONINTERCEPTING ELECTRON-BEAM DIAGNOSTICS USING SPONTANEOUS EMISSION
Alex H. Lumpkin 1989 25 p Presented at the 11th International Free Electron Laser Conference, Naples, FL, 28 Aug. - 1 Sep. 1989
(Contract W-7405-eng-36)
(DE90-003211; LA-UR-89-3786; CONF-8908134-17) Avail: NTIS HC A03/MF A01

Characterization and optimization of electron-beam parameters are important aspects of optimizing free-electron laser (FEL) performance. The visible spontaneous emission (lambda approximately 650 nm) from the 5-meter long undulator of the Boeing FEL experiment can be characterized in sufficient detail with a streak/spectrometer to deduce time-resolved electron-beam spatial position and profile, micropulse duration, and energy. DOE

N90-15415# Texas Univ., Austin. Dept. of Physics.
KINETIC STUDIES FOLLOWING STATE-SELECTIVE LASER EXCITATION Progress Report, 15 Mar. 1987 - 14 Mar. 1990
J. W. Keto Oct. 1989 30 p
(Contract DE-FG05-84ER-13191)
(DE90-003232; DOE/ER-13191/10) Avail: NTIS HC A03/MF A01

The objective is the study of state-to-state, electronic energy transfer reactions following two-photon laser excitation. Reactions of Xe 5p(sup 5)np were chosen because of their relevance to the XeCl excimer laser. Deactivation reactions in collisions with heavy atoms such as Ar, Kr, and Xe and reactive collisions with chlorides are being studied. The reactants are excited by multiphoton laser absorption. Product channels are observed by their fluorescence, or by laser induced fluorescence using a second color laser. DOE

N90-15416# Los Alamos National Lab., NM. Physics Div.
INITIAL OPTICAL TRANSITION RADIATION MEASUREMENTS OF THE ELECTRON BEAM FOR THE BOEING FREE-ELECTRON LASER EXPERIMENT
Alex H. Lumpkin, R. B. Fiorito, D. W. Rule, D. H. Dowell, W. Sellyey, and A. R. Lowrey (Boeing Aerospace Co., Seattle, WA.) 1989 25 p Presented at the 11th International Free Electron Laser Conference, Naples, FL, 28 Aug. - 1 Sep. 1989
(Contract W-7405-eng-36)
(DE90-003396; LA-UR-89-3763; CONF-8908134-18) Avail: NTIS HC A03/MF A01

The potential for characterization of electron beams at (approximately) 100 MeV at the Boeing Free-Electron Laser (FEL) facility by optical transition radiation (OTR) techniques has been demonstrated as an important complement to other diagnostic means. Electron beam properties such as spatial profile and position, current intensity, emittance, and energy were made accessible in an on-line manner. Initial examples including transport through the 5-m wiggler and the resolution of Cerenkov radiation and spontaneous emission radiation competitive sources are discussed. DOE

N90-15417# Lawrence Livermore National Lab., CA. Beam Research Program.
WAVEGUIDE EFFECTS IN SUPERRADIANT FREE-ELECTRON LASERS
W. M. Sharp, S. S. Yu, P. Pierini, and G. Cerchioni (Istituto Nazionale di Fisica Nucleare, Milan, Italy) 1989 24 p Presented at the 11th International Free Electron Laser Conference, Naples, FL, 28 Aug. - 1 Sep. 1989
(Contract W-7405-eng-48)
(DE90-003605; UCRL-101071; CONF-8908134-19) Avail: NTIS HC A03/MF A01

A quasi 3-D time dependent particle simulation was developed to model slippage effects in a single-pass microwave free electron laser. The code is used here to model the large-amplitude superradiant signal that can develop in the slippage region of constant current beams. Results are presented for single mode and multiple-code cases, and the effects of the waveguide dimensions, detuning, energy spread, and the initial power in the modes are discussed. DOE

N90-15418# Brookhaven National Lab., Upton, NY.
A MICROWIGGLER FREE-ELECTRON LASER AT THE BROOKHAVEN ACCELERATOR TEST FACILITY
K. Batchelor, I. Ben-Zvi, R. Fernow, J. Gallardo, H. Kirk, C. Pellegrini, A. vanSteenbergen, and A. Bhowmik (Rockwell International Corp., Canoga Park, CA.) 26 Sep. 1989 14 p
(Contract DE-AC02-76CH-00016)
(DE90-003643; BNL-43306) Avail: NTIS HC A03/MF A01

The design and status of an FEL experiment at the Brookhaven National Laboratory Accelerator Test Facility is reported. A 50 MeV high brightness electron beam will be utilized for an oscillator experiment in the visible wavelength region. The microwiggler to be used is a superferric planar undulator with a 0.88 cm period, 60 cm length and K = 0.35. The optical cavity is a 368 cm long stable resonator with broadband dielectric coated mirrors. DOE

N90-15419# Argonne National Lab., IL. Materials Science Div.
LASER-INDUCED SURFACE ABLATION AND OPTICAL DAMAGE OF ZnS CRYSTALS CAUSED BY SINGLE- AND MULTIPLE-PULSE LASER-IRRADIATION
H. F. Arlinghaus, W. F. Calaway, D. M. Gruen, and L. L. Chase (Lawrence Livermore National Lab., CA.) 1989 13 p Presented at the 20th Annual Symposium on Optical Materials for High-Power Lasers, Boulder, CO, 26-28 Oct. 1988
(Contracts W-31-109-eng-38; W-7405-eng-48)
(DE90-003807; CONF-8810246-6) Avail: NTIS HC A03/MF A01

Velocity distributions and yields of neutral Zn atoms emitted from laser-irradiated ZnS crystals at power densities far below the single-pulse damage threshold have been analyzed by high-resolution two-photon laser-induced fluorescence spectroscopy and also by electron impact ionization mass spectrometry. Large differences in the measured kinetic temperatures have been found between the single- and multiple-pulse laser irradiation experiments. The high-kinetic temperatures, obtained in multiple-pulse experiments, may be caused by cumulative surface modification, such as thermally-induced cracking, leading to a reduction of the thermal conductivity compared to the bulk value. Optical damage was related to the interaction of a plasma formed at a critical combination of particle density and laser intensity, with the surface. DOE

N90-15420# Lawrence Livermore National Lab., CA.
NOISE: A NONLINEAR OPTIMIZATION INDUCTION FREE-ELECTRON LASER SYSTEMS ENGINEERING CODE
D. T. Blackfield (TRW, Inc., Redondo Beach, CA.) Aug. 1989 36 p
(Contract W-7405-eng-48)
(DE90-004438; UCID-21543) Avail: NTIS HC A03/MF A01

A computer code was developed to assist in the design of a ground-based induction free-electron laser (FEL) proposed for construction at the White Sands Missile Range. Called the Nonlinear Optimization Induction Free-Electron Laser Systems Engineering (NOISE), the code contains algorithms for modeling and costing the eight basic IFEL assemblies (accelerator, amplifier, master oscillator, optical conditioning, controls and data acquisition, ancillary and alignment systems, prime power, and technical facilities). A set of nonlinear equations is used to optimize a figure of merit (FOM) subject to various engineering constraints. The FOM is typically total cost (less facilities costs) but may be any combination of variables used by NOISE. The NOISE architecture is highly modular so that assembly routines can be easily modified. Trade studies can be quickly performed over a wide range of dimensions (up to 34 variables with up to 12 constraints). In addition, NOISE contains a spreadsheet or benchmark mode that calculates feasible, but not necessarily optimized, design points. Various nonlinear optimization techniques are reviewed, showing how the techniques influenced NOISE development, and describing in detail the code's subroutines and capabilities. DOE

N90-15421# Rice Univ., Houston, TX. Dept. of Electrical and Computer Engineering.
DEVELOPMENT OF TUNABLE EXCIMER LASERS Final Report, 1 Oct. 1985 - 31 Dec. 1988
Frank K. Tittel, R. Sauerbrey, and William L. Wilson 1 Mar. 1989 11 p
(Contract N00014-80-C-0807; RR0-1107)
(AD-A213521) Avail: NTIS HC A03/MF A01 CSCL 09/3

An investigation of the fundamental processes affecting the operation, performance and application of electrically excited lasers having potential utility in a variety of areas of importance to the Navy was conducted. Particular attention was focused on the broadband XeF laser, which has the potential for efficient, tunable operation throughout the blue-green spectral region. This report summarizes the results of this investigation, and lists published papers and conference reports in which specific results and conclusions of the research are described in detail. GRA

N90-15422# Air Force Systems Command, Wright-Patterson AFB, OH. Foreign Technology Div.
CHINA-BUILT AIRBORNE SYNCHRONOUS LASER RANGER THE NEW L-8 JET TRAINER AIRCRAFT
Chang Shan Su 1 Sep. 1989 9 p Transl. into ENGLISH from Guoji Hangkong, (China), no. 3, Mar. 1988 p 56
(AD-A213835; FTD-ID(RS)T-0221-89) Avail: NTIS HC A02/MF A01 CSCL 15/3

The airborne synchronous laser ranger designed and built by the China Aviation Technology Import Export Corporation Electrooptics Equipment Research Institute passed flight testing and in September of 1987 was evaluated for design model technology in Luoyang in Honan Province. This ranger is mainly used in attack aircraft for air-to-ground ranging. It provides highly accurate target distance and location information for the fire control systems, improving the firing accuracy of airborne weapons systems. It can also be used in bombers and armed helicopters as well as surface vessels and vehicles for fire control system ranging. It can also be used in combination with aerial cartography, terrain avoidance and terrain allowing systems. GRA

N90-15423# Boston Univ., MA. Dept. of Chemistry.
DEVELOPMENT OF GLASS-CERAMIC LASERS Final Report, 1 Feb. 1986 - 31 May 1989
A. Lempicki, T. Keyes, A. J. Wojtowicz, M. Kazmierczak, and J. J. Chen Aug. 1989 195 p
(Contract DAAL03-86-K-0016)
(AD-A214146; ARO-23241.8-PH) Avail: NTIS HC A09/MF A02 CSCL 09/3

The goal of this program was to ascertain the possibility of developing a Tunable Solid State Laser, based on Cr-doped transparent glass ceramics. To this end the spectroscopy of Cr in mullite ceramics and related aluminosilicate crystals was studied in detail. The results indicate an extremely large inhomogenous broadening, interpreted in terms of a statistical distribution of crystal fields. The main limitation of these materials is the high scattering loss which should be reduced by at least a factor of 10, before laser applications are contemplated. Work on scattering led to the discovery of un-averaged, angularly distributed intensity fluctuations in amorphous materials. This work was carried out on CVD silica as well as on ceramics and led to new insights concerning the statistics of speckle phenomena. GRA

N90-15424# Naval Research Lab., Washington, DC. Beam Physics Branch.
FREQUENCY SHIFT INDUCED IN LASER PULSES BY PLASMA DENSITY VARIATIONS Interim Report
E. Esarey, A. Ting, and P. Sprangle 25 Oct. 1989 20 p

Sponsored by ONR and DOE
(AD-A214195; NRL-MR-6541) Avail: NTIS HC A02/MF A01 CSCL 09/3

An analytical theory is developed which describes how a radiation pulse becomes modified as it propagates through a plasma with arbitrary temporal and spatial density variations. Expressions are derived for the shifts induced in both the frequency and the wavenumber of the radiation pulse. It is shown that temporal variations in the plasma density result in frequency shifts of the radiation. The possibility of up shifting the frequency of the laser pulse using plasma waves is analyzed, and it is found that maximum shifts occur when the phase velocity of the plasma wave is equal to the group velocity of the laser pulse. GRA

N90-15425# New Mexico Univ., Albuquerque. Center for High Technology Materials.
LASER-MATERIAL INTERACTIONS Final Technical Report, 1 Apr. 1988 - 31 Mar. 1989
S. R. J. Brueck Sep. 1989 136 p
(Grant AF-AFOSR-0120-86; AF Proj. 2301)
(AD-A214421; AFOSR-89-1337TR) Avail: NTIS HC A07/MF A01 CSCL 09/3

The Laser-Materials Interaction Laboratory at the Center for High Technology Materials of the University of New Mexico is devoted to the study of a broad range of laser spectroscopic probes of semiconductor and nonlinear-materials, fabrication processes and optoelectronic devices. Much of this work is being performed in conjunction with the Optoelectronics Research Center Program at CHTM which is also partially funded by the Air Force Office of Scientific Research. Significant progress was made in this reporting period in a number of areas including: laser-induced photo-degradation of the GaAs surface, studies of grating-coupling into surface-plasma modes at a metal-dielectric interface, electro-optic and nonlinear optical effects in PLZT thin films, and resonant-periodic-gain surface-emitting semiconductor lasers. Brief synopses of this work are presented here. More details are provided in the attached reprints and preprints. GRA

N90-15426# Department of the Navy, Washington, DC.
LASER DETECTION AND DISCRIMINATION SYSTEM Patent Application
S. Charkrabarti, inventor (to Navy), V. K. Mathur, inventor (to Navy), and G. P. Summers, inventor (to Navy) 16 Aug. 1989 15 p
(AD-D014301; US-Patent-Appl-SN-394457) Avail: NTIS HC A03/MF A01 CSCL 17/5

Magnesium oxide sensing material is pretreated and charged by UV radiation to identify impingement thereon of radiation from a near infrared laser source by detection of blue emissions which persist for an unusually long period of time, avoiding frequent respotting and recharging. When heated to thermoluminescence peaks above room temperature by irradiation from a far infrared laser source, the magnesium oxide exhibits green luminescence enabling wavelength discrimination between detection of near and far infrared laser sources. Such pretreated magnesium oxide also produces green emissions when irradiated by UV laser sources, to distinguish between detection of the UV laser sources and the far infrared laser sources by discrimination between different fading behaviors of the green emissions. GRA

N90-15427# Department of the Navy, Washington, DC.
LASER COMMUNICATION SYSTEM WITH WIDE BAND MAGNETOSTRICTIVE MODULATION Patent Application
Lawrence T. Kabacoff, inventor (to Navy) 15 Sep. 1989 14 p
(AD-D014302; US-Patent-Appl-SN-408377) Avail: NTIS HC A03/MF A01 CSCL 25/3

A laser beam conducted through an optical fiber cable is phase modulated for communication purposes by a signal encoder operative through a source of current to generate a modulated magnetic field applied to a magnetostrictive sheathing. The magnetostrictive sheathing is annealed and covers a portion of the fiber cable which undergoes dimensional change to effect modulation. GRA

N90-15428# New Mexico State Univ., Las Cruces. Dept. of Physics.
AEROSOL HEATING AND VAPORIZATION OF HIGH-FLUX LASER BEAMS Final Report
R. L. Armstrong, L. J. Radziemski, and B.-S. Park May 1989 6 p Prepared for Lawrence Livermore National Lab., CA
(Contract W-7405-eng-48)
(DE90-003471; UCRL-21245) Avail: NTIS HC A02/MF A01

Research has emphasized theoretical modeling of laser-aerosol interactions and compared the results of some of the modeling calculations with experiment. When a high irradiance laser beam propagates through the atmosphere a broad spectrum of interaction can occur. These range from linear scattering and absorption which occur at low irradiance, to Joule heating and vaporization, superheating, hydrodynamics, nonlinear optics and plasma formation which become significant as the irradiance increases. Of particular interest are interactions which occur at moderate irradiance levels. By moderate, it is meant that those interactions occurring at higher irradiances such as plasma irritation, and strong hydrodynamic processes (shocks) may be neglected. Nonlinear optical interactions were not considered. There remains the interactions centered around Joule heating and superheating together with the heat and mass transport processes which constitutes the response of the aerosol to these heating effects. Accordingly, the modeling efforts and comparison with experimental results were restricted to those latter effects. DOE

37 MECHANICAL ENGINEERING

Includes auxiliary systems (nonpower); machine elements and processes; and mechanical equipment.

N90-15429 Virginia Univ., Charlottesville.
THERMAL ANALYSIS OF FIXED AND TILTING PAD JOURNAL BEARINGS INCLUDING CROSS-FILM VISCOSITY VARIATIONS AND DEFORMATIONS Ph.D. Thesis
Lyle Arthur Branagan 1988 382 p
Avail: Univ. Microfilms Order No. DA8914628

Presented here are several enhancements to the thermal analysis of fixed geometry and tilting pad journal bearings. An approximate solution for a generalized Reynolds equation coupled with an approximate form of the energy equation is used to find the static and dynamic characteristics of several bearing geometries. The effect of including a cross-film viscosity variation in the solution is considered and found to be computationally expensive while generating changes greater than ten percent only for a few dynamic characteristics. Several models for the effect of cavitation on the cross-film heat conduction are studied and found to be helpful in determining the temperature field of the unloaded pads in fixed geometry bearings. Comparison with a published thermohydrodynamic solution indicate that this approximate analysis gives characteristic temperatures within ten degrees Fahrenheit, if boundary conditions are matched. Comparisons with two experimental investigations show correlation wthin eight degrees Fahrenheit of measured babbitt temperatures. Lack of agreement with measured eccentricities for a two axial groove bearing are attributed to modeling differences near the oil inlet. The work with tilting pad bearings includes the cross-film viscosity variation and the thermal cavitation models. Neither of these effects is demonstrated to be important. Deformation models for the pivots and for the pads are outlined and investigated.
Dissert. Abstr.

N90-15430 California Univ., Los Angeles.
NUMERICAL ANALYSIS AND SIMULATION OF FRICTIONAL PARTICLE SYSTEMS Ph.D. Thesis
Jihad A. Issa 1988 93 p
Avail: Univ. Microfilms Order No. DA8907575

The results of a numerical investigation of the micromechanical behavior of an assembly of frictional particles, i.e., a frictional material, under the action of applied forces, are presented. The analysis of frictional granular systems is conducted using a new

computer program MASOM (Micro Analysis and Simulation of Materials) developed as a part of the research. The computer program is used to investigate the behavior of frictional materials in standard uniaxial and triaxial compression tests. The computer simulation using MASOM is shown to realistically capture (macroscopic) behavior observed in physical tests. The effects of several important processes are revealed by the numerical simulation, namely: (1) the effect of granular movement and rotation; (2) elasticity and fracture of the grains; (3) inhomogeneous behavior of the particle assembly during loading, including the buildup of loading chains and islands of quasistatic subassemblies; and (4) the relationship between the number of intragranular contacts and microscopic strain. The behavior of the frictional material is shown to be very complex, involving a number of different physical processes. To gain a better understanding of the micromechanical behavior, a video tape was generated of the response of the particle assembly throughout the numerical simulation. A review of the response of the frictional material during the test shows the development of inhomogeneities associated with the acretion of particles to quasistatic islands of particles in the sample. Dissert. Abstr.

N90-15431*# Martin Marietta Corp., New Orleans, LA. Michoud Assembly Facility.
ONORBIT ELECTRON BEAM WELDING EXPERIMENT DEFINITION Final Report
27 Sep. 1989 60 p
(Contract NAS8-37756)
(NASA-CR-183847; NAS 1.26:183847) Avail: NTIS HC A04/MF A01 CSCL 13H

The proposed experiment design calls for six panels to be welded, each having unique characteristics selected to yield specific results and information. The experiment is completely automated and the concept necessitated the design of a new, miniaturized, self-contained electron beam (EB) welding system, for which purpose a separate IR and D was funded by the contractor, Martin Marietta Corporation. Since future tasks beyond the proposed experiment might call for astronauts to perform hand-held EB gun repairs or for the gun to be interfaced with a dexterous robot such as the planned flight telerobotic servicer (FTS), the EB gun is designed to be dismountable from the automated system. In the experiment design, two separate, identical sets of weld panels will be welded, one on earth in a vacuum chamber and the other onorbit in the aft cargo bay of an orbiter. Since the main objective of the experiment is to demonstrate that high quality welds can be achieved under onorbit conditions, the welds produced will be subjected to a wide range of discriminating non-destructive Q.C. procedures and destructive physical tests. However, advantage will be taken of the availability of a fairly large quantity of welded material in the two series of welded specimens to widen the circle of investigative talent by providing material to academic and scientific institutions for examination. Author

N90-15432 California Univ., Berkeley.
CONTROL OF MECHANICAL MANIPULATORS Ph.D. Thesis
Ping Hsu 1988 125 p
Avail: Univ. Microfilms Order No. DA8916707

The issue of developing model based control algorithms for several manipulator applications are examined. Because of the versatility of robot manipulators, the problems of controlling them are diverse. A number of control problems which arise from several manipulator applications are studied. The Lagrangian formulation and a number of well known control schemes are introduced. The problems of coordination of multiple manipulators are studied. The problems are: trajectory tracking, load distribution, internal force control, and decentralization of control algorithm. Also discussed are several considerations when controlling a multi-fingered hand. For a model based control law to be effective, the model of the system must closely match the actual system. However, a good system model may not be always available to the designer. Three adaptive model based control laws are introduced which identify the unknown system parameters on-line so that the desirable performance of a true model-matching controller is achieved. The control problem arises when the control loop is closed around the gripper position/orientation of a redundant manipulator, since the extra degree of freedom is unobservable from the gripper position/orientation and therefore no control action will be generated by the controller to correct any undesirable behavior in this unobservable set of state variables. The control law proposed not only controls the gripper position/orientation but also utilizes the redundant degree of freedom to optimize the manipulator configuration in a sense that is made precise in the chapter. It is intuitively clear that, if the sampling frequency is high enough, the performance of the closed loop system with a digital computer in the loop will be close to the performance of the system with a true continuous time controller or, at least, the stability can be preserved. Dissert. Abstr.

N90-15433 Rutgers - The State Univ., New Brunswick, NJ.
ON THE ANALYSIS AND OPTIMIZATION OF A PLATFORM MANIPULATOR Ph.D. Thesis
Martin Cwiakala 1988 115 p
Avail: Univ. Microfilms Order No. DA8914201

A platform manipulator (closed-loop manipulator) is a spatial mechanism used to position and orient a platform. In consulting literature concerning open- and closed-loop manipulators, the topic of statis analysis was found to be missing for the closed-loop manipulator. By combining static analysis and workspace evaluation, a design of optimum geometry for a closed-loop manipulator is developed. Based on application, this research has two distinct parts: analysis and workspace optimization with regard to actuator load; and a feasibility study concerning the use of cables for legs of the manipulator. The work presented is based on a special configuration of an applied static load which is restricted to a plane. This load configuration results in the polar plots of actuator loads to be circled when plotted against load direction. Extending this concept for the general loads, work volume in which the actuators remained below a specified force for a specified platform orientation was found. A search is performed on the geometric parameters to maximize this work volume. The cable leg feasibility study also utilized the special form of the applied load. Two configurations are investigated: inverting the manipulator and using the force of gravity to keep all legs in tension, and using an additional leg mounted between the centers of the platforms. A method is presented to determine the range of force orientations that result in all legs being in tension, a necessary condition if cables are used. For specified platform orientation and disturbance/tension-force ratio, workspace shape and volume is determined in which all legs remain in tension. Again, a search is performed on the geometric parameters of the manipulator to maximize the workspace volume for each configuration. Dissert. Abstr.

N90-15434*# Cincinnati Univ., OH. Dept. of Mechanical and Industrial Engineering.
MESH REFINEMENT IN FINITE ELEMENT ANALYSIS BY MINIMIZATION OF THE STIFFNESS MATRIX TRACE Final Report
Madan G. Kittur and Ronald L. Huston Nov. 1989 108 p
Prepared in cooperation with Army Aviation Systems Command, Cleveland, OH
(Grant NsG-3188; DA Proj. 1L1-62209-A-47-A)
(NASA-CR-185170; USAAVSCOM-TR-89-C-019; NAS 1.26:185170) Avail: NTIS HC A06/MF A01 CSCL 13I

Most finite element packages provide means to generate meshes automatically. However, the user is usually confronted with the problem of not knowing whether the mesh generated is appropriate for the problem at hand. Since the accuracy of the finite element results is mesh dependent, mesh selection forms a very important step in the analysis. Indeed, in accurate analyses, meshes need to be refined or rezoned until the solution converges to a value so that the error is below a predetermined tolerance. A-posteriori methods use error indicators, developed by using the theory of interpolation and approximation theory, for mesh refinements. Some use other criterions, such as strain energy density variation and stress contours for example, to obtain near

optimal meshes. Although these methods are adaptive, they are expensive. Alternatively, a priori methods, until now available, use geometrical parameters, for example, element aspect ratio. Therefore, they are not adaptive by nature. An adaptive a-priori method is developed. The criterion is that the minimization of the trace of the stiffness matrix with respect to the nodal coordinates, leads to a minimization of the potential energy, and as a consequence provide a good starting mesh. In a few examples the method is shown to provide the optimal mesh. The method is also shown to be relatively simple and amenable to development of computer algorithms. When the procedure is used in conjunction with a-posteriori methods of grid refinement, it is shown that fewer refinement iterations and fewer degrees of freedom are required for convergence as opposed to when the procedure is not used. The mesh obtained is shown to have uniform distribution of stiffness among the nodes and elements which, as a consequence, leads to uniform error distribution. Thus the mesh obtained meets the optimality criterion of uniform error distribution. Author

N90-15435*# Old Dominion Univ., Norfolk, VA. Dept. of Mechanical Engineering and Mechanics.

LUNAR CONSTRUCTION UTILITY VEHICLE

Jul. 1989 143 p

(Contract NASw-4435)

(NASA-CR-186231; NAS 1.26:186231) Avail: NTIS HC A07/MF A01 CSCL 13F

The lunar construction utility vehicle (LCUV) is an all-purpose construction vehicle which will aid in the robotic assembly of a lunar outpost. The LCUV will have the following capabilities: (1) must be self supporting including repairs; (2) must offload itself from a lunar lander; (3) must be telerobotic and semi-autonomous; (4) must be able to transport one space station common module; (5) must allow for man-rated operation; and (6) must be able to move lunar regolith for site preparation. This study recommends the use of an elastic tracked vehicle. Detailed material analyses of most of the LCUV components were accomplished. The body frame, made of pinned truss elements, was stress analyzed using NASTRAN. A track connection system was developed; however, kinematic and stress analyses are still required. This design recommends the use of hydrogen-oxygen fuel cells for power. Thermal control has proven to be a problem which may be the most challenging technically. A tentative solution has been proposed which utilizes an onboard and towable radiator. Detailed study of the heat dissipation requirements is needed to finalize radiator sizing. Preliminary work on a man-rated cabin has begun; however, this is not required during the first mission phase of the LCUV. Finally, still in the conceptual phases, are the communication, navigation and mechanical arm systems. Author

N90-15436# Oak Ridge National Lab., TN. Advanced Computing and Integrated Sensor Systems.

SENSOR INTEGRATION USING CONCURRENT COMPUTING ON-BOARD THE ORNL MOBILE ROBOT

R. C. Mann, J. P. Jones, M. Beckerman, C. W. Glover, L. Farkas, and J. R. Einstein 1989 12 p Presented at the International Conference on Robotics and Automation, Scottsdale, AZ, May 14, 1989

(Contract DE-AC05-84OR-21400)

(DE89-008740; CONF-890522-6) Avail: NTIS HC A03/MF A01

The mobile robot prototypes developed at the Center for Engineering Systems Advanced Research (CESAR) at the Oak Ridge National Laboratory (ORNL) are equipped with sonar sensors, CCD cameras and a laser range camera that are used to support autonomous navigation and inspection tasks in an a priori unknown and unstructured dynamic environment. This paper summarizes work directed at extracting information from data collected with these sensors and integrating it, in order to produce reliable descriptions of the robot's environment. The approach consists in studying different world models and mappings among them, sensor models and parallel algorithms for sensor information processing, and appropriate integration strategies. Specifically, the paper describes the integration of two-dimensional vision and sonar range information, and the integration of laser range and luminance images. DOE

N90-15437# Sandia National Labs., Albuquerque, NM. Strategic Defense Studies Div.

STAND-OFF SHIELDS FOR HYPERVELOCITY PARTICLES

R. Jeffery Lawrence 1989 4 p Presented at the American Physical Society Topical Conference on Shock Compression of Condensed Matter, Albuquerque, NM, 14-17 Aug. 1989

(Contract DE-AC04-76DP-00789)

(DE89-016182; SAND-89-0919C; CONF-890812-8) Avail: NTIS HC A01/MF A01

Stand-off hypervelocity particle shields offer potential weight savings of an order of magnitude or more over conventional homogeneous armors. Based on an earlier complete model for the design and optimization of a stand-of shield system, a more restricted model appropriate for retrofit shields is described. Procedures to minimize the shield mass are provided, and scaling laws for many of the important parameter relationships are illustrated. DOE

N90-15438# Los Alamos National Lab., NM.

MESA 3-D CALCULATIONS OF ARMOR PENETRATION BY PROJECTILES WITH COMBINED OBLIQUITY AND YAW

D. J. Cagliostro, D. A. Mandell, L. A. Schwalbe, T. F. Adams, and E. J. Chapyak 1989 28 p Presented at the 1989 Hypervelocity Impact Symposium, San Antonio, TX, 12-14 Dec. 1989 Sponsored in part by DARPA; Army; and Marine Corps

(Contract W-7405-eng-36)

(DE89-015265; LA-UR-89-2342; CONF-891214-3) Avail: NTIS HC A03/MF A01

MESA, a new 3-D hydrodynamic code, developed specifically for simulations of armor and anti-armor systems is introduced and briefly described. The code's current capabilities and its planned model improvements and additions are discussed. An Eulerian code using state-of-the-art numerical methods, MESA runs faster and is less affected by spurious numerical diffusion than older codes. It models hydrodynamic flow and the dynamic deformation of solid materials. It uses simple elastic-perfectly plastic material strength models as well as models with strain and strainrate hardening and thermal softening. Future versions will incorporate advanced fracture models. It treats detonations in explosives using a programmed burn. The code's current capabilities are illustrated with simulations of experiments on yawed rods obliquely impacting armor plates at 1.29 km/s. DOE

N90-15439# Los Alamos National Lab., NM. Computing and Communications Div.

HYDRODYNAMICS CODE CALCULATIONS OF DEBRIS CLOUDS PRODUCED BY BALL-PLATE IMPACTS

Kathleen S. Holian 1989 30 p Presented at the Hypervelocity Impact Symposium, San Antonio, TX, 12-14 Dec. 1989

(Contract W-7405-eng-36)

(DE89-015270; LA-UR-89-2309; CONF-891214-4) Avail: NTIS HC A03/MF A01

When a metal projectile hits a thin metal plate at a high enough velocity to penetrate it, a cloud of debris is produced, whose structure for normal impacts provides a unique test for hydrodynamic computer simulation. Since the equations of state of the materials involved are a vital ingredient for hydrocode calculations, how important it is to use an accurate equation of state is determined. Results are reported of benchmark calculations of hypervelocity impacts of a lead sphere on a lead plate where significant vaporization occurs. The results are somewhat sensitive to the equation of state used, particularly in the regime where the material is expanded. The results are greatly affected when an attempt is made to include nonequilibrium effects by allowing negative pressures in the EOS. DOE

N90-15440# Los Alamos National Lab., NM. Mechanical and Electronic Engineering Div.

COMPARISON OF MULTIDIMENSIONAL CALCULATIONS OF LONG-ROD IMPACTS ON OBLIQUE PLATES

Robert K. Fujita and G. Edward Cort 1989 9 p Presented at the 1989 ASME Winter Annual Meeting, San Francisco, CA, 10-15 Dec. 1989
(Contract W-7405-eng-36)
(DE89-015275; LA-UR-89-2595; CONF-891208-12) Avail: NTIS HC A02/MF A01

The justification for 3-D versus 2-D simulations of non-symmetric armor penetration problems has been a topic of discussion for many years. Two-dimensional plane-strain approximations are generally not quantitatively accurate, especially at later times, but they can be performed efficiently and the results are usually acceptable. Although 3-D calculations provide better results, they are very time consuming and expensive to perform. But with the improved speed and memory capabilities of modern computers, it is now more feasible to perform 3-D calculations. Two- and 3-D Eulerian calculations performed with the HULL hydrodynamic computer code with experimental data from oblique impacts of uranium-alloy penetrators into rolled homogeneous armor targets are compared. The results indicate that the 3-D calculations provide the best predictions of experimental data and are reasonably efficient to perform considering the improved accuracy of the calculation over comparable 2-D calculations. DOE

N90-15441# Japan Atomic Energy Research Inst., Tokyo. Dept. of Reactor Engineering.
NEW APPROACH TO THE INVERSE PROBLEM OF SIX-LINK MANIPULATORS VIA THE OPTIMIZATION TECHNIQUE
Shinobu Sasaki Jun. 1989 23 p In JAPANESE; ENGLISH summary
(DE90-710044; JAERI-M-89-067) Avail: NTIS (US Sales Only) HC A03/MF A01

An approach is presented to solve the inverse kinematics of manipulators by associating an expression as to manipulator hand position and orientation with an optimization technique. The key point in this approach is to depart from the fixed and customary idea of dealing with all given articulated variables at a time and to pay attention to only three of them while the remaining three variables are considered to have dependent relationships with the first three variables. The linearized model of a specified performance index composed of these three variables plays an important role in determining the desired solutions. The results of computer simulation show that numerical solutions are sufficiently reliable. Theoretically, this approach is applicable to all types of six link manipulators with rotational and/or revolute joints. DOE

N90-15442*# National Aeronautics and Space Administration. Langley Research Center, Hampton, VA.
SINGLE ELEMENT MAGNETIC SUSPENSION ACTUATOR Patent Application
Nelson J. Groom, inventor (to NASA) 11 Sep. 1989 16 p
(NASA-Case-LAR-13981-1; NAS 1.71:LAR-13981-1; US-Patent-Appl-SN-405154) Avail: NTIS HC A03/MF A01 CSCL 13I

The invention, a single element magnetic suspension actuator with bidirectional force capability along a single axis, includes an electromagnet and a nonmagnetic suspended element. A permanent magnet mounted on the suspended element interacts with a magnetic field established by the electromagnet to produce bidirectional forces in response to a variable force command voltage V(sub FC) applied to the electromagnet. A sensor measures the position of the suspended element on the single axis which is a function of force command voltage V(sub FC). NASA

N90-15443*# National Aeronautics and Space Administration. Marshall Space Flight Center, Huntsville, AL.
HYBRID BUTTERFLY VALVE Patent Application
Laurence deQuay, inventor (to NASA) 7 Sep. 1989 15 p
(NASA-Case-SSC-00004; US-Patent-Appl-SN-404292; NAS 1.71:SSC-00004) Avail: NTIS HC A03/MF A01 CSCL 13K

A hybrid butterfly valve has a stationary seat and a valve closure disk which may rotate together with an actuating shaft from the fully open position to a position wherein the disk is aligned with the seat, and may be moved linearly into a sealing relationship with the seat. The disk is supported by brackets having an elongated slot through which the shaft extends, the brackets being adapted to move linearly relative to the shaft. Cams fastened to the shaft initiate a 90 degree rotation of the disk from the fully open position to the position where the valve disk is aligned with the seat, and the cams act in conjunction with followers carried by the disk to move the disk and the brackets linearly. The disk carries guide members which are positioned in a guide slot, the guide slot having an arcuate portion and a linear portion, and the disk is guided by the guide members guided in the arcuate portion when the disk is fully opened to and until the disk is aligned with the seat, and the guide members are guided by the linear portion of the slot. A portion of each cam is spring biased so that the cams tightly engage follower rollers carried by the brackets during the rotational portion of the movement of the disk. NASA

N90-15444*# National Aeronautics and Space Administration. Lewis Research Center, Cleveland, OH.
HIGH TEMPERATURE, FLEXIBLE, THERMAL BARRIER SEAL Patent Application
Paul J. Siroccky and Bruce M. Steinetz 27 Nov. 1989 13 p
(NASA-Case-LEW-14672-1; NAS 1.71:LEW-14672-1; US-Patent-Appl-SN-441672) Avail: NTIS HC A03/MF A01 CSCL 11A

This device seals the sliding interfaces between structural panels that are roughly perpendicular to each other or whose edges are butted against one another. The nonuniformity of the gap between the panels requires significant flexibility along the seal length. The seal is mounted in a rectangular groove in a moveable structural panel. A plurality of particles or balls is densely packed in an outer sheathing. The balls are laterally preloaded to maintain sealing contact with the adjacent wall using a pressurized linear bellows. Distortions in the adjacent panel are accommodated by rearrangement of the particles within the outer sheathing. Leakage through the seal is minimized by densely compacting the internal particles and by maintaining positive preload along the back side of the seal. The braid architecture of the outer sheathing is selected to minimize leakage through the seal and to resist mechanical abrasion. NASA

N90-15445*# National Aeronautics and Space Administration. Lewis Research Center, Cleveland, OH.
FULLY ARTICULATED FOUR-POINT-BEND LOADING FIXTURE Patent Application
Anthony M. Calomino, inventor (to NASA) 28 Dec. 1989 11 p
(NASA-Case-LEW-14776-1; US-Patent-Appl-SN-458274; NAS 1.71:LEW-14776-1) Avail: NTIS HC A03/MF A01 CSCL 13I

A fully articulated four-point bend loading fixture for Modulus of Rupture (MOR) and fracture toughness specimens utilizes an upper loading plate in combination with a lower loading plate. The lower plate has a pair of spring loaded ball bearings which seat in V-shaped grooves located in the upper plate. The ball bearings are carried in the arms of the lower plate. A load is applied to the specimen through steel rollers, one large roller and one smaller roller each located on both the upper and lower plates. The large rollers have needle roller bearings which enable a single loading roller to rotate relative to the plate to which it is attached. NASA

N90-15446 ESDU International Ltd., London (England).
A PROCEDURE FOR FORCE-BALANCING PLANAR LINKAGES USING COUNTERWEIGHTS
Sep. 1989 49 p
(ESDU-89028; ISBN-0-85679-700-6; ISSN-0141-4046) Avail: ESDU

This data item gives a step-by-step procedure for force-balancing planar single degree of freedom linkages. Balance is achieved by the addition of counterweights so that the resulting center of mass of the linkage remains stationary throughout the motion cycle. The procedure, each step of which is illustrated by its application to a six bar linkage with a slider, calculates the counterweight masses and their locations. Although the method applies to most linkages composed of rigid links, with revolute

and sliding joints, a test is included to identify those linkages that cannot be completely force balanced. Advice is given on the optimum shape of the counterweights and on allowable combinations for common linkages. A further fully worked example of a twelve bar linkage driven by a gear pair is included. ESDU

N90-15447*# Carnegie-Mellon Univ., Pittsburgh, PA. The Robotics Inst.
BASE REACTION OPTIMIZATION OF REDUNDANT MANIPULATORS FOR SPACE APPLICATIONS
C. L. Chung, S. Desa, and C. W. deSilva (British Columbia Univ., Vancouver.) 1988 32 p
(Grant NAG3-811)
(NASA-CR-186274; NAS 1.26:186274; CMU-RI-TR-88-17)
Copyright Avail: NTIS HC A03/MF A01 CSCL 13I

One of the problems associated with redundant manipulators which were proposed for space applications is that the reactions transmitted to the base of the manipulator as a result of the motion of the manipulator will cause undesirable effects on the dynamic behavior of the supporting space structure. It is therefore necessary to minimize the magnitudes of the forces and moments transmitted to the base. It is shown that kinematic redundancy can be used to solve the dynamic problem of minimizing the magnitude of the base reactions. The methodology described is applied to a four degree-of-freedom spatial manipulator with one redundant degree-of-freedom. Author

N90-15448# Lawrence Livermore National Lab., CA.
COMPARISON OF ENGINE KNOCK PREDICTIONS USING A FULLY-DETAILED AND A REDUCED CHEMICAL KINETIC MECHANISM
J. S. Cowart, J. C. Keck, J. B. Heywood, Charles K. Westbrook, and William J. Pitz (Massachusetts Inst. of Tech., Cambridge.) 13 Oct. 1989 62 p Presented at the Western States Section Meeting of the Combustion Institute, Livermore, CA, 23-24 Oct. 1989 Submitted for publication Sponsored in part by Ford Motor Co.; Chrysler Corp.; Peugeot Societe Anonyme; and Regie Nationale des Usines Renault
(Contract W-7405-eng-48)
(DE90-002805; UCRL-102147; CONF-8910289-1) Avail: NTIS HC A04/MF A01

Two different chemical kinetic models are used to interpret engine knock data obtained in a laboratory internal combustion engine. These consisted of a detailed chemical kinetic model and a global kinetic model, both calibrated to be able to describe these conditions. Both models are found to provide accurate simulations of the experimental data, but both models required calibration and/or updating. The comparisons of both models with experimental results are discussed, and the two models are compared together. The relationships between the detailed kinetic model and the global reaction steps intended to simulate those steps are examined in detail, and the relative strengths and weaknesses of the two approaches are discussed. DOE

N90-15449# Sandia National Labs., Albuquerque, NM. Dept. of Solid Dynamics.
FRAGMENTATION STATISTICS FROM EULERIAN HYDROCODE CALCULATIONS
Timothy G. Trucano, Dennis E. Grady, and J. Michael McGlaun 1989 27 p Presented at the Hypervelocity Impact Symposium, San Antonio, TX, 12-14 Dec. 1989
(Contract DE-AC04-76DP-00789)
(DE90-002906; SAND-89-0597C; CONF-891214-10) Avail: NTIS HC A03/MF A01

In this paper, we discuss a procedure for computing discrete fragmentation information for terminal ballistics events from the continuum data that emerges from two-dimensional Eulerian hydrocode simulations of these events. The present examples deal with the normal impact of lead cylinders on lead plates at velocities below 1600 m/s. In this regime, the resulting debris is almost exclusively solid lead fragments. We have experimental data of sufficient accuracy to evaluate the extraction of such fragmentation information from code simulations. The problem is interesting because the observed distribution of fragment size would require extreme subgrid resolution in the hydrocode if the statistics were computed directly. Our approach is different. We ask whether or not the general continuum description predicted by the code contains enough information to allow coupling of an analytic fragmentation theory that successfully predicts fragmentation statistics. We believe that this approach is valid, and discuss our current success in matching experimental data. DOE

N90-15450# Los Alamos National Lab., NM. Technical Engineering Support Group.
EFFECTS OF PARAMETRIC VARIATIONS OF COMPLEX TARGETS ON DAMAGE FROM PROJECTILE IMPACT
Robert W. Meier 1989 14 p Presented at the Hypervelocity Impact Symposium, San Antonio, TX, 12-14 Dec. 1989 Submitted for publication
(Contract W-7405-eng-36)
(DE90-003214; LA-UR-89-3791; CONF-891214-11) Avail: NTIS HC A03/MF A01

The effects of a hypervelocity projectile striking complex targets have been investigated. The targets consisted of metallic and low-density shock attenuating layers and void regions. The major features of the targets were systematically varied to correlate changes in the targets with the projectile's effectiveness in damaging the targets. Two-dimensional numerical simulations were done with the Eulerian computational fluid dynamics program PINON. Projectile effectiveness against the various targets was measured by determining the maximum pressure, pressure integral, P(sup 2)(tau) value, and hole size at several locations in the targets. DOE

N90-15451# Ricardo-ITI, Westmont, IL.
MULTI-DIMENSIONAL MODELING OF CONVECTIVE HEAT TRANSFER WITH APPLICATION TO I.C. ENGINES Final Report
30 Nov. 1989 9 p
(Contract DE-AC04-86AL-33183)
(DE90-003245; DOE/AL-33183/T12; Rept-89-154) Avail: NTIS HC A02/MF A01

This report summarizes the major findings of a research program in the area of convective heat transfer modeling for internal combustion engine flows. The modeling effort has been performed in the context of multi-dimensional flow calculation procedures with the following objectives: (1) develop better techniques for representing the key heat transfer phenomena in multi-dimensional calculation procedures, and (2) utilize these to develop a more comprehensive understanding of convective heat transfer in complex, unsteady, reacting flows characteristic of those found in I.C. engines. DOE

N90-15452# Massachusetts Inst. of Tech., Cambridge. Dept. of Materials Science and Engineering.
SUBMERGED ARC WELDING CONSUMABLES FOR HSLA (HIGH STRENGTH LOW ALLOY)-100 STEEL M.S. Thesis
Daniel J. Peters Jun. 1989 122 p
(Contract N00014-88-K-0215)
(AD-A213433) Avail: NTIS HC A06/MF A01 CSCL 11/6

The development of a class of high strength, a low alloy steel with strength levels of 690 MPa (100 ksi) has made it necessary to formulate new welding consumables to take advantage of the potential benefits of this steel, HSLA-100. The possible benefits include welding without pre or post heating resulting in improved productivity. Optimizing the consumables for higher heat inputs further improve productivity and reduce construction costs when using this steel. The optimum titanium content for the welds in this investigation was 0.012 wt percent, the lowest level in this study. The range over which the titanium content varied was found to have little direct effect on the acicular ferrite fraction in the weld metal. The result indicated that the number of metallic oxide inclusions per unit volume and the inclusion size distribution were controlled by titanium bearing, faceted particles found within the spherical inclusions. Manganese

also has little effect on the acicular ferrite fraction, but influenced the formation of martensite and retained austenite islands within the microstructure. GRA

N90-15453# University of Southern California, Los Angeles. Inst. for Robotics and Intelligent Systems.
RESEARCH IN KNOWLEDGE-BASED VISION TECHNIQUES FOR THE AUTONOMOUS LAND VEHICLE PROGRAM Final Annual Report, 1 Jun. 1988 - 31 May 1989
R. Nevatia, ed., K. Price, ed., W. Franzen, S. Gazit, G. Medioni, S. Peng, and P. Saint-Marc Aug. 1989 59 p
(Contract DACA76-85-C-0009)
(AD-A213440; IRIS-255; ETL-0545) Avail: NTIS HC A04/MF A01 CSCL 17/7

The authors' basic approach to detecting and tracking motion is to extract and match features, such as lines and regions, from a sequence and to generate motion estimates from these. They present one report on spatio-temporal analysis for tracking edges through very closely spaced sequences. They also present a report on matching edge-based contours using edges from multiple scales with low resolution guiding high resolution matches. They also present an analysis of estimating 3-D motion and structure of moving object with uniform acceleration. GRA

N90-15454# Naval Surface Warfare Center, Silver Spring, MD.
EPOXY-RESIN CABLE TERMINATIONS
Peter B. Keller 3 Feb. 1989 25 p
(AD-A213789; NSWC-TR-88-400) Avail: NTIS HC A03/MF A01 CSCL 13/5

The general function of end fittings, also referred to as terminations, is to allow the attachment of wire to a system in a manner that approaches 100 percent of the strength of the cable. This report addresses investigations made into the use of epoxy-resin terminations. An initial investigation into the application of Epoxy-Resin Terminations, for end-fitting, to small diameter cables was conducted. Test samples were made using steel, titanium, and amorphous metal cables. Though some difficulty was encountered during termination installation, tensile testing produced results equal to cable strength. Recommendations to enhance installation, and provide broad base testing and evaluation are given. GRA

N90-15455# Illinois Univ., Chicago. Dept. of Mechanical Engineering.
SPATIAL DYNAMICS OF DEFORMABLE MULTIBODY SYSTEMS WITH VARIABLE KINEMATIC STRUCTURE Final Report, 21 Sep. 1987 - 20 Sep. 1989
A. A. Shabana Oct. 1989 11 p
(Contract DAAL03-87-K-0124)
(AD-A214098; ARO-25170.14-EG) Avail: NTIS HC A03/MF A01 CSCL 12/1

A method of the spatial kinematic and dynamic analysis of deformable multibody systems subject to topology changes and impacts is presented. A pieced interval analysis scheme that accounts for the change in the spatial system topology due to the changes on the connectivity between bodies is developed. Deformable bodies in the system are discretized using the finite element method and accordingly a finite set of deformation modes is employed to characterize the system vibration. Even though there are infinitely many arrangements for deformable body axes, computational difficulties may be encountered due to the use of a limited number of deformation modes. Therefore, the deformable body references have to be carefully selected, and accordingly as the system topology changes, new bases for the configuration space to another, a set of spatial interface conditions or compatibility conditions that are formulated using a set of nonlinear algebraic equations are developed. The solution of these equations uniquely defines the spatial configuration of the deformable multibody system after the change in the system kinematic structure. The techniques proposed in this research are applied to several technological system such as robotic manipulators and weapon systems. GRA

N90-15456# Army Construction Engineering Research Lab., Champaign, IL.
AUTOMATION AND ROBOTICS IN CONSTRUCTION: JAPANESE RESEARCH AND DEVELOPMENT Final Report
Thomas M. Gatton and Frank W. Kearney Oct. 1989 38 p
(DA Proj. 4A1-62731-AT-41)
(AD-A214170; CERL-TR-M-90/03) Avail: NTIS HC A03/MF A01 CSCL 12/9

The U.S. Army Corps of Engineers' construction program needs to reduce costs and improve quality. Productivity is decreasing in the U.S. construction industry, which is the opposite of the manufacturing segment, where productivity is improving. One reason for this is the use of advanced computer and machine technologies. The introduction of advanced construction technologies is particularly evident in Japan. This report presents information gathered during a study of Japanese construction industry. Much of the information was gained through interviews with company representatives. Particular focus was placed on identifying the methodology and organization that the Japanese use in their research and development for automated construction systems, including development of robotics. The information gathered shows that the Japanese are considerably ahead of other countries in their applied research towards construction automation. The organization and methodology that each Japanese company used toward this effort seem very similar. The differences between Japanese companies and their U.S. counterparts as they affect the introduction of new construction technologies are discussed. GRA

N90-15457# Naval Postgraduate School, Monterey, CA. Dept. of Computer Science.
PLANNING MINIMUM-ENERGY PATHS IN AN OFF-ROAD ENVIRONMENT WITH ANISOTROPIC TRAVERSAL COSTS AND MOTION CONSTRAINTS Ph.D. Thesis
Ron S. Ross Jun. 1989 280 p
(Contract MIPR-ATEC-88-86)
(AD-A214181; NPS52-89-040) Avail: NTIS HC A13/MF A02 CSCL 12/9

For a vehicle operating across arbitrarily-contoured terrain, finding the most fuel-efficient route between two points can be viewed as a high-level global path-planning problem with traversal costs and stability dependent on the direction of travel (anisotropic). The problem assumes a two-dimensional polygonal map of homogeneous cost regions for terrain representation constructed from elevation information. The anisotropic energy cost of vehicle motion has a non-braking component dependent on horizontal distance, a braking component dependent on vertical distance, and a constant path-independent component. The behavior of minimum-energy paths is then proved to be restricted to a small, but optimal set of traversal types. An optimal-path-planning algorithm, using a heuristic search technique, reduces the infinite number of paths between the start and goal points to a finite number by generating sequences of goal-feasible window lists from analyzing the polygonal map and applying pruning criteria. The pruning criteria consist of visibility analysis, heading analysis, and region-boundary constraints. Each goal-feasible window lists specifies an associated convex optimization problem, and the best of all locally-optimal paths through the goal-feasible window lists is the globally-optimal path. These ideas have been implemented in a computer program, with results showing considerably better performance than the exponential average-case behavior predicted. GRA

N90-15458# Environmental Research Inst. of Michigan, Ann Arbor.
PLANNING SYSTEMS FOR AUTONOMOUS LEGGED VEHICLES Final Technical Report, Jul. 1986 - Aug. 1987
May 1989 67 p Sponsored in part by Wisconsin Univ., Madison
(Contract DAAE07-86-C-R013; ARPA Order 5575)
(AD-A214242; ERIM-196000-7-F) Avail: NTIS HC A04/MF A01 CSCL 13/6

This report describes efforts to integrate the areas of mobility

research and autonomous navigation in support of the Adaptive Suspension Vehicle program. Experimental research on the locomotion of Nubian goats is summarized. A decision model of terrain navigation based upon the experimental results is reported. The Computer Simulation of Animal based upon the experimental results is reported. The Computer Simulation of Animal Navigation, which implements the decision model, is presented. The need for increased flexibility in planning systems is discussed, and a sliding vehicle simulation which incorporates some of the desired features (the Blackboard Planning System) is described. A paper discussing the fundamental notions of search and exploration in autonomous navigation is included. GRA

N90-15459# Air Force Wright Research and Development Center, Wright-Patterson AFB, OH.
ANALYSIS OF AN ELASTOHYDRODYNAMIC LUBRICATED POINT CONTACT: USER'S MANUAL Final Report, Apr. 1987 - Apr. 1988
Lewis Rosado Aug. 1989 41 p
(AD-A214257; WRDC-TR-89-2106) Avail: NTIS HC A03/MF A01 CSCL 12/5

In this report, a PC-based computer program is described. The computer program calculates the descriptive characteristics of a general elastohydrodynamic (ehd) lubricated point contact typically found in bearings, gears, and cams. The following characteristics of the contact are calculated: (1) the contact maximum and mean Hertzian stress; (2) the contact ellipse dimensions; (3) the ehd isothermal minimum and central film thickness; and (4) a thermal film thickness correction factor accounting for the effect of shear heating because of sliding and rolling. In addition, it provides the basic theoretical background and equations used. GRA

N90-15460# Westinghouse Savannah River Co., Aiken, SC. Generation Technology Div.
SIMON (SUPERINTELLIGENT MOBILE OBSERVING NAVIGATOR): A HIGH-RELIABILITY ROBOT FOR A RADIATION ENVIRONMENT
A. W. Gartner 1989 15 p Presented at the Annual Westinghouse Computer Symposium, Pittsburgh, PA, 6-7 Nov. 1989
(Contracts DE-AC09-89SR-18035; DE-AC09-76SR-00001)
(DE90-003888; WSRC-RP-89-345; CONF-891192-23) Avail: NTIS HC A03/MF A01

The Robotics Group at the Savannah River Site is developing an autonomous robot to perform monitoring in a reactor radiation zone while the reactor is in operation. The robot will be sealed into a room where it cannot be serviced for the six month reactor cycle. The robot is radio controlled, uses dead reckoning to determine vehicle position, and will dock with a charging stand to replenish its batteries. The system will provide video, temperature, and radiation information. In addition to hardening the robot for the harsh reactor environment, the robot will include many features to ensure that a component failure has minimal impact on the robot with a minimum of redundant systems. Emphasis is being placed on ease of use with a minimal of training and controls to prevent damage by an inexperienced operator. Paths for the robot are preprogrammed and are selected on a graphic map of the room. Additional paths can be entered by authorized personnel. Under manual control, the robot and equipment is protected by a highly effective ultra-sonic collision avoidance system. Under development is a system that will anticipate an unsatisfactory video image and attempt to adjust the receiving antenna's angle for best reception. DOE

N90-15461# California Univ., Davis. Dept. of Electrical Engineering and Computer Science.
FEASIBILITY STUDY OF USING INDUSTRIAL ROBOT FOR ULTRASOUND TESTING Final Progress Report
T. C. Hsia 13 Feb. 1989 22 p Prepared for Lawrence Livermore National Lab., CA
(Contract W-7405-eng-48)
(DE90-002977; UCRL-21243) Avail: NTIS HC A03/MF A01

The purpose of this program is to study the feasibility of employing an articulated industrial robot arm to perform ultrasound scanning of a work piece. The robot arm suitable for such application is the Unimation PUMA 560 manipulator with six degrees of freedom. This research is intended to study the basic properties of several issues which arise in the operations of the UTB facility at LLNL. These issues involve the understanding of control algorithms for collision-free motions of the robot arm with and without redundant kinematics, trajectory generation schemes for automated surface tracking based on 3D CAD/CAM model of the work piece, and the effective use of computer vision and ultrasound sensor to achieve position calibration of a work piece and on-line trajectory modification for accurate surface tracking. The robotics research laboratory at UC Davis has a research robotic system based on a six degrees-of-freedom Unimation PUMA 560 arm and a VAL-II controller. This system is used as a research tool for the investigation. DOE

38 QUALITY ASSURANCE AND RELIABILITY

Includes product sampling procedures and techniques; and quality control.

N90-15462*# Oak Ridge National Lab., TN.
EDDY-CURRENT INSPECTION OF SHUTTLE HEAT EXCHANGER TUBE WELDS
C. V. Dodd, G. W. Scott, and L. D. Chitwood 1989 17 p Presented at the 2nd Conference on Non-Destructive Evaluation for Aerospace Requirements, Huntsville, AL, 22-24 Aug. 1989 Prepared in cooperation with Martin Marietta Corp., New Orleans, LA Sponsored in part by NASA
(Contract DE-AC05-84OR-21400)
(NASA-CR-186302; NAS 1.26:186302; DE90-001335; CONF-8908160-2) Avail: NTIS HC A03/MF A01 CSCL 14D

The goal of this project was to develop the system necessary to demonstrate in the laboratory that an eddy current system can inspect the tubes and welds described, screening for the existence of flaws equal in size to, or larger than, the target flaw. The laboratory system was to include the probe necessary to traverse the tubing, the electronics to drive (i.e., electrically excite) the probe and receive and process signals from it, a data display, data recording and playback devices, and microprocessor software or firmware necessary to operate the system. DOE

N90-15463# Pacific Northwest Lab., Richland, WA.
BACK TO BASICS
James E. Ruffin Sep. 1989 7 p Presented at the 16th Annual Conference of the American Society for Quality Control, Fort Lauderdale, FL, 17-20 Sep. 1989
(Contract DE-AC06-76RL-01830)
(DE90-002734; PNL-SA-16968; CONF-8909110-9) Avail: NTIS HC A02/MF A01

Quality control/quality assurance controls were originally developed and selected for application because they were effective in preventing, reducing, or detecting specific problems that were occurring in manufacturing processes. With the development and use of quality assurance program standards, there has been a movement toward determining the requirements of a quality program standard that are applicable to a certain process as the starting point in the determination of the QA controls to be applied. The advantages are discussed of reviewing and addressing the problems, past or potential, associated with a process as the initial step in the QA control determination. DOE

N90-15464# California Univ., Berkeley. Lawrence Berkeley Lab. Materials and Chemical Sciences Div.
ISOTHERMAL FATIGUE BEHAVIOR OF Sn-Pb SOLAR JOINTS
T. S. E. Summers and J. W. Morris, Jr. Sep. 1989 16 p Presented at the Winter Annual Meeting of the American Society of Mechanical Engineers, San Francisco, CA, 10-15 Dec. 1989 Prepared in cooperation with California Univ., Berkeley
(Contract DE-AC03-76SF-00098)

(DE90-003280; LBL-27774; CONF-891208-25) Avail: NTIS HC A03/MF A01

Isothermal fatigue data were collected for the compositions 5Sn--95Pb, 20Sn--80Pb, 40Sn--60Pb, 50Sn--50Pb and 63Sn--37Pb within the binary Sn--Pb system. All of these compositions are commercially available and include those most commonly used. Because Sn-rich solders are rarely used, they were not investigated here. The fatigue life was defined by a 30 percent load drop. The solders were tested in a double shear configuration joined to copper at 75 C. The displacement rate chosen was 0.01 mm/min, which corresponds to a strain rate of 1.5 x 10(sup -4) s(sup -1) for the specimen configuration, over a 10 percent plastic strain range. Additionally, the microstructural changes during fatigue are presented. The various solder compositions studied exhibit strikingly different as-solidified microstructures. These differences are discussed in terms of their effect on the isothermal joint failure mechanism and joint isothermal fatigue life. DOE

N90-15465# Maryland Univ., College Park. Inst. for Advanced Computer Studies.

INTEGRATED APPROACH FAULT TOLERANCE-CURRENT STATE AND FUTURE REQUIREMENTS Final Report

Pankaj Jalote, comp. and Satish K. Tripathi, comp. 1989 19 p (Contract N00014-89-J-1867)

(AD-A214402) Avail: NTIS HC A03/MF A01 CSCL 12/5

Fault tolerance is a very broad topic. There are many valuable results in the area with many important areas of research remaining. This workshop brought together researchers in four areas; applications, operating systems, hardware, and modelling, in an attempt to take an integrated view of fault tolerance. The outcome is presented of the discussion of the different groups, and a description of the presentations made at the start of the workshop. The use of computers in critical applications such as aircraft flight control and industrial processes continues to increase. As it does so, there is a corresponding increase in the need for computing systems that will continue to operate despite failures. Perhaps the best approach for achieving such dependable computing is the use of integrated fault tolerance, where the system is designed from the ground up to support dependable computing for the given application. With a clean slate, the system designer can allocate portions of the functionality required to implement dependability to the different levels of the system rather than being forced a priori to use a given architecture or operating system. It is with this view that a workshop was organized to discuss the issues involved in an integrated approach to fault tolerance. GRA

N90-15466# Sandia National Labs., Albuquerque, NM. Reliability Dept.

AN ITERATIVE BAYES PROCEDURE FOR RELIABILITY ASSESSMENT

R. R. Prairie and W. J. Zimmer (New Mexico Univ., Albuquerque.) 1990 10 p Presented at the Reliability and Maintainability Symposium, Los Angeles, CA, Jan. 1990

(Contract DE-AC04-76DP-00789)

(DE90-002106; SAND-89-2592C; CONF-900108-2) Avail: NTIS HC A02/MF A01

In component reliability assessment programs, three major sources of data are available for reliability assessment: a development program, production data, and field test data. In practice, reliability assessments are required at the end of each of these stages, and a common method of assessment is to simply combine the test data and provide a pooled estimate. The method suggested in this paper is Bayesian in that the uncertainty about the unreliability is expressed by means of a prior distribution with a specified upper limit. The method is hierarchical Bayes in that the uncertainty about the limit of that prior distribution is also expressed by means of a prior distribution. The data from the development program are incorporated with the prior on the unreliability and with the prior on the upper limit of the prior to obtain a new prior on unreliability. The production data are then used to obtain a revised estimate of the unreliability as well as a modified value for the limit of the prior distribution. This same concept will be carried through when the field data are obtained. The result is a final Bayesian reliability assessment that is iterative in nature and incorporates in a sequential fashion data from each of the three stages common to a component development, production, and surveillance program. DOE

N90-15467# Westinghouse Savannah River Co., Aiken, SC. Scientific Computations Div.

AN EXPERT SYSTEM FOR QUALITY ASSURANCE (A.K.A.) QA EXPRESS

Mary Beth McGrath 1989 15 p Presented at the Annual Westinghouse Computer Symposium, Pittsburgh, PA, 6-7 Nov. 1989

(Contract DE-AC09-89SR-18035)

(DE90-003887; WSRC-RP-89-524; CONF-891192-22) Avail: NTIS HC A03/MF A01

An Expert System to assist and advise engineers and programmers with quality assurance computational software applications was developed using Level 5 software. The expert system was created using production rule language (logic programming) which launches external Hypercard applications and prompts the user for simple answers in order to print out the appropriate QA forms for a specific quality assurance application. The Level 5 and Hypercard interfaces make for a friendly and reliable system which allows for simply maintenance and accessible modifications. DOE

39 STRUCTURAL MECHANICS

Includes structural element design and weight analysis; fatigue; and thermal stress.

For applications see *05 Aircraft Design, Testing and Performance* and *18 Spacecraft Design, Testing and Performance.*

N90-15468 California Inst. of Tech., Pasadena.

ON THE DOMAIN OF DOMINANCE OF THE ASYMPTOTIC ELASTODYNAMIC CRACK-TIP FIELDS Ph.D. Thesis

Sridhar Krishnaswamy 1989 119 p

Avail: Univ. Microfilms Order No. DA8908418

A substantial part of the experimental data in dynamic fracture mechanics has been obtained under the assumption that the asymptotic elastodynamic stress-intensity factor field is dominant over the region around the crack-tip from which the experimental measurements are made. The validity of this assumption is investigated here both experimentally and through simulations of the experiments. The experiments reported in this work were on 4340 steel, three-point bend specimens loaded dynamically using a drop-weight tower. The two cases of dynamically loaded stationary cracks and dynamically propagating cracks were considered. An optical configuration is proposed that leads to a bifocal high-speed camera capable of focussing on two different planes simultaneously. This was used in conjunction with the method of caustics to measure the apparent stress-intensity factor simultaneously from two different regions (initial-curves) around the crack-tip. The experimentally obtained boundary loads were subsequently used in dynamic two- and three-dimensional finite-element simulations of the experiments which were carried only up to the point of crack initiation. On the basis of both the experimental results as well as the numerical simulations, no sizeable region of dominance for the asymptotic elastodynamic field was found for the laboratory situation studied.

Dissert. Abstr.

N90-15469 Northwestern Univ., Evanston, IL.

DAMAGE EVALUATION FROM SURFACE DISPLACEMENT DATA Ph.D. Thesis

Zhanjun Gao 1989 142 p

Avail: Univ. Microfilms Order No. DA8913975

The problem of evaluating plastic damages by using the residual surface displacement data is discussed. The plastic damages are caused by a series of unknown loadings and accumulated in an unknown sub-domain of the material. The general problem of the

damage evaluation from the residual surface displacement data is an ill-posed nonlinear problem. The residual surface displacements are not sufficient to recover the shape of the damage domain and the exact distribution of the residual plastic strains. However, some important characteristic quantities associated with the damages of the material can be obtained. These quantities include stresses in the vicinity of the damage domain, lower bounds of the strain energy and any quadratic functions of the plastic strains. The problem addressed here is an inverse problem of continuum mechanics, which is different substantially from the conventional forward analyses. Satisfactory numerical results can be obtained only if a suitable algorithm is employed. The nature of the ill-posed problem is discussed and a very powerful method is presented to convert an ill-posed problem into a well-posed one. The surface displacements serve as sensors for the damages inside the materials. The inversion of the characteristic damage quantities requires no knowledge of the loading history. Coordinating with appropriate damage models, we can determine the mechanical effects of the material deterioration, and elucidate the process leading to the final failure. Dissert. Abstr.

N90-15470# Sydney Univ. (Australia). School of Civil and Mining Engineering.

NONLINEAR STRAIN-DISPLACEMENT RELATIONS FOR THIN AXISYMMETRIC SHELLS

J. Michael Rotter and Paul T. Jumikis Feb. 1988 48 p
(PB89-226013; R-563) Avail: NTIS HC A03/MF A01 CSCL 20K

Nonlinear deformation and stability analyses are based on nonlinear relations between the strains and the corresponding displacements of the body. Many attempts were made to develop nonlinear strain-displacement relations for thin shells, and many of these are quoted in specialized form for shells of revolution. A new set of nonlinear strain-displacement relations is described for thin shells, subject to large displacements with moderate rotations, and which retains more terms than most existing theories. The new relations are proposed only for use in finite element calculations. The chief difference between the new relations and previous work is the recognition that nonlinear strains arising from products of in-plane strain terms may be important in certain buckling problems. It is shown that the widely-used relations of Sanders (1963) lead to the wrong answer for a simple practical proble, and that this disadvantage is overcome by the present formulation. GRA

N90-15471 George Washington Univ., Washington, DC.

DEVELOPMENT OF A RATE INDEPENDENT PLASTICITY THEORY FOR GENERAL CYCLIC LOADING Ph.D. Thesis

Keyvan Ahdut 1989 164 p
Avail: Univ. Microfilms Order No. DA8910825

Rate independent cyclic plasticity under general cyclic loading conditions are studied. Different existing cyclic plasticity theories are discussed and the constitutive relation for each theory is evaluated. A general rate independent cyclic plasticity theory is formulated for general loading conditions and for multidimensional stress states. The main feature of this theory is that three stages are identified for describing the associated constitutive relation of the model. The plastic modulus is the most important quantity employed in formulating this new theory for general cyclic loading. The functional form of the plastic modulus depends on the loading history, the accumulated plastic strain, and the location of the yield surface in stress space. A general hardening model for combined kinematic and isotropic hardening is considered, the specific hardening rules are discussed, and equations are derived for the translation and deformation of the yield surface. The simulative and predictive capabilities of this new theory are compared with a variety of experimental data on materials under different uniaxial loading conditions. Specifically, different types of predicted uniaxial behavior, including monotonic loading, cyclic creep, and cyclic stabilization under controlled strain range, are compared with test data. The results of these comparisons show good agreement between the predicted material behavior and the experimental results. Dissert. Abstr.

N90-15472 Notre Dame Univ., IN.

PARAMETRIC IDENTIFICATION OF DISCRETE TIME SERIES MODELS FOR STRUCTURAL RESPONSE PREDICTION Ph.D. Thesis

Joseph Jay Hollkamp 1989 319 p
Avail: Univ. Microfilms Order No. DA8914275

Methods are studied for the identification of discrete time series models for dynamic structural systems. Experimental data in time series form is used to estimate the model parameters and the model is then used to predict the transient response of the structural system when subjected to arbitrary input. The linear, structural transfer function is expressed in the form of an autoregressive moving average discrete time series model. Accurate estimation of the model parameters for a given system is often limited due to the influence of measurement noise. Numerous algorithms were developed to treat the noise bias problem and were successful in varying degrees. The focus is the evaluation of current methods and the development of alternative methods for the estimation of the discrete time series models in the presence of experimental noise. A new procedure, the Reduced Backward Method, was developed to estimate models form the noise corrupted data. The Reduced Backward Method uses model order overspecification to reduce the noise bias errors. Unfortunately, overspecified models are excessively large and contain noise related modes. Unlike other procedures, the Reduced Backward Method automatically reduces the model order by eliminating the noise related portions of the model. The result is a low order model that provides accurate prediction of transient response. Simulated numerical data and experimental data from structural systems ranging from single degree of freedom oscillators to a complex subscale sailplane are used to verify the effectiveness of the Reduced Backward Method. Results show that predictions of experimental acceleration response are accurate to within a few percent. Extensions to multiple input multiple output systems, nonlinear systems and a two-stage algorithm for estimation of reduced order models are also presented. Dissert. Abstr.

N90-15473# Sandia National Labs., Albuquerque, NM.

CHARACTERIZING TRANSIENT VIBRATIONS USING BAND LIMITED MOMENTS

David O. Smallwood 1989 25 p Presented at the 60th Shock and Vibration Symposium, Virginia Beach, VA, 14-16 Nov. 1989
(Contract DE-AC04-76DP-00789)
(DE90-000799; SAND-89-1512C; CONF-891152-2) Avail: NTIS HC A03/MF A01

A method is described to characterize shocks (transient time histories) in terms of the Fourier energy spectrum and the moments in the time domain of the shock passed through a contiguous set of bandpass filters. It is then shown how realizations of a random process can be generated which in the mean will have the same energy and moments as the characterization of the transient event. DOE

N90-15474# Sandia National Labs., Albuquerque, NM. Experimental Mechanics Dept.

LOCATION OF INTERIOR IMPACT SOURCE IN RANDOMLY EXCITED STRUCTURES

Thomas L. Paez, Terry Ernest, and Scott McBride 1989 13 p Presented at the 60th Shock and Vibration Symposium, Virginia Beach, VA, 14-16 Nov. 1989
(Contract DE-AC04-76DP-00789)
(DE90-001092; SAND-89-1680C; CONF-891152-4) Avail: NTIS HC A03/MF A01

A technique for identifying the location of an internal impact source in a randomly excited structure is developed in this paper. It is shown that when an impact source can be modelled as a shot noise random process, a straightforward procedure can be used along with standard testing and measurement procedures to find the impact source. The results of a laboratory experiment are presented; these demonstrate the applicability of the technique. DOE

N90-15475# Lawrence Livermore National Lab., CA.
A SIMPLE SHELL ELEMENT FORMULATION FOR LARGE-SCALE ELASTOPLASTIC ANALYSIS
Bruce E. Engelmann, Robert G. Whirley, and Gerald L. Goudreau Jul. 1989 18 p Presented at the ASME Winter Annual Meeting, San Francisco, CA, 10-15 Dec. 1989
(Contract W-7405-eng-48)
(DE89-015452; UCRL-99677; CONF-891208-9) Avail: NTIS HC A03/MF A01

Nonlinear structural mechanics problems arise in a wide variety of disciplines, from automotive crashdynamics to earthquake engineering to nuclear power plant analysis. An important aspect of many of these problems involves the study of shell structures undergoing potentially large displacement but small strains. In addition, material nonlinearity may play a major role. Due to the complexity of solution strategies for nonlinear problems, these analyses can require large amounts of computer time to achieve a solution. Thus, practical developments for nonlinear analysis must balance accuracy and robustness against computational speed. A recently developed four-node quadrilateral shell element with good accuracy properties is described. The element combines many components from other successful mixed formulations in a three-field variational framework, and is formulated in a large-displacement small-strain context. Emphasis was placed on the development of a simple, low order formulation with good accuracy in a wide range of loading situations. Implementation of complex constitutive models is straightforward in this formulation. In addition, this four-node flat shell element is suitable for most widely used contact algorithms. These characteristics make the present formulation amenable to implementation in a general purpose analysis environment. A description of the shell kinematics and governing equations is given. This is followed by a detailed description of the finite element formulation with particular emphasis on the fields chosen for in-place and transverse variables. Finally, several numerical examples are given to illustrate the performance of the proposed element on both linear and nonlinear problems. DOE

N90-15476# Lawrence Livermore National Lab., CA.
STATISTICAL MODEL FOR PARTICLE-VOID DEFORMATION KINETICS IN GRANULAR MATERIALS DURING SHOCK WAVE PROPAGATION
R. B. Stout 25 Jul. 1989 24 p Presented at the International Symposium on Wave Propagation in Granular Media, San Francisco, CA, 10-14 Dec. 1989 Submitted for publication
(Contract W-7405-eng-48)
(DE89-017729; UCRL-101623; CONF-891241-1) Avail: NTIS HC A03/MF A01

The object is a physically based theory for the shock response of granular materials. The approach applied concepts from classical statistical mechanics to represent physical attributes and their time rates of change that are descriptive of particle-void kinetics in deforming granular materials. Mathematically, an arbitrary volume in a granular material is viewed as a set of particles and a set of void spaces. A statistical description for the set of particles is defined in the context of physical attributes that characterize a given species of particle. Similarly, a statistical description for the set of void spaces is defined in the context of physical attributes that characterize a given species of void. For a statistical formulation that describes deformation kinematics across a propagating shock front, field expressions for the relative deformation and its associated kinematic measures are represented with functionals that depend on the probability density functions for the sets of particles and voids. In deriving field equations for the shock analysis, a thermodynamic model for particle-void kinetics was developed. As part of this development, a thermodynamic potential for the particle-void kinetics was defined. DOE

N90-15477# International Centre for Theoretical Physics, Trieste (Italy).
FRACTAL DIMENSION OF THE FRACTURED SURFACE OF MATERIALS
C. W. Lung and S. Z. Zhang (Academia Sinica, Shenyang, China) May 1989 11 p Conference held in Nice, Franc, 1-4 Oct. 1989 Submitted for publication
(DE89-635764; IC-89/76) Avail: NTIS (US Sales Only) HC A03/MF A01

Fractal dimension of the fractured surface of materials is discussed to show that the origin of the negative correlation between D(sub F) and toughness lies in the method of fractal dimension measurement with perimeter-area relation and also in the physical mechanism of crack propagation. DOE

N90-15478# Edgerton, Germeshausen and Grier, Inc., Idaho Falls, ID.
EXPERIENCE WITH J TESTING OF 304/308 STAINLESS STEEL WELDMENT
S. M. Graham, W. R. Lloyd, and W. G. Reuter 1989 28 p Presented at the 2nd Symposium on User Experience With Elastic-Plastic Test Methods, Orlando, FL, 8-9 Nov. 1989
(Contract DE-AC07-76ID-01570)
(DE90-002046; EGG-M-88501; CONF-8911118-1) Avail: NTIS HC A03/MF A01

Crack initiation toughness tests were conducted using the J-Integral as a fracture characterizing parameter according to the ASTM Standard Test Method for J(sub Ic), A Measure of Fracture toughness, E813-87. The specimens were made from a weldment of 304 stainless steel (SS) base metal and 308 SS weld metal, and were fabricated such that the crack initiation toughness J(sub Ic) of the weld metal could be measured. A peculiar feature of all of the tests was that crack growth occurred in an inverse tunneling mode. The provisional initiation toughness J(sub Q) calculated from the test results was determined to be invalid because the validation requirements on change in crack front curvature and on accuracy of the predicted crack extension were not met. The accuracy of the predicted extensions was improved by applying correction factors to the measured compliances to account for crack front curvature, plastic deformation, friction, and indention. The excessive change in crack front curvature was caused by the transition from tunneling growth during fatigue precracking (before the specimens were side grooved) to inverse tunneling during slow stable crack growth. Crack growth by inverse tunneling may indicate a constraint condition higher than plane strain at the root of the side-grooves. If this is the case, the overall stress state is more severe than plane strain, and the measured initiation toughness should be a valid indication of the lower bound for high constraint. DOE

N90-15479# Oak Ridge National Lab., TN. Metals and Ceramics Div.
A SEMIAUTOMATED COMPUTER-INTERACTIVE DYNAMIC IMPACT TESTING SYSTEM
D. J. Alexander, R. K. Nanstad, W. R. Corwin, and J. T. Hutton 1989 27 p Presented at the ASTM Symposium on the Applications of Automation Technology to Fatigue and Fracture Testing, Kansas City, MO, 22-23 May 1989
(Contract DE-AC05-84OR-21400)
(DE90-002721; CONF-8905112-2) Avail: NTIS HC A03/MF A01

A computer assisted semiautomated system was developed for testing a variety of specimen types under dynamic impact conditions. The primary use of this system is for the testing of Charpy specimens. Full-, half-, and third-size specimens were tested, both in the lab and remotely in a hot cell for irradiated specimens. Specimens are loaded into a transfer device which moves the specimen into a chamber, where a hot air gun is used to heat the specimen, or cold nitrogen gas is used for cooling, as required. The specimen is then quickly transferred from the furnace to the anvils and then broken. This system incorporates an instrumented tup to determine the change in voltage during the fracture process. These data are analyzed by the computer system after the test is complete. The voltage-time trace is recorded with a digital oscilloscope, transferred to the computer, and analyzed. The analysis program incorporates several unique features. It interacts with the operator and identifies the maximum voltage during the test, the amount of rapid fracture during the test (if any), and the end of the fracture process. The program then

calculates the area to maximum voltage and the total area under the voltage-time curve. The data acquisition and analysis part of the system can also be used to conduct other dynamic testing. Dynamic tear and precracked specimens can be tested with an instrumented tup and analyzed in a similar manner. DOE

N90-15480 ESDU International Ltd., London (England).
RESULTANT FORCES AND MOMENTS IN COMPLETELY RESTRAINED PLATES SUBJECTED TO A RECOVERY TEMPERATURE VARYING LINEARLY WITH TIME
Aug. 1989 5 p Supersedes ESDU-Struct-H.02.00.02
(ESDU-89024; ESDU-Struct-H.02.00.02; ISBN-0-85679-696-4; ISSN-0141-4097) Avail: ESDU

This Data Item ESDU 89024, an addition to the Structures Subseries, treats the transient situation of the variation of the forces and moments in a thick plate insulated on one side when the aerodynamic heating temperature on the other side is changing, from an initially constant temperature condition, linearly with time. Curves are given that allow the force and moment to be obtained at any time in a plate with fully clamped edges. The curves can be applied when there is a thin insulating layer at the heated surface. A fully worked example illustrates the use of the method. ESDU

N90-15481 ESDU International Ltd., London (England).
THERMAL STRESSES IN UNRESTRAINED PLATES SUBJECTED TO A RECOVERY TEMPERATURE VARYING LINEARLY WITH TIME
Aug. 1989 4 p Supersedes ESDU-Struct-H.02.00.04
(ESDU-89025; ESDU-Struct-H.02.00.04; ISBN-0-85679-697-2; ISSN-0141-4097) Avail: ESDU

This data item treats the transient situation of the variation of the surface stresses in a thick plate insulated on one side when the aerodynamic heating temperature on the other side is changing, from an initially constant temperature condition, linearly with time. Curves are given that allow the stresses to be obtained at both the heated and insulated surfaces at any time for a plate with completely free edges. The curves can be applied when there is a thin insulating layer at the heated surface. A fully worked example illustrates the use of the method. ESDU

N90-15482*# Virginia Polytechnic Inst. and State Univ., Blacksburg. Dept. of Engineering Science and Mechanics.
FATIGUE LOADING HISTORY RECONSTRUCTION BASED ON THE RAIN-FLOW TECHNIQUE
A. K. Khosrovaneh and N. E. Dowling Dec. 1989 73 p
(Grant NAG1-822)
(NASA-CR-181942; NAS 1.26:181942) Avail: NTIS HC A04/MF A01 CSCL 20K

Methods are considered for reducing a non-random fatigue loading history to a concise description and then for reconstructing a time history similar to the original. In particular, three methods of reconstruction based on a rain-flow cycle counting matrix are presented. A rain-flow matrix consists of the numbers of cycles at various peak and valley combinations. Two methods are based on a two dimensional rain-flow matrix, and the third on a three dimensional rain-flow matrix. Histories reconstructed by any of these methods produce a rain-flow matrix identical to that of the original history, and as a result the resulting time history is expected to produce a fatigue life similar to that for the original. The procedures described allow lengthy loading histories to be stored in compact form. Author

N90-15483# Westinghouse Electric Corp., Pittsburgh, PA. Science and Technology Center.
ADVANCED STUDY IN SOLID TRANSPORT: RHEOLOGICAL BEHAVIOR OF DENSE SUSPENSION Quarterly Report No. 4, 1 Jul. - 30 Sep. 1989
H. J. Kim, J. L. Chen (Pittsburgh Univ., PA.), R. M. Roidt, and H. A. Burgman 10 Oct. 1989 40 p
(Contract DE-AC22-88PC-88949)
(DE90-003369; DOE/PC-88949/T4) Avail: NTIS HC A03/MF A01

The dynamic shear stress of glass beads has been measured for various combinations of water content, shearing zone height, speed, and normal stress. Equipment and a procedure have been developed to mix uniformly the glass beads with water. A procedure for performing dynamic shear stress experiments has been established. The effects of parameters are discussed. From the results of the present experiments, it is concluded that a smaller shearing zone height and a precise measure of water content are required. In the next experiment, the effects of glass bead particle size and size distribution will be examined. The velocity distribution will also be measured. In addition, we will measure packing fraction as a function of load in order to correct for water void fraction. DOE

N90-15484# Illinois Univ., Urbana.
THIN FILMS UNDER CHEMICAL STRESS Progress Report, 1-31 Jul. 1989
1989 10 p
(Contract DE-FG02-88ER-13949)
(DE90-003754; DOE/ER-13949/T1) Avail: NTIS HC A02/MF A01

The purpose of this research is to enable workers in a variety of fields to understand the chemical and physical changes which take place when thin films (primarily organic films) are placed under chemical stress. This stress may occur because the film is being swelled by a penetrant entrained in solvent, because interfacial reactions are occurring at one or more boundaries within the film structure, or because some component of the film is responding to an external stimulus (e.g., pH, temperature, electric field, or radiation). The efforts build upon the optical depth profiling (ODP) capability developed in our laboratory, using these techniques as starting points for the description of film behavior under chemical stress. In the past year we have concentrated on the following objectives: (1) development of experimental protocols for probing the film-liquid system in real time; and (2) understanding the diffusion behavior of model systems containing all the complications likely to be present in more general systems. Progress in meeting each of these objectives will be described separately below. DOE

N90-15485# California Univ., Los Angeles. Dept. of Civil Engineering.
MICROMECHANICS OF AN EXTRUSION IN HIGH-CYCLE FATIGUE WITH CREEP
T. H. Lin, S. R. Lin (Aerospace Corp., El Segundo, CA.), and X. Q. Wu 1988 24 p
(Contract N00014-86-K-0153)
(AD-A213509; UCLA-ENG-89-09) Avail: NTIS HC A03/MF A01 CSCL 20/11

A most favorably oriented crystal located at a free surface of a f.c.c. polycrystal subject to creep under cyclic tension and compression of high cycle fatigue is considered. An extrusion in this crystal is shown to be produced by a positive slip in one thin slice P and a negative slip in a closely located slice Q. An initial tensile strain in the thin slice R sandwiched between P and Q causes a positive initial shear stress in P and a negative one in Q. It is shown that the extrusion growth causes a tensile strain in R, which can activate second slip system giving a creep stain with a tensor component. It has the same effect as the initial strain in causing this difference in shear stresses in P and Q and gives much additional extrusion growth. The extent of intrusion and extrusion is important in this study of crack initiation. GRA

N90-15486# Air Force Wright Research and Development Center, Wright-Patterson AFB, OH. Materials Lab.
PROCEEDINGS OF THE 1988 STRUCTURAL INTEGRITY PROGRAM CONFERENCE Final Report
Thomas D. Cooper, ed. and John W. Lincoln, ed. May 1989 958 p Conference held in San Antonio, TX, 29 Nov. - 1 Dec. 1988
(AF Proj. 2418)
(AD-A213545; WRDC-TR-89-4071) Avail: NTIS HC A99/MF A04 CSCL 11/6

A compilation of the papers presented at the 1988 Structural Integrity Program Conference is presented. Some topics of discussion include: Propulsion and Power System Integrity; The Integrity Process as Applied to the F-119-PW-100 Advanced Tactical Fighter Engine; Structural Analysis, Fasteners and Testing; Predicting Fatigue Crack Growth Under Combined Tension and Out of Plane Bending in Transitional Thickness Plates; Inspection of Fatigue Critical Fastener Holes Using Capacitance Measurement System Equipment; An update on the Study of the Quality of Screw Threaded Products; CF116 Full Scale Durability and Damage Tolerance Test; F-16 Full Scale Airframe Durability Test; T37B Damage Tolerance Analysis Results; The C-17 Aircraft Structural Integrity Overview; The X-30 Structural Integrity Program; Structural Risk Analysis in Aging Aircraft Fleets; Metallic/Composite Structures; and Low Velocity Impact Damage Detector Development. GRA

N90-15487# Air Force Academy, CO.
TWO DIMENSIONAL LAMINATED SHELL THEORY INCLUDING PARABOLIC TRANSVERSE SHEAR Final Report
Scott T. Dennis Oct. 1989 85 p
(AD-A213817; USAFA-TR-89-6) Avail: NTIS HC A05/MF A01 CSCL 20/11

An approach is presented for a general laminated shell geometry describable by orthogonal curvilinear coordinates. The theory includes a through the thickness parabolic distribution of transverse shear stress. Additionally, a simplified approach that allows large displacements and rotations is incorporated. The theory is cast into a displacement based finite element formulation and then specialized to a cylindrical shell geometry. Linear results are compared to exact elasticity solutions of a laminated cylindrical shell in cylindrical bending. The approach predicts displacement and stress for the unidirectional cases very well even for the very thick laminates. GRA

N90-15488# Office of Naval Research,
DUCTILE FAILURE
Alan Needleman and R. Barsoum 13 Oct. 1989 6 p Submitted for publication
(Contract N00014-89-J-3054)
(AD-A213864) Avail: NTIS HC A02/MF A01 CSCL 20/11

Work has proceeded in two areas: combined experimental and numerical studies of the plastic response of metal matrix composites and analyses of dynamic crack growth in porous plastic solids. Dynamic crack growth was analyzed numerically for a plane strain double edge cracked specimen subject to symmetric impulsive tensile loading at the two ends. The material behavior is described in terms of an elastic-viscoplastic constitutive model that accounts for ductile fracture by the nucleation and subsequent growth of voids to coalescence. Two populations of second phase particles are represented, including large inclusions or inclusion colonies with low strength, which result in large voids near the crack tip at an early stage, and small second phase particles, which require large strains before cavities nucleate. The crack growth velocities determined were entirely based on the ductile failure predictions of the material model, and thus is free from ad hoc assumptions regarding appropriate dynamic crack growth criteria. GRA

N90-15489# Cornell Univ., Ithaca, NY. Dept. of Computer Science.
ON THE MOTION OF COMPLIANTLY-CONNECTED RIGID BODIES IN CONTACT. PART 1: THE MOTION PREDICTION PROBLEM
Dinesh K. Pai and Bruce R. Donald 1989 20 p Prepared for presentation at the IEEE International Conference on Robotics and Automation, 1990 Sponsored in part by the Presidential Young Investigator Award, and by the Mathematical Sciences Inst. Submitted for publication
(Contracts N00014-88-K-0591; N00014-86-K-0281; NSF DMC-86-17355; NSF IRI-88-02390)
(AD-A214135) Avail: NTIS HC A03/MF A01 CSCL 20/11

Consider the problem of planning and predicting the motion of a flexible object amidst obstacles in the plane by modelling the flexible object as a rigid root body, attached to compliant members of torsional springs. The root's position may be controlled, but the compliant members move in response to forces from contact with the environment. Such a model encompasses several important and complicated mechanisms in mechanical design and automated assembly: snap-fasteners, latches, ratchet and pawl mechanisms, and escapements. The problem is to predict the motion of such a mechanism amidst fixed obstacles. For example, our algorithm could be used to determine whether a snap-fastener design can be assembled with a certain plan. This paper analyzes the physics of these flexible devices, and develops the first combinatorially precise algorithm for predicting their movement under a motion plan. This algorithm determines when and where the motion will terminate, and also computes the time-history of contacts. In addition to providing the first known exact algorithm that addresses flexibility in motion planning, we also note that our approach to compliance permits an exact algorithm for predicting motions under rotational compliance, which was not possible in earlier work. GRA

N90-15490# Cornell Univ., Ithaca, NY. Dept. of Computer Science.
ON THE MOTION OF COMPLIANTLY-CONNECTED RIGID BODIES IN CONTACT. PART 2: A SYSTEM FOR ANALYZING DESIGNS FOR ASSEMBLY
Dinesh K. Pai and Bruce R. Donald 1989 70 p Prepared for presentation at the IEEE International Conference on Robotics and Automation, 1990 Sponsored in part by the Presidential Young Investigator Award, and by the Mathematical Sciences Inst.
(Contracts N00014-88-K-0591; N00014-86-K-0281; NSF DMC-86-17355; NSF IRI-88-02390)
(AD-A214136) Avail: NTIS HC A04/MF A01 CSCL 20/11

The design of mechanical devices and the planning to assemble then should not be independent activities. A new, fully algorithmic, combinatorially precise approach is introduced to designing devices so that they are easy to assemble and (optionally) hard to disassemble. This analysis can be used to validate good designs, and can be iterated to generate improved designs. The approach is based on an algorithm for predicting the motion of flexible objects in contact; the flexible objects have rotationally passively compliant members, which deform when they experience contact forces from the environment. Such objects are intended to model snap-fastener-type devices, which are very useful in design for assembly. The algorithm is based on the theory in AD-A214135; this paper describes the details of the algorithm, its implementation in a system for predicting and analyzing the motion of snap-fastener-type devices, and experiments we ran using the system to analyze and design particular devices. GRA

N90-15491 ESDU International Ltd., London (England).
PIPELINE VIBRATIONS. FLUID TRANSIENTS IN NON-RIGID, UNBRANCHED PLANAR PIPING SYSTEMS
Oct. 1989 118 p
(ESDU-89030; ISBN-0-85679-702-2; ISSN-0141-4011) Avail: ESDU

This Data Item ESDU 89030, an addition to the Fluid Mechanics Subseries, provides a computer program for predicting, following pump trip and/or valve operation, the changing values at a junction of liquid pressure and flow velocity, structural displacement, velocity and acceleration, and piping forces in a liquid-filled planar system. The effect of the mutual coupling of the fluid and pipe behavior is included in the analysis (or if desired, can be neglected). Guidance is included on modeling the pump characteristics and the valve closure/time behavior. Values of friction factor and wave speed are required for each pipe, or can be computed by the program. Data on the natural vibration characteristics of the system are also necessary, and can be generated by ESDU 88022, in which case they will be in the format required by the program. The effects of axial strain in the pipe walls are neglected, and the program assumes elastic structural behavior and a homogeneous fluid. Thus, although gas release and cavitation are predicted,

their subsequent effect on the system behavior cannot be modeled. Steady-state values of pressure, flow velocity, structural displacement, and piping forces are calculated before the transient analysis. A detailed explanation of the input data and their format is given, together with a worked example illustrating the use of the program and the presentation of the output. Graphs produced from the program show the comparison between a coupled and uncoupled calculation of the structural parameters and fluid pressure at two points in the system. The FORTRAN program is available on magnetic media as ESDUpac 8930. ESDU

42 GEOSCIENCES (GENERAL)

No abstracts in this category.

43 EARTH RESOURCES AND REMOTE SENSING

Includes remote sensing of earth resources by aircraft and spacecraft; photogrammetry; and aerial photography.

For instrumentation see *35 Instrumentation and Photography.*

N90-15492 Texas Univ., Austin.
GEOSAT/ERM ALTIMETER DATA ANALYSIS FOR THE DETERMINATION OF GLOBAL OCEANIC MESOSCALE VARIABILITY Ph.D. Thesis
Bohai Zhang 1988 160 p
Avail: Univ. Microfilms Order No. DA8909772

The goal of this dissertation is to develop methods for reducing radial orbit error and to apply these methods to Geosat altimeter data. An efficient and generalized method is developed which is applicable to both single and dual satellite crossover measurements. Evaluations of the radial orbit error show that the operational Geosat Exact Repeat Mission (ERM) orbits have 3 to 4 m crossover rms residuals and the predominating radial orbit error occurs at the frequency of once per revolution (40,000 km wavelength). Based on this orbit error analysis, a new technique was developed for extracting global mesoscale variability from collinear satellite altimeter profiles which have large radial orbit error. Long wavelength radial orbit error is suppressed by taking the derivative of each altimeter profile. The resulting mean sea surface slope profiles, averaged from 22 repeat slope profiles, have a precision about 0.1 microrad. Slopes due to mesoscale dynamic topography are typically 1 microrad. Root mean square (rms) slope variability as low as 0.2 microrad are found in the Southeast Pacific and maximum slope variations up to 6 to 8 microrad are found in major western boundary currents (e.g., Gulf Stream, Kuroshio, Falkland and Agulhas) and in the Antarctic Circumpolar Current (ACC) systems. The global rms variability map shows previously unknown spatial details that are highly correlated with sea floor topography. At mid-latitudes, the variability is generally high in deep water and low in shallow water. Eddy kinetic energy associated with the Gulf Stream and Kuroshio Current is also examined. Good agreement with previous altimeter results is obtained in both magnitude and spatial distribution.
Dissert. Abstr.

N90-15493# Utah Univ., Salt Lake City.
A LOGIC FOR THE PIXEL ASSIGNMENT STEP OF IMAGERY CLASSIFICATION PREDICATED ON CLASS STRUCTURE Ph.D. Thesis
Perry James Hardin 1989 282 p
Avail: Univ. Microfilms Order No. DA8921015

A logic for optimizing the pixel assignment step in semisupervised classification is presented. The logic includes: (1) the extraction of a random sample from the clustered image; (2) the statistical and graphic exploration of the class structure; (3) the prediction of error potential using nearest neighbor distance values as confusion threshold criteria; (4) the prediction of classification accuracy rate and error distribution; (5) the prediction of potential classifier success; (6) the assignment of each sample pixel to a predicted class using each potential classifier; (7) the comparison of the predicted and known pixel class labels for agreement; (8) the quantification of exclusion and exclusion error rates; and (9) the classification of the entire image using the optimum classifier identified in the previous step. In an initial experiment, five classifiers were compared for assignment efficiency and quality on 81 synthesized data sets with differing class centroid and covariance matrix characteristics. Generally, the linear discriminant function with prior probabilities and quadratic discriminant function with prior probabilities generated statistically equivalent accuracy values, but the quadratic discriminant function produced a more equitable distribution of errors between the several classes. In a second experiment on two multiband satellite scenes, it was found that deviations from normality made the modeled results of the first experiment difficult to apply to the classifications of the real scenes. Dissert. Abstr.

N90-15494# Aerospace Corp., El Segundo, CA. Space Systems Div.
RAIDS: AN ORBITING OBSERVATORY FOR IONOSPHERIC REMOTE SENSING FROM SPACE
R. P. McCoy, L. J. Paxton, R. R. Meier, D. D. Cleary, D. K. Printz, K. D. Wolfram (Naval Research Lab., Washington, DC.), A. B. Christensen, J. B. Pranke, and D. C. Kayser 10 Aug. 1989 28 p
(Contract F04701-85-C-0086)
(AD-A213717; TR-0086A(2940-04)-3; SD-TR-89-60) Avail: NTIS HC A03/MF A01 CSCL 04/1

A NOAA TIROS satellite currently scheduled to be launched in mid 1990 will contain a payload of optical sensors for ionospheric remote sensing known as RAIDS (Remote Atmospheric and Ionospheric Detection System). The RAIDS experiment consists of eight separate optical instruments which have a combined spectral coverage of 500 to 8700 A. Seven of the instruments will be mounted to a scan platform and will mechanically scan the earth's limb from 75 to 750 km, while the eighth obtains height images without being scanned. These instruments will measure naturally occurring airglow emissions from the upper atmosphere and ionosphere and will provide altitude profiles of ion and neutral atmospheric constituents along the satellite track on both the day and night side of the earth. The purpose of the RAIDS experiment is to demonstrate a technique for ionospheric remote sensing from space and to produce a global data base of ionospheric and neutral atmospheric composition. GRA

N90-15495# Aerospace Corp., El Segundo, CA. Space Sciences Lab.
DEVELOPMENT OF THE RAIDS (REMOTE ATMOSPHERIC AND IONOSPHERIC DETECTOR SYSTEM) EXTREME ULTRAVIOLET WEDGE AND STRIP DETECTOR
D. C. Kayser, W. T. Chater, A. B. Christensen, C. K. Howey, J. B. Pranke, S. Chakrabarti, and O. H. W. Siegmund (California Univ., Berkeley.) 28 Aug. 1989 18 p
(Contract F04701-85-C-0086)
(AD-A213730; TR-0088(3940-04)-2; SSD-TR-89-66) Avail: NTIS HC A03/MF A01 CSCL 17/5

In the next few years the Remote Atmospheric and Ionospheric Detector System (RAIDS) package will be flown on a TRIOS spacecraft. The Extreme Ultraviolet Spectrometer (EUVS) experiment contains a position-sensitive detector based on wedge and strip anode technology. A detector design has been implemented in brazed alumina and Kovar to provide a rugged bakeable housing and anode. A stack of three 80:1 microchannel plates is operated at 3500 to 4100 V to achieve a gain of about 10 to the 7th power. The top MCP is to be coated with MgF for increased quantum efficiency in the range of 500 to 1150 A. Fabrication of the wedge and strip anode on brazed alumina has

presented some challenging problems. In this report, a summary of fabrication techniques and detector performance characteristics is presented. GRA

N90-15496# Kapteyn Astronomical Lab., Groningen (Netherlands).
IMAGE ENHANCEMENT USING THE IRAS (INFRARED ASTRONOMY SATELLITE) SURVEY DATA Final Report, Mar. 1986 - Mar. 1989
P. R. Wesselius Mar. 1989 38 p
(Grant AF-AFOSR-0140-86; AF Proj. 7670)
(AD-A213811; GL-TR-89-0180) Avail: NTIS HC A03/MF A01 CSCL 03/1

An improved global calibration was derived and image enhancement techniques developed to increase the image quality, sensitivity, and spatial resolution of maps from the Infrared Astronomy Satellite (IRAS) survey data. These goals were achieved by augmenting and extending GEISHA (Groningen Exportable IRAS High-resolution Analysis) system. A completely new calibration scheme using the zodiacal light emission as a standard candle has been designed and implemented. This calibration is better suited for smaller spatial frequencies. Comparison of the zodiacal light calibration and that of IPAC (IRAS Processing and Analysis), for point sources, gives very satisfactory results (less than 10 percent) at the wavelengths 12, 25, and 60 microns, but a 50 percent error at 100 microns. Scans making an angle larger than 5 deg with the plane perpendicular to the line Sun-IRAS cannot be calibrated properly. An iterative least squares (ILSQ) routine has been prepared that makes it possible to enhance the resolution of an IRAS image to slightly better than 2 arc minutes for most regions of sky. The output of this routine is directly traceable to the input and the method is rather straightforward. Our ILSQ program is ideal for creating large spatial resolution enhanced images, and for checking e.g., maximum entropy results. A spline-smoothed plate system was created as well, consisting of 40 instead of 363 tapes. GRA

N90-15497# Photometrics, Inc., Woburn, MA.
MEASUREMENT OF OPTICAL RADIATIONS IN SPACECRAFT ENVIRONMENTS Scientific Report No. 1
I. L. Kofsky, N. H. Tran, M. A. Maris, and C. A. Trowbridge 15 Jun. 1989 52 p
(Contract F19628-88-C-0070)
(AD-A213814; PHM-P-06-89; GL-TR-89-0168; SR-1) Avail: NTIS HC A04/MF A01 CSCL 04/1

Three topics in remote sensing of the gaseous and particulate environment of spacecraft are reported and several further optical contamination and induced-glow phenomenology issues now under consideration are briefly reviewed. The transmission to ground stations of the near-ultraviolet radiation from OH* excited when high-kinetic energy water molecules in thruster rocket exhaust react with the ambient oxygen atoms is calculated from band and atmosphere models, and the measurement signal/noise is shown to depend on the concentrations of both (UV-absorbing) ozone molecules and (UV sky background-producing) O atoms along the view path as well as on the spatial distribution of radiance from the exoatmospheric collision volume. Vacuum-ultraviolet photolysis of water vapor off spacecraft with radiometry of the resulting electronically-excited, microsecond lifetime hydroxyl radicals is shown to be a feasible means for determining its rates of offgassing, and preliminary designs for such active probes are presented. An initial review of the potential for identification of spaceborne particulates from their chemical composition-dependent scattering and emission of visible and infrared quanta indicates these synthetic (instrument response-convolved) spectra of candidate contaminant particles are need to evaluate the concept. GRA

44 ENERGY PRODUCTION AND CONVERSION

Includes specific energy conversion systems, e.g., fuel cells; global sources of energy; geophysical conversion; and windpower.

For related information see also *07 Aircraft Propulsion and Power, 20 Spacecraft Propulsion and Power,* and *28 Propellants and Fuels.*

N90-15498# California Inst. of Tech., Pasadena.
INSTABILITY OF A-Si:H/Ag INTERFACE AT 150 DEG C Annual Subcontract Report, 1 Sep. 1987 - 31 Aug. 1988
M. A. Nicolet and L. T. Tran May 1989 18 p Prepared for Midwest Research Inst., Golden, CO
(Contract DE-AC02-83CH-10093)
(DE89-009419; SERI/STR-211-3508) Avail: NTIS HC A03/MF A01

This report documents the results of an investigation of the interaction of silver (Ag) with a-Si:H films in order to evaluate the possible effect of Ag on solar cell degradation. After 5 hours at 250 C, grains of polycrystalline silicon are found in the Ag layer. No difference is detected in the behavior between i-, n-, p-type a-Si:H thin films. The process also occurs in a-Si:H/Al where it is even more pronounced. After annealing at 150(degree)C for 120 hours, some polycrystalline silicon is detected in a-Si:H/Al, but none in the a-Si:H/Ag system. DOE

N90-15499# Harvard Univ., Cambridge, MA. Div. of Applied Sciences.
RESEARCH ON AMORPHOUS SILICON-GERMANIUM ALLOYS FOR TANDEM SOLAR CELLS Annual Subcontract Report, 1 Sep. 1987 - 31 Aug. 1988
W. Paul Jun. 1989 131 p
(Contract DE-AC02-83CH-10093)
(DE89-009436; SERI/STR-211-3525) Avail: NTIS HC A07/MF A01

This report presents results of research on amorphous silicon-germanium alloys for tandem solar-cell applications. A study was completed of a-Si(1-x)Ge(x):H and a-Si(1-x)Ge(x):H:F alloys. This included extensive structural examination by transmission electron spectroscopy, gas evolution, and differential scanning calorimetry, and also a measurement of the dependence of the mobility-lifetime product for electrons in the two types al alloys. It also included a project to deposit for electron in the two types of alloys. It also included a project to deposit a-Si:H and its alloys by photochemical vapor deposition, which is described. Microstructure, on a scale of 100 angstroms, appears to be an important determinant of film properties. Structure can also be modified by altering the proportions of SiH4, GeH4, and H2 used in growing the films. Films grown by photo-CVD were compared with those grown by conventional glow discharge. DOE

N90-15500# Oak Ridge National Lab., TN. Engineering Technology Div.
THERMAL ENERGY STORAGE Technical Progress Report, Apr. 1987 - Mar. 1988
J. J. Tomlinson and R. J. Kedl Sep. 1989 48 p
(Contract DE-AC05-84OR-21400)
(DE90-000953; ORNL/TM-11233) Avail: NTIS HC A03/MF A01

Progress in the development of thermal energy storage (TES) technology under Oak Ridge National Laboratory's TES Program for the period April 1987 to March 1988 is reported. Program goals and project structures are presented. Each of the projects active during this report period is discussed, and the contribution of specific projects to major technology transfer activities is described. DOE

N90-15501# International Fuel Cells Corp., South Windsor, CT.
MOLTEN CARBONATE FUEL CELL TECHNOLOGY IMPROVEMENT Quarterly Technical Progress Report No. 17, period ending May 1989

Sep. 1989 26 p
(Contract DE-AC21-87MC-23270)
(DE90-001934; DOE/MC-23270/2751) Avail: NTIS HC A03/MF A01

The overall objective of this program is to define a competitive CG/MCFC (Molten Carbonate Fuel Cell) power plant and the associated technology development requirements and to develop an improved cell configuration for molten carbonate fuel cells which has improved performance, has reduced cell creep and electrolyte management consistent with 40,000 hour projected life, reduces existing cell cost, and is adaptable to a range of power plant applications. Component design specifications for the end-cells of the alternative cell configuration were completed. Testing to evaluate new components was performed on 14 cells during this reporting period with eight tests started and terminated, and six tests continuing into the next reporting period. A test and performance summary of all the single cell tests conducted to date on this program is presented. A single cell test to qualify new matrix materials and matrix reinforcement was successfully completed. Integrated cell testing of new anode- and cathode-side components was completed. Single cell tests were conducted to identify the electrolyte fill procedure for the new cell configuration. Methods of fabricating manifold seals from the new candidate materials are being developed. Preparation of construction drawings for the 1-ft(sup 2) short stack was continued. Fabrication of repeating cell components for the 1-ft(sup 2) short stack was initiated. Trials to tape cast electrodes and matrices were initiated, tooling to form current collectors is being fabricated, and existing tooling to form separator plates is being modified. Non-repeat components from the previous 1-ft(sup 2) short stack that are acceptable for re-use were identified. New non-repeat components that are required have been ordered. Preparation of the test stand for the 1-ft(sup 2) short stack test was initiated. DOE

N90-15502# Midwest Research Inst., Golden, CO. Solar Energy Research Inst.
RESEARCH ON HIGH-EFFICIENCY, SINGLE-JUNCTION, MONOLITHIC, THIN-FILM AMORPHOUS SILICON SOLAR CELLS, PHASE 1 Annual Subcontract Report, 1 Feb. 1987 - 31 Jan. 1988
A. W. Catalano, D. E. Carlson, R. R. Ayra, M. S. Bennett, R. V. DAiello, C. R. Dickson, C. M. Fortmann, B. Goldstein, J. McVeigh, and J. Morris et al Oct. 1989 142 p Prepared in cooperation with Solarex Corp., Newtown, PA
(Contract DE-AC02-83CH-10093)
(DE89-009495; SERI/STR-211-3582) Avail: NTIS HC A08/MF A01

This document describes the progress made in obtaining stable, a-Si-based submodules that have a large area and high efficiency. Conversion efficiencies of up to 11.95 percent were obtained in small-area, single-junction a-Si solar cells using textured TiO2, superlattice p-layers, graded carbon concentrations near the p/i interface, and highly reflective ITO/silver back contacts. Single-junction a-SiC and a-SiGe p-i-n cells were also fabricated that had conversion efficiencies of 9 to 11 percent, and some recently fabricated stacked-junction cells had conversion efficiencies of about 10 percent. In materials research boron-doped microcrystalline SiC films were recently developed containing up to 6 at. percent carbon with conductivities of 3 times 10(-3) (Omega)-cm at room temperature and activation energies of 0.11 eV. Microcrystalline film growth was shown to be strongly influenced by the nature of the substrate, with nucleation occurring more readily on a-Si substrates than on TiO2. Stability studies show that light-induced degradation is usually enhanced by the presence of carbon grading near the p/i interface. In general, adding either germanium (from GeH4), or carbon (from CH4) to the i-layer of a p-i-n cell leads to enhanced light-induced degradation. DOE

N90-15503# Midwest Research Inst., Golden, CO. Solar Energy Research Inst.
RESEARCH ON HIGH-EFFICIENCY, SINGLE-JUNCTION, MONOLITHIC, THIN-FILM AMORPHOUS SILICON SOLAR CELLS, PHASE 2 Semiannual Report, 1 Feb. 1988 - 31 Jul. 1989
R. R. Ayra, M. S. Bennett, C. R. Dickson, B. Fieselmann, C. M. Fortmann, B. Goldstein, J. Morris, J. G. ODowd, R. S. Oswald, and S. Wiedeman et al Oct. 1989 120 p Prepared in cooperation with Solarex Corp., Newtown, PA
(Contract DE-AC02-83CH-10093)
(DE89-009496; SERI/STR-211-3583) Avail: NTIS HC A06/MF A01

This document describes efforts to improve the quality of candidate photovoltaic materials used in amorphous wide- and narrow-band-gap materials, namely, a-Si sub 1-x C sub x and a-Si sub 1-x Ge sub x. Although these alloys show a decrease in mobility-lifetime product as the fraction of silicon decreases, their optical properties show marked differences. Microcrystalline p-layer films containing carbon were prepared to evaluate their importance for achieving high open-circuit voltages. Silicon-germanium cells were studied to optimize their performance in multijunction, stacked cell structures. The best cells fabricated from the silicon-germanium alloys yielded a conversion efficiency of 10.1 percent with a band gap of 1.55 eV. Several alloy-based stacked cells had conversion efficiencies of more than 10 percent: an a-SiC/a-SiGe cell yielded 10.5 percent and an a-SiC:H/a-Si:H structure yielded 10.2 percent. Stacked-junction cells showed far less susceptibility to light-induced degradation. DOE

N90-15504# Midwest Research Inst., Golden, CO. Solar Energy Research Inst.
US POLYCRYSTALLINE THIN FILM SOLAR CELLS PROGRAM
Harin S. Ullal, Kenneth Zweibel, and Richard L. Mitchell Nov. 1989 8 p Presented at the Materials Research Society Fall Meeting, Boston, MA, 27 Nov. - 2 Dec. 1989
(Contract DE-AC02-83CH-10093)
(DE89-009506; SERI/TP-211-3595; CONF-891119-5) Avail: NTIS HC A02/MF A01

The Polycrystalline Thin Film Solar Cells Program, part of the United States National Photovoltaic Program, performs R and D on copper indium diselenide and cadmium telluride thin films. The objective of the program is to support research to develop cells and modules that meet the U.S. Department of Energy's long-term goals by achieving high efficiencies (15 to 20 percent), low-cost ($50/m(sup 2)), and long-time reliability (30 years). The importance of work in this area is due to the fact that the polycrystalline thin-film CuInSe2 and CdTe solar cells and modules have made rapid advances. They have become the leading thin films for PV in terms of efficiency and stability. The U.S. Department of Energy has increased its funding through an initiative through the Solar Energy Research Institute in CuInSe2 and CdTe with subcontracts to start in spring 1990. DOE

N90-15505# Sandia National Labs., Albuquerque, NM. Dept. of Fluid and Thermal Sciences.
ANALYSIS OF CATALYTICALLY ENHANCED SOLAR ABSORPTION CHEMICAL REACTORS: 1 - NUMERICAL MODEL DESCRIPTION
R. E. Hogan, Jr. and R. D. Skocypec 1989 16 p Presented at the ASME Winter Annual Meeting, San Francisco, CA, 10-15 Dec. 1989
(Contract DE-AC04-76DP-00789)
(DE89-014742; SAND-89-0246C; CONF-891208-4) Avail: NTIS HC A03/MF A01

A detailed numerical model is presented for the Catalytically Enhanced Solar Absorption Receiver (CAESAR). CAESAR is a high temperature chemical reactor for the carbon dioxide reforming of methane. Concentrated solar energy is volumetrically absorbed throughout a porous absorber matrix impregnated with a rhodium catalyst. The catalyst promotes heterogeneous reactions with fluid phase reactant species flowing through the absorber. The numerical model was developed to provide guidance in the catalytic matrix

design for CAESAR, to evaluate the reactor performance, and to evaluate test data. There are a number of applications of this concept, including thermochemical energy transport, methanol production, and the destruction of certain classes of hazardous chemical waste. DOE

N90-15506*# Oak Ridge National Lab., TN.
SELECTION OF PHASE-CHANGE AND CONTAINMENT MATERIALS FOR THERMAL ENERGY STORAGE
D. F. Wilson, J. H. DeVan, and M. Howell 1989 14 p Presented at the ASME Winter Annual Meeting, San Francisco, CA, 10-15 Dec. 1989
(Contract NASA Order C-3003-J; DE-AC05-84OR-21400)
(NASA-CR-186228; NAS 1.26:186228; DE89-014778; CONF-891208-6) Avail: NTIS HC A03/MF A01 CSCL 10A

The high thermal conductivity and generally low volume change on melting of germanium and alloys based on silicon make then attractive for storage of thermal energy in space power systems. However, this application obviously depends on identification of suitable container materials that are compatible with these metals at the temperature of interest (greater than 1223 K). An approach to solving the containment problem, involving both chemical and physical compatibility, preparation of NiSi/NiSi2, and initial results for containment of germanium and NiSi/NiSi2 are presented. DOE

N90-15507# Oak Ridge National Lab., TN. Metals and Ceramics Div.
SATELLITE THERMAL STORAGE SYSTEMS USING METALLIC PHASE-CHANGE MATERIALS
R. J. Lauf and C. Hamby 1989 5 p Presented at the ASME Winter Annual Meeting, San Francisco, CA, 10-15 Dec. 1989
(Contract DE-AC05-84OR-21400)
(DE89-016872; CONF-891208-17) Avail: NTIS HC A02/MF A01

Solar (thermal) dynamic power systems for satellites require a heat storage system capable of operating the engine during eclipse. A system is described in which the phase-change material (PCM) is a metal rather than the more conventional fluoride salts. Thermal storage modules consisting of germanium contained in graphite have good thermal conductivity, low parasitic mass, and are physically and chemically stable. The result is described for thermal cycle testing of graphite capsules containing germanium and several germanium- and silicon-based alloys, as well as some initial tests of the compatibility of graphite with Nb-1 percent Zr structural materials. DOE

N90-15508# Argonne National Lab., IL. Chemical Technology Div.
AN ASSESSMENT AND COMPARISON OF FUEL CELLS FOR TRANSPORTATION APPLICATIONS
M. Krumpelt and C. C. Christianson Sep. 1989 20 p
(Contract W-31-109-eng-38)
(DE90-001807; ANL-89/28) Avail: NTIS HC A03/MF A01

Fuel cells offer the potential of a clean, efficient power source for buses, cars, and other transportation applications. When the fuel cell is run on methanol, refueling would be as rapid as with gasoline-powered internal combustion engines, providing a virtually unlimited range while still maintaining the smooth and quiet acceleration that is typical for electric vehicles. The advantages and disadvantages of five types of fuel cells are reviewed and analyzed for a transportation application: alkaline, phosphoric acid, proton exchange membrane, molten carbonate, and solid oxide. The status of each technology is discussed, system designs are reviewed, and preliminary comparisons of power densities, start-up times, and dynamic response capabilities are made. To test the concept, a fuel cell/battery powered urban bus appears to be a good first step that can be realized today with phosphoric acid cells. In the longer term, the proton exchange membrane and solid oxide fuel cells appear to be superior. DOE

N90-15509# Sandia National Labs., Albuquerque, NM.
HIGH-EFFICIENCY SILICON CONCENTRATOR SOLAR CELLS FOR USE WITH PRISMATIC COVERS
Jerome S. Culik and Edward L. Jackson (Astrosystems International, Inc., Newark, DE.) Oct. 1989 30 p
(Contract DE-AC04-76DP-00789)
(DE90-002644; SAND-89-7039) Avail: NTIS HC A03/MF A01

Advanced-design 20X concentration silicon solar cells that are compatible with prismatic covers have been designed and fabricated. Our design is based upon a micro-machined, deeply grooved, three-dimensional silicon structure and incorporates a dual-layer emitter, oxide surface passivation layers for front and rear surfaces, and back surface reflector light-trapping technologies. Using solar grade Czochralski-grown silicon with a resistivity of 1.25 ohm-cm, we obtained open-circuit voltages as high as 679 mV and active-area current densities of up to 38.4 mA/cm(sup 2). The best efficiency for a full-sized (50 cm(sup 2)) solar cell with prismatic cover is 17.8 percent. The performance of these devices is limited primarily by series resistance in the emitter and emitter contact due to the wide grid finger spacing (504 microns) and reflection from a groove ridgetop between the fingers. Increasing the density of front-contact fingers to eliminate the center ridge, together with a matched prismatic cover, will yield significant improvements in fill-factor and short-circuit current. Preliminary modeling of this design using PC-1D/2 indicates that efficiencies of up to 24 percent are feasible. With optimization of the fabrication sequence, the conversion efficiency of the deeply grooved concentrator solar cell should approach this level of performance. DOE

N90-15510# Texas A&M Univ., College Station. Center for Electrochemical Systems and Hydrogen Research.
OXYGEN ELECTRODE IN MOLTEN CARBONATE FUEL CELLS Quarterly Progress Report No. 7, 1 Feb. - 30 Apr. 1989
B. B. Dave, P. K. Adanuvor, M. A. Enayetullah, R. E. White, S. Srinivasan, and A. J. Appleby 1989 24 p
(Contract DE-FG22-87PC-79931)
(DE90-002871; DOE/PC-79931/T4) Avail: NTIS HC A03/MF A01

Effects of partial pressure of oxygen and temperature on oxygen reduction kinetics on a submerged gold electrode in lithium carbonate melt were investigated using cyclic voltammetry and impedance analysis. Cyclic voltammetry measurements show that the peroxide reduction reaction in Li2CO3 melt is reversible up to 200 mV/s. The impedance analysis was carried out using a Complex Nonlinear Least Square (CNLS) parameter estimation program based upon the Randles-Ershler equivalent circuit. This analysis estimated electrode kinetics and mass transfer related parameters such as charge transfer resistance and Warburg coefficient. The mass transfer related parameters obtained from cyclic voltammetry and impedance analysis show good agreement. The oxygen reaction orders for mass transfer parameter and exchange current density at 800 C were calculated to be 0.5 and 0.377 respectively; these values are consistent with the peroxide mechanism. DOE

N90-15511# Sandia National Labs., Albuquerque, NM.
IN-SITU ION BEAM MEASUREMENTS OF DEUTERIUM LOADING IN THIN FOIL ELECTROCHEMICAL CELLS
J. A. Knapp, T. R. Guilinger, M. J. Kelly, D. Walsh, and B. L. Doyle 1989 12 p Presented at the Materials Research Society Fall Meeting, Boston, MA, 27 Nov. - 2 Dec. 1989
(Contract DE-AC04-76DP-00789)
(DE90-003162; SAND-89-1711C; CONF-891119-8) Avail: NTIS HC A03/MF A01

A key element of recent assertions of cold fusion has been the claim that electrochemical loading of deuterium into Pd electrodes can produce D:Pd levels exceeding 1:1. Using external beam nuclear reaction analysis of Pd foil electrodes in operating electrochemical cells, we have directly monitored deuterium content in-situ. No conditions were found which resulted in loadings higher than (approximately) 0.9. DOE

N90-15512# Midwest Research Inst., Golden, CO. Solar Energy Research Inst.
OCEAN THERMAL ENERGY CONVERSION: AN OVERVIEW
Nov. 1989 36 p
(Contract DE-AC02-83CH-10093)
(DE89-000838; SERI/SP-220-3024) Avail: NTIS HC A03/MF A01

Ocean thermal energy conversion, or OTEC is a technology that extracts power from the ocean's natural thermal gradient. This technology is being pursued by researchers from many nations; in the United States, OTEC research is funded by the U.S. Department of Energy's Ocean Energy Technology program. The program's goal is to develop the technology so that industry can make a competent assessment of its potential; either as an alternative or as a supplement to conventional energy sources. Federally funded research in components and systems will help OTEC to the threshold of commercialization. An overview of the OTEC technology is provided. DOE

N90-15513# Hawaii Natural Energy Inst., Honolulu.
THE THIRD PACIFIC BASIN BIOFUELS WORKSHOP: PROCEEDINGS
1989 173 p Workshop held in Waianae, HI, 27-28 Mar. 1989
(Contract DE-AC02-83CH-10093)
(DE90-002523; CONF-8903174) Avail: NTIS HC A08/MF A01

Among the many compelling reasons for the development of biofuels on remote Pacific islands, several of the most important include: (1) a lack of indigenous fossil fuels necessitates their import at great economic loss to local island economics, (2) ideal conditions for plant growth exist on many Pacific islands to produce yields of biomass feedstocks, (3) gaseous and liquid fuels such as methane, methanol and ethanol manufactured locally from biomass feedstocks are the most viable alternatives to gasoline and diesel fuels for transportation, and (4) the combustion of biofuels is cleaner than burning petroleum products and contributes no net atmospheric CO2 to aggravate the greenhouse effect and the subsequent threat of sea level rise to low islands. Dr. Vic Phillips, HNEI Program Manager of the Hawaii Integrated Biofuels Research Program welcomed 60 participants to the Third Pacific Basin Biofuels Workshop at the Sheraton Makaha Hotel, Waianae, Oahu, on March 27 and 28, 1989. The objectives of the workshop were to update progress since the Second Pacific Basin Biofuels Workshop in April 1987 and to develop a plan for action for biofuels R and D, technology transfer, and commercialization now (immediate attention), in the near-term (less than two years), in the mid-term (three to five years), and in the long-term (more than six years). An emerging theme of the workshop was how the production, conversion, and utilization of biofuels can help increase environmental and economic security locally and globally. Individual papers are processed separately for the data base. DOE

N90-15514# Massachusetts Inst. of Tech., Cambridge.
INTERFACIAL SYSTEMS FOR PHOTOCHEMICAL ENERGY CONVERSION Progress Report, 1 Dec. 1988 - 30 Nov. 1989
Mark S. Wrighton 1989 26 p
(Contract DE-FG02-88ER-13914)
(DE90-003181; DOE/ER-13914/13) Avail: NTIS HC A03/MF A01

Research supported by the DOE falls in the areas of: (1) multicomponent redox molecules; (2) polymer-modified electrodes and semiconductor photoelectrodes; (3) semiconductor surface chemistry; and (4) multielectron transfer biological catalysts for redox energy conversion processes. Highlights of research in these areas are given. Plans for the concluding year of the grant are also summarized. DOE

N90-15515# Syracuse Univ., NY. Dept. of Chemistry.
PHOTOCHEMICAL SOLAR ENERGY CONVERSION UTILIZING SEMICONDUCTORS LOCALIZED IN MEMBRANE MIMETIC SYSTEMS
Janos H. Fendler and Subhash Baral 1989 3 p Presented at the 13th DOE Solar Photochemistry Conference, Silvercreek, CO, 11-15 Jun. 1989
(Contract DE-FG02-86ER-13506)
(DE90-003450; DOE/ER-13506/24; CONF-8906129-2) Avail: NTIS HC A02/MF A01

Different membrane mimetic systems continue to be exploited as media for organizing components of the artificial photosynthetic apparatus. Surfactant vesicles, polymerized surfactant vesicles, Bilayer Lipid Membranes (BLMs), and Langmuir-Blodgett (LB) films are used as membrane mimetic systems. Catalyst-coated colloidal semiconductor particles are employed as sensitizers and relays in sacrificial half cells. Emphasis in our studies is placed on obtaining fundamental information on photoelectron transport. The BLM-supported colloidal semiconductors provide the most suitable media since photoelectron transfer processes can be monitored by simultaneous electrical and spectroscopic measurements. Advantage is taken of the insight gained from mechanistic investigations of vesicles and BLMs in the construction of more elaborate semiconductor-particle-containing LB films. DOE

N90-15516# Argonne National Lab., IL. Electrochemical Technology Program.
CHARACTERIZATION OF NEW CATHODE MATERIALS FOR MOLTEN CARBONATE FUEL CELLS
Alan P. Brown, James L. Smith, and Gene H. Kucera 1989 8 p Presented at the American Institute of Chemical Engineers Annual Meeting, San Francisco, CA, 5-10 Nov. 1989
(Contract W-31-109-eng-38)
(DE90-003547; CONF-891113-9) Avail: NTIS HC A02/MF A01

The in-cell performance is reported for molten carbonate fuel cell cathodes fabricated from fibrous agglomerates of LiFeO2. Both 25 sq cm full-cell tests with an Ni-Cr anode and half-cell tests with a gold reference electrode are described. Cathode materials tested were undoped LiFeO2 and LiFeO2 doped with Cu, Co, or Mn. Parameters varied included the electrode pore structure and the size of the particles forming the agglomerates. These tests demonstrated that the LiFeO2 cathodes are morphologically and chemically stable; these cathodes do not suffer from the dissolution/reprecipitation problem that limits the long-term performance of conventional NiO cathodes. The LiFeO2 cathodes, however, have not yet achieved state-of-the-art performance. They currently have an electron-transfer-limited reaction rate and a high IR drop. Methods are discussed for improving the cathode performance by, for example, modifying the electrode structure to reduce the porosity. DOE

N90-15517# Argonne National Lab., IL. Electrochemical Technology Program.
FABRICATION OF POROUS CERAMIC ELECTRODE STRUCTURES
Gene H. Kucera, James L. Smith, and Alan P. Brown 1989 10 p Presented at the American Institute of Chemical Engineers Annual Meeting, San Francisco, CA, 5-10 Nov. 1989
(Contract W-31-109-eng-38)
(DE90-003548; CONF-891113-8) Avail: NTIS HC A02/MF A01

The conventional cathode material in molten carbonate fuel cells, NiO, has a limited lifetime due to dissolution under cathodic conditions and precipitation as the metal under anodic conditions. Alternative ceramic materials, identified as stable in the cathode environment, were made electronically conductive through doping. Techniques to fabricate dual-porosity electrodes from these alternative ceramic materials were developed and are reported. Cell tests, using NiO cathodes, have ascertained the viability of the new techniques for obtaining the desired electrode structure; these data are also presented. DOE

N90-15518# Massachusetts Inst. of Tech., Cambridge. Dept. of Ocean Engineering.
DESIGN STUDY OF A MODULAR GAS-COOLED, CLOSED-BRAYTON CYCLE REACTOR FOR MARINE USE M.S. Thesis
Richard D. Lantz Jun. 1989 171 p
(Contract N00228-89-G-0580)
(AD-A213453) Avail: NTIS HC A08/MF A01 CSCL 13/10

A conceptual design of a direct Brayton cycle marine power plant is presented. The design is a modification of the commercial MGR-GT, as proposed by James Staudt, sized to produce 40,000 shaft horsepower (SHP) and 5 MW of ship service electrical power. The requirements of a shipboard power plant are discussed and the design changes that must be made to the components of a commercial power plant in order to fit them into the demanding environment of a ship at sea are detailed. The final design consists of an 80-MWth passively safe pebble bed reactor with an outlet temperature of 850. GRA

N90-15519# Midwest Research Inst., Golden, CO. Solar Energy Research Inst.

INCLUSION OF NONLINEAR AERODYNAMICS IN THE FLAP CODE

Tim L. Weber Nov. 1989 8 p Presented at the 9th ASME Wind Energy Symposium, New Orleans, LA, 14-17 Jan. 1990
(Contract DE-AC02-83CH-10093)
(DE89-009507; SERI/TP-257-3558; CONF-900136-5) Avail: NTIS HC A02/MF A01

Horizontal axis wind turbines usually operate with significant portions of the blade in deep stall. This contradicts the assumption in the FLAP code that a linear relation exists between the angle of attack and the lift coefficient. The objective is to determine the importance of nonlinear aerodynamics in the prediction of loads. The FLAP code was modified to include the nonlinear relationships between the lift and drag coefficients with the angle of attack. The modification affects the calculation of the induced velocities and the aerodynamic loads. This requires an iterative procedure to determine the induced velocities instead of a closed form solution. A more advanced tower interference model was also added that accounts for both upwind and downwind tower effects. DOE

N90-15520# Midwest Research Inst., Golden, CO. Solar Energy Research Inst.

PREDICTION OF STOCHASTIC BLADE LOADS FOR THREE-BLADED, RIGID-HUB ROTORS

A. D. Wright, Tim L. Weber, R. W. Thresher, and C. P. Butterfield Nov. 1989 7 p Presented at the 9th ASME Wind Energy Symposium, New Orleans, LA, 14-17 Jan. 1990
(Contract DE-AC02-83CH-10093)
(DE89-009508; SERI/TP-257-3589; CONF-900136-6) Avail: NTIS HC A02/MF A01

Accurately predicting wind turbine blade loads and response is important for the design of future wind turbines. The need to include turbulent wind inputs in structural dynamics models is widely recognized. The Force and Loads Analysis Program (FLAP) code is used to predict turbulence induced bending moments for the SERI Combined Experiment rotor blade and the Howden 330 kW blade. FLAP code predictions is compared to the power spectra of measured blade bending moments. Two methods are used to generate turbulent wind inputs to FLAP: a theoretical simulation: the Pacific Northwest Laboratories (PNL) simulation theory; and measured wind speed data taken from an array of anemometers upwind of the turbine. Turbulent wind speed time series are input to FLAP for both methods outlined above. Power spectra of predicted flap bending moments are compared to measured results for different wind conditions. Conclusions are also drawn as to the ability of the turbulence simulation models to provide accurate wind input to FLAP and to FLAP's ability to accurately simulate blade response to turbulence. Finally, suggestions are made as to needed improvements in the theoretical model. DOE

N90-15521# Sandia National Labs., Albuquerque, NM. Fluid and Thermal Sciences Dept.

ANALYSIS OF CATALYTICALLY ENHANCED SOLAR ABSORPTION CHEMICAL REACTORS. 2: PREDICTED CHARACTERISTICS OF A 100 kW CHEMICAL REACTOR

R. D. Skocypec and R. E. Hogan, Jr. 1989 22 p Presented at the Winter Annual Meeting of the American Society of Mechanical Engineers, San Francisco, CA, 10-15 Dec. 1989
(Contract DE-AC04-76DP-00789)
(DE89-014743; SAND-89-0247C-2; CONF-891208-5-2) Avail: NTIS HC A03/MF A01

The CAtalytically Enhanced Solar Absorption Receiver (CAESAR) volumetrically absorbs concentrated solar energy throughout a catalyzed porous absorber matrix volume, promoting heterogeneous reactions with fluid phase reactant species flowing through the absorber. There are a number of applications of this concept, including thermochemical energy transport, methanol production, and the destruction of certain classes of hazardous chemical waste. A numerical model of these reactors was developed to provide guidance in the catalytic matrix design for CAESAR, which is intended for the carbon dioxide reforming of methane. In addition, the model is being used to evaluate both the 100 kW chemical reactor performance and test data. The effects are presented on the thermal and chemical characteristics of the reactor of varying the incident solar flux, the fluid mass flow, the convective heat transfer coefficient, the solar and infrared optical thicknesses, and the catalyst loading. Predicted CAESAR performance is based on a prototype absorber and anticipated operating conditions. Model results suggest the mass flux must be proportioned to the incident solar flux radial distribution to prevent unacceptably high local temperatures and to provide a reactor having more uniform exit conditions. Either the catalytic loading or geometric thickness of the absorber should be increased for conversion to approach equilibrium levels. Also, the optical density of the matrix (particularly at the sunlit side of the reactor) should be decreased to distribute solar energy more uniformly in depth and decrease matrix temperatures at the front of the absorber. DOE

N90-15522# Los Alamos National Lab., NM. Advanced Engineering Technology Dept.

NIOBIUM 1 PERCENT ZIRCONIUM/POTASSIUM AND TITANIUM/POTASSIUM LIFE-TEST HEAT PIPE DESIGN AND TESTING

J. Tom Sena and Michael A. Merrigan 1989 7 p Presented at the 7th Symposium on Space Nuclear Power Systems, Albuquerque, NM, 7-11 Jan. 1990
(Contract W-7405-eng-36)
(DE90-002430; LA-UR-89-3363; CONF-900109-11) Avail: NTIS HC A02/MF A01

Experimental lifetime performance studies currently in progress use Niobium 1 percent Zirconium (Nb-1Zr) and Titanium (Ti) heat pipes with potassium (K) as the working fluid. A heat pipe life test matrix was developed for testing the heat pipes. Because the corrosion rates in alkali metal heat pipes are affected by temperature and working fluid evaporation flux, the variable parameters of the experimental matrix are established as steady operating temperature and input heat flux density. Total impurity inventory is a factor in corrosion rate so impurity levels are being evaluated in the heat pipe materials before and after testing. Eight Nb-1Zr/K heat pipes were designed, fabricated, and tested. Two of the heat pipes have completed testing whereas the other six are currently in test. These are gravity assist heat pipes operating in a reflux mode. The heat pipes are tested by sets, one set of two and two sets of three heat pipes. Three Ti/K heat pipes are also in life test. These heat pipes are tested as a set in a horizontal position in a capillary pumped annular flow mode. Each of the heat pipes is encapsulated in a quartz vacuum container with a water calorimeter over the vacuum container for power throughput measurements. Thermocouples are attached to the heat pipes for measuring temperature. Heat input to the heat pipes is via an RF coil. The heat pipes are operating at between 800 and 900 K, with heat input fluxes of 13.8 to 30 W/sq cm. Of the Nb-1Zr/K heat pipes, two of the heat pipes have been in operation for 14,000 hours, three over 10,000 hours, and three over 7,000 hours. The Ti/K heat pipes have been in operation for 1,266 hours. DOE

N90-15523# Sandia National Labs., Albuquerque, NM.
AERODYNAMIC DESIGN AND INITIAL PERFORMANCE MEASUREMENTS FOR THE SANDIA 34-METRE DIAMETER VERTICAL-AXIS WIND TURBINE
Dale E. Berg, Paul C. Klimas, and William A. Stephenson 1989 7 p Presented at the 9th ASME Wind Energy Symposium, New Orleans, LA, 14-17 Jan. 1990
(Contract DE-AC04-76DP-00789)
(DE90-002574; SAND-89-2597C; CONF-900136-2) Avail: NTIS HC A02/MF A01

The DOE/Sandia 34-m diameter Vertical-Axis Wind turbine (VAWT) utilizes a step-tapered, multiple-airfoil section blade. One of the airfoil sections is a natural laminar flow profile, the SAND 0018/50, designed specifically for use on VAWTs. The turbine has now been fully operational for more than a year, and extensive turbine aerodynamic performance data have been obtained. This paper reviews the design and fabrication of the rotor blade, with emphasis on the SAND 0018/50 airfoil, and compares the performance measurements to date with the performance predictions. Possible sources of the discrepancies between measured and predicted performance are identified, and plans for additional aerodynamic testing on the turbine are briefly discussed. DOE

N90-15524# Sandia National Labs., Albuquerque, NM. Wind Energy Research Div.
STRUCTURAL RESPONSE MEASUREMENTS AND PREDICTIONS FOR THE SANDIA 34-METER TEST BED
Thomas D. Ashwill and Paul S. Veers 1989 8 p Presented at the 9th ASME Wind Energy Symposium, New Orleans, LA, 14-17 Jan. 1990
(Contract DE-AC04-76DP-00789)
(DE90-002575; SAND-89-2476C; CONF-900136-1) Avail: NTIS HC A02/MF A01

Measurements of structural response during operation of the 34-Meter Test Bed vertical axis wind turbine are compared with analytical predictions. Measured structural data include stationary and rotating modal frequencies, cable natural frequencies, and operating stresses. These data are compared to analytical results obtained with the use of NASTRAN-based structural codes. In the case of operating stresses, analytical results with and without turbulence are compared to measured stresses. Data taken during two significant events, a high wind over-speed condition with an emergency stop and a cable resonance that couples with a tower natural frequency, are shown. DOE

N90-15525# Rockwell International Corp., Thousand Oaks, CA. Science Center.
FATIGUE BEHAVIOR OF VERTICAL AXIS WIND TURBINE AIRFOILS WITH TWO WELD CONFIGURATIONS
M. R. Mitchell and A. R. Murphy Oct. 1989 37 p Prepared for Sandia National Labs., Albuquerque, NM
(Contract DE-AC04-76DP-00789)
(DE90-002628; SAND-89-7037) Avail: NTIS HC A03/MF A01

A series of narrowband, pseudo-random cyclic fatigue tests on sections of 6063-T651 aluminum, Darrius-type, vertical axis wind turbine (VAWT) airfoils were performed. A load member was designed and constructed that was mounted within the frame of a rigid 200-kip servohydraulic, closed-loop test system to hold the VAWT section and permit cantilever bending along the shear centerline of the beam. A computer program was developed to synthesize a narrow band, pseudo-random load history with fixed root mean square (RMS) stress levels at a given bandwidth and central frequency. Six specimens each of two different weld configurations at the flange mounting plate were tested at several RMS stress levels with failure defined as visual observation of a 3 inch long crack in the VAWT. In order to test at as great a frequency as possible, a 20-kip hydraulic ram with a 10 GPM servovalve was employed with a 20 GPM pump. Tests were performed from 2 to 1.3 ksi RMS on the two-weld configurations. The conclusions are obvious that the fillet weld design is far superior to the butt weld design in the range of variables used in this program. DOE

N90-15526# Oak Ridge National Lab., TN. Energy Div.
A GUIDE FOR ESTIMATING POTENTIAL ENERGY SAVINGS FROM INCREASED SOLAR REFLECTANCE OF A LOW-SLOPED ROOF
J. M. MacDonald, G. E. Courville, E. I. Griggs, and T. R. Sharp 1989 14 p Presented at the 4th Thermal Performance of the Exterior Envelopes of Buildings, Orlando, FL, 4-7 Dec. 1989
(Contract DE-AC05-84OR-21400)
(DE90-003720; CONF-891202-8) Avail: NTIS HC A03/MF A01

A guidebook was developed that can be used to evaluate the net energy savings and resultant cost savings associated with changing the solar reflectance of low-sloped roofs. This paper presents an overview of the guide and excerpts to illustrate its use. The guide provides data and calculation procedures for estimating energy and cost savings. In most instances, the cooling cost savings associated with a change to a white roof surface (one with higher solar reflectance) exceed the heating cost penalty. If the difference between reduced cooling costs and increased heating costs is significant, it can affect the choice of membrane for a new roof or a re-roofed building. The guide helps the user estimate this energy cost difference and also describes how various factors influenced potential energy savings and actual roof surface temperatures for different solar reflectances. DOE

N90-15527# Brookhaven National Lab., Upton, NY. Dept. of Applied Science.
ANNUAL OPERATING PLAN FOR FISCAL YEAR 1990 FOR CHEMICAL/HYDROGEN ENERGY SYSTEMS PROGRAM
James Wegrzyn and A. Mezzina Jun. 1989 20 p
(Contract DE-AC02-76CH-00016)
(DE90-003964; BNL-43426) Avail: NTIS HC A03/MF A01

Since 1975, Brookhaven National Laboratory (BNL) has served the U.S. Department of Energy (DOE) as Field Manager for The Chemical/Hydrogen Energy Systems (C/HES) subprogram. In this capacity, BNL has provided technical and management support in accordance with DOE policy and budgetary guidance, which has resulted in several programmatic transitions reflecting: revised perceptions of future conventional resources costs and availability; redefinition of R and D priorities; and changes in technical scope through budgetary constraints. These changes are best summarized as: the transfer of the programmatic management mission to solar/renewable derived hydrogen (SERI), the phase out of BNL's hydrogen facilities, and the strengthening of BNL's interest in advanced hydrogen storage concepts. Hydrogen storage, although not primary, still remains a major concern because problems of accommodating the temporal mismatches of renewable energy supply with load center demands remains as a technical barrier to implementing a comprehensive hydrogen program. DOE

N90-15841*# California Univ., San Diego, La Jolla.
LUNAR POWER SYSTEM SUMMARY OF STUDIES FOR THE LUNAR ENTERPRISE TASK FORCE NASA-OFFICE OF EXPLORATION
David R. Criswell *In* NASA, Langley Research Center, Report of NASA Lunar Energy Enterprise Case Study Task Force Jul. 1989 p 84-96 (For primary document see N90-15836 07-81)
Avail: NTIS HC A09/MF A02 CSCL 10B

N90-15842*# Boeing Aerospace Co., Huntsville, AL.
TRANSPORTATION AND OPERATIONS ASPECTS OF SPACE ENERGY SYSTEMS
Gordon R. Woodcock *In* NASA, Langley Research Center, Report of NASA Lunar Energy Enterprise Case Study Task Force Jul. 1989 p 97-149 (For primary document see N90-15836 07-81)
Avail: NTIS HC A09/MF A02 CSCL 10B

45 ENVIRONMENT POLLUTION

Includes atmospheric, noise, thermal, and water pollution.

N90-15528# California Univ., Riverside. Statewide Air Pollution Research Center.
VARIABILITY OF CULTIVAR RESPONSES TO OZONE Final Report, 25 Jun. 1987 - 31 Dec. 1988
Patrick J. Temple Jun. 1989 80 p
(Contract ARB-A6-201-33)
(PB89-225460; ARB-R-89/402) Avail: NTIS HC A05/MF A01 CSCL 13B

Four cultivars each of dry beans, processing tomatoes, cotton, lettuce, broccoli, and onions were exposed to oxidant air pollutants at three levels: charcoal filtered air, ambient air, and ambient air with ozone added to equal 1.5 times ambient concentrations. Stomatal conductance, visible injury, yield, and vegetative biomass were measured. In beans, varieties with higher rates of stomatal conductance exhibited greater amounts of visible injury and greater yield losses. For processing tomatoes, cultivars with potentially greater yields seemed more susceptible to oxidant induced yield losses. There was no relationship between visible injury or rates of stomatal conductance and yield reductions. For cotton, short season cultivars suffered greater yield losses than late maturing cultivars. All lettuce cultivars showed visible injury symptons on their outer leaves, but no consistent effects on yield due to oxidant exposure. None of the broccoli cultivars showed a significant yield reduction in response to oxidant exposure. Exposure to elevated oxidant levels resulted in visible injury and accelerated senescence of onion plants. GRA

N90-15529# IIT Research Inst., Chicago, IL.
ANALYSIS OF AMBIENT POLAR VOLATILE ORGANIC COMPOUNDS USING CHEMICAL IONIZATION-ION TRAP DETECTOR Report, Jul. 1988 - May 1989
Sydney M. Gordon and Michael Miller May 1989 37 p
(Contract EPA-68-D8-0002)
(PB90-106451; EPA/600/3-89/070) Avail: NTIS HC A03/MF A01 CSCL 13B

The current approach to measuring trace levels of Volatile Organic Compounds (VOCs) in ambient air required cryogenic trapping of the analytes, followed by thermal desorption and low-temperature refocusing onto a column for analysis by capillary Gas Chromatography/Mass Spectrometry (GC/MS). The approach was successfully applied to nonpolar VOCs, but its use for more polar species was complicated by the problems associated with the ambient water vapor collected with the VOCs. A promising technique for measuring polar VOCs is chemical ionization GC/MS (GC/CI-MS) in the quadrupole ion trap. The approach allows whole air samples to be taken since the water present in the air is used as the CI reagent gas. Water CI leads to appreciable intensities for the proton transfer agent H30+, which produces intense pseudomolecular ions and class-specific fragmentation patterns for various low molecular weight polar compounds. Standard mixtures of polar species at low concentrations in humidified zero air were analyzed without a membrane dryer, using a cryogenic trap and CI-GC/MS with the ion trap detector in the full scan model. GRA

N90-15530# Illinois Association of Recycling Centers, Naperville.
MANAGING THE WASTE STREAM: BACKGROUND INFORMATION FOR PLANNING SOURCE SEPARATION PROGRAMS Final Report
Greg Lindsey and Lynne Lechner Jul. 1989 79 p Sponsored by Illinois Dept. of Energy and Natural Resources, Springfield
(PB90-100223; IL/ENR/RE/EA-89/16) Avail: NTIS HC A05/MF A01 CSCL 13B

A variety of data that can be used to help plan recycling and yard waste collection and composting programs is reported. The report was written primarily as a reference for people using the Recycling Planning and Evaluation Program (REPRP), a simple, spreadsheet computer program for planning recycling programs. Much of the information and some of the default data in REPEP were developed as part of a review of the first two years of the Illinois Recycling Grants Program. Data are organized so that readers can easily look up estimates of the impact that different types of source separation programs have on the waste stream. The terminology and framework for evaluation of the performance of source separation programs is consistent with standards being developed by the National Recycling Coalition (NRC). Included is an overview of different types of recycling programs and a discussion of the NRC framework for measuring program performance. Waste generation and composition data from a number of jurisdictions in Illinois are summarized. Collection statistics for materials recovery programs supported by recycling grants are summarized. Yard waste programs are described.
Author

N90-15531# Oxford Univ. (England). Tropical Palaeoenvironmental Research Group.
GLOBAL LAKE-LEVEL VARIATIONS FROM 18,000 TO 0 YEARS AGO: A PALAEOCLIMATE ANALYSIS
F. A. Street-Perrott, D. S. Marchand, N. Roberts, and S. P. Harrison Sep. 1989 213 p
(Contract DE-FG02-85ER-60304)
(DE90-000998; DOE/ER-60304/H1) Avail: NTIS HC A10/MF A01

Fluctuations in the water levels of lakes are an important source of information about past climates, and can be used to validate paleoclimatic simulations made with atmospheric general-circulation models. The Oxford Lake-Level Data bank contains information about variations in the water levels of approximately 360 lake basins during the last 30,000 years. This data set was compiled as part of COHMAP (the Climates of the Holocene Mapping Project). In this report, regional and global maps of lake status (coded as high, intermediate or low) at 18, 15, 12, 9, 6, 3, and 0 thousand years (Before Present) are presented and compared with numerical simulations for the same time slices carried out with NCAR Community Climate Model. Although agreement between the data and the model is generally excellent, significant discrepancies occur. These may reflect the effects of changes in boundary conditions that were not included in the experiments, for example increased glacial-age aerosol loadings, as well as the inability of the model to portray some of the complexities of the climate system such as oceanic circulation and orographic effects. DOE

N90-15532# Oak Ridge National Lab., TN.
ENVIRONMENTAL SURVEILLANCE DATA Quarterly Report No. 1, 1989
K. L. Daniels, P. Y. Goldberg, B. M. Horwedel, I. L. McCollough, A. E. Osborne-Lee, M. F. Tardiff, S. W. Teeters, C. K. Valentine, C. J. Wear, and D. A. Wolf Sep. 1989 134 p
(Contract DE-AC05-84OR-21400)
(DE90-001275; ORNL/M-836) Avail: NTIS HC A07/MF A01

During the first quarter of 1989, over 4100 samples, which represent more than 9100 analyses and measurements, were collected by the Environmental Monitoring and Compliance Section. A network of real-time monitoring stations that telemeter 10-min averaged readings of radiation levels, total precipitation, flows, water quality parameters, and air quality parameters around Oak Ridge National Laboratory (ORNL) also reported data. In addition, three meteorological towers sent weather data at various heights to a host computer every 15 min. The environmental monitoring program at ORNL was reviewed during this quarter and revisions are currently being implemented to reflect changing requirements and historical results. DOE

N90-15533# Brookhaven National Lab., Upton, NY. Dept. of Applied Science.
LONG-TERM WORLDWIDE ENVIRONMENTAL EFFECTS CAUSED BY ACID RAIN FROM FOSSIL FUELS
B. Manowitz and F. W. Lipfert 1989 16 p Presented at the International Workshop on Safety of Nuclear Installations of the Next Generation and Beyond, Chicago, IL, 28-31 Aug. 1989

(Contract DE-AC02-76CH-00016)
(DE90-001534; BNL-43240; CONF-890841-2) Avail: NTIS HC A03/MF A01

Acid rain is regarded as an environmental problem of growing importance in many parts of the world; it is one of the adverse effects of air pollution. This paper presents data on emissions of air pollutants from combustion of fossil fuels and discusses atmospheric processes that act on these emissions, various effects of air pollution and acid deposition, and some of the aspects of regulation of these pollutants. Evidence of worldwide concern is shown by contrasting the perceived adverse effects of air pollution with ambient levels and the status of regulation. DOE

N90-15534# Pacific Northwest Lab., Richland, WA.
INTERNATIONAL ASPECTS OF RESTRICTIONS OF OZONE-DEPLETING SUBSTANCES
S. C. McDonald Oct. 1989 54 p
(Contract DE-AC06-76RL-01830)
(DE90-001813; PNL-7163) Avail: NTIS HC A04/MF A01

This report summarizes international efforts to protect stratospheric ozone. Also included in this report is a discussion of activities in other countries to meet restrictions in the production and use of ozone-depleting substances. Finally, there is a brief presentation of trade and international competitiveness issues relating to the transition to alternatives for the regulated chlorofluorocarbons (CFCs) and halons. The stratosphere knows no international borders. Just as the impact of reduced stratospheric ozone will be felt internationally, so protection of the ozone layer is properly an international effort. Unilateral action, even by a country that produces and used large quantities of ozone-depleting substances, will not remedy the problem of ozone depletion if other countries do not follow suit. DOE

N90-15535# Lawrence Livermore National Lab., CA. Atmospheric and Geophysical Sciences Div.
GREENHOUSE GASES: CHANGING THE GLOBAL CLIMATE
Michael C. MacCracken Sep. 1989 20 p Presented at the 9th Session of the International Seminars on Nuclear War, Erice, Italy, 19-24 Aug. 1989
(Contract W-7405-eng-48)
(DE90-002788; UCRL-101837; CONF-8908182-1) Avail: NTIS HC A03/MF A01

The increasing atmospheric concentrations of carbon dioxide and other radiatively active gases will enhance the ability of the atmosphere to trap infrared radiation and thereby lead to warming of the climate. Numerical models suggest that the global average surface air temperature can be expected to increase a few degrees during the 21st century. This estimate is probably uncertain by a factor of at least two. The uncertainties in estimates of regional changes of temperature and precipitation are even greater. Despite these uncertainties, there is broad agreement that the persistence of such changes would be unprecedented in historical times. To moderate the projected climatic and environmental changes, the rate of emissions of greenhouse gases must be slowed while alternative energy technologies are developed. DOE

N90-15536# Pacific Northwest Lab., Richland, WA.
EVALUATE AND CHARACTERIZE MECHANISMS CONTROLLING TRANSPORT, FATE, AND EFFECTS OF ARMY SMOKES IN THE AEROSOL WIND TUNNEL: TRANSPORT, TRANSFORMATIONS, FATE, AND TERRESTRIAL ECOLOGICAL EFFECTS OF HEXACHLOROETHANE OBSCURANT SMOKES Final Report
Dominic A. Cataldo, Michael W. Ligotke, Harry Bolton, Jr., Robert J. Fellows, Peter VanVoris, Bruce D. McVeety, Shu-mei W. Li, and Kristin M. McFadden 1 Sep. 1989 195 p
(Contract DE-AC06-76RL-01830; DA Proj. 3E1-62720-A-835)
(DE90-002923; PNL-7166) Avail: NTIS HC A09/MF A02

The terrestrial transport, chemical fate, and ecological effects of hexachloroethane (HC) smoke were evaluated under controlled wind tunnel conditions. The primary objectives of this research program are to characterize and assess the impacts of smoke and obscurants on: (1) natural vegetation characteristic of U.S. Army training sites in the United States; (2) physical and chemical properties of soils representative of these training sites; and (3) soil microbiological and invertebrate communities. Impacts and dose/responses were evaluated based on exposure scenarios, including exposure duration, exposure rate, and sequential cumulative dosing. Key to understanding the environmental impacts of HC smoke/obscurants is establishing the importance of environmental parameters such as relative humidity and wind speed on airborne aerosol characteristics and deposition to receptor surfaces. Direct and indirect biotic effects were evaluated using five plant species and two soil types. HC aerosols were generated in a controlled atmosphere wind tunnel by combustion of hexachloroethane mixtures prepared to simulate normal pot burn rates and conditions. The aerosol was characterized and used to expose plant, soil, and other test systems. Particle sizes of airborne HC ranged from 1.3 to 2.1 micron mass median aerodynamic diameter (MMAD), and particle size was affected by relative humidity over a range of 20 to 85 percent. Air concentrations employed ranged from 130 to 680 mg/cu m, depending on exposure scenario. Chlorocarbon concentrations within smokes, deposition rates for plant and soil surfaces, and persistence were determined. The fate of principal inorganic species (Zn, Al, and Cl) in a range of soils was assessed. DOE

N90-15537# Oak Ridge National Lab., TN.
ACID RAIN RESEARCH Foreign Trip Report, 26 Oct. - 6 Nov. 1989
Robert H. Gardner 15 Nov. 1989 11 p
(Contract DE-AC05-84OR-21400)
(DE90-003283; ORNL/FTR-3468) Avail: NTIS HC A03/MF A01

This report describes the foreign travel of Robert H. Gardner of the Environmental Sciences Division (ESD), Oak Ridge National Laboratory (ORNL), who was invited by The Free University, Amsterdam, to participate in the presentation and defense of the doctoral thesis of Jean-Paul Hettelingh. The opportunity to visit The Netherlands also allowed the traveler to confer with Dr. M.B. Beck at The Imperial College, London; to present a lecture on the theory and methods of assessing the uncertainties associated with environmental models to the Institute for Environmental Studies (IVM) at The Free University; to confer with scientists at The National Institute of Public Health and Environmental Protection (RIVM) at RIVM headquarters in Bilthoven and present a seminar on recent developments in theoretical ecology; and to confer with Dr. Paul Opdam and Jana Verboom of the Research Institute for Nature Management (RIN) concerning our similar research activities in landscape ecology. DOE

N90-15538# State Univ. of New York, Albany. Research Foundation.
RESEARCH PROJECT ON CO2-INDUCED CLIMATE CHANGE Progress Report
Robert D. Cess and Sultan Hameed 1989 9 p
(Contract DE-FG02-85ER-60314)
(DE90-003531; DOE/ER-60314/T1) Avail: NTIS HC A02/MF A01

The following pages summarize the work completed to date in the second year of the Research Project on CO2-Induced Climate Change which is funded by the Department of Energy. The three major areas of study are discussed separately. The first task deals with an intercomparison of general circulation model capabilities with the aim of improving their parameterizations of important physical processes, so that model predictions of CO2 induced climate change become more reliable. Task 2 encompasses analysis of climate data for the purpose of understanding climate change and climate variability. The third task is concerned with analyzing climatic variability in General Circulation Models and its comparison with observations. DOE

N90-15539# Argonne National Lab., IL. Environmental Assessment and Information Sciences Div.
RESPONDING TO THE THREAT OF GLOBAL WARMING: OPTIONS FOR THE PACIFIC AND ASIA

Neeloo Bhatti, David G. Streets, and Toufiq A. Siddiqi (Environment and Policy Inst., Honolulu, HI.) 1989 22 p Presented at the Symposium on Environmental Perspectives Towards the Year 2000 and Beyond, Bangkok, Thailand, 9-10 Nov. 1989
(Contract W-31-109-eng-38)
(DE90-003553; CONF-8911110-2) Avail: NTIS HC A03/MF A01

During the past few years, global climate change was rapidly transformed from an esoteric topic of interest mainly to scientists to one of worldwide concern to policymakers, the business communities, the media, and the general public. In response to this heightened interest, a number of high-level international meetings dealing with this issue were held in the past two years. With growing recognition that the global climate change phenomenon would result in different regional (and local) effects, a workshop was organized by Argonne National Laboratory and the East-West Center to assess the likely consequences of this threat and the possible remediation options available to the countries of the Pacific Asia. The deliberations and conclusion of the workshop are summarized. DOE

N90-15540# Oak Ridge National Lab., TN. Environment Sciences Div.
GLOBAL CLIMATE CHANGE AND NEPA (NATIONAL ENVIRONMENTAL POLICY ACT) ANALYSES
Robert M. Cushman, Donald B. Hunsaker, Jr., Martha S. Salk, and Robert M. Reed 1989 25 p Presented at the The Scientific Challenge of NEPA: Future Directions Based on 20 Years of Experience, Knoxville, TN, 24-27 Oct. 1989
(Contract DE-AC05-84OR-21400)
(DE90-003704; CONF-891098-4) Avail: NTIS HC A03/MF A01

Energy production and use, industrial activity, and land-use change are expected to cause a global climate change that would have local and regional manifestations during the next century. Although the resulting impacts are not yet known with certainty, potential effects on agriculture, water, forests, ecosystems, fisheries, coastal areas (from rising sea level), and other environmental resources have been predicted. The National Environmental Policy Act of 1969 (NEPA) provides for consideration of such topics as global climate change. However, the implementation of the environmental impact statement (EIS) requirements of NEPA has seldom been used to address the issue. Climate change and its consequent effects have three important implications for NEPA determinations: (1) the potential for an action to individually alter climate must be assessed, (2) cumulative impacts of the action in concert with other actions must be considered, and (3) the potential for future climate change to alter the baseline environment (and thus to affect the action or to alter the impact of the action) must be assessed, even if the action under consideration will not in itself contribute to climate change. In this paper, we evaluate the climate-change issue (including the uncertainty of the temporal and spatial distribution of impacts) in a NEPA context. We discuss the kinds of actions to which NEPA is applicable, the types of analyses that might be appropriate, and the problems they might involve. In particular, the opportunities and limitations under current Council on Environmental Quality regulations for addressing climate change through the environmental assessment (EA)/EIS process are addressed. We also discuss changes that have been proposed for NEPA and its implementing regulation and how they could affect the analysis of global climate change. DOE

N90-15541# Argonne National Lab., IL.
GLOBAL CLIMATE CHANGE: A FOSSIL ENERGY PERSPECTIVE
Robert Kane (Department of Energy, Washington, DC.) and David W. South 1989 7 p Presented at the 6th International Coal Trade, Transportation and Handling Conference, London, England, 16-18 Oct. 1989
(Contract W-31-109-eng-38)
(DE90-003770; CONF-891080-1) Avail: NTIS HC A02/MF A01

Global climate change has attracted considerable attention recently as an emerging environmental problem. While substantial uncertainties still exist regarding the ability to accurately predict climate change, some scientists and policymakers believe immediate action is required. As a result, legislative proposals have been introduced and policies/programs proposed to address the perceived problem. Since fossil fuel combustion has been identified as a major contributor to the growth in atmospheric greenhouse gases, curtailing the emissions from fossil-fired facilities is a primary focus of many proposals. This paper discusses global climate change from a fossil, energy development and utilization perspective and demonstrates that if it is determined that greenhouse gas emissions should be reduced, fossil fuels and fossil-fuel-based technologies can, and must, play a role. DOE

N90-15542# Spectral Sciences, Inc., Burlington, MA.
HCl MONITOR, PHASE 2 Final Report, 1 Jul. 1986 - 3 Jun. 1988
Lawrence S. Bernstein, F. Bien, W. K. Cheng, R. P. Domingue, and S. C. Richtsmeier Mar. 1989 94 p
(Contract F08635-86-C-0137; AF Proj. 3005)
(AD-A213572; SSI-TR-137-Phase-2;
AFESC/ESL-TR-88-51-Phase-2) Avail: NTIS HC A05/MF A01
CSCL 21/8

At present, the short- and long-term environmental impacts of massive HCl releases from the Space Shuttle and other solid-rocket launches are not well characterized. It is important to measure the atmospheric HCl content in both the vapor and aerosol forms. Spectral Sciences, Inc., (SSI) has developed a combination vapor-aerosol HCl monitor under a Phase 2 SBIR (Small Business Innovative Research program) contract from the Air Force Engineering Services Center (AFESC), Tyndall AFB, Florida. The instrument consists of four major components: (1) an air sampling, optical measurement unit; (2) a power supply and analog signal output unit; (3) an analog-to-digital (a/d) converter and timing pulse unit; and (4) a personal computer (PC). An air sample is drawn through an aerosol evaporator which vaporizes the aerosols and releases the dissolved HCl into the gas phase. By turning the aerosol heater on and off, one can determine both the total HCl (aerosol and vapor) and the vapor phase HCl. The device is based on measuring the infrared absorption of gas phase HCl in the 3.4 micrometer wavelength region. GRA

N90-15543# Oak Ridge National Lab., TN. Energy Div.
FACTORS THAT MAY INFLUENCE RESPONSES OF THE US TRANSPORTATION SECTOR TO POLICIES FOR REDUCING GREENHOUSE GAS EMISSIONS
Edward L. Hillsman and Frank Southworth 1990 30 p Presented at the Transportation Research Board Meeting, Washington, DC, Jan. 1990
(Contract DE-AC05-84OR-21400)
(DE90-000704; CONF-900121-3) Avail: NTIS HC A03/MF A01

Transportation vehicle operations in the U.S. contribute 32 percent of the nation's emissions of carbon dioxide, and 7 percent of the world's emissions from energy use. Technical options exist to reduce emissions rates, but policies to reduce emissions must recognize the fragmentation of responsibility for key transportation activities among diverse groups of decision makers, and the need to coordinate their decisionmaking. Policies to increase vehicle fuel efficiency affect decisions by vehicle suppliers, transportation service suppliers, and those who demand transportation services. Policies to shift to alternative transportation fuels affect decisions by these decision makers, by fuel suppliers, and possibly by infrastructure developers as well. Long-term increases projected in the demand for transportation services will offset emission reductions from these policies unless service can be delivered by modes with lower emissions, or unless demand growth can be managed as is now occurring in other sectors of the economy. Additional research is needed to determine the most effective demand management strategies. DOE

N90-15544# Brookhaven National Lab., Upton, NY. Environmental Chemistry Div.
ACID DEPOSITION
Stephen E. Schwartz Nov. 1989 18 p Presented at the 9th

Session of the International Seminars on Nuclear War, Erice, Italy, 19-24 Aug. 1989 Submitted for publication
(Contract DE-AC02-76CH-00016)
(DE90-003959; BNL-43550; CONF-8908182-2) Avail: NTIS HC A03/MF A01

The acid deposition phenomenon is a well documented example of the influence of industrial activities on atmospheric composition and precipitation composition. This phenomenon consists of emissions of sulfur and nitrogen oxides into the atmosphere, largely from fossil-fueled combustion, followed by transport, chemical transformation, and deposition to the surface. This deposition consists principally of deposition of sulfuric and nitric acids in precipitation (wet deposition) and deposition of gaseous SO2, NO2, and HNO3 in the absence of precipitation (dry deposition). The acid deposition phenomenon is widely held to be responsible for deleterious effects on ecological systems, structural and ornamental materials, and visibility in the atmosphere. Because of the density of emission sources in eastern North America, it is not yet possible to specify precisely the contribution to deposition at particular receptor sites to particulate emission sources. Present understanding of atmosphere transport velocities and rates of transformation and deposition processes suggest mean source-receptor distances of 500 to 1500 km. Regional emission densities in the Northeast United States substantially exceed standards that have been suggested to protect sensitive ecosystems. Recognition of the properties of the acid deposition phenomenon is explicitly noted in prospective legislation in the United States. DOE

46 GEOPHYSICS

Includes aeronomy; upper and lower atmosphere studies; ionospheric and magnetospheric physics; and geomagnetism.

For space radiation see *93 Space Radiation.*

N90-15545*# National Aeronautics and Space Administration. Marshall Space Flight Center, Huntsville, AL.
SUPERCONDUCTING GRAVITY GRADIOMETER MISSION. VOLUME 1: STUDY TEAM EXECUTIVE SUMMARY
Samuel H. Morgan, ed. and Ho Jung Paik, ed. (Maryland Univ., College Park.) Aug. 1989 42 p
(NASA-TM-4091-Vol-1; NAS 1.15:4091-Vol-1) Avail: NTIS HC A03/MF A01 CSCL 08G

An executive summary is presented based upon the scientific and engineering studies and developments performed or directed by a Study Team composed of various Federal and University activities involved with the development of a three-axis Superconducting Gravity Gradiometer integrated with a six-axis superconducting accelerometer. This instrument is being developed for a future orbital mission to make precise global gravity measurements. The scientific justification and requirements for such a mission are discussed. This includes geophysics, the primary mission objective, as well as secondary objectives, such as navigation and tests of fundamental laws of physics, i.e., a null test of the inverse square law of gravitation and tests of general relativity. The instrument design and status along with mission analysis, engineering assessments, and preliminary spacecraft concepts are discussed. In addition, critical spacecraft systems and required technology advancements are examined. The mission requirements and an engineering assessment of a precursor flight test of the instrument are discussed. Author

N90-15546 Texas A&M Univ., College Station.
IDENTIFICATION AND QUANTIFICATION OF SYNOPTIC STRUCTURE IN SIMULATED TIROS N RADIANCE SOUNDINGS Ph.D. Thesis
G. Anderson White, III 1988 162 p
Avail: Univ. Microfilms Order No. DA8913468

There was continual improvement in the accuracy of retrieved atmospheric soundings from satellite radiance measurements; however, satellite data still provide an overly smooth product which is of limited use for synoptic scale analysis. Considerable smoothing occurs when information present in satellite radiance measurements is lost in the retrieval process. Techniques are described and developed which identify synoptic features and quantify their fine structures directly from TIROS N satellite radiance data. A series of nine, overlapping, synthetic temperature and moisture soundings is constructed which contains synoptic features representative of the tropical eastern Pacific Ocean. Each of the soundings in the series is perturbed randomly, within limits, to create a statistically meaningful training data set. The training data set is processed through a radiative transfer algorithm to generate equivalent TIROS N satellite observations. In a two-step process, the training data observations first are separated according to synoptic features, and, second, the fine structure of the synoptic feature is quantified. Three clasisification techniques are developed to partition the training data observations into synoptic groups and to classify new soundings: a subjective, graphical, interpretative procedure; canonical discriminant analysis; and, discriminant analysis. Two experiments of feature qualification are described: a prediction of trade wind and frontal inversion height and strength using both synthetic and observed soundings; and, a prediction of frontal structure based on discriminant analysis of a training data set containing frontal inversion soundings. Dissert. Abstr.

N90-15547 California Univ., Los Angeles.
OBSERVATIONAL STUDY OF THE MACROSCOPIC BEHAVIOR OF MOIST-CONVECTIVE PROCESSES Ph.D. Thesis
Jeng-Ming Chen 1989 288 p
Avail: Univ. Microfilms Order No. DA8919908

The cumulus parameterization problem is a closure problem, in which relationships are sought between the collective effects of moist-convective processes and their large-scale environment. Closures used in existing parameterization schemes can be classified into four types. The focus is on the first two types. Type 1 is a constraint on coupling of net moistening and net warming. Type 2 is a constraint on coupling of the apparent heat source, Q(sub 1), and the apparent moist sink, Q(sub 2), through a cumulus ensemble model. The main objectives are to directly verify closures and assess the parameterizability of moist-convective processes using observations under a variety of large-scale conditions. A statistical method, which combines principal component analysis (PCA) and conventional canonical component analysis (CCA), is developed for this purpose. The statistical method is applied to the GATE dataset and the Asian dataset. Using the results from these analyses, estimates are determined for the Q(sub 1) and Q(sub 2) fields from a linear combination of both, gamma Q(sub 1) = Q(sub 2), for example. From these results, it was found that Type 2 coupling is quasi-universally strong. An empirical cumulus parameterization scheme, conceptually guided by the Arakawa-Schubert parameterization, is constructed based on the CCA results of the Asian dataset. In this scheme, gamma Q(sub 1) = Q(sub 2) is determined for a given large-scale condition through type 1 coupling, introducing the concept of empirical cloud work function. The scheme has been tested against an independent dataset, the GATE dataset. From the results of this study, we can conclude that cumulus convection is basically parameterizable.
Dissert. Abstr.

N90-15548 California Univ., Irvine.
FLUX PARAMETERIZATION TECHNIQUES IN THE ATMOSPHERIC SURFACE LAYER Ph.D. Thesis
Steven Philip Oncley 1989 225 p
Avail: Univ. Microfilms Order No. DA8915442

The relationship used to determine the fluxes of momentum, sensible and latent heat in the atmospheric surface layer are explored using a new, extensive data set taken over uniform terrain. After these relationships are found, an estimate is made of the accuracy to which fluxes are obtained from a sonic anemometer with co-located dry and and wet thermocouples. Wind speed, temperature, and humidity profiles are reduced suing flux-profile relations. Measurements of the dissipation rate of turbulent kinetic energy (TKE) taken by a high-frequency hot-wire anemometer are

compared to momentum flux using the TKE budget. The dissipation rate of TKE also is estimated from velocity power spectra in the inertial subrange using the lower frequency response sonic anemometer. The dissipation rate of temperature variance from a cold-wire thermometer and thermocouple sensor are also explored. An energy balance system is used to estimate the sensible and latent heat flux using the Bowen ratio method. Finally, statistical time series analysis is performed on the data to explore simple methods to determine fluxes. The eddy-correlation and flux-profile methods are found to yield the best estimates of the fluxes. The Bowen ratio estimates were within 30 W/m squared, which was similar to the accuracy from the dissipation technique. Single-point statistics show some promise for use in flux determinations, but are not well understood. All methods require extensive data handling to ensure reliable results. Dissert. Abstr.

N90-15549# Brookhaven National Lab., Upton, NY. Atmospheric Sciences Div.

VERTICAL DISTRIBUTION OF POLLUTANTS IN THE PRESENCE OF CONVECTIVE STORMS

Lawrence Kleinman 1989 6 p Presented at the 28th Liege International Astrophysical Colloquium on our Changing Atmosphere, Liege, Belgium, 26-30 Jun. 1989

(Contract DE-AC02-76CH-00016)

(DE90-002590; BNL-43361; CONF-8906154-2) Avail: NTIS HC A02/MF A01

During the PRECP V field program vertical profiles of CO, NO(y), SO2, O3, H2O2, aerosol particles and water vapor were measured in the vicinity of convective storms or in air masses which had experienced convection in their recent past. Peak concentrations occur at the altitudes at which the various substances are emitted or formed in the atmosphere. For water vapor, SO2, CO, NO(y) and submicron aerosol particles this is the boundary layer. High concentrations of O3 occur in the boundary layer where it is photochemically formed and in the upper troposphere as a result of downward transport from the stratosphere. The peak formation rate and the highest concentration of H2O2 occurs above the boundary layer. The insoluble pollutants CO and NO(y) can be efficiently transported from the boundary layer to upper troposphere. Soluble species such as SO2 and aerosol particles cannot be similarly transported from the boundary layer to upper troposphere. The observed proportionality between aerosol particles and water vapor is consistent with limits on the upward transport imposed by the sequence of cooling, cloud formation, and removal in precipitation. DOE

N90-15550# Lawrence Livermore National Lab., CA.

BERYLLIUM DISPERSION NEAR EXPLOSIVE FIRING TABLES: A COMPARISON OF COMPUTED AND OBSERVED RESULTS

Joseph H. Shinn, R. T. Cederwall, K. C. Lamson, and C. S. Mitchell Jul. 1989 57 p

(Contract W-7405-eng-48)

(DE90-002635; UCID-21682) Avail: NTIS HC A04/MF A01

It was demonstrated that evaluation of vertical atmospheric Be profiles, extensive deposition samples, a few strategically located air concentration measuring devices, and ambient meteorological conditions can be used to characterize the high-explosives tests at Site 300. The application of modeling simulation using the detailed description of Be particle size and air concentrations in the stem and cap cloud formed during a detonation has resulted in a high level of physical realism and objectivity in the assessment of downwind Be deposition and short term elevated air concentrations. DOE

N90-15551# Japan Atomic Energy Research Inst., Tokyo.

DEVELOPMENT OF A THREE-DIMENSIONAL LOCAL SCALE ATMOSPHERIC MODEL WITH TURBULENCE CLOSURE MODEL

Hiromi Yamazawa May 1989 27 p

(DE90-710045; JAERI-M-89-062) Avail: NTIS (US Sales Only) HC A03/MF A01

Through the study to improve SPEEDI's capability, a three-dimensional numerical atmospheric model Prognostic HYdroStatic model Including turbulence Closure (PHYSIC) developed to apply it to the transport and diffusion evaluation over complex terrains. The detailed description of the atmospheric model was given. This model consists of five prognostic equations; the momentum equations of horizontal components with the so-called Boussinesq and hydrostatic assumptions, the conservation equations of heat, turbulence kinetic energy and turbulence length scale. The coordinate system used is the terrain following z(sub *) coordinate system which allows the existence of complex terrain. The minute formula of the turbulence closure calculation, the surface layer process, the ground surface heat budget, and the atmospheric and solar radiation were also presented. The time integration method used in this model is the Alternating Direction Implicit (A.D.I.) method with a vertically and horizontally staggered grid system. The memory storage needed to execute this model with 31 x 31 x 16 grid points, five layers in soil and double precision variables is about 5.3 MBytes. The CPU time is about 2.2 x 10(exp -5) s per one step per one grid point with a vector processor FACOM VP-100. DOE

N90-15552# California Inst. of Tech., Pasadena.

SALTATION AND SUSPENSION OF PARTICULATE MATTER IN AIR Final Report, 1 Aug. 1986 - 15 Apr. 1989

Peter K. Haff and Robert S. Anderson 28 Aug. 1989 30 p

(Contract DAAL03-86-K-0132)

(AD-A213618; ARO-23900.9-GS) Avail: NTIS HC A03/MF A01 CSCL 04/1

A summary of progress which was made on the computer simulated and modeling of wind blown sand transport is presented. GRA

N90-15553# Air Force Inst. of Tech., Wright-Patterson AFB, OH.

IDENTIFICATION AND QUANTIFICATION OF SYNOPTIC STRUCTURE IN SIMULATED TIROS N RADIANCE SOUNDINGS Ph.D. Thesis

G. Anderson White, III 1989 162 p

(AD-A213729; AFIT/CI/CIA-88-230) Avail: NTIS HC A08/MF A01 CSCL 04/2

There has been continual improvement in the accuracy of retrieved atmospheric soundings from satellite radiance measurements; however, satellite data still provide an overly smooth product which is of limited use for synoptic scale analysis. Considerable smoothing occurs when information present in satellite radiance measurements is lost in the retrieval process. This research describes and develops techniques which: (1) identify synoptic features and (2) quantify their fine structures directly from TIROS N satellite radiance data. A series of nine, overlapping, synthetic temperature and moisture soundings is constructed which contains synoptic features representative of the tropical eastern Pacific Ocean. Each of the soundings in the series is perturbed randomly, within limits, to create a statistically meaningful training data set. The training data set is processed through a radiative transfer algorithm to generate equivalent TIROS N satellite observations. In a two-step process, the training data observations first are separated according to synoptic feature, and, second, the fine structure of the synoptic feature is quantified. Three classification techniques are developed to partition the training data observations into synoptic groups and to classify new soundings: a subjective, graphical, interpretative procedure; canonical discriminant analysis; and, discriminant analysis. GRA

N90-15554# Illinois Univ., Urbana.

DETERMINATION OF Q AS A FUNCTION OF DEPTH AND TECTONIC PROVINCE Final Report, 20 Jan. 1987 - 22 Jan. 1989

Stephen Grand and Xiao-Yang Ding 14 Jun. 1989 69 p

(Contract F19628-87-K-0025)

(AD-A213805; GL-TR-89-0157) Avail: NTIS HC A04/MF A01 CSCL 08/11

The goal of this study is to determine the relation between upper mantle shear velocity at a particular depth and Q sub u at

the depth. Such a relation would provide a means of finding t asterisk biases for any test site by using well developed techniques for remotely sensing shear velocity structure. We have developed upper mantle Q models, to 700 km depth, beneath two distinctly different tectonic regions, the East Pacific Rise and the North American craton. These two regions are end members in terms of upper mantle velocity structure with the East Pacific Rise having the lowest shear velocities and the Canadian shield the highest. The NTS test site overlies an upper mantle similar to the East Pacific Rise. The Soviet and French Saharan test sites overlie mantle with intermediate shear structures. The upper mantle Q structures were derived by modeling the amplitude decay of multiple bounce shear waves as a function of distance. For the East Pacific Rise, S, SS, SSS, and SSSS waves were included for distances from 30 to 80 deg. For the shield data only phases up to SSS were used and the distance range was limited to 60 deg due to the geographic extent of the craton. The data have predominant periods from 20 to 30 sec. The PREM lower mantle Q model was assumed for below 700 km depth and mechanisms for the earthquakes were taken from the literature. GRA

N90-15555# Air Force Geophysics Lab., Hanscom AFB, MA.
DESCRIPTION OF SHARC: THE STRATEGIC HIGH-ALTITUDE RADIANCE CODE Environmental Research Papers, Sep. 1987 - Jun. 1989
R. D. Sharma, A. J. Ratkowski, R. L. Sundberg, J. W. Duff, and L. S. Bernstein 16 Aug. 1989 226 p
(AF Proj. S321)
(AD-A213806; GL-TR-89-0229; GL-ERP-1036) Avail: NTIS HC A11/MF A02 CSCL 12/5

The Strategic High-Altitude Radiance Code (SHARC) is a new computer code that calculates atmospheric radiation and transmittance for paths from 60 to 300 km altitude in the 2 to 40 microns spectral region. It models radiation due to NLTE (Non-Local Thermodynamic Equilibrium) molecular emissions. This initial version of SHARC includes the five strongest IR radiators, NO, CO, H2, O3, and CO2. This report describes the code and models used to calculate the NLTE molecular populations and the resulting atmospheric radiance. The SHARC Manual is reproduced in the appendix. GRA

N90-15556# Colorado Univ., Boulder. Cooperative Inst. for Research in Environmental Science.
THEORETICAL MODELS OF EARTHQUAKE PHENOMENA AND THE PHYSICAL SIGNIFICANCE OF SEISMIC MOMENT TENSOR EXPANSIONS Final Scientific Report, May 1987 - May 1989
Charles B. Archambeau and John Scales 1 Jun. 1989 89 p
(Contract F19628-87-K-0019; ARPA Order 5299)
(AD-A213813; GL-TR-89-0156) Avail: NTIS HC A05/MF A01 CSCL 08/11

The objective of this study is to formulate a physically sound analytical representation of the seismic radiation field produced by spontaneous failure in an arbitrarily prestressed solid. Such formulations, usually given in terms of a Green's function integral equation, may then be expanded in a moment series which is used as a basis of interpretation of observed seismic wave fields from naturally occuring earthquakes. Consequently, a meaningful understanding of the physics involved in such an event, as can be gained from an inversion of observed seismic wave fields, as well as the ability to provide reliable predictions of the seismic radiation to be expected from such events, is dependent on the completeness and accuracy with which the basic integral equation (or numerically based formulation) represents the conservation laws involved in both the failure process and the energy release associated with the seismic radiation. The present study develops an approach that incorporates the (nonlinear) conservation relations on the failure surface, as well as those appropriate in the surrounding linear zone, to generate a Greens function integral equation describing both the failure growth and the (interacting) seismic radiation field. GRA

N90-15557# Yale Univ., New Haven, CT. Dept. of Chemistry.
OXYGEN AND OTHER ATMOSPHERIC GASES Final Report, 15 Sep. 1986 - 30 Sep. 1988
W. A. Chupka, S. D. Colson, and E. E. Eyler 27 Feb. 1989 128 p
(Contract F19628-86-C-0214; AF Proj. 2310)
(AD-A214296; AFGL-TR-89-0064) Avail: NTIS HC A07/MF A01 CSCL 04/1

Laser multiphoton, mass, and photoelectron spectroscopy was used to investigate the energy level structure and photophysics of oxygen and other atmospheric gases. Particular emphasis was placed on determining the location, predissociation and photoionization processes of the previously unknown lower ns and nd gerade Rydberg states and their interactions with valence states. A shape resonance in the ionization continuum near threshold was found to play a large role in inducing non-Franck-Condon transitions. Optimum transitions for production of vibrationally state-selected O2+ ions were found. The effects of dissociation continua and strongly mixed Rydberg-valence states as intermediates in multiphoton processes were demonstrated and explored. GRA

N90-15558# Pennsylvania State Univ., University Park.
CALCULATION OF SOURCE AND STRUCTURE PARAMETERS AT REGIONAL AND TELESEISMIC DISTANCES Final Report, 1 Feb. 1987 - 31 Jan. 1989
Charles A. Langston and Roy J. Greenfield 13 Apr. 1989 129 p
(Contract F19628-87-K-0024; AF Proj. 7A10)
(AD-A214297; GL-TR-89-0108) Avail: NTIS HC A07/MF A01 CSCL 08/11

Teleseismic receiver functions for structure under Pasadena, California (PAS) are derived from azimuthally distributed teleseismic P waves recorded on Benioff 1-90 instrumentation. The broadband three-component Benioff 1-90 system is peaked at a 1-s period allows resolution of major crustal interfaces from large Ps conversions seen in the receiver function data. The observed body wave data are quite complex, showing exceptionally large Ps conversions and scattered waves on horizontal components. Radial and tangential motions are of equal magnitude and show major off-azimuth converted Ps waves, suggesting large-scale crustal heterogeneity beneath the station. Stochastic simulations of one-dimensional plane layered structure show that geologically unreasonable one-dimensional models are required to fit the data. The observed coda decay yields a scattering Q estimate of 239 at a 2-s period using an energy flux model for a propagating plane wave interacting with a scattering layer over a homogeneous half-space. PAS coda is compared to coda from deep teleseisms, it is seen that scattering is more severe at PAS, as reflected in higher coda levels and slower decay rate. Consideration of energy partitioning and coda amplitude suggests that much of the coda consists of scattered surface waves. Analysis of a major Ps conversion arriving 3 s after direct P indicates that a major crustal discontinuity at about 20 km depth dips at moderate angles to the north under the San Gabriel Mountains. GRA

N90-15559*# National Aeronautics and Space Administration. Goddard Space Flight Center, Greenbelt, MD.
A HIGH SPATIAL RESOLUTION STUDY OF THE THERMOSPHERIC RESPONSE TO A DISCRETE AURORAL ARC Final Report
R. W. Eastes, T. L. Killeen, G. R. Carrignan, A. E. Hedin, N. W. Spencer, L. H. Brace, W. R. Hoegy, R. A. Heelis, J. D. Winningham, and B. A. Emery (National Center for Atmospheric Research, Boulder, CO.) 16 Feb. 1989 20 p
(AF Proj. 4643)
(NASA-TM-102904; NAS 1.15:102904; AD-A214400; AFGL-TR-89-0043; AFGL-ERP-1021) Avail: NTIS HC A03/MF A01 CSCL 04/1

A sequence of three high latitude passes by the De-2 spacecraft has been studied using high spatial resolution data from several instruments to investigate the local thermospheric response to a discrete auroral arc. Three passes, orbits 1847, 1848, and 1849,

which occurred on 6 December 1981, cross an isolated, discrete arc in the evening auroral oval. Observations of neutral winds, ion winds, neutral densities, energetic electron spectrum, and neutral temperatures were examined at a spatial resolution of approximately 8 km. The observations illustrate the response of the thermosphere to the local insertion of energy and momentum and provide the basis for a more critical test of the various theoretical models that have predicted local thermospheric phenomena. The results are presented and discussed in relation to the predictions of three such local models. GRA

N90-15560# SRI International Corp., Menlo Park, CA.
NO2 PHOTODISSOCIATION DYNAMICS Final Report, 1 Nov. 1986 - 30 Sep. 1989
Tom G. Slanger Sep. 1989 89 p
(Contract F49620-87-K-0004; SRI Proj. PYU-2891; AF Proj. 2303)
(AD-A214422; MP-89-187; AFOSR-89-1338TR) Avail: NTIS HC A05/MF A01 CSCL 07/4

The studies carried out under the present contract have all involved investigations of the photophysics and photochemistry of two nitrogen oxide molecules, NO and NO2. As well as being intrinsically interesting, these molecules are important from the point of view of atmospheric chemistry, and the NO2 molecule is a leading candidate as the emitting molecule that has been observed in the space shuttle glow. Major findings of these studies include the following observations: Multiphoton dissociation of NO2 by green light produces highly excited products, specifically, highly vibrationally excited O2 and NO, and O(S); and two-photon absorption of 268 to 280 nm radiation by NO results in production of the first excited state of the N-atom, N(2D), an atmospherically important species that is difficult to produce by any other photodissociative technique. GRA

N90-15561# International Centre for Theoretical Physics, Trieste (Italy).
STABLE SUPERMEMBRANE VACUUM WITH A DISCRETE SPECTRUM
M. J. Duff, C. N. Pope (Texas A&M Univ., College Station.), and E. Sezgin Apr. 1989 9 p Submitted for publication
(DE89-635722; IC-89/71; CTP-TAMU-1/89) Avail: NTIS (US Sales Only) HC A02/MF A01

The massless spectrum of the supermembrane was examined in the background of four-dimensional anti-de Sitter space times a compact internal space, by considering quantization about a collapsed membrane configuration. It was also observed that the vacuum is stable and that the spectrum of massive states is necessarily discrete. In this respect, the supermembrane favors anti-de Sitter over Minkowski space, where the spectrum seems likely to be continuous. DOE

N90-15043# Office National d'Etudes et de Recherches Aerospatiales, Paris (France).
DESCRIPTION OF ATMOSPHERIC TURBULENCE [DESCRIPTION DE LA TURBULENCE ATMOSPHERIQUE]
Pierre-Marie Hutin *In* AGARD, Flight in Adverse Environmental Conditions Sep. 1989 14 p In FRENCH Previously announced in IAA as A89-48750 (For primary document see N90-15041 07-01)
Copyright Avail: NTIS HC A17/MF A03; Non-NATO Nationals requests available only from AGARD/Scientific Publications Executive

47 METEOROLOGY AND CLIMATOLOGY

Includes weather forecasting and modification.

N90-15562# Bureau of Reclamation, Denver, CO. Water Augmentation Group.
WINTER CLOUD SEEDING POTENTIAL ON THE MOGOLLON RIM Final Report
Arlin B. Super, Edmond W. Holroyd, III, and Jack T. McPartland Jan. 1989 191 p Sponsored by Central Arizona Project Association; Central Arizona Water Conservation District; Maricopa Water District; and Salt River Project
(Contract IGA-88-6189-000-0051)
(PB89-190540; R-89-02) Avail: NTIS HC A09/MF A01 CSCL 04B

Natural cloud and precipitation processes were investigated on the Mogollon Rim of Arizona during mid-January to mid-March of 1987 and 1988. The primary goal was to evaluate the cloud seeding potential of winter storms prior to attempting any seeding. It was crucial to monitor the availability of supercooled CLW (cloud liquid water) required for precipitation development, and this was accomplished with a ground-based microwave radiometer and instrumented aircraft. Other measurements of importance included cloud depth and structure, atmospheric stability, winds, cloud ice particles and water droplets, and surface precipitation. The field measurements were put in the context of large-scale weather patterns using standard weather maps and satellite photographs. A secondary goal involved evaluation of ground-based seeding simulated by transport and diffusion experiments using a tracer gas. Several important findings emerged from the various analyses of the data. Cloud liquid water was available during portions of most storm episodes. The flux of liquid water passing over the crestline during a 4-month winter was estimated at 30 to 100 percent of the mean annual runoff from the study areas. Thus, the raw material required for successful cloud seeding was available in reasonable abundance. Author

N90-15563 Princeton Univ., NJ.
DYNAMICS OF BAROCLINIC INSTABILITY IN RAPID CYCLOGENESIS Ph.D. Thesis
Noboru Nakamura 1989 174 p
Avail: Univ. Microfilms Order No. DA8908056

In order to aid the understanding of intense midlatitude cyclogenesis, linear and nonlinear aspects of the life cycle of baroclinic instability are investigated in the parameter settings representing meso- to synoptic-scale spectral ranges of a dry atmosphere. Scale selectivity is examined in a 2-D(x-z) nongeostrophic stability analysis. It was found that low level weak stability leads to a modal separation of baroclinic instability between fast growing, shallow waves and deep, long waves. When the Richardson number of the flow is small, a short wave ageostrophic unstable mode exists besides the conventional baroclinic instability, that is sustained by a resonance between a boundary wave and Doppler-shifted inertia-gravity wave. The nonlinear evolution of the instability is examined in a numerical integration of 2-D(x-z) Eady waves using a primitive equation model. An oscillation in the amplitude of the wave is observed, following a rapid frontogenesis. Examination reveals that this is caused by an increase in static stability of the flow, not directly by the frontal dynamics and dissipation. The corresponding maximum amplitude of the velocity field is roughly proportional to the initial buoyancy frequency. Generally, shallow baroclinic waves cease to grow at a low energy level despite a rapid growth. Therefore, explosive cyclogenesis on the mesoscale is unlikely to be sustained solely by dry, single wave baroclinic instability. Such processes as moist boundary layer dynamics and resonance with a synoptic scale disturbance should be taken into account for a more realistic representation.
Dissert. Abstr.

N90-15564 Reading Univ. (England).
POTENTIAL VORTICITY IN EXTRATROPICAL CYCLONES Ph.D. Thesis
Paul Berrisford 1988 172 p
Avail: Univ. Microfilms Order No. BRDX86070

The physical processes that are important in a number of cases of extratropical cyclogenesis are investigated using the quasi-conservative quantity potential vorticity (p.v.). The focus is on the storm over the south of England in October 1987 which deepened rapidly and had associated strong low level winds. The cases with extreme surface winds exhibit stratospheric values of p.v. in the lower troposphere. For the October storm the advective properties and sources of p.v. are investigated in detail. Advections on 350 K suggest that in the region of the tropopause the source

of p.v. can be as large as +1p.v.u.d(sup -1). Continuity of the tropopause p.v. on 350 K is poor. On 305 K the source of p.v. is seen to be less than -1p.v.u.d(sup -1) in some regions of the tropopause. Large scale moist ascent is seen to produce a source of p.v. greater than +5p.v.u.d(sup -1) in the lower tropopause. For isentropic surfaces within about 2 km of the sea surface the results of advection calculations suggest that turbulent fluxes of heat can provide a sink of p.v. of comparable magnitude to that due to large scale latent heat release. Towards the end of development friction is seen to produce a sink of magnitude 2p.v.u.d(sup -1). For the October storm a semi-geostrophic inversion is carried out. It is found that various components of the p.v. field are associated with the strong low level winds. The sloping nature of the tropopause and the low level p.v. maximum both contribute to the high winds while the surface baroclinity actually reduces them. In another explosive cyclone it is seen that the mature cyclone core consists of high low level p.v. and warm air at the ground. Both of these features contribute to the strong low level winds. Dissert. Abstr.

N90-15565# Oak Ridge National Lab., TN.
ANTARCTIC SURFACE TEMPERATURE AND PRESSURE DATA
P. D. Jones, ed., D. W. S. Limbert, ed. (British Antarctic Survey, Cambridge, England), and T. A. Boden, ed. Sep. 1989 60 p
(Contract DE-AC05-84OR-21400)
(DE90-000971; ORNL/CDIAC-27; NDP-032) Avail: NTIS HC A05/MF A01

Monthly mean surface temperature and pressure data from 30 Antarctic stations are presented. These data were assembled primarily from World Weather Records volumes for 1951 to 1960 and 1961 to 1979 and from Monthly Climatic Data for the World records since 1961. The periods of record vary by station. The earliest data are from 1903, and the most recent data are from 1988. All the assembled data were assessed for quality and for long-term homogeneity through the use of interstation comparison techniques. These data are available free of charge as a numeric data package (NDP) from the Carbon Dioxide Information Analysis Center. The NDP consists of this document and a magnetic tape containing machine-readable data files. Tabular listings are provided for the temperature and pressure data, the processing of the data is described, the limitations and restrictions of the data are defined, and reprints of pertinent literature provided. DOE

N90-15566# Oklahoma Univ., Norman. Cooperative Inst. for Mesoscale Meteorological Studies.
TURBULENCE SPECTRAL WIDTHS VIEW ANGLE INDEPENDENCE AS OBSERVED BY DOPPLER RADAR Final Report
J. T. Lee and K. Thomas Oct. 1989 56 p
(Contract DTFA01-80-Y-10524)
(DOT/FAA/SA-89/2) Avail: NTIS HC A04/MF A01

As air traffic density increases, effective use of airspace must include consideration of weather. Accurate identification of turbulent volumes is of paramount importance to flight safety. The advent of Doppler radar has made it possible to observe wind motion in convective clouds. Over a number of years, research has lead to the spectral width (standard deviation) of the Doppler velocity measurements as an indicator of turbulence. The hypotheses that turbulence is essentially isotropic in convective systems, and therefore, observations of turbulence are independent of viewing angle, is addressed. Radar observations made during the months of April, May, and June in 1980 to 1985 were scanned to locate storms amenable to analysis. A number of cases are presented in which a dual-Doppler network provided the essential data. Each case is in a different quadrant with respect to the Norman Doppler. Forty-four horizontal planes were studied from six different storms. The results of four of these storms included range from near surface to 7 km. At these altitudes the maximum spectral width was 12 ms(exp -1). For these cases, involving nearly 30,000 data points, 70 percent of the spectral width observations from CIM and NRO were within 1 ms(exp -1) or less. These results indicate that the use of Doppler radar to detect turbulent regions within thunderstorms has a high probability of success, and the turbulent regions can be detected independent of the direction from which they are viewed. Author

N90-15567# Central Research Inst. of Electric Power Industry, Tokyo (Japan). Energy and Environment Lab.
CHARACTERISTICS OF ELECTROMAGNETIC WAVE FORMS WITH LIGHTNING IN WINTER SEASON
Seietsu Tomita Sep. 1988 26 p In JAPANESE; ENGLISH summary
(DE89-901256; CRIE-T-87097) Avail: NTIS (US Sales Only) HC A03/MF A01

From measured results of lightning electromagnetic wave forms, the electromagnetic wave forms in winter season were classified, wave propagation under the thunder cloud was clarified and a countermeasure of direction finder (DF) singularity was described. Typical electromagnetic wave forms are one shot signal of positive polarity and bi-polar shot, and each of them is about a half. Sawteeth-like electromagnetic wave forms of negative polar lightning in summer are found smaller and the rate is only about 13 percent. Return stroke can appear immediately after bi-polar shot of shallow generation period. Received signal is sometimes larger from the distant lightning and smaller from the near lightning. Cause of DF singularity as self-discharge from the top of antenna was clarified and effectiveness of the loop antenna was identified. Electromagnetic wave forms of lightning triggered by a rocket were measured to confirm that some lightnings in winter cannot be judged as lightning by LLS, and that wave propagation under the thunder cloud is inhomogeneous. DOE

N90-15568# Air Force Inst. of Tech., Wright-Patterson AFB, OH.
APPLICATION OF A MASS-CONSISTENT WIND MODEL TO CHINOOK WINDSTORMS M.S. Thesis - San Jose State Univ.
Neil J. Muranaka Jun. 1988 105 p Sponsored in part by Murdock Charitable Trust, Vancouver, WA
(AD-A213622; AFIT/CI/CIA-88-231) Avail: NTIS HC A06/MF A01 CSCL 04/2

The applicability of a simple objective analysis technique on a personal computer to determine the detailed distribution of surface winds during strong downslope windstorms was examined. A 3-D, mass-consistent, diagnostic wind flow model applicable to complex terrain (COMPLEX) was modified to analyze surface wind fields for two severe chinook windstorms in southern Alberta. Realistic results were produced in the case study analyses where maximum winds followed the position of the hydrostatic wave trough, with the highest model wind speeds produced when the wave trough was closest to the mountains. Problems caused by the assumed 2-D wave structure included unrealistic changes in wind direction at some boundary points where the model flow surfaces passed beneath the terrain surface. Similarly, the intersection of flow surfaces with the terrain occasionally caused wind speed maxima to occur between, rather than over, hilltops as normally observed. The most significant error was found at the base of the terrain slope where windspeeds were underestimated as the hydrostatic wave trough was moved away from the mountains. Recommended improvements include the use of a hydraulic jump-like flow field in place of the hydrostatic wave perturbation in the model flow surfaces, and a more realistic treatment of the neutral boundary layer. GRA

N90-15569# Air Force Inst. of Tech., Wright-Patterson AFB, OH.
PRECIPITATION DISTRIBUTIONS ASSOCIATED WITH CYCLONES ORIGINATING OVER THE GULF OF MEXICO AND SURROUNDING COASTAL REGIONS M.S. Thesis
David I. Knapp 1988 109 p
(AD-A213644; AFIT/CI/CIA-88-229) Avail: NTIS HC A06/MF A01 CSCL 04/2

An investigation of the evolution of precipitation patterns associated with intensity and movement of winter surface lows across the southeast United States was undertaken. A 24-year climatology (1960 to 1983) of the 66 storms producing wide areas

of precipitation totals in excess of 25 mm revealed three dominant storm tracks. Six-hour totals of hourly precipitation data were objectively analyzed and contoured. Grid point values were extracted from the contour charts and compiled for all storms plotted along each track. Mean precipitation distribution charts and frequency of occurrence charts (for specified amounts) revealed the evolving precipitation field surrounding storms in each track. Precipitation maxima for storms tracking from the Gulf of Mexico to the Ohio Valley were found to extend across the Appalachians to the Atlantic coast, best explained by Miller's (1946) Type B cyclones and found to have occurred in 5 of the 12 cyclones following this inland track. Precipitation patterns for storms tracking along the Gulf coast across the Florida panhandle to the Atlantic coast suggest that the Atlantic Ocean joins the Gulf of Mexico as a second moisture source. The central Gulf coast area tended to receive the brunt of the precipitation from these lows. Multiple linear regression equations revealed the importance of storm longitude, surface geostrophic relative vorticity, and surface central pressure for forecasting various precipitation parameters. GRA

N90-15570# Naval Ocean Systems Center, San Diego, CA.
SPECIFICATION FOR EVAPORATION DUCT HEIGHT CALCULATIONS Final Report, Oct. 1988 - Jun. 1989
Richard A. Paulus Jul. 1989 34 p
(AD-A213841; NOSC/TD-1596) Avail: NTIS HC A03/MF A01 CSCL 04/2

The propagation of microwaves at altitudes close to the surface of the sea depends upon the refractive structure in the first few tens of meters. This height interval is called the atmospheric surface layer and is usually dominated by mechanical and buoyant turbulence. The average profile of wind temperature, humidity, or any scalar is determined by the turbulent motions. Roll presents an overview of the wind, temperature, and moisture fields in the first few meters above the sea surface. Meteorological measurements to directly determine these profiles in the surface layer over the ocean are quite difficult, semiempirical relationships between the profiles and the fluxes of momentum, heat, and moisture were developed. GRA

N90-15571# District of Columbia Univ., Washington, DC. Dept. of Mechanical Engineering.
FURTHER RESEARCH ON DYNAMICS OF MARINE ATMOSPHERES IN TROPICAL CYCLONES Final Technical Report
Joseph Chi Sep. 1989 60 p
(Contract N00014-84-K-0610)
(AD-A213882) Avail: NTIS HC A04/MF A01 CSCL 04/2

Basic research was undertaken on dynamics of marine atmospheres in tropical cyclones with an objective of improving understanding of turbulence in cyclone vortices and efficiency of computer simulation for transfer of heat, moisture and momentum in marine planetary boundary layers of tropical cyclones. For this objective, the following four phase of effort were performed: Develop a mathematical model, using the second order turbulent closure equations, for simulating planetary boundary layers of tropical cyclones over the sea surface; calculate velocity, enthalpy and moisture distributions in planetary boundary layers of tropical cyclones over the sea surface; develop and instrument a laboratory vortex chamber for measuring the air/water interface turbulence and heat, moisture and momentum transfer; and develop a graphics-oriented interactive finite-element compute model to simulate transfer of heat, moisture and momentum in marine planetary boundary layers of tropical cyclones. GRA

N90-15572# Chemical Research and Development Center, Aberdeen Proving Ground, MD.
ANOMALOUS ABSORPTION BY ATMOSPHERIC WATER VAPOR AND STABILIZED WATER FOGS IN THE INFRARED AND CM-WAVE REGIONS Technical Report, Jan. 1978 - Dec. 1982
Hugh R. Carlon Oct. 1989 22 p
(DA Proj. 1L1-61101-A-91A)
(AD-A214202; CRDEC-TR-111) Avail: NTIS HC A02/MF A01 CSCL 04/2

Measurements of anomalous or excessive absorption by atmospheric water vapor, i.e., absorption in excess of water monomer absorption and droplet scattering predictions, are analyzed for the infrared and 5-17/cm regions. Both fair weather and fog data are considered. It is found that observations in both spectral regions can be explained by clustering (hydrogen bonding) of approx. .001 of vapor molecules. The development leads to several tentative conclusions: (1) equilibrium cluster populations (and maximum absorption) are only attained for vapor in contact with liquid water; (2) the clusters are formed by evaporation, are large, and cannot be modeled by Boltzmann statistics; (3) cluster modes can account for unexplained spectral features at 5 to 17/cm; (4) excessive absorption both in the infrared and 5 to 17/cm regions probably can be explained by the same cluster species. In the appendix, the visible and infrared optical properties of evaporation stabilized water fogs also are considered. Evaporation of artificial water fogs can be retarded by the application of coatings of long-chain fatty alcohols to the droplets during generation. Measurements are described, and droplet diameters and mass extinction coefficients are reported for water fogs coated with cetyl alcohol (1-hexadecanol) from a commercial generator. GRA

N90-15573# Air Force Systems Command, Wright-Patterson AFB, OH. Foreign Technology Div.
FRONTAL CLOUDS AND FLIGHT CONDITIONS IN THEM
A. M. Baranov 8 Sep. 1989 10 p Transl. into ENGLISH from Frontalnyye Oblaka i Isloviya Poletov, v. Nikh, Leningrad (USSR), 1964 p 236-238
(AD-A214250; FTD-ID(RS)T-0793-89) Avail: NTIS HC A02/MF A01 CSCL 04/2

An outline of the contents of a book is given. Part 1 includes chapters on three-dimensional structure of frontal clouds. Part 2 includes chapters on meteorological flight conditions in frontal clouds. GRA

N90-15574# Washington Univ., Seattle. Dept. of Atmospheric Sciences.
GLOBAL DISTRIBUTION OF TOTAL CLOUD COVER AND CLOUD TYPE AMOUNTS OVER THE OCEAN
Stephen G. Warren, Carole J. Hahn, Julius London, Robert M. Chervin, and Roy L. Jenne (National Center for Atmospheric Research, Boulder, CO.) Dec. 1988 305 p Sponsored by DOE, Washington; National Center for Atmospheric Research, Boulder, CO and NSF, Washington, DC
(DE90-003187; DOE/ER-0406; NCAR/TN-317-STR) Avail: NTIS HC A14/MF A02

This is the fourth of a series of atlases to result from a study of the global cloud distribution from ground-based observations. The first two atlases (NCAR/TN-201+STR and NCAR/TN-241+STR) described the frequency of occurrence of each cloud type and the co-occurrence of different types, but included no information about cloud amounts. The third atlas (NCAR/TN-273+STR) described, for the land areas of the earth, the average total cloud cover and the amounts of each cloud type, and their geographical, diurnal, seasonal, and interannual variations, as well as the average base heights of the low clouds. The present atlas does the same for the ocean areas of the earth. DOE

N90-15044# Technische Univ., Brunswick (Germany, F.R.). Inst. of Guidance and Control.
WIND SHEAR MODELS FOR AIRCRAFT HAZARD INVESTIGATION
Manfred Swolinsky *In* AGARD, Flight in Adverse Environmental Conditions Sep. 1989 17 p (For primary document see N90-15041 07-01)
Copyright Avail: NTIS HC A17/MF A03; Non-NATO Nationals requests available only from AGARD/Scientific Publications Executive

N90-15045*# National Aeronautics and Space Administration. Ames Research Center, Moffett Field, CA.
ANALYSIS OF SEVERE ATMOSPHERIC DISTURBANCES FROM AIRLINE FLIGHT RECORDS
R. C. Wingrove, R. E. Bach, Jr., and T. A. Schultz *In* AGARD, Flight in Adverse Environmental Conditions Sep. 1989 7 p Previously announced as N89-25977 (For primary document see N90-15041 07-01)
Copyright Avail: NTIS HC A17/MF A03; Non-NATO Nationals requests available only from AGARD/Scientific Publications Executive CSCL 04B

N90-15046# Aerodata Flugmesstechnik G.m.b.H., Brunswick (Germany, F.R.).
SYSTEMS FOR AIRBORNE WIND AND TURBULENCE MEASUREMENT
Peter Voersmann *In* AGARD, Flight in Adverse Environmental Conditions Sep. 1989 12 p (For primary document see N90-15041 07-01)
Copyright Avail: NTIS HC A17/MF A03; Non-NATO Nationals requests available only from AGARD/Scientific Publications Executive

N90-15049# Royal Aircraft Establishment, Bedford (England).
CLASSIFICATION OF WINDSHEAR SEVERITY
A. A. Woodfield *In* AGARD, Flight in Adverse Environmental Conditions Sep. 1989 13 p (For primary document see N90-15041 07-01)
Copyright Avail: NTIS HC A17/MF A03; Non-NATO Nationals requests available only from AGARD/Scientific Publications Executive

N90-15052# National Aeronautical Establishment, Ottawa (Ontario). Flight Research Lab.
ADVERSE WEATHER OPERATIONS DURING THE CANADIAN ATLANTIC STORMS PROGRAM
J. I. MacPherson and G. A. Isaac (Atmospheric Environment Service, Downsview, Ontario) *In* AGARD, Flight in Adverse Environmental Conditions Sep. 1989 13 p (For primary document see N90-15041 07-01)
Copyright Avail: NTIS HC A17/MF A03; Non-NATO Nationals requests available only from AGARD/Scientific Publications Executive

N90-15059# Technische Univ., Hanover (Germany, F.R.). Inst. fuer Meteorologie und Klimatologie.
MEASUREMENTS OF HORIZONTAL VISIBILITY IN THE LOWEST 300 m OVER NORTHERN GERMANY
R. Roth and A. R. Siemer *In* AGARD, Flight in Adverse Environmental Conditions Sep. 1989 10 p (For primary document see N90-15041 07-01)
Copyright Avail: NTIS HC A17/MF A03; Non-NATO Nationals requests available only from AGARD/Scientific Publications Executive

48 OCEANOGRAPHY

Includes biological, dynamic, and physical oceanography; and marine resources.

For related information see also *43 Earth Resources and Remote Sensing.*

N90-15575 Princeton Univ., NJ.
DYNAMICS OF MID-OCEAN RIDGE SYSTEMS Ph.D. Thesis
Yongshun Chen 1989 233 p
Avail: Univ. Microfilms Order No. DA8920417

Models of the thermal and mechanical properties of spreading centers and transform faults are developed. The resistance force at oceanic transform faults is estimated based on a model of a brittle plate with strength increasing with depth over a ductile fluid. A thermal model of the transform fault is developed which includes the effects of the lateral heat conduction across the fault and the shear heating along the fault. This raises the temperature along the fault, consistent with the observed shallow focal depths of major transform fault earthquakes. The increase in shear traction with depth within the brittle part of the transform fault generates a net twisting moment along the fault. The observed inside corner uplift can be partly explained by flexure of the oceanic plate due to the twisting moment of this traction along the fault. A model of the mid-ocean ridge axis based on a weaker crust over a strong mantle is developed. This model can produce the observed transition of large rift valley, rough topography, and large gravity variations for slow spreading rates to no-rift valley, smooth topography, small gravity variations for fast spreading rates. The essential premise is that a low ductile strength chamber (decoupling chamber) exists beneath the ridge axis in the lower crust, and its size relative to the size of the failure zone within the brittle plate determines the first order axial topography (whether or not an axial rift valley exists) and the style of the local isostatic compensation. A finite element program was implemented to compute both the temperature and the flow field of the oceanic lithosphere using a nonlinear rheology. The numerical results show the importance of the oceanic crust in controlling the nature of the axial topography and gravity variations for different spreading rates. Dissert. Abstr.

N90-15576# California Univ., Santa Barbara. Dept. of Geological Sciences.
EVOLUTION OF OVERLAPPING SPREADING CENTERS: A SEA MARK 2 INVESTIGATION Final Technical Report
K. C. Macdonald and P. J. Fox (Rhode Island Univ., Narragansett.) 1988 15 p
(Contract N00014-85-K-0649)
(AD-A214278) Avail: NTIS HC A03/MF A01 CSCL 08/3

The long term goal is to further the understanding of mid-ocean ridge processes and their relation to seafloor morphology. With recent advances in high resolution sonar swath mapping technology the detection of discontinuities currently along the spread axis and to trace related features which were rafted off onto the ridge flanks was made easier. The temporal and spatial interactions between the processes of volcanism and tectonism which shape the seafloor were investigated. Study of these ridge segmentation processes should tell a great deal about the timing and spacing of major melting events in the upper mantle and their relation to axial magma chamber. During a major Sea Marc 2 expedition in May to June 1987 all the overlapping spreading centers (OSC's) north of the equator between 8 and 18 degrees N and all their related off-axis scars were mapped. The main results include: The finding that OSC's leave abandoned ridge tips and fossil overlap basins as distinctive scars on the flanks of the EPR, disrupting a significant amount (more than 20 percent) of the normal seafloor fabric; Traces of the discordant zones indicate that OSC's have migrated both to the north and to the south, not necessarily following pole of opening or hot spot traces; and large OSC's can persist for 0.5 to 2.0 my whereas small offset OSC's are transient, persisting less than 10,000 years. The character of the axial summit graben can be used to predict the presence and size of the underlying crustal magma chamber. GRA

51 LIFE SCIENCES (GENERAL)

N90-15577*# National Aeronautics and Space Administration. Ames Research Center, Moffett Field, CA.
EFFECT OF CONTRAST ON THE PERCEPTION OF DIRECTION OF A MOVING PATTERN
L. S. Stone, A. B. Watson, and J. B. Mulligan Dec. 1989 30 p
(NASA-TM-102234; A-89242; NAS 1.15:102234) Avail: NTIS HC A03/MF A01 CSCL 06C

A series of experiments examining the effect of contrast on the perception of moving plaids was performed to test the hypothesis that the human visual system determines the direction of a moving plaid in a two-staged process: decomposition into component motion followed by application of the intersection-

of-constraints rule. Although there is recent evidence that the first tenet of the hypothesis is correct, i.e., that plaid motion is initially decomposed into the motion of the individual grating components, the nature of the second-stage combination rule has not yet been established. It was found that when the gratings within the plaid are of different contrast the preceived direction is not predicted by the intersection-of-constraints rule. There is a strong (up to 20 deg) bias in the direction of the higher-contrast grating. A revised model, which incorporates a contrast-dependent weighting of perceived grating speed as observed for one-dimensional patterns, can quantitatively predict most of the results. The results are then discussed in the context of various models of human visual motion processing and of physiological responses of neurons in the primate visual system.
Author

N90-15578# Pacific Northwest Lab., Richland, WA.
INTRODUCTION TO EXTREMELY-LOW-FREQUENCY ELECTRIC AND MAGNETIC FIELDS
T. S. Tenforde Jul. 1989 6 p Presented at the 8th Annual American Statistical Association Conference on Radiation and Health: Health Effects of Electric and Magnetic Fields: Statistical Support for Research Strategies, Cooper Mountain, CO, 9-13 Jul. 1989
(Contract DE-AC06-76RL-01830)
(DE90-002662; PNL-SA-17179; CONF-8907166-1) Avail: NTIS HC A02/MF A01

The interaction with living systems of electromagnetic fields in the extremely-low-frequency (ELF) range below 300 Hz are summarized briefly. In materials with the electrical and magnetic properties of living tissues, these fields have a long wavelength (5000 m) and skin depth (150 m). As a consequence, in their interactions with humans and other living organisms ELF fields behave as though they are composed of independent electric and magnetic components of an ELF field is commonly referred to as the quasi-static approximation, which permits the radiating properties of the field to be neglected in describing its interaction with living organisms. The electric and magnetic components of an ELF field have several distinctly different features in their interactions with humans and other living organisms. First, the electrical conductivity of tissue is approximately 14 to 15 orders of magnitude greater than that of air at ELF electric fields. Consequently, the body behaves like a good electrical conductor in ELF electric fields. As a result, an electrical charge is developed on the surface of a living object in an external ELF field, but the electric field penetrates into the body only to a very limited extent. DOE

52 AEROSPACE MEDICINE

Includes physiological factors; biological effects of radiation; and effects of weightlessness on man and animals.

N90-15579# JIL Systems, Inc., Arlington, VA.
DOCTORD DATABASE SYSTEM USER'S GUIDE, JUNE 1989: dBASE 3 PLUS PHYSICIAN/(PART B MEDICARE): PERSONAL COMPUTER REFERENCE SYSTEM AND USER'S GUIDE
Judith Stevenson, Jim Melendez, and Julie Walton Jun. 1989 151 p
(Contract HCFA-500-87-0005)
(PB90-100181; HCFA/DF/DK-90/001A) Avail: NTIS HC A08/MF A01 CSCL 05B

The DOCTORD System is based on a dBase 3 PLUS database which contains information on completed and active physician and other Part B studies, projects and reports sponsored by ORD. Its function is to act as a reference tool to assist management is accessing past studies and tracing present ones. The DOCTORD System is run by a menu-driven applications program, which allows the user to perform such tasks as appending new records, searching for specific data and printing out abstracts and indexes. The program is designed to make using the system as easy as possible; the manual provides detailed instructions and examples to illustrate how the system should be operated. GRA

N90-15580# Los Alamos National Lab., NM. Center for Nonlinear Studies.
MONITORING CHAOS OF CARDIAC RHYTHMS
Gottfried Mayer-Kress 1989 10 p Presented at BIOTECH USA: 6th Annual Industry Conference and Exhibition, San Francisco, CA, 2-4 Oct. 1989
(Contract W-7405-eng-36)
(DE90-000692; LA-UR-89-3192; CONF-8910223-1) Avail: NTIS HC A02/MF A01

Chaos theory provides a new paradigm in monitoring complexity changes in heart rate variability. Even in cases where the spectral analysis only shows broad band characteristics, estimations of dimensional complexity parameters can show quantitative changes in the degree of chaos present in the interbeat interval dynamics. We introduce the concept of dimensional complexity as a dynamical monitoring parameter and discuss its properties in connection with control data and data taken during cardiac arrest. Whereas dimensional complexity provides a quantitative indicator of overall chaotic behavior, recurrence plots allow direct visualization of recurrences in arbitrary high dimensional pattern-space. In combination these two methods from non-linear dynamics exemplify a new approach in the problem of heart rate monitoring and identification of precursors of cardiac arrest. Finally we mention a new method of chaotic control, by which selective and highly effective perturbations of nonlinear dynamical systems could be used for improved pacing patterns. DOE

N90-15581# Krug International, San Antonio, TX. Technology Services Div.
POTENTIAL FOR REDUCTION OF DECOMPRESSION SICKNESS BY PREBREATHING WITH 100 PERCENT OXYGEN WHILE EXERCISING Interim Report
James T. Webb, Gene A. Dixon (School of Aerospace Medicine, Brooks AFB, TX.), and Janet F. Wiegman 1989 7 p
(Contract F33615-85-C-4503)
(AD-A213449; USAFSAM-JA-89-21) Avail: NTIS HC A02/MF A01 CSCL 06/10

Exercise performed for at least 30 min while prebreathing 100 percent oxygen prior to decompression was reported to increase efficiency of denitrogenation by 100 to 500 percent. The incidence of decompression sickness following such a prebreathe was decreased by 50 percent compared to resting prebreathe. If prebreathing with exercise is to have an operational application, it must be brief, it must significantly reduce standard prebreathing times, it must not create excess fatigue, and it must use exercise equipment compatible with aerospace operations. This article provides background and recommends parameters for a test to determine the operational feasibility of prebreathing with exercise.
GRA

N90-15582# Rockefeller Univ., New York, NY.
CARBOXYALKYLATED HEMOGLOBIN AS A POTENTIAL BLOOD SUBSTITUTE Annual Report, 1 Sep. 1988 - 31 Aug. 1989
James M. Manning 20 Sep. 1989 20 p
(Contract DAMD17-88-C-8169)
(AD-A213886) Avail: NTIS HC A02/MF A01 CSCL 06/1

Emphasis was on two major objectives. First, the properties were characterized of the carboxymethyl derivative of hemoglobin to determine whether they are consistent with its possible future use as a blood substitute. Evidence was found that this derivative is analogous to that formed in the reaction of hemoglobin with CO2. This natural product results in a very low oxygen affinity for hemoglobin, which is a very desirable property for a blood substitute. The second major objective of the research was to crosslink this hemoglobin derivative in a manner that will maintain the essential functional properties of hemoglobin. GRA

N90-15583# Wright State Univ., Dayton, OH.
USE OF LOWER BODY NEGATIVE PRESSURE AS A COUNTERMEASURE TO NEGATIVE Gz ACCELERATION Final Report, Dec. 1987 - Dec. 1989
Bradley Gerard Beck and Lloyd D. Tripp, Jr. (Aerospace Medical Research Labs., Wright-Patterson AFB, OH.) Apr. 1989 108 p (AF Proj. 7231)
(AD-A213927; AAMRL-TR-89-025) Avail: NTIS HC A06/MF A01 CSCL 06/10

Lower body negative pressure (LBNP) was used at levels of 0, -50, and -100 torr as a countermeasure prior to centrifuge exposures of subjects to negative Gz at levels of -1.0, -1.5, and -2.0. EKG, echocardiographic, and subjective data were gathered. Physiological variables for end diastolic volume (EDV), end systolic volume (ESV), stroke volume (SV), heart rate (HR), and cardiac output (CO) were obtained at baseline values, then percent of baseline after LBNP was started, then during the -Gz exposure plateau. ANOVA revealed that the LBNP main effects were significant for EDV, ESV, SV, and HR (p is less than .0027). The negative Gz main effects were not significant for EDV, ESV, and SV (p is greater than .3821), but were significant for HR and CO (p is less than .0001). Paired T-tests showed the LBNP of -50 and -100 torr lessened the HR changes during -Gz as compared to 0 LBNP (p is less than .0199). LBNP retained its effects for EDV, ESV, HR, and CO (p is less than .0017). The subjective results showed pairwise differences ($p = .0312$) in ratings between -2.0 Gz exposure unprotected and -2.0 Gz protected for facial congestion, sinus pain, and degree of comfort. Overall rankings of exposures also demonstrated that LBNP protected against negative Gz effects at $p = .028$. GRA

53 BEHAVIORAL SCIENCES

Includes psychological factors; individual and group behavior; crew training and evaluation; and psychiatric research.

N90-15584# Chief of Naval Education and Training Support, Pensacola, FL.
HUMAN BEHAVIOR
May 1989 163 p
(PB90-780008; NAVEDTRA-10058-C1) Avail: NTIS HC A08/MF A01 CSCL 05I

A basic presentation is given of human behavior theory and utilization techniques as applied to basic assumptions about human behavior and motivation, the influence of perception, the effects of stress and conflict on human reactions, the formation and influence of attitudes, communication, problem solving, and teaching learning. Human behavior is designed to serve as a basic course on leadership concepts and principles for senior enlisted personnel, especially those in paygrades E-6, E-7, E-8, and E-9, who spend most of their time in supervisory duties. Author

N90-15585# Idaho National Engineering Lab., Idaho Falls.
MODEL FOR MEASURING COMPLEX PERFORMANCE IN AN AVIATION ENVIRONMENT
Heidi Ann Hahn 1988 5 p Presented at the 32nd Human Factors Society Annual Meeting, Anaheim, CA, 24-28 Oct. 1988 Previously announced in IAA as A89-31648 Sponsored in part by AF
(Contract DE-AC07-76ID-01570)
(DE90-002055; EGG-M-88271; CONF-881058-5) Avail: NTIS HC A01/MF A01

An experiment was conducted to identify models of pilot performance through the attainment and analysis of concurrent verbal protocols. Sixteen models were identified. Novice and expert pilots differed with respect to the models they used. Models were correlated to performance, particularly in the case of expert subjects. Models were not correlated to performance shaping factors (i.e., workload). DOE

N90-15586# Edgerton, Germeshausen and Grier, Inc., Idaho Falls, ID.
WHERE TO FROM HERE. FUTURE APPLICATIONS OF MENTAL MODELS OF COMPLEX PERFORMANCE
Heidi Ann Hahn, William R. Nelson, and Harold S. Blackman 1988 2 p Presented at the Human Factors Society Annual Meeting, Anaheim, CA, 24-28 Oct. 1988
(Contract DE-AC07-76ID-01570)
(DE90-002091; EGG-M-88288; CONF-881058-7) Avail: NTIS HC A02/MF A01

The purpose of this paper is to raise issues for discussion regarding the applications of mental models in the study of complex performance. Applications for training, expert systems and decision aids, job selection, workstation design, and other complex environments are considered. DOE

N90-15587# Maryland Univ., College Park. Center for Automation Research.
VISION IN DYNAMIC ENVIRONMENTS Final Report
Azriel Rosenfeld 15 Aug. 1989 27 p
(Contract DAAB07-86-K-F073)
(AD-A213434) Avail: NTIS HC A03/MF A01 CSCL 23/3

Research conducted on the contract was primarily concerned with real-time, three-dimensional computer vision and image understanding. Abstracts include: Tracing Finite Motions without Correspondence; Group Theoretical Methods in Image Understanding; Interpreting Aerial Photographs by Segmentation and Search; Straight Line Fitting in a Noisy Image; Calibration of a Stereo System with Small Relative Angles; Cylindrical Shape from Contour and Shading without Knowledge of Lighting Conditions or Surface Albedo; A Robust Algorithm for Determining the Translation of a Rigidly Moving Surface without Correspondence, for Robotics Applications; Finding Motion Parameters from Spherical Flow Fields (Or the Advantages of Having Eyes in the Back of your Head). GRA

N90-15588# Washington Univ., Saint Louis, MO.
THE ROLE OF ATTENTION IN VISUAL PROCESSING Progress Report
Gordon L. Shulman 1989 4 p
(Contract N00014-89-J-1426)
(AD-A214158) Avail: NTIS HC A02/MF A01 CSCL 06/4

This is the first reported instance in which attention modulates the strength of a visual aftereffect and supports the basic idea underlying the grant: that one can use adaptation phenomena to relate the action of attention to specific visual mechanisms. If one views an object on a monitor whose direction of rotation is specified through perspective, then a subsequent object presented without perspective, whose direction of rotation is normally ambiguous, will be seen to rotate in the opposite direction. Adapting to the unambiguous stimulus has desensitized mechanisms specific for a particular direction of rotation in depth. Data indicating that the extent to which this adaption process occurs depends on the extent to which the adapting stimulus is attended. This result suggests that the mechanisms that are being adapted in these experiments are also capable of being attentionally influenced. GRA

N90-15589# Rochester Univ., NY. Dept. of Computer Science.
AN ARCHITECTURAL MODEL OF VISUAL MOTION UNDERSTANDING Ph.D. Thesis
Thomas Jeremy Olson Aug. 1989 151 p
(Contracts N00014-84-K-0655; DACA76-85-C-0001)
(AD-A214327; TR-305) Avail: NTIS HC A08/MF A01 CSCL 12/9

The past few years have seen an explosion of interest in the recovery and use of visual motion information by biological and machine vision systems. In the area of computer vision, a variety of algorithms were developed for extracting various types of motion information from images. The central claim is that many puzzling aspects of motion perception can be understood by assuming a particular architecture for the human motion processing system. The architecture consists of three functional units or subsystems.

The first or low level subsystem computes simple mathematical properties of the visual signal. It is entirely bottom-up, and prone to error when its implicit assumptions are violated. The intermediate-level subsystem combines the low-level system's output with world knowledge, segmentation information and other inputs to construct a representation of the world in terms of primitive forms and their trajectories. In order to compute the trajectories of primitive shapes it is necessary to design mechanisms for handling time and Gestalt grouping effects in connectionist networks. Solutions to these problems are developed and used to construct a network that interprets continuous and apparent motion stimuli in a limited domain. Simulation results show that its interpretations are in qualitative agreement with human perception. GRA

54 MAN/SYSTEM TECHNOLOGY AND LIFE SUPPORT

Includes human engineering; biotechnology; and space suits and protective clothing.

For related information see also *16 Space Transportation.*

N90-15590 Maryland Univ., College Park.
THE APPLICATION OF OPTIMAL CONTROL THEORY FOR ANALYSIS OF HUMAN JUMPING AND PEDALING Ph.D. Thesis
Eunsup Sim 1988 204 p
Avail: Univ. Microfilms Order No. DA8912351

Human jumping and pedaling are analyzed using optimal control theory. The human body is mechanically modeled as 3 rigid links with 8 group muscles for each leg and 1 rigid link for the upper body. The jumps which maximize the vertical height reached by the subject's center of mass while jumping from an initial squat posture or an erect posture are studied. The pedaling process is a bicycle-rider system. The rider's hips are fixed on the saddle, the feet are rigidly attached to the pedals and the upper body is stationary. So, the process is modeled as 2-five bar linkages moving in the plane, fixed at the hip joint and at a crank axis. The performance criterion is minimization of the time required for one cycle of the crank. The system is described mathematically by nonlinear differential equations which are linear in the controls. The system equations consist of limb mechanics, muscle dynamics and muscle activation dynamics. The optimal control is assumed to be of bang-bang type with a finite number of switchings. A new computation algorithm for bang-bang control of these highly nonlinear and large scale dynamic systems is developed. The controls are determined by using the projection of the gradient of the cost function with respect to the control input switching times on the control Hamiltonian function of the system. The controls maximize this Hamiltonian function, holding the state and costate trajectories fixed. An optimization algorithm to get the best values for unknown initial state variables on a constraint set defined by linear equalities and inequalities is developed. The necessary conditions for optimal control of a redundant dynamic system and a reduced dynamic system to represent the pedaling process are developed. This along with the algorithm for bang-bang control is used to obtain the optimal control inputs of the pedaling process. The computational results for human jumping are compared with experimental results. Dissert. Abstr.

N90-15591*# Massachusetts Inst. of Tech., Cambridge. Dept. of Applied Biological Sciences.
UTILIZATION OF NON-CONVENTIONAL SYSTEMS FOR CONVERSION OF BIOMASS TO FOOD COMPONENTS
M. Karel and Z. Nakhost Dec. 1989 37 p
(Contract NCC2-231)
(NASA-CR-177545; NAS 1.26:177545) Avail: NTIS HC A03/MF A01 CSCL 06F

Described here is work accomplished in investigating the potential use of micro-algae in yielding useful macronutrients for closed ecological life support systems in space habitats. Analysis of the chemical composition of the blue-green alga Synechoccus 6311 was done in the present work, and was compared to values found in previous work on the green algae Scenedesmus obliquus. Similar values were obtained for proteins, and lower values for nucleic acids and lipids. A second part of the work involved fabrication of food products containing various levels of incorporated algae (S. obliquus) proteins and/or lipids. Protein isolate was incorporated into a variety of food products such as bran muffins, fettuccine (spinach noodle imitation), and chocolate chip cookies. In the sensory analysis, the greenish color of the bran muffins and cookies was not found to be objectionable. The mild spinachy flavor was less detectable in chocolate chip cookies than in bran muffins. The color and taste of the algae noodles were found to be pleasant and compared well with commercially available spinach noodles. Author

N90-15592# Anacapa Sciences, Inc., Fort Rucker, AL.
DEVELOPMENT OF THE AH-64 DISPLAY SYMBOLOGY TRAINING MODULE Interim Report, Dec. 1986 - Apr. 1989
John W. Ruffner, Gary W. Coker, and Richard D. Weeter Aug. 1989 337 p
(Contract MDA903-87-C-0523)
(AD-A213456; ASI690-322-89; ARI-RN-89-41) Avail: NTIS HC A15/MF A02 CSCL 05/8

To become fully qualified in the AH-64A attack helicopter, a student aviator must learn to identify and interpret the individual symbols presented on the helicopter's visual displays and to interpret the information provided by groups of symbols. A training module for teaching aviators to identify and interpret the symbology used on the AH-64A visual displays is described. The training module, known as the Symbology Tutor, consists of an introductory section, a help system, and five lessons that provide instruction on the symbols contained in the AH-64A flight symbology set. The lessons cover symbols dealing with: (1) position and movement, (2) attitude and altitude, (3) heading and navigation, (4) cueing and reference, and (5) weapons usage. Each lesson is divided into a tutorial and a quiz. Storyboards were developed for each of the five lessons and are included in the appendixes. Computer programs were completed for the first two lessons. The completed portions of the Symbology Tutor is described and the required computer hardware is identified. GRA

N90-15593# Dynamics Research Corp., Wilmington, MA.
MANPRINT METHODS MONOGRAPH: AIDING THE DEVELOPMENT OF MANNED SYSTEM PERFORMANCE CRITERIA Final Report, Nov. 1986 - May 1987
Jonathan D. Kaplan Jun. 1989 269 p
(Contracts MDA903-86-C-0412; MDA903-86-C-0414; MDA903-86-C-0416)
(AD-A213543) Avail: NTIS HC A12/MF A01 CSCL 23/2

This monograph consists of three papers on a common subject: The development of complete, rigorous, and operationally measurable performance criteria for manned systems. Each of these papers presents a concept for building an aiding method. The U.S. Army Research Institute for the Behavioral and Social Sciences began the program to develop methods to integrate available operations and maintenance personnel with hardware and software. The first stage of this process was to develop three alternate, competitive concepts for each method. The three concept papers in this monograph were written in response to requirements for a method to develop rigorous and ultimately measurable performance criteria. These criteria would enable hardware and software designers to better understand what a manned, fully integrated system would have to do to achieve operations and maintenance success. Success would be described in terms of required performance levels of operations and maintenance tasks under specified conditions. The concept papers written in response to this requirement have three significantly different focuses and bring powerful but different approaches to the problem of developing rigorous and meaningful performance criteria. Ultimately, the ARI study advisory group decided to implement the concept proposed by Micro-Analysis and Design. GRA

N90-15594# Dayton Univ., OH.
COCKPIT RESOURCE MANAGEMENT: A SELECTED ANNOTATED BIBLIOGRAPHY Interim Report, Jul. 1987 - May 1989
H. Kingsley Povenmire Oct. 1989 52 p
(Contracts F33615-84-C-0066; F33615-87-C-0012)
(AD-A214272; UDR-TR-88-104; AFHRL-TR-89-22) Avail: NTIS HC A04/MF A01 CSCL 05/9

The concepts of cockpit resource management (CRM) emerged during a 1979 study by the National Aeronautics and Space Administration which was intended to study the interaction of pilot workload with errors. During this study, researchers began to realize that the stereo-typical airline captain who can do no wrong was not feasible in today's complex jet aircraft. Several accidents and incidents may be traced directly to improper crew management or lack of coordination by the crew. NASA began to explore the feasibility of teaching generic management principles to flight crews. Several training programs have been developed, and some significant research has been conducted which further defines optimum CRM training and practice. Line-Oriented Flight Training (LOFT) is a training method developed originally to relate simulator training more closely to actual line flying. Airlines found that they could enhance the sharing of experiences by simulating an entire flight, complete with incidents experienced in the real world, rather than repeated malfunctions taken out of context. It is important to note that LOFT is often utilized by airlines and other simulator users without employing the principles of CRM. However, LOFT is a valuable tool in CRM training. This bibliography addresses current training practices, techniques which enhance crew coordination, and questions appropriate for systematic research. GRA

N90-15060# Army Aeromedical Research Lab., Fort Rucker, AL. Aviation Research and Development Activity.
IMAGING PROBABILITIES, GEOMETRY AND ERGONOMICS IN LIMITED VISIBILITY HELICOPTER OPERATIONS
Robert H. Wright *In* AGARD, Flight in Adverse Environmental Conditions Sep. 1989 11 p (For primary document see N90-15041 07-01)
Copyright Avail: NTIS HC A17/MF A03; Non-NATO Nationals requests available only from AGARD/Scientific Publications Executive

55 SPACE BIOLOGY

Includes exobiology; planetary biology; and extraterrestrial life.

No abstracts in this category.

59 MATHEMATICAL AND COMPUTER SCIENCES (GENERAL)

N90-15595# Argonne National Lab., IL. Mathematics and Computer Science Div.
RESEARCH IN MATHEMATICS AND COMPUTER SCIENCE AT ARGONNE Research Activity Report, Jan. 1988 - Aug 1989
Gail W. Pieper Aug. 1989 70 p
(Contract W-31-109-eng-38)
(DE90-000975; ANL-89/12) Avail: NTIS HC A04/MF A01

The research activities in the Mathematics and Computer Science Division at Argonne National Laboratory for the period January 1988 - August 1989 are reviewed. A brief look at the MCS staff and the research facilities is given, and various projects are discussed which were performed in two major areas of research: analytical and numerical methods and advanced computing concepts. Projects funded by non-DOE sources are also discussed, and new technology transfer activities are described. Further information on division staff, visitors, workshops, and seminars is found in the appendices. DOE

60 COMPUTER OPERATIONS AND HARDWARE

Includes hardware for computer graphics, firmware, and data processing.

For components see *33 Electronics and Electrical Engineering.*

N90-15596# Fermi National Accelerator Lab., Batavia, IL.
DESIGNING MACHINES FOR LATTICE PHYSICS AND ALGORITHM INVESTIGATION
M. Fischler, R. Atac, A. Cook, J. Deppe, E. Eichten, I. Gaines, M. Gao, G. Hockney, D. Husby, and A. Kronfeld et al Oct. 1989 5 p Presented at the Lattice 1989 International Workshop, Isola di Capri, Italy, 18-21 Sep. 1989 Submitted for publication
(Contract DE-AC02-76CH-03000)
(DE90-003543; FNAL/C-89/220; CONF-8909249-2) Avail: NTIS HC A01/MF A01

Special-purpose computers are appropriate tools for the study of lattice gauge theory. While these machines deliver considerable processing power, it is also important to be able to program complex physics ideas and investigate algorithms on them. Features are examined that facilitate coding of physics problems, and flexibility in algorithms. Appropriate balances among power, memory, communications and I/O capabilities are presented. DOE

N90-15597# Lawrence Livermore National Lab., CA.
LLNL'S PLAN FOR A PROTOTYPE CIRCUIT SWITCH, A POTENTIAL GIGABIT LAN OF THE FUTURE
Paul R. Rupert Oct. 1989 7 p Presented at the Cray User's Group Conference, Los Angeles, CA, 24-28 Apr. 1989
(Contract W-7405-eng-48)
(DE90-003614; UCRL-101076-Rev-1; CONF-8904210-4-Rev-1)
Avail: NTIS HC A02/MF A01

LLNL's High Speed Communication project will prototype a communications system designed to foster distributed computing and to provide visualization from supercomputers to scientists and engineers. High quality graphics images require 24 MBits per frame and 750 MBits/sec for animation; it is fully anticipated that the next generation of Supercomputers will provide animated results for general users. Local visualization machines will be available for rendering and graphics manipulation, but visualization of meaningful physics will require communications of large blocks of computed results between Supercomputers and local devices. In addition to visualization, a distributed computing environment is being developed. The required transfer of data between supercomputers and other local mini-supers or special purpose floating point accelerators, will sorely tax the existing communications ability. Improved communications mechanisms will be necessary before distributed applications can become truly effective. The plans to demonstrate, through the use of a prototype system, data transmission at 800 MBits/sec per channel is described along with aggregate bandwidth growth that is linear with the number of connected users and computers. DOE

N90-15598# Massachusetts Inst. of Tech., Cambridge. Lab. for Computer Science.
TEMPORAL, PROCESSOR, AND SPATIAL LOCALITY IN MULTIPROCESSOR MEMORY REFERENCES
Anant Agarwal and Anoop Gupta Jun. 1989 22 p
(Contract N00014-87-K-0825)
(AD-A213790; MIT/LCS/TM-397) Avail: NTIS HC A03/MF A01 CSCL 12/6

The performance of cache-coherent multiprocessors is strongly influenced by locality in the memory reference behavior of parallel applications. While the notions of temporal and spatial locality in uniprocessor memory references are well understood, the

corresponding notions of locality in multiprocessors and their impact on multiprocessor cache behavior are not clear. A locality model suitable for multiprocessor cache evaluation is derived by viewing memory references as streams of processor identifiers directed at specific cache/memory blocks. This viewpoint differs from the traditional uniprocessor approach that uses streams of addresses to different blocks emanating from specific processors. The view here is based on the intuition that cache coherence traffic in multiprocessor is largely determined by the number of processors accessing a location, the frequency with which they access the location, and the sequence in which their accesses occur. The specific locations accessed by each processor, the time order of access to different locations, and the size of the working set play a smaller role in determining the cache coherence traffic, although they still influence intrinsic cache performance. Looking at traces from the viewpoint of a memory block leads to a new notion of reference locality for multiprocessors, called processor locality. The temporal, spatial, and processor locality in the memory reference patterns of three parallel applications is studied. Based on the observed locality, the expected cache behavior of the three applications is then reexamined. GRA

N90-15599# New Mexico State Univ., Las Cruces.
ARGOS (A RESEARCH GMMP OPERATING SYSTEM): OVERVIE W AND INTERFACES
Eric E. Johnson Aug. 1989 78 p Sponsored in part by AT and T Foundation
(Contract DAAL03-87-K-0106)
(AD-A213871; NMSU-ECE-89-007A; ARO-25173.20-EL) Avail: NTIS HC A05/MF A01 CSCL 12/6

An overview is presented of A Research GMMP Operating System (ARGOS) developed at the NMSU Parallel Architecture Research Laboratory for the prototype Virtual Port Memory multiprocessor. ARGOS is an initial attempt to realize the reliability and performance benefits expected of GMMP multiprocessors. After a review of GMMP architectures and the Virtual Port Memory machine, the structure and philosophy of ARGOS are presented, followed by interface-level descriptions of each of the system modules. Later reports will present detailed individual discussion of the implementations of these modules. GRA

N90-15600# Rochester Univ., NY. Dept. of Computer Science.
THE IMPLEMENTATION OF A COHERENT MEMORY ABSTRACTION ON A NUMA (NON-UNIFORM MEMORY ACCESS) MULTIPROCESSOR: EXPERIENCES WITH PLATINUM (PLATFORM FOR INVESTIGATING NON-UNIFORM MEMORY)
Alan L. Cox and Robert J. Fowler 6 May 1989 27 p Revised
(Contracts DACA76-85-C-0001; N00014-84-K-0655; NSF CCR-87-04492)
(AD-A213909; TR-263) Avail: NTIS HC A03/MF A01 CSCL 12/5

PLATINUM is an operating system kernel with a novel memory management system for Non-uniform Memory Access (NUMA) multiprocessor architectures. This memory management system implements a coherent memory abstraction. Coherent memory is uniformly accessible from all processors in the system. When used by applications coded with appropriate programming styles it appears to be nearly as fast as local physical memory and it reduces memory contention. Coherent memory makes programming NUMA multiprocessors easier for the user while attaining a level of performance comparable with hand-tuned programs. The design of the PLATINUM memory management system is described with emphasis on the implementation of coherent memory and the factors that affect its performance. The cost is measured of basic operations implementing coherent memory. Also measured is the performance of a set of application programs running on PLATINUM. Finally, the interaction between architecture and the coherent memory system is measured. Platinum currently runs on the BBN Butterfly Plys (TM) Multiprocessor. GRA

N90-15601# Rochester Univ., NY. Dept. of Computer Science.
MEMORY MANAGEMENT FOR LARGE-SCALE NUMA (NON-UNIFORM MEMORY ACCESS) MULTIPROCESSORS
Thomas J. LeBlanc, Brian D. Marsh, and Michael L. Scott Mar. 1989 24 p
(Contract DACA76-85-C-0001; NSF DCR-83-20136)
(AD-A213910; TR-311) Avail: NTIS HC A02/MF A01 CSCL 12/6

Large scale shared memory multiprocessors such as the BBN Butterfly and IBM RP3 introduce a new level in the memory hierarchy; multiple physical memories with different memory access times. An operating system for these NUMA (Non-Uniform Memory Access) multiprocessors should provide traditional virtual memory management, facilitate dynamic and widespread memory sharing, and minimize the apparent disparity between local and nonlocal memory. In addition, the implementation must be scalable to configurations with hundreds or thousands of processors. Memory management in the PSYCHE multiprocessor operating system is described. The PSYCHE kernel manages a multi-level memory hierarchy consisting of local memory, nonlocal memory, and backing store. Local memory stores private data and serves as a cache for shared data; nonlocal memory stores shared data and serves as a disk cache. The system structure isolates the policies and mechanisms that manage different layers in the memory hierarchy, so that customized data structures and policies can be constructed for each layer. Local memory management policies are implemented using mechanisms that are independent of the architectural configuration; global policies are implemented using multiple processes that increase in number as the architecture scales. PSYCHE currently runs on the BBN Butterfly Plus multiprocessor. GRA

N90-15602# Rochester Univ., NY. Dept. of Computer Science.
AN OVERVIEW OF PLATINUM: A PLATFORM FOR INVESTIGA TING NON-UNIFORM MEMORY (PRELIMINARY VERSION)
Robert J. Fowler and Alan L. Cox Nov. 1988 23 p
(Contracts DACA76-85-C-0001; N00014-84-K-0655; NSF CCR-87-04492)
(AD-A213911; TR-262) Avail: NTIS HC A02/MF A01 CSCL 12/5

PLATINUM is an experimental operating system kernel designed to facilitate research on memory management systems for Non-Uniform Memory Access (NUMA) Multiprocessor Architectures. It exports to user programs a simple abstraction of a shared memory multiprocessor in which all memory appears to be uniformly and rapidly accessible from all processors in the machine. The perceived uniformity on top of a non-uniform physical memory architecture is supported by an abstraction called coherent memory. Implemented in software as an extension of a directory-based caching mechanism using invalidation, coherent memory attempts to transparently migrate and replicate data to locations that are physically close to the processors that use it. A fundamental property of PLATINUM coherent memory is that it automatically reverts to the use of remote memory access for data that is not amenable to caching. PLATINUM (Platform for Investigation Non-Uniform Memory) currently runs on BBN Butterfly Plus Computers. An overview is presented of PLATINUM. In addition to motivating the project and presenting the reseach plans, the interface that the kernel provides to its users is described. GRA

N90-15603# Rochester Univ., NY. Dept. of Computer Science.
EVOLUTION OF AN OPERATING SYSTEM FOR LARGE-SCALE SHARED-MEMORY MULTIPROCESSORS
Michael L. Scott, Thomas J. LeBlanc, and Brian D. Marsh Mar. 1989 28 p Sponsored in part by IBM
(Contract DACA76-85-C-0001; NSF DCR-83-20136)
(AD-A213912; TR-309) Avail: NTIS HC A03/MF A01 CSCL 12/5

Scalable shared-memory multiprocessors (those with non-uniform memory access times) are among the most flexible architectures for high performance parallel computing, admitting efficient implementations of a wide range of process models,

communication mechanisms, and granularities of parallelism. Such machines present opportunities for general purpose parallel computing that cannot be exploited by existing operating systems, because the traditional approach to operating system design presents a virtual machine in which the definition of process, communication, and grain size are outside the control of the user. PSYCHE is an operating system designed to enable the most effective use possible of large scale shared memory multiprocessors. The PSYCHE project is characterized by: (1) a design that permits the implementation of multiple models of parallelism, both within and among applications, (2) the ability to trade protection for performance, with information sharing as the default, rather than the exception, (3) explicit, user level control of process structure and scheduling, and (4) a kernel implementation that uses shared memory itself, and that provides users with the illusion of uniform memory access times. GRA

N90-15604# Massachusetts Inst. of Tech., Cambridge. Lab. for Computer Science.
PARALATION VIEWS: ABSTRACTIONS FOR EFFICIENT SCIENTIFIC COMPUTING ON THE CONNECTION MACHINE
Kenneth J. Goldman Jun. 1989 28 p
(Contracts N00014-85-K-0168; N00014-83-K-0125; NSF CCR-86-11442)
(AD-A213935; MIT/LCS/TM-398) Avail: NTIS HC A03/MF A01 CSCL 12/5

An ideal parallel programming language for scientific applications should provide flexible abstraction mechanisms for writing organized and readable programs, encourage a modular programming style that permits using libraries of tested routines, and, above all, permit the programming to write efficient programs for the target machine. These criteria are used to evaluate the languages Lisp, Connection Machine Lisp, and Paralation Lisp for writing scientific programs on the Connection Machine. As a vehicle for this exploration, a particular non-trivial algorithm (LU decomposition with partial pivoting) and study code were fixed for implementing it in the three languages. GRA

N90-15605# Georgia Inst. of Tech., Atlanta. School of Civil Engineering.
UTILIZATION OF A PC FOR FINITE ELEMENT MODELING M.S. Thesis
Robin A. Collins Aug. 1989 204 p
(Contract N00228-85-G-3247)
(AD-A214173) Avail: NTIS HC A10/MF A02 CSCL 12/5

This document provides an individual that has no finite element experience and/or NISA II program experience with a more clarified user's manual, highlighting the problem areas the author encountered, and some comparisons between NISA answers and those provided by theory or another finite element program (GTSTRUDL). Appendix A provides a list of the equipment required to operate the NISA II program and appendix B provides an idea of the time required to perform analyses of various sizes. GRA

N90-15606# California Univ., Berkeley. Computer Science Div.
XNUSIM: GRAPHICAL INTERFACE FOR A MULTIPROCESSOR SIMULATOR
Swee-Chee Pang 8 Sep. 1989 69 p Sponsored in part by NCR Corp., Dayton, OH and NSF
(Contract N00014-88-K-0579)
(AD-A214176; UCB/CSD-89/532) Avail: NTIS HC A04/MF A01 CSCL 12/6

Xnusim is an X11 Window Interface for the Multi-Processor simulator Nusim. It is a display oriented interface between the simulator and the user via UNIX1 sockets with graphical objects such as menus, buttons, etc. It is designed in such a way that would allow it to be used with other simulators of the same class. This paper intends to describe the functionality of the objects, structures and program modules of XNUSIM in detail. GRA

N90-15607# Department of the Navy, Washington, DC.
RECONFIGURABLE N-DIMENSIONAL COMPUTER MEMORY Patent Application
Allen D. Parks, inventor (to Navy) and Albert P. Shuler, inventor (to Navy) 18 Sep. 1989 20 p
(AD-D014309; US-Patent-Appl-SN-408970) Avail: NTIS HC A03/MF A01 CSCL 12/6

The invention is a computer memory architecture wherein a multiply partitioned N-dimensional memory for serial and parallel computers provides a specialized storage and retrieval media. It can efficiently service associated computational processes with one 1-D hyperplanes of data that are accessible from any of the N-directions in a single access, or fewer accesses than required of conventional computer memory. This architecture reduces access time and complexity in parallel and array processing. GRA

61 COMPUTER PROGRAMMING AND SOFTWARE

Includes computer programs, routines, alogorithms, and specific applications, e.g., CAD/CAM.

N90-15608 Open Univ., Oxford (England).
UNDERSTANDING DEVELOPMENTS IN COMPUTER TECHNOLOGY: A PRAGMATIC AND SYNTHETIC INTERPRETATION Ph.D. Thesis
Peter William Conroy 1987 368 p
Avail: Univ. Microfilms Order No. BRDX84101

A new concept of technology is used to explain developments in computers and their practical application. The need for this reconceptualization is demonstrated by a survey illustrating the variability and contradictions between existing uses of the term technology, in particular the tendency to emphasize either its concrete or abstract attributes. The possibility of using positivist principles as the basis for a comprehensive concept which can synthesize these two orientations is examined and rejected. Instead, the new concept is constructed with ideas drawn from the work of various non-positivist theorists, principally Marx and Foucault. The result is not a definitive list of characteristics, but a description of the relationships in which technology is used and through which it changes. In order to explore the potential of this concept, it is used to develop an understanding of various aspects of computer technology. Firstly, historical events which let to the construction of the first modern computers are described and their interpretation in terms of the synthetic concept of technology contrasted with ones derived from a positivist casual analysis. In its second application to computer technology, the synthetic concept is used to interpret changes in contemporary methods of developing commercial data processing systems. Dissert. Abstr.

N90-15609# Fermi National Accelerator Lab., Batavia, IL. Computing Dept.
HIGH LEVEL LANGUAGE MEMORY MANAGEMENT ON PARALLEL ARCHITECTURES
P. Lebrun and A. Kreymer May 1989 6 p Presented at the Computing in High Energy Physics, Oxford, England, 10-14 Apr. 1989
(Contract DE-AC02-76CH-03000)
(DE89-015018; FNAL/C-89/124; CONF-890415-8) Avail: NTIS HC A02/MF A01

The HEP memory management packages such as YBOS and ZEBRA have been implemented and are currently running on a variety of mainframe computers. These packages were originally designed to run on single CPU engines. Implementation of these packages on parallel machines, loosely or tightly coupled architectures is discussed. The ZEBRA (CERN package) on ACP (Fermilab) is presented in detail. Design of memory management system for the new generation of ACP systems or similar parallel architectures are presented. The future of packages such as ZEBRA is not only linked to system architecture, but also to languages issues. We briefly mention penalties in using F77 with respect to other increasingly popular languages in HEP, such as C, on parallel systems. DOE

N90-15610# Los Alamos National Lab., NM. Computing and Communications Div.
AN EFFICIENT UNICOS RUN-TIME SYSTEM FOR FUNCTIONAL PROGRAMS ON A CRAY X-MP
Jeffrey P. Hammes, Bonnie Yantis, Randy Michelsen, Joseph H. Fasel, III, and Patricia K. Fasel 1989 9 p Presented at the Supercomputing '89 Conference, Reno, NV, 13-17 Nov. 1989
(Contract W-7405-eng-36)
(DE89-016603; LA-UR-89-2974; CONF-891149-4) Avail: NTIS HC A02/MF A01

The ParaGraph (Parallel Graph reduction) project at Los Alamos National Laboratory is an investigation of the use of functional languages for scientific applications; efficient implementation strategies are a primary concern. The initial version of the ParaGraph run-time system, ParaGraph-RTS 1.0, was not targeted for the X-MP architecture specifically. We examine the new Cray X-MP UNICOS single processor implementation, ParaGraph-RTS 2.0, and describe the CRAY specific optimizations employed. Optimizations include novel use of the CRAY X-MP register set and the generation of optimized assembly code. Performance improvements over ParaGraph-RTS 1.0 have been significant; initial measurements are presented. DOE

N90-15611# Oak Ridge National Lab., TN.
ELICITATION OF NATURAL LANGUAGE REPRESENTATIONS OF UNCERTAINTY USING COMPUTER TECHNOLOGY
Bruce Tonn, Richard Goeltz, and Cheryl Travis (Tennessee Univ., Knoxville.) 1989 16 p Presented at the Annual Meeting of the Society for Risk Analysis, Washington, DC, 31 Oct. - 2 Nov. 1989
(Contract DE-AC05-84OR-21400)
(DE90-001416; CONF-8910246-1) Avail: NTIS HC A03/MF A01

Knowledge elicitation is an important aspect of risk analysis. Knowledge about risks must be accurately elicited from experts for use in risk assessments. Knowledge and perceptions of risks must also be accurately elicited from the public in order to intelligently perform policy analysis and develop and implement programs. Oak Ridge National Laboratory is developing computer technology to effectively and efficiently elicit knowledge from experts and the public. This paper discusses software developed to elicit natural language representations of uncertainty. The software is written in Common Lisp and resides on VAX Computers System and Symbolics Lisp machines. The software has three goals, to determine preferences for using natural language terms for representing uncertainty; likelihood rankings of the terms; and how likelihood estimates are combined to form new terms. The first two goals relate to providing useful results for those interested in risk communication. The third relates to providing cognitive data to further our understanding of people's decision making under uncertainty. The software is used to elicit natural language terms used to express the likelihood of various agents causing cancer in humans and cancer resulting in various maladies, and the likelihood of everyday events. DOE

N90-15612# Texas Univ., Austin. Fusion Research Center.
TRANSPORT MODELING AND ADVANCED COMPUTER TECHNIQUES
J. C. Wiley, D. W. Ross, and W. H. Miner, Jr. Nov. 1988 19 p
(Contract DE-FG05-88ER-53266)
(DE90-001481; DOE/ER-53266/16; FRCR-321) Avail: NTIS HC A03/MF A01

The current state of transport codes and whether improved user interfaces would make the codes more usable and accessible to the fusion community was considered. Also considered was the possibility that a software standard could be devised to ease the exchange of routines between groups. It was noted that two of the major obstacles to exchanging routines now are the variety of geometrical representation and choices of units. While the workshop formulated no standards, it was generally agreed that good software engineering would aid in the exchange of routines, and that a continued exchange of ideas between groups would be worthwhile. It seems that before software standards are discussed, the current state of computer technology (both hardware and software) should be reviewed to see what influence recent advances might have on the software goals. This is done. DOE

N90-15613# Argonne National Lab., IL. Mathematics and Computer Science Div.
A BLOCK QR FACTORIZATION ALGORITHM USING RESTRICTED PIVOTING
Christian H. Bischof 29 Apr. 1989 22 p Presented at the Supercomputing 1989 Conference, Reno, NV, 13-17 Nov. 1989
(Contract W-31-109-eng-38; NSF ASC-87-15728)
(DE90-001921; CONF-891149-8) Avail: NTIS HC A03/MF A01

This paper presents a new algorithm for computing the QR factorization of a rank-deficient matrix on high-performance machines. The algorithm is based on the Householder QR factorization algorithm with column pivoting. The traditional pivoting strategy is not well suited for machines with a memory hierarchy since it precludes the use of matrix-matrix operations. However, matrix-matrix operations perform better on those machines than matrix-vector or vector-vector operations since they involve significantly less data movement per floating point operation. We suggest a restricted pivoting strategy which allows us to formulate a block QR factorization algorithm where the bulk of the work is in matrix-matrix operations. Incremental condition estimation is used to ensure the reliability of the restricted pivoting scheme. Implementation results on the Cray 2, Cray X-MP and Cray-Y-MP show that the new algorithm performs significantly better than the traditional scheme and can more than halve the cost of computing the QR factorization. DOE

N90-15614# Pacific Northwest Lab., Richland, WA.
THE COMPONENTS OF SCIENTIFIC VISUALIZATION
T. D. Desmarais Oct. 1989 6 p Presented at the Supercomputing World Conference, San Francisco, CA, 17-20 Oct. 1989
(Contract DE-AC06-76RL-01830)
(DE90-001992; PNL-SA-17406; CONF-8910103-2) Avail: NTIS HC A02/MF A01

The purpose of scientific visualization is to improve the ability of a human to analyze and understand data. A goal of visualization is improving productivity. If we measure the success of our visualization by measuring only the increase in productivity, we are missing a key capability of proper visualization: the improvement in our ability to discover through exploration. This paper presents a breakdown of the components that improve the success of visualization as measured in both productivity and discovery. Important concepts associated with these components are described in order to give the supercomputer user practical guidelines during construction of a visualization system. DOE

N90-15615# Lawrence Livermore National Lab., CA.
KNOWLEDGE REPRESENTATIONS FOR THE AUTOMATIC GENERATION OF NUMERICAL SIMULATORS FOR PDES
David Balaban, Joseph Garbarini, William Greiman, and Mark Durst 21 Feb. 1989 9 p Presented at the International Association of Mathematics and Computers Simulation Conference, West Lafayette, IN, 5-7 Dec. 1989 Submitted for publication
(Contract W-7405-eng-48)
(DE89-008036; UCRL-100557; CONF-891213-1) Avail: NTIS HC A03/MF A01

In this paper we describe an Automatic Programming (AP) system which generates numerical discretization schemes for Partial Differential Equation (PDE) problems. This system is based on the observation that a wide variety of discretization schemes can be mechanically produced by computing surface integrals of spacetime currents. However, surface integration is difficult to carry out using conventional vector calculus. For this reason, the system is structured to include the differential geometry formalisms which make high dimensional surface integration simple. The differential geometry formalisms have also simplified the representation of continuous physics problems and increased the domain of applicability of the system. DOE

N90-15616# Stanford Univ., CA. Systems Optimization Lab.
ON THE IDENTIFICATION OF LOCAL MINIMIZERS IN INERTIA-CONTROLLING METHODS FOR QUADRATIC PROGRAMMING
Anders L. Forsgren, Philip E. Gill (California Univ., San Diego, La Jolla.), and Walter Murray Jul. 1989 24 p Sponsored in part by Goeran Gustafsson Foundation
(Contracts DE-FG03-87ER-25030; N00014-87-K-0142; NSF CCR-84-13211)
(DE89-017330; SU-SOL-89-11) Avail: NTIS HC A03/MF A01

The verification of a local minimizer of a general (i.e., nonconvex) quadratic program is in general an NP-hard problem. The difficulty concerns the optimality of certain points (which we call dead points) at which the first-order necessary conditions for optimality are satisfied, but strict complementarity does not hold. One important class of methods for solving general quadratic programming problems are called inertia-controlling quadratic programming (ICQP) methods. We derive a computational scheme for proceeding at a dead point that is appropriate for a general ICQP method. DOE

N90-15617# Stanford Univ., CA. Systems Optimization Lab.
SEQUENTIAL QUADRATIC PROGRAMMING ALGORITHMS FOR OPTIMIZATION
Francisco J. Prieto Aug. 1989 158 p Sponsored in part by the Bank of Spain
(Contracts DE-FG03-87ER-25030; N00014-87-K-0142; NSF ECS-87-15153)
(DE90-000022; SU-SOL-89-7) Avail: NTIS HC A08/MF A01

The problem considered is that of finding local minimizers for a function subject to general nonlinear inequality constraints, when first and perhaps second derivatives are available. The methods studied belong to the class of sequential quadratic programming (SQP) algorithms. In particular, the methods are based on the SQP algorithm embodied in the code NPSOL, which was developed at the Systems Optimization Laboratory, Stanford University. The goal of this paper is to develop SQP algorithms that allow some flexibility in their design. Specifically, we are interested in introducing modifications that enable the algorithms to solve large-scale problems efficiently. The following issues are considered in detail: instead of trying to obtain the search direction as a minimizer for the QP, the solution process is terminated after a limited number of iterations. Suitable termination criteria are defined that ensure convergence for an algorithm that uses a quasi-Newton approximation for the full Hessian. For many problems the reduced Hessian is considerably smaller than the full Hessian. Consequently, there are considerable practical benefits to be gained by only requiring an approximation to the reduced Hessian. DOE

N90-15618# Argonne National Lab., IL. Mathematics and Computer Science Div.
GRADIENT PROJECTION TECHNIQUES FOR LARGE-SCALE OPTIMIZATION PROBLEMS
Jorge J. More 1989 4 p Presented at the 28th IEEE Conference on Decision and Control, Tampa, FL, 13-15 Dec. 1989
(Contract W-31-109-eng-38)
(DE90-001986; CONF-891251-2) Avail: NTIS HC A02/MF A01

The impact of the identification properties of the gradient projection method on algorithms for the solution of large-scale optimization problems with bound constraints, is described. In particular, recent results of More and Toraldo are described which show that the gradient projection method can be combined with the conjugate gradient method to solve an important class of large-scale (number of variables between 5000 and 15000) bound constrained quadratic programming problems with a few (less than 15) iterations. DOE

N90-15619# California Univ., Berkeley. Lawrence Berkeley Lab.
OPTIMIZING AND EVALUATING ALGORITHMS FOR REPLICATED DATA CONCURRENCY CONTROL
Akhil Kumar and Arie Segev Feb. 1989 27 p Presented at the 9th International Conference on Distributed Computing Systems, Newport Beach, CA, 5-9 Jun. 1989
(Contract DE-AC03-76SF-00098)
(DE90-003080; LBL-25435; CONF-8906250-1) Avail: NTIS HC A03/MF A01

Techniques for optimizing a static voting type algorithm are presented. Our optimization model is based on minimizing communications cost subject to a given availability constraint. We describe a semi-exhaustive algorithm for solving this model. This algorithm utilizes a novel signature-based method for identifying equivalent vote combinations, and also an efficient algorithm for computing availability. Static algorithms naturally have the advantage of simplicity; however, votes and quorum sizes are not allowed to vary. Therefore, the optimized static algorithm was compared against the available copies method, a dynamic algorithm, to understand the relative performance of the two types of algorithms. We found that if realistic reconfiguration times are assumed, then no one type of algorithm is uniformly better. The factors that influence relative performance have been identified. The available copies algorithm does better when the update traffic ratio is small, and the variability in the inter-site communications cost is low. DOE

N90-15620# Stanford Univ., CA. Dept. of Operations Research.
A BASIC THEOREM OF COMPLEMENTARITY FOR THE GENERALIZED VARIATIONAL-LIKE INEQUALITY PROBLEM
Jen-Chih Yao Nov. 1989 21 p
(Contract DE-FG03-87ER-25028)
(DE90-003102; SU-SOL-89-16) Avail: NTIS HC A03/MF A01

In this report, a basic theorem of complementarity is established for the generalized variational-like inequality problem introduced by Parida and Sen. Some existence results for both generalized variational inequality and complementarity problems are established by employing this basic theorem of complementarity. In particular, some sets of conditions that are normally satisfied by a nonsolvable generalized complementarity problem are investigated. DOE

N90-15621# California Univ., Berkeley. Lawrence Berkeley Lab. Information and Computing Sciences Div.
SCRY: A DISTRIBUTED IMAGE HANDLING SYSTEM, VERSION 1.1
David W. Robertson, William E. Johnston, Teck-Joo Chua, James Huang, Fritz Renema, Max Rible, Nicole Texier, and B. J. Wishinsky Apr. 1989 60 p
(Contract DE-AC03-76SF-00098)
(DE90-003105; LBL-26796) Avail: NTIS HC A04/MF A01

Scry is a distributed image handling system that provides both image compression and transport on local and wide area networks, and a collection of higher level graphics and scientific visualization functions. The system can be distributed among workstations, between supercomputers and workstations, and between supercomputers, workstations and video animation controllers. The system is most commonly used to produce video based movie displays of time dependent data and complex 3D data sets, and to handle the images resulting from certain image processing operations. In the scientific visualization process, the system is typically used in one of two configurations. In the first, the supercomputer application generates data (e.g., flow field vectors) that are compressed and sent to a graphics workstation over a wide area network. The graphics workstation environment is used to design and debug the graphics visualization for a movie. Finally, the raster images that represent the frames of the movie are compressed and sent over a local area network to the video animation controller. This report discusses the use of this program. DOE

N90-15622*# National Aeronautics and Space Administration. Lewis Research Center, Cleveland, OH.
CRYOTRAN USER'S MANUAL, VERSION 1.0
Glenn R. Cowgill, David J. Chato, and Ehab Saad (Analex Corp., Cleveland, OH.) Dec. 1989 326 p
(NASA-TM-102468; E-5256; NAS 1.15:102468) Avail: NTIS HC A15/MF A02 CSCL 09B

The development of cryogenic fluid management systems for space operation is a major portion of the efforts of the Cryogenic Fluids Technology Office (CFTO) at the NASA Lewis Research Center. Analytical models are a necessary part of experimental programs which are used to verify the results of experiments and are also used as a predictor for parametric studies. The CryoTran computer program is a bridge to obtain analytical results. The object of CryoTran is to coordinate these separate analyses into an integrated framework with a user-friendly interface and a common cryogenic property database. CryoTran is an integrated software system designed to help solve a diverse set of problems involving cryogenic fluid storage and transfer in both ground and low-g environments. Author

N90-15623# California Univ., Berkeley. Lawrence Berkeley Lab. Dept. of Computer Science Research.
NAME ASSIGNMENT TECHNIQUES FOR RELATIONAL SCHEMAS REPRESENTING EXTENDED ENTITY-RELATIONSHIP SCHEMAS
Victor M. Markowitz and Arie Shoshani Aug. 1989 27 p Presented at the 8th International Conference on Enity-Relationship Approach, Toronto, Ontario, 18-20 Oct. 1989 Submitted for publication
(Contract DE-AC03-76SF-00098)
(DE90-003269; LBL-27070; CONF-8910295-2) Avail: NTIS HC A03/MF A01

The mapping of Extended Entity-Relationship (EER) schemas into relational schemas involves the assignment of names to relational attributes. We propose several criteria for such name assignment, such as brevity and clarity. These name assignments must satisfy certain assumptions underlying relational normalization. We develop two name assignment algorithms that satisfy these assumptions and follow the criteria mentioned above. The first algorithm is intended for regular relational interfaces where users know both relations and attributes. The second algorithm is designed for special relational (Universal Relation) interfaces where users interact at the attribute level only and are not expected to know how attributes are grouped into relations. Both algorithms employ well known graph algorithms in order to devise appropriate name assignment strategies. DOE

N90-15624# Pacific Northwest Lab., Richland, WA.
DEVELOPMENTAL VERSIONS OF FORTRAN/77 ROUTINES FOR THE DESIGN AND ANALYSIS OF MIXTURE EXPERIMENTS
G. F. Piepel and B. M. Linbo-Terhaar Nov. 1989 107 p
(Contract DE-AC06-76RL-01830)
(DE90-003513; PNL-SA-17603) Avail: NTIS HC A06/MF A01

Preliminary, developmental FORTRAN/77 codes that implement several techniques for the statistical design and analysis of mixture experiments are presented. The codes contained are as they existed at the end of August 1988 when funding of their development ceased. A list of the attached FORTRAN/77 source codes is contained. The documentation for each code is built-in at the beginning of each source code. Descriptions of the code capabilities are given in this built-in documentation. Potential users should use extreme caution because of the preliminary, developmental nature of the codes. Some of the codes were partially tested, while others were not tested at all. All of the codes were still under development and should be treated accordingly. DOE

N90-15625# Stanford Univ., CA. Systems Optimization Lab.
THE PARALLEL DECOMPOSITION OF LINEAR PROGRAMS Thesis
Robert Entriken Nov. 1989 167 p
(Contracts DE-FG03-87ER-25028; DE-FG03-87ER-25030; N00014-89-J-1659; N00014-87-K-0142; NSF DMS-89-13089; NSF DDM-88-14253; NSF ECS-87-15153)
(DE90-003538; SU-SOL-89-17) Avail: NTIS HC A08/MF A01

A new calculus is introduced for manipulating linear-program decomposition schemes. A linear program is represented by a communication network, which is decomposed by splitting nodes in two, and a transformation is defined to recover subproblems from the network. Also defined is a dual-symmetric oracle that provides solutions to linear programs, and can be performed by the simplex method, nested decomposition, and finally, parallel decomposition. Two important classes of linear program serve as examples for the above calculus: staircase linear programs and stochastic linear programs. For the former case, a sophisticated yet experimental computer code was written for an IBM 3090/600E with six processors. The code performs the parallel decomposition algorithm and is tested on twenty-two small to medium sized real-world problems. Experiments show that in addition to speedups provided by decomposition alone, performance is improved by using parallel processors. DOE

N90-15626# Brookhaven National Lab., Upton, NY. AGS Dept.
PROGRAMS FOR CONTROL OF AN ANALOG-SIGNAL SWITCHING NETWORK
T. DOttavio, R. Enriquez, R. Katz, and J. Skelly 1989 18 p Presented at the International Conference on Accelerator and Large Experimental Physics Control Systems, Vancouver, British Columbia, 30 Oct. - 3 Nov. 1989
(Contract DE-AC02-76CH-00016)
(DE90-003645; BNL-43066; CONF-891094-4) Avail: NTIS HC A03/MF A01

A suite of programs was developed to control the network of analog-signal switching multiplexers in the AGS complex. The software is driven by a relational database which describes the architecture of the multiplexer tree and the set of available analog signals. Signals are routed through a three-layer multiplexer tree, to be made available at four consoles each with three 4-trace oscilloscopes. A menu-structured operator interface program is available at each console, to accept requests to route any available analog signal to any of that console's 12 oscilloscope traces. A common routing-server program provides automatic routing of requested signals through the layers of multiplexers, maintaining a reservation database to denote free and in-use trunks. Expansion of the analog signal system is easily accommodated in software by adding new signals, trunks, multiplexers, or consoles to the database. Programmatic control of the triggering signals for each of the oscilloscopes is also provided. DOE

N90-15627# Massachusetts Inst. of Tech., Cambridge. Dept. of Ocean Engineering.
AN EXECUTIVE SYSTEM FOR MODELING WITH RATIONAL B-SPLINES M.S. Thesis
Glenn Roy Hottel, Sr. May 1989 190 p
(Contract N00228-89-G-0580)
(AD-A213460) Avail: NTIS HC A09/MF A01 CSCL 12/5

An editor for use in the modeling of surfaces and curves with non-uniform rational B-splines (NURBS) was developed. A comprehensive menu structure has been generated and a method for interfacing future modules into this structure was developed and discussed with examples. Surface modules interfaced include: Gaussian, mean, normal and principal curvature presentations; shading with light source and color editing; presentation editing with full positioning and rotation capabilities; and, isophote line calculation. Curve modules interfaced include entering and editing points in the parametric space of a B-spline surface; generation of a B-spline curve interpolating these points while staying on the surface; and, fairing of the curve to get a smoother shape for a curve on a surface. Implementation of the editor uses a DEC VAX Station 2 with the NAG Mark 11 library. The display graphics are performed on a Silicon Graphics IRIS 3030 Workstation networked with the VAX station. GRA

N90-15628# Naval Postgraduate School, Monterey, CA.
A SIMULATION MODEL FOR DYNAMIC SYSTEM AVAILABILITY ANALYSIS M.S. Thesis
Dister L. Deoss, Jr. May 1989 280 p
(AD-A213499) Avail: NTIS HC A13/MF A01 CSCL 12/4

A dynamic Monte Carlo system availability simulation model is developed. DYMCAM is based on 3 fundamental modeling objectives: (1) to provide the ability to analyze time dependent

availability of dynamic systems; (2) to provide a model which is easy to apply and interpret; And (3) to create a model which can easily be modified to incorporate additional features as needed. The output generated by the program includes time dependent system unavailability information and average system unavailability over the duration of the simulated time period. DYMCAM is tested on several basic availability analysis problems to demonstrate program capabilities. These tests include a single component with exponential failure and repair times, a single component with two repair states, a two-out-of-three pump failure system, and a phased mission problem requiring the forced change of a system component state after the start of the analysis. A modification of the DYMCAM program was also developed to demonstrate the capability of treating continuous process variables in a dynamic simulation model. Results were compared with analytical results where possible, and with Markovian analysis techniques in other cases. The simulation model provided accurate unavailability results on all example problems tested. Further work needs to be done to expand the capabilities of the basic DYMCAM model and to continue program testing on more complex problems. GRA

N90-15629# Office of the Under Secretary of Defense (Acquisitions), Washington, DC.
ADA 9X PROJECT REPORT. REVISION REQUEST REPORT
Aug. 1989 344 p
(AD-A213503) Avail: NTIS HC A15/MF A01 CSCL 12/5

The overall goal of the Ada 9X Project is to revise ANSI/MIL-STD-1815A to reflect current essential requirements with minimum negative impact and maximum positive impact to the Ada community. The Ada 9X process is a revision and not a redesign of the language and should be viewed as a natural part of the maturation process. Requirements for the revision are based on input from the Ada community in the form of special studies, workshops, public meetings, Ada Language Issues, and revision requests. This document contains all the revision requests submitted as of 25 July 1989. Requests are organized according to relevant sections in the Language Reference Manual, ANSI/MIL-STD-1815A. If a request is relevant to more than one section, it will physically appear in the first section designated by the author as a reference, and appear by reference in other sections. Indices are provided to support referencing by key words, submitter, organization, and revision request number. This document will be updated and reissued periodically throughout the duration of the Ada 9X Project. GRA

N90-15630# Colorado Univ., Boulder. Dept. of Computer Science.
SOFTWARE FOR A NEW MODIFIED CHOLESKY FACTORIZATION Technical Report, 15 May 1989 - 15 May 1990
Elizabeth Eskow and Robert B. Schnabel 31 Aug. 1989 29 p
(Contract DAAL03-88-K-0086; NSF CCR-87-02403; NSF DCR-84-20944)
(AD-A213643; CU-CS-443-89; ARO-24923.5-MA) Avail: NTIS HC A03/MF A01 CSCL 12/5

The software for a new modified Cholesky factorization is described. Given a symmetric but not necessarily positive definite matrix A, the modified Cholesky factorization computes a Cholesky factorization of A + E, where E = 0 if A is safely positive definite, and E is a diagonal matrix chosen to make A + E positive definite otherwise. The modified Cholesky factorization was introduced by Gill and Murray and refined by Gill, Murray and Wright, and is commonly used in optimization algorithms. This version, which is based upon new techniques, has a considerably smaller a priori upper bound on the size of E than the Gill, Murray and Wright factorization, and appears to generally produce a smaller E, and a well-conditioned A + E, in practice. Its cost, like the Gill, Murray and Wright version, is only a small multiple of n squared operations greater than the standard Cholesky factorization. Thus it may be useful in optimization algorithms. The algorithm is summarized and the code and its use is described. GRA

N90-15631# Rochester Univ., NY. Dept. of Computer Science.
AN OVERVIEW OF LYNX
Michael L. Scott Aug. 1989 30 p
(Contract DACA76-85-C-0001)
(AD-A213714; TR-308) Avail: NTIS HC A03/MF A01 CSCL 12/5

A programming language can provide much better support for interprocess communication that a library package can. Most message-passing languages limit this support to communication between the pieces of a single program, but this need not be the case. Lynx facilitates convenient, typesafe message passing not only within applications, but also between applications, and among distributed collections of servers. Specifically, it addresses issues of compiler statelessness, late binding, and protection that allow runtime interaction between processes that were developed independently and that do not trust each other. Implementation experience with Lynx has yielded important insights into the relationship between distributed operating systems and language run-time support packages, and into the inherent costs of high-level message-passing semantics. GRA

N90-15632# Massachusetts Inst. of Tech., Cambridge. Lab. for Computer Science.
ON THE CORRECTNESS OF ORPHAN MANAGEMENT ALGORITHMS
Maurice Herlihy, Nancy A. Lynch, Michael Merritt, and William Weihl Aug. 1989 58 p
(Contracts N00014-83-K-0125; N00014-85-K-0168)
(AD-A213777; MIT/LCS/TM-406) Avail: NTIS HC A04/MF A01 CSCL 12/7

In a distributed system, node failures, network delays and other unpredictable occurrences can result in orphan computations; subcomputations that continue to run but whose results are no longer needed. Several algorithms have been proposed to prevent such computations from seeing inconsistent states of the shared data. Herein, two such orphan management algorithms are analyzed. The first is an algorithm proposed at Carnegie-Mellon. The algorithms are described formally, and complete proofs of their correctness are given. The proofs show that the fundamental concepts underlying the two algorithms are very similar in that each can be regarded as an implementation of the same high level algorithm. By exploiting properties of information flow within transaction management systems, the algorithms ensure that orphans only see states of the shared data that they could also see if they are not orphans. When the algorithms are used in combination with any correct concurrency control algorithm, they guarantee that all computations, orphan as well as non-orphan see consistent states of the shared data. GRA

N90-15633# Massachusetts Inst. of Tech., Cambridge. Lab. for Computer Science.
TIME BOUNDS FOR REAL-TIME PROCESS CONTROL IN THE PRESENCE OF TIMING UNCERTAINTY
Hagit Attiya and Nancy A. Lynch Jul. 1989 52 p
(Contracts N00014-83-K-0125; N00014-85-K-0168)
(AD-A213791; MIT/LCS/TM-403) Avail: NTIS HC A04/MF A01 CSCL 12/7

An important area of computer applications is real-time process control, in which a computer system interacts with a real-world system in order to guarantee certain desirable real-world behavior. In most interesting cases, the real-world requirements involve timing properties, and so the behavior of the computer system is required to satisfy certain timing constraints. In order to be able to guarantee timing constraints, the computer system must satisfy some assumptions about time - for example, its various components should operate at known speeds. A timing-based variant of the mutual exclusion problem is considered. In this variant, only an upper-bound on the time it takes to release the resource is known, and no explicit signal is sent when the resource is released; furthermore; the only mechanism to measure real time is an inaccurate clock, whose tick intervals take time between two constants. GRA

N90-15634# Massachusetts Inst. of Tech., Cambridge. Lab. for Computer Science.
OPTIMISTIC CONCURRENCY CONTROL FOR NESTED DISTRIBUTED TRANSACTIONS
Robert Edward Gruber Jun. 1989 110 p
(Contract N00014-83-K-0125; NSF DCR-85-03662)
(AD-A213828; MIT/LCS/TR-453) Avail: NTIS HC A06/MF A01 CSCL 12/7

Optimistic concurrency control techniques allow atomic transactions (or actions for short) to execute without synchronization, relying on commit-time validation to ensure serializability. Previous work in this area has focussed on single-level actions. This thesis extends previous work on optimistic concurrency control to distributed systems with nested actions. The thesis presents two contrasting models for managing nested actions, which we call the fixed action model and the fixed object model. In the fixed action model, an action executes at only a single network node; if an action accesses an object whose storage is provided by another node, it brings a copy of the object to its node. In this model, caching copies of non-local objects can be used to improve performance by reducing the number of non-local object requests. We show that optimistic concurrency control has an advantage over pessimistic concurrency control with respect to this object caching. In the fixed object model, actions can span network nodes: an action at one node can start a nested action at another node. However, an object's state is never moved from the node providing its storage. While there is a clear reason for using optimistic concurrency control for systems following the fixed action model, there is no clear reason for choosing either optimism or pessimism for systems following the fixed object model; however, the development of this model is an important step in the study of hybrid models. GRA

N90-15635# Massachusetts Inst. of Tech., Cambridge. Lab. for Computer Science.
A SIGNAL PROCESSING LANGUAGE FOR COARSE GRAIN DATA FLOW MULTIPROCESSORS M.S. Thesis
Janice S. Onanian Jun. 1989 122 p Sponsored in part by Raytheon Co., Sudbury, MA
(Contract N00014-84-K-0099)
(AD-A213863; MIT/LCS/TR-449) Avail: NTIS HC A06/MF A01 CSCL 12/5

A language and graph representation designed to aid in the partitioning of large signal processing applications into tasks to run on a multiprocessor are presented. This language compiles directly into a program graph upon which optimizations are performed to find the optimal task configuration. The optimal task configuration is one in which computation-to-communication is minimized while throughput is maximized. The language and graph are designed to express coarse-grain parallelism so that large communication delays and task overhead do not outweigh the speedup achieved by exploiting the parallelism in the application. The data flow model underlying the graph representation is based on a distributed, loosely-coupled multiprocessor concept which supports tagged data flow at the operating system level. The approach utilized in the graph and language is to insert specific, data, routing operators into the data flow graph defined by the application. These operators shape and route data through the application and express all the coarse-grain parallelism which is exploitable in the model. Data routing operators are parameterized to reflect the degree of parallelism, i.e., the number of parallel tasks in a partition of the application. The graph constructs also contain sufficient information to describe fully the task structure of the application. GRA

N90-15636# Utah State Univ., Logan.
FAST ALGORITHMS FOR ESTIMATING MIXTURE PARAMETERS Final Report, 1 Jul. 1988 - 30 Jun. 1989
Homer F. Walker and Michael P. Windham 30 Aug. 1989 8 p
(Contract DAAL03-88-K-0051)
(AD-A213869; ARO-25333.5-MA-SDI) Avail: NTIS HC A02/MF A01 CSCL 12/3

The investigation and results for the work on the accelerated scoring techniques was completed and prepared for publication, and the numerical testing of the accelerated fixed-point method was completed. The work on relaxation methods will be done during the coming year. GRA

N90-15637# Carnegie-Mellon Univ., Pittsburgh, PA. Optical Data Processing.
OPTICAL NEURAL NETS FOR SCENE ANALYSIS Semiannual Technical Report, 1 Apr. - 1 Oct. 1989
David Cassent 23 Oct. 1989 10 p
(Contract DAAH01-89-C-0418; ARPA Order 6671)
(AD-A213986; CMU-DARPA/SEMI/1089) Avail: NTIS HC A02/MF A01 CSCL 12/9

A hybrid optical/digital neural net for scene an analysis described. It combines pattern recognition and neural net techniques. New algorithms, architectures and applications are described for optimization neural nets (a mixture neural net for image spectrometry, cubic and quadratic neural nets for multitarget tracking, and a matrix inversion neural net), production system neural nets, symbolic neural nets and a new adaptive learning neural net (the adaptive clustering neural net). Progress in the first six months on these seven neural nets and our hardware are presented. GRA

N90-15638# Lowell Univ., MA. Dept. of Electrical Engineering.
STUDIES OF QUANTITATIVE METHODS FOR IMAGING FROM SCATTERED FIELDS Report, for 1 Feb. - 1 Oct. 1989
M. A. Fiddy 1 Oct. 1989 16 p
(Contract N00014-89-J-1158)
(AD-A214047) Avail: NTIS HC A03/MF A01 CSCL 17/9

The objective of this project remains reconstructing images from scattered field data. Concern is with targets or objects that cannot be considered weakly scattering, which makes the well known inversion schemes based on the first Born approximation of limited use. Methods based on distorted wave Born and Rytov approximations are under study, as well as techniques which treat the inversion procedure as a spectral estimation exercise. Owing to the difficulty in testing these new procedures with simulated data, due to the inherent difficulty in computing such data sets reliably, focus is on the use of real data from known simple targets. Work continues on the collection and interpretation of such scattered field data, which has been collected at the RADC Radar Cross Section Facility. Software has been developed to allow easy manipulation and display of these data sets as well as the images reconstructed from them. The capability exists for placing each scattered field data set on an arc of arbitrary radius and center in the Fourier domain and then interpolate these data to a cartesian grid; this was important for the evaluation of one of the inversion methods under consideration. GRA

N90-15639# Surveillance Research Lab., Salisbury (Australia).
EVALUATION OF A SIMPLE ALGORITHM FOR ESTIMATING INFRARED SIGNATURES FROM MULTI-PIXEL TO SUB-PIXEL TARGETS APPLIED TO AGA THERMOVISION IMAGERY
G. W. McQuistan May 1989 31 p
(AD-A214103; SRL-0020-TM; DODA-AR-005-450) Avail: NTIS HC A03/MF A01 CSCL 17/5

Evaluation of a simple algorithm for estimating the infrared signatures of small multi-pixel and sub-pixel targets in calibrated digital imagery is described. It is concluded that the only errors in the algorithm arise from the digitizing process. The algorithm is simple and the target area does not have to be defined, nor does it have to be visible on the displayed imagery. GRA

N90-15640# Army Construction Engineering Research Lab., Champaign, IL.
GUIDELINES FOR EVALUATING ENERGY ANALYSIS SOFTWARE Final Report
Linda Lawrie and William Bahnfleth Sep. 1989 61 p
(DA Proj. 4A1-62781-AT-45)
(AD-A214171; CERL-TR-E-89/15) Avail: NTIS HC A04/MF A01 CSCL 12/5

Design criteria documents used by Army designers require

that an energy analysis of buildings be performed during the design process. However, designers are are given little guidance either on modeling buildings of energy analysis or on using computer programs to perform the analysis. This report describes methods designers can use to evaluate energy related software used for whole building energy analysis and proves an Energy Analysis Calculation Tool Worksheet to use during evaluation. The suitability of an energy analysis program depends to a large extent on the intended use. Rather than using a separate program for each application, it may be better to learn a very detailed program that will be suitable for all applications. Agreement between programs during evaluation does not guarantee agreement with real data. The program's successful solution of a simple problem may not be a good indicator of its ability to give similar accuracy for a complex problem. Energy Analysis is the process of estimating energy requirements and fuel consumption of heating, ventilating, and air conditioning, electrical, and other consuming systems for either short or long terms of operation. Three common elements associated with building energy analysis are the calculation of: (1) space load, (2) secondary equipment load, and (3) primary equipment energy requirements. Here, secondary refers to the equipment that distributes the heating, cooling, or ventilating medium to the conditioned spaces. GRA

N90-15641# Naval Postgraduate School, Monterey, CA. Dept. of Computer Science.
ENVIRONMENT FOR FAILURE REGION ANALYSIS: REACHER - A REACHABILITY CONDITION DERIVATION TOOL Progress Report, Sep. 1988 - Sep. 1989
Timothy J. Shimeall 25 Sep. 1989 18 p
(AD-A214183; NPS52-89-050) Avail: NTIS HC A02/MF A01 CSCL 12/5

REACHER is a tool that derives the conditions under which each program block in a Pascal program, procedure or function may be executed (i.e., the reachability conditions for each subprocedure, subfunction and begin-end block). The tool shall accept compilable Pascal program source code and shall produce both an annotated listing and an augmented control flow graph. REACHER is one of a series of four tools that work in an integrated fashion to analyze Pascal programs to determine the failure regions associated with identified faults in the programs. The augmented control flow graph produced by REACHER will used as input by the programs FALTER and SPACER, and shall be customized for such usage. The annotated source listing provides includes a correspondence between Pascal statements and control flow graph nodes. The users may access REACHER, FALTER and SPACER through a screen-oriented user interface called VIEWER. This document describes the operation of REACHER and its direct user interface. GRA

N90-15642# Virginia Univ., Charlottesville. Dept. of Computer Science.
THE STARLITE PROJECT Annual Report, 1 Oct. 1988 - 30 Sep. 1989
R. P. Cook and S. H. Son Oct. 1989 56 p
(Contract N00014-86-K-0245)
(AD-A214193; UVA/525410/CS90/103) Avail: NTIS HC A04/MF A01 CSCL 12/7

The Starlike Project has the goal of constructing a program library for real-time applications. The initial focus of the project is on operating system and database support. The project also invcIves the construction of a prototyping environment that supports experimentation with concurrent and distributed algorithms in a host environment before down-loading to a target system for performance testing. The components of the project include a Modula-2 compiler, a symbolic Modula-2 debugger, an interpreter/runtime package, the Pheonix operating system, the meta-file system, a visual simulation package, a database system, and documentation. GRA

N90-15643# Brown Univ., Providence, RI.
A RENORMALIZATION GROUP APPROACH TO IMAGE PROCESSING: A NEW COMPUTATIONAL METHOD FOR THREE-DIMENSIONAL SHAPES IN ROBOT VISION, AND THE COMPUTATION COMPLEXITY OF THE COOLING ALGORITHMS Final Report, 15 Jun. 1986 - 31 Jul. 1989
Basilis Gidas 30 Sep. 1989 8 p
(Contract DAAL03-86-K-0110)
(AD-A214247; ARO-24371.11-MA-SDI) Avail: NTIS HC A02/MF A01 CSCL 12/9

During this contract period, the following work was accomplished: (1) A parallel multilevel, multiresolution algorithm for image processing and low-level robot vision tasks; (2) A Bayesian/geometric framework for 3-D shape estimation from 2-D images, appropriate for object recognition and other robot tasks; (3) A procedure for rotation and scale invariant representation (coding) and recognition of textures; a computationally efficient algorithm for estimating Markov random fields; and (4) mathematical results were obtained concerning the convergence and speed of convergence of computational algorithms such as the annealing algorithm. Also studied mathematically were the consistency and asymptotic normality of Maximum Likelihood Estimators for Gibbs distributions. GRA

N90-15644# Rochester Univ., NY. Dept. of Computer Science.
PRINCIPLES AND ALGORITHMS FOR CAUSAL REASONING WITH UNCERTAINTY
Jay Weber May 1989 113 p
(Contract N00014-82-K-0193)
(AD-A214248; TR-287) Avail: NTIS HC A06/MF A01 CSCL 12/4

This thesis examines representational issues that arise when reasoning about causes and effects given incomplete and uncertain knowledge about the domain. These issues are largely covered by the famous frame and qualification problems. This thesis shows how traditional nonmonotonic logic approaches can be modified to address these problems in a simple, domain-dependent way. this nonmonotonic approach is then generalized to manipulate statistically-founded beliefs, allowing for more consistent and fine-grained representation of causal knowledge. In addition, this thesis presents an algorithmic approach for efficient parallel computation of statistical predictions. This approach involves two heuristics, highest impact first and highest impact remaining, which control the speed of convergence and error estimation for an algorithm that iteratively refines degrees of belief. This algorithm has been implemented and tested by a program called HITEST, which runs on parallel hardware. GRA

N90-15645# Rome Air Development Center, Griffiss AFB, NY.
KNOWLEDGE BASED TEXT GENERATION Final Report, Oct. 1987 - Oct. 1988 M.S. Thesis - Cambridge Univ., England
Mark T. Maybury Aug. 1989 108 p
(AD-A214273; RADC-TR-89-93) Avail: NTIS HC A06/MF A01 CSCL 12/5

A theory is developed for text generation and describes an implemented computational model of this theory. The theory attempts both domain independency at the knowledge level and language independency at the linguistic level by drawing and expanding upon previous work in discourse schema and grammatical relations, respectively. The implemented system, GENNY, generates coherent texts by employing discourse strategies (which occur in human produced text) in parallel with pragmatic constraints (e.g., focus and context). The report begins with an introduction and summary of the research performed. This is followed by a survey of the text generation literature which places GENNY in the context of past language production research. Next, the motivation for the theoretical position adopted is discussed followed by detail of the theory on a knowledge, pragmatic, semantic, relational, and syntactic level, with illustration of the practical implementation throughout. Results of GENNY's test production from two frame knowledge bases (neuropsychology and photography) are then presented together with preliminary interlingual test results (English and Italian). GENNY is evaluated

with respect to state-of-the-art generators and is shown to be equivalent and, in some respects, superior, in competence and performance. In conclusion, the contributions and limitations of the system are discussed for further development are suggested. GRA

N90-15646# University of Southern California, Redondo Beach. Behavioral Technology Labs.
TOOLS FOR SIMULATION-BASED TRAINING Final Report, Jun. 1987 - Aug. 1989
Douglas M. Towne and Allen Munro 2 Oct. 1989 54 p Sponsored in cooperation with AF Human Resources Lab.
(Contract N00014-87-C-0489)
(AD-A214307; TR-113) Avail: NTIS HC A04/MF A01 CSCL 05/6

The Intelligent Maintenance Training System (IMTS) is a set of software tools that permits the composition and presentation of interactive graphical simulations for computer-based technical training. IMTS is designed to support training on the operation and maintenance of complex devices. Simulations are authored by device experts, who use the IMTS tools to draw the components of the device to describe their behavior, and to create simulations made up of the components. IMTS provides special support for maintenance training. An artificial expert on troubleshooting strategy, called Profile, generates instruction and advice for students. RAPIDS is an additional set of tools, built on the foundation of IMTS, that enables the authoring of a wide variety of simulation-based training courses. Using RAPIDS, an expert creates lessons by performing in the simulation the tasks that are to be taught to students. GRA

N90-15647# Cornell Univ., Ithaca, NY. Dept. of Computer Science.
A PARADIGM FOR ROBUST GEOMETRIC ALGORITHMS
John E. Hopcroft and Peter J. Kahn Oct. 1989 66 p Sponsored in cooperation with ARO
(Contracts N00014-86-K-0281; N00014-88-K-0591; NSF DMC-86-17355; NSF DMS-87-02070)
(AD-A214324; TR-89-1044) Avail: NTIS HC A04/MF A01 CSCL 12/5

Geometrical algorithms in use in computer aided design systems today often fail for numerical reasons. The cause of these failures usually can be traced to logical decisions such as branch on zero that depend on the results of numerical calculations. Numerical inaccuracies, introduced either in the initial data or in the finite-precision arithmetic that is used, may result in a set of logical decisions that are inconsistent. This loss of logical consistency usually proves fatal to the algorithm. Interest is in geometric algorithms that are robust in the sense that they are provably immune to such potential problems. A paradigm is explored that should have wide applicability for producing robust algorithms, and it applies the paradigm to the task of intersecting two convex polyhedral objects. The paradigm was previously used in an implementation of an algorithm for intersecting polyhedral objects that was substantially more robust than algorithms implemented earlier. This paper is a first step in developing a mathematical framework that justifies the underlying ideas in this implementation. In particular, an important tool in this work is a method of manipulating embedded polyhedra in ways consistent with their topology. GRA

N90-15648# Rochester Univ., NY. Dept. of Computer Science.
HIERARCHICAL PROCESS COMPOSITION: DYNAMIC MAINTENANCE OF STRUCTURE IN A DISTRIBUTED ENVIRONMENT Ph.D. Thesis
Stuart Arthur Friedberg 1988 166 p
(Contracts N00014-80-C-0197; N00014-82-K-0193; DACA76-85-C-0001; NSF DCR-83-20136)
(AD-A214325; TR-294) Avail: NTIS HC A08/MF A01 CSCL 12/5

A method, called Hierarchial Process Composition (HPC), is studied for organizing, developing, and maintaining large distributed programs. HPC extends the process abstraction to nested collections of processes, allowing a multiprocess program in place of any single process, and provides a rich set of structuring mechanisms for building distributed applications. The emphasis in HPC is on structural and architectural issues in distributed software systems, especially interactions involving dynamic reconfiguration, protection, and distribution. The major contributions come from the detailed consideration, based on case studies, formal analysis, and a prototype implementation, of how abstraction and composition interact in unexpected ways with each other and with a distributed environment. HPC ties processes together with heterogeneous interprocess communication mechanisms, such as TCP/IP and remote procedure call. Explicit structure determines the logical connectivity between processes, masking differences in communication mechanisms. HPC supports one-to-one, parallel channel, and many-to-many (multicasting) connectivity. Efficient computation of end-to-end connectivity from the communication structure is a challenging problem, and a third-party connection facility is needed to implement dynamic reconfiguration when the logical connectivity changes. GRA

N90-15649# Rochester Univ., NY. Dept. of Computer Science.
A STRUCTURED CONNECTIONIST APPROACH TO DIRECT INFERENCES AND FIGURATIVE ADJECTIVE-NOUN COMBINATIONS Ph.D. Thesis
Susan Hollbach Weber May 1989 182 p
(Contracts N00014-82-K-0193; N00014-84-K-0655)
(AD-A214326; TR-289) Avail: NTIS HC A09/MF A02 CSCL 12/5

This work was motivated by the observation that categories have internal structure sufficiently sophisticated to capture a variety of effects, ranging from the direct inferences arising from adjectival modification of nouns to the ability to comprehend figurative usages. The design of the internal structure of category representation is constrained by the model requirements of the connectionist implementation and by the observable behaviors exhibited in direct inferences. The former dictates the use of a spreading activation format, and the latter indicates some to the topology and connectivity of the resultant semantic network. The connectionist knowledge representation scheme described in this thesis is based on the idea that categories and concepts are context sensitive and functionally structured. Each functional property value of a category motivates a distinct aspect of that category's internal structure. This model of cognition, as implemented in a structured connectionist knowledge representation system, permits the system to draw immediate inferences, and, when augmented with property inheritance mechanisms, mediated inferences about the full meaning of adjective-noun combinations. These inferences are used not only to understand the implicit references to correlated properties (a green peach is unripe) but also to make sense of figurative adjective uses, by drawing on the connotations of the adjective in literal contexts. GRA

N90-15650# Spectral Sciences, Inc., Burlington, MA.
MODTRAN: A MODERATE RESOLUTION MODEL FOR LOWTRAN 7 Final Report, 12 May 1986 - Apr. 1989
Alexander Berk, Lawrence S. Bernstein, and David C. Robertson 30 Apr. 1989 48 p
(Contract F19628-86-C-0079; AF Proj. 7670)
(AD-A214337; SSI-TR-154; GL-TR-89-0122) Avail: NTIS HC A03/MF A01 CSCL 12/5

The LOWTRAN computer codes, with LOWTRAN 7 being the most current version, are widely used to calculate atmospheric transmittance and/or radiance in the infrared, visible and near ultraviolet spectral regions; LOWTRAN 7 was extended to include the microwave spectral region. The code is easily used, runs quickly and provides the user with a wide variety of atmospheric models and options. Its spectral resolution is 20 1/cm Full Width/Half Maximum (FWHM) with calculations being done in 5 1/cm increments. This report describes work done to increase LOWTRAN's spectral resolution from 20 to 2 1/cm (FWHM). Specifically, the technical objectives for this program were: to develop algorithms providing 2 1/cm resolution (FWHM); to model molecular absorption of atmospheric molecules as a function of

temperature and pressure; to calculate band model parameters for twelve LOWTRAN molecular species; and to integrate the LOWTRAN 7 capabilities into the new algorithms, maintaining compatibility with the multiple scattering option. MODTRAN, the final product of this effort, is a moderate resolution LOWTRAN code. Molecular absorption is calculated in 1 1/cm spectral bins, while the other parts of the calculation remain unchanged. The molecular species affected are: water vapor, carbon dioxide, ozone, nitrous oxide, carbon monoxide, methane, oxygen, nitric oxide, sulfur dioxide, nitrogen dioxide, ammonia, and nitric acid. GRA

N90-15651# Oak Ridge National Lab., TN. Engineering Physics and Mathematics Div.
NEURAL NETWORK MODELS FOR LINEAR PROGRAMMING
Jean-Christophe Culioli, Vladimir Protopopescu, Charles L. Britton, Jr., and Milton N. Ericson 1989 5 p Presented at the International Joint Conference on Neural Networks, Washington, DC, 15-19 Jan. 1990
(Contract DE-AC05-84OR-21400)
(DE89-015974; CONF-900116-2) Avail: NTIS HC A01/MF A01

A neural network is presented that solves the general Linear Programming (LP) problem. In the first part, Hopfield and Tank's circuit for LP is recalled and it shows that although it converges to stable states, it does not, in general, yield admissible solutions. This is due to the penalization treatment of the constraints. In the second part, an approach is proposed based on Lagragrange multipliers that converges to primal and dual admissible solutions. It is also shown that the duality gap (measuring the optimality) can be rendered, in principle, as small as needed. DOE

N90-15652# Oak Ridge National Lab., TN. Engineering Physics and Mathematics Div.
A NEURAL NETWORK FOR BOUNDED LINEAR PROGRAMMING
Jean-Christophe Culioli, Vladimir Protopopescu, Charles L. Britton, Jr., and Milton N. Ericson 1989 5 p Presented at the International Joint Conference on Neural Networks, Washington, DC, 15-19 Jan. 1990
(Contract DE-AC05-84OR-21400)
(DE89-015975; CONF-900116-3; CESAR-89/33) Avail: NTIS HC A01/MF A01

The purpose of this paper is to describe a neural network implementation of an algorithm recently designed to solve the Transportation and the Assignment Problems, and, more generally, any explicitly bounded linear program. DOE

N90-15653# Oak Ridge National Lab., TN. Energy Div.
ESTIMATING DEPARTURE TIMES FROM TRAFFIC COUNTS USING DYNAMIC ASSIGNMENT
Bruce N. Janson and Frank Southworth Jul. 1989 20 p Presented at the Transportation Research Board Meeting, Washington, DC, Jan. 1990
(Contract DE-AC05-84OR-21400)
(DE89-016259; CONF-900121-1) Avail: NTIS HC A03/MF A01

A dynamic traffic assignment algorithm and observed traffic counts are used to estimate the distribution of departure times in a trip matrix. The objective is to find the maximum entropy distribution of departure times by origin zone subject to observed traffic counts on a subset of network links. The procedure results in the estimated number of trip departures from each origin in 10 to 15 minute time intervals of the full analysis period. Such an analysis period will typically range from one to three hours long. We first review the dynamic assignment algorithm developed and tested in a previous paper, and then describe its use with traffic counts to estimate the departure times of a trip matrix. We present an application to a Pittsburgh network in which trip departures are estimated for each 10-minute interval of a peak-hour survey trip matrix. Computational advances such as parallel computing will enable the procedure to be run on large networks while counts are being monitored. Such an application may provide near real-time detection of temporal trip departure profiles by origin zone. DOE

62 COMPUTER SYSTEMS

Includes computer networks and special application computer systems.

N90-15654*# Draper (Charles Stark) Lab., Inc., Cambridge, MA.
INVESTIGATION OF THE APPLICABILITY OF A FUNCTIONAL PROGRAMMING MODEL TO FAULT-TOLERANT PARALLEL PROCESSING FOR KNOWLEDGE-BASED SYSTEMS Final Report
Richard Harper Dec. 1989 31 p
(Contract NAS1-18565)
(NASA-CR-181938; NAS 1.26:181938) Avail: NTIS HC A03/MF A01 CSCL 09B

In a fault-tolerant parallel computer, a functional programming model can facilitate distributed checkpointing, error recovery, load balancing, and graceful degradation. Such a model has been implemented on the Draper Fault-Tolerant Parallel Processor (FTPP). When used in conjunction with the FTPP's fault detection and masking capabilities, this implementation results in a graceful degradation of system performance after faults. Three graceful degradation algorithms have been implemented and are presented. A user interface has been implemented which requires minimal cognitive overhead by the application programmer, masking such complexities as the system's redundancy, distributed nature, variable complement of processing resources, load balancing, fault occurrence and recovery. This user interface is described and its use demonstrated. The applicability of the functional programming style to the Activation Framework, a paradigm for intelligent systems, is then briefly described. Author

N90-15655# Lawrence Livermore National Lab., CA. User Systems Div.
SIMULATING THE SCHEDULING OF PARALLEL SUPERCOMPUTER APPLICATIONS
Mark K. Seager and James M. Stichnoth 19 Sep. 1989 30 p Presented at the Parallelization Discussions, Yorktown Heights, NY, 2-3 Nov. 1989
(Contract W-7405-eng-48)
(DE90-003604; UCRL-102059; CONF-8911132-1) Avail: NTIS HC A03/MF A01

An Event Driven Simulator for Evaluating Multiprocessing Scheduling (EDSEMS) disciplines is presented. The simulator is made up of three components: machine model; parallel workload characterization; and scheduling disciplines for mapping parallel applications (many processes cooperating on the same computation) onto processors. A detailed description of how the simulator is constructed, how to use it and how to interpret the output is also given. Initial results are presented from the simulation of parallel supercomputer workloads using Dog-Eat-Dog, Family and Gang scheduling disciplines. These results indicate that Gang scheduling is far better at giving the number of processors that a job requests than Dog-Eat-Dog or Family scheduling. In addition, the system throughput and turnaround time are not adversely affected by this strategy. DOE

N90-15656# Unisys Corp., Paoli, PA. Research Center.
MASC: MULTIPROCESSOR ARCHITECTURE FOR SYMBOLIC PROCESSING Final Report, Mar. 1986 - Sep. 1988
William C. Hopkins, Tom M. Blenko, Keith Cassell, Judy P. Clark, Joel B. Coltoff, Daniel R. Corpron, Massoud Farhang, Lynette Hirschman, Donald P. McKay, and Robert C. Smith Aug. 1989 358 p
(Contract F30602-86-C-0093)
(AD-A213504; RADC-TR-89-108) Avail: NTIS HC A16/MF A02 CSCL 12/5

The MASC program addresses the support of symbolic computation for Artificial Intelligence (AI), as part of the DARPA Strategic Computing Program. The work has been aimed at the fundamental questions of choosing an appropriate programming model for AI and finding efficient implementation techniques to support it on multiprocessor systems. The Strategic Computing Program is motivated by the need to provide real-time response by AI subsystems in planned or contemplated DOD systems. Our

efforts have directly supported this goal, contributing fundamental results in language design, language implementation, and application parallelism. The work has been driven by the needs of real AI applications, drawn from our substantial experience in natural language processing, knowledge representation, and expert systems. The technologies we have developed are broadly applicable, and several specific recommendations for their further development and application are presented. The most profound result is the design and demonstration of a powerful technique for the compilation of logic programs to applicative form. This brings the power of compilation and optimization techniques for functional programming to bear on logic programming languages. We recommend that these technology be extended and applied to current research efforts in language design for very high level programming and program prototyping. GRA

N90-15657# Royal Norwegian Council for Scientific and Industrial Research, Kjeller.

A MULTICHANNEL PROCESSING APPROACH TO REAL TIME NETWORK DETECTION, PHASE ASSOCIATION, AND THRESHOLD MONITORING Scientific Report No. 1, 1 Feb. - 30 Apr. 1989

Frode Ringdal and Tormod Kvaerna 31 May 1989 39 p
(Contract F49620-89-C-0038; ARPA Order 5307)
(AD-A213940; NORSAR-CONTRIB-406; GL-TR-89-0171) Avail: NTIS HC A03/MF A01 CSCL 12/7

This paper presents an approach to multichannel processing of data recorded by a network of stations which represents an extension of the delay-and-sum beamforming traditionally applied in array processing. A number of geographical beam-steering points are defined, and for each beam a set of time-aligned traces derived from the network stations are processed together so as to extract, for each step in time, a set of features corresponding to that particular beam. Applying this approach to the network of the three regional arrays NORESS, ARCESS and FINESA in Fennoscandia, we demonstrate its usefulness for associating regional phases detected at individual arrays and originating from the same event. We also give an example of application addressing the problem of continuously monitoring the seismic noise field. GRA

N90-15658# Massachusetts Inst. of Tech., Cambridge. Lab. for Computer Science.

ADAPTIVE BACKOFF SYNCHRONIZATION TECHNIQUES

Anant Agarwal and Mathews Cherian Jun. 1989 23 p Presented at the 16th Annual Symposium on Computer Architecture, Jerusalem, Israel, Jun. 1989 Sponsored in part by IBM
(Contract N00014-87-K-0825)
(AD-A213966; MIT/LCS/TM-396) Avail: NTIS HC A02/MF A01 CSCL 12/6

Shared-memory multiprocessors commonly use shared variables for synchronization. Our simulations of real parallel applications show that large-scale cache-coherent multiprocessors suffer significant amounts of invalidation traffic due to synchronization. Large multiprocessors that do not cache synchronization variables are often more severely impacted. If this synchronization traffic is not reduced or managed adequately, synchronization references can cause severe congestion in the network. We propose a class of adaptive backoff methods that do not use any extra hardware and can significantly reduce the memory traffic to synchronization variables. These methods use synchronization state to reduce polling of synchronization variables. Our simulations show that when the number of processors participating in a barrier synchronization is small compared to the time of arrival of the processors, reductions of 20 percent to over 95 percent in synchronization traffic can be achieved at no extra cost. In other situations adaptive backoff techniques result in a tradeoff between reduced network accesses and increased processor idle time. GRA

N90-15659# Florida Univ., Gainesville. Dept. of Electrical Engineering.

ULTRA HIGH PERFORMANCE, HIGHLY RELIABLE, NUMERIC INTENSIVE PROCESSORS AND SYSTEMS Final Report, 20 May 1987 - 19 Sep. 1989

Fred J. Taylor Oct. 1989 36 p
(Contract DAAL03-87-K-0080)
(AD-A214100; ARO-24116.13-EL) Avail: NTIS HC A03/MF A01 CSCL 12/6

Arithmetic bandwidth remains one of the principal bottlenecks in real-time-high-end signal, image, and data processing applications. The problem is compounded when complex arithmetic is required. The problem, unfortunately, does not stop there. For military applications, size (volume) and power dissipation often are as important as bandwidth. Unfortunately speed and complexity (size-power) metrics are often in conflict. As a result, the defense signal processing systems designer finds that performance requirements often cannot be satisfied with contemporary hardware. As performance demands escalate, the gap between computational bandwidth and packaging will also increase. This will further stress a defense signal processing system. To achieve the numeric data processing speeds required in very high-end applications, a highly parallel arithmetic system called the residue number system (RNS) is considered. Recent results in this field have provided a framework in which very fast, reliable, and compact VLSI digital systems can be fabricated. It will be shown that the developed system exhibits a number of advantages which including speed and compactness. The reported technology is a central processing element for a signal processing system under development called the Gauss Machine. GRA

N90-15660# Naval Postgraduate School, Monterey, CA.

POLYNOMIAL TRANSFER LOT SIZING TECHNIQUES FOR BATCH PROCESSING ON CONSECUTIVE MACHINES Final Report

Dan Trietsch Sep. 1989 52 p
(AD-A214198; NPS54-89-011) Avail: NTIS HC A04/MF A01 CSCL 13/8

Using transfer lots, we can overlap the processing of a batch on several consecutive machines, and thus reduce the makespan considerably. This in turn promotes work-in-process reduction. In this paper we investigate the transfer lots sizing problem for a given batch size under two operating procedures. Our objective is to minimize the makespan subject to a transferring budget. An important part of the solution involves partitioning the problem to subsets of machines without losing optimality. For each part (subset), the first and the last machines operate continuously while intermediate machines may idle intermittently. The first operating procedure we consider calls for the lots to be identical across all machines in each subset. The second operating procedure allows sub-lots for some of the machines or for some of the lots. Through more elaborate, the second operating procedure yields demonstrably superior results. The techniques provide satisfying feasible solutions, which can also serve as efficient bounds for an exact branch and bound inter linear programming model. GRA

N90-15661# Sandia National Labs., Albuquerque, NM. Exploratory Systems Development Div.

ONE-CLASS GENERALIZATION IN SECOND-ORDER BACKPROPAGATION NETWORKS FOR IMAGE CLASSIFICATION

Mary M. Moya and Larry D. Hostetler 1989 5 p Presented at the International Joint Conference on Neural Networks, Washington, DC, 15-19 Jan. 1990
(Contract DE-AC04-76DP-00789)
(DE89-015845; SAND-89-1916C; CONF-900116-1) Avail: NTIS HC A01/MF A01

It was earlier reported that it is possible to train a first order multilayer feedforward network with backpropagation to classify raw 8-bit images of vehicles. It was concluded that a linear feedforward network is capable of within-class generalization when trained with perspective views taken every 10 degree, but it is

incapable of one-class generalization. The results are described of a set of experiments to train a feedforward network with second order inputs to perform one-class classification on image data. The results are compared of the first order network and the second-order network and show that the second order network is better able to generalize as a one-class classifier. DOE

63 CYBERNETICS

Includes feedback and control theory, artificial intelligence, robotics and expert systems.

For related information see also *54 Man/System Technology and Life Support.*

N90-15662# Montana State Univ., Bozeman. Dept. of Electrical Engineering.
COMPUTER CONTROLLED MHD POWER CONSOLIDATION AND PULSE-GENERATION SYSTEM Technical Progress Report, Oct. 1988 - Mar. 1989
R. Johnson, K. Marcotte, and M. Donnelly 1989 9 p
(Contract DE-AC22-87PC-79680)
(DE90-001224; DOE/PC-79680/T2; ERL-290666-1) Avail: NTIS HC A03/MF A01

The major goal of this research project is to establish the feasibility of a power conversion technology which will permit the direct synthesis of computer programmable pulse power. Feasibility will be established by demonstration of direct synthesis of commercial frequency power by means of computer control. The power input to the conversion system is assumed to be a MHD Faraday connected generator which may be viewed as a multi-terminal d.c. source. This consolidation/inversion process is referred to subsequently as Pulse Amplitude Synthesis and Control (PASC). A secondary goal is to deliver a controller subsystem consisting of a computer, software, and computer interface board which can serve as one of the building blocks for a possible phase 2 prototype system. This report contains discussions on the following areas: description of test transformer configurations for preliminary testing of the PASC power supply and computer control subsystems; results of test transformer testing; conclusions from preliminary testing results and new PASC configuration; control algorithms and data acquisition; feasibility demonstration testing. DOE

N90-15663# Oak Ridge National Lab., TN. Intelligent Systems Section.
DESIGN AND IMPLEMENTATION OF TWO CONCURRENT MULTI-SENSOR INTEGRATION ALGORITHMS FOR MOBILE ROBOTS
J. P. Jones, M. Beckerman, and R. C. Mann 1989 13 p Presented at the SPIE Symposium on Advances in Intelligent Robotic Systems, Philadelphia, PA, 5-8 Nov. 1989
(Contract DE-AC05-84OR-21400)
(DE90-003041; CONF-8911125-1) Avail: NTIS HC A03/MF A01

Two multi-sensor integration algorithms useful in mobile robotics applications are reviewed. A minimal set of utilities are then developed which enable implementation of these algorithms on a distributed memory concurrent computer. DOE

N90-15664*# Texas Univ., Austin. Dept. of Mechanical Engineering.
ARCHITECTURAL STUDY OF THE DESIGN AND OPERATION OF ADVANCED FORCE FEEDBACK MANUAL CONTROLLERS Final Report, 1 Nov. 1988 - 31 Jan. 1990
Delbert Tesar and Whee-kuk Kim Jan. 1990 235 p
(Grant NAG9-320)
(NASA-CR-185948; NAS 1.26:185948) Avail: NTIS HC A11/MF A02 CSCL 09B

A teleoperator system consists of a manual controller, control hardware/software, and a remote manipulator. It was employed in either hazardous or unstructured, and/or remote environments. In teleoperation, the main-in-the-loop is the central concept that brings human intelligence to the teleoperator system. When teleoperation involves contact with an uncertain environment, providing the feeling of telepresence to the human operator is one of desired characteristics of the teleoperator system. Unfortunately, most available manual controllers in bilateral or force-reflecting teleoperator systems can be characterized by their bulky size, high costs, or lack of smoothness and transparency, and elementary architectures. To investigate other alternatives, a force-reflecting, 3 degree of freedom (dof) spherical manual controller is designed, analyzed, and implemented as a test bed demonstration in this research effort. To achieve an improved level of design to meet criteria such as compactness, portability, and a somewhat enhanced force-reflecting capability, the demonstration manual controller employs high gear-ratio reducers. To reduce the effects of the inertia and friction on the system. various force control strategies are applied and their performance investigated. The spherical manual controller uses a parallel geometry to minimize inertial and gravitational effects on its primary task of transparent information transfer. As an alternative to the spherical 3-dof manual controller, a new conceptual (or parallel) spherical 3-dof module is introduced with a full kinematic analysis. Also, the resulting kinematic properties are compared to those of other typical spherical 3-dof systems. The conceptual design of a parallel 6-dof manual controller and its kinematic analysis is presented. This 6-dof manual controller is similar to the Stewart Platform with the actuators located on the base to minimize the dynamic effects. Finally, a combination of the new 3-dof and 6-dof concepts is presented as a feasible test-bed for enhanced performance in a 9-dof system. Author

N90-15665# Rochester Univ., NY. Dept. of Computer Science.
SOME COMPUTATIONAL PROPERTIES OF ROTATION REPRESENTATIONS
Christopher M. Brown 23 Aug. 1989 27 p
(Contracts DACA76-85-C-0001; F30602-85-C-0008)
(AD-A213888; TR-303) Avail: NTIS HC A03/MF A01 CSCL 12/9

There are four main parameterizations of the rotation group SO3. Two of them (rotation angle and axis, and the closely related quaternion components) as well as the matrix form of rotation representation are particularly of interest in computer vision, graphics, and robotics. Some of their computational properties are explored here. Operation counts are given for primitive operations of normalization, conversion, and application of the same or different rotations. The measure of accuracy is taken to be the length and direction of the resulting rotated vector. Some analytical analysis appears, but most conclusions are based on empirical tests at artificially reduced numerical precision. GRA

N90-15666# Massachusetts Inst. of Tech., Cambridge. Lab. for Computer Science.
USING MAPPINGS TO PROVE TIMING PROPERTIES
Nancy A. Lynch and Hagit Attiya 26 Sep. 1989 47 p
(Contracts N00014-85-K-0168; N00014-83-K-0125; N00014-89-J-1988; NSF CCR-86-11442)
(AD-A213967; MIT/LCS/TM-412) Avail: NTIS HC A03/MF A01 CSCL 12/5

A new technique for proving timing properties for timing-based algorithms is described; it is an extension of the mapping techniques previously used in proofs of safety properties for asynchronous concurrent systems. The key to the method is a way of representing timing information. Timing assumptions and timing requirements for the system are both represented in this way. A multivalued mapping from the assumptions automation to the requirements automation is then used to show that the given system satisfies the requirements. The technique is illustrated with two simple examples, a resource manager and a signal relay. GRA

N90-15667# Rochester Univ., NY. Dept. of Computer Science.
GAZE CONTROLS WITH INTERACTIONS AND DELAYS
Christopher M. Brown Mar. 1989 22 p
(Contract DACA76-85-C-0001)

(AD-A214286; TR-278) Avail: NTIS HC A03/MF A01 CSCL 12/9

Five control systems loosely corresponding to primate saccadic, vergence, pursuit, vestibulo-ocular, and head control operate on a simulated two-eyed robot head maneuvered by a robot arm. The goal is to get some qualitative understanding of the interaction of such reflexes under various assumptions. The simulation is meant to be relevant to U. Rochester's robot. Thus it incorporates kinematics of the robot head but assumes a tool-coordinate system available to robot arm commands, so that arm kinematic calculations are unnecessary. Dynamics are not modeled, since they are handled by the commercial controllers currently used in the Rochester robot. Even small delays render the effect of delay-free controllers unstable, but multi-delay version of a Smith predictor can cope with delays. If each controller acts on the predicted system and ignores other controllers, the situation is improved but still potentially unstable if controllers with different delays act on the same control output. The system's performance is much improved if controllers consider the effect of other controllers, and the resulting system is stable in the presence of a certain amount of stochastic disturbance of control delays and inputs, and also in the presence of systematic error arising from inaccurate plant and world models. GRA

N90-15668# Naval Postgraduate School, Monterey, CA. Dept. of Computer Science.

A NOTE ON THE MAXIMUM SIZE OF A RECTILINEAR MAZE

Technical Report, Sep. 1988 - Aug. 1989

Man-Tak Shing, Michael M. Mayer, and Kim A. S. Hefner Sep. 1989 11 p

(AD-A214445; NPS52-89-057) Avail: NTIS HC A03/MF A01 CSCL 12/9

The problem of searching through an unknown maze by a robot is studied and it is shown that the size of the largest rectilinear maze the robot can explore in at most k steps is bounded by 2K squred + 2k + 1 for mazes with circuits, and is bounded by 4k squared/3 + 8k/3 + 1 for mazes without circuits. Furthermore, it is shown that the bounds are tight. GRA

64 NUMERICAL ANALYSIS

Includes iteration, difference equations, and numerical approximation.

N90-15669# Technische Univ., Delft (Netherlands). Faculty of Technical Mathematics and Informatics.

ON THE SUM OF TWO MAXIMAL MONOTONE OPERATORS

Ph. Clement and P. Egberts 1989 20 p

(Rept-89-31; ISSN-0922-5641) Avail: NTIS HC A03/MF A01

Theorems are presented concerning nonlinear and linear equivalently maximal monotone operators in a real Hilbert space. Remarks on, and proofs of, the theorems are given, and a counterexample is included. Applications in an elliptic system are presented. ESA

N90-15670# Los Alamos National Lab., NM. Theoretical Div.

GENERAL MANY-BODY SYSTEMS

S. A. Trugman 1989 27 p Presented at the NATO Advanced Summer School on Applications of Statistical and Field Theory To Condensed Matter, Evora, Portugal, May 1989

(Contract W-7405-eng-36)

(DE90-000685; LA-UR-89-3249; CONF-8905225-1) Avail: NTIS HC A03/MF A01

The problem of how to visualize and sometimes solve a general many-body system is considered. The ideas are established in the context of very simple small systems, a Hubbard model and a coupled electron-phonon model, both on two lattice sites. These models are also solved to good approximation in the thermodynamic limit, although the Hubbard model is restricted to a small number of holes away from the Mott insulating state. Response functions are also considered. A fairly general many-body Hamiltonian is considered. It consists of an electron or other fermion kinetic energy and electron-electron interactions, which may be coupled to a bose field such as a phonon. The phonons themselves may be nonlinear (have self-interactions). The system may be strongly coupled. One may also add coupling to an external driving field, such as an ac electric field. The methods discussed are nonperturbative, and so differ from the standard methods of diagrammatic perturbation theory. A comparison is made with diagrammatic methods in the context of the random phase approximation. DOE

N90-15671# International Centre for Theoretical Physics, Trieste (Italy).

MODULAR INVARIANTS FOR THETA-FUNCTIONS WITH CHARACTERISTICS AND THE TWISTED N=2 SUPERCONFORMAL AND SU(2) KAC-MOODY ALGEBRAS

V. K. Dobrev and A. H. Ganchev (Bulgarian Academy of Sciences, Sofia.) May 1989 16 p Submitted for publication Sponsored in part by Ministry of Science, Culture, and Education of Bulgaria

(DE89-635701; IC-89/84) Avail: NTIS (US Sales Only) HC A03/MF A01

The modular invariants are classified for theta-functions with characteristics relevant for the twisted N=2 super-Virasoro and the twisted SU(2) Kac-Moody algebras. Detailed and complete proofs are given. Based on this the classification of the modular invariants are given for the above algebras. DOE

N90-15672# Sandia National Labs., Albuquerque, NM.

OUTLIER DETECTION IN MULTIVARIATE CALIBRATION

Edward V. Thomas and David M. Haaland 1989 22 p Presented at the American Institute of Chemical Engineers Annual Meeting, San Francisco, CA, 5-10 Nov. 1989

(Contract DE-AC04-76DP-00789)

(DE90-001502; SAND-89-0965C; CONF-891113-3) Avail: NTIS HC A03/MF A01

Outlier samples can have very detrimental effects on the performances of multivariate calibration methods, as these methods are generally not very robust. Often, the software implementations of these methods do not check for outliers. If outliers are not detected, invalid predictions may result. This paper illustrates some simple exploratory procedures for detecting outliers with examples from near-infrared and mid-infrared spectroscopy using partial least-squares regression as the calibration method. DOE

N90-15673# Texas Univ., Austin. Inst. for Fusion Studies.

INTRODUCTION TO BIFURCATION THEORY

John David Crawford, Chris Kueny, Bill Saphir, and Brad Shadwick Nov. 1989 73 p

(Contract DE-FG05-80ET-53088)

(DE90-003319; DOE/ET-53088/407; IFSR-407) Avail: NTIS HC A05/MF A01

Bifurcation theory is a subject with classical mathematical origins. The modern development of the subject starts with Poincare and the qualitative theory of differential equations. In recent years, the theory has undergone a tremendous development with the infusion of new ideas and methods from dynamical systems theory, singularity theory, group theory, and computer-assisted studies of dynamics. As a result, it is difficult to draw the boundaries of the theory with any confidence. In this review, the objects in question are parameterized families of dynamical systems (vector fields or maps). In the sciences these families commonly arise when one formulates equations of motion to model a physical system. We specifically analyze how the time evolution near an equilibrium can change as parameters are varied; for simplicity we consider the case of a single parameter only. DOE

N90-15674# International Centre for Theoretical Physics, Trieste (Italy).

MIXED SINGULAR LINEAR ELLIPTIC EQUATIONS

Duong Minh Duc and Stephan Luckhaus (Bonn Univ., Germany, F.R.) May 1989 19 p Submitted for publication

(DE90-600722; IC-89/57) Avail: NTIS (US Sales Only) HC A03/MF A01

The existence and nontangent convergence properties of solutions of mixed singular elliptic equations are established.
DOE

N90-15675# International Centre for Theoretical Physics, Trieste (Italy).
SL(2,R) CURRENT ALGEBRA IN TWO-DIMENSIONAL CONFORMAL QUANTUM GRAVITY
E. Abdalla, M. C. B. Abdalla, and A. Zadra Apr. 1989 8 p Prepared in cooperation with Sao Paulo Univ., and Universidade Estadual de Paulista Submitted for publication
(DE90-600755; IC-89/56) Avail: NTIS (US Sales Only) HC A02/MF A01

The SL(2,R) current algebra in conformal two-dimensional gravity is obtained directly from the residual symmetries of the theory in light-cone gauge. The relation of the theory with previous results is discussed.
DOE

N90-15676# Maryland Univ., College Park. Dept. of Mathematics.
HIGHER ORDER CROSSINGS FROM A PARAMETRIC FAMILY OF LINEAR FILTERS
Benjamin Kedem and Ta-hsin Li Sep. 1989 46 p
(Contract N00014-89-J-1051; AF-AFOSR-0049-89)
(AD-A213427; MD89-47-KDM/THL; TR89-47) Avail: NTIS HC A03/MF A01 CSCL 12/1

When a time series is filtered, the effect of the filter can be described by counting the resulting number of zero-crossings. By extension, a time series can be applied to a family of filters and obtain the corresponding family of zero-crossing counts. The resulting family of counts is referred to as Higher Order Crossings or HOC. Thus, HOC are zero-crossing counts observed in a time series and in its filtered versions. The main application of HOC is in the description of the oscillation observed in oscillatory time series. Moreover, in the special case of stationary Gaussian time series there are quite a few HOC families and also HOC sequences that determine the spectrum up to a constant. Examples are defined and given for HOC from parametric families of linear filters. The motivation for studying HOC is outlined in connection with oscillatory time series. An adaptive HOC sequence form (0.1) is constructed that converges to a frequency in the presence of noise. As a matter of fact, the main result there, Corollary 1, has prompted interest in pursuing HOC in connection with parametric linear operations. More results about the HOC family from (0.1) were obtained. The main result there is the connection between the zero-crossing rate, as a function of the parameter, and the correlation generating function under the Gaussian assumption. A vocal sound time series of a megaptera novaeangliae whale is analyzed.
GRA

N90-15677# Washington Univ., Seattle. Dept. of Statistics.
RECURRENCE AND ERGODICITY FOR EXPONENTIAL FAMILY STATE-SPACE MODELS Technical Report, 1 Sep. 1988 - 31 Aug. 1989
Gary Grunwald (Melbourne Univ., Carlton, Australia), Peter Guttorp, and Adrian Raftery Aug. 1989 13 p
(Contract N00014-88-K-0265)
(AD-A213466; TR-173) Avail: NTIS HC A03/MF A01 CSCL 12/3

Two results are given concerning the properties of state-space models with exponential family observation distribution and conjugate state distribution. The first result gives a simple and general interpretation of the parameters of the predictive state distribution in terms of the observation forecast distribution. The second result shows how the first result can be used to check the long term model properties of recurrence and ergodicity for a class of non-Gaussian observation distributions. In particular, these results apply to models with Poisson, binomial and multinomial observation distributions.
GRA

N90-15678# Wisconsin Univ., Madison. Center for Mathematical Sciences.
QUASI INTERPOLANTS AND APPROXIMATION POWER OF MULTIVARIATE SPLINES Technical Summary Report
Carl deBoor 25 Sep. 1989 36 p
(Contract DAAL03-87-K-0030; NSF DMS-87-01275)
(AD-A213535; CMS-TSR-90-12) Avail: NTIS HC A03/MF A01 CSCL 12/1

The determination of the approximation power of spaces of multivariate splines with the aid of quasi interpolants is reviewed. In the process, streamlined description of the existing quasi interpolants theory is given. A brief review is given of the approximation power of univariate splines since the techniques for its investigation are also those with which people have tried to understand the multivariate setup. (That may in fact be the reason why so little is known about it.) Three examples are then discussed to illustrate some basic limitations of the standard univariate approach.
GRA

N90-15679# Wisconsin Univ., Madison. Center for the Mathematical Sciences.
SOME RESULTS ON CONNECTING ORBITS FOR A CLASS OF HAMILTONIAN SYSTEMS
Paul H. Rabinowitz and Kazunaka Tanaka 17 Oct. 1989 34 p
(Contracts DAAL03-87-K-0043; N00014-88-K-0134; NSF MCS-81-10556)
(AD-A213536; CMS-TSR-90-17) Avail: NTIS HC A03/MF A01 CSCL 12/1

The existence of various kinds of connecting orbits is established for a certain Hamiltonian system as well as its time dependent analogue. For the autonomous case, the main assumption is that V has a global maximum, e.g., at $X = O$ and various kinds of orbits terminating at O are found. For the time dependent case V has a local but not global maximum at $X = O$ and a homoclinic orbit emanating from and terminating at O was found.
GRA

N90-15680# Missouri Univ., Columbia. Dept. of Psychology.
NUMERICAL FACILITY: CONVERGENCE OF COGNITIVE AND FACTOR ANALYTIC MODELS Final Scientific Report, 1 Aug. 1988 - 31 Jul. 1989
David C. Geary 30 Sep. 1989 97 p
(Grant AF-AFOSR-0239-88; AF Proj. 2313)
(AD-A213627; AFOSR-89-1273TR) Avail: NTIS HC A05/MF A01 CSCL 12/9

Results are reported for a study comparing the pattern of convergent and discriminant validity in relating information processing variables which represent basic numerical operations, an index of the facility of performing these operations within working memory, and ability measures defining Numerical Facility, Perceptual Speed, General Reasoning, and Memory Span. Analyses supported theoretically expected patterns of convergent and discriminant validity in relating process variables to individual-differences measures. The data also indicated that the relationship between distinct ability factors was due to common underlying operations. Different sets of ability factors, however, were found to correlate for different reasons, and not because of a pervasive general ability spanning all cognitive domains. Finally, implications for the nature of individual differences in human abilities were discussed.
GRA

N90-15681# Colorado Univ., Boulder. Dept. of Computer Science.
TENSOR METHODS FOR UNCONSTRAINED OPTIMIZATION USING SECOND DERIVATIVES Technical Report, 15 May 1989 - 14 May 1990
Robert B. Schnabel and Ta-Tung Chow 25 Jul. 1989 41 p
(Contract DAAL03-88-K-0086; NSF CCR-87-02403)
(AD-A213642; CU-CS-439-89; ARO-24923.4-MA) Avail: NTIS HC A03/MF A01 CSCL 12/4

A new type of method is introduced for unconstrained optimization, which is called a tensor method. It is related in its basic philosophy to the tensor methods for nonlinear equations of

Schnabel and Frank, but beyond that the methods have significant differences. The tensor method for unconstrained optimization bases each iteration upon a 4th order model of the objective function. This model consists of the quadratic portion of the Taylor series, plus low rank 3rd and 4th order terms that cause the model to interpolate already calculated function and gradient values from one or more previous iterates. It is shown that the costs of forming, storing, and solving the tensor model are not significantly more than these costs for a standard method based upon a quadratic Taylor series model. Test results are presented for sets of problems where the Hessian at the minimizer is nonsingular, and where it is singular. On all the test sets, the tensor method solves considerably more problems than a comparable standard method. On problems solved by both methods, the tensor method requires about half as many iterations, and half as many function and derivative evaluations as the standard method, on the average. GRA

N90-15682# Florida State Univ., Tallahassee.
TWO BASIC PARTIAL ORDERINGS FOR DISTRIBUTIONS DERIVED FROM SCHUR FUNCTIONS AND MAJORIZATION
Kumar Joag-Dev (Illinois Univ., Chicago.) and Jayaram Sethuraman Sep. 1989 13 p
(Contract DAAL03-86-K-0094)
(AD-A213703; FSU-TR-M-814; ARO-23699.25-MA) Avail: NTIS HC A03/MF A01 CSCL 12/1

Researchers in applied fields have long recognized the usefulness of inequalities when exact results are not available. The use of inequalities allows one to state that one estimate is better than another, that one maintenance policy is better than another or that a certain selection procedure is better than another or that a certain selection procedure is better than another etc., even though, the best estimator may not be known, nor the best maintenance policy or the best selection procedure. Such results are generally obtained from inequalities between two probability measures or random variables. Inequalities between random variables are in turn obtained from deterministic inequalities or deterministic partial orderings. Herein, the essentials of stochastic majorization and DT ordering are described and some applications demonstrated. A new proof of a slight generalization of earlier result on DT functions is given. GRA

N90-15683# Rome Univ. (Italy). Dept. of Mathematics.
NUMERICAL OPTIMIZATION Periodic Report No. 6, Jul. 1988 - Jan. 1989
Francesco Zirilli Jan. 1989 11 p
(Contract DAJA45-86-C-0028)
(AD-A213758) Avail: NTIS HC A03/MF A01 CSCL 12/1

This is the Sixth Periodic Report on Contract DAJA 45-86-0028. It contains a statement of the scientific work done during the reporting period and research plans for the immediate future. GRA

N90-15684# Stanford Univ., CA. Dept. of Operations Research.
LIKELIHOOD RATIO DERIVATIVE ESTIMATORS FOR STOCHASTIC SYSTEMS
Peter W. Glynn Aug. 1989 9 p
(Contract DAAL03-88-K-0063)
(AD-A213787; TR-41; ARO-25839.16-MA) Avail: NTIS HC A02/MF A01 CSCL 12/4

The likelihood ratio derivative estimation techniques for stochastic systems is discussed. After a brief review of the basic concepts, likelihood ratio derivative estimators are presented for the following classes of stochastic processes: time homogeneous discrete-time Markov chains, non-time homogeneous discrete-time Markov chains, time homogeneous continuous-time Markov chains, semi-Markov processes, non-time homogeneous continuous-time Markov chains, and generalized semi-Markov processes. GRA

N90-15685# Notre Dame Univ., IN. Dept. of Electrical and Computer Engineering.
MEMBERSHIP-SET PARAMETER ESTIMATION VIA OPTIMAL BOUNDING ELLIPSOIDS Semiannual Progress Report Ph.D. Thesis
Ashok K. Rao and Yih-Fang Huang Oct. 1989 123 p
(Contracts N00014-89-J-1788; N00014-87-K-0284)
(AD-A213807; UND-TR-89-10-01) Avail: NTIS HC A06/MF A01 CSCL 12/3

In the last few years, there seems to have been a resurgence of interest in the membership-set-theoretic approach to parameter estimation. This report concentrates on the optimal bounding ellipsoid (OBE) approach to membership-set parameter estimation, with emphasis being placed on the performance of one particular OBE algorithm in nonideal conditions. It is first shown that OBE algorithms offer distinct advantages over commonly used recursive parameter estimation algorithms like the recursive least-squares (RLS) algorithm in some real-life environments. Then the extension of a particular OBE algorithm to the problem of parameter estimation with unobservable but bounded inputs (ARMA parameter estimation) is discussed in some detail. The problem is important because, in many signal processing applications, the inputs to the system under consideration are unknown. Analysis of the extended algorithm shows that under some conditions, the extended algorithm yields 100 percent confidence intervals for the parameters at every sampling instant. This feature does not appear to be present in any other existing ARMA parameter estimation algorithms. Furthermore, the transient performance of this algorithm is observed to be superior to that of the extended least-squares algorithm. Finite precision effects of one of the OBE algorithms are also studied via analysis of error propagation in the algorithm and through simulations. GRA

N90-15686# Massachusetts Inst. of Tech., Cambridge. Lab. for Computer Science.
BOUNDED POLYNOMIAL RANDOMIZED CONSENSUS
Hagit Attiya, Danny Dolev, and Nir Shavit Jun. 1989 16 p
(Contracts N00014-85-K-0168; N00014-83-K-0125)
(AD-A213808; MIT/LCS/TM-392) Avail: NTIS HC A03/MF A01 CSCL 12/7

In (A88), Abrahamson presented a solution to the randomized consensus problem of Chor, Israeli and Li (CIL87), without assuming the existence of anatomic coin flip operation. This elegant algorithm uses unbounded memory, and has expected exponential running time. In (AH89), Aspens and Herlihy provide a breakthrough polynomial-time algorithm. However, it too is based on the use of unbounded memory. In this paper, we present a solution to the randomized consensus problem, that is bounded in space and runs in polynomial expected time. GRA

N90-15687# Stanford Univ., CA. Dept. of Operations Research.
QUEUES WITH NEGATIVE ARRIVALS
Erol Gelenbe, Peter W. Glynn, and Karl Sigman (Columbia Univ., New York, NY.) 20 Aug. 1989 10 p Sponsored in part by Centre National de la Recherche Scientifique
(Contract DAAL03-88-K-0063; NSF DDM-89-57825)
(AD-A213860; TR-42; ARO-25839.17-MA) Avail: NTIS HC A02/MF A01 CSCL 12/4

Single server queueing models where in addition to regular arriving customers, there are negative arrivals, are presented. A negative arrival has the effect of removing a customer from the queue. The way in which this removal is specified gives rise to several different models. Unlike the standard FIFO GI/GI/1 model, the stability conditions for these new models may depend upon more than just the arrival and service rates; the entire distributions of interarrival and service times may be involved. GRA

N90-15688# Illinois Univ., Urbana-Champaign. Coordinated Science Lab.
AN IMPROVED TOEPLITZ APPROXIMATION METHOD
K. S. Arun and Bhaskar D. Rao (California Univ., San Diego, La Jolla.) 1988 5 p

(Contract DAAL03-86-K-0111)
(AD-A213994; ARO-24370.38-MA-SDI) Avail: NTIS HC A02/MF A01 CSCL 12/1

This reprint suggests a modification of the Toeplitz approximation method for estimating frequencies of multiple sinusoids from covariance measurements. The method constructs a state-feedback matrix following a low-rank approximation of the Toeplitz covariance matrix via singular value decomposition. Ideally, the eigenvalues of this state-feedback matrix will be on the unit circle in the complex plane, and the angles that they make with the real axis will be equal to the unknown sinusoid frequencies. The modification proposed here exploits this prior knowledge of the modulus of the eigenvalues, and guarantees that even the presence of noise, the eigenvalues of the estimated state-feedback matrix will lie on the unit circle. GRA

N90-15689# Stanford Univ., CA. Dept. of Operations Research.
OPTIMIZATION OF STOCHASTIC SYSTEMS VIA SIMULATION
Peter W. Glynn Aug. 1989 18 p
(Contract DAAL03-88-K-0063)
(AD-A214011; TR-43; ARO-25839.18-MA) Avail: NTIS HC A03/MF A01 CSCL 12/3

Some research issues related to the general topic of optimizing a stochastic system via simulation are discussed. In particular, extensive attention is devoted to finite difference estimators of objective function gradients and a number of new limit theorems is presented. A new family of orthogonal function approximations to the global behavior of the objective function is discussed. It is shown that if the objective function is sufficiently smooth, the convergence rate can be made arbitrarily close to n to the minus half power in the number of observations required. A brief discussion of how these ideas can be integrated into an optimization algorithm is presented. GRA

N90-15690# Houston Univ., TX. Dept. of Mathematics.
NUMERICAL METHODS FOR PARABOLIC EQUATIONS AND INEQUALITIES IN VERY HIGH DIMENSIONS Final Report, May 1986 - May 1989
Roland Glowinski 5 Oct. 1989 21 p
(Contract DAAL03-86-K-0138)
(AD-A214102; ARO-24409.3-MA) Avail: NTIS HC A03/MF A01 CSCL 12/1

The main goal of this projects was to investigate the numerical solution of parabolic equations in very high dimension, the principal motivation being the solution of the so-called Zakai equation from nonlinear filtering. As it will be seen in Section 2, below, this equation is of the advection-diffusion type and therefore is closely related to other equations of this type such as the Navier-Stokes equations from Fluid Dynamics; since these equations are also of interest for the Department of Defense some aspects of their numerical solution will be considered in the present document. The content of this report is the following: In section 2, we describe the Zakai and its origin. In Section 3, we consider the solution of time dependent problems by operator splitting methods, and show in Sections 4, 5, 6, how these methods apply to the Zakai equation, to parabolic inequalities of obstacle type and to Navier-Stokes equations. In Section 7 we comment on the solution of advection-diffusion problems by up winding, particle and characteristics methods. In Section 8 we go back to the Zakai equation and its stochastic dynamical system origin and comment about the feasibility of the Zakai equation approach for the analysis of such systems. GRA

N90-15691# International Centre for Theoretical Physics, Trieste (Italy).
CONTINUUM ANALOGUES OF CONTRAGREDIENT LIE ALGEBRAS: LIE ALGEBRAS WITH A CARTAN OPERATOR AND NONLINEAR DYNAMICAL SYSTEMS
M. V. Saveliev and A. M. Vershik (Leningrad State Univ., USSR) Mar. 1989 14 p Submitted for publication
(DE89-635698; IC-89/55) Avail: NTIS (US Sales Only) HC A03/MF A01

An axiomatic formulation is presented for a new class of infinite-dimensional Lie algebras - the generalizations of Z-graded Lie algebras with, generally speaking, an infinite-dimensional Cartan subalgebra and a contiguous set of roots. Such algebras are called continuum Lie algebras. The simple Lie algebras of constant growth are encapsulated in the formulation. Particular attention is paid to the case when the local algebra is parametrized by a commutative algebra while the Cartan operator (the generalization of the Cartan matrix) is a linear operator. Special examples of these algebras are the Kac-Moody algebras, algebras of Poisson brackets, algebras of vector fields on a manifold, current algebras, and algebras with differential or integro-differential Cartan operator. The nonlinear dynamical systems associated with the continuum contragredient Lie algebras are also considered. DOE

N90-15692# International Centre for Theoretical Physics, Trieste (Italy).
FLOW OF HARMONIC APPLICATIONS OF A COMPACT VARIETY ON A BORDERED VARIETY
Yun Mei Chen and Roberta Musina May 1989 5 p In FRENCH Submitted for publication
(DE89-635699; IC-89/67) Avail: NTIS (US Sales Only) HC A01/MF A01

If M is a compact riemannian variety and C a riemannian variety closed to border, a weak harmonic application (mu):M yields C is defined as being a solution of a differential inclusion. A theorem of existence and partial regularity is presented for the weak solution of the evolution inclusion for harmonic applications. This solution converges to a weak harmonic application when the time tends appropriately to infinity. DOE

N90-15693 ESDU International Ltd., London (England).
PARAMETER ESTIMATION OF LINEAR SYSTEMS IN THE PRESENCE OF PROCESS NOISE USING THE MAXIMUM LIKLIHOOD METHOD
Sep. 1989 29 p
(ESDU-89032; ISBN-0-85679-704-9; ISSN-0141-3988) Avail: ESDU

This data item extends methods of parameter identification in ESDU 87039 and 88011 that treated systems with measurement noise alone to deal with the case of a system subject to both measurement and process noise. The method used is to formulate an Objective Function in terms of the maximum likelihood estimator and to minimize it by a Gauss-Newton iterative procedure to find the unknown parameters. State estimation is formulated in terms of both time-varying and steady state Kalman filters. The procedure is first developed for a first order state system with only a single unknown parameter and driven by a combination of known and random inputs. For the time-varying Kalman filter the unknown parameter set is the unknown in the state equation and the variances of the measurement noise and of the process noise. For the steady state Kalman filter the variance of the process noise is replaced by the constant Kalman gain in the set of unknown parameters and is subsequently found once the parameter set has been determined. An example of an aircraft executing a pure rolling maneuver illustrates the procedure. The fully generalized method for a multiparameter system with many degrees of freedom is described. ESDU

65 STATISTICS AND PROBABILITY

Includes data sampling and smoothing; Monte Carlo method; and stochastic processes.

N90-15694# Los Alamos National Lab., NM.
USE OF THE LINEAR VARIATE METHOD OF MONTE CARLO FOR ESTIMATING UNCERTAINTY IN THERMAL-HYDRAULIC CODES
William L. Kubic, Jr. and A. M. White (Westinghouse Savannah River Co., Aiken, SC.) 1989 7 p Presented at the Winter Meeting of the American Nuclear Society, San Francisco, CA, 26-30 Nov. 1989

(Contract DE-AC09-89SR-18035)
(DE89-017871; WSRC-RP-89-385; CONF-891103-28) Avail: NTIS HC A02/MF A01

Thermal-hydraulic computer codes represent non-linear functions that may contain discontinuities. Monte Carlo methods are an effective means of accurately evaluating the effect of uncertainty on a nonlinear function with discontinuities, but the computational requirements of standard Monte Carlo methods may be prohibitive. The linear variate Monte Carlo method is a means of reducing the computational requirements. The linear variate method combines the linear response surface method with Monte Carlo analysis to obtain an efficient and accurate method of nonlinear uncertainty analysis. The method is applied to the power limit analysis for the Savannah River Site reactors. DOE

N90-15695# Oak Ridge National Lab., TN. Engineering Physics and Mathematics.
NONLINEAR MAPS WITH COMPETITIVE INTERACTIONS: FIXED-POINTS, BIFURCATIONS, AND CHAOTIC ATTRACTORS
D. F. Scollan (Pennsylvania State Univ., University Park.), Y. Y. Azmy, and V. Protopopescu Sep. 1989 70 p Sponsored in part by DARPA
(Contract DE-AC05-84OR-21400)
(DE90-001858; ORNL/TM-11315) Avail: NTIS HC A04/MF A01

Several aspects are examined of the dynamical behavior of competitive systems modeled by nonlinear maps. Some features of special cases of such maps are analytical investigated and the symbolic manipulator MACSYMA is used to derive expressions for the linearized systems' eigenvalues. These enables the determination of the linear stability of some of the fixed and periodic points of these maps, and in some cases, yield the regions of attraction in phase space. The analysis is extended to a more general form of competitive systems. The two-species one-index system and the one-species two-index map are numerically explored in search for interesting bifurcation and/or chaotic regimes over a large range of parameters. It is shown that system with linear attrition displays stable, interesting behavior for a large region of parameter space even if the quadratic self-repression is taken very small. It is also shown that small quadratic self-repression combined with bilinear attrition generally results in steady-state solutions with one species zero or in unbounded iterates. The method is described which is used to obtain an approximate estimate of the correlation dimensions of the chaotic attractor. A new method is proposed to evaluate the correlation dimension of a chaotic attractor using statistical analysis methods. DOE

N90-15696# Los Alamos National Lab., NM.
UNIFORM VERSUS RANDOM SAMPLING IN PHYSICAL CALCULATIONS: MONTE CARLO
Joseph J. Devaney Sep. 1989 16 p
(Contract W-7405-eng-36)
(DE90-003247; LA-11681-MS) Avail: NTIS HC A03/MF A01

It is argued that whenever the sampling of the mean physical behavior of a system can be broken up into the successive sampling of a sequence of independent basic probability functions, then a uniform deterministic sampling of each such function for a fixed number of trials is always superior, or at least as good as, uniformly distributed (or probable) random sampling of each such function. Elementary numerical examples are given. A brief discussion is given of the relative merits of uniform deterministic sampling versus uniformly distributed random sampling in practical problems, e.g., the Monte Carlo methods. It is concluded that in such problems other advantages of sampling often overweigh the superior accuracy of uniform deterministic sampling. Thus uniform deterministic sampling should properly be thought of as an addition to present Monte Carlo techniques and not as a replacement. DOE

N90-15697# College of William and Mary, Williamsburg, VA. Dept. of Mathematics.
A STRUCTURAL FACTORING APPROACH FOR ANALYZING PROBABILISTIC NETWORKS M.S. Thesis
Kelly Jeanne Hayhurst 1989 64 p
Avail: NTIS HC A04/MF A01

The problem of finding the shortest path through a stochastic network is analyzed by applying a structural factoring approach. A broad class of stochastic networks with the following characteristics is considered: (1) arc values (length, duration, cost, etc.) are discrete random variables; (2) these random variables are statistically independent; and (3) nodes do not fail. A general algorithm for determining the exact distribution of the shortest path length in such directed networks is presented. The algorithm is based on the concept of structural factoring, in which a stochastic network is decomposed into an equivalent set of smaller, generally less complex subnetworks. Several network constructs are identified and exploited to reduce significantly the computational effort required to solve a network problem relative to complete enumeration. This algorithm can be applied to two important classes of stochastic path problems: determining the critical path distribution for acyclic networks and the exact two-terminal reliability for probabilistic networks. Computational experience with the algorithm has been encouraging and has allowed the exact solution of networks previously analyzed only by approximation techniques. Author

N90-15698# Old Dominion Univ., Norfolk, VA. Dept. of Mathematics and Statistics.
STRONG LARGE DEVIATION AND LOCAL LIMIT THEOREMS
Narasinga Rao Chaganty and Jayaram Sethuraman Aug. 1989 38 p Prepared in cooperation with Florida State Univ., Tallahassee
(Contract DAAL03-86-K-0094)
(AD-A213610; FSU-TR-M-813; ARO-23699.23-MA) Avail: NTIS HC A03/MF A01 CSCL 12/3

An event is loosely called a large deviation event if the dominant term in the probability of that event goes to zero exponentially. Most papers give asymptotic expressions only to the algorithm of the probability of a large deviation event. Herein, strong deviation results are obtained which give asymptotic expressions to the actual probability of a large deviation event based on an arbitrary sequence of random variables, under some conditions on the moment generating functions. The proof of these results depends on local limit theorems, which also are proved, by imposing some conditions on the characteristic functions. A local limit theorem states that the pseudo-densities of random variables converge, which is stronger than the convergence of these random variables in distribution. GRA

66 SYSTEMS ANALYSIS

Includes mathematical modeling; network analysis; and operations research.

N90-15699*# Cornell Univ., Ithaca, NY. Dept. of Computer Science.
CONCURRENCE CONTROL FOR TRANSACTIONS WITH PRIORITIES
Keith Marzullo May 1989 19 p
(Contract NAG2-593; N00140-87-C-8904; ARPA Order 6037)
(NASA-CR-186241; NAS 1.26:186241; TR-89-996) Avail: NTIS HC A03/MF A01 CSCL 12B

Priority inversion occurs when a process is delayed by the actions of another process with less priority. With atomic transactions, the concurrency control mechanism can cause delays, and without taking priorities into account can be a source of priority inversion. Three traditional concurrency control algorithms are extended so that they are free from unbounded priority inversion. Author

N90-15700# Los Alamos National Lab., NM.
PROSPECTS FOR SPACE ARMS CONTROL
Joseph F. Pilat 1989 7 p Presented at the Research in Air Space Law Symposium, Montreal, Quebec, Sep. 1989
(Contract W-7405-eng-36)
(DE90-003392; LA-UR-89-3684; CONF-8909272-1) Avail: NTIS HC A02/MF A01

At the recent Wyoming Ministerial, US Secretary of State Baker and Soviet Foreign Minister Shevardnadze signed a memorandum of understanding on a bilateral verification experiment and data exchange related to a prohibition on chemical weapons, an agreement on advance notification of certain strategic exercises, and an umbrella agreement on START trial verification and stability measures. Despite these substantive achievements in high priority areas for the United States and the Soviet Union, media attention on the ministerial focused on an offer by the Soviets that would allow a START agreement to be concluded without a resolution of US-Soviet differences in the Defense and Space (D and S) talks. Of course, the Soviet offer did not delink START and D and S, because the Soviets continued to demand the right to withdraw from START if the United States deployed space-based defenses. A more substantial proposal on Defense and Space was the US initiative inviting a group of Soviet experts to visit Los Alamos and the TRW Corporation's test facility in San Juan Capistrano to learn more about US SDI research activities. The US invitation was proposed in the context of the Predictability Measures Protocol to a Defense and Space Treaty, tabled by the United States, which calls for regular exchanges of data, briefings, visits to laboratories, and observation of tests designed to foster transparency and predictability. DOE

N90-15701# Illinois Univ. at Urbana-Champaign, Savoy. Coordinated Science Lab.
SYSTOLIC ALGORITHMS FOR IMAGING FROM SPACE Final Report, 1 Aug. 1986 - 30 Jun. 1989
K. S. Arun, T. S. Huang, W. K. Jensins, Hua Lee, and D. C. Munson, Jr. 31 Jul. 1989 28 p
(Contract DAAL03-86-K-0111)
(AD-A213870; ARO-24370.20-MA-SDI) Avail: NTIS HC A03/MF A01 CSCL 15/3

The goal of the Strategic Defense Initiative is to develop technologies that can be used to defend against the threat of nuclear ballistic missiles. Primary components of a strategic defense system would be a high resolution sensing or imaging system for surveillance, acquisition, tracking, and overall monitoring of targets, and a weapons system possible utilizing directed energy or kinetic energy technologies for destroying targets. The research was aimed at developing algorithms and VLSI architectures for high resolution imaging from space. The problems studied were from two major, related categories: algorithm definition and development, and VLSI implementation of signal and image processing algorithms. In the first category, the imaging problems studied were from synthetic aperture radar, high resolution, sensor array systems, and motion estimation and target tracking. The primary objective of the work was to find high performance algorithms suitable for high speed implementation on multi processor arrays. The second aspect of the work focussed on VLSI implementation of signal processors, the analysis of finite register length effects, and the development of short wordlength, low noise structures for signal and image processing. GRA

67 THEORETICAL MATHEMATICS

Includes topology and number theory.

N90-15702# Rochester Univ., NY. Dept. of Physics and Astronomy.
NIJENHUIS TENSOR AND INTEGRABLE MODELS
Susumu Okubo 18 Aug. 1989 13 p Presented at the Annual Seminar of the Canadian Mathematical Society, Montreal, Quebec, 1-11 Aug. 1989
(Contract DE-AC02-76ER-13065)
(DE90-001403; DOE/ER-13065/589; CONF-8908166-1; UR-1126)
Avail: NTIS HC A03/MF A01

Let M be a differential manifold admitting two symplectic tensors f(sub mu nu) and F(sub mu nu). If the Nijenhuis tensor constructed out of S(sub mu)(sup nu) = F(sub mu lambda) f(sup lambda nu) vanishes identically, then integrable dynamical system with hierarchy relation can be constructed. Also, it was shown that the zero Nijenhuis tensor condition is associated with various Lie and Lie-super algebraic structures. DOE

N90-15703# International Centre for Theoretical Physics, Trieste (Italy).
CHERN-SIMONS THEORIES OF SYMPLECTIC SUPER-DIFFEOMORPHISMS
E. Sezgin and E. Sokatchev Apr. 1989 12 p Submitted for publication
(DE89-635700; IC-89/72) Avail: NTIS (US Sales Only) HC A03/MF A01

The symplectic diffeomorphisms are discussed for a class of supermanifolds and the structure of the underlying infinite dimensional superalgebras. A Chern-Simons (CS) gauge theory was constructed in 2+1 dimensions for these algebras. There exists a finite dimensional supersymmetric truncation which is the (2/sup n/-1)-dimensional Hamiltonian superalgebra H-tilde(n). With a central charge added, it is a superalgebra, C(n), associated with a Clifford algebra. An embedding of d=3, N=2 anti-de Sitter superalgebra OSp(2 2)+OSp(2 2) in C(4) was found, and a Cs action constructed for its infinite dimensional extension. The construction of a CS action was also constructed for the infinite dimensional extension of the d=3, N=2 superconformal algebra OSp(2,4). DOE

70 PHYSICS (GENERAL)

For precision time and time interval (PTTI) see *35 Instrumentation and Photography;* for geophysics, astrophysics or solar physics see *46 Geophysics, 90 Astrophysics,* or *92 Solar Physics.*

N90-15704 Texas Univ., Austin.
OPTIMAL PERIODIC CONTROL AND REGULATOR THEORY BASED ON THE SECOND VARIATION Ph.D. Thesis
Qinghong Wang 1989 181 p
Avail: Univ. Microfilms Order No. DA8920863

A class of optimal periodic control problems are investigated which are characterized by an autonomous nonlinear system and Lagrangian with periodic boundary condition forcing the path to be closed. An average cost criterion is to be minimized with respect to a piecewise continuous control, the initial state vector, and the period. For this class of optimal control problems, the second variation about both a single-period process and an infinitely-repeated periodic process produces necessary and sufficient conditions for weak local optimality which are compactly established. For the single-period process, the existence of a real symmetric solution to the Riccati differential equation on a certain time interval is required for the non-existence of the conjugate point. This requirement is strengthened to the existence of a periodic solution to the Riccati differential equation for the infinitely-repeated periodic process. Accessory minimum problems for variations in the initial state and period are then solved, and the conditions for the second variation to be non-negative and strongly positive are stated. For a local optimal periodic path satisfying the given sufficient optimality conditions, a periodic regulator is constructed based on the second variation to bring state deviations back to the nominal periodic path. This regulator is derived through minimizing an infinite-time, second variation problem around the nominal optical periodic path. A projection method using the eigenvectors associated with the stable eigenvalues of the monodromy matrix is used to determine the index point on the nominal optimal periodic path. By using the index point, state and control perturbations from the nominal and

associated gains are determined to preserve optimality. In addition, a regulator including small parameter variations is derived. Finally, the periodic regulator is applied to a hypersonic scram-jet cruiser problem. Convergence of state variation due to initial state perturbation and parameter variation are demonstrated. The results show the applicability of this periodic regulator in implementation of optimal periodic processes. Dissert. Abstr.

N90-15705# Texas Univ., Austin. Dept. of Physics.
THE FREE ENERGY OF MAXWELL-VLASOV EQUILIBRIA
P. J. Morrison and D. Pfirsch (Max-Planck-Inst. fuer Plasmaphysik, Garching, Germany, F.R.) Oct. 1989 25 p
(Contract DE-FG05-80ET-53088)
(DE90-003318; DOE/ET-53088/401; IFSR-401) Avail: NTIS HC A03/MF A01

A previously derived expression for the energy of arbitrary perturbations about arbitrary Vlasov-Maxwell equilibria is transformed into a very compact form. The new form is also obtained by a canonical transformation method for solving Vlasov's equation, which is based on Lie group theory. This method is simpler than the one used before and provides better physical insight. Finally a procedure is presented for determining the existence of negative-energy modes. In this context the question of why there is an accessibility constraint for the particles, but not for the fields, is discussed. DOE

N90-15706# Sandia National Labs., Albuquerque, NM.
BROWNIAN TRAIL RECTIFIED
Alan J. Hurd and Pauline Ho 1989 5 p Presented at the Materials Research Society Fall Meeting, Boston, MA, 27 Nov. - 2 Dec. 1989
(Contract DE-AC04-76DP-00789)
(DE90-003339; SAND-89-2536C; CONF-891119-7) Avail: NTIS HC A01/MF A01

The experiments described here indicate when one of Nature's best fractals -- the Brownian trail -- becomes nonfractal. In most ambient fluids, the trail of a Brownian particle is self-similar over many decades of length. For example, the trail of a submicron particle suspended in an ordinary liquid, recorded at equal time intervals, exhibits apparently discontinuous changes in velocity from macroscopic lengths down to molecular lengths: the trail is a random walk with no velocity memory from one step to the next. In ideal Brownian motion, the kinks in the trail persist to infinitesimal time intervals, i.e., it is a curve without tangents. Even in real Brownian motion in a liquid, the time interval must be shortened to approximately 10(-8) s before the velocity appears continuous. In sufficiently rarefied environments, this time resolution at which a Brownian trail is rectified from a curve without tangents to a smoothly varying trajectory is greatly lengthened, making it possible to study the kinetic regime by dynamic light scattering. Our recent experiments with particles in a plasma have demonstrated this capability. In this regime, the particle velocity persists over a finite step length allowing an analogy to an ideal gas with Maxwell-Boltzmann velocities; the particle mass could be obtained from equipartition. The crossover from ballistic flight to hydrodynamic diffusion was also seen. DOE

N90-15707# Florida State Univ., Tallahassee. Dept. of Statistics.
A DIFFUSION ON A FRACTAL STATE SPACE
William Bernard Krebs Sep. 1989 42 p
(Contract DAAL03-86-K-0094)
(AD-A213555; FSU-STATISTICS-M-812; TR-D-108; ARO-23699.24-MA) Avail: NTIS HC A03/MF A01 CSCL 12/3

A fractal is defined in the plane known as the Vicsek Snowflake by constructing a skeletal lattice graph and then rescaling spatial dimensions to give a sequence of lattices that converges to a fractal. By defining a simple random walk on the skeletal lattice and then rescaling both time and space, we define a sequence of random walks on the approximating lattices that converge weakly to a limiting process on the snowflake. This limit has continuous sample paths and the strong Markov property, and that it is the unique diffusion limit of random walk on the snowflake in a natural sense. This diffusion has a scaling property reminiscent of Brownian motion, and we introduce a coupling argument to show that the diffusion has transition densities with respect to Hausdorff measure on the snowflake. GRA

N90-15708# Naval Ocean Systems Center, San Diego, CA.
PERIODIC PHASE ADJUSTMENT DISTRIBUTED CLOCK SYNCHRONIZATION IN THE HARD REALTIME ENVIRONMENT Final Report
D. R. Wilcox Aug. 1989 25 p
(AD-A213842; NOSC/TR-1310) Avail: NTIS HC A03/MF A01 CSCL 12/7

Many multiprocessing and distributed-processing system applications require the various components of the system to have access to the same knowledge of the current time of day. Uses for time-of-day data include the generation of timestamps for the coordination of transactions in a database system, the detection of process faults without the limitations of timeout in distributed fault-tolerant systems, and the recording and predicting of physical world events in a realtime system. There are various alternative methods of coordinating database transactions which avoid time-of-day timestamps, such as traditional locking mechanisms and timestamps employing virtual time. There is no alternative for time-of-day facilities in a system designed to act upon real-world, time-oriented events. This paper describes the operation and rationale underlying an approach to synchronizing a set of time-of-day realtime clocks located on the respective processors of a distributed processing system. The approach is called periodic phase adjustment. The paper also shows how to integrate this approach into rate monotonic hard-deadline realtime scheduling technology. GRA

71 ACOUSTICS

Includes sound generation, transmission and attenuation. For noise pollution see *45 Environmental Pollution.*

N90-15709# Pacific Northwest Lab., Richland, WA.
PULSED EMAT (ELECTROMAGNETIC ACOUSTIC TRANSDUCER) ACOUSTIC MEASUREMENTS ON A HORIZONTAL CONTINUOUS CASTER FOR INTERNAL TEMPERATURE DETERMINATION
Donald M. Boyd Oct. 1989 15 p Presented at the Metallurgical Society Fall Meeting: Materials Week, Indianapolis, IN, 1-5 Oct. 1989
(Contract DE-AC06-76RL-01830)
(DE90-002735; PNL-SA-16885; CONF-891024-4) Avail: NTIS HC A03/MF A01

Development of a Pulsed Electromagnetic Acoustic Transducer (EMAT) through transmission system for acoustic measurements on steel billets up to 1300 C was completed. Laboratory measurements of acoustic velocity were made, and used to determine the average internal temperature of hot stainless and carbon steel billets. Following the success of the laboratory system development, the laboratory EMAT system was subsequently tested successfully at the Baltimore Specialty Steel Co. on a horizontal continuous caster. Details of the sensor system development and the steel plant demonstration results are presented. Future directions for the high temperature pulsed EMAT internal temperature concept are discussed for potential material processing applications. DOE

N90-15710*# National Aeronautics and Space Administration. Langley Research Center, Hampton, VA.
SOUND ATTENUATION APPARATUS Patent Application
Kevin P. Shepherd, inventor (to NASA) and M. W. A. Ferdinand Grosveld, inventor (to NASA) (Planning Research Corp., Hampton, VA.) 10 Aug. 1989 11 p
(NASA-Case-LAR-13968-1; NAS 1.71:LAR-13968-1; US-Patent-Appl-SN-392165) Avail: NTIS HC A03/MF A01 CSCL 20A

An apparatus is disclosed for reducing acoustic transmission from mechanical or acoustic sources by means of a double wall partition, within which an acoustic pressure field is generated by at least one secondary acoustic source. The secondary acoustic source is advantageously placed within the partition, around its edges, or it may be an integral part of a wall of the partition.
NASA

N90-15711# Washington State Univ., Pullman. Dept. of Physics.
RESEARCH ON ACOUSTICAL SCATTERING, DIFFRACTION CATASTROPHES, OPTICS OF BUBBLES, ACOUSTICAL PHASE CONJUGATION, AND WAKE OF AN OSCILLATING CIRCULAR CYLINDER Annual Summary Report, 16 Oct. 1988 - 15 Oct. 1989
Philip L. Marston 31 Oct. 1989 58 p
(Contract N00014-85-C-0141)
(AD-A214168) Avail: NTIS HC A04/MF A01 CSCL 20/1

The research summarized concerns several aspects of the propagation and scattering of acoustical and optical waves. The topics discussed fall under the following five categories: (1) Project to extend GTD (Ray methods) to guided waves on smooth elastic objects in water as tested by synthesis of the forward and backward scattering amplitudes of a spherical shell and the total scattering cross section; (2) Acoustical and optical caustics and associated wavefields: opening rate in the transverse cusp in light scattered from oblate water drops; scaling laws and wavefront shape for light backscattered from oblate drops; (3) Physical optics of bubbles in water: an asymptotic series for critical angle scattering useful for determining bubble sizes; (4) Acoustics phase conjugation and aspects of wavefront reversal: the present status of experiments on three-wave mixing in a layer of microbubbles in water; and preliminary aspects of an experiment with phase conjugation of ripples on layer of water; (5) Response of the wake of a circular cylinder to forced torsional oscillations: waves on shear layers and effects on primary and secondary vortices. GRA

N90-15712# Naval Underwater Systems Center, West Palm Beach, FL. Test and Evaluation Dept.
WIND SPEED DEPENDENCE OF ACOUSTIC AMBIENT VERTICAL DIRECTIONAL SPECTRA AT HIGH FREQUENCY Final Report
R. M. Kennedy, T. K. Szlyk, and S. M. Wentworth Jun. 1989 64 p
(AD-A214293; NUSC-TR-8537) Avail: NTIS HC A04/MF A01 CSCL 17/1

A measurement of the acoustic ambient arriving from a horizontal direction along with total acoustic intensity spectra allows one to infer both the total directional spectra and some physical characteristics of the sources of sea surface sound. A long-term measurement of these two quantities was made at high frequency, i.e., 8 kHz to 64 kHz, in the Tongue of the Ocean, the Bahamas. The horizontally directed ambient was measured using vertically oriented line arrays and was observed for wind speeds ranging from 1 to 30 knots. The resulting data base was used to estimate the statistics of anisotropic noise gain relative to the isotropic noise gain. Differences in the functional dependence and residual statistics were found for two cases: whitecaps present and not present. The relation of these results to the total directional spectra and a model of the near-surface distribution of acoustic sources are discussed. GRA

N90-15713# Florida State Univ., Tallahassee. Dept. of Mathematics.
COMPUTATION OF BROADBAND MIXING NOISE FROM TURBOMACHINERY Semiannual Progress Report, 1 Mar. - 31 Aug. 1989
Christopher Tam Aug. 1989 2 p
(Contract N00014-89-J-1836)
(AD-A214448) Avail: NTIS HC A02/MF A01 CSCL 20/1

Broadband mixing noise is generated by a number of sources inside a turbomachine. The most important sources are the turbulent boundary layers (on the casing walls or on the blades), the turbulent free shear layers (separated flows) and turbulent wakes (from blades). High quality noise data are currently not available. A set of reliable near and far field mixing noise data from the free shear layers of a low speed jet was obtained. Work concentrated on broadband mixing noise theory on free shear flows. One began the theory by adopting the Kappa-Epsilon turbulence modelling equations as the basis. Although at this stage the formalism is the same yet a slightly different interpretation of the physical variables is needed. The averaging process is to be a volume average. On assuming there is a distinct separation of scales between the large turbulence structures and fine scale turbulence a closed set of governing equations can be derived in the usual way by using a volume average. The volume is to be small compared with the large turbulence structures but large compared to the fine scale turbulence. The semi-empirical constants used in turbulence calculation will be adopted. The next stage of work is to develop ways of solving the time dependent equations and to determine the radiated noise intensity and spectrum. GRA

N90-15714 ESDU International Ltd., London (England).
THE CALCULATION OF OVERGROUND SOUND PROPAGATION IN THE PRESENCE OF WIND AND TEMPERATURE GRADIENTS
Oct. 1989 25 p
(ESDU-89036; ISBN-0-85679-709-X; ISSN-0307-0115) Avail: ESDU

This data item ESDU 89036, an addition to the Noise Subseries, gives a computer program listing in FORTRAN for calculating a difference noise spectrum in one-third octave bands which, when subtracted from a measured spectrum, will yield the free-field values. The method assumes a linear sound speed gradient, and was validated against limited experimental data drawn from the literature for distances up to 120 m (400 ft) and for source and receiver heights up to 2 m (6.5 ft) in the frequency range 100 Hz to 5 kHz. The accuracy was within 3 dB. The method represents the acoustic impedance of the ground in terms of porosity and specific flow resistance, and guidance is given of the values to be taken for those quantities. The theory is outlined, and a worked example illustrates the form of the input data and the output results. The program is available on magnetic media as ESDUpac 8936.
ESDU

72 ATOMIC AND MOLECULAR PHYSICS

Includes atomic structure, electron properties, and molecular spectra.

N90-15715# Lund Univ. (Sweden).
RAPIDITY DENSITIES AND THEIR FLUCTUATIONS IN CENTRAL 200 A GeV S32 INTERATIONS WITH Au AND Ag,Br NUCLEI
M. I. Adamovich, M. M. Aggarwal, N. P. Andreeva, Z. V. Anson, Z. V. Ameeva, R. Arora, Y. A. Alexandrov, S. A. Azimov, E. Basova, and K. B. Bhalla (Rajasthan Univ., Jaipur, India) Jun. 1989 13 p
(LUIP-8905; LUNFD6/(NFFK-7102)1-12(1989); ISSN-0348-9329)
Avail: NTIS HC A03/MF A01

The pseudo-rapidity density distributions of shower particles (n sub s) are measured in central inelastic S + Au and S + Ag,Br interactions. The extracted maximum energy densities, while being higher for Au than for Ag,Br interactions, were found to be similar to those obtained for oxygen emulsion interactions. The correlation between rapidity density and shower particle multiplicity shows a small deviation from the Lund Model Fritiof for the highest energy densities in S + Au interactions, whereas the bulk of the data yields satisfactory agreement. Author

N90-15716# Lund Univ. (Sweden).
SUBSTRUCTURAL DEPENDENCE OF THE MULTIPARTICLE PRODUCTION IN RELATIVISTIC HEAVY-ION INTERACTIONS
M. I. Adamovich, M. M. Aggarwal, R. Arora, Y. A. Alexandrov, E.

Basova, K. B. Bhalla, A. Bhasin, V. S. Bhatia, R. A. Bondarenko, and T. H. Burnett (Washington Univ., Seattle.) et al May 1989 10 p
(LUIP-8904; LUNFD6/(NFFK-7101)1-9(1989); ISSN-0348-9329)
Avail: NTIS HC A02/MF A01

The average multiplicities of singly charged relativistic particles in oxygen-induced interactions with a nuclear emulsion target are studied over the energy range 2.1 to 200 A GeV. A similar energy dependence as for proton-induced interactions is observed. Both the number of participating nucleons and the number of binary collisions are shown to be of importance for the particle production. Author

N90-15717# California Univ., Berkeley. Lawrence Berkeley Lab. Nuclear Science Div.
THERMAL AND STATISTICAL PROPERTIES OF NUCLEI AND NUCLEAR SYSTEMS
L. G. Moretto and G. J. Wozniak Jul. 1989 102 p Presented at the Enrico Fermi Summer Course CX11: Nuclear Collisions From the Mean Field Into the Fragmentation Regime, Varenna, Italy, 11-21 Jul. 1989
(Contract DE-AC03-76SF-00098)
(DE90-000183; LBL-27502; CONF-8907154-1) Avail: NTIS HC A06/MF A01

The term statistical decay, statistical or thermodynamic equilibrium, thermalization, temperature, etc., have been used in nuclear physics since the introduction of the compound nucleus (CN) concept, and they are still used, perhaps even more frequently, in the context of intermediate- and high-energy heavy-ion reactions. Unfortunately, the increased popularity of these terms has not made them any clearer, and more often than not one encounters sweeping statements about the alleged statisticity of a nuclear process where the statistical connotation is a more apt description of the state of the speaker's mind than of the nuclear reaction. It is our goal, in this short set of lectures, to set at least some ideas straight on this broad and beautiful subject, on the one hand by clarifying some fundamental concepts, on the other by presenting some interesting applications to actual physical cases. DOE

N90-15718# Argonne National Lab., IL.
STRUCTURE AND DYNAMICS OF DISORDERED SYSTEMS
David L. Price 1989 18 p Presented at the Conference on Neutron Scattering Days At Studsvik, Studsvik, Sweden, 22-24 May 1989
(Contract W-31-109-eng-38)
(DE90-001408; CONF-8905231-1) Avail: NTIS HC A03/MF A01

Neutron scattering has proved to be a powerful tool in the study of glasses and liquids: structures are investigated by neutron diffraction, and dynamics by inelastic neutron scattering. Evidence of current interest in this field is provided by the new instruments for diffraction from amorphous systems being constructed at IPNS, ISIS and the R2-reactor at Studsvik, in addition to existing instruments such as the D4B diffractometer at ILL. DOE

N90-15719# Iowa Univ., Iowa City.
DETERMINATION OF STEPSIZE PARAMETERS FOR INTERMOLECULAR VIBRATIONAL ENERGY TRANSFER Progress Report, 1 May 1988 - 30 Apr. 1989
D. C. Tardy Jun. 1989 15 p
(Contract DE-FG02-87ER-13700)
(DE90-003346; DOE/ER-13700/2) Avail: NTIS HC A

The understanding of intermolecular vibrational energy transfer (IVET) is important since it is involved in any mechanism in which internal energy is added or removed from molecules. The database for the details of IVET for highly excited polyatomic molecules is inadequate and must be expanded. The overall objectives of this project are: (1) to determine the dependence of energy relaxation on excitation energy and on the molecular complexity of substrate and deactivator, (2) to assess the importance of intermolecular attractions on IVET, (3) to obtain more detailed information on the energy distribution after collision, and (4) to evaluate the importance of IVET on high temperature unimolecular reactions. The first three objectives are being met by experimentally measuring the time evolution of the average energy of the vibrationally excited species (hydro- and fluoro- carbons excited by a pulsed CO(sub 2) laser) and the average energy transferred into relative translation via time resolved IR spectrometry, interferometry and optoacoustic techniques. Trajectory calculations simulating IVET are being performed for model substrate/deactivator pairs to provide additional details and insight on the critical parameters. Our calculations for high temperature unimolecular reactions indicate that IVET effects are significant and must be correctly taken into account. DOE

N90-15720# Sandia National Labs., Albuquerque, NM.
BAND-TO-BAND TRANSITIONS IN POLY (PHENYL METHYL SILANE)
R. G. Kepler and J. M. Zeigler 1989 9 p Presented at the Materials Research Society Fall Meeting, Boston, MA, 27 Nov. - 2 Dec. 1989
(Contract DE-AC04-76DP-00789)
(DE90-003575; SAND-89-1653C; CONF-891119-21) Avail: NTIS HC A02/MF A01

The quantum efficiency was measured for carrier generation as a function of photon energy and the electroabsorption spectrum in poly (phenyl methyl silane). The experimental data are consistent with a band gap of about 4.6 eV. A strong absorption peak which is observed at 3.7 eV is an exciton band. DOE

N90-15721# California Inst. of Tech., Pasadena. Lab. of Chemical Physics.
DYNAMICS OF ELECTRON TRANSFER FOR A NONSUPEREXCHANGE COHERENT MECHANISM, 1 Technical Report, 1 Aug. 1988 - 13 Oct. 1989
R. A. Marcus and R. Almeida 13 Oct. 1989 27 p
(Contract N00014-89-J-1278)
(AD-A213450; TR-11) Avail: NTIS HC A03/MF A01 CSCL 07/4

In addition to mechanisms such as superexchange and a chemical intermediate mechanism for electron transfer from a donor D* to an acceptor A via a molecular bridge B, and third possibility occurs when the BA electronic coupling is very strong and the D asterisk B and D(+)B(-) states have energies moderately close to each other. This mechanism is discussed. Like superexchange, it is a coherent one, in contrast to the chemical intermediate mechanism, where the transfer is sequential and incoherent. The dynamics of the mechanism are discussed, particularly the maximum population of B- and the question of whether an effective rate constant. There are, as yet, no experimental data on the mechanism, though the synthesis of suitable D8BA's may permit is observation. In the treatment three collective nuclear coordinates are introduced, permitting independent reorganization energies for each reactive center. With certain approximations, namely, equal vibration frequencies and a nonadiabatic first step, the problem is reduced analytically to a one-coordinate one, which can be readily treated numerically. One rough but simple analytical result for the latter is also given. GRA

N90-15722# California Inst. of Tech., Pasadena. Lab. of Chemical Physics.
DYNAMICS OF ELECTRON TRANSFER FOR A NON-SUPEREXCHANGE COHERENT MECHANISMS. 2: NUMERICAL CALCULATIONS Technical Report No. 12, 1 Aug. 1988 - 13 Oct. 1989
R. Almeida and R. A. Marcus 13 Oct. 1989 39 p
(Contract N00014-89-J-1278)
(AD-A213511) Avail: NTIS HC A03/MF A01 CSCL 07/4

The expressions previously derived are used to treat the dynamics of electron transfer in the donor acceptor system D asterisk BA, via a molecular bridge B. Using a Fast Fourier Transform method results are obtained for the maximum population of B- and for other properties for this coherent but nonsuperexchange model. Several approximate ideas on rate

populations and energy distributions are tested using various values for the numerical parameters. GRA

N90-15723# Georgia State Univ., Atlanta.
INVESTIGATIONS OF THE INTERACTIONS OF RADIATION WITH MATTER Final Report, May 1986 - May 1989
Steven T. Manson 15 Sep. 1989 13 p
(Contract DAAL03-86-K-0085)
(AD-A213554; ARO-23570.23-PH) Avail: NTIS HC A02/MF A01 CSCL 20/5

Work on the interaction of radiation with matter is described. In particular charged particle impact ionization of atoms and molecules is discussed, along with photoabsorption by excited states and ground stat atoms, and atomic ions. GRA

N90-15724# Puerto Rico Univ., Rio Piedras. Dept. of Chemistry.
RELATIVISTIC SELF-CONSISTENT FIELD STUDIES OF ATOMS AND MOLECULES Final Report, 1 Sep. 1985 - 31 Aug. 1989
Yasuyuki Ishikawa Oct. 1989 5 p
(Contract DAAG29-85-G-0118)
(AD-A214101; ARO-22983.17-CH-H) Avail: NTIS HC A02/MF A01 CSCL 20/10

Dirac-Fock balanced Gaussian basis method that employs an extended nucleus model has been implemented, and applied to a number of atoms and the hydrogen molecular ion. The balanced expansion method does not introduce any of the variational instabilities that have plagued the early Dirac-Fock basis expansion calculations. Relativistic diagrammatic perturbation theory method has been developed and applied to a number of atoms in order to simultaneously take into account both relativistic and correlation effects. These studies showed that the Dirac-Fock balanced Gaussian basis expansion and the relativistic many-body methods are capable of providing accurate Dirac-Fock and correlation energies. GRA

N90-15725# State Univ. of New York, Buffalo. Dept. of Chemistry.
OBSERVATION OF ATOMIC RELAXATION NEAR AN INTERFACE THROUGH DETECTION OF EMITTED FLUORESCENCE
Henk F. Arnoldus and Thomas F. George Nov. 1989 20 p Submitted for publication
(Contract N00014-86-K-0043)
(AD-A214308; TR-115) Avail: NTIS HC A03/MF A01 CSCL 20/5

The general features of spontaneous decay of an atom which is close to the surface of a dielectric (or metal) layer are discussed, and compared to atomic decay near a four-wave mixing phase conjugator. It is pointed out that the decay or relaxation constants can be expressed entirely in terms of the classical Fresnel coefficients for reflection and transmission of a plane wave, independent of what the explicit forms of these coefficients are. For decay near a dielectric the relaxation constants can be measured directly by counting the number of fluorescent photons per unit of time, after excitation by a laser. For relaxation near a phase conjugator this procedure would require a spectral resolution in the photon detection, since there are two distinct contributions to the fluorescent yield of a two-state atom. The two possible decay mechanisms have different relaxation constants and produce radiation with different frequencies. GRA

N90-15726# Los Alamos National Lab., NM.
LARGE SCALE CALCULATIONS OF THE STRUCTURE AND DYNAMICS OF DENSE MATTER
Stephen M. Younger 1989 12 p Presented at the 7th Topical Conference on Atomic Processes in Plasma, Gaithersburg, MD, 2-6 Oct. 1989; sponsored by American Physical Society
(Contract W-7405-eng-36)
(DE90-003654; LA-UR-89-3982; CONF-891052-1) Avail: NTIS HC A03/MF A01

The physics of matter at high density has been found to be strongly influenced by transient quasi-molecular phenomena, the distribution of electron charge density among several nearby atoms. Calculations performed using the self-consistent field molecular dynamics approximation, a synthesis of techniques derived from quantum chemistry and molecular dynamics, have shown that such effects can result in more than a 30 percent increase in the diffusion coefficient of helium at 1 g/cc. The effect of finite electron temperature is to weaken many-electron collective phenomena, but significant effects are expected to occur even in fully ionized dense plasmas. DOE

73 NUCLEAR AND HIGH-ENERGY PHYSICS

Includes elementary and nuclear particles; and reactor theory.

For space radiation see *93 Space Radiation.*

N90-15727# Lund Univ. (Sweden).
TARGET NUCLEUS FRAGMENTATION IN O16 + (Ag,Br) INTERACTIONS AT 200 A GeV
M. I. Adamovich, M. M. Aggarwal, R. Arora, Y. A. Alexandrov, E. Basova, K. B. Bhalla, A. Bhasin, V. S. Bhatia, R. A. Bondarenko, and T. H. Burnett (Washington Univ., Seattle.) et al Jun. 1989 13 p
(LUIP-8906; LUNFD6/(NFFK-7103)1-11(1989); ISSN-0348-9329)
Avail: NTIS HC A03/MF A01

The multiplicity distributions of low energetic target-associated particles from 200 A GeV Oxygen-induced interactions with emulsion nuclei are presented. The experimental distributions are compared with distributions obtained using the Ranft and Fritiof simulation codes. It is found that the intra-nuclear cascade plays an important role for the target break-up in ion-induced interactions, similar to what is the case for hadron-induced interactions.
Author

N90-15839*# Spectra Technology, Inc., Bellevue, WA.
INTRODUCTION TO D-He(3) FUSION REACTORS
G. C. Vlases and L. C. Steinhauer *In* NASA, Langley Research Center, Report of NASA Lunar Energy Enterprise Case Study Task Force Jul. 1989 p 56-67 (For primary document see N90-15836 07-81)
Avail: NTIS HC A09/MF A02 CSCL 18L

N90-15843*# Wisconsin Univ., Madison.
IMPORTANCE OF HELIUM-3 FOR THE FUTURE
Gerald L. Kulcinski *In* NASA, Langley Research Center, Report of NASA Lunar Energy Enterprise Case Study Task Force Jul. 1989 p 150-171 (For primary document see N90-15836 07-81)
Avail: NTIS HC A09/MF A02 CSCL 18L

74 OPTICS

Includes light phenomena; and optical devices.

For lasers see *36 Lasers and Masers.*

N90-15728# Los Alamos National Lab., NM.
OPTICAL SOLITONS IN LIQUID CRYSTALS
Y. S. Yung and L. Lam (San Jose State Univ., CA.) 1989 7 p Presented at the Conference on Solitons and Chaotic Behavior in Optical Systems, San Jose, CA, 6-7 Jan. 1988 Submitted for publication
(Contract W-7405-eng-36)
(DE90-000694; LA-UR-89-3175; CONF-8801171-1) Avail: NTIS HC A02/MF A01

In this paper, we will discuss theoretically the possible existence of optical solitons in the isotropic liquid and in the nematic phase. For the same compound, when heated, the nematic phase will go through a first order transition at temperature T sub c to the isotropic liquid phase. As temperature increases from below T

sub c, the orientation order parameter, Q, decreases, drops to zero abruptly at T sub c and remains zero for T greater than T sub c. DOE

N90-15729# Naval Research Lab., Washington, DC.
INTERLABORATORY COMPARISON OF RADIATION-INDUCED ATTENUATION IN OPTICAL FIBERS. PART 3: TRANSIENT EXPOSURES
E. J. Friebele, P. B. Lyons, J. C. Blackburn, H. Henschel, A. Johan, J. A. Krinsky, A. Robinson, W. Schneider, D. Smith, and E. W. Taylor (Air Force Weapons Lab., Kirtland AFB, NM.) et al Aug. 1989 49 p Prepared in cooperation with Commissariat a l'Energie Atomique, Bruyeres-le-Chatel, France; Royal Military Coll. of Science, Shrivenham, England and Edgerton, Germeshausen and Grier, Inc., Santa Barbara, CA
(Contract W-7405-eng-48)
(DE90-000859; UCID-21753-Pt-3) Avail: NTIS HC A03/MF A01

A comparison of the losses induced in step index multimode, graded index multimode and single mode fibers by pulsed radiation exposure has been made among 12 laboratories over a period of 5 years. The recoveries of the incremental attenuations from 10(exp -9) to 10(exp 1) s are reported. Although a standard set of measurement parameters was attempted, differences between the laboratories are evident; possible origins for these are discussed. DOE

N90-15730# Central Research Inst. of Electric Power Industry, Tokyo (Japan). Energy and Environment Lab.
OPTICAL ACOUSTIC SENSOR USING OPTICAL FIBER
Kazuo Tanabe Oct. 1988 35 p In JAPANESE; ENGLISH summary
(DE89-901267; CRIE-T-87077) Avail: NTIS (US Sales Only) HC A03/MF A01

Microphone or sensor utilizing optical technique (optical microphone or sensor) of optical acoustic conversion technique was surveyed. The optical sensor is composed of OF functional type in which optical fiber (OF) is used as a sensor and of transmission line type (fiber acoustic sensor) in which other acousto-optic transducer part is fitted at the top of OF or in the line. Both types intend to measure acoustic pressure at one point in a space. In case of fiber interferometer device of OF functional type, minimum detectable pressure level is 100 to 120 dB (sub ref) microPa which is not yet sufficient, but may be possible to measure the pressure distribution in future. In case of latter type, it was 57 dB (sub ref) microPa which can be used practically. The quantity 55 dB (sub ref) microPa or less may be detectable when utilizing side hole fiber, coating plastic on fiber to raise the acoustic sensitivity and constructing single optical path heterodyne detection system. This system may enable the measurement of pressure distribution. Acoustic fiber sensor having high sensitivity to sound may be useful for a part of the diagnosis and monitoring system for electric power system. DOE

N90-15731# Lawrence Livermore National Lab., CA.
SBS (STIMULATED BRILLOUIN SCATTERING) PULSE DISTORTION IN MULTIMODE OPTICAL FIBERS: PRELIMINARY RESULTS
J. R. Smith, R. J. Hawkins, C. W. Laumann, and J. Hatch 1989 8 p Presented at the 33rd SPIE Annual International Technical Symposium on Optical and Optoelectronic Applied Science and Engineering, San Diego, CA, 6-11 Aug. 1989
(Contract W-7405-eng-48)
(DE90-003023; UCRL-101649; CONF-890836-18) Avail: NTIS HC A02/MF A01

We have observed severe temporal-pulse-shape distortion due to stimulated Brillouin scattering (SBS) in multimode optical fibers used to diagnose 351 nm laser pulses on the Nova laser system. Our measurements can be fit by a basic model of SBS and provide a clear indication of the intensity and temporal regimes where significant SBS-induced temporal-pulse-shape distortion can be avoided. DOE

N90-15732# California Univ., Berkeley. Lawrence Berkeley Lab. Accelerator and Fusion Research Div.
CENTER FOR X RAY OPTICS, 1988
Apr. 1989 24 p
(Contract DE-AC03-76SF-00098)
(DE90-003300; LBL-27001) Avail: NTIS HC A03/MF A01

This report briefly reviews the following topics: soft-x ray imaging; reflective optics for hard x rays; coherent XUV sources; spectroscopy with x rays; detectors for coronary artery imaging; synchrotron-radiation optics; and support for the advanced light source. DOE

N90-15733*# National Aeronautics and Space Administration. Lewis Research Center, Cleveland, OH.
FIBER OPTIC SENSING SYSTEM Patent Application
Grigory Adamovsky, inventor (to NASA) 7 Sep. 1989 14 p
(NASA-Case-LEW-14795-1; NAS 1.71:LEW-14795-1; US-Patent-Appl-SN-404291) Avail: NTIS HC A03/MF A01 CSCL 20F

A fiber optic interferometer utilizes a low coherence light emitting diode (LED) laser as a light source which is filtered and driven at two RF frequencies, high and low, that are specific to the initial length of the resonator chamber. A displacement of a reflecting mirror changes the length traveled by the nonreferencing signal. The low frequency light undergoes destructive interference which reduces the average intensity of the wave while the high frequency light undergoes constructive interference which increases the average intensity of the wave. The ratio of these two intensity measurements is proportional to the displacement incurred. NASA

N90-15734# Stanford Linear Accelerator Center, CA.
CANONICAL FORMALISM FOR COUPLED BEAM OPTICS
S. A. Kheifets Sep. 1989 22 p
(Contract DE-AC03-76SF-00515)
(DE90-003764; SU-SLAC/AP-77) Avail: NTIS HC A03/MF A01

Beam optics of a lattice with an inter-plane coupling is treated using a canonical Hamiltonian formalism. The method developed is equally applicable both to a circular (periodic) machine and to an open transport line. A solution of the equation of a particle motion (and correspondingly, the transfer matrix between two arbitrary points of the lattice) are described in terms of two amplitude functions (and their derivatives and corresponding phases of oscillations) and four coupling functions, defined by a solution of the system of the first-order nonlinear differential equations derived in the paper. Thus the total number of independent parameters is equal to ten. DOE

N90-15735# Massachusetts Inst. of Tech., Lexington. Lincoln Lab.
BINARY OPTICS TECHNOLOGY: THE THEORY AND DESIGN OF MULTI-LEVEL DIFFRACTIVE OPTICAL ELEMENTS
G. J. Swanson 14 Aug. 1989 55 p
(Contract F19628-85-C-0002)
(AD-A213404; AD-E501157; TR-854) Avail: NTIS HC A04/MF A01 CSCL 20/6

Multi-level diffractive phase have the potential to significantly improve the performance of many conventional lens systems. The theory, design and fabrication of these diffractive profiles are described in detail. Basic examples illustrate the potential usefulness, as well as the limitations, of these elements. GRA

N90-15736# JAYCOR, Vienna, VA.
ASPECTS OF RAMAN SCATTERING Final Report, 1 Dec. 1986 - 30 Apr. 1989
Rita Mahon, David G. Cooper, and James L. Dexter 25 Aug. 1989 77 p
(Contract N00014-87-C-2013)
(AD-A213926; J206-89-002/6264) Avail: NTIS HC A05/MF A01 CSCL 20/6

Aspects of stimulated Raman scattering are investigated to better understand the propagation of intense light beams through

the atmosphere. In addition, a new unstable resonator cavitie was developed for the long pulse excimer laser used in the Raman beam-cleanup experiments and have made preliminary measurements on an anti-Stokes Raman laser which operates in the vacuum ultra violet region of the spectrum. Experiments demonstrate the Raman gain suppression observed on-axis, or at very small angles, for rotational Raman gain using linearly polarized beams in hydrogen and deuterium. The reduction in vibrational Raman gain at the phase matching angle is noted in hydrogen and deuterium. The normal exponential gain observed in the transient limit was modeled to fit the experiment. The theory had to take account of the actual beam shapes, both spatially and temporally, as well as the self-phase modulation, in order to correctly predict the observed gain functions. Experiments were made on the beam quality and gain dependence of the 2nd Stokes. In particular, a study of the seeding mechanism responsible for generating the 2nd Stokes through the threshold level, has required statistical, spectral, beam profile and gain parameter studies. The far field pattern was then compared with the Fourier transform of the near field pattern to give a measure of the beam quality. GRA

N90-15737# New Mexico Univ., Albuquerque. Center for Advanced Studies.
NONLINEAR OPTICAL MATERIAL STUDIES Final Report, Sep. 1987 - Sep. 1988
M. O. Scully, J. Bergou, W. Becker, and J. K. McIver Sep. 1989 49 p
(Contract F29601-87-C-0059; AF Proj. 3326)
(AD-A213938; WL-TR-89-37) Avail: NTIS HC A03/MF A01 CSCL 20/6

This report covers research on nonlinear optics theory. An analytical theory of the reflection and transmission of light from nonlinear optical interfaces is described. The general theory is applied to some simple two-dimensional nonlinear waveguide configurations. The intensity dependence of total versus differential ionization rates in laser-induced above-threshold ionization is also discussed. GRA

N90-15738# Air Force Systems Command, Wright-Patterson AFB, OH. Foreign Technology Div.
DESIGN OF A LARGE ANGULAR APERTURE TeO2 ACOUSTO-OPTIC TUNABLE FILTER
M. Fuquin 23 Aug. 1989 9 p Transl. into ENGLISH from Guangxue Xuebao (Peoples Republic of China), v. 6, no. 5, 1986 p 446-449
(AD-A213999; FTD-ID(RS)T-0487-89) Avail: NTIS HC A02/MF A01 CSCL 09/6

The design of a large angular aperture acousto-optic tunable filter (AOTF) using TeO2 crystals is described. A new crystal orientation with theta(sub a) = 100 degree and theta(sub i) = 23.4 degree is proposed. It was proven in the experiments that this AOTF meets the exact condition of tangent momentum match. The measured tuning relation is in good agreement with theoretical calculations and the spectral resolution was improved by nearly 10 A. After compensation, the change in deflection angle is decreased to + or - 0.06 degrees. GRA

N90-15739# University of Southern California, Los Angeles.
RESEARCH IN OPTICAL INTERCONNECTION TECHNIQUES Final Report, 1 May 1984 - 31 Mar. 1989
Alexander A. Sawchuk, B. K. Jenkins, and C. S. Raghavendra 30 Sep. 1989 108 p
(Contract DAAG29-84-K-0066)
(AD-A214028; ARO-21739.6-PH-A) Avail: NTIS HC A06/MF A01 CSCL 12/7

This report summarizes results of basic research on the application of bulk (3-D) optical signal processing and communication technology to the interconnection of digital systems. Emphasis is on the typical distances and bandwidths found at the board and processor level of interconnection. Results are relevant to telecommunications, data networks, and parallel computer architectures. Important issues in the design of any interconnection network (electronic or optical) are: reconfiguration time; synchronous/asynchronous operation; data word size; uni-directional/bidirectional data transfer; broadcast capability; and propagation delay. Crossbar networks are very desirable in that arbitrary 1:1 interconnection of N inputs to N outputs is possible without connection. More than 14 basic optical matrix-vector and matrix-matrix multiplier designs (having binary weights) for implementation of crossbars are given. These systems may use acousto-optic, magneto-optic or electro-optic spatial light modulator, have data bandwidths of up to 1 GHz, and can reconfigure in times as low as 1 microsec. A related result is a design for an optical crossbar network using variable-grating-mode liquid crystal devices. Several types of 3-D dynamic optical networks that interconnect a 2-D array (consisting of N x N input lines) with a similar 2-D array of N x N output lines are given. These 3-D networks are intended to make specific use of the volume (non-planar) aspects of optics. GRA

N90-15740# Army Missile Command, Redstone Arsenal, AL. Guidance and Control Directorate.
MECHANICAL EVALUATION OF THE DIFFERENTIAL DRUM CONCEPT FOR OPTICAL FIBER PAY-OUT Technical Report, Mar. - Apr. 1989
Stephen C. Cayson Jul. 1989 47 p
(AD-A214149; AD-E951392; AMSMI/TR-RD-GC-89-17) Avail: NTIS HC A03/MF A01 CSCL 20/6

This report describes the design of a differential drum system for optical fiber pay-out. The critical design parameters, such as the stresses and deflections in high-speed machinery, are discussed and the equations that govern them are developed. These equations are then applied and two systems are designed which meet the requirements. GRA

N90-15741# Washington Univ., Seattle. Aerospace and Energetics Research Program.
GAS OPTICS APPLICABLE TO FREE ELECTRON LASER TECHNOLOGY Final Technical Report, 15 Dec. 1983 - 31 May 1989
Walter H. Christiansen 23 Oct. 1989 28 p
(Contract N00014-84-K-0113)
(AD-A214285) Avail: NTIS HC A03/MF A01 CSCL 09/3

The free electron laser has the potential of being a highly efficient short wavelength laser. The designs of these lasers are hampered by excessively long optical cavities required by practical considerations of the mirror reflectors. A solution to this problem may be the use of defocussing gas optics in conjunction with the traditional mirror optics. Estimates show that the length of the optical cavity may be reduced by over an order of magnitude with this approach. A program of experimental and theoretical research was carried out to study the various aspects of gas optics for use with the free electron laser. GRA

75 PLASMA PHYSICS

Includes magnetohydrodynamics and plasma fusion.

For ionospheric plasmas see *46 Geophysics*. For space plasmas see *90 Astrophysics*.

N90-15742 Oxford Univ. (England).
THEORY OF INTERACTING PLASMAS IN SPACE Ph.D. Thesis
Carol M. C. Nairn 1988 124 p
Avail: Univ. Microfilms Order No. BRD-85951

Using theoretical techniques the physics of plasma interactions observed in space by the Active Magnetospheric Particle Tracer Explorers (AMPTE) satellite project is explained. The spacecraft carried out artificial plasma release experiments involving the release of lithium and barium plasmas in the flowing solar wind. As the released plasmas expanded, diamagnetic cavities formed which were bounded on the sun-ward side by large shock-like magnetic field structures. The magnetic wave activity observed upstream of the barium plasma cloud is shown to have the characteristics of finite-amplitude magnetosonic waves and is

described using the Adlam-Allen wave model. It is shown that the equations describing the Adlam-Allen waves can be reduced using a perturbation technique to one nonlinear equation, namely the Korteweg-de Vries equation. Using a Vlasov stability analysis electrostatic wave generation by ion-acoustic-like instabilities and the modified two-stream instability is investigated for both the plasma releases. Data obtained in the earth's foreshock region show a correlation between the observation of high-frequency electrostatic noise and the appearance of a feature, which may be an unresolved bump, in the distribution functions of the field-aligned electrons backstreaming from the bow shock. It is shown that if there is a region of positive slope in the distribution function the waves may be generated by an electron-beam instability in which the Langmuir mode couples to the electron-beam mode. Dissert. Abstr.

N90-15743*# Southwest Research Inst., San Antonio, TX. Dept. of Space Sciences.
SIMULATION OF RADIAL EXPANSION OF AN ELECTRON BEAM INJECTED INTO A BACKGROUND PLASMA
J. Koga and C. S. Lin 1989 22 p
(Grant NAGw-1231)
(NASA-CR-186188; NAS 1.26:186188) Avail: NTIS HC A03/MF A01 CSCL 20I

A 2-D electrostatic particle code was used to study the beam radial expansion of a nonrelativistic electron beam injected from an isolated equipotential conductor into a background plasma. The simulations indicate that the beam radius is generally proportional to the beam electron gyroradius when the conductor is charged to a large potential. The simulations also suggest that the charge buildup at the beam stagnation point causes the beam radial expansion. From a survey of the simulation results, it is found that the ratio of the beam radius to the beam electron gyroradius increases with the square root of beam density and decreases inversely with beam injection velocity. This dependence is explained in terms of the ratio of the beam electron Debye length to the ambient electron Debye length. These results are most applicable to the SEPAC electron beam injection experiments from Spacelab 1, where high charging potential was observed. Author

N90-15744# Oak Ridge National Lab., TN.
FUSION REACTOR MATERIALS Semiannual Progress Report, period ending 31 Mar. 1989
1989 423 p
(Contract DE-AC05-84OR-21400)
(DE90-000976; DOE/ER-0313/6; ORNL/M-919) Avail: NTIS HC A17/MF A01

This paper discuses the following topics on fusion reactor materials: irradiation, facilities, test matrices, and experimental methods; dosimetry, damage parameters, and activation calculations; materials engineering and design requirements; fundamental mechanical behavior; radiation effects; development of structural alloys; solid breeding materials; and ceramics. DOE

N90-15745# Washington Univ., Seattle.
EXPERIMENTS ON LINEAR HIGH BETA HELICAL AXIS STELLARATORS TO STUDY SIMULATED TOROIDAL EFFECTS AND ALFVEN-WAVE HEATING Progress Report No. 3, 16 Jul. 1988 - 15 Jul. 1989
F. L. Ribe and B. A. Nelson 1989 61 p
(Contract DE-FG06-87ER-53242)
(DE90-001704; DOE/ER-53242/3; UWAERP-20) Avail: NTIS HC A03/MF A01

This report discusses the following topics: nonaxisymmetric radio-frequency heating in an $l = 1$ stellarator and in a linear plasma column; measurement of induced current in a hardcore theta pinch; externally driven tilt mode study on a field reversed configuration (FRC); elimination of induced plasma current in a hardcore theta pinch; and simulated toroidicity studies. DOE

N90-15746# Oak Ridge National Lab., TN.
STUDIES OF PLASMA PERFORMANCE AND TRANSPORT IN THE ADVANCED TOROIDAL FACILITY (ATF)
G. H. Neilson, T. S. Bigelow, B. A. Carreras, R. J. Colchin, E. C. Crume, J. L. Dunlap, G. R. Dyer, A. C. England, J. C. Glowienka, and J. W. Halliwell et al 1989 6 p Presented at the 13th International Symposium on Fusion Engineering, Knoxville, TN, 2-6 Oct. 1989
(Contract DE-AC05-84OR-21400)
(DE90-001737; CONF-891007-24) Avail: NTIS HC A02/MF A01

An overview of recent ATF experimental results and program plans is presented, with emphasis on the role of magnetic configuration controls in transport studies. The ATF operating space is bounded by a density limit that effectively sets a limit on the energy confinement time tau (sub E). Although this limit is not solely due to impurities, it has recently been raised by improved cleanliness following titanium gettering. This has led to collapse-free neutral beam injection (NBI) discharges with global tau (sub E) (approx) 16 ms. Preliminary experiments show that stored energy and bootstrap current are sensitive to details of the magnetic configuration. DOE

N90-15747# Oak Ridge National Lab., TN.
TECHNOLOGY OF FAST-WAVE CURRENT DRIVE ANTENNAS
D. J. Hoffman, F. W. Baity, R. H. Goulding, G. R. Haste, P. M. Ryan, D. J. Taylor, D. W. Swain, M. J. Mayberry (General Atomic Co., San Diego, CA.), and J. J. Yugo 1989 13 p Presented at the 13th International Symposium on Fusion Engineering, Knoxville, TN, 2-6 Oct. 1989
(Contract DE-AC05-84OR-21400)
(DE90-001972; CONF-891007-30) Avail: NTIS HC A03/MF A01

The design of Fast-Wave Current Drive (FWCD) antennas combines the usual antenna considerations (e.g., the plasma/antenna interface, disruptions, high currents and voltages, and thermal loads) with new requirements for spectral shaping and phase control. The internal configuration of the antenna array has a profound effect on the spectrum and the ability to control phasing. This paper elaborates on these considerations, as epitomized by a Proof-Of-Principle (POP) experiment designed for the D3-D tokamak. The extension of FWCD for machines such as the International Thermonuclear Engineering Reactor (ITER) will require combining ideas implemented in the POP experiment with reactor-relevant antenna concepts, such as the folded waveguide. DOE

N90-15748# California Univ., Los Angeles. Dept. of Physics.
COMPUTER SIMULATION OF LASER PLASMA INTERACTION Progress Report
John M. Dawson 1988 7 p Prepared for Lawrence Livermore National Lab., CA
(Contract W-7405-eng-48)
(DE90-002828; UCRL-21250) Avail: NTIS HC A02/MF A01

During the past year, some new ideas on laser plasma interactions were investigated. In particular, the possibility is studied of using plasmas to upshift the frequency of laser light in a tunable fashion. Two techniques are discussed. DOE

N90-15749# Lawrence Livermore National Lab., CA.
INTENSE REB (RELATIVISTIC ELECTRON BEAM) TRANSPORT IN A WEAKLY MAGNETIZED PLASMA
J. F. Camacho, B. R. Poole, and B. Chang 1989 9 p Presented at the 7th IEEE Pulsed Power Conference, Monterey, CA, 11-14 Jul. 1989
(Contract W-7405-eng-48)
(DE90-002978; UCRL-100359; CONF-8907168-2) Avail: NTIS HC A02/MF A01

Intense relativistic electron beams (REBs) have been used in various applications for the purpose of high-power microwave (HPM) generation. By injecting the beam into a plasma, it is possible to overcome the space-charge limiting current because of charge and current neutralization provided by the plasma. Our goal in this experiment was to study beam transport issues which may be relevant to the development of HPM sources which use intense REBs. We conducted high-power REB-plasma interaction

experiments by injecting a 1.4 MeV, 25 kA electron beam with n(sub b) approx. 4 times 10(10) cm(-3) into a performed, partially ionized (less than 1 percent) argon background situated within a 15 cm ID Lucite tube, with n sub e approx. 10(11) cm(-3). Our experimental apparatus consisted of the electron beam accelerator, a plasma source, magnetic field coils, and beam, plasma, and microwave diagnostics. The beam diagnostics included a streak camera and Rogowski coils to measure beam profiles and net current in the system, respectively. A microwave interferometer provided plasma density measurements around the time of the beam-plasma interaction. We also measured RF emission using a microwave spectrometer. These data will be presented. Particle-in-cell code simulations have been performed to help us understand the relevant physics. We shall present the results of these computations. DOE

N90-15750# General Atomic Co., San Diego, CA.
UPGRADE PLANS TO HANDLE 30 TO 40 MBYTES OF DATA FOR D3-D
Pamela Henline Nov. 1989 6 p Presented at the 13th International Symposium on Fusion Engineering, Knoxville, TN, 2-6 Oct. 1989
(Contract DE-AC03-89ER-51114)
(DE90-003291; GA-A-19741; CONF-891007-93) Avail: NTIS HC A02/MF A01

The Department of Energy funds the D3-D tokamak program which carries out plasma physics and fusion energy research experiments. The machine began operations in February 1986; at that time, approximately 7 Mbytes of data was collected for each shot. Since that time, the shot size has steadily increased to a maximum of over 30 Mbytes. The average shot size is now about 25 Mbytes and over 1 Gigabyte of data has been collected during some operation days. The computer systems were designed to handle a maximum shot size of 25 Mbytes. In order to meet the increased demands, changes to hardware and software are being made and each experiment reviewed before being added to a shot. The area of data transfer now increasing the most is data transferred from small diagnostic DEC VAX systems to the main VAX cluster. Plans in this area include upgrading the VAX which receives data (possibly to a VAX 6310) to have both more CPU power and a faster interface to the Network Systems Hyperchannel which transfers data to the VAX. The new machine will be more easily upgraded with additional CPU's, communication devices and storage devices. Software changes are being incorporated on diagnostic VAXes so that subsets of data, or calculated results are included with the shot data file, rather than the often large (6 to 20 Mbytes) amount of data collected locally. DOE

N90-15751# General Atomic Co., San Diego, CA.
MECHANICAL DESIGN OF THE INSIDE LAUNCH SYSTEM FOR ELECTRON CYCLOTRON HEATING IN D3-D
E. H. Hoffmann, C. P. Moeller, and R. Prater Nov. 1989 3 p Presented at the 13th International Symposium on Fusion Engineering, Knoxville, TN, 2-6 Oct. 1989
(Contract DE-AC03-89ER-51114)
(DE90-003292; GA-A-19739; CONF-891007-94) Avail: NTIS HC A02/MF A01

A description is presented of the elements which form a transmission and launching system for the 2 MW Electron Cyclotron Heating (ECH) Inside Launch experiment on the DIII-D tokamak. The design of various system components, such as mode converters, waveguide bends, couplings, split waveguides, and launching mirrors are described. The DIII-D ECH system has ten gyrotrons which each produce 200 kW of power at 60 GHz. Each gyrotron has its own run of waveguide, about 46 m in length, to connect it to a vacuum window at the tokamak. A taper after the window reduces the diameter of the waveguide to the size that meets the requirements of the vacuum vessel port. A split waveguide which is electrostatically biased carries the microwave power across the location of the magnetic field resonance. The launch point is at the centerpost at midplane. The launching mirrors are adjustable to different angles of injection. DOE

N90-15752# General Atomic Co., San Diego, CA.
DESIGN OF DIII-D ADVANCED DIVERTOR
J. P. Smith, C. B. Baxi, E. Reis, M. Schaffer, and G. Thurston Nov. 1989 4 p Presented at the 13th International Symposium on Fusion Engineering, Knoxville, TN, 2-6 Oct. 1989 Submitted for publication
(Contract DE-AC03-89ER-51114)
(DE90-003343; GA-A-19742; CONF-891007-95) Avail: NTIS HC A02/MF A01

The Advanced Divertor is a modification being designed for the plasma chamber of the DIII-D tokamak in order to optimize the divertor configuration and allow a broader range of experiments to be carried out. The Advanced Divertor will enable two classes of physics experiments to be run in DIII-D: Divertor biasing and Divertor baffling. The Advanced Divertor has two principal components: a toroidally symmetric baffle; and a continuous ring electrode. The tokamak can be run in baffle, bias, or standard DIII-D divertor modes by accurate positioning of the outer divertor strike point through the use of the DIII-D plasma control system. The baffle will contain approximately 50,000 l/s pumping for particle removal in the outer bottom corner of the vacuum vessel. The strike point will be positioned at the entrance aperture for the baffle mode. The aperture geometry is designed to facilitate a large particle influx plus a high probability that backstreaming particles will be reionized and redirected to the aperture. Where the baffling plates meet, gas sealing is required to prevent recycling of neutrals back into the plasma. The electrode is a continuous water-cooled ring, armored with graphite. The ring is electrically isolated from the vessel wall and is biasable to 1 kV and 20 kA. The outer leg of the divertor will be positioned on the graphite covered ring during biasing experiments. DOE

N90-15753# InterScience, Inc., Troy, NY.
MAGNETIC MIRROR CONFINEMENT CONCEPTS SYSTEM STUDIES Final Report
1989 22 p
(Contract DE-AC01-84ER-51051)
(DE90-003667; DOE/ER-51051/T1) Avail: NTIS HC A03/MF A01

The following topics are discussed: world survey of mirror confinement research facilities; data base on mirror confinement program budget milestone; Fokker-Planck modeling of tandem mirror confinement; review of diagnostic capabilities for tandem mirror research; tandem mirror reactor concept development; tandem mirror data base; and primer on tokamak confinement. DOE

N90-15754# Los Alamos National Lab., NM.
INITIAL RESULTS FROM FRC (FIELD-REVERSED CONFIGURATION) COMPRESSION EXPERIMENTS ON FRX-C/LSM
D. J. Rej, G. A. Barnes, M. H. Baron, R. E. Chrien, R. E. Siemon, J. T. Slough, D. P. Taggart, T. Takahashi (Nihon Univ., Tokyo, Japan), M. Tuszewski, and B. L. Wright 1989 6 p Presented at the 11th US/Japan Workshop on Field-Reversed Configurations and Compact Toroids, Los Alamos, NM, 8-9 Nov. 1989
(Contract W-7405-eng-36)
(DE90-003390; LA-UR-89-3687; CONF-8911130-1) Avail: NTIS HC A02/MF A01

After more than two years of preparation, high-power FRC compression heating studies are now underway on the Los Alamos FRX-C/LSM facility. Field-reversed configuration plasmas are formed and translated out of the theta-pinch source, and into a compressor where the external B-field can be increased from 0.4 to 2 T in 55 microseconds. A principal experimental goal is to study FRC confinement at the high energy density, n(T(sub e) + T(sub i)) less than or equal 1.0 x 10(exp 22) keV/cu m, associated with the large external field. In this paper, we report on the first experiments which were performed between April and July, 1989. DOE

N90-15755# Lawrence Livermore National Lab., CA. Dept. of Physics.
THE MEASUREMENT OF TRANSPORT PROPERTIES IN STRONGLY COUPLED PLASMAS
R. L. Shepherd, D. R. Kania, L. A. Jones (Los Alamos National Lab., NM.), D. H. Schneider, and R. E. Stewart Dec. 1989 7 p Presented at the 24th Yamada Conference on Strongly Coupled Plasma Physics, Tokyo, Japan, 29 Aug. - 2 Sep. 1989 Submitted for publication
(Contract W-7405-eng-48)
(DE90-003451; UCRL-100805; CONF-8908133-8) Avail: NTIS HC A02/MF A01

Transport properties of strongly coupled plasmas are of interest in solid state physics, astrophysics, and high-density plasma physics. Many theoretical models have been presented to describe transport phenomena in strongly coupled plasmas, however few experiments have been performed to compare with calculations. We present the results of an experiment which measure the low-frequency electron resistivity in a partially degenerate (1.2 less than theta less than 1.9), strongly coupled (0.6 less than gamma less than 1.8) plasma. In addition, we suggest experiments to measure the stopping power and the energy transport in strongly coupled plasmas. DOE

N90-15756# Oak Ridge National Lab., TN.
DESTABILIZATION OF TOKAMAK PRESSURE-GRADIENT DRIVEN INSTABILITIES BY ENERGETIC ALPHA POPULATIONS
D. A. Spong, J. A. Holmes, J-N. Leboeuf, and P. J. Christenson (Michigan Univ., Ann Arbor.) 1989 22 p Presented at the IAEA Technical Committee Meeting on Alpha Particles/Confinement and Heating, Kiev, USSR, 23-26 Oct. 1989
(Contract DE-AC05-84OR-21400)
(DE90-003716; CONF-8910259-3) Avail: NTIS HC A03/MF A01

Alpha particle populations can significantly alter existing magnetohydrodynamic (MHD) instabilities in tokamaks through kinetic effects and coupling to otherwise stable shear Alfven waves. Here we consider resonances of the trapped alpha precessional drift with both the usual ballooning mode diamagnetic frequency, omega (sub star i)/2, and the toroidicity induced Alfven eigenmode (TAE). This is examined for noncircular tokamaks in the high-n ballooning limit using an isotropic alpha slowing down distribution and retaining the full energy and pitch angle dispersion in the alpha drift frequency. Applying this to CIT and ITER indicates that ballooning instabilities can persist at beta's below the ideal MHD threshold. These are especially dominated by the destabilization of the TAE mode. In addition, a hybrid fluid-particle approach for simulating alpha effects on pressure-gradient driven instabilities is described. DOE

N90-15757# Sandia National Labs., Albuquerque, NM.
THEORETICAL AND COMPUTATIONAL STUDIES OF MAGNETIC INSULATION AND OTHER PLASMA-OPENING-SWITCH PHENOMENA
Erick L. Lindeman, Jr. (Mission Research Corp., Los Alamos, NM.) Nov. 1989 86 p
(Contract DE-AC04-76DP-00789)
(DE90-004421; SAND-89-7111) Avail: NTIS HC A05/MF A01

The following topics are discussed: electron trajectories and magnetic insulation; blade-load simulation studies; azimuthal asymmetries; MAGIC simulation studies of a segmented plasma opening switch; PBFA II calculations with different spatial resolution; and analytic solution of the electron current layer in the magnetic front. DOE

N90-15758# Argonne National Lab., IL. Fusion Power Program.
NEAR-SURFACE SPUTTERED PARTICLE TRANSPORT FOR AN OBLIQUE INCIDENCE MAGNETIC FIELD PLASMA
Jeffrey N. Brooks Nov. 1989 17 p
(Contract W-31-109-eng-38)
(DE90-004422; ANL/FPP/TM-244) Avail: NTIS HC A03/MF A01

Near-surface sputtered particle transport has been analyzed numerically using models of sputtering, sheath parameters, and impurity collisions with a background D-T plasma. Tungsten and carbon sputtering was examined, for tokamak divertor plasma conditions. Redeposited ion parameters computed include the charge state, transit time, energy and angle of incidence. A regime of operation for finite self-sputtering of tungsten has been identified. This regime is broader than previous estimates. Results for energetically sputtered and thermally sputtered carbon are compared. DOE

N90-15759# Australian Inst. of Nuclear Science and Engineering, Lucas Heights.
THE 17TH AINSE PLASMA PHYSICS CONFERENCE: CONFERENCE HANDBOOK
1989 90 p Conference held in Lucas Heights, Australia, 6-8 Feb. 1989
(DE90-600936; INIS-mf-11537; CONF-8902130) Avail: NTIS (US Sales Only) HC A05/MF A01

The conference sessions covered stellarators, alfven waves, rotamak research, plasmas, RF current drives, laser fusion, high power ion cyclotron resonance, RF plasmas and magnetic confinement. DOE

N90-15760# Nauchno-Issledovatelskii Inst. Ehlekt- Rofizicheskoj Apparatury, Leningrad (USSR).
MICROFLUCTUATIONS OF PLASMA DENSITY IN A THETA-PINCH AND SPATIAL COHERENCY OF A PROBING LASER BEAM
A. B. Berezin, V. A. Burtsev, V. M. Kozhevin, V. G. Smirnov, and Yu. I. Sholokhov 1988 46 p In RUSSIAN
(DE90-603347; NIIEFA-P-K-0782) Avail: NTIS (US Sales Only) HC A03/MF A01

Spatial distribution of RMS value of density fluctuations and perturbation wave lengths determined by low hybrid drift (LHD)-instability is obtained on the basis of 1-D MHD model describing the behavior of the linear theta pinch plasma taking account of the process of classical and anomalous transfer. The assumption about spatial uniform distribution of electron density fluctuations inside the plasma layer is introduced proceeding from the results of these calculations. The angular spectrum of laser radiation passing through the plasma is obtained analytically in the framework of this assumption. Comparison of the spectrum shape obtained in the paper with the experiment has shown that anomalously great increase of divergence of coherent probing radiation can be explained by LHD-instability development. Such a sharp change in spatial coherency (divergency) may be used for diagnosis as a method to study microinstabilities of plasma in pinch discharges. DOE

N90-15761# Massachusetts Inst. of Tech., Cambridge. Dept. of Aeronautics and Astronautics.
PHYSICAL PROCESS IN MPD PLASMAS Final Report, 1 May 1988 - 31 Apr. 1989
Daniel Hastings 19 Jul. 1989 49 p
(Grant AF-AFOSR-0119-86; AF Proj. 2308)
(AD-A213679; AFOSR-89-1275TR) Avail: NTIS HC A03/MF A01 CSCL 21/3

Magnetoplasmadynamic, or MPD, thrusters are a promising method of propulsion for a variety of different space missions. This research develops and analyzes a numerical simulation of a quasi one dimensional model for an MPD thruster. A finite difference scheme is used to integrate the fluid equations for each species and a magnetic field equation derived from Maxwell's laws. The model includes separate electron and heavy species temperatures, varying conductivity, varying ionization fraction, collisional energy transfer between heavy particles and electrons, averaged viscosity and ambipolar diffusion, and electron heat conduction. Both constant area and variable area channels are examined.The applied current in the cases studied ranges from 79.6 kAmp/meter depth to 159 kAmp/meter depth for an inlet mass flow of 0.5 kg/sqm sec. It is shown that thermal equilibrium is not a valid assumption

in a typical thruster. It is also found that viscosity plays a significant role in determining thruster performance. Area variation is also found to have a significant effect on performance. GRA

N90-15762# Air Force Astronautics Lab., Edwards AFB, CA.
TUNNELLING EFFECTS ON LOW ENERGY FUSION CROSS SECTIONS Special Report, Jun. - Aug. 1989
Christopher L. Leakeas Sep. 1989 18 p
(AD-A214010; AL-TR-89-053) Avail: NTIS HC A03/MF A01 CSCL 20/10

Recently, the claim of discovery of cold fusion among the isotopes of hydrogen in a metal lattice has raised many questions as to the cross sections of some fusion reactions at low energies. The quantum phenomenon of tunneling and its effects on the fusion process are investigated. Special attention is paid to penetrabilities in the Hulthen potential, which gives a reasonably accurate approximation of the potential inside the metal lattice. Cross section data for the DD, ST and pD reactions are included. Also given are graphs showing the fusion cross section crossover point between the DD and DT reactions and the increased penetrabilities due to enhance tunneling effects. GRA

N90-15763# Naval Research Lab., Washington, DC. Beam Physics Branch.
OPTICAL GUIDING BY PLASMA WAVES IN THE PLASMA BEAT WAVE ACCELERATOR
E. Esarey and A. Ting 25 Oct. 1989 25 p
(AD-A214288; NRL-MR-6542) Avail: NTIS HC A03/MF A01 CSCL 20/9

As the resonantly driven plasma wave grows to sufficiently large amplitudes, it strongly affects the diffractive properties of the radiation beams in the plasma beat wave accelerator (PBWA). In particular, a large amplitude plasma wave (with phase velocity approximately the speed of light) will break up an initially uniform radiation beam into periodic beamlet segments, of length less than or equal to half a plasma wavelength, which remain optically guided as they propagate. In the PBWA, for an optimal choice of the mismatch between the radiation beat frequency and the ambient plasma frequency, the resonantly driven plasma wave may lead to enhanced focusing of the radiation beams. GRA

N90-15764# Los Alamos National Lab., NM.
PROGRESS IN LTE AND NON-LTE TRANSPORT CALCULATIONS
J. J. Keady, W. F. Huebner (Southwest Research Inst., San Antonio, TX.), J. Abdallah, Jr., and N. H. Magee, Jr. 1989 15 p Presented at the Advanced NATO Research Workshop: Physical Processes in Hot Cosmic Plasmas, Sicily, Italy, May 1989
(Contract W-7405-eng-36)
(DE90-003394; LA-UR-89-3769; CONF-8905245-1) Avail: NTIS HC A03/MF A01

The physical processes in ionized gases are reviewed along with recent calculations of particular processes. Ongoing opacity calculations at Los Alamos are described. Some of the open issues in the calculation of physical processes relevant to opacities are discussed. DOE

N90-15765# Argonne National Lab., IL. Analytical Chemistry Lab.
ICP/AES (INDUCTIVELY COUPLED PLASMA/ATOMIC EMISSION SPECTROSCOPY): A MODERN ANALYTICAL TOOL
Carmen S. Sabau 1989 18 p Presented at the 14th Annual ARA Congress, Los Angeles, CA, 20-22 Apr. 1989
(Contract W-31-109-eng-38)
(DE90-003822; CONF-8904296-1) Avail: NTIS HC A03/MF A01

A historical evolution of Inductively Coupled Plasma/Atomic Emission Spectroscopy (ICP/AES) is presented, along with the basic principles and equipment of this technique. The method of ICP/AES has developed rapidly since 1965 as an analytical tool. This modern method, which replaced combustion flames with a plasma, has proven to be superior to the traditional excitation sources in terms of precision, accuracy, and sensitivity. Several examples of analyses using this method demonstrate its advantages and multiple uses. DOE

76 SOLID-STATE PHYSICS

Includes superconductivity.

For related information, see also *33 Electronics and Electrical Engineering* and *36 Lasers and Masers.*

N90-15766*# Clarkson Univ., Potsdam, NY.
BRIDGMAN CRYSTAL GROWTH Final Report
Frederick Carlson Jan. 1990 59 p
(Grant NAG1-397)
(NASA-CR-186204; NAS 1.26:186204) Avail: NTIS HC A04/MF A01 CSCL 20B

The objective of this theoretical research effort was to improve the understanding of the growth of Pb(x)Sn(1-x)Te and especially how crystal quality could be improved utilizing the microgravity environment of space. All theoretical growths are done using the vertical Bridgman method. It is believed that improved single crystal yields can be achieved by systematically identifying and studying system parameters both theoretically and experimentally. A computational model was developed to study and eventually optimize the growth process. The model is primarily concerned with the prediction of the thermal field, although mass transfer in the melt and the state of stress in the crystal were of considerable interest. The evolution is presented of the computer simulation and some of the important results obtained. Diffusion controlled growth was first studied since it represented a relatively simple, but nontheless realistic situation. In fact, results from this analysis prompted a study of the triple junction region where the melt, crystal, and ampoule wall meet. Since microgravity applications were sought because of the low level of fluid movement, the effect of gravitational field strength on the thermal and concentration field was also of interest. A study of the strength of coriolis acceleration on the growth process during space flight was deemed necessary since it would surely produce asymmetries in the flow field if strong enough. Finally, thermosolutal convection in a steady microgravity field for thermally stable conditions and both stable and unstable solutal conditions was simulated.

Author

N90-15767# Oak Ridge National Lab., TN. Metals and Ceramics Div.
DEFORMATION TWINNING IN ORDERED INTERMETALLIC COMPOUNDS
M. H. Yoo, C. L. Fu, and J. K. Lee 1989 8 p Presented at the Materials Research Society Fall Meeting, Boston, MA, 27 Nov. - 2 Dec. 1989
(Contract DE-AC05-84OR-21400)
(DE89-014779; CONF-891119-1) Avail: NTIS HC A02/MF A01

Mechanistic understanding of deformation twinning in ordered superlattice structures is reviewed, and the inter-relationships between twinning and generalized plastic flow or fracture toughness are discussed. While general discussions refer to all the fcc-based and bcc-based cubic and noncubic ordered intermetallic alloys, specific calculations of the energetic and kinetic aspects of deformation twinning are made for TiAl. The importance of the twin-slip conjugate relationship on high temperature mechanical properties is emphasized. Discussion is given of possible effects of macro- and micro-alloying on twinning propensity. DOE

N90-15768# Los Alamos National Lab., NM. Theoretical Div.
PHONONS AND CHARGE-TRANSFER EXCITATIONS IN HTS SUPERCONDUCTORS
A. R. Bishop 1989 25 p Presented at the International School of Materials Science and Technology: Earlier and Recent Aspects of Superconductivity, Erice, Italy, 4-16 Jul. 1989
(Contract W-7405-eng-36)
(DE89-016616; LA-UR-89-2885; CONF-8907139-1) Avail: NTIS HC A03

Some of the experimental and theoretical evidence implicating phonons and charge-transfer excitations in HTS superconductors is reviewed. It is suggested that superconductivity may be driven by a synergistic interplay of (anharmonic) phonons and electronic degrees of freedom (e.g., charge fluctuations, excitons). DOE

N90-15769# Sandia National Labs., Albuquerque, NM.
SURFACE ROUGHENING OF Ge(001) DURING 200 eV Xe ION BOMBARDMENT AND Ge MOLECULAR BEAM EPITAXY
E. Chason, J. Y. Tsao, K. M. Horn, S. T. Picraux, and H. A. Atwater 1989 19 p. Presented at the 36th American Vacuum Society National Vacuum Symposium, Boston, MA, 23-27 Oct. 1989
(Contract DE-AC04-76DP-00789)
(DE90-000674; SAND-89-1322C; CONF-891093-6) Avail: NTIS HC A03/MF A01

The kinetics of surface roughening of Ge (001) during 200 eV Xe ion bombardment and during Ge molecular beam epitaxy are studied by real time reflection high energy electron diffraction. In both cases, initially smooth surfaces reach a steady state roughness which depends on temperature and incident ion or adatom flux. The data are analyzed in terms of a model in which defect-induced roughening competes with defect-induced smoothening, and in which the defect creation rate and surface diffusivity are fitting parameters. For comparable fluxes, the temperature dependences for the net roughening induced by ions and adatoms are strikingly similar, implying a similarity in the surface diffusivities of vacancies and adatoms. For the case of ion-induced roughening, a defect creation rate of 3 per ion is obtained which is consistent with calculations and which indicates that the majority of atomic displacements produce surface defects at these ion energies. DOE

N90-15770# Lawrence Livermore National Lab., CA.
SPECTROSCOPIC AND LASER PROPERTIES OF Cr:LiCaAlF6 AND Cr:LiSrAlF6 CRYSTALS
William F. Krupke, Stephen A. Payne, and Lloyd A. Chase Aug. 1989 8 p Presented at the 5th International Tunable Laser Conference, Irkutsk, USSR, 20-23 Sep. 1989
(Contract W-7405-eng-48)
(DE90-000783; UCRL-100786; CONF-8909211-2) Avail: NTIS HC A02/MF A01

Cr:LiCAF and Cr:LiSAF have been found to be excellent materials for efficient, tunable, chromium lasers. Their physical, thermal, optical, and spectroscopic properties permit efficient laser emission at the watt level under laser pumping, tunable over the range 740 to 920 nm. Flashlamp pumping has generated joule level output energy without appearance of deleterious solarization effects. Further improvements in laser performance are anticipated as laser crystals of higher quality become available. This report covers work on the laser properties of Cr:LiCAF and Cr:LiSAF crystals. DOE

N90-15771# Oak Ridge National Lab., TN.
THEORETICAL STUDIES ON THE ELECTRONIC STRUCTURE OF HIGH-TEMPERATURE SUPERCONDUCTORS
W. A. Shelton, Jr. Oct. 1988 6 p
(Contract DE-AC05-84OR-21400)
(DE90-001301; ORNL/FTR-3067) Avail: NTIS HC A02/MF A01

Large scale computer codes for calculating the electronic structure of ordered and disordered high temperature superconductors were developed. These codes were used to calculate the electronic structure of Ba(1-x)K(x)BiO3 alloys and the Mott insulator NiO. DOE

N90-15772# Lawrence Livermore National Lab., CA.
MICRON-THIN Nb FILMS RECOVERED FROM MBAR SHOCK PRESSURES
W. J. Nellis, R. Koch, H. Davidson, J. W. Hunter, W. F. Brocius, A. Marshall, and T. H. Geballe (Stanford Univ., CA.) Sep. 1989 4 p Presented at the American Physical Society Topical Conference on Shock Compression of Condensed Matter, Albuquerque, NM, 14-17 Aug. 1989 Sponsored in part by Strategic Defense Initiative
(Contract W-7405-eng-48)
(DE90-001509; UCRL-100833; CONF-890812-59) Avail: NTIS HC A02/MF A01

Niobium films of thickness 1, 2.5, 5, and 10 microns were subjected to shock pressures of 0.72 and 0.97 Mbar. The recovery technique and the results of microstructural investigations of the recovered films are described. DOE

N90-15773# Oak Ridge National Lab., TN. Instrumentation and Controls Div.
CHARACTERISTICS OF CMOS ANALOG INTEGRATED STRUCTURES USING MOSIS (METAL OXIDE SEMICONDUCTOR IMPLEMENTATION SYSTEM)
Charles L. Britton, Jr., J. M. Rochelle, G. T. Alley, D. F. Newport (Tennessee Univ., Knoxville.), W. L. Bryan, and Milton N. Ericson 1989 7 p Presented at the IEEE Nuclear Science Symposium and Exhibits, San Francisco, CA, 25-27 Oct. 1989 Sponsored in part by the Navy RADIAC Development Program and DARPA
(Contract DE-AC05-84OR-21400)
(DE90-001630; CONF-891087-5) Avail: NTIS HC A02/MF A01

The performance of analog functions and subcircuits designed at Oak Ridge National Laboratory (ORNL) and successfully implemented using metal oxide semiconductor implementation system (MOSIS) fabrication is summarized. Among the topics discussed are operational amplifiers, a low-voltage comparator, solar cells, an improved low-voltage bilateral analog switch a subthreshold reference circuit for supply independent biasing, and a variety of CMOS transistor measurements. The suitability of MOSIS SPICE parameters in strong and weak inversion modeling as well as dc, ac, and noise performance are discussed. Finally, the application to analog design of low-cost, high-performance CAD tools, such as MAGIC, is examined. DOE

N90-15774# California Univ., Berkeley. Lawrence Berkeley Lab. Materials and Chemical Sciences Div.
THERMALLY STABLE METAL/GaAs CONTACTS Ph.D. Thesis
Jian Ding (California Univ., Berkeley.) Jun. 1989 132 p
(Contract DE-AC03-76SF-00098)
(DE90-002122; LBL-27661) Avail: NTIS HC A07/MF A01

Further improvement of electrical properties and thermal stability of reactively sputtered refractory metal nitride contacts on GaAs and In-based ohmic contacts to GaAs require a systematic study of the relationships between structural and electrical characteristics at the interface. The interface morphologies and structures of Nb/GaAs, NbN/GaAs, TiN/GaAs, WN/GaAs and In/GaAs contacts were investigated before and after annealing at temperatures up to 950 C by transmission electron microscopy and diffraction, energy dispersive spectrometry of x rays, x ray diffractometry and cross-sectional high resolution transmission electron microscopy. The results from these techniques were combined to provide detailed descriptions of the structural evolution of the interface region in refractor metal nitride/GaAs and In/GaAs heterojunctions. Structural details were related to the corresponding electrical characteristics. DOE

N90-15775# International Centre for Theoretical Physics, Trieste (Italy).
ON THE FREE CARRIER-NEGATIVE U CENTER INTERACTING MODEL FOR THE HIGH-T(SUB c) OXIDE SUPERCONDUCTOR
Li-Yuan Zhang (Peking Univ., China) Mar. 1989 8 p Submitted for publication
(DE89-635908; IC-89/39) Avail: NTIS (US Sales Only) HC A02/MF A01

Using the free carrier-negative U center interacting model, we have investigated the superconducting transition temperature T sub c, the specific heat jump at T sub c, the coherence length, the penetration depth, the thermodynamic critical field and the isotope effect for the high T sub c oxide superconductor. The theoretical values of these physical quantities are consistent with the experimental values. Further, the residual electronic specific

heat in the superconducting state is explained as the result of the inherent instability in this superconductive mechanism. DOE

N90-15776# Argonne National Lab., IL. Materials Science Div.
TUNNELING SPECTROSCOPY AND THE ELECTRON-PHONON INTERACTION IN Ba(1-x)K(x)BiO3
J. F. Zasadzinski, N. Tralshawala, J. Timpf (Illinois Inst. of Tech., Chicago.), D. G. Hinks, B. Dabrowski, A. W. Mitchell, and D. R. Richards 1989 13 p Presented at the International Conference on High T(sub c) Thin Films and Single Crystals, Ustron, Poland, 30 Sep. - 4 Oct. 1989
(Contract W-31-109-eng-38)
(DE90-002842; CONF-890939-2) Avail: NTIS HC A03/MF A01

Tunneling spectroscopy measurements were performed on bulk samples of Ba(1-x)K(x)BiO3 for the compositions, x=0.375, 0.4 and 0.5, using the natural, surface oxide as the tunnel barrier. The data show structures which are characteristic of phonon effects as seen in conventional superconductors and suggest that alpha (sup 2)F omega is strongest for the high frequency optical modes. These results are consistent with other experiments and with recent microscopic calculations which indicate that phonon-mediated pairing is responsible for the superconductivity in this compound. DOE

N90-15777# Argonne National Lab., IL.
THE POSSIBLE OCCURRENCE OF MULTI-PHASE BEHAVIOR IN THE HIGH T(SUB c) SUPERCONDUCTOR YBa2Cu3O(SUB x)
Mark A. Beno, L. Soderholm, D. W. Capone, II, D. G. Hinks, J. D. Jorgensen, J. D. Grace, I. K. Schuller, Boyd W. Veal, L. J. Nowicki, and A. P. Paulikas et al 1989 17 p Prepared in cooperation with Illinois Inst. of Tech., Chicago
(Contract W-31-109-eng-38)
(DE90-002999; ANL/PPRNT-89-185) Avail: NTIS HC A03/MF A01

We report here the results obtained for powder diffraction studies on four YBa2, Cu3, O sub x samples in which a model with two orthorhombic phases was used to obtain an improved agreement. The implications of this structural model on the systematic variation of (Tc) with oxygen content will be discussed. DOE

N90-15778# Argonne National Lab., IL.
SYNTHESIS CONDUCTIVITY, AND X RAY PHOTOELECTRON SPECTRUM OF Bi2Sr2Cu(SUB 7+x). A NEW TERNARY BISMUTH-OXIDE SYSTEM EXHIBITING METALLIC CONDUCTIVITY
Leigh Christopher Porter, Evan Appleman, Mark A. Beno, Carolyn S. Cariss, K. Douglas Carlson, Harry Cohen, Urs Geiser, R. J. Thorn, and John M. Williams 1989 10 p
(Contract W-31-109-eng-38)
(DE90-003010; ANL/PPRNT-89-199) Avail: NTIS HC A02/MF A01

The preparation and some of the properties relating to the superconductive state of the newly discovered ternary bismuth oxides, Bi2Sr2Cu2O(7+x), are described. Conductivity behavior ranging from semiconductive to metallic is observed when four-probe ac resistivity measurements are carried out on pressed pellet specimens that have been annealed under different conditions. From a determination of the total oxygen present by an iodometric titration, it was found that metallic conductivity was associated with a higher oxygen content. An x ray photoelectron experiment was carried out in order to determine whether bismuth or copper was present as the mixed valent species. The XPS spectrum of the Bi 4f orbital electrons in the oxides was nearly identical to that observed in Bi2O3, with no evidence of any Bi5(+). DOE

N90-15779# Argonne National Lab., IL. Chemistry Div.
LINEAR ELECTRON-HOLE-ELECTRON PAIR MODEL OF HIGH-TEMPERATURE SUPERCONDUCTIVITY IN La(2-x)M(x)CuO4 AND YBa2Cu3O(7-y): PART 2. DEPENDENCE OF THE SUPERCONDUCTING TRANSITION TEMPERATURES ON PRESSURE AND ON HOLE CONCENTRATION
Myung-Hwan Whangbo, Michel Evain, Enric Canadell (Paris-Sud Univ., Orsay, France), and Jack M. Williams 1989 14 p
(Contracts W-31-109-eng-38; DE-FG05-86ER-45259)
(DE90-003012; ANL/PPRNT-89-197) Avail: NTIS HC A03/MF A01

On the basis of the linear electron-hole-electron (e-h-e) pair model, the number of holes (i.e., formal Cu3(+) sites), and an applied pressure, affect the superconducting transition temperatures (Tc) of La(2-x)M(x)CuO4 and LBa2Cu3O(7-y) with (L = Y, Sm, Eu, Gd, Dy, Ho, Yb). The origin is also examined of the plateaus in the (Tc) vs oxygen content pilot of YBa2Cu3O(7-y) within the framework of the linear e-h-e pair model. DOE

N90-15780# Lawrence Livermore National Lab., CA.
ELECTRON-POSITRON MOMENTUM DISTRIBUTION MEASUREMENTS OF HIGH-T SUPERCONDUCTORS AND RELATED SYSTEMS
A. L. Wachs, P. E. A. Turchi, R. J. Howell, Y. C. Jean, M. J. Fluss, R. N. West, J. H. Kaiser, S. Rayner, H. Hahgighi, and K. L. Merkle (Argonne National Lab., IL.) et al Aug. 1989 3 p Presented at the International Conference on Materials and Mechanisms of Superconductivity - High-Temperature Superconductors, Stanford, CA, 23-28 Jul. 1989
(Contract W-7405-eng-48)
(DE90-002974; UCRL-100596-Rev-1; CONF-890718-Rev-1)
Avail: NTIS HC A01/MF A01

Measurements are discussed of the 2-D angular correlation of positron annihilation radiation (ACAR) in La2CuO4, YBa2Cu3O7 (YBCO), and NiO. The measurements for NiO are the first such 2-D ACAR measurements; the YBCO results are of a higher statistical quality than previously reported in the literature. The data are compared with complementary theoretical calculations and with each other. The implication is discussed of the analysis for ACAR studies of similar and related systems. DOE

N90-15781# California Univ., Berkeley. Lawrence Berkeley Lab. Materials and Chemical Sciences Div.
VARIATIONAL QUANTUM MONTE CARLO CALCULATION OF ELECTRONIC AND STRUCTURAL PROPERTIES OF CRYSTALS
Steven G. Louie Sep. 1989 15 p Presented at the Los Alamos Workshop on Quantum Simulations of Condensed Matter Phenomena, Los Alamos, NM, 8-11 Aug. 1989
(Contract DE-AC03-76SF-00098)
(DE90-003265; LBL-27806; CONF-8908106-5) Avail: NTIS HC A03/MF A01

Calculation of the electronic and structural properties of solids using a variational quantum Monte Carlo nonlocal pseudopotential approach is described. Ionization potentials and electron affinities for atoms, and binding energies and structural properties for crystals are found to be in very good agreement with experiment. The approach employs a correlated many-electron wavefunction of the Jastrow-Slater form and the exact Coulomb interaction between valence electrons. One- and two-body terms in the Jastrow factor are used and found necessary for an accurate description of the electron-electron energy for the systems considered. The method has further been applied to compute various single-particle properties for solids including the single-particle orbital occupancy, electron pair correlation functions, and quasiparticle excitation energies. DOE

N90-15782# Los Alamos National Lab., NM.
PARTIAL REDUCTION OF RE-OXIDATION PROCESSING OF Y-Ba-Cu-O SPUTTERED THIN FILMS
F. H. Garzon, J. G. Beery, D. K. Wilde, and I. D. Raistrick 1989 9 p Presented at the Materials Research Society Fall Meeting, Boston, MA, 27 Nov. - 2 Dec. 1989 Submitted for publication

(Contract W-7405-eng-36)
(DE90-003655; LA-UR-89-3963; CONF-891119-11) Avail: NTIS HC A02/MF A01

Thin films of Y--Ba--Cu--O were produced by RF sputtering of YBa2 Cu3 O7-x ceramic targets, using a variety of plasma compositions, RF power levels, and substrate temperatures. Post annealing of these films in oxygen produced superconducting films with T sub c values between 40 to 60 K, broad transition widths and semiconductor-like electrical behavior above T sub c. Subsequent annealing at 850 C in an inert gas with a residual oxygen partial pressure of 10 ppM followed by an oxygen anneal produced high quality thin films: T sub c greater than 85 K with narrow transition widths. The structure and morphology of these films during reduction-oxidation processing were monitored using x ray diffraction and electron microscopy. DOE

N90-15783# International Centre for Theoretical Physics, Trieste (Italy).
FURTHER STUDIES ON POSSIBLE COEXISTENCE OF ANTIFERROMAGNETISM AND SUPERCONDUCTIVITY IN 2D HEISENBERG MODEL
Hao Chen, Zhao-Bin Su, and Lu Yu (Academia Sinica, Beijing, China) May 1989 19 p Submitted for publication
(DE90-601082; IC-89/89) Avail: NTIS (US Sales Only) HC A03/MF A01

The question of possible coexistence of antiferromagnetism (AF) and superconductivity (SC) is re-examined with the t - J model by using an improved mean field treatment. The renormalization of the effective Hamiltonian and the symmetry of the order parameters are properly taken into account. Our calculations reconfirm the possible coexistence of AF and SC below critical doping concentrations delta sub c = 0.04 and 0.06 for t/J = 5 and 2.5, respectively, in good agreement with recent variational Monte Carlo results. This conclusion is consistent with the (mu)SR data. Among pairings of various symmetries, the d-wave pairing has the lowest energy. DOE

N90-15784# Aerospace Corp., El Segundo, CA. Chemistry and Physics Lab.
ORIENTATION OF rf-SPUTTER-DEPOSITED MoS2 FILMS
P. A. Bertrand 15 Jan. 1989 23 p
(Contract F04701-88-C-0089)
(ATR-89(4752)-1) Avail: NTIS HC A03/MF A01

A theory to predict the orientation of radio frequency (rf) sputter deposited MoS2 films with respect to the substrate surface is presented. Oxygen containing species such as H2O and -OH are postulated to be active sites that force crystallites to form with their basal planes perpendicular to the surface. X ray diffraction is used to determine the crystallite orientation in films deposited on smooth, rough, or oxidized Si surfaces, as well as on fused silica or gold surfaces. The results support the theory. To produce MoS2 films with their crystallite basal planes parallel to a substrate surface (which has been suggested to be the low friction orientation), the active sites must be removed from the substrate by, for instance, heating in vacuum. Author

N90-15785# Brookhaven National Lab., Upton, NY. Physics Dept.
MAGNETIC AND ELECTRONIC CORRELATIONS IN YBa2Cu3O(SUB 6+x)
J. M. Tranquada 1989 20 p Presented at the International School of Materials Science and Technology: Earlier and Recent Aspects of Superconductivity, Erice, Italy, 4-16 Jul. 1989
(Contract DE-AC02-76CH-00016)
(DE89-017604; BNL-43107; CONF-8907139-3) Avail: NTIS HC A03/MF A01

YBa2Cu3O(6+x) is an antiferromagnetic insulator in its tetragonal phase at small x, and it becomes a superconducting metal in the large x orthorhombic phase. The transition between the two phases is controlled by the orientational ordering of CuO(x) chain segments and dielectric screening by the BaO layers. In the orthorhombic phase, holes from the chains are transferred to the CuO2 planes, and the superconducting transition temperature scales with the density of O 2p holes. The antiferromagnetic ordering in the tetragonal phase is dominated by localized Cu moments in the CuO2 planes. The two-dimensional (2-D) coupling between those spins is unusually strong. The interaction between nearest-neighbor planes is sufficiently strong that spins in bilayers remain highly correlated well above the Neel temperature. Long-range order is destroyed when a significant density of O 2p holes is present in the planes; however, there is evidence that Cu moments survive and interact in the metallic phase. DOE

N90-15786# Lawrence Livermore National Lab., CA.
PICOSECOND PHOTOCONDUCTIVITY USING A GRADED BANDGAP Al(x)Ga(1-x)As ACTIVE DETECTING LAYER
J. D. Morse, R. P. Mariella, and R. W. Dutton (Stanford Univ., CA.) Nov. 1989 6 p Presented at the IEEE International Electronic Devices Meeting, Washington, DC, 3-6 Dec. 1989 Submitted for publication
(Contract W-7405-eng-48)
(DE90-003452; UCRL-101579; CONF-891205-2) Avail: NTIS HC A02/MF A01

This paper presents a concept where improved responsivity for picosecond photoconductors is achieved by utilizing a graded bandgap Al(x)Ga(1-x)As active detecting layer grown on a high defect density. Low temperature GaAs layer by MBE. By taking advantage of the superior transport properties of the graded Al(x)Ga(1-x)As layer, order of magnitude improvement in responsivity was demonstrated, along with 2 to 6 times improvement in peak photo-current response. DOE

N90-15787# Cornell Univ., Ithaca, NY. Dept. of Materials Science.
AN INVESTIGATION OF MECHANICAL BEHAVIOR OF CRYSTALLINE SOLIDS Final Report, Mar. 1984 - Jun. 1988
C.-Y. Li 1988 8 p
(Contract DE-FG02-84ER-45055)
(DE90-003530; DOE/ER-45055/24) Avail: NTIS HC A02/MF A01

Brief summaries of twenty-four research programs on the mechanical behavior of crystalline solids are presented. Materials studied include Incoloys, copper, stainless steel 316, and aluminum-magnesium alloys. DOE

N90-15788# Argonne National Lab., IL. Materials Science Div.
TWO-DIMENSIONAL MAGNETIC PHASE TRANSITION OF ULTRATHIN IRON FILMS ON Pd(100)
C. Liu and S. D. Bader 1989 12 p Presented at the 34th Conference on Magnetism and Magnetic Materials, Boston, MA, 28 Nov. - 1 Dec. 1989
(Contract W-31-109-eng-38)
(DE90-003555; CONF-891117-10) Avail: NTIS HC A03/MF A01

Epitaxial Fe films grown on Pd(100) are used to study monolayer magnetism, critical behavior, and surface magnetic anisotropy, by means of in-situ surface magneto-optical Kerr-effect measurements. Auxilliary LEED-Auger observations in 10(exp -11) Torr vacuum are used to characterize the (1 x 1) epitaxy and the layer-by-layer film-growth mode. Ferromagnetic hysteresis loops were detected for all Fe thickness from 0.6 to 4 monolayers (ML) with the (Tc) monotonically increasing with thickness, independent of the easy-axis orientation. The easy axis is perpendicular to the film plane below a critical thickness of 2.5 ML for 100-K film growth, and reorients in-plane above this thickness, and for all thicknesses for films grown at 300 K. The temperature dependence of the magnetization was obtained from the height of the Kerr loops in the remanent state and used to extract an effective magnetization exponent (beta) for different film thicknesses and spin orientations. A value of beta = 0.127 + or - 0.004 is reported for a 1.2-ML Fe film with perpendicular spin orientation from a log-log plot for T is greater than 0.9 (Tc), in agreement with the value of the theoretical 2-dimensional Ising critical exponent beta(sub c) = 1/8 = 0.125. DOE

N90-15789# Argonne National Lab., IL. Materials and Components Technology Div.
PROCESSING AND FABRICATION OF YBa2Cu4O8 AND YBa2Cu4O8/YBa2Cu3O(x) COMPOSITES
U. Balachandran, M. E. Biznek, K. C. Goretta, Boyd W. Veal, R. B. Poeppel, and T. O. Mason (Northwestern Univ., Evanston, IL.) Nov. 1989 9 p Presented at the Materials Research Society Fall Meeting, Boston, MA, 27 Nov. - 2 Dec. 1989 Submitted for publication
(Contract W-31-109-eng-38; NSF DMR-88-09854)
(DE90-003559; CONF-891119-19) Avail: NTIS HC A02/MF A01

Powders of YBa2Cu4O8 (124) were prepared via solid state reaction of Y2O3, BaCO3, and CuO. The mixed precursors were heated in flowing oxygen of reduced total pressure, followed by cooling and annealing at 750 C under ambient pressure oxygen. The procedure produced orthorhombic 124 as the main phase with YBa2Cu3O(x) (123) as a minor impurity phase. The phase purity improved and nearly phase-pure 124 was obtained upon annealing the as-calcined powder in flowing oxygen at 800 C. DOE

N90-15790# Argonne National Lab., IL. Materials Science Div.
CHARACTERIZATION OF MOCVD (METAL ORGANIC CHEMICAL VAPOR DEPOSITION) GROWN EPITAXIAL CERAMIC OXIDE THIN FILMS
J. C. Parker, H. L. M. Chang, J. J. Xu, and D. J. Lam Nov. 1989 6 p Presented at the Materials Research Society Fall Meeting, Boston, MA, 27 Nov. - 2 Dec. 1989
(Contract W-31-109-eng-38)
(DE90-003561; CONF-891119-24) Avail: NTIS HC A02/MF A01

Characterization of TiO2 films grown by the MOCVD technique using micro-Raman scattering is discussed. The effects of processing parameters on the film composition and morphology have been investigated. The micro-Raman technique is shown to be a useful tool for characterizing oxide thin films grown by the MOCVD technique. DOE

N90-15791# Argonne National Lab., IL. Materials Science Div.
MOLECULAR-DYNAMICS STUDY OF THE AMORPHIZATION OF CuTi
Michael J. Sabochick (Air Force Inst. of Tech., Wright-Patterson AFB, OH.) and Nghi Q. Lam Nov. 1989 7 p Presented at the Materials Research Society Fall Meeting, Boston, MA, 27 Nov. - 2 Dec. 1989 Sponsored in part by Air Force Inst. of Technology, Wright-Patterson AFB, OH
(Contract W-31-109-eng-38)
(DE90-003563; CONF-891119-26) Avail: NTIS HC A02/MF A01

Radiation-induced amorphization of the crystalline compound CuTi was investigated by molecular-dynamics simulations using new interatomic potentials derived from the embedded-atom method. Two different approaches to amorphization were tried: one in which Cu and Ti atoms were randomly exchanged, and another in which Frenkel pairs were introduced at random. The potential energy, volume expansion and pair-correlation function were calculated as functions of chemical disorder and atomic displacements. The results indicate that, although both chemical disordering and point-defect introduction increase the system energy and volume, the presence of Frenkel pairs is essential to trigger the crystalline-to-amorphous transition. DOE

N90-15792# Argonne National Lab., IL. Materials Science Div.
IRRADITION-INDUCED GRAIN GROWTH: ROLE OF DISLOCATIONS
Charles W. Allen and Lynn E. Rehn Nov. 1989 8 p Presented at the Materials Research Society Fall Meeting, Boston, MA, 27 Nov. - 2 Dec. 1989 Submitted for publication
(Contract W-31-109-eng-38)
(DE90-003565; CONF-891119-16) Avail: NTIS HC A02/MF A01

Existing theories of irradiation-induced grain growth assume that growth occurs by the boundary migration mechanism commonly observed for thermal growth and that it is only the point defects generated at boundaries during the irradiation which are responsible for boundary migration. In contrast, in situ observations during ion irradiation of Au films at temperatures less than 20 K have clearly demonstrated that growth occurs both by boundary migration and by grain coalescence. Here we present further evidence for the latter. Furthermore, the substantial defect cluster activity observed during irradiation suggests that dislocations play a significant role in the growth phenomenon. Here, we also demonstrate qualitatively that glide of such dislocations to or through a boundary can produce essentially the same effect on boundary position or structure that the original point defects would have had if they had migrated individually to or through the boundary. Via dislocation motion, point defects originating far from a boundary may induce boundary migration or boundary structure change, and hence, grain growth. DOE

N90-15793# Argonne National Lab., IL. Materials Science Div.
PREPARATION, STRUCTURE AND PROPERTIES OF VO(SUB x) AND TiO2 THIN FILMS BY MOCVD
H. L. M. Chang, J. C. Parker, H. You, J. J. Xu, and D. J. Lam Nov. 1989 7 p Presented at the Materials Research Society Fall Meeting, Boston, MA, 27 Nov. - 2 Dec. 1989
(Contract W-31-109-eng-38)
(DE90-003566; CONF-891119-17) Avail: NTIS HC A02/MF A01

Titanium and vanadium oxide thin films have been prepared in a cold wall low pressure MOCVD system for the study of MOCVD processing of epitaxial oxide films. Films were deposited on Si(111) and sapphire (0001) and (1120) at temperatures from 400 to 800 C. Processing parameter-structure-property relationship was examined in detail and the result is presented. DOE

N90-15794# Argonne National Lab., IL. Materials and Components Technology Div.
PROCESSING YBa2Cu3O(x) WIRES IN O3/O2
S. E. Dorris, K. C. Goretta, B. Hajyousif, U. Balachandran, J. T. Dusek, D. Shi, and R. B. Poeppel Sep. 1989 8 p Presented at the 1st International Ceramic Science and Technology Congress, Anaheim, CA, 31 Oct. - 3 Nov. 1989
(Contract W-31-109-eng-38)
(DE90-003570; CONF-8910120-5) Avail: NTIS HC A02/MF A01

Plastically extruded wires were heat treated in O2 or a mixture of O2/3 percent O3. The presence of O3 during the burnoff of organics resulted in measurable increases in critical current density J(sub c), while post-sintering annealing in the O3/O2 mixture rather than in O2 had no effect. Maximum zero-field J(sub c) values exceeded 1000 A/sq cm. DOE

N90-15795# Sandia National Labs., Albuquerque, NM.
CATION DISORDERING IN THE Tl-2122 SUPERCONDUCTORS
B. Morosin, D. S. Ginley, E. L. Venturini, R. J. Baughman, J. E. Schirber, and C. P. Tigges 1989 8 p Presented at the Materials Research Society Fall Meeting, Boston, MA, 27 Nov. - 2 Dec. 1989
(Contract DE-AC04-76DP-00789)
(DE90-003579; SAND-89-2793C; CONF-891119-22) Avail: NTIS HC A02/MF A01

Several crystals belonging to the Tl-2122 structure type (Tl2CaBa2Cu2O8 with c = 29A), and have shown that cation solid solution occurs. Such cation disorder appears to be responsible for the observed small differences in lattice parameters reported by various investigators and to contribute towards the substantial variation in the superconducting transition temperatures. DOE

N90-15796# Brookhaven National Lab., Upton, NY.
MAGNETIC MECHANISMS OF HIGH TEMPERATURE SUPERCONDUCTIVITY
V. J. Emery 1989 13 p Presented at the 34th Conference on Magnetism and Magnetic Materials, Boston, MA, 28 Nov. - 1 Dec.

1989
(Contract DE-AC02-76CH-00016)
(DE90-003625; BNL-43407; CONF-891117-11) Avail: NTIS HC A03/MF A01

A survey of the relationship between magnetism and superconductivity in high temperature superconductors is presented. It is shown that strong electron correlations are responsible for magnetic behavior and for the specific electronic structure of the charge carriers. A survey of various proposals for a magnetic origin of high temperature superconductivity is given, including the possibilities of unconventional pairing, new mechanisms and new forms of many body theory. An important issue is whether superconductivity is an intrinsic property of mobile holes in an antiferromagnet. This possibility is compared and contrasted with more conventional approaches to the problem. DOE

N90-15797# Brookhaven National Lab., Upton, NY. Dept. of Physics.
X RAY ABSORPTION STUDIES OF YBa2Cu3O(6+x), La(2-x)Sr(x)CuO4, AND Nd(2-x)Ce(x)CuO4
C. L. Lin, S. L. Qiu, Jie Chen, Myron Strongin, J. E. Crow, and C. W. Chu (Houston Univ., TX.) 1989 7 p Presented at the 36th American Vacuum Society National Vacuum Symposium, Boston, MA, 23-27 Oct. 1989
(Contract DE-AC02-76CH-00016)
(DE90-003640; BNL-43461; CONF-891093-15) Avail: NTIS HC A02/MF A01

O K-edge absorption studies show that the density of O 2p empty states near the Fermi level increases with increasing oxygen content for YBa2Cu3O(6+x), and Sr concentration in La(2-x)Sr(x)CuO4. With Zn substitution for Cu in YBa2Cu3O7, (Tc) does not correlate with the density of O 2p empty states. In this case Tc dramatically decreases with Zn substitution while the pre-edge feature remains unchanged. The O K-edge spectrum of Nd(2-x)Ce(x)CuO4 barely changes from the undoped, insulating, to the Ce doped superconducting sample. The lack of unoccupied O 2p states near the Fermi level in this case is consistent with naive expectations for electron-doping. DOE

N90-15798# Oak Ridge National Lab., TN.
THE KIND OF MATHEMATICS INVOLVED IN APPLIED SUPERCONDUCTIVITY RESEARCH
Lawrence Dresner 19 Oct. 1989 7 p
(Contract DE-AC05-84OR-21400)
(DE90-003706; DOE/OR-21400/T407) Avail: NTIS HC A02/MF A01

This paper discusses the mathematic process used in studying the property of superconductivity. DOE

N90-15799# Oak Ridge National Lab., TN.
MAGNETIC FLUX PINNING IN YBa2Cu3O7 FILMS
H. R. Kerchner, R. Feenstra, J. O. Thomson, J. R. Thompson, D. K. Christen, S. T. Sekula, and L. A. Boatner Nov. 1989 5 p Presented at the Materials Research Society Fall Meeting, Boston, MA, 27 Nov. - 2 Dec. 1989
(Contract DE-AC05-84OR-21400)
(DE90-003709; CONF-891119-27) Avail: NTIS HC A01/MF A01

The magnetic hysteresis was studied for YBa2Cu3O7 films of different epitaxial orientations on single-crystal SrTiO3 and KTaO3 substrates. Deposition by coevaporation of Y, BaF2, and Cu was followed by annealing in flowing, wet oxygen at 800 to 850 C. The critical current density J(sub c) deduced from magnetic hysteresis loops was compared with four-terminal transport-current results. Thermally activated magnetic flux flow was manifest in the audio-frequency data. The J(sub c) fits a scaling law similar to one used for describing Nb3Sn and other A15 materials. DOE

N90-15800# Argonne National Lab., IL. Materials Science Div.
HIGH RESOLUTION ELECTRON MICROSCOPY OF GRAIN BOUNDARIES IN NANOPHASE PALLADIUM
G. J. Thomas (Sandia National Labs., Albuquerque, NM.), R. W. Siegel, and J. A. Eastman Sep. 1989 8 p Presented at Symposium J: Interfaces between Polymers, Metals and Ceramics, San Diego, CA, 24-29 Apr. 1989 Submitted for publication
(Contracts W-31-109-eng-38; DE-AC04-76DP-00789)
(DE90-003823; CONF-8904290-4) Avail: NTIS HC A02/MF A01

Using high resolution electron microscopy, considered nanophase palladium samples were examined following electrolytic thinning after a hydriding-dehydriding cycle at 310 K. Due to the small size and random orientations of the individual grains, a large number of grain boundaries were available for examination. Some of these yielded adequate imaging conditions to allow observation of the lattice structure in the grain boundary regions. Image simulations were performed to determine the sensitivity of the technique to lattice disorder. The results of these studies suggest that grain boundary structures in nanophase palladium are similar to those in conventional coarse-grained polycrystals. DOE

N90-15801# Sandia National Labs., Albuquerque, NM.
SUPERCONDUCTIVITY AND STOICHIOMETRY IN Tl2Ca2Ba2Cu3O(x) SINGLE CRYSTALS
E. L. Venturini, C. P. Tigges, R. J. Baughman, D. S. Ginley, and B. Morosin 1989 4 p Presented at the Materials Research Society Fall Meeting, Boston, MA, 27 Nov. - 2 Dec. 1989
(Contract DE-AC04-76DP-00789)
(DE90-003838; SAND-89-1723C; CONF-891119-33) Avail: NTIS HC A01/MF A01

Magnetization and resistivity data are presented which show a substantial difference in superconducting transitions for nominal Tl2Ca2Ba2Cu3O(x) plates with identical crystal structures grown from two different melt compositions. A CuO-rich starting composition yielded approximately stoichiometric plates which have sharp transitions beginning near 111 K, while a second composition with less CuO produced plates containing more Tl and less Ba with very broad transitions starting near 96 K. These data demonstrate the extreme sensitivity of superconductivity to cation site disorder in the Tl-Ca-Ba-Cu-O system. DOE

N90-15802# Sandia National Labs., Albuquerque, NM.
ION-IRRADIATION EFFECTS IN Tl2Ca2Ba2Cu3O10 SUPERCONDUCTORS
J. C. Barbour, J. F. Kwak, E. L. Venturini, D. S. Ginley, and P. S. Peercy 1989 4 p Presented at the Materials Research Society Fall Meeting, Boston, MA, 27 Nov. - 2 Dec. 1989
(Contract DE-AC04-76DP-00789)
(DE90-003840; SAND-89-1727C; CONF-891119-32) Avail: NTIS HC A01/MF A01

The effects of oxygen and helium ion irradiation on the superconducting properties of Tl2Ca2Ba2Cu3O10 thin films were investigated. The transition temperature and width were monitored as a function of ion fluence using both magnetization and resistivity measurements. These data suggest that superconductivity is completely suppressed at 0.020 dpa for both He and O ion irradiation. Further, the rate of decrease in (Tc) as a function of deposited energy showed that the dominant mechanism causing damage-induced suppression of (Tc) in these films was from atomic collisions. DOE

N90-15803# Centro Brasileiro de Pesquisas Fisicas, Rio de Janeiro.
PROCEEDINGS OF THE LATIN AMERICAN CONFERENCE ON THE APPLICATIONS OF THE MOESSBAUER EFFECT
1988 128 p Conference held in Rio de Janeiro, Brazil, 31 Oct. - 4 Nov. 1988
(DE90-600819; INIS-BR-1610; CONF-8810423) Avail: NTIS (US Sales Only) HC A07/MF A01

Several applications of the Moessbauer effect, such as determination of crystal structure, study of physical properties of metals, ceramics and amorphous materials, are presented. DOE

N90-15804# Joint Inst. for Nuclear Research, Dubna (USSR).
ON FUNCTIONAL INTEGRAL REPRESENTATIONS IN THE LOWER HUBBARD BAND BASED ON GENERALIZED COHERENT STATES
W. Weller 1988 6 p
(DE90-602936; JINR-E-17-88-510) Avail: NTIS (US Sales Only) HC A02/MF A01

The Hubbard Hamiltonian is considered after the elimination (to first order in t/U) of transitions between singly and doubly occupied sites by means of a canonical transformation. Using generalized coherent states functional integral representations excluding double occupation are investigated. A special representation is constructed, which needs only one Grassman field psi and one c-number field (beta) (in the simplest form beta = + or - 1) in exact correspondence to the restricted number of degrees of freedom. DOE

N90-15805# Joint Inst. for Nuclear Research, Dubna (USSR). Lab. of Computing Techniques and Automation.
Cu-O CHAINS IN YBa2Cu3O(7-DELTA) AND THE PHONON MECHANISM OF HIGH-Tc SUPERCONDUCTIVITY
T. Galbaatar, R. J. Rakauskas, and J. Sulskus 1988 10 p Submitted for publication
(DE90-603502; JINR-E-17-88-624) Avail: NTIS (US Sales Only) HC A02/MF A01

Within the phonon mechanisms the effect of the interplay of high and low frequency quasi-local modes, involving the longitudinal and transversal vibrations of oxygen atoms in the Cu-O chains on the superconductivity in YBa2Cu3O(7-delta) is studied. The possibility of enhancing T(sub c) due to this interplay is demonstrated numerically. A strong normal isotope effect is predicted. The adiabatic potential for the high-frequency mode is obtained by considering the cluster (Cu-O-Cu)(2+) by the Hartree-Fock method with pseudopotential. It is shown that the in-chain copper ions are 1(+) valence state. The calculations including vectorized codes have been performed on the array processor EC 2706. DOE

N90-15806# Massachusetts Inst. of Tech., Lexington. Lincoln Lab.
SOLID STATE RESEARCH Quarterly Technical Report, 1 Nov. 1988 - 31 Jan. 1989
Alan L. McWhorter 15 Feb. 1989 103 p
(Contract F19628-85-C-0002)
(AD-A213405; AD-E501157; Rept-1989:; Rept-1) Avail: NTIS HC A06/MF A01 CSCL 20/12

The research work of the Solid State Division at Lincoln Laboratory is detailed. The topics covered are Electrooptical Devices, Quantum Electronics, Materials Research, Submicrometer Technology, Microelectronics, and Analog Device Technology. Funding is provided primarily by the Air Force, with additional support provided by the Army, DARPA, Navy SDIO, NASA, and DOE. GRA

N90-15807# Minnesota Univ., Minneapolis. School of Physics and Astronomy.
EPITAXIAL IRON FILMS Final Report, 15 Jul. 1986 - 15 Jul. 1989
E. D. Dahlberg and P. I. Cohen 15 Sep. 1989 22 p
(Grant AF-AFOSR-0201-86; AF Proj. 2306)
(AD-A213551; AFOSR-89-1280TR) Avail: NTIS HC A02/MF A01 CSCL 20/2

The research program focused on the growth and the magnetic properties of epitaxial iron films grown on GaAs/InAs alloy substrates. Pseudomorphic growth of magnetic films on semiconductor substrates provides the potential for tuning of the magnetic properties of thin film magnets by varying the lattice constant and the morphology of the growth surface; this type of research has both device and fundamental research applications. The studies of Fe films grown on GaAs revealed a number of interesting phenomena including a dynamic Fe-FeO coupling, and a correlation between surface morphology and the coercivity of the films. In the growth studies reflection high energy electron diffraction determines the quality of the material (surfaces and interfaces) and the growth mechanisms of the metal films. The magnetic studies relied on the transport properties of the films supplemented by magnetization measurements. GRA

N90-15808# Harry Diamond Labs., Adelphi, MD.
HOST MATERIALS FOR TRANSITION-METAL IONS Interim Report, Jul. 1983 - Jul. 1988
Clyde A. Morrison Sep. 1989 164 p Sponsored by Night-Vision and Electro-Optics Lab, Fort Belvior, VA
(AD-A213605; HDL-DS-89-1) Avail: NTIS HC A08/MF A01 CSCL 09/3

Data are given on host materials for lasers that use the transition metal ions. Included in each section are the crystallographic data, x ray data, crystal field components crystal field parameters, and spin-orbit constants. One section contains the phenomenological free ion parameters which were obtained by fitting the reported free ion data. There is a bibliography for each host which, depending on the host, is more or less complete. The data contained on each host material will be updated periodically, and data on new host materials will be added. GRA

N90-15809# Stanford Univ., CA. Center for Materials Research.
PHASE EQUILIBRIUM AND CRYSTAL GROWTH STUDIES ON AgGaSe2 AND RELATED NONLINEAR OPTICAL MATERIALS Final Technical Report, 1 Jun. 1986 - 31 Dec. 1988
Robert S. Feigelson Sep. 1989 70 p
(Contract N00014-86-K-0343)
(AD-A213650; CMR-89-6) Avail: NTIS HC A04/MF A01 CSCL 20/6

A 31 month research program is summarized. The principal objectives were: (1) to improve the crystal growth technology for AgGaSe2 to facilitate the growth and yield of useful size nonlinear optical elements; (2) to gain an increased understanding of the optical scattering precipitates that form in melt-grown crystals; (3) to determine the cause of residual optical absorption remaining after post-growth heat-treatment; (4) to refine the heat-treatment procedure so as to eliminate residual optical absorption; and (5) to elucidate the chemistry and thermodynamics of the heat-treatment procedure. The first four objectives were met successfully and are described fully. The final objective, the topic of a graduate student dissertation research project is still ongoing, and progress to date is described in detail. GRA

N90-15810# State Univ. of New York at Buffalo, Amherst. Dept. of Physics and Astronomy.
INTERFACE PHONONS IN SEMICONDUCTOR DOUBLE HETEROSTRUCTURES
D. L. Lin, R. Chen, and Thomas F. George Oct. 1989 20 p
(Contract N00014-86-K-0043)
(AD-A213732; UBUFFALO/DC/89/TR-113) Avail: NTIS HC A03/MF A01 CSCL 20/12

Within the framework of the continuum model, the equation of motion for the polarization vector in a semiconductor double heterostructure is solved exactly for the interface phonon modes. Both the eigenvectors and dispersion relations are obtained analytically. It is shown that the slab modes observed in right-angle Raman scattering in a Gallium Arsenides quantum can be understood in terms of the interface modes found in this paper. GRA

N90-15811# California Univ., San Diego, La Jolla. Dept. of Electrical and Computer Engineering.
RESEARCH ON MATERIALS AND COMPONENTS FOR OPTO-ELECTRONIC SIGNAL PROCESSING AND COMPUTING Final Scientific Report, 1 Oct. 1984 - 30 Nov. 1988
William S. Chang, Timothy VanEck, Shigeru Niki, Andrew Williams, Albert L. Kellner, and H. H. Wieder 20 Jul. 1989 79 p
(Grant AF-AFOSR-0389-84; AF Proj. 2305)
(AD-A213740; AFOSR-89-1150TR) Avail: NTIS HC A05/MF A01 CSCL 20/12

Electro-absorption and electro-refraction properties of

heterostructures and multiple quantum well structures in GaInAs/GaAs were demonstrated and optimized for spatial light modulation applications. Techniques to generate and to confine dislocations near the substrate interface to grow a large number of strained quantum wells were developed. Modulation at 1.06 micron wavelength were observed using strained layer quantum wells. Optical optical interaction in a multiple quantum well detector modulator pair was demonstrated. A new device, the gate controlled photodiode was conceived and demonstrated. GRA

N90-15812# North Carolina State Univ., Raleigh. Dept. of Materials Science and Engineering.
COMPUTER-CONTROLLED ION BEAM SPUTTER-DEPOSITION OF SUPERCONDUCTING OXIDE FILMS Technical Report, 1 Jul. 1988 - 30 Jun. 1989
Orlando H. Auciello (Microelectronics Center of North Carolina, Research Triangle Park.), Angus I. Kingon, and Robert F. Davis 30 Jun. 1989 76 p
(Contract N00014-88-K-0525)
(AD-A213921) Avail: NTIS HC A05/MF A01 CSCL 20/12

The goals are: the development of a new method for the fabrication of superconducting oxide thin films, viz computer controlled ion beam sputter deposition; and the fabrication of YBa2Cu3O(7-delta) thin films and devices using this method. In the early stage of the project it was demonstrated that the use of complex multicomponent sputter targets (such as ceramic YBa2Cu3O(7-delta)) present significant problems for compositional control. The new computer-controlled ion beam sputter deposition system was developed. The key features include: a rotatable target holder assembly, which serves to position elemental targets under the ion beam in a rapid sequence, a primary ion beam to produce a sputtered flux from the targets, a secondary oxygen beam (ionic, atomic, or reactive oxygen (ozone)) to oxygenate the film and lower the required deposition temperature, complete computer interfacing to provide real time feedback on the thickness of the depositing species and control of the above items. In terms of the superconductor device objectives, the system is designed to allow for low temperature deposition for integrated devices, compositional control and flexibility, and for scaling to a commercial system. The capability of the system for controlled sequential deposition of layered structures is fundamental for the production of heterostructuers and sandwich junctions (superconductor-insulator-superconductor and superconductor-normal-superconductor). GRA

N90-15813# Wisconsin Univ., Milwaukee. Dept. of Physics.
BULK WAVE CHARACTERIZATION OF HIGH T(SUB c) SUPERCONDUCTORS Annual Report, 1 Nov. 1988 - 1 Nov. 1989
Moises Levy and Bimal Sarma 1 Nov. 1989 11 p
(Contract N00014-88-K-0046)
(AD-A214030) Avail: NTIS HC A03/MF A01 CSCL 20/3

The objective of this research is to characterize high T sub c superconductors with ultrasonic waves. A peak in ultrasonic attenuation has been observed at the superconducting phase transition of the thalium superconducting compound with a T sub c = 103 K. The position of this peak is independent of frequency and therefore should not be produced by a relaxation mechanism. It may be produced by interactions with fluctuations associated with the superconducting phase transition. The magnitude of the peak decreases in magnetic fields up to 6 Tesla. This appears to be the first time that an attenuation effect has been observed which is directly associated with the superconducting state of a high T sub c superconductor. Shear waves propagating parallel to the Copper Oxide planes and polarized in the CuO planes of a sinter forged YBa2Cu3O7 sample exhibit only one maximum in attenuation at around 180 K. Velocity measurements in the copper free high T sub c superconductors Ba(1-x)K(x)BiO3 show a definite change in slope at the phase transition. Measurements in the heavy Fermion superconductor UPt(3) show a 40 ppm change in velocity around 4.5 K, its antiferromagnetic phase transition temperature. GRA

N90-15814# Carnegie-Mellon Univ., Pittsburgh, PA. Dept. of Electrical and Computer Engineering.
DEFECT CONTROL AND DENUDED TRAP ZONES IN THE 3-5 SEMICONDUCTORS Final Report, 1 May 1986 - 31 Aug. 1989
Arthur G. Milnes and Tuviah E. Schlesinger 20 Oct. 1989 7 p
(Contract DAAL03-86-K-0066)
(AD-A214099; ARO-23520.17-EL) Avail: NTIS HC A02/MF A01 CSCL 20/12

The effects of a variety of different treatments on the diffusion lengths in GaAs wafers were investigated. Sealed ampule proximity-capped anneals of 16 hours at 950 C were found to increase minority carrier (hole) diffusion lengths in 1 x 10 to the 17th power Si doped GaAs from initial values of about 0.8 microns to 1.9 microns. This improvement appears to be associated with the reduction in density of a hole trap at E sub v + 0.3 eV which has a capture cross-section in the 10 to the minus 14th to 10 to the minus 15th sq cm range. The proximity anneal also greatly reduced the densities of electron traps, including EL2, but there was no direct correlation of electron trap density and improved carrier lifetime. In other studies the effects of isoelectronic In and Sb doping on the hole traps in Be-doped p-GaAs and electron traps in Si-doped n-GaAs (100) grown by molecular beam epitaxy (MBE) were investigated. The addition of 0.2 to 1 percent indium causes large reductions of electron trap densities in layers grown at 550 C and also reduces certain hole traps. Homojunction GaAs bipolar transistors npn and pnp have been fabricated with base layers containing In isoelectronic doping and are found to have significantly better characteristics than if the In is omitted. GRA

N90-15815# Cornell Univ., Ithaca, NY.
INNOVATIVE OPTOELECTRONIC MATERIALS AND STRUCTURES USING OMVPE Final Technical Report, 1 Jan. - 31 Dec. 1989
James R. Shealy 27 Oct. 1989 12 p
(Contract N00014-89-J-1311)
(AD-A214192) Avail: NTIS HC A02/MF A01 CSCL 09/5

An advanced OMVPE process is being developed for the deposition of III-V semiconductor materials and structures. There are important optoelectronic device structures which can not be realized by conventional means. These include AlGaAs semiconductor lasers with improved coherence using embedded diffraction gratings, and GaInP pseudomorphic structures on GaP substrates for short wavelength semiconductor lasers. The structure on GaP result in improved laser performance compared to the 650 nm AlGaInP devices previously developed in this program. The new OMVPE apparatus combines the multichamber reaction cell with deep UV photo-assisted growth and modulation flow epitaxial techniques. Using a combination of such processes, the growth temperature requirements for III-V alloys can be substantially reduced. Selective growth on a sub-micron scale will be attempted with in-situ interference holography. GRA

N90-15816# State Univ. of New York, Buffalo. Dept. of Chemistry.
OPTICAL PHONON MODES IN A DOUBLE HETEROSTRUCTURE OF POLAR CRYSTALS
R. Chen, D. L. Lin, and Thomas F. George Oct. 1989 34 p Submitted for publication
(Contracts N00014-86-K-0043; F49620-86-C-0009)
(AD-A214208; UBUFFALO/DC/89/TR-114) Avail: NTIS HC A03/MF A01 CSCL 20/12

The equation of motion for the polarization vector for a double heterostructure of polar crystals is solved exactly within the framework of the continuum model. There exist only two types of phonon modes, the interface modes and the confined bulk modes, whose eigenvectors are obtained explicity. Dispersion relations are derived analytically for the interface modes, while the confined bulk modes are dispersionless, a fact consistent with the model. It is also found that in Raman scattering experiments, the symmetric interface modes are predominantly longitudinal (LO) and the antisymmetric interface modes transversal (TO). In the central region of the Brillouin zone, however, they both split into two

branches oscillating at LO and TO frequencies, respectively. Possibly reinterpretation of various experiments are briefly discussed. GRA

N90-15817# Carnegie-Mellon Univ., Pittsburgh, PA. Dept. of Electrical and Computer Engineering.
THE EFFECT OF ANNEALING TREATMENTS ON DEFECT STRUCTURE AND DIFFUSION LENGTHS IN n-TYPE GaAs
A. G. Milnes, D. Wong, H. K. Kim, Z. Q. Fang, and Tuviah E. Schlesinger 1 Sep. 1989 10 p Repr. from J. Appl. Phys., v. 66, no. 5, 1 Sep. 1989 p 2002-2010
(Contracts DAAL03-86-K-0066; SERI-XB-6-06005-3)
(AD-A214215; ARO-23520.15-EL) Avail: NTIS HC A02/MF A01 CSCL 10/2

Gallium arsenide is a material with properties which make it well suited for solar cell applications. In fact, some of the highest efficiencies reported to date for single-junction solar cells have been achieved by GaAs cells. However, the long minority-carrier diffusion lengths necessary to obtain such efficiencies are, by and large, found only in epitaxially grown layers. Bulk-grown material generally has a relatively short diffusion length, and solar cells designed with active regions in the bulk substrate show significantly lower efficiencies than the best epitaxial GaAs cells. Short minority-carrier diffusion lengths in bulk substrates are a manifestation of the presence of high concentrations of defects which act as recombination centers in this type of material. Since GaAs is a direct band-gap material, solar cell applications require a high-quality active region of only a few micrometers depth. GRA

N90-15818# General Atomic Co., San Diego, CA.
HIGH-TEMPERATURE CERAMIC SUPERCONDUCTORS Report, 1 Jul. - 30 Sep. 1989
K. S. Mazdiyasni, K. C. Chen, W. J. DeHope, D. M. Duggan, Y. R. Lin-Lui, F. C. Montgomery, S. S. Pak, R. B. Stephens, M. B. Maple, and L. Paulius et al 10 Oct. 1989 54 p
(Contract N00014-88-C-0714)
(AD-A214251; GA-C19465) Avail: NTIS HC A04/MF A01 CSCL 09/1

The principal objectives of this program are: (1) to demonstrate fabrication of high-temperature ceramic superconductors that can operate at or above 90 K with appropriate current density, Jc, in forms useful for application in resonant cavities, magnets, motors, sensors, computers, and other devices; and (2) to fabricate and demonstrate selected components made of these materials, including microwave cavities and magnetic shields. GRA

N90-15819# Sandia National Labs., Albuquerque, NM. Power System Electronics Div.
POWER SEMICONDUCTOR DEVICES FOR SPACE NUCLEAR POWER SYSTEMS
D. H. Loescher and William R. Dawes, Jr. 1989 6 p Presented at the 7th Symposium on Space Nuclear Power Systems, Albuquerque, NM, 7-11 Jan. 1990 Sponsored in part by Wright Research and Development Center, Wright-Patterson AFB, OH
(Contract DE-AC04-76DP-00789)
(DE90-001178; SAND-89-2374C; CONF-900109-9) Avail: NTIS HC A02/MF A01

Silicon power diodes, transistors, thyristors and other devices can be damaged by elevated temperatures, temperature cycling, and radiation. The vulnerability is discussed of devices that integrate bipolar and MOSFET (metal oxide semiconductor field effect transistor) devices onto a single chip. Such devices offer the advantages of good current carrying capability that is characteristic of bipolar structures and high impedance control nodes that are characteristic of MOSFET devices. Devices located near a space based fission power source will be subjected to high temperatures, temperature cycling, naturally occurring radiation, radiation from the reactor; and these devices may be subjected to radiation from or caused by weapons used to attack the power source. Damaging radiation includes electrons and protons trapped in naturally occurring radiation belts, electrons pumped into these belts as a result of nuclear explosions, cosmic rays, neutrons from the reactor, and high energy photons (gamma rays and x rays). DOE

N90-15820# Los Alamos National Lab., NM.
TRITIUM AND NEUTRON MEASUREMENTS OF A SOLID STATE CELL
T. N. Claytor, P. A. Seeger, R. K. Rohwer, D. G. Tuggle, and W. R. Doty 1989 16 p Presented at the NSF/EPRI Workshop on Anomalous Effects in Deuterated Materials, Washington, DC, 16-18 Oct. 1989
(Contract W-7405-eng-36)
(DE90-003657; LA-UR-89-3946; CONF-8910313-1) Avail: NTIS HC A03/MF A01

A solid state cold fusion cell was constructed to test for non-equilibrium fusion in a solid. The stimulus for the design was the hypothesis that the electrochemical surface layer in the Pons-Fleischmann cell could be replaced with a metal-insulator-semiconductor (MIS) barrier. Cells were constructed of alternating layers of palladium and silicon powders pressed into a ceramic form and exposed to deuterium gas at 110 psia resulting in a D/Pd ratio of 0.7. Pulses of current were passed through the cells to populate non-equilibrium states at the MIS barriers. One cell showed neutron activity and was found to have a large amount of tritium, other cells have produced tritium at a low rate consistent with neutron emission below the threshold of observability. The branching ratio for n/p has been about 1 x 10(exp -9) in all the experiments where a substantial amount of tritium has been found. DOE

N90-15821# Argonne National Lab., IL. Materials Science Div.
PROPERTIES OF HIGH Tc SUPERCONDUCTING OXIDES
Boyd W. Veal and S.-K. Chan Oct. 1989 16 p Presented at the 7th World Round Table Conference on Sintering, Herceg-Novi, Yugoslavia, 28 Aug. - 1 Sep. 1989
(Contract W-31-109-eng-38)
(DE90-003792; CONF-8908192-1) Avail: NTIS HC A03/MF A01

In this paper we shall first briefly consider the history of oxide superconductor discoveries followed by a brief sketch of the current state of theory. We then consider crystallographic structures of the high-(Tc) oxide superconductors. We will then examine some phase fields (Tc) of the oxide superconductors. Since these phase fields show continuous variation between superconducting (metallic) and insulating behavior, they contain both these elements favorable to superconductivity and those detrimental. Particularly well studied are the remarkably variable physical properties of the 123 superconductor that are associated with varied oxygen stoichiometry and cation substitution. We present selected results to provide a brief overview of this problem. Then recent work on electronic properties, providing insight into the fundamental nature of electronic conduction will be examined. These consideration impact on the problem of sintering. Sample density, grain size, grain boundary impurities and texture all affect the physical properties. Of particular importance to superconducting properties is the control of oxygen stoichiometry and sample homogeneity associated with dispersal of dopant ions. DOE

N90-15822# Brookhaven National Lab., Upton, NY. Materials Science Div.
EFFECTS OF NON-LINEARITY IN THE VARIATION OF PINNING POTENTIAL WITH CURRENT-DENSITY ON MAGNETIC FLUX CREEP IN HIGH AND LOW T(SUB c) SUPERCONDUCTORS
D. O. Welch, M. Suenaga, Youwen Xu, and A. K. Ghosh 1989 4 p Presented at the 2d International Symposium on Superconductivity, Tsukuba, Japan, 14-17 Nov. 1989
(Contract DE-AC02-76CH-00016)
(DE90-003952; BNL-43137; CONF-891137-1) Avail: NTIS HC A01/MF A01

A theoretical analysis is presented of the effects on magnetic flux creep of non-linearity in the relation between the activation energy required for the depinning of magnetic flux and the current density. The non-linearity results in an apparent temperature

dependence of the depinning energy as deduced by the conventional methods of analysis of flux-creep data. The discussion is illustrated with data for YBa2Cu3O7 and Nb3Sn. DOE

N90-15823# Brookhaven National Lab., Upton, NY. Dept. of Applied Science.
ATOMIC SCALE STRUCTURE OF TWIN BOUNDARY IN Y-Ba-Cu-O SUPERCONDUCTORS
Yimei Zhu, M. Suenaga, Youwen Xu, and M. Kawasaki (JEOL USA, Inc., Peabody, MA.) 1989 7 p Presented at the Materials Research Society Fall Meeting, Boston, MA, 27 Nov. - 2 Dec. 1989
(Contract DE-AC02-76CH-00016)
(DE90-003955; BNL-43068; CONF-891119-36) Avail: NTIS HC A02/MF A01

High resolution electron microscopy of the twin boundary layers in Y-Ba2Cu(sub 1-x)M(sub x)3O(sub 7-delta) for x=0 and 0.02 and M=Zn, Fe and Al showed that the boundary widths are approximately 1 nm for the pure and the Zn substituted Y-Ba2Cu3O7, 2.5 approximately 3 nm for the Fe and Al substituted oxide. It was found that the lattice plane is shifted across the twin boundary by 1/3 approximately 1/2 2d sub 110 along the boundary. The broadening of the layer for the cases of Fe and Al is also thought to be associated with a reduction of the twin boundary energy, which also leads to an increased twin density. DOE

N90-15824# Brookhaven National Lab., Upton, NY. Materials Science Div.
THE FABRICATION OF YBa2Cu3O7 THIN FILMS BY THERMAL COEVAPORATION IN OXYGEN
H. Wiesmann and De Huai Chen 1989 5 p Presented at the Materials Research Society Fall Meeting, Boston, MA, 27 Nov. - 2 Dec. 1989
(Contract DE-AC02-76CH-00016)
(DE90-003960; BNL-43576; CONF-891119-35) Avail: NTIS HC A01/MF A01

Thin films of YBa2Cu3O7 have been fabricated by the technique of thermal coevaporation in oxygen. Details of the deposition system design and process are presented. Preliminary results are presented for films grown on magnesium oxide substrates. The films are characterized by x ray diffraction and the quality of their superconducting transition. DOE

N90-15825# Brookhaven National Lab., Upton, NY. Physics Dept.
AUGER AND X RAY ABSORPTION STUDIES OF SOLID MOLECULAR OXYGEN
Jie Chen, C. L. Lin, S. L. Qui, Myron Strongin, and M. L. denBoer (Hunter Coll., New York, NY.) 1989 15 p Presented at the 36th American Vacuum Society National Vacuum Symposium, Boston, MA, 23-27 Oct. 1989
(Contract DE-AC02-76CH-00016)
(DE90-003966; BNL-43462; CONF-891093-16) Avail: NTIS HC A03/MF A01

We have studied the x ray absorption spectrum (XAS) and the Auger electron spectrum (AES) of condensed molecular oxygen in the vicinity of the O 1s (K) core level. The XAS spectrum, which is similar to that previously reported for gas phase O(sub 2), has sharp peaks at about 530.8 eV and 540.3 eV which we attribute to excitations from the 1s level into (pi) asterisk and (sigma) askerisk states respectively. We assign a third peak at 543.3 eV to Rydberg transitions. Compared with gas phase O(sub 2), the (sigma) askerisk and Rydberg states are shifted to higher energies, an effect which we attribute to solid state effects in the condensed layer. The AES spectra of the ionized molecule and excited molecule are both shifted relative to the spectra of gas phase O(sub 2), but by different amounts, 10 eV and 2 eV respectively, which may be due to different final state screening effects. A tentative assignment of the features in the AES spectra is also made. DOE

77 THERMODYNAMICS AND STATISTICAL PHYSICS

Includes quantum mechanics; theoretical physics; and Bose and Fermi statistics.

For related information see also *25 Inorganic and Physical Chemistry* and *34 Fluid Mechanics and Heat Transfer.*

N90-15826*# Fermi National Accelerator Lab., Batavia, IL. Astrophysics Center.
AN EXACT SOLUTION FOR A THICK DOMAIN WALL IN GENERAL RELATIVITY
Guenter Goetz and Dirk Noetzold (Chicago Univ., IL.) Nov. 1989 8 p Submitted for publication Sponsored in part by Alexander-von-Humboldt Foundation
(Grants NAGw-1321; NAGw-1340; NSF AST-88-22595)
(NASA-CR-185013; NAS 1.26:185013; FERMILAB-Pub-89/235-A) Avail: NTIS HC A02/MF A01 CSCL 20C

An exact solution of the Einstein equations for a static, planar domain wall with finite thickness is presented. At infinity, density and pressure vanish and the space-time tends to the Minkowski vacuum on one side of the wall and to the Taub vacuum on the other side. A surprising feature of this solution is that the density and pressure distribution are symmetric about the central plane of the wall whereas the space-time metric and therefore also the gravitational field experienced by a test particle is asymmetric. M.G.

N90-15827# Argonne National Lab., IL. Materials Science Div.
MAXIMUM ENTROPY AND EQUATIONS OF STATE FOR RANDOM CELLULAR STRUCTURES
N. Rivier 1989 13 p Presented at the Conference on Maximum Entropy and Bayesian Methods, Hanover, NH, 14-18 Aug. 1989
(Contract W-31-109-eng-38)
(DE90-002840; CONF-8908179-2) Avail: NTIS HC A03/MF A01

Random, space-filling cellular structures (biological tissues, metallurgical grain aggregates, foams, etc.) are investigated. Maximum entropy inference under a few constraints yields structural equations of state, relating the size of cells to their topological shape. These relations are known empirically as Lewis's law in Botany, or Desch's relation in Metallurgy. Here, the functional form of the constraints is now known as a priori, and one takes advantage of this arbitrariness to increase the entropy further. The resulting structural equations of state are independent of priors, they are measurable experimentally and constitute therefore a direct test for the applicability of MaxEnt inference (given that the structure is in statistical equilibrium, a fact which can be tested by another simple relation (Aboav's law)). DOE

N90-15828# International Centre for Theoretical Physics, Trieste (Italy).
NON NEWTONIAN GRAVITY CREEPING FLOW
Julio Gratton, Swadesh M. Mahajan, and Fernando Minotti (Buenos Aires Univ., Argentina) Nov. 1988 18 p Submitted for publication Sponsored in part by Organization of American States and Buenos Aires Univ.
(Contract DE-AS05-85ER-53193)
(DE90-600816; IC-88/370) Avail: NTIS (US Sales Only) HC A03/MF A01

We derive the governing equations for creeping gravity currents of non Newtonian liquids having a power law rheology, using a lubrication approximation. We consider unidirectional and axisymmetric currents. The equations differ from those for Newtonian liquids, being nonlinear in the spatial derivative of the thickness of the current. However, many solutions are closely analogous to those for Newtonian rheology; in particular the spreading relations can also be expressed as power laws of time, with exponents that depend on the rheological index. Similarity solutions for currents whose volume varies as a power of time are obtained. For the spread of a constant volume of liquid, analytic solutions are found. We also derive solutions of the waiting-time type, as well as the ones describing steady flows from a constant

source to a sink. General travelling wave solutions are given, and analytic formulae for a simple case are derived. A phase plane formalism, that allows the systematic derivation of self similar solutions, is introduced. The application of the Boltzmann transform is briefly discussed. Present results are closely analogous to those for Newtonian liquids; all the solutions obtained here have their counterparts in Newtonian flows. DOE

N90-15829# Hiroshima Univ., Takehara (Japan). Research Inst. for Theoretical Physics.
A (2+1)-DIMENSIONAL PURE GRAVITY FOR AN ARBITRARY CLOSED INITIAL SURFACE
Akio Hosoya and Ken-ichi Nakao Apr. 1989 25 p
(DE90-701754; RRK-89-11) Avail: NTIS (US Sales Only) HC A03/MF A01

The (2+1)-dimensional pure Einstein gravity is studied in the ADM formalism. We completely solve the initial value and the time evolution problems with a closed Riemann surface being an initial surface, choosing the time slicing so that the trace of the extrinsic curvature is independent of spatial coordinates. The possible topology of the two-surface is either a torus or a Riemann surface of genus g greater than or equal to 2. It is shown that the moduli parameters of the torus follow the geodesic curve in the moduli space, while the motion of the moduli is static for the case g greater than or equal to 2. DOE

N90-15830# Hiroshima Univ., Takehara (Japan). Research Inst. for Theoretical Physics.
ABELIAN GAUGE THEORY IN TOPOLOGICALLY NON-TRIVIAL SPACE
Akio Hosoya and Jiro Soda May 1989 10 p
(DE90-710100; RRK-89-13) Avail: NTIS (US Sales Only) HC A02/MF A01

The (1+1)-dimensional Abelian gauge theory on cylinder was quantized to illustrate the extraction of global modes of topological origin. A new analysis is made for the (2+1)-dimensional Maxwell theory on T squared (torus) x R(time). The dynamics is explicitly given for the Wilson loops around cycles of the torus with arbitrary moduli parameters. We also discuss an extension to antisymmetric tensor fields in higher dimensions. DOE

N90-15831 ESDU International Ltd., London (England).
TEMPERATURES IN PLATES SUBJECTED TO A RECOVERY TEMPERATURE VARYING LINEARLY WITH TIME
Aug. 1989 6 p Supersedes ESDU-Struct-H.02.00.01
(ESDU-89023; ESDU-Struct-H.02.00.01; ISBN-0-85679-695-6; ISSN-0141-4097) Avail: ESDU

This data item treats the transient situation of the variation of the temperature distribution through a thick plate insulated on one side when the aerodynamic heating temperature on the other side is changing, from an initially constant temperature condition, linearly with time. Curves are given that allow the temperature change from the initial constant temperature condition to be obtained at both surfaces and at three surfaces at equal intervals through the plate. The method can be applied also when there is a thin insulating layer at the heated face. A fully worked example illustrates the use of the method. ESDU

N90-15832*# Fermi National Accelerator Lab., Batavia, IL. Astrophysics Center.
THE DYNAMICS OF DOMAIN WALLS AND STRINGS
Ruth Gregory, David Haws, and David Garfinkle (California Univ., Santa Barbara.) Nov. 1989 16 p Sponsored in part by DOE (Grants NAGw-1340; NSF PHY-85-06686)
(NASA-CR-186255; NAS 1.26:186255; FERMILAB-Pub-89/249-A) Avail: NTIS HC A03/MF A01 CSCL 20C

The leading order finite-width corrections to the equation of motion describing the motion of a domain wall are derived. The regime in which this equation of motion is invalid is discussed. Spherically and cylindrically symmetric solutions to this equation of motion are found. A misconception that has arisen in recent years regarding the rigidity (or otherwise) of cosmic strings is also clarified. Author

N90-15833# Joint Inst. for Nuclear Research, Dubna (USSR). Lab. of Theoretical Physics.
NONLOCALITY AND STOCHASTIC QUANTIZATION OF FIELD THEORY
M. Dineykhan and Kh. Namsrai 1988 52 p Submitted for publication
(DE89-633913; JINR-E-2-88-557) Avail: NTIS (US Sales Only) HC A04/MF A01

Concept of nonlocality is introduced into physics by means of stochastic context using Langevin and Schwinger-Dyson techniques. This allows the reformulation of the finite theory of quantum field, free from ultraviolet divergences, based on the stochastic quantization method with nonlocal regulators. As a nonlocal regulator, any entire analytic function in the momentum space was chosen, which guarantees that the regularization method for any theory of interest does not violate basic physical principles such as unitarity, causality, and gauge invariance of the theory. Here, regularization scheme are presented for scalar, gauge and scalar electrodynamics theories. DOE

N90-15834# Naval Postgraduate School, Monterey, CA. Dept. of Physics.
ANNUAL SUMMARY OF BASIC RESEARCH IN THERMOACOUSTIC HEAT TRANSPORT Annual Report, 1 Mar. - 30 Sep. 1989
Anthony A. Atchley 19 Sep. 1989 28 p
(Contract N00014-89-WR-24017)
(AD-A214185; NPS61-89-015PR) Avail: NTIS HC A03/MF A01 CSCL 20/13

This annual report details progress in basic research in thermoacoustic heat transport. The approach and progress of three projects are discussed. The first project involves measurements of thermoacoustic phenomena using thermoacoustics couples (TACs). The second is an investigation of heat driven prime movers and heat pumps. The purpose of the third project is to examine means of visualizing thermoacoustic processes. A publication, patents, presentations, and honors report is also included. GRA

N90-15835# International Centre for Theoretical Physics, Trieste (Italy).
LEFSCHETZ TRACE FORMULA AND BRST
A. S. Schwarz Apr. 1989 7 p Submitted for publication
(DE89-635705; IC-89/73) Avail: NTIS (US Sales Only) HC A02/MF A01

Quantum systems with constraints showing how the BRST-transformation and the BFV-method of quantization can be understood directly in this case are studied in this paper. The results concerning the quantization of classical constrained systems can be derived from the results for quantum systems. DOE

80 SOCIAL SCIENCES (GENERAL)

Includes educational matters.

No abstracts in this category.

81 ADMINISTRATION AND MANAGEMENT

Includes management planning and research.

N90-15836*# National Aeronautics and Space Administration. Langley Research Center, Hampton, VA.
REPORT OF NASA LUNAR ENERGY ENTERPRISE CASE STUDY TASK FORCE
John J. Kearney Jul. 1989 176 p
(NASA-TM-101652; NAS 1.15:101652) Avail: NTIS HC A09/MF A02 CSCL 03B

The Lunar Energy Enterprise Case Study Task Force was asked to determine the economic viability and commercial potential of mining and extracting He-3 from the lunar soil, and transporting the material to Earth for use in a power-generating fusion reactor. Two other space energy projects, the Space Power Station (SPS) and the Lunar Power Station (LPS), were also reviewed because of several interrelated aspects of these projects. The specific findings of the Task Force are presented. Appendices contain related papers generated by individual Task Force Members. For individual titles, see N90-15837 through N90-15843.

N90-15837*# National Aeronautics and Space Administration. Langley Research Center, Hampton, VA.
REPORT OF THE NASA LUNAR ENERGY ENTERPRISE CASE STUDY TASK FORCE
In its Report of NASA Lunar Energy Enterprise Case Study Task Force Jul. 1989 p 1-37 (For primary document see N90-15836 07-81)
Avail: NTIS HC A09/MF A02 CSCL 03B

The Lunar Energy Enterprise Cast Study Task Force was formed to determine the economic viability and commercial business potential of mining and extracting He-3 from the lunar soil for use in earth-based fusion reactors. In addition, the Solar Power Satellite (SPS) and the Lunar Power Station (LPS) were also evaluated because they involve the use of lunar materials and could provide energy for lunar-based activities. The Task Force considered: (1) the legal and liability aspects of the space energy projects; (2) the long-range terrestrial energy needs and options; (3) the technical maturity of the three space energy projects; and (4) their commercial potential. The use of electricity is expected to increase, but emerging environmental concerns and resource availability suggest changes for the national energy policy. All three options have the potential to provide a nearly inexhaustible, clean source of electricity for the U.S. and worldwide, without major adverse impacts on the Earth's environment. Assumption by industry of the total responsibility for these energy projects is not yet possible. Pursuit of these energy concepts requires the combined efforts of government and industry. The report identifies key steps necessary for the development of these concepts and an evolving industrial role. M.G.

N90-15838*# Wisconsin Univ., Madison.
ANALYSIS OF THE FINANCIAL FACTORS GOVERNING THE PROFITABILITY OF LUNAR HELIUM-3
G. L. Kulcinski, H. Thompson, and S. Ott *In* NASA, Langley Research Center, Report of NASA Lunar Energy Enterprise Case Study Task Force Jul. 1989 p 40-55 (For primary document see N90-15836 07-81)
Avail: NTIS HC A09/MF A02 CSCL 03B

Financial factors influencing the profitability of the mining and utilization of lunar helium-3 are examined. The analysis addressed the following questions: (1) which financial factors have the greatest leverage on the profitability of He-3; (2) over what range can these factors be varied to keep the He-3 option profitable; and (3) what ultimate effect could this energy source have on the price of electricity for U.S. consumers. Two complementary methods of analysis were used in the assessment: rate of return on incremental investment required and reduction revenue requirements (total cost to customers) achieved. Some of the factors addressed include energy demand, power generation costs with and without fusion, profitability for D-He(3) fusion, annual capital and operating costs, launch mass and costs, He-3 price, and government funding. Specific conclusions are made with respect to each of the companies considered: utilities, lunar mining company, and integrated energy company. M.G.

N90-15839*# Spectra Technology, Inc., Bellevue, WA.
INTRODUCTION TO D-He(3) FUSION REACTORS **c73**
G. C. Vlases and L. C. Steinhauer *In* NASA, Langley Research Center, Report of NASA Lunar Energy Enterprise Case Study Task Force Jul. 1989 p 56-67 (For primary document see N90-15836 07-81)
Avail: NTIS HC A09/MF A02 CSCL 18L

A review and evaluation of D-He(3) fusion reactor technology is presented. The advantages and disadvantages of the D-He(3) and D-T reactor cycles are outlined and compared. In addition, the general design features of D-He(3) tokamaks and field reversed configuration (FRC) reactors are described and the relative merits of each are compared. It is concluded that both tokamaks and FRC's offer certain advantages, and that the ultimate decision as to which to persue for terrestrial power generation will depend heavily on how the physics performance of each of them develops over the next few years. It is clear that the D-He(3) fuel cycle offers marked advantages over the D-T cycle. Although the physics requirements for D-He(3) are more demanding, the overwhelming advantages resulting from the two order of magnitude reduction of neutron flux are expected to lead to a shorter time to commercialization than for the D-T cycle. M.G.

N90-15840*# Little (Arthur D.), Inc., Cambridge, MA.
THE SOLAR POWER SATELLITE (SPS): PROGRESS SO FAR **c18**
Peter E. Glaser *In* NASA, Langley Research Center, Report of NASA Lunar Energy Enterprise Case Study Task Force Jul. 1989 p 68-83 (For primary document see N90-15836 07-81)
Avail: NTIS HC A09/MF A02 CSCL 22B

Major developments in key Solar Power Satellite (SPS)-related technologies are outlined and the significance of these developments are evaluated considering the SPS, both as an alternate energy option for use on Earth and as a potential stimulus for space infrastructure developments and expansion of the use of extraterrestrial resources. B.G.

N90-15841*# California Univ., San Diego, La Jolla.
LUNAR POWER SYSTEM SUMMARY OF STUDIES FOR THE LUNAR ENTERPRISE TASK FORCE NASA-OFFICE OF EXPLORATION **c44**
David R. Criswell *In* NASA, Langley Research Center, Report of NASA Lunar Energy Enterprise Case Study Task Force Jul. 1989 p 84-96 (For primary document see N90-15836 07-81)
Avail: NTIS HC A09/MF A02 CSCL 10B

The capacity of global power systems must be increased by a factor of ten to provide the predicted power needs of electric power by the year 2050. The Lunar Power System (LPS) would collect solar energy at power bases located on opposing limbs of the moon as seen from Earth. LPS can provide dependable, economic, renewable, and environmentally benign solar energy to Earth. A preliminary engineering and cash flow model of the LPS was developed. Results are shown for a system scaled to a peak capacity of 355 GWe on Earth and to provide 13,600 GWe-Yrs of energy over a 70 year life cycle of construction and full operation. The growth in capacity of the reference system from start of installation on the moon in 2005 to completion of its nominal life cycle in the year 2070 is shown. World needs for power could be accommodated by expansion in capacity of the reference LPS beyond 344 GWe. This would be done by steadily incorporating newer technology during full operation and by establishing additional bases. The results presented encourage consideration of a faster paced program than is assumed herein. Author

N90-15842*# Boeing Aerospace Co., Huntsville, AL.
TRANSPORTATION AND OPERATIONS ASPECTS OF SPACE ENERGY SYSTEMS **c44**
Gordon R. Woodcock *In* NASA, Langley Research Center, Report of NASA Lunar Energy Enterprise Case Study Task Force Jul. 1989 p 97-149 (For primary document see N90-15836 07-81)
Avail: NTIS HC A09/MF A02 CSCL 10B

A brief comparative analysis was made for three concepts of supplying large-scale electrical energy to Earth from space. The concepts were: (1) mining helium-3 on the Moon and returning it to Earth; (2) constructing solar power satellites in geosynchronous orbit from lunar materials (the energy is beamed by microwave to receivers on Earth); and (3) constructing power collection and beaming systems on the Moon itself and transmitting the energy to Earth by microwave. This analysis concerned mainly space

transportation and operations, but each of the systems is briefly characterized to provide a basis for space transportation and operations analysis. Author

N90-15843*# Wisconsin Univ., Madison.
IMPORTANCE OF HELIUM-3 FOR THE FUTURE **c73**
Gerald L. Kulcinski *In* NASA, Langley Research Center, Report of NASA Lunar Energy Enterprise Case Study Task Force Jul. 1989 p 150-171 (For primary document see N90-15836 07-81)
Avail: NTIS HC A09/MF A02 CSCL 18L

Relevant plasma physics principles of thermonuclear research; the state of plasma physics as it pertains to the D-He(3) cycle; the technological benefits of the D-He(3) fuel cycle; the availability of He(3); and its location, methods of extraction and cost are discussed. A perspective on the rate of progress toward the goal of heating the confined plasma fuel to sufficiently high temperatures at high enough densities and for long enough times to cause substantial fusion of the atoms to take place is given in graphical form. The main technological advantages resulting from the D-He(3) fuel cycle, when compared with the DT cycle, are as follows: (1) increased electrical conversion efficiency; (2) reduced radiation damage to reactors; (3) reduced radioactive waste; (4) an increased level of safety in case of an accident; (5) the lower cost of electricity; and (6) the shorter time to commercialization. An account is given of mining He(3) on the Moon. Author

N90-15844# Defense Systems Management School, Fort Belvoir, VA.
PROGRAM MANAGER'S HANDBOOK
Mar. 1989 422 p
(AD-A214338) Avail: NTIS HC A18/MF A03 CSCL 05/1

A reference tool for program managers and related functional or staff managers is designed. The document is in the form of a three-ring notebook containing a series of fact sheets on the fundamentals of nearly all major facets of the program management business with references for sources of more detailed information on each subject. Recipients are provided with updated and new facts sheets as they become available. GRA

82 DOCUMENTATION AND INFORMATION SCIENCE

Includes information management; information storage and retrieval technology; technical writing; graphic arts; and micrography.

For computer documentation see *61 Computer Programming and Software.*

N90-15845 Syracuse Univ., Utica, NY.
A COMPARATIVE EVALUATION AND ANALYSIS OF END-USER SEARCH PERFORMANCE IN AN ACADEMIC ENVIRONMENT Ph.D. Thesis
Margaret Geraldene P Walker 1988 172 p
Avail: Univ. Microfilms Order No. DA8907896

The searches performed by a self-selected user population (N = 45) in an academic environment, using the BRS/After Dark search system is investigated. Two searches were performed for each query, one by the information-seeker in person and one by a trained intermediary. Performance measures, based on a comparison of the two search outputs, provide an evaluation in terms of both effectiveness (precision and recall) and efficiency (connect time and cost effectiveness). These measures are supplemented by an analysis of precision and recall failures for a random sample of the queries, which provides information regarding the causes of search failure. No significant differences between the two groups were found in terms of either precision or recall, though results for both groups varied widely. However, end-users took twice as long as intermediaries to perform their searches, and since cost effectiveness is a function of the relationship between time and performance, it showed significant differences. All search process variables also showed significant differences between the two groups, indicating wide discrepancies in searching styles. Failure analysis established that there were almost equal numbers of precision and recall failures and that they were also equally divided among end-users and intermediaries. Search vocabulary was identified as the overwhelming source for the majority of both precision (75 percent) and recall (77 percent) failures. Choice of database, Boolean logic, the system itself and failures in the judging of relevance all accounted for minimal failures individually. The findings confirm the feasibility of direct end-user searching and suggest that the further identification and development of features to simplify the search process will have a major effect on the acceptability and effectiveness of online searching in the future. Author

N90-15846*# National Aeronautics and Space Administration. Lewis Research Center, Cleveland, OH.
BIBLIOGRAPHY OF LEWIS RESEARCH CENTER TECHNICAL PUBLICATIONS ANNOUNCED IN 1988
Jul. 1989 371 p
(NASA-TM-102034; E-4780; NAS 1.15:102034) Avail: NTIS HC A16/MF A02 CSCL 05B

This bibliography contains abstracts of the technical reports that resulted from the scientific and engineering work performed and managed by the Lewis Research Center in 1988. Subject, author, and corporate source indexes are also included. All the publications were announced in the 1988 issues of STAR (Scientific and Technical Aerospace Reports) and/or IAA (International Aerospace Abstracts). Included are research reports, journal articles, conference presentations, patents and patent applications, and theses. Author

N90-15847 California Univ., Los Angeles.
ALTERNATIVE REPRESENTATIONS FOR DATABASE RESPONSES Ph.D. Thesis
Chung-Dak Shum 1989 160 p
Avail: Univ. Microfilms Order No. DA8915371

Two issues in retrieval from a database are addressed: effectiveness and efficiency. Effectiveness is concerned with the representation of answers; and efficiency is concerned with fast response to queries. Conventional responses to queries in database systems, usually consisting of lists of tuples, do not necessarily provide effective communication between a user and the system. It is suggested that when responding to a use query, the system can improve effectiveness of information transfer by providing concise intensional answers, as a set of concepts and predicates, rather than just providing the set of facts satisfying the query. Abstracting responses before presenting them to the user is an effective means of information exchange. Aggregation is a commonly used abstraction process. Next, aggregate responses that are expressions of quantified concepts are investigated. The tradeoff between the conciseness and impreciseness of an aggregate response is studied. Conciseness is measured by the length of the expression and preciseness is measured by the entropy of the expression. The objective of conventional query optimization is usually to minimize the total time required for evaluating a query. Lastly, it is argued that in some interactive environment, the initial response time of a query may also be considered important. For selection queries, a long initial response time can be shortened without compromising on the total time for completely evaluating a query. The same, however, is not always true for join queries. But the tradeoffs between the total response time and the initial response time of a query are quantifiable. Semantic query optimization techniques can also improve the initial response time of a query. Moreover, in addition to exact rules, inexact rules can be utilized to improve the initial response time.
Dissert. Abstr.

N90-15848*# National Aeronautics and Space Administration. Langley Research Center, Hampton, VA.
TECHNICAL COMMUNICATIONS IN AERONAUTICS: RESULTS OF AN EXPLORATORY STUDY. AN ANALYSIS OF PROFIT MANAGERS' AND NONPROFIT MANAGERS' RESPONSES
Thomas E. Pinelli, Myron Glassman, Rebecca O. Barclay, and

Walter E. Oliu Oct. 1989 71 p
(NASA-TM-101626; NAS 1.15:101626) Avail: NTIS HC A04/MF A01 CSCL 05B

Data collected from an exploratory study concerned with the technical communications practices of aerospace engineers and scientists were analyzed to test the primary assumption that profit and nonprofit managers in the aerospace community have different technical communications practices. Five assumptions were established for the analysis. Profit and nonprofit managers in the aerospace community were found to have different technical communications practices for one of the five assumptions tested. It was, therefore, concluded that profit and nonprofit managers in the aerospace community do not have different technical communications practices. Author

N90-15849# Westinghouse Savannah River Co., Aiken, SC.
PROCUREMENT OF AN OPTICAL DISK INFORMATION STORAGE AND RETRIEVAL SYSTEM
Barry J. Hudson 1989 10 p Presented at the Annual Westinghouse Computer Symposium, Pittsburgh, PA, 6-7 Nov. 1989
(Contract DE-AC09-89SR-18035)
(DE90-001372; WSRC-RP-89-472; CONF-891192-16) Avail: NTIS HC A03/MF A01

There are a number of factors that affect the decision to buy an optical disk based system for records management or information retrieval. The prospective buyer of an image storage system must perform a thorough requirements analysis to determine his needs. The following issues and their impact on the system requirements are discussed: Volume of records; Scanning workloads; Photographs/halftones; Standalone vs network; Use of existing index systems; Growth paths, integration to network; Legal, DOE considerations; Who are your users; Types of records; Retrieval workloads; Oversize documents; Use of existing workstations; Image quality vs file sizes; Proprietary vs standard components; Records vs information; and What is your justification. DOE

N90-15850# General Atomic Co., San Diego, CA.
DATA FILE MANAGEMENT IN THE D3-D DATA ACQUISITION AND ANALYSIS COMPUTER SYSTEMS
B. B. McHarg, Jr. Nov. 1989 6 p Presented at the 13th International Symposium on Fusion Engineering, Knoxville, TN, 2-6 Oct. 1989
(Contract DE-AC03-89ER-51114)
(DE90-003289; GA-A-19748; CONF-891007-91) Avail: NTIS HC A02/MF A01

D3-D is a large tokamak plasma physics and fusion energy research experiment funded by the Department of Energy. Each shot of the experiment results in data files containing between 20 and 30 Mbytes of data. These shots occur about once every 10 minutes with 40 to 50 shots per operating day. Over 1.2 gigabytes have been acquired in one daily session. Most of this data is acquired by MODCOMP Classic computers and is transferred via a Network Systems Hyperchannel to the D3-D DEC VAX cluster system which is connected via Ether-net to the User Service Center DEC VAX cluster system. Some other data is acquired by local MicroVAX based plasma diagnostic systems and is transferred via DECnet to the D3-D cluster. A substantial part of these VAX cluster systems is devoted to handling the large data files so as to maintain availability of the data for users, provide for shot archiving and shot restoration capabilities, and at the same time allow for new data to be received into the systems. Many of these tasks are carried out in near real time in sequence with a tokamak shot while other tasks are performed periodically throughout operations or during off hours. These tasks include disk space management, data archiving to 6250 and/or 8 mm tape drives, data file migration from the D3-D cluster to the User Service Center cluster, data file compression, and network wide data file access. DOE

N90-15851* National Aeronautics and Space Administration, Washington, DC.
NASA PATENT ABSTRACTS BIBLIOGRAPHY: A CONTINUING BIBLIOGRAPHY. SECTION 1: ABSTRACTS (SUPPLEMENT 36)
Jan. 1990 38 p
(NASA-SP-7039(36)-Sect-1; NAS 1.21:7039(36)-Sect-1) Avail: NTIS HC A04; NTIS standing order as PB89-911100, $13.75 domestic, $27.50 foreign CSCL 05B

Abstracts are provided for 63 patents and patent applications entered into the NASA scientific and technical information systems during the period July 1989 through December 1989. Each entry consists of a citation, an abstract, and in most cases, a key illustration selected from the patent or patent application. Author

N90-15852# Mission Research Corp., Santa Barbara, CA.
A SIGNAL REALIZATION DATA BASE GENERATED BY THE MULTIPLE PHASE-SCREEN METHOD Technical Report, 15 Dec. 1988 - 24 Mar. 1989
D. J. Krueger, M. O. Duff, and S. M. Frasier 24 Mar. 1989 77 p
(Contract DNA001-87-C-0169)
(AD-A214004; MRC-R-1223; DNA-TR-89-73) Avail: NTIS HC A05/MF A01 CSCL 20/14

This report is intended to serve as supporting documentation for an accompanying magnetic tape which contains realizations of signals resulting from propagation through a striated ionosphere (parameterized as fifteen different cases of carrier frequency and electron-density variance). The signals were generated with a Multiple Phase-Screen (MPS) computer code, and the simulated cases range, in their levels of effect, from very weakly scattered cases to those where the signals display intensity profiles characteristic of Rayleigh amplitude fluctuations. This report details what is represented on the magnetic tape and provides information regarding its use. The appendices present supplementary material on the MPS techniques, provide example software that may be used to read realization data, and summarize the MPS runs with plots and tables. GRA

N90-15853# Defense Applied Information Technology Center, Alexandria, VA. Textsearch Lab.
TERMINOLOGY STRATEGIES FOR INTERNATIONAL INFORMATION EXCHANGE
Gladys A. Cotter and Walter R. Blados Aug. 1989 13 p
(AD-A214147; DAITC/TR-89/9; DTIC-TR-89/20) Avail: NTIS HC A03/MF A01 CSCL 05/2

Development of a common thesaurus for every use by national and international Defense Scientific and Technical Information (STI) organizations to facilitate the exchange of information is described. The concept of a core thesaurus comprising STI terminology which is acceptable to all participants and which can be extended with specific micro vocabularies at the local level to meet specialized needs is explored. The thesaurus will be bilingual with both English and French terminology. GRA

N90-15854# Colorado Univ., Boulder.
YOUNG INVESTIGATOR'S AWARD AND DISTRIBUTED SELF-ADAPTIVE DATABASES Final Report, 22 Aug. 1988 - 30 Sep. 1989
Roger King 5 Oct. 1989 13 p
(Contracts N00014-88-K-0059; N00014-86-K-0054)
(AD-A214194; Rept-153-7639) Avail: NTIS HC A02/MF A01 CSCL 12/7

The goal of the adaptive database project at the University of Colorado is to develop techniques which will make database systems useful for newer applications, such as engineering design. In such cases, there is a need to support complex, computed data, as well a need to hand-tailor a database system to suit specific processing requirements, for example, version support and document management. Two different experimental systems, one addressing each of these concerns, are under construction. The algorithms and techniques developed for these systems are intended to help relieve the advanced database user from the

highly constrained mechanisms which traditional database management systems provide. GRA

83 ECONOMICS AND COST ANALYSIS

Includes cost effectiveness studies.

No abstracts in this category.

84 LAW, POLITICAL SCIENCE AND SPACE POLICY

Includes NASA appropriation hearings; aviation law; space law and policy; international law; international cooperation; and patent policy.

N90-15855# Defense Systems Management School, Fort Belvoir, VA.
CONGRESSIONAL INVOLVEMENT AND RELATIONS: A GUIDE FOR DEPARTMENT OF DEFENSE ACQUISITION MANAGERS
Wilbur D. Jones, Jr. Jul. 1989 98 p
(AD-A214408) Avail: NTIS HC A05/MF A01 CSCL 05/4

This guide is written to assist program managers achieving the necessary understanding of congressional involvement and relations with DOD. It describes how the congress is organized and structured to carry out its two major responsibilities in dealing with DOD: the legislative process and the oversight function. This guide covers congressional involvement in the DOD weapon system acquisitions process. GRA

85 URBAN TECHNOLOGY AND TRANSPORTATION

Includes applications of space technology to urban problems; technology transfer; technology assessment; and surface and mass transportation.

For related information see also *03 Air Transportation and Safety, 16 Space Transportation,* and *44 Energy Production and Conversion.*

No abstracts in this category.

88 SPACE SCIENCES (GENERAL)

No abstracts in this category.

89 ASTRONOMY

Includes radio, gamma-ray, and infrared astronomy, and astrometry.

N90-15856*# South African Astronomical Observatory, Cape Town.
THE SOUTH AFRICAN ASTRONOMICAL OBSERVATORY Report, period ending 31 Dec. 1988
1989 48 p
(NASA-CR-186258; NAS 1.26:186258; PB89-235840; SAAO-13; ISBN-0-7988-4647-X; ISSN-0250-0671) Avail: NTIS HC A03/MF A01 CSCL 03A

Topics discussed in the Overview of Year 1988 include the following: Supernova in the Large Magellanic Cloud; Galaxies; Ground based observations of celestial x ray sources; the Magellanic Clouds; Pulsating variables; Galactic structure; Binary star phenomena; The provision of photometric standards; Nebulae and interstellar matter; Stellar astrophysics; Astrometry; Solar system studies; Visitors programs; Publications; and General matters. Author

N90-15857 State Univ. of New York, Stony Brook.
NEAR-INFRARED POLARIMETRY AND SPECTROSCOPY OF COMETS Ph.D. Thesis
Timothy Young Brooke 1988 115 p
Avail: Univ. Microfilms Order No. DA8921208

The linear polarizations and colors of the light scattered by dust grains in comet Halley in broadband filters J(1.25 microns), H(1.65 microns), and K(2.2 microns) were measured at phase angles 9.4 deg approx. less than beta approx. less than 65.3 deg. The colors were red, characteristic of comet dust at these wavelengths. The JHK polarizations reach 25 percent at the largest phase angles with a reversal at beta = 20 deg and negative values of a few percent at smaller beta. The polarization increases with wavelength at the larger phase angles, in contrast to other solar system particulates. The data were modeled in two ways. Models using spheres required two separate components of absorbing and dielectric materials. A rough particle model based on a theory due to Wolff provided better fits and required only a single component, which could, however, be an intimate mixture of dielectric and absorbing material. A mixture of carbon and silicates fits the data. The derived carbon-to-silicon abundance for this mixture is approx. 0.7, consistent with some other results, but lower than the value derived from mass spectrometry. The wavelength dependences of the polarization and color of comet Halley require refractive indices whose real and imaginary parts increase with wavelength from the visible to the near-infrared. Absorbing material, presumably carbon-based, is essential.
Dissert. Abstr.

N90-15858# Istituto Nazionale di Fisica Nucleare, Frascati (Italy). Dept. of Physics.
FIRST RESULTS FROM THE MACRO (MONOPOLE, ASTROPHYSICS, COSMIC RAY OBSERVATORY) DETECTOR AT THE GRAN SASSO LABORATORY
M. Calicchio, G. DeCataldo, C. DeMarzo, O. Erriquez, C. Favuzzi, N. Giglietto, E. Nappi, P. Spinelli, S. Cecchini, and I. DAntone et al 1989 21 p Presented at the 2nd International Conference on Engineering Management, Toronto, Ontario, 10-13 Sep. 1989 Prepared in cooperation with Texas A and M Univ., College Station
(Contract DE-AS05-81ER-40039)
(DE90-003243; DOE/ER-40039/31; CONF-890930-3) Avail: NTIS HC A03/MF A01

The MACRO (Monopole, Astrophysics, Cosmic Ray Observatory) detector which is being installed at the underground Gran Sasso Laboratory (LNGS) is described in detail. The performance of the detector's first supermodule (approx. 800 sq mp sr), which had its initial data run from February 27 to May 30, 1989, is reported. About 245,000 muon triggers were recorded during this first run. Preliminary results are presented on: the measured vertical muon flux; the detection features of MACRO as a high energy muon and muon neutrino telescope; the measured lateral spread and multiplicity distributions of muon bundles; a search for GUT magnetic monopoles; a search for electron anti-neutrinos from stellar collapses. In addition, there are results obtained in conjunction with the EAS-TOP detector located on top of the Gran Sasso mountain. DOE

N90-15859*# Space Telescope Science Inst., Baltimore, MD.
SHAPES OF STAR-GAS WAVES IN SPIRAL GALAXIES
Stephen H. Lubow (Johns Hopkins Univ., Baltimore, MD.) Feb. 1988 7 p Submitted for publication Sponsored by NASA,

Washington, DC
(NASA-CR-186289; NAS 1.26:186289; Preprint-Series-240)
Avail: NTIS HC A02/MF A01 CSCL 03A

Density-wave profile shapes are influenced by several effects. By solving viscous fluid equations, the nonlinear effects of the gas and its gravitational interaction with the stars can be analyzed. The stars are treated through a linear theory developed by Lin and coworkers. Short wavelength gravitational forces are important in determining the gas density profile shape. With the inclusion of disk finite thickness effects, the gas gravitational field remains important, but is significantly reduced at short wavelengths. Softening of the gas equation of state results in an enhanced response and a smoothing of the gas density profile. A Newtonian stress relation is marginally acceptable for HI gas clouds, but not acceptable for giant molecular clouds. Author

N90-15860*# Space Telescope Science Inst., Baltimore, MD.
THE DISK-HALO CONNECTION AND THE NATURE OF THE INTERSTELLAR MEDIUM
Colin A. Norman and Satoru Ikeuchi (Tokyo Astronomical Observatory, Japan) Jan. 1988 8 p Submitted for publication Sponsored by NASA, Washington, DC
(NASA-CR-186286; NAS 1.26:186286; Preprint-Series-232)
Avail: NTIS HC A02/MF A01 CSCL 03A

Some results on the nature of the interstellar medium that are specifically concerned with the disk-halo interaction are discussed. Over the last five years or so it has become clear that the supernovae rate in our Galaxy is spatially clumped and the consequences of such clumping are superbubbles and supershells fed by tens or hundreds of supernovae per shell. These objects evolve and expand rapidly and soon break out of the disk of the Galaxy, feeding the halo with very significant mass, energy, and momentum. As cooling occurs, gas will rain down onto the disk of the Galaxy completing the cycle. The basic flow of physical quantities from disk to halo and vice versa are discussed. Some of the many implications are noted including aspects of dynamo theory, quasar absorption lines, the theory of galactic coronae, and the nature of the x ray background. The essential difference here with the McKee-Ostriker (1977) theory is that the filling factor of the hot gas in the disk is significantly less than unity. Author

N90-15861*# Space Telescope Science Inst., Baltimore, MD.
AUTOMATED OBSERVATION SCHEDULING FOR THE VLT
Mark D. Johnston Aug. 1988 13 p Submitted for publication Sponsored by NASA, Washington, DC
(NASA-CR-186282; NAS 1.26:186282; Preprint-Series-307)
Avail: NTIS HC A03/MF A01 CSCL 03A

It is becoming increasingly evident that, in order to optimize the observing efficiency of large telescopes, some changes will be required in the way observations are planned and executed. Not all observing programs require the presence of the astronomer at the telescope: for those programs which permit service observing it is possible to better match planned observations to conditions at the telescope. This concept of flexible scheduling has been proposed for the VLT: based on current and predicted environmental and instrumental observations which make the most efficient possible use of valuable time. A similar kind of observation scheduling is already necessary for some space observatories, such as Hubble Space Telescope (HST). Space Telescope Science Institute is presently developing scheduling tools for HST, based on the use of artificial intelligence software development techniques. These tools could be readily adapted for ground-based telescope scheduling since they address many of the same issues. The concept are described on which the HST tools are based, their implementation, and what would be required to adapt them for use with the VLT and other ground-based observatories. Author

N90-15862*# Space Telescope Science Inst., Baltimore, MD.
ARTIFICIAL INTELLIGENCE APPROACHES TO ASTRONOMICAL OBSERVATION SCHEDULING
Mark D. Johnston and Glenn Miller (Computer Sciences Corp., Baltimore, MD.) Aug. 1988 11 p Presented at the 3rd International Workshop on Data, Analysis in Astronomy, Erice, Italy, 20-27 Jun. 1988 Submitted for publication Sponsored by NASA, Washington, DC
(NASA-CR-186277; NAS 1.26:186277; Preprint-Series-304)
Avail: NTIS HC A03/MF A01 CSCL 03A

Automated scheduling will play an increasing role in future ground- and space-based observatory operations. Due to the complexity of the problem, artificial intelligence technology currently offers the greatest potential for the development of scheduling tools with sufficient power and flexibility to handle realistic scheduling situations. Summarized here are the main features of the observatory scheduling problem, how artificial intelligence (AI) techniques can be applied, and recent progress in AI scheduling for Hubble Space Telescope. Author

N90-15863*# Space Telescope Science Inst., Baltimore, MD.
AUTOMATED TELESCOPE SCHEDULING
Mark D. Johnston Aug. 1988 10 p Submitted for publication Sponsored by NASA, Washington, DC
(NASA-CR-186279; NAS 1.26:186279; Preprint-Series-306)
Avail: NTIS HC A02/MF A01 CSCL 03A

With the ever increasing level of automation of astronomical telescopes the benefits and feasibility of automated planning and scheduling are becoming more apparent. Improved efficiency and increased overall telescope utilization are the most obvious goals. Automated scheduling at some level has been done for several satellite observatories, but the requirements on these systems were much less stringent than on modern ground or satellite observatories. The scheduling problem is particularly acute for Hubble Space Telescope: virtually all observations must be planned in excruciating detail weeks to months in advance. Space Telescope Science Institute has recently made significant progress on the scheduling problem by exploiting state-of-the-art artificial intelligence software technology. What is especially interesting is that this effort has already yielded software that is well suited to scheduling groundbased telescopes, including the problem of optimizing the coordinated scheduling of more than one telescope. Author

90 ASTROPHYSICS

Includes cosmology; celestial mechanics; space plasmas; and interstellar and interplanetary gases and dust.
For related information see also *75 Plasma Physics*.

N90-15864 Alabama Univ., Huntsville.
A NUMERICAL SIMULATION MODEL FOR THE STUDY OF MAGNETOHYDRODYNAMIC (MHD) WAVES IN A STRUCTURED MEDIUM Ph.D. Thesis
Yingcai Xiao 1988 252 p
Avail: Univ. Microfilms Order No. DA8911252

This dissertation contains two basic parts: a formal development of a numerical simulation model for the study of magnetohydrodynamic (MHD) waves in a structured medium, and an application of the model to the investigation of the propagation of MHD waves in a magnetic slab and their interactions with non-magnetic surroundings. The numerical model is a time-dependent, two-dimensional, and nonlinear MHD model with gravity and radiative energy loss. The corresponding numerical code is based on the newly developed SINIL (Semi-Implicit-Non-Iterative-Lagrangian) scheme. The MHD governing equations are discretized on a Lagrangian rid, using the control-volume method. The gas dynamic properties are solved explicitly, and the magnetic field is solved implicitly without using numerical iterations. Using this numerical model, three kinds of slab waves are studied, namely, kink type slab waves, sausage type slab waves, and kink type single interface waves (which are considered as kink type slabe waves in the limit of infinite slab width). In the present study, external acoustic waves can only be excited by internal body waves. The excitation of external acoustic waves represents the energy leakage from the internal magnetized region to the external field-free region. The condition of the

excitation is the relative compressibility (the ratio of the internal body wave speed to the external sound speed) being greater than one. Dissert. Abstr.

N90-15865 Princeton Univ., NJ.
PULSARS LOST AND FOUND: THE SECOND PRINCETON-ARECIBO MILLISECOND PULSAR SEARCH Ph.D. Thesis
Andrew Steven Fruchter 1989 112 p
Avail: Univ. Microfilms Order No. DA8920419

A search for weak, nearby millisecond pulsars at the Arecibo 305 m telescope was performed. The survey covered more than 160 square degrees of sky centered on the galactic place with a sensitivity several times greater than any previous millisecond pulsar search. Fifteen new pulsars were found, including a 39.5 ms pulsar in the supernova remnant CTB 80, and a 1.6 ms pulsar in orbit with a low mass companion. While only three of the forty-seven pulsars detected in this survey have period less than 10 ms, the low average flux of these three objects suggests that there may be as many millisecond pulsars in the galaxy as slow normal pulsars. At an observing frequency of 430 MHz, the new binary millisecond pulsar, PSR 1957 + 20, is eclipsed for 45 minutes of each 9 hour orbit. Timing observations imply a companion mass of only 0.02 to 0.04 solar masses. The eclipsing matter extends well beyond the Roche lobe of the companion and appears to possess a comet-like tail, strongly suggesting that the neutron star is evaporating its companion. This pulsar may therefore represent a missing link in the evolution of millisecond pulsars for binary to solitary stars. Optical observations of the system show a 20th magnitude visual object which varies greatly in apparent intensity over the course of an orbit. The data suggest that the companion is a hydrogen white dwarf and perhaps the least massive object directly observed outside of the solar system. Dissert. Abstr.

N90-15866 California Univ., Los Angeles.
A CALCULATION OF ENERGETIC PROTON SPECTRA PRODUCEDAT SUBSTORM ONSET IN THE FIELDS OF THE EXPLOSIVE RECONNECTION MODEL Ph.D. Thesis
Richard K. Albano 1989 135 p
Avail: Univ. Microfilms Order No. DA8918024

Impulsive bursts are observed throughout the magnetosphere at the onset of the expansive phase of geomagnetic storms are sudden enhancements of the energetic particle flux. The model fields of the explosive reconnection model (Coroniti, 1985) is used to calculate impulsive burst particle spectra from an observing satellite's perspective. The explosive reconnection model evolves toward a steady state reconnection, determining the maximum particle energy gain. A satellite detector's location and time with reference to, respectively, the x-lines's location and temporal evolution, are important factors determining the characteristics of the observed burst spectrum. Therefore burst spectra are computed by approximating the averaging in energy and solid angle of an actual detector. The most energetic spectra are calculated after reconnection has reached a steady rate at onset. Plasma in the diffusion layer is heated by the current sheet acceleration mechanism. This heated plasma is not observed outside the diffussion region, near the separatrix, where only the most energetic particles have had time to reach after current sheet ejection. Particles gaining the most energy are accelerated in the diffusion region where the components of the magnetic field normal to the neutral sheet is small, allowing particles to stay in the region for relatively long periods of time. The particles are eventually turned perpendicular to the x-line by the normal component. These resonant particles originate in denser phase space volumes than unaccelerated particles and, hence, can enhance the distribution junction at the satellite. Energetic particle fluxes at the satellite are enhanced only if adequate numbers of the incident particles were accelerated along the x-line. It is found that spectra consistent with observations are obtained for a model detector positioned far enough from the x-line that the impinging resonant particle flux is aligned along the magnetic field. Dissert. Abstr.

N90-15867# Fermi National Accelerator Lab., Batavia, IL. Astrophysics Center.
SMALL SCALE STRUCTURE ON COSMIC STRINGS
Andreas Albrecht 30 Oct. 1989 20 p Presented at the Symposium on the Formation and Evolution of Cosmic Strings, Cambridge, England, 2-7 Jul. 1989
(Contract DE-AC02-76CH-03000)
(DE90-003128; FNAL/C-89/221-A; CONF-8907171-1) Avail: NTIS HC A03/MF A01

Current understanding of cosmic string evolution is discussed and the question of small scale structure on strings, where most of the disagreements lie, is focussed upon. A physical picture designed to put the role of the small scale structure into more intuitive terms, is presented. In this picture one can see how the small scale structure can feed back in a major way on the overall scaling solution. It is also argued that it is easy for small scale numerical errors to feed back in just such a way. The intuitive discussion presented here may form the basis for an analytic treatment of the small structure, which argued in any case would be extremely valuable in filling the gaps in current understanding of cosmic string evolution. DOE

N90-15868# Hiroshima Univ., Takehara (Japan). Research Inst. for Theoretical Physics.
GRAVITATIONAL LENS EFFECT ON THE COSMIC BACKGROUND RADIATION DUE TO NONLINEAR INHOMOGENEITIES
Kenji Tomita and Kazuya Watanabe Apr. 1989 25 p Sponsored in part by Ministry of Education, Science, and Culture
(DE90-701753; RRK-89-10) Avail: NTIS (US Sales Only) HC A03/MF A01

Null geodesic equations are numerically solved, in order to investigate the light propagation in inhomogeneous cosmological models. The models are derived using the N body simulation method and assuming for simplicity that clusters of galaxies are regarded as particles. Statistical properties of angular fluctuations of light paths and angular correlation functions of the cosmic background radiation are studied. It is shown that the angular fluctuation due to gravitational lensing depend much on the particle size. If it is equal to the size of the Coma cluster, the lens effect is so large as to decrease the finite-beam-smeared temperature fluctuations of the cosmic backgound radiation by a factor (ge)2, compared with those in the no-lens case, while the non-smeared temperature fluctuations are much enhanced for angles (ge)0.5 arcmin. DOE

N90-15869*# Space Telescope Science Inst., Baltimore, MD.
THE AGE OF THE GALACTIC DISK
Allan Sandage Jul. 1988 15 p Presented at a Workshop on The Calibration of Stellar Ages, Middletown, CT, 13-14 May 1988
(NASA-CR-186292; Preprint-Series-288; NAS 1.26:186292)
Avail: NTIS HC A03/MF A01 CSCL 03B

The galactic disk is a dissipative structure and must, therefore be younger than the halo if galaxy formation generally proceeds by collapse. Just how much younger the oldest stars in the galactic disk are than the oldest halo stars remains an open question. A fast collapse (on a time scale no longer than the rotation period of the extended protogalaxy) permits an age gap of the order of approximately 10 to the 9th power years. A slow collapse, governed by the cooling rate of the partially pressure supported falling gas that formed into what is now the thick stellar disk, permits a longer age gap, claimed by some to be as long as 6 Gyr. Early methods of age dating the oldest components of the disk contain implicit assumptions concerning the details of the age-metallicity relation for stars in the solar neighborhood. The discovery that this relation for open clusters outside the solar circle is different that in the solar neighborhood (Geisler 1987), complicates the earlier arguments. The oldest stars in the galactic disk are at least as old as NGC 188. The new data by Janes on NGC 6791, shown first at this conference, suggest a disk age of at least 12.5 Gyr, as do data near the main sequence termination point of metal rich, high proper motion stars of low orbital eccentricity.

Hence, a case can still be made that the oldest part of the galactic thick disk is similar in age to the halo globular clusters, if their ages are the same as 47 Tuc. Author

N90-15870*# Space Telescope Science Inst., Baltimore, MD.
RECENT PROGRESS IN UNDERSTANDING THE ERUPTIONS OF CLASSICAL NOVAE
Michael M. Shara Oct. 1988 52 p Submitted for publication Sponsored by NASA, Washington, DC
(NASA-CR-186280; NAS 1.26:186280; Preprint-Series-314)
Avail: NTIS HC A04/MF A01 CSCL 03B

Dramatic progress has occurred in the last two decades in understanding the physical processes and events leading up to, and transpiring during the eruption of a classical nova. The mechanism whereby a white dwarf accreting hydrogen-rich matter from a low-mass main-sequence companion produces a nova eruption has been understood since 1970. The mass-transferring binary stellar configuration leads inexorably to thermonuclear runaways detected at distances of megaparsecs. Summarized here are the efforts of many researchers in understanding the physical processes which generate nova eruptions; the effects upon nova eruptions of different binary-system parameters (e.g., chemical composition or mass of the white dwarf, different mass accretion rates); the possible metamorphosis from dwarf to classical novae and back again; and observational diagnostics of novae, including x ray and gamma ray emission, and the characteristics and distributions of novae in globular clusters and in extragalactic systems. While the thermonuclear-runaway model remains the successful cornerstone of nova simulation, it is now clear that a wide variety of physical processes, and three-dimensional hydrodynamic simulations, will be needed to explain the rich spectrum of behavior observed in erupting novae. Author

N90-15871*# Space Telescope Science Inst., Baltimore, MD.
THE VOLATILE COMPOSITION OF COMETS
H. A. Weaver Nov. 1988 8 p Submitted for publication Sponsored by NASA, Washington, DC
(NASA-CR-186281; NAS 1.26:186281; Preprint-Series-316)
Avail: NTIS HC A02/MF A01 CSCL 03B

Comets may be our best probes of the physical and chemical conditions in the outer regions of the solar nebula during that crucial period when the planets formed. The volatile composition of cometary nuclei can be used to decide whether comets are the product of a condensation sequence similar to that invoked to explain the compositions of the planets and asteroids, or if comets are simply agglomerations of interstellar grains which have been insignificantly modified by the events that shaped the other bodies in the solar system. Although cometary nuclei are not generally accessible to observation, observations of cometary comae can illuminate at least some of the mysteries of the nuclei provided one has a detailed knowledge of the excitation conditions in the coma and also has access to basic atomic and molecular data on the many species present in comets. Examined here is the status of our knowledge of the volatile composition of cometary nuclei and how these data are obtained. Author

N90-15872# Lawrence Livermore National Lab., CA. High Temperature Div.
ASTOPHYSICAL OPACITIES AT LLNL
Carlos A. Iglesias and Forrest J. Rogers 2 Aug. 1989 10 p Presented at the International Conference: Inside the Sun, Versailles, France, 22-26 May 1989
(Contract W-7405-eng-48)
(DE90-003599; UCRL-102150; CONF-890520-3) Avail: NTIS HC A03/MF A01

In an effort to reduce uncertainties in the theoretical radiative opacities a new code was developed at LLNL which removes several of the approximation present in past calculations. Results from the new code with comparisons to other available opacity calculations are presented as well as experiments. DOE

N90-15873*# Arizona Univ., Tucson.
DUST BANDS IN THE ASTEROID BELT
M. Sykes, R. Greenberg, S. Dermott, P. Nicholson, J. Burns, and T. N. Gautier 8 Sep. 1989 144 p Submitted for publication Sponsored in part by Infrared Processing and Analysis Center
(Contract NAGw-1029; F19628-87-K-0045)
(NASA-CR-186301; NAS 1.26:186301; AD-A213549; GL-TR-89-0262) Avail: NTIS HC A07/MF A01 CSCL 03/1

The Infrared Astronomical Satellite (IRAS) discovered three bands of dust: one above, below, and approximately in the plane of the ecliptic. These bands are located in the asteroid belt and are believed to arise from collisional activity. Debris from an asteroid collision, over time, fills a torus having peaks in particle number density near its inner and outer corners, corresponding to the locus of perihelia and aphelia, respectively. As a consequence of this geometry, such a swarm should produce two pairs of bands that straddle the ecliptic - a perihelion band pair and an aphelion band pair (which generally overlap along the line of sight from earth). Indeed, processing of the IRAS data now resolves the band structure into at least three such band pairs, with indications of several more pairs distributed over a large range of ecliptic latitudes. Some of these bands appear to be associated with major Hirayama asteroid families, while others are not. Possible origins of the observed dust bands include: (1) the gradual comminution of the asteroid belts as a whole, in which the local dust population is maximum where the concentration of asteroids is greatest (e.g., families); (2) one or a few large random asteroid collisions enhancing the local population of small debris, which in turn is comminuted into dust; and (3) the disintegration of one or more large comets. GRA

91 LUNAR AND PLANETARY EXPLORATION

Includes planetology; and manned and unmanned flights.
For spacecraft design or space stations see *18 Spacecraft Design, Testing and Performance.*

N90-15874 Cornell Univ., Ithaca, NY.
THE MIDDLE MARTIAN ATMOSPHERE Ph.D. Thesis
Robert Frederick Jaquin, III 1989 135 p
Avail: Univ. Microfilms Order No. DA8915153

Profiles of scattered light above the planetary limb from 116 Viking Orbiter images are used to constrain the temporal and spatial behavior of aerosols suspended in the Martian atmosphere. The data cover a wide range of seasons, locations, and viewing geometry, providing information about the aerosol optical properties and vertical distribution. The potential role of stationary gravity gravity waves in modifying the middle atmosphere circulation is explored using a linear theory applied to a realistic Martian environment. Martian topography derived from radar observations is decomposed into Fourier harmonics and used to linearly superpose gravity waves arising from each component. Gravity waves are found to become unstable and break between the near-surface and 90 km elevation, depending on season and terrain type. This establishes a wave drag that accelerates the mean flow. Insight into the character of the middle atmosphere circulation is examined using the seasonal variation in the equator-to-pole equilibrium temperature difference. The circulation of the middle atmosphere is examined using a two-dimensional, linearized, axisymmetric model successfully employed in the study of the terrestrial mesosphere. Radiative equilibrium temperatures are calculated using a general random band model for the transmission of radiation through the 2.0, 2.7, 4.3, and 15 micrometer bands of CO2. The breakdown of local thermodynamic equilibrium is treated using a two level model. Various profiles of the Rayleigh friction timescale are used but the most satisfactory in reproducing observations is a two level profile consistent with the breaking of internal gravity waves near 50 km elevation on a global annual average. Illustrations of temperature and wind speeds are presented for the southern summer solstice and southern spring equinox. Dissert. Abstr.

N90-15875 California Univ., Riverside.
LABORATORY SIMULATIONS OF THE SOLAR WIND-COMET INTERACTIONS Ph.D. Thesis
Tsuey-Fen Chang 1988 156 p
Avail: Univ. Microfilms Order No. DA8909857

The laboratory simulation of the solar wind interaction with a comet is performed to study the cometary neutral gas ionization and the influence of the ionization process on bow shock formation. The UCR T-1 facility is used for the simulations, an ice ball as a comet model and photographs and data are taken under a variety of solar wind velocity, interplanetary magnetic field and comet configurations. The results show that the cometary neutral gas ionization depends on both the velocity of the solar wind and the interplanetary magnetic field. The plasma cloud surrounding the comet is visible only when the solar wind velocity and IMF are both above minimum values. This velocity dependent phenomena is explained by Alfven's critical ionization velocity effect. This critical magnetic field effect may be caused by the lower hybrid instability triggering ionization of the neutral gas by plasma flow. The magnetic component of electromagnetic instabilities are investigated both with and without the CIV effect. Four groups of waves are found and identified to lie in the range of lower hybrid waves. The cometary bow shock formation is studied with the neutral gas ionization conditions satisfied. A contact discontinuity and a collisional bow shock are found. Dissert. Abstr.

N90-15876# Los Alamos National Lab., NM. Earth and Environmental Sciences Div.
A QUASI-ECONOMIC ROLE FOR LUNAR SCIENCE
Eric M. Jones 1989 12 p Presented at the 40th Congress of the International Astronautical Federation, Malaga, Spain, 7-13 Oct. 1989
(Contract W-7405-eng-36)
(DE90-000679; LA-UR-89-3288; CONF-8910229-1) Avail: NTIS HC A03/MF A01

In broad economic terms, the development of lunar products will begin with a sequence of technology, production, and delivery demonstrations which will have to precede the emergence of markets. Economically viable products will tend to be those for which the sum of production and transport costs are lower for lunar suppliers than for terrestrial suppliers. As long as lunar production costs exceed terrestrial production costs - as will be the case for most lunar products until such time as lunar development has reached a mature stage - the most viable industries will be those producing low-tech products for lunar markets. The scale of initial lunar markets will depend on the size of a lunar base and/or its rate of growth. For a given level of public support, maximum base size can be achieved through the conduct, at the base, of a vigorous program of scientific and engineering research making use of as much local production and as many permanently-resident support staff as feasible.
DOE

92 SOLAR PHYSICS

Includes solar activity, solar flares, solar radiation and sunspots.

For related information see *93 Space Radiation.*

N90-15877# Los Alamos National Lab., NM.
A SIMPLE MODEL FOR THE STELLAR ANALOGY OF COMPACT SOLAR FLARES
R. A. Kopp and G. Poletto (Osservatorio Astrofisico di Arcetri, Florence, Italy) 1989 4 p Presented at the 6th Cambridge Workshop on Cool Stars, Stellar Systems and the Sun, Seattle, WA, 11-14 Sep. 1989
(Contract W-7405-eng-36)
(DE90-003215; LA-UR-89-3788; CONF-8909276-1) Avail: NTIS HC A01/MF A01

We have developed a simple point model to describe the average thermodynamical properties of a compact flare loop as a function of time during the flare decay phase. The model includes thermal conduction, chromospheric evaporation, and radiative losses; moreover, it assumes lateral (gas + magnetic) pressure balance with the background corona at all times. For the case of a low-(beta) plasma (rigid flux tube), detailed 1-D hydrodynamical simulations are available in the literature for comparison; we show that the temporal variation of average loop properties predicted by the point model are in good agreement with these numerical simulations for a loop with the same energy input. DOE

93 SPACE RADIATION

Includes cosmic radiation; and inner and outer earth's radiation belts.

For biological effects of radiation see *52 Aerospace Medicine.* For theory see *73 Nuclear and High-Energy Physics.*

N90-15878 Arizona Univ., Tucson.
LEAP: A BALLOON-BORNE SEARCH FOR LOW-ENERGY COSMIC RAY ANTIPROTONS Ph.D. Thesis
Anne Rosalie Myers Moats 1989 163 p
Avail: Univ. Microfilms Order No. DA8919046

The LEAP (Low Energy Antiproton) experiment is a search for cosmic ray antiprotons in the 120 MeV to 1.2 GeV kinetic energy range. The motivation for this project was the result announced by Buffington et al. (1981) that indicated an anomalously high antiproton flux below 300 MeV; this result has compelled theorists to propose sources of primary antiprotons above the small secondary antiproton flux produced by high energy cosmic ray collisions with nuclei in the interstellar medium. LEAP consisted of the NMSU magnet spectrometer, a time-of-flight system designed at NASA-Goddard, two scintillation detectors, and a Cherenkov counter. Analysis of flight data performed by the high energy astrophysics group at Goddard Space Flight Center revealed no antiproton candidates found in the 120 MeV to 360 MeV range; 3 possible antiproton candidate events were found in the 500 MeV to 1.2 GeV range in an analysis done here at the University of Arizona. However, since it will be necessary to sharpen the calibration on all of the LEAP systems in order to positively identify these events as antiprotons, only an upper limit has been determined at present. Thus, combining the analyses performed at the University of Arizona and NASA-Goddard, 90 percent confidence upper limits of 3.5 x 10(exp -5) in the 120 MeV to 360 MeV range and 2.3 x 10(exp -4) in the 500 MeV to 1.2 GeV range for the antiproton/proton ratio is indicated by the LEAP results. LEAP disagrees sharply with the results of the Buffington group, indicating a low antiproton flux at these energies. Thus, a purely secondary antiproton flux may be adequate at low energies. Dissert. Abstr.

N90-15879# Stanford Linear Accelerator Center, CA.
THE DIGITAL DATA ACQUISITION CHAIN AND THE COSMIC RAY TRIGGER SYSTEM FOR THE SLD WARM IRON CALORIMETER
A. Benvenuti, L. Piemontese, A. Calcaterra, R. DeSangro, P. DeSimone, P. N. Burrows, S. L. Cartwright, S. Gonzales, A. Lath, and U. Schneekloth (Massachusetts Inst. of Tech., Cambridge.) et al Aug. 1989 8 p Presented at the 4th Pisa Meeting on Advanced Detectors: Frontier Detectors From Frontier Physics, La Biodola, Italy, 21-26 May 1989 Sponsored in part by Instituto Nazionale di Fiscia Nucleare, Italy
(Contracts DE-AC03-76SF-00515; DE-AC02-76ER-03069; DE-AC02-76ER-00881)
(DE90-000943; SU-SLAC-PUB-5066; CONF-8905194-6) Avail: NTIS HC A02/MF A01

The entire data-acquisition chain, from the custom-made front-end electronics to the Fastbus readout and data-reduction module, for the digital readout of the SLD limited streamer tube Warm Iron Calorimeter and Muon Identifier is described. Also described is a Fastbus Cosmic Logic Unit being developed to achieve the capability of reading cosmic ray events, also during

the inter-crossing time, for apparatus monitoring and calibration purposes. DOE

N90-15880# California Univ., Berkeley. Lawrence Berkeley Lab. Nuclear Science Div.
COSMIC RAY HALF LIFE OF (54)Mn
E. B. Norman, B. Sur, K. R. Vogel, K. T. Lesko, R.-M. Larimer, and E. Browne Aug. 1989 3 p Presented at the 21st International Cosmic Ray Conference, Adelaide, Australia, 6-19 Jan. 1990
(Contract DE-AC03-76SF-00098)
(DE90-000134; LBL-27672; CONF-900129-1) Avail: NTIS HC A01/MF A01

A search for the beta(+) decay of Mn-54 has established an upper limit of 4.4 x 10(exp -8) for this branching ratio, and a lower limit of 13.3 for the log ft value for this second forbidden unique transition. Assuming that the beta(-) decay branch has the same log ft value, then its partial half life must be greater than 4 x 10(exp 4) years. Experiments to directly measure the beta(-) decay rate of Mn-54 are now in progress. DOE

99 GENERAL

N90-15881# General Accounting Office, Washington, DC. Information Management and Technology Div.
SPACE OPERATIONS: LISTING OF NASA SCIENTIFIC MISSIONS, 1980-2000. FACT SHEET FOR THE CHAIRMAN, SUBCOMMITTEE ON SPACE SCIENCE AND APPLICATIONS, COMMITTEE ON SCIENCE, SPACE, AND TECHNOLOGY, HOUSE OF REPRESENTATIVES
Apr. 1989 24 p
(AD-A213493; GAO/IMTEC-89-46FS) Avail: NTIS HC A03/MF A01 CSCL 22/1

As requested GAO provided a list of the National Aeronautics and Space Administration's (NASA) active and planned scientific missions, 1980-2000. Included are missions with the following status: launches prior to 1980, and those since 1980 that either ended after 1980 or are currently approved by NASA and remain active; and planned launches that were approved or proposed by NASA. This compilation covers the following four major scientific disciplines: planetary and lunar, earth sciences, space physics, and astrophysics. Appendixes 2-5 present this information, including mission names and acronyms, actual or anticipated launch dates, and the actual or expected end-of-mission dates, in tables and figures. As requested, other types of NASA missions in biology and life sciences, manufacturing sciences, and communication technology are not listed. GRA

Typical Subject Index Listing

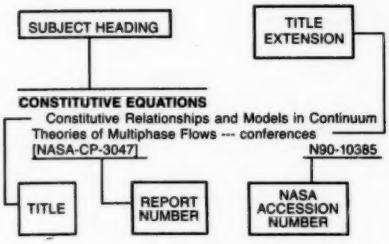

The subject heading is a key to the subject content of the document. Titles, report numbers, and accession numbers of pertinent documents are provided under each subject heading. When the title is insufficiently descriptive of the document content, a title extension has been added, separated from the title by three hyphens. The report number helps to indicate the type of document cited (e.g., NASA report, NASA translation, NASA contractor report). The NASA accession number is the number by which the document abstracts are arranged in this journal and by which the document is sold or requested. The titles, with title extensions if present, are arranged under each subject heading in ascending accession number order. The subject headings have been selected from the latest revision of the *NASA Thesaurus* (NASA SP-7064).

A

ABEL FUNCTION
Abelian gauge theory in topologically non-trivial space
[DE90-710100] N90-15830

ABILITIES
Numerical facility: Convergence of cognitive and factor analytic models
[AD-A213627] N90-15680

ABLATION
Laser-induced surface ablation and optical damage of ZnS crystals caused by single- and multiple-pulse laser-irradiation
[DE90-003807] N90-15419

ABSORBERS (MATERIALS)
Analysis of catalytically enhanced solar absorption chemical reactors: 1 - numerical model description
[DE89-014742] N90-15505

ABSORPTION SPECTRA
Anomalous absorption by atmospheric water vapor and stabilized water fogs in the infrared and CM-wave regions
[AD-A214202] N90-15572
X ray absorption studies of YBa2Cu3O(6+x), La(2-x)Sr(x)CuO4, and Nd(2-x)Ce(x)CuO4
[DE90-003640] N90-15797
Auger and x ray absorption studies of solid molecular oxygen
[DE90-003966] N90-15825

ABSORPTION SPECTROSCOPY
Spectral studies of solid propellant combustion. 2: Emission and absorption results for M-30 and HMX1 propellants
[AD-A213857] N90-15292

ABSORPTIVITY
Kinetic studies following state-selective laser excitation
[DE90-003232] N90-15415

ACCELERATED LIFE TESTS
Accelerated aging embrittlement of cast duplex stainless steel: Activation energy for extrapolation
[DE90-001773] N90-15221
Status and results of ANL life evaluation of valve-regulated lead-acid load-leveling batteries
[DE90-001918] N90-15329
Life evaluation of valve-regulated lead-acid batteries for load-leveling applications
[DE90-002188] N90-15336
Fast algorithms for estimating mixture parameters
[AD-A213869] N90-15636

ACCELERATION (PHYSICS)
VIBRAFUGE: Combined vibration and centrifuge testing
[DE90-001091] N90-15114
Research in knowledge-based vision techniques for the Autonomous Land Vehicle Program
[AD-A213440] N90-15453
Use of lower body negative pressure as a countermeasure to negative Gz acceleration
[AD-A213927] N90-15583

ACCELERATION TOLERANCE
Use of lower body negative pressure as a countermeasure to negative Gz acceleration
[AD-A213927] N90-15583

ACCELEROMETERS
Superconducting gravity gradiometer mission. Volume 1: Study team executive summary
[NASA-TM-4091-VOL-1] N90-15545

ACCESS CONTROL
On the privacy problems involved in allowing access to computers via the public telephone system
[RSRE-88006] N90-15303
Reconfigurable N-dimensional computer memory
[AD-D014309] N90-15607

ACCESS TIME
Temporal, processor, and spatial locality in multiprocessor memory references
[AD-A213790] N90-15598
The implementation of a coherent memory abstraction on a NUMA (Non-Uniform Memory Access) multiprocessor: Experiences with PLATINUM (Platform for Investigating Non-Uniform Memory)
[AD-A213909] N90-15600
Memory management for large-scale NUMA (Non-Uniform Memory Access) multiprocessors
[AD-A213910] N90-15601
An overview of PLATINUM: A Platform for Investiga ting Non-Uniform Memory (preliminary version)
[AD-A213911] N90-15602
Evolution of an operating system for large-scale shared-memory multiprocessors
[AD-A213912] N90-15603
Reconfigurable N-dimensional computer memory
[AD-D014309] N90-15607

ACCIDENT PREVENTION
Improved lighting of taxiway/taxiway intersections for Instrument Flight Rules (IFR) operations
[DOT/FAA/CT-TN89/64] N90-15089

ACETONITRILE
Electrochemistry in near-critical and supercritical fluids. 8: Methyl viologen, decamethylferrocene, Os(bpy)3(sup 2+) and ferrocene in acetonitrile and the effect of pressure on diffusion coefficients under supercritical conditions
[AD-A213407] N90-15172

ACID RAIN
Long-term worldwide environmental effects caused by acid rain from fossil fuels
[DE90-001534] N90-15533
Acid rain research
[DE90-003283] N90-15537

ACOUSTIC ATTENUATION
Sound attenuation apparatus
[NASA-CASE-LAR-13968-1] N90-15710

ACOUSTIC MEASUREMENT
Pulsed EMAT (Electromagnetic Acoustic Transducer) acoustic measurements on a horizontal continuous caster for internal temperature determination
[DE90-002735] N90-15709
Wind speed dependence of acoustic ambient vertical directional spectra at high frequency
[AD-A214293] N90-15712

ACOUSTIC PROPERTIES
Annual summary of basic research in thermoacoustic heat transport
[AD-A214185] N90-15834

ACOUSTIC SCATTERING
Research on acoustical scattering, diffraction catastrophes, optics of bubbles, acoustical phase conjugation, and wake of an oscillating circular cylinder
[AD-A214168] N90-15711

ACOUSTICS
Sound attenuation apparatus
[NASA-CASE-LAR-13968-1] N90-15710

ACOUSTO-OPTICS
Laser glass (1989)
[DE90-002754] N90-15257
Optical acoustic sensor using optical fiber
[DE89-901267] N90-15730
Design of a large angular aperture TeO2 acousto-optic tunable filter
[AD-A213999] N90-15738

ACRYLIC RESINS
Crosslinked, flexible, low-molecular-weight polyacrylamide gels for mobility control
[DE90-000202] N90-15280

ACTIVATION ENERGY
Accelerated aging embrittlement of cast duplex stainless steel: Activation energy for extrapolation
[DE90-001773] N90-15221
Effects of non-linearity in the variation of pinning potential with current-density on magnetic flux creep in high and low T(sub c) superconductors
[DE90-003952] N90-15822

ACTIVE CONTROL
Active control system for gust load alleviation and structural damping N90-15056
Numerical investigation of transition control of a flat plate boundary layer N90-15361

ACTUATORS
A versatile stepping motor controller for systems with many motors
[DE90-001556] N90-15327
Single element magnetic suspension actuator
[NASA-CASE-LAR-13981-1] N90-15442

ADA (PROGRAMMING LANGUAGE)
Ada 9X project report. Revision request report
[AD-A213503] N90-15629

ADAPTATION
The role of attention in visual processing
[AD-A214158] N90-15588
Young Investigator's Award and distributed self-adaptive databases
[AD-A214194] N90-15854

ADAPTIVE CONTROL
Adaptive control of helicopter vibrations via the impulse response method
[AD-A213728] N90-15113
Gaze controls with interactions and delays
[AD-A214286] N90-15667

ADAPTIVE FILTERS
Adaptive canceller limitations caused by I,Q mismatch errors
[AD-A214287] N90-15318

ADHESION
Characterization and in situ testing of diamond films
[DE90-003155] N90-15265
Benefits from combining electroplating and physical vapor deposition technologies
[DE90-002700] N90-15301

ADHESIVE BONDING
Bonding aerogels with polyurethanes
[DE90-003050] N90-15258

ADSORPTION
Studies of the adsorption/desorption behavior of explosive-like molecules
[DE90-001867] N90-15283

ADVECTION
Potential vorticity in extratropical cyclones N90-15564

Numerical methods for parabolic equations and inequalities in very high dimensions
[AD-A214102] N90-15690
AERIAL PHOTOGRAPHY
Vision in dynamic environments
[AD-A213434] N90-15587
AERODYNAMIC CHARACTERISTICS
Flight and wind tunnel investigation of aerodynamic effects of aircraft ground deicing/antiicing fluids N90-15064
Serrated trailing edges for improving lift and drag characteristics of lifting surfaces
[NASA-CASE-LAR-13870-1] N90-15094
AERODYNAMIC COEFFICIENTS
The maximum lift coefficient of plain wings at subsonic speeds
[ESDU-89034] N90-15082
Inclusion of nonlinear aerodynamics in the FLAP code
[DE89-009507] N90-15519
AERODYNAMIC CONFIGURATIONS
Application of the joined wing to tiltrotor aircraft
[NASA-CR-177543] N90-15093
AERODYNAMIC DRAG
Serrated trailing edges for improving lift and drag characteristics of lifting surfaces
[NASA-CASE-LAR-13870-1] N90-15094
AERODYNAMIC HEATING
Numerical investigation of transition control of a flat plate boundary layer N90-15361
Resultant forces and moments in completely restrained plates subjected to a recovery temperature varying linearly with time
[ESDU-89024] N90-15480
Thermal stresses in unrestrained plates subjected to a recovery temperature varying linearly with time
[ESDU-89025] N90-15481
Temperatures in plates subjected to a recovery temperature varying linearly with time
[ESDU-89023] N90-15831
AERODYNAMIC INTERFERENCE
An experimental investigation of wall-interference effects for parachutes in closed wind tunnels
[DE90-001802] N90-15076
Installed tailplane lift-curve slope at subsonic speeds
[ESDU-89029] N90-15081
AERODYNAMIC LOADS
Description of atmospheric turbulence N90-15043
The interference of flightmechanical control laws with those of load alleviation and its influence on structural design N90-15054
An examination of helicopter rotor load calculations
[AD-A214295] N90-15098
AERODYNAMIC STALLING
Schleicher ASK-21 glider (TG-9) stall and spin
[AD-A213513] N90-15096
Aircraft performance enhancement with active compressor stabilization
[AD-A213652] N90-15097
AERODYNAMICS
Aeronautical engineering: A continuing bibliography with indexes (supplement 246)
[NASA-SP-7037(246)] N90-15068
An alternative derivation for an integral equation for linearized subsonic flow over a wing
[AD-A214140] N90-15079
Aerodynamic design and initial performance measurements for the SANDIA 34-metre diameter vertical-axis wind turbine
[DE90-002574] N90-15523
AEROELASTICITY
Nonlinear phenomena in computational transonic aeroelasticity N90-15070
Current status of the application of conventional aluminium-lithium alloys and the potential for future developments N90-15203
Solution of potential flow past an elastic body using the boundary element technique
[AD-A213843] N90-15390
AERONAUTICAL ENGINEERING
Aeronautical engineering: A continuing bibliography with indexes (supplement 246)
[NASA-SP-7037(246)] N90-15068
Bibliography of Lewis Research Center technical publications announced in 1988
[NASA-TM-102034] N90-15846
AERONAUTICS
Technical communications in aeronautics: Results of an exploratory study. An analysis of profit managers' and nonprofit managers' responses
[NASA-TM-101626] N90-15848
AEROSOLS
Aerosol heating and vaporization of high-flux laser beams
[DE90-003471] N90-15428
Evaluate and characterize mechanisms controlling transport, fate, and effects of army smokes in the aerosol wind tunnel: Transport, transformations, fate, and terrestrial ecological effects of hexachloroethane obscurant smokes
[DE90-002923] N90-15536
HCl monitor, phase 2
[AD-A213572] N90-15542
Vertical distribution of pollutants in the presence of convective storms
[DE90-002590] N90-15549
The middle Martian atmosphere N90-15874
AEROSPACE ENGINEERING
Manned spacecraft
[AD-A214218] N90-15129
Al-Li alloy developed by Pechiney N90-15186
The microstructure and properties of aluminum-lithium alloys N90-15187
Current status of the application of conventional aluminium-lithium alloys and the potential for future developments N90-15203
Magnesium alloy technology for aerospace applications N90-15209
Bibliography of Lewis Research Center technical publications announced in 1988
[NASA-TM-102034] N90-15846
NASA patent abstracts bibliography: A continuing bibliography. Section 1: Abstracts (supplement 36)
[NASA-SP-7039(36)-SECT-1] N90-15851
AEROSPACE INDUSTRY
Technical communications in aeronautics: Results of an exploratory study. An analysis of profit managers' and nonprofit managers' responses
[NASA-TM-101626] N90-15848
AEROSPACE PLANES
Hypersonic nozzle design
[NASA-CR-186261] N90-15077
AEROSPACE VEHICLES
Effects of lightning on operations of aerospace vehicles N90-15065
AGING (METALLURGY)
Accelerated aging embrittlement of cast duplex stainless steel: Activation energy for extrapolation
[DE90-001773] N90-15221
Cast stainless steel aging: Mechanisms and predictions
[DE90-003772] N90-15241
AGREEMENTS
Prospects for space arms control
[DE90-003392] N90-15700
AIR
Reduction of erosion in elbows due to flow modifications, phase 2
[DE89-011702] N90-15394
AIR CONDITIONING EQUIPMENT
Design and fabricate a metallic hydride heat pump with a cooling capacity of 9000 BTU/H
[AD-A213756] N90-15388
Guidelines for evaluating energy analysis software
[AD-A214171] N90-15640
AIR CONDUCTIVITY
Transport processes through monomolecular films
[AD-A213609] N90-15342
AIR NAVIGATION
Control outside of independent surveillance coverage operational concept
[AD-A214163] N90-15090
AIR POLLUTION
Characterization of chemicals on engine exhaust particles
[AD-A213566] N90-15106
A methodology for evaluating heavy gas dispersion models
[AD-A214009] N90-15131
Variability of cultivar responses to ozone
[PB89-225460] N90-15528
Long-term worldwide environmental effects caused by acid rain from fossil fuels
[DE90-001534] N90-15533
International aspects of restrictions of ozone-depleting substances
[DE90-001813] N90-15534
Acid deposition
[DE90-003959] N90-15544
Vertical distribution of pollutants in the presence of convective storms
[DE90-002590] N90-15549
AIR QUALITY
Variability of cultivar responses to ozone
[PB89-225460] N90-15528
Environmental surveillance data
[DE90-001275] N90-15532
AIR SAMPLING
Analysis of ambient polar volatile organic compounds using chemical ionization-ion trap detector
[PB90-106451] N90-15529
HCl monitor, phase 2
[AD-A213572] N90-15542
AIR TRAFFIC
Turbulence spectral widths view angle independence as observed by Doppler radar
[DOT/FAA/SA-89/2] N90-15566
AIR TRAFFIC CONTROL
Control outside of independent surveillance coverage operational concept
[AD-A214163] N90-15090
AIR WATER INTERACTIONS
Further research on dynamics of marine atmospheres in tropical cyclones
[AD-A213882] N90-15571
AIRBORNE LASERS
China-built airborne synchronous laser ranger the new L-8 jet trainer aircraft
[AD-A213835] N90-15422
AIRCRAFT ACCIDENTS
Flight in Adverse Environmental Conditions
[AGARD-CP-470] N90-15041
The human element: The key to safe, civil operations in adverse weather N90-15042
See and avoid/cockpit visibility
[AD-A214214] N90-15084
International Aircraft Occupant Safety Conference and Workshop proceedings
[AD-A214452] N90-15085
AIRCRAFT COMMUNICATION
The application of queuing theory to the modelling of CP-140 aircraft communications
[AD-A213479] N90-15310
AIRCRAFT CONFIGURATIONS
Installed tailplane lift-curve slope at subsonic speeds
[ESDU-89029] N90-15081
AIRCRAFT CONSTRUCTION MATERIALS
New Light Alloys
[AGARD-CP-444] N90-15185
Properties of Al-Li alloys N90-15191
Putting alloy 2091 to work N90-15197
AIRCRAFT CONTROL
Turbulence effects of aircraft flight dynamics and control N90-15055
Aircraft performance enhancement with active compressor stabilization
[AD-A213652] N90-15097
Relative merits of reactive and forward-look detection for wind-shear encounters during landing approach for various microburst escape strategies
[NASA-TM-4158] N90-15108
AIRCRAFT DESIGN
Canard versus aft-tail ride qualities performance and pilot command response N90-15053
The interference of flightmechanical control laws with those of load alleviation and its influence on structural design N90-15054
Turbulence effects of aircraft flight dynamics and control N90-15055
Aircraft performance enhancement with active compressor stabilization
[AD-A213652] N90-15097
Aluminum-lithium: Application of plate and sheet to fighter aircraft N90-15202
AIRCRAFT ENGINES
X.2 limited flight test plan
[AD-A214412] N90-15099
AIRCRAFT GUIDANCE
Relative merits of reactive and forward-look detection for wind-shear encounters during landing approach for various microburst escape strategies
[NASA-TM-4158] N90-15108
Guidance analysis of the aeroglide plane change maneuver as a turning point problem
[NASA-TM-101639] N90-15110
AIRCRAFT HAZARDS
Wind shear models for aircraft hazard investigation N90-15044
NASA's program on icing research and technology N90-15062
Principal characteristics of lightning on aircraft N90-15067
International Aircraft Occupant Safety Conference and Workshop proceedings
[AD-A214452] N90-15085
AIRCRAFT INSTRUMENTS
Principal characteristics of lightning on aircraft N90-15067
Display interface concepts for automated fault diagnosis
[NASA-TM-101610] N90-15102
AIRCRAFT MANEUVERS
Flow visualization of the effect of pitch rate on the vortex development on the scale model of a F-18 fighter aircraft
[AD-A214244] N90-15080

Relative merits of reactive and forward-look detection for wind-shear encounters during landing approach for various microburst escape strategies
[NASA-TM-4158] N90-15108

AIRCRAFT PERFORMANCE
Influence of windshear, downdraft and turbulence on flight safety N90-15048
Classification of windshear severity N90-15049
A pitch control law for compensation of the phugoid mode induced by windshears N90-15051
Aircraft response and pilot behaviour during a wake vortex encounter perpendicular to the vortex axis N90-15057
Ice induced aerodynamic performance degradation of rotorcraft: An overview N90-15063
Aircraft performance enhancement with active compressor stabilization
[AD-A213652] N90-15097

AIRCRAFT PILOTS
Cockpit resource management: A selected annotated bibliography
[AD-A214272] N90-15594

AIRCRAFT SAFETY
Adverse weather operations during the Canadian Atlantic storms program N90-15052
See and avoid/cockpit visibility
[AD-A214214] N90-15084
International Aircraft Occupant Safety Conference and Workshop proceedings
[AD-A214452] N90-15085

AIRCRAFT STRUCTURES
The microstructure and properties of aluminum-lithium alloys N90-15187
Fabrication of test-articles from Al-Li 2091 for Fokker 100 N90-15196
Current status of the application of conventional aluminium-lithium alloys and the potential for future developments N90-15203

AIRFOIL OSCILLATIONS
Nonlinear phenomena in computational transonic aeroelasticity N90-15070

AIRFOILS
Unsteady aerodynamics of oscillating and rapidly pitched airfoils N90-15074
Experimental measurements of the laminar separation bubble on an Eppler 387 airfoil at low Reynolds numbers
[NASA-CR-186263] N90-15380

AIRFRAMES
Application of the joined wing to tiltrotor aircraft
[NASA-CR-177543] N90-15093

AIRGLOW
Measurement of optical radiations in spacecraft environments
[AD-A213814] N90-15497

AIRPORTS
National airspace system: Airport movement area control operational concept
[WP-89W00181] N90-15086

AIRSPEED
Evaluation of the improved OV-ID anti-icing system, phase 2
[AD-A213928] N90-15083

ALCOHOLS
Orthobaric densities and molar volumes of liquids: Alcohols
[ESDU-89037] N90-15184

ALGAE
Utilization of non-conventional systems for conversion of biomass to food components
[NASA-CR-177545] N90-15591

ALGEBRA
Modular invariants for theta-functions with characteristics and the twisted N=2 superconformal and SU(2) Kac-Moody algebras
[DE89-635701] N90-15671
Chern-Simons theories of symplectic super-diffeomorphisms
[DE89-635700] N90-15703

ALGORITHMS
Advanced detection, isolation, and accommodation of sensor failures in turbofan engines: Real-time microcomputer implementation
[NASA-TP-2925] N90-15112
More efficient sensitivity testing
[DE90-002639] N90-15298
Component presence-absence detection for automated visual inspection of hybrid microcircuits
[KCP-613-4050] N90-15335
Array signal processing: New techniques for direction finding and spectrum estimation
[AD-A213883] N90-15345
New transient algorithms for non-Newtonian flows
[AD-A213494] N90-15385
Control of mechanical manipulators N90-15432
Mesh refinement in finite element analysis by minimization of the stiffness matrix trace
[NASA-CR-185170] N90-15434
A simple shell element formulation for large-scale elastoplastic analysis
[DE89-015452] N90-15475
On the motion of compliantly-connected rigid bodies in contact. Part 1: The motion prediction problem
[AD-A214135] N90-15489
On the motion of compliantly-connected rigid bodies in contact. Part 2: A system for analyzing designs for assembly
[AD-A214136] N90-15490
Fatigue behavior of vertical axis wind turbine airfoils with two weld configurations
[DE90-002628] N90-15525
An architectural model of visual motion understanding
[AD-A214327] N90-15589
Designing machines for lattice physics and algorithm investigation
[DE90-003543] N90-15596
A block QR factorization algorithm using restricted pivoting
[DE90-001921] N90-15613
Sequential quadratic programming algorithms for optimization
[DE90-000022] N90-15617
Optimizing and evaluating algorithms for replicated data concurrency control
[DE90-003080] N90-15619
Software for a new modified Cholesky factorization
[AD-A213643] N90-15630
On the correctness of orphan management algorithms
[AD-A213777] N90-15632
Evaluation of a simple algorithm for estimating infrared signatures from multi-pixel to sub-pixel targets applied to AGA thermovision imagery
[AD-A214103] N90-15639
A renormalization group approach to image processing: A new computational method for three-dimensional shapes in robot vision, and the computation complexity of the cooling algorithms
[AD-A214247] N90-15643
Principles and algorithms for causal reasoning with uncertainty
[AD-A214248] N90-15644
A paradigm for robust geometric algorithms
[AD-A214324] N90-15647
MODTRAN: A moderate resolution model for LOWTRAN 7
[AD-A214337] N90-15650
Neural network models for linear programming
[DE89-015974] N90-15651
Estimating departure times from traffic counts using dynamic assignment
[DE89-016259] N90-15653
Simulating the scheduling of parallel supercomputer applications
[DE90-003604] N90-15655
Design and implementation of two concurrent multi-sensor integration algorithms for mobile robots
[DE90-003041] N90-15663
Using mappings to prove timing properties
[AD-A213967] N90-15666
Membership-set parameter estimation via optimal bounding ellipsoids
[AD-A213807] N90-15685
Bounded polynomial randomized consensus
[AD-A213808] N90-15686
Optimization of stochastic systems via simulation
[AD-A214011] N90-15689
A structural factoring approach for analyzing probabilistic networks N90-15697
Strong large deviation and local limit theorems
[AD-A213610] N90-15698
Concurrence control for transactions with priorities
[NASA-CR-186241] N90-15699
Systolic algorithms for imaging from space
[AD-A213870] N90-15701

ALIPHATIC HYDROCARBONS
Thermal conductivity of gaseous aliphatic hydrocarbons. Part 1: Alkanes
[ESDU-89035-PT-1] N90-15183

ALKALI HALIDES
On the choice of trial function in theoretical calculations of the thermal conductivity
[DE90-001733] N90-15182

ALKALINE EARTH METALS
Excimer emission from alkali diatomic and alkaline-earth-noble-gas molecules
[AD-A214246] N90-15179

ALKANES
Summary physical data tables: Alkanes
[ESDU-PD3] N90-15162
Thermal conductivity of gaseous aliphatic hydrocarbons. Part 1: Alkanes
[ESDU-89035-PT-1] N90-15183

ALKYLATION
Carboxyalkylated hemoglobin as a potential blood substitute
[AD-A213886] N90-15582

ALL-WEATHER AIR NAVIGATION
Flight in Adverse Environmental Conditions
[AGARD-CP-470] N90-15041
The human element: The key to safe, civil operations in adverse weather N90-15042
The United States Air Force approach to all-weather testing N90-15047
Adverse weather operations during the Canadian Atlantic storms program N90-15052

ALLOCATIONS
Name assignment techniques for relational schemas representing extended entity-relationship schemas
[DE90-003269] N90-15623

ALLOYING
A review of the effects of microalloying constituents on the formation and breakdown of protective oxide scales on high-temperature alloys at temperatures below 700 C
[DE90-001277] N90-15216

ALLOYS
Thermal mechanical fatigue of coated blade materials
[AD-A214258] N90-15107
Electron theory of long wavelength concentration fluctuations in liquid metal alloys
[DE89-636213] N90-15225

ALPHA PARTICLES
Destabilization of tokamak pressure-gradient driven instabilities by energetic alpha populations
[DE90-003716] N90-15756

ALTIMETERS
Geosat/ERM altimeter data analysis for the determination of global oceanic mesoscale variability N90-15492

ALUMINIDES
Thermal mechanical fatigue of coated blade materials
[AD-A214258] N90-15107

ALUMINUM
Ultrasonic evaluation of porosity in aluminum cast materials
[AD-A213548] N90-15232
Using small scale tests to estimate the failure diameter of a propellant
[DE90-001166] N90-15281

ALUMINUM ALLOYS
Fatigue properties of SiC/Al composites N90-15138
New Light Alloys
[AGARD-CP-444] N90-15185
Al-Li alloy developed by Pechiney N90-15186
The microstructure and properties of aluminum-lithium alloys N90-15187
Mechanical properties and fracture toughness of 8090-T651 plate and 2091 and 8090 sheet N90-15188
Fatigue properties of Al-Li alloys N90-15189
Corrosion and stress corrosion of aluminium-lithium alloys N90-15190
Properties of Al-Li alloys N90-15191
Investigation on sheet material of 8090 and 2091 aluminium-lithium alloy N90-15192
Aluminum lithium alloys for Navy aircraft N90-15193
Fatigue, fracture mechanics and corrosion properties of some aluminium-lithium alloys N90-15194
Fatigue and fracture behaviour of a PM Al-Li alloy N90-15195
Fabrication of test-articles from Al-Li 2091 for Fokker 100 N90-15196
Putting alloy 2091 to work N90-15197
Fabrication characteristics of 8090 alloy N90-15198
Superplastic performance and properties of the Lital Alloys N90-15199
Point of view of a civil aircraft manufacturer on Al-Li alloy N90-15200
Uses and properties of Al-Li on the new EH101 helicopter N90-15201
Aluminum-lithium: Application of plate and sheet to fighter aircraft N90-15202
Current status of the application of conventional aluminium-lithium alloys and the potential for future developments N90-15203
High performance powder metallurgy aluminum alloys: An overview N90-15204
Microstructure/mechanical property relations in a mechanically alloyed aluminum N90-15205
Report of the Advanced Neutron Source (ANS) Aluminum Cladding Corrosion Workshop
[DE90-001281] N90-15217
Properties of aluminum-uranium alloys
[DE90-003889] N90-15243

ALUMINUM COMPOUNDS
Heat treatment of pulsed Nd: YAG laser welds in a Ti-14.8 wt pct Al-21.3 wt pct Nb titanium aluminide
[DE90-003484] N90-15228
ALUMINUM GALLIUM ARSENIDES
Picosecond photoconductivity using a graded bandgap Al(x)Ga(1-x)As active detecting layer
[DE90-003452] N90-15786
ALUMINUM GRAPHITE COMPOSITES
Damping characteristics of metal matrix composites
[AD-A213712] N90-15151
ALUMINUM OXIDES
Surface engineering by high energy beams
[DE90-001296] N90-15250
Development of the RAIDS (Remote Atmospheric and Ionospheric Detector System) extreme ultraviolet wedge and strip detector
[AD-A213730] N90-15495
AMBIENCE
Wind speed dependence of acoustic ambient vertical directional spectra at high frequency
[AD-A214293] N90-15712
AMERICIUM
Magnetic behavior of curium and americium-curium alloys
[DE89-017808] N90-15213
AMMONIUM NITRATES
Properties and thermal decomposition of the double salts of uranyl nitrate-ammonium nitrate
[DE89-004909] N90-15287
AMMONIUM PERCHLORATES
Using small scale tests to estimate the failure diameter of a propellant
[DE90-001166] N90-15281
AMORPHOUS MATERIALS
Dynamical structure of liquid and amorphous metals
[DE90-003805] N90-15229
Metal film coatings on amorphous metallic alloys
[AD-D014308] N90-15240
Epoxy-resin cable terminations
[AD-A213789] N90-15454
Research on amorphous silicon-germanium alloys for tandem solar cells
[DE89-009436] N90-15499
Proceedings of the Latin American Conference on the Applications of the Moessbauer Effect
[DE90-600819] N90-15803
AMORPHOUS SILICON
Instability of a-Si:H/Ag interface at 150 deg C
[DE89-009419] N90-15498
Research on high-efficiency, single-junction, monolithic, thin-film amorphous silicon solar cells, phase 1
[DE89-009495] N90-15502
Research on high-efficiency, single-junction, monolithic, thin-film amorphous silicon solar cells, phase 2
[DE89-009496] N90-15503
AMPLIFICATION
Enhancement of microchannel plate gain by deposition of CsI on the channel walls
[DE90-003051] N90-15334
ANAEROBES
Effect of community structure on the kinetics of anaerobic degradation of aromatic compounds
[DE90-003666] N90-15134
ANALOG TO DIGITAL CONVERTERS
The 22 GHz Radioastron receiver: Development of prototype components during the year 1988
[PB89-212583] N90-15323
ANALOGIES
A simple model for the stellar analogy of compact solar flares
[DE90-003215] N90-15877
ANALOGS
Continuum analogues of contragredient Lie algebras: Lie algebras with a Cartan operator and nonlinear dynamical systems
[DE89-635698] N90-15691
ANALYSIS (MATHEMATICS)
The kind of mathematics involved in applied superconductivity research
[DE90-003706] N90-15798
ANALYTIC GEOMETRY
Geometric considerations for a waypoint guidance method
[DE90-001803] N90-15088
ANGLE OF ATTACK
Flow visualization of the effect of pitch rate on the vortex development on the scale model of a F-18 fighter aircraft
[AD-A214244] N90-15080
ANGLES (GEOMETRY)
Some computational properties of rotation representations
[AD-A213888] N90-15665
ANGULAR MOMENTUM
Electron-positron momentum distribution measurements of high-T superconductors and related systems
[DE90-002974] N90-15780
ANGULAR RESOLUTION
Design of a large angular aperture TeO2 acousto-optic tunable filter
[AD-A213999] N90-15738
ANHYDRIDES
Novel polyimide compositions based on 4,4': Isophthaloyldiphthalic anaydride (IDPA)
[NASA-CASE-LAR-14194-1] N90-15148
Wet spinning of solid polyamic acid fibers
[NASA-CASE-LAR-14162-1] N90-15259
ANNEALING
Research on mercury cadmium telluride
[AD-A213924] N90-15237
Sintering studies on high field varistors
[DE90-002626] N90-15359
Partial reduction of re-oxidation processing of Y-Ba-Cu-O sputtered thin films
[DE90-003655] N90-15782
Processing and fabrication of YBa2Cu4O8 and YBa2Cu4O8/YBa2Cu3O(x) composites
[DE90-003559] N90-15789
Defect control and denuded trap zones in the 3-5 semiconductors
[AD-A214099] N90-15814
ANODES
Development of the RAIDS (Remote Atmospheric and Ionospheric Detector System) extreme ultraviolet wedge and strip detector
[AD-A213730] N90-15495
ANOMALIES
Research on mercury cadmium telluride
[AD-A213924] N90-15237
ANTARCTIC REGIONS
Antarctic surface temperature and pressure data
[DE90-000971] N90-15565
ANTENNA ARRAYS
Proceedings of the Antenna Applications Symposium, volume 2
[AD-A213815] N90-15313
High resolution imaging by phase retrieval and discrimination using speckle, volume 1
[AD-A214243] N90-15317
Focal plane antenna array for millimeter waves
[AD-D014306] N90-15322
Investigation of broadband microstrip antenna structures for application in monolithic millimeter wave arrays
[AD-A213856] N90-15344
Scannable millimeter wave arrays, volume 1
[AD-A213895] N90-15347
Scannable millimeter wave arrays, volume 2
[AD-A213896] N90-15348
Large-aperture sparse array detector system for multiple emitter location
[AD-D014303] N90-15355
Technology of fast-wave current drive antennas
[DE90-001972] N90-15747
ANTENNA COMPONENTS
Investigation of broadband microstrip antenna structures for application in monolithic millimeter wave arrays
[AD-A213856] N90-15344
ANTENNA DESIGN
Alternative techniques for some typical MIL-STD-461/462 types of measurements
[PB89-235139] N90-15302
Scannable millimeter wave arrays, volume 1
[AD-A213895] N90-15347
Scannable millimeter wave arrays, volume 2
[AD-A213896] N90-15348
Technology of fast-wave current drive antennas
[DE90-001972] N90-15747
ANTENNA FEEDS
Scannable millimeter wave arrays, volume 1
[AD-A213895] N90-15347
Scannable millimeter wave arrays, volume 2
[AD-A213896] N90-15348
ANTENNA RADIATION PATTERNS
Proceedings of the Antenna Applications Symposium, volume 2
[AD-A213815] N90-15313
ANTENNAS
Polarimetric SAR antenna characterization
[AD-A213438] N90-15306
Proceedings of the Antenna Applications Symposium, volume 2
[AD-A213815] N90-15313
Technology of fast-wave current drive antennas
[DE90-001972] N90-15747
ANTIFERROMAGNETISM
Further studies on possible coexistence of antiferromagnetism and superconductivity in 2D Heisenberg model
[DE90-601082] N90-15783
ANTIICING ADDITIVES
Flight and wind tunnel investigation of aerodynamic effects of aircraft ground deicing/antiicing fluids
[AD-A214243] N90-15064
ANTIMISSILE DEFENSE
High resolution imaging by phase retrieval and discrimination using speckle, volume 1
[AD-A214243] N90-15317
ANTINEUTRINOS
First results from the MACRO (Monopole, Astrophysics, Cosmic Ray Observatory) detector at the Gran Sasso Laboratory
[DE90-003243] N90-15858
ANTIPROTONS
LEAP: A balloon-borne search for low-energy cosmic ray antiprotons N90-15878
APERTURES
Design of a large angular aperture TeO2 acousto-optic tunable filter
[AD-A213999] N90-15738
APPLICATIONS PROGRAMS (COMPUTERS)
Transverse (through-the-thickness) shear stiffnesses of fibre reinforced composite laminated plates (computer program)
[ESDU-89013] N90-15152
Analysis of an elastohydrodynamic lubricated point contact: User's manual
[AD-A214257] N90-15459
APPROXIMATION
Quasi interpolants and approximation power of multivariate splines
[AD-A213535] N90-15678
An improved toeplitz approximation method
[AD-A213994] N90-15688
Optimization of stochastic systems via simulation
[AD-A214011] N90-15689
A structural factoring approach for analyzing probabilistic networks N90-15697
AQUEOUS SOLUTIONS
Dimensional analysis of continuous high-capacity electrodispersion of aqueous based liquids in an organic continuous phase
[DE90-003714] N90-15136
ARC SPRAYING
Improved process for HIP canning of composites
[NASA-CASE-LEW-14990-1-CU] N90-15147
Arc-sprayed coatings for electromagnetic pulse protection: Assessment of physical and electrical properties
[AD-A213825] N90-15275
ARC WELDING
The effect of nitrogen and titanium on the toughness of high strength saw weld deposits
[AD-A213400] N90-15230
Submerged arc welding consumables for HSLA (High Strength Low Alloy)-100 steel
[AD-A213433] N90-15452
ARCHITECTURE (COMPUTERS)
Autonomous land navigation in a structured environment
[DE90-001625] N90-15087
NOISE: A nonlinear optimization induction free-electron laser systems engineering code
[DE90-004438] N90-15420
Sensor integration using concurrent computing on-board the ORNL mobile robot
[DE89-008740] N90-15436
A semiautomated computer-interactive dynamic impact testing system
[DE90-002721] N90-15479
An architectural model of visual motion understanding
[AD-A214327] N90-15589
Designing machines for lattice physics and algorithm investigation
[DE90-003543] N90-15596
ARGOS (A Research GMMP Operating System): Overvie w and interfaces
[AD-A213871] N90-15599
The implementation of a coherent memory abstraction on a NUMA (Non-Uniform Memory Access) multiprocessor: Experiences with PLATINUM (Platform for Investigating Non-Uniform Memory)
[AD-A213909] N90-15600
Memory management for large-scale NUMA (Non-Uniform Memory Access) multiprocessors
[AD-A213910] N90-15601
An overview of PLATINUM: A Platform for Investiga ting Non-Uniform Memory (preliminary version)
[AD-A213911] N90-15602
Evolution of an operating system for large-scale shared-memory multiprocessors
[AD-A213912] N90-15603
Reconfigurable N-dimensional computer memory
[AD-D014309] N90-15607

High level language memory management on parallel architectures
[DE89-015018] N90-15609
An efficient UNICOS run-time system for functional programs on a CRAY X-MP
[DE89-016603] N90-15610
Elicitation of natural language representations of uncertainty using computer technology
[DE90-001416] N90-15611
Transport modeling and advanced computer techniques
[DE90-001481] N90-15612
Name assignment techniques for relational schemas representing extended entity-relationship schemas
[DE90-003269] N90-15623
Programs for control of an analog-signal switching network
[DE90-003645] N90-15626
Optical neural nets for scene analysis
[AD-A213986] N90-15637
MASC: Multiprocessor architecture for symbolic processing
[AD-A213504] N90-15656
One-class generalization in second-order backpropagation networks for image classification
[DE89-015845] N90-15661
Systolic algorithms for imaging from space
[AD-A213870] N90-15701
Upgrade plans to handle 30 to 40 Mbytes of data for D3-D
[DE90-003291] N90-15750
Procurement of an optical disk information storage and retrieval system
[DE90-001372] N90-15849
Data file management in the D3-D data acquisition and analysis computer systems
[DE90-003289] N90-15850

ARCTIC REGIONS
A compact acoustic recorder
[AD-A213581] N90-15403

ARITHMETIC
Ultra high performance, highly reliable, numeric intensive processors and systems
[AD-A214100] N90-15659

ARIZONA
Winter cloud seeding potential on the Mogollon Rim
[PB89-190540] N90-15562

ARMOR
Stand-off shields for hypervelocity particles
[DE89-016182] N90-15437
Comparison of multidimensional calculations of long-rod impacts on oblique plates
[DE89-015275] N90-15440

AROMATIC COMPOUNDS
High temperature chemistry of aromatic hydrocarbons
[DE90-003664] N90-15133
Effect of community structure on the kinetics of anaerobic degradation of aromatic compounds
[DE90-003666] N90-15134

ARRIVALS
Queues with negative arrivals
[AD-A213860] N90-15687

ARTIFICIAL INTELLIGENCE
Automation and robotics in construction: Japanese research and development
[AD-A214170] N90-15456
An architectural model of visual motion understanding
[AD-A214327] N90-15589
Understanding developments in computer technology: A pragmatic and synthetic interpretation N90-15608
Optical neural nets for scene analysis
[AD-A213986] N90-15637
Tools for simulation-based training
[AD-A214307] N90-15646
MASC: Multiprocessor architecture for symbolic processing
[AD-A213504] N90-15656
Some computational properties of rotation representations
[AD-A213888] N90-15665
Gaze controls with interactions and delays
[AD-A214286] N90-15667
Automated observation scheduling for the VLT
[NASA-CR-186282] N90-15861
Artificial intelligence approaches to astronomical observation scheduling
[NASA-CR-186277] N90-15862
Automated telescope scheduling
[NASA-CR-186279] N90-15863

ASIA
Responding to the threat of global warming: Options for the Pacific and Asia
[DE90-003553] N90-15539

ASPHALT
Design temperatures for flexible airfield pavement design
[AD-A214141] N90-15115

ASSAYING
ROBOCAL (Robotic Calorimetry): An automated NDA (Nondestructive Assay) calorimetry and gamma isotopic system
[DE90-003217] N90-15168

ASSESSMENTS
Safety evaluation report for Galileo, volume 2
[DE90-003087] N90-15123
An assessment and comparison of fuel cells for transportation applications
[DE90-001807] N90-15508

ASTEROID BELTS
Dust bands in the asteroid belt
[NASA-CR-186301] N90-15873

ASTEROIDS
The volatile composition of comets
[NASA-CR-186281] N90-15871
Dust bands in the asteroid belt
[NASA-CR-186301] N90-15873

ASTRONOMICAL MODELS
Near-infrared polarimetry and spectroscopy of comets N90-15857
Laboratory simulations of the solar wind-comet interactions N90-15875

ASTRONOMICAL OBSERVATORIES
The South African Astronomical Observatory
[NASA-CR-186258] N90-15856

ASTRONOMICAL SPECTROSCOPY
Near-infrared polarimetry and spectroscopy of comets N90-15857

ASTRONOMY
Artificial intelligence approaches to astronomical observation scheduling
[NASA-CR-186277] N90-15862

ASTROPHYSICS
Astophysical opacities at LLNL
[DE90-003599] N90-15872
Space operations: Listing of NASA scientific missions, 1980-2000. Fact sheet for the Chairman, Subcommittee on Space Science and Applications, Committee on Science, Space, and Technology, House of Representatives
[AD-A213493] N90-15881

ASYMMETRY
Products of the hypochlorite oxidation of hydrazine fuels
[AD-A213557] N90-15291

ASYMPTOTIC SERIES
Strong large deviation and local limit theorems
[AD-A213610] N90-15698

ATMOSPHERIC ATTENUATION
MODTRAN: A moderate resolution model for LOWTRAN 7
[AD-A214337] N90-15650

ATMOSPHERIC BOUNDARY LAYER
Dynamics of baroclinic instability in rapid cyclogenesis N90-15563

ATMOSPHERIC CHEMISTRY
Long-term worldwide environmental effects caused by acid rain from fossil fuels
[DE90-001534] N90-15533
HCl monitor, phase 2
[AD-A213572] N90-15542
Oxygen and other atmospheric gases
[AD-A214296] N90-15557
NO2 photodissociation dynamics
[AD-A214422] N90-15560
Anomalous absorption by atmospheric water vapor and stabilized water fogs in the infrared and CM-wave regions
[AD-A214202] N90-15572
MODTRAN: A moderate resolution model for LOWTRAN 7
[AD-A214337] N90-15650

ATMOSPHERIC CIRCULATION
Beryllium dispersion near explosive firing tables: A comparison of computed and observed results
[DE90-002635] N90-15550

ATMOSPHERIC COMPOSITION
Factors that may influence responses of the US transportation sector to policies for reducing greenhouse gas emissions
[DE90-000704] N90-15543
Oxygen and other atmospheric gases
[AD-A214296] N90-15557
The middle Martian atmosphere N90-15874

ATMOSPHERIC EFFECTS
Flight in Adverse Environmental Conditions
[AGARD-CP-470] N90-15041
Adverse weather operations during the Canadian Atlantic storms program N90-15052

ATMOSPHERIC GENERAL CIRCULATION MODELS
Research project on CO2-induced climate change
[DE90-003531] N90-15538

ATMOSPHERIC MODELS
Description of atmospheric turbulence N90-15043
A methodology for evaluating heavy gas dispersion models
[AD-A214009] N90-15131
Application of a mass-consistent wind model to chinook windstorms
[AD-A213622] N90-15568
MODTRAN: A moderate resolution model for LOWTRAN 7
[AD-A214337] N90-15650
A calculation of energetic proton spectra producedat substorm onset in the fields of the explosive reconnection model N90-15866
The middle Martian atmosphere N90-15874

ATMOSPHERIC MOISTURE
Dynamics of baroclinic instability in rapid cyclogenesis N90-15563
Anomalous absorption by atmospheric water vapor and stabilized water fogs in the infrared and CM-wave regions
[AD-A214202] N90-15572

ATMOSPHERIC PHYSICS
Description of SHARC: The Strategic High-Altitude Radiance Code
[AD-A213806] N90-15555
Oxygen and other atmospheric gases
[AD-A214296] N90-15557
Anomalous absorption by atmospheric water vapor and stabilized water fogs in the infrared and CM-wave regions
[AD-A214202] N90-15572
MODTRAN: A moderate resolution model for LOWTRAN 7
[AD-A214337] N90-15650

ATMOSPHERIC SCATTERING
A methodology for evaluating heavy gas dispersion models
[AD-A214009] N90-15131

ATMOSPHERIC SOUNDING
Identification and quantification of synoptic structure in simulated Tiros N radiance soundings N90-15546
Identification and quantification of synoptic structure in simulated TIROS N radiance soundings
[AD-A213729] N90-15553

ATMOSPHERIC STRATIFICATION
Flux parameterization techniques in the atmospheric surface layer N90-15548

ATMOSPHERIC TURBULENCE
Description of atmospheric turbulence N90-15043

ATOMIC STRUCTURE
Exchange coupling in metals as understood then and now
[DE90-001271] N90-15214
Phase transition in polymer blends and structure of ionomers
[DE90-003525] N90-15266
Band-to-band transitions in poly (phenyl methyl silane)
[DE90-003575] N90-15720
Relativistic self-consistent field studies of atoms and molecules
[AD-A214101] N90-15724
Theoretical studies on the electronic structure of high-temperature superconductors
[DE90-001301] N90-15771
Variational quantum Monte Carlo calculation of electronic and structural properties of crystals
[DE90-003265] N90-15781
Magnetic and electronic correlations in YBa2Cu3O(sub 6+x)
[DE89-017604] N90-15785
Magnetic mechanisms of high temperature superconductivity
[DE90-003625] N90-15796
X ray absorption studies of YBa2Cu3O(6+x), La(2-x)Sr(x)CuO4, and Nd(2-x)Ce(x)CuO4
[DE90-003640] N90-15797
Atomic scale structure of twin boundary in Y-Ba-Cu-O superconductors
[DE90-003955] N90-15823

ATOMIZING
Fundamental mechanism of atomization
[AD-A213859] N90-15293

ATOMS
Observation of atomic relaxation near an interface through detection of emitted fluorescence
[AD-A214308] N90-15725

ATTENTION
The role of attention in visual processing
[AD-A214158] N90-15588

ATTITUDE (INCLINATION)
Thermal analysis of fixed and tilting pad journal bearings including cross-film viscosity variations and deformations N90-15429
AUGER SPECTROSCOPY
Auger and x ray absorption studies of solid molecular oxygen
[DE90-003966] N90-15825
AUGMENTATION
Enhancement of microchannel plate gain by deposition of CsI on the channel walls
[DE90-003051] N90-15334
AURORAL ARCS
A high spatial resolution study of the thermospheric response to a discrete auroral arc
[NASA-TM-102904] N90-15559
AUSTENITIC STAINLESS STEELS
An investigation of the sensitization behavior of Fe-Mn-Cr austenitic steels
[DE90-002719] N90-15226
Fusion reactor materials
[DE90-000976] N90-15744
AUTOMATA THEORY
Time bounds for real-time process control in the presence of timing uncertainty
[AD-A213791] N90-15633
Using mappings to prove timing properties
[AD-A213967] N90-15666
AUTOMATIC CONTROL
Automated convection soldering
[KCP-613-4005] N90-15300
Computer controlled MHD power consolidation and pulse-generation system
[DE90-001224] N90-15662
AUTONOMOUS NAVIGATION
Autonomous land navigation in a structured environment
[DE90-001625] N90-15087
Research in knowledge-based vision techniques for the Autonomous Land Vehicle Program
[AD-A213440] N90-15453
Planning systems for autonomous legged vehicles
[AD-A214242] N90-15458
AVAILABILITY
A simulation model for dynamic system availability analysis
[AD-A213499] N90-15628
AVALANCHES
Avalanche photoconductive switching
[DE90-002980] N90-15337
AVIATION METEOROLOGY
Description of atmospheric turbulence N90-15043
AVIATION PSYCHOLOGY
Model for measuring complex performance in an aviation environment
[DE90-002055] N90-15585
AVIONICS
Aircraft testing in the electromagnetic environment N90-15066
AXES OF ROTATION
Some computational properties of rotation representations
[AD-A213888] N90-15665
AXISYMMETRIC FLOW
A numerical model for the axisymmetric equilibrium shape of drops in uniform motion: Effects of external flow, electric field and surface charge N90-15071

B

BACKGROUND RADIATION
The disk-halo connection and the nature of the interstellar medium
[NASA-CR-186286] N90-15860
Gravitational lens effect on the cosmic background radiation due to nonlinear inhomogeneities
[DE90-701753] N90-15868
BACKSCATTERING
N-port theory applied to backscatter polarimetry and depolarization in foliage penetration
[AD-A213437] N90-15305
Flashlight radar: A three-dimensional imaging radar
[AD-A213439] N90-15307
BACKWARD FACING STEPS
An algebraic turbulence model for flow separation caused by forward and backward facing steps
[AD-A213800] N90-15389
BACTERIOLOGY
Effect of community structure on the kinetics of anaerobic degradation of aromatic compounds
[DE90-003666] N90-15134
BAFFLES
Design of DIII-D advanced divertor
[DE90-003343] N90-15752
BAINITIC STEEL
Deformation and fracture of low alloy steels at high temperature
[DE90-001274] N90-15215
BALANCE
A procedure for force-balancing planar linkages using counterweights
[ESDU-89028] N90-15446
BALL BEARINGS
Fully articulated four-point-bend loading fixture
[NASA-CASE-LEW-14776-1] N90-15445
BALLAST (MASS)
Schleicher ASK-21 glider (TG-9) stall and spin
[AD-A213513] N90-15096
BALLOON-BORNE INSTRUMENTS
LEAP: A balloon-borne search for low-energy cosmic ray antiprotons N90-15878
BALLOONING MODES
Destabilization of tokamak pressure-gradient driven instabilities by energetic alpha populations
[DE90-003716] N90-15756
BANDWIDTH
Ultra high performance, highly reliable, numeric intensive processors and systems
[AD-A214100] N90-15659
Research in optical interconnection techniques
[AD-A214028] N90-15739
BARIUM OXIDES
Partial reduction of re-oxidation processing of Y-Ba-Cu-O sputtered thin films
[DE90-003655] N90-15782
Magnetic and electronic correlations in YBa2Cu3O(sub 6+x)
[DE89-017604] N90-15785
Magnetic flux pinning in YBa2Cu3O7 films
[DE90-003709] N90-15799
Cu-O chains in YBa2Cu3O(7-delta) and the phonon mechanism of high-Tc superconductivity
[DE90-603502] N90-15805
Atomic scale structure of twin boundary in Y-Ba-Cu-O superconductors
[DE90-003955] N90-15823
BAROCLINIC INSTABILITY
Dynamics of baroclinic instability in rapid cyclogenesis N90-15563
BARRIER LAYERS
High temperature, flexible, thermal barrier seal
[NASA-CASE-LEW-14672-1] N90-15444
BATCH PROCESSING
Adaptive control of helicopter vibrations via the impulse response method
[AD-A213728] N90-15113
Polynomial transfer lot sizing techniques for batch processing on consecutive machines
[AD-A214198] N90-15660
BAYES THEOREM
An iterative Bayes procedure for reliability assessment
[DE90-002106] N90-15466
Recurrence and ergodicity for exponential family state-space models
[AD-A213466] N90-15677
BAYS (STRUCTURAL UNITS)
Onorbit electron beam welding experiment definition
[NASA-CR-183847] N90-15431
BEAM INJECTION
Simulation of radial expansion of an electron beam injected into a background plasma
[NASA-CR-186188] N90-15743
Intense REB (Relativistic Electron Beam) transport in a weakly magnetized plasma
[DE90-002978] N90-15749
BEAM INTERACTIONS
Aerosol heating and vaporization of high-flux laser beams
[DE90-003471] N90-15428
BEAMS (RADIATION)
Canonical formalism for coupled beam optics
[DE90-003764] N90-15734
Optical guiding by plasma waves in the plasma beat wave accelerator
[AD-A214288] N90-15763
BEHAVIOR
A structured connectionist approach to direct inferences and figurative adjective-noun combinations
[AD-A214326] N90-15649
BEND TESTS
Mechanical behavior of laminated composites at elevated temperatures N90-15141
BENDING THEORY
Effects of aeroelastic tailoring on anisotropic composite material beam models of helicopter blades
[AD-A213478] N90-15095
BERYLLIUM
Beryllium dispersion near explosive firing tables: A comparison of computed and observed results
[DE90-002635] N90-15550
BERYLLIUM ALLOYS
Nickel beryllides and their properties
[DE90-001736] N90-15220
BETA PARTICLES
Cosmic ray half life of (54)Mn
[DE90-000134] N90-15880
BETATRONS
Anharmonic betatron motion in free electron lasers
[DE90-001515] N90-15407
A microwiggler Free-Electron Laser at the Brookhaven Accelerator Test Facility
[DE90-003643] N90-15418
BIBLIOGRAPHIES
Aeronautical engineering: A continuing bibliography with indexes (supplement 246)
[NASA-SP-7037(246)] N90-15068
Cockpit resource management: A selected annotated bibliography
[AD-A214272] N90-15594
Bibliography of Lewis Research Center technical publications announced in 1988
[NASA-TM-102034] N90-15846
NASA patent abstracts bibliography: A continuing bibliography. Section 1: Abstracts (supplement 36)
[NASA-SP-7039(36)-SECT-1] N90-15851
BIOCHEMISTRY
Capillary electrophoresis ionization-mass spectrometry and tandem mass spectrometry
[DE90-002664] N90-15158
Introduction to extremely-low-frequency electric and magnetic fields
[DE90-002662] N90-15578
BIOCONVERSION
The Third Pacific Basin Biofuels Workshop: Proceedings
[DE90-002523] N90-15513
BIODEGRADATION
Effect of community structure on the kinetics of anaerobic degradation of aromatic compounds
[DE90-003666] N90-15134
The Third Pacific Basin Biofuels Workshop: Proceedings
[DE90-002523] N90-15513
BIOLOGICAL EFFECTS
Introduction to extremely-low-frequency electric and magnetic fields
[DE90-002662] N90-15578
BIOMASS
Utilization of non-conventional systems for conversion of biomass to food components
[NASA-CR-177545] N90-15591
BIOMASS ENERGY PRODUCTION
The Third Pacific Basin Biofuels Workshop: Proceedings
[DE90-002523] N90-15513
BIPOLAR TRANSISTORS
Defect control and denuded trap zones in the 3-5 semiconductors
[AD-A214099] N90-15814
BISMUTH COMPOUNDS
Synthesis conductivity, and x ray photoelectron spectrum of Bi2Sr2Cu(sub 7+x). A new ternary bismuth-oxide system exhibiting metallic conductivity
[DE90-003010] N90-15778
BLOOD
Carboxyalkylated hemoglobin as a potential blood substitute
[AD-A213886] N90-15582
BLOOD CIRCULATION
Monitoring chaos of cardiac rhythms
[DE90-000692] N90-15580
BODY CENTERED CUBIC LATTICES
Energetics of BCC-FCC lattice deformation in iron
[AD-A213801] N90-15233
BODY KINEMATICS
Spatial dynamics of deformable multibody systems with variable kinematic structure
[AD-A214098] N90-15455
BODY-WING CONFIGURATIONS
An experimental study of the time-dependent behavior of the appendage-body junction vortex
[AD-A213465] N90-15384
BOILING
Radial heat flux limits in potassium heat pipes: An experimental and analytical investigation
[DE90-002655] N90-15396
BOLTZMANN DISTRIBUTION
Brownian trail rectified
[DE90-003339] N90-15706
BOMBER AIRCRAFT
Proposed activities to prepare for testing advanced/stealth weapons systems
[AD-A214453] N90-15321
BORIDES
Preparation and properties of icosahedral borides
[DE90-003574] N90-15180

BORON CARBIDES
Preparation and properties of icosahedral borides
[DE90-003574] N90-15180
BORON PHOSPHIDES
Preparation and properties of icosahedral borides
[DE90-003574] N90-15180
BOUNDARY ELEMENT METHOD
Development of an integrated BEM approach for hot fluid structure interaction
[NASA-CR-186214] N90-15364
Solution of potential flow past an elastic body using the boundary element technique
[AD-A213843] N90-15390
BOUNDARY LAYER PLASMAS
Propulsion research on the hybrid plume rocket
[AD-A214420] N90-15132
BOUNDARY LAYER SEPARATION
Experimental measurements of the laminar separation bubble on an Eppler 387 airfoil at low Reynolds numbers
[NASA-CR-186263] N90-15380
An algebraic turbulence model for flow separation caused by forward and backward facing steps
[AD-A213800] N90-15389
Computation of broadband mixing noise from turbomachinery
[AD-A214448] N90-15713
BOUNDARY LAYER TRANSITION
On strongly nonlinear vortex/wave interactions in boundary-layer transition
[NASA-CR-181963] N90-15078
Numerical investigation of transition control of a flat plate boundary layer N90-15361
BOUNDARY LAYERS
Numerical investigation of transition control of a flat plate boundary layer N90-15361
BOUNDARY VALUE PROBLEMS
A direct-inverse method for transonic and separated flows about airfoils
[NASA-CR-4270] N90-15072
Numerical simulation of the unsteady two-dimensional flow in a time-dependent doubly-connected domain N90-15073
Guidance analysis of the aeroglide plane change maneuver as a turning point problem
[NASA-TM-101639] N90-15110
New transient algorithms for non-Newtonian flows
[AD-A213494] N90-15385
Research in mathematics and computer science at Argonne
[DE90-000975] N90-15595
On functional integral representations in the lower Hubbard band based on generalized coherent states
[DE90-602936] N90-15804
BRANCHING (MATHEMATICS)
Introduction to bifurcation theory
[DE90-003319] N90-15673
Nonlinear maps with competitive interactions: Fixed-points, bifurcations, and chaotic attractors
[DE90-001858] N90-15695
BRAYTON CYCLE
Design study of a modular gas-cooled, closed-brayton cycle reactor for marine use
[AD-A213453] N90-15518
BREEDER REACTORS
Microstructural evolution of martensitic steels during fast neutron irradiation
[DE89-016231] N90-15212
Fusion reactor materials
[DE90-000976] N90-15744
BRIDGMAN METHOD
Bridgman crystal growth
[NASA-CR-186204] N90-15766
BRILLOUIN EFFECT
SBS (Stimulated Brillouin Scattering) pulse distortion in multimode optical fibers: Preliminary results
[DE90-003023] N90-15731
BRILLOUIN ZONES
Optical phonon modes in a double heterostructure of polar crystals
[AD-A214208] N90-15816
BRITTLENESS
The mechanical behavior of a fiber-reinforced brittle matrix composite N90-15139
BROADBAND
Computation of broadband mixing noise from turbomachinery
[AD-A214448] N90-15713
Near-infrared polarimetry and spectroscopy of comets N90-15857
BROADCASTING
Research in optical interconnection techniques
[AD-A214028] N90-15739
BROMINATION
Brominated graphitized carbon fibers
[NASA-CASE-LEW-14698-2] N90-15262
BROMINE
Brominated graphitized carbon fibers
[NASA-CASE-LEW-14698-2] N90-15262
Rapidity densities and their fluctuations in central 200 A GeV S32 interations with Au and Ag,Br nuclei
[LUIP-8905] N90-15715
BROWNIAN MOVEMENTS
Brownian trail rectified
[DE90-003339] N90-15706
A diffusion on a fractal state space
[AD-A213555] N90-15707
BUBBLES
Experimental measurements of the laminar separation bubble on an Eppler 387 airfoil at low Reynolds numbers
[NASA-CR-186263] N90-15380
BURNING RATE
Calculation of Einstein A coefficients and oscillator strengths for the A(perturbed)(2)A(1)-X(perturbed)(2)B(1) transition of NH(2)
[AD-A213837] N90-15176
Burning rates of two cast nitramine explosives using a hybrid closed bomb-strand burner
[DE90-002785] N90-15286
BUTT JOINTS
The effect of nitrogen and titanium on the toughness of high strength saw weld deposits
[AD-A213400] N90-15230
BUTTERFLY VALVES
Comments on compressible flow through butterfly valves
[DE89-015730] N90-15371
Hybrid butterfly valve
[NASA-CASE-SSC-00004] N90-15443

C

CALCULUS OF VARIATIONS
Variational quantum Monte Carlo calculation of electronic and structural properties of crystals
[DE90-003265] N90-15781
CALIBRATING
Design and calibration of an in-stack, low-pressure impactor
[AD-A213531] N90-15105
N-port theory applied to backscatter polarimetry and depolarization in foliage penetration
[AD-A213437] N90-15305
Flashlight radar: A three-dimensional imaging radar
[AD-A213439] N90-15307
Calibration of seven-hole pressure probes for use in fluid flows with large angularity
[NASA-TM-102200] N90-15399
Portable digital pressure indicator for calibrating magnetic tape recorders
[NASA-TM-101650] N90-15401
Image enhancement using the IRAS (Infrared Astronomy Satellite) survey data
[AD-A213811] N90-15496
Outlier detection in multivariate calibration
[DE90-001502] N90-15672
CALORIMETERS
ROBOCAL (Robotic Calorimetry): An automated NDA (Nondestructive Assay) calorimetry and gamma isotopic system
[DE90-003217] N90-15168
The digital data acquisition chain and the cosmic ray trigger system for the SLD warm iron calorimeter
[DE90-000943] N90-15879
CAMBER
The maximum lift coefficient of plain wings at subsonic speeds
[ESDU-89034] N90-15082
CAMERAS
Sensor integration using concurrent computing on-board the ORNL mobile robot
[DE89-008740] N90-15436
CANADA
Adverse weather operations during the Canadian Atlantic storms program N90-15052
CANARD CONFIGURATIONS
Canard versus aft-tail ride qualities performance and pilot command response N90-15053
CANCELLATION
Adaptive canceller limitations caused by I,Q mismatch errors
[AD-A214287] N90-15318
CANCER
Elicitation of natural language representations of uncertainty using computer technology
[DE90-001416] N90-15611
CANONICAL FORMS
Canonical formalism for coupled beam optics
[DE90-003764] N90-15734
On functional integral representations in the lower Hubbard band based on generalized coherent states
[DE90-602936] N90-15804
CANS
Improved process for HIP canning of composites
[NASA-CASE-LEW-14990-1-CU] N90-15147
CAPACITORS
Advanced double layer capacitor
[AD-A213406] N90-15341
CAPILLARY TUBES
Ceramic heat pipe wick
[NASA-CASE-GSC-13199-1] N90-15261
CARBIDES
The effects of Mo2C morphology and strain distribution on the fatigue properties of Fe-C-Mo dual-phase steels N90-15210
CARBON DIOXIDE
Rayleigh-Taylor instability in compressible fluids
[DE90-003027] N90-15376
Research project on CO2-induced climate change
[DE90-003531] N90-15538
Responding to the threat of global warming: Options for the Pacific and Asia
[DE90-003553] N90-15539
CARBON DIOXIDE CONCENTRATION
Greenhouse gases: Changing the global climate
[DE90-002788] N90-15535
Factors that may influence responses of the US transportation sector to policies for reducing greenhouse gas emissions
[DE90-000704] N90-15543
CARBON FIBERS
Brominated graphitized carbon fibers
[NASA-CASE-LEW-14698-2] N90-15262
CARBONATES
Molten carbonate fuel cell technology improvement
[DE90-001934] N90-15501
Oxygen electrode in molten carbonate fuel cells
[DE90-002871] N90-15510
Characterization of new cathode materials for molten carbonate fuel cells
[DE90-003547] N90-15516
CARBONYL COMPOUNDS
Polyimides with carbonyl and ether connecting groups between the aromatic rings
[NASA-CASE-LAR-14001-1] N90-15260
CARBOXYLATION
Carboxyalkylated hemoglobin as a potential blood substitute
[AD-A213886] N90-15582
CARCINOGENS
Elicitation of natural language representations of uncertainty using computer technology
[DE90-001416] N90-15611
CARDIOVASCULAR SYSTEM
Monitoring chaos of cardiac rhythms
[DE90-000692] N90-15580
CAST ALLOYS
Magnesium alloy technology for aerospace applications N90-15209
Cast stainless steel aging: Mechanisms and predictions
[DE90-003772] N90-15241
CASTING
Magnesium alloy technology for aerospace applications N90-15209
Fabrication of superconductor coils
[DE90-003571] N90-15338
CATALYSIS
Electronic materials high-T(sub c) superconductivity polymers and composites structural materials surface science and catalysts industry participation
[NASA-CR-186063] N90-15145
Interfacial systems for photochemical energy conversion
[DE90-003181] N90-15514
CATALYSTS
Correlations between surface structure and catalytic activity/selectivity
[DE90-003755] N90-15181
New polymers made with well-characterized organometallic catalysts
[AD-A213592] N90-15272
Survey on synthesis technologies of methanol as an alternative fuel
[DE89-901303] N90-15284
Analysis of catalytically enhanced solar absorption chemical reactors: 1 - numerical model description
[DE89-014742] N90-15505
CATHODES
Characterization of new cathode materials for molten carbonate fuel cells
[DE90-003547] N90-15516
CATIONS
Cation disordering in the Tl-2122 superconductors
[DE90-003579] N90-15795

Superconductivity and stoichiometry in Tl2Ca2Ba2Cu3O(x) single crystals
[DE90-003838] N90-15801

CAVITY RESONATORS
Review of quasi-optical gyrotron development
[AD-A213491] N90-15402

CENTRAL PROCESSING UNITS
Ultra high performance, highly reliable, numeric intensive processors and systems
[AD-A214100] N90-15659

CENTRIFUGES
VIBRAFUGE: Combined vibration and centrifuge testing
[DE90-001091] N90-15114

CERAMIC MATRIX COMPOSITES
The mechanical behavior of a fiber-reinforced brittle matrix composite N90-15139
Effects of filament-matrix interfaces on the mechanical properties of SiC-reinforced Si3N4: A review
[DE90-001863] N90-15144

CERAMICS
Critical and subcritical crack-growth behavior along toughened ceramic/metal interfaces N90-15140
Electronic materials high-T(sub c) superconductivity polymers and composites structural materials surface science and catalysts industry participation
[NASA-CR-186063] N90-15145
Laser mixing of titanium on silicon carbide
[DE90-003216] N90-15150
Processing and properties of nanophase oxides
[DE90-003826] N90-15171
Surface modification of metals by ion beams
[DE90-001285] N90-15218
Solid-state phase equilibria in the ZnS-Ga2S3 system
[AD-A213944] N90-15238
Potential applications of structural ceramic composites in gas turbines
[DE90-001273] N90-15248
Ceramic powder characterization
[DE90-001282] N90-15249
Surface engineering by high energy beams
[DE90-001296] N90-15250
Ceramic technology for advanced heat engines project
[DE90-001852] N90-15251
Solid lubrication of ceramic surfaces by IAD (Ion-Assisted Deposition)-silver coatings for heat engine applications
[DE90-002860] N90-15253
Crack tip toughening by inclusions with pairs of shear transformations
[DE89-007845] N90-15254
Predicting the performance of ceramic filters by the use of silt density index
[DE90-001316] N90-15256
Ceramic heat pipe wick
[NASA-CASE-GSC-13199-1] N90-15261
Ceramic processing using inorganic polymers
[DE90-003638] N90-15268
Development of NMR (Nuclear Magnetic Resonance) imaging probes for advanced ceramics
[DE90-003812] N90-15269
IEA/Annex 2 powder characterization cooperative program
[AD-A213540] N90-15271
Composite ceramic superconducting wires for electric motor applications
[AD-A213742] N90-15274
Hardening and toughening of ZnS-Ga2S3 ceramics by solid-state reactions
[AD-A213875] N90-15276
Silver coated superconducting ceramic powder
[AD-D014300] N90-15278
Toughening behavior and interfacial properties of fiber-reinforced ceramic composites
[DE89-015351] N90-15279
Development of glass-ceramic lasers
[AD-A214146] N90-15423
Fabrication of porous ceramic electrode structures
[DE90-003548] N90-15517
Characterization of MOCVD (Metal Organic Chemical Vapor Deposition) grown epitaxial ceramic oxide thin films
[DE90-003561] N90-15790
Proceedings of the Latin American Conference on the Applications of the Moessbauer Effect
[DE90-600819] N90-15803
High-temperature ceramic superconductors
[AD-A214251] N90-15818

CESIUM IODIDES
Enhancement of microchannel plate gain by deposition of CsI on the channel walls
[DE90-003051] N90-15334

CHANNEL FLOW
Gelled propellant flow: Boundary layer theory for power-law fluids in a converging planar channel
[DE90-000923] N90-15365
Experimental determination of the fluid velocity by spectral analysis of temperature fluctuations
[DE89-636430] N90-15372

CHAOS
Hamiltonian chaos in a nonlinear polarized optical beam
[DE90-002437] N90-15408
Monitoring chaos of cardiac rhythms
[DE90-000692] N90-15580

CHARACTERISTICS
Fabrication characteristics of 8090 alloy N90-15198

CHARACTERIZATION
Characterization of chemicals on engine exhaust particles
[AD-A213566] N90-15106
Ceramic powder characterization
[DE90-001282] N90-15249
Simultaneous thermal analysis techniques for characterization of energetic materials
[DE90-003028] N90-15289
Polarimetric SAR antenna characterization
[AD-A213438] N90-15306
Advanced double layer capacitor
[AD-A213406] N90-15341
Comprehensive, nonintercepting electron-beam diagnostics using spontaneous emission
[DE90-003211] N90-15414
Characteristics of electromagnetic wave forms with lightning in winter season
[DE89-901256] N90-15567

CHARGE CARRIERS
Magnetic mechanisms of high temperature superconductivity
[DE90-003625] N90-15796
Defect control and denuded trap zones in the 3-5 semiconductors
[AD-A214099] N90-15814

CHARGE DISTRIBUTION
A numerical model for the axisymmetric equilibrium shape of drops in uniform motion: Effects of external flow, electric field and surface charge N90-15071

CHARGE EFFICIENCY
Membrane and durability studies for the zinc/bromine battery
[DE89-016181] N90-15324

CHARGE TRANSFER
New organic synthetic metals derived from BEDT-TTF, Ni(dsit)2 and BEDO-TTF
[DE90-003793] N90-15242
Phonons and charge-transfer excitations in HTS superconductors
[DE89-016616] N90-15768

CHARGED PARTICLES
Near-surface sputtered particle transport for an oblique incidence magnetic field plasma
[DE90-004422] N90-15758

CHARPY IMPACT TEST
Cast stainless steel aging: Mechanisms and predictions
[DE90-003772] N90-15241
A semiautomated computer-interactive dynamic impact testing system
[DE90-002721] N90-15479

CHEMICAL ANALYSIS
Capillary electrophoresis ionization-mass spectrometry and tandem mass spectrometry
[DE90-002664] N90-15158
Development of a robotics system for automated chemical analysis of sediment, sludges, and soils
[DE90-003637] N90-15170
The effect of nitrogen and titanium on the toughness of high strength saw weld deposits
[AD-A213400] N90-15230
Electrochemical investigation of electronically conductive polymers
[AD-A214019] N90-15277
Properties and thermal decomposition of the double salts of uranyl nitrate-ammonium nitrate
[DE89-004909] N90-15287

CHEMICAL BONDS
The production and spectroscopy of molecular ions isolated in solid neon
[AD-A213723] N90-15174
Cu-O chains in YBa2Cu3O(7-delta) and the phonon mechanism of high-Tc superconductivity
[DE90-603502] N90-15805

CHEMICAL COMPOSITION
Novel polyimide compositions based on 4,4': Isophthaloyldiphthalic anaydride (IDPA)
[NASA-CASE-LAR-14194-1] N90-15148
Orthobaric densities and molar volumes of liquids: Alcohols
[ESDU-89037] N90-15184
Superplastic performance and properties of the Lital Alloys N90-15199
Magnetic viscosity in Ni/Cu compositionally-modulated alloys
[DE90-002303] N90-15223
The effect of dissolved chlorine on the pitting behavior of 304L stainless steel in a 0.5 N NaCl solution
[AD-A213803] N90-15234
The effect of dissolved ozone on the corrosion behavior of Cu-30 Ni and 304L stainless steel in 0.5 N NaCl solutions
[AD-A213804] N90-15235
Thermal stability of jet fuel
[DE90-002760] N90-15288
The volatile composition of comets
[NASA-CR-186281] N90-15871

CHEMICAL EFFECTS
Studies of the adsorption/desorption behavior of explosive-like molecules
[DE90-001867] N90-15283

CHEMICAL PROPERTIES
Properties of aluminum-uranium alloys
[DE90-003889] N90-15243

CHEMICAL REACTIONS
The dissociation energy of N2
[NASA-TM-101930] N90-15153
The behavior of matter under nonequilibrium conditions: Fundamental aspects and applications
[DE90-002522] N90-15157
Theoretical methods for the study of chemical dynamics
[DE90-003122] N90-15160
Dynamics of electron transfer for a nonsuperexchange coherent mechanism, 1
[AD-A213450] N90-15721

CHEMICAL REACTORS
Analysis of catalytically enhanced solar absorption chemical reactors. 2: Predicted characteristics of a 100 kW chemical reactor
[DE89-014743] N90-15521

CHEMISORPTION
Excitation lifetimes and excited-state forces in chemisorbed molecules
[DE90-002578] N90-15165
Chemisorption under stress
[AD-A213785] N90-15175

CHLORINE
The effect of dissolved chlorine on the pitting behavior of 304L stainless steel in a 0.5 N NaCl solution
[AD-A213803] N90-15234

CHLORINE COMPOUNDS
Products of the hypochlorite oxidation of hydrazine fuels
[AD-A213557] N90-15291

CHLOROCARBONS
Evaluate and characterize mechanisms controlling transport, fate, and effects of army smokes in the aerosol wind tunnel: Transport, transformations, fate, and terrestrial ecological effects of hexachloroethane obscurant smokes
[DE90-002923] N90-15536

CHOLESKY FACTORIZATION
Software for a new modified Cholesky factorization
[AD-A213643] N90-15630

CHROMIUM
Development of glass-ceramic lasers
[AD-A214146] N90-15423
Spectroscopic and laser properties of Cr:LiCaAlF6 and Cr:LiSrAlF6 crystals
[DE90-000783] N90-15770

CHROMIUM ALLOYS
Deformation and fracture of low alloy steels at high temperature
[DE90-001274] N90-15215
An investigation of the sensitization behavior of Fe-Mn-Cr austenitic steels
[DE90-002719] N90-15226

CHROMIUM STEELS
Microstructural evolution of martensitic steels during fast neutron irradiation
[DE89-016231] N90-15212

CHRONOLOGY
The age of the galactic disk
[NASA-CR-186292] N90-15869

CIRCUITS
Tuned-circuit Johnson noise thermometry
[DE89-016221] N90-15356

CIRCULAR WAVEGUIDES
Rectangular-to-circular waveguide transitions for high-power circular overmoded waveguides
[AD-A213925] N90-15349

CIVIL AVIATION
Cockpit resource management: A selected annotated bibliography
[AD-A214272] N90-15594
CLADDING
Report of the Advanced Neutron Source (ANS) Aluminum Cladding Corrosion Workshop
[DE90-001281] N90-15217
CLASSIFICATIONS
Classification of windshear severity N90-15049
Design and calibration of an in-stack, low-pressure impactor
[AD-A213531] N90-15105
A logic for the pixel assignment step of imagery classification predicated on class structure N90-15493
CLASSIFIERS
A logic for the pixel assignment step of imagery classification predicated on class structure N90-15493
CLEAR AIR TURBULENCE
Analysis of severe atmospheric disturbances from airline flight records N90-15045
CLIMATE
Antarctic surface temperature and pressure data
[DE90-000971] N90-15565
CLIMATE CHANGE
Greenhouse gases: Changing the global climate
[DE90-002788] N90-15535
Research project on CO2-induced climate change
[DE90-003531] N90-15538
Global climate change and NEPA (National Environmental Policy Act) analyses
[DE90-003704] N90-15540
Global climate change: A fossil energy perspective
[DE90-003770] N90-15541
CLIMATOLOGY
Measurements of horizontal visibility in the lowest 300 m over Northern Germany N90-15053
Global climate change: A fossil energy perspective
[DE90-003770] N90-15541
CLINICAL MEDICINE
DOCTORD Database System user's guide, June 1989: dBase 3 PLUS Physician/(Part B Medicare): Personal computer reference system and user's guide
[PB90-100181] N90-15579
CLOCKS
Periodic phase adjustment distributed clock synchronization in the hard realtime environment
[AD-A213842] N90-15708
CLOSED ECOLOGICAL SYSTEMS
Utilization of non-conventional systems for conversion of biomass to food components
[NASA-CR-177545] N90-15591
CLOSURE LAW
Development of a three-dimensional local scale atmospheric model with turbulence closure model
[DE90-710045] N90-15551
CLOSURES
Observational study of the macroscopic behavior of moist-convective processes N90-15547
CLOUD COVER
Global distribution of total cloud cover and cloud type amounts over the ocean
[DE90-003187] N90-15574
CLOUD PHYSICS
Winter cloud seeding potential on the Mogollon Rim
[PB89-190540] N90-15562
CLOUD SEEDING
Winter cloud seeding potential on the Mogollon Rim
[PB89-190540] N90-15562
CLOUDS (METEOROLOGY)
Adverse weather operations during the Canadian Atlantic storms program N90-15052
Global distribution of total cloud cover and cloud type amounts over the ocean
[DE90-003187] N90-15574
CLUSTER ANALYSIS
Fast algorithms for estimating mixture parameters
[AD-A213869] N90-15636
COASTS
Precipitation distributions associated with cyclones originating over the Gulf of Mexico and surrounding coastal regions
[AD-A213644] N90-15569
COATING
High-temperature ceramic superconductors
[AD-A214251] N90-15818
COCKPIT SIMULATORS
Cockpit resource management: A selected annotated bibliography
[AD-A214272] N90-15594
COCKPITS
Imaging probabilities, geometry and ergonomics in limited visibility helicopter operations N90-15060
See and avoid/cockpit visibility
[AD-A214214] N90-15084
Task-oriented display design: Concept and example
[NASA-TM-101685] N90-15101
Display interface concepts for automated fault diagnosis
[NASA-TM-101610] N90-15102
COGNITION
Numerical facility: Convergence of cognitive and factor analytic models
[AD-A213627] N90-15680
COHERENT LIGHT
Excimer emission from alkali diatomic and alkaline-earth-noble-gas molecules
[AD-A214246] N90-15179
COHESION
Determination of flow-regime boundaries for cohesive particles
[DE90-001405] N90-15369
COLD PLASMAS
Strategic characteristics of Dynamics Explorer 1 retarding ion mass spectrometer and the consequences for core plasma measurements
[AD-A214013] N90-15125
COLD WELDING
Microstructure/mechanical property relations in a mechanically alloyed aluminum N90-15205
COLLISION AVOIDANCE
See and avoid/cockpit visibility
[AD-A214214] N90-15084
COLLISIONLESS PLASMAS
Single fluid simulations of plasma openings switch behavior
[DE90-002643] N90-15330
COLLISIONS
Dust bands in the asteroid belt
[NASA-CR-186301] N90-15873
COLOR
Near-infrared polarimetry and spectroscopy of comets N90-15857
COMBUSTIBLE FLOW
Combustion characteristics of sprays
[AD-A213651] N90-15173
Development of an integrated BEM approach for hot fluid structure interaction
[NASA-CR-186214] N90-15364
COMBUSTION EFFICIENCY
Steady flow combustion model for solid-fuel ramjet projectiles
[BRL-TR-2987] N90-15163
Factors that may influence responses of the US transportation sector to policies for reducing greenhouse gas emissions
[DE90-000704] N90-15543
COMBUSTION PRODUCTS
Characterization of chemicals on engine exhaust particles
[AD-A213566] N90-15106
Spectral studies of solid propellant combustion. 2: Emission and absorption results for M-30 and HMX1 propellants
[AD-A213857] N90-15292
Long-term worldwide environmental effects caused by acid rain from fossil fuels
[DE90-001534] N90-15533
Global climate change: A fossil energy perspective
[DE90-003770] N90-15541
HCl monitor, phase 2
[AD-A213572] N90-15542
COMET NUCLEI
The volatile composition of comets
[NASA-CR-186281] N90-15871
COMETARY ATMOSPHERES
Near-infrared polarimetry and spectroscopy of comets N90-15857
The volatile composition of comets
[NASA-CR-186281] N90-15871
COMETS
Dust bands in the asteroid belt
[NASA-CR-186301] N90-15873
Laboratory simulations of the solar wind-comet interactions N90-15875
COMMERCE
Program manager's handbook
[AD-A214338] N90-15844
COMMERCIAL AIRCRAFT
International Aircraft Occupant Safety Conference and Workshop proceedings
[AD-A214452] N90-15085
COMMINUTION
Dust bands in the asteroid belt
[NASA-CR-186301] N90-15873
COMMUNICATION
Technical communications in aeronautics: Results of an exploratory study. An analysis of profit managers' and nonprofit managers' responses
[NASA-TM-101626] N90-15848
COMMUNICATION EQUIPMENT
Baseband development system implementation
[AD-A213464] N90-15309
COMMUNICATION NETWORKS
Network simulator definition
[AD-A213463] N90-15308
Voice/data integration in mobile radio networks: Overview and future research directions
[AD-A214289] N90-15319
COMMUNICATION SATELLITES
SLCSAT (Submarine Laser Communication Satellite) communication system design study
[AD-A213403] N90-15304
COMPACTING
Ceramic processing using inorganic polymers
[DE90-003638] N90-15268
COMPARATORS
Characteristics of CMOS analog integrated structures using MOSIS (Metal Oxide Semiconductor Implementation System)
[DE90-001630] N90-15773
COMPILERS
The StarLite project
[AD-A214193] N90-15642
COMPLEMENTS (MATHEMATICS)
A basic theorem of complementarity for the generalized variational-like inequality problem
[DE90-003102] N90-15620
COMPONENT RELIABILITY
A study of variable geometry in advanced gas turbines N90-15104
COMPOSITE MATERIALS
Effects of lightning on operations of aerospace vehicles N90-15065
Empirical and analytical determination of the fracture resistance of a TiB2 particle/SiC matrix composite
[NASA-TM-101940] N90-15143
Composite activities at Lawrence Livermore National Laboratory
[DE90-002979] N90-15149
Potential applications of structural ceramic composites in gas turbines
[DE90-001273] N90-15248
A future for LLNL (Lawrence Livermore National Laboratory) research in composite high explosives
[DE90-004442] N90-15290
COMPOSITE PROPELLANTS
Spectral studies of solid propellant combustion. 2: Emission and absorption results for M-30 and HMX1 propellants
[AD-A213857] N90-15292
COMPOSITE STRUCTURES
Improved process for HIP canning of composites
[NASA-CASE-LEW-14990-1-CU] N90-15147
New Light Alloys
[AGARD-CP-444] N90-15185
High performance powder metallurgy aluminum alloys: An overview N90-15204
Proceedings of the 1988 Structural Integrity Program Conference
[AD-A213545] N90-15486
COMPRESSIBLE FLOW
Irreversible processes from reversible mechanics
[DE90-001057] N90-15368
Comments on compressible flow through butterfly valves
[DE89-015730] N90-15371
COMPRESSIBLE FLUIDS
Rayleigh-Taylor instability in compressible fluids
[DE90-003027] N90-15376
COMPRESSION LOADS
Short fibre and particulate reinforced metal matrix composites N90-15207
COMPRESSOR ROTORS
An experimental, analytical, and computational investigation of turbomachinery rotor flow fields N90-15360
COMPUTATION
Enhanced resolution concepts in large scale scientific computing
[AD-A214095] N90-15393
Portable digital pressure indicator for calibrating magnetic tape recorders
[NASA-TM-101650] N90-15401
Multi-dimensional modeling of convective heat transfer with application to I.C. engines
[DE90-003245] N90-15451
Calculation of source and structure parameters at regional and teleseismic distances
[AD-A214297] N90-15558
Specification for evaporation duct height calculations
[AD-A213841] N90-15570
A paradigm for robust geometric algorithms
[AD-A214324] N90-15647

Hierarchical process composition: Dynamic maintenance of structure in a distributed environment [AD-A214325] N90-15648
MASC: Multiprocessor architecture for symbolic processing [AD-A213504] N90-15656

COMPUTATIONAL FLUID DYNAMICS
Unsteady aerodynamics of oscillating and rapidly pitched airfoils N90-15074
Finite difference techniques and rotor blade aeroelastic partial differential equations with quasisteady aerodynamics N90-15075
Hypersonic nozzle design [NASA-CR-186261] N90-15077
Spatially-resolved, nonintrusive measurements in a nonreacting scramjet combustor using laser-induced iodine fluorescence N90-15103
Explicit and implicit calculations of turbulent cavity flows with and without yaw angle [NASA-CR-186293] N90-15381
Research in mathematics and computer science at Argonne [DE90-000975] N90-15595

COMPUTATIONAL GRIDS
Mesh refinement in finite element analysis by minimization of the stiffness matrix trace [NASA-CR-185170] N90-15434

COMPUTER AIDED DESIGN
Aircraft performance enhancement with active compressor stabilization [AD-A213652] N90-15097
Computer aided design of monolithic microwave and millimeter wave integrated circuits and subsystems [AD-A213656] N90-15343
An executive system for modeling with rational b-splines [AD-A213460] N90-15627
A paradigm for robust geometric algorithms [AD-A214324] N90-15647

COMPUTER ASSISTED INSTRUCTION
Development of the AH-64 display symbology training module [AD-A213456] N90-15592
Tools for simulation-based training [AD-A214307] N90-15646

COMPUTER GRAPHICS
Vision in dynamic environments [AD-A213434] N90-15587
An architectural model of visual motion understanding [AD-A214327] N90-15589
LLNL's plan for a prototype circuit switch, a potential gigabit LAN of the future [DE90-003614] N90-15597
Scry: A distributed image handling system, version 1.1 [DE90-003105] N90-15621
Name assignment techniques for relational schemas representing extended entity-relationship schemas [DE90-003269] N90-15623
An executive system for modeling with rational b-splines [AD-A213460] N90-15627
A renormalization group approach to image processing: A new computational method for three-dimensional shapes in robot vision, and the computation complexity of the cooling algorithms [AD-A214247] N90-15643
Some computational properties of rotation representations [AD-A213888] N90-15665

COMPUTER INFORMATION SECURITY
On the privacy problems involved in allowing access to computers via the public telephone system [RSRE-88006] N90-15303

COMPUTER NETWORKS
On the privacy problems involved in allowing access to computers via the public telephone system [RSRE-88006] N90-15303
Temporal, processor, and spatial locality in multiprocessor memory references [AD-A213790] N90-15598
Scry: A distributed image handling system, version 1.1 [DE90-003105] N90-15621
Programs for control of an analog-signal switching network [DE90-003645] N90-15626
On the correctness of orphan management algorithms [AD-A213777] N90-15632
Neural network models for linear programming [DE89-015974] N90-15651
A neural network for bounded linear programming [DE89-015975] N90-15652
A multichannel processing approach to real time network detection, phase association, and threshold monitoring [AD-A213940] N90-15657
Adaptive backoff synchronization techniques [AD-A213966] N90-15658
One-class generalization in second-order backpropagation networks for image classification [DE89-015845] N90-15661
Upgrade plans to handle 30 to 40 Mbytes of data for D3-D [DE90-003291] N90-15750
Data file management in the D3-D data acquisition and analysis computer systems [DE90-003289] N90-15850

COMPUTER PROGRAMMING
Fatigue behavior of vertical axis wind turbine airfoils with two weld configurations [DE90-002628] N90-15525
Paralation views: Abstractions for efficient scientific computing on the connection machine [AD-A213935] N90-15604
Utilization of a PC for finite element modeling [AD-A214173] N90-15605
Scry: A distributed image handling system, version 1.1 [DE90-003105] N90-15621
An executive system for modeling with rational b-splines [AD-A213460] N90-15627
The StarLite project [AD-A214193] N90-15642
A structured connectionist approach to direct inferences and figurative adjective-noun combinations [AD-A214326] N90-15649
Investigation of the applicability of a functional programming model to fault-tolerant parallel processing for knowledge-based systems [NASA-CR-181938] N90-15654

COMPUTER PROGRAMS
Systems for airborne wind and turbulence measurement N90-15046
Nonlinear phenomena in computational transonic aeroelasticity N90-15070
A study of variable geometry in advanced gas turbines N90-15104
Design and calibration of an in-stack, low-pressure impactor [AD-A213531] N90-15105
Design limitations on ultra-high velocity projectile launchers [DE89-012933] N90-15118
Research on mercury cadmium telluride [AD-A213924] N90-15237
Automated convection soldering [KCP-613-4005] N90-15300
Rectangular-to-circular waveguide transitions for high-power circular overmoded waveguides [AD-A213925] N90-15349
Solution of potential flow past an elastic body using the boundary element technique [AD-A213843] N90-15390
Geotechnical instrumentation [PB89-198675] N90-15398
Implementing fault-tolerant sensors [NASA-CR-186251] N90-15400
Waveguide effects in superradiant free-electron lasers [DE90-003605] N90-15417
NOISE: A nonlinear optimization induction free-electron laser systems engineering code [DE90-004438] N90-15420
MESA 3-D calculations of armor penetration by projectiles with combined obliquity and yaw [DE89-015265] N90-15438
Comparison of multidimensional calculations of long-rod impacts on oblique plates [DE89-015275] N90-15440
Fragmentation statistics from Eulerian hydrocode calculations [DE90-002906] N90-15449
Planning minimum-energy paths in an off-road environment with anisotropic traversal costs and motion constraints [AD-A214181] N90-15457
A semiautomated computer-interactive dynamic impact testing system [DE90-002721] N90-15479
Pipeline vibrations. Fluid transients in non-rigid, unbranched planar piping systems [ESDU-89030] N90-15491
Inclusion of nonlinear aerodynamics in the FLAP code [DE89-009507] N90-15519
Description of SHARC: The Strategic High-Altitude Radiance Code [AD-A213806] N90-15555
Development of the AH-64 display symbology training module [AD-A213456] N90-15592
MANPRINT methods monograph: Aiding the development of manned system performance criteria [AD-A213543] N90-15593
Designing machines for lattice physics and algorithm investigation [DE90-003543] N90-15596
High level language memory management on parallel architectures [DE89-015018] N90-15609
CryoTran user's manual, version 1.0 [NASA-TM-102468] N90-15622
Developmental versions of FORTRAN/77 routines for the design and analysis of mixture experiments [DE90-003513] N90-15624
Programs for control of an analog-signal switching network [DE90-003645] N90-15626
A simulation model for dynamic system availability analysis [AD-A213499] N90-15628
Software for a new modified Cholesky factorization [AD-A213643] N90-15630
Optical neural nets for scene analysis [AD-A213986] N90-15637
Principles and algorithms for causal reasoning with uncertainty [AD-A214248] N90-15644
MODTRAN: A moderate resolution model for LOWTRAN 7 [AD-A214337] N90-15650
Use of the linear variate method of Monte Carlo for estimating uncertainty in thermal-hydraulic codes [DE89-017871] N90-15694
The calculation of overground sound propagation in the presence of wind and temperature gradients [ESDU-89036] N90-15714
Theoretical studies on the electronic structure of high-temperature superconductors [DE90-001301] N90-15771
Automated observation scheduling for the VLT [NASA-CR-186282] N90-15861
Automated telescope scheduling [NASA-CR-186279] N90-15863
Astophysical opacities at LLNL [DE90-003599] N90-15872

COMPUTER STORAGE DEVICES
New devices using ferroelectric thin films [DE90-000789] N90-15328
Temporal, processor, and spatial locality in multiprocessor memory references [AD-A213790] N90-15598
Adaptive backoff synchronization techniques [AD-A213966] N90-15658
Bounded polynomial randomized consensus [AD-A213808] N90-15686

COMPUTER SYSTEMS DESIGN
Understanding developments in computer technology: A pragmatic and synthetic interpretation N90-15608
Elicitation of natural language representations of uncertainty using computer technology [DE90-001416] N90-15611

COMPUTER SYSTEMS PERFORMANCE
Integrated approach fault tolerance-current state and future requirements [AD-A214402] N90-15485
LLNL's plan for a prototype circuit switch, a potential gigabit LAN of the future [DE90-003614] N90-15597
Temporal, processor, and spatial locality in multiprocessor memory references [AD-A213790] N90-15598
ARGOS (A Research GMMP Operating System): Overvie w and interfaces [AD-A213871] N90-15599
Simulating the scheduling of parallel supercomputer applications [DE90-003604] N90-15655
One-class generalization in second-order backpropagation networks for image classification [DE89-015845] N90-15661
Alternative representations for database responses N90-15847

COMPUTER SYSTEMS PROGRAMS
Autonomous land navigation in a structured environment [DE90-001625] N90-15087

COMPUTER TECHNIQUES
Vision in dynamic environments [AD-A213434] N90-15587
XNUSIM: Graphical interface for a multiprocessor simulator [AD-A214176] N90-15606
Name assignment techniques for relational schemas representing extended entity-relationship schemas [DE90-003269] N90-15623
Studies of quantitative methods for imaging from scattered fields [AD-A214047] N90-15638

Guidelines for evaluating energy analysis software
[AD-A214171] N90-15640
Polynomial transfer lot sizing techniques for batch processing on consecutive machines
[AD-A214198] N90-15660
Periodic phase adjustment distributed clock synchronization in the hard realtime environment
[AD-A213842] N90-15708

COMPUTER VISION
Component presence-absence detection for automated visual inspection of hybrid microcircuits
[KCP-613-4050] N90-15335
Research in knowledge-based vision techniques for the Autonomous Land Vehicle Program
[AD-A213440] N90-15453
Vision in dynamic environments
[AD-A213434] N90-15587
A renormalization group approach to image processing: A new computational method for three-dimensional shapes in robot vision, and the computation complexity of the cooling algorithms
[AD-A214247] N90-15643
Gaze controls with interactions and delays
[AD-A214286] N90-15667

COMPUTERIZED SIMULATION
Numerical simulation of the unsteady two-dimensional flow in a time-dependent doubly-connected domain N90-15073
A study of variable geometry in advanced gas turbines N90-15104
The behavior of matter under nonequilibrium conditions: Fundamental aspects and applications
[DE90-002522] N90-15157
Interaction of hydrogen in palladium as prescribed by the embedded atom method
[DE90-003893] N90-15244
More efficient sensitivity testing
[DE90-002639] N90-15298
High resolution imaging by phase retrieval and discrimination using speckle, volume 1
[AD-A214243] N90-15317
Single fluid simulations of plasma openings switch behavior
[DE90-002643] N90-15330
Explicit and implicit calculations of turbulent cavity flows with and without yaw angle
[NASA-CR-186293] N90-15381
Waveguide effects in superradiant free-electron lasers
[DE90-003605] N90-15417
Numerical analysis and simulation of frictional particle systems N90-15430
Hydrodynamics code calculations of debris clouds produced by ball-plate impacts
[DE89-015270] N90-15439
Comparison of multidimensional calculations of long-rod impacts on oblique plates
[DE89-015275] N90-15440
Fragmentation statistics from Eulerian hydrocode calculations
[DE90-002906] N90-15449
Planning systems for autonomous legged vehicles
[AD-A214242] N90-15458
Beryllium dispersion near explosive firing tables: A comparison of computed and observed results
[DE90-002635] N90-15550
Antarctic surface temperature and pressure data
[DE90-000971] N90-15565
Further research on dynamics of marine atmospheres in tropical cyclones
[AD-A213882] N90-15571
The components of scientific visualization
[DE90-001992] N90-15614
Knowledge representations for the automatic generation of numerical simulators for PDEs
[DE89-008036] N90-15615
CryoTran user's manual, version 1.0
[NASA-TM-102468] N90-15622
A simulation model for dynamic system availability analysis
[AD-A213499] N90-15628
The StarLite project
[AD-A214193] N90-15642
Tools for simulation-based training
[AD-A214307] N90-15646
Simulating the scheduling of parallel supercomputer applications
[DE90-003604] N90-15655
Optimization of stochastic systems via simulation
[AD-A214011] N90-15689
Simulation of radial expansion of an electron beam injected into a background plasma
[NASA-CR-186188] N90-15743
Computer simulation of laser plasma interaction
[DE90-002828] N90-15748
Theoretical and computational studies of magnetic insulation and other plasma-opening-switch phenomena
[DE90-004421] N90-15757
Progress in LTE and non-LTE transport calculations
[DE90-003394] N90-15764
A signal realization data base generated by the multiple phase-screen method
[AD-A214004] N90-15852
A simple model for the stellar analogy of compact solar flares
[DE90-003215] N90-15877

COMPUTERS
Automation and robotics in construction: Japanese research and development
[AD-A214170] N90-15456
Understanding developments in computer technology: A pragmatic and synthetic interpretation N90-15608

CONCENTRATION (COMPOSITION)
The effect of dissolved chlorine on the pitting behavior of 304L stainless steel in a 0.5 N NaCl solution
[AD-A213803] N90-15234

CONCURRENT PROCESSING
Concurrence control for transactions with priorities
[NASA-CR-186241] N90-15699

CONDENSATES
Reflux condensation in vertical tubes
[ESDU-89038] N90-15397

CONDENSATION
Heat transfer in condensation of lithium vapors
[DE90-002081] N90-15375

CONDENSERS (LIQUEFIERS)
Reflux condensation in vertical tubes
[ESDU-89038] N90-15397

CONDENSING
Processing and properties of nanophase oxides
[DE90-003826] N90-15171
Recent advances in magnetic heat pump technology
[DE89-013289] N90-15370

CONDUCTING POLYMERS
Novel high-rate, all solid-state, sodium and lithium/organosulfur batteries
[DE90-001014] N90-15325

CONFERENCES
Flight in Adverse Environmental Conditions
[AGARD-CP-470] N90-15041
International Aircraft Occupant Safety Conference and Workshop proceedings
[AD-A214452] N90-15085
New Light Alloys
[AGARD-CP-444] N90-15185
Proceedings of the Antenna Applications Symposium, volume 2
[AD-A213815] N90-15313
Proceedings of the 1988 Structural Integrity Program Conference
[AD-A213545] N90-15486
Acid rain research
[DE90-003283] N90-15537
Responding to the threat of global warming: Options for the Pacific and Asia
[DE90-003553] N90-15539
Ada 9X project report. Revision request report
[AD-A213503] N90-15629
The 17th AINSE Plasma Physics Conference: Conference handbook
[DE90-600936] N90-15759
Proceedings of the Latin American Conference on the Applications of the Moessbauer Effect
[DE90-600819] N90-15803
The age of the galactic disk
[NASA-CR-186292] N90-15869

CONFIGURATION INTERACTION
The dissociation energy of N2
[NASA-TM-101930] N90-15153

CONFINEMENT
Structure properties of confined systems. Hard spheres between ideal walls
[DE90-600818] N90-15378

CONGESTION
Adaptive backoff synchronization techniques
[AD-A213966] N90-15658

CONICAL BODIES
A coning motion apparatus for hydrodynamic model testing in a non-planar cross-flow
[AD-A213431] N90-15383

CONJUGATE GRADIENT METHOD
Gradient projection techniques for large-scale optimization problems
[DE90-001986] N90-15618

CONSOLIDATION
Computer controlled MHD power consolidation and pulse-generation system
[DE90-001224] N90-15662

CONSTITUTIVE EQUATIONS
Development of a rate independent plasticity theory for general cyclic loading N90-15471
Ductile failure
[AD-A213864] N90-15488

CONSTRUCTION
Geotechnical instrumentation
[PB89-198675] N90-15398

CONSUMABLES (SPACECREW SUPPLIES)
Utilization of non-conventional systems for conversion of biomass to food components
[NASA-CR-177545] N90-15591

CONTAINMENT
Selection of phase-change and containment materials for thermal energy storage
[NASA-CR-186228] N90-15506

CONTINUUM MECHANICS
Damage evaluation from surface displacement data N90-15469

CONTINUUMS
Continuum analogues of contragredient Lie algebras: Lie algebras with a Cartan operator and nonlinear dynamical systems
[DE89-635698] N90-15691

CONTRACT MANAGEMENT
Congressional involvement and relations: A guide for Department of Defense acquisition managers
[AD-A214408] N90-15855

CONTRAST
The assessment of visibility from automatic contrast Measurements N90-15061
Effect of contrast on the perception of direction of a moving pattern
[NASA-TM-102234] N90-15577

CONTROL SIMULATION
Planning systems for autonomous legged vehicles
[AD-A214242] N90-15458

CONTROL SURFACES
Numerical investigation of transition control of a flat plate boundary layer N90-15361

CONTROL SYSTEMS DESIGN
Effect of modal truncation on derivatives of closed-loop damping ratios in structural control N90-15109
Fly-by-light flight control system technology development plan
[NASA-CR-181953] N90-15111
On the privacy problems involved in allowing access to computers via the public telephone system
[RSRE-88006] N90-15303
Implementing fault-tolerant sensors
[NASA-CR-186251] N90-15400
Control of mechanical manipulators N90-15432
A semiautomated computer-interactive dynamic impact testing system
[DE90-002721] N90-15479
Concurrence control for transactions with priorities
[NASA-CR-186241] N90-15699

CONTROL THEORY
A pitch control law for compensation of the phugoid mode induced by windshears N90-15051
The interference of flightmechanical control laws with those of load alleviation and its influence on structural design N90-15054
Adaptive control of helicopter vibrations via the impulse response method
[AD-A213728] N90-15113
Control of mechanical manipulators N90-15432
The application of optimal control theory for analysis of human jumping and pedaling N90-15590
On the identification of local minimizers in inertia-controlling methods for quadratic programming
[DE89-017330] N90-15616
Optimal periodic control and regulator theory based on the second variation N90-15704

CONTROLLERS
Effect of modal truncation on derivatives of closed-loop damping ratios in structural control N90-15109
A versatile stepping motor controller for systems with many motors
[DE90-001556] N90-15327
Tuned-circuit Johnson noise thermometry
[DE89-016221] N90-15356
Architectural study of the design and operation of advanced force feedback manual controllers
[NASA-CR-185948] N90-15664

CONVECTION
Observational study of the macroscopic behavior of moist-convective processes N90-15547

CONVECTION CURRENTS
Vertical distribution of pollutants in the presence of convective storms
[DE90-002590] N90-15549

CONVECTIVE HEAT TRANSFER
Automated convection soldering
[KCP-613-4005] N90-15300
Multi-dimensional modeling of convective heat transfer with application to I.C. engines
[DE90-003245] N90-15451

Analysis of catalytically enhanced solar absorption chemical reactors. 2: Predicted characteristics of a 100 kW chemical reactor
[DE89-014743] N90-15521

CONVERGENCE
Effect of modal truncation on derivatives of closed-loop damping ratios in structural control N90-15109
Sequential quadratic programming algorithms for optimization
[DE90-000022] N90-15617
Mixed singular linear elliptic equations
[DE90-600722] N90-15674

COOLING
Retractable gas cooled leads for ASTROMAG
[DE90-002679] N90-15331
High power density spray cooling
[AD-A213575] N90-15386
Design and fabricate a metallic hydride heat pump with a cooling capacity of 9000 BTU/H
[AD-A213756] N90-15388
A renormalization group approach to image processing: A new computational method for three-dimensional shapes in robot vision, and the computation complexity of the cooling algorithms
[AD-A214247] N90-15643

COPOLYMERS
Electronic and ionic transport in polymers
[AD-A213410] N90-15270
New polymers made with well-characterized organometallic catalysts
[AD-A213592] N90-15272

COPPER
Critical and subcritical crack-growth behavior along toughened ceramic/metal interfaces N90-15140
Secondary electron emission characteristics of molybdenum-masked, ion-textured OFHC copper
[NASA-TP-2967] N90-15211

COPPER ALLOYS
Magnetic viscosity in Ni/Cu compositionally-modulated alloys
[DE90-002303] N90-15223
The effect of dissolved ozone on the corrosion behavior of Cu-30 Ni and 304L stainless steel in 0.5 N NaCl solutions
[AD-A213804] N90-15235
Fusion reactor materials
[DE90-000976] N90-15744

COPPER OXIDES
On the free carrier-negative U center interacting model for the high-T(sub c) oxide superconductor
[DE89-635908] N90-15775
Synthesis conductivity, and x ray photoelectron spectrum of Bi2Sr2Cu(sub 7+x). A new ternary bismuth-oxide system exhibiting metallic conductivity
[DE90-003010] N90-15778
Linear electron-hole-electron pair model of high-temperature superconductivity in La(2-x)M(x)CuO4 and YBa2Cu3O(7-y): Part 2. Dependence of the superconducting transition temperatures on pressure and on hole concentration
[DE90-003012] N90-15779
Partial reduction of re-oxidation processing of Y-Ba-Cu-O sputtered thin films
[DE90-003655] N90-15782
Magnetic and electronic correlations in YBa2Cu3O(sub 6+x)
[DE89-017604] N90-15785
Processing YBa2Cu3O(x) wires in O3/O2
[DE90-003570] N90-15794
Magnetic flux pinning in YBa2Cu3O7 films
[DE90-003709] N90-15799
Superconductivity and stoichiometry in Tl2Ca2Ba2Cu3O(x) single crystals
[DE90-003838] N90-15801
Ion-irradiation effects in Tl2Ca2Ba2Cu3O10 superconductors
[DE90-003840] N90-15802
Cu-O chains in YBa2Cu3O(7-delta) and the phonon mechanism of high-Tc superconductivity
[DE90-603502] N90-15805
Atomic scale structure of twin boundary in Y-Ba-Cu-O superconductors
[DE90-003955] N90-15823

CORES
Gas turbine regenerators: A method for selecting the optimum plate-finned surface pair for minimum core volume
[AD-A213430] N90-15382

CORONAS
The disk-halo connection and the nature of the interstellar medium
[NASA-CR-186286] N90-15860

CORRELATION
Correlations between surface structure and catalytic activity/selectivity
[DE90-003755] N90-15181
Relativistic self-consistent field studies of atoms and molecules
[AD-A214101] N90-15724

CORROSION
Report of the Advanced Neutron Source (ANS) Aluminum Cladding Corrosion Workshop
[DE90-001281] N90-15217
Niobium 1 percent zirconium/potassium and titanium/potassium life-test heat pipe design and testing
[DE90-002430] N90-15522

CORROSION RESISTANCE
Aluminum lithium alloys for Navy aircraft N90-15193
Fatigue, fracture mechanics and corrosion properties of some aluminium-lithium alloys N90-15194
The effect of dissolved ozone on the corrosion behavior of Cu-30 Ni and 304L stainless steel in 0.5 N NaCl solutions
[AD-A213804] N90-15235

COSMIC DUST
The volatile composition of comets
[NASA-CR-186281] N90-15871
Dust bands in the asteroid belt
[NASA-CR-186301] N90-15873

COSMIC RAYS
First results from the MACRO (Monopole, Astrophysics, Cosmic Ray Observatory) detector at the Gran Sasso Laboratory
[DE90-003243] N90-15858
Gravitational lens effect on the cosmic background radiation due to nonlinear inhomogeneities
[DE90-701753] N90-15868
The digital data acquisition chain and the cosmic ray trigger system for the SLD warm iron calorimeter
[DE90-000943] N90-15879

COSMOLOGY
Small scale structure on cosmic strings
[DE90-003128] N90-15867
Gravitational lens effect on the cosmic background radiation due to nonlinear inhomogeneities
[DE90-701753] N90-15868

COST ANALYSIS
A nickel/hydrogen battery for PV systems
[DE90-001537] N90-15358
Planning minimum-energy paths in an off-road environment with anisotropic traversal costs and motion constraints
[AD-A214181] N90-15457
Analysis of the financial factors governing the profitability of lunar helium-3 N90-15838

COST EFFECTIVENESS
Fly-by-light flight control system technology development plan
[NASA-CR-181953] N90-15111
A strategy for concurrent product and process design of aerospace components
[DE90-002926] N90-15299

COST ESTIMATES
A guide for estimating potential energy savings from increased solar reflectance of a low-sloped roof
[DE90-003720] N90-15526

COST REDUCTION
Aluminum-lithium: Application of plate and sheet to fighter aircraft N90-15202
IEA/Annex 2 powder characterization cooperative program
[AD-A213540] N90-15271

COTTON
Variability of cultivar responses to ozone
[PB89-225460] N90-15528

COUETTE FLOW
Comments on ER (Electrorheological) fluid rheology
[DE90-002892] N90-15166

COUNTERBALANCES
A procedure for force-balancing planar linkages using counterweights
[ESDU-89028] N90-15446

COUNTERMEASURES
Use of lower body negative pressure as a countermeasure to negative Gz acceleration
[AD-A213927] N90-15583

COUPLING
Canonical formalism for coupled beam optics
[DE90-003764] N90-15734

COVARIANCE
Error modeling of bias-type parameters for TOPEX orbit determination N90-15117
An improved toeplitz approximation method
[AD-A213994] N90-15688

CRACK INITIATION
On the domain of dominance of the asymptotic elastodynamic crack-tip fields N90-15468
Micromechanics of an extrusion in high-cycle fatigue with creep
[AD-A213509] N90-15485

CRACK PROPAGATION
Thermal mechanical fatigue of coated blade materials
[AD-A214258] N90-15107
Critical and subcritical crack-growth behavior along toughened ceramic/metal interfaces N90-15140
Fatigue properties of Al-Li alloys N90-15189
Fatigue and fracture behaviour of a PM Al-Li alloy N90-15195
Helium-induced weld cracking in irradiated 304 stainless steel
[DE90-001312] N90-15219
Guide to the selection of surface treatments for the improvement of fatigue strength of steels
[ESDU-89031] N90-15245
Crack tip toughening by inclusions with pairs of shear transformations
[DE89-007845] N90-15254
Fractal dimension of the fractured surface of materials
[DE89-635764] N90-15477
Experience with J testing of 304/308 stainless steel weldment
[DE90-002046] N90-15478
Ductile failure
[AD-A213864] N90-15488

CRACK TIPS
Crack tip toughening by inclusions with pairs of shear transformations
[DE89-007845] N90-15254
On the domain of dominance of the asymptotic elastodynamic crack-tip fields N90-15468

CRACKING (FRACTURING)
Thermal mechanical fatigue of coated blade materials
[AD-A214258] N90-15107
Microstructure/mechanical property relations in a mechanically alloyed aluminum N90-15205

CRACKS
Design temperatures for flexible airfield pavement design
[AD-A214141] N90-15115

CRASHES
International Aircraft Occupant Safety Conference and Workshop proceedings
[AD-A214452] N90-15085

CRASHWORTHINESS
International Aircraft Occupant Safety Conference and Workshop proceedings
[AD-A214452] N90-15085

CRAY COMPUTERS
An efficient UNICOS run-time system for functional programs on a CRAY X-MP
[DE89-016603] N90-15610

CREEP PROPERTIES
Micromechanics of an extrusion in high-cycle fatigue with creep
[AD-A213509] N90-15485
Effects of non-linearity in the variation of pinning potential with current-density on magnetic flux creep in high and low T(sub c) superconductors
[DE90-003952] N90-15822
Non Newtonian gravity creeping flow
[DE90-600816] N90-15828

CREEP STRENGTH
Dispersion strengthening of high temperature niobium alloys
[AD-A213829] N90-15236

CRITERIA
MANPRINT methods monograph: Aiding the development of manned system performance criteria
[AD-A213543] N90-15593

CRITICAL POINT
Orthobaric densities and molar volumes of liquids: Alcohols
[ESDU-89037] N90-15184

CRITICAL PRESSURE
Thermal conductivity of gaseous aliphatic hydrocarbons. Part 1: Alkanes
[ESDU-89035-PT-1] N90-15183

CRITICAL TEMPERATURE
Summary physical data tables: Alkanes
[ESDU-PD3] N90-15162
Thermal conductivity of gaseous aliphatic hydrocarbons. Part 1: Alkanes
[ESDU-89035-PT-1] N90-15183

CROSS FLOW
A coning motion apparatus for hydrodynamic model testing in a non-planar cross-flow
[AD-A213431] N90-15383

CROSSINGS
Higher order crossings from a parametric family of linear filters
[AD-A213427] N90-15676

CROSSLINKING
Crosslinked, flexible, low-molecular-weight polyacrylamide gels for mobility control
[DE90-000202] N90-15280

CRYOGENIC FLUIDS
CryoTran user's manual, version 1.0
[NASA-TM-102468] N90-15622
CRYOGENICS
Cryogenic mechanical properties of low density superplastic Al-Mg-Sc alloys
[DE90-002120] N90-15222
Retractable gas cooled leads for ASTROMAG
[DE90-002679] N90-15331
Analysis of ambient polar volatile organic compounds using chemical ionization-ion trap detector
[PB90-106451] N90-15529
CRYSTAL GROWTH
Electronic materials high-T(sub c) superconductivity polymers and composites structural materials surface science and catalysts industry participation
[NASA-CR-186063] N90-15145
Processing and properties of nanophase oxides
[DE90-003826] N90-15171
Research on mercury cadmium telluride
[AD-A213924] N90-15237
Development of high performance beta-SiC field-effect transistors
[AD-A213885] N90-15346
Research on amorphous silicon-germanium alloys for tandem solar cells
[DE89-009436] N90-15499
Bridgman crystal growth
[NASA-CR-186204] N90-15766
Irradition-induced grain growth: Role of dislocations
[DE90-003565] N90-15792
Phase equilibrium and crystal growth studies on AgGaSe2 and related nonlinear optical materials
[AD-A213650] N90-15809
CRYSTAL LATTICES
A diffusion on a fractal state space
[AD-A213555] N90-15707
Molecular-dynamics study of the amorphization of CuTi
[DE90-003563] N90-15791
Cation disordering in the Tl-2122 superconductors
[DE90-003579] N90-15795
High resolution electron microscopy of grain boundaries in nanophase palladium
[DE90-003823] N90-15800
Epitaxial iron films
[AD-A213551] N90-15807
Host materials for transition-metal ions
[AD-A213605] N90-15808
Atomic scale structure of twin boundary in Y-Ba-Cu-O superconductors
[DE90-003955] N90-15823
CRYSTAL STRUCTURE
Preparation and properties of icosahedral borides
[DE90-003574] N90-15180
Interaction of hydrogen in palladium as prescribed by the embedded atom method
[DE90-003893] N90-15244
Instability of a-Si:H/Ag interface at 150 deg C
[DE89-009419] N90-15498
Deformation twinning in ordered intermetallic compounds
[DE89-014779] N90-15767
Theoretical studies on the electronic structure of high-temperature superconductors
[DE90-001301] N90-15771
The possible occurrence of multi-phase behavior in the high T(sub c) superconductor YBa2Cu3O(sub x)
[DE90-002999] N90-15777
Variational quantum Monte Carlo calculation of electronic and structural properties of crystals
[DE90-003265] N90-15781
Orientation of rf-sputter-deposited MoS2 films
[ATR-89(4752)-1] N90-15784
Preparation, structure and properties of VO(sub x) and TiO2 thin films by MOCVD
[DE90-003566] N90-15793
Cation disordering in the Tl-2122 superconductors
[DE90-003579] N90-15795
Proceedings of the Latin American Conference on the Applications of the Moessbauer Effect
[DE90-600819] N90-15803
Optical phonon modes in a double heterostructure of polar crystals
[AD-A214208] N90-15816
Properties of high Tc superconducting oxides
[DE90-003792] N90-15821
CRYSTALLINITY
An investigation of mechanical behavior of crystalline solids
[DE90-003530] N90-15787
CRYSTALLIZATION
Novel polyimide compositions based on 4,4': Isophthaloyldiphthalic anaydride (IDPA)
[NASA-CASE-LAR-14194-1] N90-15148
CRYSTALS
Dynamical structure of liquid and amorphous metals
[DE90-003805] N90-15229
Energetics of BCC-FCC lattice deformation in iron
[AD-A213801] N90-15233
Laser-induced surface ablation and optical damage of ZnS crystals caused by single- and multiple-pulse laser-irradiation
[DE90-003807] N90-15419
Spectroscopic and laser properties of Cr:LiCaAlF6 and Cr:LiSrAlF6 crystals
[DE90-000783] N90-15770
CUES
Imaging probabilities, geometry and ergonomics in limited visibility helicopter operations N90-15060
CURING
Mechanistic modeling of epoxy resins
[DE89-015119] N90-15247
CURIUM
Magnetic behavior of curium and americium-curium alloys
[DE89-017808] N90-15213
CURRENT ALGEBRA
SL(2,R) current algebra in two-dimensional conformal quantum gravity
[DE90-600755] N90-15675
CURRENT DENSITY
Processing YBa2Cu3O(x) wires in O3/O2
[DE90-003570] N90-15794
Effects of non-linearity in the variation of pinning potential with current-density on magnetic flux creep in high and low T(sub c) superconductors
[DE90-003952] N90-15822
CYCLIC LOADS
Development of a rate independent plasticity theory for general cyclic loading N90-15471
CYCLOGENESIS
Dynamics of baroclinic instability in rapid cyclogenesis N90-15563
Potential vorticity in extratropical cyclones N90-15564
CYCLONES
Potential vorticity in extratropical cyclones N90-15564
Precipitation distributions associated with cyclones originating over the Gulf of Mexico and surrounding coastal regions
[AD-A213644] N90-15569
Further research on dynamics of marine atmospheres in tropical cyclones
[AD-A213882] N90-15571
CYCLOTRON RESONANCE
Propulsion research on the hybrid plume rocket
[AD-A214420] N90-15132
The 17th AINSE Plasma Physics Conference: Conference handbook
[DE90-600936] N90-15759
CYCLOTRON RESONANCE DEVICES
Review of quasi-optical gyrotron development
[AD-A213491] N90-15402
Mechanical design of the inside launch system for electron cyclotron heating in D3-D
[DE90-003292] N90-15751

D

DAMAGE
Design temperatures for flexible airfield pavement design
[AD-A214141] N90-15115
Point of view of a civil aircraft manufacturer on Al-Li alloy N90-15200
Damage evaluation from surface displacement data N90-15469
Fatigue loading history reconstruction based on the rain-flow technique
[NASA-CR-181942] N90-15482
DAMAGE ASSESSMENT
Damage evaluation from surface displacement data N90-15469
DAMPING
Effect of modal truncation on derivatives of closed-loop damping ratios in structural control N90-15109
Damping characteristics of metal matrix composites
[AD-A213712] N90-15151
DARK ADAPTATION
The assessment of visibility from automatic contrast Measurements N90-15061
A scheiner-principle vernier optometer
[AD-D014304] N90-15405
DATA ACQUISITION
Instrumentation for a facility for the test, analysis and active control of spacecraft truss structures
[AD-A213655] N90-15124
MF/HF multistatic mid-ocean radar experiments in support of SWOTHR (Surface-Wave Over-The-Horizon Radar)
[AD-A213830] N90-15314
NTES (Nuclear Test and Experimental Sciences) program laser facility for physics experiments Building 391 High Bay Option
[DE90-001795] N90-15411
Upgrade plans to handle 30 to 40 Mbytes of data for D3-D
[DE90-003291] N90-15750
Data file management in the D3-D data acquisition and analysis computer systems
[DE90-003289] N90-15850
The digital data acquisition chain and the cosmic ray trigger system for the SLD warm iron calorimeter
[DE90-000943] N90-15879
DATA BASE MANAGEMENT SYSTEMS
An expert system for quality assurance (a.k.a.) QA Express
[DE90-003887] N90-15467
Name assignment techniques for relational schemas representing extended entity-relationship schemas
[DE90-003269] N90-15623
Programs for control of an analog-signal switching network
[DE90-003645] N90-15626
Procurement of an optical disk information storage and retrieval system
[DE90-001372] N90-15849
Young Investigator's Award and distributed self-adaptive databases
[AD-A214194] N90-15854
DATA BASES
Current launch vehicle reliability practice and data base assessment. Volume 1: Executive summary and report body
[AD-A213600] N90-15121
Identification and quantification of synoptic structure in simulated TIROS N radiance soundings
[AD-A213729] N90-15553
DOCTORD Database System user's guide, June 1989: dBase 3 PLUS Physician/(Part B Medicare): Personal computer reference system and user's guide
[PB90-100181] N90-15579
Ultra high performance, highly reliable, numeric intensive processors and systems
[AD-A214100] N90-15659
Periodic phase adjustment distributed clock synchronization in the hard realtime environment
[AD-A213842] N90-15708
A signal realization data base generated by the multiple phase-screen method
[AD-A214004] N90-15852
Young Investigator's Award and distributed self-adaptive databases
[AD-A214194] N90-15854
DATA INTEGRATION
Voice/data integration in mobile radio networks: Overview and future research directions
[AD-A214289] N90-15319
DATA MANAGEMENT
Data file management in the D3-D data acquisition and analysis computer systems
[DE90-003289] N90-15850
DATA PROCESSING
Flashlight radar: A three-dimensional imaging radar
[AD-A213439] N90-15307
A multichannel processing approach to real time network detection, phase association, and threshold monitoring
[AD-A213940] N90-15657
Ultra high performance, highly reliable, numeric intensive processors and systems
[AD-A214100] N90-15659
Upgrade plans to handle 30 to 40 Mbytes of data for D3-D
[DE90-003291] N90-15750
DATA PROCESSING EQUIPMENT
Instrumentation for a facility for the test, analysis and active control of spacecraft truss structures
[AD-A213655] N90-15124
Understanding developments in computer technology: A pragmatic and synthetic interpretation N90-15608
Polynomial transfer lot sizing techniques for batch processing on consecutive machines
[AD-A214198] N90-15660
DATA SMOOTHING
Identification and quantification of synoptic structure in simulated Tiros N radiance soundings N90-15546
DATA STORAGE
Procurement of an optical disk information storage and retrieval system
[DE90-001372] N90-15849
DATA TRANSMISSION
Research in optical interconnection techniques
[AD-A214028] N90-15739

DEBRIS
Hydrodynamics code calculations of debris clouds produced by ball-plate impacts
[DE89-015270] N90-15439
Dust bands in the asteroid belt
[NASA-CR-186301] N90-15873
DECAY
Thermal and statistical properties of nuclei and nuclear systems
[DE90-000183] N90-15717
DECISION MAKING
Planning systems for autonomous legged vehicles
[AD-A214242] N90-15458
International aspects of restrictions of ozone-depleting substances
[DE90-001813] N90-15534
Model for measuring complex performance in an aviation environment
[DE90-002055] N90-15585
Where to from here. Future applications of mental models of complex performance
[DE90-002091] N90-15596
DECOMPOSITION
A novel heat resistant blend produced by compositional quenching: A thermoplastic polyimide impact modified with a fluoroelastomer
[AD-A213724] N90-15273
Simultaneous thermal analysis techniques for characterization of energetic materials
[DE90-003028] N90-15289
The parallel decomposition of linear programs
[DE90-003538] N90-15625
DECOMPRESSION SICKNESS
Potential for reduction of decompression sickness by prebreathing with 100 percent oxygen while exercising
[AD-A213449] N90-15581
DEEP SPACE
Manned spacecraft
[AD-A214218] N90-15129
DEFENSE PROGRAM
Prospects for space arms control
[DE90-003392] N90-15700
Congressional involvement and relations: A guide for Department of Defense acquisition managers
[AD-A214408] N90-15855
DEFOCUSING
Gas optics applicable to free electron laser technology
[AD-A214285] N90-15741
DEFORMATION
Design temperatures for flexible airfield pavement design
[AD-A214141] N90-15115
Deformation and fracture of low alloy steels at high temperature
[DE90-001274] N90-15215
Energetics of BCC-FCC lattice deformation in iron
[AD-A213801] N90-15233
Geotechnical instrumentation
[PB89-198675] N90-15398
Thermal analysis of fixed and tilting pad journal bearings including cross-film viscosity variations and deformations N90-15429
Spatial dynamics of deformable multibody systems with variable kinematic structure
[AD-A214098] N90-15455
Statistical model for particle-void deformation kinetics in granular materials during shock wave propagation
[DE89-017729] N90-15476
DEGRADATION
Ice induced aerodynamic performance degradation of rotorcraft: An overview N90-15063
A review of the effects of microalloying constituents on the formation and breakdown of protective oxide scales on high-temperature alloys at temperatures below 700 C
[DE90-001277] N90-15216
Dual task performance with LPC (Linear Predictive Coding) degraded speech in a sentence verification task
[AD-A214298] N90-15320
DEICERS
Evaluation of the improved OV-ID anti-icing system, phase 2
[AD-A213928] N90-15083
DEICING
NASA's program on icing research and technology N90-15062
Flight and wind tunnel investigation of aerodynamic effects of aircraft ground deicing/antiicing fluids N90-15064
DELAMINATING
An analysis of drilling of composite materials N90-15142
DELAY
Gaze controls with interactions and delays
[AD-A214286] N90-15667
DENITROGENATION
Properties and thermal decomposition of the double salts of uranyl nitrate-ammonium nitrate
[DE89-004909] N90-15287
DENSE PLASMAS
Large scale calculations of the structure and dynamics of dense matter
[DE90-003654] N90-15726
DENSITY (MASS/VOLUME)
Simultaneous multipoint measurements of density gradients and temperature in a flame
[DE90-001719] N90-15155
Orthobaric densities and molar volumes of liquids: Alcohols
[ESDU-89037] N90-15184
DENSITY (NUMBER/VOLUME)
Large scale calculations of the structure and dynamics of dense matter
[DE90-003654] N90-15726
DENSITY DISTRIBUTION
Rapidity densities and their fluctuations in central 200 A GeV S32 interations with Au and Ag,Br nuclei
[LUIP-8905] N90-15715
DEPLOYMENT
Modeling and control of the rapid deployment of towed airborne devices N90-15092
DEPOLARIZATION
N-port theory applied to backscatter polarimetry and depolarization in foliage penetration
[AD-A213437] N90-15305
DEPOSITION
Enhancement of microchannel plate gain by deposition of CsI on the channel walls
[DE90-003051] N90-15334
Acid deposition
[DE90-003959] N90-15544
Partial reduction of re-oxidation processing of Y-Ba-Cu-O sputtered thin films
[DE90-003655] N90-15782
Orientation of rf-sputter-deposited MoS2 films
[ATR-89(4752)-1] N90-15784
The fabrication of YBa2Cu3O7 thin films by thermal coevaporation in oxygen
[DE90-003960] N90-15824
DEPTH
Determination of Q as a function of depth and tectonic province
[AD-A213805] N90-15554
DERIVATION
Tensor methods for unconstrained optimization using second derivatives
[AD-A213642] N90-15681
DESIGN ANALYSIS
The United States Air Force approach to all-weather testing N90-15047
Task-oriented display design: Concept and example
[NASA-TM-101685] N90-15101
Shuttle-C utilization for assembly of the rephased Freedom configuration
[NASA-TM-101658] N90-15120
Modifications of the Penn State Boundary Layer Research Facility for boundary layer/structure interaction experimental research
[AD-A213874] N90-15391
On the analysis and optimization of a platform manipulator N90-15433
On the motion of compliantly-connected rigid bodies in contact. Part 1: The motion prediction problem
[AD-A214135] N90-15489
On the motion of compliantly-connected rigid bodies in contact. Part 2: A system for analyzing designs for assembly
[AD-A214136] N90-15490
High-efficiency silicon concentrator solar cells for use with prismatic covers
[DE90-002644] N90-15509
Architectural study of the design and operation of advanced force feedback manual controllers
[NASA-CR-185948] N90-15664
DESORPTION
Studies of the adsorption/desorption behavior of explosive-like molecules
[DE90-001867] N90-15283
DESTABILIZATION
Destabilization of tokamak pressure-gradient driven instabilities by energetic alpha populations
[DE90-003716] N90-15756
DETECTION
Relative merits of reactive and forward-look detection for wind-shear encounters during landing approach for various microburst escape strategies
[NASA-TM-4158] N90-15108
Laser detection and discrimination system
[AD-D014301] N90-15426
RAIDS: An orbiting observatory for ionospheric remote sensing from space
[AD-A213717] N90-15494
Observation of atomic relaxation near an interface through detection of emitted fluorescence
[AD-A214308] N90-15725
DETECTORS
Center for X Ray Optics, 1988
[DE90-003300] N90-15732
DETERIORATION
Damage evaluation from surface displacement data N90-15469
DETONATION
Using small scale tests to estimate the failure diameter of a propellant
[DE90-001166] N90-15281
DETONATION WAVES
Laser-supported detonation waves and pulsed laser propulsion
[DE90-002753] N90-15412
DEUTERIUM
In-situ ion beam measurements of deuterium loading in thin foil electrochemical cells
[DE90-003162] N90-15511
Tritium and neutron measurements of a solid state cell
[DE90-003657] N90-15820
DIAMINES
Wet spinning of solid polyamic acid fibers
[NASA-CASE-LAR-14162-1] N90-15259
Polyimides with carbonyl and ether connecting groups between the aromatic rings
[NASA-CASE-LAR-14001-1] N90-15260
DIAMONDS
Characterization and in situ testing of diamond films
[DE90-003155] N90-15265
DIATOMIC MOLECULES
Excimer emission from alkali diatomic and alkaline-earth-noble-gas molecules
[AD-A214246] N90-15179
DIELECTRICS
Laser-material interactions
[AD-A214421] N90-15425
DIESEL ENGINES
Design and fabricate a metallic hydride heat pump with a cooling capacity of 9000 BTU/H
[AD-A213756] N90-15388
DIESEL FUELS
Mutagenic responses of some petroleum-base obscurants in the Ames test
[AD-A214201] N90-15295
DIFFERENTIAL EQUATIONS
Introduction to bifurcation theory
[DE90-003319] N90-15673
Flow of harmonic applications of a compact variety on a bordered variety
[DE89-635699] N90-15692
Nonlinear maps with competitive interactions: Fixed-points, bifurcations, and chaotic attractors
[DE90-001858] N90-15695
Nonlocality and stochastic quantization of field theory
[DE89-633913] N90-15833
DIFFRACTION
Binary optics technology: The theory and design of multi-level diffractive optical elements
[AD-A213404] N90-15735
DIFFUSION
Interaction of hydrogen in palladium as prescribed by the embedded atom method
[DE90-003893] N90-15244
Time-dependent free convection in low Prandtl number fluids
[DE90-003053] N90-15377
Thin films under chemical stress
[DE90-003754] N90-15484
Defect control and denuded trap zones in the 3-5 semiconductors
[AD-A214099] N90-15814
DIFFUSION ELECTRODES
In-situ ion beam measurements of deuterium loading in thin foil electrochemical cells
[DE90-003162] N90-15511
DIGITAL DATA
The digital data acquisition chain and the cosmic ray trigger system for the SLD warm iron calorimeter
[DE90-000943] N90-15879
DIGITAL ELECTRONICS
Advanced detection, isolation, and accommodation of sensor failures in turbofan engines: Real-time microcomputer implementation
[NASA-TP-2925] N90-15112
DIGITAL FILTERS
Compensation for peak shifts and variable background responses in fluorescence spectroscopy
[DE90-001102] N90-15154

DIGITAL SIMULATION
Aircraft response and pilot behaviour during a wake vortex encounter perpendicular to the vortex axis
N90-15057
DIGITAL SYSTEMS
Research in optical interconnection techniques
[AD-A214028] N90-15739
DIMENSIONAL ANALYSIS
Dimensional analysis of continuous high-capacity electrodispersion of aqueous based liquids in an organic continuous phase
[DE90-003714] N90-15136
A renormalization group approach to image processing: A new computational method for three-dimensional shapes in robot vision, and the computation complexity of the cooling algorithms
[AD-A214247] N90-15643
DIRECTION
Effect of contrast on the perception of direction of a moving pattern
[NASA-TM-102234] N90-15577
DIRECTION FINDING
Array signal processing: New techniques for direction finding and spectrum estimation
[AD-A213883] N90-15345
Large-aperture sparse array detector system for multiple emitter location
[AD-D014303] N90-15355
DIRECTIONAL SOLIDIFICATION (CRYSTALS)
Directional solidification of superalloys
[NASA-CASE-MFS-28314-1] N90-15227
DISCONTINUITY
Evolution of overlapping spreading centers: A Sea Mark 2 investigation
[AD-A214278] N90-15576
DISK GALAXIES
The disk-halo connection and the nature of the interstellar medium
[NASA-CR-186286] N90-15860
DISKS
Hybrid butterfly valve
[NASA-CASE-SSC-00004] N90-15443
DISPERSING
A methodology for evaluating heavy gas dispersion models
[AD-A214009] N90-15131
Dimensional analysis of continuous high-capacity electrodispersion of aqueous based liquids in an organic continuous phase
[DE90-003714] N90-15136
Beryllium dispersion near explosive firing tables: A comparison of computed and observed results
[DE90-002635] N90-15550
DISPLACEMENT
Damage evaluation from surface displacement data
N90-15469
Nonlinear strain-displacement relations for thin axisymmetric shells
[PB89-226013] N90-15470
Pipeline vibrations. Fluid transients in non-rigid, unbranched planar piping systems
[ESDU-89030] N90-15491
DISPLAY DEVICES
Task-oriented display design: Concept and example
[NASA-TM-101685] N90-15101
Display interface concepts for automated fault diagnosis
[NASA-TM-101610] N90-15102
Voice Multiplex System (VMS)
[AD-A213902] N90-15315
Development of the AH-64 display symbology training module
[AD-A213456] N90-15592
Studies of quantitative methods for imaging from scattered fields
[AD-A214047] N90-15638
DISSOCIATION
The dissociation energy of N2
[NASA-TM-101930] N90-15153
DISTILLATION EQUIPMENT
Reflux condensation in vertical tubes
[ESDU-89038] N90-15397
DISTORTION
Reduction of residual stress and distortion in HY100 and HY130 high strength steels during welding
[AD-A213532] N90-15231
SBS (Stimulated Brillouin Scattering) pulse distortion in multimode optical fibers: Preliminary results
[DE90-003023] N90-15731
DISTRIBUTED PROCESSING
Implementing fault-tolerant sensors
[NASA-CR-186251] N90-15400
Optimizing and evaluating algorithms for replicated data concurrency control
[DE90-003080] N90-15619
Scry: A distributed image handling system, version 1.1
[DE90-003105] N90-15621
An overview of lynx
[AD-A213714] N90-15631
On the correctness of orphan management algorithms
[AD-A213777] N90-15632
Optimistic concurrency control for nested distributed transactions
[AD-A213828] N90-15634
Hierarchical process composition: Dynamic maintenance of structure in a distributed environment
[AD-A214325] N90-15648
Periodic phase adjustment distributed clock synchronization in the hard realtime environment
[AD-A213842] N90-15708
Young Investigator's Award and distributed self-adaptive databases
[AD-A214194] N90-15854
DISTRIBUTION FUNCTIONS
An iterative Bayes procedure for reliability assessment
[DE90-002106] N90-15466
DOMAIN WALL
An exact solution for a thick domain wall in general relativity
[NASA-CR-185013] N90-15826
The dynamics of domain walls and strings
[NASA-CR-186255] N90-15832
DOPPLER RADAR
Turbulence spectral widths view angle independence as observed by Doppler radar
[DOT/FAA/SA-89/2] N90-15566
DOWNLINKING
SLCSAT (Submarine Laser Communication Satellite) communication system design study
[AD-A213403] N90-15304
DRAG CHUTES
An experimental investigation of wall-interference effects for parachutes in closed wind tunnels
[DE90-001802] N90-15076
DRILLING
An analysis of drilling of composite materials
N90-15142
DROPS (LIQUIDS)
Dense-spray properties: Structure and turbulence modulation
[AD-A213671] N90-15387
Anomalous absorption by atmospheric water vapor and stabilized water fogs in the infrared and CM-wave regions
[AD-A214202] N90-15572
DUCTILITY
Ductile failure
[AD-A213864] N90-15488
DWARF NOVAE
Recent progress in understanding the eruptions of classical novae
[NASA-CR-186280] N90-15870
DYNAMIC CHARACTERISTICS
Theoretical methods for the study of chemical dynamics
[DE90-003122] N90-15160
Base reaction optimization of redundant manipulators for space applications
[NASA-CR-186274] N90-15447
Spatial dynamics of deformable multibody systems with variable kinematic structure
[AD-A214098] N90-15455
Further research on dynamics of marine atmospheres in tropical cyclones
[AD-A213882] N90-15571
Vision in dynamic environments
[AD-A213434] N90-15587
Hierarchical process composition: Dynamic maintenance of structure in a distributed environment
[AD-A214325] N90-15648
DYNAMIC CONTROL
Gaze controls with interactions and delays
[AD-A214286] N90-15667
DYNAMIC LOADS
Investigation of loads generated by temperature transients in pipes
[DE89-636433] N90-15395
Location of interior impact source in randomly excited structures
[DE90-001092] N90-15474
Prediction of stochastic blade loads for three-bladed, rigid-hub rotors
[DE89-009508] N90-15520
DYNAMIC MODELS
Wind shear models for aircraft hazard investigation
N90-15044
Adaptive control of helicopter vibrations via the impulse response method
[AD-A213728] N90-15113
Ductile failure
[AD-A213864] N90-15488
Theoretical models of earthquake phenomena and the physical significance of seismic moment tensor expansions
[AD-A213813] N90-15556
DYNAMIC STRUCTURAL ANALYSIS
Active control system for gust load alleviation and structural damping N90-15056
Location of interior impact source in randomly excited structures
[DE90-001092] N90-15474
DYNAMIC TESTS
VIBRAFUGE: Combined vibration and centrifuge testing
[DE90-001091] N90-15114
Geotechnical instrumentation
[PB89-198675] N90-15398
A semiautomated computer-interactive dynamic impact testing system
[DE90-002721] N90-15479
DYNAMICAL SYSTEMS
A simulation model for dynamic system availability analysis
[AD-A213499] N90-15628
Introduction to bifurcation theory
[DE90-003319] N90-15673
Continuum analogues of contragredient Lie algebras: Lie algebras with a Cartan operator and nonlinear dynamical systems
[DE89-635698] N90-15691
DYNAMO THEORY
The disk-halo connection and the nature of the interstellar medium
[NASA-CR-186286] N90-15860

E

EARTH ATMOSPHERE
Development of a three-dimensional local scale atmospheric model with turbulence closure model
[DE90-710045] N90-15551
EARTH CRUST
Dynamics of mid-ocean ridge systems N90-15575
Evolution of overlapping spreading centers: A Sea Mark 2 investigation
[AD-A214278] N90-15576
EARTH IONOSPHERE
RAIDS: An orbiting observatory for ionospheric remote sensing from space
[AD-A213717] N90-15494
Development of the RAIDS (Remote Atmospheric and Ionospheric Detector System) extreme ultraviolet wedge and strip detector
[AD-A213730] N90-15495
EARTH MAGNETOSPHERE
Strategic characteristics of Dynamics Explorer 1 retarding ion mass spectrometer and the consequences for core plasma measurements
[AD-A214013] N90-15125
EARTH MANTLE
Determination of Q as a function of depth and tectonic province
[AD-A213805] N90-15554
Evolution of overlapping spreading centers: A Sea Mark 2 investigation
[AD-A214278] N90-15576
EARTHQUAKES
Determination of Q as a function of depth and tectonic province
[AD-A213805] N90-15554
Theoretical models of earthquake phenomena and the physical significance of seismic moment tensor expansions
[AD-A213813] N90-15556
ECOLOGY
Acid rain research
[DE90-003283] N90-15537
ECONOMIC ANALYSIS
Report of NASA Lunar Energy Enterprise Case Study Task Force
[NASA-TM-101652] N90-15836
Report of the NASA lunar energy enterprise case study task force N90-15837
Analysis of the financial factors governing the profitability of lunar helium-3 N90-15838
The Solar Power Satellite (SPS): Progress so far
N90-15840
Lunar power system summary of studies for the lunar enterprise task force NASA-office of exploration
N90-15841
ECONOMIC DEVELOPMENT
A quasi-economic role for lunar science
[DE90-000679] N90-15876

ECOSYSTEMS
Utilization of non-conventional systems for conversion of biomass to food components
[NASA-CR-177545] N90-15591
EDDY CURRENTS
Eddy-current inspection of shuttle heat exchanger tube welds
[NASA-CR-186302] N90-15462
EDGE DISLOCATIONS
Crack tip toughening by inclusions with pairs of shear transformations
[DE89-007645] N90-15254
EDGES
Research in knowledge-based vision techniques for the Autonomous Land Vehicle Program
[AD-A213440] N90-15453
EDITING
An executive system for modeling with rational b-splines
[AD-A213480] N90-15627
EDUCATION
Human behavior
[PB90-780008] N90-15584
Where to from here. Future applications of mental models of complex performance
[DE90-002091] N90-15586
Cockpit resource management: A selected annotated bibliography
[AD-A214272] N90-15594
Tools for simulation-based training
[AD-A214307] N90-15646
EINSTEIN EQUATIONS
An exact solution for a thick domain wall in general relativity
[NASA-CR-185013] N90-15826
ELASTIC BENDING
Two dimensional laminated shell theory including parabolic transverse shear
[AD-A213817] N90-15487
ELASTIC BODIES
Solution of potential flow past an elastic body using the boundary element technique
[AD-A213843] N90-15390
ELASTIC DEFORMATION
Mechanical behavior of laminated composites at elevated temperatures N90-15141
The elastic properties of woven polymeric fabric
[DE89-015391] N90-15255
A simple shell element formulation for large-scale elastoplastic analysis
[DE89-015452] N90-15475
ELASTIC PROPERTIES
Nickel beryllides and their properties
[DE90-001736] N90-15220
ELASTOHYDRODYNAMICS
Analysis of an elastohydrodynamic lubricated point contact: User's manual
[AD-A214257] N90-15459
ELASTOMERS
A novel heat resistant blend produced by compositional quenching: A thermoplastic polyimide impact modified with a fluoroelastomer
[AD-A213724] N90-15273
ELASTOPLASTICITY
A simple shell element formulation for large-scale elastoplastic analysis
[DE89-015452] N90-15475
Ductile failure
[AD-A213864] N90-15488
ELECTRIC BATTERIES
Status and results of ANL life evaluation of valve-regulated lead-acid load-leveling batteries
[DE90-001918] N90-15329
Rechargable molten-electrolyte lithium batteries
[DE90-003774] N90-15339
An assessment and comparison of fuel cells for transportation applications
[DE90-001807] N90-15508
ELECTRIC FIELDS
A numerical model for the axisymmetric equilibrium shape of drops in uniform motion: Effects of external flow, electric field and surface charge N90-15071
Dimensional analysis of continuous high-capacity electrodispersion of aqueous based liquids in an organic continuous phase
[DE90-003714] N90-15136
Comments on ER (Electrorheological) fluid rheology
[DE90-002892] N90-15166
ELECTRIC FUSES
Analysis and evaluation of technical data on the photochromic and non-linear optical properties of materials. Appendix: Eye/sensor protection by an optical fuse mirror at a focal plane: Feasibility assessment
[AD-A214051] N90-15177
ELECTRIC GENERATORS
Design of a high-gain flux-compression generator
[DE90-002795] N90-15333
Design and fabricate a metallic hydride heat pump with a cooling capacity of 9000 BTU/H
[AD-A213756] N90-15388
ELECTRIC MOTORS
Composite ceramic superconducting wires for electric motor applications
[AD-A213742] N90-15274
Adjustable speed drive study, June 1985 to September 1988. Part 2: Appendices
[DE90-002771] N90-15332
ELECTRIC POTENTIAL
Single element magnetic suspension actuator
[NASA-CASE-LAR-13981-1] N90-15442
ELECTRICAL IMPEDANCE
First International Symposium on Electrochemical Impedance Spectroscopy. Extended abstracts
[AD-A214406] N90-15354
ELECTRICAL PROPERTIES
Arc-sprayed coatings for electromagnetic pulse protection: Assessment of physical and electrical properties
[AD-A213825] N90-15275
RF transistor thermal/electrical characterization
[DE90-001427] N90-15326
Development of tunable excimer lasers
[AD-A213521] N90-15421
Thermally stable metal/GaAs contacts
[DE90-002122] N90-15774
Properties of high Tc superconducting oxides
[DE90-003792] N90-15821
ELECTRICAL RESISTIVITY
Electrochemical investigation of electronically conductive polymers
[AD-A214019] N90-15277
Introduction to extremely-low-frequency electric and magnetic fields
[DE90-002662] N90-15578
The measurement of transport properties in strongly coupled plasmas
[DE90-003451] N90-15755
ELECTRO-OPTICS
Analysis and evaluation of technical data on the photochromic and non-linear optical properties of materials. Appendix: Eye/sensor protection by an optical fuse mirror at a focal plane: Feasibility assessment
[AD-A214051] N90-15177
A new kind of heterodyne fiber-optic gyroscope
[AD-A213953] N90-15404
Laser-material interactions
[AD-A214421] N90-15425
Research in optical interconnection techniques
[AD-A214028] N90-15739
Solid state research
[AD-A213405] N90-15806
Research on materials and components for opto-electronic signal processing and computing
[AD-A213740] N90-15811
Innovative optoelectronic materials and structures using OMVPE
[AD-A214192] N90-15815
ELECTROACOUSTIC TRANSDUCERS
Pulsed EMAT (Electromagnetic Acoustic Transducer) acoustic measurements on a horizontal continuous caster for internal temperature determination
[DE90-002735] N90-15709
ELECTROCHEMICAL CELLS
Electrochemistry in near-critical and supercritical fluids. 8: Methyl viologen, decamethylferrocene, Os(bpy)3(sup 2+) and ferrocene in acetonitrile and the effect of pressure on diffusion coefficients under supercritical conditions
[AD-A213407] N90-15172
Advanced double layer capacitor
[AD-A213406] N90-15341
In-situ ion beam measurements of deuterium loading in thin foil electrochemical cells
[DE90-003162] N90-15511
Tritium and neutron measurements of a solid state cell
[DE90-003657] N90-15820
ELECTROCHEMICAL CORROSION
The effect of dissolved chlorine on the pitting behavior of 304L stainless steel in a 0.5 N NaCl solution
[AD-A213803] N90-15234
The effect of dissolved ozone on the corrosion behavior of Cu-30 Ni and 304L stainless steel in 0.5 N NaCl solutions
[AD-A213804] N90-15235
ELECTROCHEMISTRY
Electrochemistry in near-critical and supercritical fluids. 8: Methyl viologen, decamethylferrocene, Os(bpy)3(sup 2+) and ferrocene in acetonitrile and the effect of pressure on diffusion coefficients under supercritical conditions
[AD-A213407] N90-15172
Electronic and ionic transport in polymers
[AD-A213410] N90-15270
Electrochemical investigation of electronically conductive polymers
[AD-A214019] N90-15277
First International Symposium on Electrochemical Impedance Spectroscopy. Extended abstracts
[AD-A214406] N90-15354
ELECTRODES
Dimensional analysis of continuous high-capacity electrodispersion of aqueous based liquids in an organic continuous phase
[DE90-003714] N90-15136
Electrochemical investigation of electronically conductive polymers
[AD-A214019] N90-15277
Advanced double layer capacitor
[AD-A213406] N90-15341
Oxygen electrode in molten carbonate fuel cells
[DE90-002871] N90-15510
Interfacial systems for photochemical energy conversion
[DE90-003181] N90-15514
Fabrication of porous ceramic electrode structures
[DE90-003548] N90-15517
Design of DIII-D advanced divertor
[DE90-003343] N90-15752
ELECTROLYTES
Rechargable molten-electrolyte lithium batteries
[DE90-003774] N90-15339
ELECTROMAGNETIC COMPATIBILITY
Alternative techniques for some typical MIL-STD-461/462 types of measurements
[PB89-235139] N90-15302
ELECTROMAGNETIC COUPLING
Metal film coatings on amorphous metallic alloys
[AD-D014308] N90-15240
ELECTROMAGNETIC FIELDS
Design of a bounded wave EMP (Electromagnetic Pulse) simulator
[AD-A214137] N90-15316
Introduction to extremely-low-frequency electric and magnetic fields
[DE90-002662] N90-15578
ELECTROMAGNETIC INTERFERENCE
Aircraft testing in the electromagnetic environment N90-15066
ELECTROMAGNETIC MEASUREMENT
RF transistor thermal/electrical characterization
[DE90-001427] N90-15326
Pulsed EMAT (Electromagnetic Acoustic Transducer) acoustic measurements on a horizontal continuous caster for internal temperature determination
[DE90-002735] N90-15709
ELECTROMAGNETIC NOISE
Adaptive canceller limitations caused by I,Q mismatch errors
[AD-A214287] N90-15318
ELECTROMAGNETIC PULSES
Flight in Adverse Environmental Conditions
[AGARD-CP-470] N90-15041
Arc-sprayed coatings for electromagnetic pulse protection: Assessment of physical and electrical properties
[AD-A213825] N90-15275
Design of a bounded wave EMP (Electromagnetic Pulse) simulator
[AD-A214137] N90-15316
Proposed activities to prepare for testing advanced/stealth weapons systems
[AD-A214453] N90-15321
Technology of fast spark gaps
[AD-A214199] N90-15353
Frequency shift induced in laser pulses by plasma density variations
[AD-A214195] N90-15424
ELECTROMAGNETIC RADIATION
Characteristics of electromagnetic wave forms with lightning in winter season
[DE89-901256] N90-15567
ELECTROMAGNETIC SCATTERING
N-port theory applied to backscatter polarimetry and depolarization in foliage penetration
[AD-A213437] N90-15305
Studies of quantitative methods for imaging from scattered fields
[AD-A214047] N90-15638
ELECTROMAGNETIC SHIELDING
Arc-sprayed coatings for electromagnetic pulse protection: Assessment of physical and electrical properties
[AD-A213825] N90-15275
ELECTRON ACCELERATORS
Intense REB (Relativistic Electron Beam) transport in a weakly magnetized plasma
[DE90-002978] N90-15749

ELECTRON BEAM WELDING
Onorbit electron beam welding experiment definition
[NASA-CR-183847] N90-15431
ELECTRON BEAMS
Surface engineering by high energy beams
[DE90-001296] N90-15250
Theory for high gain, high power free electron lasers
[DE90-003024] N90-15409
Comprehensive, nonintercepting electron-beam diagnostics using spontaneous emission
[DE90-003211] N90-15414
Initial optical transition radiation measurements of the electron beam for the Boeing free-electron laser experiment
[DE90-003396] N90-15416
Waveguide effects in superradiant free-electron lasers
[DE90-003605] N90-15417
A microwiggler Free-Electron Laser at the Brookhaven Accelerator Test Facility
[DE90-003643] N90-15418
Simulation of radial expansion of an electron beam injected into a background plasma
[NASA-CR-186188] N90-15743
ELECTRON BOMBARDMENT
Secondary electron emission characteristics of molybdenum-masked, ion-textured OFHC copper
[NASA-TP-2967] N90-15211
ELECTRON CAPTURE
Defect control and denuded trap zones in the 3-5 semiconductors
[AD-A214099] N90-15814
ELECTRON CYCLOTRON HEATING
Review of quasi-optical gyrotron development
[AD-A213491] N90-15402
Mechanical design of the inside launch system for electron cyclotron heating in D3-D
[DE90-003292] N90-15751
ELECTRON DENSITY (CONCENTRATION)
Electron theory of long wavelength concentration fluctuations in liquid metal alloys
[DE89-636213] N90-15225
Microfluctuations of plasma density in a theta-pinch and spatial coherency of a probing laser beam
[DE90-603347] N90-15760
ELECTRON DIFFRACTION
Surface roughening of Ge(001) during 200 eV Xe ion bombardment and Ge molecular beam epitaxy
[DE90-000674] N90-15769
ELECTRON IMPACT
A high spatial resolution study of the thermospheric response to a discrete auroral arc
[NASA-TM-102904] N90-15559
ELECTRON MICROSCOPY
High resolution electron microscopy of grain boundaries in nanophase palladium
[DE90-003823] N90-15800
ELECTRON MOBILITY
Band-to-band transitions in poly (phenyl methyl silane)
[DE90-003575] N90-15720
Magnetic mechanisms of high temperature superconductivity
[DE90-003625] N90-15796
ELECTRON PHONON INTERACTIONS
General many-body systems
[DE90-000685] N90-15670
Tunneling spectroscopy and the electron-phonon interaction in Ba(1-x)K(x)BiO3
[DE90-002842] N90-15776
ELECTRON SPECTROSCOPY
Auger and x ray absorption studies of solid molecular oxygen
[DE90-003966] N90-15825
ELECTRON SPIN
Aspects of Raman scattering
[AD-A213926] N90-15736
ELECTRON TRANSFER
Interfacial systems for photochemical energy conversion
[DE90-003181] N90-15514
Photochemical solar energy conversion utilizing semiconductors localized in membrane mimetic systems
[DE90-003450] N90-15515
Dynamics of electron transfer for a nonsuperexchange coherent mechanism, 1
[AD-A213450] N90-15721
Dynamics of electron transfer for a non-superexchange coherent mechanisms. 2: Numerical calculations
[AD-A213511] N90-15722
Intense REB (Relativistic Electron Beam) transport in a weakly magnetized plasma
[DE90-002978] N90-15749
ELECTRON TUNNELING
Research on GaAs quantum-coupled structures that can be used as electron devices
[AD-A214015] N90-15350
Tunnelling effects on low energy fusion cross sections
[AD-A214010] N90-15762
Tunneling spectroscopy and the electron-phonon interaction in Ba(1-x)K(x)BiO3
[DE90-002842] N90-15776
ELECTRONIC CONTROL
Advanced detection, isolation, and accommodation of sensor failures in turbofan engines: Real-time microcomputer implementation
[NASA-TP-2925] N90-15112
ELECTRONIC EQUIPMENT
Design of a custom load cell for a precision assembly application
[DE90-004439] N90-15340
Research on GaAs quantum-coupled structures that can be used as electron devices
[AD-A214015] N90-15350
Technology of fast spark gaps
[AD-A214199] N90-15353
Overview on radiation effects in electronics
[DE90-000841] N90-15357
ELECTRONIC SPECTRA
The production and spectroscopy of molecular ions isolated in solid neon
[AD-A213723] N90-15174
ELECTRONS
Physical process in MPD plasmas
[AD-A213679] N90-15761
ELECTROPHORESIS
Capillary electrophoresis ionization-mass spectrometry and tandem mass spectrometry
[DE90-002664] N90-15158
ELECTROPLATING
Benefits from combining electroplating and physical vapor deposition technologies
[DE90-002700] N90-15301
ELECTROSTATICS
A numerical model for the axisymmetric equilibrium shape of drops in uniform motion: Effects of external flow, electric field and surface charge N90-15071
ELLIPSOIDS
Geometric considerations for a waypoint guidance method
[DE90-001803] N90-15088
Membership-set parameter estimation via optimal bounding ellipsoids
[AD-A213807] N90-15685
ELLIPTIC DIFFERENTIAL EQUATIONS
Mixed singular linear elliptic equations
[DE90-600722] N90-15674
ELONGATION
Brominated graphitized carbon fibers
[NASA-CASE-LEW-14698-2] N90-15262
EMBEDDING
Interaction of hydrogen in palladium as prescribed by the embedded atom method
[DE90-003893] N90-15244
EMBRITTLEMENT
Accelerated aging embrittlement of cast duplex stainless steel: Activation energy for extrapolation
[DE90-001773] N90-15221
Cast stainless steel aging: Mechanisms and predictions
[DE90-003772] N90-15241
EMERGENCIES
A methodology for evaluating heavy gas dispersion models
[AD-A214009] N90-15131
EMISSION
Spectral studies of solid propellant combustion. 2: Emission and absorption results for M-30 and HMX1 propellants
[AD-A213857] N90-15292
Thermal and statistical properties of nuclei and nuclear systems
[DE90-000183] N90-15717
EMISSION SPECTRA
Description of SHARC: The Strategic High-Altitude Radiance Code
[AD-A213806] N90-15555
ICP/AES (Inductively Coupled Plasma/Atomic Emission Spectroscopy): A modern analytical tool
[DE90-003822] N90-15765
Spectroscopic and laser properties of Cr:LiCaAlF6 and Cr:LiSrAlF6 crystals
[DE90-000783] N90-15770
Near-infrared polarimetry and spectroscopy of comets N90-15857
EMITTANCE
Observation of atomic relaxation near an interface through detection of emitted fluorescence
[AD-A214308] N90-15725
EMITTERS
Large-aperture sparse array detector system for multiple emitter location
[AD-D014303] N90-15355
ENCAPSULATING
Selection of phase-change and containment materials for thermal energy storage
[NASA-CR-186228] N90-15506
END EFFECTORS
New approach to the inverse problem of six-link manipulators via the optimization technique
[DE90-710044] N90-15441
ENERGETIC PARTICLES
Destabilization of tokamak pressure-gradient driven instabilities by energetic alpha populations
[DE90-003716] N90-15756
ENERGY BANDS
The effect of annealing treatments on defect structure and diffusion lengths in n-type GaAs
[AD-A214215] N90-15817
ENERGY CONSERVATION
Planning minimum-energy paths in an off-road environment with anisotropic traversal costs and motion constraints
[AD-A214181] N90-15457
A guide for estimating potential energy savings from increased solar reflectance of a low-sloped roof
[DE90-003720] N90-15526
Guidelines for evaluating energy analysis software
[AD-A214171] N90-15640
ENERGY CONSUMPTION
Laboratory study of the dynamic losses of a single speed, split system air-to-air heat pump having tube and plate fin heat exchangers, 1985 to 1986
[DE90-000970] N90-15367
Planning minimum-energy paths in an off-road environment with anisotropic traversal costs and motion constraints
[AD-A214181] N90-15457
Guidelines for evaluating energy analysis software
[AD-A214171] N90-15640
ENERGY CONVERSION
Interfacial systems for photochemical energy conversion
[DE90-003181] N90-15514
Photochemical solar energy conversion utilizing semiconductors localized in membrane mimetic systems
[DE90-003450] N90-15515
ENERGY CONVERSION EFFICIENCY
Propulsion research on the hybrid plume rocket
[AD-A214420] N90-15132
Research on high-efficiency, single-junction, monolithic, thin-film amorphous silicon solar cells, phase 1
[DE89-009495] N90-15502
High-efficiency silicon concentrator solar cells for use with prismatic covers
[DE90-002644] N90-15509
ENERGY DISSIPATION
Damping characteristics of metal matrix composites
[AD-A213712] N90-15151
Flux parameterization techniques in the atmospheric surface layer N90-15548
A numerical simulation model for the study of magnetohydrodynamic (MHD) waves in a structured medium N90-15864
ENERGY DISTRIBUTION
Analysis of catalytically enhanced solar absorption chemical reactors. 2: Predicted characteristics of a 100 kW chemical reactor
[DE89-014743] N90-15521
ENERGY GAPS (SOLID STATE)
Molecules with enhanced electronic polarizabilities based on defect-like states in conjugated polymers
[NASA-CASE-NPO-17633-1-CU] N90-15263
Picosecond photoconductivity using a graded bandgap Al(x)Ga(1-x)As active detecting layer
[DE90-003452] N90-15786
The effect of annealing treatments on defect structure and diffusion lengths in n-type GaAs
[AD-A214215] N90-15817
ENERGY LEVELS
Tunnelling effects on low energy fusion cross sections
[AD-A214010] N90-15762
X ray absorption studies of YBa2Cu3O(6+x), La(2-x)Sr(x)CuO4, and Nd(2-x)Ce(x)CuO4
[DE90-003640] N90-15797
ENERGY POLICY
The Third Pacific Basin Biofuels Workshop: Proceedings
[DE90-002523] N90-15513
ENERGY SPECTRA
Characterizing transient vibrations using band limited moments
[DE90-000799] N90-15473
Substructural dependence of the multiparticle production in relativistic heavy-ion interactions
[LUIP-8904] N90-15716
Target nucleus fragmentation in O16 + (Ag,Br) interactions at 200 A GeV
[LUIP-8906] N90-15727

A calculation of energetic proton spectra producedat substorm onset in the fields of the explosive reconnection model N90-15866
LEAP: A balloon-borne search for low-energy cosmic ray antiprotons N90-15878

ENERGY STORAGE
Thermal energy storage [DE90-000953] N90-15500
Selection of phase-change and containment materials for thermal energy storage [NASA-CR-186226] N90-15506
Satellite thermal storage systems using metallic phase-change materials [DE89-016872] N90-15507

ENERGY TECHNOLOGY
Molten carbonate fuel cell technology improvement [DE90-001934] N90-15501
The Solar Power Satellite (SPS): Progress so far N90-15840

ENERGY TRANSFER
Kinetic studies following state-selective laser excitation [DE90-003232] N90-15415
Determination of stepsize parameters for intermolecular vibrational energy transfer [DE90-003346] N90-15719

ENGINE DESIGN
A study of variable geometry in advanced gas turbines N90-15104
Ceramic technology for advanced heat engines project [DE90-001852] N90-15251

ENGINE PARTS
A study of variable geometry in advanced gas turbines N90-15104
Ceramic technology for advanced heat engines project [DE90-001852] N90-15251
Development of an integrated BEM approach for hot fluid structure interaction [NASA-CR-186214] N90-15364
Proceedings of the 1988 Structural Integrity Program Conference [AD-A213545] N90-15486

ENGINE TESTS
Advanced detection, isolation, and accommodation of sensor failures in turbofan engines: Real-time microcomputer implementation [NASA-TP-2925] N90-15112

ENGINEERING MANAGEMENT
Program manager's handbook [AD-A214338] N90-15844

ENGLAND
Potential vorticity in extratropical cyclones N90-15564

ENGLISH LANGUAGE
Terminology strategies for international information exchange [AD-A214147] N90-15853

ENVIRONMENT EFFECTS
Long-term worldwide environmental effects caused by acid rain from fossil fuels [DE90-001534] N90-15533
Evaluate and characterize mechanisms controlling transport, fate, and effects of army smokes in the aerosol wind tunnel: Transport, transformations, fate, and terrestrial ecological effects of hexachloroethane obscurant smokes [DE90-002923] N90-15536

ENVIRONMENT MANAGEMENT
Global climate change and NEPA (National Environmental Policy Act) analyses [DE90-003704] N90-15540

ENVIRONMENT POLLUTION
Environmental surveillance data [DE90-001275] N90-15532

ENVIRONMENT PROTECTION
International aspects of restrictions of ozone-depleting substances [DE90-001813] N90-15534

ENVIRONMENTAL MONITORING
Environmental surveillance data [DE90-001275] N90-15532
Global climate change and NEPA (National Environmental Policy Act) analyses [DE90-003704] N90-15540

ENVIRONMENTAL SURVEYS
Global climate change and NEPA (National Environmental Policy Act) analyses [DE90-003704] N90-15540
HCl monitor, phase 2 [AD-A213572] N90-15542

ENZYMES
Electronic materials high-T(sub c) superconductivity polymers and composites structural materials surface science and catalysts industry participation [NASA-CR-186063] N90-15145

EPITAXY
Research on GaAs quantum-coupled structures that can be used as electron devices [AD-A214015] N90-15350
Epitaxial iron films [AD-A213551] N90-15807

EPOXY RESINS
Mechanistic modeling of epoxy resins [DE89-015119] N90-15247
Epoxy-resin cable terminations [AD-A213789] N90-15454

EQUATIONS OF MOTION
Design limitations on ultra-high velocity projectile launchers [DE89-012933] N90-15118
Introduction to bifurcation theory [DE90-003319] N90-15673
Interface phonons in semiconductor double heterostructures [AD-A213732] N90-15810
The dynamics of domain walls and strings [NASA-CR-186255] N90-15832

EQUATIONS OF STATE
Hydrodynamics code calculations of debris clouds produced by ball-plate impacts [DE89-015270] N90-15439
Maximum entropy and equations of state for random cellular structures [DE90-002840] N90-15827
Shapes of star-gas waves in spiral galaxies [NASA-CR-186289] N90-15859

EQUILIBRIUM EQUATIONS
The free energy of Maxwell-Vlasov equilibria [DE90-003318] N90-15705

ERGODIC PROCESS
Recurrence and ergodicity for exponential family state-space models [AD-A213466] N90-15677

ERROR ANALYSIS
Error modeling of bias-type parameters for TOPEX orbit determination N90-15117
Geosat/ERM altimeter data analysis for the determination of global oceanic mesoscale variability N90-15492

ERRORS
Adaptive canceller limitations caused by I,Q mismatch errors [AD-A214287] N90-15318

ESTIMATING
A guide for estimating potential energy savings from increased solar reflectance of a low-sloped roof [DE90-003720] N90-15526
Estimating departure times from traffic counts using dynamic assignment [DE89-016259] N90-15653
Membership-set parameter estimation via optimal bounding ellipsoids [AD-A213807] N90-15685

ETCHING
Research on GaAs quantum-coupled structures that can be used as electron devices [AD-A214015] N90-15350

ETHERS
Polyimides with carbonyl and ether connecting groups between the aromatic rings [NASA-CASE-LAR-14001-1] N90-15260

EUROPEAN AIRBUS
Properties of Al-Li alloys N90-15191

EUTECTICS
Hardening and toughening of ZnS-Ga2S3 ceramics by solid-state reactions [AD-A213875] N90-15276
Characterization of the thermal degradation of selected energetic materials and mixtures by Rapid-Scan Fourier Transform Infrared (RSFTIR) spectroscopy [AD-A214411] N90-15296

EVAPORATION
Time-dependent free convection in liquid metals [DE90-000957] N90-15386
Specification for evaporation duct height calculations [AD-A213841] N90-15570
Anomalous absorption by atmospheric water vapor and stabilized water fogs in the infrared and CM-wave regions [AD-A214202] N90-15572
The fabrication of YBa2Cu3O7 thin films by thermal coevaporation in oxygen [DE90-003960] N90-15824

EXCIMER LASERS
Laser mixing of titanium on silicon carbide [DE90-003216] N90-15150
Excimer emission from alkali diatomic and alkaline-earth-noble-gas molecules [AD-A214246] N90-15179
Kinetic studies following state-selective laser excitation [DE90-003232] N90-15415
Development of tunable excimer lasers [AD-A213521] N90-15421

EXCITATION
The effectiveness of vane-aileron excitation in the experimental determination of flutter speed by parameter identification [NASA-TP-2971] N90-15100
Kinetic studies following state-selective laser excitation [DE90-003232] N90-15415
Phonons and charge-transfer excitations in HTS superconductors [DE89-016616] N90-15768

EXCITONS
Phonons and charge-transfer excitations in HTS superconductors [DE89-016616] N90-15768

EXHAUST EMISSION
Factors that may influence responses of the US transportation sector to policies for reducing greenhouse gas emissions [DE90-000704] N90-15543

EXHAUST GASES
Design and fabricate a metallic hydride heat pump with a cooling capacity of 9000 BTU/H [AD-A213756] N90-15388
Factors that may influence responses of the US transportation sector to policies for reducing greenhouse gas emissions [DE90-000704] N90-15543

EXHAUST SYSTEMS
X.2 limited flight test plan [AD-A214412] N90-15099

EXOSPHERE
Measurement of optical radiations in spacecraft environments [AD-A213814] N90-15497

EXPERIMENT DESIGN
Physical and Electrical Standards Laboratory general operating procedures [DE90-003515] N90-15116
Onorbit electron beam welding experiment definition [NASA-CR-183847] N90-15431
Developmental versions of FORTRAN/77 routines for the design and analysis of mixture experiments [DE90-003513] N90-15624

EXPERT SYSTEMS
Autonomous land navigation in a structured environment [DE90-001625] N90-15087
An expert system for quality assurance (a.k.a.) QA Express [DE90-003887] N90-15467
Where to from here. Future applications of mental models of complex performance [DE90-002091] N90-15586
Knowledge based text generation [AD-A214273] N90-15645
Investigation of the applicability of a functional programming model to fault-tolerant parallel processing for knowledge-based systems [NASA-CR-181938] N90-15654
Gaze controls with interactions and delays [AD-A214286] N90-15667

EXPLOSIVES
Simultaneous thermal analysis techniques for characterization of energetic materials [DE90-003028] N90-15289
Characterization of the thermal degradation of selected energetic materials and mixtures by Rapid-Scan Fourier Transform Infrared (RSFTIR) spectroscopy [AD-A214411] N90-15296

EXPONENTIAL FUNCTIONS
Recurrence and ergodicity for exponential family state-space models [AD-A213466] N90-15677
Strong large deviation and local limit theorems [AD-A213610] N90-15698

EXPOSURE
Variability of cultivar responses to ozone [PB89-225460] N90-15528

EXTENSOMETERS
Geotechnical instrumentation [PB89-198675] N90-15398

EXTRATERRESTRIAL RESOURCES
Report of NASA Lunar Energy Enterprise Case Study Task Force [NASA-TM-101652] N90-15836
Report of the NASA lunar energy enterprise case study task force N90-15837

Analysis of the financial factors governing the profitability of lunar helium-3 N90-15838
Lunar power system summary of studies for the lunar enterprise task force NASA-office of exploration N90-15841
Transportation and operations aspects of space energy systems N90-15842
Importance of helium-3 for the future N90-15843

EXTREMELY LOW FREQUENCIES
Introduction to extremely-low-frequency electric and magnetic fields
[DE90-002662] N90-15578

EXTRUDING
Fabrication of superconductor coils
[DE90-003571] N90-15338
Micromechanics of an extrusion in high-cycle fatigue with creep
[AD-A213509] N90-15485

EYE PROTECTION
Analysis and evaluation of technical data on the photochromic and non-linear optical properties of materials. Appendix: Eye/sensor protection by an optical fuse mirror at a focal plane: Feasibility assessment
[AD-A214051] N90-15177
Analysis and evaluation of technical data on the photochromic and non-linear optical properties of materials
[AD-A214212] N90-15178

F

F-18 AIRCRAFT
Flow visualization of the effect of pitch rate on the vortex development on the scale model of a F-18 fighter aircraft
[AD-A214244] N90-15080

FABRICATION
Design and calibration of an in-stack, low-pressure impactor
[AD-A213531] N90-15105
Al-Li alloy developed by Pechiney N90-15186
Fabrication of test-articles from Al-Li 2091 for Fokker 100 N90-15196
Fabrication characteristics of 8090 alloy N90-15198
Aluminum-lithium: Application of plate and sheet to fighter aircraft N90-15202
High performance powder metallurgy aluminum alloys: An overview N90-15204
Short fibre and particulate reinforced metal matrix composites N90-15207
Superconducting film fabrication by the sol-gel process
[DE90-002069] N90-15252
Fabrication of superconductor coils
[DE90-003571] N90-15338
Design of a custom load cell for a precision assembly application
[DE90-004439] N90-15340
Advanced double layer capacitor
[AD-A213406] N90-15341
Laser-material interactions
[AD-A214421] N90-15425
Development of the RAIDS (Remote Atmospheric and Ionospheric Detector System) extreme ultraviolet wedge and strip detector
[AD-A213730] N90-15495
Research on amorphous silicon-germanium alloys for tandem solar cells
[DE89-009436] N90-15499
Research on high-efficiency, single-junction, monolithic, thin-film amorphous silicon solar cells, phase 2
[DE89-009496] N90-15503
High-efficiency silicon concentrator solar cells for use with prismatic covers
[DE90-002644] N90-15509
Characterization of new cathode materials for molten carbonate fuel cells
[DE90-003547] N90-15516
Fabrication of porous ceramic electrode structures
[DE90-003548] N90-15517
Characteristics of CMOS analog integrated structures using MOSIS (Metal Oxide Semiconductor Implementation System)
[DE90-001630] N90-15773
Thermally stable metal/GaAs contacts
[DE90-002122] N90-15774
Processing and fabrication of YBa2Cu4O8 and YBa2Cu4O8/YBa2Cu3O(x) composites
[DE90-003559] N90-15789
Computer-controlled ion beam sputter-deposition of superconducting oxide films
[AD-A213921] N90-15812
High-temperature ceramic superconductors
[AD-A214251] N90-15818
The fabrication of YBa2Cu3O7 thin films by thermal coevaporation in oxygen
[DE90-003960] N90-15824

FABRICS
The elastic properties of woven polymeric fabric
[DE89-015391] N90-15255

FACE CENTERED CUBIC LATTICES
Energetics of BCC-FCC lattice deformation in iron
[AD-A213801] N90-15233

FACTORIZATION
A block QR factorization algorithm using restricted pivoting
[DE90-001921] N90-15613

FAILURE
Display interface concepts for automated fault diagnosis
[NASA-TM-101610] N90-15102
Using small scale tests to estimate the failure diameter of a propellant
[DE90-001166] N90-15281
Damage evaluation from surface displacement data N90-15469

FAILURE ANALYSIS
Evaluation of the improved OV-ID anti-icing system, phase 2
[AD-A213928] N90-15083
Current launch vehicle reliability practice and data base assessment. Volume 1: Executive summary and report body
[AD-A213600] N90-15121
A study of impact damage in composite laminates N90-15137
Fatigue properties of SiC/Al composites N90-15138
Composite activities at Lawrence Livermore National Laboratory
[DE90-002979] N90-15149
Characterization and in situ testing of diamond films
[DE90-003155] N90-15265
A paradigm for robust geometric algorithms
[AD-A214324] N90-15647

FAILURE MODES
Fatigue properties of SiC/Al composites N90-15138
Fatigue, fracture mechanics and corrosion properties of some aluminium-lithium alloys N90-15194
Studies on some failure modes in latex barrier films
[PB89-209308] N90-15246

FAR ULTRAVIOLET RADIATION
Development of the RAIDS (Remote Atmospheric and Ionospheric Detector System) extreme ultraviolet wedge and strip detector
[AD-A213730] N90-15495

FAST FOURIER TRANSFORMATIONS
Dynamics of electron transfer for a non-superexchange coherent mechanisms. 2: Numerical calculations
[AD-A213511] N90-15722

FAST NEUTRONS
Microstructural evolution of martensitic steels during fast neutron irradiation
[DE89-016231] N90-15212

FASTENERS
On the motion of compliantly-connected rigid bodies in contact. Part 1: The motion prediction problem
[AD-A214135] N90-15489
On the motion of compliantly-connected rigid bodies in contact. Part 2: A system for analyzing designs for assembly
[AD-A214136] N90-15490

FATIGUE (MATERIALS)
Design temperatures for flexible airfield pavement design
[AD-A214141] N90-15115
Short fibre and particulate reinforced metal matrix composites N90-15207
Fatigue loading history reconstruction based on the rain-flow technique
[NASA-CR-181942] N90-15482
Micromechanics of an extrusion in high-cycle fatigue with creep
[AD-A213509] N90-15485

FATIGUE LIFE
Thermal mechanical fatigue of coated blade materials
[AD-A214258] N90-15107
Fatigue and fracture behaviour of a PM Al-Li alloy N90-15195
Isothermal fatigue behavior of Sn-Pb solar joints
[DE90-003280] N90-15464
Fatigue loading history reconstruction based on the rain-flow technique
[NASA-CR-181942] N90-15482

FATIGUE TESTS
Design temperatures for flexible airfield pavement design
[AD-A214141] N90-15115
Composite activities at Lawrence Livermore National Laboratory
[DE90-002979] N90-15149
Fatigue behavior of vertical axis wind turbine airfoils with two weld configurations
[DE90-002628] N90-15525

FAULT TOLERANCE
Implementing fault-tolerant sensors
[NASA-CR-186251] N90-15400
Integrated approach fault tolerance-current state and future requirements
[AD-A214402] N90-15465
Investigation of the applicability of a functional programming model to fault-tolerant parallel processing for knowledge-based systems
[NASA-CR-181938] N90-15654

FEASIBILITY ANALYSIS
Analysis and evaluation of technical data on the photochromic and non-linear optical properties of materials. Appendix: Eye/sensor protection by an optical fuse mirror at a focal plane: Feasibility assessment
[AD-A214051] N90-15177
Feasibility study of using industrial robot for ultrasound testing
[DE90-002977] N90-15481

FEEDBACK CONTROL
Turbulence effects of aircraft flight dynamics and control N90-15055
Effect of modal truncation on derivatives of closed-loop damping ratios in structural control N90-15109
Advanced detection, isolation, and accommodation of sensor failures in turbofan engines: Real-time microcomputer implementation
[NASA-TP-2925] N90-15112

FEEDFORWARD CONTROL
One-class generalization in second-order backpropagation networks for image classification
[DE89-015845] N90-15661

FERMI SURFACES
X ray absorption studies of YBa2Cu3O(6+x), La(2-x)Sr(x)CuO4, and Nd(2-x)Ce(x)CuO4
[DE90-003640] N90-15797

FERRITES
The effects of Mo2C morphology and strain distribution on the fatigue properties of Fe-C-Mo dual-phase steels N90-15210

FERRITIC STAINLESS STEELS
Fusion reactor materials
[DE90-000976] N90-15744

FERROCENES
Electrochemistry in near-critical and supercritical fluids. 8: Methyl viologen, decamethylferrocene, Os(bpy)3(sup 2+) and ferrocene in acetonitrile and the effect of pressure on diffusion coefficients under supercritical conditions
[AD-A213407] N90-15172

FERROELECTRICITY
New devices using ferroelectric thin films
[DE90-000789] N90-15328

FIBER COMPOSITES
A study of impact damage in composite laminates N90-15137
The mechanical behavior of a fiber-reinforced brittle matrix composite N90-15139
Composite activities at Lawrence Livermore National Laboratory
[DE90-002979] N90-15149
Transverse (through-the-thickness) shear stiffnesses of fibre reinforced composite laminated plates (computer program)
[ESDU-89013] N90-15152
Metal matrix composites with long inorganic fibers N90-15206
Short fibre and particulate reinforced metal matrix composites N90-15207
SESAME equation of state for a polymer composite: Phenolic refrasil
[LA-11512-MS] N90-15264
Toughening behavior and interfacial properties of fiber-reinforced ceramic composites
[DE89-015351] N90-15279

FIBER OPTICS
Fly-by-light flight control system technology development plan
[NASA-CR-181953] N90-15111
Voice Multiplex System (VMS)
[AD-A213902] N90-15315
A new kind of heterodyne fiber-optic gyroscope
[AD-A213953] N90-15404
Laser communication system with wide band magnetostrictive modulation
[AD-D014302] N90-15427
Fiber optic sensing system
[NASA-CASE-LEW-14795-1] N90-15733

FIBER STRENGTH
Toughening behavior and interfacial properties of fiber-reinforced ceramic composites
[DE89-015351] N90-15279

FIBERS
Composite activities at Lawrence Livermore National Laboratory
[DE90-002979] N90-15149
FIELD EFFECT TRANSISTORS
Development of high performance beta-SiC field-effect transistors
[AD-A213885] N90-15346
Power semiconductor devices for space nuclear power systems
[DE90-001178] N90-15819
FIELD EMISSION
Technology of fast spark gaps
[AD-A214199] N90-15353
FIELD STRENGTH
Alternative techniques for some typical MIL-STD-461/462 types of measurements
[PB89-235139] N90-15302
FIELD THEORY (PHYSICS)
Nonlocality and stochastic quantization of field theory
[DE89-633913] N90-15833
FILE MAINTENANCE (COMPUTERS)
SESAME equation of state for a polymer composite: Phenolic refrasil
[LA-11512-MS] N90-15264
ARGOS (A Research GMMP Operating System): Overvie w and interfaces
[AD-A213871] N90-15599
FILTRATION
Predicting the performance of ceramic filters by the use of silt density index
[DE90-001316] N90-15256
FINITE DIFFERENCE THEORY
Finite difference techniques and rotor blade aeroelastic partial differential equations with quasisteady aerodynamics N90-15075
An examination of helicopter rotor load calculations
[AD-A214295] N90-15098
Nonlinear maps with competitive interactions: Fixed-points, bifurcations, and chaotic attractors
[DE90-001858] N90-15695
Physical process in MPD plasmas
[AD-A213679] N90-15761
FINITE ELEMENT METHOD
Effects of aeroelastic tailoring on anisotropic composite material beam models of helicopter blades
[AD-A213478] N90-15095
Solution of potential flow past an elastic body using the boundary element technique
[AD-A213843] N90-15390
Mesh refinement in finite element analysis by minimization of the stiffness matrix trace
[NASA-CR-185170] N90-15434
Nonlinear strain-displacement relations for thin axisymmetric shells
[PB89-226013] N90-15470
Utilization of a PC for finite element modeling
[AD-A214173] N90-15605
FINNED BODIES
Laminar forced convection inside externally finned tubes
[DE89-636431] N90-15373
FIRE CONTROL
China-built airborne synchronous laser ranger the new L-8 jet trainer aircraft
[AD-A213835] N90-15422
FITTINGS
Epoxy-resin cable terminations
[AD-A213789] N90-15454
FIXED POINTS (MATHEMATICS)
Nonlinear maps with competitive interactions: Fixed-points, bifurcations, and chaotic attractors
[DE90-001858] N90-15695
FLAME PROPAGATION
A tomographic study of premixed turbulent stagnation point flames
[DE90-002462] N90-15156
FLAME SPECTROSCOPY
Spectral studies of solid propellant combustion. 2: Emission and absorption results for M-30 and HMX1 propellants
[AD-A213857] N90-15292
FLAME STABILITY
Combustion characteristics of sprays
[AD-A213651] N90-15173
FLAMES
Simultaneous multipoint measurements of density gradients and temperature in a flame
[DE90-001719] N90-15155
FLAMMABILITY
Ignitability test method and apparatus
[NASA-CASE-LAR-13996-1-SB] N90-15161
FLAT PLATES
Numerical investigation of transition control of a flat plate boundary layer N90-15361
FLEXIBILITY
The dynamics of domain walls and strings
[NASA-CR-186255] N90-15832
FLEXIBLE BODIES
On the motion of compliantly-connected rigid bodies in contact. Part 1: The motion prediction problem
[AD-A214135] N90-15489
FLIGHT CHARACTERISTICS
Influence of windshear, downdraft and turbulence on flight safety N90-15048
A pitch control law for compensation of the phugoid mode induced by windshears N90-15051
Canard versus aft-tail ride qualities performance and pilot command response N90-15053
The interference of flightmechanical control laws with those of load alleviation and its influence on structural design N90-15054
FLIGHT CONDITIONS
Frontal clouds and flight conditions in them
[AD-A214250] N90-15573
FLIGHT CONTROL
Wind shear models for aircraft hazard investigation N90-15044
How to fly windshear using the fly-by-wire concept N90-15050
Turbulence effects of aircraft flight dynamics and control N90-15055
Imaging probabilities, geometry and ergonomics in limited visibility helicopter operations N90-15060
Fly-by-light flight control system technology development plan
[NASA-CR-181953] N90-15111
Integrated approach fault tolerance-current state and future requirements
[AD-A214402] N90-15465
FLIGHT CREWS
Display interface concepts for automated fault diagnosis
[NASA-TM-101610] N90-15102
Cockpit resource management: A selected annotated bibliography
[AD-A214272] N90-15594
FLIGHT HAZARDS
Effects of lightning on operations of aerospace vehicles N90-15065
Relative merits of reactive and forward-look detection for wind-shear encounters during landing approach for various microburst escape strategies
[NASA-TM-4158] N90-15108
FLIGHT MECHANICS
Flight in Adverse Environmental Conditions
[AGARD-CP-470] N90-15041
Description of atmospheric turbulence N90-15043
A pitch control law for compensation of the phugoid mode induced by windshears N90-15051
The interference of flightmechanical control laws with those of load alleviation and its influence on structural design N90-15054
A study of the effects of Rotating Frame Turbulence (RFT) on helicopter flight mechanics N90-15058
FLIGHT PATHS
Geometric considerations for a waypoint guidance method
[DE90-001803] N90-15088
FLIGHT PLANS
Control outside of independent surveillance coverage operational concept
[AD-A214163] N90-15090
FLIGHT SAFETY
Analysis of severe atmospheric disturbances from airline flight records N90-15045
Influence of windshear, downdraft and turbulence on flight safety N90-15048
Ice induced aerodynamic performance degradation of rotorcraft: An overview N90-15063
Effects of lightning on operations of aerospace vehicles N90-15065
Aircraft testing in the electromagnetic environment N90-15066
Turbulence spectral widths view angle independence as observed by Doppler radar
[DOT/FAA/SA-89/2] N90-15566
FLIGHT SIMULATION
Wind shear models for aircraft hazard investigation N90-15044
FLIGHT TESTS
Systems for airborne wind and turbulence measurement N90-15046
The United States Air Force approach to all-weather testing N90-15047
NASA's program on icing research and technology N90-15062
Flight and wind tunnel investigation of aerodynamic effects of aircraft ground deicing/antiicing fluids N90-15064
Aircraft testing in the electromagnetic environment N90-15066
Schleicher ASK-21 glider (TG-9) stall and spin
[AD-A213513] N90-15096
X.2 limited flight test plan
[AD-A214412] N90-15099
China-built airborne synchronous laser ranger the new L-8 jet trainer aircraft
[AD-A213835] N90-15422
FLOW CHARACTERISTICS
Explicit and implicit calculations of turbulent cavity flows with and without yaw angle
[NASA-CR-186293] N90-15381
FLOW CHARTS
Environment for failure region analysis: REACHER - a reachability condition derivation tool
[AD-A214183] N90-15641
FLOW DISTRIBUTION
Unsteady aerodynamics of oscillating and rapidly pitched airfoils N90-15074
Spatially-resolved, nonintrusive measurements in a nonreacting scramjet combustor using laser-induced iodine fluorescence N90-15103
Steady flow combustion model for solid-fuel ramjet projectiles
[BRL-TR-2987] N90-15163
An experimental, analytical, and computational investigation of turbomachinery rotor flow fields N90-15360
Comments on compressible flow through butterfly valves
[DE89-015730] N90-15371
A coning motion apparatus for hydrodynamic model testing in a non-planar cross-flow
[AD-A213431] N90-15383
Reduction of erosion in elbows due to flow modifications, phase 2
[DE89-011702] N90-15394
Application of a mass-consistent wind model to chinook windstorms
[AD-A213622] N90-15568
FLOW STABILITY
Dynamics of baroclinic instability in rapid cyclogenesis N90-15563
FLOW VELOCITY
Gelled propellant flow: Boundary layer theory for power-law fluids in a converging planar channel
[DE90-000923] N90-15365
Determination of flow-regime boundaries for cohesive particles
[DE90-001405] N90-15369
Comments on compressible flow through butterfly valves
[DE89-015730] N90-15371
Experimental determination of the fluid velocity by spectral analysis of temperature fluctuations
[DE89-636430] N90-15372
Experimental measurements of the laminar separation bubble on an Eppler 387 airfoil at low Reynolds numbers
[NASA-CR-186263] N90-15380
Reduction of erosion in elbows due to flow modifications, phase 2
[DE89-011702] N90-15394
Pipeline vibrations. Fluid transients in non-rigid, unbranched planar piping systems
[ESDU-89030] N90-15491
FLOW VISUALIZATION
Flow visualization of the effect of pitch rate on the vortex development on the scale model of a F-18 fighter aircraft
[AD-A214244] N90-15080
FLUID BOUNDARIES
Solution of potential flow past an elastic body using the boundary element technique
[AD-A213843] N90-15390
FLUID DYNAMICS
Unsteady three-dimensional thin-layer Navier-Stokes solutions on dynamic blocked grids N90-15069
Saltation and suspension of particulate matter in air
[AD-A213618] N90-15552
Numerical methods for parabolic equations and inequalities in very high dimensions
[AD-A214102] N90-15690
FLUID FLOW
Single fluid simulations of plasma openings switch behavior
[DE90-002643] N90-15330
Calibration of seven-hole pressure probes for use in fluid flows with large angularity
[NASA-TM-102200] N90-15399
FLUID MANAGEMENT
CryoTran user's manual, version 1.0
[NASA-TM-102468] N90-15622
FLUID MECHANICS
Comments on ER (Electrorheological) fluid rheology
[DE90-002892] N90-15166

A coning motion apparatus for hydrodynamic model testing in a non-planar cross-flow
[AD-A213431] N90-15383
FLUORESCENCE
Compensation for peak shifts and variable background responses in fluorescence spectroscopy
[DE90-001102] N90-15154
FLUOROPOLYMERS
A novel heat resistant blend produced by compositional quenching: A thermoplastic polyimide impact modified with a fluoroelastomer
[AD-A213724] N90-15273
FLUTTER
The effectiveness of vane-aileron excitation in the experimental determination of flutter speed by parameter identification
[NASA-TP-2971] N90-15100
FLUTTER ANALYSIS
Nonlinear phenomena in computational transonic aeroelasticity N90-15070
FLUX DENSITY
Design of a high-gain flux-compression generator
[DE90-002795] N90-15333
FLUX PINNING
Magnetic flux pinning in YBa2Cu3O7 films
[DE90-003709] N90-15799
FLY BY WIRE CONTROL
How to fly windshear using the fly-by-wire concept N90-15050
FOCAL PLANE DEVICES
Focal plane antenna array for millimeter waves
[AD-D014306] N90-15322
FOCUSING
A scheiner-principle vernier optometer
[AD-D014304] N90-15405
FOG
Anomalous absorption by atmospheric water vapor and stabilized water fogs in the infrared and CM-wave regions
[AD-A214202] N90-15572
FOILS (MATERIALS)
In-situ ion beam measurements of deuterium loading in thin foil electrochemical cells
[DE90-003162] N90-15511
FOLIAGE
N-port theory applied to backscatter polarimetry and depolarization in foliage penetration
[AD-A213437] N90-15305
FOOD PRODUCTION (IN SPACE)
Utilization of non-conventional systems for conversion of biomass to food components
[NASA-CR-177545] N90-15591
FORCED CONVECTION
Laminar forced convection inside externally finned tubes
[DE89-636431] N90-15373
FORECASTING
The radar-based short term prediction of the time-space evolution of rain fields
[AD-A213802] N90-15312
FORMALISM
Canonical formalism for coupled beam optics
[DE90-003764] N90-15734
FORTRAN
Developmental versions of FORTRAN/77 routines for the design and analysis of mixture experiments
[DE90-003513] N90-15624
FORWARD SCATTERING
Research on acoustical scattering, diffraction catastrophes, optics of bubbles, acoustical phase conjugation, and wake of an oscillating circular cylinder
[AD-A214168] N90-15711
FOSSIL FUELS
Long-term worldwide environmental effects caused by acid rain from fossil fuels
[DE90-001534] N90-15533
Global climate change: A fossil energy perspective
[DE90-003770] N90-15541
FOULING
Predicting the performance of ceramic filters by the use of silt density index
[DE90-001316] N90-15256
FOURIER ANALYSIS
Characterizing transient vibrations using band limited moments
[DE90-000799] N90-15473
FOURIER SERIES
Effect of modal truncation on derivatives of closed-loop damping ratios in structural control N90-15109
FOURIER TRANSFORMATION
High resolution imaging by phase retrieval and discrimination using speckle, volume 1
[AD-A214243] N90-15317
FRACTALS
Fractal dimension of the fractured surface of materials
[DE89-635764] N90-15477
A diffusion on a fractal state space
[AD-A213555] N90-15707
FRACTURE MECHANICS
An analysis of drilling of composite materials N90-15142
Fatigue, fracture mechanics and corrosion properties of some aluminium-lithium alloys N90-15194
Fatigue and fracture behaviour of a PM Al-Li alloy N90-15195
Hardening and toughening of ZnS-Ga2S3 ceramics by solid-state reactions
[AD-A213875] N90-15276
On the domain of dominance of the asymptotic elastodynamic crack-tip fields N90-15468
Experience with J testing of 304/308 stainless steel weldment
[DE90-002046] N90-15478
FRACTURE STRENGTH
The mechanical behavior of a fiber-reinforced brittle matrix composite N90-15139
Empirical and analytical determination of the fracture resistance of a TiB2 particle/SiC matrix composite
[NASA-TM-101940] N90-15143
Mechanical properties and fracture toughness of 8090-T651 plate and 2091 and 8090 sheet N90-15188
Investigation on sheet material of 8090 and 2091 aluminium-lithium alloy N90-15192
Fatigue and fracture behaviour of a PM Al-Li alloy N90-15195
Directional solidification of superalloys
[NASA-CASE-MFS-28314-1] N90-15227
Solid-state phase equilibria in the ZnS-Ga2S3 system
[AD-A213944] N90-15238
Toughening behavior and interfacial properties of fiber-reinforced ceramic composites
[DE89-015351] N90-15279
Fully articulated four-point-bend loading fixture
[NASA-CASE-LEW-14776-1] N90-15445
Fractal dimension of the fractured surface of materials
[DE89-635764] N90-15477
A semiautomated computer-interactive dynamic impact testing system
[DE90-002721] N90-15479
FRACTURING
Critical and subcritical crack-growth behavior along toughened ceramic/metal interfaces N90-15140
Deformation and fracture of low alloy steels at high temperature
[DE90-001274] N90-15215
FRAGMENTATION
Fragmentation statistics from Eulerian hydrocode calculations
[DE90-002906] N90-15449
FRAME PHOTOGRAPHY
Knowledge based text generation
[AD-A214273] N90-15645
FRANCE
Terminology strategies for international information exchange
[AD-A214147] N90-15853
FREE CONVECTION
Time-dependent free convection in liquid metals
[DE90-000957] N90-15366
Time-dependent free convection in low Prandtl number fluids
[DE90-003053] N90-15377
FREE ELECTRON LASERS
The 17.1-GHz free-electron laser as a microwave source for TeV colliders
[DE90-001506] N90-15406
Anharmonic betatron motion in free electron lasers
[DE90-001515] N90-15407
Theory for high gain, high power free electron lasers
[DE90-003024] N90-15409
Comprehensive, nonintercepting electron-beam diagnostics using spontaneous emission
[DE90-003211] N90-15414
Initial optical transition radiation measurements of the electron beam for the Boeing free-electron laser experiment
[DE90-003396] N90-15416
Waveguide effects in superradiant free-electron lasers
[DE90-003605] N90-15417
A microwiggler Free-Electron Laser at the Brookhaven Accelerator Test Facility
[DE90-003643] N90-15418
NOISE: A nonlinear optimization induction free-electron laser systems engineering code
[DE90-004438] N90-15420
Center for X Ray Optics, 1988
[DE90-003300] N90-15732
Gas optics applicable to free electron laser technology
[AD-A214285] N90-15741
FREE ELECTRONS
Technology of fast spark gaps
[AD-A214199] N90-15353
FREE ENERGY
Electron theory of long wavelength concentration fluctuations in liquid metal alloys
[DE89-636213] N90-15225
The free energy of Maxwell-Vlasov equilibria
[DE90-003318] N90-15705
FREQUENCY SHIFT
Frequency shift induced in laser pulses by plasma density variations
[AD-A214195] N90-15424
FRICTION FACTOR
Numerical analysis and simulation of frictional particle systems N90-15430
FRONTS (METEOROLOGY)
Identification and quantification of synoptic structure in simulated Tiros N radiance soundings N90-15546
Frontal clouds and flight conditions in them
[AD-A214250] N90-15573
FUEL CELL POWER PLANTS
Molten carbonate fuel cell technology improvement
[DE90-001934] N90-15501
FUEL CELLS
Molten carbonate fuel cell technology improvement
[DE90-001934] N90-15501
An assessment and comparison of fuel cells for transportation applications
[DE90-001807] N90-15508
Oxygen electrode in molten carbonate fuel cells
[DE90-002871] N90-15510
Characterization of new cathode materials for molten carbonate fuel cells
[DE90-003547] N90-15516
Fabrication of porous ceramic electrode structures
[DE90-003548] N90-15517
FUEL COMBUSTION
Comparison of engine knock predictions using a fully-detailed and a reduced chemical kinetic mechanism
[DE90-002805] N90-15448
FUEL CONSUMPTION
Guidance analysis of the aeroglide plane change maneuver as a turning point problem
[NASA-TM-101639] N90-15110
Guidelines for evaluating energy analysis software
[AD-A214171] N90-15640
FUEL INJECTION
Extended temperature range rocket injector
[NASA-CASE-LEW-14846-1] N90-15130
FUEL SPRAYS
Fundamental mechanism of atomization
[AD-A213859] N90-15293
FUELS
Products of the hypochlorite oxidation of hydrazine fuels
[AD-A213557] N90-15291
FUNCTIONAL ANALYSIS
Flow of harmonic applications of a compact variety on a bordered variety
[DE89-635699] N90-15692
FUNCTIONS (MATHEMATICS)
Higher order crossings from a parametric family of linear filters
[AD-A213427] N90-15676
FUSELAGES
Investigation on sheet material of 8090 and 2091 aluminium-lithium alloy N90-15192
FUSION REACTORS
Fusion reactor materials
[DE90-000976] N90-15744
Introduction to D-He(3) fusion reactors N90-15839
Importance of helium-3 for the future N90-15843

G

GALACTIC EVOLUTION
The age of the galactic disk
[NASA-CR-186292] N90-15869
GALACTIC STRUCTURE
The South African Astronomical Observatory
[NASA-CR-186258] N90-15856
GALAXIES
Pulsars lost and found: The second Princeton-Arecibo millisecond pulsar search N90-15865
GALILEO SPACECRAFT
Safety evaluation report for Galileo: Volume 1
[DE90-003086] N90-15122
Safety evaluation report for Galileo, volume 2
[DE90-003087] N90-15123
GALLIUM ARSENIDES
Electronic materials high-T(sub c) superconductivity polymers and composites structural materials surface science and catalysts industry participation
[NASA-CR-186063] N90-15145
Avalanche photoconductive switching
[DE90-002980] N90-15337

Laser-material interactions
[AD-A214421] N90-15425
Thermally stable metal/GaAs contacts
[DE90-002122] N90-15774
The effect of annealing treatments on defect structure and diffusion lengths in n-type GaAs
[AD-A214215] N90-15817
GALLIUM COMPOUNDS
Phase equilibrium and crystal growth studies on AgGaSe2 and related nonlinear optical materials
[AD-A213650] N90-15809
GAMMA RAYS
ROBOCAL (Robotic Calorimetry): An automated NDA (Nondestructive Assay) calorimetry and gamma isotopic system
[DE90-003217] N90-15168
GAS ANALYSIS
HCl monitor, phase 2
[AD-A213572] N90-15542
GAS CHROMATOGRAPHY
Analysis of ambient polar volatile organic compounds using chemical ionization-ion trap detector
[PB90-106451] N90-15529
GAS COOLED REACTORS
Design study of a modular gas-cooled, closed-brayton cycle reactor for marine use
[AD-A213453] N90-15518
GAS DENSITY
A methodology for evaluating heavy gas dispersion models
[AD-A214009] N90-15131
Shapes of star-gas waves in spiral galaxies
[NASA-CR-186289] N90-15859
GAS DYNAMICS
Enhanced resolution concepts in large scale scientific computing
[AD-A214095] N90-15393
GAS FLOW
Isotopic selectivity of surface diffusion: An activated diffusion model
[DE90-003473] N90-15169
Retractable gas cooled leads for ASTROMAG
[DE90-002679] N90-15331
Comments on compressible flow through butterfly valves
[DE89-015730] N90-15371
GAS IONIZATION
Laboratory simulations of the solar wind-comet interactions N90-15875
GAS TURBINE ENGINES
A study of variable geometry in advanced gas turbines N90-15104
GAS TURBINES
Dispersion strengthening of high temperature niobium alloys
[AD-A213829] N90-15236
Potential applications of structural ceramic composites in gas turbines
[DE90-001273] N90-15248
Gas turbine regenerators: A method for selecting the optimum plate-finned surface pair for minimum core volume
[AD-A213430] N90-15382
GAS WELDING
Reduction of residual stress and distortion in HY100 and HY130 high strength steels during welding
[AD-A213532] N90-15231
GAS-METAL INTERACTIONS
Ultrasonic evaluation of porosity in aluminum cast materials
[AD-A213548] N90-15232
GASES
Gas-liquid-liquid equilibria in mixtures of water, light gases, and hydrocarbons
[DE90-003180] N90-15167
Gas optics applicable to free electron laser technology
[AD-A214285] N90-15741
GATES (CIRCUITS)
Integration of a gated microchannel plate detector into the Nova laser system
[DE90-002981] N90-15413
GAUGE INVARIANCE
Chern-Simons theories of symplectic super-diffeomorphisms
[DE89-635700] N90-15703
Nonlocality and stochastic quantization of field theory
[DE89-633913] N90-15833
GAUGE THEORY
Designing machines for lattice physics and algorithm investigation
[DE90-003543] N90-15596
Chern-Simons theories of symplectic super-diffeomorphisms
[DE89-635700] N90-15703
Abelian gauge theory in topologically non-trivial space
[DE90-710100] N90-15830
GELLED ROCKET PROPELLANTS
Gelled propellant flow: Boundary layer theory for power-law fluids in a converging planar channel
[DE90-000923] N90-15365
GELS
Bonding aerogels with polyurethanes
[DE90-003050] N90-15258
Wet spinning of solid polyamic acid fibers
[NASA-CASE-LAR-14162-1] N90-15259
Crosslinked, flexible, low-molecular-weight polyacrylamide gels for mobility control
[DE90-000202] N90-15280
GEODESIC LINES
A (2+1)-dimensional pure gravity for an arbitrary closed initial surface
[DE90-701754] N90-15829
GEODESY
Superconducting gravity gradiometer mission. Volume 1: Study team executive summary
[NASA-TM-4091-VOL-1] N90-15545
GEODYNAMICS
Dynamics of mid-ocean ridge systems N90-15575
GEOLOGICAL FAULTS
Dynamics of mid-ocean ridge systems N90-15575
GEOMETRY
A study of variable geometry in advanced gas turbines N90-15104
GEOMORPHOLOGY
Evolution of overlapping spreading centers: A Sea Mark 2 investigation
[AD-A214278] N90-15576
GEOPHYSICS
Space operations: Listing of NASA scientific missions, 1980-2000. Fact sheet for the Chairman, Subcommittee on Space Science and Applications, Committee on Science, Space, and Technology, House of Representatives
[AD-A213493] N90-15881
GEOPOTENTIAL
Error modeling of bias-type parameters for TOPEX orbit determination N90-15117
GEOSAT SATELLITES
Geosat/ERM altimeter data analysis for the determination of global oceanic mesoscale variability N90-15492
GEOSTROPHIC WIND
Precipitation distributions associated with cyclones originating over the Gulf of Mexico and surrounding coastal regions
[AD-A213644] N90-15569
GEOTECHNICAL ENGINEERING
Geotechnical instrumentation
[PB89-196675] N90-15398
GERMANIUM
Surface roughening of Ge(001) during 200 eV Xe ion bombardment and Ge molecular beam epitaxy
[DE90-000674] N90-15769
GERMANIUM ALLOYS
Research on amorphous silicon-germanium alloys for tandem solar cells
[DE89-009436] N90-15499
GLASS
Dynamical structure of liquid and amorphous metals
[DE90-003805] N90-15229
Development of glass-ceramic lasers
[AD-A214146] N90-15423
Advanced study in solid transport: Rheological behavior of dense suspension
[DE90-003369] N90-15483
GLASS FIBER REINFORCED PLASTICS
An analysis of drilling of composite materials N90-15142
GLASS LASERS
Laser glass (1989)
[DE90-002754] N90-15257
Development of glass-ceramic lasers
[AD-A214146] N90-15423
GLIDERS
Schleicher ASK-21 glider (TG-9) stall and spin
[AD-A213513] N90-15096
GLOBAL WARMING
Responding to the threat of global warming: Options for the Pacific and Asia
[DE90-003553] N90-15539
Global climate change and NEPA (National Environmental Policy Act) analyses
[DE90-003704] N90-15540
Global climate change: A fossil energy perspective
[DE90-003770] N90-15541
GLOBULAR CLUSTERS
The age of the galactic disk
[NASA-CR-186292] N90-15869
Recent progress in understanding the eruptions of classical novae
[NASA-CR-186280] N90-15870
GLOVES
Studies on some failure modes in latex barrier films
[PB89-209308] N90-15246
GOLD
Rapidity densities and their fluctuations in central 200 A GeV S32 interations with Au and Ag,Br nuclei
[LUIP-8905] N90-15715
GOVERNMENT PROCUREMENT
Congressional involvement and relations: A guide for Department of Defense acquisition managers
[AD-A214408] N90-15855
GOVERNMENT/INDUSTRY RELATIONS
Report of NASA Lunar Energy Enterprise Case Study Task Force
[NASA-TM-101652] N90-15836
Report of the NASA lunar energy enterprise case study task force N90-15837
GOVERNMENTS
Congressional involvement and relations: A guide for Department of Defense acquisition managers
[AD-A214408] N90-15855
GRADIENTS
Gradient projection techniques for large-scale optimization problems
[DE90-001986] N90-15618
GRAIN BOUNDARIES
High resolution electron microscopy of grain boundaries in nanophase palladium
[DE90-003823] N90-15800
GRAIN SIZE
Irradition-induced grain growth: Role of dislocations
[DE90-003565] N90-15792
GRANULAR MATERIALS
Statistical model for particle-void deformation kinetics in granular materials during shock wave propagation
[DE89-017729] N90-15476
GRAPHITE-EPOXY COMPOSITES
An analysis of drilling of composite materials N90-15142
GRAPHITIZATION
Brominated graphitized carbon fibers
[NASA-CASE-LEW-14698-2] N90-15262
GRATINGS (SPECTRA)
Binary optics technology: The theory and design of multi-level diffractive optical elements
[AD-A213404] N90-15735
GRAVITATION
SL(2,R) current algebra in two-dimensional conformal quantum gravity
[DE90-600755] N90-15675
Non Newtonian gravity creeping flow
[DE90-600816] N90-15828
A (2+1)-dimensional pure gravity for an arbitrary closed initial surface
[DE90-701754] N90-15829
A numerical simulation model for the study of magnetohydrodynamic (MHD) waves in a structured medium N90-15864
GRAVITATION THEORY
An exact solution for a thick domain wall in general relativity
[NASA-CR-185013] N90-15826
GRAVITATIONAL EFFECTS
Shapes of star-gas waves in spiral galaxies
[NASA-CR-186289] N90-15859
GRAVITATIONAL FIELDS
Shapes of star-gas waves in spiral galaxies
[NASA-CR-186289] N90-15859
Gravitational lens effect on the cosmic background radiation due to nonlinear inhomogeneities
[DE90-701753] N90-15868
GRAVITATIONAL LENSES
Gravitational lens effect on the cosmic background radiation due to nonlinear inhomogeneities
[DE90-701753] N90-15868
GRAVITY GRADIOMETERS
Superconducting gravity gradiometer mission. Volume 1: Study team executive summary
[NASA-TM-4091-VOL-1] N90-15545
GREAT CIRCLES
Geometric considerations for a waypoint guidance method
[DE90-001803] N90-15088
GREEN'S FUNCTIONS
Theoretical models of earthquake phenomena and the physical significance of seismic moment tensor expansions
[AD-A213813] N90-15556
GREENHOUSE EFFECT
Greenhouse gases: Changing the global climate
[DE90-002788] N90-15535
Research project on CO2-induced climate change
[DE90-003531] N90-15538
Responding to the threat of global warming: Options for the Pacific and Asia
[DE90-003553] N90-15539

Global climate change: A fossil energy perspective
[DE90-003770] N90-15541
Factors that may influence responses of the US transportation sector to policies for reducing greenhouse gas emissions
[DE90-000704] N90-15543

GRID GENERATION (MATHEMATICS)
Mesh refinement in finite element analysis by minimization of the stiffness matrix trace
[NASA-CR-185170] N90-15434

GROUND TESTS
The United States Air Force approach to all-weather testing N90-15047
NASA's program on icing research and technology N90-15062

GROUND WIND
Application of a mass-consistent wind model to chinook windstorms
[AD-A213622] N90-15568

GUIDANCE (MOTION)
Geometric considerations for a waypoint guidance method
[DE90-001803] N90-15088

GULF OF MEXICO
Precipitation distributions associated with cyclones originating over the Gulf of Mexico and surrounding coastal regions
[AD-A213644] N90-15569

GUST ALLEVIATORS
Active control system for gust load allevation and structural damping N90-15056

GUST LOADS
Active control system for gust load allevation and structural damping N90-15056

GUSTS
Turbulence effects of aircraft flight dynamics and control N90-15055

GYROSCOPES
A new kind of heterodyne fiber-optic gyroscope
[AD-A213953] N90-15404

GYROSCOPIC STABILITY
A new kind of heterodyne fiber-optic gyroscope
[AD-A213953] N90-15404

H

HALF LIFE
Cosmic ray half life of (54)Mn
[DE90-000134] N90-15880

HALL EFFECT
Single fluid simulations of plasma openings switch behavior
[DE90-002643] N90-15330

HALLEY'S COMET
Near-infrared polarimetry and spectroscopy of comets N90-15857

HALOGEN COMPOUNDS
Inorganic halogen oxidizers
[AD-A213990] N90-15294

HALOS
The disk-halo connection and the nature of the interstellar medium
[NASA-CR-186286] N90-15860

HAMILTONIAN FUNCTIONS
Hamiltonian chaos in a nonlinear polarized optical beam
[DE90-002437] N90-15408
The application of optimal control theory for analysis of human jumping and pedaling N90-15590
Some results on connecting orbits for a class of Hamiltonian systems
[AD-A213536] N90-15679
Nijenhuis tensor and integrable models
[DE90-001403] N90-15702

HANDBOOKS
Program manager's handbook
[AD-A214338] N90-15844

HARDNESS
Nickel beryllides and their properties
[DE90-001736] N90-15220
Hardening and toughening of ZnS-Ga2S3 ceramics by solid-state reactions
[AD-A213875] N90-15276

HARMONIC OSCILLATORS
Anharmonic betatron motion in free electron lasers
[DE90-001515] N90-15407

HARMONICS
An examination of helicopter rotor load calculations
[AD-A214295] N90-15098
Flow of harmonic applications of a compact variety on a bordered variety
[DE89-635699] N90-15692

HARTREE APPROXIMATION
Large scale calculations of the structure and dynamics of dense matter
[DE90-003654] N90-15726

HEART
Monitoring chaos of cardiac rhythms
[DE90-000692] N90-15580

HEART RATE
Monitoring chaos of cardiac rhythms
[DE90-000692] N90-15580

HEAT
Ceramic technology for advanced heat engines project
[DE90-001852] N90-15251

HEAT EXCHANGERS
Solid lubrication of ceramic surfaces by IAD (Ion-Assisted Deposition)-silver coatings for heat engine applications
[DE90-002860] N90-15253
Gas turbine regenerators: A method for selecting the optimum plate-finned surface pair for minimum core volume
[AD-A213430] N90-15382
Reflux condensation in vertical tubes
[ESDU-89038] N90-15397

HEAT FLUX
Calculation of surface heat transfer parameters during quenching from surface thermocouple signals
[DE89-011620] N90-15224
High power density spray cooling
[AD-A213575] N90-15386
Radial heat flux limits in potassium heat pipes: An experimental and analytical investigation
[DE90-002655] N90-15396
Flux parameterization techniques in the atmospheric surface layer N90-15548
Potential vorticity in extratropical cyclones N90-15564

HEAT PIPES
Ceramic heat pipe wick
[NASA-CASE-GSC-13199-1] N90-15261
Radial heat flux limits in potassium heat pipes: An experimental and analytical investigation
[DE90-002655] N90-15396
Niobium 1 percent zirconium/potassium and titanium/potassium life-test heat pipe design and testing
[DE90-002430] N90-15522

HEAT PUMPS
Ceramic heat pipe wick
[NASA-CASE-GSC-13199-1] N90-15261
Feasibility analysis of reciprocating magnetic heat pumps
[NASA-CR-186205] N90-15363
Laboratory study of the dynamic losses of a single speed, split system air-to-air heat pump having tube and plate fin heat exchangers, 1985 to 1986
[DE90-000970] N90-15367
Recent advances in magnetic heat pump technology
[DE89-013289] N90-15370
Design and fabricate a metallic hydride heat pump with a cooling capacity of 9000 BTU/H
[AD-A213756] N90-15388
Annual summary of basic research in thermoacoustic heat transport
[AD-A214185] N90-15834

HEAT RESISTANT ALLOYS
Deformation and fracture of low alloy steels at high temperature
[DE90-001274] N90-15215
A review of the effects of microalloying constituents on the formation and breakdown of protective oxide scales on high-temperature alloys at temperatures below 700 C
[DE90-001277] N90-15216
Directional solidification of superalloys
[NASA-CASE-MFS-28314-1] N90-15227
Dispersion strengthening of high temperature niobium alloys
[AD-A213829] N90-15236

HEAT SOURCES
Design and fabricate a metallic hydride heat pump with a cooling capacity of 9000 BTU/H
[AD-A213756] N90-15388

HEAT STORAGE
Thermal energy storage
[DE90-000953] N90-15500
Selection of phase-change and containment materials for thermal energy storage
[NASA-CR-186228] N90-15506

HEAT TRANSFER
Calculation of surface heat transfer parameters during quenching from surface thermocouple signals
[DE89-011620] N90-15224
Critical temperature analysis for a hemispherical charge of a binary explosive
[DE90-001447] N90-15282
RF transistor thermal/electrical characterization
[DE90-001427] N90-15326
High power density spray cooling
[AD-A213575] N90-15386
Radial heat flux limits in potassium heat pipes: An experimental and analytical investigation
[DE90-002655] N90-15396
Reflux condensation in vertical tubes
[ESDU-89038] N90-15397
Thermal energy storage
[DE90-000953] N90-15500
Pulsed EMAT (Electromagnetic Acoustic Transducer) acoustic measurements on a horizontal continuous caster for internal temperature determination
[DE90-002735] N90-15709
Annual summary of basic research in thermoacoustic heat transport
[AD-A214185] N90-15834

HEAT TRANSFER COEFFICIENTS
Heat transfer in condensation of lithium vapors
[DE90-002081] N90-15375

HEAT TRANSMISSION
Time-dependent free convection in low Prandtl number fluids
[DE90-003053] N90-15377

HEAT TREATMENT
Heat treatment investigation of 4330 vanadium-modified steel
[AD-A214290] N90-15239
Phase equilibrium and crystal growth studies on AgGaSe2 and related nonlinear optical materials
[AD-A213650] N90-15809

HEATING
Surface thermometry of energetic materials by laser-induced fluorescence
[AD-A214423] N90-15297
Numerical investigation of transition control of a flat plate boundary layer N90-15361
Submerged arc welding consumables for HSLA (High Strength Low Alloy)-100 steel
[AD-A213433] N90-15452

HEAVY IONS
Substructural dependence of the multiparticle production in relativistic heavy-ion interactions
[LUIP-8904] N90-15716

HEAVY LIFT LAUNCH VEHICLES
Shuttle-C utilization for assembly of the rephased Freedom configuration
[NASA-TM-101658] N90-15120

HEIGHT
Specification for evaporation duct height calculations
[AD-A213841] N90-15570

HELICOPTERS
A study of the effects of Rotating Frame Turbulence (RFT) on helicopter flight mechanics N90-15058
Imaging probabilities, geometry and ergonomics in limited visibility helicopter operations N90-15060
Effects of aeroelastic tailoring on anisotropic composite material beam models of helicopter blades
[AD-A213478] N90-15095
An examination of helicopter rotor load calculations
[AD-A214295] N90-15098
Adaptive control of helicopter vibrations via the impulse response method
[AD-A213728] N90-15113
Uses and properties of Al-Li on the new EH101 helicopter N90-15201
Design of a bounded wave EMP (Electromagnetic Pulse) simulator
[AD-A214137] N90-15316

HELIUM
Helium-induced weld cracking in irradiated 304 stainless steel
[DE90-001312] N90-15219
Rayleigh-Taylor instability in compressible fluids
[DE90-003027] N90-15376
Large scale calculations of the structure and dynamics of dense matter
[DE90-003654] N90-15726
Report of NASA Lunar Energy Enterprise Case Study Task Force
[NASA-TM-101652] N90-15836
Report of the NASA lunar energy enterprise case study task force N90-15837
Analysis of the financial factors governing the profitability of lunar helium-3 N90-15838
Introduction to D-He(3) fusion reactors N90-15839

HELIUM IONS
Ion-irradiation effects in Tl2Ca2Ba2Cu3O10 superconductors
[DE90-003840] N90-15802

HELIUM ISOTOPES
Transportation and operations aspects of space energy systems N90-15842
Importance of helium-3 for the future N90-15843

HEMOGLOBIN
Carboxyalkylated hemoglobin as a potential blood substitute
[AD-A213886] N90-15582
HETERODYNING
A new kind of heterodyne fiber-optic gyroscope
[AD-A213953] N90-15404
HETEROJUNCTIONS
Interface phonons in semiconductor double heterostructures
[AD-A213732] N90-15810
HIERARCHIES
Hierarchical process composition: Dynamic maintenance of structure in a distributed environment
[AD-A214325] N90-15648
HIGH ALTITUDE
SCATHA (Spacecraft Charging at High Altitudes) atlas data base, volume 1
[AD-A214204] N90-15127
SCATHA (Spacecraft Charging At High Altitudes) atlas data base, volume 2
[AD-A214205] N90-15128
Description of SHARC: The Strategic High-Altitude Radiance Code
[AD-A213806] N90-15555
HIGH ELECTRON MOBILITY TRANSISTORS
The 22 GHz Radioastron receiver: Development of prototype components during the year 1988
[PB89-212583] N90-15323
Computer aided design of monolithic microwave and millimeter wave integrated circuits and subsystems
[AD-A213656] N90-15343
HIGH ENERGY ELECTRONS
SCATHA (Spacecraft Charging at High Altitudes) atlas data base, volume 1
[AD-A214204] N90-15127
SCATHA (Spacecraft Charging At High Altitudes) atlas data base, volume 2
[AD-A214205] N90-15128
HIGH ENERGY INTERACTIONS
Rapidity densities and their fluctuations in central 200 A GeV S32 interations with Au and Ag,Br nuclei
[LUIP-8905] N90-15715
Substructural dependence of the multiparticle production in relativistic heavy-ion interactions
[LUIP-8904] N90-15716
HIGH ENERGY PROPELLANTS
Shock-wave characterization of energetic booster-rocket propellant WAK-2 and its simulant UGS
[DE90-002633] N90-15285
HIGH FREQUENCIES
Wind speed dependence of acoustic ambient vertical directional spectra at high frequency
[AD-A214293] N90-15712
HIGH LEVEL LANGUAGES
High level language memory management on parallel architectures
[DE89-015018] N90-15609
An overview of lynx
[AD-A213714] N90-15631
HIGH POWER LASERS
Excimer emission from alkali diatomic and alkaline-earth-noble-gas molecules
[AD-A214246] N90-15179
Optical properties and laser damage measurements of inorganic polymer films
[DE90-003633] N90-15267
Theory for high gain, high power free electron lasers
[DE90-003024] N90-15409
HIGH STRENGTH
Current status of the application of conventional aluminium-lithium alloys and the potential for future developments N90-15203
HIGH STRENGTH ALLOYS
Fatigue properties of Al-Li alloys N90-15189
HIGH STRENGTH STEELS
Deformation and fracture of low alloy steels at high temperature
[DE90-001274] N90-15215
Reduction of residual stress and distortion in HY100 and HY130 high strength steels during welding
[AD-A213532] N90-15231
Heat treatment investigation of 4330 vanadium-modified steel
[AD-A214290] N90-15239
Submerged arc welding consumables for HSLA (High Strength Low Alloy)-100 steel
[AD-A213433] N90-15452
HIGH TEMPERATURE
High temperature chemistry of aromatic hydrocarbons
[DE90-003664] N90-15133
Mechanical behavior of laminated composites at elevated temperatures N90-15141
High-temperature gel-permeation chromatography of poly(4-methyl-1-pentene)
[DE90-002967] N90-15159
Microstructural evolution of martensitic steels during fast neutron irradiation
[DE89-016231] N90-15212
Deformation and fracture of low alloy steels at high temperature
[DE90-001274] N90-15215
High power density spray cooling
[AD-A213575] N90-15386
High temperature, flexible, thermal barrier seal
[NASA-CASE-LEW-14672-1] N90-15444
HIGH TEMPERATURE GASES
The disk-halo connection and the nature of the interstellar medium
[NASA-CR-186286] N90-15860
HIGH TEMPERATURE SUPERCONDUCTORS
Electronic materials high-T(sub c) superconductivity polymers and composites structural materials surface science and catalysts industry participation
[NASA-CR-186063] N90-15145
Preparation and properties of icosahedral borides
[DE90-003574] N90-15180
Composite ceramic superconducting wires for electric motor applications
[AD-A213742] N90-15274
Theoretical studies on the electronic structure of high-temperature superconductors
[DE90-001301] N90-15771
Tunneling spectroscopy and the electron-phonon interaction in Ba(1-x)K(x)BiO3
[DE90-002842] N90-15776
Linear electron-hole-electron pair model of high-temperature superconductivity in La(2-x)M(x)CuO4 and YBa2Cu3O(7-y): Part 2. Dependence of the superconducting transition temperatures on pressure and on hole concentration
[DE90-003012] N90-15779
Electron-positron momentum distribution measurements of high-T superconductors and related systems
[DE90-002974] N90-15780
Magnetic mechanisms of high temperature superconductivity
[DE90-003625] N90-15796
Bulk wave characterization of high T(sub c) superconductors
[AD-A214030] N90-15813
High-temperature ceramic superconductors
[AD-A214251] N90-15818
HILBERT SPACE
On the sum of two maximal monotone operators
[REPT-89-31] N90-15669
General many-body systems
[DE90-000685] N90-15670
On functional integral representations in the lower Hubbard band based on generalized coherent states
[DE90-602936] N90-15804
HISTORIES
Current launch vehicle reliability practice and data base assessment. Volume 1: Executive summary and report body
[AD-A213600] N90-15121
Fatigue loading history reconstruction based on the rain-flow technique
[NASA-CR-181942] N90-15482
Understanding developments in computer technology: A pragmatic and synthetic interpretation N90-15608
HMX
Using small scale tests to estimate the failure diameter of a propellant
[DE90-001166] N90-15281
Burning rates of two cast nitramine explosives using a hybrid closed bomb-strand burner
[DE90-002785] N90-15286
Spectral studies of solid propellant combustion. 2: Emission and absorption results for M-30 and HMX1 propellants
[AD-A213857] N90-15292
HOLDERS
Ignitability test method and apparatus
[NASA-CASE-LAR-13998-1-SB] N90-15161
HOLES (ELECTRON DEFICIENCIES)
Linear electron-hole-electron pair model of high-temperature superconductivity in La(2-x)M(x)CuO4 and YBa2Cu3O(7-y): Part 2. Dependence of the superconducting transition temperatures on pressure and on hole concentration
[DE90-003012] N90-15779
Defect control and denuded trap zones in the 3-5 semiconductors
[AD-A214099] N90-15814
HORIZONTAL TAIL SURFACES
Installed tailplane lift-curve slope at subsonic speeds
[ESDU-89029] N90-15081
HOT CORROSION
A review of the effects of microalloying constituents on the formation and breakdown of protective oxide scales on high-temperature alloys at temperatures below 700 C
[DE90-001277] N90-15216
HOT ISOSTATIC PRESSING
Improved process for HIP canning of composites
[NASA-CASE-LEW-14990-1-CU] N90-15147
HOUSEHOLDER TRANSFORMATIONS
A block QR factorization algorithm using restricted pivoting
[DE90-001921] N90-15613
HOVERING
X.2 limited flight test plan
[AD-A214412] N90-15099
HUBBLE SPACE TELESCOPE
Artificial intelligence approaches to astronomical observation scheduling
[NASA-CR-186277] N90-15862
Automated telescope scheduling
[NASA-CR-186279] N90-15863
HUGONIOT EQUATION OF STATE
Hugoniot measurements with the LLNL electric gun facility
[DE90-002809] N90-15119
SESAME equation of state for a polymer composite: Phenolic refrasil
[LA-11512-MS] N90-15264
Shock-wave characterization of energetic booster-rocket propellant WAK-2 and its simulant UGS
[DE90-002633] N90-15285
HUMAN BEHAVIOR
Human behavior
[PB90-780008] N90-15584
HUMAN BEINGS
An architectural model of visual motion understanding
[AD-A214327] N90-15589
HUMAN BODY
Introduction to extremely-low-frequency electric and magnetic fields
[DE90-002662] N90-15578
The application of optimal control theory for analysis of human jumping and pedaling N90-15590
HUMAN FACTORS ENGINEERING
The human element: The key to safe, civil operations in adverse weather N90-15042
Imaging probabilities, geometry and ergonomics in limited visibility helicopter operations N90-15060
See and avoid/cockpit visibility
[AD-A214214] N90-15084
Task-oriented display design: Concept and example
[NASA-TM-101685] N90-15101
An expert system for quality assurance (a.k.a.) QA Express
[DE90-003887] N90-15467
Model for measuring complex performance in an aviation environment
[DE90-002055] N90-15585
Architectural study of the design and operation of advanced force feedback manual controllers
[NASA-CR-185948] N90-15664
HUMAN PERFORMANCE
Dual task performance with LPC (Linear Predictive Coding) degraded speech in a sentence verification task
[AD-A214298] N90-15320
A comparative evaluation and analysis of end-user search performance in an academic environment N90-15845
HYDRAZINES
Products of the hypochlorite oxidation of hydrazine fuels
[AD-A213557] N90-15291
HYDROCARBONS
High temperature chemistry of aromatic hydrocarbons
[DE90-003664] N90-15133
Gas-liquid-liquid equilibria in mixtures of water, light gases, and hydrocarbons
[DE90-003180] N90-15167
HYDROCHLORIC ACID
HCl monitor, phase 2
[AD-A213572] N90-15542
HYDROCLIMATOLOGY
Global lake-level variations from 18,000 to 0 years ago: A palaeoclimate analysis
[DE90-000998] N90-15531
HYDRODYNAMIC EQUATIONS
Determination of flow-regime boundaries for cohesive particles
[DE90-001405] N90-15369
MESA 3-D calculations of armor penetration by projectiles with combined obliquity and yaw
[DE89-015265] N90-15438
HYDRODYNAMICS
Irreversible processes from reversible mechanics
[DE90-001057] N90-15368

Rayleigh-Taylor instability in compressible fluids
[DE90-003027] N90-15376
A coning motion apparatus for hydrodynamic model testing in a non-planar cross-flow
[AD-A213431] N90-15383
Hydrodynamics code calculations of debris clouds produced by ball-plate impacts
[DE89-015270] N90-15439
Comparison of multidimensional calculations of long-rod impacts on oblique plates
[DE89-015275] N90-15440
Development of a three-dimensional local scale atmospheric model with turbulence closure model
[DE90-710045] N90-15551
Brownian trail rectified
[DE90-003339] N90-15706
Recent progress in understanding the eruptions of classical novae
[NASA-CR-186280] N90-15870

HYDROELASTICITY
Analysis of an elastohydrodynamic lubricated point contact: User's manual
[AD-A214257] N90-15459

HYDROGEN
Interaction of hydrogen in palladium as prescribed by the embedded atom method
[DE90-003893] N90-15244
Annual operating plan for fiscal year 1990 for chemical/hydrogen energy systems program
[DE90-003964] N90-15527

HYDROGEN ATOMS
Interaction of hydrogen in palladium as prescribed by the embedded atom method
[DE90-003893] N90-15244

HYDROGEN CHLORIDES
HCl monitor, phase 2
[AD-A213572] N90-15542

HYDROGEN IONS
Relativistic self-consistent field studies of atoms and molecules
[AD-A214101] N90-15724

HYDROGENOLYSIS
Correlations between surface structure and catalytic activity/selectivity
[DE90-003755] N90-15181

HYDROGEOLOGY
Evolution of overlapping spreading centers: A Sea Mark 2 investigation
[AD-A214278] N90-15576

HYPERBOLIC DIFFERENTIAL EQUATIONS
Unsteady three-dimensional thin-layer Navier-Stokes solutions on dynamic blocked grids N90-15069

HYPERSONIC NOZZLES
Hypersonic nozzle design
[NASA-CR-186261] N90-15077

HYPERSONIC VEHICLES
Manned spacecraft
[AD-A214218] N90-15129

HYPERSONIC WIND TUNNELS
Hypersonic nozzle design
[NASA-CR-186261] N90-15077

HYPERSONICS
Hypersonic nozzle design
[NASA-CR-186261] N90-15077

HYPERVELOCITY GUNS
Hugoniot measurements with the LLNL electric gun facility
[DE90-002809] N90-15119

HYPERVELOCITY IMPACT
Stand-off shields for hypervelocity particles
[DE89-016182] N90-15437
Effects of parametric variations of complex targets on damage from projectile impact
[DE90-003214] N90-15450

HYPERVELOCITY LAUNCHERS
Design limitations on ultra-high velocity projectile launchers
[DE89-012933] N90-15118

HYPERVELOCITY PROJECTILES
Design limitations on ultra-high velocity projectile launchers
[DE89-012933] N90-15118
Stand-off shields for hypervelocity particles
[DE89-016182] N90-15437
Effects of parametric variations of complex targets on damage from projectile impact
[DE90-003214] N90-15450

I

ICE FORMATION
Flight in Adverse Environmental Conditions
[AGARD-CP-470] N90-15041
NASA's program on icing research and technology N90-15062
Ice induced aerodynamic performance degradation of rotorcraft: An overview N90-15063
Flight and wind tunnel investigation of aerodynamic effects of aircraft ground deicing/antiicing fluids N90-15064
Evaluation of the improved OV-ID anti-icing system, phase 2
[AD-A213928] N90-15083

ICE PREVENTION
NASA's program on icing research and technology N90-15062
Flight and wind tunnel investigation of aerodynamic effects of aircraft ground deicing/antiicing fluids N90-15064
Evaluation of the improved OV-ID anti-icing system, phase 2
[AD-A213928] N90-15083

IDEAL GAS
Thermal conductivity of gaseous aliphatic hydrocarbons. Part 1: Alkanes
[ESDU-89035-PT-1] N90-15183

IGNITION
Ignitability test method and apparatus
[NASA-CASE-LAR-13996-1-SB] N90-15161
Shock tube ignition of octanes
[DE90-001167] N90-15164
Using small scale tests to estimate the failure diameter of a propellant
[DE90-001166] N90-15281
Critical temperature analysis for a hemispherical charge of a binary explosive
[DE90-001447] N90-15282

ILLUMINATING
Improved lighting of taxiway/taxiway intersections for Instrument Flight Rules (IFR) operations
[DOT/FAA/CT-TN89/64] N90-15089

IMAGE ENHANCEMENT
Image enhancement using the IRAS (Infrared Astronomy Satellite) survey data
[AD-A213811] N90-15496

IMAGE PROCESSING
Component presence-absence detection for automated visual inspection of hybrid microcircuits
[KCP-613-4050] N90-15335
Sensor integration using concurrent computing on-board the ORNL mobile robot
[DE89-008740] N90-15436
Image enhancement using the IRAS (Infrared Astronomy Satellite) survey data
[AD-A213811] N90-15496
Identification and quantification of synoptic structure in simulated Tiros N radiance soundings N90-15546
Vision in dynamic environments
[AD-A213434] N90-15587
The role of attention in visual processing
[AD-A214158] N90-15588
Scry: A distributed image handling system, version 1.1
[DE90-003105] N90-15621
Evaluation of a simple algorithm for estimating infrared signatures from multi-pixel to sub-pixel targets applied to AGA thermovision imagery
[AD-A214103] N90-15639
A renormalization group approach to image processing: A new computational method for three-dimensional shapes in robot vision, and the computation complexity of the cooling algorithms
[AD-A214247] N90-15643
One-class generalization in second-order backpropagation networks for image classification
[DE89-015845] N90-15661
Design and implementation of two concurrent multi-sensor integration algorithms for mobile robots
[DE90-003041] N90-15663
Systolic algorithms for imaging from space
[AD-A213870] N90-15701

IMAGE RECONSTRUCTION
Studies of quantitative methods for imaging from scattered fields
[AD-A214047] N90-15638
A renormalization group approach to image processing: A new computational method for three-dimensional shapes in robot vision, and the computation complexity of the cooling algorithms
[AD-A214247] N90-15643

IMAGE RESOLUTION
Image enhancement using the IRAS (Infrared Astronomy Satellite) survey data
[AD-A213811] N90-15496

IMAGERY
A logic for the pixel assignment step of imagery classification predicated on class structure N90-15493

IMAGES
Surface thermometry of energetic materials by laser-induced fluorescence
[AD-A214423] N90-15297
An architectural model of visual motion understanding
[AD-A214327] N90-15589
Center for X Ray Optics, 1988
[DE90-003300] N90-15732

IMAGING RADAR
Flashlight radar: A three-dimensional imaging radar
[AD-A213439] N90-15307

IMAGING TECHNIQUES
Development of NMR (Nuclear Magnetic Resonance) imaging probes for advanced ceramics
[DE90-003812] N90-15269
High resolution imaging by phase retrieval and discrimination using speckle, volume 1
[AD-A214243] N90-15317
Focal plane antenna array for millimeter waves
[AD-D014306] N90-15322
Studies of quantitative methods for imaging from scattered fields
[AD-A214047] N90-15638
Systolic algorithms for imaging from space
[AD-A213870] N90-15701

IMPACT DAMAGE
A study of impact damage in composite laminates N90-15137
Effects of parametric variations of complex targets on damage from projectile impact
[DE90-003214] N90-15450

IMPACT LOADS
Effects of parametric variations of complex targets on damage from projectile impact
[DE90-003214] N90-15450
Location of interior impact source in randomly excited structures
[DE90-001092] N90-15474

IMPACT STRENGTH
Hydrodynamics code calculations of debris clouds produced by ball-plate impacts
[DE89-015270] N90-15439

IMPACTORS
Design and calibration of an in-stack, low-pressure impactor
[AD-A213531] N90-15105

IMPULSES
Adaptive control of helicopter vibrations via the impulse response method
[AD-A213728] N90-15113

IMPURITIES
Survey on synthesis technologies of methanol as an alternative fuel
[DE89-901303] N90-15284

IN-FLIGHT MONITORING
Systems for airborne wind and turbulence measurement N90-15046

INCLUSIONS
Crack tip toughening by inclusions with pairs of shear transformations
[DE89-007845] N90-15254

INCOMPRESSIBLE FLUIDS
Numerical investigation of transition control of a flat plate boundary layer N90-15361

INDEPENDENT VARIABLES
Fast algorithms for estimating mixture parameters
[AD-A213869] N90-15636

INDEXES (DOCUMENTATION)
Aeronautical engineering: A continuing bibliography with indexes (supplement 246)
[NASA-SP-7037(246)] N90-15068
Bibliography of Lewis Research Center technical publications announced in 1988
[NASA-TM-102034] N90-15846

INELASTIC COLLISIONS
Investigations of the interactions of radiation with matter
[AD-A213554] N90-15723

INELASTIC SCATTERING
Structure and dynamics of disordered systems
[DE90-001408] N90-15718

INEQUALITIES
A basic theorem of complementarity for the generalized variational-like inequality problem
[DE90-003102] N90-15620
Two basic partial orderings for distributions derived from Schur functions and majorization
[AD-A213703] N90-15682

INERTIA
On the identification of local minimizers in inertia-controlling methods for quadratic programming
[DE89-017330] N90-15616

INERTIAL CONFINEMENT FUSION
The search for solid state fusion lasers
[DE89-012301] N90-15410

INFORMATION FLOW
A signal processing language for coarse grain data flow multiprocessors
[AD-A213863] N90-15635

INFORMATION PROCESSING (BIOLOGY)
The application of queuing theory to the modelling of CP-140 aircraft communications
[AD-A213479] N90-15310
The components of scientific visualization
[DE90-001992] N90-15614
Numerical facility: Convergence of cognitive and factor analytic models
[AD-A213627] N90-15680
INFORMATION RETRIEVAL
Identification and quantification of synoptic structure in simulated TIROS N radiance soundings
[AD-A213729] N90-15553
Reconfigurable N-dimensional computer memory
[AD-D014309] N90-15607
A comparative evaluation and analysis of end-user search performance in an academic environment
N90-15845
Alternative representations for database responses
N90-15847
Procurement of an optical disk information storage and retrieval system
[DE90-001372] N90-15849
INFORMATION SYSTEMS
DOCTORD Database System user's guide, June 1989: dBase 3 PLUS Physician/(Part B Medicare): Personal computer reference system and user's guide
[PB90-100181] N90-15579
INFORMATION TRANSFER
Research in optical interconnection techniques
[AD-A214028] N90-15739
INFRARED ASTRONOMY SATELLITE
Image enhancement using the IRAS (Infrared Astronomy Satellite) survey data
[AD-A213811] N90-15496
INFRARED IMAGERY
High resolution imaging by phase retrieval and discrimination using speckle, volume 1
[AD-A214243] N90-15317
Measurement of optical radiations in spacecraft environments
[AD-A213814] N90-15497
Evaluation of a simple algorithm for estimating infrared signatures from multi-pixel to sub-pixel targets applied to AGA thermovision imagery
[AD-A214103] N90-15639
INFRARED INSTRUMENTS
Solid-state phase equilibria in the ZnS-Ga2S3 system
[AD-A213944] N90-15238
INFRARED LASERS
Laser detection and discrimination system
[AD-D014301] N90-15426
INFRARED RADIATION
Solid-state phase equilibria in the ZnS-Ga2S3 system
[AD-A213944] N90-15238
Description of SHARC: The Strategic High-Altitude Radiance Code
[AD-A213806] N90-15555
Anomalous absorption by atmospheric water vapor and stabilized water fogs in the infrared and CM-wave regions
[AD-A214202] N90-15572
INFRARED SIGNATURES
Evaluation of a simple algorithm for estimating infrared signatures from multi-pixel to sub-pixel targets applied to AGA thermovision imagery
[AD-A214103] N90-15639
INFRARED SPECTROSCOPY
Outlier detection in multivariate calibration
[DE90-001502] N90-15672
INJECTORS
Extended temperature range rocket injector
[NASA-CASE-LEW-14846-1] N90-15130
INORGANIC COMPOUNDS
Ceramic processing using inorganic polymers
[DE90-003638] N90-15268
INSPECTION
Component presence-absence detection for automated visual inspection of hybrid microcircuits
[KCP-613-4050] N90-15335
Back to basics
[DE90-002734] N90-15463
INSTALLING
Epoxy-resin cable terminations
[AD-A213789] N90-15454
INSTRUMENT FLIGHT RULES
Improved lighting of taxiway/taxiway intersections for Instrument Flight Rules (IFR) operations
[DOT/FAA/CT-TN89/64] N90-15089
INSULATION
Resultant forces and moments in completely restrained plates subjected to a recovery temperature varying linearly with time
[ESDU-89024] N90-15480
Thermal stresses in unrestrained plates subjected to a recovery temperature varying linearly with time
[ESDU-89025] N90-15481
Theoretical and computational studies of magnetic insulation and other plasma-opening-switch phenomena
[DE90-004421] N90-15757
Temperatures in plates subjected to a recovery temperature varying linearly with time
[ESDU-89023] N90-15831
INSULATORS
Fabrication of superconductor coils
[DE90-003571] N90-15338
INTEGRAL EQUATIONS
An alternative derivation for an integral equation for linearized subsonic flow over a wing
[AD-A214140] N90-15079
INTEGRATED CIRCUITS
Computer aided design of monolithic microwave and millimeter wave integrated circuits and subsystems
[AD-A213656] N90-15343
Research on GaAs quantum-coupled structures that can be used as electron devices
[AD-A214015] N90-15350
VLSI theory and parallel supercomputing
[AD-A214035] N90-15351
A study of Inter-Injection-Locked phased arrays
[AD-A214097] N90-15352
Characteristics of CMOS analog integrated structures using MOSIS (Metal Oxide Semiconductor Implementation System)
[DE90-001630] N90-15773
Solid state research
[AD-A213405] N90-15806
INTELLECT
Numerical facility: Convergence of cognitive and factor analytic models
[AD-A213627] N90-15680
INTELLIGENCE
The components of scientific visualization
[DE90-001992] N90-15614
INTELLIGIBILITY
Dual task performance with LPC (Linear Predictive Coding) degraded speech in a sentence verification task
[AD-A214298] N90-15320
INTERFACES
Display interface concepts for automated fault diagnosis
[NASA-TM-101610] N90-15102
Rayleigh-Taylor instability in compressible fluids
[DE90-003027] N90-15376
Laser-material interactions
[AD-A214421] N90-15425
High temperature, flexible, thermal barrier seal
[NASA-CASE-LEW-14672-1] N90-15444
Interfacial systems for photochemical energy conversion
[DE90-003181] N90-15514
Interface phonons in semiconductor double heterostructures
[AD-A213732] N90-15810
INTERFEROMETERS
Fiber optic sensing system
[NASA-CASE-LEW-14795-1] N90-15733
INTERMETALLICS
Exchange coupling in metals as understood then and now
[DE90-001271] N90-15214
Selection of phase-change and containment materials for thermal energy storage
[NASA-CR-186228] N90-15506
Deformation twinning in ordered intermetallic compounds
[DE89-014779] N90-15767
Molecular-dynamics study of the amorphization of CuTi
[DE90-003563] N90-15791
INTERNAL COMBUSTION ENGINES
Comparison of engine knock predictions using a fully-detailed and a reduced chemical kinetic mechanism
[DE90-002805] N90-15448
Multi-dimensional modeling of convective heat transfer with application to I.C. engines
[DE90-003245] N90-15451
INTERNATIONAL COOPERATION
International aspects of restrictions of ozone-depleting substances
[DE90-001813] N90-15534
Prospects for space arms control
[DE90-003392] N90-15700
INTERPLANETARY DUST
Near-infrared polarimetry and spectroscopy of comets
N90-15857
INTERPLANETARY FLIGHT
Manned spacecraft
[AD-A214218] N90-15129
INTERPLANETARY MAGNETIC FIELDS
Laboratory simulations of the solar wind-comet interactions N90-15875
INTERSECTIONS
Improved lighting of taxiway/taxiway intersections for Instrument Flight Rules (IFR) operations
[DOT/FAA/CT-TN89/64] N90-15089
INTERSTELLAR MATTER
The disk-halo connection and the nature of the interstellar medium
[NASA-CR-186286] N90-15860
The volatile composition of comets
[NASA-CR-186281] N90-15871
INTRUSION
Micromechanics of an extrusion in high-cycle fatigue with creep
[AD-A213509] N90-15485
INVARIANCE
Modular invariants for theta-functions with characteristics and the twisted N=2 superconformal and SU(2) Kac-Moody algebras
[DE89-635701] N90-15671
INVISCID FLOW
Dynamics of a class of vortex rings N90-15362
IODINE
Spatially-resolved, nonintrusive measurements in a nonreacting scramjet combustor using laser-induced iodine fluorescence N90-15103
ION BEAMS
Surface modification of metals by ion beams
[DE90-001285] N90-15218
Surface roughening of Ge(001) during 200 eV Xe ion bombardment and Ge molecular beam epitaxy
[DE90-000674] N90-15769
Computer-controlled ion beam sputter-deposition of superconducting oxide films
[AD-A213921] N90-15812
ION EMISSION
RAIDS: An orbiting observatory for ionospheric remote sensing from space
[AD-A213717] N90-15494
ION EXCHANGE MEMBRANE ELECTROLYTES
An assessment and comparison of fuel cells for transportation applications
[DE90-001807] N90-15508
ION IMPLANTATION
Surface engineering by high energy beams
[DE90-001296] N90-15250
ION IRRADIATION
Ion-irradiation effects in Tl2Ca2Ba2Cu3O10 superconductors
[DE90-003840] N90-15802
ION PROPULSION
Propulsion research on the hybrid plume rocket
[AD-A214420] N90-15132
ION TRAPS (INSTRUMENTATION)
Analysis of ambient polar volatile organic compounds using chemical ionization-ion trap detector
[PB90-106451] N90-15529
IONIC MOBILITY
Transport processes through monomolecular films
[AD-A213609] N90-15342
IONIZATION
Analysis of ambient polar volatile organic compounds using chemical ionization-ion trap detector
[PB90-106451] N90-15529
IONIZATION CROSS SECTIONS
Investigations of the interactions of radiation with matter
[AD-A213554] N90-15723
IRON
Metal film coatings on amorphous metallic alloys
[AD-D014308] N90-15240
Two-dimensional magnetic phase transition of ultrathin iron films on Pd(100)
[DE90-003555] N90-15788
Epitaxial iron films
[AD-A213551] N90-15807
IRON ALLOYS
Energetics of BCC-FCC lattice deformation in iron
[AD-A213801] N90-15233
IRRADIATION
Microstructural evolution of martensitic steels during fast neutron irradiation
[DE89-016231] N90-15212
Helium-induced weld cracking in irradiated 304 stainless steel
[DE90-001312] N90-15219
Optical properties and laser damage measurements of inorganic polymer films
[DE90-003633] N90-15267
Fusion reactor materials
[DE90-000976] N90-15744
Irradition-induced grain growth: Role of dislocations
[DE90-003565] N90-15792

IRREVERSIBLE PROCESSES
Irreversible processes from reversible mechanics
[DE90-001057] N90-15368
ISOTOPE SEPARATION
Isotopic selectivity of surface diffusion: An activated diffusion model
[DE90-003473] N90-15169
ISOTOPES
On the free carrier-negative U center interacting model for the high-T(sub c) oxide superconductor
[DE89-635908] N90-15775
ISOTROPY
Turbulence spectral widths view angle independence as observed by Doppler radar
[DOT/FAA/SA-89/2] N90-15566
ITERATION
An iterative Bayes procedure for reliability assessment
[DE90-002106] N90-15486
Tensor methods for unconstrained optimization using second derivatives
[AD-A213642] N90-15681
Parameter estimation of linear systems in the presence of process noise using the maximum liklihood method
[ESDU-89032] N90-15693
ITERATIVE SOLUTION
Structure properties of confined systems. Hard spheres between ideal walls
[DE90-600818] N90-15378

J

J INTEGRAL
Experience with J testing of 304/308 stainless steel weldment
[DE90-002046] N90-15478
JAPAN
Automation and robotics in construction: Japanese research and development
[AD-A214170] N90-15456
JET AIRCRAFT NOISE
Dynamics of a class of vortex rings N90-15362
JET ENGINE FUELS
Thermal stability of jet fuel
[DE90-002760] N90-15288
Fundamental mechanism of atomization
[AD-A213859] N90-15293
JET ENGINES
Characterization of chemicals on engine exhaust particles
[AD-A213566] N90-15106
JOINED WINGS
Application of the joined wing to tiltrotor aircraft
[NASA-CR-177543] N90-15093
JOURNAL BEARINGS
Thermal analysis of fixed and tilting pad journal bearings including cross-film viscosity variations and deformations N90-15429

K

KALMAN FILTERS
Centralized and decentralized Kalman filter techniques for tracking, navigation, and control
[AD-A214245] N90-15091
KINEMATICS
New approach to the inverse problem of six-link manipulators via the optimization technique
[DE90-710044] N90-15441
Spatial dynamics of deformable multibody systems with variable kinematic structure
[AD-A214098] N90-15455
Architectural study of the design and operation of advanced force feedback manual controllers
[NASA-CR-185948] N90-15664
KINETIC ENERGY
Flux parameterization techniques in the atmospheric surface layer N90-15548
KINETICS
Critical temperature analysis for a hemispherical charge of a binary explosive
[DE90-001447] N90-15282
Statistical model for particle-void deformation kinetics in granular materials during shock wave propagation
[DE89-017729] N90-15476
KNOWLEDGE REPRESENTATION
Principles and algorithms for causal reasoning with uncertainty
[AD-A214248] N90-15644
A structured connectionist approach to direct inferences and figurative adjective-noun combinations
[AD-A214326] N90-15649

L

LAGRANGE MULTIPLIERS
Neural network models for linear programming
[DE89-015974] N90-15651
LAKES
Global lake-level variations from 18,000 to 0 years ago: A palaeoclimate analysis
[DE90-000998] N90-15531
LAMINAR BOUNDARY LAYER
Unsteady three-dimensional thin-layer Navier-Stokes solutions on dynamic blocked grids N90-15069
A direct-inverse method for transonic and separated flows about airfoils
[NASA-CR-4270] N90-15072
Experimental measurements of the laminar separation bubble on an Eppler 387 airfoil at low Reynolds numbers
[NASA-CR-186263] N90-15380
LAMINAR FLOW
Laminar forced convection inside externally finned tubes
[DE89-636431] N90-15373
Time-dependent free convection in low Prandtl number fluids
[DE90-003053] N90-15377
LAMINAR HEAT TRANSFER
Time-dependent free convection in liquid metals
[DE90-000957] N90-15366
LAMINATES
Effects of aeroelastic tailoring on anisotropic composite material beam models of helicopter blades
[AD-A213478] N90-15095
A study of impact damage in composite laminates N90-15137
Mechanical behavior of laminated composites at elevated temperatures N90-15141
Transverse (through-the-thickness) shear stiffnesses of fibre reinforced composite laminated plates (computer program)
[ESDU-89013] N90-15152
Two dimensional laminated shell theory including parabolic transverse shear
[AD-A213817] N90-15487
LANDFORMS
Dynamics of mid-ocean ridge systems N90-15575
LANDING
Relative merits of reactive and forward-look detection for wind-shear encounters during landing approach for various microburst escape strategies
[NASA-TM-4158] N90-15108
LANDING SIMULATION
Wind shear models for aircraft hazard investigation N90-15044
LANTHANUM COMPOUNDS
Linear electron-hole-electron pair model of high-temperature superconductivity in La(2-x)M(x)CuO4 and YBa2Cu3O(7-y): Part 2. Dependence of the superconducting transition temperatures on pressure and on hole concentration
[DE90-003012] N90-15779
LASER APPLICATIONS
Laser mixing of titanium on silicon carbide
[DE90-003216] N90-15150
China-built airborne synchronous laser ranger the new L-8 jet trainer aircraft
[AD-A213835] N90-15422
Gas optics applicable to free electron laser technology
[AD-A214285] N90-15741
LASER BEAMS
Analysis and evaluation of technical data on the photochromic and non-linear optical properties of materials. Appendix: Eye/sensor protection by an optical fuse mirror at a focal plane: Feasibility assessment
[AD-A214051] N90-15177
Analysis and evaluation of technical data on the photochromic and non-linear optical properties of materials
[AD-A214212] N90-15178
Surface engineering by high energy beams
[DE90-001296] N90-15250
High resolution imaging by phase retrieval and discrimination using speckle, volume 1
[AD-A214243] N90-15317
Frequency shift induced in laser pulses by plasma density variations
[AD-A214195] N90-15424
Aerosol heating and vaporization of high-flux laser beams
[DE90-003471] N90-15428
Microfluctuations of plasma density in a theta-pinch and spatial coherency of a probing laser beam
[DE90-603347] N90-15760
LASER CAVITIES
Gas optics applicable to free electron laser technology
[AD-A214285] N90-15741
LASER DAMAGE
Analysis and evaluation of technical data on the photochromic and non-linear optical properties of materials. Appendix: Eye/sensor protection by an optical fuse mirror at a focal plane: Feasibility assessment
[AD-A214051] N90-15177
Analysis and evaluation of technical data on the photochromic and non-linear optical properties of materials
[AD-A214212] N90-15178
Optical properties and laser damage measurements of inorganic polymer films
[DE90-003633] N90-15267
Laser-induced surface ablation and optical damage of ZnS crystals caused by single- and multiple-pulse laser-irradiation
[DE90-003807] N90-15419
LASER FUSION
The 17th AINSE Plasma Physics Conference: Conference handbook
[DE90-600936] N90-15759
LASER INDUCED FLUORESCENCE
Spatially-resolved, nonintrusive measurements in a nonreacting scramjet combustor using laser-induced iodine fluorescence N90-15103
Surface thermometry of energetic materials by laser-induced fluorescence
[AD-A214423] N90-15297
Kinetic studies following state-selective laser excitation
[DE90-003232] N90-15415
Observation of atomic relaxation near an interface through detection of emitted fluorescence
[AD-A214308] N90-15725
LASER MATERIALS
Development of glass-ceramic lasers
[AD-A214146] N90-15423
Host materials for transition-metal ions
[AD-A213605] N90-15808
LASER OUTPUTS
The 17.1-GHz free-electron laser as a microwave source for TeV colliders
[DE90-001506] N90-15406
Fiber optic sensing system
[NASA-CASE-LEW-14795-1] N90-15733
Aspects of Raman scattering
[AD-A213926] N90-15736
LASER PLASMA INTERACTIONS
Computer simulation of laser plasma interaction
[DE90-002828] N90-15748
LASER PLASMAS
The search for solid state fusion lasers
[DE89-012301] N90-15410
Computer simulation of laser plasma interaction
[DE90-002828] N90-15748
LASER POWER BEAMING
The Solar Power Satellite (SPS): Progress so far N90-15840
LASER PROPULSION
Laser-supported detonation waves and pulsed laser propulsion
[DE90-002753] N90-15412
LASER RANGE FINDERS
China-built airborne synchronous laser ranger the new L-8 jet trainer aircraft
[AD-A213835] N90-15422
LASER SPECTROSCOPY
The production and spectroscopy of molecular ions isolated in solid neon
[AD-A213723] N90-15174
LASER TARGETS
NTES (Nuclear Test and Experimental Sciences) program laser facility for physics experiments Building 391 High Bay Option
[DE90-001795] N90-15411
LASER WELDING
Heat treatment of pulsed Nd: YAG laser welds in a Ti-14.8 wt pct Al-21.3 wt pct Nb titanium aluminide
[DE90-003484] N90-15228
LASERS
High power density spray cooling
[AD-A213575] N90-15386
NTES (Nuclear Test and Experimental Sciences) program laser facility for physics experiments Building 391 High Bay Option
[DE90-001795] N90-15411
Optical guiding by plasma waves in the plasma beat wave accelerator
[AD-A214288] N90-15763
Innovative optoelectronic materials and structures using OMVPE
[AD-A214192] N90-15815
LATEX
Studies on some failure modes in latex barrier films
[PB89-209308] N90-15246

LATTICES (MATHEMATICS)
Designing machines for lattice physics and algorithm investigation
[DE90-003543] N90-15596
LAUNCH VEHICLES
Current launch vehicle reliability practice and data base assessment. Volume 1: Executive summary and report body
[AD-A213600] N90-15121
LAUNCHING
Shuttle-C utilization for assembly of the rephased Freedom configuration
[NASA-TM-101658] N90-15120
Laser-supported detonation waves and pulsed laser propulsion
[DE90-002753] N90-15412
Mechanical design of the inside launch system for electron cyclotron heating in D3-D
[DE90-003292] N90-15751
LAW (JURISPRUDENCE)
Congressional involvement and relations: A guide for Department of Defense acquisition managers
[AD-A214408] N90-15855
LAY-UP
Transverse (through-the-thickness) shear stiffnesses of fibre reinforced composite laminated plates (computer program)
[ESDU-89013] N90-15152
LEAD ACID BATTERIES
Status and results of ANL life evaluation of valve-regulated lead-acid load-leveling batteries
[DE90-001918] N90-15329
Life evaluation of valve-regulated lead-acid batteries for load-leveling applications
[DE90-002188] N90-15336
LEAD ALLOYS
Isothermal fatigue behavior of Sn-Pb solar joints
[DE90-003280] N90-15464
LEAD TELLURIDES
Bridgman crystal growth
[NASA-CR-186204] N90-15766
LEADERSHIP
Human behavior
[PB90-780008] N90-15584
LEAST SQUARES METHOD
Outlier detection in multivariate calibration
[DE90-001502] N90-15672
LEGUMINOUS PLANTS
Variability of cultivar responses to ozone
[PB89-225460] N90-15528
LENS DESIGN
Binary optics technology: The theory and design of multi-level diffractive optical elements
[AD-A213404] N90-15735
LENSES
A scheiner-principle vernier optometer
[AD-D014304] N90-15405
Binary optics technology: The theory and design of multi-level diffractive optical elements
[AD-A213404] N90-15735
Gas optics applicable to free electron laser technology
[AD-A214285] N90-15741
LIBRARIES
The StarLite project
[AD-A214193] N90-15642
LIE GROUPS
Continuum analogues of contragredient Lie algebras: Lie algebras with a Cartan operator and nonlinear dynamical systems
[DE89-635698] N90-15691
Nijenhuis tensor and integrable models
[DE90-001403] N90-15702
Lefschetz trace formula and BRST
[DE89-635705] N90-15835
LIFE (DURABILITY)
Status and results of ANL life evaluation of valve-regulated lead-acid load-leveling batteries
[DE90-001918] N90-15329
LIFE SCIENCES
Space operations: Listing of NASA scientific missions, 1980-2000. Fact sheet for the Chairman, Subcommittee on Space Science and Applications, Committee on Science, Space, and Technology, House of Representatives
[AD-A213493] N90-15881
LIFT
A direct-inverse method for transonic and separated flows about airfoils
[NASA-CR-4270] N90-15072
The maximum lift coefficient of plain wings at subsonic speeds
[ESDU-89034] N90-15082
Serrated trailing edges for improving lift and drag characteristics of lifting surfaces
[NASA-CASE-LAR-13870-1] N90-15094
LIFT DEVICES
Installed tailplane lift-curve slope at subsonic speeds
[ESDU-89029] N90-15081
The maximum lift coefficient of plain wings at subsonic speeds
[ESDU-89034] N90-15082
Serrated trailing edges for improving lift and drag characteristics of lifting surfaces
[NASA-CASE-LAR-13870-1] N90-15094
LIFTING BODIES
Unsteady aerodynamics of oscillating and rapidly pitched airfoils N90-15074
LIGHT EMITTING DIODES
Fiber optic sensing system
[NASA-CASE-LEW-14795-1] N90-15733
LIGHT GAS GUNS
Design limitations on ultra-high velocity projectile launchers
[DE89-012933] N90-15118
LIGHT MODULATION
Research on materials and components for opto-electronic signal processing and computing
[AD-A213740] N90-15811
LIGHT SCATTERING
Research on acoustical scattering, diffraction catastrophes, optics of bubbles, acoustical phase conjugation, and wake of an oscillating circular cylinder
[AD-A214168] N90-15711
SBS (Stimulated Brillouin Scattering) pulse distortion in multimode optical fibers: Preliminary results
[DE90-003023] N90-15731
The middle Martian atmosphere N90-15874
LIGHT TRANSMISSION
Solid-state phase equilibria in the ZnS-Ga2S3 system
[AD-A213944] N90-15238
Nonlinear optical material studies
[AD-A213938] N90-15737
LIGHTNING
Effects of lightning on operations of aerospace vehicles N90-15055
Principal characteristics of lightning on aircraft N90-15067
Characteristics of electromagnetic wave forms with lightning in winter season
[DE89-901256] N90-15567
LIKELIHOOD RATIO
Likelihood ratio derivative estimators for stochastic systems
[AD-A213787] N90-15684
LINEAR ACCELERATORS
The 17.1-GHz free-electron laser as a microwave source for TeV colliders
[DE90-001506] N90-15406
LINEAR EQUATIONS
Mixed singular linear elliptic equations
[DE90-600722] N90-15674
LINEAR FILTERS
Higher order crossings from a parametric family of linear filters
[AD-A213427] N90-15676
LINEAR PREDICTION
Dual task performance with LPC (Linear Predictive Coding) degraded speech in a sentence verification task
[AD-A214298] N90-15320
LINEAR PROGRAMMING
The parallel decomposition of linear programs
[DE90-003538] N90-15625
Neural network models for linear programming
[DE89-015974] N90-15651
A neural network for bounded linear programming
[DE89-015975] N90-15652
Polynomial transfer lot sizing techniques for batch processing on consecutive machines
[AD-A214198] N90-15660
Numerical optimization
[AD-A213758] N90-15683
LINEAR SYSTEMS
Parameter estimation of linear systems in the presence of process noise using the maximum liklihood method
[ESDU-89032] N90-15693
LINGUISTICS
Knowledge based text generation
[AD-A214273] N90-15645
LINKAGES
A procedure for force-balancing planar linkages using counterweights
[ESDU-89028] N90-15446
LIPIDS
Transport processes through monomolecular films
[AD-A213609] N90-15342
LIQUID CHROMATOGRAPHY
Compensation for peak shifts and variable background responses in fluorescence spectroscopy
[DE90-001102] N90-15154
High-temperature gel-permeation chromatography of poly(4-methyl-1-pentene)
[DE90-002967] N90-15159
LIQUID CRYSTALS
Optical solitons in liquid crystals
[DE90-000694] N90-15728
LIQUID FLOW
Pipeline vibrations. Fluid transients in non-rigid, unbranched planar piping systems
[ESDU-89030] N90-15491
LIQUID METAL FAST BREEDER REACTORS
Static pressure distribution in an angular channel with helicoidal wire
[DE89-636474] N90-15374
LIQUID METALS
Electron theory of long wavelength concentration fluctuations in liquid metal alloys
[DE89-636213] N90-15225
Dynamical structure of liquid and amorphous metals
[DE90-003805] N90-15229
Time-dependent free convection in liquid metals
[DE90-000957] N90-15366
Time-dependent free convection in low Prandtl number fluids
[DE90-003053] N90-15377
LIQUID PHASES
Survey on synthesis technologies of methanol as an alternative fuel
[DE89-901303] N90-15284
LIQUID ROCKET PROPELLANTS
Extended temperature range rocket injector
[NASA-CASE-LEW-14846-1] N90-15130
LIQUID-GAS MIXTURES
Gas-liquid-liquid equilibria in mixtures of water, light gases, and hydrocarbons
[DE90-003180] N90-15167
LIQUID-LIQUID INTERFACES
Gas-liquid-liquid equilibria in mixtures of water, light gases, and hydrocarbons
[DE90-003180] N90-15167
LIQUID-VAPOR EQUILIBRIUM
Gas-liquid-liquid equilibria in mixtures of water, light gases, and hydrocarbons
[DE90-003180] N90-15167
LIQUID-VAPOR INTERFACES
Transport processes through monomolecular films
[AD-A213609] N90-15342
LIQUIDS
Structure properties of confined systems. Hard spheres between ideal walls
[DE90-600818] N90-15378
LITHIUM
Heat transfer in condensation of lithium vapors
[DE90-002081] N90-15375
LITHIUM ALLOYS
New Light Alloys
[AGARD-CP-444] N90-15185
Al-Li alloy developed by Pechiney N90-15186
The microstructure and properties of aluminum-lithium alloys N90-15187
Mechanical properties and fracture toughness of 8090-T651 plate and 2091 and 8090 sheet N90-15188
Fatigue properties of Al-Li alloys N90-15189
Corrosion and stress corrosion of aluminium-lithium alloys N90-15190
Properties of Al-Li alloys N90-15191
Investigation on sheet material of 8090 and 2091 aluminium-lithium alloy N90-15192
Aluminum lithium alloys for Navy aircraft N90-15193
Fatigue, fracture mechanics and corrosion properties of some aluminium-lithium alloys N90-15194
Fatigue and fracture behaviour of a PM Al-Li alloy N90-15195
Fabrication of test-articles from Al-Li 2091 for Fokker 100 N90-15196
Putting alloy 2091 to work N90-15197
Fabrication characteristics of 8090 alloy N90-15198
Superplastic performance and properties of the Lital Alloys N90-15199
Point of view of a civil aircraft manufacturer on Al-Li alloy N90-15200
Uses and properties of Al-Li on the new EH101 helicopter N90-15201
Aluminum-lithium: Application of plate and sheet to fighter aircraft N90-15202
Current status of the application of conventional aluminium-lithium alloys and the potential for future developments N90-15203
Rechargable molten-electrolyte lithium batteries
[DE90-003774] N90-15339
LITHIUM COMPOUNDS
Spectroscopic and laser properties of Cr:LiCaAlF6 and Cr:LiSrAlF6 crystals
[DE90-000783] N90-15770

LITHIUM SULFUR BATTERIES
Novel high-rate, all solid-state, sodium and lithium/organosulfur batteries
[DE90-001014] N90-15325
LITHOSPHERE
Dynamics of mid-ocean ridge systems N90-15575
LOAD TESTING MACHINES
Fully articulated four-point-bend loading fixture
[NASA-CASE-LEW-14776-1] N90-15445
LOAD TESTS
Characterization and in situ testing of diamond films
[DE90-003155] N90-15265
LOADS (FORCES)
Design of a custom load cell for a precision assembly application
[DE90-004439] N90-15340
Investigation of loads generated by temperature transients in pipes
[DE89-636433] N90-15395
Single element magnetic suspension actuator
[NASA-CASE-LAR-13981-1] N90-15442
A procedure for force-balancing planar linkages using counterweights
[ESDU-89028] N90-15446
Fatigue loading history reconstruction based on the rain-flow technique
[NASA-CR-181942] N90-15482
LOCAL AREA NETWORKS
Voice Multiplex System (VMS)
[AD-A213902] N90-15315
LLNL's plan for a prototype circuit switch, a potential gigabit LAN of the future
[DE90-003614] N90-15597
LOCOMOTION
Planning systems for autonomous legged vehicles
[AD-A214242] N90-15458
LOGIC DESIGN
A logic for the pixel assignment step of imagery classification predicated on class structure N90-15493
Principles and algorithms for causal reasoning with uncertainty
[AD-A214248] N90-15644
LOGIC PROGRAMMING
Research in mathematics and computer science at Argonne
[DE90-000975] N90-15595
LOGISTICS MANAGEMENT
Program manager's handbook
[AD-A214338] N90-15844
LONGITUDINAL WAVES
On strongly nonlinear vortex/wave interactions in boundary-layer transition
[NASA-CR-181963] N90-15078
LOOP ANTENNAS
Characteristics of electromagnetic wave forms with lightning in winter season
[DE89-901256] N90-15567
LOOPS
Portable digital pressure indicator for calibrating magnetic tape recorders
[NASA-TM-101650] N90-15401
LOW MOLECULAR WEIGHTS
Crosslinked, flexible, low-molecular-weight polyacrylamide gels for mobility control
[DE90-000202] N90-15280
LOW PASS FILTERS
Adaptive canceller limitations caused by I,Q mismatch errors
[AD-A214287] N90-15318
LOW VISIBILITY
Flight in Adverse Environmental Conditions
[AGARD-CP-470] N90-15041
LOWER BODY NEGATIVE PRESSURE
Use of lower body negative pressure as a countermeasure to negative Gz acceleration
[AD-A213927] N90-15583
LUBRICATION
Solid lubrication of ceramic surfaces by IAD (Ion-Assisted Deposition)-silver coatings for heat engine applications
[DE90-002860] N90-15253
Analysis of an elastohydrodynamic lubricated point contact: User's manual
[AD-A214257] N90-15459
LUMINAIRES
Improved lighting of taxiway/taxiway intersections for Instrument Flight Rules (IFR) operations
[DOT/FAA/CT-TN89/64] N90-15089
LUNAR BASES
Lunar construction utility vehicle
[NASA-CR-186231] N90-15435
Lunar power system summary of studies for the lunar enterprise task force NASA-office of exploration N90-15841
Transportation and operations aspects of space energy systems N90-15842
A quasi-economic role for lunar science
[DE90-000679] N90-15876
LUNAR PROGRAMS
Lunar construction utility vehicle
[NASA-CR-186231] N90-15435
LUNAR SOIL
Report of NASA Lunar Energy Enterprise Case Study Task Force
[NASA-TM-101652] N90-15836
Report of the NASA lunar energy enterprise case study task force N90-15837
Importance of helium-3 for the future N90-15843
LUNAR SURFACE
Report of NASA Lunar Energy Enterprise Case Study Task Force
[NASA-TM-101652] N90-15836
Report of the NASA lunar energy enterprise case study task force N90-15837
Analysis of the financial factors governing the profitability of lunar helium-3 N90-15838
Transportation and operations aspects of space energy systems N90-15842
LUNAR SURFACE VEHICLES
Lunar construction utility vehicle
[NASA-CR-186231] N90-15435

M

MACHINING
An analysis of drilling of composite materials N90-15142
MAGELLANIC CLOUDS
The South African Astronomical Observatory
[NASA-CR-186258] N90-15856
MAGNESIUM ALLOYS
New Light Alloys
[AGARD-CP-444] N90-15185
Magnesium alloy technology for aerospace applications N90-15209
Cryogenic mechanical properties of low density superplastic Al-Mg-Sc alloys
[DE90-002120] N90-15222
MAGNESIUM OXIDES
Processing and properties of nanophase oxides
[DE90-003826] N90-15171
Laser detection and discrimination system
[AD-D014301] N90-15426
MAGNET COILS
Retractable gas cooled leads for ASTROMAG
[DE90-002679] N90-15331
Fabrication of superconductor coils
[DE90-003571] N90-15338
MAGNETIC COMPRESSION
Design of a high-gain flux-compression generator
[DE90-002795] N90-15333
The 17th AINSE Plasma Physics Conference: Conference handbook
[DE90-600936] N90-15759
MAGNETIC COOLING
Feasibility analysis of reciprocating magnetic heat pumps
[NASA-CR-186205] N90-15363
MAGNETIC CORES
Tuned-circuit Johnson noise thermometry
[DE89-016221] N90-15356
MAGNETIC FIELD CONFIGURATIONS
Studies of plasma performance and transport in the Advanced Toroidal Facility (ATF)
[DE90-001737] N90-15746
Initial results from FRC (Field-Reversed Configuration) compression experiments on FRX-C/LSM
[DE90-003390] N90-15754
MAGNETIC FIELDS
SCATHA (Spacecraft Charging at High Altitudes) atlas data base, volume 1
[AD-A214204] N90-15127
SCATHA (Spacecraft Charging At High Altitudes) atlas data base, volume 2
[AD-A214205] N90-15128
Exchange coupling in metals as understood then and now
[DE90-001271] N90-15214
Anharmonic betatron motion in free electron lasers
[DE90-001515] N90-15407
Theory of interacting plasmas in space N90-15742
Simulation of radial expansion of an electron beam injected into a background plasma
[NASA-CR-186188] N90-15743
Intense REB (Relativistic Electron Beam) transport in a weakly magnetized plasma
[DE90-002978] N90-15749
Initial results from FRC (Field-Reversed Configuration) compression experiments on FRX-C/LSM
[DE90-003390] N90-15754
Theoretical and computational studies of magnetic insulation and other plasma-opening-switch phenomena
[DE90-004421] N90-15757
Near-surface sputtered particle transport for an oblique incidence magnetic field plasma
[DE90-004422] N90-15758
A numerical simulation model for the study of magnetohydrodynamic (MHD) waves in a structured medium N90-15864
MAGNETIC FILMS
Epitaxial iron films
[AD-A213551] N90-15807
MAGNETIC FLUX
Design of a high-gain flux-compression generator
[DE90-002795] N90-15333
Magnetic flux pinning in YBa2Cu3O7 films
[DE90-003709] N90-15799
Effects of non-linearity in the variation of pinning potential with current-density on magnetic flux creep in high and low T(sub c) superconductors
[DE90-003952] N90-15822
MAGNETIC MIRRORS
Magnetic mirror confinement concepts system studies
[DE90-003667] N90-15753
MAGNETIC PROBES
Development of NMR (Nuclear Magnetic Resonance) imaging probes for advanced ceramics
[DE90-003812] N90-15289
MAGNETIC PROPERTIES
Magnetic behavior of curium and americium-curium alloys
[DE89-017808] N90-15213
Magnetic viscosity in Ni/Cu compositionally-modulated alloys
[DE90-002303] N90-15223
Magnetic and electronic correlations in YBa2Cu3O(sub 6+x)
[DE89-017604] N90-15785
Two-dimensional magnetic phase transition of ultrathin iron films on Pd(100)
[DE90-003555] N90-15788
Magnetic mechanisms of high temperature superconductivity
[DE90-003625] N90-15796
Effects of non-linearity in the variation of pinning potential with current-density on magnetic flux creep in high and low T(sub c) superconductors
[DE90-003952] N90-15822
MAGNETIC RECORDING
Portable digital pressure indicator for calibrating magnetic tape recorders
[NASA-TM-101650] N90-15401
MAGNETIC STORMS
A calculation of energetic proton spectra producedat substorm onset in the fields of the explosive reconnection model N90-15866
MAGNETIC SUSPENSION
Single element magnetic suspension actuator
[NASA-CASE-LAR-13981-1] N90-15442
MAGNETIC TAPES
A signal realization data base generated by the multiple phase-screen method
[AD-A214004] N90-15852
MAGNETIC VARIATIONS
Physical process in MPD plasmas
[AD-A213679] N90-15761
MAGNETO-OPTICS
Laser glass (1989)
[DE90-002754] N90-15257
MAGNETOHYDRODYNAMIC STABILITY
Theory of interacting plasmas in space N90-15742
Destabilization of tokamak pressure-gradient driven instabilities by energetic alpha populations
[DE90-003716] N90-15756
Microfluctuations of plasma density in a theta-pinch and spatial coherency of a probing laser beam
[DE90-603347] N90-15760
MAGNETOHYDRODYNAMIC WAVES
Experiments on linear high beta helical axis stellarators to study simulated toroidal effects and Alfven-wave heating
[DE90-001704] N90-15745
The 17th AINSE Plasma Physics Conference: Conference handbook
[DE90-600936] N90-15759
A numerical simulation model for the study of magnetohydrodynamic (MHD) waves in a structured medium N90-15864
MAGNETOHYDRODYNAMICS
Computer controlled MHD power consolidation and pulse-generation system
[DE90-001224] N90-15662
A numerical simulation model for the study of magnetohydrodynamic (MHD) waves in a structured medium N90-15864

MAGNETOPLASMADYNAMICS
Physical process in MPD plasmas
[AD-A213679] N90-15761
MAGNETRON SPUTTERING
Metal film coatings on amorphous metallic alloys
[AD-D014308] N90-15240
MAIN SEQUENCE STARS
The age of the galactic disk
[NASA-CR-186292] N90-15869
MAINTENANCE
Life evaluation of valve-regulated lead-acid batteries for load-leveling applications
[DE90-002188] N90-15336
MANPRINT methods monograph: Aiding the development of manned system performance criteria
[AD-A213543] N90-15593
Tools for simulation-based training
[AD-A214307] N90-15646
Hierarchical process composition: Dynamic maintenance of structure in a distributed environment
[AD-A214325] N90-15648
MAINTENANCE TRAINING
Tools for simulation-based training
[AD-A214307] N90-15646
MAN MACHINE SYSTEMS
Task-oriented display design: Concept and example
[NASA-TM-101685] N90-15101
Automation and robotics in construction: Japanese research and development
[AD-A214170] N90-15456
SIMON (SuperIntelligent Mobile Observing Navigator): A high-reliability robot for a radiation environment
[DE90-003888] N90-15460
Model for measuring complex performance in an aviation environment
[DE90-002055] N90-15585
Architectural study of the design and operation of advanced force feedback manual controllers
[NASA-CR-185948] N90-15664
MAN-COMPUTER INTERFACE
Development of a robotics system for automated chemical analysis of sediment, sludges, and soils
[DE90-003637] N90-15170
The components of scientific visualization
[DE90-001992] N90-15614
MANAGEMENT METHODS
DOCTORD Database System user's guide, June 1989: dBase 3 PLUS Physician/(Part B Medicare): Personal computer reference system and user's guide
[PB90-100181] N90-15579
Guidelines for evaluating energy analysis software
[AD-A214171] N90-15640
MANAGEMENT PLANNING
Program manager's handbook
[AD-A214338] N90-15844
MANEUVERABILITY
Centralized and decentralized Kalman filter techniques for tracking, navigation, and control
[AD-A214245] N90-15091
MANGANESE ALLOYS
An investigation of the sensitization behavior of Fe-Mn-Cr austenitic steels
[DE90-002719] N90-15226
MANGANESE ISOTOPES
Cosmic ray half life of (54)Mn
[DE90-000134] N90-15880
MANGANESE OXIDES
Sintering studies on high field varistors
[DE90-002626] N90-15359
MANIFOLDS
Extended temperature range rocket injector
[NASA-CASE-LEW-14846-1] N90-15130
MANIFOLDS (MATHEMATICS)
Chern-Simons theories of symplectic super-diffeomorphisms
[DE89-635700] N90-15703
MANIPULATORS
Control of mechanical manipulators N90-15432
On the analysis and optimization of a platform manipulator N90-15433
New approach to the inverse problem of six-link manipulators via the optimization technique
[DE90-710044] N90-15441
Base reaction optimization of redundant manipulators for space applications
[NASA-CR-186274] N90-15447
Spatial dynamics of deformable multibody systems with variable kinematic structure
[AD-A214098] N90-15455
Feasibility study of using industrial robot for ultrasound testing
[DE90-002977] N90-15461
MANNED SPACECRAFT
Manned spacecraft
[AD-A214218] N90-15129
MANUAL CONTROL
Architectural study of the design and operation of advanced force feedback manual controllers
[NASA-CR-185948] N90-15664
MANUFACTURING
A strategy for concurrent product and process design of aerospace components
[DE90-002926] N90-15299
Back to basics
[DE90-002734] N90-15463
MANY BODY PROBLEM
Irreversible processes from reversible mechanics
[DE90-001057] N90-15368
General many-body systems
[DE90-000685] N90-15670
Relativistic self-consistent field studies of atoms and molecules
[AD-A214101] N90-15724
MAPPING
Surface thermometry of energetic materials by laser-induced fluorescence
[AD-A214423] N90-15297
China-built airborne synchronous laser ranger the new L-8 jet trainer aircraft
[AD-A213835] N90-15422
SIMON (SuperIntelligent Mobile Observing Navigator): A high-reliability robot for a radiation environment
[DE90-003888] N90-15460
Evolution of overlapping spreading centers: A Sea Mark 2 investigation
[AD-A214278] N90-15576
MAPS
Nonlinear maps with competitive interactions: Fixed-points, bifurcations, and chaotic attractors
[DE90-001858] N90-15695
MARINE ENVIRONMENTS
MF/HF multistatic mid-ocean radar experiment in support of SWOTHR (Surface-Wave Over-The-Horizon Radar)
[AD-A213830] N90-15314
Further research on dynamics of marine atmospheres in tropical cyclones
[AD-A213882] N90-15571
MARINE TECHNOLOGY
Design study of a modular gas-cooled, closed-brayton cycle reactor for marine use
[AD-A213453] N90-15518
MARKOV CHAINS
Likelihood ratio derivative estimators for stochastic systems
[AD-A213787] N90-15684
MARS ATMOSPHERE
The middle Martian atmosphere N90-15874
MARTENSITE
Microstructural evolution of martensitic steels during fast neutron irradiation
[DE89-016231] N90-15212
Heat treatment investigation of 4330 vanadium-modified steel
[AD-A214290] N90-15239
MARTENSITIC TRANSFORMATION
Energetics of BCC-FCC lattice deformation in iron
[AD-A213801] N90-15233
MASS DISTRIBUTION
A procedure for force-balancing planar linkages using counterweights
[ESDU-89028] N90-15446
MASS FLOW
Physical process in MPD plasmas
[AD-A213679] N90-15761
MASS FLOW FACTORS
Annual summary of basic research in thermoacoustic heat transport
[AD-A214185] N90-15834
MASS SPECTROMETERS
Strategic characteristics of Dynamics Explorer 1 retarding ion mass spectrometer and the consequences for core plasma measurements
[AD-A214013] N90-15125
MASS SPECTROSCOPY
Capillary electrophoresis ionization-mass spectrometry and tandem mass spectrometry
[DE90-002664] N90-15158
Analysis of ambient polar volatile organic compounds using chemical ionization-ion trap detector
[PB90-106451] N90-15529
MASS TRANSFER
Advanced study in solid transport: Rheological behavior of dense suspension
[DE90-003369] N90-15483
MASSIVELY PARALLEL PROCESSORS
Paralation views: Abstractions for efficient scientific computing on the connection machine
[AD-A213935] N90-15604
MATERIAL ABSORPTION
Phase equilibrium and crystal growth studies on AgGaSe2 and related nonlinear optical materials
[AD-A213650] N90-15809
MATERIALS RECOVERY
Managing the waste stream: Background information for planning source separation programs
[PB90-100223] N90-15530
MATHEMATICAL MODELS
Analysis of severe atmospheric disturbances from airline flight records N90-15045
Systems for airborne wind and turbulence measurement N90-15046
A pitch control law for compensation of the phugoid mode induced by windshears N90-15051
Aircraft response and pilot behaviour during a wake vortex encounter perpendicular to the vortex axis N90-15057
A numerical model for the axisymmetric equilibrium shape of drops in uniform motion: Effects of external flow, electric field and surface charge N90-15071
Numerical simulation of the unsteady two-dimensional flow in a time-dependent doubly-connected domain N90-15073
Modeling and control of the rapid deployment of towed airborne devices N90-15092
Error modeling of bias-type parameters for TOPEX orbit determination N90-15117
Propulsion research on the hybrid plume rocket
[AD-A214420] N90-15132
A tomographic study of premixed turbulent stagnation point flames
[DE90-002462] N90-15156
Steady flow combustion model for solid-fuel ramjet projectiles
[BRL-TR-2987] N90-15163
Shock tube ignition of octanes
[DE90-001167] N90-15164
Isotopic selectivity of surface diffusion: An activated diffusion model
[DE90-003473] N90-15169
The effects of Mo2C morphology and strain distribution on the fatigue properties of Fe-C-Mo dual-phase steels N90-15210
Ceramic technology for advanced heat engines project
[DE90-001852] N90-15251
The elastic properties of woven polymeric fabric
[DE89-015391] N90-15255
More efficient sensitivity testing
[DE90-002639] N90-15298
A strategy for concurrent product and process design of aerospace components
[DE90-002926] N90-15299
The application of queuing theory to the modelling of CP-140 aircraft communications
[AD-A213479] N90-15310
Design of a high-gain flux-compression generator
[DE90-002795] N90-15333
Numerical investigation of transition control of a flat plate boundary layer N90-15361
Development of an integrated BEM approach for hot fluid structure interaction
[NASA-CR-186214] N90-15364
Determination of flow-regime boundaries for cohesive particles
[DE90-001405] N90-15369
An algebraic turbulence model for flow separation caused by forward and backward facing steps
[AD-A213800] N90-15389
Aerosol heating and vaporization of high-flux laser beams
[DE90-003471] N90-15428
Control of mechanical manipulators N90-15432
Comparison of engine knock predictions using a fully-detailed and a reduced chemical kinetic mechanism
[DE90-002805] N90-15448
Multi-dimensional modeling of convective heat transfer with application to I.C. engines
[DE90-003245] N90-15451
Development of a rate independent plasticity theory for general cyclic loading N90-15471
Parametric identification of discrete time series models for structural response prediction N90-15472
Characterizing transient vibrations using band limited moments
[DE90-000799] N90-15473
Statistical model for particle-void deformation kinetics in granular materials during shock wave propagation
[DE89-017729] N90-15476
Analysis of catalytically enhanced solar absorption chemical reactors: 1 - numerical model description
[DE89-014742] N90-15505
Prediction of stochastic blade loads for three-bladed, rigid-hub rotors
[DE89-009508] N90-15520

Calculation of source and structure parameters at regional and teleseismic distances
[AD-A214297] N90-15558
Further research on dynamics of marine atmospheres in tropical cyclones
[AD-A213882] N90-15571
The application of optimal control theory for analysis of human jumping and pedaling N90-15590
CryoTran user's manual, version 1.0
[NASA-TM-102468] N90-15622
Knowledge based text generation
[AD-A214273] N90-15645
Neural network models for linear programming
[DE89-015974] N90-15651
Recurrence and ergodicity for exponential family state-space models
[AD-A213466] N90-15677
Numerical facility: Convergence of cognitive and factor analytic models
[AD-A213627] N90-15680
Queues with negative arrivals
[AD-A213860] N90-15687
Use of the linear variate method of Monte Carlo for estimating uncertainty in thermal-hydraulic codes
[DE89-017871] N90-15694
Theory of interacting plasmas in space N90-15742
Progress in LTE and non-LTE transport calculations
[DE90-003394] N90-15764
Bridgman crystal growth
[NASA-CR-186204] N90-15766
A numerical simulation model for the study of magnetohydrodynamic (MHD) waves in a structured medium N90-15864

MATRICES (MATHEMATICS)
A block QR factorization algorithm using restricted pivoting
[DE90-001921] N90-15613
An improved toeplitz approximation method
[AD-A213994] N90-15688
Canonical formalism for coupled beam optics
[DE90-003764] N90-15734

MATRIX MATERIALS
Effects of filament-matrix interfaces on the mechanical properties of SiC-reinforced Si3N4: A review
[DE90-001863] N90-15144
Metal matrix composites: A promising alternative to conventional alloys N90-15208

MATTER (PHYSICS)
Large scale calculations of the structure and dynamics of dense matter
[DE90-003654] N90-15726
Pulsars lost and found: The second Princeton-Arecibo millisecond pulsar search N90-15865
Recent progress in understanding the eruptions of classical novae
[NASA-CR-186280] N90-15870

MAXIMUM ENTROPY METHOD
Maximum entropy and equations of state for random cellular structures
[DE90-002840] N90-15827

MAXIMUM LIKELIHOOD ESTIMATES
Parameter estimation of linear systems in the presence of process noise using the maximum liklihood method
[ESDU-89032] N90-15693

MAXWELL EQUATION
The free energy of Maxwell-Vlasov equilibria
[DE90-003318] N90-15705

MAZE LEARNING
A note on the maximum size of a rectilinear maze
[AD-A214445] N90-15668

MEASURING INSTRUMENTS
The assessment of visibility from automatic contrast Measurements N90-15061

MECHANICAL DEVICES
On the motion of compliantly-connected rigid bodies in contact. Part 2: A system for analyzing designs for assembly
[AD-A214136] N90-15490

MECHANICAL DRIVES
Adjustable speed drive study, June 1985 to September 1988. Part 2: Appendices
[DE90-002771] N90-15332

MECHANICAL PROPERTIES
Fatigue properties of SiC/Al composites N90-15138
The mechanical behavior of a fiber-reinforced brittle matrix composite N90-15139
Mechanical behavior of laminated composites at elevated temperatures N90-15141
Effects of filament-matrix interfaces on the mechanical properties of SiC-reinforced Si3N4: A review
[DE90-001863] N90-15144
New Light Alloys
[AGARD-CP-444] N90-15185
Al-Li alloy developed by Pechiney N90-15186
The microstructure and properties of aluminum-lithium alloys N90-15187
Mechanical properties and fracture toughness of 8090-T651 plate and 2091 and 8090 sheet N90-15188
Fatigue properties of Al-Li alloys N90-15189
Microstructure/mechanical property relations in a mechanically alloyed aluminum N90-15205
Metal matrix composites: A promising alternative to conventional alloys N90-15208
Magnesium alloy technology for aerospace applications N90-15209
Cryogenic mechanical properties of low density superplastic Al-Mg-Sc alloys
[DE90-002120] N90-15222
Heat treatment of pulsed Nd: YAG laser welds in a Ti-14.8 wt pct Al-21.3 wt pct Nb titanium aluminide
[DE90-003484] N90-15228
The effect of nitrogen and titanium on the toughness of high strength saw weld deposits
[AD-A213400] N90-15230
Dispersion strengthening of high temperature niobium alloys
[AD-A213829] N90-15236
Properties of aluminum-uranium alloys
[DE90-003889] N90-15243
Bonding aerogels with polyurethanes
[DE90-003050] N90-15258
Modifications of the Penn State Boundary Layer Research Facility for boundary layer/structure interaction experimental research
[AD-A213874] N90-15391
Epoxy-resin cable terminations
[AD-A213789] N90-15454
Ductile failure
[AD-A213864] N90-15488
An investigation of mechanical behavior of crystalline solids
[DE90-003530] N90-15787

MECHANICAL TWINNING
Deformation twinning in ordered intermetallic compounds
[DE89-014779] N90-15767

MEDICAL EQUIPMENT
A scheiner-principle vernier optometer
[AD-D014304] N90-15405

MELTING POINTS
Summary physical data tables: Alkanes
[ESDU-PD3] N90-15162
Orthobaric densities and molar volumes of liquids: Alcohols
[ESDU-89037] N90-15184

MEMBRANES
Electrochemical investigation of electronically conductive polymers
[AD-A214019] N90-15277
Membrane and durability studies for the zinc/bromine battery
[DE89-016181] N90-15324
Advanced double layer capacitor
[AD-A213406] N90-15341
Transport processes through monomolecular films
[AD-A213609] N90-15342
Photochemical solar energy conversion utilizing semiconductors localized in membrane mimetic systems
[DE90-003450] N90-15515

MEMORY (COMPUTERS)
New devices using ferroelectric thin films
[DE90-000789] N90-15328
Temporal, processor, and spatial locality in multiprocessor memory references
[AD-A213790] N90-15598
The implementation of a coherent memory abstraction on a NUMA (Non-Uniform Memory Access) multiprocessor: Experiences with PLATINUM (Platform for Investigating Non-Uniform Memory)
[AD-A213909] N90-15600
Memory management for large-scale NUMA (Non-Uniform Memory Access) multiprocessors
[AD-A213910] N90-15601
An overview of PLATINUM: A Platform for Investiga ting Non-Uniform Memory (preliminary version)
[AD-A213911] N90-15602
Evolution of an operating system for large-scale shared-memory multiprocessors
[AD-A213912] N90-15603
Reconfigurable N-dimensional computer memory
[AD-D014309] N90-15607
High level language memory management on parallel architectures
[DE89-015018] N90-15609
Bounded polynomial randomized consensus
[AD-A213808] N90-15686

MENTAL PERFORMANCE
Where to from here. Future applications of mental models of complex performance
[DE90-002091] N90-15586

MERCURY CADMIUM TELLURIDES
Research on mercury cadmium telluride
[AD-A213924] N90-15237

MESOSCALE PHENOMENA
Geosat/ERM altimeter data analysis for the determination of global oceanic mesoscale variability N90-15492

MESSAGE PROCESSING
An overview of lynx
[AD-A213714] N90-15631

METAL BONDING
Critical and subcritical crack-growth behavior along toughened ceramic/metal interfaces N90-15140

METAL COATINGS
Thermal mechanical fatigue of coated blade materials
[AD-A214258] N90-15107
Metal film coatings on amorphous metallic alloys
[AD-D014308] N90-15240
Arc-sprayed coatings for electromagnetic pulse protection: Assessment of physical and electrical properties
[AD-A213825] N90-15275
Silver coated superconducting ceramic powder
[AD-D014300] N90-15278

METAL FATIGUE
Fatigue properties of Al-Li alloys N90-15189
Investigation on sheet material of 8090 and 2091 aluminium-lithium alloy N90-15192
Aluminum lithium alloys for Navy aircraft N90-15193
Fatigue, fracture mechanics and corrosion properties of some aluminium-lithium alloys N90-15194
Fatigue and fracture behaviour of a PM Al-Li alloy N90-15195
Uses and properties of Al-Li on the new EH101 helicopter N90-15201
The effects of Mo2C morphology and strain distribution on the fatigue properties of Fe-C-Mo dual-phase steels N90-15210
Directional solidification of superalloys
[NASA-CASE-MFS-28314-1] N90-15227
Guide to the selection of surface treatments for the improvement of fatigue strength of steels
[ESDU-89031] N90-15245
Proceedings of the 1988 Structural Integrity Program Conference
[AD-A213545] N90-15486
Fatigue behavior of vertical axis wind turbine airfoils with two weld configurations
[DE90-002628] N90-15525

METAL FILMS
Critical and subcritical crack-growth behavior along toughened ceramic/metal interfaces N90-15140
Correlations between surface structure and catalytic activity/selectivity
[DE90-003755] N90-15181
Metal film coatings on amorphous metallic alloys
[AD-D014308] N90-15240
Micron-thin Nb films recovered from Mbar shock pressures
[DE90-001509] N90-15772
Two-dimensional magnetic phase transition of ultrathin iron films on Pd(100)
[DE90-003555] N90-15788
Epitaxial iron films
[AD-A213551] N90-15807

METAL FOILS
Arc-sprayed coatings for electromagnetic pulse protection: Assessment of physical and electrical properties
[AD-A213825] N90-15275

METAL IONS
Host materials for transition-metal ions
[AD-A213605] N90-15808

METAL MATRIX COMPOSITES
Fatigue properties of SiC/Al composites N90-15138
Metal matrix composites with long inorganic fibers N90-15206
Short fibre and particulate reinforced metal matrix composites N90-15207
Metal matrix composites: A promising alternative to conventional alloys N90-15208
Ductile failure
[AD-A213864] N90-15488

METAL OXIDE SEMICONDUCTORS
Characteristics of CMOS analog integrated structures using MOSIS (Metal Oxide Semiconductor Implementation System)
[DE90-001630] N90-15773

METAL OXIDES
Studies of organo phosphorus-, nitrogen-, and sulfur-containing molecules
[AD-A213518] N90-15135

METAL PLATES
Comparison of multidimensional calculations of long-rod impacts on oblique plates
[DE89-015275] N90-15440

METAL SHEETS
Corrosion and stress corrosion of aluminium-lithium alloys N90-15190
Investigation on sheet material of 8090 and 2091 aluminium-lithium alloy N90-15192
Superplastic performance and properties of the Lital Alloys N90-15199
Uses and properties of Al-Li on the new EH101 helicopter N90-15201
Aluminum-lithium: Application of plate and sheet to fighter aircraft N90-15202
METAL SURFACES
Surface modification of metals by ion beams [DE90-001285] N90-15218
Laser-material interactions [AD-A214421] N90-15425
METAL VAPORS
Heat transfer in condensation of lithium vapors [DE90-002081] N90-15375
METAL WORKING
Putting alloy 2091 to work N90-15197
METALLIC PLASMAS
Theory of interacting plasmas in space N90-15742
METALS
Proceedings of the Latin American Conference on the Applications of the Moessbauer Effect [DE90-600819] N90-15803
METEOROLOGICAL CHARTS
Precipitation distributions associated with cyclones originating over the Gulf of Mexico and surrounding coastal regions [AD-A213644] N90-15569
Global distribution of total cloud cover and cloud type amounts over the ocean [DE90-003187] N90-15574
METEOROLOGICAL PARAMETERS
Winter cloud seeding potential on the Mogollon Rim [PB89-190540] N90-15562
Frontal clouds and flight conditions in them [AD-A214250] N90-15573
METEOROLOGICAL SATELLITES
Identification and quantification of synoptic structure in simulated TIROS N radiance soundings [AD-A213729] N90-15553
METEOROLOGY
Antarctic surface temperature and pressure data [DE90-000971] N90-15565
METHANE
Greenhouse gases: Changing the global climate [DE90-002788] N90-15535
METHYL ALCOHOL
Survey on synthesis technologies of methanol as an alternative fuel [DE89-901303] N90-15284
METHYL COMPOUNDS
Electrochemistry in near-critical and supercritical fluids. 8: Methyl viologen, decamethylferrocene, Os(bpy)3(sup 2+) and ferrocene in acetonitrile and the effect of pressure on diffusion coefficients under supercritical conditions [AD-A213407] N90-15172
Band-to-band transitions in poly (phenyl methyl silane) [DE90-003575] N90-15720
MICROANALYSIS
ICP/AES (Inductively Coupled Plasma/Atomic Emission Spectroscopy): A modern analytical tool [DE90-003822] N90-15765
MICROBURSTS (METEOROLOGY)
Analysis of severe atmospheric disturbances from airline flight records N90-15045
Influence of windshear, downdraft and turbulence on flight safety N90-15048
Relative merits of reactive and forward-look detection for wind-shear encounters during landing approach for various microburst escape strategies [NASA-TM-4158] N90-15108
MICROCHANNEL PLATES
Enhancement of microchannel plate gain by deposition of CsI on the channel walls [DE90-003051] N90-15334
Integration of a gated microchannel plate detector into the Nova laser system [DE90-002981] N90-15413
Development of the RAIDS (Remote Atmospheric and Ionospheric Detector System) extreme ultraviolet wedge and strip detector [AD-A213730] N90-15495
MICROCOMPUTERS
Utilization of a PC for finite element modeling [AD-A214173] N90-15605
MICROCRACKS
Critical and subcritical crack-growth behavior along toughened ceramic/metal interfaces N90-15140
MICROELECTRONICS
Component presence-absence detection for automated visual inspection of hybrid microcircuits [KCP-613-4050] N90-15335
A study of Inter-Injection-Locked phased arrays [AD-A214097] N90-15352
Overview on radiation effects in electronics [DE90-000841] N90-15357
Solid state research [AD-A213405] N90-15806
MICROHARDNESS
Dispersion strengthening of high temperature niobium alloys [AD-A213829] N90-15236
MICROMECHANICS
Numerical analysis and simulation of frictional particle systems N90-15430
Micromechanics of an extrusion in high-cycle fatigue with creep [AD-A213509] N90-15485
MICROORGANISMS
Effect of community structure on the kinetics of anaerobic degradation of aromatic compounds [DE90-003666] N90-15134
MICROSTRIP ANTENNAS
Investigation of broadband microstrip antenna structures for application in monolithic millimeter wave arrays [AD-A213856] N90-15344
MICROSTRUCTURE
Critical and subcritical crack-growth behavior along toughened ceramic/metal interfaces N90-15140
The microstructure and properties of aluminum-lithium alloys N90-15187
Microstructure/mechanical property relations in a mechanically alloyed aluminum N90-15205
Metal matrix composites: A promising alternative to conventional alloys N90-15208
The effects of Mo2C morphology and strain distribution on the fatigue properties of Fe-C-Mo dual-phase steels N90-15210
Microstructural evolution of martensitic steels during fast neutron irradiation [DE89-016231] N90-15212
Accelerated aging embrittlement of cast duplex stainless steel: Activation energy for extrapolation [DE90-001773] N90-15221
Cryogenic mechanical properties of low density superplastic Al-Mg-Sc alloys [DE90-002120] N90-15222
Heat treatment of pulsed Nd: YAG laser welds in a Ti-14.8 wt pct Al-21.3 wt pct Nb titanium aluminide [DE90-003484] N90-15228
Cast stainless steel aging: Mechanisms and predictions [DE90-003772] N90-15241
Properties of aluminum-uranium alloys [DE90-003889] N90-15243
Submerged arc welding consumables for HSLA (High Strength Low Alloy)-100 steel [AD-A213433] N90-15452
Research on amorphous silicon-germanium alloys for tandem solar cells [DE89-009436] N90-15499
Fabrication of porous ceramic electrode structures [DE90-003548] N90-15517
Micron-thin Nb films recovered from Mbar shock pressures [DE90-001509] N90-15772
Atomic scale structure of twin boundary in Y-Ba-Cu-O superconductors [DE90-003955] N90-15823
MICROWAVE AMPLIFIERS
Mechanical design of the inside launch system for electron cyclotron heating in D3-D [DE90-003292] N90-15751
MICROWAVE ANTENNAS
Scannable millimeter wave arrays, volume 1 [AD-A213895] N90-15347
Scannable millimeter wave arrays, volume 2 [AD-A213896] N90-15348
MICROWAVE CIRCUITS
Computer aided design of monolithic microwave and millimeter wave integrated circuits and subsystems [AD-A213656] N90-15343
MICROWAVE EQUIPMENT
RF transistor thermal/electrical characterization [DE90-001427] N90-15326
A study of Inter-Injection-Locked phased arrays [AD-A214097] N90-15352
The 17.1-GHz free-electron laser as a microwave source for TeV colliders [DE90-001506] N90-15406
MICROWAVE POWER BEAMING
Lunar power system summary of studies for the lunar enterprise task force NASA-office of exploration N90-15841
MICROWAVE SCATTERING
MODTRAN: A moderate resolution model for LOWTRAN 7 [AD-A214337] N90-15650
MICROWAVE TRANSMISSION
Rectangular-to-circular waveguide transitions for high-power circular overmoded waveguides [AD-A213925] N90-15349
The Solar Power Satellite (SPS): Progress so far N90-15840
Lunar power system summary of studies for the lunar enterprise task force NASA-office of exploration N90-15841
MICROWAVES
Intense REB (Relativistic Electron Beam) transport in a weakly magnetized plasma [DE90-002978] N90-15749
MIDCOURSE TRAJECTORIES
High resolution imaging by phase retrieval and discrimination using speckle, volume 1 [AD-A214243] N90-15317
MILLIMETER WAVES
Flashlight radar: A three-dimensional imaging radar [AD-A213439] N90-15307
Focal plane antenna array for millimeter waves [AD-D014306] N90-15322
Computer aided design of monolithic microwave and millimeter wave integrated circuits and subsystems [AD-A213656] N90-15343
Scannable millimeter wave arrays, volume 1 [AD-A213895] N90-15347
Scannable millimeter wave arrays, volume 2 [AD-A213896] N90-15348
MINERAL OILS
Mutagenic responses of some petroleum-base obscurants in the Ames test [AD-A214201] N90-15295
MINING
Report of NASA Lunar Energy Enterprise Case Study Task Force [NASA-TM-101652] N90-15836
Report of the NASA lunar energy enterprise case study task force N90-15837
Analysis of the financial factors governing the profitability of lunar helium-3 N90-15838
Transportation and operations aspects of space energy systems N90-15842
Importance of helium-3 for the future N90-15843
MINKOWSKI SPACE
Stable supermembrane vacuum with a discrete spectrum [DE89-635722] N90-15561
MIRRORS
Review of quasi-optical gyrotron development [AD-A213491] N90-15402
MIS (SEMICONDUCTORS)
Tritium and neutron measurements of a solid state cell [DE90-003657] N90-15820
MISSION PLANNING
Superconducting gravity gradiometer mission. Volume 1: Study team executive summary [NASA-TM-4091-VOL-1] N90-15545
MIXING
Laser mixing of titanium on silicon carbide [DE90-003216] N90-15150
MIXTURES
Simultaneous thermal analysis techniques for characterization of energetic materials [DE90-003028] N90-15289
Developmental versions of FORTRAN/77 routines for the design and analysis of mixture experiments [DE90-003513] N90-15624
Fast algorithms for estimating mixture parameters [AD-A213869] N90-15636
MOBILE COMMUNICATION SYSTEMS
Spread spectrum mobile radio communications [AD-A213726] N90-15311
Voice/data integration in mobile radio networks: Overview and future research directions [AD-A214289] N90-15319
MOBILITY
Crosslinked, flexible, low-molecular-weight polyacrylamide gels for mobility control [DE90-000202] N90-15280
Planning systems for autonomous legged vehicles [AD-A214242] N90-15458
MODAL RESPONSE
Effect of modal truncation on derivatives of closed-loop damping ratios in structural control N90-15109
MODEL REFERENCE ADAPTIVE CONTROL
Control of mechanical manipulators N90-15432
MODELS
Research on GaAs quantum-coupled structures that can be used as electron devices [AD-A214015] N90-15350
MODULUS OF ELASTICITY
The elastic properties of woven polymeric fabric [DE89-015391] N90-15255

MOISTURE
Observational study of the macroscopic behavior of moist-convective processes N90-15547
Specification for evaporation duct height calculations [AD-A213841] N90-15570
MOLECULAR BEAM EPITAXY
Surface roughening of Ge(001) during 200 eV Xe ion bombardment and Ge molecular beam epitaxy [DE90-000674] N90-15769
Defect control and denuded trap zones in the 3-5 semiconductors [AD-A214099] N90-15814
MOLECULAR CLOUDS
Shapes of star-gas waves in spiral galaxies [NASA-CR-186289] N90-15859
MOLECULAR COLLISIONS
Measurement of optical radiations in spacecraft environments [AD-A213814] N90-15497
Investigations of the interactions of radiation with matter [AD-A213554] N90-15723
MOLECULAR EXCITATION
Excitation lifetimes and excited-state forces in chemisorbed molecules [DE90-002578] N90-15165
MOLECULAR IONS
The production and spectroscopy of molecular ions isolated in solid neon [AD-A213723] N90-15174
MOLECULAR ORBITALS
Electronic and ionic transport in polymers [AD-A213410] N90-15270
MOLECULAR OSCILLATIONS
Determination of stepsize parameters for intermolecular vibrational energy transfer [DE90-003346] N90-15719
MOLECULAR RELAXATION
Determination of stepsize parameters for intermolecular vibrational energy transfer [DE90-003346] N90-15719
MOLECULAR STRUCTURE
Studies of organo phosphorus-, nitrogen-, and sulfur-containing molecules [AD-A213518] N90-15135
Energetics of BCC-FCC lattice deformation in iron [AD-A213801] N90-15233
MODTRAN: A moderate resolution model for LOWTRAN 7 [AD-A214337] N90-15650
Dynamics of electron transfer for a non-superexchange coherent mechanisms. 2: Numerical calculations [AD-A213511] N90-15722
Relativistic self-consistent field studies of atoms and molecules [AD-A214101] N90-15724
Large scale calculations of the structure and dynamics of dense matter [DE90-003654] N90-15726
Irradition-induced grain growth: Role of dislocations [DE90-003565] N90-15792
MOLECULAR WEIGHT
High-temperature gel-permeation chromatography of poly(4-methyl-1-pentene) [DE90-002967] N90-15159
Summary physical data tables: Alkanes [ESDU-PD3] N90-15162
MOLECULES
Molecules with enhanced electronic polarizabilities based on defect-like states in conjugated polymers [NASA-CASE-NPO-17633-1-CU] N90-15263
Studies of the adsorption/desorption behavior of explosive-like molecules [DE90-001867] N90-15283
Relativistic self-consistent field studies of atoms and molecules [AD-A214101] N90-15724
MOLTEN SALT ELECTROLYTES
Molten carbonate fuel cell technology improvement [DE90-001934] N90-15501
An assessment and comparison of fuel cells for transportation applications [DE90-001807] N90-15508
Oxygen electrode in molten carbonate fuel cells [DE90-002871] N90-15510
MOLTEN SALTS
Molten carbonate fuel cell technology improvement [DE90-001934] N90-15501
Characterization of new cathode materials for molten carbonate fuel cells [DE90-003547] N90-15516
MOLYBDENUM
Secondary electron emission characteristics of molybdenum-masked, ion-textured OFHC copper [NASA-TP-2967] N90-15211
MOLYBDENUM ALLOYS
Deformation and fracture of low alloy steels at high temperature [DE90-001274] N90-15215
MOLYBDENUM COMPOUNDS
The effects of Mo2C morphology and strain distribution on the fatigue properties of Fe-C-Mo dual-phase steels N90-15210
MOLYBDENUM DISULFIDES
Orientation of rf-sputter-deposited MoS2 films [ATR-89(4752)-1] N90-15784
MONITORS
Display interface concepts for automated fault diagnosis [NASA-TM-101610] N90-15102
HCl monitor, phase 2 [AD-A213572] N90-15542
MONOCHROMATIC RADIATION
A scheiner-principle vernier optometer [AD-D014304] N90-15405
MONOMERS
New polymers made with well-characterized organometallic catalysts [AD-A213592] N90-15272
MONOMOLECULAR FILMS
Transport processes through monomolecular films [AD-A213609] N90-15342
MONTE CARLO METHOD
Theoretical methods for the study of chemical dynamics [DE90-003122] N90-15160
A simulation model for dynamic system availability analysis [AD-A213499] N90-15628
Use of the linear variate method of Monte Carlo for estimating uncertainty in thermal-hydraulic codes [DE89-017871] N90-15694
Uniform versus random sampling in physical calculations: Monte Carlo [DE90-003247] N90-15696
Variational quantum Monte Carlo calculation of electronic and structural properties of crystals [DE90-003265] N90-15781
MOON
A quasi-economic role for lunar science [DE90-000679] N90-15876
MORPHOLOGY
The effects of Mo2C morphology and strain distribution on the fatigue properties of Fe-C-Mo dual-phase steels N90-15210
Thermally stable metal/GaAs contacts [DE90-002122] N90-15774
MOSSBAUER EFFECT
Proceedings of the Latin American Conference on the Applications of the Moessbauer Effect [DE90-600819] N90-15803
MOTION
Effect of contrast on the perception of direction of a moving pattern [NASA-TM-102234] N90-15577
MOTION PERCEPTION
An architectural model of visual motion understanding [AD-A214327] N90-15589
MOTIVATION
Human behavior [PB90-780008] N90-15584
MULTIPATH TRANSMISSION
Spread spectrum mobile radio communications [AD-A213726] N90-15311
MULTIPHASE FLOW
Dense-spray properties: Structure and turbulence modulation [AD-A213671] N90-15387
MULTIPLEXING
Voice Multiplex System (VMS) [AD-A213902] N90-15315
MULTIPROCESSING (COMPUTERS)
Temporal, processor, and spatial locality in multiprocessor memory references [AD-A213790] N90-15598
ARGOS (A Research GMMP Operating System): Overvie w and interfaces [AD-A213871] N90-15599
The implementation of a coherent memory abstraction on a NUMA (Non-Uniform Memory Access) multiprocessor: Experiences with PLATINUM (Platform for Investigating Non-Uniform Memory) [AD-A213909] N90-15600
Memory management for large-scale NUMA (Non-Uniform Memory Access) multiprocessors [AD-A213910] N90-15601
An overview of PLATINUM: A Platform for Investiga ting Non-Uniform Memory (preliminary version) [AD-A213911] N90-15602
Evolution of an operating system for large-scale shared-memory multiprocessors [AD-A213912] N90-15603
XNUSIM: Graphical interface for a multiprocessor simulator [AD-A214176] N90-15606
A signal processing language for coarse grain data flow multiprocessors [AD-A213863] N90-15635
MASC: Multiprocessor architecture for symbolic processing [AD-A213504] N90-15656
Adaptive backoff synchronization techniques [AD-A213966] N90-15658
Systolic algorithms for imaging from space [AD-A213870] N90-15701
Periodic phase adjustment distributed clock synchronization in the hard realtime environment [AD-A213842] N90-15708
MULTISENSOR APPLICATIONS
Design and implementation of two concurrent multi-sensor integration algorithms for mobile robots [DE90-003041] N90-15663
MULTIVARIATE STATISTICAL ANALYSIS
Outlier detection in multivariate calibration [DE90-001502] N90-15672
Quasi interpolants and approximation power of multivariate splines [AD-A213535] N90-15678
MUTAGENS
Mutagenic responses of some petroleum-base obscurants in the Ames test [AD-A214201] N90-15295

N

N-TYPE SEMICONDUCTORS
Defect control and denuded trap zones in the 3-5 semiconductors [AD-A214099] N90-15814
NASA PROGRAMS
Bibliography of Lewis Research Center technical publications announced in 1988 [NASA-TM-102034] N90-15846
NASA patent abstracts bibliography: A continuing bibliography. Section 1: Abstracts (supplement 36) [NASA-SP-7039(36)-SECT-1] N90-15851
Space operations: Listing of NASA scientific missions, 1980-2000. Fact sheet for the Chairman, Subcommittee on Space Science and Applications, Committee on Science, Space, and Technology, House of Representatives [AD-A213493] N90-15881
NATIONAL AIRSPACE SYSTEM
National airspace system: Airport movement area control operational concept [WP-89W00181] N90-15086
Control outside of independent surveillance coverage operational concept [AD-A214163] N90-15090
NATURAL LANGUAGE (COMPUTERS)
Elicitation of natural language representations of uncertainty using computer technology [DE90-001416] N90-15611
NAVIER-STOKES EQUATION
Numerical simulation of the unsteady two-dimensional flow in a time-dependent doubly-connected domain N90-15073
An algebraic turbulence model for flow separation caused by forward and backward facing steps [AD-A213800] N90-15389
Nonlinear viscous waves produced by an impulsively moving plate [AD-A214014] N90-15392
Numerical methods for parabolic equations and inequalities in very high dimensions [AD-A214102] N90-15690
NAVIGATION
Centralized and decentralized Kalman filter techniques for tracking, navigation, and control [AD-A214245] N90-15091
Sensor integration using concurrent computing on-board the ORNL mobile robot [DE89-008740] N90-15436
SIMON (SuperIntelligent Mobile Observing Navigator): A high-reliability robot for a radiation environment [DE90-003888] N90-15460
Design and implementation of two concurrent multi-sensor integration algorithms for mobile robots [DE90-003041] N90-15663
NAVIGATION AIDS
Control outside of independent surveillance coverage operational concept [AD-A214163] N90-15090

NEAR FIELDS
Aspects of Raman scattering
[AD-A213926] N90-15736
NEAR WAKES
An experimental, analytical, and computational investigation of turbomachinery rotor flow fields
N90-15360
NEON
The production and spectroscopy of molecular ions isolated in solid neon
[AD-A213723] N90-15174
NETWORK ANALYSIS
Network simulator definition
[AD-A213463] N90-15308
On the correctness of orphan management algorithms
[AD-A213777] N90-15632
Optimistic concurrency control for nested distributed transactions
[AD-A213828] N90-15634
A structural factoring approach for analyzing probabilistic networks N90-15697
NETWORK CONTROL
Voice/data integration in mobile radio networks: Overview and future research directions
[AD-A214289] N90-15319
Programs for control of an analog-signal switching network
[DE90-003645] N90-15626
On the correctnesa of orphan management algorithms
[AD-A213777] N90-15632
Optimistic concurrency control for nested distributed transactions
[AD-A213828] N90-15634
NEURAL NETS
Optical neural nets for scene analysis
[AD-A213986] N90-15637
Neural network models for linear programming
[DE89-015974] N90-15651
A neural network for bounded linear programming
[DE89-015975] N90-15652
NEUTRAL GASES
Laboratory simulations of the solar wind-comet interactions N90-15875
NEUTRON DIFFRACTION
Str. cture and dynamics of disordered systems
[DE90-001408] N90-15718
The possible occurrence of multi-phase behavior in the high T(sub c) superconductor YBa2Cu3O(sub x)
[DE90-002999] N90-15777
NEUTRON EMISSION
Tritium and neutron measurements of a solid state cell
[DE90-003657] N90-15820
NEUTRON SCATTERING
Structure and dynamics of disordered systems
[DE90-001408] N90-15718
NEUTRON SOURCES
Report of the Advanced Neutron Source (ANS) Aluminum Cladding Corrosion Workshop
[DE90-001281] N90-15217
NEUTRON STARS
Pulsars lost and found: The second Princeton-Arecibo millisecond pulsar search N90-15865
NEUTRONS
Tritium and neutron measurements of a solid state cell
[DE90-003657] N90-15820
NICKEL ALLOYS
Nickel beryllides and their properties
[DE90-001736] N90-15220
Magnetic viscosity in Ni/Cu compositionally-modulated alloys
[DE90-002303] N90-15223
The effect of dissolved ozone on the corrosion behavior of Cu-30 Ni and 304L stainless steel in 0.5 N NaCl solutions
[AD-A213804] N90-15235
NICKEL COMPOUNDS
New organic synthetic metals derived from BEDT-TTF, Ni(dait)2 and BEDO-TTF
[DE90-003793] N90-15242
NICKEL HYDROGEN BATTERIES
A nickel/hydrogen battery for PV systems
[DE90-001537] N90-15358
NIGHT VISION
Imaging probabilities, geometry and ergonomics in limited visibility helicopter operations N90-15060
The assessment of visibility from automatic contrast Measurements N90-15061
NIOBIUM
Niobium 1 percent zirconium/potassium and titanium/potassium life-test heat pipe design and testing
[DE90-002430] N90-15522
Micron-thin Nb films recovered from Mbar shock pressures
[DE90-001509] N90-15772
NIOBIUM ALLOYS
Dispersion strengthening of high temperature niobium alloys
[AD-A213829] N90-15236
NITRAMINE PROPELLANTS
Calculation of Einstein A coefficients and oscillator strengths for the A(perturbed)(2)A(1)-X(perturbed)(2)B(1) transition of NH(2)
[AD-A213837] N90-15176
NITRIC OXIDE
Excitation lifetimes and excited-state forces in chemisorbed molecules
[DE90-002578] N90-15165
NITROGEN
The dissociation energy of N2
[NASA-TM-101930] N90-15153
NITROGEN COMPOUNDS
Studies of organo phosphorus-, nitrogen-, and sulfur-containing molecules
[AD-A213518] N90-15135
NITROGEN OXIDES
Acid deposition
[DE90-003959] N90-15544
NOISE (SOUND)
Wind speed dependence of acoustic ambient vertical directional spectra at high frequency
[AD-A214293] N90-15712
Computation of broadband mixing noise from turbomachinery
[AD-A214448] N90-15713
NOISE GENERATORS
Dynamics of a class of vortex rings N90-15362
NOISE REDUCTION
Sound attenuation apparatus
[NASA-CASE-LAR-13968-1] N90-15710
NOISE SPECTRA
Dynamics of a class of vortex rings N90-15362
The calculation of overground sound propagation in the presence of wind and temperature gradients
[ESDU-89036] N90-15714
NONDESTRUCTIVE TESTS
ROBOCAL (Robotic Calorimetry): An automated NDA (Nondestructive Assay) calorimetry and gamma isotopic system
[DE90-003217] N90-15168
NONLINEAR OPTICS
Molecules with enhanced electronic polarizabilities based on defect-like states in conjugated polymers
[NASA-CASE-NPO-17633-1-CU] N90-15263
Nonlinear optical material studies
[AD-A213938] N90-15737
Phase equilibrium and crystal growth studies on AgGaSe2 and related nonlinear optical materials
[AD-A213650] N90-15809
NONLINEAR PROGRAMMING
On the identification of local minimizers in inertia-controlling methods for quadratic programming
[DE89-017330] N90-15616
Sequential quadratic programming algorithms for optimization
[DE90-000022] N90-15617
NONLINEAR SYSTEMS
On strongly nonlinear vortex/wave interactions in boundary-layer transition
[NASA-CR-181963] N90-15078
Nonlinear viscous waves produced by an impulsively moving plate
[AD-A214014] N90-15392
Nonlinear strain-displacement relations for thin axisymmetric shells
[PB89-226013] N90-15470
Continuum analogues of contragredient Lie algebras: Lie algebras with a Cartan operator and nonlinear dynamical systems
[DE89-635698] N90-15691
Optimal periodic control and regulator theory based on the second variation N90-15704
NONLINEARITY
Hamiltonian chaos in a nonlinear polarized optical beam
[DE90-002437] N90-15408
Use of the linear variate method of Monte Carlo for estimating uncertainty in thermal-hydraulic codes
[DE89-017871] N90-15694
Nonlinear optical material studies
[AD-A213938] N90-15737
NONNEWTONIAN FLUIDS
New transient algorithms for non-Newtonian flows
[AD-A213494] N90-15385
NORMALITY
A renormalization group approach to image processing: A new computational method for three-dimensional shapes in robot vision, and the computation complexity of the cooling algorithms
[AD-A214247] N90-15643
NORMALIZING (STATISTICS)
Some computational properties of rotation representations
[AD-A213888] N90-15665
NOVA LASER SYSTEM
Integration of a gated microchannel plate detector into the Nova laser system
[DE90-002981] N90-15413
NOZZLE DESIGN
Hypersonic nozzle design
[NASA-CR-186261] N90-15077
NUCLEAR ELECTRIC POWER GENERATION
Report of the NASA lunar energy enterprise case study task force N90-15837
Analysis of the financial factors governing the profitability of lunar helium-3 N90-15838
Introduction to D-He(3) fusion reactors N90-15839
Importance of helium-3 for the future N90-15843
NUCLEAR ELECTRIC PROPULSION
Design study of a modular gas-cooled, closed-brayton cycle reactor for marine use
[AD-A213453] N90-15518
NUCLEAR EMULSIONS
Target nucleus fragmentation in O16 + (Ag,Br) interactions at 200 A GeV
[LUIP-8906] N90-15727
NUCLEAR FUSION
In-situ ion beam measurements of deuterium loading in thin foil electrochemical cells
[DE90-003162] N90-15511
Upgrade plans to handle 30 to 40 Mbytes of data for D3-D
[DE90-003291] N90-15750
Tunnelling effects on low energy fusion cross sections
[AD-A214010] N90-15762
Tritium and neutron measurements of a solid state cell
[DE90-003657] N90-15820
Analysis of the financial factors governing the profitability of lunar helium-3 N90-15838
NUCLEAR MAGNETIC RESONANCE
Development of NMR (Nuclear Magnetic Resonance) imaging probes for advanced ceramics
[DE90-003812] N90-15269
NUCLEAR PHYSICS
NTES (Nuclear Test and Experimental Sciences) program laser facility for physics experiments Building 391 High Bay Option
[DE90-001795] N90-15411
Thermal and statistical properties of nuclei and nuclear systems
[DE90-000183] N90-15717
On the free carrier-negative U center interacting model for the high-T(sub c) oxide superconductor
[DE89-635908] N90-15775
NUCLEAR POWER PLANTS
Design study of a modular gas-cooled, closed-brayton cycle reactor for marine use
[AD-A213453] N90-15518
NUCLEAR REACTORS
Tuned-circuit Johnson noise thermometry
[DE89-016221] N90-15356
NUCLEATION
Energetics of BCC-FCC lattice deformation in iron
[AD-A213801] N90-15233
NUCLEI
Thermal and statistical properties of nuclei and nuclear systems
[DE90-000183] N90-15717
NUCLEI (NUCLEAR PHYSICS)
Rapidity densities and their fluctuations in central 200 A GeV S32 interations with Au and Ag,Br nuclei
[LUIP-8905] N90-15715
Target nucleus fragmentation in O16 + (Ag,Br) interactions at 200 A GeV
[LUIP-8906] N90-15727
NUMERICAL ANALYSIS
Investigation of broadband microstrip antenna structures for application in monolithic millimeter wave arrays
[AD-A213856] N90-15344
Stability of numerical solutions for stratified two-phase flow
[DE90-701646] N90-15379
Numerical analysis and simulation of frictional particle systems N90-15430
Ultra high performance, highly reliable, numeric intensive processors and systems
[AD-A214100] N90-15659
Numerical optimization
[AD-A213758] N90-15683
Numerical methods for parabolic equations and inequalities in very high dimensions
[AD-A214102] N90-15690
Dynamics of electron transfer for a non-superexchange coherent mechanisms. 2: Numerical calculations
[AD-A213511] N90-15722

NUMERICAL CONTROL
Time bounds for real-time process control in the presence of timing uncertainty
[AD-A213791] N90-15633
Computer controlled MHD power consolidation and pulse-generation system
[DE90-001224] N90-15662
Computer-controlled ion beam sputter-deposition of superconducting oxide films
[AD-A213921] N90-15812
NUMERICAL FLOW VISUALIZATION
Dynamics of a class of vortex rings N90-15362
NUTRITION
Utilization of non-conventional systems for conversion of biomass to food components
[NASA-CR-177545] N90-15591

O

O RING SEALS
High temperature, flexible, thermal barrier seal
[NASA-CASE-LEW-14672-1] N90-15444
OBSERVATORIES
Artificial intelligence approaches to astronomical observation scheduling
[NASA-CR-186277] N90-15862
OCEAN BOTTOM
Dynamics of mid-ocean ridge systems N90-15575
Evolution of overlapping spreading centers: A Sea Mark 2 investigation
[AD-A214278] N90-15576
OCEAN SURFACE
Geosat/ERM altimeter data analysis for the determination of global oceanic mesoscale variability N90-15492
Specification for evaporation duct height calculations
[AD-A213841] N90-15570
Further research on dynamics of marine atmospheres in tropical cyclones
[AD-A213882] N90-15571
Global distribution of total cloud cover and cloud type amounts over the ocean
[DE90-003187] N90-15574
Wind speed dependence of acoustic ambient vertical directional spectra at high frequency
[AD-A214293] N90-15712
OCEAN TEMPERATURE
Specification for evaporation duct height calculations
[AD-A213841] N90-15570
OCEAN THERMAL ENERGY CONVERSION
Ocean thermal energy conversion: An overview
[DE89-000838] N90-15512
OCTANES
Shock tube ignition of octanes
[DE90-001167] N90-15164
OHMIC DISSIPATION
Aerosol heating and vaporization of high-flux laser beams
[DE90-003471] N90-15428
ON-LINE SYSTEMS
A comparative evaluation and analysis of end-user search performance in an academic environment N90-15845
OPACITY
Astophysical opacities at LLNL
[DE90-003599] N90-15872
OPEN CLUSTERS
The age of the galactic disk
[NASA-CR-186292] N90-15869
OPENINGS
Single fluid simulations of plasma openings switch behavior
[DE90-002643] N90-15330
OPERATING SYSTEMS (COMPUTERS)
Integrated approach fault tolerance-current state and future requirements
[AD-A214402] N90-15465
ARGOS (A Research GMMP Operating System): Overvie w and interfaces
[AD-A213871] N90-15599
The implementation of a coherent memory abstraction on a NUMA (Non-Uniform Memory Access) multiprocessor: Experiences with PLATINUM (Platform for Investigating Non-Uniform Memory)
[AD-A213909] N90-15600
Memory management for large-scale NUMA (Non-Uniform Memory Access) multiprocessors
[AD-A213910] N90-15601
An overview of PLATINUM: A Platform for Investiga ting Non-Uniform Memory (preliminary version)
[AD-A213911] N90-15602
Evolution of an operating system for large-scale shared-memory multiprocessors
[AD-A213912] N90-15603
An executive system for modeling with rational b-splines
[AD-A213460] N90-15627
OPERATIONS RESEARCH
Research in optical interconnection techniques
[AD-A214028] N90-15739
OPERATOR PERFORMANCE
The application of queuing theory to the modelling of CP-140 aircraft communications
[AD-A213479] N90-15310
Where to from here. Future applications of mental models of complex performance
[DE90-002091] N90-15586
OPERATORS (MATHEMATICS)
On the sum of two maximal monotone operators
[REPT-89-31] N90-15669
Continuum analogues of contragredient Lie algebras: Lie algebras with a Cartan operator and nonlinear dynamical systems
[DE89-635698] N90-15691
OPTICAL COMMUNICATION
SLCSAT (Submarine Laser Communication Satellite) communication system design study
[AD-A213403] N90-15304
Laser communication system with wide band magnetostrictive modulation
[AD-D014302] N90-15427
OPTICAL DATA PROCESSING
New devices using ferroelectric thin films
[DE90-000789] N90-15328
OPTICAL DENSITY
Analysis of catalytically enhanced solar absorption chemical reactors. 2: Predicted characteristics of a 100 kW chemical reactor
[DE89-014743] N90-15521
OPTICAL DISKS
Procurement of an optical disk information storage and retrieval system
[DE90-001372] N90-15849
OPTICAL EQUIPMENT
Analysis and evaluation of technical data on the photochromic and non-linear optical properties of materials. Appendix: Eye/sensor protection by an optical fuse mirror at a focal plane: Feasibility assessment
[AD-A214051] N90-15177
OPTICAL FIBERS
Interlaboratory comparison of radiation-induced attenuation in optical fibers. Part 3: Transient exposures
[DE90-000859] N90-15729
Optical acoustic sensor using optical fiber
[DE89-901267] N90-15730
SBS (Stimulated Brillouin Scattering) pulse distortion in multimode optical fibers: Preliminary results
[DE90-003023] N90-15731
Mechanical evaluation of the differential drum concept for optical fiber pay-out
[AD-A214149] N90-15740
OPTICAL FILTERS
Design of a large angular aperture TeO2 acousto-optic tunable filter
[AD-A213999] N90-15738
OPTICAL MATERIALS
Nonlinear optical material studies
[AD-A213938] N90-15737
Phase equilibrium and crystal growth studies on AgGaSe2 and related nonlinear optical materials
[AD-A213650] N90-15809
OPTICAL MEASUREMENT
Measurement of optical radiations in spacecraft environments
[AD-A213814] N90-15497
HCl monitor, phase 2
[AD-A213572] N90-15542
OPTICAL MEASURING INSTRUMENTS
Optical acoustic sensor using optical fiber
[DE89-901267] N90-15730
OPTICAL POLARIZATION
Optical phonon modes in a double heterostructure of polar crystals
[AD-A214208] N90-15816
OPTICAL PROPERTIES
Analysis and evaluation of technical data on the photochromic and non-linear optical properties of materials
[AD-A214212] N90-15178
Laser-material interactions
[AD-A214421] N90-15425
Thin films under chemical stress
[DE90-003754] N90-15484
Research on high-efficiency, single-junction, monolithic, thin-film amorphous silicon solar cells, phase 2
[DE89-009496] N90-15503
Nonlinear optical material studies
[AD-A213938] N90-15737
Picosecond photoconductivity using a graded bandgap Al(x)Ga(1-x)As active detecting layer
[DE90-003452] N90-15786
Research on materials and components for opto-electronic signal processing and computing
[AD-A213740] N90-15811
Innovative optoelectronic materials and structures using OMVPE
[AD-A214192] N90-15815
The middle Martian atmosphere N90-15874
OPTICAL SWITCHING
Laser glass (1989)
[DE90-002754] N90-15257
OPTICAL THICKNESS
Analysis of catalytically enhanced solar absorption chemical reactors. 2: Predicted characteristics of a 100 kW chemical reactor
[DE89-014743] N90-15521
OPTICAL TRANSITION
Initial optical transition radiation measurements of the electron beam for the Boeing free-electron laser experiment
[DE90-003396] N90-15416
OPTICAL WAVEGUIDES
Optical guiding by plasma waves in the plasma beat wave accelerator
[AD-A214288] N90-15763
OPTICS
Canonical formalism for coupled beam optics
[DE90-003764] N90-15734
Gas optics applicable to free electron laser technology
[AD-A214285] N90-15741
OPTIMAL CONTROL
Guidance analysis of the aeroglide plane change maneuver as a turning point problem
[NASA-TM-101639] N90-15110
The application of optimal control theory for analysis of human jumping and pedaling N90-15590
Optimal periodic control and regulator theory based on the second variation N90-15704
OPTIMIZATION
Centralized and decentralized Kalman filter techniques for tracking, navigation, and control
[AD-A214245] N90-15091
Guidance analysis of the aeroglide plane change maneuver as a turning point problem
[NASA-TM-101639] N90-15110
Investigation of broadband microstrip antenna structures for application in monolithic millimeter wave arrays
[AD-A213856] N90-15344
Gas turbine regenerators: A method for selecting the optimum plate-finned surface pair for minimum core volume
[AD-A213430] N90-15382
Comprehensive, nonintercepting electron-beam diagnostics using spontaneous emission
[DE90-003211] N90-15414
NOISE: A nonlinear optimization induction free-electron laser systems engineering code
[DE90-004438] N90-15420
On the analysis and optimization of a platform manipulator N90-15433
New approach to the inverse problem of six-link manipulators via the optimization technique
[DE90-710044] N90-15441
Base reaction optimization of redundant manipulators for space applications
[NASA-CR-186274] N90-15447
Planning minimum-energy paths in an off-road environment with anisotropic traversal costs and motion constraints
[AD-A214181] N90-15457
Oxygen and other atmospheric gases
[AD-A214296] N90-15557
On the identification of local minimizers in inertia-controlling methods for quadratic programming
[DE89-017330] N90-15616
Sequential quadratic programming algorithms for optimization
[DE90-000022] N90-15617
Gradient projection techniques for large-scale optimization problems
[DE90-001986] N90-15618
Optimizing and evaluating algorithms for replicated data concurrency control
[DE90-003080] N90-15619
Tensor methods for unconstrained optimization using second derivatives
[AD-A213642] N90-15681
Numerical optimization
[AD-A213758] N90-15683
Optimization of stochastic systems via simulation
[AD-A214011] N90-15689
OPTOMETRY
A scheiner-principle vernier optometer
[AD-D014304] N90-15405

ORBIT CALCULATION
Error modeling of bias-type parameters for TOPEX orbit determination N90-15117
ORBIT PERTURBATION
Some results on connecting orbits for a class of Hamiltonian systems
[AD-A213536] N90-15679
ORBITAL ASSEMBLY
Onorbit electron beam welding experiment definition
[NASA-CR-183847] N90-15431
ORBITAL MANEUVERS
Guidance analysis of the aeroglide plane change maneuver as a turning point problem
[NASA-TM-101639] N90-15110
ORBITS
Some results on connecting orbits for a class of Hamiltonian systems
[AD-A213536] N90-15679
ORDER-DISORDER TRANSFORMATIONS
Structure and dynamics of disordered systems
[DE90-001408] N90-15718
Theoretical studies on the electronic structure of high-temperature superconductors
[DE90-001301] N90-15771
ORGANIC CHARGE TRANSFER SALTS
New organic synthetic metals derived from BEDT-TTF, Ni(dsit)2 and BEDO-TTF
[DE90-003793] N90-15242
ORGANIC COMPOUNDS
Analysis of ambient polar volatile organic compounds using chemical ionization-ion trap detector
[PB90-106451] N90-15529
ORGANIC LIQUIDS
Dimensional analysis of continuous high-capacity electrodispersion of aqueous based liquids in an organic continuous phase
[DE90-003714] N90-15136
ORGANIC MATERIALS
Analysis and evaluation of technical data on the photochromic and non-linear optical properties of materials
[AD-A214212] N90-15178
ORGANIC PHOSPHORUS COMPOUNDS
Studies of organo phosphorus-, nitrogen-, and sulfur-containing molecules
[AD-A213518] N90-15135
ORGANIC SULFUR COMPOUNDS
Novel high-rate, all solid-state, sodium and lithium/organosulfur batteries
[DE90-001014] N90-15325
ORGANOMETALLIC COMPOUNDS
New organic synthetic metals derived from BEDT-TTF, Ni(dsit)2 and BEDO-TTF
[DE90-003793] N90-15242
ORGANOMETALLIC POLYMERS
New polymers made with well-characterized organometallic catalysts
[AD-A213592] N90-15272
ORTHOGONALITY
Two dimensional laminated shell theory including parabolic transverse shear
[AD-A213817] N90-15487
OSCILLATIONS
Unsteady aerodynamics of oscillating and rapidly pitched airfoils N90-15074
OSCILLATOR STRENGTHS
Calculation of Einstein A coefficients and oscillator strengths for the A(perturbed)(2)A(1)-X(perturbed)(2)B(1) transition of NH(2)
[AD-A213837] N90-15176
OSCILLATORS
A study of Inter-Injection-Locked phased arrays
[AD-A214097] N90-15352
OUTGASSING
Improved process for HIP canning of composites
[NASA-CASE-LEW-14990-1-CU] N90-15147
OUTLIERS (STATISTICS)
Outlier detection in multivariate calibration
[DE90-001502] N90-15672
OVER-THE-HORIZON RADAR
MF/HF multistatic mid-ocean radar experiments in support of SWOTHR (Surface-Wave Over-The-Horizon Radar)
[AD-A213830] N90-15314
OXIDATION
Novel polyimide compositions based on 4,4': Isophthaloyldiphthalic anaydride (IDPA)
[NASA-CASE-LAR-14194-1] N90-15148
A review of the effects of microalloying constituents on the formation and breakdown of protective oxide scales on high-temperature alloys at temperatures below 700 C
[DE90-001277] N90-15216
Report of the Advanced Neutron Source (ANS) Aluminum Cladding Corrosion Workshop
[DE90-001281] N90-15217
Products of the hypochlorite oxidation of hydrazine fuels
[AD-A213557] N90-15291
Partial reduction of re-oxidation processing of Y-Ba-Cu-O sputtered thin films
[DE90-003655] N90-15782
OXIDATION RESISTANCE
Nickel beryllides and their properties
[DE90-001736] N90-15220
OXIDE FILMS
Computer-controlled ion beam sputter-deposition of superconducting oxide films
[AD-A213921] N90-15812
OXIDES
A review of the effects of microalloying constituents on the formation and breakdown of protective oxide scales on high-temperature alloys at temperatures below 700 C
[DE90-001277] N90-15216
Design of a large angular aperture TeO2 acousto-optic tunable filter
[AD-A213999] N90-15738
OXIDIZERS
Inorganic halogen oxidizers
[AD-A213990] N90-15294
OXYGEN
Oxygen electrode in molten carbonate fuel cells
[DE90-002871] N90-15510
OXYGEN BREATHING
Potential for reduction of decompression sickness by prebreathing with 100 percent oxygen while exercising
[AD-A213449] N90-15581
OXYGEN ISOTOPES
Target nucleus fragmentation in O16 + (Ag,Br) interactions at 200 A GeV
[LUIP-8906] N90-15727
OXYGEN PRODUCTION
Oxygen and other atmospheric gases
[AD-A214296] N90-15557
OZONE
Variability of cultivar responses to ozone
[PB89-225460] N90-15528
OZONE DEPLETION
International aspects of restrictions of ozone-depleting substances
[DE90-001813] N90-15534

P

P-N JUNCTIONS
Development of high performance beta-SiC field-effect transistors
[AD-A213885] N90-15346
P-TYPE SEMICONDUCTORS
Defect control and denuded trap zones in the 3-5 semiconductors
[AD-A214099] N90-15814
PACIFIC OCEAN
Responding to the threat of global warming: Options for the Pacific and Asia
[DE90-003553] N90-15539
Identification and quantification of synoptic structure in simulated TIROS N radiance soundings
[AD-A213729] N90-15553
PAIR PRODUCTION
Rapidity densities and their fluctuations in central 200 A GeV S32 interations with Au and Ag,Br nuclei
[LUIP-8905] N90-15715
Linear electron-hole-electron pair model of high-temperature superconductivity in La(2-x)M(x)CuO4 and YBa2Cu3O(7-y): Part 2. Dependence of the superconducting transition temperatures on pressure and on hole concentration
[DE90-003012] N90-15779
PALEOCLIMATOLOGY
Global lake-level variations from 18,000 to 0 years ago: A palaeoclimate analysis
[DE90-000998] N90-15531
PALLADIUM
Interaction of hydrogen in palladium as prescribed by the embedded atom method
[DE90-003893] N90-15244
Two-dimensional magnetic phase transition of ultrathin iron films on Pd(100)
[DE90-003555] N90-15788
High resolution electron microscopy of grain boundaries in nanophase palladium
[DE90-003823] N90-15800
PANELS
Onorbit electron beam welding experiment definition
[NASA-CR-183847] N90-15431
High temperature, flexible, thermal barrier seal
[NASA-CASE-LEW-14672-1] N90-15444
PARABOLAS
Two dimensional laminated shell theory including parabolic transverse shear
[AD-A213817] N90-15487
PARABOLIC DIFFERENTIAL EQUATIONS
Numerical methods for parabolic equations and inequalities in very high dimensions
[AD-A214102] N90-15690
PARALLEL COMPUTERS
Reconfigurable N-dimensional computer memory
[AD-D014309] N90-15607
High level language memory management on parallel architectures
[DE89-015018] N90-15609
Investigation of the applicability of a functional programming model to fault-tolerant parallel processing for knowledge-based systems
[NASA-CR-181938] N90-15654
PARALLEL PROCESSING (COMPUTERS)
VLSI theory and parallel supercomputing
[AD-A214035] N90-15351
Research in mathematics and computer science at Argonne
[DE90-000975] N90-15595
The parallel decomposition of linear programs
[DE90-003538] N90-15625
Investigation of the applicability of a functional programming model to fault-tolerant parallel processing for knowledge-based systems
[NASA-CR-181938] N90-15654
Adaptive backoff synchronization techniques
[AD-A213966] N90-15658
PARALLEL PROGRAMMING
Paralation views: Abstractions for efficient scientific computing on the connection machine
[AD-A213935] N90-15604
An overview of lynx
[AD-A213714] N90-15631
Principles and algorithms for causal reasoning with uncertainty
[AD-A214248] N90-15644
MASC: Multiprocessor architecture for symbolic processing
[AD-A213504] N90-15656
PARAMETER IDENTIFICATION
The effectiveness of vane-aileron excitation in the experimental determination of flutter speed by parameter identification
[NASA-TP-2971] N90-15100
Error modeling of bias-type parameters for TOPEX orbit determination N90-15117
Parametric identification of discrete time series models for structural response prediction N90-15472
Parameter estimation of linear systems in the presence of process noise using the maximum liklihood method
[ESDU-89032] N90-15693
PARAMETERIZATION
Shock tube ignition of octanes
[DE90-001167] N90-15164
Observational study of the macroscopic behavior of moist-convective processes N90-15547
Flux parameterization techniques in the atmospheric surface layer N90-15548
Calculation of source and structure parameters at regional and teleseismic distances
[AD-A214297] N90-15558
Fast algorithms for estimating mixture parameters
[AD-A213869] N90-15636
Some computational properties of rotation representations
[AD-A213888] N90-15665
Higher order crossings from a parametric family of linear filters
[AD-A213427] N90-15676
Membership-set parameter estimation via optimal bounding ellipsoids
[AD-A213807] N90-15685
PARTIAL DIFFERENTIAL EQUATIONS
Finite difference techniques and rotor blade aeroelastic partial differential equations with quasisteady aerodynamics N90-15075
Knowledge representations for the automatic generation of numerical simulators for PDEs
[DE89-008036] N90-15615
Physical process in MPD plasmas
[AD-A213679] N90-15761
PARTICLE ACCELERATION
A calculation of energetic proton spectra producedat substorm onset in the fields of the explosive reconnection model N90-15866
PARTICLE COLLISIONS
Progress in LTE and non-LTE transport calculations
[DE90-003394] N90-15764
Electron-positron momentum distribution measurements of high-T superconductors and related systems
[DE90-002974] N90-15780

LEAP: A balloon-borne search for low-energy cosmic ray antiprotons N90-15878
PARTICLE DENSITY (CONCENTRATION)
Dense-spray properties: Structure and turbulence modulation
[AD-A213671] N90-15387
PARTICLE DIFFUSION
Numerical methods for parabolic equations and inequalities in very high dimensions
[AD-A214102] N90-15690
PARTICLE EMISSION
Characterization of chemicals on engine exhaust particles
[AD-A213566] N90-15106
PARTICLE ENERGY
A calculation of energetic proton spectra producedat substorm onset in the fields of the explosive reconnection model N90-15866
LEAP: A balloon-borne search for low-energy cosmic ray antiprotons N90-15878
PARTICLE INTERACTIONS
Target nucleus fragmentation in O16 + (Ag,Br) interactions at 200 A GeV
[LUIP-8906] N90-15727
PARTICLE LADEN JETS
Dense-spray properties: Structure and turbulence modulation
[AD-A213671] N90-15387
PARTICLE MOTION
Dense-spray properties: Structure and turbulence modulation
[AD-A213671] N90-15387
Canonical formalism for coupled beam optics
[DE90-003764] N90-15734
PARTICLE PRODUCTION
Substructural dependence of the multiparticle production in relativistic heavy-ion interactions
[LUIP-8904] N90-15716
PARTICLE SIZE DISTRIBUTION
Advanced study in solid transport: Rheological behavior of dense suspension
[DE90-003369] N90-15483
Beryllium dispersion near explosive firing tables: A comparison of computed and observed results
[DE90-002635] N90-15550
PARTICLE TELESCOPES
First results from the MACRO (Monopole, Astrophysics, Cosmic Ray Observatory) detector at the Gran Sasso Laboratory
[DE90-003243] N90-15858
PARTICLES
Processing and properties of nanophase oxides
[DE90-003826] N90-15171
Numerical analysis and simulation of frictional particle systems N90-15430
Stand-off shields for hypervelocity particles
[DE89-016182] N90-15437
PARTICULATE SAMPLING
Design and calibration of an in-stack, low-pressure impactor
[AD-A213531] N90-15105
PARTICULATES
Saltation and suspension of particulate matter in air
[AD-A213618] N90-15552
PASCAL (PROGRAMMING LANGUAGE)
Environment for failure region analysis: REACHER - a reachability condition derivation tool
[AD-A214183] N90-15641
PASSENGER AIRCRAFT
International Aircraft Occupant Safety Conference and Workshop proceedings
[AD-A214452] N90-15085
PATENT APPLICATIONS
Molecules with enhanced electronic polarizabilities based on defect-like states in conjugated polymers
[NASA-CASE-NPO-17633-1-CU] N90-15263
PATENT POLICY
NASA patent abstracts bibliography: A continuing bibliography. Section 1: Abstracts (supplement 36)
[NASA-SP-7039(36)-SECT-1] N90-15851
PATHOLOGY
Mutagenic responses of some petroleum-base obscurants in the Ames test
[AD-A214201] N90-15295
PATTERN RECOGNITION
Vision in dynamic environments
[AD-A213434] N90-15587
Optical neural nets for scene analysis
[AD-A213986] N90-15637
PATTERNS
Effect of contrast on the perception of direction of a moving pattern
[NASA-TM-102234] N90-15577
PAVEMENTS
Design temperatures for flexible airfield pavement design
[AD-A214141] N90-15115
PAYLOAD CONTROL
Modeling and control of the rapid deployment of towed airborne devices N90-15092
PEBBLE BED REACTORS
Design study of a modular gas-cooled, closed-brayton cycle reactor for marine use
[AD-A213453] N90-15518
PENETRATION
N-port theory applied to backscatter polarimetry and depolarization in foliage penetration
[AD-A213437] N90-15305
MESA 3-D calculations of armor penetration by projectiles with combined obliquity and yaw
[DE89-015265] N90-15438
Hydrodynamics code calculations of debris clouds produced by ball-plate impacts
[DE89-015270] N90-15439
Comparison of multidimensional calculations of long-rod impacts on oblique plates
[DE89-015275] N90-15440
PERCEPTION
Effect of contrast on the perception of direction of a moving pattern
[NASA-TM-102234] N90-15577
PERCEPTUAL ERRORS
An architectural model of visual motion understanding
[AD-A214327] N90-15589
PERFORMANCE PREDICTION
An analysis of drilling of composite materials N90-15142
Predicting the performance of ceramic filters by the use of silt density index
[DE90-001316] N90-15256
Parametric identification of discrete time series models for structural response prediction N90-15472
PERFORMANCE TESTS
Current launch vehicle reliability practice and data base assessment. Volume 1: Executive summary and report body
[AD-A213600] N90-15121
The effect of nitrogen and titanium on the toughness of high strength saw weld deposits
[AD-A213400] N90-15230
A future for LLNL (Lawrence Livermore National Laboratory) research in composite high explosives
[DE90-004442] N90-15290
MF/HF multistatic mid-ocean radar experiments in support of SWOTHR (Surface-Wave Over-The-Horizon Radar)
[AD-A213830] N90-15314
A nickel/hydrogen battery for PV systems
[DE90-001537] N90-15358
High power density spray cooling
[AD-A213575] N90-15386
SIMON (SuperIntelligent Mobile Observing Navigator): A high-reliability robot for a radiation environment
[DE90-003888] N90-15460
Structural response measurements and predictions for the SANDIA 34-meter test bed
[DE90-002575] N90-15524
Knowledge based text generation
[AD-A214273] N90-15645
PERIODIC VARIATIONS
Optimal periodic control and regulator theory based on the second variation N90-15704
PERSONAL COMPUTERS
Utilization of a PC for finite element modeling
[AD-A214173] N90-15605
PERSONNEL
Physical and Electrical Standards Laboratory general operating procedures
[DE90-003515] N90-15116
MANPRINT methods monograph: Aiding the development of manned system performance criteria
[AD-A213543] N90-15593
PERTURBATION THEORY
General many-body systems
[DE90-000685] N90-15670
Relativistic self-consistent field studies of atoms and molecules
[AD-A214101] N90-15724
PETN
Critical temperature analysis for a hemispherical charge of a binary explosive
[DE90-001447] N90-15282
PHASE CHANGE MATERIALS
Selection of phase-change and containment materials for thermal energy storage
[NASA-CR-186228] N90-15506
Satellite thermal storage systems using metallic phase-change materials
[DE89-016872] N90-15507
PHASE DIAGRAMS
Gas-liquid-liquid equilibria in mixtures of water, light gases, and hydrocarbons
[DE90-003180] N90-15167
PHASE LOCKED SYSTEMS
The 22 GHz Radioastron receiver: Development of prototype components during the year 1988
[PB89-212583] N90-15323
PHASE MATCHING
Aspects of Raman scattering
[AD-A213926] N90-15736
PHASE SHIFT
Aspects of Raman scattering
[AD-A213926] N90-15736
PHASE TRANSFORMATIONS
Crack tip toughening by inclusions with pairs of shear transformations
[DE89-007845] N90-15254
Phase transition in polymer blends and structure of ionomers
[DE90-003525] N90-15266
The possible occurrence of multi-phase behavior in the high T(sub c) superconductor YBa2Cu3O(sub x)
[DE90-002999] N90-15777
Bulk wave characterization of high T(sub c) superconductors
[AD-A214030] N90-15813
PHASE VELOCITY
Optical guiding by plasma waves in the plasma beat wave accelerator
[AD-A214288] N90-15763
PHASED ARRAYS
Proceedings of the Antenna Applications Symposium, volume 2
[AD-A213815] N90-15313
A study of Inter-Injection-Locked phased arrays
[AD-A214097] N90-15352
A multichannel processing approach to real time network detection, phase association, and threshold monitoring
[AD-A213940] N90-15657
PHILOSOPHY
Understanding developments in computer technology: A pragmatic and synthetic interpretation N90-15608
PHONONS
On the choice of trial function in theoretical calculations of the thermal conductivity
[DE90-001733] N90-15182
General many-body systems
[DE90-000685] N90-15670
Phonons and charge-transfer excitations in HTS superconductors
[DE89-016616] N90-15768
Cu-O chains in YBa2Cu3O(7-delta) and the phonon mechanism of high-Tc superconductivity
[DE90-603502] N90-15805
Interface phonons in semiconductor double heterostructures
[AD-A213732] N90-15810
PHOTOABSORPTION
Investigations of the interactions of radiation with matter
[AD-A213554] N90-15723
PHOTOCATHODES
Enhancement of microchannel plate gain by deposition of CsI on the channel walls
[DE90-003051] N90-15334
Center for X Ray Optics, 1988
[DE90-003300] N90-15732
PHOTOCHEMICAL REACTIONS
Characterization of chemicals on engine exhaust particles
[AD-A213566] N90-15106
Excimer emission from alkali diatomic and alkaline-earth-noble-gas molecules
[AD-A214246] N90-15179
Interfacial systems for photochemical energy conversion
[DE90-003181] N90-15514
Photochemical solar energy conversion utilizing semiconductors localized in membrane mimetic systems
[DE90-003450] N90-15515
NO2 photodissociation dynamics
[AD-A214422] N90-15560
PHOTOCHROMISM
Analysis and evaluation of technical data on the photochromic and non-linear optical properties of materials
[AD-A214212] N90-15178
PHOTOCONDUCTIVITY
Picosecond photoconductivity using a graded bandgap Al(x)Ga(1-x)As active detecting layer
[DE90-003452] N90-15786
PHOTOCONDUCTORS
Avalanche photoconductive switching
[DE90-002980] N90-15337

PHOTODIODES
Research on materials and components for opto-electronic signal processing and computing
[AD-A213740] N90-15811
PHOTODISSOCIATION
NO2 photodissociation dynamics
[AD-A214422] N90-15560
PHOTOELECTRIC EFFECT
Technology of fast spark gaps
[AD-A214199] N90-15353
PHOTOELECTRON SPECTROSCOPY
Synthesis conductivity, and x ray photoelectron spectrum of Bi2Sr2Cu(sub 7+x). A new ternary bismuth-oxide system exhibiting metallic conductivity
[DE90-003010] N90-15778
PHOTOIONIZATION
Oxygen and other atmospheric gases
[AD-A214296] N90-15557
Investigations of the interactions of radiation with matter
[AD-A213554] N90-15723
PHOTOLITHOGRAPHY
Critical and subcritical crack-growth behavior along toughened ceramic/metal interfaces N90-15140
Research on GaAs quantum-coupled structures that can be used as electron devices
[AD-A214015] N90-15350
PHOTONS
NO2 photodissociation dynamics
[AD-A214422] N90-15560
PHOTOSENSITIVITY
New devices using ferroelectric thin films
[DE90-000789] N90-15328
Center for X Ray Optics, 1988
[DE90-003300] N90-15732
PHOTOVOLTAIC CELLS
A nickel/hydrogen battery for PV systems
[DE90-001537] N90-15358
PHYSICAL EXERCISE
Potential for reduction of decompression sickness by prebreathing with 100 percent oxygen while exercising
[AD-A213449] N90-15581
The application of optimal control theory for analysis of human jumping and pedaling N90-15590
PHYSIOLOGICAL EFFECTS
Use of lower body negative pressure as a countermeasure to negative Gz acceleration
[AD-A213927] N90-15583
PILE FOUNDATIONS
Geotechnical instrumentation
[PB89-196675] N90-15398
PILOT PERFORMANCE
The human element: The key to safe, civil operations in adverse weather N90-15042
Classification of windshear severity N90-15049
Canard versus aft-tail ride qualities performance and pilot command response N90-15053
Aircraft response and pilot behaviour during a wake vortex encounter perpendicular to the vortex axis N90-15057
Imaging probabilities, geometry and ergonomics in limited visibility helicopter operations N90-15060
Model for measuring complex performance in an aviation environment
[DE90-002055] N90-15585
PILOT TRAINING
Development of the AH-64 display symbology training module
[AD-A213456] N90-15592
PINNING
Effects of non-linearity in the variation of pinning potential with current-density on magnetic flux creep in high and low T(sub c) superconductors
[DE90-003952] N90-15822
PIPE FLOW
Reduction of erosion in elbows due to flow modifications, phase 2
[DE89-011702] N90-15394
PIPELINES
Pipeline vibrations. Fluid transients in non-rigid, unbranched planar piping systems
[ESDU-89030] N90-15491
PIPES (TUBES)
Laminar forced convection inside externally finned tubes
[DE89-636431] N90-15373
Investigation of loads generated by temperature transients in pipes
[DE89-636433] N90-15395
Eddy-current inspection of shuttle heat exchanger tube welds
[NASA-CR-186302] N90-15462
PITCH (INCLINATION)
A pitch control law for compensation of the phugoid mode induced by windshears N90-15051
PITCHING MOMENTS
Flow visualization of the effect of pitch rate on the vortex development on the scale model of a F-18 fighter aircraft
[AD-A214244] N90-15080
PITTING
The effect of dissolved chlorine on the pitting behavior of 304L stainless steel in a 0.5 N NaCl solution
[AD-A213803] N90-15234
The effect of dissolved ozone on the corrosion behavior of Cu-30 Ni and 304L stainless steel in 0.5 N NaCl solutions
[AD-A213804] N90-15235
PIXELS
A logic for the pixel assignment step of imagery classification predicated on class structure N90-15493
PLANE WAVES
A new technique for simulating composite material. Task 2: Analytical solutions with Generalized Impedance Boundary Conditions (GIBCs)
[NASA-CR-186249] N90-15146
Focal plane antenna array for millimeter waves
[AD-D014306] N90-15322
Observation of atomic relaxation near an interface through detection of emitted fluorescence
[AD-A214308] N90-15725
PLANETARY EVOLUTION
The volatile composition of comets
[NASA-CR-186281] N90-15871
PLANETARY ORBITS
Manned spacecraft
[AD-A214218] N90-15129
PLANNING
An expert system for quality assurance (a.k.a.) QA Express
[DE90-003887] N90-15467
Annual operating plan for fiscal year 1990 for chemical/hydrogen energy systems program
[DE90-003964] N90-15527
PLASMA ACCELERATORS
Theoretical and computational studies of magnetic insulation and other plasma-opening-switch phenomena
[DE90-004421] N90-15757
Optical guiding by plasma waves in the plasma beat wave accelerator
[AD-A214288] N90-15763
PLASMA COMPRESSION
Initial results from FRC (Field-Reversed Configuration) compression experiments on FRX-C/LSM
[DE90-003390] N90-15754
PLASMA CONTROL
Studies of plasma performance and transport in the Advanced Toroidal Facility (ATF)
[DE90-001737] N90-15746
Design of DIII-D advanced divertor
[DE90-003343] N90-15752
Magnetic mirror confinement concepts system studies
[DE90-003667] N90-15753
Theoretical and computational studies of magnetic insulation and other plasma-opening-switch phenomena
[DE90-004421] N90-15757
PLASMA DENSITY
Strategic characteristics of Dynamics Explorer 1 retarding ion mass spectrometer and the consequences for core plasma measurements
[AD-A214013] N90-15125
Frequency shift induced in laser pulses by plasma density variations
[AD-A214195] N90-15424
Microfluctuations of plasma density in a theta-pinch and spatial coherency of a probing laser beam
[DE90-603347] N90-15760
PLASMA DIAGNOSTICS
Microfluctuations of plasma density in a theta-pinch and spatial coherency of a probing laser beam
[DE90-603347] N90-15760
PLASMA DYNAMICS
Strategic characteristics of Dynamics Explorer 1 retarding ion mass spectrometer and the consequences for core plasma measurements
[AD-A214013] N90-15125
PLASMA ENGINES
Physical process in MPD plasmas
[AD-A213679] N90-15761
PLASMA HEATING
Propulsion research on the hybrid plume rocket
[AD-A214420] N90-15132
PLASMA INTERACTIONS
Frequency shift induced in laser pulses by plasma density variations
[AD-A214195] N90-15424
Theory of interacting plasmas in space N90-15742
Laboratory simulations of the solar wind-comet interactions N90-15875
PLASMA PHYSICS
Upgrade plans to handle 30 to 40 Mbytes of data for D3-D
[DE90-003291] N90-15750
Data file management in the D3-D data acquisition and analysis computer systems
[DE90-003289] N90-15850
PLASMA POWER SOURCES
Review of quasi-optical gyrotron development
[AD-A213491] N90-15402
PLASMA SHEATHS
Near-surface sputtered particle transport for an oblique incidence magnetic field plasma
[DE90-004422] N90-15758
PLASMA SPECTRA
ICP/AES (Inductively Coupled Plasma/Atomic Emission Spectroscopy): A modern analytical tool
[DE90-003822] N90-15765
PLASMA SPRAYING
Improved process for HIP canning of composites
[NASA-CASE-LEW-14990-1-CU] N90-15147
PLASMA WAVES
Optical guiding by plasma waves in the plasma beat wave accelerator
[AD-A214288] N90-15763
PLASMAS (PHYSICS)
SCATHA (Spacecraft Charging At High Altitudes) atlas data base, volume 2
[AD-A214205] N90-15128
Intense REB (Relativistic Electron Beam) transport in a weakly magnetized plasma
[DE90-002978] N90-15749
The 17th AINSE Plasma Physics Conference: Conference handbook
[DE90-600936] N90-15759
Physical process in MPD plasmas
[AD-A213679] N90-15761
PLASTIC DEFORMATION
Isothermal fatigue behavior of Sn-Pb solar joints
[DE90-003280] N90-15464
PLASTIC PROPERTIES
Development of a rate independent plasticity theory for general cyclic loading N90-15471
PLATES
Mechanical properties and fracture toughness of 8090-T651 plate and 2091 and 8090 sheet N90-15188
Uses and properties of Al-Li on the new EH101 helicopter N90-15201
Aluminum-lithium: Application of plate and sheet to fighter aircraft N90-15202
Fully articulated four-point-bend loading fixture
[NASA-CASE-LEW-14776-1] N90-15445
PLATES (STRUCTURAL MEMBERS)
Transverse (through-the-thickness) shear stiffnesses of fibre reinforced composite laminated plates (computer program)
[ESDU-89013] N90-15152
PLATES (TECTONICS)
Dynamics of mid-ocean ridge systems N90-15575
PLATINUM
Correlations between surface structure and catalytic activity/selectivity
[DE90-003755] N90-15181
PLUMES
Propulsion research on the hybrid plume rocket
[AD-A214420] N90-15132
POINCARE PROBLEM
The behavior of matter under nonequilibrium conditions: Fundamental aspects and applications
[DE90-002522] N90-15157
POINT DEFECTS
Molecular-dynamics study of the amorphization of CuTi
[DE90-003563] N90-15791
POLARIMETRY
N-port theory applied to backscatter polarimetry and depolarization in foliage penetration
[AD-A213437] N90-15305
Polarimetric SAR antenna characterization
[AD-A213438] N90-15306
Flashlight radar: A three-dimensional imaging radar
[AD-A213439] N90-15307
Near-infrared polarimetry and spectroscopy of comets N90-15857
POLARIZATION (WAVES)
Hamiltonian chaos in a nonlinear polarized optical beam
[DE90-002437] N90-15408
POLICIES
Global climate change and NEPA (National Environmental Policy Act) analyses
[DE90-003704] N90-15540
POLLUTION MONITORING
Environmental surveillance data
[DE90-001275] N90-15532

POLLUTION TRANSPORT
Vertical distribution of pollutants in the presence of convective storms
[DE90-002590] N90-15549
POLYAMIDE RESINS
Wet spinning of solid polyamic acid fibers
[NASA-CASE-LAR-14162-1] N90-15259
Crosslinked, flexible, low-molecular-weight polyacrylamide gels for mobility control
[DE90-000202] N90-15280
POLYATOMIC MOLECULES
Determination of stepsize parameters for intermolecular vibrational energy transfer
[DE90-003346] N90-15719
POLYCRYSTALS
US Polycrystalline Thin Film Solar Cells Program
[DE89-009506] N90-15504
POLYETHYLENE TEREPHTHALATE
Electronic and ionic transport in polymers
[AD-A213410] N90-15270
POLYIMIDE RESINS
A novel heat resistant blend produced by compositional quenching: A thermoplastic polyimide impact modified with a fluoroelastomer
[AD-A213724] N90-15273
POLYIMIDES
Novel polyimide compositions based on 4,4': Isophthaloyldiphthalic anaydride (IDPA)
[NASA-CASE-LAR-14194-1] N90-15148
Wet spinning of solid polyamic acid fibers
[NASA-CASE-LAR-14162-1] N90-15259
Polyimides with carbonyl and ether connecting groups between the aromatic rings
[NASA-CASE-LAR-14001-1] N90-15260
POLYMER BLENDS
Phase transition in polymer blends and structure of ionomers
[DE90-003525] N90-15266
POLYMER CHEMISTRY
Interfacial systems for photochemical energy conversion
[DE90-003181] N90-15514
POLYMER MATRIX COMPOSITES
SESAME equation of state for a polymer composite: Phenolic refrasil
[LA-11512-MS] N90-15264
POLYMERIC FILMS
Electronic materials high-T(sub c) superconductivity polymers and composites structural materials surface science and catalysts industry participation
[NASA-CR-186063] N90-15145
Optical properties and laser damage measurements of inorganic polymer films
[DE90-003633] N90-15267
Thin films under chemical stress
[DE90-003754] N90-15484
POLYMERIZATION
Superconducting film fabrication by the sol-gel process
[DE90-002069] N90-15252
Molecules with enhanced electronic polarizabilities based on defect-like states in conjugated polymers
[NASA-CASE-NPO-17633-1-CU] N90-15263
New polymers made with well-characterized organometallic catalysts
[AD-A213592] N90-15272
Electrochemical investigation of electronically conductive polymers
[AD-A214019] N90-15277
POLYMERS
The elastic properties of woven polymeric fabric
[DE89-015391] N90-15255
POLYMORPHISM
Energetics of BCC-FCC lattice deformation in iron
[AD-A213801] N90-15233
POLYNOMIALS
Bounded polynomial randomized consensus
[AD-A213808] N90-15686
POLYPHENYLS
Band-to-band transitions in poly (phenyl methyl silane)
[DE90-003575] N90-15720
POLYPROPYLENE
High-temperature gel-permeation chromatography of poly(4-methyl-1-pentene)
[DE90-002967] N90-15159
POPULATIONS
Destabilization of tokamak pressure-gradient driven instabilities by energetic alpha populations
[DE90-003716] N90-15756
POROSITY
Ultrasonic evaluation of porosity in aluminum cast materials
[AD-A213548] N90-15232
Characterization of new cathode materials for molten carbonate fuel cells
[DE90-003547] N90-15516
Fabrication of porous ceramic electrode structures
[DE90-003548] N90-15517
POSITION (LOCATION)
National airspace system: Airport movement area control operational concept
[WP-89W00181] N90-15086
Feasibility study of using industrial robot for ultrasound testing
[DE90-002977] N90-15461
Location of interior impact source in randomly excited structures
[DE90-001092] N90-15474
POSITRON ANNIHILATION
Electron-positron momentum distribution measurements of high-T superconductors and related systems
[DE90-002974] N90-15780
POTASSIUM
Radial heat flux limits in potassium heat pipes: An experimental and analytical investigation
[DE90-002655] N90-15396
Niobium 1 percent zirconium/potassium and titanium/potassium life-test heat pipe design and testing
[DE90-002430] N90-15522
POTENTIAL ENERGY
A guide for estimating potential energy savings from increased solar reflectance of a low-sloped roof
[DE90-003720] N90-15526
POTENTIAL FLOW
Solution of potential flow past an elastic body using the boundary element technique
[AD-A213843] N90-15390
POWDER (PARTICLES)
Ceramic powder characterization
[DE90-001282] N90-15249
IEA/Annex 2 powder characterization cooperative program
[AD-A213540] N90-15271
Processing and fabrication of YBa2Cu4O8 and YBa2Cu4O8/YBa2Cu3O(x) composites
[DE90-003559] N90-15789
POWDER METALLURGY
New Light Alloys
[AGARD-CP-444] N90-15185
Fatigue and fracture behaviour of a PM Al-Li alloy N90-15195
High performance powder metallurgy aluminum alloys: An overview N90-15204
POWER BEAMING
Transportation and operations aspects of space energy systems N90-15842
POWER CONDITIONING
Research on GaAs quantum-coupled structures that can be used as electron devices
[AD-A214015] N90-15350
POWER EFFICIENCY
X.2 limited flight test plan
[AD-A214412] N90-15099
POWER FACTOR CONTROLLERS
Adjustable speed drive study, June 1985 to September 1988. Part 2: Appendices
[DE90-002771] N90-15332
POWER SPECTRA
Array signal processing: New techniques for direction finding and spectrum estimation
[AD-A213883] N90-15345
PRANDTL NUMBER
Time-dependent free convection in low Prandtl number fluids
[DE90-003053] N90-15377
PRECIPITATION (METEOROLOGY)
Adverse weather operations during the Canadian Atlantic storms program N90-15052
PREDICTION ANALYSIS TECHNIQUES
Parametric identification of discrete time series models for structural response prediction N90-15472
On the motion of compliantly-connected rigid bodies in contact. Part 1: The motion prediction problem
[AD-A214135] N90-15489
Identification and quantification of synoptic structure in simulated Tiros N radiance soundings N90-15546
PREDICTIONS
The radar-based short term prediction of the time-space evolution of rain fields
[AD-A213802] N90-15312
Comparison of engine knock predictions using a fully-detailed and a reduced chemical kinetic mechanism
[DE90-002805] N90-15448
Pipeline vibrations. Fluid transients in non-rigid, unbranched planar piping systems
[ESDU-89030] N90-15491
Elicitation of natural language representations of uncertainty using computer technology
[DE90-001416] N90-15611
Gradient projection techniques for large-scale optimization problems
[DE90-001986] N90-15618
PREMIXED FLAMES
A tomographic study of premixed turbulent stagnation point flames
[DE90-002462] N90-15156
PRESSURE DISTRIBUTION
Static pressure distribution in an angular channel with helicoidal wire
[DE89-636474] N90-15374
Modifications of the Penn State Boundary Layer Research Facility for boundary layer/structure interaction experimental research
[AD-A213874] N90-15391
Nonlinear viscous waves produced by an impulsively moving plate
[AD-A214014] N90-15392
Optical acoustic sensor using optical fiber
[DE89-901267] N90-15730
PRESSURE EFFECTS
Shock-wave characterization of energetic booster-rocket propellant WAK-2 and its simulant UGS
[DE90-002633] N90-15285
Burning rates of two cast nitramine explosives using a hybrid closed bomb-strand burner
[DE90-002785] N90-15286
Oxygen electrode in molten carbonate fuel cells
[DE90-002871] N90-15510
Micron-thin Nb films recovered from Mbar shock pressures
[DE90-001509] N90-15772
PRESSURE GAGES
Portable digital pressure indicator for calibrating magnetic tape recorders
[NASA-TM-101650] N90-15401
PRESSURE GRADIENTS
An experimental study of the time-dependent behavior of the appendage-body junction vortex
[AD-A213465] N90-15384
Destabilization of tokamak pressure-gradient driven instabilities by energetic alpha populations
[DE90-003716] N90-15756
PRESSURE MEASUREMENT
Portable digital pressure indicator for calibrating magnetic tape recorders
[NASA-TM-101650] N90-15401
Antarctic surface temperature and pressure data
[DE90-000971] N90-15565
PRESSURE REDUCTION
Potential for reduction of decompression sickness by prebreathing with 100 percent oxygen while exercising
[AD-A213449] N90-15581
PRESSURE SENSORS
Calibration of seven-hole pressure probes for use in fluid flows with large angularity
[NASA-TM-102200] N90-15399
PRESSURE SUITS
Manned spacecraft
[AD-A214218] N90-15129
Use of lower body negative pressure as a countermeasure to negative Gz acceleration
[AD-A213927] N90-15583
PRESTRESSING
Theoretical models of earthquake phenomena and the physical significance of seismic moment tensor expansions
[AD-A213813] N90-15556
PRINCIPAL COMPONENTS ANALYSIS
Observational study of the macroscopic behavior of moist-convective processes N90-15547
PRIORITIES
Concurrence control for transactions with priorities
[NASA-CR-186241] N90-15699
PRIVACY
On the privacy problems involved in allowing access to computers via the public telephone system
[RSRE-88006] N90-15303
PROBABILITY DISTRIBUTION FUNCTIONS
Uniform versus random sampling in physical calculations: Monte Carlo
[DE90-003247] N90-15696
Strong large deviation and local limit theorems
[AD-A213610] N90-15698
PROBABILITY THEORY
Centralized and decentralized Kalman filter techniques for tracking, navigation, and control
[AD-A214245] N90-15091
Two basic partial orderings for distributions derived from Schur functions and majorization
[AD-A213703] N90-15682
PROBLEM SOLVING
On the identification of local minimizers in inertia-controlling methods for quadratic programming
[DE89-017330] N90-15616
A note on the maximum size of a rectilinear maze
[AD-A214445] N90-15668

PROCESS CONTROL (INDUSTRY)
Processing and properties of nanophase oxides
[DE90-003826] N90-15171
Mechanistic modeling of epoxy resins
[DE89-015119] N90-15247
Automated convection soldering
[KCP-613-4005] N90-15300
Back to basics
[DE90-002734] N90-15463
Integrated approach fault tolerance-current state and future requirements
[AD-A214402] N90-15465
Time bounds for real-time process control in the presence of timing uncertainty
[AD-A213791] N90-15633
Processing and fabrication of YBa2Cu4O8 and YBa2Cu4O8/YBa2Cu3O(x) composites
[DE90-003559] N90-15789
PROCUREMENT MANAGEMENT
Program manager's handbook
[AD-A214338] N90-15844
PRODUCTION ENGINEERING
Current launch vehicle reliability practice and data base assessment. Volume 1: Executive summary and report body
[AD-A213600] N90-15121
PRODUCTION MANAGEMENT
Current launch vehicle reliability practice and data base assessment. Volume 1: Executive summary and report body
[AD-A213600] N90-15121
PRODUCTIVITY
Submerged arc welding consumables for HSLA (High Strength Low Alloy)-100 steel
[AD-A213433] N90-15452
PROGRAM VERIFICATION (COMPUTERS)
Environment for failure region analysis: REACHER - a reachability condition derivation tool
[AD-A214183] N90-15641
The StarLite project
[AD-A214193] N90-15642
PROGRAMMING LANGUAGES
Paralation views: Abstractions for efficient scientific computing on the connection machine
[AD-A213935] N90-15604
A signal processing language for coarse grain data flow multiprocessors
[AD-A213863] N90-15635
PROJECT MANAGEMENT
Physical and Electrical Standards Laboratory general operating procedures
[DE90-003515] N90-15116
Back to basics
[DE90-002734] N90-15463
PROJECTILES
MESA 3-D calculations of armor penetration by projectiles with combined obliquity and yaw
[DE89-015265] N90-15438
PROPELLANT ADDITIVES
Calculation of Einstein A coefficients and oscillator strengths for the A(perturbed)(2)A(1)-X(perturbed)(2)B(1) transition of NH(2)
[AD-A213837] N90-15176
PROPELLANT BINDERS
Using small scale tests to estimate the failure diameter of a propellant
[DE90-001166] N90-15281
PROPELLANT CHEMISTRY
Calculation of Einstein A coefficients and oscillator strengths for the A(perturbed)(2)A(1)-X(perturbed)(2)B(1) transition of NH(2)
[AD-A213837] N90-15176
PROPELLANT COMBUSTION
Spectral studies of solid propellant combustion. 2: Emission and absorption results for M-30 and HMX1 propellants
[AD-A213857] N90-15292
PROPELLANT DECOMPOSITION
Calculation of Einstein A coefficients and oscillator strengths for the A(perturbed)(2)A(1)-X(perturbed)(2)B(1) transition of NH(2)
[AD-A213837] N90-15176
PROPELLANT SENSITIVITY
Shock-wave characterization of energetic booster-rocket propellant WAK-2 and its simulant UGS
[DE90-002633] N90-15285
PROPELLANTS
Ignitability test method and apparatus
[NASA-CASE-LAR-13996-1-SB] N90-15161
PROPELLER DRIVE
X.2 limited flight test plan
[AD-A214412] N90-15099
PROPELLERS
Evaluation of the improved OV-ID anti-icing system, phase 2
[AD-A213928] N90-15083
PROTECTION
Effects of lightning on operations of aerospace vehicles N90-15065
PROTECTIVE COATINGS
A review of the effects of microalloying constituents on the formation and breakdown of protective oxide scales on high-temperature alloys at temperatures below 700 C
[DE90-001277] N90-15216
PROTONS
A calculation of energetic proton spectra producedat substorm onset in the fields of the explosive reconnection model N90-15866
PSYCHOLOGY
Human behavior
[PB90-780008] N90-15584
PULSARS
Pulsars lost and found: The second Princeton-Arecibo millisecond pulsar search N90-15865
PULSE COMMUNICATION
Network simulator definition
[AD-A213463] N90-15308
PULSE GENERATORS
Design of a bounded wave EMP (Electromagnetic Pulse) simulator
[AD-A214137] N90-15316
Avalanche photoconductive switching
[DE90-002980] N90-15337
Computer controlled MHD power consolidation and pulse-generation system
[DE90-001224] N90-15662
PULSED LASERS
Laser-supported detonation waves and pulsed laser propulsion
[DE90-002753] N90-15412
Frequency shift induced in laser pulses by plasma density variations
[AD-A214195] N90-15424
PULSED RADIATION
Interlaboratory comparison of radiation-induced attenuation in optical fibers. Part 3: Transient exposures
[DE90-000859] N90-15729
PULSES
SBS (Stimulated Brillouin Scattering) pulse distortion in multimode optical fibers: Preliminary results
[DE90-003023] N90-15731
PYROLYSIS
New polymers made with well-characterized organometallic catalysts
[AD-A213592] N90-15272
Characterization of the thermal degradation of selected energetic materials and mixtures by Rapid-Scan Fourier Transform Infrared (RSFTIR) spectroscopy
[AD-A214411] N90-15296
PYRROLES
Electrochemical investigation of electronically conductive polymers
[AD-A214019] N90-15277

Q

QUADRATIC PROGRAMMING
On the identification of local minimizers in inertia-controlling methods for quadratic programming
[DE89-017330] N90-15816
Sequential quadratic programming algorithms for optimization
[DE90-000022] N90-15617
Gradient projection techniques for large-scale optimization problems
[DE90-001986] N90-15618
QUALITY CONTROL
Physical and Electrical Standards Laboratory general operating procedures
[DE90-003515] N90-15116
Back to basics
[DE90-002734] N90-15463
An expert system for quality assurance (a.k.a.) QA Express
[DE90-003887] N90-15467
QUANTUM EFFICIENCY
Research on high-efficiency, single-junction, monolithic, thin-film amorphous silicon solar cells, phase 2
[DE89-009496] N90-15503
QUANTUM ELECTRONICS
Chemisorption under stress
[AD-A213785] N90-15175
Research on GaAs quantum-coupled structures that can be used as electron devices
[AD-A214015] N90-15350
Solid state research
[AD-A213405] N90-15806
QUANTUM MECHANICS
Theoretical methods for the study of chemical dynamics
[DE90-003122] N90-15160
Lefschetz trace formula and BRST
[DE89-635705] N90-15835
QUANTUM THEORY
Chemisorption under stress
[AD-A213785] N90-15175
Research on GaAs quantum-coupled structures that can be used as electron devices
[AD-A214015] N90-15350
Relativistic self-consistent field studies of atoms and molecules
[AD-A214101] N90-15724
Tunnelling effects on low energy fusion cross sections
[AD-A214010] N90-15762
Interface phonons in semiconductor double heterostructures
[AD-A213732] N90-15810
QUANTUM WELLS
Research on materials and components for opto-electronic signal processing and computing
[AD-A213740] N90-15811
QUASARS
The disk-halo connection and the nature of the interstellar medium
[NASA-CR-186286] N90-15860
QUENCHING (COOLING)
Calculation of surface heat transfer parameters during quenching from surface thermocouple signals
[DE89-011620] N90-15224
QUEUEING THEORY
The application of queuing theory to the modelling of CP-140 aircraft communications
[AD-A213479] N90-15310
Queues with negative arrivals
[AD-A213860] N90-15687

R

RADAR
The radar-based short term prediction of the time-space evolution of rain fields
[AD-A213802] N90-15312
Adaptive canceller limitations caused by I,Q mismatch errors
[AD-A214287] N90-15318
RADAR CROSS SECTIONS
Flashlight radar: A three-dimensional imaging radar
[AD-A213439] N90-15307
RADAR IMAGERY
Flashlight radar: A three-dimensional imaging radar
[AD-A213439] N90-15307
RADAR MEASUREMENT
Flashlight radar: A three-dimensional imaging radar
[AD-A213439] N90-15307
RADAR TARGETS
Studies of quantitative methods for imaging from scattered fields
[AD-A214047] N90-15638
RADAR TRACKING
Turbulence spectral widths view angle independence as observed by Doppler radar
[DOT/FAA/SA-89/2] N90-15566
RADIANCE
Identification and quantification of synoptic structure in simulated Tiros N radiance soundings N90-15546
Identification and quantification of synoptic structure in simulated TIROS N radiance soundings
[AD-A213729] N90-15553
Description of SHARC: The Strategic High-Altitude Radiance Code
[AD-A213806] N90-15555
RADIATION ABSORPTION
Analysis of catalytically enhanced solar absorption chemical reactors: 1 - numerical model description
[DE89-014742] N90-15505
RADIATION DAMAGE
Microstructural evolution of martensitic steels during fast neutron irradiation
[DE89-016231] N90-15212
Fusion reactor materials
[DE90-000976] N90-15744
RADIATION EFFECTS
Aircraft testing in the electromagnetic environment N90-15066
Helium-induced weld cracking in irradiated 304 stainless steel
[DE90-001312] N90-15219
Cast stainless steel aging: Mechanisms and predictions
[DE90-003772] N90-15241
Overview on radiation effects in electronics
[DE90-000841] N90-15357
Interlaboratory comparison of radiation-induced attenuation in optical fibers. Part 3: Transient exposures
[DE90-000859] N90-15729

Fusion reactor materials
[DE90-000976] N90-15744
Progress in LTE and non-LTE transport calculations
[DE90-003394] N90-15764
Irradition-induced grain growth: Role of dislocations
[DE90-003565] N90-15792
Ion-irradiation effects in Tl2Ca2Ba2Cu3O10 superconductors
[DE90-003840] N90-15802
Power semiconductor devices for space nuclear power systems
[DE90-001178] N90-15819

RADIATION HARDENING
Design of a bounded wave EMP (Electromagnetic Pulse) simulator
[AD-A214137] N90-15316
Proposed activities to prepare for testing advanced/stealth weapons systems
[AD-A214453] N90-15321
Power semiconductor devices for space nuclear power systems
[DE90-001178] N90-15819

RADIATION HAZARDS
Safety evaluation report for Galileo: Volume 1
[DE90-003086] N90-15122
Safety evaluation report for Galileo, volume 2
[DE90-003087] N90-15123

RADIATION MEASUREMENT
Initial optical transition radiation measurements of the electron beam for the Boeing free-electron laser experiment
[DE90-003396] N90-15416
Environmental surveillance data
[DE90-001275] N90-15532

RADIATION PROTECTION
Safety evaluation report for Galileo: Volume 1
[DE90-003086] N90-15122
Safety evaluation report for Galileo, volume 2
[DE90-003087] N90-15123
Interlaboratory comparison of radiation-induced attenuation in optical fibers. Part 3: Transient exposures
[DE90-000859] N90-15729

RADIATION SHIELDING
Arc-sprayed coatings for electromagnetic pulse protection: Assessment of physical and electrical properties
[AD-A213825] N90-15275
Interlaboratory comparison of radiation-induced attenuation in optical fibers. Part 3: Transient exposures
[DE90-000859] N90-15729

RADIATION SOURCES
Intense REB (Relativistic Electron Beam) transport in a weakly magnetized plasma
[DE90-002978] N90-15749

RADIATIVE TRANSFER
Identification and quantification of synoptic structure in simulated TIROS N radiance soundings
[AD-A213729] N90-15553

RADIO ASTRONOMY
The 22 GHz Radioastron receiver: Development of prototype components during the year 1988
[PB89-212583] N90-15323

RADIO COMMUNICATION
Spread spectrum mobile radio communications
[AD-A213726] N90-15311
Voice/data integration in mobile radio networks: Overview and future research directions
[AD-A214289] N90-15319

RADIO FREQUENCIES
Fiber optic sensing system
[NASA-CASE-LEW-14795-1] N90-15733

RADIO FREQUENCY HEATING
Experiments on linear high beta helical axis stellarators to study simulated toroidal effects and Alfven-wave heating
[DE90-001704] N90-15745

RADIO RECEIVERS
The 22 GHz Radioastron receiver: Development of prototype components during the year 1988
[PB89-212583] N90-15323

RADIOACTIVE DECAY
Excitation lifetimes and excited-state forces in chemisorbed molecules
[DE90-002578] N90-15165
Cosmic ray half life of (54)Mn
[DE90-000134] N90-15880

RADIOACTIVE ISOTOPES
Safety evaluation report for Galileo: Volume 1
[DE90-003086] N90-15122
ROBOCAL (Robotic Calorimetry): An automated NDA (Nondestructive Assay) calorimetry and gamma isotopic system
[DE90-003217] N90-15168

RADIOACTIVE MATERIALS
ROBOCAL (Robotic Calorimetry): An automated NDA (Nondestructive Assay) calorimetry and gamma isotopic system
[DE90-003217] N90-15168
Technology of fast spark gaps
[AD-A214199] N90-15353

RAIN
The radar-based short term prediction of the time-space evolution of rain fields
[AD-A213802] N90-15312

RAINDROPS
A numerical model for the axisymmetric equilibrium shape of drops in uniform motion: Effects of external flow, electric field and surface charge N90-15071

RAMAN SPECTRA
Aspects of Raman scattering
[AD-A213926] N90-15736
Characterization of MOCVD (Metal Organic Chemical Vapor Deposition) grown epitaxial ceramic oxide thin films
[DE90-003561] N90-15790
Optical phonon modes in a double heterostructure of polar crystals
[AD-A214208] N90-15816

RAMJET MISSILES
Steady flow combustion model for solid-fuel ramjet projectiles
[BRL-TR-2987] N90-15163

RANDOM PROCESSES
Location of interior impact source in randomly excited structures
[DE90-001092] N90-15474

RANDOM SAMPLING
A logic for the pixel assignment step of imagery classification predicated on class structure N90-15493
Uniform versus random sampling in physical calculations: Monte Carlo
[DE90-003247] N90-15696

RANDOM VARIABLES
Strong large deviation and local limit theorems
[AD-A213610] N90-15698

RANDOM WALK
A diffusion on a fractal state space
[AD-A213555] N90-15707

RANGEFINDING
China-built airborne synchronous laser ranger the new L-8 jet trainer aircraft
[AD-A213835] N90-15422

RARE GASES
Excimer emission from alkali diatomic and alkaline-earth-noble-gas molecules
[AD-A214246] N90-15179

REACTION KINETICS
Effect of community structure on the kinetics of anaerobic degradation of aromatic compounds
[DE90-003666] N90-15134
Theoretical methods for the study of chemical dynamics
[DE90-003122] N90-15160
Shock tube ignition of octanes
[DE90-001167] N90-15164
Mechanistic modeling of epoxy resins
[DE89-015119] N90-15247
Burning rates of two cast nitramine explosives using a hybrid closed bomb-strand burner
[DE90-002785] N90-15286
Comparison of engine knock predictions using a fully-detailed and a reduced chemical kinetic mechanism
[DE90-002805] N90-15448
Dynamics of electron transfer for a nonsuperexchange coherent mechanism, 1
[AD-A213450] N90-15721

REACTOR DESIGN
Design of DIII-D advanced divertor
[DE90-003343] N90-15752

REACTOR MATERIALS
Microstructural evolution of martensitic steels during fast neutron irradiation
[DE89-016231] N90-15212
Report of the Advanced Neutron Source (ANS) Aluminum Cladding Corrosion Workshop
[DE90-001281] N90-15217
Fusion reactor materials
[DE90-000976] N90-15744

REACTOR SAFETY
Niobium 1 percent zirconium/potassium and titanium/potassium life-test heat pipe design and testing
[DE90-002430] N90-15522

REACTOR TECHNOLOGY
Static pressure distribution in an angular channel with helicoidal wire
[DE89-636474] N90-15374
The search for solid state fusion lasers
[DE89-012301] N90-15410
Design of DIII-D advanced divertor
[DE90-003343] N90-15752
Introduction to D-He(3) fusion reactors N90-15839

REAL TIME OPERATION
Implementing fault-tolerant sensors
[NASA-CR-186251] N90-15400
Time bounds for real-time process control in the presence of timing uncertainty
[AD-A213791] N90-15633
A multichannel processing approach to real time network detection, phase association, and threshold monitoring
[AD-A213940] N90-15657
Ultra high performance, highly reliable, numeric intensive processors and systems
[AD-A214100] N90-15659
Concurrence control for transactions with priorities
[NASA-CR-186241] N90-15699
Periodic phase adjustment distributed clock synchronization in the hard realtime environment
[AD-A213842] N90-15708

RECEIVERS
SLCSAT (Submarine Laser Communication Satellite) communication system design study
[AD-A213403] N90-15304

RECIPROCATION
Feasibility analysis of reciprocating magnetic heat pumps
[NASA-CR-186205] N90-15363

RECTANGULAR WAVEGUIDES
Rectangular-to-circular waveguide transitions for high-power circular overmoded waveguides
[AD-A213925] N90-15349

RECURSIVE FUNCTIONS
Membership-set parameter estimation via optimal bounding ellipsoids
[AD-A213807] N90-15685

RECYCLING
Managing the waste stream: Background information for planning source separation programs
[PB90-100223] N90-15530

REDOX CELLS
Interfacial systems for photochemical energy conversion
[DE90-003181] N90-15514

REDUCED GRAVITY
Bridgman crystal growth
[NASA-CR-186204] N90-15766

REDUNDANCY
Base reaction optimization of redundant manipulators for space applications
[NASA-CR-186274] N90-15447

REELS
Mechanical evaluation of the differential drum concept for optical fiber pay-out
[AD-A214149] N90-15740

REFLECTION
A guide for estimating potential energy savings from increased solar reflectance of a low-sloped roof
[DE90-003720] N90-15526

REFRACTIVITY
Optical solitons in liquid crystals
[DE90-000694] N90-15728

REFRACTORY MATERIALS
A novel heat resistant blend produced by compositional quenching: A thermoplastic polyimide impact modified with a fluoroelastomer
[AD-A213724] N90-15273

REFRACTORY METALS
Thermally stable metal/GaAs contacts
[DE90-002122] N90-15774

REFRIGERATING MACHINERY
Recent advances in magnetic heat pump technology
[DE89-013289] N90-15370

REGENERATIVE COOLING
Feasibility analysis of reciprocating magnetic heat pumps
[NASA-CR-186205] N90-15363

REGENERATORS
Gas turbine regenerators: A method for selecting the optimum plate-finned surface pair for minimum core volume
[AD-A213430] N90-15382

REGRESSION ANALYSIS
Precipitation distributions associated with cyclones originating over the Gulf of Mexico and surrounding coastal regions
[AD-A213644] N90-15569

REGULATIONS
International aspects of restrictions of ozone-depleting substances
[DE90-001813] N90-15534

REINFORCING FIBERS
Metal matrix composites with long inorganic fibers N90-15206
Metal matrix composites: A promising alternative to conventional alloys N90-15208

REINFORCING MATERIALS
Composite activities at Lawrence Livermore National Laboratory
[DE90-002979] N90-15149
RELATIVISTIC ELECTRON BEAMS
Intense REB (Relativistic Electron Beam) transport in a weakly magnetized plasma
[DE90-002978] N90-15749
RELATIVISTIC PARTICLES
Substructural dependence of the multiparticle production in relativistic heavy-ion interactions
[LUIP-8904] N90-15716
RELATIVITY
An exact solution for a thick domain wall in general relativity
[NASA-CR-185013] N90-15826
RELIABILITY ANALYSIS
Reliability analysis of the space station freedom electrical power system
[AD-A214105] N90-15126
An iterative Bayes procedure for reliability assessment
[DE90-002106] N90-15466
REMOTE CONTROL
X.2 limited flight test plan
[AD-A214412] N90-15099
A versatile stepping motor controller for systems with many motors
[DE90-001556] N90-15327
SIMON (SuperIntelligent Mobile Observing Navigator): A high-reliability robot for a radiation environment
[DE90-003888] N90-15460
REMOTE SENSING
RAIDS: An orbiting observatory for ionospheric remote sensing from space
[AD-A213717] N90-15494
REMOTE SENSORS
RAIDS: An orbiting observatory for ionospheric remote sensing from space
[AD-A213717] N90-15494
Development of the RAIDS (Remote Atmospheric and Ionospheric Detector System) extreme ultraviolet wedge and strip detector
[AD-A213730] N90-15495
REPRESENTATIONS
Principles and algorithms for causal reasoning with uncertainty
[AD-A214248] N90-15644
REQUIREMENTS
MANPRINT methods monograph: Aiding the development of manned system performance criteria
[AD-A213543] N90-15593
A structured connectionist approach to direct inferences and figurative adjective-noun combinations
[AD-A214326] N90-15649
Ultra high performance, highly reliable, numeric intensive processors and systems
[AD-A214100] N90-15659
RESEARCH
The kind of mathematics involved in applied superconductivity research
[DE90-003706] N90-15798
RESEARCH AND DEVELOPMENT
Automation and robotics in construction: Japanese research and development
[AD-A214170] N90-15456
RESEARCH FACILITIES
Hypersonic nozzle design
[NASA-CR-186261] N90-15077
NTES (Nuclear Test and Experimental Sciences) program laser facility for physics experiments Building 391 High Bay Option
[DE90-001795] N90-15411
Magnetic mirror confinement concepts system studies
[DE90-003667] N90-15753
RESEARCH PROJECTS
The StarLite project
[AD-A214193] N90-15642
RESEARCH VEHICLES
Research in knowledge-based vision techniques for the Autonomous Land Vehicle Program
[AD-A213440] N90-15453
RESIDUAL STRESS
Reduction of residual stress and distortion in HY100 and HY130 high strength steels during welding
[AD-A213532] N90-15231
RESINS
Composite activities at Lawrence Livermore National Laboratory
[DE90-002979] N90-15149
RESOLUTION
Flashlight radar: A three-dimensional imaging radar
[AD-A213439] N90-15307
RESONANT FREQUENCIES
Structural response measurements and predictions for the SANDIA 34-meter test bed
[DE90-002575] N90-15524
RESOURCES MANAGEMENT
Cockpit resource management: A selected annotated bibliography
[AD-A214272] N90-15594
RESPONSE TIME (COMPUTERS)
Alternative representations for database responses N90-15847
REVISIONS
Ada 9X project report. Revision request report
[AD-A213503] N90-15629
RHEOLOGY
Comments on ER (Electrorheological) fluid rheology
[DE90-002892] N90-15166
Gelled propellant flow: Boundary layer theory for power-law fluids in a converging planar channel
[DE90-000923] N90-15365
Determination of flow-regime boundaries for cohesive particles
[DE90-001405] N90-15369
Advanced study in solid transport: Rheological behavior of dense suspension
[DE90-003369] N90-15483
Non Newtonian gravity creeping flow
[DE90-600816] N90-15828
RIBBON PARACHUTES
An experimental investigation of wall-interference effects for parachutes in closed wind tunnels
[DE90-001802] N90-15076
RIDING QUALITY
Canard versus aft-tail ride qualities performance and pilot command response N90-15053
RIEMANN MANIFOLD
A (2+1)-dimensional pure gravity for an arbitrary closed initial surface
[DE90-701754] N90-15829
RIGID STRUCTURES
On the motion of compliantly-connected rigid bodies in contact. Part 1: The motion prediction problem
[AD-A214135] N90-15489
RISK
Elicitation of natural language representations of uncertainty using computer technology
[DE90-001416] N90-15611
ROBOT ARMS
Control of mechanical manipulators N90-15432
Feasibility study of using industrial robot for ultrasound testing
[DE90-002977] N90-15461
Gaze controls with interactions and delays
[AD-A214286] N90-15667
ROBOT DYNAMICS
Centralized and decentralized Kalman filter techniques for tracking, navigation, and control
[AD-A214245] N90-15091
SIMON (SuperIntelligent Mobile Observing Navigator): A high-reliability robot for a radiation environment
[DE90-003888] N90-15460
ROBOT SENSORS
Sensor integration using concurrent computing on-board the ORNL mobile robot
[DE89-008740] N90-15436
ROBOTICS
Autonomous land navigation in a structured environment
[DE90-001625] N90-15087
New approach to the inverse problem of six-link manipulators via the optimization technique
[DE90-710044] N90-15441
Spatial dynamics of deformable multibody systems with variable kinematic structure
[AD-A214098] N90-15455
Vision in dynamic environments
[AD-A213434] N90-15587
ROBOTS
Centralized and decentralized Kalman filter techniques for tracking, navigation, and control
[AD-A214245] N90-15091
ROBOCAL (Robotic Calorimetry): An automated NDA (Nondestructive Assay) calorimetry and gamma isotopic system
[DE90-003217] N90-15168
Development of a robotics system for automated chemical analysis of sediment, sludges, and soils
[DE90-003637] N90-15170
Lunar construction utility vehicle
[NASA-CR-186231] N90-15435
Sensor integration using concurrent computing on-board the ORNL mobile robot
[DE89-008740] N90-15436
Research in knowledge-based vision techniques for the Autonomous Land Vehicle Program
[AD-A213440] N90-15453
Feasibility study of using industrial robot for ultrasound testing
[DE90-002977] N90-15461
Design and implementation of two concurrent multi-sensor integration algorithms for mobile robots
[DE90-003041] N90-15663
Gaze controls with interactions and delays
[AD-A214286] N90-15667
A note on the maximum size of a rectilinear maze
[AD-A214445] N90-15668
ROBUSTNESS (MATHEMATICS)
A paradigm for robust geometric algorithms
[AD-A214324] N90-15647
ROCKET ENGINES
Extended temperature range rocket injector
[NASA-CASE-LEW-14846-1] N90-15130
Development of an integrated BEM approach for hot fluid structure interaction
[NASA-CR-186214] N90-15364
ROCKET EXHAUST
Measurement of optical radiations in spacecraft environments
[AD-A213814] N90-15497
ROCKET OXIDIZERS
Gelled propellant flow: Boundary layer theory for power-law fluids in a converging planar channel
[DE90-000923] N90-15365
ROLLERS
Fully articulated four-point-bend loading fixture
[NASA-CASE-LEW-14776-1] N90-15445
ROOFS
A guide for estimating potential energy savings from increased solar reflectance of a low-sloped roof
[DE90-003720] N90-15526
ROTARY GYROSCOPES
A new kind of heterodyne fiber-optic gyroscope
[AD-A213953] N90-15404
ROTARY WING AIRCRAFT
NASA's program on icing research and technology N90-15062
ROTARY WINGS
Effects of aeroelastic tailoring on anisotropic composite material beam models of helicopter blades
[AD-A213478] N90-15095
An examination of helicopter rotor load calculations
[AD-A214295] N90-15098
ROTATION
A study of the effects of Rotating Frame Turbulence (RFT) on helicopter flight mechanics N90-15058
The role of attention in visual processing
[AD-A214158] N90-15588
Some computational properties of rotation representations
[AD-A213888] N90-15665
Mechanical evaluation of the differential drum concept for optical fiber pay-out
[AD-A214149] N90-15740
ROTOR AERODYNAMICS
Finite difference techniques and rotor blade aeroelastic partial differential equations with quasisteady aerodynamics N90-15075
ROTOR BLADES (TURBOMACHINERY)
A study of the effects of Rotating Frame Turbulence (RFT) on helicopter flight mechanics N90-15058
ROTOR DYNAMICS
Application of the joined wing to tiltrotor aircraft
[NASA-CR-177543] N90-15093
ROTORS
Prediction of stochastic blade loads for three-bladed, rigid-hub rotors
[DE89-009508] N90-15520
ROUTES
A structural factoring approach for analyzing probabilistic networks N90-15697
RUBBER
A novel heat resistant blend produced by compositional quenching: A thermoplastic polyimide impact modified with a fluoroelastomer
[AD-A213724] N90-15273
RUN TIME (COMPUTERS)
An efficient UNICOS run-time system for functional programs on a CRAY X-MP
[DE89-016603] N90-15610
Systolic algorithms for imaging from space
[AD-A213870] N90-15701
RUNWAYS
Design temperatures for flexible airfield pavement design
[AD-A214141] N90-15115
RUPTURING
Fully articulated four-point-bend loading fixture
[NASA-CASE-LEW-14776-1] N90-15445

S

S MATRIX THEORY
A new technique for simulating composite material. Task 2: Analytical solutions with Generalized Impedance Boundary Conditions (GIBCs)
[NASA-CR-186249] N90-15146
SAFETY
Evaluation of the improved OV-ID anti-icing system, phase 2
[AD-A213928] N90-15083
X.2 limited flight test plan
[AD-A214412] N90-15099
Safety evaluation report for Galileo: Volume 1
[DE90-003086] N90-15122
Safety evaluation report for Galileo, volume 2
[DE90-003087] N90-15123
SAFETY FACTORS
The United States Air Force approach to all-weather testing N90-15047
SAMPLING
Environmental surveillance data
[DE90-001275] N90-15532
SANDWICH STRUCTURES
Computer-controlled ion beam sputter-deposition of superconducting oxide films
[AD-A213921] N90-15812
SAPPHIRE
Preparation, structure and properties of VO(sub x) and TiO2 thin films by MOCVD
[DE90-003566] N90-15793
SATELLITE ANTENNAS
Proceedings of the Antenna Applications Symposium, volume 2
[AD-A213815] N90-15313
SATELLITE COMMUNICATION
SLCSAT (Submarine Laser Communication Satellite) communication system design study
[AD-A213403] N90-15304
A signal realization data base generated by the multiple phase-screen method
[AD-A214004] N90-15852
SATELLITE OBSERVATION
Geosat/ERM altimeter data analysis for the determination of global oceanic mesoscale variability N90-15492
SCALARS
An exact solution for a thick domain wall in general relativity
[NASA-CR-185013] N90-15826
Nonlocality and stochastic quantization of field theory
[DE89-633913] N90-15833
SCALE (CORROSION)
A review of the effects of microalloying constituents on the formation and breakdown of protective oxide scales on high-temperature alloys at temperatures below 700 C
[DE90-001277] N90-15216
SCANDIUM
Cryogenic mechanical properties of low density superplastic Al-Mg-Sc alloys
[DE90-002120] N90-15222
SCANNING
Scannable millimeter wave arrays, volume 1
[AD-A213895] N90-15347
Scannable millimeter wave arrays, volume 2
[AD-A213896] N90-15348
SCATHA SATELLITE
SCATHA (Spacecraft Charging at High Altitudes) atlas data base, volume 1
[AD-A214204] N90-15127
SCATHA (Spacecraft Charging At High Altitudes) atlas data base, volume 2
[AD-A214205] N90-15128
SCATTERING
Dynamical structure of liquid and amorphous metals
[DE90-003805] N90-15229
Progress in LTE and non-LTE transport calculations
[DE90-003394] N90-15764
SCATTERING COEFFICIENTS
Anomalous absorption by atmospheric water vapor and stabilized water fogs in the infrared and CM-wave regions
[AD-A214202] N90-15572
SCATTERING CROSS SECTIONS
A new technique for simulating composite material. Task 2: Analytical solutions with Generalized Impedance Boundary Conditions (GIBCs)
[NASA-CR-186249] N90-15146
Research on acoustical scattering, diffraction catastrophes, optics of bubbles, acoustical phase conjugation, and wake of an oscillating circular cylinder
[AD-A214168] N90-15711
SCENE ANALYSIS
A logic for the pixel assignment step of imagery classification predicated on class structure N90-15493
Optical neural nets for scene analysis
[AD-A213986] N90-15637
SCHEDULING
Simulating the scheduling of parallel supercomputer applications
[DE90-003604] N90-15655
Automated observation scheduling for the VLT
[NASA-CR-186282] N90-15861
Artificial intelligence approaches to astronomical observation scheduling
[NASA-CR-186277] N90-15862
Automated telescope scheduling
[NASA-CR-186279] N90-15863
SCIENTISTS
Technical communications in aeronautics: Results of an exploratory study. An analysis of profit managers' and nonprofit managers' responses
[NASA-TM-101626] N90-15848
SCINTILLATION COUNTERS
First results from the MACRO (Monopole, Astrophysics, Cosmic Ray Observatory) detector at the Gran Sasso Laboratory
[DE90-003243] N90-15858
SEA LEVEL
Global lake-level variations from 18,000 to 0 years ago: A palaeoclimate analysis
[DE90-000998] N90-15531
SEALING
High temperature, flexible, thermal barrier seal
[NASA-CASE-LEW-14672-1] N90-15444
SEARCH PROFILES
A comparative evaluation and analysis of end-user search performance in an academic environment N90-15845
Alternative representations for database responses N90-15847
SEARCHING
A note on the maximum size of a rectilinear maze
[AD-A214445] N90-15668
SECONDARY COSMIC RAYS
LEAP: A balloon-borne search for low-energy cosmic ray antiprotons N90-15878
SECONDARY EMISSION
Secondary electron emission characteristics of molybdenum-masked, ion-textured OFHC copper
[NASA-TP-2967] N90-15211
Technology of fast spark gaps
[AD-A214199] N90-15353
SECONDARY FLOW
Research on acoustical scattering, diffraction catastrophes, optics of bubbles, acoustical phase conjugation, and wake of an oscillating circular cylinder
[AD-A214168] N90-15711
SEDIMENT TRANSPORT
Saltation and suspension of particulate matter in air
[AD-A213618] N90-15552
SEDIMENTS
Development of a robotics system for automated chemical analysis of sediment, sludges, and soils
[DE90-003637] N90-15170
Predicting the performance of ceramic filters by the use of silt density index
[DE90-001316] N90-15256
SEISMIC WAVES
Determination of Q as a function of depth and tectonic province
[AD-A213805] N90-15554
Theoretical models of earthquake phenomena and the physical significance of seismic moment tensor expansions
[AD-A213813] N90-15556
A multichannel processing approach to real time network detection, phase association, and threshold monitoring
[AD-A213940] N90-15657
SEISMOLOGY
Theoretical models of earthquake phenomena and the physical significance of seismic moment tensor expansions
[AD-A213813] N90-15556
Calculation of source and structure parameters at regional and teleseismic distances
[AD-A214297] N90-15558
SELECTIVITY
Correlations between surface structure and catalytic activity/selectivity
[DE90-003755] N90-15181
SELENIUM COMPOUNDS
Phase equilibrium and crystal growth studies on AgGaSe2 and related nonlinear optical materials
[AD-A213650] N90-15809
SELF CONSISTENT FIELDS
Relativistic self-consistent field studies of atoms and molecules
[AD-A214101] N90-15724
Large scale calculations of the structure and dynamics of dense matter
[DE90-003654] N90-15726
SELF EXCITATION
The behavior of matter under nonequilibrium conditions: Fundamental aspects and applications
[DE90-002522] N90-15157
SEMANTICS
An overview of lynx
[AD-A213714] N90-15631
A structured connectionist approach to direct inferences and figurative adjective-noun combinations
[AD-A214326] N90-15649
SEMICONDUCTOR DEVICES
RF transistor thermal/electrical characterization
[DE90-001427] N90-15326
Avalanche photoconductive switching
[DE90-002980] N90-15337
Picosecond photoconductivity using a graded bandgap Al(x)Ga(1-x)As active detecting layer
[DE90-003452] N90-15786
SEMICONDUCTOR DIODES
Power semiconductor devices for space nuclear power systems
[DE90-001178] N90-15819
SEMICONDUCTOR LASERS
SLCSAT (Submarine Laser Communication Satellite) communication system design study
[AD-A213403] N90-15304
Fiber optic sensing system
[NASA-CASE-LEW-14795-1] N90-15733
SEMICONDUCTORS (MATERIALS)
Research on GaAs quantum-coupled structures that can be used as electron devices
[AD-A214015] N90-15350
Interfacial systems for photochemical energy conversion
[DE90-003181] N90-15514
Photochemical solar energy conversion utilizing semiconductors localized in membrane mimetic systems
[DE90-003450] N90-15515
Proceedings of the Latin American Conference on the Applications of the Moessbauer Effect
[DE90-600819] N90-15803
Epitaxial iron films
[AD-A213551] N90-15807
Interface phonons in semiconductor double heterostructures
[AD-A213732] N90-15810
Innovative optoelectronic materials and structures using OMVPE
[AD-A214192] N90-15815
SENSITIVITY
An investigation of the sensitization behavior of Fe-Mn-Cr austenitic steels
[DE90-002719] N90-15226
More efficient sensitivity testing
[DE90-002639] N90-15298
SENTENCES
Dual task performance with LPC (Linear Predictive Coding) degraded speech in a sentence verification task
[AD-A214298] N90-15320
SEPARATED FLOW
A direct-inverse method for transonic and separated flows about airfoils
[NASA-CR-4270] N90-15072
SEPARATORS
Membrane and durability studies for the zinc/bromine battery
[DE89-016181] N90-15324
SERVICE LIFE
Ceramic technology for advanced heat engines project
[DE90-001852] N90-15251
Membrane and durability studies for the zinc/bromine battery
[DE89-016181] N90-15324
Life evaluation of valve-regulated lead-acid batteries for load-leveling applications
[DE90-002188] N90-15336
Niobium 1 percent zirconium/potassium and titanium/potassium life-test heat pipe design and testing
[DE90-002430] N90-15522
SERVOMECHANISMS
Automation and robotics in construction: Japanese research and development
[AD-A214170] N90-15456
Feasibility study of using industrial robot for ultrasound testing
[DE90-002977] N90-15461
SET THEORY
Membership-set parameter estimation via optimal bounding ellipsoids
[AD-A213807] N90-15685

SHAPES
A renormalization group approach to image processing: A new computational method for three-dimensional shapes in robot vision, and the computation complexity of the cooling algorithms
[AD-A214247] N90-15643
Shapes of star-gas waves in spiral galaxies
[NASA-CR-186289] N90-15859
SHEAR FLOW
New transient algorithms for non-Newtonian flows
[AD-A213494] N90-15385
SHEAR LAYERS
Computation of broadband mixing noise from turbomachinery
[AD-A214448] N90-15713
SHEAR PROPERTIES
Heat treatment investigation of 4330 vanadium-modified steel
[AD-A214290] N90-15239
Two dimensional laminated shell theory including parabolic transverse shear
[AD-A213817] N90-15487
SHEAR STRESS
Transverse (through-the-thickness) shear stiffnesses of fibre reinforced composite laminated plates (computer program)
[ESDU-89013] N90-15152
New transient algorithms for non-Newtonian flows
[AD-A213494] N90-15385
SHELL THEORY
Two dimensional laminated shell theory including parabolic transverse shear
[AD-A213817] N90-15487
SHELLS (STRUCTURAL FORMS)
Two dimensional laminated shell theory including parabolic transverse shear
[AD-A213817] N90-15487
SHOCK FRONTS
Shapes of star-gas waves in spiral galaxies
[NASA-CR-186289] N90-15859
SHOCK TESTS
Using small scale tests to estimate the failure diameter of a propellant
[DE90-001166] N90-15281
SHOCK TUBES
Shock tube ignition of octanes
[DE90-001167] N90-15164
Rayleigh-Taylor instability in compressible fluids
[DE90-003027] N90-15376
SHOCK WAVE INTERACTION
Enhanced resolution concepts in large scale scientific computing
[AD-A214095] N90-15393
SHOCK WAVE PROPAGATION
Statistical model for particle-void deformation kinetics in granular materials during shock wave propagation
[DE89-017729] N90-15476
SHOCK WAVES
Hugoniot measurements with the LLNL electric gun facility
[DE90-002809] N90-15119
Shock-wave characterization of energetic booster-rocket propellant WAK-2 and its simulant UGS
[DE90-002633] N90-15285
Rayleigh-Taylor instability in compressible fluids
[DE90-003027] N90-15376
Characterizing transient vibrations using band limited moments
[DE90-000799] N90-15473
Micron-thin Nb films recovered from Mbar shock pressures
[DE90-001509] N90-15772
SHUTTLE DERIVED VEHICLES
Shuttle-C utilization for assembly of the rephased Freedom configuration
[NASA-TM-101658] N90-15120
SIDELOBES
Large-aperture sparse array detector system for multiple emitter location
[AD-D014303] N90-15355
SIGNAL DETECTION
A multichannel processing approach to real time network detection, phase association, and threshold monitoring
[AD-A213940] N90-15657
SIGNAL DETECTORS
Large-aperture sparse array detector system for multiple emitter location
[AD-D014303] N90-15355
Optical acoustic sensor using optical fiber
[DE89-901267] N90-15730
SIGNAL DISTORTION
Baseband development system implementation
[AD-A213464] N90-15309
A compact acoustic recorder
[AD-A213581] N90-15403
SIGNAL ENCODING
SLCSAT (Submarine Laser Communication Satellite) communication system design study
[AD-A213403] N90-15304
SIGNAL FADING
Spread spectrum mobile radio communications
[AD-A213726] N90-15311
SIGNAL PROCESSING
Fly-by-light flight control system technology development plan
[NASA-CR-181953] N90-15111
Flashlight radar: A three-dimensional imaging radar
[AD-A213439] N90-15307
Baseband development system implementation
[AD-A213464] N90-15309
Focal plane antenna array for millimeter waves
[AD-D014306] N90-15322
Array signal processing: New techniques for direction finding and spectrum estimation
[AD-A213883] N90-15345
Identification and quantification of synoptic structure in simulated TIROS N radiance soundings
[AD-A213729] N90-15553
A signal processing language for coarse grain data flow multiprocessors
[AD-A213863] N90-15635
Ultra high performance, highly reliable, numeric intensive processors and systems
[AD-A214100] N90-15659
Membership-set parameter estimation via optimal bounding ellipsoids
[AD-A213807] N90-15685
An improved toeplitz approximation method
[AD-A213994] N90-15688
Research in optical interconnection techniques
[AD-A214028] N90-15739
Research on materials and components for opto-electronic signal processing and computing
[AD-A213740] N90-15811
A signal realization data base generated by the multiple phase-screen method
[AD-A214004] N90-15852
SILANES
Band-to-band transitions in poly (phenyl methyl silane)
[DE90-003575] N90-15720
SILICA GLASS
Bonding aerogels with polyurethanes
[DE90-003050] N90-15258
SILICON
Preparation, structure and properties of VO(sub x) and TiO2 thin films by MOCVD
[DE90-003566] N90-15793
SILICON CARBIDES
Fatigue properties of SiC/Al composites N90-15138
Empirical and analytical determination of the fracture resistance of a TiB2 particle/SiC matrix composite
[NASA-TM-101940] N90-15143
Effects of filament-matrix interfaces on the mechanical properties of SiC-reinforced Si3N4: A review
[DE90-001863] N90-15144
Laser mixing of titanium on silicon carbide
[DE90-003216] N90-15150
Potential applications of structural ceramic composites in gas turbines
[DE90-001273] N90-15248
IEA/Annex 2 powder characterization cooperative program
[AD-A213540] N90-15271
SILICON COMPOUNDS
Research on amorphous silicon-germanium alloys for tandem solar cells
[DE89-009436] N90-15499
SILICON DIOXIDE
Laser glass (1989)
[DE90-002754] N90-15257
SILICON FILMS
Instability of a-Si:H/Ag interface at 150 deg C
[DE89-009419] N90-15498
SILICON NITRIDES
Effects of filament-matrix interfaces on the mechanical properties of SiC-reinforced Si3N4: A review
[DE90-001863] N90-15144
Ceramic technology for advanced heat engines project
[DE90-001852] N90-15251
IEA/Annex 2 powder characterization cooperative program
[AD-A213540] N90-15271
SILOXANES
Ceramic processing using inorganic polymers
[DE90-003638] N90-15268
SILVER
Solid lubrication of ceramic surfaces by IAD (Ion-Assisted Deposition)-silver coatings for heat engine applications
[DE90-002860] N90-15253
Instability of a-Si:H/Ag interface at 150 deg C
[DE89-009419] N90-15498
Rapidity densities and their fluctuations in central 200 A GeV S32 interations with Au and Ag,Br nuclei
[LUIP-8905] N90-15715
SILVER COMPOUNDS
Phase equilibrium and crystal growth studies on AgGaSe2 and related nonlinear optical materials
[AD-A213650] N90-15809
SILVER NITRATES
Silver coated superconducting ceramic powder
[AD-D014300] N90-15278
SIMULATION
Principal characteristics of lightning on aircraft N90-15067
Using small scale tests to estimate the failure diameter of a propellant
[DE90-001166] N90-15281
Network simulator definition
[AD-A213463] N90-15308
Baseband development system implementation
[AD-A213464] N90-15309
On the domain of dominance of the asymptotic elastodynamic crack-tip fields N90-15468
Calculation of source and structure parameters at regional and teleseismic distances
[AD-A214297] N90-15558
Molecular-dynamics study of the amorphization of CuTi
[DE90-003563] N90-15791
Laboratory simulations of the solar wind-comet interactions N90-15875
SIMULATORS
Design of a bounded wave EMP (Electromagnetic Pulse) simulator
[AD-A214137] N90-15316
XNUSIM: Graphical interface for a multiprocessor simulator
[AD-A214176] N90-15606
Knowledge representations for the automatic generation of numerical simulators for PDEs
[DE89-008036] N90-15615
SINGLE CRYSTALS
Micromechanics of an extrusion in high-cycle fatigue with creep
[AD-A213509] N90-15485
Superconductivity and stoichiometry in Tl2Ca2Ba2Cu3O(x) single crystals
[DE90-003838] N90-15801
SINGULARITY (MATHEMATICS)
Mixed singular linear elliptic equations
[DE90-600722] N90-15674
SINTERING
Sintering studies on high field varistors
[DE90-002626] N90-15359
Properties of high Tc superconducting oxides
[DE90-003792] N90-15821
SLIDING
Hybrid butterfly valve
[NASA-CASE-SSC-00004] N90-15443
A procedure for force-balancing planar linkages using counterweights
[ESDU-89028] N90-15446
SLOPES
Installed tailplane lift-curve slope at subsonic speeds
[ESDU-89029] N90-15081
SLUDGE
Development of a robotics system for automated chemical analysis of sediment, sludges, and soils
[DE90-003637] N90-15170
SMOKE
Evaluate and characterize mechanisms controlling transport, fate, and effects of army smokes in the aerosol wind tunnel: Transport, transformations, fate, and terrestrial ecological effects of hexachloroethane obscurant smokes
[DE90-002923] N90-15536
SMOOTHING
Shapes of star-gas waves in spiral galaxies
[NASA-CR-186289] N90-15859
SNOW
A diffusion on a fractal state space
[AD-A213555] N90-15707
SODIUM CHLORIDES
The effect of dissolved chlorine on the pitting behavior of 304L stainless steel in a 0.5 N NaCl solution
[AD-A213803] N90-15234
SODIUM SULFUR BATTERIES
Novel high-rate, all solid-state, sodium and lithium/organosulfur batteries
[DE90-001014] N90-15325
SOFTWARE ENGINEERING
XNUSIM: Graphical interface for a multiprocessor simulator
[AD-A214176] N90-15606

Transport modeling and advanced computer techniques
[DE90-001481] N90-15612
Environment for failure region analysis: REACHER - a reachability condition derivation tool
[AD-A214183] N90-15641

SOFTWARE TOOLS
Guidelines for evaluating energy analysis software
[AD-A214171] N90-15640
Environment for failure region analysis: REACHER - a reachability condition derivation tool
[AD-A214183] N90-15641
Young Investigator's Award and distributed self-adaptive databases
[AD-A214194] N90-15854

SOILS
Development of a robotics system for automated chemical analysis of sediment, sludges, and soils
[DE90-003637] N90-15170

SOL-GEL PROCESSES
Superconducting film fabrication by the sol-gel process
[DE90-002069] N90-15252
High-temperature ceramic superconductors
[AD-A214251] N90-15818

SOLAR CELLS
Instability of a-Si:H/Ag interface at 150 deg C
[DE89-009419] N90-15498
Research on amorphous silicon-germanium alloys for tandem solar cells
[DE89-009436] N90-15499
Research on high-efficiency, single-junction, monolithic, thin-film amorphous silicon solar cells, phase 1
[DE89-009495] N90-15502
Research on high-efficiency, single-junction, monolithic, thin-film amorphous silicon solar cells, phase 2
[DE89-009496] N90-15503
US Polycrystalline Thin Film Solar Cells Program
[DE89-009506] N90-15504
High-efficiency silicon concentrator solar cells for use with prismatic covers
[DE90-002644] N90-15509
Characteristics of CMOS analog integrated structures using MOSIS (Metal Oxide Semiconductor Implementation System)
[DE90-001630] N90-15773
The effect of annealing treatments on defect structure and diffusion lengths in n-type GaAs
[AD-A214215] N90-15817

SOLAR ENERGY
Analysis of catalytically enhanced solar absorption chemical reactors: 1 - numerical model description
[DE89-014742] N90-15505
Satellite thermal storage systems using metallic phase-change materials
[DE89-016872] N90-15507

SOLAR ENERGY ABSORBERS
Analysis of catalytically enhanced solar absorption chemical reactors. 2: Predicted characteristics of a 100 kW chemical reactor
[DE89-014743] N90-15521

SOLAR ENERGY CONVERSION
Photochemical solar energy conversion utilizing semiconductors localized in membrane mimetic systems
[DE90-003450] N90-15515
The Solar Power Satellite (SPS): Progress so far N90-15840
Lunar power system summary of studies for the lunar enterprise task force NASA-office of exploration N90-15841

SOLAR FLARES
A simple model for the stellar analogy of compact solar flares
[DE90-003215] N90-15877

SOLAR POWER SATELLITES
The Solar Power Satellite (SPS): Progress so far N90-15840
Transportation and operations aspects of space energy systems N90-15842

SOLAR RADIATION
Analysis of catalytically enhanced solar absorption chemical reactors: 1 - numerical model description
[DE89-014742] N90-15505
A guide for estimating potential energy savings from increased solar reflectance of a low-sloped roof
[DE90-003720] N90-15526

SOLAR SEA POWER PLANTS
Ocean thermal energy conversion: An overview
[DE89-000838] N90-15512

SOLAR WIND
Laboratory simulations of the solar wind-comet interactions N90-15875

SOLDERED JOINTS
Isothermal fatigue behavior of Sn-Pb solar joints
[DE90-003280] N90-15464

SOLDERING
Automated convection soldering
[KCP-613-4005] N90-15300

SOLID CRYOGENS
Auger and x ray absorption studies of solid molecular oxygen
[DE90-003966] N90-15825

SOLID ELECTROLYTES
Novel high-rate, all solid-state, sodium and lithium/organosulfur batteries
[DE90-001014] N90-15325

SOLID LUBRICANTS
Solid lubrication of ceramic surfaces by IAD (Ion-Assisted Deposition)-silver coatings for heat engine applications
[DE90-002860] N90-15253

SOLID PROPELLANT COMBUSTION
Steady flow combustion model for solid-fuel ramjet projectiles
[BRL-TR-2987] N90-15163
Spectral studies of solid propellant combustion. 2: Emission and absorption results for M-30 and HMX1 propellants
[AD-A213857] N90-15292

SOLID PROPELLANT IGNITION
Calculation of Einstein A coefficients and oscillator strengths for the A(perturbed)(2)A(1)-X(perturbed)(2)B(1) transition of NH(2)
[AD-A213837] N90-15176

SOLID ROCKET PROPELLANTS
HCl monitor, phase 2
[AD-A213572] N90-15542

SOLID STATE
Solid-state phase equilibria in the ZnS-Ga2S3 system
[AD-A213944] N90-15238
Novel high-rate, all solid-state, sodium and lithium/organosulfur batteries
[DE90-001014] N90-15325
Solid state research
[AD-A213405] N90-15806
Tritium and neutron measurements of a solid state cell
[DE90-003657] N90-15820

SOLID STATE DEVICES
A study of Inter-Injection-Locked phased arrays
[AD-A214097] N90-15352

SOLID STATE LASERS
SLCSAT (Submarine Laser Communication Satellite) communication system design study
[AD-A213403] N90-15304
The search for solid state fusion lasers
[DE89-012301] N90-15410
SBS (Stimulated Brillouin Scattering) pulse distortion in multimode optical fibers: Preliminary results
[DE90-003023] N90-15731

SOLID STATE PHYSICS
The effect of annealing treatments on defect structure and diffusion lengths in n-type GaAs
[AD-A214215] N90-15817

SOLID WASTES
Managing the waste stream: Background information for planning source separation programs
[PB90-100223] N90-15530

SOLID-SOLID INTERFACES
Effects of filament-matrix interfaces on the mechanical properties of SiC-reinforced Si3N4: A review
[DE90-001863] N90-15144
Energetics of BCC-FCC lattice deformation in iron
[AD-A213801] N90-15233
Instability of a-Si:H/Ag interface at 150 deg C
[DE89-009419] N90-15498

SOLIDIFIED GASES
Auger and x ray absorption studies of solid molecular oxygen
[DE90-003966] N90-15825

SOLIDS
Theoretical models of earthquake phenomena and the physical significance of seismic moment tensor expansions
[AD-A213813] N90-15556

SOLITARY WAVES
Optical solitons in liquid crystals
[DE90-000694] N90-15728

SONAR
Sensor integration using concurrent computing on-board the ORNL mobile robot
[DE89-008740] N90-15436

SOUND GENERATORS
Dynamics of a class of vortex rings N90-15362

SOUND PRESSURE
Optical acoustic sensor using optical fiber
[DE89-901267] N90-15730

SOUND PROPAGATION
Sound attenuation apparatus
[NASA-CASE-LAR-13968-1] N90-15710
The calculation of overground sound propagation in the presence of wind and temperature gradients
[ESDU-89036] N90-15714

SOUND TRANSMISSION
Sound attenuation apparatus
[NASA-CASE-LAR-13968-1] N90-15710

SOUND WAVES
A compact acoustic recorder
[AD-A213581] N90-15403
Bulk wave characterization of high T(sub c) superconductors
[AD-A214030] N90-15813

SOURCE PROGRAMS
Managing the waste stream: Background information for planning source separation programs
[PB90-100223] N90-15530

SOVIET SPACECRAFT
Manned spacecraft
[AD-A214218] N90-15129

SPACE CHARGE
Intense REB (Relativistic Electron Beam) transport in a weakly magnetized plasma
[DE90-002978] N90-15749

SPACE COMMERCIALIZATION
Report of NASA Lunar Energy Enterprise Case Study Task Force
[NASA-TM-101652] N90-15836
Report of the NASA lunar energy enterprise case study task force N90-15837
Analysis of the financial factors governing the profitability of lunar helium-3 N90-15838
Transportation and operations aspects of space energy systems N90-15842

SPACE COMMUNICATION
Spread spectrum mobile radio communications
[AD-A213726] N90-15311

SPACE COOLING (BUILDINGS)
Guidelines for evaluating energy analysis software
[AD-A214171] N90-15640

SPACE DENSITY
Theory of interacting plasmas in space N90-15742

SPACE EXPLORATION
Space operations: Listing of NASA scientific missions, 1980-2000. Fact sheet for the Chairman, Subcommittee on Space Science and Applications, Committee on Science, Space, and Technology, House of Representatives
[AD-A213493] N90-15881

SPACE HABITATS
Utilization of non-conventional systems for conversion of biomass to food components
[NASA-CR-177545] N90-15591

SPACE INDUSTRIALIZATION
A quasi-economic role for lunar science
[DE90-000679] N90-15876

SPACE MISSIONS
Physical process in MPD plasmas
[AD-A213679] N90-15761
Space operations: Listing of NASA scientific missions, 1980-2000. Fact sheet for the Chairman, Subcommittee on Space Science and Applications, Committee on Science, Space, and Technology, House of Representatives
[AD-A213493] N90-15881

SPACE PLASMAS
Theory of interacting plasmas in space N90-15742
Simulation of radial expansion of an electron beam injected into a background plasma
[NASA-CR-186188] N90-15743

SPACE PLATFORMS
On the analysis and optimization of a platform manipulator N90-15433

SPACE POWER REACTORS
Power semiconductor devices for space nuclear power systems
[DE90-001178] N90-15819

SPACE SHUTTLE BOOSTERS
HCl monitor, phase 2
[AD-A213572] N90-15542

SPACE SHUTTLES
Measurement of optical radiations in spacecraft environments
[AD-A213814] N90-15497

SPACE STATION POWER SUPPLIES
Reliability analysis of the space station freedom electrical power system
[AD-A214105] N90-15126

SPACE STATIONS
Shuttle-C utilization for assembly of the rephased Freedom configuration
[NASA-TM-101658] N90-15120
Reliability analysis of the space station freedom electrical power system
[AD-A214105] N90-15126
Manned spacecraft
[AD-A214218] N90-15129

Onorbit electron beam welding experiment definition
[NASA-CR-183847] N90-15431

SPACE WEAPONS
Prospects for space arms control
[DE90-003392] N90-15700

SPACECRAFT CHARGING
Strategic characteristics of Dynamics Explorer 1 retarding ion mass spectrometer and the consequences for core plasma measurements
[AD-A214013] N90-15125
SCATHA (Spacecraft Charging at High Altitudes) atlas data base, volume 1
[AD-A214204] N90-15127
SCATHA (Spacecraft Charging At High Altitudes) atlas data base, volume 2
[AD-A214205] N90-15128

SPACECRAFT COMPONENTS
Instrumentation for a facility for the test, analysis and active control of spacecraft truss structures
[AD-A213655] N90-15124
A strategy for concurrent product and process design of aerospace components
[DE90-002926] N90-15299
Satellite thermal storage systems using metallic phase-change materials
[DE89-016872] N90-15507

SPACECRAFT CONSTRUCTION MATERIALS
Manned spacecraft
[AD-A214218] N90-15129

SPACECRAFT CONTAMINATION
Measurement of optical radiations in spacecraft environments
[AD-A213814] N90-15497

SPACECRAFT CONTROL
Instrumentation for a facility for the test, analysis and active control of spacecraft truss structures
[AD-A213655] N90-15124

SPACECRAFT DESIGN
Shuttle-C utilization for assembly of the rephased Freedom configuration
[NASA-TM-101658] N90-15120
A strategy for concurrent product and process design of aerospace components
[DE90-002926] N90-15299

SPACECRAFT ENVIRONMENTS
SCATHA (Spacecraft Charging at High Altitudes) atlas data base, volume 1
[AD-A214204] N90-15127
SCATHA (Spacecraft Charging At High Altitudes) atlas data base, volume 2
[AD-A214205] N90-15128
Measurement of optical radiations in spacecraft environments
[AD-A213814] N90-15497

SPACECRAFT ORBITS
SCATHA (Spacecraft Charging at High Altitudes) atlas data base, volume 1
[AD-A214204] N90-15127

SPACECRAFT POWER SUPPLIES
Safety evaluation report for Galileo, volume 2
[DE90-003087] N90-15123
Tuned-circuit Johnson noise thermometry
[DE89-016221] N90-15356

SPACECRAFT SHIELDING
Stand-off shields for hypervelocity particles
[DE89-016182] N90-15437

SPACECRAFT STRUCTURES
Instrumentation for a facility for the test, analysis and active control of spacecraft truss structures
[AD-A213655] N90-15124
Base reaction optimization of redundant manipulators for space applications
[NASA-CR-186274] N90-15447

SPALLATION
Shock-wave characterization of energetic booster-rocket propellant WAK-2 and its simulant UGS
[DE90-002633] N90-15285

SPARK GAPS
Technology of fast spark gaps
[AD-A214199] N90-15353

SPATIAL DISTRIBUTION
The radar-based short term prediction of the time-space evolution of rain fields
[AD-A213802] N90-15312
Spatial dynamics of deformable multibody systems with variable kinematic structure
[AD-A214098] N90-15455
Global distribution of total cloud cover and cloud type amounts over the ocean
[DE90-003187] N90-15574

SPATIAL RESOLUTION
Image enhancement using the IRAS (Infrared Astronomy Satellite) survey data
[AD-A213811] N90-15496

SPECIFIC HEAT
Summary physical data tables: Alkanes
[ESDU-PD3] N90-15162
Thermal conductivity of gaseous aliphatic hydrocarbons. Part 1: Alkanes
[ESDU-89035-PT-1] N90-15183
On the free carrier-negative U center interacting model for the high-T(sub c) oxide superconductor
[DE89-635908] N90-15775

SPECIFICATIONS
National airspace system: Airport movement area control operational concept
[WP-89W00181] N90-15086

SPECTRA
Array signal processing: New techniques for direction finding and spectrum estimation
[AD-A213883] N90-15345
Stable supermembrane vacuum with a discrete spectrum
[DE89-635722] N90-15561
Studies of quantitative methods for imaging from scattered fields
[AD-A214047] N90-15638
Wind speed dependence of acoustic ambient vertical directional spectra at high frequency
[AD-A214293] N90-15712

SPECTRAL THEORY
Design of a large angular aperture TeO2 acousto-optic tunable filter
[AD-A213999] N90-15738

SPECTROMETERS
Capillary electrophoresis ionization-mass spectrometry and tandem mass spectrometry
[DE90-002664] N90-15158

SPECTROSCOPIC ANALYSIS
ICP/AES (Inductively Coupled Plasma/Atomic Emission Spectroscopy): A modern analytical tool
[DE90-003822] N90-15765

SPECTROSCOPY
Compensation for peak shifts and variable background responses in fluorescence spectroscopy
[DE90-001102] N90-15154
First International Symposium on Electrochemical Impedance Spectroscopy. Extended abstracts
[AD-A214406] N90-15354
Outlier detection in multivariate calibration
[DE90-001502] N90-15672
Spectroscopic and laser properties of Cr:LiCaAlF6 and Cr:LiSrAlF6 crystals
[DE90-000783] N90-15770

SPECTRUM ANALYSIS
Experimental determination of the fluid velocity by spectral analysis of temperature fluctuations
[DE89-636430] N90-15372

SPEECH
Dual task performance with LPC (Linear Predictive Coding) degraded speech in a sentence verification task
[AD-A214298] N90-15320

SPEED CONTROL
Adjustable speed drive study, June 1985 to September 1988. Part 2: Appendices
[DE90-002771] N90-15332

SPEED REGULATORS
Adjustable speed drive study, June 1985 to September 1988. Part 2: Appendices
[DE90-002771] N90-15332

SPIN DYNAMICS
Electronic and ionic transport in polymers
[AD-A213410] N90-15270
Two-dimensional magnetic phase transition of ultrathin iron films on Pd(100)
[DE90-003555] N90-15788

SPIRAL GALAXIES
Shapes of star-gas waves in spiral galaxies
[NASA-CR-186289] N90-15859

SPLINE FUNCTIONS
An executive system for modeling with rational b-splines
[AD-A213460] N90-15627
Quasi interpolants and approximation power of multivariate splines
[AD-A213535] N90-15678

SPONTANEOUS EMISSION
Comprehensive, nonintercepting electron-beam diagnostics using spontaneous emission
[DE90-003211] N90-15414

SPRAY CHARACTERISTICS
Combustion characteristics of sprays
[AD-A213651] N90-15173
Dense-spray properties: Structure and turbulence modulation
[AD-A213671] N90-15387

SPRAYERS
High power density spray cooling
[AD-A213575] N90-15386

SPREAD SPECTRUM TRANSMISSION
Spread spectrum mobile radio communications
[AD-A213726] N90-15311

SPUTTERING
Characterization and in situ testing of diamond films
[DE90-003155] N90-15265
Near-surface sputtered particle transport for an oblique incidence magnetic field plasma
[DE90-004422] N90-15758
Partial reduction of re-oxidation processing of Y-Ba-Cu-O sputtered thin films
[DE90-003655] N90-15782
Orientation of rf-sputter-deposited MoS2 films
[ATR-89(4752)-1] N90-15784
Computer-controlled ion beam sputter-deposition of superconducting oxide films
[AD-A213921] N90-15812

STABILITY
Stability of numerical solutions for stratified two-phase flow
[DE90-701646] N90-15379
Stable supermembrane vacuum with a discrete spectrum
[DE89-635722] N90-15561

STAGNATION POINT
A tomographic study of premixed turbulent stagnation point flames
[DE90-002462] N90-15156

STAGNATION PRESSURE
An experimental, analytical, and computational investigation of turbomachinery rotor flow fields
N90-15360

STAINLESS STEELS
Helium-induced weld cracking in irradiated 304 stainless steel
[DE90-001312] N90-15219
Accelerated aging embrittlement of cast duplex stainless steel: Activation energy for extrapolation
[DE90-001773] N90-15221
The effect of dissolved chlorine on the pitting behavior of 304L stainless steel in a 0.5 N NaCl solution
[AD-A213803] N90-15234
The effect of dissolved ozone on the corrosion behavior of Cu-30 Ni and 304L stainless steel in 0.5 N NaCl solutions
[AD-A213804] N90-15235
Cast stainless steel aging: Mechanisms and predictions
[DE90-003772] N90-15241
Experience with J testing of 304/308 stainless steel weldment
[DE90-002046] N90-15478

STANDARDIZATION
Terminology strategies for international information exchange
[AD-A214147] N90-15853

STANDARDS
An expert system for quality assurance (a.k.a.) QA Express
[DE90-003887] N90-15467

STATE ESTIMATION
Parameter estimation of linear systems in the presence of process noise using the maximum liklihood method
[ESDU-89032] N90-15683

STATIC LOADS
Design of a custom load cell for a precision assembly application
[DE90-004439] N90-15340

STATIC PRESSURE
Static pressure distribution in an angular channel with helicoidal wire
[DE89-636474] N90-15374

STATISTICAL ANALYSIS
Measurements of horizontal visibility in the lowest 300 m over Northern Germany N90-15059
The radar-based short term prediction of the time-space evolution of rain fields
[AD-A213802] N90-15312
Statistical model for particle-void deformation kinetics in granular materials during shock wave propagation
[DE89-017729] N90-15476
Observational study of the macroscopic behavior of moist-convective processes N90-15547
Flux parameterization techniques in the atmospheric surface layer N90-15548
Developmental versions of FORTRAN/77 routines for the design and analysis of mixture experiments
[DE90-003513] N90-15624
Two basic partial orderings for distributions derived from Schur functions and majorization
[AD-A213703] N90-15682
Likelihood ratio derivative estimators for stochastic systems
[AD-A213787] N90-15684

STATISTICAL DISTRIBUTIONS
Precipitation distributions associated with cyclones originating over the Gulf of Mexico and surrounding coastal regions
[AD-A213644] N90-15569
Recurrence and ergodicity for exponential family state-space models
[AD-A213466] N90-15677
Thermal and statistical properties of nuclei and nuclear systems
[DE90-000183] N90-15717
STATISTICAL MECHANICS
Estimating departure times from traffic counts using dynamic assignment
[DE89-016259] N90-15653
Outlier detection in multivariate calibration
[DE90-001502] N90-15672
Brownian trail rectified
[DE90-003339] N90-15706
STATISTICAL TESTS
More efficient sensitivity testing
[DE90-002639] N90-15298
STATORS
Design of a high-gain flux-compression generator
[DE90-002795] N90-15333
STEADY FLOW
Steady flow combustion model for solid-fuel ramjet projectiles
[BRL-TR-2987] N90-15163
Irreversible processes from reversible mechanics
[DE90-001057] N90-15368
STEELS
The effects of Mo2C morphology and strain distribution on the fatigue properties of Fe-C-Mo dual-phase steels N90-15210
Guide to the selection of surface treatments for the improvement of fatigue strength of steels
[ESDU-89031] N90-15245
On the domain of dominance of the asymptotic elastodynamic crack-tip fields N90-15468
STELLAR MASS
Pulsars lost and found: The second Princeton-Arecibo millisecond pulsar search N90-15865
STELLAR PHYSICS
The South African Astronomical Observatory
[NASA-CR-186258] N90-15856
STELLARATORS
Experiments on linear high beta helical axis stellarators to study simulated toroidal effects and Alfven-wave heating
[DE90-001704] N90-15745
The 17th AINSE Plasma Physics Conference: Conference handbook
[DE90-600936] N90-15759
STEPPING MOTORS
A versatile stepping motor controller for systems with many motors
[DE90-001556] N90-15327
STIFFNESS
Transverse (through-the-thickness) shear stiffnesses of fibre reinforced composite laminated plates (computer program)
[ESDU-89013] N90-15152
Current status of the application of conventional aluminium-lithium alloys and the potential for future developments N90-15203
STIFFNESS MATRIX
Mesh refinement in finite element analysis by minimization of the stiffness matrix trace
[NASA-CR-185170] N90-15434
STOCHASTIC PROCESSES
Prediction of stochastic blade loads for three-bladed, rigid-hub rotors
[DE89-009508] N90-15520
The parallel decomposition of linear programs
[DE90-003538] N90-15625
Two basic partial orderings for distributions derived from Schur functions and majorization
[AD-A213703] N90-15682
Optimization of stochastic systems via simulation
[AD-A214011] N90-15689
Numerical methods for parabolic equations and inequalities in very high dimensions
[AD-A214102] N90-15690
A structural factoring approach for analyzing probabilistic networks N90-15697
Nonlocality and stochastic quantization of field theory
[DE89-633913] N90-15833
STOICHIOMETRY
Superconductivity and stoichiometry in Tl2Ca2Ba2Cu3O(x) single crystals
[DE90-003838] N90-15801
STOPPING
Epoxy-resin cable terminations
[AD-A213789] N90-15454
STORAGE
Annual operating plan for fiscal year 1990 for chemical/hydrogen energy systems program
[DE90-003964] N90-15527
STORMS
Application of a mass-consistent wind model to chinook windstorms
[AD-A213622] N90-15568
STORMS (METEOROLOGY)
Vertical distribution of pollutants in the presence of convective storms
[DE90-002590] N90-15549
STRAIN DISTRIBUTION
The effects of Mo2C morphology and strain distribution on the fatigue properties of Fe-C-Mo dual-phase steels N90-15210
Nonlinear strain-displacement relations for thin axisymmetric shells
[PB89-226013] N90-15470
STRAIN RATE
New transient algorithms for non-Newtonian flows
[AD-A213494] N90-15385
STRATIFIED FLOW
Stability of numerical solutions for stratified two-phase flow
[DE90-701646] N90-15379
STRATOSPHERIC WARMING
Greenhouse gases: Changing the global climate
[DE90-002788] N90-15535
STRESS (PHYSIOLOGY)
Potential for reduction of decompression sickness by prebreathing with 100 percent oxygen while exercising
[AD-A213449] N90-15581
STRESS ANALYSIS
Toughening behavior and interfacial properties of fiber-reinforced ceramic composites
[DE89-015351] N90-15279
Nonlinear viscous waves produced by an impulsively moving plate
[AD-A214014] N90-15392
Investigation of loads generated by temperature transients in pipes
[DE89-636433] N90-15395
STRESS CONCENTRATION
On the domain of dominance of the asymptotic elastodynamic crack-tip fields N90-15468
STRESS CORROSION
Corrosion and stress corrosion of aluminium-lithium alloys N90-15190
Fabrication of test-articles from Al-Li 2091 for Fokker 100 N90-15196
An investigation of the sensitization behavior of Fe-Mn-Cr austenitic steels
[DE90-002719] N90-15226
STRESS CORROSION CRACKING
Corrosion and stress corrosion of aluminium-lithium alloys N90-15190
Fabrication of test-articles from Al-Li 2091 for Fokker 100 N90-15196
STRESS DISTRIBUTION
A study of impact damage in composite laminates N90-15137
Development of a rate independent plasticity theory for general cyclic loading N90-15471
STRESS INTENSITY FACTORS
Critical and subcritical crack-growth behavior along toughened ceramic/metal interfaces N90-15140
On the domain of dominance of the asymptotic elastodynamic crack-tip fields N90-15468
STRESS-STRAIN RELATIONSHIPS
Mechanical behavior of laminated composites at elevated temperatures N90-15141
A simple shell element formulation for large-scale elastoplastic analysis
[DE89-015452] N90-15475
Mechanical evaluation of the differential drum concept for optical fiber pay-out
[AD-A214149] N90-15740
STRESSES
Thin films under chemical stress
[DE90-003754] N90-15484
Structural response measurements and predictions for the SANDIA 34-meter test bed
[DE90-002575] N90-15524
Mechanical evaluation of the differential drum concept for optical fiber pay-out
[AD-A214149] N90-15740
An investigation of mechanical behavior of crystalline solids
[DE90-003530] N90-15787
STRING THEORY
The dynamics of domain walls and strings
[NASA-CR-186255] N90-15832
Small scale structure on cosmic strings
[DE90-003128] N90-15867
STRIP TRANSMISSION LINES
Investigation of broadband microstrip antenna structures for application in monolithic millimeter wave arrays
[AD-A213856] N90-15344
STRONGLY COUPLED PLASMAS
The measurement of transport properties in strongly coupled plasmas
[DE90-003451] N90-15755
STRONTIUM COMPOUNDS
Spectroscopic and laser properties of Cr:LiCaAlF6 and Cr:LiSrAlF6 crystals
[DE90-000783] N90-15770
STRUCTURAL ANALYSIS
An examination of helicopter rotor load calculations
[AD-A214295] N90-15098
Instrumentation for a facility for the test, analysis and active control of spacecraft truss structures
[AD-A213655] N90-15124
Solution of potential flow past an elastic body using the boundary element technique
[AD-A213843] N90-15390
Modifications of the Penn State Boundary Layer Research Facility for boundary layer/structure interaction experimental research
[AD-A213874] N90-15391
Proceedings of the 1988 Structural Integrity Program Conference
[AD-A213545] N90-15486
Structural response measurements and predictions for the SANDIA 34-meter test bed
[DE90-002575] N90-15524
STRUCTURAL DESIGN
The interference of flightmechanical control laws with those of load alleviation and its influence on structural design N90-15054
Design and calibration of an in-stack, low-pressure impactor
[AD-A213531] N90-15105
Design of a custom load cell for a precision assembly application
[DE90-004439] N90-15340
NOISE: A nonlinear optimization induction free-electron laser systems engineering code
[DE90-004438] N90-15420
On the analysis and optimization of a platform manipulator N90-15433
Hybrid butterfly valve
[NASA-CASE-SSC-00004] N90-15443
Pipeline vibrations. Fluid transients in non-rigid, unbranched planar piping systems
[ESDU-89030] N90-15491
STRUCTURAL DESIGN CRITERIA
Point of view of a civil aircraft manufacturer on Al-Li alloy N90-15200
Uses and properties of Al-Li on the new EH101 helicopter N90-15201
STRUCTURAL ENGINEERING
Automation and robotics in construction: Japanese research and development
[AD-A214170] N90-15456
STRUCTURAL FAILURE
Proceedings of the 1988 Structural Integrity Program Conference
[AD-A213545] N90-15486
STRUCTURAL RELIABILITY
Proceedings of the 1988 Structural Integrity Program Conference
[AD-A213545] N90-15486
STRUCTURAL VIBRATION
Active control system for gust load alleviation and structural damping N90-15056
Effect of modal truncation on derivatives of closed-loop damping ratios in structural control N90-15109
SUBMARINES
SLCSAT (Submarine Laser Communication Satellite) communication system design study
[AD-A213403] N90-15304
SUBSONIC FLOW
An alternative derivation for an integral equation for linearized subsonic flow over a wing
[AD-A214140] N90-15079
SUBSONIC SPEED
Installed tailplane lift-curve slope at subsonic speeds
[ESDU-89029] N90-15081
The maximum lift coefficient of plain wings at subsonic speeds
[ESDU-89034] N90-15082
SULFUR COMPOUNDS
Studies of organo phosphorus-, nitrogen-, and sulfur-containing molecules
[AD-A213518] N90-15135
SULFUR OXIDES
Acid deposition
[DE90-003959] N90-15544

SUN
Astophysical opacities at LLNL
[DE90-003599] N90-15872
SUPERCOMPUTERS
VLSI theory and parallel supercomputing
[AD-A214035] N90-15351
LLNL's plan for a prototype circuit switch, a potential gigabit LAN of the future
[DE90-003614] N90-15597
Transport modeling and advanced computer techniques
[DE90-001481] N90-15612
The components of scientific visualization
[DE90-001992] N90-15614
Simulating the scheduling of parallel supercomputer applications
[DE90-003604] N90-15655
SUPERCONDUCTING FILMS
Superconducting film fabrication by the sol-gel process
[DE90-002069] N90-15252
Partial reduction of re-oxidation processing of Y-Ba-Cu-O sputtered thin films
[DE90-003655] N90-15782
Ion-irradiation effects in Tl2Ca2Ba2Cu3O10 superconductors
[DE90-003840] N90-15802
SUPERCONDUCTING MAGNETS
Retractable gas cooled leads for ASTROMAG
[DE90-002679] N90-15331
Feasibility analysis of reciprocating magnetic heat pumps
[NASA-CR-186205] N90-15363
Recent advances in magnetic heat pump technology
[DE89-013289] N90-15370
SUPERCONDUCTING POWER TRANSMISSION
Silver coated superconducting ceramic powder
[AD-D014300] N90-15278
Processing YBa2Cu3O(x) wires in O3/O2
[DE90-003570] N90-15794
SUPERCONDUCTING SUPER COLLIDER
The 17.1-GHz free-electron laser as a microwave source for TeV colliders
[DE90-001506] N90-15406
SUPERCONDUCTIVITY
Superconducting gravity gradiometer mission. Volume 1: Study team executive summary
[NASA-TM-4091-VOL-1] N90-15545
Phonons and charge-transfer excitations in HTS superconductors
[DE89-016616] N90-15768
Tunneling spectroscopy and the electron-phonon interaction in Ba(1-x)K(x)BiO3
[DE90-002842] N90-15776
The possible occurrence of multi-phase behavior in the high T(sub c) superconductor YBa2Cu3O(sub x)
[DE90-002999] N90-15777
Synthesis conductivity, and x ray photoelectron spectrum of Bi2Sr2Cu(sub 7+x). A new ternary bismuth-oxide system exhibiting metallic conductivity
[DE90-003010] N90-15778
Further studies on possible coexistence of antiferromagnetism and superconductivity in 2D Heisenberg model
[DE90-601082] N90-15783
Magnetic and electronic correlations in YBa2Cu3O(sub 6+x)
[DE89-017604] N90-15785
Magnetic mechanisms of high temperature superconductivity
[DE90-003625] N90-15796
The kind of mathematics involved in applied superconductivity research
[DE90-003706] N90-15798
Magnetic flux pinning in YBa2Cu3O7 films
[DE90-003709] N90-15799
Superconductivity and stoichiometry in Tl2Ca2Ba2Cu3O(x) single crystals
[DE90-003838] N90-15801
Cu-O chains in YBa2Cu3O(7-delta) and the phonon mechanism of high-Tc superconductivity
[DE90-603502] N90-15805
Bulk wave characterization of high T(sub c) superconductors
[AD-A214030] N90-15813
Properties of high Tc superconducting oxides
[DE90-003792] N90-15821
Effects of non-linearity in the variation of pinning potential with current-density on magnetic flux creep in high and low T(sub c) superconductors
[DE90-003952] N90-15822
Atomic scale structure of twin boundary in Y-Ba-Cu-O superconductors
[DE90-003955] N90-15823
The fabrication of YBa2Cu3O7 thin films by thermal coevaporation in oxygen
[DE90-003960] N90-15824
SUPERCONDUCTORS
New organic synthetic metals derived from BEDT-TTF, Ni(dsit)2 and BEDO-TTF
[DE90-003793] N90-15242
Fabrication of superconductor coils
[DE90-003571] N90-15338
Phonons and charge-transfer excitations in HTS superconductors
[DE89-016616] N90-15768
On the free carrier-negative U center interacting model for the high-T(sub c) oxide superconductor
[DE89-635908] N90-15775
The possible occurrence of multi-phase behavior in the high T(sub c) superconductor YBa2Cu3O(sub x)
[DE90-002999] N90-15777
Processing and fabrication of YBa2Cu4O8 and YBa2Cu4O8/YBa2Cu3O(x) composites
[DE90-003559] N90-15789
Cation disordering in the Tl-2122 superconductors
[DE90-003579] N90-15795
X ray absorption studies of YBa2Cu3O(6+x), La(2-x)Sr(x)CuO4, and Nd(2-x)Ce(x)CuO4
[DE90-003640] N90-15797
On functional integral representations in the lower Hubbard band based on generalized coherent states
[DE90-602936] N90-15804
Computer-controlled ion beam sputter-deposition of superconducting oxide films
[AD-A213921] N90-15812
Properties of high Tc superconducting oxides
[DE90-003792] N90-15821
Effects of non-linearity in the variation of pinning potential with current-density on magnetic flux creep in high and low T(sub c) superconductors
[DE90-003952] N90-15822
Atomic scale structure of twin boundary in Y-Ba-Cu-O superconductors
[DE90-003955] N90-15823
SUPERCRITICAL AIRFOILS
A direct-inverse method for transonic and separated flows about airfoils
[NASA-CR-4270] N90-15072
SUPERCRITICAL FLUIDS
Electrochemistry in near-critical and supercritical fluids. 8: Methyl viologen, decamethylferrocene, Os(bpy)3(sup 2+) and ferrocene in acetonitrile and the effect of pressure on diffusion coefficients under supercritical conditions
[AD-A213407] N90-15172
SUPERCRITICAL PRESSURES
Electrochemistry in near-critical and supercritical fluids. 8: Methyl viologen, decamethylferrocene, Os(bpy)3(sup 2+) and ferrocene in acetonitrile and the effect of pressure on diffusion coefficients under supercritical conditions
[AD-A213407] N90-15172
SUPERHEATING
Aerosol heating and vaporization of high-flux laser beams
[DE90-003471] N90-15428
SUPERNOVA REMNANTS
Pulsars lost and found: The second Princeton-Arecibo millisecond pulsar search N90-15865
SUPERNOVAE
The disk-halo connection and the nature of the interstellar medium
[NASA-CR-186286] N90-15860
SUPERPLASTICITY
Aluminum lithium alloys for Navy aircraft N90-15193
Superplastic performance and properties of the Lital Alloys N90-15199
Cryogenic mechanical properties of low density superplastic Al-Mg-Sc alloys
[DE90-002120] N90-15222
SUPERSONIC COMBUSTION RAMJET ENGINES
Spatially-resolved, nonintrusive measurements in a nonreacting scramjet combustor using laser-induced iodine fluorescence N90-15103
SUPERSONIC FLOW
Explicit and implicit calculations of turbulent cavity flows with and without yaw angle
[NASA-CR-186293] N90-15381
An algebraic turbulence model for flow separation caused by forward and backward facing steps
[AD-A213800] N90-15389
SUPERSYMMETRY
Modular invariants for theta-functions with characteristics and the twisted N=2 superconformal and SU(2) Kac-Moody algebras
[DE89-635701] N90-15671
Lefschetz trace formula and BRST
[DE89-635705] N90-15835
SURFACE DIFFUSION
Isotopic selectivity of surface diffusion: An activated diffusion model
[DE90-003473] N90-15169
SURFACE FINISHING
Guide to the selection of surface treatments for the improvement of fatigue strength of steels
[ESDU-89031] N90-15245
Characterization and in situ testing of diamond films
[DE90-003155] N90-15265
SURFACE LAYERS
Flux parameterization techniques in the atmospheric surface layer N90-15548
Specification for evaporation duct height calculations
[AD-A213841] N90-15570
SURFACE NAVIGATION
Autonomous land navigation in a structured environment
[DE90-001625] N90-15087
Planning minimum-energy paths in an off-road environment with anisotropic traversal costs and motion constraints
[AD-A214181] N90-15457
SURFACE PROPERTIES
A numerical model for the axisymmetric equilibrium shape of drops in uniform motion: Effects of external flow, electric field and surface charge N90-15071
Correlations between surface structure and catalytic activity/selectivity
[DE90-003755] N90-15181
Studies of the adsorption/desorption behavior of explosive-like molecules
[DE90-001867] N90-15283
A coning motion apparatus for hydrodynamic model testing in a non-planar cross-flow
[AD-A213431] N90-15383
Laser-induced surface ablation and optical damage of ZnS crystals caused by single- and multiple-pulse laser-irradiation
[DE90-003807] N90-15419
Fractal dimension of the fractured surface of materials
[DE89-635764] N90-15477
Resultant forces and moments in completely restrained plates subjected to a recovery temperature varying linearly with time
[ESDU-89024] N90-15480
Orientation of rf-sputter-deposited MoS2 films
[ATR-89(4752)-1] N90-15784
SURFACE REACTIONS
Studies of organo phosphorus-, nitrogen-, and sulfur-containing molecules
[AD-A213518] N90-15135
Interfacial systems for photochemical energy conversion
[DE90-003181] N90-15514
SURFACE ROUGHNESS
Surface roughening of Ge(001) during 200 eV Xe ion bombardment and Ge molecular beam epitaxy
[DE90-000674] N90-15769
SURFACE TEMPERATURE
Numerical investigation of transition control of a flat plate boundary layer N90-15361
Antarctic surface temperature and pressure data
[DE90-000971] N90-15565
SURFACE VEHICLES
Research in knowledge-based vision techniques for the Autonomous Land Vehicle Program
[AD-A213440] N90-15453
SURFACES
Damage evaluation from surface displacement data N90-15469
SURVEILLANCE
Control outside of independent surveillance coverage operational concept
[AD-A214163] N90-15090
Geotechnical instrumentation
[PB89-198675] N90-15398
SURVEYS
Image enhancement using the IRAS (Infrared Astronomy Satellite) survey data
[AD-A213811] N90-15496
SUSPENDING (MIXING)
Advanced study in solid transport: Rheological behavior of dense suspension
[DE90-003369] N90-15483
Saltation and suspension of particulate matter in air
[AD-A213618] N90-15552
SUSPENSION SYSTEMS (VEHICLES)
Planning systems for autonomous legged vehicles
[AD-A214242] N90-15458
SWITCHES
Single fluid simulations of plasma openings switch behavior
[DE90-002643] N90-15330

Portable digital pressure indicator for calibrating magnetic tape recorders
[NASA-TM-101650] N90-15401

SWITCHING
Avalanche photoconductive switching
[DE90-002980] N90-15337

SWITCHING CIRCUITS
LLNL's plan for a prototype circuit switch, a potential gigabit LAN of the future
[DE90-003614] N90-15597
Programs for control of an analog-signal switching network
[DE90-003645] N90-15626
Theoretical and computational studies of magnetic insulation and other plasma-opening-switch phenomena
[DE90-004421] N90-15757

SYMBOLS
Development of the AH-64 display symbology training module
[AD-A213456] N90-15592
MASC: Multiprocessor architecture for symbolic processing
[AD-A213504] N90-15656

SYMMETRY
SL(2,R) current algebra in two-dimensional conformal quantum gravity
[DE90-600755] N90-15675

SYNCHRONISM
Adaptive backoff synchronization techniques
[AD-A213966] N90-15658
Using mappings to prove timing properties
[AD-A213967] N90-15666
Periodic phase adjustment distributed clock synchronization in the hard realtime environment
[AD-A213842] N90-15708

SYNCHRONOUS SATELLITES
SCATHA (Spacecraft Charging at High Altitudes) atlas data base, volume 1
[AD-A214204] N90-15127

SYNCHROTRON RADIATION
Center for X Ray Optics, 1988
[DE90-003300] N90-15732

SYNTAX
Knowledge based text generation
[AD-A214273] N90-15645

SYNTHESIS (CHEMISTRY)
Novel polyimide compositions based on 4,4': Isophthaloyldiphthalic anaydride (IDPA)
[NASA-CASE-LAR-14194-1] N90-15148
Wet spinning of solid polyamic acid fibers
[NASA-CASE-LAR-14162-1] N90-15259
Polyimides with carbonyl and ether connecting groups between the aromatic rings
[NASA-CASE-LAR-14001-1] N90-15260
Optical properties and laser damage measurements of inorganic polymer films
[DE90-003633] N90-15267
Survey on synthesis technologies of methanol as an alternative fuel
[DE89-901303] N90-15284
Inorganic halogen oxidizers
[AD-A213990] N90-15294

SYNTHETIC APERTURE RADAR
Polarimetric SAR antenna characterization
[AD-A213438] N90-15306

SYNTHETIC FUELS
Survey on synthesis technologies of methanol as an alternative fuel
[DE89-901303] N90-15284
The Third Pacific Basin Biofuels Workshop: Proceedings
[DE90-002523] N90-15513

SYNTHETIC METALS
New organic synthetic metals derived from BEDT-TTF, Ni(dsit)2 and BEDO-TTF
[DE90-003793] N90-15242

SYSTEMS ANALYSIS
Ocean thermal energy conversion: An overview
[DE89-000838] N90-15512
A simulation model for dynamic system availability analysis
[AD-A213499] N90-15628
A structured connectionist approach to direct inferences and figurative adjective-noun combinations
[AD-A214326] N90-15649

SYSTEMS ENGINEERING
NOISE: A nonlinear optimization induction free-electron laser systems engineering code
[DE90-004438] N90-15420
Young Investigator's Award and distributed self-adaptive databases
[AD-A214194] N90-15854

SYSTEMS INTEGRATION
Integration of a gated microchannel plate detector into the Nova laser system
[DE90-002981] N90-15413

T

TAIL ASSEMBLIES
Canard versus aft-tail ride qualities performance and pilot command response N90-15053

TANDEM MIRRORS
Magnetic mirror confinement concepts system studies
[DE90-003667] N90-15753

TAPE RECORDERS
Portable digital pressure indicator for calibrating magnetic tape recorders
[NASA-TM-101650] N90-15401
A compact acoustic recorder
[AD-A213581] N90-15403

TARGET RECOGNITION
High resolution imaging by phase retrieval and discrimination using speckle, volume 1
[AD-A214243] N90-15317
Research in knowledge-based vision techniques for the Autonomous Land Vehicle Program
[AD-A213440] N90-15453

TARGET THICKNESS
Effects of parametric variations of complex targets on damage from projectile impact
[DE90-003214] N90-15450

TARGETS
MF/HF multistatic mid-ocean radar experiments in support of SWOTHR (Surface-Wave Over-The-Horizon Radar)
[AD-A213830] N90-15314
Effects of parametric variations of complex targets on damage from projectile impact
[DE90-003214] N90-15450
Evaluation of a simple algorithm for estimating infrared signatures from multi-pixel to sub-pixel targets applied to AGA thermovision imagery
[AD-A214103] N90-15639

TASKS
Task-oriented display design: Concept and example
[NASA-TM-101685] N90-15101
Dual task performance with LPC (Linear Predictive Coding) degraded speech in a sentence verification task
[AD-A214298] N90-15320
MANPRINT methods monograph: Aiding the development of manned system performance criteria
[AD-A213543] N90-15593

TASTE
Utilization of non-conventional systems for conversion of biomass to food components
[NASA-CR-177545] N90-15591

TATB
A future for LLNL (Lawrence Livermore National Laboratory) research in composite high explosives
[DE90-004442] N90-15290

TAYLOR SERIES
Tensor methods for unconstrained optimization using second derivatives
[AD-A213642] N90-15681

TECHNOLOGY ASSESSMENT
Proceedings of the Antenna Applications Symposium, volume 2
[AD-A213815] N90-15313
Ocean thermal energy conversion: An overview
[DE89-000838] N90-15512
Introduction to D-He(3) fusion reactors N90-15839
The Solar Power Satellite (SPS): Progress so far N90-15840
Importance of helium-3 for the future N90-15843

TECHNOLOGY TRANSFER
Point of view of a civil aircraft manufacturer on Al-Li alloy N90-15200
Research in mathematics and computer science at Argonne
[DE90-000975] N90-15595

TECHNOLOGY UTILIZATION
Base reaction optimization of redundant manipulators for space applications
[NASA-CR-186274] N90-15447

TECTONICS
Determination of Q as a function of depth and tectonic province
[AD-A213805] N90-15554
Evolution of overlapping spreading centers: A Sea Mark 2 investigation
[AD-A214278] N90-15576

TELEMETRY
X.2 limited flight test plan
[AD-A214412] N90-15099
Identification and quantification of synoptic structure in simulated TIROS N radiance soundings
[AD-A213729] N90-15553

TELEOPERATORS
Architectural study of the design and operation of advanced force feedback manual controllers
[NASA-CR-185948] N90-15664

TELEPHONY
On the privacy problems involved in allowing access to computers via the public telephone system
[RSRE-88006] N90-15303

TELLURIUM COMPOUNDS
Design of a large angular aperture TeO2 acousto-optic tunable filter
[AD-A213999] N90-15738

TEMPERATURE DEPENDENCE
Accelerated aging embrittlement of cast duplex stainless steel: Activation energy for extrapolation
[DE90-001773] N90-15221

TEMPERATURE DISTRIBUTION
Temperatures in plates subjected to a recovery temperature varying linearly with time
[ESDU-89023] N90-15831

TEMPERATURE EFFECTS
Microstructural evolution of martensitic steels during fast neutron irradiation
[DE89-016231] N90-15212
Nickel beryllides and their properties
[DE90-001736] N90-15220
Solid lubrication of ceramic surfaces by IAC (Ion-Assisted Deposition)-silver coatings for heat engine applications
[DE90-002860] N90-15253
Studies of the adsorption/desorption behavior of explosive-like molecules
[DE90-001867] N90-15283
Investigation of loads generated by temperature transients in pipes
[DE89-636433] N90-15395
Innovative optoelectronic materials and structures using OMVPE
[AD-A214192] N90-15815
Power semiconductor devices for space nuclear power systems
[DE90-001178] N90-15819

TEMPERATURE GRADIENTS
Simultaneous multipoint measurements of density gradients and temperature in a flame
[DE90-001719] N90-15155
Experimental determination of the fluid velocity by spectral analysis of temperature fluctuations
[DE89-636430] N90-15372
Ocean thermal energy conversion: An overview
[DE89-000838] N90-15512
The calculation of overground sound propagation in the presence of wind and temperature gradients
[ESDU-89036] N90-15714

TEMPERATURE MEASUREMENT
Simultaneous multipoint measurements of density gradients and temperature in a flame
[DE90-001719] N90-15155
Surface thermometry of energetic materials by laser-induced fluorescence
[AD-A214423] N90-15297
Tuned-circuit Johnson noise thermometry
[DE89-016221] N90-15356
Pulsed EMAT (Electromagnetic Acoustic Transducer) acoustic measurements on a horizontal continuous caster for internal temperature determination
[DE90-002735] N90-15709

TENSILE PROPERTIES
Heat treatment investigation of 4330 vanadium-modified steel
[AD-A214290] N90-15239

TENSILE TESTS
Epoxy-resin cable terminations
[AD-A213789] N90-15454

TENSOR ANALYSIS
Tensor methods for unconstrained optimization using second derivatives
[AD-A213642] N90-15681
Nijenhuis tensor and integrable models
[DE90-001403] N90-15702

TENSORS
Nijenhuis tensor and integrable models
[DE90-001403] N90-15702

TERMINAL BALLISTICS
MESA 3-D calculations of armor penetration by projectiles with combined obliquity and yaw
[DE89-015265] N90-15438
Fragmentation statistics from Eulerian hydrocode calculations
[DE90-002906] N90-15449

TERMINOLOGY
Terminology strategies for international information exchange
[AD-A214147] N90-15853

TERRAIN
Measurements of horizontal visibility in the lowest 300 m over Northern Germany N90-15059

TEST EQUIPMENT
Ignitability test method and apparatus
[NASA-CASE-LAR-13996-1-SB] N90-15161

TEST FACILITIES
VIBRAFUGE: Combined vibration and centrifuge testing
[DE90-001091] N90-15114
Hugoniot measurements with the LLNL electric gun facility
[DE90-002809] N90-15119
Instrumentation for a facility for the test, analysis and active control of spacecraft truss structures
[AD-A213655] N90-15124
NTES (Nuclear Test and Experimental Sciences) program laser facility for physics experiments Building 391 High Bay Option
[DE90-001795] N90-15411
TETHERLINES
Modeling and control of the rapid deployment of towed airborne devices N90-15092
TEXTS
Knowledge based text generation
[AD-A214273] N90-15645
THALLIUM COMPOUNDS
Cation disordering in the Tl-2122 superconductors
[DE90-003579] N90-15795
THEOREMS
A basic theorem of complementarity for the generalized variational-like inequality problem
[DE90-003102] N90-15620
On the sum of two maximal monotone operators
[REPT-89-31] N90-15669
Strong large deviation and local limit theorems
[AD-A213610] N90-15698
THEORETICAL PHYSICS
Theory of interacting plasmas in space N90-15742
THERMAL ANALYSIS
Simultaneous thermal analysis techniques for characterization of energetic materials
[DE90-003028] N90-15289
Thermal analysis of fixed and tilting pad journal bearings including cross-film viscosity variations and deformations N90-15429
THERMAL CONDUCTIVITY
Summary physical data tables: Alkanes
[ESDU-PD3] N90-15162
On the choice of trial function in theoretical calculations of the thermal conductivity
[DE90-001733] N90-15182
Thermal conductivity of gaseous aliphatic hydrocarbons. Part 1: Alkanes
[ESDU-89035-PT-1] N90-15183
Short fibre and particulate reinforced metal matrix composites N90-15207
Laser-induced surface ablation and optical damage of ZnS crystals caused by single- and multiple-pulse laser-irradiation
[DE90-003807] N90-15419
Selection of phase-change and containment materials for thermal energy storage
[NASA-CR-186228] N90-15506
Satellite thermal storage systems using metallic phase-change materials
[DE89-016872] N90-15507
Physical process in MPD plasmas
[AD-A213679] N90-15761
THERMAL DECOMPOSITION
Properties and thermal decomposition of the double salts of uranyl nitrate-ammonium nitrate
[DE89-004909] N90-15287
THERMAL DEGRADATION
Hardening and toughening of ZnS-Ga2S3 ceramics by solid-state reactions
[AD-A213875] N90-15276
Thermal stability of jet fuel
[DE90-002760] N90-15288
Characterization of the thermal degradation of selected energetic materials and mixtures by Rapid-Scan Fourier Transform Infrared (RSFTIR) spectroscopy
[AD-A214411] N90-15296
THERMAL ENERGY
Thermal energy storage
[DE90-000953] N90-15500
Selection of phase-change and containment materials for thermal energy storage
[NASA-CR-186228] N90-15506
Satellite thermal storage systems using metallic phase-change materials
[DE89-016872] N90-15507
THERMAL EXPANSION
Short fibre and particulate reinforced metal matrix composites N90-15207
THERMAL FATIGUE
Thermal mechanical fatigue of coated blade materials
[AD-A214258] N90-15107
Isothermal fatigue behavior of Sn-Pb solar joints
[DE90-003280] N90-15464
THERMAL STABILITY
A novel heat resistant blend produced by compositional quenching: A thermoplastic polyimide impact modified with a fluoroelastomer
[AD-A213724] N90-15273
Thermal stability of jet fuel
[DE90-002760] N90-15288
Characterization of the thermal degradation of selected energetic materials and mixtures by Rapid-Scan Fourier Transform Infrared (RSFTIR) spectroscopy
[AD-A214411] N90-15296
Instability of a-Si:H/Ag interface at 150 deg C
[DE89-009419] N90-15498
Physical process in MPD plasmas
[AD-A213679] N90-15761
Thermally stable metal/GaAs contacts
[DE90-002122] N90-15774
THERMAL STRESSES
Thermal stresses in unrestrained plates subjected to a recovery temperature varying linearly with time
[ESDU-89025] N90-15481
THERMOCHEMISTRY
High temperature chemistry of aromatic hydrocarbons
[DE90-003664] N90-15133
Guide to the selection of surface treatments for the improvement of fatigue strength of steels
[ESDU-89031] N90-15245
THERMODYNAMIC EFFICIENCY
Annual summary of basic research in thermoacoustic heat transport
[AD-A214185] N90-15834
THERMODYNAMIC EQUILIBRIUM
Progress in LTE and non-LTE transport calculations
[DE90-003394] N90-15764
Phase equilibrium and crystal growth studies on AgGaSe2 and related nonlinear optical materials
[AD-A213650] N90-15809
THERMODYNAMIC PROPERTIES
Properties of aluminum-uranium alloys
[DE90-003889] N90-15243
Surface thermometry of energetic materials by laser-induced fluorescence
[AD-A214423] N90-15297
RF transistor thermal/electrical characterization
[DE90-001427] N90-15326
A high spatial resolution study of the thermospheric response to a discrete auroral arc
[NASA-TM-102904] N90-15559
Thermal and statistical properties of nuclei and nuclear systems
[DE90-000183] N90-15717
THERMODYNAMICS
A study of variable geometry in advanced gas turbines N90-15104
Irreversible processes from reversible mechanics
[DE90-001057] N90-15368
On the free carrier-negative U center interacting model for the high-T(sub c) oxide superconductor
[DE89-635908] N90-15775
THERMOELECTRIC GENERATORS
Safety evaluation report for Galileo: Volume 1
[DE90-003086] N90-15122
Safety evaluation report for Galileo, volume 2
[DE90-003087] N90-15123
THERMOHYDRAULICS
Use of the linear variate method of Monte Carlo for estimating uncertainty in thermal-hydraulic codes
[DE89-017871] N90-15694
THERMOLUMINESCENCE
Laser detection and discrimination system
[AD-D014301] N90-15426
THERMOMECHANICAL TREATMENT
Aluminum lithium alloys for Navy aircraft N90-15193
Superplastic performance and properties of the Lital Alloys N90-15199
THERMOPLASTIC RESINS
A novel heat resistant blend produced by compositional quenching: A thermoplastic polyimide impact modified with a fluoroelastomer
[AD-A213724] N90-15273
THERMOPLASTICITY
A novel heat resistant blend produced by compositional quenching: A thermoplastic polyimide impact modified with a fluoroelastomer
[AD-A213724] N90-15273
THERMOSPHERE
A high spatial resolution study of the thermospheric response to a discrete auroral arc
[NASA-TM-102904] N90-15559
THESAURI
Terminology strategies for international information exchange
[AD-A214147] N90-15853
THETA PINCH
Initial results from FRC (Field-Reversed Configuration) compression experiments on FRX-C/LSM
[DE90-003390] N90-15754
Microfluctuations of plasma density in a theta-pinch and spatial coherency of a probing laser beam
[DE90-603347] N90-15760
THICK PLATES
Resultant forces and moments in completely restrained plates subjected to a recovery temperature varying linearly with time
[ESDU-89024] N90-15480
Thermal stresses in unrestrained plates subjected to a recovery temperature varying linearly with time
[ESDU-89025] N90-15481
Temperatures in plates subjected to a recovery temperature varying linearly with time
[ESDU-89023] N90-15831
THIN FILMS
Electronic materials high-T(sub c) superconductivity polymers and composites structural materials surface science and catalysts industry participation
[NASA-CR-186063] N90-15145
Superconducting film fabrication by the sol-gel process
[DE90-002069] N90-15252
Characterization and in situ testing of diamond films
[DE90-003155] N90-15265
Optical properties and laser damage measurements of inorganic polymer films
[DE90-003633] N90-15267
New devices using ferroelectric thin films
[DE90-000789] N90-15328
Analysis of an elastohydrodynamic lubricated point contact: User's manual
[AD-A214257] N90-15459
Thin films under chemical stress
[DE90-003754] N90-15484
Research on high-efficiency, single-junction, monolithic, thin-film amorphous silicon solar cells, phase 1
[DE89-009495] N90-15502
Research on high-efficiency, single-junction, monolithic, thin-film amorphous silicon solar cells, phase 2
[DE89-009496] N90-15503
US Polycrystalline Thin Film Solar Cells Program
[DE89-009506] N90-15504
Phonons and charge-transfer excitations in HTS superconductors
[DE89-016616] N90-15768
Micron-thin Nb films recovered from Mbar shock pressures
[DE90-001509] N90-15772
Partial reduction of re-oxidation processing of Y-Ba-Cu-O sputtered thin films
[DE90-003655] N90-15782
Orientation of rf-sputter-deposited MoS2 films
[ATR-89(4752)-1] N90-15784
Two-dimensional magnetic phase transition of ultrathin iron films on Pd(100)
[DE90-003555] N90-15788
Characterization of MOCVD (Metal Organic Chemical Vapor Deposition) grown epitaxial ceramic oxide thin films
[DE90-003561] N90-15790
Preparation, structure and properties of VO(sub x) and TiO2 thin films by MOCVD
[DE90-003566] N90-15793
Magnetic flux pinning in YBa2Cu3O7 films
[DE90-003709] N90-15799
Computer-controlled ion beam sputter-deposition of superconducting oxide films
[AD-A213921] N90-15812
High-temperature ceramic superconductors
[AD-A214251] N90-15818
The fabrication of YBa2Cu3O7 thin films by thermal coevaporation in oxygen
[DE90-003960] N90-15824
THIN WALLED SHELLS
Nonlinear strain-displacement relations for thin axisymmetric shells
[PB89-226013] N90-15470
THREE DIMENSIONAL BOUNDARY LAYER
Numerical investigation of transition control of a flat plate boundary layer N90-15361
THREE DIMENSIONAL FLOW
Explicit and implicit calculations of turbulent cavity flows with and without yaw angle
[NASA-CR-186293] N90-15381
An experimental study of the time-dependent behavior of the appendage-body junction vortex
[AD-A213465] N90-15384
THREE DIMENSIONAL MODELS
Development of a three-dimensional local scale atmospheric model with turbulence closure model
[DE90-710045] N90-15551

THREE DIMENSIONAL MOTION
Vision in dynamic environments
[AD-A213434] N90-15587
THYRISTORS
Power semiconductor devices for space nuclear power systems
[DE90-001178] N90-15819
TIME
Using mappings to prove timing properties
[AD-A213967] N90-15666
Periodic phase adjustment distributed clock synchronization in the hard realtime environment
[AD-A213842] N90-15708
TIME DEPENDENCE
Numerical simulation of the unsteady two-dimensional flow in a time-dependent doubly-connected domain N90-15073
Time-dependent free convection in liquid metals
[DE90-000957] N90-15366
Time-dependent free convection in low Prandtl number fluids
[DE90-003053] N90-15377
An experimental study of the time-dependent behavior of the appendage-body junction vortex
[AD-A213465] N90-15384
TIME SERIES ANALYSIS
Parametric identification of discrete time series models for structural response prediction N90-15472
Higher order crossings from a parametric family of linear filters
[AD-A213427] N90-15676
Recurrence and ergodicity for exponential family state-space models
[AD-A213466] N90-15677
TIME SHARING
The implementation of a coherent memory abstraction on a NUMA (Non-Uniform Memory Access) multiprocessor: Experiences with PLATINUM (Platform for Investigating Non-Uniform Memory)
[AD-A213909] N90-15600
Memory management for large-scale NUMA (Non-Uniform Memory Access) multiprocessors
[AD-A213910] N90-15601
An overview of PLATINUM: A Platform for Investiga ting Non-Uniform Memory (preliminary version)
[AD-A213911] N90-15602
Evolution of an operating system for large-scale shared-memory multiprocessors
[AD-A213912] N90-15603
TIN ALLOYS
Isothermal fatigue behavior of Sn-Pb solar joints
[DE90-003280] N90-15464
TIN TELLURIDES
Bridgman crystal growth
[NASA-CR-186204] N90-15766
TIROS SATELLITES
RAIDS: An orbiting observatory for ionospheric remote sensing from space
[AD-A213717] N90-15494
TITANIUM
Laser mixing of titanium on silicon carbide
[DE90-003216] N90-15150
Epoxy-resin cable terminations
[AD-A213789] N90-15454
TITANIUM BORIDES
Empirical and analytical determination of the fracture resistance of a TiB2 particle/SiC matrix composite
[NASA-TM-101940] N90-15143
TITANIUM CARBIDES
Laser mixing of titanium on silicon carbide
[DE90-003216] N90-15150
TITANIUM COMPOUNDS
Heat treatment of pulsed Nd: YAG laser welds in a Ti-14.8 wt pct Al-21.3 wt pct Nb titanium aluminide
[DE90-003484] N90-15228
TITANIUM OXIDES
Processing and properties of nanophase oxides
[DE90-003826] N90-15171
Research on high-efficiency, single-junction, monolithic, thin-film amorphous silicon solar cells, phase 1
[DE89-009495] N90-15502
Characterization of MOCVD (Metal Organic Chemical Vapor Deposition) grown epitaxial ceramic oxide thin films
[DE90-003561] N90-15790
Preparation, structure and properties of VO(sub x) and TiO2 thin films by MOCVD
[DE90-003566] N90-15793
TOKAMAK DEVICES
Upgrade plans to handle 30 to 40 Mbytes of data for D3-D
[DE90-003291] N90-15750
Design of DIII-D advanced divertor
[DE90-003343] N90-15752
Magnetic mirror confinement concepts system studies
[DE90-003667] N90-15753
Destabilization of tokamak pressure-gradient driven instabilities by energetic alpha populations
[DE90-003716] N90-15756
The 17th AINSE Plasma Physics Conference: Conference handbook
[DE90-600936] N90-15759
Introduction to D-He(3) fusion reactors N90-15839
Data file management in the D3-D data acquisition and analysis computer systems
[DE90-003289] N90-15850
TOLERANCES (MECHANICS)
Point of view of a civil aircraft manufacturer on Al-Li alloy N90-15200
Overview on radiation effects in electronics
[DE90-000841] N90-15357
TOMOGRAPHY
A tomographic study of premixed turbulent stagnation point flames
[DE90-002462] N90-15156
TOPEX
Error modeling of bias-type parameters for TOPEX orbit determination N90-15117
TOPOGRAPHY
Geosat/ERM altimeter data analysis for the determination of global oceanic mesoscale variability N90-15492
Evolution of overlapping spreading centers: A Sea Mark 2 investigation
[AD-A214278] N90-15576
TOPOLOGY
Spatial dynamics of deformable multibody systems with variable kinematic structure
[AD-A214098] N90-15455
A (2+1)-dimensional pure gravity for an arbitrary closed initial surface
[DE90-701754] N90-15829
Abelian gauge theory in topologically non-trivial space
[DE90-710100] N90-15830
TOROIDAL PLASMAS
Experiments on linear high beta helical axis stellarators to study simulated toroidal effects and Alfven-wave heating
[DE90-001704] N90-15745
Studies of plasma performance and transport in the Advanced Toroidal Facility (ATF)
[DE90-001737] N90-15746
TOUGHNESS
Hardening and toughening of ZnS-Ga2S3 ceramics by solid-state reactions
[AD-A213875] N90-15276
TOWED BODIES
Modeling and control of the rapid deployment of towed airborne devices N90-15092
TOXINS AND ANTITOXINS
Mutagenic responses of some petroleum-base obscurants in the Ames test
[AD-A214201] N90-15295
TRACKED VEHICLES
Lunar construction utility vehicle
[NASA-CR-186231] N90-15435
TRACKING (POSITION)
Research in knowledge-based vision techniques for the Autonomous Land Vehicle Program
[AD-A213440] N90-15453
TRAFFIC
Estimating departure times from traffic counts using dynamic assignment
[DE89-016259] N90-15653
Adaptive backoff synchronization techniques
[AD-A213966] N90-15658
TRAILING EDGES
Serrated trailing edges for improving lift and drag characteristics of lifting surfaces
[NASA-CASE-LAR-13870-1] N90-15094
TRAINING ANALYSIS
Where to from here. Future applications of mental models of complex performance
[DE90-002091] N90-15586
TRAINING DEVICES
Development of the AH-64 display symbology training module
[AD-A213456] N90-15592
TRAINING SIMULATORS
Cockpit resource management: A selected annotated bibliography
[AD-A214272] N90-15594
TRAJECTORIES
Geometric considerations for a waypoint guidance method
[DE90-001803] N90-15088
Anharmonic betatron motion in free electron lasers
[DE90-001515] N90-15407
MESA 3-D calculations of armor penetration by projectiles with combined obliquity and yaw
[DE89-015265] N90-15438
Feasibility study of using industrial robot for ultrasound testing
[DE90-002977] N90-15461
TRAJECTORY OPTIMIZATION
Guidance analysis of the aeroglide plane change maneuver as a turning point problem
[NASA-TM-101639] N90-15110
TRANSFORMERS
Computer controlled MHD power consolidation and pulse-generation system
[DE90-001224] N90-15662
TRANSIENT RESPONSE
Parametric identification of discrete time series models for structural response prediction N90-15472
TRANSISTORS
RF transistor thermal/electrical characterization
[DE90-001427] N90-15326
TRANSITION METALS
Host materials for transition-metal ions
[AD-A213605] N90-15808
TRANSITION TEMPERATURE
Optical solitons in liquid crystals
[DE90-000694] N90-15728
Linear electron-hole-electron pair model of high-temperature superconductivity in La(2-x)M(x)CuO4 and YBa2Cu3O(7-y): Part 2. Dependence of the superconducting transition temperatures on pressure and on hole concentration
[DE90-003012] N90-15779
Cation disordering in the TI-2122 superconductors
[DE90-003579] N90-15795
TRANSMISSION LINES
Silver coated superconducting ceramic powder
[AD-D014300] N90-15278
Laser communication system with wide band magnetostrictive modulation
[AD-D014302] N90-15427
Processing YBa2Cu3O(x) wires in O3/O2
[DE90-003570] N90-15794
TRANSMISSION LOSS
Rectangular-to-circular waveguide transitions for high-power circular overmoded waveguides
[AD-A213925] N90-15349
TRANSMITTANCE
Description of SHARC: The Strategic High-Altitude Radiance Code
[AD-A213806] N90-15555
TRANSMITTERS
SLCSAT (Submarine Laser Communication Satellite) communication system design study
[AD-A213403] N90-15304
TRANSONIC FLOW
Nonlinear phenomena in computational transonic aeroelasticity N90-15070
A direct-inverse method for transonic and separated flows about airfoils
[NASA-CR-4270] N90-15072
TRANSPORT AIRCRAFT
Relative merits of reactive and forward-look detection for wind-shear encounters during landing approach for various microburst escape strategies
[NASA-TM-4158] N90-15108
TRANSPORT PROPERTIES
Preparation and properties of icosahedral borides
[DE90-003574] N90-15180
Electronic and ionic transport in polymers
[AD-A213410] N90-15270
The measurement of transport properties in strongly coupled plasmas
[DE90-003451] N90-15755
Near-surface sputtered particle transport for an oblique incidence magnetic field plasma
[DE90-004422] N90-15758
Progress in LTE and non-LTE transport calculations
[DE90-003394] N90-15764
TRANSPORT THEORY
Evaluate and characterize mechanisms controlling transport, fate, and effects of army smokes in the aerosol wind tunnel: Transport, transformations, fate, and terrestrial ecological effects of hexachloroethane obscurant smokes
[DE90-002923] N90-15536
Transport modeling and advanced computer techniques
[DE90-001481] N90-15612
Studies of plasma performance and transport in the Advanced Toroidal Facility (ATF)
[DE90-001737] N90-15746
TRANSPORTATION
An assessment and comparison of fuel cells for transportation applications
[DE90-001807] N90-15508

TRANSVERSE OSCILLATION
Research on acoustical scattering, diffraction catastrophes, optics of bubbles, acoustical phase conjugation, and wake of an oscillating circular cylinder
[AD-A214168] N90-15711
TRAVELING WAVE TUBES
Secondary electron emission characteristics of molybdenum-masked, ion-textured OFHC copper
[NASA-TP-2967] N90-15211
TRIBOLOGY
Characterization and in situ testing of diamond films
[DE90-003155] N90-15265
TRIGGER CIRCUITS
First results from the MACRO (Monopole, Astrophysics, Cosmic Ray Observatory) detector at the Gran Sasso Laboratory
[DE90-003243] N90-15858
TRITIUM
Tritium and neutron measurements of a solid state cell
[DE90-003657] N90-15820
TROPICAL STORMS
Further research on dynamics of marine atmospheres in tropical cyclones
[AD-A213882] N90-15571
TRUCKS
Autonomous land navigation in a structured environment
[DE90-001625] N90-15087
TUBE HEAT EXCHANGERS
Laboratory study of the dynamic losses of a single speed, split system air-to-air heat pump having tube and plate fin heat exchangers, 1985 to 1986
[DE90-000970] N90-15367
Eddy-current inspection of shuttle heat exchanger tube welds
[NASA-CR-186302] N90-15462
TUNABLE LASERS
Development of tunable excimer lasers
[AD-A213521] N90-15421
Development of glass-ceramic lasers
[AD-A214146] N90-15423
Computer simulation of laser plasma interaction
[DE90-002828] N90-15748
Spectroscopic and laser properties of Cr:LiCaAlF6 and Cr:LiSrAlF6 crystals
[DE90-000783] N90-15770
TURBINE BLADES
Inclusion of nonlinear aerodynamics in the FLAP code
[DE89-009507] N90-15519
Prediction of stochastic blade loads for three-bladed, rigid-hub rotors
[DE89-009508] N90-15520
Aerodynamic design and initial performance measurements for the SANDIA 34-metre diameter vertical-axis wind turbine
[DE90-002574] N90-15523
TURBINE ENGINES
Aircraft performance enhancement with active compressor stabilization
[AD-A213652] N90-15097
Characterization of chemicals on engine exhaust particles
[AD-A213566] N90-15106
TURBOFAN ENGINES
Advanced detection, isolation, and accommodation of sensor failures in turbofan engines: Real-time microcomputer implementation
[NASA-TP-2925] N90-15112
TURBOMACHINERY
An experimental, analytical, and computational investigation of turbomachinery rotor flow fields
N90-15360
Computation of broadband mixing noise from turbomachinery
[AD-A214448] N90-15713
TURBULENCE
Systems for airborne wind and turbulence measurement N90-15046
Influence of windshear, downdraft and turbulence on flight safety N90-15048
Dense-spray properties: Structure and turbulence modulation
[AD-A213671] N90-15387
Inclusion of nonlinear aerodynamics in the FLAP code
[DE89-009507] N90-15519
Turbulence spectral widths view angle independence as observed by Doppler radar
[DOT/FAA/SA-89/2] N90-15566
Specification for evaporation duct height calculations
[AD-A213841] N90-15570
TURBULENCE EFFECTS
Turbulence effects of aircraft flight dynamics and control N90-15055
A study of the effects of Rotating Frame Turbulence (RFT) on helicopter flight mechanics N90-15058
TURBULENCE MODELS
Turbulence effects of aircraft flight dynamics and control N90-15055
A study of the effects of Rotating Frame Turbulence (RFT) on helicopter flight mechanics N90-15058
Explicit and implicit calculations of turbulent cavity flows with and without yaw angle
[NASA-CR-186293] N90-15381
An algebraic turbulence model for flow separation caused by forward and backward facing steps
[AD-A213800] N90-15389
Development of a three-dimensional local scale atmospheric model with turbulence closure model
[DE90-710045] N90-15551
TURBULENT BOUNDARY LAYER
An experimental study of the time-dependent behavior of the appendage-body junction vortex
[AD-A213465] N90-15384
Modifications of the Penn State Boundary Layer Research Facility for boundary layer/structure interaction experimental research
[AD-A213874] N90-15391
Further research on dynamics of marine atmospheres in tropical cyclones
[AD-A213882] N90-15571
Computation of broadband mixing noise from turbomachinery
[AD-A214448] N90-15713
TURBULENT FLOW
Simultaneous multipoint measurements of density gradients and temperature in a flame
[DE90-001719] N90-15155
Combustion characteristics of sprays
[AD-A213651] N90-15173
Explicit and implicit calculations of turbulent cavity flows with and without yaw angle
[NASA-CR-186293] N90-15381
TURBULENT WAKES
An experimental, analytical, and computational investigation of turbomachinery rotor flow fields
N90-15360
Computation of broadband mixing noise from turbomachinery
[AD-A214448] N90-15713
TURNING FLIGHT
Guidance analysis of the aeroglide plane change maneuver as a turning point problem
[NASA-TM-101639] N90-15110
TWO DIMENSIONAL BOUNDARY LAYER
Application of a mass-consistent wind model to chinook windstorms
[AD-A213622] N90-15568
TWO DIMENSIONAL FLOW
Numerical simulation of the unsteady two-dimensional flow in a time-dependent doubly-connected domain
N90-15073
TWO DIMENSIONAL MODELS
Further studies on possible coexistence of antiferromagnetism and superconductivity in 2D Heisenberg model
[DE90-601082] N90-15783
The middle Martian atmosphere N90-15874
TWO PHASE FLOW
Stability of numerical solutions for stratified two-phase flow
[DE90-701646] N90-15379

U

ULTRASONIC SPECTROSCOPY
Ultrasonic evaluation of porosity in aluminum cast materials
[AD-A213548] N90-15232
ULTRASONIC TESTS
Ultrasonic evaluation of porosity in aluminum cast materials
[AD-A213548] N90-15232
ULTRASONICS
Feasibility study of using industrial robot for ultrasound testing
[DE90-002977] N90-15461
Bulk wave characterization of high T(sub c) superconductors
[AD-A214030] N90-15813
ULTRAVIOLET LASERS
Laser detection and discrimination system
[AD-D014301] N90-15426
ULTRAVIOLET SPECTROMETERS
Development of the RAIDS (Remote Atmospheric and Ionospheric Detector System) extreme ultraviolet wedge and strip detector
[AD-A213730] N90-15495
UNDERWATER ACOUSTICS
A compact acoustic recorder
[AD-A213581] N90-15403
Wind speed dependence of acoustic ambient vertical directional spectra at high frequency
[AD-A214293] N90-15712
UNSATURATION (CHEMISTRY)
Correlations between surface structure and catalytic activity/selectivity
[DE90-003755] N90-15181
UNSTEADY AERODYNAMICS
Canard versus aft-tail ride qualities performance and pilot command response N90-15053
Unsteady aerodynamics of oscillating and rapidly pitched airfoils N90-15074
UNSTEADY FLOW
An alternative derivation for an integral equation for linearized subsonic flow over a wing
[AD-A214140] N90-15079
Dynamics of a class of vortex rings N90-15362
Nonlinear viscous waves produced by an impulsively moving plate
[AD-A214014] N90-15392
UPWASH
Aircraft response and pilot behaviour during a wake vortex encounter perpendicular to the vortex axis
N90-15057
URANIUM ALLOYS
Properties of aluminum-uranium alloys
[DE90-003889] N90-15243
URANIUM OXIDES
Properties and thermal decomposition of the double salts of uranyl nitrate-ammonium nitrate
[DE89-004909] N90-15287
USER MANUALS (COMPUTER PROGRAMS)
Analysis of an elastohydrodynamic lubricated point contact: User's manual
[AD-A214257] N90-15459
CryoTran user's manual, version 1.0
[NASA-TM-102468] N90-15622
USER REQUIREMENTS
A comparative evaluation and analysis of end-user search performance in an academic environment
N90-15845

V

VACUUM
Stable supermembrane vacuum with a discrete spectrum
[DE89-635722] N90-15561
VACUUM CHAMBERS
Onorbit electron beam welding experiment definition
[NASA-CR-183847] N90-15431
VANADIUM ALLOYS
Heat treatment investigation of 4330 vanadium-modified steel
[AD-A214290] N90-15239
Fusion reactor materials
[DE90-000976] N90-15744
VANES
The effectiveness of vane-aileron excitation in the experimental determination of flutter speed by parameter identification
[NASA-TP-2971] N90-15100
VAPOR DEPOSITION
Benefits from combining electroplating and physical vapor deposition technologies
[DE90-002700] N90-15301
Characterization of MOCVD (Metal Organic Chemical Vapor Deposition) grown epitaxial ceramic oxide thin films
[DE90-003561] N90-15790
Preparation, structure and properties of VO(sub x) and TiO2 thin films by MOCVD
[DE90-003566] N90-15793
VAPOR PHASES
Heat transfer in condensation of lithium vapors
[DE90-002081] N90-15375
VAPORIZING
Time-dependent free convection in low Prandtl number fluids
[DE90-003053] N90-15377
Aerosol heating and vaporization of high-flux laser beams
[DE90-003471] N90-15428
VAPORS
Reflux condensation in vertical tubes
[ESDU-89038] N90-15397
VARIABILITY
Geosat/ERM altimeter data analysis for the determination of global oceanic mesoscale variability
N90-15492
VARIATIONAL PRINCIPLES
On the choice of trial function in theoretical calculations of the thermal conductivity
[DE90-001733] N90-15182

A basic theorem of complementarity for the generalized variational-like inequality problem
[DE90-003102] N90-15620

VARIATIONS
Experimental determination of the fluid velocity by spectral analysis of temperature fluctuations
[DE89-636430] N90-15372
Global lake-level variations from 18,000 to 0 years ago: A palaeoclimate analysis
[DE90-000998] N90-15531

VARISTORS
Sintering studies on high field varistors
[DE90-002626] N90-15359

VEGETABLES
Variability of cultivar responses to ozone
[PB89-225460] N90-15528

VEHICULAR TRACKS
Lunar construction utility vehicle
[NASA-CR-186231] N90-15435

VELOCITY
Application of the joined wing to tiltrotor aircraft
[NASA-CR-177543] N90-15093
Effects of parametric variations of complex targets on damage from projectile impact
[DE90-003214] N90-15450

VENTILATION
Guidelines for evaluating energy analysis software
[AD-A214171] N90-15640

VERTICAL AIR CURRENTS
Vertical distribution of pollutants in the presence of convective storms
[DE90-002590] N90-15549

VERTICAL DISTRIBUTION
Vertical distribution of pollutants in the presence of convective storms
[DE90-002590] N90-15549
Beryllium dispersion near explosive firing tables: A comparison of computed and observed results
[DE90-002635] N90-15550

VERY LARGE ARRAY (VLA)
Automated observation scheduling for the VLT
[NASA-CR-186282] N90-15861

VERY LARGE SCALE INTEGRATION
VLSI theory and parallel supercomputing
[AD-A214035] N90-15351
Systolic algorithms for imaging from space
[AD-A213870] N90-15701

VIBRATION
VIBRAFUGE: Combined vibration and centrifuge testing
[DE90-001091] N90-15114
Characterizing transient vibrations using band limited moments
[DE90-000799] N90-15473
Pipeline vibrations. Fluid transients in non-rigid, unbranched planar piping systems
[ESDU-89030] N90-15491

VIBRATION DAMPING
Active control system for gust load allevation and structural damping N90-15056

VIBRATION TESTS
VIBRAFUGE: Combined vibration and centrifuge testing
[DE90-001091] N90-15114

VIBRATIONAL SPECTRA
The production and spectroscopy of molecular ions isolated in solid neon
[AD-A213723] N90-15174
Dynamics of electron transfer for a nonsuperexchange coherent mechanism, 1
[AD-A213450] N90-15721

VIDEO DATA
Scry: A distributed image handling system, version 1.1
[DE90-003105] N90-15621

VIDEO SIGNALS
Focal plane antenna array for millimeter waves
[AD-D014306] N90-15322

VISCOELASTICITY
Investigation of loads generated by temperature transients in pipes
[DE89-636433] N90-15395

VISCOPLASTICITY
Ductile failure
[AD-A213864] N90-15488

VISCOSITY
Summary physical data tables: Alkanes
[ESDU-PD3] N90-15162
New transient algorithms for non-Newtonian flows
[AD-A213494] N90-15385
Nonlinear viscous waves produced by an impulsively moving plate
[AD-A214014] N90-15392
Thermal analysis of fixed and tilting pad journal bearings including cross-film viscosity variations and deformations N90-15429
Physical process in MPD plasmas
[AD-A213679] N90-15761

VISCOUS FLOW
Development of an integrated BEM approach for hot fluid structure interaction
[NASA-CR-186214] N90-15364
Irreversible processes from reversible mechanics
[DE90-001057] N90-15368

VISIBILITY
Measurements of horizontal visibility in the lowest 300 m over Northern Germany N90-15059
Imaging probabilities, geometry and ergonomics in limited visibility helicopter operations N90-15060
The assessment of visibility from automatic contrast Measurements N90-15061

VISION
Effect of contrast on the perception of direction of a moving pattern
[NASA-TM-102234] N90-15577

VISUAL AIDS
Improved lighting of taxiway/taxiway intersections for Instrument Flight Rules (IFR) operations
[DOT/FAA/CT-TN89/64] N90-15089

VISUAL PERCEPTION
The role of attention in visual processing
[AD-A214158] N90-15588

VISUAL SIGNALS
An architectural model of visual motion understanding
[AD-A214327] N90-15589

VLASOV EQUATIONS
The free energy of Maxwell-Vlasov equilibria
[DE90-003318] N90-15705

VOICE COMMUNICATION
Baseband development system implementation
[AD-A213464] N90-15309
Voice Multiplex System (VMS)
[AD-A213902] N90-15315
Voice/data integration in mobile radio networks: Overview and future research directions
[AD-A214289] N90-15319
Dual task performance with LPC (Linear Predictive Coding) degraded speech in a sentence verification task
[AD-A214298] N90-15320

VOIDS
Wet spinning of solid polyamic acid fibers
[NASA-CASE-LAR-14162-1] N90-15259
Statistical model for particle-void deformation kinetics in granular materials during shock wave propagation
[DE89-017729] N90-15476

VOLCANOLOGY
Evolution of overlapping spreading centers: A Sea Mark 2 investigation
[AD-A214278] N90-15576

VORTEX RINGS
Analysis of severe atmospheric disturbances from airline flight records N90-15045
Dynamics of a class of vortex rings N90-15362

VORTEX SHEDDING
Flow visualization of the effect of pitch rate on the vortex development on the scale model of a F-18 fighter aircraft
[AD-A214244] N90-15080
A coning motion apparatus for hydrodynamic model testing in a non-planar cross-flow
[AD-A213431] N90-15383

VORTICES
Aircraft response and pilot behaviour during a wake vortex encounter perpendicular to the vortex axis N90-15057
On strongly nonlinear vortex/wave interactions in boundary-layer transition
[NASA-CR-181963] N90-15078
Dynamics of a class of vortex rings N90-15362
Rayleigh-Taylor instability in compressible fluids
[DE90-003027] N90-15376
An experimental study of the time-dependent behavior of the appendage-body junction vortex
[AD-A213465] N90-15384

VORTICITY
Dynamics of a class of vortex rings N90-15362
Potential vorticity in extratropical cyclones N90-15564

W

WAFERS
Defect control and denuded trap zones in the 3-5 semiconductors
[AD-A214099] N90-15814

WAKES
An experimental, analytical, and computational investigation of turbomachinery rotor flow fields N90-15360

WALL FLOW
An experimental investigation of wall-interference effects for parachutes in closed wind tunnels
[DE90-001802] N90-15076

WALL PRESSURE
Modifications of the Penn State Boundary Layer Research Facility for boundary layer/structure interaction experimental research
[AD-A213874] N90-15391

WALLS
Enhancement of microchannel plate gain by deposition of CsI on the channel walls
[DE90-003051] N90-15334
Numerical investigation of transition control of a flat plate boundary layer N90-15361
Structure properties of confined systems. Hard spheres between ideal walls
[DE90-600818] N90-15378
Sound attenuation apparatus
[NASA-CASE-LAR-13968-1] N90-15710
Computation of broadband mixing noise from turbomachinery
[AD-A214448] N90-15713

WARNING SYSTEMS
How to fly windshear using the fly-by-wire concept N90-15050
Improved lighting of taxiway/taxiway intersections for Instrument Flight Rules (IFR) operations
[DOT/FAA/CT-TN89/64] N90-15089
Relative merits of reactive and forward-look detection for wind-shear encounters during landing approach for various microburst escape strategies
[NASA-TM-4158] N90-15108

WASTE ENERGY UTILIZATION
Design and fabricate a metallic hydride heat pump with a cooling capacity of 9000 BTU/H
[AD-A213756] N90-15388

WASTE HEAT
Design and fabricate a metallic hydride heat pump with a cooling capacity of 9000 BTU/H
[AD-A213756] N90-15388

WASTE TREATMENT
Managing the waste stream: Background information for planning source separation programs
[PB90-100223] N90-15530

WATER
Gas-liquid-liquid equilibria in mixtures of water, light gases, and hydrocarbons
[DE90-003180] N90-15167
Advanced study in solid transport: Rheological behavior of dense suspension
[DE90-003369] N90-15483

WATER QUALITY
Environmental surveillance data
[DE90-001275] N90-15532

WATER VAPOR
Analysis of ambient polar volatile organic compounds using chemical ionization-ion trap detector
[PB90-106451] N90-15529
Vertical distribution of pollutants in the presence of convective storms
[DE90-002590] N90-15549

WATER WAVES
Nonlinear viscous waves produced by an impulsively moving plate
[AD-A214014] N90-15392

WAVE DIFFRACTION
A new technique for simulating composite material. Task 2: Analytical solutions with Generalized Impedance Boundary Conditions (GIBCs)
[NASA-CR-186249] N90-15146

WAVE DISPERSION
Optical phonon modes in a double heterostructure of polar crystals
[AD-A214208] N90-15816

WAVE EQUATIONS
Enhanced resolution concepts in large scale scientific computing
[AD-A214095] N90-15393

WAVE FUNCTIONS
The dissociation energy of N2
[NASA-TM-101930] N90-15153
Variational quantum Monte Carlo calculation of electronic and structural properties of crystals
[DE90-003265] N90-15781

WAVE INTERACTION
On strongly nonlinear vortex/wave interactions in boundary-layer transition
[NASA-CR-181963] N90-15078
Excimer emission from alkali diatomic and alkaline-earth-noble-gas molecules
[AD-A214246] N90-15179

WAVE PROPAGATION
Hamiltonian chaos in a nonlinear polarized optical beam
[DE90-002437] N90-15408

Laser-supported detonation waves and pulsed laser propulsion
[DE90-002753] N90-15412
Determination of Q as a function of depth and tectonic province
[AD-A213805] N90-15554
Bulk wave characterization of high T(sub c) superconductors
[AD-A214030] N90-15813
A numerical simulation model for the study of magnetohydrodynamic (MHD) waves in a structured medium N90-15864

WAVEGUIDES
Waveguide effects in superradiant free-electron lasers
[DE90-003605] N90-15417
Thin films under chemical stress
[DE90-003754] N90-15484

WAVELENGTHS
Electron theory of long wavelength concentration fluctuations in liquid metal alloys
[DE89-636213] N90-15225

WEAPON SYSTEMS
The United States Air Force approach to all-weather testing N90-15047
Proposed activities to prepare for testing advanced/stealth weapons systems
[AD-A214453] N90-15321
China-built airborne synchronous laser ranger the new L-8 jet trainer aircraft
[AD-A213835] N90-15422

WEAR TESTS
Solid lubrication of ceramic surfaces by IAD (Ion-Assisted Deposition)-silver coatings for heat engine applications
[DE90-002860] N90-15253

WEATHER
Measurements of horizontal visibility in the lowest 300 m over Northern Germany N90-15059
Effects of lightning on operations of aerospace vehicles N90-15065
Environmental surveillance data
[DE90-001275] N90-15532
Winter cloud seeding potential on the Mogollon Rim
[PB89-190540] N90-15562

WEIGHT REDUCTION
Aluminum-lithium: Application of plate and sheet to fighter aircraft N90-15202

WELD TESTS
Reduction of residual stress and distortion in HY100 and HY130 high strength steels during welding
[AD-A213532] N90-15231
Eddy-current inspection of shuttle heat exchanger tube welds
[NASA-CR-186302] N90-15462

WELDED JOINTS
Helium-induced weld cracking in irradiated 304 stainless steel
[DE90-001312] N90-15219
The effect of nitrogen and titanium on the toughness of high strength saw weld deposits
[AD-A213400] N90-15230
Onorbit electron beam welding experiment definition
[NASA-CR-183847] N90-15431
Submerged arc welding consumables for HSLA (High Strength Low Alloy)-100 steel
[AD-A213433] N90-15452
Eddy-current inspection of shuttle heat exchanger tube welds
[NASA-CR-186302] N90-15462
Experience with J testing of 304/308 stainless steel weldment
[DE90-002046] N90-15478
Fatigue behavior of vertical axis wind turbine airfoils with two weld configurations
[DE90-002628] N90-15525

WEST GERMANY
Measurements of horizontal visibility in the lowest 300 m over Northern Germany N90-15059

WHEATSTONE BRIDGES
Design of a custom load cell for a precision assembly application
[DE90-004439] N90-15340

WHITE DWARF STARS
Pulsars lost and found: The second Princeton-Arecibo millisecond pulsar search N90-15865

WICKS
Ceramic heat pipe wick
[NASA-CASE-GSC-13199-1] N90-15261

WIENER HOPF EQUATIONS
A new technique for simulating composite material. Task 2: Analytical solutions with Generalized Impedance Boundary Conditions (GIBCs)
[NASA-CR-186249] N90-15146

WIGGLER MAGNETS
A microwiggler Free-Electron Laser at the Brookhaven Accelerator Test Facility
[DE90-003643] N90-15418

WIND (METEOROLOGY)
Saltation and suspension of particulate matter in air
[AD-A213618] N90-15552
The calculation of overground sound propagation in the presence of wind and temperature gradients
[ESDU-89036] N90-15714

WIND DIRECTION
Application of a mass-consistent wind model to chinook windstorms
[AD-A213622] N90-15568

WIND EFFECTS
Evaluate and characterize mechanisms controlling transport, fate, and effects of army smokes in the aerosol wind tunnel: Transport, transformations, fate, and terrestrial ecological effects of hexachloroethane obscurant smokes
[DE90-002923] N90-15536

WIND MEASUREMENT
Systems for airborne wind and turbulence measurement N90-15046

WIND PRESSURE
Inclusion of nonlinear aerodynamics in the FLAP code
[DE89-009507] N90-15519
Prediction of stochastic blade loads for three-bladed, rigid-hub rotors
[DE89-009508] N90-15520

WIND SHEAR
Flight in Adverse Environmental Conditions
[AGARD-CP-470] N90-15041
Wind shear models for aircraft hazard investigation N90-15044
Analysis of severe atmospheric disturbances from airline flight records N90-15045
Influence of windshear, downdraft and turbulence on flight safety N90-15048
Classification of windshear severity N90-15049
How to fly windshear using the fly-by-wire concept N90-15050
A pitch control law for compensation of the phugoid mode induced by windshears N90-15051
Relative merits of reactive and forward-look detection for wind-shear encounters during landing approach for various microburst escape strategies
[NASA-TM-4158] N90-15108

WIND TUNNEL TESTS
NASA's program on icing research and technology N90-15062
Flight and wind tunnel investigation of aerodynamic effects of aircraft ground deicing/antiicing fluids N90-15064
An experimental investigation of wall-interference effects for parachutes in closed wind tunnels
[DE90-001802] N90-15076

WIND TUNNEL WALLS
An experimental investigation of wall-interference effects for parachutes in closed wind tunnels
[DE90-001802] N90-15076

WIND TUNNELS
Evaluate and characterize mechanisms controlling transport, fate, and effects of army smokes in the aerosol wind tunnel: Transport, transformations, fate, and terrestrial ecological effects of hexachloroethane obscurant smokes
[DE90-002923] N90-15536

WIND TURBINES
Inclusion of nonlinear aerodynamics in the FLAP code
[DE89-009507] N90-15519
Aerodynamic design and initial performance measurements for the SANDIA 34-metre diameter vertical-axis wind turbine
[DE90-002574] N90-15523
Structural response measurements and predictions for the SANDIA 34-meter test bed
[DE90-002575] N90-15524
Fatigue behavior of vertical axis wind turbine airfoils with two weld configurations
[DE90-002628] N90-15525

WIND VELOCITY
Application of a mass-consistent wind model to chinook windstorms
[AD-A213622] N90-15568
Wind speed dependence of acoustic ambient vertical directional spectra at high frequency
[AD-A214293] N90-15712

WINDSHIELDS
Evaluation of the improved OV-ID anti-icing system, phase 2
[AD-A213928] N90-15083

WINGS
Unsteady three-dimensional thin-layer Navier-Stokes solutions on dynamic blocked grids N90-15069
An alternative derivation for an integral equation for linearized subsonic flow over a wing
[AD-A214140] N90-15079
The maximum lift coefficient of plain wings at subsonic speeds
[ESDU-89034] N90-15082
Evaluation of the improved OV-ID anti-icing system, phase 2
[AD-A213928] N90-15083

WINTER
Winter cloud seeding potential on the Mogollon Rim
[PB89-190540] N90-15562
Characteristics of electromagnetic wave forms with lightning in winter season
[DE89-901256] N90-15567

WIRE
Composite ceramic superconducting wires for electric motor applications
[AD-A213742] N90-15274
Epoxy-resin cable terminations
[AD-A213789] N90-15454
Processing YBa2Cu3O(x) wires in O3/O2
[DE90-003570] N90-15794

WORDS (LANGUAGE)
A structured connectionist approach to direct inferences and figurative adjective-noun combinations
[AD-A214326] N90-15649

WORKING FLUIDS
Ceramic heat pipe wick
[NASA-CASE-GSC-13199-1] N90-15261

WORKLOADS (PSYCHOPHYSIOLOGY)
The application of queuing theory to the modelling of CP-140 aircraft communications
[AD-A213479] N90-15310

X

X RAY ABSORPTION
X ray absorption studies of YBa2Cu3O(6+x), La(2-x)Sr(x)CuO4, and Nd(2-x)Ce(x)CuO4
[DE90-003640] N90-15797
Auger and x ray absorption studies of solid molecular oxygen
[DE90-003966] N90-15825

X RAY ASTRONOMY
The South African Astronomical Observatory
[NASA-CR-186258] N90-15856

X RAY DIFFRACTION
Synthesis conductivity, and x ray photoelectron spectrum of Bi2Sr2Cu(sub 7+x). A new ternary bismuth-oxide system exhibiting metallic conductivity
[DE90-003010] N90-15778

X RAY IMAGERY
Integration of a gated microchannel plate detector into the Nova laser system
[DE90-002981] N90-15413

X RAY SPECTROSCOPY
Center for X Ray Optics, 1988
[DE90-003300] N90-15732

XV-15 AIRCRAFT
Ice induced aerodynamic performance degradation of rotorcraft: An overview N90-15063
Application of the joined wing to tiltrotor aircraft
[NASA-CR-177543] N90-15093

Y

YAW
Explicit and implicit calculations of turbulent cavity flows with and without yaw angle
[NASA-CR-186293] N90-15381

YIELD POINT
Investigation on sheet material of 8090 and 2091 aluminium-lithium alloy N90-15192

YTTRIUM COMPOUNDS
Magnetic and electronic correlations in YBa2Cu3O(sub 6+x)
[DE89-017604] N90-15785

YTTRIUM OXIDES
Linear electron-hole-electron pair model of high-temperature superconductivity in La(2-x)M(x)CuO4 and YBa2Cu3O(7-y): Part 2. Dependence of the superconducting transition temperatures on pressure and on hole concentration
[DE90-003012] N90-15779
Partial reduction of re-oxidation processing of Y-Ba-Cu-O sputtered thin films
[DE90-003655] N90-15782
Magnetic flux pinning in YBa2Cu3O7 films
[DE90-003709] N90-15799
Cu-O chains in YBa2Cu3O(7-delta) and the phonon mechanism of high-Tc superconductivity
[DE90-603502] N90-15805

Properties of high Tc superconducting oxides
[DE90-003792] N90-15821
Atomic scale structure of twin boundary in Y-Ba-Cu-O superconductors
[DE90-003955] N90-15823

Z

ZINC OXIDES
Processing and properties of nanophase oxides
[DE90-003826] N90-15171
Sintering studies on high field varistors
[DE90-002626] N90-15359
ZINC SULFIDES
Laser-induced surface ablation and optical damage of ZnS crystals caused by single- and multiple-pulse laser-irradiation
[DE90-003807] N90-15419
ZINC-BROMIDE BATTERIES
Membrane and durability studies for the zinc/bromine battery
[DE89-016181] N90-15324
ZIRCONIUM OXIDES
Potential applications of structural ceramic composites in gas turbines
[DE90-001273] N90-15248
IEA/Annex 2 powder characterization cooperative program
[AD-A213540] N90-15271
ZODIACAL LIGHT
Image enhancement using the IRAS (Infrared Astronomy Satellite) survey data
[AD-A213811] N90-15496

Typical Personal Author Index Listing

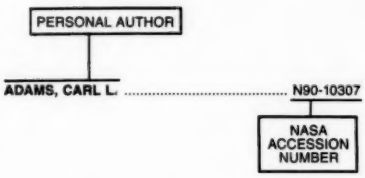

Listings in this index are arranged alphabetically by personal author. The NASA accession number denotes the number by which the citation is identified.

A

ABBOTT, TERENCE S. N90-15101
ABDALLA, E. N90-15675
ABDALLA, M. C. B. N90-15675
ABDALLAH, J., JR. N90-15764
ABE, D. K. N90-15333
ADAMOVICH, M. I. N90-15715
N90-15716
N90-15727
ADAMOVSKY, GRIGORY N90-15733
ADAMS, T. F. N90-15438
ADANUVOR, P. K. N90-15510
ADLER, L. N90-15232
AGARWAL, ANANT N90-15598
N90-15658
AGGARWAL, M. M. N90-15715
N90-15716
N90-15727
AGULAR, A. J. N. M. N90-15051
AHDUT, KEYVAN N90-15471
AKSAY, I. A. N90-15268
ALBANO, RICHARD K. N90-15866
ALBRECHT, ANDREAS N90-15867
ALEXANDER, D. J. N90-15479
ALEXANDROV, Y. A. N90-15715
N90-15716
N90-15727
ALLEN, CHARLES W. N90-15792
ALLEY, G. T. N90-15773
ALMEIDA, R. N90-15721
N90-15722
ALMLOEF, JAN N90-15153
ALTER, WENDY SUE N90-15227
AMEEVA, Z. V. N90-15715
ANDERSON, ROBERT S. N90-15552
ANDERSON, WILLIAM R. N90-15176
ANDREEVA, N. P. N90-15715
ANSON, Z. V. N90-15715
APPLEBY, A. J. N90-15510
APPLEMAN, EVAN N90-15778
ARCHAMBEAU, CHARLES B. N90-15556
ARDELL, ALAN J. N90-15238
N90-15276
ARLINGHAUS, H. F. N90-15419
ARMAND, MICHEL B. N90-15325
ARMSTRONG, JOSEPH H. N90-15151
ARMSTRONG, R. L. N90-15428
ARNOLD, C., JR. N90-15324
ARNOLDUS, HENK F. N90-15725
ARORA, R. N90-15715
N90-15716
N90-15727
ARUN, K. S. N90-15688
N90-15701
ASELAGE, T. L. N90-15180
ASHWILL, THOMAS D. N90-15524
ASSINK, R. A. N90-15324
ATAC, R. N90-15596
ATCHLEY, ANTHONY A. N90-15834
ATTIYA, HAGIT N90-15633
N90-15666
N90-15686
ATWATER, H. A. N90-15769
ATZMONY, U. N90-15223
AUCIELLO, ORLANDO H. N90-15812
AYRA, R. R. N90-15502
N90-15503
AZIMOV, S. A. N90-15715
AZINHEIRA, J. R. C. N90-15051
AZMY, Y. Y. N90-15695

B

BACH, R. E., JR. N90-15045
BADER, S. D. N90-15788
BAESLACK, W. A., III N90-15228
BAHNFLETH, WILLIAM N90-15640
BAILEY, JAMES W. N90-15161
BAITY, F. W. N90-15747
BALABAN, DAVID N90-15615
BALACHANDRAN, U. N90-15789
N90-15794
BANERJEE, P. K. N90-15364
BARAL, SUBHASH N90-15515
BARANOV, A. M. N90-15573
BARBAUX, Y. N90-15191
BARBOUR, J. C. N90-15802
BARCLAY, REBECCA O. N90-15848
BARD, ALLEN J. N90-15172
BARICH, J. J. N90-15170
BARINAGA, CHARLES J. N90-15158
BARNARD, JOHN J. N90-15407
BARNES, G. A. N90-15754
BARNES, RICHARD M. N90-15305
N90-15306
N90-15307
BARON, M. H. N90-15754
BARSOUM, R. N90-15488
BASOVA, E. N90-15715
N90-15716
N90-15727
BASS, RICHARD A. N90-15231
BATCHELOR, K. N90-15418
BATE, R. T. N90-15350
BAUGHMAN, R. J. N90-15795
N90-15801
BAUSCHLICHER, CHARLES W., JR. N90-15153
BAXI, C. B. N90-15752
BEATTY, JOHN HENRY N90-15210
BECHER, P. F. N90-15254
BECK, BRADLEY GERARD N90-15583
BECKER, W. N90-15737
BECKERMAN, M. N90-15436
N90-15663
BEERY, J. G. N90-15782
BELL, G. E. C. N90-15226
BELL, P. M. N90-15413
BEMENT, LAURENCE J. N90-15161
BEN-HARUSH, YITZHAK N90-15093
BEN-ZVI, I. N90-15418
BENNETT, GLORIA A. N90-15326
BENNETT, L. H. N90-15223
BENNETT, M. S. N90-15502
N90-15503
BENO, MARK A. N90-15242
N90-15777
N90-15778
BENVENUTI, A. N90-15879
BENZ, FRANK J. N90-15122
N90-15123
BERATAN, DAVID N. N90-15263
BEREZIN, A. B. N90-15760
BERG, DALE E. N90-15523
BERGOU, J. N90-15737
BERK, ALEXANDER N90-15650
BERNSTEIN, L. S. N90-15555
BERNSTEIN, LAWRENCE S. N90-15542
N90-15650
BERNSTEIN, S. L. N90-15304
BERRISFORD, PAUL N90-15564
BERRY, DON TRAVIS N90-15092
BERTRAND, P. A. N90-15784
BERWICK, J. W. N90-15111
BEVALOT, J. N90-15197
BHALLA, K. B. N90-15715
N90-15716
N90-15727
BHASIN, A. N90-15716
N90-15727
BHATIA, V. S. N90-15716
N90-15727
BHATTI, NEELOO N90-15539
BHOWMIK, A. N90-15418
BIEN, F. N90-15542
BIGELOW, T. S. N90-15746
BIRCHENALL, A. K. N90-15219
BISCHOF, CHRISTIAN H. N90-15613
BISHOP, A. R. N90-15768
BISHOP, D. O. N90-15413
BISHOP, HAROLD T. N90-15321
BIZNEK, M. E. N90-15789
BLACKBURN, J. C. N90-15729
BLACKFIELD, D. T. N90-15420
BLACKMAN, HAROLD S. N90-15586
BLADOS, WALTER R. N90-15853
BLAKENSHIP, JOHN G. N90-15371
BLALOCK, T. V. N90-15356
BLEJER, DENNIS J. N90-15306
N90-15307
BLENKO, TOM M. N90-15656
BOATNER, L. A. N90-15799
BODEN, T. A. N90-15565
BOEHRET, HARTMUT N90-15056
BOETTGER, J. C. N90-15264
BOLTON, HARRY, JR. N90-15536
BONAFE, J. L. N90-15050
BONDARENKO, R. A. N90-15716
N90-15727
BONDURANT, R. S. N90-15304
BONGERS, J. E. N90-15116
BONILLA, JOSE V. N90-15291
BONNER, C. A. N90-15168
BONNER, R. N90-15334
BOOGERS, J. A. M. N90-15190
BOOTH, LEWIE N90-15121
BOPARAI, AMRIT S. N90-15291
BOSCHETTI, F. N90-15194
BOTTO, R. E. N90-15269
BOUDH-HIR, M.-E. N90-15378
BOULAY, J. L. N90-15067
BOYD, DONALD M. N90-15709
BRACE, L. H. N90-15559
BRANAGAN, LYLE ARTHUR N90-15429
BRAUN, R. N90-15190
BRAY, D. J. N90-15209
BREWER, DAVID H. N90-15299
BRILL, THOMAS B. N90-15296
BRITTON, CHARLES L., JR. N90-15651
N90-15652
N90-15773
BRITTON, R. K. N90-15063
BROCIUS, W. F. N90-15772
BROOKE, TIMOTHY YOUNG N90-15857
BROOKS, JEFFREY N. N90-15758
BROWN, ALAN P. N90-15516
N90-15517
BROWN, BERNARD J. N90-15295
BROWN, CHARLES R. N90-15289
BROWN, CHRISTOPHER M. N90-15091
N90-15665
N90-15667
BROWN, ROBERT H. N90-15122
N90-15123
BROWNE, E. N90-15880
BRUBAKER, KENNETH L. N90-15291
BRUECK, S. R. J. N90-15425
BRYAN, W. L. N90-15773
BUCHER, E. A. N90-15304
BUFFINGTON, ROBERT J. N90-15076
BUHL, H. N90-15190
BUNK, W. N90-15208
BURCAT, ALEXANDER N90-15164
BURGMAN, H. A. N90-15483
BURNETT, T. H. N90-15716
N90-15727
BURNS, A. R. N90-15165

BURNS, ALAN A. N90-15314
BURNS, J. N90-15873
BURROUGHS, C. B. N90-15391
BURROWS, P. N. N90-15879
BURTSEV, V. A. N90-15760
BUSH, DONALD M. N90-15358
BUSHNELL, DENNIS M. N90-15094
BUTLER, M. A. N90-15328
BUTLER, P. C. N90-15324
BUTLER, R. G. N90-15199
BUTTERFIELD, C. P. N90-15520

C

CABRERA, CARLOS R. N90-15172
CAGLIOSTRO, D. J. N90-15438
CAIN, STEVEN M. N90-15256
CALAWAY, W. F. N90-15419
CALCATERRA, A. N90-15879
CALICCHIO, M. N90-15858
CALOMINO, ANTHONY M. N90-15445
CAMACHO, J. F. N90-15749
CAMPBELL, E. L. N90-15310
CAMPBELL, JOSEPH F., JR. N90-15382
CAMPOS, I. M. B. C. N90-15051
CANADELL, ENRIC N90-15779
CAPONE, D. W., II N90-15777
CARISS, CAROLYN S. N90-15778
CARLON, HUGH R. N90-15572
CARLSON, D. E. N90-15502
CARLSON, FREDERICK N90-15766
CARLSON, K. DOUGLAS N90-15242
N90-15778
CARLSON, LELAND A. N90-15072
CARRERAS, B. A. N90-15746
CARRIGNAN, G. R. N90-15559
CARTWRIGHT, S. L. N90-15879
CASSELL, KEITH N90-15656
CASSENT, DAVID N90-15637
CATALANO, A. W. N90-15502
CATALDO, DOMINIC A. N90-15536
CAVALLINI, G. N90-15194
CAYSON, STEPHEN C. N90-15740
CAZZATO, A. N90-15338
CECCHINI, S. N90-15858
CEDERQUIST, J. N. N90-15317
CEDERWALL, R. T. N90-15550
CERCHIONI, G. N90-15417
CERICOLA, F. N90-15114
CESS, ROBERT D. N90-15538
CHAGANTY, NARASINGA RAO N90-15698
CHAKRABARTI, S. N90-15495
CHAKRAVARTY, A. N90-15111
CHAN, S.-K. N90-15821
CHAN, V. W. N90-15304
CHANG-DIAZ, F. R. N90-15132
CHANG, B. N90-15749
CHANG, CHERNG N90-15289
CHANG, DAVID C. N90-15344
CHANG, H. L. M. N90-15790
N90-15793
CHANG, S.-J. N90-15254
CHANG, TSUEY-FEN N90-15875
CHANG, WILLIAM S. N90-15811
CHANNELL, DEWEY B. N90-15122
N90-15123
CHAO, K. C. N90-15167
CHAPYAK, E. J. N90-15438
CHARKRABARTI, K. N90-15426
CHASE, J. B. N90-15333
CHASE, L. L. N90-15419
CHASE, LLOYD A. N90-15770
CHASON, E. N90-15769
CHATER, W. T. N90-15495
CHATO, DAVID J. N90-15622
CHAU, H. H. N90-15119
CHEN, DE HUAI N90-15824
CHEN, HAO N90-15783
CHEN, J. J. N90-15423
CHEN, J. L. N90-15483
CHEN, JENG-MING N90-15547
CHEN, JIE N90-15797
N90-15825
CHEN, K. C. N90-15818
CHEN, R. N90-15810
N90-15816
CHEN, WILLIAM W. N90-15238
N90-15276
CHEN, YEN-MING N90-15073
CHEN, YONGSHUN N90-15575
CHEN, YUN MEI N90-15692
CHEN, Z. N90-15312
CHENG, R. K. N90-15156
CHENG, W. K. N90-15542
CHERAY, D. L. N90-15335
CHERIAN, MATHEWS N90-15658
CHERVIN, ROBERT M. N90-15574
CHI, JOSEPH N90-15571
CHIAO, LEROY N90-15247
CHITWOOD, L. D. N90-15462
CHOPRA, O. K. N90-15221
N90-15241
CHOW, LOUIS C. N90-15386
CHOW, TA-TUNG N90-15681
CHRIEN, R. E. N90-15754
CHRISTE, K. O. N90-15294
CHRISTEN, D. K. N90-15799
CHRISTENSEN, A. B. N90-15494
N90-15495
CHRISTENSON, P. J. N90-15756
CHRISTIANSEN, WALTER H. N90-15741
CHRISTIANSON, C. C. N90-15508
CHRISTIE, D. J. N90-15411
CHU, BENJAMIN N90-15266
CHU, C. W. N90-15797
CHUA, TECK-JOO N90-15621
CHUANG, CHIEN-HUA CATHERINE N90-15071
CHUANG, J. C. N90-15106
CHUNG, C. L. N90-15447
CHUNG, H. M. N90-15221
N90-15241
CHUPKA, W. A. N90-15557
CHWANG, ALLEN T. N90-15392
CIESLAK, M. J. N90-15228
CIFTAN, MIKAEL N90-15175
CIOFFI, L. V. N90-15053
CLARK, JUDY P. N90-15656
CLAYTOR, T. N. N90-15820
CLEARY, D. D. N90-15494
CLEMENT, PH. N90-15669
COHEN, HARRY N90-15778
COHEN, M. R. N90-15150
COHEN, P. I. N90-15807
COKER, GARY W. N90-15592
COLCHIN, R. J. N90-15746
COLE, GREGORY M. N90-15380
COLLINS, ROBIN A. N90-15605
COLSON, S. D. N90-15557
COLSON, WILLIAM B. N90-15409
COLTOFF, JOEL B. N90-15656
COLWELL, J. A. N90-15216
CONRAD, FRANK J. N90-15283
CONROY, PETER WILLIAM N90-15608
CONSTANT, D. N90-15186
COOK, A. N90-15596
COOK, R. P. N90-15642
COOPER, DAVID G. N90-15736
COOPER, THOMAS D. N90-15486
COPENHAVER, RONALD M. N90-15288
CORPRON, DANIEL R. N90-15656
CORT, G. EDWARD N90-15440
CORWIN, W. R. N90-15479
COSTANTINO, MARC S. N90-15286
COTTA, R. M. N90-15373
COTTER, GLADYS A. N90-15853
COURVILLE, G. E. N90-15526
COWART, J. S. N90-15448
COWGILL, GLENN R. N90-15622
COWLES, B. A. N90-15107
COX, ALAN L. N90-15600
N90-15602
COZZENS, ROBERT F. N90-15177
N90-15178
CRAIG, ERROL A. N90-15368
CRAWFORD, JOHN DAVID N90-15673
CRISWELL, DAVID R. N90-15841
CROSBY, KEVIN M. N90-15267
CROW, J. E. N90-15797
CRUME, E. C. N90-15746
CRUZ, J. E. N90-15302
CULIK, JEROME S. N90-15509
CULIOLI, JEAN-CHRISTOPHE N90-15651
N90-15652
CURREN, ARTHUR N. N90-15211
CUSHMAN, ROBERT M. N90-15540
CUSHMAN, WILLIAM B. N90-15405
CWIAKALA, MARTIN N90-15433

D

DABROWSKI, B. N90-15776
DAHLBERG, E. D. N90-15807
DAIELLO, R. V. N90-15502
DANBERG, JAMES E. N90-15389
DANIELS, K. L. N90-15532
DANTONE, I. N90-15858
DARGUSH, G. F. N90-15364
DAVE, B. B. N90-15510
DAVID, D. N90-15408
DAVIDSON, H. N90-15772
DAVIS, BYRON A. N90-15202
DAVIS, ROBERT F. N90-15812
DAWES, WILLIAM R., JR. N90-15357
N90-15819
DAWSON, JOHN M. N90-15748
DEBOOR, CARL N90-15678
DEBSIKDAR, J. C. N90-15252
DECATALDO, G. N90-15858
DEHOPE, W. J. N90-15818
DEJONGHE, LUTGARD C. N90-15325
DELAAT, JOHN C. N90-15112
DELEEUW, BRADLEY J. N90-15153
DELEMOS, MARCELO J. S. N90-15374
DELUCA, W. H. N90-15329
N90-15336
DEMARZO, C. N90-15858
DENBOER, M. L. N90-15825
DENNIS, SCOTT T. N90-15487
DEOSS, DISTER L., JR. N90-15628
DEPPE, J. N90-15596
DEQUAY, LAURENCE N90-15443
DERMOTT, S. N90-15873
DERYDER, LEONARD J. N90-15120
DESA, S. N90-15447
DESANCTIS, M. N90-15194
DESANGRO, R. N90-15879
DESILVA, C. W. N90-15447
DESIMONE, P. N90-15879
DESMARAIS, T. D. N90-15614
DEVAN, J. H. N90-15506
DEVANEY, JOSEPH J. N90-15696
DEXTER, JAMES L. N90-15736
DICKSON, C. R. N90-15502
N90-15503
DIECKMAN, S. L. N90-15269
DINEYKHAN, M. N90-15833
DING, JIAN N90-15774
DING, XIAO-YANG N90-15554
DINI, J. W. N90-15301
DIX, DAVID W. N90-15239
DIXON, GENE A. N90-15581
DOBREV, V. K. N90-15671
DODD, C. V. N90-15462
DODSON, M. G. N90-15170
DOGGETT, J. W. N90-15114
DOLEV, DANNY N90-15686
DOMINGUE, R. P. N90-15542
DONALD, BRUCE R. N90-15489
N90-15490
DONNELLY, M. N90-15662
DOROGY, WILLIAM E., JR. N90-15259
DORRIS, S. E. N90-15338
N90-15794
DOTTAVIO, T. N90-15626
DOTY, W. R. N90-15820
DOUDEAU, M. N90-15186
DOWDING, C. H. N90-15398
DOWELL, D. H. N90-15416
DOWLING, N. E. N90-15482
DOYLE, B. L. N90-15511
DRAGOO, ALAN L. N90-15271
DRESNER, LAWRENCE N90-15798
DRUCE, R. L. N90-15337
DUC, DUONG MINH N90-15674
DUFF, J. W. N90-15555
DUFF, M. J. N90-15561
DUFF, M. O. N90-15852
DUGGAN, D. M. N90-15818
DUNLAP, J. L. N90-15746
DUNN, BRUCE N90-15238
N90-15276
DUNWOODY, B. J. N90-15199
DUQUETTE, D. J. N90-15234
N90-15235
DURRANT-WHYTE, HUGH N90-15091
DURST, MARK N90-15615
DUSEK, J. T. N90-15338
N90-15794
DUTTON, R. W. N90-15786
DYER, G. R. N90-15746

E

EASTES, R. W. N90-15559
EASTMAN, J. A. N90-15171
N90-15800
EDMONDS, CHARLES G. N90-15158
EDWARDS, GEORGE, JR. N90-15159
EGBERTS, P. N90-15669
EICHTEN, E. N90-15596
EINSTEIN, J. R. N90-15436
ELLINGSON, W. A. N90-15269
EMERY, B. A. N90-15559
EMERY, V. J. N90-15796
ENAYETULLAH, M. A. N90-15510

ENDERS, JOHN H. N90-15042
ENGELMANN, BRUCE E. N90-15475
ENGLAND, A. C. N90-15746
ENRIQUEZ, R. N90-15626
ENTRIKEN, ROBERT N90-15625
EPHREMIDES, ANTHONY N90-15319
ERCK, R. A. N90-15253
ERDEMIR, A. N90-15253
ERICSON, MILTON N. N90-15651
N90-15652
N90-15773
ERMAK, DONALD L. N90-15131
ERNEST, TERRY N90-15474
ERRIQUEZ, O. N90-15858
ESAREY, E. N90-15424
N90-15763
ESER, SEMIN N90-15288
ESKOW, ELIZABETH N90-15630
ETTEDGUI, H. N90-15223
EVAIN, MICHEL N90-15779
EVANS, WILL J. N90-15368
EXARHOS, GREGORY J. N90-15267
EYLER, E. E. N90-15557

F

FAETH, G. M. N90-15387
FALLONE, JOSEPH F. N90-15384
FANG, Z. Q. N90-15817
FARHANG, MASSOUD N90-15656
FARKAS, L. N90-15436
FASEL, JOSEPH H., III N90-15610
FASEL, PATRICIA K. N90-15610
FAVUZZI, C. N90-15858
FAYA, ARTUR J. G. N90-15372
FEENSTRA, R. N90-15799
FEIGELSON, ROBERT S. N90-15809
FELLOWS, ROBERT J. N90-15536
FENDLER, JANOS H. N90-15515
FENG, SHUCHEN K. N90-15327
FENSKE, G. R. N90-15253
FERNOW, R. N90-15418
FERRANDO, WILLIAM N90-15278
FERRANTI, RICHARD L. N90-15307
FIDDY, M. A. N90-15638
FIELDS, STEVEN M. N90-15158
FIENUP, J. R. N90-15317
FIESELMANN, B. N90-15503
FIORITO, R. B. N90-15416
FISCHER, R. P. N90-15402
FISCHLER, M. N90-15596
FISHER, BRUCE D. N90-15065
FLETCHER, DOUGLAS GERALD N90-15103
FLETCHER, ROBERT F. N90-15122
N90-15123
FLIFLET, A. W. N90-15402
FLUSS, M. J. N90-15780
FLYNN, KATHLEEN M. N90-15246
FOLEY, R. J. N90-15411
FORD, JAMES A. N90-15047
FORRESTER, PATRICK GRAHAM N90-15095
FORSGREN, ANDERS L. N90-15616
FORSTER, G. A. N90-15269
FORTMANN, C. M. N90-15502
N90-15503
FOUCRIER, MICHEL JEAN N90-15372
FOWLER, ROBERT J. N90-15600
N90-15602
FOX, P. J. N90-15576
FRAGOLA, JOSEPH R. N90-15121
FRANK, D. N. N90-15411
FRANZEN, W. N90-15453
FRASIER, S. M. N90-15852
FRENSLEY, W. R. N90-15350
FRESE, MICHAEL H. N90-15330
FRIEBELE, E. J. N90-15729
FRIEDBERG, STUART ARTHUR N90-15648
FRONTROTH, R. L. N90-15243
FROST, D. D. N90-15398
FRUCHTER, ANDREW STEVEN N90-15865
FU, C. L. N90-15767
FUJITA, ROBERT K. N90-15440
FUKUZAWA, HISASHI N90-15284
FULLER, EDWARD N. N90-15159
FUQUIN, M. N90-15738
FURNO, JOHN S. N90-15273

G

GABRIEL, W. F. N90-15355
GAINES, I. N90-15596
GALBAATAR, T. N90-15805
GALLARDO, J. N90-15418
GANCHEV, A. H. N90-15671
GAO, H. W. N90-15280
GAO, M. N90-15596
GAO, ZHANJUN N90-15469
GAONKAR, G. H. N90-15058
GARBARINI, JOSEPH N90-15615
GARDNER, ROBERT H. N90-15537
GARFINKLE, DAVID N90-15832
GARINO, T. J. N90-15359
GARTNER, A. W. N90-15460
GARZON, F. H. N90-15782
GATHERS, G. R. N90-15119
GATTON, THOMAS M. N90-15456
GAUTIER, T. N. N90-15873
GAZIT, S. N90-15453
GEARY, DAVID C. N90-15680
GEBALLE, T. H. N90-15772
GEISER, URS N90-15242
N90-15778
GELENBE, EROL N90-15687
GELLER, A. S. N90-15365
GEORGE, THOMAS F. N90-15725
N90-15810
N90-15816
GERLACH, KARL N90-15318
GHANDHI, SORAB K. N90-15237
GHOSH, A. K. N90-15822
GIBSON, G. W. N90-15217
GIDAS, BASILIS N90-15643
GIESKE, J. H. N90-15180
GIESS, S. C. N90-15303
GIGLIETTO, N. N90-15858
GILL, PHILIP E. N90-15616
GINLEY, D. S. N90-15795
N90-15801
N90-15802
GLASER, PETER E. N90-15840
GLASSMAN, MYRON N90-15848
GLENN, LEWIS A. N90-15118
GLICK, J. H. N90-15365
GLIMM, JAMES N90-15393
GLOVER, C. W. N90-15436
GLOWIENKA, J. C. N90-15746
GLOWINSKI, ROLAND N90-15690
GLYNN, PETER W. N90-15684
N90-15687
N90-15689
GOBIN, P. F. N90-15206
GOELTZ, RICHARD N90-15611
GOETZ, GUENTER N90-15826
GOIX, P. N90-15156
GOLBEN, P. M. N90-15388
GOLDBERG, P. Y. N90-15532
GOLDMAN, KENNETH J. N90-15604
GOLDSTEIN, B. N90-15502
N90-15503
GOMEZ, JOSE PANTALEON, III N90-15138
GONZALES, S. N90-15879
GOODMAN, D. W. N90-15181
GOPALSAMI, N. N90-15269
GORDON, SYDNEY M. N90-15529
GORETTA, K. C. N90-15789
N90-15794
GOSS, LARRY P. N90-15297
GOUDREAU, GERALD L. N90-15475
GOULDING, R. H. N90-15747
GRACE, J. D. N90-15777
GRACEY, CHRISTOPHER N90-15110
GRADY, DENNIS E. N90-15449
GRAHAM, S. M. N90-15478
GRAHAM, WALTON N90-15084
GRAND, STEPHEN N90-15554
GRATTON, JULIO N90-15828
GRAY, J. A. N90-15190
GRAY, LEVEN B. N90-15122
N90-15123
GREEN, G. E. N90-15398
GREEN, LEROY G. N90-15281
GREEN, M. A. N90-15331
GREENBERG, R. N90-15873
GREENFIELD, ROY J. N90-15558
GREGORY, RUTH N90-15832
GREIMAN, WILLIAM N90-15615
GRIESS, J. C. N90-15217
GRIFFITH, D. M. N90-15111
GRIFFITH, WAYLAND C. N90-15077
GRIGGS, E. I. N90-15526
GROOM, NELSON J. N90-15442
GROSVELD, M. W. A. FERDINAND N90-15710
GROVES, SCOTT E. N90-15149
GRUBER, ROBERT EDWARD N90-15634
GRUEN, D. M. N90-15419
GRUNWALD, GARY N90-15677
GUDERLEY, KARL G. N90-15079
GUILINGER, T. R. N90-15511
GUPTA, ANOOP N90-15598
GUPTA, S. C. N90-15311
GUSSENHOVEN, M. S. N90-15127
N90-15128
GUTTMAN, CHARLES M. N90-15246
GUTTORP, PETER N90-15677

H

HA, SUNG KYU N90-15141
HAALAND, DAVID M. N90-15672
HAAS, PAUL A. N90-15287
HAFF, PETER K. N90-15552
HAHGIGHI, H. N90-15780
HAHN, CAROLE J. N90-15574
HAHN, HEIDI ANN N90-15585
N90-15586
HAIRE, R. G. N90-15213
HAJYOUSIF, B. N90-15794
HALL, PHILIP N90-15078
HALLIWELL, J. W. N90-15746
HALLORAN, JOHN W. N90-15274
HAMBY, C. N90-15507
HAMEED, SULTAN N90-15538
HAMILTON, WILLIAM DAVID N90-15227
HAMMES, JEFFREY P. N90-15610
HANKS, R. L. N90-15413
HANSON, G. H. N90-15217
HARDIN, PERRY JAMES N90-15493
HARGREAVES, T. A. N90-15402
HARPER, RICHARD N90-15654
HARRINGTON, M. S. N90-15359
HARRIS, S. J. N90-15207
HARRISON, S. P. N90-15531
HARTE, C. G. N90-15300
HARTLEY, J. G. N90-15363
HASTE, G. R. N90-15747
HASTINGS, DANIEL N90-15761
HATCH, J. N90-15731
HAUSNER, HANS N90-15271
HAVENS, STEPHEN J. N90-15260
HAVILAND, J. K. N90-15113
HAWKINS, R. J. N90-15731
HAWS, DAVID N90-15832
HAYHURST, KELLY JEANNE N90-15697
HEADLEY, T. J. N90-15228
HEDIN, A. E. N90-15559
HEDSTROM, JAMES C. N90-15326
HEELIS, R. A. N90-15559
HEFNER, KIM A. S. N90-15668
HEINE, J. E. N90-15107
HENESIAN, M. A. N90-15411
HENLINE, PAMELA N90-15750
HENSCHEL, H. N90-15729
HERGENROTHER, PAUL M. N90-15260
HERLIHY, MAURICE N90-15632
HERMES, G. L. N90-15411
HEYWOOD, J. B. N90-15448
HICKEY, CHARLES F., JR. N90-15239
HICKMAN, ROBERT G. N90-15290
HILL, EUGENE G. N90-15064
HILLSMAN, EDWARD L. N90-15543
HINKS, D. G. N90-15776
N90-15777
HINTON, DAVID A. N90-15108
HIRANO, MASASHI N90-15379
HIRSCHMAN, LYNETTE N90-15656
HIRVONEN, J.-P. N90-15150
HO, PAULINE N90-15706
HOCKNEY, G. N90-15596
HOEGY, W. R. N90-15559
HOFER, W. W. N90-15337
HOFFMAN, D. J. N90-15747
HOFFMAN, D. MARK N90-15258
HOFFMANN, E. H. N90-15751
HOGAN, R. E., JR. N90-15505
N90-15521
HOGREFE, R. L. N90-15329
N90-15336
HOLIAN, KATHLEEN S. N90-15439
HOLLKAMP, JOSEPH JAY N90-15472
HOLM, D. D. N90-15408
HOLMES, BRUCE J. N90-15094
HOLMES, J. A. N90-15756
HOLROYD, EDMOND W., III N90-15562
HONG, HO-CHENG N90-15142
HOOVER, CAROL G. N90-15368
HOOVER, WILLIAM G. N90-15368
HOPCROFT, JOHN E. N90-15647
HOPKINS, D. B. N90-15406
HOPKINS, WILLIAM C. N90-15656
HORN, K. M. N90-15769
HORWEDEL, B. M. N90-15532
HOSOYA, AKIO N90-15829
N90-15830
HOSTETLER, LARRY D. N90-15661
HOTTEL, GLENN ROY, SR. N90-15627

HOWARD, FLOYD G. N90-15094
HOWELL, M. N90-15506
HOWELL, R. J. N90-15780
HOWEY, C. K. N90-15495
HSIA, T. C. N90-15461
HSU, PING N90-15432
HSU, STEVEN M. N90-15271
HSUEH, CHUN-HWAY N90-15279
HUANG, JAMES N90-15621
HUANG, SHANGYUAN N90-15404
HUANG, T. S. N90-15701
HUANG, YIH-FANG N90-15685
HUDSON, BARRY J. N90-15849
HUEBNER, W. F. N90-15764
HUENNEKENS, JOHN P. N90-15179
HUFF, DARREL A. N90-15122
N90-15123
HULL, JOHN R. N90-15370
HUNG, CHING-CHEN N90-15262
HUNSAKER, DONALD B., JR. N90-15540
HUNT, J. T. N90-15411
HUNTER, J. W. N90-15772
HURD, ALAN J. N90-15706
HURD, J. R. N90-15168
HUSBY, D. N90-15596
HUSTON, E. L. N90-15388
HUSTON, RONALD L. N90-15434
HUTIN, PIERRE-MARIE N90-15043
HUTING, WILLIAM A. N90-15349
HUTTON, J. T. N90-15479
HWANG, JENG-YIH N90-15299

I

IGLESIAS, CARLOS A. N90-15872
IKEUCHI, SATORU N90-15860
IRVING, WILLIAM W. N90-15307
ISAAC, G. A. N90-15052
ISHIKAWA, YASUYUKI N90-15724
ISSA, JIHAD A. N90-15430

J

JABBOUR, KAMAL N90-15309
JACKSON, EDWARD L. N90-15509
JACOX, MARILYN E. N90-15174
JALOTE, PANKAJ N90-15465
JANSON, BRUCE N. N90-15653
JANZEN, DOYLE B. N90-15096
JAQUIN, ROBERT FREDERICK, III N90-15874
JEAN, Y. C. N90-15780
JENKINS, B. K. N90-15739
JENKINS, MICHAEL G. N90-15143
JENNE, ROY L. N90-15574
JENNISON, D. R. N90-15165
JENSEN, KENNETH A. N90-15211
JENSINS, W. K. N90-15701
JERVIS, THOMAS R. N90-15150
JOAG-DEV, KUMAR N90-15682
JOHAN, A. N90-15729
JOHNSON, D. RAY N90-15271
JOHNSON, DAVID C. N90-15383
JOHNSON, E. K. N90-15394
JOHNSON, ERIC E. N90-15599
JOHNSON, R. N90-15662
JOHNSON, WAYNE N90-15093
JOHNSTON, MARK D. N90-15861
N90-15862
N90-15863
JOHNSTON, WILLIAM E. N90-15621
JONES, ERIC M. N90-15876
JONES, J. P. N90-15436
N90-15663
JONES, L. A. N90-15755
JONES, P. D. N90-15565
JONES, WILBUR D., JR. N90-15855
JONG, R. A. N90-15406
JORGENSEN, J. D. N90-15777
JOYCE, JOHN P. N90-15122
N90-15123
JUHAS, JOHN J. N90-15147
JUKKALA, PETRI N90-15323
JUMIKIS, PAUL T. N90-15470

K

KABACOFF, LAWRENCE T. N90-15240
N90-15427
KAHN, PETER J. N90-15647
KAISER, J. H. N90-15780
KAISLER, KENNETH L. N90-15122
N90-15123
KALLMAN, HOWARD J. N90-15320
KANE, ROBERT N90-15541
KANGASMAA, SEPPO N90-15323
KANIA, D. R. N90-15755
KAPLAN, JONATHAN D. N90-15593
KARE, JORDIN T. N90-15412
KAREL, M. N90-15591
KATZ, ERIC S. N90-15089
KATZ, R. N90-15626
KAUN, T. D. N90-15339
KAVVAS, M. L. N90-15312
KAWASAKI, M. N90-15823
KAYSER, D. C. N90-15494
N90-15495
KAZMIERCZAK, M. N90-15423
KEADY, J. J. N90-15764
KEARNEY, FRANK W. N90-15456
KEARNEY, JOHN J. N90-15836
KECK, J. C. N90-15448
KEDDY, E. S. N90-15396
KEDEM, BENJAMIN N90-15676
KEDL, R. J. N90-15500
KELLER, PETER B. N90-15454
KELLNER, ALBERT L. N90-15811
KELLY, F. R. N90-15413
KELLY, M. J. N90-15511
KENIK, E. A. N90-15226
KENNA, BERNARD T. N90-15283
KENNEDY, R. M. N90-15712
KEPLER, R. G. N90-15720
KERCHNER, H. R. N90-15799
KETO, J. W. N90-15415
KEYES, T. N90-15423
KHEIFETS, S. A. N90-15734
KHOSROVANEH, A. K. N90-15482
KILLEEN, T. L. N90-15559
N90-15483
KIM, H. J. N90-15817
KIM, H. K. N90-15664
KIM, WHEE-KUK N90-15854
KING, ROGER N90-15812
KINGON, ANGUS I. N90-15242
KINI, ARAVINDA M. N90-15418
KIRK, H. N90-15434
KITTUR, MADAN G. N90-15087
KLARER, PAUL R. N90-15549
KLEINMAN, LAWRENCE N90-15523
KLIMAS, PAUL C. N90-15569
KNAPP, DAVID I. N90-15511
KNAPP, J. A. N90-15113
KNOSPE, CARL R. N90-15369
KNOWLTON, T. M. N90-15346
KOBA, RICHARD N90-15143
KOBAYASHI, ALBERT S. N90-15772
KOCH, R. N90-15315
KOCHANSKI, R. J. N90-15204
KOCZAK, M. J. N90-15057
KOENIG, REINHARD N90-15497
KOFSKY, I. L. N90-15743
KOGA, J. N90-15385
KOLKKA, ROBERT W. N90-15877
KOPP, R. A. N90-15063
KORKAN, K. D. N90-15200
KOSHORST, JOHANNES N90-15070
KOUSEN, KENNETH ARTHUR N90-15760
KOZHEVIN, V. M. N90-15361
KRAL, LINDA DEE N90-15233
KRASKO, GENRICH L. N90-15166
KRAYNIK, ANDREW M. N90-15365
KREBS, WILLIAM BERNARD N90-15707
KREYMER, A. N90-15609
KRINSKY, J. A. N90-15729
KRISHNASWAMY, SRIDHAR N90-15468
KRONFELD, A. N90-15596
KRUEGER, D. J. N90-15852
KRUMPELT, M. N90-15508
KRUPKE, WILLIAM F. N90-15770
KU, WALTER H. N90-15343
KUBIC, WILLIAM L., JR. N90-15694
KUCERA, GENE H. N90-15516
N90-15517
KUENY, CHRIS N90-15673
KUESTER, E. F. N90-15344
KUHLMAN, M. R. N90-15106
KULCINSKI, G. L. N90-15838
KULCINSKI, GERALD L. N90-15843
KUMAR, AKHIL N90-15619
KVAERNA, TORMOD N90-15657
KWAK, J. F. N90-15802

L

LABIAK, W. G. N90-15411
LACONTI, ANTHONY B. N90-15341
LAHTINEN, ARI N90-15323
LAM, D. J. N90-15790
N90-15793
LAM, L. N90-15728
LAM, NGHI Q. N90-15791
LAMSON, K. C. N90-15550
LAND, C. E. N90-15328
LANGSTON, CHARLES A. N90-15558
LANNUTTI, J. J. N90-15268
LANTZ, RICHARD D. N90-15518
LARIMER, R.-M. N90-15880
LARKIN, TIMOTHY H. N90-15326
LARSEN, E. B. N90-15302
LARSON, A. V. N90-15383
LARSON, D. W. N90-15411
LASHMORE, D. S. N90-15223
LATH, A. N90-15879
LAUF, R. J. N90-15507
LAUMANN, C. W. N90-15731
LAWRENCE, R. JEFFERY N90-15437
LAWRIE, LINDA N90-15640
LAWSON, J. K. N90-15411
LAZZERI, L. N90-15194
LEAKEAS, CHRISTOPHER L. N90-15762
LEBLANC, THOMAS J. N90-15601
N90-15603
LEBOEUF, J-N. N90-15756
LEBRUN, P. N90-15609
LECHNER, LYNNE N90-15530
LECKIE, FREDERICK A. N90-15215
LEE, E. W. N90-15193
LEE, FRED K., JR. N90-15295
LEE, HUA N90-15701
LEE, J. K. N90-15767
LEE, J. T. N90-15566
LEE, MARK R. N90-15079
LEIGHTY, BRADLEY D. N90-15401
LEINO, ANNE-TUULIA N90-15323
LEISERSON, CHARLES E. N90-15351
LEMPICKI, A. N90-15423
LEONARD, JOHN N90-15091
LESKO, K. T. N90-15880
LESSNER, PHILIP N90-15341
LEU, H. J. N90-15338
LEVATIN, JOANNE A. N90-15368
LEVY, MOISES N90-15813
LI, C.-Y. N90-15787
LI, SHU-MEI W. N90-15536
LI, TA-HSIN N90-15676
LI, WANG N90-15225
LIAO, Y. X. N90-15171
LIGOTKE, MICHAEL W. N90-15536
LIMBERT, D. W. S. N90-15565
LIN-LUI, Y. R. N90-15818
LIN, C. L. N90-15797
N90-15825
LIN, C. S. N90-15743
LIN, D. L. N90-15810
N90-15816
LIN, S. P. N90-15293
LIN, S. R. N90-15485
LIN, T. H. N90-15485
LIN, ZHONGQI N90-15404
LINBO-TERHAAR, B. M. N90-15624
LINCOLN, JOHN W. N90-15486
LINDEMAN, ERICK L., JR. N90-15757
LINDSEY, GREG N90-15530
LIPFERT, F. W. N90-15533
LIU, C. N90-15788
LIU, C. T. N90-15220
LIU, MEILIN N90-15325
LLOYD, W. R. N90-15478
LOESCHER, D. H. N90-15819
LONDON, JULIUS N90-15574
LONG, MARSHALL B. N90-15155
LOO, JOSEPH A. N90-15158
LOUIE, STEVEN G. N90-15781
LOWREY, A. R. N90-15416
LU, H. H. N90-15234
N90-15235
LUBOW, STEPHEN H. N90-15859
LUCKHAUS, STEPHAN N90-15674
LUDTKA, G. M. N90-15224
LUH, ELLICE YENG N90-15139
LUMPKIN, ALEX H. N90-15414
N90-15416
LUNDGREN, D. A. N90-15105
LUNG, C. W. N90-15477
LYNCH, NANCY A. N90-15632
N90-15633
N90-15666
LYONS, P. B. N90-15729

M

MACCRACKEN, MICHAEL C. N90-15535
MACDONALD, J. M. N90-15526
MACDONALD, K. C. N90-15576

MACHA, J. MICHAEL N90-15076
MACPHERSON, J. I. N90-15052
MAGEE, N. H., JR. N90-15764
MAHAJAN, SWADESH M. N90-15828
MAHON, RITA N90-15736
MAIER, THOMAS H. N90-15098
MAKRI, NANCY N90-15160
MALKUS, DAVID S. N90-15385
MANDELL, D. A. N90-15438
MANESCHY, C. E. N90-15395
MANGIACASALE, L. N90-15053
MANHEIMER, W. M. N90-15402
MANN, R. C. N90-15436
N90-15663
MANNING, JAMES M. N90-15582
MANOWITZ, B. N90-15533
MANSON, STEVEN T. N90-15723
MAPLE, M. B. N90-15818
MARCHAND, D. S. N90-15531
MARCOTTE, K. N90-15662
MARCUS, R. A. N90-15721
N90-15722
MARIELLA, R. P. N90-15786
MARIS, M. A. N90-15497
MARKOWITZ, VICTOR M. N90-15623
MARRIOTT, DOUGLAS L. N90-15215
MARRON, J. C. N90-15317
MARSH, BRIAN D. N90-15601
N90-15603
MARSHALL, A. N90-15772
MARSHALL, JOHN W. N90-15122
N90-15123
MARSTON, PHILIP L. N90-15711
MARSTON, S. E. N90-15111
MARTIN, CHARLES R. N90-15277
MARTIN, S. J. N90-15328
MARYNICK, DENNIS S. N90-15270
MARZULLO, KEITH N90-15400
N90-15699
MASON, T. O. N90-15789
MATHUR, V. K. N90-15426
MATTHEWS, FLORIDA N90-15258
MAYBERRY, M. J. N90-15747
MAYBURY, MARK T. N90-15645
MAYER-KRESS, GOTTFRIED N90-15580
MAYER, MICHAEL M. N90-15668
MAYES, PAUL N90-15313
MAYNE, P. W. N90-15398
MAYO, S. E. N90-15411
MAZDIYASNI, K. S. N90-15818
MAZIASZ, P. J. N90-15212
MCBRIDE, SCOTT N90-15474
MCCAULEY, JAMES W. N90-15271
MCCLELLAND, MATTHEW A. N90-15366
N90-15377
MCCOLLOUGH, I. L. N90-15532
MCCORMACK, RAY G. N90-15275
MCCORMICK, ROYCE F. N90-15401
MCCOY, R. P. N90-15494
MCDANIEL, JOHN A. N90-15289
MCDARMAID, D. S. N90-15188
N90-15189
MCDONALD, S. C. N90-15534
MCFADDEN, KRISTIN M. N90-15536
MCGLAUN, J. MICHAEL N90-15449
MCGRAIL, B. P. N90-15170
MCGRATH, MARY BETH N90-15467
MCHARG, B. B., JR. N90-15850
MCHARGUE, C. J. N90-15218
N90-15250
MCINERNEY, MICHAEL J. N90-15134
MCIVER, J. K. N90-15737
MCKAY, DONALD P. N90-15656
MCKENNA, GREGORY B. N90-15246
MCPARTLAND, JACK T. N90-15562
MCQUISTAN, G. W. N90-15639
MCVANEY, GARY N90-15083
MCVEETY, BRUCE D. N90-15536
MCVEIGH, J. N90-15502
MCWHORTER, ALAN L. N90-15806
MEANS, K. H. N90-15394
MEDIONI, G. N90-15453
MEIER, R. R. N90-15494
MEIER, ROBERT W. N90-15450
MEIJER, CORINNE N90-15320
MELENDEZ, JIM N90-15579
MENGER, FREDERIC M. N90-15342
MERKLE, K. L. N90-15780
MERRIGAN, MICHAEL A. N90-15396
N90-15522
MERRILL, WALTER C. N90-15112
MERRITT, MICHAEL N90-15632
MERRY, MICHAEL N90-15131
MEYER, P. N90-15186
MEYER, PAMELA J. N90-15366
MEZZINA, A. N90-15527
MICHELSEN, RANDY N90-15610
MIESS, JOSEPH C. N90-15083
MIKKELSEN, P. E. N90-15398
MILEY, D. V. N90-15252
MILLER, GLENN N90-15862
MILLER, J. F. N90-15329
N90-15336
MILLER, MICHAEL N90-15529
MILLER, W. A. N90-15367
MILNES, A. G. N90-15817
MILNES, ARTHUR G. N90-15814
MINER, W. H., JR. N90-15612
MINOTTI, FERNANDO N90-15828
MISRA, MOHAN S. N90-15151
MITCHELL, A. W. N90-15776
MITCHELL, C. S. N90-15550
MITCHELL, M. R. N90-15525
MITCHELL, RICHARD L. N90-15504
MOATS, ANNE ROSALIE MYERS N90-15878
MOEBEST, R. N90-15054
MOELLER, C. P. N90-15751
MOLZOW, M. N90-15054
MONTGOMERY, F. C. N90-15818
MOORE, J. R. N90-15213
MORAN, BILL N90-15368
MORE, JORGE J. N90-15618
MORETTO, L. G. N90-15717
MORGAN, SAMUEL H. N90-15545
MOROSIN, B. N90-15795
N90-15801
MORRIS, J. N90-15502
N90-15503
MORRIS, J. W., JR. N90-15222
N90-15464
MORRISON, CLYDE A. N90-15808
MORRISON, P. J. N90-15705
MORSE, J. D. N90-15786
MOULD, V. H. N90-15198
MOYA, MARY M. N90-15661
MUDDLE, BARRIE N90-15215
MUELLER, THOMAS J. N90-15380
MULLEN, E. G. N90-15127
N90-15128
MULLIGAN, J. B. N90-15577
MUNRO, ALLEN N90-15646
MUNSON, D. C., JR. N90-15701
MURANAKA, NEIL J. N90-15568
MURPHY, A. R. N90-15525
MURRAY, WALTER N90-15616
MUSE, WILLIAM T., JR. N90-15295
MUSINA, ROBERTA N90-15692

N

NAAR, DANIEL S. N90-15314
NAGY, P. B. N90-15232
NAIRN, CAROL M. C. N90-15742
NAKAMURA, NOBORU N90-15563
NAKAO, KEN-ICHI N90-15829
NAKHOST, Z. N90-15591
NAMSRAI, KH. N90-15833
NANSTAD, R. K. N90-15479
NAPPI, E. N90-15858
NARAYANASAMY, A. N90-15171
NASTASI, MICHAEL N90-15150
NAUMAN, E. BRUCE N90-15273
NAVE, S. E. N90-15213
NEEDLEMAN, ALAN N90-15488
NEILSON, G. H. N90-15746
NELLIS, W. J. N90-15772
NELSON, B. A. N90-15745
NELSON, WILLIAM R. N90-15586
NEVATIA, R. N90-15453
NEWPORT, D. F. N90-15773
NEWTON, P. M. N90-15066
NEYER, BARRY T. N90-15298
NICHOLS, F. A. N90-15253
NICHOLSON, P. N90-15873
NICOLET, M. A. N90-15498
NIEH, T. G. N90-15220
NIKI, SHIGERU N90-15811
NISSIM, ELI N90-15100
NOETZOLD, DIRK N90-15826
NORMAN, COLIN A. N90-15860
NORMAN, E. B. N90-15880
NORTON, R. L. N90-15111
NOTZ, KARL J. N90-15287
NOWICKI, L. J. N90-15777
NUSCA, MICHAEL J. N90-15163

O

ODONOVAN, MARY E. N90-15239
ODOWD, J. G. N90-15503
OH, C. H. N90-15375
OH, TAE SUNG N90-15140
OKUBO, SUSUMU N90-15702
OLINER, ARTHUR A. N90-15347
N90-15348
OLIU, WALTER E. N90-15848
OLSEN, R. C. N90-15125
OLSON, GREGORY B. N90-15233
OLSON, THOMAS JEREMY N90-15589
ONANIAN, JANICE S. N90-15635
ONCLEY, STEVEN PHILIP N90-15548
ORNELLAS, DONALD L. N90-15286
OSBORNE-LEE, A. E. N90-15532
OSHER, J. E. N90-15119
OSTENAK, C. A. N90-15168
OSWALD, R. S. N90-15503
OTT, S. N90-15838
OYAMA, SEIICHI N90-15284
OZAWA, YASUSHI N90-15284
OZISIK, M. N. N90-15373

P

PACE, N. E. N90-15217
PAEZ, THOMAS L. N90-15474
PAI, DINESH K. N90-15489
N90-15490
PAIK, HO JUNG N90-15545
PAIS, MARTIN R. N90-15386
PAK, S. S. N90-15818
PALMER, MICHAEL T. N90-15102
PANG, SWEE-CHEE N90-15606
PARK, B.-S. N90-15428
PARK, J. E. N90-15224
PARK, SUNG-NAM N90-15080
PARKER, J. C. N90-15790
N90-15793
PARKS, ALLEN D. N90-15607
PARKS, W. P., JR. N90-15248
PARTHASARATHY, R. N. N90-15387
PATEL, NISHEETH R. N90-15389
PAUL, W. N90-15499
PAULIKAS, A. P. N90-15777
PAULIUS, L. N90-15818
PAULUS, RICHARD A. N90-15570
PAWEL, R. E. N90-15217
PAXTON, L. J. N90-15494
PAYNE, STEPHEN A. N90-15770
PAYNE, STEVEN S. N90-15330
PEACOCK, H. B. N90-15243
PEEBLES, D. E. N90-15265
PEEL, C. J. N90-15203
PEERCY, P. S. N90-15802
PELLEGRINI, C. N90-15418
PELTONEN, JUHANI N90-15323
PENG, GANGDING N90-15404
PENG, S. N90-15453
PENNER, REGINALD M. N90-15277
PERDREAUVILLE, FARRELL J. N90-15088
PERISON, JANICE N90-15288
PETERKIN, ROBERT E., JR. N90-15330
PETERS, DANIEL J. N90-15452
PETERS, M. N90-15188
N90-15189
PETTERSSON, S. N90-15182
PFIRSCH, D. N90-15705
PHELAN, P. F. N90-15168
PICCIOLO, J. J. N90-15338
PICKARD, JAMES M. N90-15282
PICRAUX, S. T. N90-15769
PIEMONTESE, L. N90-15879
PIEPEL, G. F. N90-15624
PIEPER, GAIL W. N90-15595
PIERINI, P. N90-15417
PIIRONEN, PETRI N90-15323
PILAT, JOSEPH F. N90-15700
PILKEY, W. D. N90-15113
PILLAI, S. UNNIKRISHNA N90-15345
PINCOSY, P. A. N90-15333
PINELLI, THOMAS E. N90-15848
PITZ, WILLIAM J. N90-15164
N90-15448
POCHA, M. D. N90-15337
POELLAENEN, OSSI N90-15323
POEPPEL, R. B. N90-15338
N90-15789
N90-15794
POLETTO, G. N90-15877
POMERANTZ, MARTIN N90-15270
POMPE, ROBERT N90-15271
PONOMAREV, A. N. N90-15129
POOLE, B. R. N90-15749
POPE, C. N. N90-15561
POPE, LARRY E. N90-15265
POPE, W. L. N90-15331

PORTER, LEIGH CHRISTOPHER N90-15778
POST, MICHAEL E. N90-15297
POVENMIRE, H. KINGSLEY N90-15594
POWELL, W. D. N90-15168
POWER, G. D. N90-15334
N90-15413
PRAIRIE, R. R. N90-15466
PRANKE, J. B. N90-15494
N90-15495
PRASAD, J. V. B. N90-15058
PRATER, R. N90-15751
PRATT, J. RICHARD N90-15148
PRECOURT, CHARLES J. N90-15096
PREMKUMAR, M. K. N90-15204
PRICE, DAVID L. N90-15229
N90-15718
PRICE, J. R. N90-15248
PRICE, K. N90-15453
PRIETO, FRANCISCO J. N90-15617
PRIGOGINE, ILYA N90-15157
PRINTZ, D. K. N90-15494
PROTOPOPESCU, V. N90-15695
PROTOPOPESCU, VLADIMIR N90-15651
N90-15652
PUFFETT, A. W. N90-15061

Q

QIU, S. L. N90-15797
QUI, S. L. N90-15825
QUIST, WILLIAM E. N90-15187

R

RABINOWITZ, PAUL H. N90-15679
RADZIEMSKI, L. J. N90-15428
RAEISAENEN, ANTTI N90-15323
RAFTERY, ADRIAN N90-15677
RAGHAVENDRA, C. S. N90-15739
RAISTRICK, I. D. N90-15782
RAJASENAN, C. N90-15117
RAJESHWAR, KRISHNAN N90-15270
RAKAUSKAS, R. J. N90-15805
RAMEY, R. R. N90-15248
RANAUDO, RICHARD J. N90-15062
RANDLETT, JILL B. N90-15090
RAO, ASHOK K. N90-15685
RAO, BHASKAR D. N90-15688
RAO, BOBBY N90-15091
RATKOWSKI, A. J. N90-15555
RAWAL, SURAJ P. N90-15151
RAWLINS, D. C. N90-15248
RAYNER, S. N90-15780
REED, M. A. N90-15350
REED, ROBERT M. N90-15540
REFAI, W. N90-15311
REHN, LYNN E. N90-15792
REINMANN, JOHN J. N90-15062
REIS, E. N90-15752
REJ, D. J. N90-15754
RENDIGS, K. H. N90-15192
RENEMA, FRITZ N90-15621
RESETAR, THERESA M. N90-15271
REUTER, W. G. N90-15478
REYNOLDS, JOHN R. N90-15270
RIBE, F. L. N90-15745
RIBLE, MAX N90-15621
RICHARDS, D. R. N90-15776
RICHTSMEIER, S. C. N90-15542
RICOY, M. A. N90-15146
RINGDAL, FRODE N90-15657
RIVIER, N. N90-15827
ROBERTS, M. J. N90-15358
ROBERTS, N. N90-15531
ROBERTSON, DAVID C. N90-15650
ROBERTSON, DAVID W. N90-15621
ROBINSON, A. N90-15729
ROCHELLE, J. M. N90-15773
ROGERS, FORREST J. N90-15872
ROGERS, J. D. N90-15114
ROHWER, R. K. N90-15820
ROIDT, R. M. N90-15483
ROMAN, ROBERT F. N90-15211
ROSADO, LEWIS N90-15459
ROSE, J. H. N90-15232
ROSENFELD, AZRIEL N90-15587
ROSS, D. W. N90-15612
ROSS, RON S. N90-15457
ROTH, R. N90-15059
ROTTER, J. MICHAEL N90-15470
ROY-AIKINS, J. E. A. N90-15104
RUFF, G. A. N90-15387
RUFFIN, JAMES E. N90-15463
RUFFNER, JOHN W. N90-15592
RULE, D. W. N90-15416
RUNYAN, L. JAMES N90-15064
RUPERT, PAUL R. N90-15597
RUSSELL, THOMAS P. N90-15296
RUTAN, SARAH C. N90-15154
RYAN, P. M. N90-15747
RYNE, R. D. N90-15406
RYPIEN, D. V. N90-15232
RYSKAMP, J. M. N90-15217

S

SAAD, EHAB N90-15622
SABAU, CARMEN S. N90-15765
SABOCHICK, MICHAEL J. N90-15791
SAINT-MARC, P. N90-15453
SAINTCLAIR, ANNE K. N90-15259
SAINTCLAIR, TERRY L. N90-15148
SALEM, JONATHAN A. N90-15143
SALK, MARTHA S. N90-15540
SAMSEL, E. G. N90-15252
SANDAGE, ALLAN N90-15869
SANDEEP, C. N90-15311
SANDRIDGE, CHRISTOPHER ALAN N90-15109
SANTOS, C. A. C. N90-15373
SAPHIR, BILL N90-15673
SARANGAPANI, S. N90-15341
SARMA, BIMAL N90-15813
SASAKI, SHINOBU N90-15441
SASAMOTO, WASHITO A. N90-15120
SAUERBREY, R. N90-15421
SAVAGE, HOWARD S. N90-15275
SAVELIEV, M. V. N90-15691
SAWCHUK, ALEXANDER A. N90-15739
SCALES, JOHN N90-15556
SCHAEFER, RAINER N90-15195
SCHAENZER, GUNTHER N90-15048
SCHAFER, GLENN E. N90-15271
SCHAFFER, M. N90-15752
SCHEIHING, PAUL E. N90-15370
SCHILLING, C. H. N90-15144
N90-15268
SCHIMMEL, MORRY L. N90-15161
SCHIRBER, J. E. N90-15795
SCHLESINGER, TUVIAH E. N90-15814
N90-15817
SCHMIDT-NIELSEN, ASTRID N90-15320
SCHMIDT, DEBORAH DIANE N90-15227
SCHNABEL, ROBERT B. N90-15630
N90-15681
SCHNEEKLOTH, U. N90-15879
SCHNEIDER, D. H. N90-15755
SCHNEIDER, D. N. N90-15168
SCHNEIDER, STEVEN J. N90-15130
SCHNEIDER, W. N90-15729
SCHOBERT, HAROLD H. N90-15288
SCHRA, L. N90-15188
N90-15190
SCHRAGE, D. P. N90-15058
SCHROCK, RICHARD R. N90-15272
SCHULLER, I. K. N90-15777
SCHULTE, K. N90-15208
SCHULTZ, T. A. N90-15045
SCHWALBE, L. A. N90-15438
SCHWARMANN, L. N90-15192
SCHWARTZ, STEPHEN E. N90-15544
SCHWARZ, A. S. N90-15835
SCOLARIS, M. N90-15194
SCOLLAN, D. F. N90-15695
SCOTT, G. W. N90-15462
SCOTT, JOHN J. N90-15340
SCOTT, L. T. N90-15133
SCOTT, MICHAEL L. N90-15601
N90-15603
N90-15631
SCOTT, TIMOTHY C. N90-15136
SCULLY, M. O. N90-15737
SEAGER, MARK K. N90-15655
SEEGER, P. A. N90-15820
SEGEV, ARIE N90-15619
SEIDENBERG, BENJAMIN N90-15261
SEKULA, S. T. N90-15799
SELLERS, C. H. N90-15252
SELLYEY, W. N90-15416
SENA, J. TOM N90-15396
N90-15522
SESSLER, A. M. N90-15406
SETHURAMAN, JAYARAM N90-15682
N90-15698
SEVAT, P. A. A. N90-15316
SEYMOUR, JOHN G. N90-15097
SEZGIN, E. N90-15561
N90-15703
SHABANA, A. A. N90-15455
SHADWICK, BRAD N90-15673
SHARA, MICHAEL M. N90-15870
SHARIFF, KARIM R. N90-15362
SHARMA, R. D. N90-15555
SHARP, T. R. N90-15526
SHARP, W. M. N90-15417
SHAVIT, NIR N90-15686
SHAW, ROBERT J. N90-15062
SHAW, W. J. D. N90-15205
SHEALY, JAMES R. N90-15815
SHEER, N. L. N90-15168
SHELTON, SAM V. N90-15363
SHELTON, W. A., JR. N90-15771
SHEN, YU N90-15121
SHEPARD, R. L. N90-15356
SHEPHERD, I. G. N90-15156
SHEPHERD, KEVIN P. N90-15710
SHEPHERD, R. L. N90-15755
SHERIFEL-GIZAWY, A. N90-15299
SHI, D. N90-15794
SHIMEALL, TIMOTHY J. N90-15641
SHING, MAN-TAK N90-15668
SHINN, JOSEPH H. N90-15550
SHOLOKHOV, YU. I. N90-15760
SHOSHANI, ARIE N90-15623
SHULER, ALBERT P. N90-15607
SHULMAN, GORDON L. N90-15588
SHUM, CHUNG-DAK N90-15847
SIDDIQI, TOUFIQ A. N90-15539
SIDDONS, D. PETER N90-15327
SIEGBAHN, PER N90-15153
SIEGEL, R. W. N90-15171
N90-15800
SIEGMUND, O. H. W. N90-15495
SIEMER, A. R. N90-15059
SIEMON, R. E. N90-15754
SIGMAN, KARL N90-15687
SIM, EUNSUP N90-15590
SIMPSON, BRUCE N90-15069
SINGH, J. P. N90-15338
SIROCCKY, PAUL J. N90-15444
SKELLY, J. N90-15626
SKOCYPEC, R. D. N90-15505
N90-15521
SKORPIK, J. R. N90-15170
SLANGER, TOM G. N90-15560
SLOUGH, J. T. N90-15754
SMALLWOOD, DAVID O. N90-15473
SMIRNOV, V. G. N90-15760
SMITH, A. F. N90-15201
SMITH, C. J. E. N90-15190
SMITH, D. N90-15729
SMITH, FRANK T. N90-15078
SMITH, J. P. N90-15752
SMITH, J. R. N90-15731
SMITH, JAMES L. N90-15516
N90-15517
SMITH, M. M. N90-15363
SMITH, RICHARD D. N90-15158
SMITH, ROBERT C. N90-15656
SODA, JIRO N90-15830
SODERHOLM, L. N90-15777
SOHRAB, SIAVASHI H. N90-15173
SOKATCHEV, E. N90-15703
SOLINA, A. N90-15194
SOMERMA, HANS N90-15323
SON, S. H. N90-15642
SOUTH, DAVID W. N90-15541
SOUTHWORTH, FRANK N90-15543
N90-15653
SPENCER, N. W. N90-15559
SPINELLI, P. N90-15858
SPONG, D. A. N90-15756
SPRANGLE, P. N90-15402
N90-15424
SPRINGEN, A. LUCILLE N90-15086
SRINIVASAN, S. N90-15510
STALEY, H. C. N90-15168
STANDLER, RONALD B. N90-15353
STANKO, STEPHEN W. N90-15230
STARKE, EDGAR A., JR. N90-15187
STECHEL, E. B. N90-15165
STEER, BARRY N90-15091
STEIN, RONALD N90-15403
STEINETZ, BRUCE M. N90-15444
STEINHAUER, L. C. N90-15839
STEPHAN, KARL D. N90-15352
STEPHENS, R. B. N90-15818
STEPHENSON, WILLIAM A. N90-15523
STEVENSON, JUDITH N90-15579
STEWART, R. E. N90-15755
STICHNOTH, JAMES M. N90-15655
STOCK, A. F. N90-15115
STONE, L. S. N90-15577
STOUT, R. B. N90-15476
STRACHAN, D. M. N90-15170
STREET-PERROTT, F. A. N90-15531

STREETS, DAVID G. N90-15539
STRONGIN, MYRON N90-15797
N90-15825
STUBBINS, JAMES F. N90-15215
STURTEVANT, B. N90-15376
SU, CHANG SHAN N90-15422
SU, ZHAO-BIN N90-15783
SUENAGA, M. N90-15822
N90-15823
SULSKUS, J. N90-15805
SUMMERS, G. P. N90-15426
SUMMERS, T. S. E. N90-15464
SUNDBERG, R. L. N90-15555
SUPER, ARLIN B. N90-15562
SUR, B. N90-15880
SWAIM, ROBERT L. N90-15055
SWAIN, D. W. N90-15747
SWANSON, G. J. N90-15735
SWANSON, THEODORE N90-15261
SWARTZENDRUBER, L. J. N90-15223
SWOLINSKY, MANFRED N90-15044
SYKES, M. N90-15873
SZLYK, T. K. N90-15712

T

TACKETT, JUANITA R. N90-15289
TAGGART, D. P. N90-15754
TAKAHASHI, T. N90-15754
TALBOTT, MICHAEL C. N90-15126
TALLANT, D. R. N90-15180
TAM, CHRISTOPHER N90-15713
TANABE, KAZUO N90-15730
TANAKA, KAZUNAKA N90-15679
TAO, WILLIAM C. N90-15286
TARDIFF, M. F. N90-15532
TARDY, D. C. N90-15719
TARVER, CRAIG M. N90-15281
TAYA, MINORU N90-15143
TAYLOR, D. J. N90-15747
TAYLOR, E. W. N90-15729
TAYLOR, FRED J. N90-15659
TAYLOR, NORMA F. N90-15390
TAYLOR, PETER R. N90-15153
TEETERS, S. W. N90-15532
TELSCHOW, K. L. N90-15252
TEMPLE, PATRICK J. N90-15528
TENFORDE, T. S. N90-15578
TENNERY, V. J. N90-15249
TESAR, DELBERT N90-15664
TEXIER, NICOLE N90-15621
THART, W. G. J. N90-15188
N90-15189
THOMAS, EDWARD V. N90-15672
THOMAS, G. J. N90-15800
THOMAS, K. N90-15566
THOMPSON, H. N90-15838
THOMPSON, J. R. N90-15799
THOMPSON, M. CLARK N90-15326
THOMPSON, WARREN E. N90-15174
THOMSON, J. O. N90-15799
THORN, R. J. N90-15778
THRESHER, R. W. N90-15520
THURSTON, G. N90-15752
TIETBOHL, G. L. N90-15413
TIGGES, C. P. N90-15795
N90-15801
TILTON, DONALD E. N90-15386
TIMPF, J. N90-15776
TING, A. N90-15424
N90-15763
TISSOT, R. G. N90-15180
TITTEL, FRANK K. N90-15421
TOMITA, KENJI N90-15868
TOMITA, SEIETSU N90-15567
TOMLINSON, J. J. N90-15500
TOMPKINS, CLIFFORD D. N90-15047
TONN, BRUCE N90-15611
TORTORELLI, P. F. N90-15226
TOSI, M. P. N90-15225
TOWNE, DOUGLAS M. N90-15646
TRALSHAWALA, N. N90-15776
TRAN, L. T. N90-15498
TRAN, N. H. N90-15497
TRANQUADA, J. M. N90-15785
TRATNIK, M. V. N90-15408
TRAVIS, CHERYL N90-15611
TRIETSCH, DAN N90-15660
TRIPATHI, SATISH K. N90-15465
TRIPP, LLOYD D., JR. N90-15583
TROUT, TODD K. N90-15246
TROUTMAN, PATRICK A. N90-15120
TROWBRIDGE, C. A. N90-15497
TROWBRIDGE, L. D. N90-15169
TRUCANO, TIMOTHY G. N90-15449
TRUGMAN, S. A. N90-15670
TSAI, YI-CHENG N90-15385
TSAO, J. Y. N90-15789
TUGGLE, D. G. N90-15820
TUNCER, ISMAIL HAKKI N90-15074
TURCHI, P. E. A. N90-15780
TUSZEWSKI, M. N90-15754
TUTTLE, B. A. N90-15359

U

UDSETH, HAROLD R. N90-15158
UHERKA, KENNETH L. N90-15370
ULLAL, HARIN S. N90-15504
ULLIAN, LOUIS J. N90-15122
N90-15123

V

VAESSEN, G. J. H. N90-15190
N90-15196
VALENTINE, C. K. N90-15532
VANDERHOFF, JOHN A. N90-15292
VANDERPOOL, R. W. N90-15105
VANDEUSEN, S. B. N90-15180
VANDYKE, LEON S. N90-15277
VANECK, TIMOTHY N90-15811
VANROODE, M. N90-15248
VANROOIJEN, H. W. N90-15196
VANSTEENBERGEN, A. N90-15418
VANTILBORGH, C. N90-15196
VANVORIS, PETER N90-15536
VARSHNEY, PRAMOD K. N90-15308
VEAL, BOYD W. N90-15777
N90-15789
N90-15821
VEERS, PAUL S. N90-15524
VENTURINI, E. L. N90-15795
N90-15801
N90-15802
VERBOUT, SHAWN M. N90-15307
VERSHIK, A. M. N90-15691
VERZASCONI, S. L. N90-15222
VIJGEN, PAUL M. H. W. N90-15094
VISCO, STEVEN J. N90-15325
VLASES, G. C. N90-15839
VOERSMANN, PETER N90-15046
VOGEL, K. R. N90-15880
VOLAKIS, J. L. N90-15146
VONFLOTOW, ANDREAS H. N90-15124

W

WACHS, A. L. N90-15780
WADKINS, R. P. N90-15375
WADSWORTH, J. N90-15220
WAINFAN, BARNABY N90-15093
WALDMAN, J. N90-15193
WALKER, HOMER F. N90-15636
WALKER, MARGARET GERALDENE PROBERT
N90-15845
WALLACE, ALAN N90-15332
WALSH, D. N90-15511
WALTHER, F. G. N90-15304
WALTON, JULIE N90-15579
WANG, CHUNG-YUE N90-15137
WANG, HAU H. N90-15242
WANG, QINGHONG N90-15704
WARREN, J. R. N90-15107
WARREN, STEPHEN G. N90-15574
WARREN, WILLIAM E. N90-15255
WATANABE, KAZUYA N90-15868
WATANABE, TADASHI N90-15379
WATERS, WILLIAM M. N90-15322
WATSON, A. B. N90-15577
WATSON, R. E. N90-15214
N90-15223
WEAR, C. J. N90-15532
WEAVER, H. A. N90-15871
WEBB, JAMES T. N90-15581
WEBER, JAY N90-15644
WEBER, MARVIN J. N90-15257
N90-15410
WEBER, SUSAN HOLLBACH N90-15649
WEBER, TIM L. N90-15519
N90-15520
WEBSTER, C. E. N90-15329
N90-15336
WEETER, RICHARD D. N90-15592
WEGRZYN, JAMES N90-15527
WEIHL, WILLIAM N90-15632
WEILKE, J. N90-15192
WEINGART, R. C. N90-15119
WEIRICK, L. J. N90-15285
WEISS, BRIGITTE N90-15195
WELCH, D. O. N90-15822
WELLER, W. N90-15804
WELPMANN, K. N90-15189
WENTWORTH, S. M. N90-15712
WESSELIUS, P. R. N90-15496
WEST, R. N. N90-15780
WESTBROOK, CHARLES K. N90-15164
N90-15448
WESTENSKOW, G. A. N90-15406
WHANGBO, MYUNG-HWAN N90-15779
WHIRLEY, ROBERT G. N90-15475
WHITAKER, RUTH B. N90-15289
WHITE, A. M. N90-15694
WHITE, G. ANDERSON, III N90-15548
N90-15553
WHITE, J. M. N90-15135
WHITE, R. E. N90-15510
WIEDEMAN, S. N90-15503
WIEDER, H. H. N90-15811
WIEDWALD, J. D. N90-15413
WIEGMAN, JANET F. N90-15581
WIESELTHIER, JEFFREY E. N90-15319
WIESMANN, H. N90-15824
WILCOX, D. R. N90-15708
WILDE, D. K. N90-15782
WILEY, J. C. N90-15612
WILLIAMS, ANDREW N90-15811
WILLIAMS, JACK M. N90-15242
N90-15779
WILLIAMS, JOHN M. N90-15778
WILLIAMS, MARC H. N90-15079
WILSON, D. F. N90-15506
WILSON, M. J. N90-15337
WILSON, WILLIAM L. N90-15421
WINDHAM, MICHAEL P. N90-15636
WINGROVE, R. C. N90-15045
WINNINGHAM, J. D. N90-15559
WINTER, JOACHIM N90-15056
WISHINSKY, B. J. N90-15621
WOJTOWICZ, A. J. N90-15423
WOLF, D. A. N90-15532
WOLF, RALPH J. N90-15244
WOLFRAM, K. D. N90-15494
WOLKOVITCH, JULIAN N90-15093
WOLOSHUN, K. A. N90-15396
WONG, D. N90-15817
WOODCOCK, GORDON R. N90-15842
WOODFIELD, A. A. N90-15049
WOZNIAK, G. J. N90-15717
WRIGHT, A. D. N90-15520
WRIGHT, B. L. N90-15754
WRIGHT, I. G. N90-15216
WRIGHT, ROBERT H. N90-15060
WRIGHTON, MARK S. N90-15514
WU, X. Q. N90-15485

X

XIAO, YINGCAI N90-15864
XU, J. J. N90-15790
N90-15793
XU, YOUWEN N90-15822
N90-15823

Y

YAMAZAWA, HIROMI N90-15551
YANG, S. A. N90-15392
YANG, T. F. N90-15132
YANTIS, BONNIE N90-15610
YAO, JEN-CHIH N90-15620
YEN, GUAN-WEI N90-15381
YILLIKCI, YILDIRIM KEMAL N90-15075
YIO, J. L. N90-15359
YLINEN, JUHANA N90-15323
YOO, M. H. N90-15767
YOU, H. N90-15793
YOUNG, M. L. N90-15114
YOUNGER, STEPHEN M. N90-15726
YU, LU N90-15783
YU, S. S. N90-15406
N90-15417
YUGO, J. J. N90-15747
YUNG, Y. S. N90-15728

Z

ZADRA, A. N90-15675
ZASADZINSKI, J. F. N90-15776
ZEIGLER, J. M. N90-15720
ZENNARO, G. N90-15194
ZHANG, BOHAI N90-15492
ZHANG, J. N90-15276

ZHANG, JIANJUN N90-15360
ZHANG, JIMIN M. N90-15238
ZHANG, LI-YUAN N90-15775
ZHANG, S. Z. N90-15477
ZHU, YIMEI N90-15823
ZIERTEN, THOMAS A. N90-15064
ZILLIAC, GREGORY G. N90-15399
ZIMMER, W. J. N90-15466
ZINK, W. N90-15192
ZIRILLI, FRANCESCO N90-15683
ZWEIBEL, KENNETH N90-15504

Typical Corporate Source Index Listing

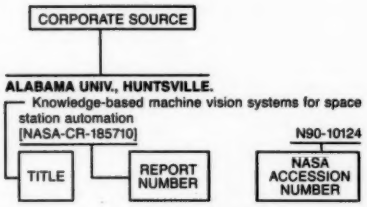

Listings in this index are arranged alphabetically by corporate source. The title of the document provides the user with a brief description of the subject matter. The report number helps to indicate the type of document cited (e.g., NASA report, translation, NASA contractor report). The NASA accession number denotes the number by which the citation is identified. The titles are arranged under each corporate source in ascending accession number order.

A

ACA INDUSTRIES, INC., RANCHO PALOS VERDES, CA.
Application of the joined wing to tiltrotor aircraft
[NASA-CR-177543] N90-15093

ADVISORY GROUP FOR AEROSPACE RESEARCH AND DEVELOPMENT, NEUILLY-SUR-SEINE (FRANCE).
Flight in Adverse Environmental Conditions
[AGARD-CP-470] N90-15041
New Light Alloys
[AGARD-CP-444] N90-15185

AERODATA FLUGMESSTECHNIK G.M.B.H., BRUNSWICK (GERMANY, F.R.).
Systems for airborne wind and turbulence measurement N90-15046

AEROLIFT, INC., TILLAMOOK, OR.
X.2 limited flight test plan
[AD-A214412] N90-15099

AERONAUTICA MACCHI S.P.A., VARESE (ITALY).
Canard versus aft-tail ride qualities performance and pilot command response N90-15053

AEROPLANE AND ARMAMENT EXPERIMENTAL ESTABLISHMENT, BOSCOMBE DOWN (ENGLAND).
Aircraft testing in the electromagnetic environment N90-15066

AEROSPACE CORP., EL SEGUNDO, CA.
RAIDS: An orbiting observatory for ionospheric remote sensing from space
[AD-A213717] N90-15494
Development of the RAIDS (Remote Atmospheric and Ionospheric Detector System) extreme ultraviolet wedge and strip detector
[AD-A213730] N90-15495
Orientation of rf-sputter-deposited MoS2 films
[ATR-89(4752)-1] N90-15784

AEROSPATIALE, TOULOUSE (FRANCE).
How to fly windshear using the fly-by-wire concept N90-15050

AIR FORCE ACADEMY, CO.
Two dimensional laminated shell theory including parabolic transverse shear
[AD-A213817] N90-15487

AIR FORCE ASTRONAUTICS LAB., EDWARDS AFB, CA.
Tunnelling effects on low energy fusion cross sections
[AD-A214010] N90-15762

AIR FORCE FLIGHT TEST CENTER, EDWARDS AFB, CA.
Schleicher ASK-21 glider (TG-9) stall and spin
[AD-A213513] N90-15096

AIR FORCE GEOPHYSICS LAB., HANSCOM AFB, MA.
SCATHA (Spacecraft Charging at High Altitudes) atlas data base, volume 1
[AD-A214204] N90-15127
SCATHA (Spacecraft Charging At High Altitudes) atlas data base, volume 2
[AD-A214205] N90-15128
Description of SHARC: The Strategic High-Altitude Radiance Code
[AD-A213806] N90-15555

AIR FORCE INST. OF TECH., WRIGHT-PATTERSON AFB, OH.
Aircraft performance enhancement with active compressor stabilization
[AD-A213652] N90-15097
Solution of potential flow past an elastic body using the boundary element technique
[AD-A213843] N90-15390
Identification and quantification of synoptic structure in simulated TIROS N radiance soundings
[AD-A213729] N90-15553
Application of a mass-consistent wind model to chinook windstorms
[AD-A213622] N90-15568
Precipitation distributions associated with cyclones originating over the Gulf of Mexico and surrounding coastal regions
[AD-A213644] N90-15569

AIR FORCE SYSTEMS COMMAND, WRIGHT-PATTERSON AFB, OH.
Manned spacecraft
[AD-A214218] N90-15129
A new kind of heterodyne fiber-optic gyroscope
[AD-A213953] N90-15404
China-built airborne synchronous laser ranger the new L-8 jet trainer aircraft
[AD-A213835] N90-15422
Frontal clouds and flight conditions in them
[AD-A214250] N90-15573
Design of a large angular aperture TeO2 acousto-optic tunable filter
[AD-A213999] N90-15738

AIR FORCE WEAPONS LAB., KIRTLAND AFB, NM.
Proposed activities to prepare for testing advanced/stealth weapons systems
[AD-A214453] N90-15321

AIR FORCE WRIGHT RESEARCH AND DEVELOPMENT CENTER, WRIGHT-PATTERSON AFB, OH.
An alternative derivation for an integral equation for linearized subsonic flow over a wing
[AD-A214140] N90-15079
Analysis of an elastohydrodynamic lubricated point contact: User's manual
[AD-A214257] N90-15459
Proceedings of the 1988 Structural Integrity Program Conference
[AD-A213545] N90-15486

AIRBUS INDUSTRIE, BLAGNAC (FRANCE).
Point of view of a civil aircraft manufacturer on Al-Li alloy N90-15200

ALABAMA UNIV., HUNTSVILLE.
A numerical simulation model for the study of magnetohydrodynamic (MHD) waves in a structured medium N90-15864

ALLIED-SIGNAL AEROSPACE CO., KANSAS CITY, MO.
High-temperature gel-permeation chromatography of poly(4-methyl-1-pentene)
[DE90-002967] N90-15159
A strategy for concurrent product and process design of aerospace components
[DE90-002926] N90-15299
Automated convection soldering
[KCP-613-4005] N90-15300
Component presence-absence detection for automated visual inspection of hybrid microcircuits
[KCP-613-4050] N90-15335

ANACAPA SCIENCES, INC., FORT RUCKER, AL.
Development of the AH-64 display symbology training module
[AD-A213456] N90-15592

ARGONNE NATIONAL LAB., IL.
Processing and properties of nanophase oxides
[DE90-003826] N90-15171
Accelerated aging embrittlement of cast duplex stainless steel: Activation energy for extrapolation
[DE90-001773] N90-15221
Dynamical structure of liquid and amorphous metals
[DE90-003805] N90-15229
Cast stainless steel aging: Mechanisms and predictions
[DE90-003772] N90-15241
New organic synthetic metals derived from BEDT-TTF, Ni(dsit)2 and BEDO-TTF
[DE90-003793] N90-15242
Solid lubrication of ceramic surfaces by IAD (Ion-Assisted Deposition)-silver coatings for heat engine applications
[DE90-002860] N90-15253
Development of NMR (Nuclear Magnetic Resonance) imaging probes for advanced ceramics
[DE90-003812] N90-15269
Products of the hypochlorite oxidation of hydrazine fuels
[AD-A213557] N90-15291
Status and results of ANL life evaluation of valve-regulated lead-acid load-leveling batteries
[DE90-001918] N90-15329
Life evaluation of valve-regulated lead-acid batteries for load-leveling applications
[DE90-002188] N90-15336
Fabrication of superconductor coils
[DE90-003571] N90-15338
Rechargable molten-electrolyte lithium batteries
[DE90-003774] N90-15339
Recent advances in magnetic heat pump technology
[DE89-013289] N90-15370
Laser-induced surface ablation and optical damage of ZnS crystals caused by single- and multiple-pulse laser-irradiation
[DE90-003807] N90-15419
An assessment and comparison of fuel cells for transportation applications
[DE90-001807] N90-15508
Characterization of new cathode materials for molten carbonate fuel cells
[DE90-003547] N90-15516
Fabrication of porous ceramic electrode structures
[DE90-003548] N90-15517
Responding to the threat of global warming: Options for the Pacific and Asia
[DE90-003553] N90-15539
Global climate change: A fossil energy perspective
[DE90-003770] N90-15541
Research in mathematics and computer science at Argonne
[DE90-000975] N90-15595
A block QR factorization algorithm using restricted pivoting
[DE90-001921] N90-15613
Gradient projection techniques for large-scale optimization problems
[DE90-001986] N90-15618
Structure and dynamics of disordered systems
[DE90-001408] N90-15718
Near-surface sputtered particle transport for an oblique incidence magnetic field plasma
[DE90-004422] N90-15758
ICP/AES (Inductively Coupled Plasma/Atomic Emission Spectroscopy): A modern analytical tool
[DE90-003822] N90-15765
Tunneling spectroscopy and the electron-phonon interaction in Ba(1-x)K(x)BiO3
[DE90-002842] N90-15776
The possible occurrence of multi-phase behavior in the high T(sub c) superconductor YBa2Cu3O(sub x)
[DE90-002999] N90-15777
Synthesis conductivity, and x ray photoelectron spectrum of Bi2Sr2Cu(sub 7+x). A new ternary bismuth-oxide system exhibiting metallic conductivity
[DE90-003010] N90-15778
Linear electron-hole-electron pair model of high-temperature superconductivity in La(2-x)M(x)CuO4 and YBa2Cu3O(7-y): Part 2. Dependence of the superconducting transition temperatures on pressure and on hole concentration
[DE90-003012] N90-15779

Two-dimensional magnetic phase transition of ultrathin iron films on Pd(100)
[DE90-003555] N90-15758
Processing and fabrication of YBa2Cu4O8 and YBa2Cu4O8/YBa2Cu3O(x) composites
[DE90-003559] N90-15789
Characterization of MOCVD (Metal Organic Chemical Vapor Deposition) grown epitaxial ceramic oxide thin films
[DE90-003561] N90-15790
Molecular-dynamics study of the amorphization of CuTi
[DE90-003563] N90-15791
Irradition-induced grain growth: Role of dislocations
[DE90-003565] N90-15792
Preparation, structure and properties of VO(sub x) and TiO2 thin films by MOCVD
[DE90-003566] N90-15793
Processing YBa2Cu3O(x) wires in O3/O2
[DE90-003570] N90-15794
High resolution electron microscopy of grain boundaries in nanophase palladium
[DE90-003823] N90-15800
Properties of high Tc superconducting oxides
[DE90-003792] N90-15821
Maximum entropy and equations of state for random cellular structures
[DE90-002840] N90-15827

ARIZONA UNIV., TUCSON.
Numerical simulation of the unsteady two-dimensional flow in a time-dependent doubly-connected domain N90-15073
Numerical investigation of transition control of a flat plate boundary layer N90-15361
Dust bands in the asteroid belt
[NASA-CR-186301] N90-15873
LEAP: A balloon-borne search for low-energy cosmic ray antiprotons N90-15870

ARMY AEROMEDICAL RESEARCH LAB., FORT RUCKER, AL.
Imaging probabilities, geometry and ergonomics in limited visibility helicopter operations N90-15060

ARMY AVIATION ENGINEERING FLIGHT ACTIVITY, EDWARDS AFB, CA.
Evaluation of the improved OV-ID anti-icing system, phase 2
[AD-A213928] N90-15083

ARMY AVIATION RESEARCH AND DEVELOPMENT COMMAND, MOFFETT FIELD, CA.
An examination of helicopter rotor load calculations
[AD-A214295] N90-15098

ARMY AVIATION SYSTEMS COMMAND, CLEVELAND, OH.
Mesh refinement in finite element analysis by minimization of the stiffness matrix trace
[NASA-CR-185170] N90-15434

ARMY CONSTRUCTION ENGINEERING RESEARCH LAB., CHAMPAIGN, IL.
Arc-sprayed coatings for electromagnetic pulse protection: Assessment of physical and electrical properties
[AD-A213825] N90-15275
Automation and robotics in construction: Japanese research and development
[AD-A214170] N90-15456
Guidelines for evaluating energy analysis software
[AD-A214171] N90-15640

ARMY LAB. COMMAND, WATERTOWN, MA.
Energetics of BCC-FCC lattice deformation in iron
[AD-A213801] N90-15233
Heat treatment investigation of 4330 vanadium-modified steel
[AD-A214290] N90-15239

ARMY MATERIALS TECHNOLOGY LAB., WATERTOWN, MA.
IEA/Annex 2 powder characterization cooperative program
[AD-A213540] N90-15271

ARMY MISSILE COMMAND, REDSTONE ARSENAL, AL.
Mechanical evaluation of the differential drum concept for optical fiber pay-out
[AD-A214149] N90-15740

ASSOCIACAO BRASILEIRA DE CIENCIAS MECANICAS, RIO DE JANEIRO.
Experimental determination of the fluid velocity by spectral analysis of temperature fluctuations
[DE89-636430] N90-15372
Laminar forced convection inside externally finned tubes
[DE89-636431] N90-15373
Static pressure distribution in an angular channel with helicoidal wire
[DE89-636474] N90-15374
Investigation of loads generated by temperature transients in pipes
[DE89-636433] N90-15395

AUSTRALIAN INST. OF NUCLEAR SCIENCE AND ENGINEERING, LUCAS HEIGHTS.
The 17th AINSE Plasma Physics Conference: Conference handbook
[DE90-600936] N90-15759

AVIONS MARCEL DASSAULT-BREGUET AVIATION, SAINT-CLOUD (FRANCE).
Putting alloy 2091 to work N90-15197

B

BALLISTIC RESEARCH LABS., ABERDEEN PROVING GROUND, MD.
Steady flow combustion model for solid-fuel ramjet projectiles
[BRL-TR-2987] N90-15163
Calculation of Einstein A coefficients and oscillator strengths for the A(perturbed)(2)A(1)-X(perturbed)(2)B(1) transition of NH(2)
[AD-A213837] N90-15176
Spectral studies of solid propellant combustion. 2: Emission and absorption results for M-30 and HMX1 propellants
[AD-A213857] N90-15292
An algebraic turbulence model for flow separation caused by forward and backward facing steps
[AD-A213800] N90-15389

BATTELLE COLUMBUS LABS., OH.
Characterization of chemicals on engine exhaust particles
[AD-A213566] N90-15106

BERKELEY RESEARCH ASSOCIATION, CA.
Theory for high gain, high power free electron lasers
[DE90-003024] N90-15409

BOEING AEROSPACE CO., HUNTSVILLE, AL.
Transportation and operations aspects of space energy systems N90-15842

BOEING COMMERCIAL AIRPLANE CO., RENTON, WA.
Flight and wind tunnel investigation of aerodynamic effects of aircraft ground deicing/antiicing fluids N90-15064

BOEING COMMERCIAL AIRPLANE CO., SEATTLE, WA.
Fly-by-light flight control system technology development plan
[NASA-CR-181953] N90-15111

BONNEVILLE POWER ADMINISTRATION, PORTLAND, OR.
Adjustable speed drive study, June 1985 to September 1988. Part 2: Appendices
[DE90-002771] N90-15332

BOSTON UNIV., MA.
Development of glass-ceramic lasers
[AD-A214146] N90-15423

BRITISH AEROSPACE PUBLIC LTD. CO., BRISTOL (ENGLAND).
Fabrication characteristics of 8090 alloy N90-15198

BROOKHAVEN NATIONAL LAB., UPTON, NY.
Exchange coupling in metals as understood then and now
[DE90-001271] N90-15214
A versatile stepping motor controller for systems with many motors
[DE90-001556] N90-15327
A microwiggler Free-Electron Laser at the Brookhaven Accelerator Test Facility
[DE90-003643] N90-15418
Annual operating plan for fiscal year 1990 for chemical/hydrogen energy systems program
[DE90-003964] N90-15527
Long-term worldwide environmental effects caused by acid rain from fossil fuels
[DE90-001534] N90-15533
Acid deposition
[DE90-003959] N90-15544
Vertical distribution of pollutants in the presence of convective storms
[DE90-002590] N90-15549
Programs for control of an analog-signal switching network
[DE90-003645] N90-15626
Magnetic and electronic correlations in YBa2Cu3O(sub 6+x)
[DE89-017604] N90-15785
Magnetic mechanisms of high temperature superconductivity
[DE90-003625] N90-15796
X ray absorption studies of YBa2Cu3O(6+x), La(2-x)Sr(x)CuO4, and Nd(2-x)Ce(x)CuO4
[DE90-003640] N90-15797
Effects of non-linearity in the variation of pinning potential with current-density on magnetic flux creep in high and low T(sub c) superconductors
[DE90-003952] N90-15822
Atomic scale structure of twin boundary in Y-Ba-Cu-O superconductors
[DE90-003955] N90-15823
The fabrication of YBa2Cu3O7 thin films by thermal coevaporation in oxygen
[DE90-003960] N90-15824
Auger and x ray absorption studies of solid molecular oxygen
[DE90-003966] N90-15825

BROWN UNIV., PROVIDENCE, RI.
A renormalization group approach to image processing: A new computational method for three-dimensional shapes in robot vision, and the computation complexity of the cooling algorithms
[AD-A214247] N90-15643

BUREAU OF RECLAMATION, DENVER, CO.
Winter cloud seeding potential on the Mogollon Rim
[PB89-190540] N90-15562

C

CALGARY UNIV. (ALBERTA).
Microstructure/mechanical property relations in a mechanically alloyed aluminum N90-15205

CALIFORNIA INST. OF TECH., PASADENA.
Rayleigh-Taylor instability in compressible fluids
[DE90-003027] N90-15376
On the domain of dominance of the asymptotic elastodynamic crack-tip fields N90-15468
Instability of a-Si:H/Ag interface at 150 deg C
[DE89-009419] N90-15498
Saltation and suspension of particulate matter in air
[AD-A213618] N90-15552
Dynamics of electron transfer for a nonsuperexchange coherent mechanism, 1
[AD-A213450] N90-15721
Dynamics of electron transfer for a non-superexchange coherent mechanisms. 2: Numerical calculations
[AD-A213511] N90-15722

CALIFORNIA UNIV., BERKELEY.
The mechanical behavior of a fiber-reinforced brittle matrix composite N90-15139
Critical and subcritical crack-growth behavior along toughened ceramic/metal interfaces N90-15140
An analysis of drilling of composite materials N90-15142
Control of mechanical manipulators N90-15432
Isothermal fatigue behavior of Sn-Pb solar joints
[DE90-003280] N90-15464
XNUSIM: Graphical interface for a multiprocessor simulator
[AD-A214176] N90-15606
Optimizing and evaluating algorithms for replicated data concurrency control
[DE90-003080] N90-15619

CALIFORNIA UNIV., BERKELEY. LAWRENCE BERKELEY LAB.
Electronic materials high-T(sub c) superconductivity polymers and composites structural materials surface science and catalysts industry participation
[NASA-CR-186063] N90-15145
A tomographic study of premixed turbulent stagnation point flames
[DE90-002462] N90-15156
Theoretical methods for the study of chemical dynamics
[DE90-003122] N90-15160
Cryogenic mechanical properties of low density superplastic Al-Mg-Sc alloys
[DE90-002120] N90-15222
Novel high-rate, all solid-state, sodium and lithium/organosulfur batteries
[DE90-001014] N90-15325
Retractable gas cooled leads for ASTROMAG
[DE90-002679] N90-15331
Isothermal fatigue behavior of Sn-Pb solar joints
[DE90-003280] N90-15464
Optimizing and evaluating algorithms for replicated data concurrency control
[DE90-003080] N90-15619
Scry: A distributed image handling system, version 1.1
[DE90-003105] N90-15621
Name assignment techniques for relational schemas representing extended entity-relationship schemas
[DE90-003269] N90-15623
Thermal and statistical properties of nuclei and nuclear systems
[DE90-000183] N90-15717
Center for X Ray Optics, 1988
[DE90-003300] N90-15732
Thermally stable metal/GaAs contacts
[DE90-002122] N90-15774
Variational quantum Monte Carlo calculation of electronic and structural properties of crystals
[DE90-003265] N90-15781

Cosmic ray half life of (54)Mn
[DE90-000134] N90-15880

CALIFORNIA UNIV., DAVIS.
The radar-based short term prediction of the time-space evolution of rain fields
[AD-A213802] N90-15312
Feasibility study of using industrial robot for ultrasound testing
[DE90-002977] N90-15461

CALIFORNIA UNIV., IRVINE.
Flux parameterization techniques in the atmospheric surface layer N90-15548

CALIFORNIA UNIV., LOS ANGELES.
Solid-state phase equilibria in the ZnS-Ga2S3 system
[AD-A213944] N90-15238
Hardening and toughening of ZnS-Ga2S3 ceramics by solid-state reactions
[AD-A213875] N90-15276
Numerical analysis and simulation of frictional particle systems N90-15430
Micromechanics of an extrusion in high-cycle fatigue with creep
[AD-A213509] N90-15485
Observational study of the macroscopic behavior of moist-convective processes N90-15547
Computer simulation of laser plasma interaction
[DE90-002828] N90-15748
Alternative representations for database responses N90-15847
A calculation of energetic proton spectra producedat substorm onset in the fields of the explosive reconnection model N90-15866

CALIFORNIA UNIV., RIVERSIDE.
Variability of cultivar responses to ozone
[PB89-225460] N90-15528
Laboratory simulations of the solar wind-comet interactions N90-15875

CALIFORNIA UNIV., SAN DIEGO.
Computer aided design of monolithic microwave and millimeter wave integrated circuits and subsystems
[AD-A213656] N90-15343

CALIFORNIA UNIV., SAN DIEGO, LA JOLLA.
Research on materials and components for opto-electronic signal processing and computing
[AD-A213740] N90-15811
Lunar power system summary of studies for the lunar enterprise task force NASA-office of exploration N90-15841

CALIFORNIA UNIV., SANTA BARBARA.
Evolution of overlapping spreading centers: A Sea Mark 2 investigation
[AD-A214278] N90-15576

CALSPAN-BUFFALO UNIV. RESEARCH CENTER, NY.
Development of an integrated BEM approach for hot fluid structure interaction
[NASA-CR-186214] N90-15364

CARNEGIE-MELLON UNIV., PITTSBURGH, PA.
Base reaction optimization of redundant manipulators for space applications
[NASA-CR-186274] N90-15447
Optical neural nets for scene analysis
[AD-A213986] N90-15637
Defect control and denuded trap zones in the 3-5 semiconductors
[AD-A214099] N90-15814
The effect of annealing treatments on defect structure and diffusion lengths in n-type GaAs
[AD-A214215] N90-15817

CASE WESTERN RESERVE UNIV., CLEVELAND, OH.
Reliability analysis of the space station freedom electrical power system
[AD-A214105] N90-15126

CEGEDUR PECHINEY CENTRE DE RECHERCHE ET DEVELOPPEMENT, VOREPPE (FRANCE).
Al-Li alloy developed by Pechiney N90-15186

CENTRAL RESEARCH INST. OF ELECTRIC POWER INDUSTRY, TOKYO (JAPAN).
Survey on synthesis technologies of methanol as an alternative fuel
[DE89-901303] N90-15284
Characteristics of electromagnetic wave forms with lightning in winter season
[DE89-901256] N90-15567
Optical acoustic sensor using optical fiber
[DE89-901267] N90-15730

CENTRO BRASILEIRO DE PESQUISAS FISICAS, RIO DE JANEIRO.
Proceedings of the Latin American Conference on the Applications of the Moessbauer Effect
[DE90-600819] N90-15803

CERAMIC PROCESS SYSTEMS CORP., MILFORD, MA.
Composite ceramic superconducting wires for electric motor applications
[AD-A213742] N90-15274

CHEMICAL RESEARCH AND DEVELOPMENT CENTER, ABERDEEN PROVING GROUND, MD.
Mutagenic responses of some petroleum-base obscurants in the Ames test
[AD-A214201] N90-15295
Anomalous absorption by atmospheric water vapor and stabilized water fogs in the infrared and CM-wave regions
[AD-A214202] N90-15572

CHIEF OF NAVAL EDUCATION AND TRAINING SUPPORT, PENSACOLA, FL.
Human behavior
[PB90-780008] N90-15584

CINCINNATI UNIV., OH.
Mesh refinement in finite element analysis by minimization of the stiffness matrix trace
[NASA-CR-185170] N90-15434

CLARKSON UNIV., POTSDAM, NY.
Fundamental mechanism of atomization
[AD-A213859] N90-15293
Bridgman crystal growth
[NASA-CR-186204] N90-15766

COLLEGE OF WILLIAM AND MARY, WILLIAMSBURG, VA.
A structural factoring approach for analyzing probabilistic networks N90-15697

COLORADO UNIV., BOULDER.
Investigation of broadband microstrip antenna structures for application in monolithic millimeter wave arrays
[AD-A213856] N90-15344
Theoretical models of earthquake phenomena and the physical significance of seismic moment tensor expansions
[AD-A213813] N90-15556
Software for a new modified Cholesky factorization
[AD-A213643] N90-15630
Tensor methods for unconstrained optimization using second derivatives
[AD-A213642] N90-15681
Young Investigator's Award and distributed self-adaptive databases
[AD-A214194] N90-15854

COMMISSARIAT A L'ENERGIE ATOMIQUE, BRUYERES-LE-CHATEL (FRANCE).
Interlaboratory comparison of radiation-induced attenuation in optical fibers. Part 3: Transient exposures
[DE90-000859] N90-15729

CORNELL UNIV., ITHACA, NY.
Implementing fault-tolerant sensors
[NASA-CR-186251] N90-15400
On the motion of compliantly-connected rigid bodies in contact. Part 1: The motion prediction problem
[AD-A214135] N90-15489
On the motion of compliantly-connected rigid bodies in contact. Part 2: A system for analyzing designs for assembly
[AD-A214136] N90-15490
A paradigm for robust geometric algorithms
[AD-A214324] N90-15647
Concurrence control for transactions with priorities
[NASA-CR-186241] N90-15699
An investigation of mechanical behavior of crystalline solids
[DE90-003530] N90-15787
Innovative optoelectronic materials and structures using OMVPE
[AD-A214192] N90-15815
The middle Martian atmosphere N90-15874

COUNCIL FOR NATIONAL ACADEMIC AWARDS (ENGLAND).
A study of variable geometry in advanced gas turbines N90-15104

D

DAYTON UNIV., OH.
Cockpit resource management: A selected annotated bibliography
[AD-A214272] N90-15594

DEFENCE AND CIVIL INST. OF ENVIRONMENTAL MEDICINE, DOWNSVIEW (ONTARIO).
The application of queuing theory to the modelling of CP-140 aircraft communications
[AD-A213479] N90-15310

DEFENCE RESEARCH ESTABLISHMENT, OTTAWA (ONTARIO).
Design of a bounded wave EMP (Electromagnetic Pulse) simulator
[AD-A214137] N90-15316

DEFENSE APPLIED INFORMATION TECHNOLOGY CENTER, ALEXANDRIA, VA.
Terminology strategies for international information exchange
[AD-A214147] N90-15853

DEFENSE SYSTEMS MANAGEMENT SCHOOL, FORT BELVOIR, VA.
Program manager's handbook
[AD-A214338] N90-15844
Congressional involvement and relations: A guide for Department of Defense acquisition managers
[AD-A214408] N90-15855

DELAWARE UNIV., NEWARK.
Characterization of the thermal degradation of selected energetic materials and mixtures by Rapid-Scan Fourier Transform Infrared (RSFTIR) spectroscopy
[AD-A214411] N90-15296

DENVER UNIV., CO.
Damping characteristics of metal matrix composites
[AD-A213712] N90-15151

DEPARTMENT OF ENERGY, WASHINGTON, DC.
Relative merits of reactive and forward-look detection for wind-shear encounters during landing approach for various microburst escape strategies
[NASA-TM-4158] N90-15108

DEPARTMENT OF THE NAVY, WASHINGTON, DC.
Metal film coatings on amorphous metallic alloys
[AD-D014308] N90-15240
Silver coated superconducting ceramic powder
[AD-D014300] N90-15278
Focal plane antenna array for millimeter waves
[AD-D014306] N90-15322
Large-aperture sparse array detector system for multiple emitter location
[AD-D014303] N90-15355
A scheiner-principle vernier optometer
[AD-D014304] N90-15405
Laser detection and discrimination system
[AD-D014301] N90-15426
Laser communication system with wide band magnetostrictive modulation
[AD-D014302] N90-15427
Reconfigurable N-dimensional computer memory
[AD-D014309] N90-15607

DEUTSCHE FORSCHUNGS- UND VERSUCHSANSTALT FUER LUFT- UND RAUMFAHRT, BRUNSWICK (GERMANY, F.R.).
Aircraft response and pilot behaviour during a wake vortex encounter perpendicular to the vortex axis N90-15057

DEUTSCHE FORSCHUNGS- UND VERSUCHSANSTALT FUER LUFT- UND RAUMFAHRT, COLOGNE (GERMANY, F.R.).
Fatigue properties of Al-Li alloys N90-15189
Metal matrix composites: A promising alternative to conventional alloys N90-15208

DIAMOND MATERIALS, INC., STATE COLLEGE, PA.
Development of high performance beta-SiC field-effect transistors
[AD-A213885] N90-15346

DISTRICT OF COLUMBIA UNIV., WASHINGTON, DC.
Further research on dynamics of marine atmospheres in tropical cyclones
[AD-A213882] N90-15571

DORNIER-WERKE G.M.B.H., FRIEDRICHSHAFEN (GERMANY, F.R.).
Active control system for gust load allevation and structural damping N90-15056

DRAPER (CHARLES STARK) LAB., INC., CAMBRIDGE, MA.
Investigation of the applicability of a functional programming model to fault-tolerant parallel processing for knowledge-based systems
[NASA-CR-181938] N90-15654

DREXEL UNIV., PHILADELPHIA, PA.
High performance powder metallurgy aluminum alloys: An overview N90-15204

DUKE UNIV., DURHAM, NC.
Chemisorption under stress
[AD-A213785] N90-15175

DUNDEE UNIV. (SCOTLAND).
Design temperatures for flexible airfield pavement design
[AD-A214141] N90-15115

DYNAMICS RESEARCH CORP., WILMINGTON, MA.
MANPRINT methods monograph: Aiding the development of manned system performance criteria
[AD-A213543] N90-15593

E

EDGERTON, GERMESHAUSEN AND GRIER, INC., IDAHO FALLS, ID.
Experience with J testing of 304/308 stainless steel weldment
[DE90-002046] N90-15478
Where to from here. Future applications of mental models of complex performance
[DE90-002091] N90-15586

EDGERTON, GERMESHAUSEN AND GRIER, INC., SANTA BARBARA, CA.
Interlaboratory comparison of radiation-induced attenuation in optical fibers. Part 3: Transient exposures
[DE90-000859] N90-15729
EG AND G MOUND APPLIED TECHNOLOGIES, MIAMISBURG, OH.
More efficient sensitivity testing
[DE90-002639] N90-15298
EMORY UNIV., ATLANTA, GA.
Transport processes through monomolecular films
[AD-A213609] N90-15342
ENVIRONMENTAL RESEARCH INST. OF MICHIGAN, ANN ARBOR.
High resolution imaging by phase retrieval and discrimination using speckle, volume 1
[AD-A214243] N90-15317
Planning systems for autonomous legged vehicles
[AD-A214242] N90-15458
ERGENICS, INC., WYCKOFF, NJ.
Design and fabricate a metallic hydride heat pump with a cooling capacity of 9000 BTU/H
[AD-A213756] N90-15388
ESDU INTERNATIONAL LTD., LONDON (ENGLAND).
Installed tailplane lift-curve slope at subsonic speeds
[ESDU-89029] N90-15081
The maximum lift coefficient of plain wings at subsonic speeds
[ESDU-89034] N90-15082
Transverse (through-the-thickness) shear stiffnesses of fibre reinforced composite laminated plates (computer program)
[ESDU-89013] N90-15152
Summary physical data tables: Alkanes
[ESDU-PD3] N90-15162
Thermal conductivity of gaseous aliphatic hydrocarbons. Part 1: Alkanes
[ESDU-89035-PT-1] N90-15183
Orthobaric densities and molar volumes of liquids: Alcohols
[ESDU-89037] N90-15184
Guide to the selection of surface treatments for the improvement of fatigue strength of steels
[ESDU-89031] N90-15245
Reflux condensation in vertical tubes
[ESDU-89038] N90-15397
A procedure for force-balancing planar linkages using counterweights
[ESDU-89028] N90-15446
Resultant forces and moments in completely restrained plates subjected to a recovery temperature varying linearly with time
[ESDU-89024] N90-15480
Thermal stresses in unrestrained plates subjected to a recovery temperature varying linearly with time
[ESDU-89025] N90-15481
Pipeline vibrations. Fluid transients in non-rigid, unbranched planar piping systems
[ESDU-89030] N90-15491
Parameter estimation of linear systems in the presence of process noise using the maximum liklihood method
[ESDU-89032] N90-15693
The calculation of overground sound propagation in the presence of wind and temperature gradients
[ESDU-89036] N90-15714
Temperatures in plates subjected to a recovery temperature varying linearly with time
[ESDU-89023] N90-15831

F

FEDERAL AVIATION ADMINISTRATION, ATLANTIC CITY, NJ.
Improved lighting of taxiway/taxiway intersections for Instrument Flight Rules (IFR) operations
[DOT/FAA/CT-TN89/64] N90-15089
FERMI NATIONAL ACCELERATOR LAB., BATAVIA, IL.
Designing machines for lattice physics and algorithm investigation
[DE90-003543] N90-15596
High level language memory management on parallel architectures
[DE89-015018] N90-15609
An exact solution for a thick domain wall in general relativity
[NASA-CR-185013] N90-15826
The dynamics of domain walls and strings
[NASA-CR-186255] N90-15832
Small scale structure on cosmic strings
[DE90-003128] N90-15867
FLIGHT SAFETY FOUNDATION, INC., ARLINGTON, VA.
The human element: The key to safe, civil operations in adverse weather N90-15042
International Aircraft Occupant Safety Conference and Workshop proceedings
[AD-A214452] N90-15085
FLORIDA STATE UNIV., TALLAHASSEE.
Two basic partial orderings for distributions derived from Schur functions and majorization
[AD-A213703] N90-15682
Strong large deviation and local limit theorems
[AD-A213610] N90-15698
A diffusion on a fractal state space
[AD-A213555] N90-15707
Computation of broadband mixing noise from turbomachinery
[AD-A214448] N90-15713
FLORIDA UNIV., GAINESVILLE.
Design and calibration of an in-stack, low-pressure impactor
[AD-A213531] N90-15105
Ultra high performance, highly reliable, numeric intensive processors and systems
[AD-A214100] N90-15659
FOKKER B.V., SCHIPOL-OOST (NETHERLANDS).
Fabrication of test-articles from Al-Li 2091 for Fokker 100 N90-15196

G

GENERAL ACCOUNTING OFFICE, WASHINGTON, DC.
Space operations: Listing of NASA scientific missions, 1980-2000. Fact sheet for the Chairman, Subcommittee on Space Science and Applications, Committee on Science, Space, and Technology, House of Representatives
[AD-A213493] N90-15881
GENERAL ATOMIC CO., SAN DIEGO, CA.
Upgrade plans to handle 30 to 40 Mbytes of data for D3-D
[DE90-003291] N90-15750
Mechanical design of the inside launch system for electron cyclotron heating in D3-D
[DE90-003292] N90-15751
Design of DIII-D advanced divertor
[DE90-003343] N90-15752
High-temperature ceramic superconductors
[AD-A214251] N90-15818
Data file management in the D3-D data acquisition and analysis computer systems
[DE90-003289] N90-15850
GEORGE MASON UNIV., FAIRFAX, VA.
Analysis and evaluation of technical data on the photochromic and non-linear optical properties of materials. Appendix: Eye/sensor protection by an optical fuse mirror at a focal plane: Feasibility assessment
[AD-A214051] N90-15177
Analysis and evaluation of technical data on the photochromic and non-linear optical properties of materials
[AD-A214212] N90-15178
GEORGE WASHINGTON UNIV., WASHINGTON, DC.
Development of a rate independent plasticity theory for general cyclic loading N90-15471
GEORGIA INST. OF TECH., ATLANTA.
A study of the effects of Rotating Frame Turbulence (RFT) on helicopter flight mechanics N90-15058
Unsteady aerodynamics of oscillating and rapidly pitched airfoils N90-15074
Finite difference techniques and rotor blade aeroelastic partial differential equations with quasisteady aerodynamics N90-15075
Feasibility analysis of reciprocating magnetic heat pumps
[NASA-CR-186205] N90-15363
Utilization of a PC for finite element modeling
[AD-A214173] N90-15605
GEORGIA STATE UNIV., ATLANTA.
Investigations of the interactions of radiation with matter
[AD-A213554] N90-15723
GINER, INC., WALTHAN, MA.
Advanced double layer capacitor
[AD-A213406] N90-15341

H

HARRY DIAMOND LABS., ADELPHI, MD.
Host materials for transition-metal ions
[AD-A213605] N90-15808
HARVARD UNIV., CAMBRIDGE, MA.
Research on amorphous silicon-germanium alloys for tandem solar cells
[DE89-009436] N90-15499
HAWAII NATURAL ENERGY INST., HONOLULU.
The Third Pacific Basin Biofuels Workshop: Proceedings
[DE90-002523] N90-15513
HELSINKI UNIV. OF TECHNOLOGY, ESPOO (FINLAND).
The 22 GHz Radioastron receiver: Development of prototype components during the year 1988
[PB89-212583] N90-15323
HIROSHIMA UNIV., TAKEHARA (JAPAN).
A (2+1)-dimensional pure gravity for an arbitrary closed initial surface
[DE90-701754] N90-15829
Abelian gauge theory in topologically non-trivial space
[DE90-710100] N90-15830
Gravitational lens effect on the cosmic background radiation due to nonlinear inhomogeneities
[DE90-701753] N90-15868
HOUSTON UNIV., TX.
Numerical methods for parabolic equations and inequalities in very high dimensions
[AD-A214102] N90-15690

I

IDAHO NATIONAL ENGINEERING LAB., IDAHO FALLS.
Superconducting film fabrication by the sol-gel process
[DE90-002069] N90-15252
Heat transfer in condensation of lithium vapors
[DE90-002081] N90-15375
Model for measuring complex performance in an aviation environment
[DE90-002055] N90-15585
IIT RESEARCH INST., BARTLESVILLE, OK.
Crosslinked, flexible, low-molecular-weight polyacrylamide gels for mobility control
[DE90-000202] N90-15280
IIT RESEARCH INST., CHICAGO, IL.
Analysis of ambient polar volatile organic compounds using chemical ionization-ion trap detector
[PB90-106451] N90-15529
ILLINOIS ASSOCIATION OF RECYCLING CENTERS, NAPERVILLE.
Managing the waste stream: Background information for planning source separation programs
[PB90-100223] N90-15530
ILLINOIS INST. OF TECH., CHICAGO.
The possible occurrence of multi-phase behavior in the high T(sub c) superconductor YBa2Cu3O(sub x)
[DE90-002999] N90-15777
ILLINOIS UNIV., CHICAGO.
Spatial dynamics of deformable multibody systems with variable kinematic structure
[AD-A214098] N90-15455
ILLINOIS UNIV., URBANA.
Thin films under chemical stress
[DE90-003754] N90-15484
Determination of Q as a function of depth and tectonic province
[AD-A213805] N90-15554
ILLINOIS UNIV., URBANA-CHAMPAIGN.
A numerical model for the axisymmetric equilibrium shape of drops in uniform motion: Effects of external flow, electric field and surface charge N90-15071
Deformation and fracture of low alloy steels at high temperature
[DE90-001274] N90-15215
An improved toeplitz approximation method
[AD-A213994] N90-15688
ILLINOIS UNIV. AT URBANA-CHAMPAIGN, SAVOY.
Systolic algorithms for imaging from space
[AD-A213870] N90-15701
INDUSTRIEANLAGEN-BETRIEBSGESELLSCHAFT M.B.H., OTTOBRUNN (GERMANY, F.R.).
Fatigue and fracture behaviour of a PM Al-Li alloy N90-15195
INSTITUT NATIONAL DES SCIENCES APPLIQUEES DE LYON, VILLEURBANNE (FRANCE).
Metal matrix composites with long inorganic fibers N90-15206
INSTITUTE FOR COMPUTER APPLICATIONS IN SCIENCE AND ENGINEERING, HAMPTON, VA.
On strongly nonlinear vortex/wave interactions in boundary-layer transition
[NASA-CR-181963] N90-15078
INSTITUTE OF GAS TECHNOLOGY, CHICAGO, IL.
Determination of flow-regime boundaries for cohesive particles
[DE90-001405] N90-15369
INSTITUTO SUPERIOR TECNICO, LISBON (PORTUGAL).
A pitch control law for compensation of the phugoid mode induced by windshears N90-15051

INTERNATIONAL CENTRE FOR THEORETICAL PHYSICS, TRIESTE (ITALY).
Electron theory of long wavelength concentration fluctuations in liquid metal alloys
[DE89-636213] N90-15225
Structure properties of confined systems. Hard spheres between ideal walls
[DE90-600818] N90-15378
Fractal dimension of the fractured surface of materials
[DE89-635764] N90-15477
Stable supermembrane vacuum with a discrete spectrum
[DE89-635722] N90-15561
Modular invariants for theta-functions with characteristics and the twisted N=2 superconformal and SU(2) Kac-Moody algebras
[DE89-635701] N90-15671
Mixed singular linear elliptic equations
[DE90-600722] N90-15674
SL(2,R) current algebra in two-dimensional conformal quantum gravity
[DE90-600755] N90-15675
Continuum analogues of contragredient Lie algebras: Lie algebras with a Cartan operator and nonlinear dynamical systems
[DE89-635698] N90-15691
Flow of harmonic applications of a compact variety on a bordered variety
[DE89-635699] N90-15692
Chern-Simons theories of symplectic super-diffeomorphisms
[DE89-635700] N90-15703
On the free carrier-negative U center interacting model for the high-T(sub c) oxide superconductor
[DE89-635908] N90-15775
Further studies on possible coexistence of antiferromagnetism and superconductivity in 2D Heisenberg model
[DE90-601082] N90-15783
Non Newtonian gravity creeping flow
[DE90-600816] N90-15828
Lefschetz trace formula and BRST
[DE89-635705] N90-15835

INTERNATIONAL FUEL CELLS CORP., SOUTH WINDSOR, CT.
Molten carbonate fuel cell technology improvement
[DE90-001934] N90-15501

INTERSCIENCE, INC., TROY, NY.
Magnetic mirror confinement concepts system studies
[DE90-003667] N90-15753

IOWA UNIV., IOWA CITY.
Nonlinear viscous waves produced by an impulsively moving plate
[AD-A214014] N90-15392
Determination of stepsize parameters for intermolecular vibrational energy transfer
[DE90-003346] N90-15719

ISTITUTO NAZIONALE DI FISICA NUCLEARE, FRASCATI (ITALY).
First results from the MACRO (Monopole, Astrophysics, Cosmic Ray Observatory) detector at the Gran Sasso Laboratory
[DE90-003243] N90-15858

J

JAPAN ATOMIC ENERGY RESEARCH INST., TOKYO.
Stability of numerical solutions for stratified two-phase flow
[DE90-701646] N90-15379
New approach to the inverse problem of six-link manipulators via the optimization technique
[DE90-710044] N90-15441
Development of a three-dimensional local scale atmospheric model with turbulence closure model
[DE90-710045] N90-15551

JAYCOR, VIENNA, VA.
Aspects of Raman scattering
[AD-A213926] N90-15736

JET PROPULSION LAB., CALIFORNIA INST. OF TECH., PASADENA.
Molecules with enhanced electronic polarizabilities based on defect-like states in conjugated polymers
[NASA-CASE-NPO-17633-1-CU] N90-15263

JIL SYSTEMS, INC., ARLINGTON, VA.
DOCTORD Database System user's guide, June 1989: dBase 3 PLUS Physician/(Part B Medicare): Personal computer reference system and user's guide
[PB90-100181] N90-15579

JOHNS HOPKINS UNIV., LAUREL, MD.
Rectangular-to-circular waveguide transitions for high-power circular overmoded waveguides
[AD-A213925] N90-15349

JOINT INST. FOR NUCLEAR RESEARCH, DUBNA (USSR).
On functional integral representations in the lower Hubbard band based on generalized coherent states
[DE90-602936] N90-15804
Cu-O chains in YBa2Cu3O(7-delta) and the phonon mechanism of high-Tc superconductivity
[DE90-603502] N90-15805
Nonlocality and stochastic quantization of field theory
[DE89-633913] N90-15833

K

KAPTEYN ASTRONOMICAL LAB., GRONINGEN (NETHERLANDS).
Image enhancement using the IRAS (Infrared Astronomy Satellite) survey data
[AD-A213811] N90-15496

KENTUCKY UNIV., LEXINGTON.
High power density spray cooling
[AD-A213575] N90-15386

KRUG INTERNATIONAL, SAN ANTONIO, TX.
Potential for reduction of decompression sickness by prebreathing with 100 percent oxygen while exercising
[AD-A213449] N90-15581

L

LABORATOIRE CENTRAL AEROSPATIALE, SURESNES CEDEX (FRANCE).
Properties of Al-Li alloys N90-15191

LAWRENCE LIVERMORE NATIONAL LAB., CA.
Design limitations on ultra-high velocity projectile launchers
[DE89-012933] N90-15118
Hugoniot measurements with the LLNL electric gun facility
[DE90-002809] N90-15119
Safety evaluation report for Galileo: Volume 1
[DE90-003086] N90-15122
Safety evaluation report for Galileo, volume 2
[DE90-003087] N90-15123
A methodology for evaluating heavy gas dispersion models
[AD-A214009] N90-15131
Composite activities at Lawrence Livermore National Laboratory
[DE90-002979] N90-15149
Shock tube ignition of octanes
[DE90-001167] N90-15164
Mechanistic modeling of epoxy resins
[DE89-015119] N90-15247
Laser glass (1989)
[DE90-002754] N90-15257
Bonding aerogels with polyurethanes
[DE90-003050] N90-15258
Using small scale tests to estimate the failure diameter of a propellant
[DE90-001166] N90-15281
Burning rates of two cast nitramine explosives using a hybrid closed bomb-strand burner
[DE90-002785] N90-15286
A future for LLNL (Lawrence Livermore National Laboratory) research in composite high explosives
[DE90-004442] N90-15290
Benefits from combining electroplating and physical vapor deposition technologies
[DE90-002700] N90-15301
Design of a high-gain flux-compression generator
[DE90-002795] N90-15333
Enhancement of microchannel plate gain by deposition of CsI on the channel walls
[DE90-003051] N90-15334
Avalanche photoconductive switching
[DE90-002980] N90-15337
Design of a custom load cell for a precision assembly application
[DE90-004439] N90-15340
Time-dependent free convection in liquid metals
[DE90-000957] N90-15366
Irreversible processes from reversible mechanics
[DE90-001057] N90-15368
Rayleigh-Taylor instability in compressible fluids
[DE90-003027] N90-15376
Time-dependent free convection in low Prandtl number fluids
[DE90-003053] N90-15377
The 17.1-GHz free-electron laser as a microwave source for TeV colliders
[DE90-001506] N90-15406
Anharmonic betatron motion in free electron lasers
[DE90-001515] N90-15407
Theory for high gain, high power free electron lasers
[DE90-003024] N90-15409
The search for solid state fusion lasers
[DE89-012301] N90-15410
NTES (Nuclear Test and Experimental Sciences) program laser facility for physics experiments Building 391 High Bay Option
[DE90-001795] N90-15411
Laser-supported detonation waves and pulsed laser propulsion
[DE90-002753] N90-15412
Integration of a gated microchannel plate detector into the Nova laser system
[DE90-002981] N90-15413
Waveguide effects in superradiant free-electron lasers
[DE90-003805] N90-15417
NOISE: A nonlinear optimization induction free-electron laser systems engineering code
[DE90-004438] N90-15420
Aerosol heating and vaporization of high-flux laser beams
[DE90-003471] N90-15428
Comparison of engine knock predictions using a fully-detailed and a reduced chemical kinetic mechanism
[DE90-002805] N90-15448
Feasibility study of using industrial robot for ultrasound testing
[DE90-002977] N90-15461
A simple shell element formulation for large-scale elastoplastic analysis
[DE89-015452] N90-15475
Statistical model for particle-void deformation kinetics in granular materials during shock wave propagation
[DE89-017729] N90-15476
Greenhouse gases: Changing the global climate
[DE90-002788] N90-15535
Beryllium dispersion near explosive firing tables: A comparison of computed and observed results
[DE90-002635] N90-15550
LLNL's plan for a prototype circuit switch, a potential gigabit LAN of the future
[DE90-003614] N90-15597
Knowledge representations for the automatic generation of numerical simulators for PDEs
[DE89-008036] N90-15615
Simulating the scheduling of parallel supercomputer applications
[DE90-003604] N90-15655
SBS (Stimulated Brillouin Scattering) pulse distortion in multimode optical fibers: Preliminary results
[DE90-003023] N90-15731
Computer simulation of laser plasma interaction
[DE90-002828] N90-15748
Intense REB (Relativistic Electron Beam) transport in a weakly magnetized plasma
[DE90-002978] N90-15749
The measurement of transport properties in strongly coupled plasmas
[DE90-003451] N90-15755
Spectroscopic and laser properties of Cr:LiCaAlF6 and Cr:LiSrAlF6 crystals
[DE90-000783] N90-15770
Micron-thin Nb films recovered from Mbar shock pressures
[DE90-001509] N90-15772
Electron-positron momentum distribution measurements of high-T superconductors and related systems
[DE90-002974] N90-15780
Picosecond photoconductivity using a graded bandgap Al(x)Ga(1-x)As active detecting layer
[DE90-003452] N90-15786
Astophysical opacities at LLNL
[DE90-003599] N90-15872

LEHIGH UNIV., BETHLEHEM, PA.
Excimer emission from alkali diatomic and alkaline-earth-noble-gas molecules
[AD-A214246] N90-15179

LITTLE (ARTHUR D.), INC., CAMBRIDGE, MA.
The Solar Power Satellite (SPS): Progress so far N90-15840

LOCKHEED MISSILES AND SPACE CO., PALO ALTO, CA.
Nickel beryllides and their properties
[DE90-001736] N90-15220

LOS ALAMOS NATIONAL LAB., NM.
Laser mixing of titanium on silicon carbide
[DE90-003216] N90-15150
ROBOCAL (Robotic Calorimetry): An automated NDA (Nondestructive Assay) calorimetry and gamma isotopic system
[DE90-003217] N90-15168
SESAME equation of state for a polymer composite: Phenolic refrasil
[LA-11512-MS] N90-15264
RF transistor thermal/electrical characterization
[DE90-001427] N90-15326

Radial heat flux limits in potassium heat pipes: An experimental and analytical investigation
[DE90-002655] N90-15396
Hamiltonian chaos in a nonlinear polarized optical beam
[DE90-002437] N90-15408
Comprehensive, nonintercepting electron-beam diagnostics using spontaneous emission
[DE90-003211] N90-15414
Initial optical transition radiation measurements of the electron beam for the Boeing free-electron laser experiment
[DE90-003396] N90-15416
MESA 3-D calculations of armor penetration by projectiles with combined obliquity and yaw
[DE89-015265] N90-15438
Hydrodynamics code calculations of debris clouds produced by ball-plate impacts
[DE89-015270] N90-15439
Comparison of multidimensional calculations of long-rod impacts on oblique plates
[DE89-015275] N90-15440
Effects of parametric variations of complex targets on damage from projectile impact
[DE90-003214] N90-15450
Niobium 1 percent zirconium/potassium and titanium/potassium life-test heat pipe design and testing
[DE90-002430] N90-15522
Monitoring chaos of cardiac rhythms
[DE90-000692] N90-15580
An efficient UNICOS run-time system for functional programs on a CRAY X-MP
[DE89-016603] N90-15610
General many-body systems
[DE90-000685] N90-15670
Use of the linear variate method of Monte Carlo for estimating uncertainty in thermal-hydraulic codes
[DE89-017871] N90-15694
Uniform versus random sampling in physical calculations: Monte Carlo
[DE90-003247] N90-15696
Prospects for space arms control
[DE90-003392] N90-15700
Large scale calculations of the structure and dynamics of dense matter
[DE90-003654] N90-15726
Optical solitons in liquid crystals
[DE90-000694] N90-15728
Initial results from FRC (Field-Reversed Configuration) compression experiments on FRX-C/LSM
[DE90-003390] N90-15754
Progress in LTE and non-LTE transport calculations
[DE90-003394] N90-15764
Phonons and charge-transfer excitations in HTS superconductors
[DE89-016616] N90-15768
Partial reduction of re-oxidation processing of Y-Ba-Cu-O sputtered thin films
[DE90-003655] N90-15782
Tritium and neutron measurements of a solid state cell
[DE90-003657] N90-15820
A quasi-economic role for lunar science
[DE90-000679] N90-15876
A simple model for the stellar analogy of compact solar flares
[DE90-003215] N90-15877

LOWELL UNIV., MA.
Studies of quantitative methods for imaging from scattered fields
[AD-A214047] N90-15638

LUND UNIV. (SWEDEN).
Rapidity densities and their fluctuations in central 200 A GeV S32 interations with Au and Ag,Br nuclei
[LUIP-8905] N90-15715
Substructural dependence of the multiparticle production in relativistic heavy-ion interactions
[LUIP-8904] N90-15716
Target nucleus fragmentation in O16 + (Ag,Br) interactions at 200 A GeV
[LUIP-8906] N90-15727

M

MARTIN MARIETTA CORP., NEW ORLEANS, LA.
Onorbit electron beam welding experiment definition
[NASA-CR-183847] N90-15431
Eddy-current inspection of shuttle heat exchanger tube welds
[NASA-CR-186302] N90-15462

MARTIN MARIETTA SPACE SYSTEMS, INC., DENVER, CO.
Damping characteristics of metal matrix composites
[AD-A213712] N90-15151

MARYLAND UNIV., COLLEGE PARK.
Integrated approach fault tolerance-current state and future requirements
[AD-A214402] N90-15465
Vision in dynamic environments
[AD-A213434] N90-15587
The application of optimal control theory for analysis of human jumping and pedaling N90-15590
Higher order crossings from a parametric family of linear filters
[AD-A213427] N90-15676

MASSACHUSETTS INST. OF TECH., CAMBRIDGE.
Instrumentation for a facility for the test, analysis and active control of spacecraft truss structures
[AD-A213655] N90-15124
Propulsion research on the hybrid plume rocket
[AD-A214420] N90-15132
The effect of nitrogen and titanium on the toughness of high strength saw weld deposits
[AD-A213400] N90-15230
Reduction of residual stress and distortion in HY100 and HY130 high strength steels during welding
[AD-A213532] N90-15231
New polymers made with well-characterized organometallic catalysts
[AD-A213592] N90-15272
VLSI theory and parallel supercomputing
[AD-A214035] N90-15351
Gas turbine regenerators: A method for selecting the optimum plate-finned surface pair for minimum core volume
[AD-A213430] N90-15382
A coning motion apparatus for hydrodynamic model testing in a non-planar cross-flow
[AD-A213431] N90-15383
An experimental study of the time-dependent behavior of the appendage-body junction vortex
[AD-A213465] N90-15384
Submerged arc welding consumables for HSLA (High Strength Low Alloy)-100 steel
[AD-A213433] N90-15452
Interfacial systems for photochemical energy conversion
[DE90-003181] N90-15514
Design study of a modular gas-cooled, closed-brayton cycle reactor for marine use
[AD-A213453] N90-15518
Utilization of non-conventional systems for conversion of biomass to food components
[NASA-CR-177545] N90-15591
Temporal, processor, and spatial locality in multiprocessor memory references
[AD-A213790] N90-15598
Paralation views: Abstractions for efficient scientific computing on the connection machine
[AD-A213935] N90-15604
An executive system for modeling with rational b-splines
[AD-A213460] N90-15627
On the correctness of orphan management algorithms
[AD-A213777] N90-15632
Time bounds for real-time process control in the presence of timing uncertainty
[AD-A213791] N90-15633
Optimistic concurrency control for nested distributed transactions
[AD-A213828] N90-15634
A signal processing language for coarse grain data flow multiprocessors
[AD-A213863] N90-15635
Adaptive backoff synchronization techniques
[AD-A213966] N90-15658
Using mappings to prove timing properties
[AD-A213967] N90-15666
Bounded polynomial randomized consensus
[AD-A213808] N90-15686
Physical process in MPD plasmas
[AD-A213679] N90-15761

MASSACHUSETTS INST. OF TECH., LEXINGTON.
SLCSAT (Submarine Laser Communication Satellite) communication system design study
[AD-A213403] N90-15304
N-port theory applied to backscatter polarimetry and depolarization in foliage penetration
[AD-A213437] N90-15305
Polarimetric SAR antenna characterization
[AD-A213438] N90-15306
Flashlight radar: A three-dimensional imaging radar
[AD-A213439] N90-15307
Binary optics technology: The theory and design of multi-level diffractive optical elements
[AD-A213404] N90-15735
Solid state research
[AD-A213405] N90-15806

MASSACHUSETTS UNIV., AMHERST.
A study of Inter-Injection-Locked phased arrays
[AD-A214097] N90-15352

MCDONNELL AIRCRAFT CO., SAINT LOUIS, MO.
Aluminum-lithium: Application of plate and sheet to fighter aircraft N90-15202

MESSERSCHMITT-BOELKOW-BLOHM G.M.B.H., BREMEN (GERMANY, F.R.).
Investigation on sheet material of 8090 and 2091 aluminium-lithium alloy N90-15192

MESSERSCHMITT-BOELKOW-BLOHM G.M.B.H., HAMBURG (GERMANY, F.R.).
The interference of flightmechanical control laws with those of load alleviation and its influence on structural design N90-15054

MICHIGAN UNIV., ANN ARBOR.
A new technique for simulating composite material. Task 2: Analytical solutions with Generalized Impedance Boundary Conditions (GIBCs)
[NASA-CR-186249] N90-15146
Dense-spray properties: Structure and turbulence modulation
[AD-A213671] N90-15387

MIDWEST RESEARCH INST., GOLDEN, CO.
Instability of a-Si:H/Ag interface at 150 deg C
[DE89-009419] N90-15498
Research on high-efficiency, single-junction, monolithic, thin-film amorphous silicon solar cells, phase 1
[DE89-009495] N90-15502
Research on high-efficiency, single-junction, monolithic, thin-film amorphous silicon solar cells, phase 2
[DE89-009496] N90-15503
US Polycrystalline Thin Film Solar Cells Program
[DE89-009506] N90-15504
Ocean thermal energy conversion: An overview
[DE89-000838] N90-15512
Inclusion of nonlinear aerodynamics in the FLAP code
[DE89-009507] N90-15519
Prediction of stochastic blade loads for three-bladed, rigid-hub rotors
[DE89-009508] N90-15520

MINNESOTA UNIV., MINNEAPOLIS.
Epitaxial iron films
[AD-A213551] N90-15807

MISSION RESEARCH CORP., SANTA BARBARA, CA.
A signal realization data base generated by the multiple phase-screen method
[AD-A214004] N90-15852

MISSISSIPPI STATE UNIV., STATE COLLEGE.
Unsteady three-dimensional thin-layer Navier-Stokes solutions on dynamic blocked grids N90-15069

MISSOURI UNIV., COLUMBIA.
Numerical facility: Convergence of cognitive and factor analytic models
[AD-A213627] N90-15680

MITRE CORP., MCLEAN, VA.
National airspace system: Airport movement area control operational concept
[WP-89W00181] N90-15086
Control outside of independent surveillance coverage operational concept
[AD-A214163] N90-15090

MONTANA STATE UNIV., BOZEMAN.
Computer controlled MHD power consolidation and pulse-generation system
[DE90-001224] N90-15662

MOUND LAB., MIAMISBURG, OH.
Critical temperature analysis for a hemispherical charge of a binary explosive
[DE90-001447] N90-15282
Simultaneous thermal analysis techniques for characterization of energetic materials
[DE90-003028] N90-15289

N

NATIONAL AERONAUTICAL ESTABLISHMENT, OTTAWA (ONTARIO).
Adverse weather operations during the Canadian Atlantic storms program N90-15052

NATIONAL AERONAUTICS AND SPACE ADMINISTRATION, WASHINGTON, DC.
Aeronautical engineering: A continuing bibliography with indexes (supplement 246)
[NASA-SP-7037(246)] N90-15068
NASA patent abstracts bibliography: A continuing bibliography. Section 1: Abstracts (supplement 36)
[NASA-SP-7039(36)-SECT-1] N90-15851

NATIONAL AERONAUTICS AND SPACE ADMINISTRATION. AMES RESEARCH CENTER, MOFFETT FIELD, CA.
Analysis of severe atmospheric disturbances from airline flight records N90-15045

The effectiveness of vane-aileron excitation in the experimental determination of flutter speed by parameter identification
[NASA-TP-2971] N90-15100
The dissociation energy of N2
[NASA-TM-101930] N90-15153
Calibration of seven-hole pressure probes for use in fluid flows with large angularity
[NASA-TM-102200] N90-15399
Effect of contrast on the perception of direction of a moving pattern
[NASA-TM-102234] N90-15577

NATIONAL AERONAUTICS AND SPACE ADMINISTRATION. GODDARD SPACE FLIGHT CENTER, GREENBELT, MD.
Ceramic heat pipe wick
[NASA-CASE-GSC-13199-1] N90-15261
A high spatial resolution study of the thermospheric response to a discrete auroral arc
[NASA-TM-102904] N90-15559

NATIONAL AERONAUTICS AND SPACE ADMINISTRATION. LANGLEY RESEARCH CENTER, HAMPTON, VA.
Effects of lightning on operations of aerospace vehicles N90-15065
Serrated trailing edges for improving lift and drag characteristics of lifting surfaces
[NASA-CASE-LAR-13870-1] N90-15094
Task-oriented display design: Concept and example
[NASA-TM-101685] N90-15101
Display interface concepts for automated fault diagnosis
[NASA-TM-101610] N90-15102
Relative merits of reactive and forward-look detection for wind-shear encounters during landing approach for various microburst escape strategies
[NASA-TM-4158] N90-15108
Guidance analysis of the aeroglide plane change maneuver as a turning point problem
[NASA-TM-101639] N90-15110
Shuttle-C utilization for assembly of the rephased Freedom configuration
[NASA-TM-101658] N90-15120
Novel polyimide compositions based on 4,4': Isophthaloyldiphthalic anaydride (IDPA)
[NASA-CASE-LAR-14194-1] N90-15148
Ignitability test method and apparatus
[NASA-CASE-LAR-13996-1-SB] N90-15161
Wet spinning of solid polyamic acid fibers
[NASA-CASE-LAR-14162-1] N90-15259
Polyimides with carbonyl and ether connecting groups between the aromatic rings
[NASA-CASE-LAR-14001-1] N90-15260
Portable digital pressure indicator for calibrating magnetic tape recorders
[NASA-TM-101650] N90-15401
Single element magnetic suspension actuator
[NASA-CASE-LAR-13981-1] N90-15442
Sound attenuation apparatus
[NASA-CASE-LAR-13968-1] N90-15710
Report of NASA Lunar Energy Enterprise Case Study Task Force
[NASA-TM-101652] N90-15836
Report of the NASA lunar energy enterprise case study task force N90-15837
Technical communications in aeronautics: Results of an exploratory study. An analysis of profit managers' and nonprofit managers' responses
[NASA-TM-101626] N90-15848

NATIONAL AERONAUTICS AND SPACE ADMINISTRATION. LEWIS RESEARCH CENTER, CLEVELAND, OH.
NASA's program on icing research and technology N90-15062
Advanced detection, isolation, and accommodation of sensor failures in turbofan engines: Real-time microcomputer implementation
[NASA-TP-2925] N90-15112
Extended temperature range rocket injector
[NASA-CASE-LEW-14846-1] N90-15130
Empirical and analytical determination of the fracture resistance of a TiB2 particle/SiC matrix composite
[NASA-TM-101940] N90-15143
Improved process for HIP canning of composites
[NASA-CASE-LEW-14990-1-CU] N90-15147
Secondary electron emission characteristics of molybdenum-masked, ion-textured OFHC copper
[NASA-TP-2967] N90-15211
Brominated graphitized carbon fibers
[NASA-CASE-LEW-14698-2] N90-15262
High temperature, flexible, thermal barrier seal
[NASA-CASE-LEW-14672-1] N90-15444
Fully articulated four-point-bend loading fixture
[NASA-CASE-LEW-14776-1] N90-15445
CryoTran user's manual, version 1.0
[NASA-TM-102468] N90-15622
Fiber optic sensing system
[NASA-CASE-LEW-14795-1] N90-15733
Bibliography of Lewis Research Center technical publications announced in 1988
[NASA-TM-102034] N90-15846

NATIONAL AERONAUTICS AND SPACE ADMINISTRATION. MARSHALL SPACE FLIGHT CENTER, HUNTSVILLE, AL.
Directional solidification of superalloys
[NASA-CASE-MFS-28314-1] N90-15227
Hybrid butterfly valve
[NASA-CASE-SSC-00004] N90-15443
Superconducting gravity gradiometer mission. Volume 1: Study team executive summary
[NASA-TM-4091-VOL-1] N90-15545

NATIONAL AERONAUTICS AND SPACE ADMINISTRATION. PASADENA OFFICE, CA.
Molecules with enhanced electronic polarizabilities based on defect-like states in conjugated polymers
[NASA-CASE-NPO-17633-1-CU] N90-15263

NATIONAL AEROSPACE LAB., EMMELOORD (NETHERLANDS).
Mechanical properties and fracture toughness of 8090-T651 plate and 2091 and 8090 sheet N90-15188

NATIONAL CHENG KUNG UNIV., TAINAN (TAIWAN).
Explicit and implicit calculations of turbulent cavity flows with and without yaw angle
[NASA-CR-186293] N90-15381

NATIONAL INST. OF STANDARDS AND TECHNOLOGY, BOULDER, CO.
Alternative techniques for some typical MIL-STD-461/462 types of measurements
[PB89-235139] N90-15302

NATIONAL INST. OF STANDARDS AND TECHNOLOGY, GAITHERSBURG, MD.
The production and spectroscopy of molecular ions isolated in solid neon
[AD-A213723] N90-15174
Magnetic viscosity in Ni/Cu compositionally-modulated alloys
[DE90-002303] N90-15223
Studies on some failure modes in latex barrier films
[PB89-209308] N90-15246

NAUCHNO-ISSLEDOVATELSKII INST. EHLEKTROFIZICHESKOJ APPARATURY, LENINGRAD (USSR).
Microfluctuations of plasma density in a theta-pinch and spatial coherency of a probing laser beam
[DE90-603347] N90-15760

NAVAL AIR DEVELOPMENT CENTER, WARMINSTER, PA.
Aluminum lithium alloys for Navy aircraft N90-15193

NAVAL OCEAN SYSTEMS CENTER, SAN DIEGO, CA.
Voice Multiplex System (VMS)
[AD-A213902] N90-15315
Specification for evaporation duct height calculations
[AD-A213841] N90-15570
Periodic phase adjustment distributed clock synchronization in the hard realtime environment
[AD-A213842] N90-15708

NAVAL POSTGRADUATE SCHOOL, MONTEREY, CA.
Flow visualization of the effect of pitch rate on the vortex development on the scale model of a F-18 fighter aircraft
[AD-A214244] N90-15080
Strategic characteristics of Dynamics Explorer 1 retarding ion mass spectrometer and the consequences for core plasma measurements
[AD-A214013] N90-15125
Planning minimum-energy paths in an off-road environment with anisotropic traversal costs and motion constraints
[AD-A214181] N90-15457
A simulation model for dynamic system availability analysis
[AD-A213499] N90-15628
Environment for failure region analysis: REACHER - a reachability condition derivation tool
[AD-A214183] N90-15641
Polynomial transfer lot sizing techniques for batch processing on consecutive machines
[AD-A214198] N90-15660
A note on the maximum size of a rectilinear maze
[AD-A214445] N90-15668
Annual summary of basic research in thermoacoustic heat transport
[AD-A214185] N90-15834

NAVAL RESEARCH LAB. WASHINGTON, DC.
Adaptive canceller limitations caused by I,Q mismatch errors
[AD-A214287] N90-15318
Voice/data integration in mobile radio networks: Overview and future research directions
[AD-A214289] N90-15319
Dual task performance with LPC (Linear Predictive Coding) degraded speech in a sentence verification task
[AD-A214298] N90-15320
Review of quasi-optical gyrotron development
[AD-A213491] N90-15402
Frequency shift induced in laser pulses by plasma density variations
[AD-A214195] N90-15424
Interlaboratory comparison of radiation-induced attenuation in optical fibers. Part 3: Transient exposures
[DE90-000859] N90-15729
Optical guiding by plasma waves in the plasma beat wave accelerator
[AD-A214288] N90-15763

NAVAL SURFACE WARFARE CENTER, SILVER SPRING, MD.
Epoxy-resin cable terminations
[AD-A213789] N90-15454

NAVAL UNDERWATER SYSTEMS CENTER, WEST PALM BEACH, FL.
Wind speed dependence of acoustic ambient vertical directional spectra at high frequency
[AD-A214293] N90-15712

NEVADA UNIV., RENO.
High temperature chemistry of aromatic hydrocarbons
[DE90-003664] N90-15133

NEW MEXICO STATE UNIV., LAS CRUCES.
Aerosol heating and vaporization of high-flux laser beams
[DE90-003471] N90-15428
ARGOS (A Research GMMP Operating System): Overvie w and interfaces
[AD-A213871] N90-15599

NEW MEXICO UNIV., ALBUQUERQUE.
Laser-material interactions
[AD-A214421] N90-15425
Nonlinear optical material studies
[AD-A213938] N90-15737

NEW YORK UNIV., NEW YORK.
Enhanced resolution concepts in large scale scientific computing
[AD-A214095] N90-15393

NORTH CAROLINA STATE UNIV., RALEIGH.
Hypersonic nozzle design
[NASA-CR-186261] N90-15077
Computer-controlled ion beam sputter-deposition of superconducting oxide films
[AD-A213921] N90-15812

NORTHWESTERN UNIV., EVANSTON, IL.
Combustion characteristics of sprays
[AD-A213651] N90-15173
Damage evaluation from surface displacement data N90-15469

NOTRE DAME UNIV., IN.
Experimental measurements of the laminar separation bubble on an Eppler 387 airfoil at low Reynolds numbers
[NASA-CR-186263] N90-15380
Parametric identification of discrete time series models for structural response prediction N90-15472
Membership-set parameter estimation via optimal bounding ellipsoids
[AD-A213807] N90-15685

NOTTINGHAM UNIV. (ENGLAND).
Short fibre and particulate reinforced metal matrix composites N90-15207

O

OAK RIDGE GASEOUS DIFFUSION PLANT, TN.
Isotopic selectivity of surface diffusion: An activated diffusion model
[DE90-003473] N90-15169
Calculation of surface heat transfer parameters during quenching from surface thermocouple signals
[DE89-011620] N90-15224
Comments on compressible flow through butterfly valves
[DE89-015730] N90-15371

OAK RIDGE NATIONAL LAB., TN.
Dimensional analysis of continuous high-capacity electrodispersion of aqueous based liquids in an organic continuous phase
[DE90-003714] N90-15136
On the choice of trial function in theoretical calculations of the thermal conductivity
[DE90-001733] N90-15182
Microstructural evolution of martensitic steels during fast neutron irradiation
[DE89-016231] N90-15212
Deformation and fracture of low alloy steels at high temperature
[DE90-001274] N90-15215

A review of the effects of microalloying constituents on the formation and breakdown of protective oxide scales on high-temperature alloys at temperatures below 700 C
[DE90-001277] N90-15216
Report of the Advanced Neutron Source (ANS) Aluminum Cladding Corrosion Workshop
[DE90-001281] N90-15217
Surface modification of metals by ion beams
[DE90-001285] N90-15218
An investigation of the sensitization behavior of Fe-Mn-Cr austenitic steels
[DE90-002719] N90-15226
Potential applications of structural ceramic composites in gas turbines
[DE90-001273] N90-15248
Ceramic powder characterization
[DE90-001282] N90-15249
Surface engineering by high energy beams
[DE90-001296] N90-15250
Ceramic technology for advanced heat engines project
[DE90-001852] N90-15251
Crack tip toughening by inclusions with pairs of shear transformations
[DE89-007845] N90-15254
Toughening behavior and interfacial properties of fiber-reinforced ceramic composites
[DE89-015351] N90-15279
Properties and thermal decomposition of the double salts of uranyl nitrate-ammonium nitrate
[DE89-004909] N90-15287
Tuned-circuit Johnson noise thermometry
[DE89-016221] N90-15356
Laboratory study of the dynamic losses of a single speed, split system air-to-air heat pump having tube and plate fin heat exchangers, 1985 to 1986
[DE90-000970] N90-15367
Sensor integration using concurrent computing on-board the ORNL mobile robot
[DE89-008740] N90-15436
Eddy-current inspection of shuttle heat exchanger tube welds
[NASA-CR-186302] N90-15462
A semiautomated computer-interactive dynamic impact testing system
[DE90-002721] N90-15479
Thermal energy storage
[DE90-000953] N90-15500
Selection of phase-change and containment materials for thermal energy storage
[NASA-CR-186228] N90-15506
Satellite thermal storage systems using metallic phase-change materials
[DE89-016872] N90-15507
A guide for estimating potential energy savings from increased solar reflectance of a low-sloped roof
[DE90-003720] N90-15526
Environmental surveillance data
[DE90-001275] N90-15532
Acid rain research
[DE90-003283] N90-15537
Global climate change and NEPA (National Environmental Policy Act) analyses
[DE90-003704] N90-15540
Factors that may influence responses of the US transportation sector to policies for reducing greenhouse gas emissions
[DE90-000704] N90-15543
Antarctic surface temperature and pressure data
[DE90-000971] N90-15565
Elicitation of natural language representations of uncertainty using computer technology
[DE90-001416] N90-15611
Neural network models for linear programming
[DE89-015974] N90-15651
A neural network for bounded linear programming
[DE89-015975] N90-15652
Estimating departure times from traffic counts using dynamic assignment
[DE89-016259] N90-15653
Design and implementation of two concurrent multi-sensor integration algorithms for mobile robots
[DE90-003041] N90-15663
Nonlinear maps with competitive interactions: Fixed-points, bifurcations, and chaotic attractors
[DE90-001858] N90-15695
Fusion reactor materials
[DE90-000976] N90-15744
Studies of plasma performance and transport in the Advanced Toroidal Facility (ATF)
[DE90-001737] N90-15746
Technology of fast-wave current drive antennas
[DE90-001972] N90-15747
Destabilization of tokamak pressure-gradient driven instabilities by energetic alpha populations
[DE90-003716] N90-15756
Deformation twinning in ordered intermetallic compounds
[DE89-014779] N90-15767
Theoretical studies on the electronic structure of high-temperature superconductors
[DE90-001301] N90-15771
Characteristics of CMOS analog integrated structures using MOSIS (Metal Oxide Semiconductor Implementation System)
[DE90-001630] N90-15773
The kind of mathematics involved in applied superconductivity research
[DE90-003706] N90-15798
Magnetic flux pinning in YBa2Cu3O7 films
[DE90-003709] N90-15799

OFFICE NATIONAL D'ETUDES ET DE RECHERCHES AEROSPATIALES, PARIS (FRANCE).
Description of atmospheric turbulence N90-15043
Principal characteristics of lightning on aircraft N90-15067

OFFICE OF NAVAL RESEARCH,
Ductile failure
[AD-A213864] N90-15488

OFFICE OF THE UNDER SECRETARY OF DEFENSE (ACQUISITIONS), WASHINGTON, DC.
Ada 9X project report. Revision request report
[AD-A213503] N90-15629

OHIO STATE UNIV., COLUMBUS.
Ultrasonic evaluation of porosity in aluminum cast materials
[AD-A213548] N90-15232

OKLAHOMA STATE UNIV., STILLWATER.
Turbulence effects of aircraft flight dynamics and control N90-15055

OKLAHOMA UNIV., NORMAN.
Effect of community structure on the kinetics of anaerobic degradation of aromatic compounds
[DE90-003666] N90-15134
Turbulence spectral widths view angle independence as observed by Doppler radar
[DOT/FAA/SA-89/2] N90-15566

OLD DOMINION UNIV., NORFOLK, VA.
Explicit and implicit calculations of turbulent cavity flows with and without yaw angle
[NASA-CR-186293] N90-15381
Lunar construction utility vehicle
[NASA-CR-186231] N90-15435
Strong large deviation and local limit theorems
[AD-A213610] N90-15698

OPEN UNIV., OXFORD (ENGLAND).
Understanding developments in computer technology: A pragmatic and synthetic interpretation N90-15608

OREGON STATE UNIV., CORVALLIS.
Adjustable speed drive study, June 1985 to September 1988. Part 2: Appendices
[DE90-002771] N90-15332

OXFORD UNIV. (ENGLAND).
Global lake-level variations from 18,000 to 0 years ago: A palaeoclimate analysis
[DE90-000998] N90-15531
Theory of interacting plasmas in space N90-15742

P

PACIFIC NORTHWEST LAB., RICHLAND, WA.
Effects of filament-matrix interfaces on the mechanical properties of SiC-reinforced Si3N4: A review
[DE90-001863] N90-15144
Capillary electrophoresis ionization-mass spectrometry and tandem mass spectrometry
[DE90-002664] N90-15158
Development of a robotics system for automated chemical analysis of sediment, sludges, and soils
[DE90-003637] N90-15170
Optical properties and laser damage measurements of inorganic polymer films
[DE90-003633] N90-15267
Ceramic processing using inorganic polymers
[DE90-003638] N90-15268
Back to basics
[DE90-002734] N90-15463
International aspects of restrictions of ozone-depleting substances
[DE90-001813] N90-15534
Evaluate and characterize mechanisms controlling transport, fate, and effects of army smokes in the aerosol wind tunnel: Transport, transformations, fate, and terrestrial ecological effects of hexachloroethane obscurant smokes
[DE90-002923] N90-15536
Introduction to extremely-low-frequency electric and magnetic fields
[DE90-002662] N90-15578
The components of scientific visualization
[DE90-001992] N90-15614
Developmental versions of FORTRAN/77 routines for the design and analysis of mixture experiments
[DE90-003513] N90-15624
Pulsed EMAT (Electromagnetic Acoustic Transducer) acoustic measurements on a horizontal continuous caster for internal temperature determination
[DE90-002735] N90-15709

PARIS-SUD UNIV., ORSAY (FRANCE).
Electron-positron momentum distribution measurements of high-T superconductors and related systems
[DE90-002974] N90-15780

PARIS UNIV. (FRANCE).
First International Symposium on Electrochemical Impedance Spectroscopy. Extended abstracts
[AD-A214406] N90-15354

PENNSYLVANIA STATE UNIV., UNIVERSITY PARK.
Thermal stability of jet fuel
[DE90-002760] N90-15288
Technology of fast spark gaps
[AD-A214199] N90-15353
An experimental, analytical, and computational investigation of turbomachinery rotor flow fields N90-15360
Modifications of the Penn State Boundary Layer Research Facility for boundary layer/structure interaction experimental research
[AD-A213874] N90-15391
Calculation of source and structure parameters at regional and teleseismic distances
[AD-A214297] N90-15558

PHOTOMETRICS, INC., WOBURN, MA.
Measurement of optical radiations in spacecraft environments
[AD-A213814] N90-15497

PISA UNIV. (ITALY).
Fatigue, fracture mechanics and corrosion properties of some aluminium-lithium alloys N90-15194

POLYTECHNIC UNIV., BROOKLYN, NY.
Array signal processing: New techniques for direction finding and spectrum estimation
[AD-A213883] N90-15345

POLYTECHNIC UNIV., FARMINGDALE, NY.
Scannable millimeter wave arrays, volume 1
[AD-A213895] N90-15347
Scannable millimeter wave arrays, volume 2
[AD-A213896] N90-15348

PRATT AND WHITNEY AIRCRAFT, WEST PALM BEACH, FL.
Thermal mechanical fatigue of coated blade materials
[AD-A214258] N90-15107

PRINCETON UNIV., NJ.
Nonlinear phenomena in computational transonic aeroelasticity N90-15070
Dynamics of baroclinic instability in rapid cyclogenesis N90-15563
Dynamics of mid-ocean ridge systems N90-15575
Electron-positron momentum distribution measurements of high-T superconductors and related systems
[DE90-002974] N90-15780
Pulsars lost and found: The second Princeton-Arecibo millisecond pulsar search N90-15865

PUERTO RICO UNIV., RIO PIEDRAS.
Relativistic self-consistent field studies of atoms and molecules
[AD-A214101] N90-15724

PURDUE UNIV., WEST LAFAYETTE, IN.
Gas-liquid-liquid equilibria in mixtures of water, light gases, and hydrocarbons
[DE90-003180] N90-15167

Q

QUESTEK, INC., CENTERPORT, NY.
See and avoid/cockpit visibility
[AD-A214214] N90-15084

R

READING UNIV. (ENGLAND).
Potential vorticity in extratropical cyclones N90-15564

RENSSELAER POLYTECHNIC INST., TROY, NY.
The effect of dissolved chlorine on the pitting behavior of 304L stainless steel in a 0.5 N NaCl solution
[AD-A213803] N90-15234
The effect of dissolved ozone on the corrosion behavior of Cu-30 Ni and 304L stainless steel in 0.5 N NaCl solutions
[AD-A213804] N90-15235
Research on mercury cadmium telluride
[AD-A213924] N90-15237

A novel heat resistant blend produced by compositional quenching: A thermoplastic polyimide impact modified with a fluoroelastomer
[AD-A213724] N90-15273

RICARDO-ITI, WESTMONT, IL.
Multi-dimensional modeling of convective heat transfer with application to I.C. engines
[DE90-003245] N90-15451

RICE UNIV., HOUSTON, TX.
Development of tunable excimer lasers
[AD-A213521] N90-15421

ROCHESTER UNIV., NY.
Centralized and decentralized Kalman filter techniques for tracking, navigation, and control
[AD-A214245] N90-15091
An architectural model of visual motion understanding
[AD-A214327] N90-15589
The implementation of a coherent memory abstraction on a NUMA (Non-Uniform Memory Access) multiprocessor: Experiences with PLATINUM (Platform for Investigating Non-Uniform Memory)
[AD-A213909] N90-15600
Memory management for large-scale NUMA (Non-Uniform Memory Access) multiprocessors
[AD-A213910] N90-15601
An overview of PLATINUM: A Platform for Investiga ting Non-Uniform Memory (preliminary version)
[AD-A213911] N90-15602
Evolution of an operating system for large-scale shared-memory multiprocessors
[AD-A213912] N90-15603
An overview of lynx
[AD-A213714] N90-15631
Principles and algorithms for causal reasoning with uncertainty
[AD-A214248] N90-15644
Hierarchical process composition: Dynamic maintenance of structure in a distributed environment
[AD-A214325] N90-15648
A structured connectionist approach to direct inferences and figurative adjective-noun combinations
[AD-A214326] N90-15649
Some computational properties of rotation representations
[AD-A213888] N90-15665
Gaze controls with interactions and delays
[AD-A214286] N90-15667
Nijenhuis tensor and integrable models
[DE90-001403] N90-15702

ROCKEFELLER UNIV., NEW YORK, NY.
Carboxyalkylated hemoglobin as a potential blood substitute
[AD-A213886] N90-15582

ROCKWELL INTERNATIONAL CORP., CANOGA PARK, CA.
Inorganic halogen oxidizers
[AD-A213990] N90-15294

ROCKWELL INTERNATIONAL CORP., THOUSAND OAKS, CA.
Fatigue behavior of vertical axis wind turbine airfoils with two weld configurations
[DE90-002628] N90-15525

ROME AIR DEVELOPMENT CENTER, GRIFFISS AFB, NY.
Proceedings of the Antenna Applications Symposium, volume 2
[AD-A213815] N90-15313
Knowledge based text generation
[AD-A214273] N90-15645

ROME UNIV. (ITALY).
Numerical optimization
[AD-A213758] N90-15683

ROYAL AEROSPACE ESTABLISHMENT, FARNBOROUGH (ENGLAND).
Corrosion and stress corrosion of aluminium-lithium alloys N90-15190
Current status of the application of conventional aluminium-lithium alloys and the potential for future developments N90-15203
Magnesium alloy technology for aerospace applications N90-15209

ROYAL AIRCRAFT ESTABLISHMENT, BEDFORD (ENGLAND).
Classification of windshear severity N90-15049
The assessment of visibility from automatic contrast Measurements N90-15061

ROYAL MILITARY COLL. OF SCIENCE, SHRIVENHAM (ENGLAND).
Interlaboratory comparison of radiation-induced attenuation in optical fibers. Part 3: Transient exposures
[DE90-000859] N90-15729

ROYAL NORWEGIAN COUNCIL FOR SCIENTIFIC AND INDUSTRIAL RESEARCH, KJELLER.
A multichannel processing approach to real time network detection, phase association, and threshold monitoring
[AD-A213940] N90-15657

ROYAL SIGNALS AND RADAR ESTABLISHMENT, MALVERN (ENGLAND).
On the privacy problems involved in allowing access to computers via the public telephone system
[RSRE-88006] N90-15303

RUTGERS - THE STATE UNIV., NEW BRUNSWICK, NJ.
On the analysis and optimization of a platform manipulator N90-15433

S

SANDIA NATIONAL LABS., ALBUQUERQUE, NM.
An experimental investigation of wall-interference effects for parachutes in closed wind tunnels
[DE90-001802] N90-15076
Autonomous land navigation in a structured environment
[DE90-001625] N90-15087
Geometric considerations for a waypoint guidance method
[DE90-001803] N90-15088
VIBRAFUGE: Combined vibration and centrifuge testing
[DE90-001091] N90-15114
Excitation lifetimes and excited-state forces in chemisorbed molecules
[DE90-002578] N90-15165
Comments on ER (Electrorheological) fluid rheology
[DE90-002892] N90-15166
Preparation and properties of icosahedral borides
[DE90-003574] N90-15180
Heat treatment of pulsed Nd: YAG laser welds in a Ti-14.8 wt pct Al-21.3 wt pct Nb titanium aluminide
[DE90-003484] N90-15228
The elastic properties of woven polymeric fabric
[DE89-015391] N90-15255
Characterization and in situ testing of diamond films
[DE90-003155] N90-15265
Studies of the adsorption/desorption behavior of explosive-like molecules
[DE90-001867] N90-15283
Shock-wave characterization of energetic booster-rocket propellant WAK-2 and its simulant UGS
[DE90-002633] N90-15285
Membrane and durability studies for the zinc/bromine battery
[DE89-016181] N90-15324
New devices using ferroelectric thin films
[DE90-000789] N90-15328
Single fluid simulations of plasma openings switch behavior
[DE90-002643] N90-15330
Overview on radiation effects in electronics
[DE90-000841] N90-15357
A nickel/hydrogen battery for PV systems
[DE90-001537] N90-15358
Sintering studies on high field varistors
[DE90-002626] N90-15359
Gelled propellant flow: Boundary layer theory for power-law fluids in a converging planar channel
[DE90-000923] N90-15365
Stand-off shields for hypervelocity particles
[DE89-016182] N90-15437
Fragmentation statistics from Eulerian hydrocode calculations
[DE90-002906] N90-15449
An iterative Bayes procedure for reliability assessment
[DE90-002106] N90-15466
Characterizing transient vibrations using band limited moments
[DE90-000799] N90-15473
Location of interior impact source in randomly excited structures
[DE90-001092] N90-15474
Analysis of catalytically enhanced solar absorption chemical reactors: 1 - numerical model description
[DE89-014742] N90-15505
High-efficiency silicon concentrator solar cells for use with prismatic covers
[DE90-002644] N90-15509
In-situ ion beam measurements of deuterium loading in thin foil electrochemical cells
[DE90-003162] N90-15511
Analysis of catalytically enhanced solar absorption chemical reactors. 2: Predicted characteristics of a 100 kW chemical reactor
[DE89-014743] N90-15521
Aerodynamic design and initial performance measurements for the SANDIA 34-metre diameter vertical-axis wind turbine
[DE90-002574] N90-15523
Structural response measurements and predictions for the SANDIA 34-meter test bed
[DE90-002575] N90-15524
Fatigue behavior of vertical axis wind turbine airfoils with two weld configurations
[DE90-002628] N90-15525
One-class generalization in second-order backpropagation networks for image classification
[DE89-015845] N90-15661
Outlier detection in multivariate calibration
[DE90-001502] N90-15672
Brownian trail rectified
[DE90-003339] N90-15706
Band-to-band transitions in poly (phenyl methyl silane)
[DE90-003575] N90-15720
Theoretical and computational studies of magnetic insulation and other plasma-opening-switch phenomena
[DE90-004421] N90-15757
Surface roughening of Ge(001) during 200 eV Xe ion bombardment and Ge molecular beam epitaxy
[DE90-000674] N90-15769
Cation disordering in the Tl-2122 superconductors
[DE90-003579] N90-15795
Superconductivity and stoichiometry in Tl2Ca2Ba2Cu3O(x) single crystals
[DE90-003838] N90-15801
Ion-irradiation effects in Tl2Ca2Ba2Cu3O10 superconductors
[DE90-003840] N90-15802
Power semiconductor devices for space nuclear power systems
[DE90-001178] N90-15819

SAO PAULO UNIV. (BRAZIL).
SL(2,R) current algebra in two-dimensional conformal quantum gravity
[DE90-600755] N90-15675

SCIENCE APPLICATIONS INTERNATIONAL CORP., NEW YORK, NY.
Current launch vehicle reliability practice and data base assessment. Volume 1: Executive summary and report body
[AD-A213600] N90-15121

SOLAREX CORP., NEWTOWN, PA.
Research on high-efficiency, single-junction, monolithic, thin-film amorphous silicon solar cells, phase 1
[DE89-009495] N90-15502
Research on high-efficiency, single-junction, monolithic, thin-film amorphous silicon solar cells, phase 2
[DE89-009496] N90-15503

SOUTH AFRICAN ASTRONOMICAL OBSERVATORY, CAPE TOWN.
The South African Astronomical Observatory
[NASA-CR-186258] N90-15856

SOUTHERN METHODIST UNIV., DALLAS, TX.
Spread spectrum mobile radio communications
[AD-A213726] N90-15311

SOUTHWEST RESEARCH INST., SAN ANTONIO, TX.
Simulation of radial expansion of an electron beam injected into a background plasma
[NASA-CR-186188] N90-15743

SPACE TELESCOPE SCIENCE INST., BALTIMORE, MD.
Shapes of star-gas waves in spiral galaxies
[NASA-CR-186289] N90-15859
The disk-halo connection and the nature of the interstellar medium
[NASA-CR-186286] N90-15860
Automated observation scheduling for the VLT
[NASA-CR-186282] N90-15861
Artificial intelligence approaches to astronomical observation scheduling
[NASA-CR-186277] N90-15862
Automated telescope scheduling
[NASA-CR-186279] N90-15863
The age of the galactic disk
[NASA-CR-186292] N90-15869
Recent progress in understanding the eruptions of classical novae
[NASA-CR-186280] N90-15870
The volatile composition of comets
[NASA-CR-186281] N90-15871

SPECTRA TECHNOLOGY, INC., BELLEVUE, WA.
Introduction to D-He(3) fusion reactors N90-15839

SPECTRAL SCIENCES, INC., BURLINGTON, MA.
HCl monitor, phase 2
[AD-A213572] N90-15542
MODTRAN: A moderate resolution model for LOWTRAN 7
[AD-A214337] N90-15650

SRI INTERNATIONAL CORP., MENLO PARK, CA.
NO2 photodissociation dynamics
[AD-A214422] N90-15560

STANFORD LINEAR ACCELERATOR CENTER, CA.
Canonical formalism for coupled beam optics
[DE90-003764] N90-15734
The digital data acquisition chain and the cosmic ray trigger system for the SLD warm iron calorimeter
[DE90-000943] N90-15879

STANFORD UNIV., CA.
Mechanical behavior of laminated composites at elevated temperatures N90-15141
Dynamics of a class of vortex rings N90-15362
On the identification of local minimizers in inertia-controlling methods for quadratic programming [DE89-017330] N90-15616
Sequential quadratic programming algorithms for optimization [DE90-000022] N90-15617
A basic theorem of complementarity for the generalized variational-like inequality problem [DE90-003102] N90-15620
The parallel decomposition of linear programs [DE90-003538] N90-15625
Likelihood ratio derivative estimators for stochastic systems [AD-A213787] N90-15684
Queues with negative arrivals [AD-A213860] N90-15687
Optimization of stochastic systems via simulation [AD-A214011] N90-15689
Phase equilibrium and crystal growth studies on AgGaSe2 and related nonlinear optical materials [AD-A213650] N90-15809

STATE UNIV. OF NEW YORK, ALBANY.
Research project on CO2-induced climate change [DE90-003531] N90-15538

STATE UNIV. OF NEW YORK, BUFFALO.
Observation of atomic relaxation near an interface through detection of emitted fluorescence [AD-A214308] N90-15725
Optical phonon modes in a double heterostructure of polar crystals [AD-A214208] N90-15816

STATE UNIV. OF NEW YORK, STONY BROOK.
Phase transition in polymer blends and structure of ionomers [DE90-003525] N90-15266
Near-infrared polarimetry and spectroscopy of comets N90-15857

STATE UNIV. OF NEW YORK AT BUFFALO, AMHERST.
Interface phonons in semiconductor double heterostructures [AD-A213732] N90-15810

SUPERFORM METALS LTD., WORCESTER (ENGLAND).
Superplastic performance and properties of the Lital Alloys N90-15199

SURVEILLANCE RESEARCH LAB., SALISBURY (AUSTRALIA).
Evaluation of a simple algorithm for estimating infrared signatures from multi-pixel to sub-pixel targets applied to AGA thermovision imagery [AD-A214103] N90-15639

SYDNEY UNIV. (AUSTRALIA).
Nonlinear strain-displacement relations for thin axisymmetric shells [PB89-226013] N90-15470

SYRACUSE UNIV., NY.
Network simulator definition [AD-A213463] N90-15308
Baseband development system implementation [AD-A213464] N90-15309
Photochemical solar energy conversion utilizing semiconductors localized in membrane mimetic systems [DE90-003450] N90-15515

SYRACUSE UNIV., UTICA, NY.
A comparative evaluation and analysis of end-user search performance in an academic environment N90-15845

SYSTEMS RESEARCH LABS., INC., DAYTON, OH.
Surface thermometry of energetic materials by laser-induced fluorescence [AD-A214423] N90-15297

T

TECHNISCHE UNIV., BRUNSWICK (GERMANY, F.R.).
Wind shear models for aircraft hazard investigation N90-15044
Influence of windshear, downdraft and turbulence on flight safety N90-15048

TECHNISCHE UNIV., DELFT (NETHERLANDS).
On the sum of two maximal monotone operators [REPT-89-31] N90-15669

TECHNISCHE UNIV., HANOVER (GERMANY, F.R.).
Measurements of horizontal visibility in the lowest 300 m over Northern Germany N90-15059

TENNESSEE UNIV., KNOXVILLE.
On the choice of trial function in theoretical calculations of the thermal conductivity [DE90-001733] N90-15182
Magnetic behavior of curium and americium-curium alloys [DE89-017808] N90-15213

TEST GROUP (6520TH), EDWARDS AFB, CA.
The United States Air Force approach to all-weather testing N90-15047

TEXAS A&M UNIV., COLLEGE STATION.
Ice induced aerodynamic performance degradation of rotorcraft: An overview N90-15063
A direct-inverse method for transonic and separated flows about airfoils [NASA-CR-4270] N90-15072
Damping characteristics of metal matrix composites [AD-A213712] N90-15151
Correlations between surface structure and catalytic activity/selectivity [DE90-003755] N90-15181
Electrochemical investigation of electronically conductive polymers [AD-A214019] N90-15277
Oxygen electrode in molten carbonate fuel cells [DE90-002871] N90-15510
Identification and quantification of synoptic structure in simulated Tiros N radiance soundings N90-15548
First results from the MACRO (Monopole, Astrophysics, Cosmic Ray Observatory) detector at the Gran Sasso Laboratory [DE90-003243] N90-15858

TEXAS INSTRUMENTS, INC., DALLAS.
Research on GaAs quantum-coupled structures that can be used as electron devices [AD-A214015] N90-15350

TEXAS UNIV., ARLINGTON.
Electronic and ionic transport in polymers [AD-A213410] N90-15270

TEXAS UNIV., AUSTIN.
Modeling and control of the rapid deployment of towed airborne devices N90-15092
Error modeling of bias-type parameters for TOPEX orbit determination N90-15117
Studies of organo phosphorus-, nitrogen-, and sulfur-containing molecules [AD-A213518] N90-15135
A study of impact damage in composite laminates N90-15137
The behavior of matter under nonequilibrium conditions: Fundamental aspects and applications [DE90-002522] N90-15157
Electrochemistry in near-critical and supercritical fluids. 8: Methyl viologen, decamethylferrocene, Os(bpy)3(sup 2+) and ferrocene in acetonitrile and the effect of pressure on diffusion coefficients under supercritical conditions [AD-A213407] N90-15172
Kinetic studies following state-selective laser excitation [DE90-003232] N90-15415
Geosat/ERM altimeter data analysis for the determination of global oceanic mesoscale variability N90-15492
Transport modeling and advanced computer techniques [DE90-001481] N90-15612
Architectural study of the design and operation of advanced force feedback manual controllers [NASA-CR-185948] N90-15664
Introduction to bifurcation theory [DE90-003319] N90-15673
Optimal periodic control and regulator theory based on the second variation N90-15704
The free energy of Maxwell-Vlasov equilibria [DE90-003318] N90-15705

TRANSPORTATION RESEARCH BOARD, WASHINGTON, DC.
Geotechnical instrumentation [PB89-198675] N90-15398

U

UNISYS CORP., PAOLI, PA.
MASC: Multiprocessor architecture for symbolic processing [AD-A213504] N90-15656

UNITED TECHNOLOGIES RESEARCH CENTER, EAST HARTFORD, CT.
Dispersion strengthening of high temperature niobium alloys [AD-A213829] N90-15236

UNIVERSIDADE ESTADUAL DE PAULISTA, SAO PAULO (BRAZIL).
SL(2,R) current algebra in two-dimensional conformal quantum gravity [DE90-600755] N90-15675

UNIVERSITY OF SOUTHERN CALIFORNIA, LOS ANGELES.
Research in knowledge-based vision techniques for the Autonomous Land Vehicle Program [AD-A213440] N90-15453
Research in optical interconnection techniques [AD-A214028] N90-15739

UNIVERSITY OF SOUTHERN CALIFORNIA, REDONDO BEACH.
Tools for simulation-based training [AD-A214307] N90-15646

UTAH STATE UNIV., LOGAN.
Fast algorithms for estimating mixture parameters [AD-A213869] N90-15636

UTAH UNIV., SALT LAKE CITY.
A logic for the pixel assignment step of imagery classification predicated on class structure N90-15493

V

VIRGINIA COMMONWEALTH UNIV., RICHMOND.
Compensation for peak shifts and variable background responses in fluorescence spectroscopy [DE90-001102] N90-15154

VIRGINIA POLYTECHNIC INST. AND STATE UNIV., BLACKSBURG.
Effect of modal truncation on derivatives of closed-loop damping ratios in structural control N90-15109
Fatigue loading history reconstruction based on the rain-flow technique [NASA-CR-181942] N90-15482

VIRGINIA UNIV., CHARLOTTESVILLE.
Effects of aeroelastic tailoring on anisotropic composite material beam models of helicopter blades [AD-A213478] N90-15095
Spatially-resolved, nonintrusive measurements in a nonreacting scramjet combustor using laser-induced iodine fluorescence N90-15103
Adaptive control of helicopter vibrations via the impulse response method [AD-A213728] N90-15113
Fatigue properties of SiC/Al composites N90-15138
The microstructure and properties of aluminum-lithium alloys N90-15187
The effects of Mo2C morphology and strain distribution on the fatigue properties of Fe-C-Mo dual-phase steels N90-15210
Thermal analysis of fixed and tilting pad journal bearings including cross-film viscosity variations and deformations N90-15429
The StarLite project [AD-A214193] N90-15642

VISTA RESEARCH CORP., MOUNTAIN VIEW, CA.
MF/HF multistatic mid-ocean radar experiments in support of SWOTHR (Surface-Wave Over-The-Horizon Radar) [AD-A213830] N90-15314

W

WASHINGTON STATE UNIV., PULLMAN.
Research on acoustical scattering, diffraction catastrophes, optics of bubbles, acoustical phase conjugation, and wake of an oscillating circular cylinder [AD-A214168] N90-15711

WASHINGTON UNIV., SAINT LOUIS, MO.
The role of attention in visual processing [AD-A214158] N90-15588

WASHINGTON UNIV., SEATTLE.
A compact acoustic recorder [AD-A213581] N90-15403
Global distribution of total cloud cover and cloud type amounts over the ocean [DE90-003187] N90-15574
Recurrence and ergodicity for exponential family state-space models [AD-A213466] N90-15677
Gas optics applicable to free electron laser technology [AD-A214285] N90-15741
Experiments on linear high beta helical axis stellarators to study simulated toroidal effects and Alfven-wave heating [DE90-001704] N90-15745

WEST VIRGINIA UNIV., MORGANTOWN.
Reduction of erosion in elbows due to flow modifications, phase 2 [DE89-011702] N90-15394

WESTINGHOUSE ELECTRIC CORP., PITTSBURGH, PA.
Advanced study in solid transport: Rheological behavior of dense suspension [DE90-003389] N90-15483

WESTINGHOUSE HANFORD CO., RICHLAND, WA.
Physical and Electrical Standards Laboratory general operating procedures [DE90-003515] N90-15116

WESTINGHOUSE SAVANNAH RIVER CO., AIKEN, SC.
Helium-induced weld cracking in irradiated 304 stainless steel [DE90-001312] N90-15219

Properties of aluminum-uranium alloys
[DE90-003889] N90-15243
Interaction of hydrogen in palladium as prescribed by the embedded atom method
[DE90-003893] N90-15244
Predicting the performance of ceramic filters by the use of silt density index
[DE90-001316] N90-15256
SIMON (SuperIntelligent Mobile Observing Navigator): A high-reliability robot for a radiation environment
[DE90-003888] N90-15460
An expert system for quality assurance (a.k.a.) QA Express
[DE90-003887] N90-15467
Procurement of an optical disk information storage and retrieval system
[DE90-001372] N90-15849

WESTLAND HELICOPTERS LTD., YEOVIL (ENGLAND).
Uses and properties of Al-Li on the new EH101 helicopter N90-15201

WISCONSIN UNIV., MADISON.
New transient algorithms for non-Newtonian flows
[AD-A213494] N90-15385
Quasi interpolants and approximation power of multivariate splines
[AD-A213535] N90-15678
Some results on connecting orbits for a class of Hamiltonian systems
[AD-A213536] N90-15679
Analysis of the financial factors governing the profitability of lunar helium-3 N90-15838
Importance of helium-3 for the future N90-15843

WISCONSIN UNIV., MILWAUKEE.
Bulk wave characterization of high T(sub c) superconductors
[AD-A214030] N90-15813

WRIGHT STATE UNIV., DAYTON, OH.
Use of lower body negative pressure as a countermeasure to negative Gz acceleration
[AD-A213927] N90-15583

Y

YALE UNIV., NEW HAVEN, CT.
Simultaneous multipoint measurements of density gradients and temperature in a flame
[DE90-001719] N90-15155
Oxygen and other atmospheric gases
[AD-A214296] N90-15557

YLINEN ELECTRONICS CO., ESPOO (NETHERLANDS).
The 22 GHz Radioastron receiver: Development of prototype components during the year 1988
[PB89-212583] N90-15323

Typical Contract Number Index Listing

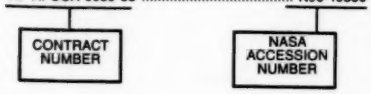

Listings in this index are arranged alphanumerically by contract number. Under each contract number the NASA accession numbers denoting documents that have been produced as a result of research done under that contract are arranged in ascending order. The NASA accession number denotes the number by which the citation is identified.

AF PROJ. ILIR N90-15312
AF PROJ. S321 ..... N90-15555
AF PROJ. 7A10 ..... N90-15558
AF PROJ. 1900 ..... N90-15106
N90-15291
AF PROJ. 2103 ..... N90-15131
AF PROJ. 2301 ..... N90-15425
AF PROJ. 2303 ..... N90-15296
N90-15560
AF PROJ. 2305 ..... N90-15311
N90-15343
N90-15347
N90-15348
N90-15811
AF PROJ. 2306 ..... N90-15807
AF PROJ. 2308 ..... N90-15132
N90-15297
N90-15387
N90-15761
AF PROJ. 2310 ..... N90-15557
AF PROJ. 2313 ..... N90-15680
AF PROJ. 2418 ..... N90-15232
N90-15486
AF PROJ. 2917 ..... N90-15124
AF PROJ. 3005 ..... N90-15542
AF PROJ. 3058 ..... N90-15121
AF PROJ. 3326 ..... N90-15737
AF PROJ. 3763 ..... N90-15321
AF PROJ. 4643 ..... N90-15559
AF PROJ. 7231 ..... N90-15583
AF PROJ. 7601 ..... N90-15127
N90-15128
AF PROJ. 7670 ..... N90-15496
N90-15650
AF-AFOSR-0031-87 ..... N90-15124
AF-AFOSR-0049-89 ..... N90-15676
AF-AFOSR-0119-86 ..... N90-15761
AF-AFOSR-0120-86 ..... N90-15425
AF-AFOSR-0140-86 ..... N90-15496
AF-AFOSR-0141-85 ..... N90-15385
AF-AFOSR-0190-84 ..... N90-15132
AF-AFOSR-0191-87 ..... N90-15385
AF-AFOSR-0201-86 ..... N90-15807
AF-AFOSR-0220-89 ..... N90-15385
AF-AFOSR-0239-88 ..... N90-15680
AF-AFOSR-0244-85 ..... N90-15387
AF-AFOSR-0309-82 ..... N90-15311
AF-AFOSR-0339-86 ..... N90-15343
AF-AFOSR-0389-84 ..... N90-15811
ARB-A6-201-33 ..... N90-15528
ARPA ORDER 5299 ..... N90-15556
ARPA ORDER 5307 ..... N90-15657
ARPA ORDER 5575 ..... N90-15458
ARPA ORDER 6037 ..... N90-15400
N90-15699
ARPA ORDER 6631 ..... N90-15178
ARPA ORDER 6671 ..... N90-15637
DA PROJ. 1C1-62622-A-552 ..... N90-15295
DA PROJ. 1L1-61101-A-91A N90-15572
DA PROJ. 1L1-62209-A-47-A N90-15434
DA PROJ. 1L1-62618-AH-80 ..... N90-15163
DA PROJ. 3E1-62720-A-835 ..... N90-15536
DA PROJ. 4A1-62731-AT-41 ..... N90-15456
DA PROJ. 4A1-62781-AT-45 ..... N90-15640
DAAB07-86-K-F073 ..... N90-15587
DAAB07-89-C-F404 ..... N90-15177
N90-15178
DAAE07-86-C-R013 ..... N90-15458
DAAG29-84-K-0066 ..... N90-15739
DAAG29-85-G-0118 ..... N90-15724
DAAH01-89-C-0418 ..... N90-15637
DAAK70-86-C-0123 ..... N90-15388
DAAL03-86-G-0026 ..... N90-15393
DAAL03-86-G-0037 ..... N90-15342
DAAL03-86-G-0043 ..... N90-15113
DAAL03-86-G-0055 ..... N90-15273
DAAL03-86-K-0016 ..... N90-15423
DAAL03-86-K-0054 ..... N90-15135
DAAL03-86-K-0066 ..... N90-15814
N90-15817
DAAL03-86-K-0072 ..... N90-15293
DAAL03-86-K-0085 ..... N90-15723
DAAL03-86-K-0087 ..... N90-15352
DAAL03-86-K-0094 ..... N90-15682
N90-15698
N90-15707
DAAL03-86-K-0110 ..... N90-15643
DAAL03-86-K-0111 ..... N90-15688
N90-15701
DAAL03-86-K-0132 ..... N90-15552
DAAL03-86-K-0138 ..... N90-15690
DAAL03-86-K-0161 ..... N90-15179
DAAL03-87-C-0009 ..... N90-15175
DAAL03-87-K-0030 ..... N90-15678
DAAL03-87-K-0036 ..... N90-15385
DAAL03-87-K-0043 ..... N90-15679
DAAL03-87-K-0078 ..... N90-15353
DAAL03-87-K-0080 ..... N90-15659
DAAL03-87-K-0106 ..... N90-15599
DAAL03-87-K-0124 ..... N90-15455
DAAL03-88-K-0051 ..... N90-15636
DAAL03-88-K-0063 ..... N90-15684
N90-15687
N90-15689
DAAL03-88-K-0086 ..... N90-15630
N90-15681
DACA76-85-C-0001 ..... N90-15091
N90-15589
N90-15600
N90-15601
N90-15602
N90-15603
N90-15631
N90-15648
N90-15665
N90-15667
DACA76-85-C-0009 ..... N90-15453
DAJA45-86-C-0028 ..... N90-15683
DAJA45-87-M-0484 ..... N90-15115
DAJA45-89-M-0187 ..... N90-15354
DAMD17-88-C-8169 ..... N90-15582
DARPA ORDER 9525 ..... N90-15274
DASG60-88-C-0014 ..... N90-15314
DE-AC01-84ER-51051 ..... N90-15753
DE-AC02-76CH-00016 ..... N90-15214
N90-15223
N90-15327
N90-15418
N90-15527
N90-15533
N90-15544
N90-15549
N90-15626
N90-15785
N90-15796
N90-15797
N90-15822
N90-15823
N90-15824
N90-15825
DE-AC02-76CH-03000 ..... N90-15596
N90-15609
N90-15867
DE-AC02-76ER-00881 ..... N90-15879
DE-AC02-76ER-03069 ..... N90-15879
DE-AC02-76ER-13065 ..... N90-15702
DE-AC02-83CH-10093 ..... N90-15498
N90-15499
N90-15502
N90-15503
N90-15504
N90-15512
N90-15513
N90-15519
N90-15520
DE-AC03-76SF-00098 ..... N90-15145
N90-15156
N90-15160
N90-15222
N90-15325
N90-15331
N90-15406
N90-15464
N90-15619
N90-15621
N90-15623
N90-15717
N90-15732
N90-15774
N90-15781
N90-15880
DE-AC03-76SF-00515 ..... N90-15734
N90-15879
DE-AC03-89ER-51114 ..... N90-15750
N90-15751
N90-15752
N90-15850
DE-AC04-76DP-00613 ..... N90-15159
N90-15299
N90-15300
N90-15335
DE-AC04-76DP-00789 ..... N90-15076
N90-15087
N90-15088
N90-15114
N90-15165
N90-15166
N90-15180
N90-15228
N90-15255
N90-15265
N90-15283
N90-15285
N90-15324
N90-15328
N90-15330
N90-15357
N90-15358
N90-15359
N90-15365
N90-15437
N90-15449
N90-15466
N90-15473
N90-15474
N90-15505
N90-15509
N90-15511
N90-15521
N90-15523
N90-15524
N90-15525
N90-15661
N90-15672
N90-15706
N90-15720
N90-15757
N90-15769
N90-15795
N90-15800
N90-15801
N90-15802
N90-15819
DE-AC04-86AL-33183 ..... N90-15451
DE-AC04-88DP-43495 ..... N90-15282
N90-15289
N90-15298

DE-AC05-84OR-21400 ..... N90-15136
N90-15143
N90-15169
N90-15182
N90-15212
N90-15215
N90-15216
N90-15217
N90-15218
N90-15220
N90-15224
N90-15226
N90-15248
N90-15249
N90-15250
N90-15251
N90-15254
N90-15279
N90-15287
N90-15356
N90-15367
N90-15371
N90-15436
N90-15462
N90-15479
N90-15500
N90-15506
N90-15507
N90-15526
N90-15532
N90-15537
N90-15540
N90-15543
N90-15565
N90-15611
N90-15651
N90-15652
N90-15653
N90-15663
N90-15695
N90-15744
N90-15746
N90-15747
N90-15756
N90-15767
N90-15771
N90-15773
N90-15798
N90-15799
DE-AC06-76RL-01830 ..... N90-15144
N90-15158
N90-15170
N90-15267
N90-15268
N90-15463
N90-15534
N90-15536
N90-15578
N90-15614
N90-15624
N90-15709
DE-AC06-87RL-10930 ..... N90-15116
DE-AC07-76ID-01570 ..... N90-15252
N90-15375
N90-15478
N90-15585
N90-15586
DE-AC09-76SR-00001 ..... N90-15244
N90-15460
DE-AC09-89SR-18035 ..... N90-15219
N90-15243
N90-15244
N90-15256
N90-15460
N90-15467
N90-15694
N90-15849
DE-AC21-84MC-21349 ..... N90-15394
DE-AC21-87MC-23270 ..... N90-15501
DE-AC22-87PC-79680 ..... N90-15662
DE-AC22-88PC-88827 ..... N90-15288
DE-AC22-88PC-88949 ..... N90-15483
DE-AC22-88PC-88951 ..... N90-15369
DE-AI05-84OR-21411 ..... N90-15271
DE-AI79-85BP-23169 ..... N90-15332
DE-AS05-81ER-40039 ..... N90-15858
DE-AS05-85ER-53193 ..... N90-15828
DE-FC22-83FE-60149 ..... N90-15280
DE-FG02-84ER-13288 ..... N90-15167
DE-FG02-84ER-45055 ..... N90-15787
DE-FG02-85ER-13427 ..... N90-15155
DE-FG02-85ER-60304 ..... N90-15531
DE-FG02-85ER-60314 ..... N90-15538
DE-FG02-86ER-13506 ..... N90-15515
DE-FG02-86ER-45237 ..... N90-15266
DE-FG02-87ER-13700 ..... N90-15719
DE-FG02-88ER-13914 ..... N90-15514
DE-FG02-88ER-13949 ..... N90-15484
DE-FG03-87ER-25028 ..... N90-15620
N90-15625
DE-FG03-87ER-25030 ..... N90-15616
N90-15617
N90-15625
DE-FG05-80ET-53088 ..... N90-15673
N90-15705
DE-FG05-84ER-13191 ..... N90-15415
DE-FG05-86ER-45259 ..... N90-15779
DE-FG05-88ER-13833 ..... N90-15154
DE-FG05-88ER-13834 ..... N90-15213
DE-FG05-88ER-13897 ..... N90-15157
DE-FG05-88ER-13954 ..... N90-15181
DE-FG05-88ER-53266 ..... N90-15612
DE-FG05-89ER-14003 ..... N90-15134
DE-FG06-87ER-53242 ..... N90-15745
DE-FG08-88ER-13945 ..... N90-15133
DE-FG22-87PC-79931 ..... N90-15510
DEW-88-24 ..... N90-15150
DNA001-87-C-0169 ..... N90-15852
DTFA01-80-Y-10524 ..... N90-15566
DTFA01-88-C-0020 ..... N90-15085
DTFA01-89-C-0001 ..... N90-15090
DTFA01-89-C-00001 ..... N90-15086
EPA-68-D6-0002 ..... N90-15529
FDA-224-79-5023 ..... N90-15246
FY1457-89-O-5004 ..... N90-15265
F04611-87-K-0067 ..... N90-15173
F04611-88-C-0014 ..... N90-15121
F04701-85-C-0086 ..... N90-15494
N90-15495
F04701-88-C-0089 ..... N90-15784
F08635-83-C-0136 ..... N90-15105
F08635-85-C-0122 ..... N90-15106
F08635-86-C-0137 ..... N90-15542
F08635-87-C-0130 ..... N90-15296
F19628-84-K-0025 ..... N90-15347
N90-15348
F19628-85-C-0002 ..... N90-15304
N90-15305
N90-15306
N90-15307
N90-15735
N90-15806
F19628-86-C-0079 ..... N90-15650
F19628-86-C-0214 ..... N90-15557
F19628-87-K-0019 ..... N90-15556
F19628-87-K-0024 ..... N90-15558
F19628-87-K-0025 ..... N90-15554
F19628-87-K-0045 ..... N90-15873
F19628-88-C-0070 ..... N90-15497
F29601-87-C-0059 ..... N90-15737
F30602-81-C-0169 ..... N90-15308
N90-15309
F30602-85-C-0008 ..... N90-15091
N90-15665
F30602-86-C-0093 ..... N90-15656
F33615-84-C-0066 ..... N90-15594
F33615-84-C-5027 ..... N90-15107
F33615-85-C-4503 ..... N90-15581
F33615-87-C-0012 ..... N90-15594
F33615-87-C-2777 ..... N90-15386
F49620-86-C-0009 ..... N90-15816
F49620-86-C-0053 ..... N90-15236
F49620-87-C-0040 ..... N90-15297
F49620-87-K-0004 ..... N90-15560
F49620-89-C-0038 ..... N90-15657
HCFA-500-87-0005 ..... N90-15579
IGA-88-6189-000-0051 ..... N90-15562
MCAIR PROJ. 7-220 ..... N90-15202
MDA903-86-C-0412 ..... N90-15593
MDA903-86-C-0414 ..... N90-15593
MDA903-86-C-0416 ..... N90-15593
MDA903-87-C-0523 ..... N90-15592
MDA972-88-C-0058 ..... N90-15099
MIPR-ATEC-88-86 ..... N90-15457
MIPR-FY1457-89-N-5014 ..... N90-15232
MIPR-FY7121-88-03752 ..... N90-15312
MIPR-117-89 ..... N90-15174
NAGW-1029 ..... N90-15873
NAGW-1231 ..... N90-15743
NAGW-1321 ..... N90-15826
NAGW-1340 ..... N90-15826
N90-15832
NAG1-397 ..... N90-15766
NAG1-664 ..... N90-15381
NAG1-822 ..... N90-15482
NAG2-541 ..... N90-15146
NAG2-593 ..... N90-15400
N90-15699
NAG3-600 ..... N90-15363
NAG3-712 ..... N90-15364
NAG3-811 ..... N90-15447
NAG9-320 ..... N90-15664
NASA ORDER C-3003-J N90-15506
NASW-4435 ..... N90-15435
NAS1-18027 ..... N90-15111
NAS1-18565 ..... N90-15654
NAS1-18605 ..... N90-15078
NAS2-12988 ..... N90-15093
NAS7-918 ..... N90-15263
NAS8-37756 ..... N90-15431
NCA2-266 ..... N90-15058
NCC1-109 ..... N90-15077
NCC2-231 ..... N90-15591
NCC2-371 ..... N90-15153
NSF ASC-87-15726 ..... N90-15613
NSF AST-88-22595 ..... N90-15826
NSF CCR-84-13211 ..... N90-15616
NSF CCR-86-11442 ..... N90-15604
N90-15666
NSF CCR-87-02403 ..... N90-15630
N90-15681
NSF CCR-87-04492 ..... N90-15600
N90-15602
NSF CHE-86-10809 ..... N90-15153
NSF CTS-89-10518 ..... N90-15385
NSF DCR-83-20136 ..... N90-15601
N90-15603
N90-15648
NSF DCR-84-20944 ..... N90-15630
NSF DCR-85-03662 ..... N90-15634
NSF DDM-88-14253 ..... N90-15625
NSF DDM-89-57825 ..... N90-15687
NSF DMC-86-17355 ..... N90-15489
N90-15490
N90-15647
NSF DMR-84-18718 ..... N90-15272
NSF DMR-88-09854 ..... N90-15789
NSF DMS-86-20303 ..... N90-15385
NSF DMS-87-01275 ..... N90-15678
NSF DMS-87-02070 ..... N90-15647
NSF DMS-87-12058 ..... N90-15385
NSF DMS-89-07264 ..... N90-15385
NSF DMS-89-13089 ..... N90-15625
NSF ECS-87-15153 ..... N90-15617
N90-15625
NSF IRI-88-02390 ..... N90-15489
N90-15490
NSF MCS-81-10556 ..... N90-15679
NSF MSM-88-17372 ..... N90-15293
NSF PHY-85-06686 ..... N90-15832
NSG-1174 ..... N90-15072
NSG-1419 ..... N90-15380
NSG-3188 ..... N90-15434
N00014-80-C-0197 ..... N90-15648
N00014-80-C-0807 ..... N90-15421
N00014-82-K-0193 ..... N90-15644
N90-15648
N90-15649
N00014-82-K-0612 ..... N90-15277
N00014-83-C-0531 ..... N90-15294
N00014-83-K-0125 ..... N90-15604
N90-15632
N90-15633
N90-15634
N90-15666
N90-15686
N00014-84-K-0099 ..... N90-15635
N00014-84-K-0113 ..... N90-15741
N00014-84-K-0428 ..... N90-15172
N00014-84-K-0610 ..... N90-15571
N00014-84-K-0655 ..... N90-15589
N90-15600
N90-15602
N90-15649
N00014-85-C-0141 ..... N90-15711
N00014-85-C-0857 ..... N90-15151
N00014-85-K-0151 ..... N90-15237
N00014-85-K-0168 ..... N90-15604
N90-15632
N90-15633
N90-15666
N90-15686
N00014-85-K-0649 ..... N90-15576
N00014-86-C-0587 ..... N90-15317
N00014-86-J-1218 ..... N90-15384
N00014-86-K-0043 ..... N90-15725
N90-15810
N90-15816
N00014-86-K-0054 ..... N90-15854
N00014-86-K-0153 ..... N90-15485
N00014-86-K-0245 ..... N90-15642
N00014-86-K-0281 ..... N90-15489
N90-15490
N90-15647
N00014-86-K-0343 ..... N90-15809
N00014-86-K-0417 ..... N90-15344
N00014-86-K-0769 ..... N90-15270
N00014-87-C-0489 ..... N90-15646

N00014-87-C-0700 ..... N90-15350
N00014-87-C-2013 ..... N90-15736
N00014-87-K-0099 ..... N90-15272
N00014-87-K-0142 ..... N90-15616
N90-15617
N90-15625
N00014-87-K-0284 ..... N90-15685
N00014-87-K-0422 ..... N90-15384
N00014-87-K-0531 ..... N90-15238
N90-15276
N00014-87-K-0825 ..... N90-15351
N90-15598
N90-15658
N00014-88-C-0391 ..... N90-15341
N00014-88-C-0512 ..... N90-15274
N00014-88-C-0714 ..... N90-15818
N00014-88-K-0046 ..... N90-15813
N00014-88-K-0059 ..... N90-15854
N00014-88-K-0134 ..... N90-15679
N00014-88-K-0215 ..... N90-15452
N00014-88-K-0265 ..... N90-15677
N00014-88-K-0525 ..... N90-15812
N00014-88-K-0579 ..... N90-15606
N00014-88-K-0591 ..... N90-15489
N90-15490
N90-15647
N00014-89-C-0207 ..... N90-15346
N00014-89-J-1051 ..... N90-15676
N00014-89-J-1125 ..... N90-15234
N90-15235
N00014-89-J-1158 ..... N90-15638
N00014-89-J-1278 ..... N90-15721
N90-15722
N00014-89-J-1311 ..... N90-15815
N00014-89-J-1426 ..... N90-15588
N00014-89-J-1512 ..... N90-15345
N00014-89-J-1581 ..... N90-15392
N00014-89-J-1659 ..... N90-15625
N00014-89-J-1788 ..... N90-15685
N00014-89-J-1836 ..... N90-15713
N00014-89-J-1867 ..... N90-15465
N00014-89-J-1988 ..... N90-15666
N00014-89-J-3054 ..... N90-15488
N00014-89-WR-24017 ..... N90-15834
N00039-88-C-0051 ..... N90-15391
N00039-89-C-5301 ..... N90-15349
N00140-87-C-8904 ..... N90-15400
N90-15699
N00228-85-G-3247 ..... N90-15605
N00228-89-G-0580 ..... N90-15231
N90-15382
N90-15383
N90-15518
N90-15627
RR0-1107 ..... N90-15421
SERI-XB-6-06005-3 ..... N90-15817
SRI PROJ. PYU-2891 ..... N90-15560
W-31-109-ENG-38 ..... N90-15171
N90-15221
N90-15229
N90-15241
N90-15242
N90-15253
N90-15269
N90-15329
N90-15336
N90-15338
N90-15339
N90-15370
N90-15419
N90-15508
N90-15516
N90-15517
N90-15539
N90-15541
N90-15595
N90-15613
N90-15618
N90-15718
N90-15758
N90-15765
N90-15776
N90-15777
N90-15778
N90-15779
N90-15788
N90-15789
N90-15790
N90-15791
N90-15792
N90-15793
N90-15794
N90-15800
N90-15821
N90-15827
W-7405-ENG-36 ..... N90-15150
N90-15168
N90-15264
N90-15326
N90-15396
N90-15408
N90-15414
N90-15416
N90-15438
N90-15439
N90-15440
N90-15450
N90-15522
N90-15580
N90-15610
N90-15670
N90-15696
N90-15700
N90-15726
N90-15728
N90-15754
N90-15764
N90-15768
N90-15782
N90-15820
N90-15876
N90-15877
W-7405-ENG-48 ..... N90-15118
N90-15119
N90-15122
N90-15123
N90-15149
N90-15164
N90-15247
N90-15257
N90-15258
N90-15281
N90-15286
N90-15290
N90-15301
N90-15333
N90-15334
N90-15337
N90-15340
N90-15366
N90-15368
N90-15376
N90-15377
N90-15406
N90-15407
N90-15409
N90-15410
N90-15411
N90-15412
N90-15413
N90-15417
N90-15419
N90-15420
N90-15428
N90-15448
N90-15461
N90-15475
N90-15476
N90-15535
N90-15550
N90-15597
N90-15615
N90-15655
N90-15729
N90-15731
N90-15748
N90-15749
N90-15755
N90-15770
N90-15772
N90-15780
N90-15786
N90-15872
W31RPD-9-D5007 ..... N90-15407
W7405-ENG-48 ..... N90-15131
199-61-12 ..... N90-15591
486-14-06-01 ..... N90-15120
505-61-01 ..... N90-15399
505-61-01-05 ..... N90-15401
505-61-21-03 ..... N90-15072
505-61-51 ..... N90-15093
505-62-01 ..... N90-15112
505-63-01-05 ..... N90-15482
505-63-51 ..... N90-15434
505-66-01-02 ..... N90-15110
505-66-41-41 ..... N90-15108
505-66-41-43 ..... N90-15111
505-66-71 ..... N90-15100
505-67-01-02 ..... N90-15101
505-67-21 ..... N90-15102
505-90-00 ..... N90-15848
505-90-21-01 ..... N90-15078
506-44-21 ..... N90-15211
506-47-11 ..... N90-15577
549-03-31-03 ..... N90-15654
591-23-00 ..... N90-15622
676-59-33 ..... N90-15545

REPORT/ACCESSION NUMBER INDEX

Typical Report Number Index Listing

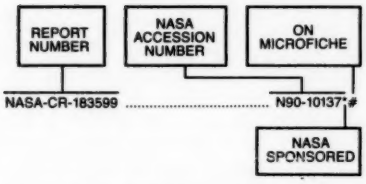

Listings in this index are arranged alphanumerically by report number. The NASA accession number denotes the number by which the citation is identified. An asterisk (*) indicates that the item is a NASA report. A pound sign (#) indicates that the item is available on microfiche.

A-89163 ..... N90-15399* #
A-89242 ..... N90-15577* #

AAMRL-TR-89-025 ..... N90-15583 #

AD-A213400 ..... N90-15230 #
AD-A213403 ..... N90-15304 #
AD-A213404 ..... N90-15735 #
AD-A213405 ..... N90-15806 #
AD-A213406 ..... N90-15341 #
AD-A213407 ..... N90-15172 #
AD-A213410 ..... N90-15270 #
AD-A213427 ..... N90-15676 #
AD-A213430 ..... N90-15382 #
AD-A213431 ..... N90-15383 #
AD-A213433 ..... N90-15452 #
AD-A213434 ..... N90-15587 #
AD-A213437 ..... N90-15305 #
AD-A213438 ..... N90-15306 #
AD-A213439 ..... N90-15307 #
AD-A213440 ..... N90-15453 #
AD-A213449 ..... N90-15581 #
AD-A213450 ..... N90-15721 #
AD-A213453 ..... N90-15518 #
AD-A213456 ..... N90-15592 #
AD-A213460 ..... N90-15627 #
AD-A213463 ..... N90-15308 #
AD-A213464 ..... N90-15309 #
AD-A213465 ..... N90-15384 #
AD-A213466 ..... N90-15677 #
AD-A213478 ..... N90-15095 #
AD-A213479 ..... N90-15310 #
AD-A213491 ..... N90-15402 #
AD-A213493 ..... N90-15881 #
AD-A213494 ..... N90-15385 #
AD-A213499 ..... N90-15628 #
AD-A213503 ..... N90-15629 #
AD-A213504 ..... N90-15656 #
AD-A213509 ..... N90-15485 #
AD-A213511 ..... N90-15722 #
AD-A213513 ..... N90-15096 #
AD-A213518 ..... N90-15135 #
AD-A213521 ..... N90-15421 #
AD-A213531 ..... N90-15105 #
AD-A213532 ..... N90-15231 #
AD-A213535 ..... N90-15678 #
AD-A213536 ..... N90-15679 · #
AD-A213540 ..... N90-15271 #
AD-A213543 ..... N90-15593 #
AD-A213545 ..... N90-15486 #
AD-A213548 ..... N90-15232 #
AD-A213549 ..... N90-15873* #
AD-A213551 ..... N90-15807 #
AD-A213554 ..... N90-15723 #
AD-A213555 ..... N90-15707 #
AD-A213557 ..... N90-15291 #
AD-A213566 ..... N90-15106 #
AD-A213572 ..... N90-15542 #
AD-A213575 ..... N90-15386 #
AD-A213581 ..... N90-15403 #
AD-A213592 ..... N90-15272 #

AD-A213600 ..... N90-15121 #
AD-A213605 ..... N90-15808 #
AD-A213609 ..... N90-15342 #
AD-A213610 ..... N90-15698 #
AD-A213618 ..... N90-15552 #
AD-A213622 ..... N90-15568 #
AD-A213627 ..... N90-15680 #
AD-A213642 ..... N90-15681 #
AD-A213643 ..... N90-15630 #
AD-A213644 ..... N90-15569 #
AD-A213650 ..... N90-15809 #
AD-A213651 ..... N90-15173 #
AD-A213652 ..... N90-15097 #
AD-A213655 ..... N90-15124 #
AD-A213656 ..... N90-15343 #
AD-A213671 ..... N90-15387 #
AD-A213679 ..... N90-15761 #
AD-A213703 ..... N90-15682 #
AD-A213712 ..... N90-15151 #
AD-A213714 ..... N90-15631 #
AD-A213717 ..... N90-15494 #
AD-A213723 ..... N90-15174 #
AD-A213724 ..... N90-15273 #
AD-A213726 ..... N90-15311 #
AD-A213728 ..... N90-15113 #
AD-A213729 ..... N90-15553 #
AD-A213730 ..... N90-15495 #
AD-A213732 ..... N90-15810 #
AD-A213740 ..... N90-15811 #
AD-A213742 ..... N90-15274 #
AD-A213756 ..... N90-15388 #
AD-A213758 ..... N90-15683 #
AD-A213777 ..... N90-15632 #
AD-A213785 ..... N90-15175 #
AD-A213787 ..... N90-15684 #
AD-A213789 ..... N90-15454 #
AD-A213790 ..... N90-15598 #
AD-A213791 ..... N90-15633 #
AD-A213800 ..... N90-15389 #
AD-A213801 ..... N90-15233 #
AD-A213802 ..... N90-15312 #
AD-A213803 ..... N90-15234 #
AD-A213804 ..... N90-15235 #
AD-A213805 ..... N90-15554 #
AD-A213806 ..... N90-15555 #
AD-A213807 ..... N90-15685 #
AD-A213808 ..... N90-15686 #
AD-A213811 ..... N90-15496 #
AD-A213813 ..... N90-15556 #
AD-A213814 ..... N90-15497 #
AD-A213815 ..... N90-15313 #
AD-A213817 ..... N90-15487 #
AD-A213825 ..... N90-15275 #
AD-A213828 ..... N90-15634 #
AD-A213829 ..... N90-15236 #
AD-A213830 ..... N90-15314 #
AD-A213835 ..... N90-15422 #
AD-A213837 ..... N90-15176 #
AD-A213841 ..... N90-15570 #
AD-A213842 ..... N90-15708 #
AD-A213843 ..... N90-15390 #
AD-A213856 ..... N90-15344 #
AD-A213857 ..... N90-15292 #
AD-A213859 ..... N90-15293 #
AD-A213860 ..... N90-15687 #
AD-A213863 ..... N90-15635 #
AD-A213864 ..... N90-15488 #
AD-A213869 ..... N90-15636 #
AD-A213870 ..... N90-15701 #
AD-A213871 ..... N90-15599 #
AD-A213874 ..... N90-15391 #
AD-A213875 ..... N90-15276 #
AD-A213882 ..... N90-15571 #
AD-A213883 ..... N90-15345 #
AD-A213885 ..... N90-15346 #
AD-A213886 ..... N90-15582 #
AD-A213888 ..... N90-15665 #
AD-A213895 ..... N90-15347 #
AD-A213896 ..... N90-15348 #
AD-A213902 ..... N90-15315 #
AD-A213909 ..... N90-15600 #
AD-A213910 ..... N90-15601 #
AD-A213911 ..... N90-15602 #

AD-A213912 ..... N90-15603 #
AD-A213921 ..... N90-15812 #
AD-A213924 ..... N90-15237 #
AD-A213925 ..... N90-15349 #
AD-A213926 ..... N90-15736 #
AD-A213927 ..... N90-15583 #
AD-A213928 ..... N90-15083 #
AD-A213935 ..... N90-15604 #
AD-A213938 ..... N90-15737 #
AD-A213940 ..... N90-15657 #
AD-A213944 ..... N90-15238 #
AD-A213953 ..... N90-15404 #
AD-A213966 ..... N90-15658 #
AD-A213967 ..... N90-15666 #
AD-A213986 ..... N90-15637 #
AD-A213990 ..... N90-15294 #
AD-A213994 ..... N90-15688 #
AD-A213999 ..... N90-15738 #
AD-A214004 ..... N90-15852 #
AD-A214009 ..... N90-15131 #
AD-A214010 ..... N90-15762 #
AD-A214011 ..... N90-15689 #
AD-A214013 ..... N90-15125 #
AD-A214014 ..... N90-15392 #
AD-A214015 ..... N90-15350 #
AD-A214019 ..... N90-15277 #
AD-A214028 ..... N90-15739 #
AD-A214030 ..... N90-15813 #
AD-A214035 ..... N90-15351 #
AD-A214047 ..... N90-15638 #
AD-A214051 ..... N90-15177 #
AD-A214095 ..... N90-15393 #
AD-A214097 ..... N90-15352 #
AD-A214098 ..... N90-15455 #
AD-A214099 ..... N90-15814 #
AD-A214100 ..... N90-15659 #
AD-A214101 ..... N90-15724 #
AD-A214102 ..... N90-15690 #
AD-A214103 ..... N90-15639 #
AD-A214105 ..... N90-15126 #
AD-A214135 ..... N90-15489 #
AD-A214136 ..... N90-15490 #
AD-A214137 ..... N90-15316 #
AD-A214140 ..... N90-15079 #
AD-A214141 ..... N90-15115 #
AD-A214146 ..... N90-15423 #
AD-A214147 ..... N90-15853 #
AD-A214149 ..... N90-15740 #
AD-A214158 ..... N90-15588 #
AD-A214163 ..... N90-15090 #
AD-A214168 ..... N90-15711 #
AD-A214170 ..... N90-15456 #
AD-A214171 ..... N90-15640 #
AD-A214173 ..... N90-15605 #
AD-A214176 ..... N90-15606 #
AD-A214181 ..... N90-15457 #
AD-A214183 ..... N90-15641 #
AD-A214185 ..... N90-15834 #
AD-A214192 ..... N90-15815 #
AD-A214193 ..... N90-15642 #
AD-A214194 ..... N90-15854 #
AD-A214195 ..... N90-15424 #
AD-A214198 ..... N90-15660 #
AD-A214199 ..... N90-15353 #
AD-A214201 ..... N90-15295 #
AD-A214202 ..... N90-15572 #
AD-A214204 ..... N90-15127 #
AD-A214205 ..... N90-15128 #
AD-A214208 ..... N90-15816 #
AD-A214212 ..... N90-15178 #
AD-A214214 ..... N90-15084 #
AD-A214215 ..... N90-15817 #
AD-A214218 ..... N90-15129 #
AD-A214242 ..... N90-15458 #
AD-A214243 ..... N90-15317 #
AD-A214244 ..... N90-15080 #
AD-A214245 ..... N90-15091 #
AD-A214246 ..... N90-15179 #
AD-A214247 ..... N90-15643 #
AD-A214248 ..... N90-15644 #
AD-A214250 ..... N90-15573 #
AD-A214251 ..... N90-15818 #
AD-A214257 ..... N90-15459 #

AD-A214258 ..... N90-15107 #
AD-A214272 ..... N90-15594 #
AD-A214273 ..... N90-15645 #
AD-A214278 ..... N90-15576 #
AD-A214285 ..... N90-15741 #
AD-A214286 ..... N90-15667 #
AD-A214287 ..... N90-15318 #
AD-A214288 ..... N90-15763 #
AD-A214289 ..... N90-15319 #
AD-A214290 ..... N90-15239 #
AD-A214293 ..... N90-15712 #
AD-A214295 ..... N90-15098 #
AD-A214296 ..... N90-15557 #
AD-A214297 ..... N90-15558 #
AD-A214298 ..... N90-15320 #
AD-A214307 ..... N90-15646 #
AD-A214308 ..... N90-15725 #
AD-A214324 ..... N90-15647 #
AD-A214325 ..... N90-15648 #
AD-A214326 ..... N90-15649 #
AD-A214327 ..... N90-15589 #
AD-A214337 ..... N90-15850 #
AD-A214338 ..... N90-15844 #
AD-A214400 ..... N90-15559* #
AD-A214402 ..... N90-15465 #
AD-A214406 ..... N90-15354 #
AD-A214408 ..... N90-15855 #
AD-A214411 ..... N90-15296 #
AD-A214412 ..... N90-15099 #
AD-A214420 ..... N90-15132 #
AD-A214421 ..... N90-15425 #
AD-A214422 ..... N90-15560 #
AD-A214423 ..... N90-15297 #
AD-A214445 ..... N90-15668 #
AD-A214448 ..... N90-15713 #
AD-A214452 ..... N90-15085 #
AD-A214453 ..... N90-15321 #

AD-D014300 ..... N90-15278 #
AD-D014301 ..... N90-15426 #
AD-D014302 ..... N90-15427 #
AD-D014303 ..... N90-15355 #
AD-D014304 ..... N90-15405 #
AD-D014306 ..... N90-15322 #
AD-D014308 ..... N90-15240 #
AD-D014309 ..... N90-15607 #

AD-E501157 ..... N90-15172 #
AD-E501157 ..... N90-15230 #
AD-E501157 ..... N90-15270 #
AD-E501157 ..... N90-15304 #
AD-E501157 ..... N90-15341 #
AD-E501157 ..... N90-15735 #
AD-E501157 ..... N90-15806 #
AD-E951392 ..... N90-15740 #

AFATL-TR-89-55 ..... N90-15296 #

AFESC/ESL-TR-87-51 ..... N90-15291 #
AFESC/ESL-TR-88-31 ..... N90-15105 #
AFESC/ESL-TR-88-37 ..... N90-15131 #
AFESC/ESL-TR-88-50 ..... N90-15106 #
AFESC/ESL-TR-88-51-PHASE-2 ..... N90-15542 #

AFFTC-TR-89-27 ..... N90-15096 #

AFGL-ERP-1021 ..... N90-15559* #

AFGL-TR-89-0043 ..... N90-15559* #
AFGL-TR-89-0064 ..... N90-15557 #

AFHRL-TR-89-22 ..... N90-15594 #

AFIT/CI/CIA-88-228 ..... N90-15097 #
AFIT/CI/CIA-88-229 ..... N90-15569 #
AFIT/CI/CIA-88-230 ..... N90-15553 #
AFIT/CI/CIA-88-231 ..... N90-15568 #

AFIT/GAE/AA/88D-37 ..... N90-15390 #

AFOSR-89-1150TR ..... N90-15811 #
AFOSR-89-1265TR ..... N90-15124 #
AFOSR-89-1266TR ..... N90-15343 #
AFOSR-89-1267TR ..... N90-15236 #
AFOSR-89-1273TR ..... N90-15680 #
AFOSR-89-1275TR ..... N90-15761 #
AFOSR-89-1280TR ..... N90-15807 #
AFOSR-89-1284TR ..... N90-15387 #
AFOSR-89-1286TR ..... N90-15311 #
AFOSR-89-1337TR ..... N90-15425 #
AFOSR-89-1338TR ..... N90-15560 #
AFOSR-89-1343TR ..... N90-15132 #
AFOSR-89-1351TR ..... N90-15297 #

AGARD-CP-444 ..... N90-15185 #
AGARD-CP-470 ..... N90-15041 #

AL-TR-89-013-VOL-1 ..... N90-15121 #
AL-TR-89-015 ..... N90-15173 #
AL-TR-89-053 ..... N90-15762 #

AMSMI/TR-RD-GC-89-17 ..... N90-15740 #

ANL-89/12 ..... N90-15595 #
ANL-89/28 ..... N90-15508 #

ANL/FPP/TM-244 ..... N90-15758 #

ANL/PPRNT-89-185 ..... N90-15777 #
ANL/PPRNT-89-197 ..... N90-15779 #
ANL/PPRNT-89-199 ..... N90-15778 #

ARB-R-89/402 ..... N90-15528 #

ARI-RN-89-41 ..... N90-15592 #

ARO-21178.15-PH ..... N90-15175 #
ARO-21739.6-PH-A ..... N90-15739 #
ARO-22983.17-CH-H ..... N90-15724 #
ARO-23241.8-PH ..... N90-15423 #
ARO-23297.10-EG ..... N90-15293 #
ARO-23397.14-EL ..... N90-15352 #
ARO-23520.15-EL ..... N90-15817 #
ARO-23520.17-EL ..... N90-15814 #
ARO-23570.23-PH ..... N90-15723 #
ARO-23591.11-CH ..... N90-15135 #
ARO-23699.23-MA ..... N90-15698 #
ARO-23699.24-MA ..... N90-15707 #
ARO-23699.25-MA ..... N90-15682 #
ARO-23761.2-EG-F ..... N90-15113 #
ARO-23770.1-MAF ..... N90-15393 #
ARO-23780.1-CH-F ..... N90-15342 #
ARO-23797.2-MS-F ..... N90-15273 #
ARO-23900.9-GS ..... N90-15552 #
ARO-24007.8-PH ..... N90-15179 #
ARO-24116.13-EL ..... N90-15659 #
ARO-24370.20-MA-SDI ..... N90-15701 #
ARO-24370.38-MA-SDI ..... N90-15688 #
ARO-24371.11-MA-SDI ..... N90-15643 #
ARO-24409.3-MA ..... N90-15690 #
ARO-24923.4-MA ..... N90-15681 #
ARO-24923.5-MA ..... N90-15630 #
ARO-25170.14-EG ..... N90-15455 #
ARO-25173.20-EL ..... N90-15599 #
ARO-25333.5-MA-SDI ..... N90-15636 #
ARO-25664.5-CH ..... N90-15174 #
ARO-25839.16-MA ..... N90-15684 #
ARO-25839.17-MA ..... N90-15687 #
ARO-25839.18-MA ..... N90-15689 #

ASI690-322-89 ..... N90-15592 #

ATR-89(4752)-1 ..... N90-15784 #

BNL-43066 ..... N90-15626 #
BNL-43068 ..... N90-15823 #
BNL-43107 ..... N90-15785 #
BNL-43108 ..... N90-15223 #
BNL-43137 ..... N90-15822 #
BNL-43240 ..... N90-15533 #
BNL-43296 ..... N90-15214 #
BNL-43306 ..... N90-15418 #
BNL-43328 ..... N90-15327 #
BNL-43361 ..... N90-15549 #
BNL-43407 ..... N90-15796 #
BNL-43426 ..... N90-15527 #
BNL-43461 ..... N90-15797 #
BNL-43462 ..... N90-15825 #
BNL-43550 ..... N90-15544 #
BNL-43576 ..... N90-15824 #

BRA-89-342R ..... N90-15409 #

BRL-MR-3791 ..... N90-15389 #

BRL-TR-2987 ..... N90-15163 #
BRL-TR-3032 ..... N90-15176 #
BRL-TR-3055 ..... N90-15292 #

BR106837 ..... N90-15303 #

CERL-TR-E-89/15 ..... N90-15640 #

CERL-TR-M-89/15 ..... N90-15275 #
CERL-TR-M-90/03 ..... N90-15456 #

CESAR-89/33 ..... N90-15652 #

CMR-89-6 ..... N90-15809 #

CMS-TSR-90-12 ..... N90-15678 #
CMS-TSR-90-14 ..... N90-15385 #
CMS-TSR-90-17 ..... N90-15679 #

CMU-DARPA/SEMI/1089 ..... N90-15637 #

CMU-RI-TR-88-17 ..... N90-15447* #

CONF-880139-5 ..... N90-15375 #
CONF-881058-5 ..... N90-15585 #
CONF-881058-7 ..... N90-15586 #
CONF-890415-8 ..... N90-15609 #
CONF-890426-31 ..... N90-15268 #
CONF-890426-32 ..... N90-15171 #
CONF-890520-3 ..... N90-15872 #
CONF-890522-6 ..... N90-15436 #
CONF-890701-13 ..... N90-15222 #
CONF-890701-19 ..... N90-15331 #
CONF-890710-22 ..... N90-15333 #
CONF-890718-REV-1 ..... N90-15780 #
CONF-890756-4 ..... N90-15412 #
CONF-890770-7 ..... N90-15269 #
CONF-890802-8 ..... N90-15327 #
CONF-890811-39 ..... N90-15281 #
CONF-890812-8 ..... N90-15437 #
CONF-890812-59 ..... N90-15772 #
CONF-890812-62 ..... N90-15119 #
CONF-890820-5 ..... N90-15221 #
CONF-890836-18 ..... N90-15731 #
CONF-890836-19 ..... N90-15413 #
CONF-890841-2 ..... N90-15533 #
CONF-890926-3 ..... N90-15286 #
CONF-890930-3 ..... N90-15858 #
CONF-890939-2 ..... N90-15776 #
CONF-891007-24 ..... N90-15746 #
CONF-891007-30 ..... N90-15747 #
CONF-891007-91 ..... N90-15850 #
CONF-891007-93 ..... N90-15750 #
CONF-891007-94 ..... N90-15751 #
CONF-891007-95 ..... N90-15752 #
CONF-891013-9 ..... N90-15136 #
CONF-891024-2 ..... N90-15220 #
CONF-891024-3 ..... N90-15219 #
CONF-891024-4 ..... N90-15709 #
CONF-891036-2 ..... N90-15253 #
CONF-891052-1 ..... N90-15726 #
CONF-891080-1 ..... N90-15541 #
CONF-891087-5 ..... N90-15773 #
CONF-891093-8 ..... N90-15769 #
CONF-891093-15 ..... N90-15797 #
CONF-891093-16 ..... N90-15825 #
CONF-891094-4 ..... N90-15626 #
CONF-891098-4 ..... N90-15540 #
CONF-891103-24 ..... N90-15212 #
CONF-891103-28 ..... N90-15694 #
CONF-891103-48 ..... N90-15168 #
CONF-891103-58 ..... N90-15170 #
CONF-891113-3 ..... N90-15672 #
CONF-891113-7 ..... N90-15377 #
CONF-891113-8 ..... N90-15517 #
CONF-891113-9 ..... N90-15516 #
CONF-891116-1 ..... N90-15143* #
CONF-891117-3 ..... N90-15214 #
CONF-891117-6 ..... N90-15223 #
CONF-891117-10 ..... N90-15788 #
CONF-891117-11 ..... N90-15796 #
CONF-891119-1 ..... N90-15767 #
CONF-891119-5 ..... N90-15504 #
CONF-891119-7 ..... N90-15706 #
CONF-891119-8 ..... N90-15511 #
CONF-891119-11 ..... N90-15782 #
CONF-891119-16 ..... N90-15792 #
CONF-891119-17 ..... N90-15793 #
CONF-891119-19 ..... N90-15789 #
CONF-891119-21 ..... N90-15720 #
CONF-891119-22 ..... N90-15795 #
CONF-891119-24 ..... N90-15790 #
CONF-891119-26 ..... N90-15791 #
CONF-891119-27 ..... N90-15799 #
CONF-891119-32 ..... N90-15802 #
CONF-891119-33 ..... N90-15801 #
CONF-891119-35 ..... N90-15824 #
CONF-891119-36 ..... N90-15823 #
CONF-891132-4 ..... N90-15324 #
CONF-891132-6 ..... N90-15325 #
CONF-891132-8 ..... N90-15329 #
CONF-891137-1 ..... N90-15822 #
CONF-891149-4 ..... N90-15610 #
CONF-891149-8 ..... N90-15613 #
CONF-891152-2 ..... N90-15473 #
CONF-891152-4 ..... N90-15474 #
CONF-891152-5 ..... N90-15114 #
CONF-891153-1 ..... N90-15247 #
CONF-891163-1 ..... N90-15267 #
CONF-891192-16 ..... N90-15849 #
CONF-891192-22 ..... N90-15467 #
CONF-891192-23 ..... N90-15460 #
CONF-891192-24 ..... N90-15244 #
CONF-891202-8 ..... N90-15526 #
CONF-891204-3 ..... N90-15226 #

CONF-891205-1 ..... N90-15328 #
CONF-891205-2 ..... N90-15786 #
CONF-891206-1 ..... N90-15287 #
CONF-891208-1 ..... N90-15254 #
CONF-891208-3 ..... N90-15224 #
CONF-891208-4 ..... N90-15505 #
CONF-891208-5-2 ..... N90-15521 #
CONF-891208-6 ..... N90-15506* #
CONF-891208-7 ..... N90-15370 #
CONF-891208-9 ..... N90-15475 #
CONF-891208-10 ..... N90-15371 #
CONF-891208-12 ..... N90-15440 #
CONF-891208-17 ..... N90-15507 #
CONF-891208-24 ..... N90-15299 #
CONF-891208-25 ..... N90-15464 #
CONF-891213-1 ..... N90-15615 #
CONF-891214-2 ..... N90-15118 #
CONF-891214-3 ..... N90-15438 #
CONF-891214-4 ..... N90-15439 #
CONF-891214-10 ..... N90-15449 #
CONF-891214-11 ..... N90-15450 #
CONF-891220-1 ..... N90-15410 #
CONF-891230-1 ..... N90-15255 #
CONF-891241-1 ..... N90-15476 #
CONF-891251-2 ..... N90-15618 #
CONF-900102-2 ..... N90-15279 #
CONF-900108-2 ..... N90-15466 #
CONF-900109-5 ..... N90-15356 #
CONF-900109-6 ..... N90-15357 #
CONF-900109-9 ..... N90-15819 #
CONF-900109-11 ..... N90-15522 #
CONF-900109-14 ..... N90-15396 #
CONF-900116-1 ..... N90-15661 #
CONF-900116-2 ..... N90-15651 #
CONF-900116-3 ..... N90-15652 #
CONF-900121-1 ..... N90-15653 #
CONF-900121-3 ..... N90-15543 #
CONF-900129-1 ..... N90-15880 #
CONF-900136-1 ..... N90-15524 #
CONF-900136-2 ..... N90-15523 #
CONF-900136-5 ..... N90-15519 #
CONF-900136-6 ..... N90-15520 #
CONF-900138-1 ..... N90-15358 #
CONF-8801171-1 ..... N90-15728 #
CONF-8810246-6 ..... N90-15419 #
CONF-8810423 ..... N90-15803 #
CONF-8811203 ..... N90-15217 #
CONF-8812106 ..... N90-15372 #
CONF-8812106 ..... N90-15373 #
CONF-8812106 ..... N90-15374 #
CONF-8812106 ..... N90-15395 #
CONF-8902130 ..... N90-15759 #
CONF-8903174 ..... N90-15513 #
CONF-8904210-4-REV-1 ..... N90-15597 #
CONF-8904290-4 ..... N90-15800 #
CONF-8904292-1 ..... N90-15301 #
CONF-8904296-1 ..... N90-15765 #
CONF-8905112-2 ..... N90-15479 #
CONF-8905118-13 ..... N90-15228 #
CONF-8905194-6 ..... N90-15879 #
CONF-8905225-1 ..... N90-15670 #
CONF-8905231-1 ..... N90-15718 #
CONF-8905241-1 ..... N90-15258 #
CONF-8905245-1 ..... N90-15764 #
CONF-8906129-2 ..... N90-15515 #
CONF-8906154-2 ..... N90-15549 #
CONF-8906239-1 ..... N90-15408 #
CONF-8906250-1 ..... N90-15619 #
CONF-8907139-1 ..... N90-15768 #
CONF-8907139-3 ..... N90-15785 #
CONF-8907154-1 ..... N90-15717 #
CONF-8907166-1 ..... N90-15578 #
CONF-8907167-1 ..... N90-15149 #
CONF-8907168-1 ..... N90-15337 #
CONF-8907168-2 ..... N90-15749 #
CONF-8907170-1 ..... N90-15336 #
CONF-8907171-1 ..... N90-15867 #
CONF-8908106-5 ..... N90-15781 #
CONF-8908133-8 ..... N90-15755 #
CONF-8908134-6 ..... N90-15407 #
CONF-8908134-7 ..... N90-15406 #
CONF-8908134-17 ..... N90-15414 #
CONF-8908134-18 ..... N90-15416 #
CONF-8908134-19 ..... N90-15417 #
CONF-8908158-1 ..... N90-15368 #
CONF-8908160-2 ..... N90-15462* #
CONF-8908166-1 ..... N90-15702 #
CONF-8908176-1 ..... N90-15159 #
CONF-8908179-2 ..... N90-15827 #
CONF-8908181-1 ..... N90-15158 #
CONF-8908182-1 ..... N90-15535 #
CONF-8908182-2 ..... N90-15544 #
CONF-8908183-1 ..... N90-15166 #
CONF-8908185-1 ..... N90-15334 #
CONF-8908191-1 ..... N90-15242 #
CONF-8908192-1 ..... N90-15821 #

CONF-8909110-9 ..... N90-15463 #
CONF-8909168-3 ..... N90-15282 #
CONF-8909211-2 ..... N90-15770 #
CONF-8909225-1 ..... N90-15213 #
CONF-8909249-2 ..... N90-15596 #
CONF-8909267-2 ..... N90-15229 #
CONF-8909272-1 ..... N90-15700 #
CONF-8909274-1 ..... N90-15180 #
CONF-8909276-1 ..... N90-15877 #
CONF-8910103-2 ..... N90-15614 #
CONF-8910107-4 ..... N90-15339 #
CONF-8910120-4 ..... N90-15338 #
CONF-8910120-5 ..... N90-15794 #
CONF-8910157-3 ..... N90-15289 #
CONF-8910222-9 ..... N90-15241 #
CONF-8910223-1 ..... N90-15580 #
CONF-8910229-1 ..... N90-15876 #
CONF-8910246-1 ..... N90-15611 #
CONF-8910259-3 ..... N90-15756 #
CONF-8910276-2 ..... N90-15165 #
CONF-8910289-1 ..... N90-15448 #
CONF-8910289-2 ..... N90-15156 #
CONF-8910289-3 ..... N90-15164 #
CONF-8910295-2 ..... N90-15623 #
CONF-8910313-1 ..... N90-15820 #
CONF-8910319-1 ..... N90-15182 #
CONF-8911102-1 ..... N90-15087 #
CONF-8911110-2 ..... N90-15539 #
CONF-8911118-1 ..... N90-15478 #
CONF-8911121-1 ..... N90-15257 #
CONF-8911125-1 ..... N90-15663 #
CONF-8911129-2 ..... N90-15265 #
CONF-8911130-1 ..... N90-15754 #
CONF-8911132-1 ..... N90-15655 #
CONF-8911139-1 ..... N90-15150 #

CPS-89-013 ..... N90-15274 #

CRDEC-TR-071 ..... N90-15295 #
CRDEC-TR-111 ..... N90-15572 #

CRIE-T-87077 ..... N90-15730 #
CRIE-T-87097 ..... N90-15567 #
CRIE-T-87110 ..... N90-15284 #

CTP-TAMU-1/89 ..... N90-15561 #

CU-CS-439-89 ..... N90-15681 #
CU-CS-443-89 ..... N90-15630 #

C87A-25 ..... N90-15341 #

DAITC/TR-89/9 ..... N90-15853 #

DCIEM-89-TR-23 ..... N90-15310 #

DE89-000838 ..... N90-15512 #
DE89-004909 ..... N90-15287 #
DE89-007845 ..... N90-15254 #
DE89-008036 ..... N90-15615 #
DE89-008740 ..... N90-15436 #
DE89-009419 ..... N90-15498 #
DE89-009436 ..... N90-15499 #
DE89-009495 ..... N90-15502 #
DE89-009496 ..... N90-15503 #
DE89-009506 ..... N90-15504 #
DE89-009507 ..... N90-15519 #
DE89-009508 ..... N90-15520 #
DE89-011620 ..... N90-15224 #
DE89-011702 ..... N90-15394 #
DE89-012301 ..... N90-15410 #
DE89-012331 ..... N90-15143* #
DE89-012933 ..... N90-15118 #
DE89-013289 ..... N90-15370 #
DE89-014742 ..... N90-15505 #
DE89-014743 ..... N90-15521 #
DE89-014778 ..... N90-15506* #
DE89-014779 ..... N90-15767 #
DE89-015018 ..... N90-15609 #
DE89-015119 ..... N90-15247 #
DE89-015265 ..... N90-15438 #
DE89-015270 ..... N90-15439 #
DE89-015275 ..... N90-15440 #
DE89-015351 ..... N90-15279 #
DE89-015391 ..... N90-15255 #
DE89-015452 ..... N90-15475 #
DE89-015730 ..... N90-15371 #
DE89-015845 ..... N90-15661 #
DE89-015974 ..... N90-15651 #
DE89-015975 ..... N90-15652 #
DE89-016181 ..... N90-15324 #
DE89-016182 ..... N90-15437 #
DE89-016221 ..... N90-15356 #
DE89-016231 ..... N90-15212 #
DE89-016259 ..... N90-15653 #
DE89-016603 ..... N90-15610 #

DE89-016616 ..... N90-15788 #
DE89-016872 ..... N90-15507 #
DE89-017330 ..... N90-15616 #
DE89-017604 ..... N90-15785 #
DE89-017729 ..... N90-15476 #
DE89-017808 ..... N90-15213 #
DE89-017871 ..... N90-15694 #
DE89-633913 ..... N90-15633 #
DE89-635698 ..... N90-15691 #
DE89-635699 ..... N90-15692 #
DE89-635700 ..... N90-15703 #
DE89-635701 ..... N90-15671 #
DE89-635705 ..... N90-15835 #
DE89-635722 ..... N90-15561 #
DE89-635764 ..... N90-15477 #
DE89-635908 ..... N90-15775 #
DE89-636213 ..... N90-15225 #
DE89-636430 ..... N90-15372 #
DE89-636431 ..... N90-15373 #
DE89-636433 ..... N90-15395 #
DE89-636474 ..... N90-15374 #
DE89-901256 ..... N90-15567 #
DE89-901267 ..... N90-15730 #
DE89-901303 ..... N90-15284 #
DE90-000022 ..... N90-15617 #
DE90-000134 ..... N90-15880 #
DE90-000183 ..... N90-15717 #
DE90-000202 ..... N90-15280 #
DE90-000674 ..... N90-15769 #
DE90-000679 ..... N90-15876 #
DE90-000685 ..... N90-15670 #
DE90-000692 ..... N90-15580 #
DE90-000694 ..... N90-15728 #
DE90-000704 ..... N90-15543 #
DE90-000783 ..... N90-15770 #
DE90-000789 ..... N90-15328 #
DE90-000799 ..... N90-15473 #
DE90-000841 ..... N90-15357 #
DE90-000859 ..... N90-15729 #
DE90-000923 ..... N90-15365 #
DE90-000943 ..... N90-15879 #
DE90-000953 ..... N90-15500 #
DE90-000957 ..... N90-15366 #
DE90-000970 ..... N90-15367 #
DE90-000971 ..... N90-15565 #
DE90-000975 ..... N90-15595 #
DE90-000976 ..... N90-15744 #
DE90-000998 ..... N90-15531 #
DE90-001014 ..... N90-15325 #
DE90-001057 ..... N90-15368 #
DE90-001091 ..... N90-15114 #
DE90-001092 ..... N90-15474 #
DE90-001102 ..... N90-15154 #
DE90-001166 ..... N90-15281 #
DE90-001167 ..... N90-15164 #
DE90-001178 ..... N90-15819 #
DE90-001224 ..... N90-15662 #
DE90-001271 ..... N90-15214 #
DE90-001273 ..... N90-15248 #
DE90-001274 ..... N90-15215 #
DE90-001275 ..... N90-15532 #
DE90-001277 ..... N90-15216 #
DE90-001281 ..... N90-15217 #
DE90-001282 ..... N90-15249 #
DE90-001285 ..... N90-15218 #
DE90-001296 ..... N90-15250 #
DE90-001301 ..... N90-15771 #
DE90-001312 ..... N90-15219 #
DE90-001316 ..... N90-15256 #
DE90-001335 ..... N90-15462* #
DE90-001372 ..... N90-15849 #
DE90-001403 ..... N90-15702 #
DE90-001405 ..... N90-15369 #
DE90-001408 ..... N90-15718 #
DE90-001416 ..... N90-15611 #
DE90-001427 ..... N90-15326 #
DE90-001447 ..... N90-15282 #
DE90-001481 ..... N90-15612 #
DE90-001502 ..... N90-15672 #
DE90-001506 ..... N90-15406 #
DE90-001509 ..... N90-15772 #
DE90-001515 ..... N90-15407 #
DE90-001534 ..... N90-15533 #
DE90-001537 ..... N90-15358 #
DE90-001556 ..... N90-15327 #
DE90-001625 ..... N90-15087 #
DE90-001630 ..... N90-15773 #
DE90-001704 ..... N90-15745 #
DE90-001719 ..... N90-15155 #
DE90-001733 ..... N90-15182 #
DE90-001736 ..... N90-15220 #
DE90-001737 ..... N90-15746 #
DE90-001773 ..... N90-15221 #
DE90-001795 ..... N90-15411 #
DE90-001802 ..... N90-15076 #
DE90-001803 ..... N90-15088 #

DE90-001807 ..... N90-15508 #
DE90-001813 ..... N90-15534 #
DE90-001852 ..... N90-15251 #
DE90-001858 ..... N90-15695 #
DE90-001863 ..... N90-15144 #
DE90-001867 ..... N90-15283 #
DE90-001918 ..... N90-15329 #
DE90-001921 ..... N90-15613 #
DE90-001934 ..... N90-15501 #
DE90-001972 ..... N90-15747 #
DE90-001986 ..... N90-15618 #
DE90-001992 ..... N90-15614 #
DE90-002046 ..... N90-15476 #
DE90-002055 ..... N90-15585 #
DE90-002069 ..... N90-15252 #
DE90-002081 ..... N90-15375 #
DE90-002091 ..... N90-15586 #
DE90-002106 ..... N90-15466 #
DE90-002120 ..... N90-15222 #
DE90-002122 ..... N90-15774 #
DE90-002188 ..... N90-15336 #
DE90-002303 ..... N90-15223 #
DE90-002377 ..... N90-15145* #
DE90-002430 ..... N90-15522 #
DE90-002437 ..... N90-15408 #
DE90-002462 ..... N90-15156 #
DE90-002522 ..... N90-15157 #
DE90-002523 ..... N90-15513 #
DE90-002574 ..... N90-15523 #
DE90-002575 ..... N90-15524 #
DE90-002578 ..... N90-15165 #
DE90-002590 ..... N90-15549 #
DE90-002626 ..... N90-15359 #
DE90-002628 ..... N90-15525 #
DE90-002633 ..... N90-15285 #
DE90-002635 ..... N90-15550 #
DE90-002639 ..... N90-15298 #
DE90-002643 ..... N90-15330 #
DE90-002644 ..... N90-15509 #
DE90-002655 ..... N90-15396 #
DE90-002662 ..... N90-15578 #
DE90-002664 ..... N90-15158 #
DE90-002679 ..... N90-15331 #
DE90-002700 ..... N90-15301 #
DE90-002719 ..... N90-15226 #
DE90-002721 ..... N90-15479 #
DE90-002734 ..... N90-15483 #
DE90-002735 ..... N90-15709 #
DE90-002753 ..... N90-15412 #
DE90-002754 ..... N90-15257 #
DE90-002760 ..... N90-15288 #
DE90-002771 ..... N90-15332 #
DE90-002785 ..... N90-15286 #
DE90-002788 ..... N90-15535 #
DE90-002795 ..... N90-15333 #
DE90-002805 ..... N90-15448 #
DE90-002809 ..... N90-15119 #
DE90-002826 ..... N90-15748 #
DE90-002840 ..... N90-15827 #
DE90-002842 ..... N90-15776 #
DE90-002860 ..... N90-15253 #
DE90-002871 ..... N90-15510 #
DE90-002892 ..... N90-15166 #
DE90-002906 ..... N90-15449 #
DE90-002923 ..... N90-15536 #
DE90-002926 ..... N90-15299 #
DE90-002967 ..... N90-15159 #
DE90-002974 ..... N90-15780 #
DE90-002977 ..... N90-15461 #
DE90-002978 ..... N90-15749 #
DE90-002979 ..... N90-15149 #
DE90-002980 ..... N90-15337 #
DE90-002981 ..... N90-15413 #
DE90-002999 ..... N90-15777 #
DE90-003010 ..... N90-15778 #
DE90-003012 ..... N90-15779 #
DE90-003023 ..... N90-15731 #
DE90-003024 ..... N90-15409 #
DE90-003027 ..... N90-15376 #
DE90-003028 ..... N90-15289 #
DE90-003041 ..... N90-15663 #
DE90-003050 ..... N90-15258 #
DE90-003051 ..... N90-15334 #
DE90-003053 ..... N90-15377 #
DE90-003080 ..... N90-15619 #
DE90-003086 ..... N90-15122 #
DE90-003087 ..... N90-15123 #
DE90-003102 ..... N90-15620 #
DE90-003105 ..... N90-15621 #
DE90-003122 ..... N90-15160 #
DE90-003128 ..... N90-15867 #
DE90-003155 ..... N90-15265 #
DE90-003162 ..... N90-15511 #
DE90-003180 ..... N90-15167 #
DE90-003181 ..... N90-15514 #
DE90-003187 ..... N90-15574 #
DE90-003211 ..... N90-15414 #
DE90-003214 ..... N90-15450 #
DE90-003215 ..... N90-15877 #
DE90-003216 ..... N90-15150 #
DE90-003217 ..... N90-15168 #
DE90-003232 ..... N90-15415 #
DE90-003243 ..... N90-15858 #
DE90-003245 ..... N90-15451 #
DE90-003247 ..... N90-15696 #
DE90-003265 ..... N90-15781 #
DE90-003269 ..... N90-15623 #
DE90-003280 ..... N90-15464 #
DE90-003283 ..... N90-15537 #
DE90-003289 ..... N90-15850 #
DE90-003291 ..... N90-15750 #
DE90-003292 ..... N90-15751 #
DE90-003300 ..... N90-15732 #
DE90-003318 ..... N90-15705 #
DE90-003319 ..... N90-15673 #
DE90-003339 ..... N90-15706 #
DE90-003343 ..... N90-15752 #
DE90-003346 ..... N90-15719 #
DE90-003369 ..... N90-15483 #
DE90-003390 ..... N90-15754 #
DE90-003392 ..... N90-15700 #
DE90-003394 ..... N90-15764 #
DE90-003396 ..... N90-15416 #
DE90-003450 ..... N90-15515 #
DE90-003451 ..... N90-15755 #
DE90-003452 ..... N90-15786 #
DE90-003471 ..... N90-15428 #
DE90-003473 ..... N90-15169 #
DE90-003484 ..... N90-15228 #
DE90-003513 ..... N90-15624 #
DE90-003515 ..... N90-15116 #
DE90-003525 ..... N90-15266 #
DE90-003530 ..... N90-15787 #
DE90-003531 ..... N90-15538 #
DE90-003538 ..... N90-15625 #
DE90-003543 ..... N90-15596 #
DE90-003547 ..... N90-15516 #
DE90-003548 ..... N90-15517 #
DE90-003553 ..... N90-15539 #
DE90-003555 ..... N90-15788 #
DE90-003559 ..... N90-15789 #
DE90-003561 ..... N90-15790 #
DE90-003563 ..... N90-15791 #
DE90-003565 ..... N90-15792 #
DE90-003566 ..... N90-15793 #
DE90-003570 ..... N90-15794 #
DE90-003571 ..... N90-15338 #
DE90-003574 ..... N90-15180 #
DE90-003575 ..... N90-15720 #
DE90-003579 ..... N90-15795 #
DE90-003599 ..... N90-15872 #
DE90-003604 ..... N90-15655 #
DE90-003605 ..... N90-15417 #
DE90-003614 ..... N90-15597 #
DE90-003625 ..... N90-15796 #
DE90-003633 ..... N90-15267 #
DE90-003637 ..... N90-15170 #
DE90-003638 ..... N90-15268 #
DE90-003640 ..... N90-15797 #
DE90-003643 ..... N90-15418 #
DE90-003645 ..... N90-15626 #
DE90-003654 ..... N90-15726 #
DE90-003655 ..... N90-15782 #
DE90-003657 ..... N90-15820 #
DE90-003664 ..... N90-15133 #
DE90-003666 ..... N90-15134 #
DE90-003667 ..... N90-15753 #
DE90-003704 ..... N90-15540 #
DE90-003706 ..... N90-15798 #
DE90-003709 ..... N90-15799 #
DE90-003714 ..... N90-15136 #
DE90-003716 ..... N90-15756 #
DE90-003720 ..... N90-15526 #
DE90-003754 ..... N90-15484 #
DE90-003755 ..... N90-15181 #
DE90-003764 ..... N90-15734 #
DE90-003770 ..... N90-15541 #
DE90-003772 ..... N90-15241 #
DE90-003774 ..... N90-15339 #
DE90-003792 ..... N90-15821 #
DE90-003793 ..... N90-15242 #
DE90-003805 ..... N90-15229 #
DE90-003807 ..... N90-15419 #
DE90-003812 ..... N90-15269 #
DE90-003822 ..... N90-15765 #
DE90-003823 ..... N90-15800 #
DE90-003826 ..... N90-15171 #
DE90-003838 ..... N90-15801 #
DE90-003840 ..... N90-15802 #
DE90-003887 ..... N90-15467 #
DE90-003888 ..... N90-15460 #
DE90-003889 ..... N90-15243 #
DE90-003893 ..... N90-15244 #
DE90-003952 ..... N90-15822 #
DE90-003955 ..... N90-15823 #
DE90-003959 ..... N90-15544 #
DE90-003960 ..... N90-15824 #
DE90-003964 ..... N90-15527 #
DE90-003966 ..... N90-15825 #
DE90-004421 ..... N90-15757 #
DE90-004422 ..... N90-15758 #
DE90-004438 ..... N90-15420 #
DE90-004439 ..... N90-15340 #
DE90-004442 ..... N90-15290 #
DE90-600722 ..... N90-15674 #
DE90-600755 ..... N90-15675 #
DE90-600816 ..... N90-15828 #
DE90-600818 ..... N90-15378 #
DE90-600819 ..... N90-15803 #
DE90-600936 ..... N90-15759 #
DE90-601062 ..... N90-15783 #
DE90-602936 ..... N90-15804 #
DE90-603347 ..... N90-15760 #
DE90-603502 ..... N90-15805 #
DE90-701646 ..... N90-15379 #
DE90-701753 ..... N90-15868 #
DE90-701754 ..... N90-15829 #
DE90-710044 ..... N90-15441 #
DE90-710045 ..... N90-15551 #
DE90-710100 ..... N90-15830 #

DMI-TR-89014 ..... N90-15346 #

DNA-TR-89-73 ..... N90-15852 #

DODA-AR-005-450 ..... N90-15639 #

DOE/AL-33183/T12 ..... N90-15451 #

DOE/BP-23169/2 ..... N90-15332 #

DOE/ER-0313/6 ..... N90-15744 #
DOE/ER-0406 ..... N90-15574 #
DOE/ER-13065/589 ..... N90-15702 #
DOE/ER-13191/10 ..... N90-15415 #
DOE/ER-13288/5 ..... N90-15167 #
DOE/ER-13427/2 ..... N90-15155 #
DOE/ER-13506/24 ..... N90-15515 #
DOE/ER-13700/2 ..... N90-15719 #
DOE/ER-13833/3 ..... N90-15154 #
DOE/ER-13834/8 ..... N90-15213 #
DOE/ER-13897/10 ..... N90-15157 #
DOE/ER-13914/13 ..... N90-15514 #
DOE/ER-13945/1 ..... N90-15133 #
DOE/ER-13949/T1 ..... N90-15484 #
DOE/ER-13954/1 ..... N90-15181 #
DOE/ER-14003/1 ..... N90-15134 #
DOE/ER-40039/31 ..... N90-15858 #
DOE/ER-45055/24 ..... N90-15787 #
DOE/ER-45237/T1 ..... N90-15266 #
DOE/ER-51051/T1 ..... N90-15753 #
DOE/ER-53242/3 ..... N90-15745 #
DOE/ER-53266/16 ..... N90-15612 #
DOE/ER-60304/H1 ..... N90-15531 #
DOE/ER-60314/T1 ..... N90-15538 #

DOE/ET-53088/401 ..... N90-15705 #
DOE/ET-53088/407 ..... N90-15673 #

DOE/MC-21349/2738 ..... N90-15394 #
DOE/MC-23270/2751 ..... N90-15501 #

DOE/OR-21400/T407 ..... N90-15798 #

DOE/PC-79680/T2 ..... N90-15662 #
DOE/PC-79931/T4 ..... N90-15510 #
DOE/PC-88827/T4 ..... N90-15288 #
DOE/PC-88949/T4 ..... N90-15483 #
DOE/PC-88951/2 ..... N90-15369 #

DOT/FAA/CT-TN89/64 ..... N90-15089 #

DOT/FAA/CT-89/18 ..... N90-15084 #

DOT/FAA/DS-89/26 ..... N90-15090 #
DOT/FAA/DS-89/33 ..... N90-15086 #
DOT/FAA/DS-89/35 ..... N90-15108* #

DOT/FAA/OV-89/2 ..... N90-15085 #

DOT/FAA/SA-89/2 ..... N90-15566 #

DP-MS-89-41 ..... N90-15219 #

DREO-1006 ..... N90-15316 #

DTIC-TR-89/20 ..... N90-15853 #

E-4391 ..... N90-15112* #
E-4780 ..... N90-15846* #
E-5009 ..... N90-15211* #
E-5256 ..... N90-15622* #

EGG-M-36587 ..... N90-15375 #
EGG-M-88271 ..... N90-15585 #
EGG-M-88288 ..... N90-15586 #
EGG-M-88501 ..... N90-15478 #

EGG-MS-8696 ..... N90-15252 #

EPA/600/3-89/070 ..... N90-15529 #

ERIM-196000-7-F ..... N90-15458 #
ERIM-201600-11-F-VOL-1 ..... N90-15317 #

ERL-290666-1 ..... N90-15662 #

ESD-TR-89-166 ..... N90-15306 #
ESD-TR-89-167 ..... N90-15307 #
ESD-TR-89-173 ..... N90-15305 #

ESDU-PD3 ..... N90-15162

ESDU-STRUCT-H.02.00.01 ..... N90-15831
ESDU-STRUCT-H.02.00.02 ..... N90-15480
ESDU-STRUCT-H.02.00.04 ..... N90-15481

ESDU-89013 ..... N90-15152
ESDU-89023 ..... N90-15831
ESDU-89024 ..... N90-15480
ESDU-89025 ..... N90-15481
ESDU-89028 ..... N90-15446
ESDU-89029 ..... N90-15081
ESDU-89030 ..... N90-15491
ESDU-89031 ..... N90-15245
ESDU-89032 ..... N90-15693
ESDU-89034 ..... N90-15082
ESDU-89035-PT-1 ..... N90-15183
ESDU-89036 ..... N90-15714
ESDU-89037 ..... N90-15184
ESDU-89038 ..... N90-15397

ETL-0545 ..... N90-15453 #

FERMILAB-PUB-89/235-A ..... N90-15826* #
FERMILAB-PUB-89/249-A ..... N90-15832* #

FNAL/C-89/124 ..... N90-15609 #
FNAL/C-89/220 ..... N90-15596 #
FNAL/C-89/221-A ..... N90-15867 #

FRCR-321 ..... N90-15612 #

FSU-STATISTICS-M-812 ..... N90-15707 #

FSU-TR-M-813 ..... N90-15698 #
FSU-TR-M-814 ..... N90-15682 #

FTD-ID(RS)T-0221-89 ..... N90-15422 #
FTD-ID(RS)T-0487-89 ..... N90-15738 #
FTD-ID(RS)T-0574-89 ..... N90-15404 #
FTD-ID(RS)T-0592-89 ..... N90-15129 #
FTD-ID(RS)T-0793-89 ..... N90-15573 #

GA-A-19739 ..... N90-15751 #
GA-A-19741 ..... N90-15750 #
GA-A-19742 ..... N90-15752 #
GA-A-19748 ..... N90-15850 #

GA-C19465 ..... N90-15818 #

GAO/IMTEC-89-46FS ..... N90-15881 #

GL-ERP-1036 ..... N90-15555 #
GL-ERP-1037-VOL-1 ..... N90-15127 #
GL-ERP-1038-VOL-2 ..... N90-15128 #

GL-TR-89-0103 ..... N90-15312 #
GL-TR-89-0108 ..... N90-15558 #
GL-TR-89-0122 ..... N90-15650 #
GL-TR-89-0156 ..... N90-15556 #
GL-TR-89-0157 ..... N90-15554 #
GL-TR-89-0168 ..... N90-15497 #
GL-TR-89-0171 ..... N90-15657 #
GL-TR-89-0180 ..... N90-15496 #
GL-TR-89-0229 ..... N90-15555 #
GL-TR-89-0249(1)-VOL-1 ..... N90-15127 #
GL-TR-89-0249(2)-VOL-2 ..... N90-15128 #
GL-TR-89-0262 ..... N90-15873* #

H-1516 ..... N90-15100* #

HCFA/DF/DK-90/001A ..... N90-15579 #

HDL-CR-89-078-1 ..... N90-15353 #

HDL-DS-89-1 ..... N90-15808 #

IC-88/370 ..... N90-15828 #
IC-89/39 ..... N90-15775 #
IC-89/55 ..... N90-15691 #
IC-89/56 ..... N90-15675 #
IC-89/57 ..... N90-15674 #
IC-89/67 ..... N90-15692 #
IC-89/69 ..... N90-15378 #
IC-89/71 ..... N90-15561 #
IC-89/72 ..... N90-15703 #
IC-89/73 ..... N90-15835 #
IC-89/76 ..... N90-15477 #
IC-89/77 ..... N90-15225 #
IC-89/84 ..... N90-15671 #
IC-89/89 ..... N90-15783 #

ICASE-89-82 ..... N90-15078* #

IFSR-401 ..... N90-15705 #
IFSR-407 ..... N90-15673 #

IIHR-332 ..... N90-15392 #

IL/ENR/RE/EA-89/16 ..... N90-15530 #

INIS-BR-1577 ..... N90-15374 #
INIS-BR-1578 ..... N90-15372 #
INIS-BR-1579 ..... N90-15373 #
INIS-BR-1581 ..... N90-15395 #
INIS-BR-1610 ..... N90-15803 #

INIS-MF-11537 ..... N90-15759 #

INSRP-89-01-VOL-1 ..... N90-15122 #
INSRP-89-01-VOL-2 ..... N90-15123 #

IRIS-255 ..... N90-15453 #

ISBN-0-309-04705-6 ..... N90-15398 #
ISBN-0-7966-4647-X ..... N90-15856* #
ISBN-0-85679-684-0 ..... N90-15152
ISBN-0-85679-685-9 ..... N90-15162
ISBN-0-85679-695-6 ..... N90-15831
ISBN-0-85679-696-4 ..... N90-15480
ISBN-0-85679-697-2 ..... N90-15481
ISBN-0-85679-700-6 ..... N90-15446
ISBN-0-85679-701-4 ..... N90-15081
ISBN-0-85679-702-2 ..... N90-15491
ISBN-0-85679-703-0 ..... N90-15245
ISBN-0-85679-704-9 ..... N90-15693
ISBN-0-85679-707-3 ..... N90-15082
ISBN-0-85679-708-1 ..... N90-15183
ISBN-0-85679-709-X N90-15714
ISBN-0-85679-710-3 ..... N90-15184
ISBN-0-85679-711-1 ..... N90-15397
ISBN-92-835-0519-0 ..... N90-15185 #
ISBN-92-835-0527-1 ..... N90-15041 #
ISBN-951-754-825-7 ..... N90-15323 #

ISSN-0141-397X N90-15081
ISSN-0141-397X N90-15082
ISSN-0141-402X N90-15397
ISSN-0141-3968 ..... N90-15693
ISSN-0141-4011 ..... N90-15491
ISSN-0141-4046 ..... N90-15446
ISSN-0141-4062 ..... N90-15183
ISSN-0141-4062 ..... N90-15184
ISSN-0141-4070 ..... N90-15162
ISSN-0141-4089 ..... N90-15245
ISSN-0141-4097 ..... N90-15152
ISSN-0141-4097 ..... N90-15480
ISSN-0141-4097 ..... N90-15481
ISSN-0141-4097 ..... N90-15831
ISSN-0250-0671 ..... N90-15856* #
ISSN-0307-0115 ..... N90-15714
ISSN-0348-9329 ..... N90-15715 #
ISSN-0348-9329 ..... N90-15716 #
ISSN-0348-9329 ..... N90-15727 #
ISSN-0355-5712 ..... N90-15323 #
ISSN-0922-5641 ..... N90-15669 #
ISSN-0958-0360 ..... N90-15152

JAERI-M-89-029 ..... N90-15379 #
JAERI-M-89-062 ..... N90-15551 #
JAERI-M-89-067 ..... N90-15441 #

JHU/APL-TG-1375 ..... N90-15349 #

JINR-E-2-88-557 ..... N90-15833 #
JINR-E-17-88-510 ..... N90-15804 #
JINR-E-17-88-524 ..... N90-15805 #

J206-89-002/6264 ..... N90-15736 #

K/CSD/INF-89/5 ..... N90-15224 #

K/ETO-4 ..... N90-15169 #

K/QT-279 ..... N90-15371 #

KCP-613-4005 ..... N90-15300 #
KCP-613-4050 ..... N90-15335 #
KCP-613-4127 ..... N90-15159 #
KCP-613-4145 ..... N90-15299 #

L-16622 ..... N90-15108* #

LA-UR-89-2309 ..... N90-15439 #
LA-UR-89-2342 ..... N90-15438 #
LA-UR-89-2595 ..... N90-15440 #
LA-UR-89-2885 ..... N90-15768 #
LA-UR-89-2974 ..... N90-15610 #
LA-UR-89-3175 ..... N90-15728 #
LA-UR-89-3192 ..... N90-15580 #
LA-UR-89-3249 ..... N90-15670 #
LA-UR-89-3288 ..... N90-15876 #
LA-UR-89-3337 ..... N90-15408 #
LA-UR-89-3363 ..... N90-15522 #
LA-UR-89-3365 ..... N90-15396 #
LA-UR-89-3684 ..... N90-15700 #
LA-UR-89-3687 ..... N90-15754 #
LA-UR-89-3763 ..... N90-15416 #
LA-UR-89-3769 ..... N90-15764 #
LA-UR-89-3786 ..... N90-15414 #
LA-UR-89-3788 ..... N90-15877 #
LA-UR-89-3791 ..... N90-15450 #
LA-UR-89-3837 ..... N90-15168 #
LA-UR-89-3841 ..... N90-15150 #
LA-UR-89-3946 ..... N90-15820 #
LA-UR-89-3963 ..... N90-15782 #
LA-UR-89-3982 ..... N90-15726 #

LA-11512-MS ..... N90-15264 #
LA-11633-MS ..... N90-15326 #
LA-11681-MS ..... N90-15696 #

LBL-25435 ..... N90-15619 #
LBL-26796 ..... N90-15621 #
LBL-27001 ..... N90-15732 #
LBL-27070 ..... N90-15623 #
LBL-27381 ..... N90-15222 #
LBL-27502 ..... N90-15717 #
LBL-27593 ..... N90-15325 #
LBL-27657 ..... N90-15145* #
LBL-27661 ..... N90-15774 #
LBL-27672 ..... N90-15880 #
LBL-27746 ..... N90-15331 #
LBL-27774 ..... N90-15464 #
LBL-27806 ..... N90-15781 #
LBL-27904 ..... N90-15156 #
LBL-27938 ..... N90-15160 #

LC-88-34472 ..... N90-15398 #

LUIP-8904 ..... N90-15716 #
LUIP-8905 ..... N90-15715 #
LUIP-8906 ..... N90-15727 #

LUNFD6/(NFFK-7101)1-9(1989) ..... N90-15716 #
LUNFD6/(NFFK-7102)1-12(1989) ..... N90-15715 #
LUNFD6/(NFFK-7103)1-11(1989) ..... N90-15727 #

MCR-89-506 ..... N90-15151 #

MD89-47-KDM/THL ..... N90-15676 #

MIT/LCS/TM-392 ..... N90-15686 #
MIT/LCS/TM-396 ..... N90-15658 #
MIT/LCS/TM-397 ..... N90-15598 #
MIT/LCS/TM-398 ..... N90-15604 #
MIT/LCS/TM-402 ..... N90-15351 #
MIT/LCS/TM-403 ..... N90-15633 #
MIT/LCS/TM-406 ..... N90-15632 #
MIT/LCS/TM-412 ..... N90-15666 #

MIT/LCS/TR-449 ..... N90-15635 #
MIT/LCS/TR-453 ..... N90-15634 #

MLM-3608(OP) ..... N90-15282 #
MLM-3609 ..... N90-15298 #
MLM-3612(OP) ..... N90-15289 #

MP-89-187 ..... N90-15560 #

MRC-R-1223 ..... N90-15852 #

MTL-TR-89-53 ..... N90-15271 #
MTL-TR-89-84 ..... N90-15239 #
MTL-TR-89-86 ..... N90-15233 #

NAS 1.15:4091-VOL-1 ..... N90-15545* #
NAS 1.15:4158 ..... N90-15108* #
NAS 1.15:101610 ..... N90-15102* #
NAS 1.15:101626 ..... N90-15848* #
NAS 1.15:101639 ..... N90-15110* #
NAS 1.15:101650 ..... N90-15401* #
NAS 1.15:101652 ..... N90-15836* #
NAS 1.15:101658 ..... N90-15120* #
NAS 1.15:101685 ..... N90-15101* #
NAS 1.15:101930 ..... N90-15153* #
NAS 1.15:101940 ..... N90-15143* #
NAS 1.15:102034 ..... N90-15846* #
NAS 1.15:102200 ..... N90-15399* #
NAS 1.15:102234 ..... N90-15577* #
NAS 1.15:102468 ..... N90-15622* #
NAS 1.15:102904 ..... N90-15559* #
NAS 1.21:7037(246) N90-15068*
NAS 1.21:7039(36)-SECT-1 ..... N90-15851*
NAS 1.26:4270 ..... N90-15072* #
NAS 1.26:177543 ..... N90-15093* #
NAS 1.26:177545 ..... N90-15591* #
NAS 1.26:181938 ..... N90-15654* #
NAS 1.26:181942 ..... N90-15482* #
NAS 1.26:181953 ..... N90-15111* #
NAS 1.26:181963 ..... N90-15078* #
NAS 1.26:183847 ..... N90-15431* #
NAS 1.26:185013 ..... N90-15826* #
NAS 1.26:185170 ..... N90-15434* #
NAS 1.26:185948 ..... N90-15664* #
NAS 1.26:186063 ..... N90-15145* #
NAS 1.26:186188 ..... N90-15743* #
NAS 1.26:186204 ..... N90-15766* #
NAS 1.26:186205 ..... N90-15363* #
NAS 1.26:186214 ..... N90-15364* #
NAS 1.26:186226 ..... N90-15506* #
NAS 1.26:186231 ..... N90-15435* #
NAS 1.26:186241 ..... N90-15699* #
NAS 1.26:186249 ..... N90-15146* #
NAS 1.26:186251 ..... N90-15400* #
NAS 1.26:186255 ..... N90-15832* #
NAS 1.26:186258 ..... N90-15856* #
NAS 1.26:186261 ..... N90-15077* #
NAS 1.26:186263 ..... N90-15380* #
NAS 1.26:186274 ..... N90-15447* #
NAS 1.26:186277 ..... N90-15862* #
NAS 1.26:186279 ..... N90-15863* #
NAS 1.26:186280 ..... N90-15870* #
NAS 1.26:186281 ..... N90-15871* #
NAS 1.26:186282 ..... N90-15861* #
NAS 1.26:186286 ..... N90-15860* #
NAS 1.26:186289 ..... N90-15859* #
NAS 1.26:186292 ..... N90-15869* #
NAS 1.26:186293 ..... N90-15381* #
NAS 1.26:186301 ..... N90-15873* #
NAS 1.26:186302 ..... N90-15462* #
NAS 1.60:2925 ..... N90-15112* #
NAS 1.60:2967 ..... N90-15211* #
NAS 1.60:2971 ..... N90-15100* #
NAS 1.71:GSC-13199-1 ..... N90-15261* #
NAS 1.71:LAR-13870-1 ..... N90-15094* #
NAS 1.71:LAR-13968-1 ..... N90-15710* #
NAS 1.71:LAR-13981-1 ..... N90-15442* #
NAS 1.71:LAR-13996-1-SB ..... N90-15161* #
NAS 1.71:LAR-14001-1 ..... N90-15260* #
NAS 1.71:LAR-14162-1 ..... N90-15259* #
NAS 1.71:LAR-14194-1 ..... N90-15148* #
NAS 1.71:LEW-14672-1 ..... N90-15444* #
NAS 1.71:LEW-14698-2 ..... N90-15262* #
NAS 1.71:LEW-14776-1 ..... N90-15445* #
NAS 1.71:LEW-14795-1 ..... N90-15733* #
NAS 1.71:LEW-14846-1 ..... N90-15130* #
NAS 1.71:LEW-14990-1-CU ..... N90-15147* #
NAS 1.71:MFS-28314-1 ..... N90-15227* #
NAS 1.71:NPO-17633-1-CU ..... N90-15263* #
NAS 1.71:SSC-00004 ..... N90-15443* #

NAS-SR-1324 ..... N90-15090 #
NAS-SR-13211 ..... N90-15086 #

NASA-CASE-GSC-13199-1 ..... N90-15261* #

NASA-CASE-LAR-13870-1 ..... N90-15094* #
NASA-CASE-LAR-13968-1 ..... N90-15710* #
NASA-CASE-LAR-13981-1 ..... N90-15442* #
NASA-CASE-LAR-13996-1-SB ..... N90-15161* #
NASA-CASE-LAR-14001-1 ..... N90-15260* #
NASA-CASE-LAR-14162-1 ..... N90-15259* #
NASA-CASE-LAR-14194-1 ..... N90-15148* #

NASA-CASE-LEW-14672-1 ..... N90-15444* #
NASA-CASE-LEW-14698-2 ..... N90-15262* #
NASA-CASE-LEW-14776-1 ..... N90-15445* #
NASA-CASE-LEW-14795-1 ..... N90-15733* #
NASA-CASE-LEW-14846-1 ..... N90-15130* #
NASA-CASE-LEW-14990-1-CU ..... N90-15147* #

NASA-CASE-MFS-28314-1 ..... N90-15227* #

NASA-CASE-NPO-17633-1-CU ..... N90-15263* #

NASA-CASE-SSC-00004 ..... N90-15443* #

NASA-CR-4270 ..... N90-15072* #
NASA-CR-177543 ..... N90-15093* #
NASA-CR-177545 ..... N90-15591* #
NASA-CR-181938 ..... N90-15654* #
NASA-CR-181942 ..... N90-15482* #
NASA-CR-181953 ..... N90-15111* #
NASA-CR-181963 ..... N90-15078* #
NASA-CR-183847 ..... N90-15431* #
NASA-CR-185013 ..... N90-15826* #
NASA-CR-185170 ..... N90-15434* #
NASA-CR-185948 ..... N90-15664* #
NASA-CR-186063 ..... N90-15145* #
NASA-CR-186188 ..... N90-15743* #
NASA-CR-186204 ..... N90-15766* #
NASA-CR-186205 ..... N90-15363* #
NASA-CR-186214 ..... N90-15364* #
NASA-CR-186226 ..... N90-15506* #
NASA-CR-186231 ..... N90-15435* #
NASA-CR-186241 ..... N90-15699* #
NASA-CR-186249 ..... N90-15146* #
NASA-CR-186251 ..... N90-15400* #
NASA-CR-186255 ..... N90-15832* #
NASA-CR-186258 ..... N90-15856* #
NASA-CR-186261 ..... N90-15077* #
NASA-CR-186263 ..... N90-15380* #
NASA-CR-186274 ..... N90-15447* #
NASA-CR-186277 ..... N90-15862* #
NASA-CR-186279 ..... N90-15863* #
NASA-CR-186280 ..... N90-15870* #
NASA-CR-186281 ..... N90-15871* #
NASA-CR-186282 ..... N90-15861* #
NASA-CR-186286 ..... N90-15860* #
NASA-CR-186289 ..... N90-15859* #
NASA-CR-186292 ..... N90-15869* #
NASA-CR-186293 ..... N90-15381* #
NASA-CR-186301 ..... N90-15873* #
NASA-CR-186302 ..... N90-15462* #

NASA-SP-7037(246) N90-15068*
NASA-SP-7039(36)-SECT-1 ..... N90-15851*

NASA-TM-4091-VOL-1 ..... N90-15545* #
NASA-TM-4158 ..... N90-15108* #
NASA-TM-101610 ..... N90-15102* #
NASA-TM-101626 ..... N90-15848* #
NASA-TM-101639 ..... N90-15110* #
NASA-TM-101650 ..... N90-15401* #
NASA-TM-101652 ..... N90-15836* #
NASA-TM-101658 ..... N90-15120* #
NASA-TM-101685 ..... N90-15101* #
NASA-TM-101930 ..... N90-15153* #
NASA-TM-101940 ..... N90-15143* #
NASA-TM-102034 ..... N90-15846* #
NASA-TM-102200 ..... N90-15399* #
NASA-TM-102234 ..... N90-15577* #
NASA-TM-102468 ..... N90-15622* #
NASA-TM-102904 ..... N90-15559* #

NASA-TP-2925 ..... N90-15112* #
NASA-TP-2967 ..... N90-15211* #
NASA-TP-2971 ..... N90-15100* #

NAVEDTRA-10058-C1 ..... N90-15584 #

NCAR/TN-317-STR ..... N90-15574 #

NDP-032 ..... N90-15565 #

NIIEFA-P-K-0782 ..... N90-15760 #

NIPER-432 ..... N90-15280 #

NIST/TN-1320 ..... N90-15302 #

NISTIR-89/4084 ..... N90-15246 #

NMSU-ECE-89-007A ..... N90-15599 #

NORDA-CONTRIB-PR-89 ..... N90-15403 #

NORSAR-CONTRIB-406 ..... N90-15657 #

NOSC/TD-1596 ..... N90-15570 #

NOSC/TR-1310 ..... N90-15708 #

NPS52-89-040 ..... N90-15457 #
NPS52-89-050 ..... N90-15641 #
NPS52-89-057 ..... N90-15668 #
NPS54-89-011 ..... N90-15660 #

NPS61-89-014 ..... N90-15125 #
NPS61-89-015PR ..... N90-15834 #

NRL-MR-6538 ..... N90-15402 #
NRL-MR-6541 ..... N90-15424 #
NRL-MR-6542 ..... N90-15763 #
NRL-MR-6557 ..... N90-15320 #

NRL-9115 ..... N90-15318 #
NRL-9189 ..... N90-15319 #

NSWC-TR-88-400 ..... N90-15454 #

NUSC-TR-8537 ..... N90-15712 #

ORNL/CDIAC-27 ..... N90-15565 #

ORNL/CON-253 ..... N90-15367 #

ORNL/FTR-3067 ..... N90-15771 #
ORNL/FTR-3096 ..... N90-15218 #
ORNL/FTR-3097 ..... N90-15249 #
ORNL/FTR-3422 ..... N90-15250 #
ORNL/FTR-3468 ..... N90-15537 #

ORNL/M-836 ..... N90-15532 #
ORNL/M-919 ..... N90-15744 #

ORNL/SUB-82-22239/01 ..... N90-15215 #
ORNL/SUB-86-57444/01 ..... N90-15216 #
ORNL/SUB-88-SA798/01 ..... N90-15248 #

ORNL/TM-11233 ..... N90-15500 #
ORNL/TM-11239 ..... N90-15251 #
ORNL/TM-11315 ..... N90-15695 #

PB89-190540 ..... N90-15562 #
PB89-198675 ..... N90-15398 #
PB89-209308 ..... N90-15246 #
PB89-212583 ..... N90-15323 #
PB89-225460 ..... N90-15528 #
PB89-226013 ..... N90-15470 #
PB89-235139 ..... N90-15302 #
PB89-235840 ..... N90-15856* #
PB90-100181 ..... N90-15579 #
PB90-100223 ..... N90-15530 #
PB90-106451 ..... N90-15529 #
PB90-780008 ..... N90-15584 #

PFC/RR-89-15 ..... N90-15132 #

PHM-P-06-89 ..... N90-15497 #

PNL-SA-16112 ..... N90-15170 #
PNL-SA-16838 ..... N90-15158 #
PNL-SA-16885 ..... N90-15709 #
PNL-SA-16968 ..... N90-15463 #
PNL-SA-17179 ..... N90-15578 #
PNL-SA-17327 ..... N90-15267 #
PNL-SA-17406 ..... N90-15614 #
PNL-SA-17603 ..... N90-15624 #
PNL-SA-17607 ..... N90-15268 #

PNL-7104 ..... N90-15144 #
PNL-7163 ..... N90-15534 #
PNL-7166 ..... N90-15536 #

POLY-WRI-1543-88-VOL-1 ..... N90-15347 #
POLY-WRI-1543-88-VOL-2 ..... N90-15348 #

PREPRINT-SERIES-232 ..... N90-15860* #
PREPRINT-SERIES-240 ..... N90-15859* #
PREPRINT-SERIES-288 ..... N90-15869* #
PREPRINT-SERIES-304 ..... N90-15862* #
PREPRINT-SERIES-306 ..... N90-15863* #
PREPRINT-SERIES-307 ..... N90-15861* #
PREPRINT-SERIES-314 ..... N90-15870* #
PREPRINT-SERIES-316 ..... N90-15871* #

PW/FL/FR-20505 ..... N90-15107 #

R-89-02 ..... N90-15562 #
R-563 ..... N90-15470 #

R/D-5852-EN-01 ..... N90-15115 #
R/D-6204-CH-02 ..... N90-15354 #

RADC-TR-89-8-VOL-1 ..... N90-15347 #
RADC-TR-89-8-VOL-2 ..... N90-15348 #
RADC-TR-89-93 ..... N90-15645 #
RADC-TR-89-108 ..... N90-15656 #
RADC-TR-89-121-VOL-2 ..... N90-15313 #
RADC-TR-89-167 ..... N90-15308 #
RADC-TR-89-168 ..... N90-15309 #

REPT-1 ..... N90-15806 #

REPT-89-31 ..... N90-15669 #
REPT-89-154 ..... N90-15451 #
REPT-047 ..... N90-15403 #
REPT-153-7639 ..... N90-15854 #
REPT-242 ..... N90-15403 #
REPT-1989: ..... N90-15806 #

RI/RD89-241 ..... N90-15294 #

RRK-89-10 ..... N90-15868 #
RRK-89-11 ..... N90-15829 #
RRK-89-13 ..... N90-15830 #

RSRE-88006 ..... N90-15303 #

S-177 ..... N90-15323 #

SAAO-13 ..... N90-15856* #

SAND-86-0141 ..... N90-15283 #
SAND-89-0246C ..... N90-15505 #
SAND-89-0247C-2 ..... N90-15521 #
SAND-89-0319C ..... N90-15087 #
SAND-89-0597C ..... N90-15449 #
SAND-89-0623 ..... N90-15088 #
SAND-89-0782 ..... N90-15359 #
SAND-89-0917 ..... N90-15285 #
SAND-89-0919C ..... N90-15437 #
SAND-89-0965C ..... N90-15672 #
SAND-89-1118C ..... N90-15165 #
SAND-89-1322C ..... N90-15769 #
SAND-89-1485 ..... N90-15076 #
SAND-89-1512C ..... N90-15473 #
SAND-89-1607C ..... N90-15328 #
SAND-89-1653C ..... N90-15720 #
SAND-89-1656C ..... N90-15114 #
SAND-89-1680C ..... N90-15474 #
SAND-89-1711C ..... N90-15511 #
SAND-89-1720 ..... N90-15365 #
SAND-89-1723C ..... N90-15801 #
SAND-89-1727C ..... N90-15802 #
SAND-89-1764C ..... N90-15228 #
SAND-89-1791C ..... N90-15180 #
SAND-89-1820C ..... N90-15255 #
SAND-89-1914C ..... N90-15324 #
SAND-89-1916C ..... N90-15661 #
SAND-89-2214C ..... N90-15358 #
SAND-89-2277C ..... N90-15357 #
SAND-89-2374C ..... N90-15819 #
SAND-89-2476C ..... N90-15524 #
SAND-89-2536C ..... N90-15706 #
SAND-89-2592C ..... N90-15466 #
SAND-89-2597C ..... N90-15523 #
SAND-89-2604C ..... N90-15166 #
SAND-89-2767C ..... N90-15265 #
SAND-89-2793C ..... N90-15795 #
SAND-89-7037 ..... N90-15525 #
SAND-89-7039 ..... N90-15509 #
SAND-89-7106 ..... N90-15330 #
SAND-89-7111 ..... N90-15757 #

SD-TR-89-60 ..... N90-15494 #

SERI/SP-220-3024 ..... N90-15512 #

SERI/STR-211-3508 ..... N90-15498 #
SERI/STR-211-3525 ..... N90-15499 #
SERI/STR-211-3582 ..... N90-15502 #
SERI/STR-211-3583 ..... N90-15503 #

SERI/TP-211-3595 ..... N90-15504 #
SERI/TP-257-3558 ..... N90-15519 #
SERI/TP-257-3589 ..... N90-15520 #

SR-1 ..... N90-15497 #

SRL-0020-TM ..... N90-15639 #
SRL-5510-F ..... N90-15297 #

SSD-TR-89-66 ..... N90-15495 #

SSI-TR-137-PHASE-2 ..... N90-15542 #
SSI-TR-154 ..... N90-15650 #

STD-15 ..... N90-15306 #

SU-SLAC-PUB-5066 ..... N90-15879 #

SU-SLAC/AP-77 ..... N90-15734 #

SU-SOL-89-7 ..... N90-15617 #
SU-SOL-89-11 ..... N90-15616 #
SU-SOL-89-16 ..... N90-15620 #
SU-SOL-89-17 ..... N90-15625 #

TAMRF-3224-85-12 ..... N90-15072* #

TI-08-89-54 ..... N90-15350 #

TM-89-38 ..... N90-15391 #

TR-D-108 ..... N90-15707 #

TR-3 ..... N90-15276 #
TR-4 ..... N90-15238 #
TR-11 ..... N90-15721 #
TR-15 ..... N90-15172 #
TR-17 ..... N90-15270 #
TR-41 ..... N90-15277 #
TR-41 ..... N90-15684 #
TR-42 ..... N90-15687 #
TR-43 ..... N90-15689 #
TR-89-996 ..... N90-15699* #
TR-89-997 ..... N90-15400* #
TR-89-1044 ..... N90-15647 #
TR-113 ..... N90-15646 #
TR-115 ..... N90-15725 #
TR-173 ..... N90-15677 #
TR-262 ..... N90-15602 #
TR-263 ..... N90-15600 #
TR-277-REV ..... N90-15091 #
TR-278 ..... N90-15667 #
TR-287 ..... N90-15644 #
TR-289 ..... N90-15649 #
TR-294 ..... N90-15648 #
TR-303 ..... N90-15665 #
TR-305 ..... N90-15589 #
TR-308 ..... N90-15631 #
TR-309 ..... N90-15603 #
TR-311 ..... N90-15601 #
TR-854 ..... N90-15735 #
TR-872 ..... N90-15304 #
TR-0086A(2940-04)-3 ..... N90-15494 #
TR-0088(3940-04)-2 ..... N90-15495 #

TRB/TRR-1169 ..... N90-15398 #

TR89-47 ..... N90-15676 #

TT-74 ..... N90-15307 #
TT-75 ..... N90-15305 #

UBUFFALO/DC/89/TR-113 ..... N90-15810 #
UBUFFALO/DC/89/TR-114 ..... N90-15816 #

UCB/CSD-89/532 ..... N90-15606 #

UCID-21543 ..... N90-15420 #
UCID-21619 ..... N90-15340 #
UCID-21682 ..... N90-15550 #
UCID-21753-PT-3 ..... N90-15729 #
UCID-21763 ..... N90-15290 #
UCID-21775-VOL-1 ..... N90-15122 #
UCID-21775-VOL-2 ..... N90-15123 #
UCID-21800 ..... N90-15366 #
UCID-21810 ..... N90-15411 #

UCLA-ENG-89-09 ..... N90-15485 #

UCRL-21230 ..... N90-15376 #
UCRL-21243 ..... N90-15461 #
UCRL-21245 ..... N90-15428 #
UCRL-21250 ..... N90-15748 #
UCRL-21254 ..... N90-15409 #
UCRL-98989 ..... N90-15410 #
UCRL-99677 ..... N90-15475 #
UCRL-100354 ..... N90-15337 #
UCRL-100359 ..... N90-15749 #
UCRL-100432 ..... N90-15333 #
UCRL-100496 ..... N90-15118 #
UCRL-100557 ..... N90-15615 #
UCRL-100596-REV-1 ..... N90-15780 #
UCRL-100649 ..... N90-15301 #
UCRL-100786 ..... N90-15770 #
UCRL-100805 ..... N90-15755 #
UCRL-100810 ..... N90-15119 #
UCRL-100833 ..... N90-15772 #
UCRL-100847 ..... N90-15377 #
UCRL-101066 ..... N90-15407 #
UCRL-101071 ..... N90-15417 #
UCRL-101076-REV-1 ..... N90-15597 #
UCRL-101108 ..... N90-15247 #
UCRL-101193 ..... N90-15406 #
UCRL-101381 ..... N90-15149 #
UCRL-101579 ..... N90-15786 #
UCRL-101602 ..... N90-15258 #
UCRL-101623 ..... N90-15476 #
UCRL-101630 ..... N90-15413 #
UCRL-101649 ..... N90-15731 #
UCRL-101663 ..... N90-15334 #
UCRL-101677 ..... N90-15412 #
UCRL-101837 ..... N90-15535 #
UCRL-101879 ..... N90-15286 #

UCRL-101907 ..... N90-15368 #
UCRL-101953 ..... N90-15281 #
UCRL-102001 ..... N90-15164 #
UCRL-102044 ..... N90-15257 #
UCRL-102059 ..... N90-15655 #
UCRL-102147 ..... N90-15448 #
UCRL-102150 ..... N90-15872 #

UDR-TR-88-104 ..... N90-15594 #

UILU-ENG-88-4019 ..... N90-15215 #

UK-ME-88-07 ..... N90-15386 #

UM-025921-8-T ..... N90-15146* #

UND-TR-89-10-01 ..... N90-15685 #

UNDAS-1419-FR ..... N90-15380* #

UR-1126 ..... N90-15702 #

US-PATENT-APPL-SN-275873 ..... N90-15355 #
US-PATENT-APPL-SN-304147 ..... N90-15261* #
US-PATENT-APPL-SN-344877 ..... N90-15148* #
US-PATENT-APPL-SN-370521 ..... N90-15405 #
US-PATENT-APPL-SN-372963 ..... N90-15322 #
US-PATENT-APPL-SN-377997 ..... N90-15240 #
US-PATENT-APPL-SN-389220 ..... N90-15278 #
US-PATENT-APPL-SN-392165 ..... N90-15710* #
US-PATENT-APPL-SN-394457 ..... N90-15426 #
US-PATENT-APPL-SN-404289 ..... N90-15227* #
US-PATENT-APPL-SN-404291 ..... N90-15733* #
US-PATENT-APPL-SN-404292 ..... N90-15443* #
US-PATENT-APPL-SN-405154 ..... N90-15442* #
US-PATENT-APPL-SN-408377 ..... N90-15427 #
US-PATENT-APPL-SN-408970 ..... N90-15607 #
US-PATENT-APPL-SN-410572 ..... N90-15259* #
US-PATENT-APPL-SN-418611 ..... N90-15263* #
US-PATENT-APPL-SN-426345 ..... N90-15161* #
US-PATENT-APPL-SN-429516 ..... N90-15094* #
US-PATENT-APPL-SN-433812 ..... N90-15260* #
US-PATENT-APPL-SN-433863 ..... N90-15147* #
US-PATENT-APPL-SN-441672 ..... N90-15444* #
US-PATENT-APPL-SN-443289 ..... N90-15262* #
US-PATENT-APPL-SN-443523 ..... N90-15130* #
US-PATENT-APPL-SN-458274 ..... N90-15445* #

USAAEFA-87-25-1-PHASE-2 ..... N90-15083 #

USAAVSCOM-TR-89-C-019 ..... N90-15434* #

USAFA-TR-89-6 ..... N90-15487 #

USAFSAM-JA-89-21 ..... N90-15581 #

UTRC-R89-917437-3 ..... N90-15236 #

UVA/525410/CS90/103 ..... N90-15642 #

UVA525167/MAE90/101 ..... N90-15113 #

UWAERP-20 ..... N90-15745 #

WHC-SP-0446 ..... N90-15116 #

WL-TR-89-37 ..... N90-15737 #

WL/NTA-TP-89-001 ..... N90-15321 #

WP-89W00181 ..... N90-15086 #

WRDC-TR-89-2082 ..... N90-15386 #
WRDC-TR-89-2106 ..... N90-15459 #
WRDC-TR-89-3097 ..... N90-15079 #
WRDC-TR-89-4023 ..... N90-15232 #
WRDC-TR-89-4027 ..... N90-15107 #
WRDC-TR-89-4071 ..... N90-15486 #

WSRC-RP-89-345 ..... N90-15460 #
WSRC-RP-89-385 ..... N90-15694 #
WSRC-RP-89-472 ..... N90-15849 #
WSRC-RP-89-476 ..... N90-15244 #
WSRC-RP-89-489 ..... N90-15243 #
WSRC-RP-89-524 ..... N90-15467 #
WSRC-RP-89-792 ..... N90-15256 #

Appendix—About STAR

Scientific and Technical Aerospace Reports (STAR) is a major component of a comprehensive National Aeronautics and Space Administration information system covering aeronautics, space, and supporting disciplines. *STAR* is issued on the 8th and 23rd of each month and announces current publications of the following types:

- NASA, NASA contractor, and NASA grantee reports
- Reports issued by other U.S. Government agencies, domestic and foreign institutions, universities, and private firms
- Translations in report form
- NASA-owned patents and patent applications
- Other U.S. Government agency and foreign patents and patent applications
- Domestic and foreign dissertations and theses

Journal, book, and conference literature, cover-to-cover journal translations, and certain foreign dissertations are announced in a companion journal, *International Aerospace Abstracts (IAA),* available on subscription from the American Institute of Aeronautics and Astronautics, Technical Information Service, 555 West 57th Street, 12th Floor, New York, NY 10019.

SUBJECT SCOPE

The subject scope of *STAR* and *IAA* includes all aspects of aeronautics and space research and development, supporting basic and applied research, and applications. Aerospace aspects of earth resources, energy development, conservation, oceanography, environmental protection, urban transportation, and other topics of high national priority are also covered.

OTHER NASA PUBLICATIONS

Other NASA publications and information services are described in the publication, *The NASA Scientific and Technical Information System ... and How to Use It,* available without charge from the NASA Scientific and Technical Information Facility, P.O. Box 8757, BWI Airport, MD 21240.

HOW TO USE *STAR* SUBJECT CATEGORIES

STAR is categorized by 10 major subject divisions broken down further into 76 specific subject categories and one general division/category. The major subject divisions are listed on page ii in the Table of Contents, together with a note for each that defines its scope and provides any cross-references. For example:

AERONAUTICS

Includes aeronautics (general); aerodynamics; air transportation and safety; aircraft communications and navigation; aircraft design, testing and performance; aircraft instrumentation; aircraft propulsion and power; aircraft stability and control; and research and support facilities (air).

For related information see also *Astronautics.*

Each major division is further divided into as many as nine specific categories, which are identified by category numbers.

Abstracts in *STAR* are grouped by subject category, the categories appearing in sequential order. Category breaks in the abstract section are identified by the category number and title, and a scope note. Cross-references to other categories are provided as appropriate. For example:

02 AERODYNAMICS

Includes aerodynamics of bodies, combinations, wings, rotors, and control surfaces; and internal flow in ducts and turbomachinery.

For related information see also *34 Fluid Mechanics and Heat Transfer.*

CROSS-REFERENCES

Individual *STAR* abstracts are not ordinarily cross-referenced, except for certain conference reports or book translations that have had separate abstracts written for their component papers or chapters. Citations and abstracts of the components follow immediately after those of the parent document. When the subject content of a component differs sufficiently from the general content of the parent, a cross-reference citation also is printed at the end of the category to which it normally would have been assigned if it were independent.

DOCUMENTS ON MICROFICHE

Documents on microfiche[1] are designated by a pound sign (#) following the accession number. The pound sign is used without regard to the source or quality of the microfiche.

LIMITED REPRODUCIBILITY

A Note of Limited Reproducibility appears in the citation, if one or a combination of the following factors affect the reproducibility of more than 20% of the document. These factors include: faint or broken type, color photographs, black and white photographs, foldouts, dot matrix print, charts/graphs with script notation, non-Roman alphabet, or some other factor that limits the reproducibility of that document. This notation also appears on the microfiche header, with the specific causing factor checked off on a list visible in the second frame.

AVAILABILITIES

One or more sources from which a document announced in *STAR* is available to the public is given in each citation. The most commonly indicated sources and their acronyms or abbreviations are listed below. If the publication is available from a source other than those listed, the publisher and his address will be displayed on the availability line or in combination with the corporate source line.

Avail: NTIS. Sold by the National Technical Information Service. Prices for hard copy (HC) and microfiche (MF) are indicated by a price code following the letters HC or MF in the *STAR* citation. Current values for the price codes are given in the tables on page A-7.

Initially distributed microfiche under the NTIS SRIM (Selected Research in Microfiche) is available at greatly reduced unit prices. For this service and for information concerning subscription to NASA printed reports, consult the NTIS Subscription Section, Springfield, VA 22161.

NOTE ON ORDERING DOCUMENTS: When ordering NASA publications (those followed by the * symbol), use the N accession number. NASA patent applications (only the specifications are offered) should be ordered by the US-Patent-Appl-SN number. Non-NASA publications (no asterisk) should be ordered by the AD, PB, or other *report number* shown on the last line of the citation, not by the N accession number. It is also advisable to cite the title and other bibliographic identification.

(1) A microfiche is a transparent sheet of film, 105 by 148 mm in size, containing as many as 60 to 98 pages of information reduced to micro images (not to exceed 26:1 reduction).

Avail: SOD (or GPO). Sold by the Superintendent of Documents, U.S. Government Printing Office, in hard copy. The current price and order number are given following the availability line. (NTIS will fill microfiche requests, as indicated above, for those documents identified by a # symbol.)

Avail: BLL (formerly NLL): British Library Lending Division, Boston Spa, Wetherby, Yorkshire, England. Photocopies available from this organization at the price shown. (If none is given, inquiry should be addressed to the BLL.)

Avail: DOE Depository Libraries. Organizations in U.S. cities and abroad that maintain collections of Department of Energy reports, usually in microfiche form, are listed in *Energy Research Abstracts*. Services available from the DOE and its depositories are described in a booklet, *DOE Technical Information Center - Its Functions and Services* (TID-4660), which may be obtained without charge from the DOE Technical Information Center.

Avail: ESDU. Pricing information on specific data, computer programs, and details on Engineering Sciences Data Unit (ESDU) topic categories can be obtained from ESDU International Ltd. Requesters in North America should use the Virginia address while all other requesters should use the London address, both of which are on page A-6.

Avail: Fachinformationszentrum, Karlsruhe. Sold by the Fachinformationszentrum Energie, Physik, Mathematik GMBH, Eggenstein Leopoldshafen, Federal Republic of Germany, at the price shown in deutschmarks (DM).

Avail: HMSO. Publications of Her Majesty's Stationery Office are sold in the U.S. by Pendragon House, Inc. (PHI), Redwood City, CA. The U.S. price (including a service and mailing charge) is given, or a conversion table may be obtained from PHI.

Avail: NASA Public Document Rooms. Documents so indicated may be examined at or purchased from the National Aeronautics and Space Administration, Public Documents Room (Room 126), 600 Independence Ave., S.W., Washington, DC 20546, or public document rooms located at NASA installations, and the NASA Pasadena Office at the Jet Propulsion Laboratory.

Avail: Univ. Microfilms. Documents so indicated are dissertations selected from *Dissertation Abstracts* and are sold by University Microfilms as xerographic copy (HC) and microfilm. All requests should cite the author and the Order Number as they appear in the citation.

Avail: US Patent and Trademark Office. Sold by Commissioner of Patents and Trademarks, U.S. Patent and Trademark Office, at the standard price of $1.50 each, postage free. (See discussion of NASA patents and patent applications below.)

Avail: (US Sales Only). These foreign documents are available to users within the United States from the National Technical Information Service (NTIS). They are available to users outside the United States through the International Nuclear Information Service (INIS) representative in their country, or by applying directly to the issuing organization.

Avail: USGS. Originals of many reports from the U.S. Geological Survey, which may contain color illustrations, or otherwise may not have the quality of illustrations preserved in the microfiche or facsimile reproduction may be examined by the public at the libraries of the USGS field offices whose addresses are listed in this Introduction. The libraries may be queried

concerning the availability of specific documents and the possible utilization of local copying services, such as color reproduction.

Avail: Issuing Activity, or Corporate Author, or no indication of availability. Inquiries as to the availability of these documents should be addressed to the organization shown in the citation as the corporate author of the document.

NASA PATENTS AND PATENT APPLICATIONS

Patents and patent applications owned by NASA are announced in *STAR* under appropriate subject categories and are referenced in the *STAR* indexes. In the Report/Accession Number Index, patents are indexed by the NASA Case Number (which appears in lieu of the report number in other indexes), the U.S. Patent Number, the U.S. Patent Application Serial Number, and the U.S. Patent Class. Patent applications for which patents have not yet been issued are indexed by the NASA Case Number and the U.S. Patent Application Serial Number.

NASA *patent application specifications* are sold in paper copy and microfiche by the National Technical Information Service (NTIS). The US-Patent-Appl-SN- number should be used in ordering either paper copy or microfiche from NTIS. Printed copies of *patents* (which are not microfiched) are available for purchase from:

Commissioner of Patents and Trademarks
U.S. Patent and Trademark Office
Washington, DC 20231

When ordering patents, the U.S. Patent Number should be used, and payment must be remitted in advance, by money order or check payable to the Commissioner of Patents and Trademarks. Prepaid purchase coupons for ordering are also available from the Patent and Trademark Office. The patents and patent applications announced in *STAR* are owned by NASA and are available for royalty-free licensing. Requests for licensing terms and further information should be addressed to:

Associate General Counsel for Intellectual Property/Code GP
National Aeronautics and Space Administration
Washington, DC 20546

ELIGIBILITY AND REGISTRATION FOR NASA INFORMATION PRODUCTS AND SERVICES

A variety of services is available to organizations of the following types that have registered with NASA to receive specific services or products:

1. NASA offices and installations, contractors, subcontractors, grantees, and consultants;
2. Other U.S. Government agencies and their contractors;
3. Libraries in the United States that have arrangements with NASA to maintain collections of NASA documents for public reference;
4. Other organizations in the United States having a need for NASA documents in work related to aeronautics and space research;
5. Organizations abroad that have established reciprocal document exchange arrangements with NASA.

Only the central service points or central points of document acquisition and control within qualified organizations are eligible to register for NASA products and services. Domestic organizations that may be eligible to receive various classes of NASA publications and services should address their requests for registration or for further information to:

NASA Scientific and Technical Information Facility
ATTN: Registration Services
P.O. Box 8757
BWI Airport, MD 21240
301-621-0153

Organizations abroad should direct requests to Manager, International STI Activities, NTT, NASA Headquarters, Washington, DC 20546.

AVAILABILITY OF *STAR* ABSTRACTS ON MICROFICHE

Microfiche of the abstract sections of this issue and other issues of *STAR* are available on annual subscription from NTIS as PB90-911300, Attn: Subscriptions, 5285 Port Royal Road, Springfield, VA 22161. Annual subscription rates are $75.50 North America; $151.00 foreign. Abstract sections for previous years retroactive to 1964 are available at the current rates. Microfiche for individual *STAR* issue abstract sections are not available.

PUBLIC COLLECTIONS OF NASA DOCUMENTS

DOMESTIC: NASA and NASA-sponsored documents and a large number of aerospace publications are available to the public for reference purposes at the library maintained by the American Institute of Aeronautics and Astronautics, Technical Information Service, 555 West 57th Street, 12th Floor, New York, NY 10019

EUROPEAN: An extensive collection of NASA and NASA-sponsored publications is maintained by the British Library Lending Division, Boston Spa, Wetherby, Yorkshire, England, for public access. The British Library Lending Division also has available many of the non-NASA publications cited in *STAR*. European requesters may purchase facsimile copy or microfiche of NASA and NASA-sponsored documents, those identified by both the symbols # and * from ESA - Information Retrieval Service, European Space Agency, 8-10 rue Mario-Nikis, 75738 Paris CEDEX 15, France.

FEDERAL DEPOSITORY LIBRARY PROGRAM

In order to provide the general public with greater access to U.S. Government publications, Congress established the Federal Depository Library Program under the Government Printing Office (GPO), with 51 regional depositories responsible for permanent retention of material, inter-library loan, and reference services. At least one copy of nearly every NASA and NASA-sponsored publication, either in printed or microfiche format, is received and retained by the 51 regional depositories. A list of the regional GPO libraries, arranged alphabetically by state, appears on the inside back cover. These libraries are *not* sales outlets. A local library can contact a Regional Depository to help locate specific reports, or direct contact may be made by an individual.

ADDRESSES OF ORGANIZATIONS

American Institute of Aeronautics and Astronautics
Technical Information Service
555 West 57th Street, 12th Floor
New York, New York 10019

British Library Lending Division,
Boston Spa, Wetherby, Yorkshire,
England

Commissioner of Patents and Trademarks
U.S. Patent and Trademark Office
Washington, DC 20231

Department of Energy
Technical Information Center
P.O. Box 62
Oak Ridge, Tennessee 37830

European Space Agency-Information Retrieval Service
ESRIN
Via Galileo Galilei
00044 Frascati (Rome) Italy

Engineering Sciences Data Unit International
P.O. Box 1633
Manassas, Virginia 22110

Engineering Sciences Data Unit International, Ltd.
251-259 Regent Street
London, W1R 7AD, England

Fachinformationszentrum Energie, Physik, Mathematik
GMBH
7514 Eggenstein Leopoldshafen
Federal Republic of Germany

Her Majesty's Stationery Office
P.O. Box 569, S.E. 1
London, England

NASA Scientific and Technical Information Facility
P.O. Box 8757
BWI Airport, Maryland 21240

National Aeronautics and Space Administration
Scientific and Technical Information Division (NTT)
Washington, DC 20546

National Technical Information Service
5285 Port Royal Road
Springfield, Virginia 22161

Pendragon House, Inc.
899 Broadway Avenue
Redwood City, California 94063

Superintendent of Documents
U.S. Government Printing Office
Washington, DC 20402

University Microfilms
A Xerox Company
300 North Zeeb Road
Ann Arbor, Michigan 48106

University Microfilms, Ltd.
Tylers Green
London, England

U.S. Geological Survey Library National Center
MS 950
12201 Sunrise Valley Drive
Reston, Virginia 22092

U.S. Geological Survey Library
2255 North Gemini Drive
Flagstaff, Arizona 86001

U.S. Geological Survey
345 Middlefield Road
Menlo Park, California 94025

U.S. Geological Survey Library
Box 25046
Denver Federal Center, MS914
Denver, Colorado 80225

NTIS PRICE SCHEDULES

(Effective January 1, 1990)

Schedule A
STANDARD PRICE DOCUMENTS AND MICROFICHE

PRICE CODE	NORTH AMERICAN PRICE	FOREIGN PRICE
A01	$ 8.00	$ 16.00
A02	11.00	22.00
A03	15.00	30.00
A04-A05	17.00	34.00
A06-A09	23.00	46.00
A10-A13	31.00	62.00
A14-A17	39.00	78.00
A18-A21	45.00	90.00
A22-A25	53.00	106.00
A99	*	*
N01	60.00	120.00
N02	59.00	118.00
N03	20.00	40.00

Schedule E
EXCEPTION PRICE DOCUMENTS AND MICROFICHE

PRICE CODE	NORTH AMERICAN PRICE	FOREIGN PRICE
E01	$10.00	$ 20.00
E02	12.00	24.00
E03	14.00	28.00
E04	16.50	33.00
E05	18.50	37.00
E06	21.50	43.00
E07	24.00	48.00
E08	27.00	54.00
E09	29.50	59.00
E10	32.50	65.00
E11	35.00	70.00
E12	38.50	77.00
E13	41.00	82.00
E14	45.00	90.00
E15	48.50	97.00
E16	53.00	106.00
E17	57.50	115.00
E18	62.00	124.00
E19	69.00	138.00
E20	80.00	160.00
E99	*	*

* Contact NTIS for price quote.

IMPORTANT NOTICE

NTIS Shipping and Handling Charges

U.S., Canada, Mexico — ADD $3.00 per TOTAL ORDER

All Other Countries — ADD $4.00 per TOTAL ORDER

Exceptions — Does NOT apply to:

ORDERS REQUESTING NTIS RUSH HANDLING
ORDERS FOR SUBSCRIPTION OR STANDING ORDER PRODUCTS *ONLY*

NOTE: Each additional delivery address on an order requires a separate shipping and handling charge.

FEDERAL REGIONAL DEPOSITORY LIBRARIES

ALABAMA

AUBURN UNIV. AT MONTGOMERY LIBRARY
Documents Department
Montgomery, AL 36193
(205) 279-9110 ext.253

UNIV. OF ALABAMA LIBRARY
Reference Department/Documents
Box S
Tuscaloosa, AL 35486
(205) 348-6046

ARIZONA

DEPT. OF LIBRARY, ARCHIVES, AND PUBLIC RECORDS
Third Floor State Capitol
1700 West Washington
Phoenix, AZ 85007
(602) 255-4121

ARKANSAS

ARKANSAS STATE LIBRARY
Documents Service Section
One Capitol Mall
Little Rock, AR 72201
(501) 371-2090

CALIFORNIA

CALIFORNIA STATE LIBRARY
Govt. Publications Section
914 Capitol Mall
Sacramento, CA 95814
(916) 322-4572

COLORADO

UNIV. OF COLORADO
Norlin Library
Government Publications Division
Campus Box 184
Boulder, CO 80309
(303) 492-8834

DENVER PUBLIC LIBRARY
Govt. Pub. Department
1357 Broadway
Denver, CO 80203
(303) 571-2346

CONNECTICUT

CONNECTICUT STATE LIBRARY
231 Capitol Avenue
Hartford, CT 06106
(203) 566-4971

FLORIDA

UNIV. OF FLORIDA LIBRARIES
Documents Department
Library West
Gainesville, FL 32611
(904) 392-0367

GEORGIA

UNIV. OF GEORGIA LIBRARIES
Government Documents Dept.
Athens, GA 30602
(404) 542-8949

HAWAII

UNIV. OF HAWAII
Hamilton Library
Government Documents Collection
2550 The Mall
Honolulu, HI 96822
(808) 948-8230

IDAHO

UNIV. OF IDAHO LIBRARY
Documents Section
Moscow, ID 83843
(208) 885-6344

ILLINOIS

ILLINOIS STATE LIBRARY
Federal Documents
Centennial Building
Springfield, IL 62756
(217) 782-5012

INDIANA

INDIANA STATE LIBRARY
Serials Section
140 North Senate Avenue
Indianapolis, IN 46204
(317) 232-3686

IOWA

UNIV. OF IOWA LIBRARIES
Government Publications Dept.
Iowa City, IA 52242
(319) 335-5926

KANSAS

UNIVERSITY OF KANSAS
Spencer Research Library
Government Documents
Lawrence, KS 66045
(913) 864-4662

KENTUCKY

UNIV. OF KENTUCKY LIBRARIES
Government Publications/Maps Dept.
Lexington, KY 40506
(606) 257-8400

LOUISIANA

LOUISIANA STATE UNIVERSITY
Middleton Library
Government Documents Dept.
Baton Rouge, LA 70803
(504) 388-2570

LOUISIANA TECHNICAL UNIV.
Prescott Memorial Library
Government Documents Dept.
Ruston, LA 71272
(318) 257-4962

MAINE

UNIVERSITY OF MAINE
Raymond H. Fogler Library
Govt. Documents & Microforms Dept.
Orono, ME 04469
(207) 581-1680

MARYLAND

UNIVERSITY OF MARYLAND
McKeldin Library
Documents/Maps Room
College Park, MD 20742
(301) 454-3034

MASSACHUSETTS

BOSTON PUBLIC LIBRARY
Government Documents Dept.
666 Boylston Street
Boston, MA 02117
(617) 536-5400 ext.226

MICHIGAN

DETROIT PUBLIC LIBRARY
5201 Woodward Avenue
Detroit, MI 48202
(313) 833-1409

LIBRARY OF MICHIGAN
Government Documents
P.O. Box 30007
735 E. Michigan Avenue
Lansing, MI 48909
(517) 373-1593

MINNESOTA

UNIVERSITY OF MINNESOTA
Wilson Library
Government Publications
309 Nineteenth Avenue South
Minneapolis, MN 55455
(612) 373-7813

MISSISSIPPI

UNIV. OF MISSISSIPPI LIB.
Government Documents Dept.
106 Old Gym Bldg.
University, MS 38677
(601) 232-5857

MISSOURI

University of Missouri at Columbia Library
Government Documents
Columbia, MO 65201
(314) 882-6733

MONTANA

UNIV. OF MONTANA
Mansfield Library
Documents Division
Missoula, MT 59812
(406) 243-6700

NEBRASKA

UNIVERSITY OF NEBRASKA - LINCOLN
Love Memorial Library
Documents Department
Lincoln, NE 68588
(402) 472-2562

NEVADA

UNIV. OF NEVADA-RENO LIB.
Govt. Pub. Department
Reno, NV 89557
(702) 784-6579

NEW JERSEY

NEWARK PUBLIC LIBRARY
U.S. Documents Division
5 Washington Street
P.O. Box 630
Newark, NJ 07101
(201) 733-7812

NEW MEXICO

UNIVERSITY OF NEW MEXICO
General Library
Government Publications/Maps Dept.
Albuquerque, NM 87131
(505) 277-5441

NEW MEXICO STATE LIBRARY
325 Don Gaspar Avenue
Santa Fe, NM 87501
(505) 827-3826

NEW YORK

NEW YORK STATE LIBRARY
Documents Sect. Cultural Educ. Ctr.
Empire State Plaza
Albany, NY 12230
(518) 474-5563

NORTH CAROLINA

UNIVERSITY OF NORTH CAROLINA AT CHAPEL HILL
Davis Library 080A
BA/SS Department Documents
Chapel Hill, NC 27514
(919) 962-1151

NORTH DAKOTA

NORTH DAKOTA STATE UNIVERSITY LIBRARY
Government Documents Dept.
Fargo, ND 58105
(701) 237-8352
In cooperation with Univ. of North Dakota, Chester Fritz Library
Grand Forks

OHIO

STATE LIBRARY OF OHIO
Documents Section
65 South Front Street
Columbus, OH 43266
(614) 644-7051

OKLAHOMA

OKLAHOMA DEPT. OF LIBRARIES
Government Documents
200 NE 18th Street
Oklahoma City, OK 73105
(405) 521-2502, ext. 252

OKLAHOMA STATE UNIV. LIB.
Documents Department
Stillwater, OK 74078
(405) 624-0489

OREGON

PORTLAND STATE UNIV.
Millar Library
934 SW Harrison - P.O. Box 1151
Portland, OR 97207
(503) 229-3673

PENNSYLVANIA

STATE LIBRARY OF PENN.
Government Publications Section
Box 1601
Walnut St. & Commonwealth Ave.
Harrisburg, PA 17105
(717) 787-3752

SOUTH CAROLINA

CLEMSON UNIV. COOPER LIB.
Documents Department
Clemson, SC 29634
(803) 656-5174
In cooperation with Univ. of South Carolina, Thomas Cooper Library, Columbia

TEXAS

TEXAS STATE LIBRARY
Public Services Department
P.O. Box 12927 - 1201 Brazos
Austin, TX 78711
(512) 463-5455

TEXAS TECH. UNIV. LIBRARY
Documents Department
Lubbock, TX 79409
(806) 742-2268

UTAH

UTAH STATE UNIVERSITY
Merrill Library & Learning Resources Center, UMC-30
Documents Department
Logan, UT 84322
(801) 750-2682

VIRGINIA

UNIVERSITY OF VIRGINIA
Alderman Library
Government Documents
Charlottesville, VA 22903
(804) 924-3133

WASHINGTON

WASHINGTON STATE LIBRARY
Document Section
Olympia, WA 98504
(206) 753-4027

WEST VIRGINIA

WEST VIRGINIA UNIV. LIB.
Government Documents Section
P.O. Box 6069
Morgantown, WV 26506
(304) 293-3640

WISCONSIN

ST. HIST SOC. OF WISCONSIN LIB.
Government Pub. Section
816 State Street
Madison, WI 53706
(608) 262-2781
In cooperation with Univ. of Wisconsin-Madison, Memorial Library

MILWAUKEE PUBLIC LIBRARY
Documents Division
814 West Wisconsin Avenue
Milwaukee, WI 53233
(414) 278-3065

WYOMING

WYOMING STATE LIBRARY
Supreme Court & Library Bldg.
Cheyenne, WY 82002
(307) 777-5919

National Aeronautics and
Space Administration
Code NTT
Washington, D.C.
20546
Official Business
Penalty for Private Use, $300

SPECIAL FOURTH-CLASS RATE
POSTAGE & FEES PAID
NASA
PERMIT No. G27

NASA

POSTMASTER: If Undeliverable (Section 158
Postal Manual) Do Not Return